C5320 Theoretical Concepts of NMR

Lukáš Žídek

May 16, 2023

ii

Contents

How to use this text

After couple years of teaching the course C5320 Theoretical Concepts of NMR, I have decided to convert my handwritten notes to an electronic format. My students soon asked me to share my notes with them. I have agreed, warning them that the text was not supposed to serve as a textbook. Its purpose was not to explain NMR to students, but to keep the background information in a single file for the teacher. More recently, I have added introductions summarizing content of individual lectures. You recognize them by a larger font and less technical details. But my original notes are still there, labeled Supporting Information. They represent a very heterogeneous collections of derivations, lists, technical issues, without much explanation. Intentionally, I have not tried to safe space and included details usually omitted in textbooks. I have also found useful to incorporate discussion from the original literature instead of providing reference to old articles. Feel free to use it as a source of information but do not expect educational approach.

I would like to stress that the course expects a regular attendance of lectures and of the related practical exercises. Fortunately, there are also excellent textbooks explaining NMR. Our course does not follow any of them specifically, but I strongly recommend to check them especially if you find my lectures confusing. At the beginning of each Lecture, I refer to the textbooks by a one-letter symbol defining the book, followed by the number specifying the section. The one-letter symbols followed by the full citation and a short description are listed below

- **K:** J. Keeler, Understanding NMR spectroscopy, 2nd. ed., Wiley 2010. Very educational, easy to read, but physically correct, written for chemists.

- **L:** M. Levitt: Spin dynamics, 2nd. ed., Wiley 2008. Also very educational, with many pictures, physically correct, going more to physics than Keeler and including topics not covered by Keeler or by our course.

- **C:** J. Cavanagh et al., Protein NMR spectroscopy, 2nd. ed., Academic Press 2006 .Extremely useful and detailed, but more difficult to read, the only book of the list discussing applications to large molecules (proteins), but including also rigorous description of physical principles.

- **B:** K. Brown: Essential mathematics for NMR and MRI spectroscopists, Royal Society of Chemistry 2017. Detailed description of many mathematical background, providing details omitted in textbooks, written for chemists without advanced prior knowledge of mathematics.

Finally, I should also clearly describe the content and purpose of the course. It is curiosity-oriented course, attempting to explain the theory of NMR and to answer the "why" questions. The

course does not teach you how to analyze NMR spectra or set up NMR experiments, but it should tell you why are the NMR experiments designed as they are. As NMR has roots in physics but its fruit is mostly picked by chemists, the course must take into account that students of chemistry and biochemistry are less trained in classical mechanics and electromagnetism than the students of physics and biophysics. I try to cope with this fact by including the "zeroth" chapter in this study text. Its content is not covered by a lecture, but the students should read it individually (ideally before the course starts) to check how much they understand the basics and to fill the gaps. The "zeroth" chapter also contains a homework that should guide the students.

Part I

Classical Introduction

Before we start:
Classical electromagnetism

Literature: Classical electromagnetism is discussed in L2 and B11, with the mathematical background covered by B4.

0.1 Electric field, electric charge, electric dipole

Objects having a property known as the *electric charge* (Q) experience forces ($\vec{F}$) described as the *electric field*. Since the force depends on both charge and field, a quantity $\vec{E} = \vec{F}/Q$ known as the *electric intensity* has been introduced:

$$\vec{F} = Q\vec{E}. \tag{1}$$

Field lines are often used to visualize the fields: direction of the line shows the direction of $\vec{E}$, density of the lines describes the size of $\vec{E}$ ($|E|$). A homogeneous static electric field is described by straight parallel field lines.

Two point electric charges of the same size and opposite sign ($+Q$ and $-Q$) separated by a distance $2r$ constitute an *electric dipole*. Electric dipoles in a homogeneous static electric field experience a *moment of force*, or *torque* $\vec{\tau}$:

$$\vec{\tau} = 2\vec{r} \times \vec{F} = 2\vec{r} \times Q\vec{E} = 2Q\vec{r} \times \vec{E} = \vec{\mu}_{\mathrm{e}} \times \vec{E}, \tag{2}$$

where $\vec{\mu}_{\mathrm{e}}$ is the *electric dipole moment*.

$$\vec{\tau} = \vec{\mu}_{\mathrm{e}} \times \vec{E} \tag{3}$$

is another possible definition of $\vec{E}$. As derived in Section 0.6.1, potential energy of an electric dipole is

$$\mathcal{E} = -\vec{\mu}_{\mathrm{e}} \cdot \vec{E}. \tag{4}$$

0.2 Magnetic field and magnetic dipole

There is no "magnetic charge", but magnetic moments exist:

$$\vec{\tau} = \vec{\mu}_{\mathrm{m}} \times \vec{B}, \tag{5}$$

where $\vec{\mu}_{\mathrm{m}}$ is the *magnetic dipole moment* (because this course is about magnetic resonance, we will write simply $\vec{\mu}$). This is *the definition* of the *magnetic induction* $\vec{B}$ as a quantity describing magnetic field. As a consequence, potential energy of a magnetic dipole can be derived as described by Eq. 27 for the electric dipole.

Potential energy of a magnetic moment $\vec{\mu}$ is

$$\mathcal{E} = -\vec{\mu} \cdot \vec{B}. \tag{6}$$

The magnetic induction $\vec{B}$ is related to the force acting on a charged object, but in a different way than the electric intensity $\vec{E}$ (cf. Eq. 1). The magnetic force depends not only on the electric charge Q but also on the speed of the charge $\vec{v}$ (i.e., on the *electric current*)

$$\vec{F} = Q(\vec{v} \times \vec{B}). \tag{7}$$

Therefore, the torque $\vec{\tau}$ cannot be described by an equation similar to Eq. 2. Instead,

$$\vec{\tau} = \vec{r} \times \vec{F} = Q\vec{r} \times (\vec{v} \times \vec{B}). \tag{8}$$

Due to the fundamental difference between Eqs. 2 and 8, it is more difficult to describe relation between the magnetic force, magnetic moment and energy. We experience it in Sections 0.6.2 and 4.9.1.

0.3 Source of the electric field

The source of the electric field is the *electric charge*. The charge (i) feels (a surrounding) field and (ii) makes (its own) field. Charge at rest is a source of a static electric field. Parallel plates with homogeneous distribution of charges (a capacitor) are a source of a homogeneous static electric field.

Force between charges is described by the *Coulomb's law*. The force between two charges is given by

$$\vec{F} = \frac{1}{4\pi\epsilon_0} \frac{Q_1 Q_2}{r^2} \frac{\vec{r}}{|r|}, \tag{9}$$

where $\epsilon_0 = 8.854187817 \times 10^{-12}\,\mathrm{F\,m^{-1}}$ is the vacuum electric permittivity.

Consequently, the electric intensity generated by a point charge is

$$\vec{E} = \frac{1}{4\pi\epsilon_0} \frac{Q}{r^2} \frac{\vec{r}}{|r|}. \tag{10}$$

The electric intensity generated by a charge density ρ is

$$\vec{E} = \frac{1}{4\pi\epsilon_0} \int_V \mathrm{d}V \frac{\rho}{r^2} \frac{\vec{r}}{|r|} \tag{11}$$

Coulomb's law implies that electric fields lines of a resting charge

1. are going out of the charge (diverge), i.e., the static electric field has a source (the charge)

2. are not curved (do not have curl or rotation), i.e., the static electric field does not circulate

This can been written mathematically in the form of *Maxwell equations*:[1]

$$\text{div } \vec{E} = \frac{\rho}{\epsilon_0}, \tag{12}$$

$$\text{rot } \vec{E} = 0. \tag{13}$$

where div $\vec{E}$ is a scalar equal to $\frac{\partial E_x}{\partial x} + \frac{\partial E_y}{\partial y} + \frac{\partial E_z}{\partial z}$ and rot $\vec{E}$ is a vector with the x, y, z components equal to $\frac{\partial E_z}{\partial y} - \frac{\partial E_y}{\partial z}, \frac{\partial E_x}{\partial z} - \frac{\partial E_z}{\partial x}, \frac{\partial E_y}{\partial x} - \frac{\partial E_x}{\partial y}$, respectively. These expressions can be written in a much more compact form, if we introduce a vector operator $\vec{\nabla} = \left(\frac{\partial}{\partial x}, \frac{\partial}{\partial y}, \frac{\partial}{\partial z} \right)$. Using this formalism, the Maxwell equations have the form

$$\vec{\nabla} \cdot \vec{E} = \frac{\rho}{\epsilon_0}, \tag{14}$$

$$\vec{\nabla} \times \vec{E} = 0. \tag{15}$$

0.4 Origin of the magnetic field

Electric charge at rest does not generate a magnetic field, but a *moving* charge does. The magnetic force is a *relativistic effect* (consequence of the contraction of distances in the direction of the motion, described by Lorentz transformation).[2] Magnetic field of a moving point charge is moving with the charge. Constant *electric current* generates a stationary magnetic field. Constant electric current in an *ideal solenoid* generates a *homogeneous* stationary magnetic field inside the solenoid.

Magnetic induction generated by a current density $\vec{j}$ (*Biot-Savart law*):

$$\vec{B} = \frac{1}{4\pi\epsilon_0 c^2} \int\limits_V \mathrm{d}V \frac{\vec{j}}{r^2} \times \frac{\vec{r}}{|r|} = \frac{\mu_0}{4\pi} \int\limits_V \mathrm{d}V \frac{\vec{j}}{r^2} \times \frac{\vec{r}}{|r|} \tag{16}$$

Biot-Savart law implies that magnetic field lines of a constant current in a straight wire

1. do not diverge, i.e., the static magnetic field does not have a source

---

[1]The first equation is often written using *electric induction* $\vec{D}$ as div $\vec{D} = \rho$. If electric properties are described in terms of individual charges in vacuum, $\vec{D} = \epsilon_0 \vec{E}$. If behavior of charges bound in molecules is described in terms of polarization $\vec{P}$ of the material, $\vec{D} = \epsilon_0 \vec{E} + \vec{P}$.

[2]A charge close to a very long straight wire which is uniformly charged experiences an electrical force $F_\perp$ in the direction perpendicular to the wire. If the charges in the wire move with a velocity v_0 and the charge close to the wire moves along the wire with a velocity v_1, the perpendicular force changes to $F_\perp(1 - \frac{v_0 v_1}{c^2})$, were c is the speed of light in vacuum. The modifying factor is clearly relativistic (B11.5).

2. make closed loops around the wire (have curl or rotation), i.e., the magnetic field circulates around the wire

This can been written mathematically in the form of *Maxwell equations*:[3]

$$\vec{\nabla} \cdot \vec{B} = 0, \tag{17}$$

$$\vec{\nabla} \times \vec{B} = \mu_0 \vec{j}. \tag{18}$$

A simple example of a moving charge is a circular loop with an electric current. As derived in Section 0.6.2, magnetic moment of a current loop is proportional the angular momentum of the circulating charge.

Magnetic dipolar moment $\vec{\mu}$ is proportional to the angular momentum $\vec{L}$

$$\vec{\mu} = \gamma \vec{L}, \tag{19}$$

where γ is known as the *magnetogyric ratio*.

The classical theory does not explain why particles like electrons or nuclei have their own magnetic moments, even when they do not move in circles (because the classical theory does not explain why such particles have their own angular momenta). However, if we take the nuclear magnetic moment as a fact (or if we obtain it using a better theory), the classical results are useful. It can be shown that the magnetic moment is *always* proportional to the angular momentum,[4] but the proportionality constant is not always $Q/2m$; it is difficult to obtain for nuclei.

Analysis of the current loop in a static homogeneous external magnetic field, presented in Section 0.6.2, shows that if the direction of the magnetic moment $\vec{\mu}$ of the loop differs from the direction of $\vec{B}$, a torque trying to align $\vec{\mu}$ with $\vec{B}$. However, the magnetic dipole does not adopt the energetically most favored orientation (with the same direction of $\vec{\mu}$ as $\vec{B}$), but rotates around $\vec{B}$ without changing the angle between $\vec{\mu}$ and $\vec{B}$. This motion on a cone is known as *precession*.

This is not a result of quantum mechanics, but a classical consequence of the relation between the magnetic moment and angular momentum of the current loop. The spinning top also precess in the Earth's gravitational field and riding a bicycle is based on the same effect.[5] The precession frequency can be derived easily for the classical current loop in a magnetic field (see Section 0.6.3):

Angular frequency of the precession of a magnetic dipolar moment $\vec{\mu}$ in a magnetic field $\vec{B}$ is

$$\vec{\omega} = -\gamma \vec{B}. \tag{20}$$

---

[3]The second equation is often written using *magnetic intensity* $\vec{H}$ as $\vec{\nabla} \times \vec{H} = \vec{j}$. If magnetism is described as behavior of individual charges and magnetic moments in vacuum, $\vec{H} = \vec{B}/\mu_0$. If properties of a magnetic materials are described in terms of its *magnetization* $\vec{M}$, then $\vec{H} = \vec{B}/\mu_0 - \vec{M}$.

[4]A consequence of the rotational symmetry of space described mathematically by the Wigner-Eckart theorem.

[5]If you sit on a bike which does not move forward, gravity soon pulls you down to the ground. But if the bike has a certain speed and you lean to one side, you do not fall down, you just turn a corner. A qualitative discussion of precession using the spinning top and riding a bicycle is presented in L2.4–L2.5.

0.5 Electrodynamics and magnetodynamics

Similarly to the electric charge, the magnetic dipole (i) feels the surrounding magnetic field and (ii) generates its own magnetic field. The magnetic field generated by a precessing magnetic dipole is not stationary, it varies. To describe variable fields, the Maxwell equations describing rotation must be modified:[6]

$$\vec{\nabla} \times \vec{E} = -\frac{\mathrm{d}\vec{B}}{\mathrm{d}t}, \tag{21}$$

$$\vec{\nabla} \times \vec{B} = \frac{1}{c^2}\frac{\mathrm{d}\vec{E}}{\mathrm{d}t} + \mu_0 \vec{j}. \tag{22}$$

Note that electric and magnetic fields are coupled in the dynamic equations. Not only electric currents current, but also temporal variation of $\vec{E}$ induces circulation of $\vec{B}$, and circulation of $\vec{E}$ is possible if $\vec{B}$ varies. This has many important consequences: it explains electromagnetic waves in vacuum and has numerous fundamental applications in electrical engineering, including those used in NMR spectroscopy.

Eq. 21 shows us how the frequency of the precession motion can be measured. A magnetic dipole in a magnetic field $\vec{B}_0$ generates a magnetic field $\vec{B}'$ with the component $\parallel \vec{B}_0$ constant and the component $\perp \vec{B}_0$ rotating around $\vec{B}_0$. If we place a loop of wire next to the precessing dipole, with the axis of the loop perpendicular to the axis of precession, the rotating component of $\vec{B}'$ induces circulation of $\vec{E}$ which creates a measurable oscillating electromotive force (voltage) in the loop (see Section 0.6.4).

$$U = \frac{\mu_0}{4\pi}\frac{2|\mu|S}{r^3}\omega \sin(\omega t). \tag{23}$$

As a consequence, an oscillating electric current flows in the loop (L2.8).

HOMEWORK

First check that you understand Section 0.6.1. Then, derive how is the magnetic moment of a current loop related to the angular momentum (Section 0.6.2) and what defines the precession frequency of a magnetic moment of a current loop in a homogeneous magnetic field (Section 0.6.3).

---

[6]The second equation can be written as $\vec{\nabla} \times \vec{H} = \frac{\mathrm{d}\vec{D}}{\mathrm{d}t} + \vec{j}$.
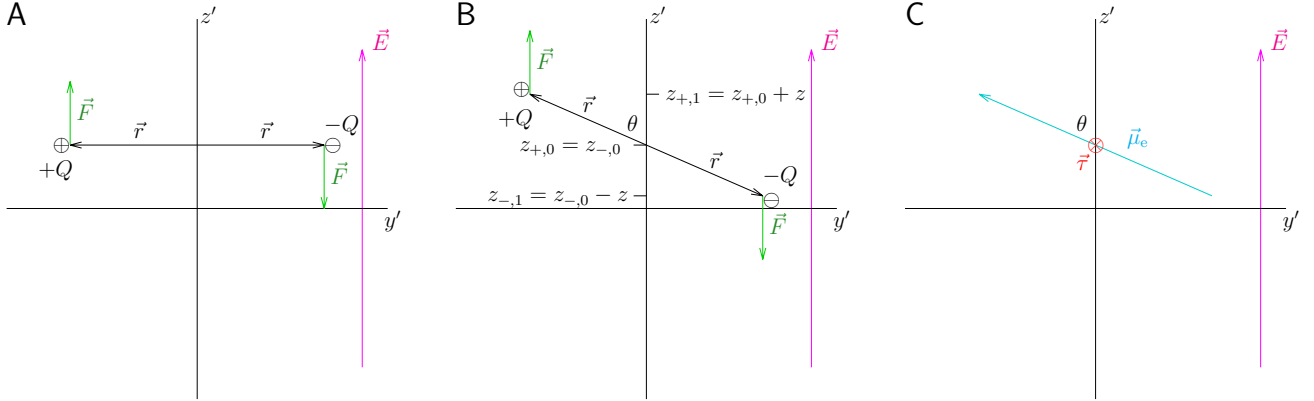
Figure 1: Potential energy of an electric dipole in a homogeneous electric field described by the intensity $\vec{E}$. The reference position of the dipole (0) is shown in Panel A, the actual position of the dipole (1) is shown in Panel B. Individual charges and forces are shown in panels A and B, the dipolar moment $\vec{\mu}_{\mathrm{e}}$ and the torque $\vec{\tau}$ (its direction $-x$ is depicted using the symbol $\otimes$) are shown in Panel C. Note that the direction of $\vec{\mu}_{\mathrm{e}}$ follows the convention used in physics, the convention used in chemistry is opposite.

0.6   SUPPORTING INFORMATION

0.6.1   Potential energy of an electric dipole

Potential energy[7] of the electric dipole can be calculated easily as a sum of potential energies of the individual charges. Potential energy is defined as the work done by the field moving the charge from a position (1) to a reference position (0). If we choose a coordinate system as defined in Figure 1, then the force acts only in the z'-direction ($F_{z'} = |\vec{F}| = Q|\vec{E}|$ for the positive charge and $F_{z'} = -|\vec{F}| = -Q|\vec{E}|$ for the negative charge). Therefore, it is sufficient to follow only how the z'-coordinates of the charges change because changes of other coordinates do not change the energy. The natural choice of the reference position is that the z' coordinates are the same for both charges, $z_{+,0} = z_{-,0}$. Changing the z' coordinate of the positive charge from $z_{+,0}$ to $z_{+,1} = z_{+,0} + z$ results in a work

$$Q|\vec{E}|(z_{+,0} - z_{+,1}) = -Q|\vec{E}|z. \tag{24}$$

Changing the z' coordinate of the negative charge from $z_{-,0}$ to $z_{-,1} = z_{-,0} - z$ results in a work

$$-Q|\vec{E}|(z_{-,0} - z_{-,1}) = -Q|\vec{E}|z. \tag{25}$$

Adding the works

$$\mathcal{E} = -2Q|\vec{E}|z = -2Q|\vec{E}|r\cos\theta = -\vec{\mu}_{\mathrm{e}} \cdot \vec{E}, \tag{26}$$

where θ is the angle between $\vec{E}$ and $\vec{\mu}_{\mathrm{e}}$.

Equivalently, the potential energy can be defined as the work done by the torque $\vec{\tau}$ on $\vec{\mu}_{\mathrm{e}}$ (Figure 1C) when rotating it from the reference orientation to the orientation described by the angle θ (between $\vec{E}$ and $\vec{\mu}_{\mathrm{e}}$). The reference angle for $z_{+,0} = z_{-,0}$ is $\pi/2$, therefore,

$$\mathcal{E} = \int_{\frac{\pi}{2}}^{\theta} |\vec{\tau}| \mathrm{d}\theta' = \int_{\frac{\pi}{2}}^{\theta} |\vec{\mu}_{\mathrm{e}}||\vec{E}| \sin\theta' \mathrm{d}\theta' = -|\vec{\mu}_{\mathrm{e}}||\vec{E}| \cos\theta = -\vec{\mu}_{\mathrm{e}} \cdot \vec{E}. \tag{27}$$

0.6.2   Current loop as a magnetic dipole

Now we derive what is the magnetic dipole of a circular loop with an electric current. The magnetic moment is defined by the torque $\vec{\tau}$ it experiences in a magnetic field $\vec{B}$ (Eq. 5):

$$\vec{\tau} = \vec{\mu} \times \vec{B}, \tag{28}$$

---

[7]Do not get confused: $\mathcal{E}$ (scalar) is the energy and $\vec{E}$ (vector) is electric intensity.

Therefore, we can calculate the magnetic moment of a current loop if we place it in a magnetic field $\vec{B}$. Let us first define the geometry of our setup. Let the axis z is the normal of the loop and let $\vec{B}$ is in the xz plane ($\Rightarrow B_y = 0$). The vector product in Eq. 5 then simplifies to

$$\tau_x = \mu_y B_z, \tag{29}$$
$$\tau_y = \mu_z B_x - \mu_x B_z, \tag{30}$$
$$\tau_z = -\mu_y B_x. \tag{31}$$

Note that we assume that the electric current in the loop and the magnetic field are independent. The current is not induced by $\vec{B}$ but has another (unspecified) origin, and $\vec{B}$ is not a result of the current, but is introduced from outside.

As the second step, we describe the electric current in the loop. The electric current is a motion of the electric charge. We describe the current as a charge Q homogeneously distributed in a ring (loop) of a mass m which rotates with a circumferential speed v. Then, each element of the loop of a infinitesimally small length $dl = r d\varphi$ contains the same fraction of the mass dm and of the charge dQ, moving with the velocity $\vec{v}$. The direction of the vector $\vec{v}$ is tangent to the loop and the amount of the charge per the length element is $Q/2\pi r$. The motion of the charge element dQ can be described, as any circular motion, by the *angular momentum*

$$d\vec{L} = \vec{r} \times d\vec{p} = dm(\vec{r} \times \vec{v}), \tag{32}$$

where $\vec{r}$ is the vector defining the position of the charge element dQ (Figure 2A). In our geometry, $\vec{r}$ is radial and therefore always perpendicular to $\vec{v}$. Since both $\vec{r}$ and $\vec{v}$ are in the xy plane, $d\vec{L}$ must have the same direction as the normal of the plane. Therefore, the x and y components of $d\vec{L}$ are equal to zero and the z component is constant and identical for all elements (note that $\vec{r}$ and $\vec{v}$ of different elements differ, but $\vec{r} \times \vec{v}$ is constant, oriented along the normal of the z axis and with the size equal to rv for all elements). It is therefore easy to integrate $d\vec{L}$ and calculate $\vec{L}$ of the loop

$$L_x = 0, \tag{33}$$
$$L_y = 0, \tag{34}$$
$$L_z = rv \int_{\text{loop}} dm = mrv. \tag{35}$$

As the third step, we examine forces acting on dQ. The force acting on a moving charge in a magnetic field (the Lorentz force) is equal to

$$\vec{F} = Q(\vec{E} + \vec{v} \times \vec{B}), \tag{36}$$

but we are now only interested in the magnetic component $\vec{F} = Q(\vec{v} \times \vec{B})$. The force acting on a single charge element dQ is

$$d\vec{F} = dQ(\vec{v} \times \vec{B}) = \frac{Q}{2\pi r} dl(\vec{v} \times \vec{B}) = \frac{Q}{2\pi}(\vec{v} \times \vec{B}) d\varphi. \tag{37}$$

The key step in our derivation is the definition of the torque

$$\vec{\tau} = \vec{r} \times \vec{F} = Q\vec{r} \times (\vec{v} \times \vec{B}), \tag{38}$$

which connects our analysis of the circular motion with the definition of $\vec{\mu}$ (Eq. 5). The torque acting on a charge element is (Figure 2B)

$$d\vec{\tau} = \vec{r} \times d\vec{F} = \frac{Q}{2\pi} \vec{r} \times (\vec{v} \times \vec{B}) d\varphi = \frac{Q}{2\pi} \left(\vec{v}(\vec{r} \cdot \vec{B}) - \vec{B} \underbrace{(\vec{r} \cdot \vec{v})}_{=0} \right) d\varphi = \frac{Q}{2\pi}(\vec{r} \cdot \vec{B}) \vec{v} d\varphi. \tag{39}$$

where a useful vector identity $\vec{a} \times (\vec{b} \times \vec{c}) = (\vec{a} \cdot \vec{c})\vec{b} - (\vec{a} \cdot \vec{b})\vec{c}$ helped us to simplify the equation because $\vec{r} \perp \vec{v}$. Eq. 39 tells us that the torque has the same direction as the velocity $\vec{v}$ ($\vec{v}$ is the only vector on the right-hand side because $\vec{r} \cdot \vec{B}$ is a scalar). In our coordinate frame, $v_x = -v \sin\varphi$, $v_y = v \cos\varphi$, $v_z = 0$, and $\vec{r} \cdot \vec{B} = r_x B_x + r_y B_y + r_z B_z = r_x B_x = B_x r \cos\varphi$ ($\vec{r} \cdot \vec{B}$ is reduced to $r_x B_x$ in our coordinate frame because $B_y = 0$ and $r_z = 0$). Therefore, we can calculate the components of the overall torque $\vec{\tau}$ as (Figure 2C)

$$\tau_x = -\frac{Qrv}{2\pi} B_x \int_0^{2\pi} \sin\varphi \cos\varphi \, d\varphi = -\frac{Qrv}{4\pi} B_x \int_0^{2\pi} \sin(2\varphi) d\varphi = 0, \tag{40}$$

$$\tau_y = \frac{Qrv}{2\pi} B_x \int_0^{2\pi} \cos^2\varphi \, d\varphi = \frac{Qrv}{4\pi} B_x \int_0^{2\pi} (1 + \cos(2\varphi)) d\varphi = \frac{Qrv}{2} B_x, \tag{41}$$

$$\tau_z = 0. \tag{42}$$

A   B   C
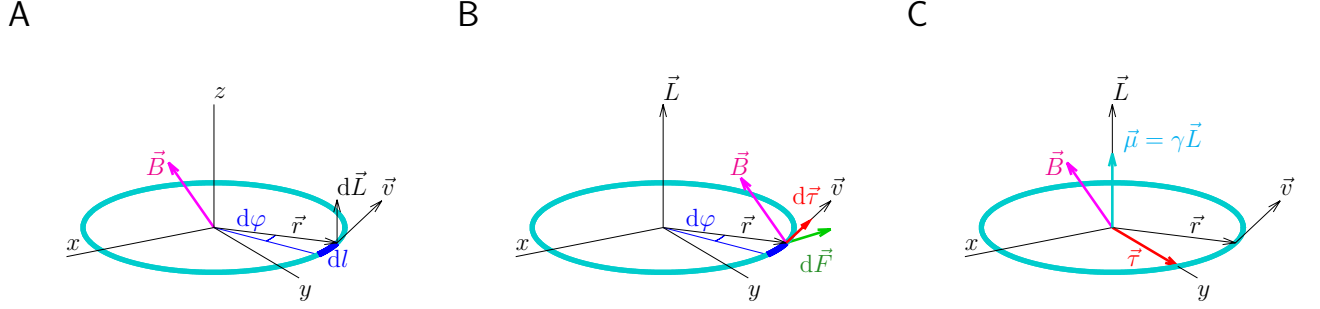
Figure 2: Current loop as a magnetic dipole. The loop of radius r and length $2\pi r$, charge Q and mass m is shown in cyan. A magnetic induction $\vec{B}$ of an external field is shown in magenta. The coordinates are chosen such that the loop is placed in the xy plane and $\vec{B}$ in the xz. An element of charge dQ (moving with the velocity $\vec{v}$), mass dm and length $dl = rd\varphi$ is shown in blue. The angular momentum of the blue element is $d\vec{L} = \vec{r} \times \vec{v}dm$ (Panel A). The total angular momentum is $\vec{L} = \vec{r} \times \vec{v}m$ (Panel B). The force $d\vec{F} = \vec{v} \times \vec{B}dQ$ and the torque $d\tau = \vec{r} \times d\vec{F}$ acting on the blue element are depicted as the green and red arrows in Panel B. The torque acting on the whole loop and the magnetic moment experiencing the torque in the field $\vec{B}$ are shown as the red and cyan arrows in Panel C.

Comparison with Eqs. 29–31 immediately shows that

$$\mu_x = 0, \tag{43}$$

$$\mu_y = 0, \tag{44}$$

$$\mu_z = \frac{Qrv}{2} \tag{45}$$

and comparison with Eqs. 33–35 reveals that the magnetic dipole moment of the current loop is closely related to the angular momentum $\vec{L} = \vec{r} \times m\vec{v}$:

$$\vec{\mu} = \frac{Q}{2m}\vec{L}. \tag{46}$$

0.6.3   Precession

Angular momentum of a particle moving in a circle is defined as $\vec{L} = m\vec{r} \times \vec{v}$ (Eq. 32), where $\vec{r}$ defines position of the particle and m and $\vec{v}$ are the mass and the velocity of the particle, respectively (Figure 3A). The change of $\vec{L}$ is described by the time derivative of $\vec{L}$.

$$\frac{d\vec{L}}{dt} = m\frac{d(\vec{r} \times \vec{v})}{dt} = m\frac{d\vec{r}}{dt} \times \vec{v} + m\vec{r} \times \frac{d\vec{v}}{dt} = m\underbrace{(\vec{v} \times \vec{v})}_{0} + \vec{r} \times m\vec{a}. \tag{47}$$

According the second Newton's law, $m\vec{a}$ is equal to the force acting on the particle (changing $\vec{L}$)

$$\frac{d\vec{L}}{dt} = \vec{r} \times m\vec{a} = \vec{r} \times \vec{F} = \vec{\tau}, \tag{48}$$

where $\vec{F}$ is the force and $\vec{\tau}$ is the corresponding torque. The change of the angular momentum of a current loop due to an external force can be calculated in the same manner (Figure 3). For an infinitesimal element of the loop,

$$\frac{d(d\vec{L})}{dt} = \vec{r} \times \vec{a}\,dm = \vec{r} \times d\vec{F} = d\vec{\tau}. \tag{49}$$

In a homogeneous magnetic field, the force acting on all elements is the same and integration of the individual elements is as easy as in Eq. 35, resulting in Eq. 48, where the force $\vec{F}$ and the torque $\vec{\tau}$ now act on the angular momentum of the whole loop. Because $\vec{\mu} = \gamma\vec{L}$ (Eq. 19) and $\vec{\tau} = \vec{\mu} \times \vec{B}$ (Eq. 5, the the magnetic moment of a current loop in a homogeneous magnetic field changes as

$$\frac{\mathrm{d}\vec{\mu}}{\mathrm{d}t} = \gamma \vec{r} \times \vec{F} = \gamma \vec{\tau} = \gamma \vec{\mu} \times \vec{B} = -\gamma \vec{B} \times \vec{\mu}. \tag{50}$$

Rotation of any vector, including $\vec{\mu}$ can be described using the angular frequency $\vec{\omega}$ (its magnitude is the speed of the rotation in radians per second and its direction is the axis of the rotation):

$$\frac{\mathrm{d}\vec{\mu}}{\mathrm{d}t} = \vec{\omega} \times \vec{\mu}. \tag{51}$$

Comparison with Eq. 50 immediately shows that $\vec{\omega} = -\gamma \vec{B}$.

0.6.4 Electromotive force (voltage)

We can use a simple example to analyze the induced voltage quantitatively. This voltage (the electromotive force) is an integral of the electric intensity along the detector loop. Stokes' theorem (see B9) allows us to calculate such integral from Eq. 21.

$$\oint_L \vec{E} \mathrm{d}\vec{l} = -\int_S \frac{\partial \vec{B}}{\partial t} \mathrm{d}\vec{S} = S \frac{\partial \vec{B}}{\partial t} \cdot \vec{n}, \tag{52}$$

where S is the area of the loop and $\vec{n}$ is the normal vector to the loop. If the distance r of the magnetic moment from the detector is much larger than the size of the loop, the magnetic induction of a field which is generated by a magnetic moment $\vec{\mu}$ rotating in a plane perpendicular to the detector loop and which crosses the loop (let us call it B_x) is[8]

$$B_x = \frac{\mu_0}{4\pi} \frac{2\mu_x}{r^3}. \tag{53}$$

As $\vec{\mu}$ rotates with the angular frequency ω, $\mu_x = |\mu|\cos(\omega t)$, and

$$\frac{\partial B_x}{\partial t} = -\frac{\mu_0}{4\pi} \frac{2}{r^3} |\mu|\omega \sin(\omega t). \tag{54}$$

Therefore, the oscillating induced voltage is

$$\oint_L \vec{E} \mathrm{d}\vec{l} = \frac{\mu_0}{4\pi} \frac{2|\mu|S}{r^3} \omega \sin(\omega t). \tag{55}$$

---

[8]We describe the field generated by a magnetic moment in more detail later in Section 8.1 when we analyze mutual interactions of magnetic moments of nuclei.
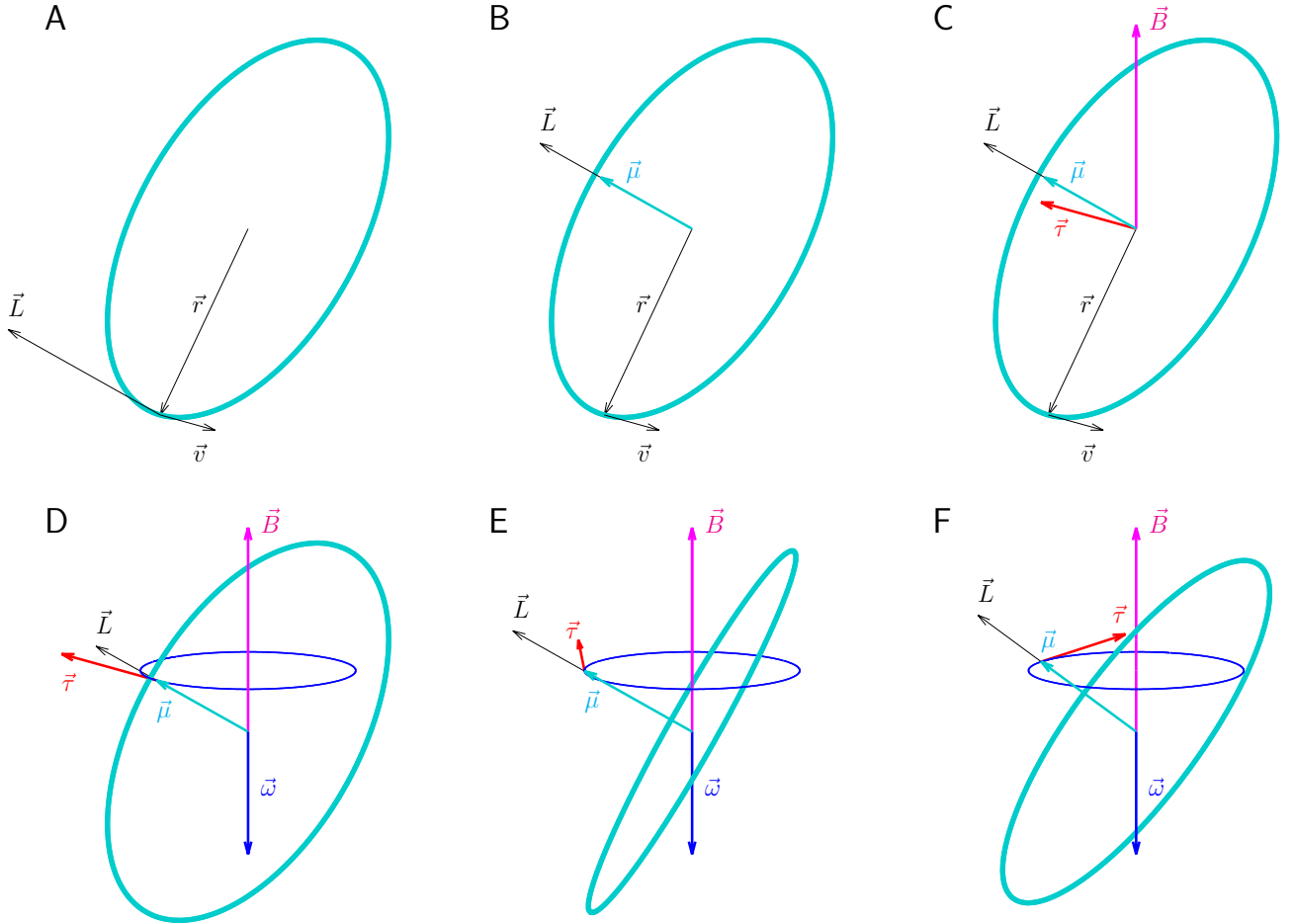
Figure 3: Classical description of precession of a current loop in a homogeneous magnetic field. Angular momentum $\vec{L}$ of a charged particle of the mass m moving in a circular loop (shown in cyan in Panel A) randomly oriented in space is given by the vector product of the actual position vector of the particle $\vec{r}$ and the actual particle's velocity $\vec{v}$ ($\vec{L} = m\vec{r} \times \vec{v}$). Note that size and direction of $\vec{L}$ is the same for all positions of the particle along the circle (for all possible vectors $\vec{r}$). The angular momentum $\vec{L}$ of a current loop of the same mass and the magnetic moment $\vec{\mu}$ (cyan arrow), proportional to $\vec{L}$ are shown in Panel B. The proportionality constant is γ (Eq. 19). In a presence of a vertical static magnetic field $\vec{B}$ (magenta arrow in Panel C), the loop experiences a torque $\vec{\tau} = \vec{\mu} \times \vec{B}$ (Eq. 5), shown as the red arrow in Panel C. This torque (red arrow moved to the tip of the cyan arrow in Panel D) acts on $\vec{\mu}$, which precesses about $\vec{B}$. Two snapshots of the precessing $\vec{\mu}$ (with the loop) are shown in Panels E and F. The tip of the cyan arrow representing $\vec{\mu}$ rotates about $\vec{B}$ (the blue circle) with the angular frequency $\vec{\omega} = -\gamma B$.

Lecture 1
Nuclear magnetic resonance

Literature: A general introduction can be found in L2.6 and L2.7. A nice and detailed discussion, emphasizing the importance of relaxation, is in Szántay et al.: Anthropic awareness, Elsevier 2015, Section 2.4. A useful review of relevant statistical concepts is presented in B6. Chemical shift is introduced by Levitt in L3.7 and discussed in detail in L9.1 (using a quantum approach, but the classical treatment can be obtained simply by using energy $\mathcal{E}_j$ instead of $\hat{H}_j$ and magnetic moment $\vec{\mu}_{jk}$ instead of $\gamma_j \hat{I}_{jk}$ in Eqs. 9.11–9.14). A nice discussion of the offset effects (and more) can be found in K4.

1.1   Nuclear magnetic moments in chemical substances

The aim of this course is to describe physical principles of the most frequent version of NMR spectroscopy, NMR analysis of chemical compounds dissolved in suitable solvents. We start by a description based on classical electrodynamics and postpone discussions based on quantum mechanics to Lecture 4. The classical theory does not explain why some nuclei in such solutions have a magnetic moment, but it describes macroscopic effects of the nuclear magnetic moments in bulk samples (i.e., in macroscopic systems composed of billions of billions of molecules). It should be emphasized that classical (non-quantum) physics provides much more relevant description of the macroscopic samples than quantum mechanics of individual particles (electrons or nuclei).

Some nuclei (e.g. ^{1}H) have permanent microscopic magnetic moments, but the macroscopic magnetic moment of non-ferromagnetic chemical substances is induced only in the magnetic field. This is the effect of symmetry. Outside a magnet, all orientations of the microscopic magnetic moments $\vec{\mu}$ have the same energy and are equally probable. Therefore, the bulk magnetic moment is zero and the bulk magnetization $\vec{M}$ (magnetic moment per unit volume) is zero (Fig. 1.1).

1.2   Polarization

In a static homogeneous magnetic field $\vec{B}_0$, the orientations of $\vec{\mu}$ are no longer equally probable: the orientation of $\vec{\mu}$ along $\vec{B}_0$ is energetically most favored and the opposite orientation is least favored. The symmetry is broken in the direction of $\vec{B}_0$, this direction is used to define the z axis of a coordinate system we work in. However, the state with all magnetic moments in the energetically most
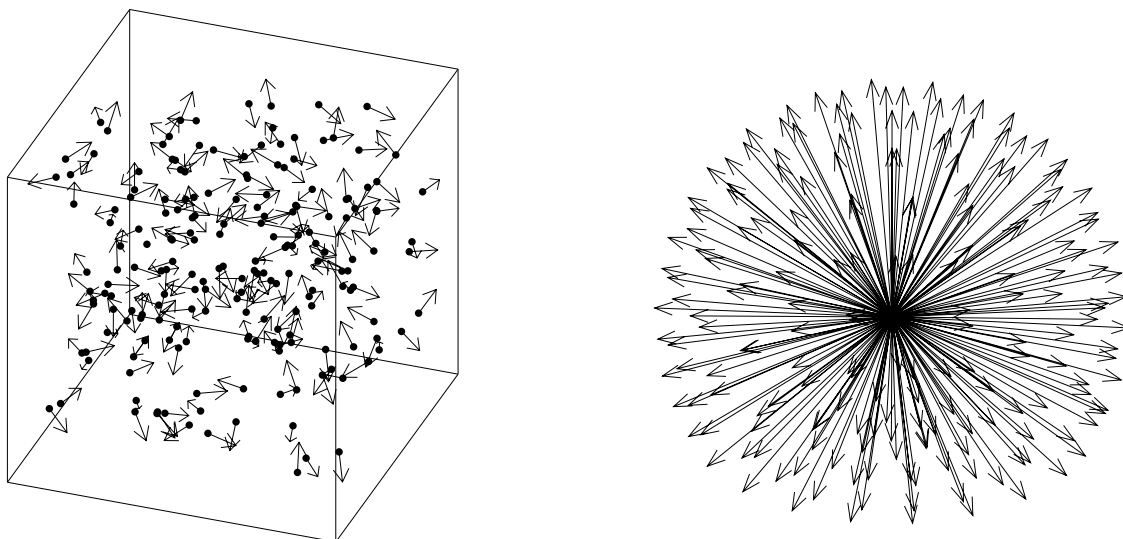
Figure 1.1: Distribution of magnetic moments in the absence of a magnetic field. Left, a schematic representation of an NMR sample. Dots represent molecules, arrows represent magnetic moments (only one magnetic moment per molecule is shown for the sake of simplicity, like e.g. in compressed $^{13}C^{16}O_2$). Right, the molecules are superimposed to make the distribution of magnetic moments visible.

favorable orientation is not most probable. Orienting all magnetic moments along the magnetic field represents only one *microstate*. In contrast, there exist a large number of microstates with somewhat higher energy. The correct balance between energy and probability is described by the Boltzmann distribution law, which can be derived from purely statistical arguments. Thermodynamics thus helps us to describe the polarization along z quantitatively.[1] Calculation of the average magnetic moment, presented in Sections 1.5.1–1.5.2, shows that the bulk magnetization of the NMR sample containing nuclei with $\vec{\mu}$:

$$M_x^{\mathrm{eq}} = 0 \qquad M_y^{\mathrm{eq}} = 0 \qquad M_z^{\mathrm{eq}} = \frac{\mathcal{N}}{3}\frac{|\mu|^2|B_0|}{k_{\mathrm{B}}T}, \tag{1.1}$$

where $\mathcal{N}$ is the number of magnetic moments per unit volume.

In summary, magnetic moments are polarized in the static homogeneous magnetic fields. In addition, all magnetic moments precess[2] with the frequency $\vec{\omega} = -\gamma\vec{B}_0$, but the precession cannot be observed at the macroscopic level because the bulk magnetization is parallel with the axis of precession (Fig. 1.2).

---

[1]Thermodynamics also tells us that the energy of the whole (isolated) system must be conserved. Decreased energy of magnetic moments is compensated by increased rotational kinetic energy of molecules of the sample, coupled with the magnetic moments via magnetic fields of the tumbling molecules, as discussed in the next chapter.

[2]Precession is described in background Section 0.6.3.
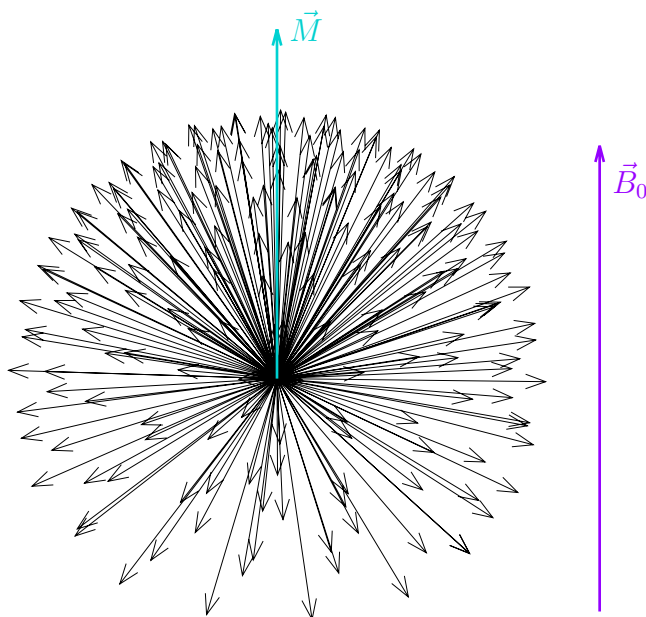
Figure 1.2: Distribution of magnetic moments in a homogeneous magnetic field $\vec{B}_0$. The cyan arrow represents the bulk magnetization.

1.3 Coherence

In order to observe precession, we need to break the axial symmetry and introduce a *coherent* motion of magnetic moments. This is achieved by applying another magnetic field $\vec{B}_1$ perpendicular to $\vec{B}_0$ and oscillating with the frequency close to (ideally equal to) $\gamma|B_0|/2\pi$. In NMR, sources of the oscillatory field are radio waves.[3] Figure 1.3 shows why a static perpendicular magnetic field cannot be used, whereas the desired effect of an oscillating perpendicular magnetic field is depicted in Figure 1.4.

If the radio waves are applied exactly for the time needed to rotate the magnetization by $90\,°$, they create a state with $\vec{M}$ perpendicular to $\vec{B}_0$. The magnetization vector (left panel in Fig. 1.4) describes a new distribution of magnetic moments (right panel in Fig. 1.4). Such magnetization vector then rotates with the precession frequency, also known as the *Larmor frequency*. The described rotation corresponds to a coherent motion of nuclear magnetic moments polarized in the direction of $\vec{M}$ and generates measurable electromotive force in the detector coil (see Section 0.6.4). As the rotation of the magnetization creates the measurable signal in NMR spectroscopy, it is important to describe it mathematically. Several mathematical approaches to rotation are presented in Sections 1.5.3–1.5.5. We even use rotation to explain effects of linear oscillations. When describing the effect of radio waves, the oscillating magnetic field of the waves is often approximated by a rotating magnetic field. Such treatment is presented in detail in Section 1.5.6. Later, after introducing quantum-mechanical description of nuclear magnetic moments, we show that rotating magnetic fields represent a good

---

[3]In the context of the NMR spectroscopy, it is important that the field *oscillates in time*, not that it travels in space as a wave.
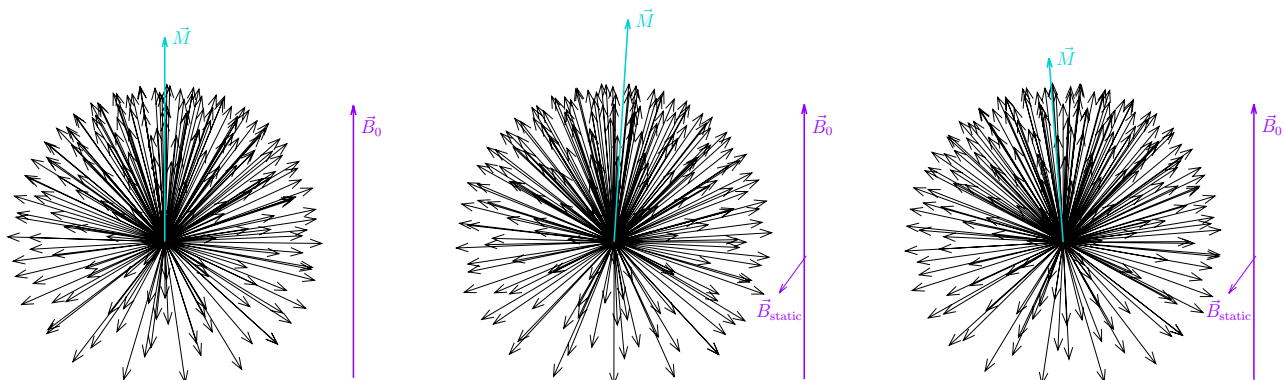
Figure 1.3: Distribution of magnetic moments in the presence of an external homogeneous magnetic field $\vec{B}_0$ (vertical purple arrow) is such that the bulk magnetization of nuclei (shown in cyan) is oriented along $\vec{B}_0$ (left). Application of another static magnetic field $\vec{B}_1$ rotates the magnetization away from the original vertical orientation down in a clockwise direction (middle). However, the magnetization also precesses about $\vec{B}_0$. After a half-turn precession (right), the clockwise rotation by the additional magnetic field $\vec{B}_1$ returns the magnetization towards its original vertical direction. Therefore, a static field cannot be used to turn the magnetization from the vertical direction to a perpendicular orientation.

approximation of radio waves oscillating in one dimension, if the magnetic induction of the radio waves is much lower than $|B_0|$ (Sections 5.7.14–5.7.18).

1.4 Chemical shift

The description of the motions of the bulk nuclear magnetization presented in the previous section is simple but boring. What makes NMR useful for chemists and biologists is the fact that the precession frequency of the magnetic moment of the observed nucleus is influenced by magnetic fields associated with motions of nearby electrons. In order to understand this effect, we need to describe the magnetic fields of moving electrons.

If a moving electron enters a homogeneous magnetic field, it experiences a Lorentz force and moves in a circle in a plane perpendicular to the field (cyclotron motion). Such an electron represents an electric current in a circular loop, and is a source of a magnetic field induced by the homogeneous magnetic field. The homogeneous magnetic field $\vec{B}_0$ in NMR spectrometers induces a similar motion of electrons in atoms, which generates microscopic magnetic fields (Figure 1.5A).

The observed nucleus feels the external magnetic field $\vec{B}_0$ slightly modified by the microscopic fields of electrons. If the electron distribution is spherically symmetric, with the observed nucleus in the center (e.g. electrons in the 1s orbital of the hydrogen atom), the induced field of the electrons decreases the effective magnetic field felt by the nucleus in the center. Since the induced field of electrons $\vec{B}_e$ is proportional to the inducing external field $\vec{B}_0$, the effective field can be described as

$$\vec{B} = \vec{B}_0 + \vec{B}_e = (1 + \delta)\vec{B}_0. \tag{1.2}$$

The constant δ is known as *chemical shift* and does not depend on the orientation of the molecule
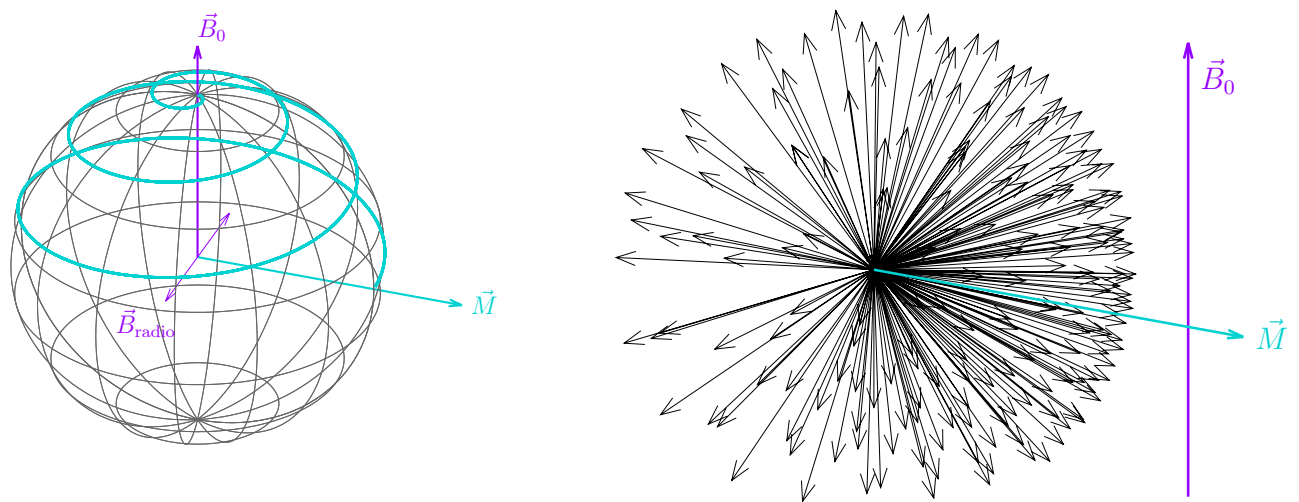
Figure 1.4: Effect of the radio waves on the bulk magnetization (left) and distribution of magnetic moments after application of the radio-wave pulse (right). The thin purple line shows oscillation of the magnetic induction vector of the radio waves, the cyan trace shows evolution of the magnetization during irradiation. If the perpendicular magnetic field oscillates with a frequency equal to the precession frequency of magnetization, it rotates the magnetization clockwise when it is tilted to the right, but counter-clockwise when the magnetization is tilted to the left. Therefore, the magnetization is more and more tilted down from the original vertical direction. The total duration of the irradiation by the radio wave was chosen so that the magnetization is rotated to the plane perpendicular to $\vec{B}_0$ (cyan arrow). Note that the ratio $|\vec{B}_0|/|\vec{B}_{\mathrm{radio}}|$ is much higher in a real experiment.

A

B

C
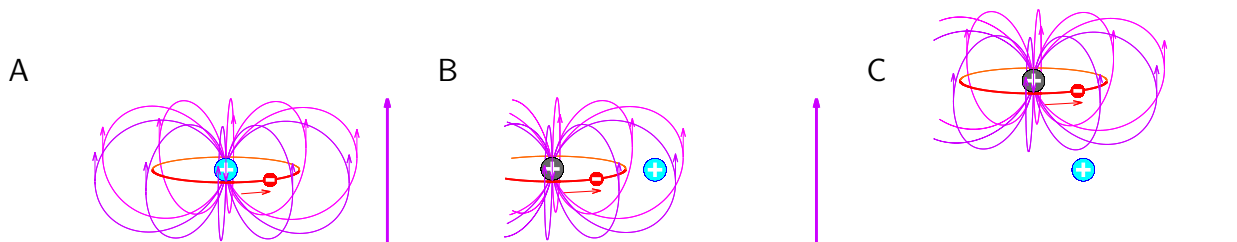
Figure 1.5: A, Classical description of interaction of an observed magnetic moment with the orbital magnetic moment of an electron of the same atom. The observed nucleus and the electron are shown in cyan and red, respectively. The thick purple arrow represents $\vec{B}_0$, the thin purple induction lines represent the magnetic field of the electron (the small purple arrows indicate its direction). The electron in $\vec{B}_0$ moves in a circle shown in red, direction of the motion is shown as the red arrow. The field of the orbital magnetic moment of the electron in the same atom decreases the total field in the place of the observed nucleus (the small purple arrow in the place of the cyan nucleus is pointing down). B, Interaction of an observed magnetic moment with the orbital magnetic moment of an electron of the another atom (its nucleus is shown in gray). In the shown orientation of the molecule, the field of the orbital magnetic moment of the electron in the other atom increases the total field in the place of the observed nucleus (the small purple arrow close the cyan nucleus is pointing up). C, As the molecule rotates, the cyan nucleus moves to a position where the field of the orbital magnetic moment of the electron in the other atom starts to decrease the total field (the induction lines reverse their direction in the place of the cyan nucleus).

in such a case[4]. The precession frequency of the nucleus is equal[5] to $\omega_0 = -\gamma(1 + \delta)B_0$.

Most molecules consist of multiple atoms and electron distribution is therefore not spherically symmetric around the observed nucleus. As a consequence, the effective field depends on the orientation of the whole molecule defining mutual positions of atoms and orientation of molecular orbitals. The currents induced in orbitals of other atoms may decrease or increase (shield or deshield) the effective magnetic field felt by the observed nucleus (Figure 1.5B,C). Therefore, the effective field fluctuates as a result of rotational diffusion of the molecule and of internal motions changing mutual positions of atoms. The induced field of electrons is still proportional to the inducing external field $\vec{B}_0$, but the proportionality constants are different for each combination of components of $\vec{B}_e$ and $\vec{B}_0$ in the coordination frame used. Therefore, we need six[6] constants δ_{jk} to describe the effect of electrons:

$$B_{e,x} = \delta_{xx}B_{0,x} + \delta_{xy}B_{0,y} + \delta_{xz}B_{0,z} \tag{1.3}$$

$$B_{e,y} = \delta_{yx}B_{0,x} + \delta_{yy}B_{0,y} + \delta_{yz}B_{0,z} \tag{1.4}$$

$$B_{e,z} = \delta_{zx}B_{0,x} + \delta_{zy}B_{0,y} + \delta_{zz}B_{0,z} \tag{1.5}$$

---

[4]Instead of δ, a constant with the opposite sign defining the *chemical shielding* is sometimes used.

[5]The value of δ in Eq. 1.2 describes how much the frequency of nuclei deviates from a hypothetical frequency of free nuclei. Such a hypothetical frequency is difficult to measure. In practice, frequencies of nuclei in certain, readily accessible chemical compounds are used instead of the frequencies of free nuclei as the reference values of δ, as is described in Section 3.1.

[6]There are nine constants in Eqs. 1.3–1.5, but $\delta_{xy} = \delta_{yx}$, $\delta_{xz} = \delta_{zx}$, and $\delta_{yz} = \delta_{zy}$.
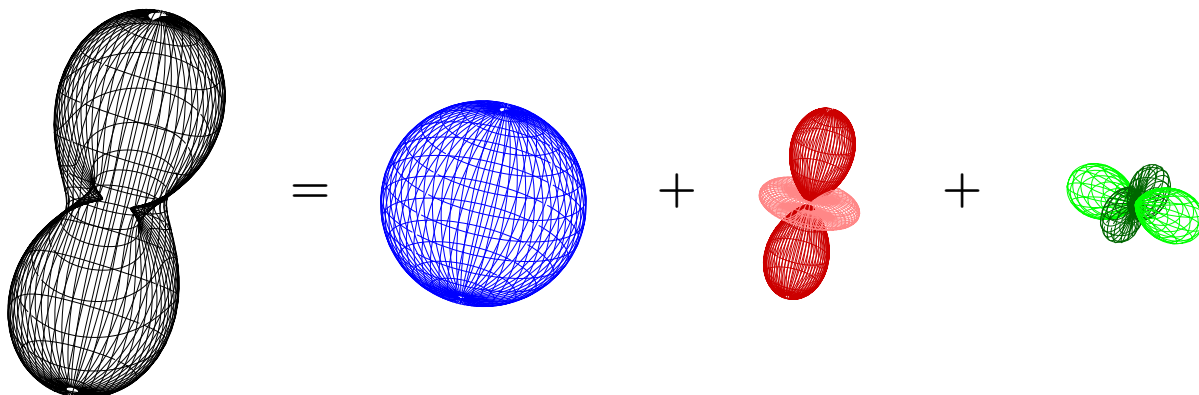
Figure 1.6: Visualization of the chemical shift tensor (black). Distance of each point at the plotted surface from its center is proportional to the magnetic induction $\vec{B}_{\mathrm{e}}$ in the given direction. The chemical shift tensor can be decomposed to its isotropic (blue), axial (red), and rhombic (green) contributions. The dark and light colors indicate positive and negative values.

Eqs. 1.3–1.5 can be written in more compact forms

$$\begin{pmatrix} B_{\mathrm{e},x} \\ B_{\mathrm{e},y} \\ B_{\mathrm{e},z} \end{pmatrix} = \begin{pmatrix} \delta_{xx} & \delta_{xy} & \delta_{xz} \\ \delta_{yx} & \delta_{yy} & \delta_{yz} \\ \delta_{zx} & \delta_{zy} & \delta_{zz} \end{pmatrix} \cdot \begin{pmatrix} B_{0,x} \\ B_{0,y} \\ B_{0,z} \end{pmatrix} \tag{1.6}$$

or

$$\vec{B}_{\mathrm{e}} = \underline{\delta} \cdot \vec{B}_0, \tag{1.7}$$

where $\underline{\delta}$ is the *chemical shift tensor*.

It is always possible to find a coordinate system X, Y, Z known as the *principal frame*, where $\underline{\delta}$ is represented by a diagonal matrix. In such a system, we need only three constants (principal values of the chemical shift tensor): $\delta_{XX}, \delta_{YY}, \delta_{ZZ}$. However, three more parameters must be specified: three *Euler angles* (written as φ, ϑ, and χ in this text) defining orientation of the coordinate system X, Y, Z in the laboratory coordinate system x, y, z. Note that $\delta_{XX}, \delta_{YY}, \delta_{ZZ}$ are true constants because they do not change as the molecule tumbles in solution (but they may change due to internal motions or chemical changes of the molecule). The orientation is completely described by the Euler angles. Graphical representation of the chemical shift tensor is shown in Figure 1.6, the algebraic description is presented in Section 1.5.7. We derive a not very simple equation describing how electrons modify the external magnetic field:

$$\vec{B}_{\mathrm{e}} = \delta_{\mathrm{i}} B_0 \begin{pmatrix} 0 \\ 0 \\ 1 \end{pmatrix} + \delta_{\mathrm{a}} B_0 \begin{pmatrix} 3\sin\vartheta\cos\vartheta\cos\varphi \\ 3\sin\vartheta\cos\vartheta\sin\varphi \\ 3\cos^2\vartheta - 1 \end{pmatrix}$$

$$+ \delta_{\mathrm{r}} B_0 \begin{pmatrix} -(2\cos^2\chi - 1)\sin\vartheta\cos\vartheta\cos\varphi + 2\sin\chi\cos\chi\sin\vartheta\sin\varphi \\ -(2\cos^2\chi - 1)\sin\vartheta\cos\vartheta\sin\varphi - 2\sin\chi\cos\chi\sin\vartheta\cos\varphi \\ +(2\cos^2\chi - 1)\sin^2\vartheta \end{pmatrix}, \tag{1.8}$$

where δ_i, δ_a, and δ_r are constants describing sizes of the isotropic, axially symmetric and asymmetric (rhombic) components of the chemical shift tensor, respectively, and ϑ, φ, χ are the aforementioned Euler angles.

Do we really need such a level of complexity? The answer is "yes and no". The blue (isotropic) term in Eq. 1.8 does not depend on the orientation. The average values of the red and green terms in Eq. 1.8 for all possible orientations are equal to zero (Section 1.5.7). It has the following consequence. When we analyze only the average value of the precession frequency, it is sufficient to consider only the isotropic component. The description of the effect of electrons then simplifies to Eq. 1.2, where δ now represents δ_i of Eq. 1.8. When we analyze also the effect of stochastic motions changing orientations of individual molecules, the other terms become important as well. The correct quantitative analysis then requires full Eq. 1.8, but the basic principles can be discussed without using the rhombic component. Therefore, we will use the axially symmetric approximation of Eq. 1.8 when we discuss effects of molecular motions in Section 2.5.1.

Practical consequences of the existence of the chemical shift, their formal description and related conventions used in the NMR literature are discussed in Section 1.5.8. In addition, Section 1.5.8 presents simplified equations of motion describing evolution of magnetization in terms of classical physics and in the absence of relaxation. Solution of these equations is described in Section 1.5.9 for a simple case of magnetization rotating in the absence of the radio waves, and in Section 1.5.10 for a general case of magnetization rotating in the presence of the radio waves. We can summarize the results of the analysis of the effect of the chemical shift as follows

- In the absence of the radio waves, the chemical shift distinguishes precession frequency of individual nuclei. In isotropic liquids (solutions of studied compounds in common solvents, investigated most frequently), the precession frequency is given by $\vec{\omega}_0 = -\gamma(1 + \delta)\vec{B}_0$, where $\delta = \delta_i$ is the isotropic chemical shift, reflecting electron distribution around the nucleus in the molecule.

- In the rotating coordinate system, the precession is described by the *frequency offset* $\vec{\Omega} = \vec{\omega}_0 - \vec{\omega}_{\mathrm{rot}} = \vec{\omega}_0 - (-\vec{\omega}_{\mathrm{radio}}) = \vec{\omega}_0 + \vec{\omega}_{\mathrm{radio}}$, where the frequency of the rotation of the coordinate frame $\vec{\omega}_{\mathrm{rot}}$ is set to the frequency $-\vec{\omega}_{\mathrm{radio}}$ defined in Section 1.5.6 (definition of the sign is a bit tricky, but the magnitude $|\omega_{\mathrm{radio}}|$ is simply frequency of the radio wave applied in the experiment.)

- During application of the radio wave, the chemical shift makes impossible to fulfill the *resonance condition* $\omega_0 = -\vec{\omega}_{\mathrm{radio}}$ (or $\Omega = 0$) for all nuclei. Only the nucleus with $\Omega = 0$ experiences exactly the desired effect of the radio wave pulse, e.g. rotation exactly by $90\,°$ exactly around axis corresponding to direction x in the rotating coordinate system. All other nuclei are affected somewhat differently, the deviations are known as *offset effects*. On one hand, the offset effects make the result of applying radio waves imperfect for nuclei with $\Omega \neq 0$. On the other hand, the chemical shift (offset effects) allow us to influence different nuclei by magnetic waves *selectively*, as described in Section 1.5.11.

Note that now (when we take into account the chemical environment of the nucleus) we describe precession of magnetic moments about $\vec{B}_0$ in isotropic liquids by three different frequencies:

- the actual *precession frequency* (*resonance frequency, chemically shifted Larmor frequency*) ω_0. Its magnitude is in the *radio frequency* range (typically 10 MHz–1 GHz), its value is $\omega_0 = -\gamma(1 + \delta)B_0$.

- *chemical shift* $\delta = \delta_i$ is a relative value expressed in units of ppm. In principle, it should be equal to $-(\omega_0 + \gamma B_0)/\gamma B_0$. In practice, it is reported relative to a reference signal from a standard compound $(\omega_0 - \omega_{0,\text{ref}})/\omega_{0,\text{ref}}$. The chemical shift is the value reported in the literature as a property of the given compound. It is given by the molecular structure, is influenced by chemical and physical conditions (temperature, ionic strength, pH) but does not depend on the experimental setup (on B_0 or frequency of radio waves used in the experiment).

- *frequency offset* $\Omega = \omega_0 - (-\omega_{\text{radio}})$. Its magnitude is in the *audio frequency* range. Frequency offset is given by the choice of the frequency of the radio waves used in the experiment. Its value is important for the experimental setup but not comparable with frequency offsets at other spectrometers. Therefore, it is usually not reported in the literature.

HOMEWORK

Derive the bulk magnetization of an NMR sample (Section 1.5.2) and solve the equations describing evolution of the magnetization in $\vec{B}_0$ (Section 1.5.9).

1.5 SUPPORTING INFORMATION

1.5.1 Calculating averages

An average value of some quantity f is calculated as

$$\overline{f} = \frac{f_1 + f_2 + \cdots + f_N}{N} = \frac{\sum\limits_{j=1}^{N} f_j}{N} = \frac{\sum\limits_{j=1}^{N} f_j}{\sum\limits_{j=1}^{N} 1}. \tag{1.9}$$

If f is a function of a variable t (e.g., time) and we measure f for regularly spaced values of t (e.g. in regular time steps Δt), we can calculate the average of f in the interval between t_0 and $t_N = t_0 + N\Delta t$ as

$$\overline{f(t_j)} = \frac{\sum\limits_{j=1}^{N} f(t_j)}{N} = \frac{\sum\limits_{j=1}^{N} f(t_j)}{\sum\limits_{j=1}^{N} 1}. \tag{1.10}$$

The same result is obtained if we multiply both the numerator and denominator by Δt:

$$\overline{f(t_j)} = \frac{\sum\limits_{j=1}^{N} f(t_j)\Delta t}{\sum\limits_{j=1}^{N} \Delta t}. \tag{1.11}$$

Shortening $\Delta t \to 0$ tells us that we can calculate an average value of a continuous function $f(t)$ by integration:

$$\overline{f(t)} = \frac{\int\limits_{t_0}^{t_N} f(t)\mathrm{d}t}{\int\limits_{t_0}^{t_N} \mathrm{d}t} = \frac{\int\limits_{t_0}^{t_N} f(t)\mathrm{d}t}{t_N - t_0}. \tag{1.12}$$

This recipe can be easily extended to functions of more variables. For example, the average value of $f(x,y)$ for $x_0 < x < x_N$ and $y_0 < y < y_N$ is

$$\overline{f(x,y)} = \frac{\int\limits_{x_0}^{x_N} \int\limits_{y_0}^{y_N} f(x,y)\mathrm{d}x\mathrm{d}y}{\int\limits_{x_0}^{x_N} \int\limits_{y_0}^{y_N} \mathrm{d}x\mathrm{d}y} = \frac{\int\limits_{x_0}^{x_N} \int\limits_{y_0}^{y_N} f(x,y)\mathrm{d}x\mathrm{d}y}{(x_N - x_0)(y_N - y_0)}. \tag{1.13}$$

The geometric interpretation is presented in Figure 1.7A. The average value is equal to the volume below the surface defined by $f(x,y)$ (pink in Figure 1.7A) above the rectangle $(x_N - x_0) \times (y_N - y_0)$, divided by the volume of the box of dimensions $(x_N - x_0) \times (y_N - y_0) \times 1$. The latter volume is numerically equal to the area of the rectangle $(x_N - x_0) \times (y_N - y_0)$. The former volume is a sum of volumes of many rectangular prisms. Each prism has the same base of the area $\mathrm{d}x \cdot \mathrm{d}y$ (shown in yellow in Figure 1.7A) and a different height (shown in magenta) equal to $f(x,y)$.

In NMR spectroscopy, we often calculate average for various orientations in space. The orientation can be described by a vector $\vec{r}$ of unit length ($|\vec{r}| = 1$) pointing in the given direction. The end points of vectors defining all possible orientations form a surface of a sphere of the radius $r = 1$ (Figure 1.7B). The orientation-dependent quantity f can be described as a function of two angles, of inclination ϑ and azimuth φ. The average value of $f(\vartheta, \varphi)$ is calculated as an integral of the values of f "above" the surface of the sphere, divided by the area of the surface. The integral "above" the surface of the sphere is a sum of integrals "above" narrow bands on the surface of the sphere. Each band (an example is shown in green in Figure 1.7B) can be decomposed into small rectangles. One rectangle is shown in yellow in Figure 1.7B. One side of the rectangle (red in Figure 1.7B) corresponds to the width of the green band. Its length is given by the arch between the vectors $\vec{r}(\vartheta, \varphi)$ (green in Figure 1.7B) and $\vec{r}(\vartheta - \mathrm{d}\vartheta, \varphi)$ (red in Figure 1.7B). The length of the arch is $r\mathrm{d}\vartheta$. The other side of the rectangle (blue in Figure 1.7B) corresponds to the arch between the *projections* of the vectors $\vec{r}(\vartheta, \varphi)$ (green in Figure 1.7B) and $\vec{r}(\vartheta, \varphi + \mathrm{d}\varphi)$ (blue in Figure 1.7B) to the horizontal plane. The length of the blue arch is $r\sin\vartheta\mathrm{d}\varphi$. Therefore, the area of the yellow rectangle is $r^2 \sin\vartheta\mathrm{d}\vartheta\mathrm{d}\varphi$, or simply $\sin\vartheta\mathrm{d}\vartheta\mathrm{d}\varphi$ because $r = 1$.

The integration is equivalent to summation of volume elements similar to the magenta prisms in Figure 1.7A. One of them is depicted in Figure 1.7C. The integral can be written as

$$\int\limits_{\vartheta=0}^{\vartheta=\pi} \int\limits_{\varphi=0}^{\varphi=2\pi} f(\vartheta, \varphi) \sin\vartheta\mathrm{d}\vartheta\mathrm{d}\varphi = \int\limits_{0}^{2\pi} \mathrm{d}\varphi \int\limits_{0}^{\pi} \sin\vartheta\mathrm{d}\vartheta f(\vartheta, \varphi) \tag{1.14}$$

A   B   C
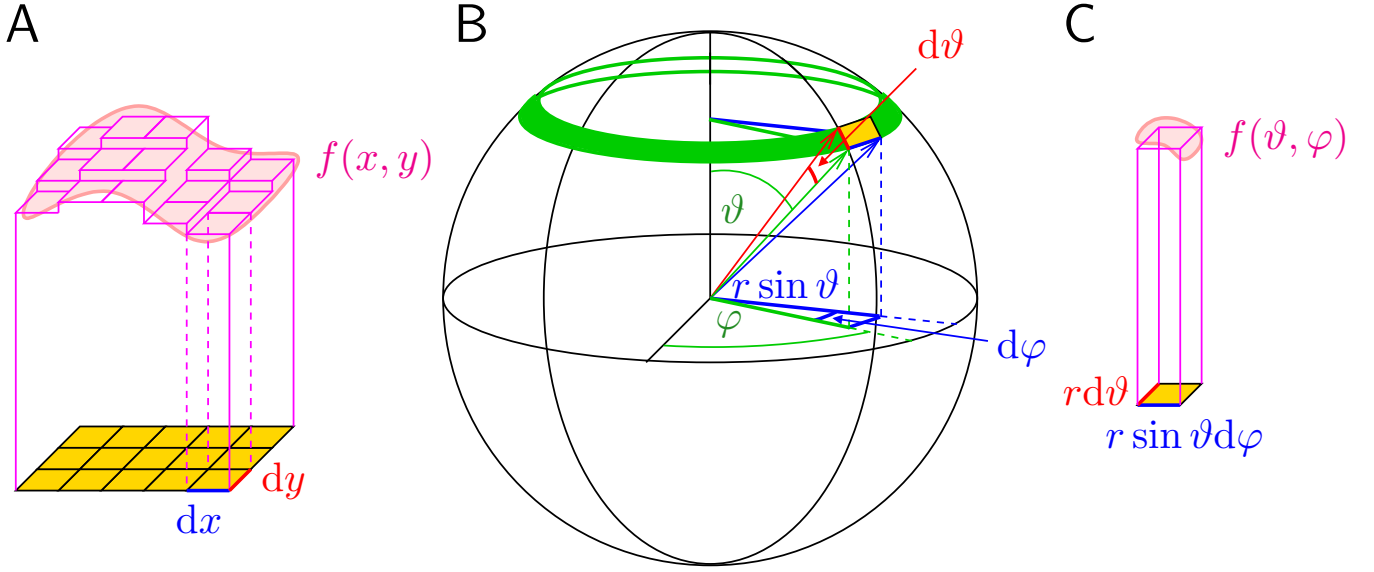
Figure 1.7: Integration in calculating averages. Integration of $f(x,y)$ (A), integration of $f(\vartheta,\varphi)$ (B), and the volume element $f(\vartheta,\varphi)r^2\sin\vartheta\mathrm{d}\vartheta\mathrm{d}\varphi$ (C). Details are described in the text.

and the average is

$$\overline{f(\vartheta,\varphi)} = \frac{\int\limits_0^{2\pi}\mathrm{d}\varphi\int\limits_0^\pi\sin\vartheta\mathrm{d}\vartheta f(\vartheta,\varphi)}{\int\limits_0^{2\pi}\mathrm{d}\varphi\int\limits_0^\pi\sin\vartheta\mathrm{d}\vartheta} = \frac{\int\limits_0^{2\pi}\mathrm{d}\varphi\int\limits_0^\pi\sin\vartheta\mathrm{d}\vartheta f(\vartheta,\varphi)}{\int\limits_0^{2\pi}\mathrm{d}\varphi\int\limits_{-1}^1\mathrm{d}u} = \frac{\int\limits_0^{2\pi}\mathrm{d}\varphi\int\limits_0^\pi\sin\vartheta\mathrm{d}\vartheta f(\vartheta,\varphi)}{4\pi}, \tag{1.15}$$

where we used the substitution

$$u = \cos\vartheta \Rightarrow \mathrm{d}u = \frac{\mathrm{d}u}{\mathrm{d}\vartheta}\mathrm{d}\vartheta = \frac{\mathrm{d}\cos\vartheta}{\mathrm{d}\vartheta}\mathrm{d}\vartheta = -\sin\vartheta\mathrm{d}\vartheta \tag{1.16}$$

1.5.2   Polarization and bulk magnetization

The average value of the z-component of $\vec{\mu}$ is calculated according to Section 1.5.1. The distribution of $\vec{\mu}$ is axially symmetric. Therefore, $\overline{\mu}_z^{\mathrm{eq}}$ does not depend on φ and we can integrate over φ and over ϑ separately in Eq. 1.15

$$\overline{\mu}_z^{\mathrm{eq}} = \frac{\left(\int\limits_0^{2\pi}\mathrm{d}\varphi\right)\left(\int\limits_0^\pi P^{\mathrm{eq}}(\vartheta)\mu_z(\vartheta\sin\vartheta)\mathrm{d}\vartheta\right)}{4\pi} = \frac{2\pi\int\limits_0^\pi P^{\mathrm{eq}}(\vartheta)\mu_z(\vartheta)\sin\vartheta\mathrm{d}\vartheta}{4\pi} = \frac{1}{2}\int\limits_0^\pi P^{\mathrm{eq}}(\vartheta)\mu_z\sin\vartheta\mathrm{d}\vartheta = \frac{1}{2}\int\limits_0^\pi P^{\mathrm{eq}}(\vartheta)|\mu|\cos\vartheta\sin\vartheta\mathrm{d}\vartheta, \tag{1.17}$$

where ϑ is the inclination (angle between $\vec{\mu}$ and axis z) and $P^{\mathrm{eq}}(\vartheta)$ is the probability of $\vec{\mu}$ to be tilted by the angle ϑ. If the magnetic dipoles are in a thermodynamic equilibrium, the angular distribution of the $\vec{\mu}$ orientation is given by the Boltzmann law: Probability of a system to be in the state with the energy $\mathcal{E}_j$ at the temperature T is given by

$$P_j^{\mathrm{eq}} = \frac{\mathrm{e}^{-\frac{\mathcal{E}_j}{k_\mathrm{B}T}}}{Z}, \tag{1.18}$$

where Z is sum of the $\mathrm{e}^{-\frac{\mathcal{E}_k}{k_\mathrm{B}T}}$ terms of all possible states.

$$P^{\mathrm{eq}}(\vartheta) = \frac{\mathrm{e}^{-\frac{\mathcal{E}(\vartheta)}{k_\mathrm{B}T}}}{\frac{\left(\int\limits_0^{2\pi}\mathrm{d}\varphi\right)\int\limits_0^\pi\mathrm{e}^{-\frac{\mathcal{E}(\vartheta')}{k_\mathrm{B}T}}\sin\vartheta'\mathrm{d}\vartheta'}{4\pi}} = P^{\mathrm{eq}}(\vartheta) = \frac{\mathrm{e}^{-\frac{\mathcal{E}(\vartheta)}{k_\mathrm{B}T}}}{\frac{1}{2}\int\limits_0^\pi\mathrm{e}^{-\frac{\mathcal{E}(\vartheta')}{k_\mathrm{B}T}}\sin\vartheta'\mathrm{d}\vartheta'}, \tag{1.19}$$

where T is the thermodynamic temperature, $k_{\mathrm{B}} = 1.38064852 \times 10^{-23}\,\mathrm{m^2\,kg\,s^{-2}\,K^{-1}}$ is the Boltzmann constant, and $\mathcal{E} = -|\mu||B_0|\cos\vartheta$ is the magnetic potential energy of the dipole. The distribution is axially symmetric, all values of the azimuth φ are equally possible.

Using the substitutions

$$u = \cos\vartheta \Rightarrow \mathrm{d}u = \frac{\mathrm{d}u}{\mathrm{d}\vartheta}\mathrm{d}\vartheta = \frac{\mathrm{d}\cos\vartheta}{\mathrm{d}\vartheta}\mathrm{d}\vartheta = -\sin\vartheta\mathrm{d}\vartheta \tag{1.20}$$

and

$$w = \frac{|\mu||B_0|}{k_{\mathrm{B}}T}, \tag{1.21}$$

$$P^{\mathrm{eq}}(\vartheta) = \frac{\mathrm{e}^{-\frac{\mathcal{E}(\vartheta)}{k_{\mathrm{B}}T}}}{\frac{1}{2}\int\limits_0^{\pi}\mathrm{e}^{-\frac{\mathcal{E}(\vartheta')}{k_{\mathrm{B}}T}}\sin\vartheta'\mathrm{d}\vartheta'} = \frac{\mathrm{e}^{uw}}{\frac{1}{2}\int\limits_1^{-1}-\mathrm{e}^{u'w}\mathrm{d}u'} = \frac{\mathrm{e}^{uw}}{\frac{1}{2}\int\limits_{-1}^{1}\mathrm{e}^{u'w}\mathrm{d}u'} = \frac{\mathrm{e}^{uw}}{\frac{1}{2w}\left[\mathrm{e}^{u'w}\right]_{-1}^1} = \frac{2w}{\mathrm{e}^w - \mathrm{e}^{-w}}\mathrm{e}^{uw} = P^{\mathrm{eq}}(u). \tag{1.22}$$

Knowing the distribution, the average z-component of $\vec{\mu}$ can be calculated

$$\overline{\mu}_z^{\mathrm{eq}} = \frac{1}{2}\int\limits_0^{\pi}P^{\mathrm{eq}}(\vartheta)|\mu|\cos\vartheta\sin\vartheta\mathrm{d}\vartheta = \frac{1}{2}\int\limits_{-1}^{1}|\mu|uP^{\mathrm{eq}}(u)\mathrm{d}u = \frac{|\mu|w}{\mathrm{e}^w - \mathrm{e}^{-w}}\int\limits_{-1}^{1}u\mathrm{e}^{uw}\mathrm{d}u. \tag{1.23}$$

The integration can be performed per parts (*per partes*), with the result

$$\overline{\mu}_z^{\mathrm{eq}} = \frac{|\mu|w}{\mathrm{e}^w - \mathrm{e}^{-w}}\left[\frac{1}{w^2}\mathrm{e}^{uw}(uw-1)\right]_{-1}^1 = \frac{|\mu|}{\mathrm{e}^w - \mathrm{e}^{-w}}\left(\frac{1}{w}\mathrm{e}^w(w-1) - \frac{1}{w}\mathrm{e}^{-w}(-w-1)\right) = |\mu|\left(\frac{\mathrm{e}^w + \mathrm{e}^{-w}}{\mathrm{e}^w - \mathrm{e}^{-w}} - \frac{1}{w}\right) = |\mu|\left(\coth(w) - \frac{1}{w}\right), \tag{1.24}$$

where we recognized that the ratio of exponential terms is the function *hyperbolic cotangent* ($\coth(w)$). The function $\coth(w)$ can be expanded as a Taylor series

$$\coth(w) \approx \frac{1}{w} + \frac{w}{3} - \frac{w^3}{45} + \frac{2w^5}{945} - \cdots \quad \Rightarrow \quad \overline{\mu}_z \approx |\mu|\left(\frac{w}{3} - \frac{w^3}{45} + \frac{2w^5}{945} - \cdots\right). \tag{1.25}$$

At the room temperature, $|\mu||B_0| \ll k_{\mathrm{B}}T$ even in the strongest NMR magnets. Therefore, w is a very small number and its high powers in the Taylor series can be neglected. In summary, the angular distribution can be approximated by

$$\overline{\mu}_z^{\mathrm{eq}} = \frac{1}{3}\frac{|\mu|^2|B_0|}{k_{\mathrm{B}}T}, \tag{1.26}$$

while

$$\overline{\mu}_x^{\mathrm{eq}} = \overline{\mu}_y^{\mathrm{eq}} = 0. \tag{1.27}$$

1.5.3   Changing Cartesian coordinate frame

Different Cartesian coordinate systems are optimal for description of different issues related to NMR spectroscopy. It is therefore useful to be able to change the coordinate system when needed. In this section, we limit the changes of coordinate systems to their rotation in space.

We start by a two-dimensional case (Figure 1.8). Let us suppose we know that a vector $\vec{a}$ has components a_x, a_y in an "original" coordinate system xy, and we wish to express components of $\vec{a}$ in a "primed" coordinate system $x'y'$. First, we have to specify relationship between the coordinate systems. This relation is a *rotation* in the xy plane. We get the "primed" coordinate frame (shown in red in Figure 1.8) if we rotate the "original" system (shown in blue in Figure 1.8) by an angle φ. Note that we now treat the original (blue) coordinate frame as a geometric object and *actively rotate* it to a new (red) orientation in the plane.

In order to describe how is the vector $\vec{a}$ represented in two rotated coordinate systems, we change the point of view. Now we are interested in how the vector $\vec{a}$ is *seen from* different coordinate frames. If we express a_x as $|a|\cos\varphi_a$ and a'_y as $|a|\sin\varphi_a$, and $a_{x'}$ as $|a|\cos\varphi'_a$ and $a'_{y'}$ as $|a|\sin\varphi'_a$, we see that $\varphi'_a = \varphi_a - \varphi$ (Figure 1.8). The coordinates of $\vec{a}$ in the "primed" coordinate system (Figure 1.8B) are the same as coordinates of $\vec{a}$ rotated "backwards" (by angle $-\varphi$) in the original system (Figure 1.8C). This manipulation of $\vec{a}$ is known as *passive rotation*. Note that the angles describing the active rotation (of the coordinate frames) and the passive rotation (of $\vec{a}$) differ in the sign. The passive rotation can written down as a set of equations relating the coordinates of $\vec{a}$ in two different frames

$$a_{x'} = |a|\cos\varphi'_a = |a|\cos(\varphi_a - \varphi) = |a|(\cos\varphi_a\cos\varphi + \sin\varphi_a\sin\varphi) = a_x\cos\varphi + a_y\sin\varphi \tag{1.28}$$

$$a_{y'} = |a|\sin\varphi'_a = |a|\sin(\varphi_a - \varphi) = |a|(\sin\varphi_a\cos\varphi - \cos\varphi_a\sin\varphi) = -a_x\sin\varphi + a_y\cos\varphi, \tag{1.29}$$
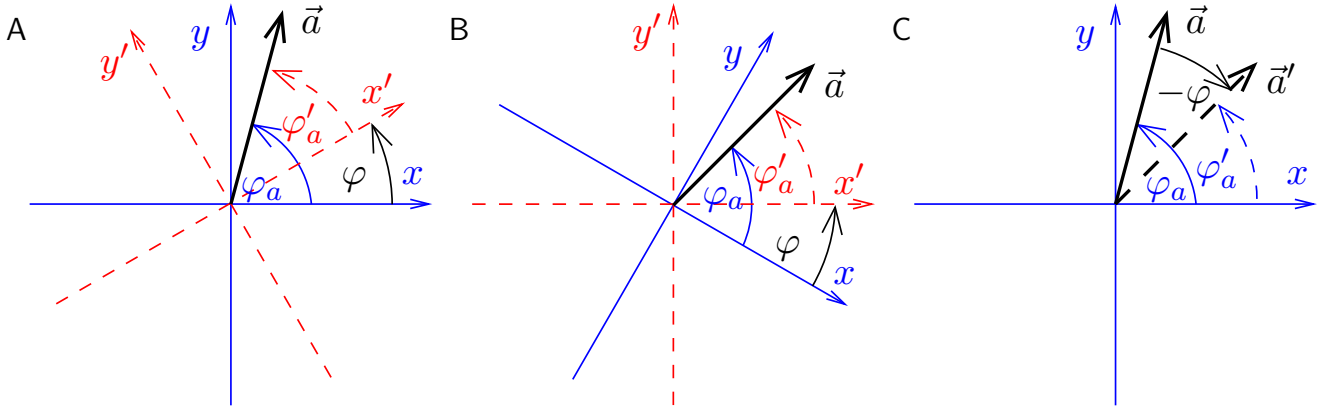
Figure 1.8: Changing two-dimensional coordinate frame. A, vector $\vec{a}$ (black) in two coordinate frames, shown in blue and red. The red coordinate system is obtained by rotating the blue frame by the angle φ. B, the same picture oriented so that the axes of the red coordinate frame are horizontal and vertical. C, Rotation of the vector $\vec{a}$ by the angle $-\varphi$ results in a vector $\vec{a}'$, which is oriented in the blue coordinate frame exactly like $\vec{a}$ is oriented in the red coordinate frame (cf. Panel B).

or in a matrix form

$$
\begin{pmatrix} a_{x'} \\ a_{y'} \end{pmatrix} = \begin{pmatrix} \cos\varphi & \sin\varphi \\ -\sin\varphi & \cos\varphi \end{pmatrix} \begin{pmatrix} a_x \\ a_y \end{pmatrix}.
\tag{1.30}
$$

In order to convert coordinates of $\vec{a}$ in the "primed" system to the coordinates of $\vec{a}$ in the "original" frame, we have to rotate by $+\varphi$. Changing sign of φ results in

$$
\begin{pmatrix} a_x \\ a_y \end{pmatrix} = \begin{pmatrix} \cos\varphi & -\sin\varphi \\ \sin\varphi & \cos\varphi \end{pmatrix} \begin{pmatrix} a_{x'} \\ a_{y'} \end{pmatrix}.
\tag{1.31}
$$

The obtained relations can be easily extended to two three-dimensional coordinate frames xyz and $x'y'z$ related by rotation about the common axis z

$$
\begin{pmatrix} a_{x'} \\ a_{y'} \\ a_{z'} \end{pmatrix} = \underbrace{\begin{pmatrix} \cos\varphi & \sin\varphi & 0 \\ -\sin\varphi & \cos\varphi & 0 \\ 0 & 0 & 1 \end{pmatrix}}_{\text{rotation by } -\varphi} \begin{pmatrix} a_x \\ a_y \\ a_z \end{pmatrix}
\qquad
\begin{pmatrix} a_x \\ a_y \\ a_z \end{pmatrix} = \underbrace{\begin{pmatrix} \cos\varphi & -\sin\varphi & 0 \\ \sin\varphi & \cos\varphi & 0 \\ 0 & 0 & 1 \end{pmatrix}}_{\text{rotation by } +\varphi} \begin{pmatrix} a_{x'} \\ a_{y'} \\ a_{z'} \end{pmatrix}.
\tag{1.32}
$$

Similar expressions can be derived for coordinated systems related by rotation about the x and y axes, respectively:

$$
\begin{pmatrix} a_{x'} \\ a_{y'} \\ a_{z'} \end{pmatrix} = \underbrace{\begin{pmatrix} 1 & 0 & 0 \\ 0 & \cos\vartheta_x & \sin\vartheta_x \\ 0 & -\sin\vartheta_x & \cos\vartheta_x \end{pmatrix}}_{\text{rotation by } -\vartheta_x} \begin{pmatrix} a_x \\ a_y \\ a_z \end{pmatrix}
\qquad
\begin{pmatrix} a_x \\ a_y \\ a_z \end{pmatrix} = \underbrace{\begin{pmatrix} 1 & 0 & 0 \\ 0 & \cos\vartheta_x & -\sin\vartheta_x \\ 0 & \sin\vartheta_x & \cos\vartheta_x \end{pmatrix}}_{\text{rotation by } +\vartheta_x} \begin{pmatrix} a_{x'} \\ a_{y'} \\ a_{z'} \end{pmatrix}
\tag{1.33}
$$

and

$$
\begin{pmatrix} a_{x'} \\ a_{y'} \\ a_{z'} \end{pmatrix} = \underbrace{\begin{pmatrix} \cos\vartheta_y & 0 & -\sin\vartheta_y \\ 0 & 1 & 0 \\ \sin\vartheta_y & 0 & \cos\vartheta_y \end{pmatrix}}_{\text{rotation by } -\vartheta_y} \begin{pmatrix} a_x \\ a_y \\ a_z \end{pmatrix}
\qquad
\begin{pmatrix} a_x \\ a_y \\ a_z \end{pmatrix} = \underbrace{\begin{pmatrix} \cos\vartheta_y & 0 & \sin\vartheta_y \\ 0 & 1 & 0 \\ -\sin\vartheta_y & 0 & \cos\vartheta_y \end{pmatrix}}_{\text{rotation by } +\vartheta_y} \begin{pmatrix} a_{x'} \\ a_{y'} \\ a_{z'} \end{pmatrix}.
\tag{1.34}
$$

We can now proceed to three-dimensional coordinate frames. Again, we start by specifying their mutual relation. In order to describe a general relation of coordinated systems xyz and $x'y'z'$, three subsequent *active rotations* of the frame xyz are needed. The choice of the actual rotations is somewhat arbitrary. Note that if a mutual orientation of two coordinate frame is described by rotations about different axes, or by rotations about the same axes but in a different order, the numerical values of the rotation angles differ. Several conventions are used in different fields of science and for different purposes, none of them is a general recommended standard. Nevertheless, all conventions allow us to relate the coordinate frames unambiguously. In this course, we use the following rotations (Figure 1.9A):

1. Rotate about the z axis of the original coordinate frame to move the y axis to the $x'y'$ plane. We call[7] the angle of this rotation χ and label a vector defining the new direction of the y axis as $\vec{n}$. Note that the direction of $\vec{n}$ is the intersection of the planes xy and $x'y'$.

2. Rotate about $\vec{n}$ to move the axis z to the direction of z'. We call the angle of this rotation ϑ.

3. Rotate about z' to move $\vec{n}$ to the direction of y'. We call the angle of this rotation φ.

Written in the matrix form, the active rotation converting the "original" frame xyz to the "primed" frame $x'y'z'$ is expressed as

$$\begin{pmatrix} \cos\varphi & -\sin\varphi & 0 \\ \sin\varphi & \cos\varphi & 0 \\ 0 & 0 & 1 \end{pmatrix} \begin{pmatrix} \cos\vartheta & 0 & \sin\vartheta \\ 0 & 1 & 0 \\ -\sin\vartheta & 0 & \cos\vartheta \end{pmatrix} \begin{pmatrix} \cos\chi & -\sin\chi & 0 \\ \sin\chi & \cos\chi & 0 \\ 0 & 0 & 1 \end{pmatrix} =$$

$$\begin{pmatrix} \cos\varphi\cos\vartheta\cos\chi - \sin\varphi\sin\chi & -\cos\varphi\cos\vartheta\sin\chi - \sin\varphi\cos\chi & \cos\varphi\sin\vartheta \\ \sin\varphi\cos\vartheta\cos\chi + \cos\varphi\sin\chi & -\sin\varphi\cos\vartheta\sin\chi + \cos\varphi\cos\chi & \sin\varphi\sin\vartheta \\ -\sin\vartheta\cos\chi & \sin\vartheta\sin\chi & \cos\vartheta \end{pmatrix}. \tag{1.35}$$

The passive rotations describing how $\vec{a}$ is seen from different coordinate frames, are performed in the reverse manner:

$$\begin{pmatrix} a_{x'} \\ a_{y'} \\ a_{z'} \end{pmatrix} = \begin{pmatrix} \cos\chi & \sin\chi & 0 \\ -\sin\chi & \cos\chi & 0 \\ 0 & 0 & 1 \end{pmatrix} \begin{pmatrix} \cos\vartheta & 0 & -\sin\vartheta \\ 0 & 1 & 0 \\ \sin\vartheta & 0 & \cos\vartheta \end{pmatrix} \begin{pmatrix} \cos\varphi & \sin\varphi & 0 \\ -\sin\varphi & \cos\varphi & 0 \\ 0 & 0 & 1 \end{pmatrix} \begin{pmatrix} a_x \\ a_y \\ a_z \end{pmatrix} \tag{1.36}$$

$$\begin{pmatrix} a_x \\ a_y \\ a_z \end{pmatrix} = \begin{pmatrix} \cos\varphi & -\sin\varphi & 0 \\ \sin\varphi & \cos\varphi & 0 \\ 0 & 0 & 1 \end{pmatrix} \begin{pmatrix} \cos\vartheta & 0 & \sin\vartheta \\ 0 & 1 & 0 \\ -\sin\vartheta & 0 & \cos\vartheta \end{pmatrix} \begin{pmatrix} \cos\chi & -\sin\chi & 0 \\ \sin\chi & \cos\chi & 0 \\ 0 & 0 & 1 \end{pmatrix} \begin{pmatrix} a_{x'} \\ a_{y'} \\ a_{z'} \end{pmatrix} \tag{1.37}$$

Expressing the product of the three rotation matrices,

$$\begin{pmatrix} a_{x'} \\ a_{y'} \\ a_{z'} \end{pmatrix} = \begin{pmatrix} \cos\chi\cos\vartheta\cos\varphi - \sin\chi\sin\varphi & \cos\chi\cos\vartheta\sin\varphi + \sin\chi\cos\varphi & -\cos\chi\sin\vartheta \\ -\sin\chi\cos\vartheta\cos\varphi - \cos\chi\sin\varphi & -\sin\chi\cos\vartheta\sin\varphi + \cos\chi\cos\varphi & \sin\chi\sin\vartheta \\ \sin\vartheta\cos\varphi & \sin\vartheta\sin\varphi & \cos\vartheta \end{pmatrix} \begin{pmatrix} a_x \\ a_y \\ a_z \end{pmatrix} \tag{1.38}$$

$$\begin{pmatrix} a_x \\ a_y \\ a_z \end{pmatrix} = \begin{pmatrix} \cos\varphi\cos\vartheta\cos\chi - \sin\varphi\sin\chi & -\cos\varphi\cos\vartheta\sin\chi - \sin\varphi\cos\chi & \cos\varphi\sin\vartheta \\ \sin\varphi\cos\vartheta\cos\chi + \cos\varphi\sin\chi & -\sin\varphi\cos\vartheta\sin\chi + \cos\varphi\cos\chi & \sin\varphi\sin\vartheta \\ -\sin\vartheta\cos\chi & \sin\vartheta\sin\chi & \cos\vartheta \end{pmatrix} \begin{pmatrix} a'_x \\ a'_y \\ a'_z \end{pmatrix}. \tag{1.39}$$

In the language of linear algebra, the matrix of the trigonometric functions of φ, ϑ, χ is a *transformation matrix*. If we label the elements of the transformation matrices $R_{k'k}$ for the transformation from the "original" to the "primed" coordinate frame and $R_{kk'}$ for the inverse transformation, the change of the coordinate frame (transformation) can be described in terms of the components of the vector $\vec{a}$ as

$$a_{k'} = \sum_k R_{k'k}(-\varphi, -\vartheta, -\chi)a_k \qquad a_k = \sum_{k'} R_{kk'}(\chi, \vartheta, \varphi)a_{k'}. \tag{1.40}$$

The elements $R_{k'k}(-\varphi, -\vartheta, -\chi)$ and $R_{kk'}(\chi, \vartheta, \varphi)$ obviously constitute inverse matrices. Using the standard notation, we can label them[8] $\hat{R}^{-1}$ and $\hat{R}$, respectively. The rotation can be then written shortly as

$$\vec{a}' = \hat{R}^{-1}\vec{a} \qquad \vec{a} = \hat{R}\vec{a}'. \tag{1.41}$$

The change of the coordinate system can be written in a similar fashion for a *tensor* T_{jk} (Figure 1.9B,C). We derive the relation in two steps. In the first step, we combine the rows of the matrix representing T_{jk} into row vectors $\vec{T}_j$

$$\begin{pmatrix} T_{xx} & T_{xy} & T_{xz} \\ T_{yx} & T_{yy} & T_{yz} \\ T_{zx} & T_{zy} & T_{zz} \end{pmatrix} = \begin{pmatrix} \vec{T}_x \\ \vec{T}_y \\ \vec{T}_z \end{pmatrix}. \tag{1.42}$$

Formally, the vectors $\vec{T}_j$ are components of a column vector that transforms according to Eq. 1.40:

---

[7]Our angles φ, ϑ, χ represent *Euler angles*, usually labeled α, β, and γ. As the Greek letters α, β, and γ are traditionally used for different purposes in NMR spectroscopy, we use other letters in our course.

[8]In our course, we use the "hat" as a symbol for both matrices and operators. In many cases, matrices represent operators (multiplying a vector by the rotation matrix is one of possible ways of describing the operation of rotating the vector in space). However, matrices and operators are different objects in mathematics and physics. Hopefully using the same symbols for both matrices and operators does not confuse the reader.

$$\vec{T}_{j'} = \sum_j R_{jj'}(-\varphi, -\vartheta, -\chi)\vec{T}_j. \tag{1.43}$$

In the second step, we describe transformation of each vector $\vec{T}_{j'}$. As $\vec{T}_{j'}$ are row vectors, they are multiplied *from right* by the transformation matrix

$$\begin{pmatrix} T_{j'x} & T_{j'y} & T_{j'z} \end{pmatrix} \begin{pmatrix} R_{xx'} & R_{xy'} & R_{xz'} \\ R_{yx'} & R_{yy'} & R_{yz'} \\ R_{zx'} & R_{zy'} & R_{zz'} \end{pmatrix} = \begin{pmatrix} T_{j'x'} & T_{j'y'} & T_{j'z'} \end{pmatrix}, \tag{1.44}$$

or

$$T_{j'k'} = \sum_k T_{j'k} R_{kk'}(-\varphi, -\vartheta, -\chi). \tag{1.45}$$

Note that if $\vec{T}_{j'}$ were written as column vectors, the transformation would be

$$\begin{pmatrix} R_{x'x} & R_{x'x} & R_{x'x} \\ R_{y'y} & R_{y'y} & R_{y'y} \\ R_{z'z} & R_{z'z} & R_{z'z} \end{pmatrix} \begin{pmatrix} T_{j'x} \\ T_{j'y} \\ T_{j'z} \end{pmatrix} = \begin{pmatrix} T_{j'x'} \\ T_{j'y'} \\ T_{j'z'} \end{pmatrix}. \tag{1.46}$$

The transformation matrices in Eqs. 1.44 and 1.46 are related by *transposition* (changing rows to columns and columns to rows), exactly like the transformation matrices in Eqs. 1.38 and 1.39. Therefore, transformation of $\vec{T}_{j'}$ can be also described as

$$T_{j'k'} = \sum_k R_{k'k}(\varphi, \vartheta, \chi) T_{j'k}. \tag{1.47}$$

Combining the first and second step of the derivation, we can describe transformation of a tensor T_{jk} as

$$T_{j'm'} = \sum_j \sum_k R_{j'j}(-\varphi, -\vartheta, -\chi) R_{kk'}(-\varphi, -\vartheta, -\chi) T_{jk} = \sum_j \sum_k R_{j'j}(-\varphi, -\vartheta, -\chi) R_{k'k}(\chi, \vartheta, \varphi) T_{jk}. \tag{1.48}$$

and

$$T_{jk} = \sum_{j'} \sum_{k'} R_{jj'}(\chi, \vartheta, \varphi) R_{k'k}(\chi, \vartheta, \varphi) T_{j'k'} = \sum_{j'} \sum_{k'} R_{jj'}(\chi, \vartheta, \varphi) R_{kk'}(-\varphi, -\vartheta, -\chi) T_{j'k'} \tag{1.49}$$

or shortly as

$$\hat{T}' = \hat{R}^{-1}\hat{T}\hat{R} \qquad \hat{T} = \hat{R}\hat{T}'\hat{R}^{-1}. \tag{1.50}$$

1.5.4 Rotation described by Wigner matrices

It is also possible to employ complex numbers to describe the rotation in space. The three-dimensional vectors in the real Cartesian coordinate system are first converted to spherical coordinates

$$a_x = |a| \sin \vartheta_a \cos \varphi_a, \tag{1.51}$$
$$a_y = |a| \sin \vartheta_a \sin \varphi_a, \tag{1.52}$$
$$a_z = |a| \cos \vartheta_a. \tag{1.53}$$

Then we use the Euler formula $\mathrm{e}^{\pm\mathrm{i}\phi} = \cos\phi \pm \mathrm{i}\sin\phi$ to express a vector $\vec{a}$ in a *different basis*. Namely we decompose $\vec{a}$ not into its three Cartesian components, but to the z component plus the linear combinations $a_x \pm \mathrm{i}a_y$:

$$a_{-1} = \frac{a_x - \mathrm{i}a_y}{\sqrt{2}} = |a| \sin \vartheta_a \frac{\cos \varphi_a - \mathrm{i} \sin \varphi_a}{\sqrt{2}} = |a| \frac{\sin \vartheta_a}{\sqrt{2}} \mathrm{e}^{-\mathrm{i}\phi_a}, \tag{1.54}$$
$$a_0 = a_z = |a| \cos \vartheta_a, \tag{1.55}$$
$$a_{+1} = \frac{a_x + \mathrm{i}a_y}{\sqrt{2}} = |a| \sin \vartheta_a \frac{\cos \varphi_a + \mathrm{i} \sin \varphi_a}{\sqrt{2}} = |a| \frac{\sin \vartheta_a}{\sqrt{2}} \mathrm{e}^{+\mathrm{i}\phi_a}. \tag{1.56}$$
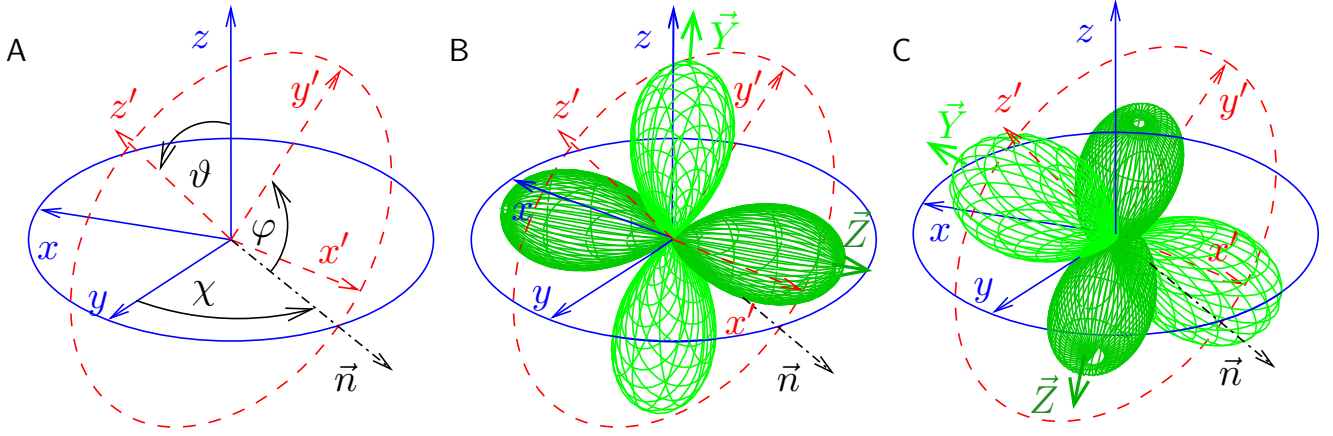
Figure 1.9: Changing three-dimensional coordinate frame. A, the red coordinate system is obtained by rotating the blue frame (i) about the axis z until the blue axis y coincides with $\vec{n}$ (angle of this rotation is χ), (ii) about $\vec{n}$ by ϑ (this determines the new direction of axis z, labeled z' and shown in red), and (iii) about z' by φ (this determines the new direction of axis y, labeled y' and shown in red). B, a graphical representation of a tensor (green) in the discussed coordinate frames. The tensor, formally corresponding to a chemical shift tensor with $\delta_{\mathrm{i}} = 0$ and $\delta_{\mathrm{a}} = \delta_{\mathrm{r}}$, is visualized as described in Figure 1.6. Dark and light green correspond to positive and negative values. C, graphical represeanation of the same tensor rotated (i) by $-\varphi$ about z', (ii) by $-\vartheta$ about $\vec{n}$, and (iii) by $-\chi$ about z. The rotated tensor has the same orientation in the blue coordinate system as the original tensor had in the red coordinate frame.

With the proper normalization (to keep $\vec{a}^* \vec{a}$ in the new basis equal to $a^2 = a_x^2 + a_y^2 + a_z^2$), $\vec{a}$ can be written as a row vector[9]

$$\vec{a} = \left(\begin{array}{ccc} \frac{a_x - \mathrm{i}a_y}{\sqrt{2}} & a_z & -\frac{a_x + \mathrm{i}a_y}{\sqrt{2}} \end{array} \right) = \left(\begin{array}{ccc} a_{-1} & a_0 & a_{+1} \end{array} \right). \tag{1.57}$$

Then, rotation of $\vec{a}$ about z is described by a transformation matrix (applied from right to row vectors, cf. Eq 1.44) which is *diagonal*:

$$\vec{a} = \left(\begin{array}{ccc} a_{-1} & a_0 & a_{+1} \end{array} \right) = \left(\begin{array}{ccc} a_{-1}(0) & a_0(0) & a_{+1}(0) \end{array} \right) \begin{pmatrix} \mathrm{e}^{-\mathrm{i}\varphi} & 0 & 0 \\ 0 & 1 & 0 \\ 0 & 0 & \mathrm{e}^{\mathrm{i}\varphi} \end{pmatrix} = \left(\begin{array}{ccc} a_{-1}(0) & a_0(0) & a_{+1}(0) \end{array} \right) \begin{pmatrix} \mathrm{e}^{\mathrm{i}\cdot(-1)\cdot\varphi} & 0 & 0 \\ 0 & \mathrm{e}^{\mathrm{i}\cdot 0\cdot\varphi} & 0 \\ 0 & 0 & \mathrm{e}^{\mathrm{i}\cdot 1\cdot\varphi} \end{pmatrix}. \tag{1.58}$$

So far, we have described only rotation about one axis (z). The discussion can be extended to a general rotation is space, relating two different coordinate systems. As described in Section 1.5.3, a Cartesian coordinate system can be transformed to another one by three successive rotations. Two of them are rotations about the z axis (about the "new" z' axis by the angle $-\varphi$ and about the "original" z axis by the angle $-\chi$ and). Such rotations are, according to Eq. 1.58, described by the functions $\mathrm{e}^{\mathrm{i}k\varphi}$ and $\mathrm{e}^{\mathrm{i}k'\chi}$, where k and k' are -1, 0, and $+1$. The middle rotation about the y axis is more difficult to describe. It is defined by a matrix with components traditionally labeled by $d^1_{k,k'}(\vartheta)$.

$$\hat{d}^1(\vartheta) = \begin{pmatrix} \frac{1}{2}(1 + \cos\vartheta) & \frac{1}{\sqrt{2}}\sin\vartheta & \frac{1}{2}(1 - \cos\vartheta) \\ -\frac{1}{\sqrt{2}}\sin\vartheta & \cos\vartheta & \frac{1}{\sqrt{2}}\sin\vartheta \\ \frac{1}{2}(1 - \cos\vartheta) & -\frac{1}{\sqrt{2}}\sin\vartheta & \frac{1}{2}(1 + \cos\vartheta) \end{pmatrix}. \tag{1.59}$$

The complete matrix, traditionally denoted $\hat{\mathscr{D}}^1$, has the following form

$$\begin{aligned}
\hat{\mathscr{D}}^1(\varphi, \vartheta, \chi) &= \begin{pmatrix} \mathrm{e}^{\mathrm{i}\varphi} & 0 & 0 \\ 0 & 1 & 0 \\ 0 & 0 & \mathrm{e}^{-\mathrm{i}\varphi} \end{pmatrix} \begin{pmatrix} \frac{1}{2}(1 + \cos\vartheta) & \frac{1}{\sqrt{2}}\sin\vartheta & \frac{1}{2}(1 - \cos\vartheta) \\ -\frac{1}{\sqrt{2}}\sin\vartheta & \cos\vartheta & \frac{1}{\sqrt{2}}\sin\vartheta \\ \frac{1}{2}(1 - \cos\vartheta) & -\frac{1}{\sqrt{2}}\sin\vartheta & \frac{1}{2}(1 + \cos\vartheta) \end{pmatrix} \begin{pmatrix} \mathrm{e}^{\mathrm{i}\chi} & 0 & 0 \\ 0 & 1 & 0 \\ 0 & 0 & \mathrm{e}^{-\mathrm{i}\chi} \end{pmatrix} \\
&= \begin{pmatrix} \frac{1}{2}\mathrm{e}^{\mathrm{i}\varphi}\mathrm{e}^{\mathrm{i}\chi}(1 + \cos\vartheta) & \mathrm{e}^{\mathrm{i}\varphi}\frac{1}{\sqrt{2}}\sin\vartheta & \frac{1}{2}\mathrm{e}^{\mathrm{i}\varphi}\mathrm{e}^{-\mathrm{i}\chi}(1 - \cos\vartheta) \\ -\frac{1}{\sqrt{2}}\mathrm{e}^{\mathrm{i}\chi}\sin\vartheta & \cos\vartheta & \frac{1}{\sqrt{2}}\mathrm{e}^{-\mathrm{i}\chi}\sin\vartheta \\ \frac{1}{2}\mathrm{e}^{-\mathrm{i}\varphi}\mathrm{e}^{\mathrm{i}\chi}(1 - \cos\vartheta) & -\mathrm{e}^{-\mathrm{i}\varphi}\frac{1}{\sqrt{2}}\sin\vartheta & \frac{1}{2}\mathrm{e}^{-\mathrm{i}\varphi}\mathrm{e}^{-\mathrm{i}\chi}(1 + \cos\vartheta) \end{pmatrix}.
\end{aligned} \tag{1.60}$$

---

[9]We present $\vec{a}$ as a row vector here because it is a convention to use row vectors (and the corresponding representations of tensors) when describing rotation in the manner discussed in Section 1.5.4.

This matrix describes *active rotation* of an object in space by the angles $(\varphi, \vartheta, \chi)$ or *passive rotation* by the angles $(-\varphi, -\vartheta, -\chi)$ describing how $\vec{a}$ is seen from different coordinate frames (cf. Section 1.5.3). Transformation of a coordinate frame can be therefore described as

$$\vec{a}' = \begin{pmatrix} a_{k'=-1} & a_{k'=0} & a_{k'=+1} \end{pmatrix} = \begin{pmatrix} a_{k=-1} & a_{k=0} & a_{k=+1} \end{pmatrix} \begin{pmatrix} \frac{1}{2}e^{i\varphi}e^{i\chi}(1+\cos\vartheta) & e^{i\varphi}\frac{1}{\sqrt{2}}\sin\vartheta & \frac{1}{2}e^{i\varphi}e^{-i\chi}(1-\cos\vartheta) \\ -\frac{1}{\sqrt{2}}e^{i\chi}\sin\vartheta & \cos\vartheta & \frac{1}{\sqrt{2}}e^{-i\chi}\sin\vartheta \\ \frac{1}{2}e^{-i\varphi}e^{i\chi}(1-\cos\vartheta) & -e^{-i\varphi}\frac{1}{\sqrt{2}}\sin\vartheta & \frac{1}{2}e^{-i\varphi}e^{-i\chi}(1+\cos\vartheta) \end{pmatrix}$$
(1.61)

or simply[10]

$$a_{k'} = \sum_{k=-1}^{1} \mathscr{D}^1_{k,k'}(\varphi, \vartheta, \chi) a_k.$$
(1.62)

Rotation of tensors discussed in Section 1.5.3 can be also described in a similar manner as presented above for vectors. The tensors of our interest can be expressed in the following basis

$$T_{0,0} = -\frac{1}{\sqrt{3}}(T_{xx} + T_{yy} + T_{zz})$$
(1.63)

$$T_{1,-1} = -\frac{1}{2}(T_{xz} - T_{zx} - i(T_{yz} - T_{zy}))$$
(1.64)

$$T_{1,0} = i\frac{1}{\sqrt{2}}(T_{xy} - T_{yx})$$
(1.65)

$$T_{1,+1} = -\frac{1}{2}(T_{xz} - T_{zx} + i(T_{yz} - T_{zy}))$$
(1.66)

$$T_{2,-2} = +\frac{1}{2}(T_{xx} - T_{yy} - i(T_{xy} - T_{yx}))$$
(1.67)

$$T_{2,-1} = +\frac{1}{2}(T_{xz} + T_{zx} - i(T_{yz} + T_{zy}))$$
(1.68)

$$T_{2,0} = -\frac{1}{\sqrt{6}}(T_{xx} + T_{yy} - 2T_{zz})$$
(1.69)

$$T_{2,+1} = -\frac{1}{2}(T_{xz} + T_{zx} + i(T_{yz} + T_{zy}))$$
(1.70)

$$T_{2,+2} = +\frac{1}{2}(T_{xx} - T_{yy} + i(T_{xy} - T_{yx}))$$
(1.71)

The first subscript defines *rank* of the component and also the transformation matrix. The zero-rank component $T_{0,0}$ is a scalar and does not change under rotation. Therefore, its transformation "matrix" is simply $\mathscr{D}^0 = 1$. An example is the atomic orbital 1s. The first-rank components $T_{1,k}$ transform as vectors[11] and their rotation is described by our familiar matrix $\hat{\mathscr{D}}^1$. Examples of first-rank tensors are the functions describing angular dependence of atomic orbitals 2p. The matrix describing transformation of the second-rank components $T_{2,k}$ is

$$\hat{\mathscr{D}}^2(\varphi, \vartheta, \chi) = \begin{pmatrix} e^{2i\varphi} & 0 & 0 & 0 & 0 \\ 0 & e^{i\varphi} & 0 & 0 & 0 \\ 0 & 0 & 1 & 0 & 0 \\ 0 & 0 & 0 & e^{-i\varphi} & 0 \\ 0 & 0 & 0 & 0 & e^{-2i\varphi} \end{pmatrix} \hat{d}^2(\vartheta) \begin{pmatrix} e^{2i\chi} & 0 & 0 & 0 & 0 \\ 0 & e^{i\chi} & 0 & 0 & 0 \\ 0 & 0 & 1 & 0 & 0 \\ 0 & 0 & 0 & e^{-i\chi} & 0 \\ 0 & 0 & 0 & 0 & e^{-2i\chi} \end{pmatrix},$$
(1.72)

where

---

[10]Here we keep notation introduced in Section 1.5.3 to describe a passive rotation corresponding to the transformation from an "original" coordinate system to a new, "primed" frame. The elements of the transformation matrix are typically marked with indices $m'm$ (summing over m') in the literature.

[11]If the Cartesian components of the tensor T are products of Cartesian components of vectors $\vec{a}$ and $\vec{b}$ ($T_{xy} = a_x b_x$ etc.), then $T_{1,k} = \frac{i}{\sqrt{2}}c_k$, where c_k are elements of $\vec{c} = \vec{a} \times \vec{b}$ in the basis defined by Eq. 1.57.

$$
\hat{d}^2(\vartheta) = \begin{pmatrix}
\frac{1}{4}(1+\cos\vartheta)^2 & \frac{1}{2}\sin\vartheta(1+\cos\vartheta) & \sqrt{\frac{3}{8}}\sin^2\vartheta & \frac{1}{2}\sin\vartheta(1-\cos\vartheta) & \frac{1}{4}(1-\cos\vartheta)^2 \\
-\frac{1}{2}\sin\vartheta(1+\cos\vartheta) & \frac{1}{2}(2\cos\vartheta-1)(1+\cos\vartheta) & \sqrt{\frac{3}{2}}\sin\vartheta\cos\vartheta & \frac{1}{2}(2\cos\vartheta+1)(1-\cos\vartheta) & \frac{1}{2}\sin\vartheta(1-\cos\vartheta) \\
\sqrt{\frac{3}{8}}\sin^2\vartheta & -\sqrt{\frac{3}{2}}\sin\vartheta\cos\vartheta & \frac{1}{2}(3\cos^2-1) & \sqrt{\frac{3}{2}}\sin\vartheta\cos\vartheta & \sqrt{\frac{3}{8}}\sin^2\vartheta \\
\frac{1}{2}\sin\vartheta(1-\cos\vartheta) & \frac{1}{2}(2\cos\vartheta+1)(1-\cos\vartheta) & -\sqrt{\frac{3}{2}}\sin\vartheta\cos\vartheta & \frac{1}{2}(2\cos\vartheta-1)(1+\cos\vartheta) & \frac{1}{2}\sin\vartheta(1+\cos\vartheta) \\
\frac{1}{4}(1-\cos\vartheta)^2 & -\frac{1}{2}\sin\vartheta(1-\cos\vartheta) & \sqrt{\frac{3}{8}}\sin^2\vartheta & -\frac{1}{2}\sin\vartheta(1+\cos\vartheta) & \frac{1}{4}(1+\cos\vartheta)^2
\end{pmatrix}. \tag{1.73}
$$

Examples of second-rank tensors are the functions describing angular dependence of the atomic orbitals 3d.
In summary, components of tensors transform as

$$
T_{j,k'} = \sum_{k=-j}^{j} \mathscr{D}_{k,k'}^{j}(\varphi,\vartheta,\chi)T_{j,k} = \sum_{k=-j}^{j} \mathrm{e}^{-\mathrm{i}k\varphi}d_{kk'}^{j}(\vartheta)\mathrm{e}^{-\mathrm{i}k'\chi} \tag{1.74}
$$

and the elements of the transformation matrices are listed in Table 1.1. Description of rotation described in this section was introduced in 1927 by Wigner and the transformation matrices are usually called Wigner matrices.

1.5.5   Rotation in spinor representation

Rotations described in Section 1.5.3 can be also analyzed in a manner that is particularly useful in NMR spectroscopy. We again start with vectors written in spherical coordinates and convert them to *two-dimensional complex vectors*, called *spinors*

$$
\begin{pmatrix} a_\alpha \\ a_\beta \end{pmatrix} = \begin{pmatrix} \sqrt{|a|}\cos\frac{\vartheta_a}{2}\mathrm{e}^{-\mathrm{i}\frac{\varphi_a}{2}} \\ \sqrt{|a|}\sin\frac{\vartheta_a}{2}\mathrm{e}^{+\mathrm{i}\frac{\varphi_a}{2}} \end{pmatrix}. \tag{1.75}
$$

We can easily check that the complex numbers a_α and a_β unambiguously define the Cartesian coordinates a_x, a_y, a_z

$$
a_\alpha a_\beta^* + a_\beta a_\alpha^* = |a|\sin\frac{\vartheta_a}{2}\cos\frac{\vartheta_a}{2}\mathrm{e}^{-\mathrm{i}\varphi_a} + |a|\sin\frac{\vartheta_a}{2}\cos\frac{\vartheta_a}{2}\mathrm{e}^{+\mathrm{i}\varphi_a} = |a|\sin\vartheta_a\frac{\mathrm{e}^{+\mathrm{i}\varphi_a}+\mathrm{e}^{-\mathrm{i}\varphi_a}}{2} = |a|\sin\vartheta_a\cos\varphi_a = a_x, \tag{1.76}
$$

$$
\mathrm{i}\left(a_\alpha a_\beta^* - a_\beta a_\alpha^*\right) = \mathrm{i}\left(|a|\sin\frac{\vartheta_a}{2}\cos\frac{\vartheta_a}{2}\mathrm{e}^{-\mathrm{i}\varphi_a} - |a|\sin\frac{\vartheta_a}{2}\cos\frac{\vartheta_a}{2}\mathrm{e}^{+\mathrm{i}\varphi_a}\right) = -\mathrm{i}|a|\sin\vartheta_a\frac{\mathrm{e}^{+\mathrm{i}\varphi_a}-\mathrm{e}^{-\mathrm{i}\varphi_a}}{2} = |a|\sin\vartheta_a\sin\varphi_a = a_y, \tag{1.77}
$$

$$
a_\alpha a_\alpha^* - a_\beta a_\beta^* = |a|\cos^2\frac{\vartheta_a}{2} - |a|\sin^2\frac{\vartheta_a}{2} = |a|\cos\vartheta_a = a_z, \tag{1.78}
$$

and

$$
a_\alpha a_\alpha^* + a_\beta a_\beta^* = |a|\cos^2\frac{\vartheta_a}{2} + |a|\sin^2\frac{\vartheta_a}{2} = |a|. \tag{1.79}
$$

Rotation of a spinor by an angle $-\vartheta_n/2$ about an axis $\vec{n}$ corresponds to the rotation of the real 3D vector about an angle $-\vartheta_n$. Rotations of spinors are described by 2×2 matrices

$$
\begin{pmatrix} \alpha_n & -\beta_n^* \\ \beta_n & \alpha_n^* \end{pmatrix}, \tag{1.80}
$$

where

$$
\alpha_n = \cos\vartheta_n/2 - \mathrm{i}n_z\sin\vartheta_n/2, \tag{1.81}
$$
$$
\beta_n = -\mathrm{i}(n_x + \mathrm{i}n_y)\sin\vartheta_n/2. \tag{1.82}
$$

For rotations about the x, y, and z axes,

$$
\begin{pmatrix} a_\alpha' \\ a_\beta' \end{pmatrix} = \begin{pmatrix} \alpha_x & -\beta_x^* \\ \beta_x & \alpha_x^* \end{pmatrix}\begin{pmatrix} a_\alpha \\ a_\beta \end{pmatrix} = \left(\begin{pmatrix} 1 & 0 \\ 0 & 1 \end{pmatrix}\cos\frac{\vartheta_x}{2} - \mathrm{i}\begin{pmatrix} 0 & 1 \\ 1 & 0 \end{pmatrix}\sin\frac{\vartheta_x}{2}\right)\begin{pmatrix} a_\alpha \\ a_\beta \end{pmatrix} = \begin{pmatrix} \cos\frac{\vartheta_x}{2} & -\mathrm{i}\sin\frac{\vartheta_x}{2} \\ -\mathrm{i}\sin\frac{\vartheta_x}{2} & \cos\frac{\vartheta_x}{2} \end{pmatrix}\begin{pmatrix} a_\alpha \\ a_\beta \end{pmatrix}, \tag{1.83}
$$

$$
\begin{pmatrix} a_\alpha' \\ a_\beta' \end{pmatrix} = \begin{pmatrix} \alpha_y & -\beta_y^* \\ \beta_y & \alpha_y^* \end{pmatrix}\begin{pmatrix} a_\alpha \\ a_\beta \end{pmatrix} = \left(\begin{pmatrix} 1 & 0 \\ 0 & 1 \end{pmatrix}\cos\frac{\vartheta_y}{2} - \mathrm{i}\begin{pmatrix} 0 & -\mathrm{i} \\ \mathrm{i} & 0 \end{pmatrix}\sin\frac{\vartheta_y}{2}\right)\begin{pmatrix} a_\alpha \\ a_\beta \end{pmatrix} = \begin{pmatrix} \cos\frac{\vartheta_y}{2} & -\sin\frac{\vartheta_y}{2} \\ \sin\frac{\vartheta_y}{2} & \cos\frac{\vartheta_y}{2} \end{pmatrix}\begin{pmatrix} a_\alpha \\ a_\beta \end{pmatrix}, \tag{1.84}
$$

Table 1.1: Elements of Wigner matrices describing rotation of vectors and tensors.

j	k	k'	$\mathrm{e}^{-\mathrm{i}k\varphi}$	$d^j_{k,k'}(\vartheta)$	$\mathrm{e}^{-\mathrm{i}k'\chi}$	$\mathscr{D}^j_{k,k'}(\varphi,\vartheta,\chi)$
0	0	0	1	1	1	$\mathscr{D}^0_{0,0} = 1$
1	-1	-1	$\mathrm{e}^{+\mathrm{i}\varphi}$	$\frac{1}{2}(1+\cos\vartheta)$	$\mathrm{e}^{+\mathrm{i}\chi}$	$\mathscr{D}^1_{-1,-1} = \frac{1}{2}\mathrm{e}^{\mathrm{i}(\varphi+\chi)}(1+\cos\vartheta)$
1	-1	0	$\mathrm{e}^{-\mathrm{i}\varphi}$	$\frac{1}{\sqrt{2}}\sin\vartheta\cos\vartheta$	1	$\mathscr{D}^1_{-1,0} = \frac{1}{\sqrt{2}}\sin\vartheta\cos\vartheta$
1	-1	$+1$	$\mathrm{e}^{+\mathrm{i}\varphi}$	$\frac{1}{2}(1-\cos\vartheta)$	$\mathrm{e}^{-\mathrm{i}\chi}$	$\mathscr{D}^1_{-1,+1} = \frac{1}{2}\mathrm{e}^{\mathrm{i}(\varphi-\chi)}\mathrm{e}^{\mathrm{i}\varphi}(1-\cos\vartheta)$
1	0	-1	1	$\frac{1}{\sqrt{2}}\sin\vartheta\cos\vartheta$	$\mathrm{e}^{+\mathrm{i}\chi}$	$\mathscr{D}^1_{0,-1} = -\frac{1}{\sqrt{2}}\mathrm{e}^{\mathrm{i}\chi}\sin\vartheta\cos\vartheta$
1	0	0	1	$\cos\vartheta$	1	$\mathscr{D}^1_{0,0} = \cos\vartheta$
1	0	$+1$	1	$\frac{1}{\sqrt{2}}\sin\vartheta\cos\vartheta$	$\mathrm{e}^{-\mathrm{i}\chi}$	$\mathscr{D}^1_{0,+1} = \frac{1}{\sqrt{2}}\mathrm{e}^{-\mathrm{i}\chi}\sin\vartheta\cos\vartheta$
1	$+1$	-1	$\mathrm{e}^{-\mathrm{i}\varphi}$	$\frac{1}{2}(1-\cos\vartheta)$	$\mathrm{e}^{+\mathrm{i}\chi}$	$\mathscr{D}^1_{+1,-1} = \frac{1}{2}\mathrm{e}^{-\mathrm{i}(\varphi-\chi)}(1-\cos\vartheta)$
1	$+1$	0	$\mathrm{e}^{-\mathrm{i}\varphi}$	$\frac{1}{\sqrt{2}}\sin\vartheta\cos\vartheta$	1	$\mathscr{D}^1_{+1,0} = -\frac{1}{\sqrt{2}}\mathrm{e}^{-\mathrm{i}\varphi}\sin\vartheta\cos\vartheta$
1	$+1$	$+1$	$\mathrm{e}^{-\mathrm{i}\varphi}$	$\frac{1}{2}(1+\cos\vartheta)$	$\mathrm{e}^{-\mathrm{i}\chi}$	$\mathscr{D}^1_{+1,+1} = \frac{1}{2}\mathrm{e}^{-\mathrm{i}(\varphi+\chi)}(1+\cos\vartheta)$
2	-2	-2	$\mathrm{e}^{+2\mathrm{i}\varphi}$	$\frac{1}{4}(1+\cos\vartheta)^2$	$\mathrm{e}^{+2\mathrm{i}\chi}$	$\mathscr{D}^2_{-2,-2} = \frac{1}{4}\mathrm{e}^{2\mathrm{i}(\varphi+\chi)}(1+\cos\vartheta)^2$
2	-2	-1	$\mathrm{e}^{+2\mathrm{i}\varphi}$	$\frac{1}{2}\sin\vartheta(1+\cos\vartheta)$	$\mathrm{e}^{+\mathrm{i}\chi}$	$\mathscr{D}^2_{-2,-1} = \frac{1}{2}\mathrm{e}^{\mathrm{i}(2\varphi+\chi)}\sin\vartheta(1+\cos\vartheta)$
2	-2	0	$\mathrm{e}^{+2\mathrm{i}\varphi}$	$\sqrt{\frac{3}{8}}\sin^2\vartheta$	1	$\mathscr{D}^2_{-2,0} = \sqrt{\frac{3}{8}}\mathrm{e}^{2\mathrm{i}\varphi}\sin^2\vartheta$
2	-2	$+1$	$\mathrm{e}^{+2\mathrm{i}\varphi}$	$\frac{1}{2}\sin\vartheta(1-\cos\vartheta)$	$\mathrm{e}^{-\mathrm{i}\chi}$	$\mathscr{D}^2_{-2,+1} = \frac{1}{2}\mathrm{e}^{\mathrm{i}(2\varphi-\chi)}\sin\vartheta(1-\cos\vartheta)$
2	-2	$+2$	$\mathrm{e}^{+2\mathrm{i}\varphi}$	$\frac{1}{4}(1-\cos\vartheta)^2$	$\mathrm{e}^{-2\mathrm{i}\chi}$	$\mathscr{D}^2_{-2,+2} = \frac{1}{4}\mathrm{e}^{2\mathrm{i}(\varphi-\chi)}(1-\cos\vartheta)^2$
2	-1	-2	$\mathrm{e}^{+\mathrm{i}\varphi}$	$-\frac{1}{2}\sin\vartheta(1+\cos\vartheta)$	$\mathrm{e}^{+2\mathrm{i}\chi}$	$\mathscr{D}^2_{-1,-2} = -\frac{1}{2}\mathrm{e}^{\mathrm{i}(\varphi+2\chi)}\sin\vartheta(1+\cos\vartheta)$
2	-1	-1	$\mathrm{e}^{+\mathrm{i}\varphi}$	$\frac{1}{2}(2\cos\vartheta-1)(1+\cos\vartheta)$	$\mathrm{e}^{+\mathrm{i}\chi}$	$\mathscr{D}^2_{-1,-1} = \frac{1}{2}\mathrm{e}^{\mathrm{i}(\varphi+\chi)}(2\cos\vartheta-1)(1+\cos\vartheta)$
2	-1	0	$\mathrm{e}^{+\mathrm{i}\varphi}$	$\sqrt{\frac{3}{2}}\sin\vartheta\cos\vartheta$	1	$\mathscr{D}^2_{-1,0} = \sqrt{\frac{3}{2}}\mathrm{e}^{\mathrm{i}\varphi}\sin\vartheta\cos\vartheta$
2	-1	$+1$	$\mathrm{e}^{+\mathrm{i}\varphi}$	$\frac{1}{2}(2\cos\vartheta+1)(1-\cos\vartheta)$	$\mathrm{e}^{-\mathrm{i}\chi}$	$\mathscr{D}^2_{-1,+1} = \frac{1}{2}\mathrm{e}^{\mathrm{i}(\varphi-\chi)}(2\cos\vartheta+1)(1-\cos\vartheta)$
2	-1	$+2$	$\mathrm{e}^{+\mathrm{i}\varphi}$	$\frac{1}{2}\sin\vartheta(1-\cos\vartheta)$	$\mathrm{e}^{-2\mathrm{i}\chi}$	$\mathscr{D}^2_{-1,+2} = \frac{1}{2}\mathrm{e}^{\mathrm{i}(\varphi-2\chi)}\sin\vartheta(1-\cos\vartheta)$
2	0	-2	1	$\sqrt{\frac{3}{8}}\sin^2\vartheta$	$\mathrm{e}^{+2\mathrm{i}\chi}$	$\mathscr{D}^2_{0,-2} = \sqrt{\frac{3}{8}}\mathrm{e}^{2\mathrm{i}\chi}\sin^2\vartheta$
2	0	-1	1	$-\sqrt{\frac{3}{2}}\sin\vartheta\cos\vartheta$	$\mathrm{e}^{+\mathrm{i}\chi}$	$\mathscr{D}^2_{0,-1} = -\sqrt{\frac{3}{2}}\mathrm{e}^{\mathrm{i}\chi}\sin\vartheta\cos\vartheta$
2	0	0	1	$\frac{1}{2}(3\cos^2\vartheta-1)$	1	$\mathscr{D}^2_{0,0} = \frac{1}{2}(3\cos^2\vartheta-1)$
2	0	$+1$	1	$\sqrt{\frac{3}{2}}\sin\vartheta\cos\vartheta$	$\mathrm{e}^{-\mathrm{i}\chi}$	$\mathscr{D}^2_{0,+1} = \sqrt{\frac{3}{2}}\mathrm{e}^{-\mathrm{i}\chi}\sin\vartheta\cos\vartheta$
2	0	$+2$	1	$\sqrt{\frac{3}{8}}\sin^2\vartheta$	$\mathrm{e}^{-2\mathrm{i}\chi}$	$\mathscr{D}^2_{0,+2} = \sqrt{\frac{3}{8}}\mathrm{e}^{-2\mathrm{i}\chi}\sin^2\vartheta$
2	$+1$	-2	$\mathrm{e}^{-\mathrm{i}\varphi}$	$-\frac{1}{2}\sin\vartheta(1-\cos\vartheta)$	$\mathrm{e}^{+2\mathrm{i}\chi}$	$\mathscr{D}^2_{+1,-2} = -\frac{1}{2}\mathrm{e}^{-\mathrm{i}(2\varphi-\chi)}\sin\vartheta(1-\cos\vartheta)$
2	$+1$	-1	$\mathrm{e}^{-\mathrm{i}\varphi}$	$\frac{1}{2}(2\cos\vartheta+1)(1-\cos\vartheta)$	$\mathrm{e}^{+\mathrm{i}\chi}$	$\mathscr{D}^2_{+1,-1} = \frac{1}{2}\mathrm{e}^{-\mathrm{i}(\varphi-\chi)}(2\cos\vartheta+1)(1-\cos\vartheta)$
2	$+1$	0	$\mathrm{e}^{-\mathrm{i}\varphi}$	$-\sqrt{\frac{3}{2}}\sin\vartheta\cos\vartheta$	1	$\mathscr{D}^2_{+1,0} = -\sqrt{\frac{3}{2}}\mathrm{e}^{-\mathrm{i}\varphi}\sin\vartheta\cos\vartheta$
2	$+1$	$+1$	$\mathrm{e}^{-\mathrm{i}\varphi}$	$\frac{1}{2}(2\cos\vartheta-1)(1+\cos\vartheta$	$\mathrm{e}^{-\mathrm{i}\chi}$	$\mathscr{D}^2_{+1,+1} = \frac{1}{2}\mathrm{e}^{-\mathrm{i}(\varphi+\chi)}(2\cos\vartheta-1)(1+\cos\vartheta)$
2	$+1$	$+2$	$\mathrm{e}^{-\mathrm{i}\varphi}$	$\frac{1}{2}\sin\vartheta(1+\cos\vartheta)$	$\mathrm{e}^{-2\mathrm{i}\chi}$	$\mathscr{D}^2_{+1,+2} = \frac{1}{2}\mathrm{e}^{-\mathrm{i}(2\varphi+\chi)}\sin\vartheta(1+\cos\vartheta)$
2	$+2$	-2	$\mathrm{e}^{-2\mathrm{i}\varphi}$	$\frac{1}{4}(1-\cos\vartheta)^2$	$\mathrm{e}^{+2\mathrm{i}\chi}$	$\mathscr{D}^2_{+2,-2} = \frac{1}{4}\mathrm{e}^{-2\mathrm{i}(\varphi-\chi)}(1-\cos\vartheta)^2$
2	$+2$	-1	$\mathrm{e}^{-2\mathrm{i}\varphi}$	$-\frac{1}{2}\sin\vartheta(1-\cos\vartheta)$	$\mathrm{e}^{+\mathrm{i}\chi}$	$\mathscr{D}^2_{+2,-1} = -\frac{1}{2}\mathrm{e}^{-\mathrm{i}(2\varphi-\chi)}\sin\vartheta(1-\cos\vartheta)$
2	$+2$	0	$\mathrm{e}^{-2\mathrm{i}\varphi}$	$\sqrt{\frac{3}{8}}\sin^2\vartheta$	1	$\mathscr{D}^2_{+2,0} = \sqrt{\frac{3}{8}}\mathrm{e}^{-2\mathrm{i}\varphi}\sin^2\vartheta$
2	$+2$	$+1$	$\mathrm{e}^{-2\mathrm{i}\varphi}$	$-\frac{1}{2}\sin\vartheta(1+\cos\vartheta)$	$\mathrm{e}^{-\mathrm{i}\chi}$	$\mathscr{D}^2_{+2,+1} = -\frac{1}{2}\mathrm{e}^{-\mathrm{i}(2\varphi+\chi)}\sin\vartheta(1+\cos\vartheta)$
2	$+2$	$+2$	$\mathrm{e}^{-2\mathrm{i}\varphi}$	$\frac{1}{4}(1+\cos\vartheta)^2$	$\mathrm{e}^{-2\mathrm{i}\chi}$	$\mathscr{D}^2_{+2,+2} = \frac{1}{4}\mathrm{e}^{-2\mathrm{i}(\varphi+\chi)}(1+\cos\vartheta)^2$

Figure 1.10: Rotation of the magnetization to direction perpendicular to $\vec{B}_0$, shown in the laboratory and rotating coordinate frame in the left and right panel, respectively. The thin purple line shows oscillation of the magnetic induction vector of the radio waves, the cyan trace shows evolution of the magnetization during irradiation.

$$\begin{pmatrix} a'_\alpha \\ a'_\beta \end{pmatrix} = \begin{pmatrix} \alpha_z & -\beta_z^* \\ \beta_z & \alpha_z^* \end{pmatrix} \begin{pmatrix} a_\alpha \\ a_\beta \end{pmatrix} = \left(\begin{pmatrix} 1 & 0 \\ 0 & 1 \end{pmatrix} \cos\frac{\vartheta_z}{2} - \mathrm{i} \begin{pmatrix} 1 & 0 \\ 0 & -1 \end{pmatrix} \sin\frac{\vartheta_z}{2} \right) \begin{pmatrix} a_\alpha \\ a_\beta \end{pmatrix} = \begin{pmatrix} \mathrm{e}^{-\mathrm{i}\frac{\vartheta_z}{2}} & 0 \\ 0 & \mathrm{e}^{+\mathrm{i}\frac{\vartheta_z}{2}} \end{pmatrix} \begin{pmatrix} a_\alpha \\ a_\beta \end{pmatrix}. \tag{1.85}$$

The rotation of a 3D real vector by the Euler angles $-\varphi, -\vartheta, -\chi$ (Eq. 1.35) thus corresponds to the following rotation of the spinor

$$\begin{pmatrix} a'_\alpha \\ a'_\beta \end{pmatrix} = \begin{pmatrix} \mathrm{e}^{-\mathrm{i}\frac{\chi}{2}} & 0 \\ 0 & \mathrm{e}^{+\mathrm{i}\frac{\chi}{2}} \end{pmatrix} \begin{pmatrix} \cos\frac{\vartheta}{2} & -\sin\frac{\vartheta}{2} \\ \sin\frac{\vartheta}{2} & \cos\frac{\vartheta}{2} \end{pmatrix} \begin{pmatrix} \mathrm{e}^{-\mathrm{i}\frac{\varphi}{2}} & 0 \\ 0 & \mathrm{e}^{+\mathrm{i}\frac{\varphi}{2}} \end{pmatrix} \begin{pmatrix} a_\alpha \\ a_\beta \end{pmatrix} = \begin{pmatrix} \cos\frac{\vartheta}{2}\mathrm{e}^{-\mathrm{i}\frac{\varphi+\chi}{2}} & -\sin\frac{\vartheta}{2}\mathrm{e}^{+\mathrm{i}\frac{\varphi-\chi}{2}} \\ \sin\frac{\vartheta}{2}\mathrm{e}^{-\mathrm{i}\frac{\varphi-\chi}{2}} & \cos\frac{\vartheta}{2}\mathrm{e}^{+\mathrm{i}\frac{\varphi+\chi}{2}} \end{pmatrix} \begin{pmatrix} a_\alpha \\ a_\beta \end{pmatrix}. \tag{1.86}$$

When we proceed to the quantum mechanical description of NMR, we again meet spinors and 2×2 matrices describing their rotations (Pauli matrices). However, what we describe here is rotation of completely classical objects, just expressed using pairs of complex numbers.

1.5.6 Rotating coordinate frame

Mathematically, the described radio field can be decomposed into two components $\vec{B}^+_{\mathrm{radio}}$ and $\vec{B}^-_{\mathrm{radio}}$ rotating with the same angular frequency but in opposite directions ($\vec{\omega}_{\mathrm{radio}}$ and $-\vec{\omega}_{\mathrm{radio}}$, respectively). The component rotating in the same direction as the precessing magnetic dipoles ($\vec{B}^-_{\mathrm{radio}} \equiv \vec{B}_1$ in this text) tilts the magnetization vector $\vec{M}$ from the z direction, the other component can be neglected as long as $|B_1| \ll |B_0|$. This process represents a double rotation, the first rotation is precession around the direction of $\vec{B}_0$, the second rotation around $\vec{B}_1$ is known as *nutation*. Although this mathematical decomposition is only formal and does not reflect the physical reality, it is frequently used to facilitate the analysis of the effect of radio waves on magnetization. The description can be simplified (the effect of the precession removed), if we use $\vec{B}_1$ to define the x axis of our coordinate frame. As $\vec{B}_1$ rotates about $\vec{B}_0$ with an angular frequency $\vec{\omega}_{\mathrm{radio}}$, we work in a coordinate frame rotating with a frequency $\vec{\omega}_{\mathrm{rot}} = -\vec{\omega}_{\mathrm{radio}}$ (*rotating frame*). In order to define the direction of x in the rotating frame, we must also define the phase ϕ_{rot}.

The components of the field $\vec{B}_1$ rotating with the angular frequency $-\vec{\omega}_{\mathrm{radio}}$ are in the laboratory frame

$$B_{1,x} = |B_1|\cos(-\omega_{\mathrm{radio}}t + \phi_{\mathrm{radio}}) = |B_1|\cos(\omega_{\mathrm{rot}}t + \phi_{\mathrm{radio}}), \tag{1.87}$$

$$B_{1,y} = |B_1|\sin(-\omega_{\mathrm{radio}}t + \phi_{\mathrm{radio}}) = |B_1|\sin(\omega_{\mathrm{rot}}t + \phi_{\mathrm{radio}}), \tag{1.88}$$

$$B_{1,z} = 0 \tag{1.89}$$

and in the rotating frame

$$B_{1,x} = |B_1| \cos(\phi_{\text{rot}}), \tag{1.90}$$
$$B_{1,y} = |B_1| \sin(\phi_{\text{rot}}), \tag{1.91}$$
$$B_{1,z} = 0. \tag{1.92}$$

Consequently, the rotation of magnetization is given by the angular frequency vector

$$\vec{\omega} = \vec{\omega}_0 + \vec{\omega}_1 = -\gamma(\vec{B}_0 + \vec{B}_1) = \begin{pmatrix} 0 \\ 0 \\ -\gamma|B_0| \end{pmatrix} + \begin{pmatrix} -\gamma|B_1|\cos(-\omega_{\text{radio}}t + \phi_{\text{rot}}) \\ -\gamma|B_1|\sin(-\omega_{\text{radio}}t + \phi_{\text{rot}}) \\ 0 \end{pmatrix} = \begin{pmatrix} -\gamma|B_1|\cos(-\omega_{\text{radio}}t + \phi_{\text{rot}}) \\ -\gamma|B_1|\sin(-\omega_{\text{radio}}t + \phi_{\text{rot}}) \\ -\gamma|B_0| \end{pmatrix} \tag{1.93}$$

in the laboratory frame, and by

$$\vec{\omega} = \vec{\omega}_1 = -\gamma\vec{B}_1 = \begin{pmatrix} -\gamma|B_1|\cos(\phi_{\text{rot}}) \\ -\gamma|B_1|\sin(\phi_{\text{rot}}) \\ 0 \end{pmatrix} \tag{1.94}$$

in the coordinate frame rotating with the angular frequency $\vec{\omega}_{\text{rot}} = -\vec{\omega}_{\text{radio}} = \vec{\omega}_0$.
What are the components of $\vec{B}_1$ in the rotating frame for different choices of ϕ_{rot}?
If $\phi_{\text{rot}} = 0$, $\cos(0) = 1$, $\sin(0) = 0$, and

$$B_{1,x} = |B_1|, \tag{1.95}$$
$$B_{1,y} = 0, \tag{1.96}$$
$$B_{1,z} = 0. \tag{1.97}$$

If $\phi_{\text{rot}} = \frac{\pi}{2}$, $\cos(\frac{\pi}{2}) = 0$, $\sin(\frac{\pi}{2}) = 1$, and

$$B_{1,x} = 0, \tag{1.98}$$
$$B_{1,y} = |B_1|, \tag{1.99}$$
$$B_{1,z} = 0. \tag{1.100}$$

If $\phi_{\text{rot}} = \pi$, $\cos(\pi) = -1$, $\sin(\pi) = 0$, and

$$B_{1,x} = -|B_1|, \tag{1.101}$$
$$B_{1,y} = 0, \tag{1.102}$$
$$B_{1,z} = 0, \tag{1.103}$$

and so on.

The typical convention is to choose $\phi_{\text{rot}} = \pi$ for nuclei with $\gamma > 0$ and $\phi_{\text{rot}} = 0$ for nuclei with $\gamma < 0$. Then, the nutation frequency is $\vec{\omega}_1 = +\gamma\vec{B}_1 = +|\gamma|\vec{B}_1$ (opposite convention to the precession frequency!) for nuclei with $\gamma > 0$ and $\vec{\omega}_1 = -\gamma\vec{B}_1 = +|\gamma|\vec{B}_1$ (the same convention as the precession frequency) for nuclei with $\gamma < 0$.

1.5.7   Chemical shift tensor

The chemical shift tensor in its principal frame can be also written as a sum of three simple matrices, each multiplied by one characteristic constant:

$$\begin{pmatrix} \delta_{XX} & 0 & 0 \\ 0 & \delta_{YY} & 0 \\ 0 & 0 & \delta_{ZZ} \end{pmatrix} = \delta_{\text{i}} \begin{pmatrix} 1 & 0 & 0 \\ 0 & 1 & 0 \\ 0 & 0 & 1 \end{pmatrix} + \delta_{\text{a}} \begin{pmatrix} -1 & 0 & 0 \\ 0 & -1 & 0 \\ 0 & 0 & 2 \end{pmatrix} + \delta_{\text{r}} \begin{pmatrix} 1 & 0 & 0 \\ 0 & -1 & 0 \\ 0 & 0 & 0 \end{pmatrix}, \tag{1.104}$$

where

$$\delta_{\text{i}} = \frac{1}{3}\text{Tr}\{\underline{\delta}\} = \frac{1}{3}(\delta_{XX} + \delta_{YY} + \delta_{ZZ}) \tag{1.105}$$

is the *isotropic component* of the chemical shift tensor,

$$\delta_{\mathrm{a}} = \frac{1}{3}\Delta_\delta = \frac{1}{6}\left(2\delta_{ZZ} - (\delta_{XX} + \delta_{YY})\right) \tag{1.106}$$

is the *axial component* of the chemical shift tensor (Δ_δ is the *chemical shift anisotropy*), and

$$\delta_{\mathrm{r}} = \frac{1}{3}\eta_\delta\Delta_\delta = \frac{1}{2}(\delta_{XX} - \delta_{YY}) \tag{1.107}$$

is the *rhombic component* of the chemical shift tensor (η_δ is the *asymmetry of the chemical shift tensor*).

The chemical shift tensor written in its principle frame is relatively simple, but we need its description in the laboratory coordinate frame. Changing the coordinate systems represents a rotation in a three-dimensional space, as described in Section 1.5.3. Equations describing such a simple operation are relatively complicated. On the other hand, the equations simplify if $\vec{B}_0$ defines the z axis of the coordinate frame (i.e., $B_{0,z} = B_0$ and $B_{0,x} = B_{0,y} = 0$):

$$\vec{B}_{\mathrm{e}} = \delta_{\mathrm{i}}B_0 \begin{pmatrix} 0 \\ 0 \\ 1 \end{pmatrix} + \delta_{\mathrm{a}}B_0 \begin{pmatrix} 3\sin\vartheta\cos\vartheta\cos\varphi \\ 3\sin\vartheta\cos\vartheta\sin\varphi \\ 3\cos^2\vartheta - 1 \end{pmatrix} + \delta_{\mathrm{r}}B_0 \begin{pmatrix} -(2\cos^2\chi - 1)\sin\vartheta\cos\vartheta\cos\varphi + 2\sin\chi\cos\chi\sin\vartheta\sin\varphi \\ -(2\cos^2\chi - 1)\sin\vartheta\cos\vartheta\sin\varphi - 2\sin\chi\cos\chi\sin\vartheta\cos\varphi \\ +(2\cos^2\chi - 1)\sin^2\vartheta \end{pmatrix}. \tag{1.108}$$

The first, isotropic contribution does not change upon rotation (it is a scalar). The second, axial contribution, is insensitive to the rotation about the symmetry axis $\vec{Z}$, described by χ. Rotation of the chemical shift anisotropy tensor from its principal frame to the laboratory frame can be also described by orientation of $\vec{Z}$ in the laboratory frame:

$$\delta_{\mathrm{a}} \begin{pmatrix} -1 & 0 & 0 \\ 0 & -1 & 0 \\ 0 & 0 & 2 \end{pmatrix} \longrightarrow \delta_{\mathrm{a}} \begin{pmatrix} 3Z_x^2 - 1 & 3Z_x Z_y & 3Z_x Z_z \\ 3Z_x Z_y & 3Z_y^2 - 1 & 3Z_y Z_z \\ 3Z_x Z_z & 3Z_y Z_z & 3Z_z^2 - 1 \end{pmatrix}, \tag{1.109}$$

where $Z_x = \sin\vartheta\cos\varphi$, $Z_y = \sin\vartheta\sin\varphi$, and $Z_z = \cos\vartheta$.

1.5.8 Offset effects

The presence of electrons makes NMR a great method for chemical analysis. The measured precession frequency depends not only on the type of nucleus (e.g. ^{1}H) but also on the electronic environment: frequencies of protons in different chemical moieties differ and can be used to identify chemical groups in organic molecules. But how do the electrons influence the physical description of the nuclear magnetization?

The effect of the isotropic component of the chemical shift on the precession frequency is simply introducing a small correction constant $1 + \delta$ modifying γ:

$$\vec{\omega}_0 = -\gamma\vec{B}_0 \quad \rightarrow \quad \vec{\omega}_0 = -\gamma(1 + \delta)\vec{B}_0. \tag{1.110}$$

The trouble is that the correction is different for each proton (or carbon etc.) in the molecule. Therefore, the frequency of the radio waves can match $\omega_0 = -\gamma(1 + \delta)|B_0|$ only for one proton in the molecule. For example, if the radio wave resonate with the frequency of the methyl proton in ethanol, it cannot resonate with the frequency of the proton in the OH or CH_2 group. In the rotating coordinate frame, only magnetization of the methyl protons rotates about $\vec{\omega}_1 = \gamma(1 + \delta_{\mathrm{methyl}})\vec{B}_1 \approx \gamma\vec{B}_1$. Magnetizations of other protons rotate about other axes (Figure 1.11). Such rotations can be described by effective angular frequencies

$$\vec{\omega}_{\mathrm{eff}} = \vec{\omega}_1 + \vec{\Omega}, \tag{1.111}$$

where

$$\vec{\Omega} = \vec{\omega}_0 - \vec{\omega}_{\mathrm{rot}} = \vec{\omega}_0 - (-\vec{\omega}_{\mathrm{radio}}) = \vec{\omega}_0 + \vec{\omega}_{\mathrm{radio}} \tag{1.112}$$

is the angular frequency *offset*. As any vector in a 3D space, $\vec{\omega}_{\mathrm{eff}}$ is characterized by three parameters: magnitude ω_{eff}, inclination ϑ, and azimuth φ.

The magnitude of the effective frequency is

$$\omega_{\mathrm{eff}} = \sqrt{\omega_1^2 + \Omega^2}. \tag{1.113}$$

The inclination can be calculated from

$$\tan\vartheta = \frac{\omega_1}{\Omega}. \tag{1.114}$$

The azimuth is given by the phase of $\vec{B}_1$ ($\varphi = \varphi_{\mathrm{rot}}$ in a single-pulse experiment).

As a result of the chemical shift, only the magnetization of the nucleus with $\Omega = 0$ (methyl protons in our case) rotates along the "meridian" in the rotating coordinate system (Figure 1.11 left). Magnetizations of other protons move in other circles (Figure 1.11 right). Therefore, if the radio transmitter is switched off when the methyl magnetization is pointing horizontally (and starts to rotate around the
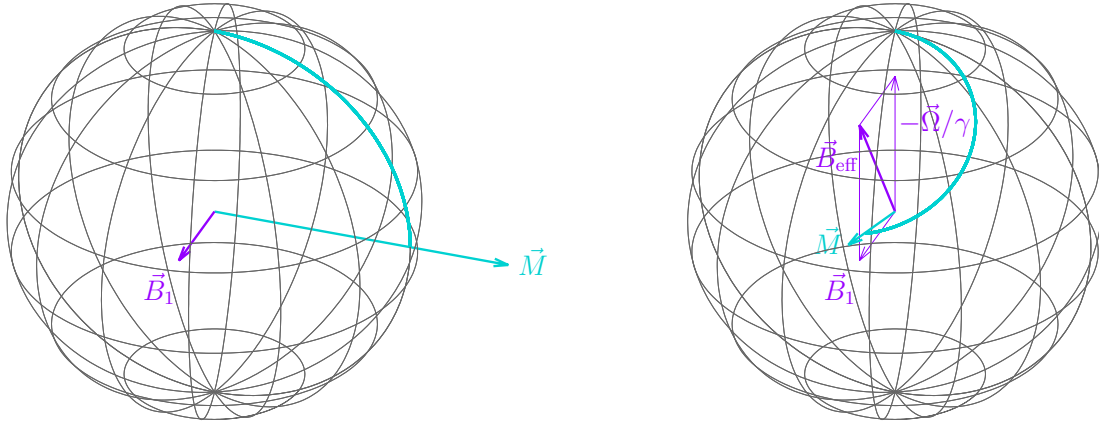
Figure 1.11: Evolution of the magnetization vectors with precession frequency exactly matching the used radio frequency (left) and slightly off-resonance (right). The evolution is shown in a coordinate frame rotating with $\vec{\omega}_{\text{rot}} = -\vec{\omega}_{\text{radio}}$.

"equator" with the precession frequency of methyl protons), vectors of magnetizations of other protons point in different directions, and start to precess on cones with different inclinations and with different initial phases. Such effects, known as the *offset effects*, influence the measured signal.[12]

The discussed motion of the magnetization vector $\vec{M}$ during irradiation is described by the following equations

$$\frac{\mathrm{d}M_x}{\mathrm{d}t} = -\Omega M_y + \omega_1 \sin\varphi M_z, \tag{1.115}$$

$$\frac{\mathrm{d}M_y}{\mathrm{d}t} = +\Omega M_x - \omega_1 \cos\varphi M_z, \tag{1.116}$$

$$\frac{\mathrm{d}M_z}{\mathrm{d}t} = -\omega_1 \sin\varphi M_x + \omega_1 \cos\varphi M_y, \tag{1.117}$$

where φ is the azimuth of $\vec{\omega}_{\text{eff}}$. The equation can be written in a compact form as

$$\frac{\mathrm{d}\vec{M}}{\mathrm{d}t} = \vec{\omega}_{\text{eff}} \times \vec{M}. \tag{1.118}$$

1.5.9 Evolution of magnetization in $\vec{B}_0$

Eqs. 1.115–1.117 are easy to solve in the absence of $\vec{B}_1$ (i.e., after turning off the radio waves):

$$\frac{\mathrm{d}M_x}{\mathrm{d}t} = -\Omega M_y \tag{1.119}$$

$$\frac{\mathrm{d}M_y}{\mathrm{d}t} = \Omega M_x \tag{1.120}$$

$$\frac{\mathrm{d}M_z}{\mathrm{d}t} = 0 \tag{1.121}$$

The trick is to multiply the second equation by i and add it to the first equation or subtract it from the first equation.

---

[12]The result is the same as if apparent effective fields of the magnitude $B_{\text{eff}} = \sqrt{B_1^2 + (\Omega/\gamma)^2}$ were applied in the direction in the directions of $\vec{\omega}_{\text{eff}}$. The apparent effective field $\vec{B}_{\text{eff}}$ is often used to describe the offset effects.

$$\frac{\mathrm{d}(M_x + \mathrm{i}M_y)}{\mathrm{d}t} = \Omega(-M_y + \mathrm{i}M_x) = +\mathrm{i}\Omega(M_x + \mathrm{i}M_y) \tag{1.122}$$

$$\frac{\mathrm{d}(M_x - \mathrm{i}M_y)}{\mathrm{d}t} = \Omega(-M_y - \mathrm{i}M_x) = -\mathrm{i}\Omega(M_x - \mathrm{i}M_y). \tag{1.123}$$

Each differential equation can be solved easily using the standard procedure. The results are

$$M_x + \mathrm{i}M_y = C_+ \mathrm{e}^{+\mathrm{i}\Omega t} \tag{1.124}$$

$$M_x - \mathrm{i}M_y = C_- \mathrm{e}^{-\mathrm{i}\Omega t}, \tag{1.125}$$

where the integration constants $C_+ = M_x(0) + \mathrm{i}M_y(0) = \sqrt{M_x^2(0) + M_y^2(0)}\mathrm{e}^{\mathrm{i}\phi_0}$ and $C_- = M_x(0) - \mathrm{i}M_y(0) = \sqrt{M_x^2(0) + M_y^2(0)}\mathrm{e}^{-\mathrm{i}\phi_0}$ are given by the initial phase ϕ_0 of $\vec{M}$ in the coordinate system (in our case, $t = 0$ is defined by switching off the radio waves):

$$M_x + \mathrm{i}M_y = \sqrt{M_x^2(0) + M_y^2(0)}\mathrm{e}^{+\mathrm{i}(\Omega t + \phi_0)} = \sqrt{M_x^2(0) + M_y^2(0)}(\cos(\Omega t + \phi_0) + \mathrm{i}(\sin(\Omega t + \phi_0))) \tag{1.126}$$

$$M_x - \mathrm{i}M_y = \sqrt{M_x^2(0) + M_y^2(0)}\mathrm{e}^{-\mathrm{i}(\Omega t + \phi_0)} = \sqrt{M_x^2(0) + M_y^2(0)}(\cos(\Omega t + \phi_0) - \mathrm{i}(\sin(\Omega t + \phi_0))), \tag{1.127}$$

$$M_x = \sqrt{M_x^2(0) + M_y^2(0)}\cos(\Omega t + \phi_0) \tag{1.128}$$

$$M_y = \sqrt{M_x^2(0) + M_y^2(0)}\sin(\Omega t + \phi_0), \tag{1.129}$$

where setting $t = 0$ shows that

$$\tan\phi_0 = \frac{\sin\phi_0}{\cos\phi_0} = \frac{M_y(0)}{M_x(0)}. \tag{1.130}$$

In order to obtain ϕ_0 and $\sqrt{M_x^2(0) + M_y^2(0)}$, we must first solve Eqs. 1.115–1.117. The solution, presented in Section 1.5.10, is

$$M_x(0) = M_0(1 - \cos(\omega_{\mathrm{eff}}\tau_{\mathrm{p}}))\sin\vartheta\cos\vartheta, \tag{1.131}$$

$$M_y(0) = M_0\sin(\omega_{\mathrm{eff}}\tau_{\mathrm{p}})\sin\vartheta, \tag{1.132}$$

$$M_z(0) = M_0(\cos^2\vartheta + \cos(\omega_{\mathrm{eff}}\tau_{\mathrm{p}})\sin^2\vartheta), \tag{1.133}$$

where M_0 is the magnitude of the bulk magnetization in the thermodynamic equilibrium, τ_{p} is duration of irradiation by the radio waves, and $\tan\vartheta = \omega_1/\Omega$.

1.5.10   Evolution of magnetization in $\vec{B}_0 + \vec{B}_1$

On one hand, Eqs. 1.115–1.117 are substantially more difficult to solve than Eqs. 1.119–1.121. On the other hand, both sets of equations (Eqs. 1.115–1.117 and Eqs. 1.119–1.121) describe the same physical process, rotation about a given axis: $\vec{\omega}_{\mathrm{eff}}$ in Eqs. 1.115–1.117 and $\vec{\Omega}$ Eqs. 1.119–1.121. This suggests that Eqs. 1.115–1.117 can be solved easily in a coordinate system with the z axis defined by the direction of $\vec{\omega}_{\mathrm{eff}}$.

The procedure is straightforward. First, the direction of the vector $\vec{M}^{\mathrm{eq}}$ is expressed in a coordinate system with the axis z given by $\vec{\omega}_{\mathrm{eff}}$, using Eq. 1.36 (or Eq. 1.38). The angles φ and ϑ in Eq. 1.36 correspond to the azimuth φ and inclination ϑ of $\vec{\omega}_{\mathrm{eff}}$, respectively, the value χ is arbitrary because we do not need to specify the x axis of the new laboratory frame. Setting $\chi = 0$,

$$\begin{pmatrix} M_{x'}^{\mathrm{eq}} \\ M_{y'}^{\mathrm{eq}} \\ M_{z'}^{\mathrm{eq}} \end{pmatrix} = \begin{pmatrix} 1\ 0\ 0 \\ 0\ 1\ 0 \\ 0\ 0\ 1 \end{pmatrix} \begin{pmatrix} \cos\vartheta & 0 & -\sin\vartheta \\ 0 & 1 & 0 \\ \sin\vartheta & 0 & \cos\vartheta \end{pmatrix} \begin{pmatrix} \cos\varphi & \sin\varphi & 0 \\ -\sin\varphi & \cos\varphi & 0 \\ 0 & 0 & 1 \end{pmatrix} \begin{pmatrix} 0 \\ 0 \\ M_0 \end{pmatrix}. \tag{1.134}$$

Second, the evolution of $\vec{M}^{\mathrm{eq}}$ is described as a rotation about z' by an angle $\omega_{\mathrm{eff}}\tau_{\mathrm{p}}$. Using Eq. 1.32,

$$\begin{pmatrix} M_{x'} \\ M_{y'} \\ M_{z'} \end{pmatrix} = \begin{pmatrix} \cos\omega_{\mathrm{eff}}\tau_{\mathrm{p}} & -\sin\omega_{\mathrm{eff}}\tau_{\mathrm{p}} & 0 \\ \sin\omega_{\mathrm{eff}}\tau_{\mathrm{p}} & \cos\omega_{\mathrm{eff}}\tau_{\mathrm{p}} & 0 \\ 0 & 0 & 1 \end{pmatrix} \begin{pmatrix} M_{x'}^{\mathrm{eq}} \\ M_{y'}^{\mathrm{eq}} \\ M_{z'}^{\mathrm{eq}} \end{pmatrix}. \tag{1.135}$$
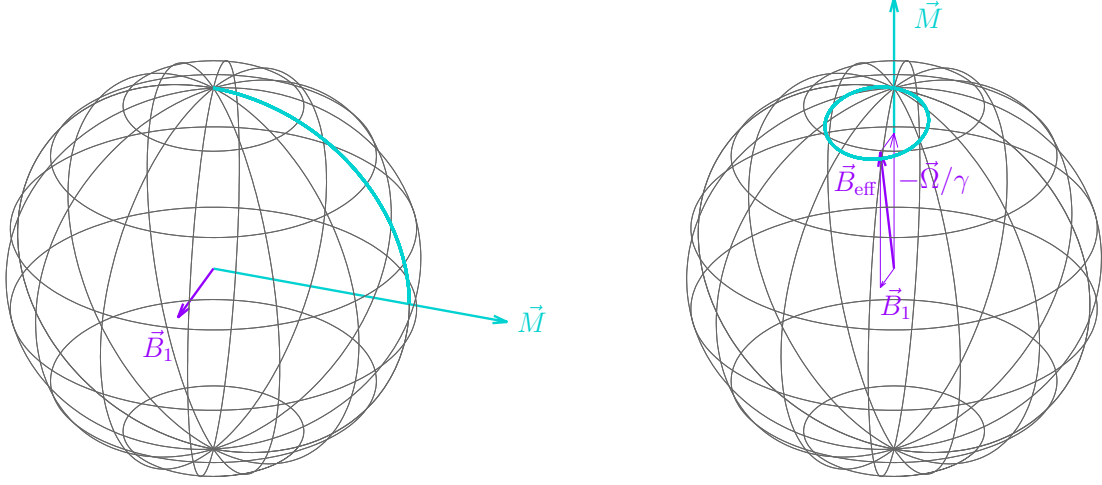
Figure 1.12: Evolution of the magnetization vectors with precession frequency exactly matching the used radio frequency (left) and with a frequency offset Ω (right), for $\omega_1 = \Omega/\sqrt{15}$. If ω_1 rotates magnetization of the former nucleus by $90\,^\circ$, then $\omega_{\mathrm{eff}} = \sqrt{1 + 15}\,\Omega = 4\Omega$ rotates magnetization of the latter nucleus by $4 \times 90\,^\circ = 360\,^\circ$, i.e., by the full circle. The evolution is shown in a coordinate frame rotating with $\vec{\omega}_{\mathrm{rot}} = -\vec{\omega}_{\mathrm{radio}}$. In both cases, magnetization rotates about the thick purple arrow with the angular frequency proportional to the length of the arrow.

Third, the components of the magnetization vector at the end of the pulse are expressed in the original coordinate system (i.e., in the rotating frame)

$$\begin{pmatrix} M_x \\ M_y \\ M_z \end{pmatrix} = \begin{pmatrix} \cos\varphi & -\sin\varphi & 0 \\ \sin\varphi & \cos\varphi & 0 \\ 0 & 0 & 1 \end{pmatrix} \begin{pmatrix} \cos\vartheta & 0 & \sin\vartheta \\ 0 & 1 & 0 \\ -\sin\vartheta & 0 & \cos\vartheta \end{pmatrix} \begin{pmatrix} 1\ 0\ 0 \\ 0\ 1\ 0 \\ 0\ 0\ 1 \end{pmatrix} \begin{pmatrix} M_{x'} \\ M_{y'} \\ M_{z'} \end{pmatrix}. \tag{1.136}$$

The whole procedure can be written in a single equation as

$$\begin{pmatrix} M_x \\ M_y \\ M_z \end{pmatrix} = \begin{pmatrix} \cos\varphi & -\sin\varphi & 0 \\ \sin\varphi & \cos\varphi & 0 \\ 0 & 0 & 1 \end{pmatrix} \begin{pmatrix} \cos\vartheta & 0 & \sin\vartheta \\ 0 & 1 & 0 \\ -\sin\vartheta & 0 & \cos\vartheta \end{pmatrix} \begin{pmatrix} \cos\omega_{\mathrm{eff}}\tau_{\mathrm{p}} & -\sin\omega_{\mathrm{eff}}\tau_{\mathrm{p}} & 0 \\ \sin\omega_{\mathrm{eff}}\tau_{\mathrm{p}} & \cos\omega_{\mathrm{eff}}\tau_{\mathrm{p}} & 0 \\ 0 & 0 & 1 \end{pmatrix} \begin{pmatrix} \cos\vartheta & 0 & -\sin\vartheta \\ 0 & 1 & 0 \\ \sin\vartheta & 0 & \cos\vartheta \end{pmatrix} \begin{pmatrix} \cos\varphi & \sin\varphi & 0 \\ -\sin\varphi & \cos\varphi & 0 \\ 0 & 0 & 1 \end{pmatrix} \begin{pmatrix} 0 \\ 0 \\ M_0 \end{pmatrix}. \tag{1.137}$$

For example, for $\varphi = \phi_{\mathrm{rot}} = 0$

$$\begin{pmatrix} M_x \\ M_y \\ M_z \end{pmatrix} = \begin{pmatrix} M_0(1 - \cos(\omega_{\mathrm{eff}}\tau_{\mathrm{p}}))\sin\vartheta\cos\vartheta \\ M_0\sin(\omega_{\mathrm{eff}}\tau_{\mathrm{p}})\sin\vartheta \\ M_0(\cos^2\vartheta + \cos(\omega_{\mathrm{eff}}\tau_{\mathrm{p}})\sin^2\vartheta) \end{pmatrix}. \tag{1.138}$$

1.5.11   Selective pulses

As discussed in Section 1.5.8, magnetization of various nuclei after applying a 90° pulse to the equilibrium distribution of magnetic moments depends on their frequency offsets Ω. Therefore, M_x, M_y, and M_z in Eq. 1.138 are in general functions of Ω (hidden in $\vec{\omega}_{\mathrm{eff}} = \vec{\omega}_1 + \vec{\Omega}$). In other words, the same radio-wave pulse will rotate magnetization of different nuclei differently, depending on their Ω. For a certain ratio of B_1 to $-\Omega/\gamma$, the magnetization makes a full circle and returns to the original direction along $\vec{B}_0$. It is therefore possible to chose such value of $\omega_1 \approx \gamma\vec{B}_1$ so that magnetization of one nucleus (with precession frequency resonating with the radio wave frequency) is flipped by $90\,^\circ$ (Figure 1.12) or $180\,^\circ$ (Figure 1.13), while magnetization of another nucleus (offset by Ω) is practically unaffected, being returned to the original direction.

The described selective manipulation of magnetic moments of different nuclei is rather limited. We can choose only which nucleus is rotated (e.g. by $90\,^\circ$) and which nucleus is not affected. Magnetization of other nuclei will end up in some direction $\vec{M}$ given by the value of Ω of the given nucleus. Such dependence of $\vec{M}$ on Ω is known as *excitation profile* (or *magnetization profile* in general, for other pulses

40
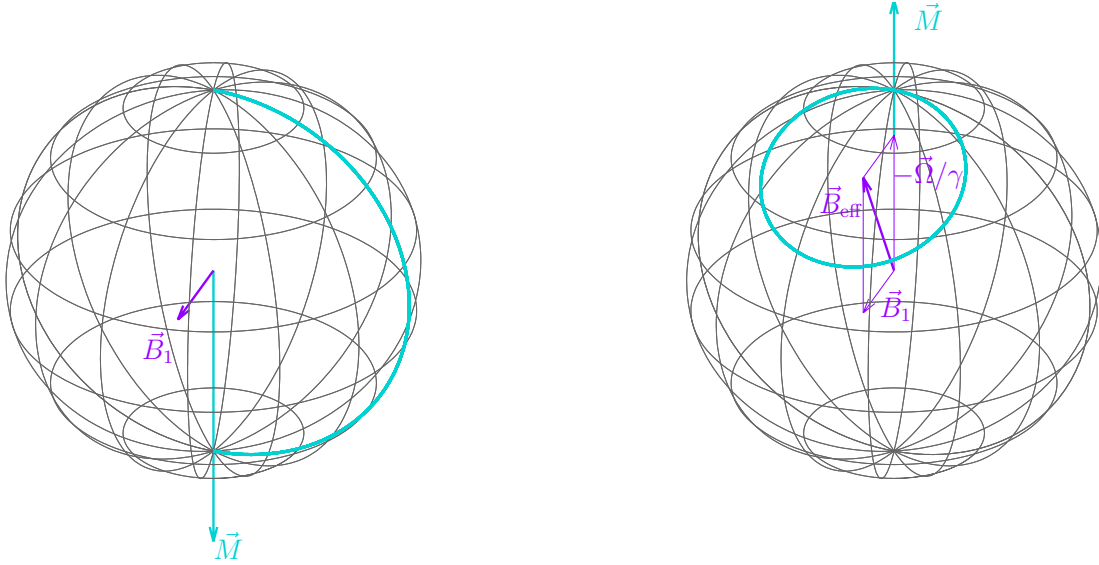
Figure 1.13: Evolution of the magnetization vectors with precession frequency exactly matching the used radio frequency (left) and with a frequency offset Ω (right), for $\omega_1 = \Omega/\sqrt{3}$. If ω_1 rotates magnetization of the former nucleus by $180\,^\circ$, then $\omega_{\text{eff}} = \sqrt{1+3}\,\Omega = 2\Omega$ rotates magnetization of the latter nucleus by $2 \times 180\,^\circ = 360\,^\circ$, i.e., by the full circle. The evolution is shown in a coordinate frame rotating with $\vec{\omega}_{\text{rot}} = -\vec{\omega}_{\text{radio}}$. In both cases, magnetization rotates about the thick purple arrow with the angular frequency proportional to the length of the arrow.

and other initial directions of $\vec{M}$). For a single pulse, the excitation profile is an explicitly defined mathematical function with only one variable parameter B_1.

Variability of the selective manipulations can be increased by applying consecutively more pulses with different B_1. Then, the excitation profile (dependence of $\vec{M}$ on Ω) depends on the actual B_1 values of all pulses. Pulses that selectively influence relatively broad ranges of frequencies are useful in advanced NMR experiments, selective excitation of a narrow frequency range is critically important in magnetic resonance imaging (see Section 13.4.5). There are several algorithms to design a series of pulses that provides a desired excitation profile. Here we comment only one of them. It is a classical approach (Shinnar–Le Roux algorithm), described by Pauly et al. in IEEE Transactions on Medical Imaging, 10 (1991) 53–65.

Magnetic moments are irradiated by a series of short radio-wave pulses. Duration of each pulse is Δt and B_1 varies. The pulses rotate $\vec{M}$ from the initial orientation (e.g. $\vec{M}^{\text{eq}}$). The rotation is expressed as described in Section 1.5.5 in terms of spinors and 2×2 matrices. During the j-th pulse, the magnetization rotates by $\Omega \Delta t$ about the z axis and by $-\omega_{1,j} = \gamma B_{1,j}$ about the direction of $\vec{B}_{1,j}$ in the xy plane. The former rotation can be described as

$$\begin{pmatrix} e^{-i\frac{\Omega \Delta t}{2}} & 0 \\ 0 & e^{+i\frac{\Omega \Delta t}{2}} \end{pmatrix} = \begin{pmatrix} z^{\frac{1}{2}} & 0 \\ 0 & z^{-\frac{1}{2}} \end{pmatrix}. \tag{1.139}$$

According to Eqs.1.80–1.82, rotation about $\vec{B}_{1,j}$ is described by the matrix

$$\begin{pmatrix} \alpha_{n,j} & -\beta_{n,j}^* \\ \beta_{n,j} & \alpha_{n,j}^* \end{pmatrix} \tag{1.140}$$

with the coefficients

$$\alpha_{n,j} = \cos\frac{\omega_{1,j}\Delta t}{2} - i\frac{\omega_{1z,j}}{|\omega_{1,j}|}\sin\frac{\omega_{1,j}\Delta t}{2} = \cos\frac{\omega_{1,j}\Delta t}{2} = C_j, \tag{1.141}$$

$$\beta_{n,j} = -i\left(\frac{\omega_{1x,j}}{|\omega_{1,j}|} + i\frac{\omega_{1y,j}}{|\omega_{1,j}|}\right)\sin\frac{\omega_{1,j}\Delta t}{2} = -ie^{-i\varphi_j}\sin\frac{\omega_{1,j}\Delta t}{2} = S_j. \tag{1.142}$$

In analogy to Eq. 1.86, rotation by each pulse is given by

$$\begin{pmatrix} \alpha_j & -\beta_j^* \\ \beta_j & \alpha_j^* \end{pmatrix} = \begin{pmatrix} C_j & -S_j^* \\ S_j & C_j \end{pmatrix} \begin{pmatrix} z^{\frac{1}{2}} & 0 \\ 0 & z^{-\frac{1}{2}} \end{pmatrix}. \tag{1.143}$$

We can define the parameters α_j, β_j by noticing that $\alpha_0 = 1$ and $\beta_0 = 0$ (i.e., no rotation in the initial state) and by calculating the recursion

$$\begin{pmatrix} \alpha_j \\ \beta_j \end{pmatrix} = \begin{pmatrix} \alpha_j & -\beta_j^* \\ \beta_j & \alpha_j^* \end{pmatrix} = \begin{pmatrix} C_j & -S_j^* \\ S_j & C_j \end{pmatrix} \begin{pmatrix} z^{\frac{1}{2}} & 0 \\ 0 & z^{-\frac{1}{2}} \end{pmatrix} \begin{pmatrix} \alpha_{j-1} \\ \beta_{j-1} \end{pmatrix} = z^{\frac{1}{2}} \begin{pmatrix} C_j & -S_j^* \\ S_j & C_j \end{pmatrix} \begin{pmatrix} 1 & 0 \\ 0 & z^{-1} \end{pmatrix} \begin{pmatrix} \alpha_{j-1} \\ \beta_{j-1} \end{pmatrix}. \tag{1.144}$$

Absorbing $z^{j/2}$ into the parameters,

$$\begin{pmatrix} \alpha_j z^{\frac{j}{2}} \\ \beta_j z^{\frac{j}{2}} \end{pmatrix} = \begin{pmatrix} \alpha_j & -\beta_j^* \\ \beta_j & \alpha_j^* \end{pmatrix} = \begin{pmatrix} C_j & -S_j^* \\ S_j & C_j \end{pmatrix} \begin{pmatrix} 1 & 0 \\ 0 & z^{-1} \end{pmatrix} \begin{pmatrix} \alpha_{j-1} z^{\frac{1}{2}} z^{\frac{j-1}{2}} \\ \beta_{j-1} z^{\frac{1}{2}} z^{\frac{j-1}{2}} \end{pmatrix} = \begin{pmatrix} C_j & -S_j^* \\ S_j & C_j \end{pmatrix} \begin{pmatrix} 1 & 0 \\ 0 & z^{-1} \end{pmatrix} \begin{pmatrix} \alpha_{j-1} z^{\frac{j}{2}} \\ \beta_{j-1} z^{\frac{j}{2}} \end{pmatrix}. \tag{1.145}$$

Labeling $\alpha_j z^{j/2} = \mathcal{A}_j$ and $\beta_j z^{j/2} = \mathcal{B}_j$, we can write

$$\begin{pmatrix} \mathcal{A}_0 \\ \mathcal{B}_0 \end{pmatrix} = \begin{pmatrix} 1 \\ 0 \end{pmatrix}, \tag{1.146}$$

$$\begin{pmatrix} \mathcal{A}_1 \\ \mathcal{B}_1 \end{pmatrix} = \begin{pmatrix} C_1 \\ S_1 \end{pmatrix}, \tag{1.147}$$

$$\begin{pmatrix} \mathcal{A}_2 \\ \mathcal{B}_2 \end{pmatrix} = \begin{pmatrix} C_2 C_1 - S_2^* S_1 z^{-1} \\ S_2 C_1 - C_2 S_1 z^{-1} \end{pmatrix}, \tag{1.148}$$

$$\begin{pmatrix} \mathcal{A}_3 \\ \mathcal{B}_3 \end{pmatrix} = \begin{pmatrix} C_3 C_2 C_1 - (C_3 S_2^* S_1 + S_3^* S_2 C_1) z^{-1} - S_3^* C_2 S_1 z^{-2} \\ S_3 C_2 C_1 - (S_3 S_2^* S_1 - C_3 S_2 C_1) z^{-1} - C_3 C_2 S_1 z^{-2} \end{pmatrix}, \tag{1.149}$$

and so on. If we define the amplitudes and phases of $\vec{B}_1$ of all pulses, defining the parameters C_j, S_j, we can express all $\mathcal{A}_j, \mathcal{B}_j$ and calculate the final dependence of the magnetization on Ω (hidden in z).

Pauly et al. describe *design* of a selective pulse, which is the opposite task: to calculate amplitudes and phases of $\vec{B}_1$ of all pulses from a set of polynomials $\mathcal{A}_j, \mathcal{B}_j$ that define the desired excitation profile (dependence of the magnetization on Ω).[13] As the first step, the recursion equation

$$\begin{pmatrix} C_j & -S_j^* z^{-1} \\ S_j & C_j z^{-1} \end{pmatrix} \begin{pmatrix} \mathcal{A}_{j-1} z^{\frac{j}{2}} \\ \mathcal{B}_{j-1} z^{\frac{j}{2}} \end{pmatrix} = \begin{pmatrix} \mathcal{A}_j \\ \mathcal{B}_j \end{pmatrix} \tag{1.150}$$

(Eq. 1.145) is inverted by multiplying both sides from left by the inversion matrix

$$\begin{pmatrix} C_j & S_j^* \\ -S_j z & C_j z \end{pmatrix} \begin{pmatrix} C_j & -S_j^* z^{-1} \\ S_j & C_j z^{-1} \end{pmatrix} \begin{pmatrix} \mathcal{A}_{j-1} \\ \mathcal{B}_{j-1} \end{pmatrix} = \begin{pmatrix} \mathcal{A}_{j-1} \\ \mathcal{B}_{j-1} \end{pmatrix} = \begin{pmatrix} C_j & S_j^* \\ -S_j z & C_j z \end{pmatrix} \begin{pmatrix} \mathcal{A}_j \\ \mathcal{B}_j \end{pmatrix} = \begin{pmatrix} C_j \mathcal{A}_j + S_j^* \mathcal{B}_j \\ -S_j z \mathcal{A}_j + C_j z \mathcal{B}_j \end{pmatrix} \begin{pmatrix} \mathcal{A}_j \\ \mathcal{B}_j \end{pmatrix}. \tag{1.151}$$

This matrix equation represents a set of two equations. The bottom one

$$\mathcal{B}_{j-1} = C_j z \mathcal{B}_j - S_j z \mathcal{A}_j \tag{1.152}$$

$$\mathcal{B}_{j-1} z^{-1} = C_j \mathcal{B}_j - S_j \mathcal{A}_j \tag{1.153}$$

provides a further clue. All polynomials start by constant terms, and continue with terms with z^{-1}, z^{-2}. However, the left-hand side of Eq. 1.153 is multiplied by z^{-1} and thus does not have any constant term, it starts with the terms with z^{-1}. Therefore, the right-hand side, $C_j \mathcal{B}_j - S_j \mathcal{A}_j$, must not have any constant term either. If we label the constant terms a_j for $\mathcal{A}_j$ and b_j for $\mathcal{B}_j$, the requirement of no constant term can be written as

$$C_j b_j - S_j a_j = 0 \quad \Rightarrow \quad \frac{b_j}{a_j} = \frac{S_j}{C_j} = \frac{-\mathrm{i} e^{-\mathrm{i}\varphi_j} \sin(\omega_{1,j}\Delta t/2)}{\cos(\omega_{1,j}\Delta t/2)} = \frac{\mathrm{i} e^{-\mathrm{i}\varphi_j} \sin(\gamma B_{1,j}\Delta t/2)}{\cos(\gamma B_{1,j}\Delta t/2)}. \tag{1.154}$$
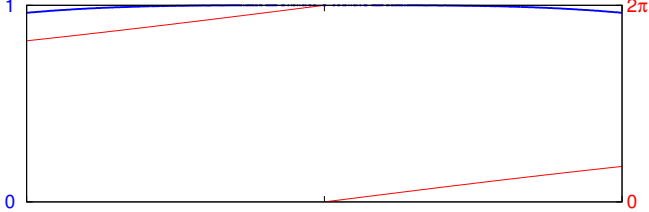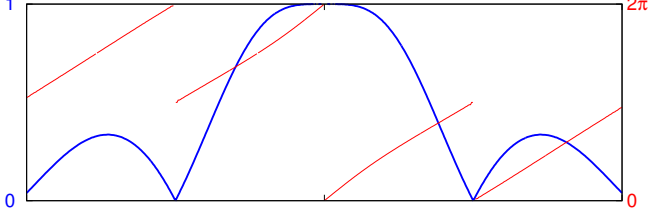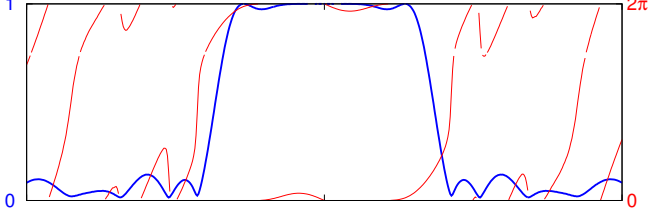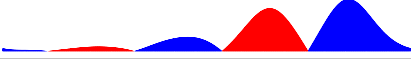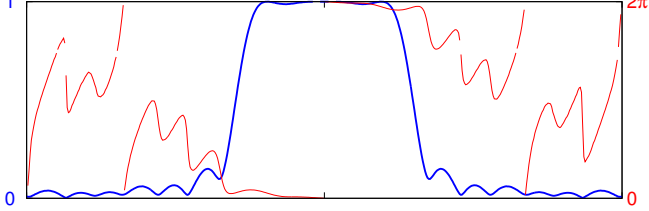
Solving this equation yields expressions defining amplitude and phase of $\vec{B}_1$ for each j. Examples of excitation profiles of several pulses are shown in Table 1.2.

$$B_{1,j} = \frac{2}{\gamma\Delta t} \arctan \left| \frac{b_j}{a_j} \right| \tag{1.155}$$

$$e^{-\mathrm{i}\varphi_j} = \frac{-\mathrm{i} b_j/a_j}{\tan(\gamma B_{1,j}\Delta t/2)}. \tag{1.156}$$

---

[13]Ideally, the pulse should rotate magnetization by $90\,^\circ$ for Ω in a small interval of offsets and have no effect outside this interval. Pauly et al. discuss how a polynomial approximation of the desired excitation profile can be found. Here, we just note that our polynomials consist of periodic functions and any shape can be approximated by a sufficient number of such periodic functions.

Table 1.2: Dependence of excitation efficiency on frequency offsets for various amplitude modulations of radio wave pulses. The pulses are shown as histograms in the second column. The lengths and amplitudes (relative $|B_1|$ values) are plotted in the real ratios, blue and red correspond to the phase of $0°$ and $180°$, respectively. The efficiency of excitation is plotted in blue, ranging from zero ($M_z = M^{\text{eq}}$, $M_x = M_y = \sqrt{M_x^2 + M_y^2} = 0$, magnetization vector in the z direction, no excitation) to one ($M_z = 0$, $\sqrt{M_x^2 + M_y^2} = M^{\text{eq}}$, magnetization vector in the xy plane). The deviations of the x and y components of the magnetization vector from the desired $-y$ direction are plotted in red (in radians). The range of the frequency offsets is $-30\,\text{kHz}$ to $+30\,\text{kHz}$. The lengths and amplitude of the hard rectangular pulse correspond to $10\,\mu s$ and $|\omega_1| = 25\,\text{kHz}$. The lengths ($64.5\,\mu s$) and amplitude ($|\omega_1| = 9.675\,\text{kHz}$) of the selective rectangular pulse are chosen so that the frequency offset of $15\,\text{kHz}$ is equal to $\sqrt{15}|\omega_1|$. The Q5 and EBURP2 pulses consist of 1000 rectangular pulses $0.3\,\mu s$ long. (the total length is $300\,\mu s$). The amplitudes of the Q5 and EBURP2 pulses were set so that the pulses rotate the magnetization by $90°$ when applied on resonance. NMR-Sim (Pavel Kessler, Bruker Biospin) was used to calculate the effects of shaped pulses.

Pulse name	Amplitude modulation (variation of $|B_1|$)	offset-dependent effect
rectangular (hard)		
rectangular (selective)		
Q5		
EBURP2		

Lecture 2
Relaxation

Literature: A nice introduction is in K9.1 and K9.3, more details can be found in L19 and L20.1–L20.3.

2.1 Relaxation due to chemical shift anisotropy

The Boltzmann law allowed us to describe the state of the system in the thermal equilibrium, but it does not tell us *how is the equilibrium reached*. The processes leading to the equilibrium states are known as *relaxation*. Relaxation takes places e.g. when the sample is placed into a magnetic field inside the spectrometer or after excitation of the sample by radio wave pulses.

Spontaneous emission is completely inefficient (because energies of nuclear magnetic moments in available magnetic fields are very small). Relaxation in NMR is due to interactions with local fluctuating magnetic fields in the molecule. One source[1] of fluctuating fields is the *anisotropy of chemical shift*, described by the axial and rhombic components of the chemical shift tensor. The chemical shift tensor is given by the distribution of electrons in a molecule. Therefore, its orientation in a coordinate frame attached to the molecule is fixed. As collisions with other molecules change orientation of the observed molecule, the isotropic component of the chemical shift tensor does not change because it is spherically symmetric (cf. Figure 1.6). However, contributions to the local fields described by the axial and rhombic components fluctuate even if the constants δ_a and δ_r do not change because the axial and rhombic parts of the chemical shift depend on the orientation of the molecule (Figure 2.1).

Here, we introduce the basic idea by analyzing the effects of fluctuating magnetic fields in a classical manner. Obviously, it is not possible to describe exactly random motions of each magnetic moment. However, it is possible to describe statistically the effect of random fluctuations of magnetic fields on the bulk magnetization. For the simplest model of molecules (rigid spherical particles in an isotropic solvent), the final equation is surprisingly simple. However, the derivation is very tedious. Therefore, we limit our analysis to the axially symmetric chemical shift tensor, and divide it to two steps.

---

[1]There are stronger sources of fluctuating fields in real molecules, but we limit our discussion to the chemical shift anisotropy in this lecture. We extend our analysis to other sources later, when we introduce quantum mechanical description of NMR.
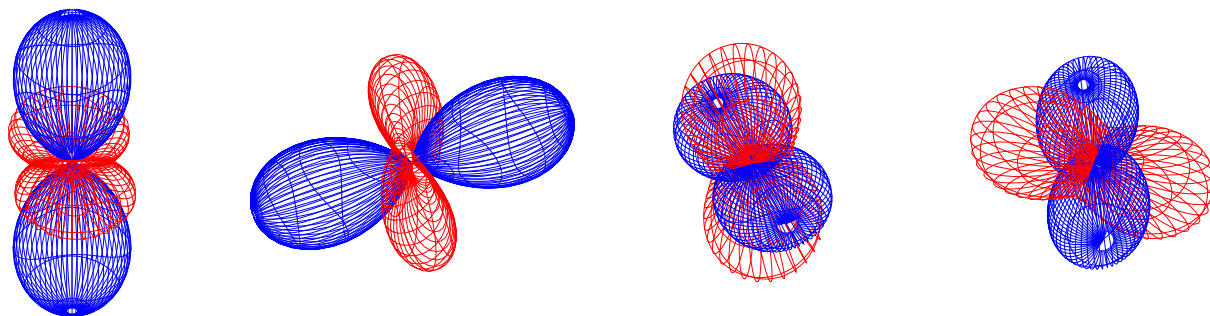
Figure 2.1: Visualization of reorientation of the anisotropic contribution to the chemical shift tensor as a result of tumbling (rotational diffusion) of the molecule. Positive and negative values are plotted in blue and red, respectively.

2.2 Adiabatic contribution to relaxation

We start by the analysis of *adiabatic* contributions to relaxation. In physics, the term *adiabatic* is used for processes that do not change energy of the studied system.

In order to distinguish fluctuations that result in adiabatic and nonadiabatic contributions to relaxation, we recall how magnetic moments move in the strong external magnetic field $\vec{B}_0$, defining the z axis of our coordinate system. We have learnt in the previous lecture that $\vec{B}_0$ causes rotation of magnetic moments about the z axis. Therefore, it does not change distribution of the z-components of magnetic moments (components parallel to $\vec{B}_0$). The energy of magnetic moments is given by $-\vec{\mu} \cdot \vec{B}_0 = -\mu_z B_0$, i.e., it depends only on the component of the magnetic moment parallel to $\vec{B}_0$.

Now we consider effects of additional fields. In this lecture, we analyze only effects of very small fields of moving electrons, introduced in the previous lecture and labeled $\vec{B}_e$. We have learnt that horizontal fields, like $B_{e,x}$ and $B_{e,y}$ have no overall effect on orientations of magnetic moments, unless their oscillate with the precession frequency of the magnetic moments. As the molecules change their orientations, components $B_{e,x}$ and $B_{e,y}$ fluctuate. However, the rate of fluctuations is in general different from the precession frequency because there is no reason why the molecular collisions causing the fluctuations should rotate our molecule with the same rate as the precession of magnetic moments in our magnet. Only very rarely and for a short time, the rate of molecular rotation may coincide with the precession frequency by accident.

In addition to $B_{e,x}$ and $B_{e,y}$, molecular collisions also change $B_{e,z}$. The vertical field $B_{e,z}$ adds to $\vec{B}_0$, changing the precession frequency $-\gamma B_z$, but not influencing μ_z. The fluctuations of $B_{e,z}$ are stochastic because the molecular collisions are random. Therefore, the average of the fluctuating field $B_{e,z}$ is zero and the average vertical field remains $\vec{B}_0$.

We can conclude that (i) fluctuations of $B_{e,z}$ does not change the energy $\mathcal{E} = -\mu_z B_z$ because they do not change μ_z or the overall B_z, (ii) $B_{e,x}$ and $B_{e,y}$ do not have any effect except for rare moments when the rate of molecular rotation coincides with the precession frequency. Most of the time, magnetic moments do not exchange energy with the environment and the process is *adiabatic*. We analyze such permanent adiabatic influence of $B_{e,z}$ in this section and complete the description by including the momentary contributions of $B_{e,x}$ and $B_{e,y}$ in Section 2.3.

As the vertical field rotates the magnetic moments about the z axis, it changes μ_x and μ_y. Therefore, stochastic fluctuations of the vertical magnetic field $B_0 + B_{e,z}$ randomize distribution of the x and y components. In other words, the adiabatic contributions to relaxation destroy *coherence* of the x and y components of magnetic moments (distributed as shown in the right panel of Figure 1.4) that was created by the radio wave pulse at the beginning of the NMR experiment.

How are the vertical fluctuations of the magnetic field related to the molecular motions? As the molecules rotate and the anisotropic components chemical shift tensors rotate with them (Figure 2.1), the vertical magnetic fields $(B_0 + B_{e,z})$ fluctuate.[2] These fluctuations are random and independent for different molecules because individual molecules in solution tumble randomly (due to collisions with other molecules) and independently. Therefore, the frequency of precession of magnetic moments in individual molecules, given by $B_0 + B_{e,z}$, also fluctuates (randomly and independently for each molecule). As a consequence, the magnetic moments in individual molecules do not precess completely coherently (with the same frequency) and their distribution shown in Figure 1.4 is slowly randomized. The cyan arrow in Figure 1.4, representing the bulk magnetization $\vec{M}$ of the given distribution of magnetic moments, shrinks but stays in the xy plane, as long as only adiabatic relaxation (fluctuations along $\vec{B}_0$) are considered. Note that we observe two processes: rotation of the cyan arrow ($\vec{M}$) in the xy plane with the (average) precession frequency, and shrinking of the cyan arrow due to the adiabatic relaxation.

In order to describe the adiabatic relaxation quantitatively, we express the precession frequency ω_z in terms of the components of the chemical shift tensor and angles[3] describing its orientation in the laboratory coordinate frame, depending on the orientation of the given molecule in the sample (Eq 1.8):

$$\omega_z = -\gamma(B_0 + B_{e,z}) = -\gamma B_0(1 + \delta_i) - \gamma B_0 \delta_a (3\cos^2 \vartheta - 1). \tag{2.1}$$

The analysis presented in Section 2.5.1 shows that the coherence disappears (the cyan arrow shrinks) with a rate constant (called R_0 in this text) proportional to the time integral of the *time correlation function*, i.e., of a mathematical function describing how quickly an ensemble of molecules (and consequently the chemical shift tensor attached to it) looses memory of its original orientation (Eq. 2.48).

$$R_0 = (\gamma B_0 \delta_a)^2 \int_0^\infty \overline{(3\cos^2 \vartheta(0) - 1)(3\cos^2 \vartheta(t) - 1)} \mathrm{d}t, \tag{2.2}$$

where the horizontal bar indicates an average value for all molecules in the sample and $\vartheta(0)$ describes orientation of the chemical shift tensor at $t = 0$. Note that statistics play the key role here: the whole analysis relies on the fact that although the product $(3\cos^2 \vartheta(0) - 1)(3\cos^2 \vartheta(t) - 1)$ changes randomly and differently for each molecule (and therefore cannot be described), the value of the time correlation function $\overline{(3\cos^2 \vartheta(0) - 1)(3\cos^2 \vartheta(t) - 1)}$ is defined statistically. If the structure of the molecule does not change (*rigid body rotational diffusion*), which is the case we analyze, the

---

[2]As the molecule rotates, $B_{e,x}$ and $B_{e,y}$ of course fluctuates too. However, fluctuating $B_{e,x}$ and $B_{e,y}$ have only the non-adiabatic effect, discussed in Section. 2.3

[3]We need only one angle, ϑ, for our analysis of adiabatic contribution to relaxation.

analytical form of $\overline{(3\cos^2\vartheta(0)-1)(3\cos^2\vartheta(t)-1)}$ can be derived. The simplest analytical form of the time correlation function is derived from the rotational diffusion equation in Section 2.5.4. The derivation shows that the time correlation function for spherically symmetric rotational diffusion is a single-exponential function:

$$\overline{\left(\frac{3}{2}\cos^2\vartheta(0)-\frac{1}{2}\right)\left(\frac{3}{2}\cos^2\vartheta(t)-\frac{1}{2}\right)}=\frac{1}{5}e^{-t/\tau_{\mathrm{c}}}\mathrm{d}t=\frac{1}{5}\mathrm{e}^{-6D^{\mathrm{rot}}t},\tag{2.3}$$

where τ_{c} is the *rotational correlation time* and D^{rot} is the *rotational diffusion coefficient*, given by the Stokes' law

$$D^{\mathrm{rot}}=\frac{k_{\mathrm{B}}T}{8\pi\eta(T)r^3},\tag{2.4}$$

where r is the radius of the spherical particle, T is the temperature, and $\eta(T)$ is the dynamic viscosity of the solvent, strongly dependent on the temperature.[4]

Analytical solutions are also available (but more difficult to derive) for axially symmetric and asymmetric rotational diffusion, with the time correlation function in a form of three- and five-exponential functions, respectively.

For the spherically symmetric rotational diffusion, the rate constant of the loss of coherence can be calculated easily:

$$R_0=\frac{4}{5}\left(\gamma B_0\delta_{\mathrm{a}}\right)^2\int\limits_{0}^{\infty}\mathrm{e}^{-t/\tau_{\mathrm{c}}}\mathrm{d}t=\frac{4}{5}\left(\gamma B_0\delta_{\mathrm{a}}\right)^2\tau_{\mathrm{c}}=\frac{4}{5}\left(\gamma B_0\delta_{\mathrm{a}}\right)^2\frac{1}{6D^{\mathrm{rot}}}.\tag{2.6}$$

2.3 Including non-adiabatic contribution to relaxation

A much more complex analysis of the *non-adiabatic* contributions to relaxation, consequences of magnetic fields fluctuations perpendicular to $\vec{B}_0$, is outlined in Section 2.5.5. Fluctuations perpendicular to $\vec{B}_0$ are also results of molecular tumbling, but now we are interested in how $B_{\mathrm{e},x}$ and $B_{\mathrm{e},y}$ fluctuate due to the reorientation of the chemical shift tensor. $B_{\mathrm{e},x}$ and $B_{\mathrm{e},y}$ have the same direction as the magnetic field of the radio waves used to rotate the magnetization form the equilibrium orientation (in the z direction) to the xy plane. Accidentally, the molecule may tumble for a short time with a rate close to the precession frequency of the magnetic moments. The resulting perpendicular fluctuations then act on the magnetic moments in a similar manner as the radio waves, i.e. rotate them about a horizontal axis. This of course changes the distribution of the z components of the magnetic moments and changes their energy in $\vec{B}_0$ (exchanges the potential magnetic energy of the magnetic moments with the kinetic rotational energy of molecules). However, there is a fundamental difference

---

[4]Dynamic viscosity of water can be approximated by

$$\eta(T)=\eta_0\times 10^{T_0/(T-T_1)},\tag{2.5}$$

where $\eta_0=2.414\times 10^{-5}\,\mathrm{kg\,m^{-1}\,s^{-1}}$, $T_0=247.8\,\mathrm{K}$, and $T_1=140\,\mathrm{K}$ (Al-Shemmeri, T., 2012. Engineering Fluid Mechanics. Ventus Publishing ApS. pp. 1718.).

between the fluctuations and the radio waves. The radio waves coherently rotate magnetic moments in all molecules, but the fluctuating fields are different in the individual molecules. And because the fluctuations are random, they randomly change distribution of magnetic moments until it returns to the equilibrium distribution. This is what happens after a sample is placed in the magnetic field of the spectrometer, and this is also what starts to happen immediately after the magnetization is tilted from the z direction by the radio waves.

The analysis in Section 2.5.5 provides values of two relaxation rates, (i) of the *longitudinal* relaxation rate R_1 describing how fast the z component of the bulk magnetization returns to its equilibrium value, and (ii) of the *transverse* relaxation rate R_2 describing how fast the x and y components of the bulk magnetization decay to zero. Note that the longitudinal and transverse relaxation are different processes. The return of M_z to its equilibrium value is identical with the process of restoring the equilibrium distribution of magnetic moments. However, the transverse relaxation has two sources, the non-adiabatic return to the equilibrium distribution of magnetic moments (with the orientation along $\vec{B}_0$ being slightly preferred) and the adiabatic loss of coherence. For large molecules, the loss of coherence is much faster than the return to the equilibrium distribution, which makes $R_2 \gg R_1$.

Quantitatively,

$$R_1 = 3 \left(\gamma B_0 \delta_\mathrm{a}\right)^2 \left(\frac{1}{2} J(\omega_0) + \frac{1}{2} J(-\omega_0)\right) \approx 3 \left(\gamma B_0 \delta_\mathrm{a}\right)^2 J(\omega_0), \tag{2.7}$$

where

$$J(\omega_0) = \int\limits_{-\infty}^{\infty} \overline{\left(\frac{3}{2}\cos^2(\theta(0)) - \frac{1}{2}\right)\left(\frac{3}{2}\cos^2(\theta(t)) - \frac{1}{2}\right)} \cos(\omega_0 t)\mathrm{d}t. \tag{2.8}$$

The function $J(\omega)$ is known as the *spectral density function.*
Note that

- The definition of R_1, describing solely the non-adiabatic effects of fluctuations perpendicular to $\vec{B}_0$ includes the same time correlation function as the definition of R_0, describing the adiabatic effects of fluctuations parallel to $\vec{B}_0$. This is possible in *isotropic solutions*, where no orientation of the molecule is preferred. Then the distribution of the orientation of the molecules in the x or y direction should be the same as in the z direction and the same time correlation function can be used. Do not get confused! The molecules may be oriented isotropically even if their tumbling is anisotropic. The anisotropic tumbling (rotational diffusion) is a result of a non-spherical shape of the molecule, whereas anisotropic orientation is a result of an external force preferring certain orientation of the molecules. The magnetic field represents such a force, but this force is very small for diamagnetic molecules and can be often neglected when describing orientations of the molecules.[5]

- The definition of R_1, unlike that of R_0, includes also the value of the (average) precession frequency ω_0. This reflects the fact that the fluctuations perpendicular to $\vec{B}_0$ rotate the magnetic

---

[5]Note, however, that the magnetic field cannot be neglected when describing the return of the magnetization to the equilibrium, as discussed in Section 2.5.5.

moments about a horizontal axis only if their rate matches the precession frequency (resonance condition).

- The term in the integral defining R_0, lacking the cosine function of ω_0, can be also written as a value of the spectral function at the zero frequency (zero in the argument converts the cosine function to unity).

Similarly, R_2 is given by

$$R_2 = 2\left(\gamma B_0 \delta_{\mathrm{a}}\right)^2 J(0) + \frac{3}{2}\left(\gamma B_0 \delta_{\mathrm{a}}\right)^2 J(\omega_0). \tag{2.9}$$

Note that

- The first term is the adiabatic contribution destroying the coherence.

- The second term is the non-adiabatic contribution, equal to $\frac{1}{2}R_1$. The factor of $\frac{1}{2}$ reflects the fact that fluctuations in a certain direction influence only components of magnetic moment vectors perpendicular to that direction. E.g., fluctuations along the x axis influence only μ_y, but not μ_x. Therefore, a fluctuation in the x direction that causes some longitudinal relaxation (described by R_1) by altering μ_z, is only half as effective at causing transverse relaxation described by R_2 (only μ_y is altered, not μ_x).

The *longitudinal relaxation rate R_1*, describing the return of M_z to the equilibrium due to the chemical shift anisotropy in randomly reorienting molecules, and the *transverse relaxation rate R_2*, describing the decay of magnetization in the xy plane, are given by

$$R_1 = \frac{3}{4}b^2 J(\omega_0), \tag{2.10}$$

$$R_2 = \frac{1}{2}b^2 J(0) + \frac{3}{8}b^2 J(\omega_0), \tag{2.11}$$

where $b = -2\gamma B_0 \delta_{\mathrm{a}}$.

The relaxation rates R_1 and R_2 can be included in the equations describing evolution of the bulk magnetization, presented in Section 2.5.6.

2.4 Internal motions, structural changes

So far, we analyzed only the rigid body motions of molecules, assuming that the structures of molecules are rigid. What happens if the structure of the molecule changes? Let us first assume that the structural changes are random internal motions which change orientation of the chemical shift tensor relative to the orientation of the whole molecule, but do not affect the size or shape of the tensor. Then, R_0 can be derived in the same manner as in the absence of molecular motions (Eq. 2.32 can be still used) and R_0 is still given by Eq. 2.2, but the correlation function is *not* mono-exponential even if the rotational diffusion of the molecule is spherically symmetric. The internal motions contribute to the dynamics together with the rotational diffusion, and in a way that is very difficult to describe exactly. Yet, useful qualitative conclusions can be made.

- If the internal motions are *much faster* than rotational diffusion, correlation between $3\cos^2\vartheta(0)-1$ and $3\cos^2\vartheta(t)-1$ is lost much faster. The faster the correlation decays, the lower is the result of integration. The internal motions faster than rotational diffusion always *decrease* the value of R_0 (make relaxation slower). Amplitude and rate of the fast internal motions can be estimated using approximative approaches.

- If the internal motions are *much slower* than rotational diffusion, the rate of the decay of the correlation function is given by the faster contribution, i.e., by the rotational diffusion. The internal motions much slower than rotational diffusion *do not change* the value of R_0 significantly. Amplitude and rate of the fast internal motions cannot be measured if the motions do not change size or shape of the diffusion tensor.

If the structural changes alter size and/or shape of the chemical shift tensor,[6] parameters δ_i and δ_a vary and cannot be treated as constants. E.g., the parameter δ_i is not absorbed into the constant (average) precession frequency (removed by introducing the rotating coordinate frame in Section 2.5.1) and $\overline{\delta_i(0)\delta_i(t)}$ contributes to R_0 even if it decays much slower than $\overline{(3\cos^2\vartheta(0)-1)(3\cos^2\vartheta(t)-1)}$.

- Internal motions or chemical processes changing size and/or shape of the chemical shift tensor may have a dramatic effect on relaxation even if their frequency is much slower than the rotational diffusion of the molecule. If the molecule is present in two inter-converting states (e.g. in two conformations or in a protonated and deprotonated state), the strongest effect is observed if the differences between the chemical shift tensors of the states are large and if the frequency of switching between the states is similar to the difference in $\gamma B_0\delta_i$ of the states. Such processes are known as *chemical* or *conformational exchange* and increase the value of R_0 and consequently R_2.

HOMEWORK

Derive the rate constant R_0 (Section 2.5.1).

---

[6]Examples of such changes are internal motions changing torsion angles and therefore distribution of electrons, or chemical changes (e.g. dissociation of protons) with similar effects.

2.5 SUPPORTING INFORMATION

2.5.1 Loss of coherence

Motion of a magnetic moment in a magnetic filed is described classically as (cf. Eq. 1.118)

$$\frac{\mathrm{d}\vec{\mu}}{\mathrm{d}t} = \vec{\omega} \times \vec{\mu} = -\gamma \vec{B} \times \vec{\mu}, \tag{2.12}$$

or for individual components:

$$\frac{\mathrm{d}\mu_x}{\mathrm{d}t} = \omega_y \mu_z - \omega_z \mu_y, \tag{2.13}$$

$$\frac{\mathrm{d}\mu_y}{\mathrm{d}t} = \omega_z \mu_x - \omega_x \mu_z, \tag{2.14}$$

$$\frac{\mathrm{d}\mu_z}{\mathrm{d}t} = \omega_x \mu_y - \omega_y \mu_x. \tag{2.15}$$

Solving a set of three equations is not so easy. Therefore, we start with a simplified case. Remember what we learnt when we tried to rotate the magnetization away from the z direction by magnetic fields perpendicular to $\vec{B}_0$, i.e., by fields with B_x and B_y components. Only B_x and B_y fields rotating with the frequency equal to the precession frequency of individual magnetic moments (*Larmor frequency*) have the desired effect. Let us start our analysis by assuming that the molecular motions are much slower than the Larmor frequency. Under such circumstances, the effects of $B_{\mathrm{e},x}$ and $B_{\mathrm{e},y}$ can be neglected and the equations of motion simplify to

$$\frac{\mathrm{d}\mu_x}{\mathrm{d}t} = -\omega_z \mu_y = \gamma B_z \mu_y \tag{2.16}$$

$$\frac{\mathrm{d}\mu_y}{\mathrm{d}t} = \omega_z \mu_x = -\gamma B_z \mu_x \tag{2.17}$$

$$\frac{\mathrm{d}\mu_z}{\mathrm{d}t} = 0 \tag{2.18}$$

Eqs. 2.16–2.18 are very similar to Eqs. 1.119–1.121, so we try the same approach and calculate

$$\frac{\mathrm{d}\mu^+}{\mathrm{d}t} \equiv \frac{\mathrm{d}(\mu_x + \mathrm{i}\mu_y)}{\mathrm{d}t} = \mathrm{i}\omega_z(\mu_x + \mathrm{i}\mu_y) = -\mathrm{i}\gamma B_z(\mu_x + \mathrm{i}\mu_y) = -\mathrm{i}\gamma B_z \mu^+ \tag{2.19}$$

According to Eq. 1.108,

$$B_z = B_0 + B_{\mathrm{e},z} = B_0(1 + \delta_{\mathrm{i}} + \delta_{\mathrm{a}}(3\cos^2\vartheta - 1) + \delta_{\mathrm{r}}(2\cos^2\chi - 1)\sin^2\vartheta). \tag{2.20}$$

For the sake of simplicity, we assume that the chemical shift tensor is axially symmetric ($\delta_{\mathrm{r}} = 0$). Then, ω_z can be written as

$$\omega_z = -\gamma(B_0 + B_{\mathrm{e},z}) = -\gamma B_0(1 + \delta_{\mathrm{i}}) - \gamma B_0 \delta_{\mathrm{a}}(3\cos^2\vartheta - 1) = \omega_0 + b\Theta^{\|}, \tag{2.21}$$

where

$$\omega_0 = -\gamma B_0(1 + \delta_{\mathrm{i}}) \tag{2.22}$$

$$b = -2\gamma B_0 \delta_{\mathrm{a}} \tag{2.23}$$

$$\Theta^{\|} = \frac{3\cos^2\vartheta - 1}{2}. \tag{2.24}$$

This looks fine, but there is a catch here: Eq. 2.19 cannot be solved as easily as we solved 1.119–1.121 because ω_z is not constant but fluctuates in time. The value of ω_z is not only changing, it is changing differently for each molecule in the sample and it is changing in a random, unpredictable way! Can we solve the equation of motion at all? The answer is "yes and no". The equation of motion cannot be solved for an individual magnetic moment. However, we can take advantage of *statistics* and solve the equation of motion for the *total magnetization* M^+, given by the statistical ensemble of magnetic moments.

We start by assuming that for a very short time Δt, shorter than the time scale of molecular motions, the orientation of the molecule does not change and $\Theta^{\|}$ remains constant. We try to describe the evolution of μ^+ in such small time steps, assuming

$$\frac{\Delta\mu^+}{\Delta t} \approx \frac{\mathrm{d}\mu^+}{\mathrm{d}t} \approx \mathrm{i}(\omega_0 + b\Theta^{\|})\mu^+ \tag{2.25}$$

$$\mu_0^+ \xrightarrow[1]{\overset{\text{i}b\Theta_1^\parallel \Delta t}{}} \mu_1^+ \xrightarrow[1]{\overset{\text{i}b\Theta_2^\parallel \Delta t}{}} \mu_2^+ \xrightarrow[1]{\overset{\text{i}b\Theta_3^\parallel \Delta t}{}} \mu_3^+ \xrightarrow[1]{\overset{\text{i}b\Theta_4^\parallel \Delta t}{}} \mu_4^+ \cdots \xrightarrow[1]{\overset{\text{i}b\Theta_k^\parallel \Delta t}{}} \mu_k^+$$
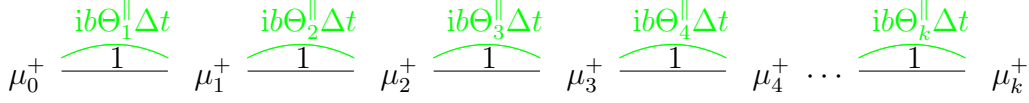
Figure 2.2: Evolution of magnetic moments due to longitudinal (parallel with $\vec{B}_0$) fluctuations of magnetic fields. The symbols μ_0^+ and μ_k^+ are connected by 2^k possible pathways composed of black and green segments. Each black segment represents multiplication by one, each green segment represents multiplication by $\text{i}b\Theta_j^\parallel \Delta t$, where j ranges from 1 to k. The product of binomials in Eq. 2.32 is a sum of 2^k terms. In order to obtain one term of the series, we walk along the corresponding pathway and multiply all black and green numbers written above the individual steps. The pathway composed of the black segments only gives the result of multiplication equal to one, the pathways containing just one green segment give results of multiplication proportional to Δt, the pathways containing two green segments give results of multiplication proportional to $(\Delta t)^2$, etc. In order to get the complete product in Eq. 2.32, we must walk through all possible pathways (all possible combinations of the segments) and sum all results of the multiplication.

If the initial value of μ^+ is μ_0^+ and if the values of $\omega_0, b, \Theta^\parallel$ during the first time step are $\omega_{0,1}, b_1, \Theta_1^\parallel$, respectively, the value of μ^+ after the first time step is

$$\mu_1^+ = \mu_0^+ + \Delta\mu_1^+ = \mu_0^+ + \text{i}(\omega_{0,1} + b_1\Theta_1^\parallel)\Delta t\mu_0^+ = [1 + \text{i}(\omega_{0,1} + b_1\Theta_1^\parallel)\Delta t]\mu_0^+. \tag{2.26}$$

After the second step,

$$\mu_2^+ = \mu_1^+ + \Delta\mu_2^+ = \mu_1^+ + \text{i}(\omega_{0,2} + b_2\Theta_2^\parallel)\Delta t\mu_1^+ = [1 + \text{i}(\omega_{0,2} + b_2\Theta_2^\parallel)\Delta t][1 + \text{i}(\omega_{0,1} + b_1\Theta_1^\parallel)\Delta t]\mu_0^+. \tag{2.27}$$

After k steps,

$$\mu_k^+ = [1 + \text{i}(\omega_{0,k} + b_k\Theta_k^\parallel)\Delta t][1 + \text{i}(\omega_{0,k-1} + b_{k-1}\Theta_{k-1}^\parallel)\Delta t]\cdots[1 + \text{i}(\omega_{0,2} + b_2\Theta_2^\parallel)\Delta t][1 + \text{i}(\omega_{0,1} + b_1\Theta_1^\parallel)\Delta t]\mu_0^+. \tag{2.28}$$

If the structure of the molecule does not change, the electron distribution is constant and the size and shape of the chemical shift tensor described by δ_i and δ_a does not change in time. Then, ω_0 and b are constant and the only time-dependent parameter is $\Theta^\parallel$, fluctuating as the orientation of the molecule (described by ϑ) changes. The parameter $\omega_0 = -\gamma B_0(1 + \delta_\text{i})$ represents a constant frequency of coherent rotation under such circumstances. The coherent rotation can be removed if we describe the evolution of μ^+ in a coordinate frame rotating with the frequency ω_0. The transformation of μ^+ to the rotating frame is given by

$$(\mu^+)_\text{rot} = \mu^+ e^{-\text{i}\omega_0 t}. \tag{2.29}$$

We also need to express the derivative of $(\mu^+)_\text{rot}$, which is done easily by applying the chain rule:

$$\frac{\text{d}(\mu^+)_\text{rot}}{\text{d}t} = \frac{\text{d}(\mu^+ e^{-\text{i}\omega_0 t})}{\text{d}t} = \frac{\text{d}\mu^+}{\text{d}t}e^{-\text{i}\omega_0 t} - \text{i}\omega_0\mu^+ e^{-\text{i}\omega_0 t}. \tag{2.30}$$

Substituting $\text{d}\mu^+/\text{d}t$ from Eq. 2.25 results in

$$\frac{\text{d}(\mu^+)_\text{rot}}{\text{d}t} = \text{i}(\omega_0 + b\Theta^\parallel)\mu^+ e^{-\text{i}\omega_0 t} - \text{i}\omega_0\mu^+ e^{-\text{i}\omega_0 t} = \text{i}b\Theta^\parallel\mu^+ e^{-\text{i}\omega_0 t} = \text{i}b\Theta^\parallel(\mu^+)_\text{rot}. \tag{2.31}$$

When compared with Eq. 2.25, we see that ω_0 disappeared, which simplifies Eq. 2.28 to

$$(\mu_k^+)_\text{rot} = [1 + \text{i}b\Theta_k^\parallel\Delta t][1 + \text{i}b\Theta_{k-1}^\parallel\Delta t]\cdots[1 + \text{i}b\Theta_2^\parallel\Delta t][1 + \text{i}b\Theta_1^\parallel\Delta t](\mu_0^+)_\text{rot}. \tag{2.32}$$

The process of calculating the product of brackets in Eq. 2.32 is shown schematically in Figure 2.2. The final product is

$$(\mu_k^+)_\text{rot} = [1 + \text{i}b\Delta t(\Theta_k^\parallel + \Theta_{k-1}^\parallel + \cdots + \Theta_1^\parallel) - b^2\Delta t^2(\Theta_k^\parallel(\Theta_{k-1}^\parallel + \cdots + \Theta_2^\parallel + \Theta_1^\parallel) + \Theta_{k-1}^\parallel(\Theta_{k-2}^\parallel + \cdots + \Theta_2^\parallel + \Theta_1^\parallel) + \cdots + \Theta_2^\parallel\Theta_1^\parallel)$$
$$- \text{i}b^3\Delta t^3(\dots) + \cdots](\mu_0^+)_\text{rot}. \tag{2.33}$$

We can now return to the question how random fluctuations change μ^+.
We first write the $(\mu^+)_\text{rot}$ value at the $k - 1$ steps

$$(\mu_{k-1}^+)_\text{rot} = [1 + \text{i}b\Delta t(\Theta_{k-1}^\parallel + \cdots + \Theta_1^\parallel) - b^2\Delta t^2(\Theta_{k-1}^\parallel(\Theta_{k-2}^\parallel + \cdots + \Theta_2^\parallel + \Theta_1^\parallel) + \cdots + \Theta_2^\parallel\Theta_1^\parallel) - \text{i}b^3\Delta t^3(\dots) + \cdots](\mu_0^+)_\text{rot}. \tag{2.34}$$

and express the difference between μ^+ after k and $k - 1$ steps:

$$\Delta(\mu_k^+)_\text{rot} = (\mu_k^+)_\text{rot} - (\mu_{k-1}^+)_\text{rot} = [\text{i}b\Delta t\Theta_k^\parallel - b^2\Delta t^2\Theta_k^\parallel(\Theta_{k-1}^\parallel + \cdots + \Theta_1^\parallel) - \text{i}b^3\Delta t^3(\dots) + \cdots](\mu_0^+)_\text{rot}. \tag{2.35}$$

We divide both sides by Δt

$$\frac{\Delta(\mu_k^+)_{\text{rot}}}{\Delta t} = \left[ib\Theta_k^\| - b^2 \Delta t \Theta_k^\|(\Theta_{k-1}^\| + \cdots + \Theta_1^\|) - ib^3 \Delta t^2(\dots) + \cdots \right](\mu_0^+)_{\text{rot}} = \left[ib\Theta_k^\| - b^2 \Theta_k^\| \sum_{j=1}^{k-1} \Theta_{k-j}^\| \Delta t - ib^3 \Delta t^2(\dots) + \cdots \right](\mu_0^+)_{\text{rot}}$$

$$(2.36)$$

and return from Δt to dt (neglecting terms with $dt^2, dt^3, \dots$, much smaller than dt). Instead of evaluating $(\mu^+)_{\text{rot}}$ after k time steps, we evaluate it at time t_k and instead of summing $\Theta^\|$ after $k - j$ time steps, we integrate $\Theta^\|$ for $t_k - t_j$ ranging from t_k to zero, where t_k is constant and t_j is variable. Therefore, the superscripts k and j no longer represent the actual values of the integer counters k and j, but they are merely distinguishing two measurements of time (from zero to t_k and from zero to t_j).

$$\frac{d(\mu^+(t_k))_{\text{rot}}}{dt} = \left[ib\Theta^\|(t_k) - b^2 \int_0^{t_k} \Theta^\|(t_k)\Theta^\|(t_k - t_j) dt_j \right](\mu_0^+)_{\text{rot}}.$$

$$(2.37)$$

We see that calculating how fluctuations of B_z affect an individual magnetic moment in time t_k requires knowledge of the orientations of the molecule during the whole evolution ($\Theta^\|(t_k - t_j)$). However, we are not interested in the evolution of a single magnetic moment, but in the evolution of the total magnetization M^+. The total magnetization is given by the sum of all magnetic moments (magnetic moments in all molecules). Therefore, we must average orientations of all molecules in the sample. In other words, we should describe $\Theta^\|$ in Eq. 2.36 using *two* indices, k and m, where k describes the time step and m the orientation of the given molecule. Calculation of the evolution of M^+ then should include summation of $\Theta_{k,m}^\|$ for all k and m in Eq. 2.36, or integration over the angles describing orientations of the molecule in addition to the time integration in Eq. 2.37. As the magnetic moments move almost independently of the molecular motions, we can average $\Theta^\|$ and μ^+ separately. In the case of the axially symmetric chemical shift tensor, the orientations of molecules are given by orientations of the symmetry axes $\vec{Z}$ of the chemical shift tensors of the observed nuclei in the molecules, described by the angles φ and ϑ. In order to simplify averaging the orientations, we assume that all orientations are equally probable. This is a very dangerous assumption. It does not introduce any error in this section, but leads to wrong results when we analyze the effects of fluctuations of magnetic fields perpendicular to $\vec{B}_0$!

As the angle $\vartheta(t)$ is hidden in the function $\Theta^\|(t) = (3\cos\vartheta^2 - 1)/2$ in our equation, the ensemble averaging can be written as[7]

$$\frac{d(M^+(t_k))_{\text{rot}}}{dt} = \left[ib\frac{1}{4\pi}\int_0^{2\pi} d\varphi \int_0^\pi \Theta^\|(t_k)\sin\vartheta d\vartheta - b^2 \int_0^{t_k} dt_j \frac{1}{4\pi}\int_0^{2\pi} d\varphi \int_0^\pi \Theta^\|(t_k)\Theta^\|(t_k - t_j)\sin\vartheta d\vartheta \right](M_0^+)_{\text{rot}},$$

$$(2.38)$$

where $\varphi \equiv \varphi(t_k)$ and $\vartheta \equiv \vartheta(t_k)$.

In order to avoid writing too many integration signs, we mark the averaging simply by a horizontal bar above the averaged function:

$$\frac{d(M^+(t_k))_{\text{rot}}}{dt} = \left[ib\overline{\Theta^\|(t_k)} - b^2 \int_0^{t_k} \overline{\Theta^\|(t_k)\Theta^\|(t_k - t_j)} dt_j \right](M_0^+)_{\text{rot}}.$$

$$(2.39)$$

The average values of $Z_z^2 = \cos^2\vartheta$, of $Z_x^2 = \cos^2\varphi\sin^2\vartheta$, and of $Z_y^2 = \sin^2\varphi\sin^2\vartheta$ must be the same because none of the directions x, y, z is preferred:

$$\overline{Z_x^2} = \overline{Z_y^2} = \overline{Z_z^2}.$$

$$(2.40)$$

Therefore,

$$\overline{Z_x^2 + Z_y^2 + Z_z^2} = \overline{3Z_z^2}$$

$$(2.41)$$

and

$$Z_x^2 + Z_y^2 + Z_z^2 = 1 \Rightarrow \overline{Z_x^2 + Z_y^2 + Z_z^2} = 1 \Rightarrow \overline{3Z_z^2 - 1} = \overline{(3\cos^2\vartheta - 1)} = 2\overline{\Theta^\|} = 0 \Rightarrow \overline{\Theta^\|} = 0.$$

$$(2.42)$$

It explains why we did not neglect already the $b^2 dt$ term – we would obtain zero on the right-hand side in the rotating coordinate frame (this level of simplification would neglect the effects of fluctuations and describe just the coherent motions).

We have derived that the equation describing the loss of coherence (resulting in a loss of transverse magnetization) is

$$\frac{d(M^+(t_k))_{\text{rot}}}{dt} = -\left[b^2 \int_0^{t_k} \overline{\Theta^\|(t_k)\Theta^\|(t_k - t_j)} dt_j \right](M_0^+)_{\text{rot}},$$

$$(2.43)$$

---

[7]Two integrals in the following equation represent calculation of an average of a function depending on the orientation. Geometrically, it is summation of the values of the function for individual surface elements (defined by inclination ϑ and azimuth φ) of a sphere with the radius $r = 1$, divided by the complete surface of the sphere 4π (see Section 1.5.1). Note that the *current* orientation of each molecule at t_k is described by $\vartheta(t_k)$ and $\varphi(t_k)$, the values $\vartheta(t_j)$ hidden in the function $\Theta^\|(t_j)$ describe only *history* of each molecule. They are *somehow* related to $\vartheta(t_k)$ and $\varphi(t_k)$ and therefore treated as an unknown function of $\vartheta(t_k)$ and $\varphi(t_k)$ during the integration.

where the value of $\overline{\Theta^{\parallel}(t_{\mathrm{k}})\Theta^{\parallel}(t_{\mathrm{k}} - t_{\mathrm{j}})}$ is clearly defined statistically (by the averaging described above). Values of $\overline{\Theta^{\parallel}(t_{\mathrm{k}})\Theta^{\parallel}(t_{\mathrm{k}} - t_{\mathrm{j}})}$ can be determined easily for two limit cases:

- $t_{\mathrm{j}} = 0$: If $t_{\mathrm{j}} = 0$, $\overline{\Theta^{\parallel}(t_{\mathrm{k}})\Theta^{\parallel}(t_{\mathrm{k}} - t_{\mathrm{j}})} = \overline{(\Theta^{\parallel}(t_{\mathrm{k}}))^2}$, i.e., $\Theta^{\parallel}(t_{\mathrm{k}})$ and $\Theta^{\parallel}(t_{\mathrm{k}} - t_{\mathrm{j}})$ are *completely correlated*.

  The average value of $\overline{\Theta^{\parallel}(t_{\mathrm{k}})^2}$ is

$$\overline{\Theta^{\parallel}(t_{\mathrm{k}})^2} = \frac{1}{4}\overline{(3\cos^2\vartheta - 1)^2} = \frac{1}{16\pi}\int_0^{2\pi}\mathrm{d}\varphi\int_0^{\pi}\mathrm{d}\vartheta(\sin\vartheta)(3\cos^2\vartheta - 1)^2 = \frac{1}{8}\int_{-1}^{1}(3u^2 - 1)^2\mathrm{d}u$$

$$= \int_{-1}^{1}\frac{9u^4 - 6u^2 + 1}{8}\mathrm{d}u = \left[\frac{9u^5 - 10u^3 + 5u}{40}\right]_{-1}^{1} = \frac{1}{5}. \tag{2.44}$$

- $t_{\mathrm{j}} \to \infty$: If the changes of orientation (molecular motions) are random, the correlation between $\Theta^{\parallel}(t_{\mathrm{k}})$ and $\Theta^{\parallel}(t_{\mathrm{k}} - t_{\mathrm{j}})$ is lost for very long t_{j} and they can be averaged separately: $\overline{\Theta^{\parallel}(t_{\mathrm{k}})\Theta^{\parallel}(t_{\mathrm{k}} - t_{\mathrm{j}})} = \overline{\Theta^{\parallel}(t_{\mathrm{k}})} \cdot \overline{\Theta^{\parallel}(t_{\mathrm{k}} - t_{\mathrm{j}})}$. But we know that average $\overline{\Theta^{\parallel}(t)} = \overline{3\cos^2\vartheta - 1} = 0$. Therefore, $\overline{\Theta^{\parallel}(t_{\mathrm{k}})\Theta^{\parallel}(t_{\mathrm{k}} - t_{\mathrm{j}})} = 0$ for $t_{\mathrm{j}} \to \infty$.

If the motions are really stochastic, it does not matter when we start to measure time. Therefore, we can start counting time from t_{k}, i.e., set $t_{\mathrm{k}} = 0$, and integrate from $-t_{\mathrm{k}}$ to zero:

$$\int_0^{t_{\mathrm{k}}}\overline{\Theta^{\parallel}(t_{\mathrm{k}})\Theta^{\parallel}(t_{\mathrm{k}} - t_{\mathrm{j}})}\mathrm{d}t_{\mathrm{j}} = \int_{-t_{\mathrm{k}}}^{0}\overline{\Theta^{\parallel}(0)\Theta^{\parallel}(-t_{\mathrm{j}})}\mathrm{d}t_{\mathrm{j}}. \tag{2.45}$$

Furthemore, orientations at $t = t_{\mathrm{k}}$ are correlated with those at $t = 0$ exactly like orientations at $t = -t_{\mathrm{k}}$ if the molecule moves really randomly (the fluctations are *stationary*). As a consequence, the integration from $-t_{\mathrm{k}}$ to zero can be replaced by integrating from zero to $+t_{\mathrm{k}}$:

$$\int_{-t_{\mathrm{k}}}^{0}\overline{\Theta^{\parallel}(0)\Theta^{\parallel}(-t_{\mathrm{j}})}\mathrm{d}t_{\mathrm{j}} = \int_0^{t_{\mathrm{k}}}\overline{\Theta^{\parallel}(0)\Theta^{\parallel}(t_{\mathrm{j}})}\mathrm{d}t_{\mathrm{j}}. \tag{2.46}$$

Finally, extending the upper integration limit from t_{k} to infinity does not change the integral significantly if t_{k} was already long enough to reduce $\overline{\Theta^{\parallel}(t_{\mathrm{k}})\Theta^{\parallel}(t_{\mathrm{k}} - t_{\mathrm{j}})}$ almost to zero. Therefore, we can describe the loss of coherence for any sufficiently long t_{k} as

$$\frac{\mathrm{d}(M^+)_{\mathrm{rot}}}{\mathrm{d}t} = -\left[b^2\int_0^{\infty}\overline{\Theta^{\parallel}(0)\Theta^{\parallel}(t)}\mathrm{d}t\right](M^+)_{\mathrm{rot}}, \tag{2.47}$$

which resembles a first-order chemical kinetics with the rate constant

$$R_0 = b^2\int_0^{\infty}\overline{\Theta^{\parallel}(0)\Theta^{\parallel}(t)}\mathrm{d}t. \tag{2.48}$$

In order to calculate the value of the rate constant R_0, we must be able to evaluate the averaged term $\overline{\Theta^{\parallel}(0)\Theta^{\parallel}(t)}$, known as the *time correlation function*. As mentioned above, statistics play the key role here. Although the product $\Theta^{\parallel}(0)\Theta^{\parallel}(t)$ changes randomly and individually, the value of the time correlation function is defined statistically.

2.5.2   Stochastic molecular motions: diffusion

Diffusion can be viewed as a result of collisions of the observed molecule with other molecules. Collisions change position of the molecule is space (cause *translation*) and orientation of the molecule (cause *rotation*). *Rotational diffusion* is important for NMR relaxation. *Translational diffusion* influences NMR experiments only if the magnetic filed is inhomogeneous. Translational diffusion can be described as a random walk in a three-dimensional space, rotational diffusion can be described as a random walk on a surface of a sphere. Although we are primarily interested in relaxation and we do not discuss magnetic field inhomogeneity at this moment, we start our discussion with the random walk in a three-dimensional space because the random walk on a surface of a sphere is just a special case of the general walk in three directions. In the following section (Section 2.5.3), we continue with the analysis of the simplest example of the random walk on a spherical surface, i.e., of the *isotropic rotational diffusion*. The analysis shows that the isotropic rotational diffusion is described by

a simple exponential time dependence (Eq. 2.56). This relation will serve as a starting point for derivation of the key component of the theory of NMR relaxation, of the *time correlation function*, described in Section 2.5.4.

We start with several definitions. Let us assume that the position of our molecule is described by coordinates x, y, z and its orientation is described by angles φ, ϑ, χ.

- Probability that the molecule is inside a cubic box of a volume $\Delta V = \Delta x \Delta y \Delta z$ centered around x, y, z is

$$P(x, y, z, t, \Delta x, \Delta y, \Delta z) = \int\limits_{x-\frac{\Delta x}{2}}^{x+\frac{\Delta x}{2}} \int\limits_{y-\frac{\Delta y}{2}}^{y+\frac{\Delta y}{2}} \int\limits_{z-\frac{\Delta z}{2}}^{z+\frac{\Delta z}{2}} \rho(x, y, z, t) \mathrm{d}x\mathrm{d}y\mathrm{d}z,$$

where $\rho(x, y, z, t)$ is *probability density* at x, y, z, corresponding to local concentration in a macroscopic picture. If the box is small enough so that $\rho(x, y, z, t)$ does not change significantly inside the box, the equation with the triple integral can be simplified to

$$P(x, y, z, t, \Delta x, \Delta y, \Delta z) = \rho(x, y, z, t)\Delta V.$$

- Probability that the molecule crosses one wall of the box centered around x, y, z and jumps into the box centered around $x + \Delta x, y, z$ during a time interval δt is proportional to the area of the wall between boxes centered around x, y, z and around $x + \Delta x, y, z$. This area is equal to $\Delta y \Delta z = \Delta V/\Delta x$ and the probability of jumping from the box centered around x, y, z to the box centered around $x + \Delta x, y, z$ can be written as

$$P(x \to x + \Delta x; x, y, z, t, \Delta x, \Delta y, \Delta z, \Delta t) = \Phi_{x \to x+\Delta x}\Delta y \Delta z = \Phi_{x \to x+\Delta x}\Delta V/\Delta x,$$

where $\Phi_{x \to x+\Delta x}$ is the *flux* from the box centered around x, y, z to the box centered around $x + \Delta x, y, z$ (per unit area). The corresponding *probability density* is

$$\rho(x \to x + \Delta x; x, y, z, t, \Delta t) = P(x \to x + \Delta x; x, y, z, t, \Delta x, \Delta y, \Delta z, \Delta t)/\Delta V = \Phi_{x \to x+\Delta x}/\Delta x.$$

The probability of jumping to the box centered around $x + \Delta x, y, z$ is also proportional to the probability that the molecule is inside the box centered around x, y, z (equal to $\rho(x, y, z, t)\Delta V$ if the box is small enough). If the probability of escaping the box is the same in all directions,

$$\rho(x \to x + \Delta x; x, y, z, t, \Delta t) = \xi\rho(x, y, z, t),$$
$$\rho(y \to y + \Delta y; x, y, z, t, \Delta t) = \xi\rho(x, y, z, t),$$
$$\rho(z \to z + \Delta z; x, y, z, t, \Delta t) = \xi\rho(x, y, z, t),$$

where ξ is a proportionality constant describing frequency of crossing a wall of a box (per unit volume and including the physical description of the collisions).

- The *net flux* in the x direction is given by

$$\Phi_x = \Phi_{x \to x+\Delta x} - \Phi_{x+\Delta x \to x} = \xi\Delta x(\rho(x, y, z, t) - \rho(x + \Delta x, y, z, t)) = -\xi\Delta x\Delta\rho = -\xi(\Delta x)^2\frac{\partial\rho}{\partial x} = -D^{\mathrm{tr}}\frac{\partial\rho}{\partial x},$$

where $D^{\mathrm{tr}} = \xi(\Delta x)^2$ is the *translational diffusion coefficient*.

- The net flux in all directions is

$$\vec{\Phi} = -D^{\mathrm{tr}}\vec{\nabla}\rho,$$

which is *the first Fick's law*.

- The *continuity equation*

$$\int\limits_V \frac{\partial\rho}{\partial t}\mathrm{d}V + \oiint\limits_S \vec{\Phi}\mathrm{d}S = 0$$

states that any time change of probability that the molecule is in a volume V is due to the total flux through a surface S enclosing the volume V (molecules are not created or annihilated). Using the divergence theorem,

$$0 = \frac{\partial\rho}{\partial t} + \vec{\nabla}\cdot\vec{\Phi} = \frac{\partial\rho}{\partial t} + \vec{\nabla}\cdot\left(-D^{\mathrm{tr}}\vec{\nabla}\rho\right) \quad \Rightarrow \quad \frac{\partial\rho}{\partial t} = D^{\mathrm{tr}}\nabla^2\rho,$$

which is *the second Fick's law*.

- If the diffusion is not isotropic, the diffusion coefficient is replaced by a diffusion tensor. If we define a coordinate frame so that the diffusion tensor is represented by a diagonal matrix with elements $D_{xx}^{\mathrm{tr}}, D_{yy}^{\mathrm{tr}}, D_{zz}^{\mathrm{tr}}$, the second Fick's law has the following form:

$$\frac{\partial\rho}{\partial t} = D_{xx}^{\mathrm{tr}}\frac{\partial}{\partial x}\frac{\partial\rho}{\partial x} + D_{yy}^{\mathrm{tr}}\frac{\partial}{\partial y}\frac{\partial\rho}{\partial y} + D_{zz}^{\mathrm{tr}}\frac{\partial}{\partial z}\frac{\partial\rho}{\partial z} = \left(D_{xx}^{\mathrm{tr}}\frac{\partial^2}{\partial x^2} + D_{yy}^{\mathrm{tr}}\frac{\partial^2}{\partial y^2} + D_{zz}^{\mathrm{tr}}\frac{\partial^2}{\partial z^2}\right)\rho.$$

2.5.3 Isotropic rotational diffusion

Isotropic rotational diffusion can be viewed as random motions of a vector describing orientation of the molecule. Such motions are equivalent to a random wandering of a point particle on a surface of a sphere with a unit diameter. In order to describe such a random walk on a spherical surface, it is convenient to express the second Fick's law in spherical coordinates

$$\frac{\partial \rho}{\partial t} = \frac{D^{\text{rot}}}{r^2 \sin \vartheta} \left(\frac{\partial}{\partial r} \left(r^2 \sin \vartheta \frac{\partial}{\partial r} \right) + \frac{\partial}{\partial \vartheta} \left(\sin \vartheta \frac{\partial}{\partial \vartheta} \right) + \frac{\partial}{\partial \varphi} \left(\frac{1}{\sin \vartheta} \frac{\partial}{\partial \varphi} \right) \right) \rho. \tag{2.49}$$

Since r is constant and equal to unity,

$$\frac{\partial \rho}{\partial t} = \frac{D^{\text{rot}}}{\sin \vartheta} \left(\frac{\partial}{\partial \vartheta} \left(\sin \vartheta \frac{\partial}{\partial \vartheta} \right) + \frac{\partial}{\partial \varphi} \left(\frac{1}{\sin \vartheta} \frac{\partial}{\partial \varphi} \right) \right) \rho. \tag{2.50}$$

Using the substitution $u = \cos \vartheta$ (and $\partial u = -\sin \vartheta \partial \vartheta$),

$$\frac{\partial \rho}{\partial t} = D^{\text{rot}} \left((1 - u^2) \frac{\partial^2}{\partial u^2} - 2u \frac{\partial}{\partial u} + \frac{1}{1 - u^2} \frac{\partial^2}{\partial \varphi^2} \right) \rho. \tag{2.51}$$

Let us now try if time and space coordinates can be separated, i.e. if ρ can be expressed as a product $\rho(\vartheta, \varphi, t) = f(\vartheta, \varphi)g(t)$.

$$f \frac{\partial g}{\partial t} = g D^{\text{rot}} \left((1 - u^2) \frac{\partial^2}{\partial u^2} - 2u \frac{\partial}{\partial u} + \frac{1}{1 - u^2} \frac{\partial^2}{\partial \varphi^2} \right) f. \tag{2.52}$$

Dividing both sides of the equation by $D^{\text{rot}} \rho = D^{\text{rot}} fg$,

$$\frac{1}{D^{\text{rot}}} \frac{1}{g} \frac{\partial g}{\partial t} = \frac{1}{f} \left((1 - u^2) \frac{\partial^2}{\partial u^2} - 2u \frac{\partial}{\partial u} + \frac{1}{1 - u^2} \frac{\partial^2}{\partial \varphi^2} \right) f. \tag{2.53}$$

If the separation of time and space coordinates is possible, i.e., if Eq. 2.53 is true for any t and any ϑ, φ independently, both sides of the equation must be equal to the same constant (called λ bellow).

$$\frac{1}{D^{\text{rot}}} \frac{1}{g} \frac{\partial g}{\partial t} = \lambda \tag{2.54}$$

$$\frac{1}{f} \left((1 - u^2) \frac{\partial^2}{\partial u^2} - 2u \frac{\partial}{\partial u} + \frac{1}{1 - u^2} \frac{\partial^2}{\partial \varphi^2} \right) f = \lambda. \tag{2.55}$$

Solution of the first equation is obviously

$$g(t) = g(0) e^{\lambda D^{\text{rot}} t}, \tag{2.56}$$

where λ is obtained by solving the second equation. We solve a simplified version of the second equation in Section 2.5.4.

2.5.4 Time correlation function

Analysis of the isotropic rotational diffusion in Section 2.5.3 allows us to calculate the time correlation function $\overline{\Theta^{\parallel}(0)\Theta^{\parallel}(t)}$ for this type of diffusion (with a spherical symmetry). The ensemble-averaged product of randomly changing $(3\cos^2 \vartheta(t) - 1)/2$, evaluated for a time difference t, can be expressed as

$$\overline{\left(\frac{3}{2} \cos^2 \vartheta(0) - \frac{1}{2} \right) \left(\frac{3}{2} \cos^2 \vartheta(t) - \frac{1}{2} \right)} \tag{2.57}$$

$$= \int\limits_{0}^{2\pi} \mathrm{d}\varphi(0) \int\limits_{0}^{\pi} \sin \vartheta(0) \mathrm{d}\vartheta(0) \rho_0 \int\limits_{0}^{2\pi} \mathrm{d}\varphi(t) \int\limits_{0}^{\pi} \sin \vartheta(t) \mathrm{d}\vartheta(t) \left(\frac{3}{2} \cos^2 \vartheta(0) - \frac{1}{2} \right) \left(\frac{3}{2} \cos^2 \vartheta(t) - \frac{1}{2} \right) G(\vartheta(0), \varphi(0) | \vartheta(t), \varphi(t)), \tag{2.58}$$

where ρ_0 is the *probability density* of the original orientation described by $\vartheta(0)$ and $\varphi(0)$, and $G(\vartheta(0), \varphi(0) | \vartheta(t), \varphi(t))$ is the *conditional probability density* or *propagator* (also known as the *Green's function*) describing what is the chance to find an orientation given by $\vartheta(t), \varphi(t)$ at time t, if the orientation at $t = 0$ was given by $\vartheta(0), \varphi(0)$.

If the molecule is present in an isotropic environment,[8] ρ_0 plays a role of a normalization constant and can be calculated easily from the condition that the overall probability of finding the molecule in *any* orientation is equal to one:

---

[8]Note that in the isotropic environment, where all orientations of the molecule are equally probable, the diffusion can be very anisotropic if the shape of the molecule greatly differs from a sphere.

$$\int\limits_0^{2\pi} \mathrm{d}\varphi(0) \int\limits_0^{\pi} \sin\vartheta(0)\mathrm{d}\vartheta(0)\rho_0 = 4\pi\rho_0 = 1 \quad \Rightarrow \quad \rho_0 = \frac{1}{4\pi}. \tag{2.59}$$

Evaluation of $G(\vartheta(0), \varphi(0)|\vartheta(t), \varphi(t))$ requires to solve the diffusion equation (Eq. 2.55). We again express G as a product of time-dependent and time-independent functions $g(t)P(\vartheta)$. The function $g(t)$ is defined by Eq. 2.54, the function $P(\vartheta)$ is a simplified version of function $f(\vartheta, \varphi)$ from Eq. 2.55. Since our correlation correlation function does not depend on φ, $\partial P/\partial\varphi = 0$, and we can further simplify Eq. 2.55 to

$$\left((1 - u^2)\frac{\mathrm{d}^2}{\mathrm{d}u^2} - 2u\frac{\mathrm{d}}{\mathrm{d}u}\right)P = \lambda P, \tag{2.60}$$

$$(1 - u^2)\frac{\mathrm{d}^2P}{\mathrm{d}u^2} - 2u\frac{\mathrm{d}P}{\mathrm{d}u} - \lambda P = 0. \tag{2.61}$$

We expand P in a Taylor series

$$P = \sum_{k=0}^{\infty} a_k u^k, \quad a_k = \frac{1}{k!}\frac{\mathrm{d}^k P(0)}{\mathrm{d}u^k}, \tag{2.62}$$

calculate its first and second derivatives

$$\frac{\mathrm{d}P}{\mathrm{d}u} = \sum_{k=0}^{\infty} k a_k u^{k-1}, \tag{2.63}$$

$$\frac{\mathrm{d}^2P}{\mathrm{d}u^2} = \sum_{k=0}^{\infty} k(k-1) a_k u^{k-2}, \tag{2.64}$$

and substitute them into Eq. 2.61

$$(1 - u^2)\sum_{k=0}^{\infty} k(k-1)a_k u^{k-2} - 2\sum_{k=0}^{\infty} k a_k u^k - \lambda\sum_{k=0}^{\infty} a_k u^k = 0 \tag{2.65}$$

$$\sum_{k=0}^{\infty} k(k-1)a_k u^{k-2} - \sum_{k=0}^{\infty} k(k-1)a_k u^k - 2\sum_{k=0}^{\infty} k a_k u^k - \lambda\sum_{k=0}^{\infty} a_k u^k = 0. \tag{2.66}$$

Note that the first two terms of the first sum are equal to zero (the first term includes multiplication by $k = 0$ and the second term includes multiplication by $k - 1 = 0$ for $k = 1$). Therefore, we can start summation from $k = 2$ in the first term

$$\sum_{k=2}^{\infty} k(k-1)a_k u^{k-2} - \sum_{k=0}^{\infty} k(k-1)a_k u^k - 2\sum_{k=0}^{\infty} k a_k u^k - \lambda\sum_{k=0}^{\infty} a_k u^k = 0. \tag{2.67}$$

We shift the index in the first sum by two to get the first sum expressed in the same power of u as the other sums

$$\sum_{k=0}^{\infty} (k+2)(k+1)a_{k+2} u^k - \sum_{k=0}^{\infty} k(k-1)a_k u^k - 2\sum_{k=0}^{\infty} k a_k u^k - \lambda\sum_{k=0}^{\infty} a_k u^k = 0 \tag{2.68}$$

$$\sum_{k=0}^{\infty} \left((k+2)(k+1)a_{k+2} - (k(k-1)+2k+\lambda)a_k\right) u^k = \sum_{k=0}^{\infty} \underbrace{\left((k+2)(k+1)a_{k+2} - (k(k+1)+\lambda)a_k\right)}_{\text{must be zero}} u^k = 0. \tag{2.69}$$

This equation is true for $u \neq 0$ only if the underbraced expression is equal to zero

$$(k+2)(k+1)a_{k+2} - (k(k+1)+\lambda)a_k = 0, \tag{2.70}$$

which gives us a recurrence formula relating a_{k+2} and a_k:

$$a_{k+2} = \frac{k(k+1)+\lambda}{(k+2)(k+1)}a_k. \tag{2.71}$$

We can use the recurrence formula to express the Taylor series in terms of a_0 and a_1:

$$P = a_0\left(1 + \frac{0\cdot 1 + \lambda}{1\cdot 2}u^2 + \frac{0\cdot 1 + \lambda}{1\cdot 2}\cdot\frac{2\cdot 3 + \lambda}{3\cdot 4}u^4 + \dots\right) + a_1\left(u + \frac{1\cdot 2 + \lambda}{2\cdot 3}u^3 + \frac{1\cdot 2 + \lambda}{2\cdot 3}\cdot\frac{3\cdot 4 + \lambda}{4\cdot 5}u^5 + \dots\right) = 0. \tag{2.72}$$

What is the value of λ? Note that $a_{k+2} = 0$ for each $\lambda = -k(k+1)$, which terminates one of the series in large parentheses, while the other series grows to infinity (for $u \neq 0$). To keep P finite, the coefficient before the large parentheses in the unterminated series must be set to zero. It tells us that we can find a possible solution for each even or odd k if $a_1 = 0$ or $a_0 = 0$, respectively.

$$k = 0 \quad a_1 = 0 \quad G = P_0 = 1 \qquad \lambda = -k(k+1) = 0 \tag{2.73}$$

$$k = 1 \quad a_0 = 0 \quad G = P_1 = u = \cos\vartheta \qquad \lambda = -k(k+1) = -2 \tag{2.74}$$

$$k = 2 \quad a_1 = 0 \quad G = P_2 = \frac{3u^2 - 1}{2} = \frac{3\cos^2\vartheta - 1}{2} \qquad \lambda = -k(k+1) = -6 \tag{2.75}$$

$$k = 3 \quad a_0 = 0 \quad G = P_3 = \frac{5u^3 - 3u}{2} = \frac{5\cos^3\vartheta - 3\cos\vartheta}{2} \qquad \lambda = -k(k+1) = -12 \tag{2.76}$$

$$\vdots \tag{2.77}$$

The value of a_0 or a_1 preceding the terminated series was chosen so that $P_k(u = 1) = P_k(\vartheta = 0) = 1$.
Which of the possible solutions is the correct one? It can be shown easily that

$$\int\limits_{-1}^{1} P_k(u) P_{k'}(u) \mathrm{d}u = \int\limits_{0}^{\pi} P_k(\vartheta) P_{k'}(\vartheta) \mathrm{d}\vartheta = \frac{2}{2k+1} \delta_{kk'}, \tag{2.78}$$

where $\delta_{kk'} = 1$ if $k = k'$ and $\delta_{kk'} = 0$ if $k \neq k'$, i.e., the integral is equal to zero for each $k \neq k'$ (P_k are orthogonal). As we are going to use $G = g(t)P(\vartheta)$ to calculate a correlation function for functions having the same form as the solutions for $k = 2$ and as the calculation of the correlation function includes the same integration as in Eq. 2.78, it is clear that the only solution which gives us a non-zero correlation function is that for $k = 2$, i.e. P_2. Our function G is therefore given by

$$G = g_0 \frac{3\cos^2\vartheta - 1}{2} \mathrm{e}^{-6D^{\mathrm{rot}}t}. \tag{2.79}$$

Still, we need to evaluate the factor g_0. This value must be chosen so that we fulfill the following conditions:

$$\int\limits_{0}^{2\pi} \mathrm{d}\varphi \int\limits_{0}^{\pi} \sin\vartheta \mathrm{d}\vartheta G = 1 \tag{2.80}$$

and

$$G(t = 0) = \delta(\vartheta - \vartheta(0)), \tag{2.81}$$

where $\delta(\vartheta - \vartheta(0))$ is a so-called Dirac delta function, defined as

$$\int\limits_{-\infty}^{\infty} f(x)\delta(x - x_0) = f(x_0). \tag{2.82}$$

The second condition says that ϑ must have its original value for $t = 0$. This is fulfilled for g_0 proportional to $(3\cos^2\vartheta(0) - 1)/2$:

$$g_0 = c_0 \frac{3\cos^2\vartheta(0) - 1}{2}. \tag{2.83}$$

We can re-write our original definition of the correlation function with the evaluated G function and in a somewhat simplified form (omitting integration over φ and $\varphi(0)$):

$$\overline{\left(\frac{3}{2}\cos^2\vartheta(0) - \frac{1}{2}\right)\left(\frac{3}{2}\cos^2\vartheta(t) - \frac{1}{2}\right)} = \int\limits_{-1}^{1} \mathrm{d}u_0 \rho_0 c_0 \int\limits_{-1}^{1} \mathrm{d}u \frac{(3u_0^2 - 1)^2}{4} \frac{(3u^2 - 1)^2}{4} \mathrm{e}^{-6D^{\mathrm{rot}}t}, \tag{2.84}$$

where ρ_0 can be evaluated from the normalization condition

$$1 = \int\limits_{-1}^{1} \mathrm{d}u_0 \rho_0 = 2\rho_0 \Rightarrow \rho_0 = \frac{1}{2} \tag{2.85}$$

and
c_0 from

$$1 = \int\limits_{-1}^{1} \mathrm{d}u_0 \int\limits_{-1}^{1} c_0 \frac{3u_0^2 - 1}{2} \frac{3u^2 - 1}{2} \delta(u - u_0) \mathrm{d}u = \int\limits_{-1}^{1} \mathrm{d}u_0 c_0 \frac{(3u_0^2 - 1)^2}{4} = \int\limits_{-1}^{1} \mathrm{d}u_0 c_0 \frac{9u_0^4 - 6u_0^2 + 1}{4} = c_0 \left[\frac{9u_0^5 - 10u_0^3 + 5u_0}{20} \right]_{-1}^{1} = \frac{2}{5} c_0, \quad (2.86)$$

showing that $c_0 = 5/2$.

Finally, the correlation function can be calculated

$$\overline{\left(\frac{3}{2} \cos^2 \vartheta(0) - \frac{1}{2} \right) \left(\frac{3}{2} \cos^2 \vartheta(t) - \frac{1}{2} \right)} = \frac{5}{4} \int\limits_{-1}^{1} \mathrm{d}u_0 \frac{(3u_0^2 - 1)^2}{4} \int\limits_{-1}^{1} \mathrm{d}u \frac{(3u^2 - 1)^2}{4} \mathrm{e}^{-6D^{\mathrm{rot}}t} = \frac{5}{4} \frac{2}{5} \frac{2}{5} \mathrm{e}^{-6D^{\mathrm{rot}}t} = \frac{1}{5} \mathrm{e}^{-6D^{\mathrm{rot}}t}. \quad (2.87)$$

We have derived that the time correlation function for spherically symmetric rotational diffusion is a single-exponential function.

2.5.5 Return to equilibrium

After introducing the correlation function, we can repeat the analysis using the same simplifications (rigid molecule, isotropic liquid), but taking the transverse (perpendicular) field fluctuations into account.

$$\frac{\mathrm{d}\mu_x}{\mathrm{d}t} = \omega_y \mu_z - \omega_z \mu_y \quad (2.88)$$

$$\frac{\mathrm{d}\mu_y}{\mathrm{d}t} = \omega_z \mu_x - \omega_x \mu_z \quad (2.89)$$

$$\frac{\mathrm{d}\mu_z}{\mathrm{d}t} = \omega_x \mu_y - \omega_y \mu_x \quad (2.90)$$

Expressing ω_x as $b\Theta^{\perp} \cos \varphi$ and ω_y as $b\Theta^{\perp} \sin \varphi$, where

$$b = -2\gamma B_0 \delta_{\mathrm{a}} \quad (2.91)$$

$$\Theta^{\perp} = \frac{3}{2} \sin \vartheta \cos \vartheta, \quad (2.92)$$

gives

$$\frac{\mathrm{d}\mu_x}{\mathrm{d}t} = (b\Theta^{\perp} \sin \varphi)\mu_z - (\omega_0 + b\Theta^{\parallel})\mu_y \quad (2.93)$$

$$\frac{\mathrm{d}\mu_y}{\mathrm{d}t} = (\omega_0 + b\Theta^{\parallel})\mu_x - (b\Theta^{\perp} \cos \varphi)\mu_z \quad (2.94)$$

$$\frac{\mathrm{d}\mu_z}{\mathrm{d}t} = (b\Theta^{\perp} \cos \varphi)\mu_y - (b\Theta^{\perp} \sin \varphi)\mu_x, \quad (2.95)$$

Introducing $\mu^{+} = \mu_x + \mathrm{i}\mu_y$ and $\mu^{-} = \mu_x - \mathrm{i}\mu_y$ results in

$$\frac{\mathrm{d}\mu^{+}}{\mathrm{d}t} = -\mathrm{i}b\Theta^{\perp}\mathrm{e}^{\mathrm{i}\varphi}\mu_z + \mathrm{i}(\omega_0 + b\Theta^{\parallel})\mu^{+} \quad (2.96)$$

$$\frac{\mathrm{d}\mu^{-}}{\mathrm{d}t} = \mathrm{i}b\Theta^{\perp}\mathrm{e}^{-\mathrm{i}\varphi}\mu_z - \mathrm{i}(\omega_0 + b\Theta^{\parallel})\mu^{-} \quad (2.97)$$

$$\frac{\mathrm{d}\mu_z}{\mathrm{d}t} = \frac{\mathrm{i}}{2}b\Theta^{\perp}\left(\mathrm{e}^{-\mathrm{i}\varphi}\mu^{+} - \mathrm{e}^{\mathrm{i}\varphi}\mu^{-} \right), \quad (2.98)$$

In a coordinate frame rotating with ω_0,

$$\frac{\mathrm{d}(\mu^{+})_{\mathrm{rot}}}{\mathrm{d}t} = -\mathrm{i}b\Theta^{\perp}\mathrm{e}^{\mathrm{i}(\varphi - \omega_0 t)}\mu_z + \mathrm{i}b\Theta^{\parallel}(\mu^{+})_{\mathrm{rot}} \quad (2.99)$$

$$\frac{\mathrm{d}(\mu^{-})_{\mathrm{rot}}}{\mathrm{d}t} = \mathrm{i}b\Theta^{\perp}\mathrm{e}^{-\mathrm{i}(\varphi - \omega_0 t)}\mu_z - \mathrm{i}b\Theta^{\parallel}(\mu^{-})_{\mathrm{rot}} \quad (2.100)$$

$$\frac{\mathrm{d}\mu_z}{\mathrm{d}t} = \frac{\mathrm{i}}{2}b\Theta^{\perp}\left(\mathrm{e}^{-\mathrm{i}(\varphi - \omega_0 t)}(\mu^{+})_{\mathrm{rot}} - \mathrm{e}^{\mathrm{i}(\varphi - \omega_0 t)}(\mu^{-})_{\mathrm{rot}} \right), \quad (2.101)$$
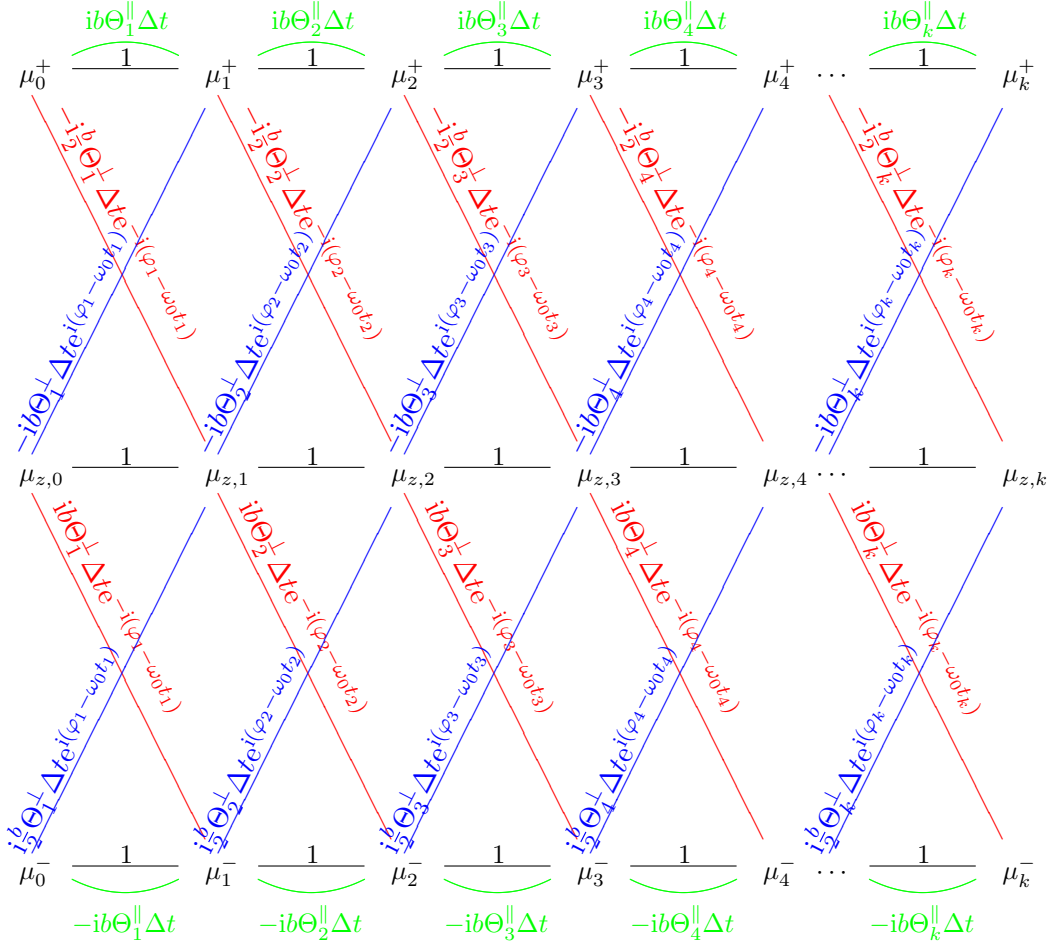
Figure 2.3: Evolution of magnetic moments due to longitudinal (parallel) and transverse (perpendicular) fluctuations of magnetic fields. The meaning of the diagram is the same as in Fig. 2.2, but additional segments (red and blue) interconnect μ_j^+, μ_j^-, and $\mu_{z,j}$, substantially increasing the number of possible pathways. The pathway composed of the black segments only gives the result of multiplication equal to one, the pathways containing just one segment of a different color give results of multiplication proportional to Δt, the pathways containing two segments of a color different than black give results of multiplication proportional to $(\Delta t)^2$, etc.

Note that now the transformation to the rotating frame did not remove ω_0 completely, it survived in the exponential terms.

Again, the set of differential equations cannot be solved because $\Theta^\parallel$, $\Theta^\perp$, and φ fluctuate in time, but we can analyze the evolution in time steps short enough to keep $\Theta^\parallel$, $\Theta^\perp$, and φ constant.

$$\mu_1^+ = \mu_0^+ + \Delta\mu_1^+ = [1 + \mathrm{i}(\omega_0 + b\Theta_1^\parallel)\Delta t]\mu_0^+ - \mathrm{i}b\Theta_1^\perp \Delta t e^{\mathrm{i}(\varphi_1 - \omega_0 t_1)}\mu_{z,0} \tag{2.102}$$

$$\mu_1^- = \mu_0^- + \Delta\mu_1^- = [1 - \mathrm{i}(\omega_0 + b\Theta_1^\parallel)\Delta t]\mu_0^- + \mathrm{i}b\Theta_1^\perp \Delta t e^{-\mathrm{i}(\varphi_1 - \omega_0 t_1)}\mu_{z,0} \tag{2.103}$$

$$\mu_{z,1} = \mu_{z,0} + \Delta\mu_{z,1} = \mu_{z,0} - \frac{\mathrm{i}}{2}b\Theta_1^\perp \Delta t e^{-\mathrm{i}(\varphi_1 - \omega_0 t_1)}\mu_0^+ + \frac{\mathrm{i}}{2}b\Theta_1^\perp \Delta t e^{\mathrm{i}(\varphi_1 - \omega_0 t_1)}\mu_0^-. \tag{2.104}$$

The μ^+, μ^-, and $\mu_{z,0}$ are now coupled which makes the step-by-step analysis much more complicated. Instead of writing the equations, we just draw a picture (Figure 2.3) similar to Fig. 2.2. Derivation of the values of relaxation rates follows the procedure described for the parallel fluctuations (Eqs. 2.32–2.38). As the number of possible pathways in Fig. 2.3 is very high, already the list of the terms proportional to Δt and Δt^2 is very long. Fortunately, we are not interested in evolution of magnetic moments in individual molecules, described in Fig. 2.3. The values of $\Theta_1^\parallel$, $\Theta_1^\perp$, φ_1, etc. are different for each molecule and we are interested in what we get after averaging results of multiplications for all molecules (all possible orientations). In order to avoid writing the long expressions for magnetic moments of individual molecules, we skip steps corresponding to Eqs. 2.32–2.37 and jump directly to the calculation of the evolution of total magnetization (corresponding to Eq. 2.38).

Let us start with the terms proportional to Δt, which give us the imaginary term proportional to b when calculating $\mathrm{d}M^+/\mathrm{d}t$ (and $\mathrm{d}M^-/\mathrm{d}t$, $\mathrm{d}M_z/\mathrm{d}t$). We have already seen that the average of $\Theta^\|$ (the green segment) is zero. The terms containing $\Theta^\perp$ (red and blue segments) contain the exponential expression with the phase including φ. If the azimuth φ is random,[9] the "red" and "blue" terms average to zero.

Let us now turn to the terms proportional to Δt^2, which give us the time integral multiplied by b^2 when calculating $\mathrm{d}M^+/\mathrm{d}t$ (and $\mathrm{d}M^-/\mathrm{d}t$, $\mathrm{d}M_z/\mathrm{d}t$). The pathways containing two red segments or two blue segments correspond to Δt^2 terms with a random phase in the exponent (random sums of $\varphi_j - \omega_0 t_j$). When averaged for all orientations, such phases tend to zero. The Δt^2 terms do not average to zero only in two cases: (i) if the pathway contains two green segments (effect of longitudinal fluctuations described above) or (ii) if the pathway contains a combination of one red and one blue segment. The former case is obvious, but the latter one is more subtle.

We can distinguish two combinations of one red and one blue segment:

$$\frac{1}{2}b^2\Delta t^2\Theta_k^\perp \mathrm{e}^{\mathrm{i}(\varphi_k - \omega_0 t_k)}\Theta_j^\perp \mathrm{e}^{-\mathrm{i}(\varphi_j - \omega_0 t_j)} = \frac{1}{2}b^2\Delta t^2\Theta_k^\perp \Theta_j^\perp \mathrm{e}^{\mathrm{i}(\varphi_k - \varphi_j - \omega_0(t_k - t_j))} \tag{2.105}$$

(with $-\omega_0(t_k - t_j)$ in the exponent) and

$$\frac{1}{2}b^2\Delta t^2\Theta_k^\perp \mathrm{e}^{-\mathrm{i}(\varphi_k - \omega_0 t_k)}\Theta_j^\perp \mathrm{e}^{\mathrm{i}(\varphi_j - \omega_0 t_j)} = \frac{1}{2}b^2\Delta t^2\Theta_k^\perp \Theta_j^\perp \mathrm{e}^{\mathrm{i}(-\varphi_k + \varphi_j + \omega_0(t_k - t_j))} \tag{2.106}$$

(with $+\omega_0(t_k - t_j)$ in the exponent). As discussed in Section 2.5.1, we can replace t_k by zero and t_j by t because the molecular motions are random:

$$\frac{1}{2}b^2\Delta t^2\Theta^\perp(0)\Theta^\perp(t)\mathrm{e}^{\mathrm{i}(-(\varphi(t) - \varphi(0)) + \omega_0 t)} \tag{2.107}$$

(with $+\omega_0 t$ in the exponent) and

$$\frac{1}{2}b^2\Delta t^2\Theta^\perp(0)\Theta^\perp(t)\mathrm{e}^{\mathrm{i}(+(\varphi(0) - \varphi(t)) - \omega_0 t)} \tag{2.108}$$

(with $-\omega_0 t$ in the exponent).

In both cases, the phase is not randomly distributed for different orientations only if $\varphi(0) - \varphi(t)$ is similar to $\omega_0 t$. The average value of $\overline{\Theta^\perp(0)^2}$ is $3/10$:

$$\overline{\Theta^\perp(t)^2} = \frac{9}{4}\overline{\cos^2\vartheta\sin^2\vartheta} = \frac{9}{16\pi}\int\limits_0^{2\pi}\mathrm{d}\varphi\int\limits_0^{\pi}\mathrm{d}\vartheta(\sin^3\vartheta\cos^2\vartheta) = \frac{9}{16\pi}\int\limits_0^{2\pi}\mathrm{d}\varphi\int\limits_{-1}^{1}\mathrm{d}u(u^2 - u^4) = \frac{9}{8}\left[\frac{u^3}{3} - \frac{u^5}{5}\right]_{-1}^{1} = \frac{9}{8}\left(\frac{2}{3} - \frac{2}{5}\right) = \frac{3}{10} \tag{2.109}$$

for any t.

The M_z component of magnetization is given by the average of the μ_z components at t_k. In order to get to $\mu_{z,k}$ through paths giving terms proportional to Δt^2, we must start at $\mu_{z,0}$ and pass one blue segment and one red segment in Figure 2.3. Eqs. 2.107 and 2.108 mathematically describe that orientations of magnetic moments are redistributed if the molecular motions (described by the azimuth φ) accidently resonate for a short time with the frequencies $\omega_0 t$ and $-\omega_0 t$. Then the magnetic energy of the magnetic moments is exchanged with the rotational kinetic energy of the molecules. This energy exchange must be taken into account when we average magnetic moments of individual molecules to calculate M_z. Let us call the total rotational energy of molecules $\mathcal{E}_0^{\mathrm{rot}}$. The exchange of the magnetic energy $\mathcal{E}_\mu$ of a magnetic moment $\vec{\mu}$ with a small amount of rotational energy of molecules $\Delta\mathcal{E}^{\mathrm{rot}}$ can be described as

$$\mathcal{E}_0^{\mathrm{rot}} \to \mathcal{E}_0^{\mathrm{rot}} + \Delta\mathcal{E}^{\mathrm{rot}} + \mathcal{E}_\mu. \tag{2.110}$$

The molecular motions have much more degrees of freedom (both directions of rotational axes and rates of rotation vary) than the magnetic moments (size is fixed, only orientation changes). We can therefore assume that the exchange perturbs distribution of the magnetic moments, but the rotating molecules stay very close to the termodynamic equilibrium. At the equilibrium, the probability to find a molecule with the rotational kinetic energy $\mathcal{E}_0^{\mathrm{rot}} + \Delta\mathcal{E}^{\mathrm{rot}}$ is proportional (Boltzmann law) to

$$\mathrm{e}^{\frac{-\Delta\mathcal{E}^{\mathrm{rot}}}{k_{\mathrm{B}}T}} \approx 1 - \frac{\Delta\mathcal{E}^{\mathrm{rot}}}{k_{\mathrm{B}}T}. \tag{2.111}$$

The conservation of energy requires

$$\mathcal{E}_0^{\mathrm{rot}} + \Delta\mathcal{E}^{\mathrm{rot}} + \mathcal{E}_\mu = \mathcal{E}_0^{\mathrm{rot}}, \tag{2.112}$$

showing that $\Delta\mathcal{E}^{\mathrm{rot}} = -\mathcal{E}_\mu$. Consequently, the population of molecules with the given rotational energy is proportional to $1 - \Delta\mathcal{E}^{\mathrm{rot}}/k_{\mathrm{B}}T = 1 + \mathcal{E}_\mu/k_{\mathrm{B}}T$. According to Eq. 1.19, the probability of finding a magnetic moment in the orientation described by a given $u = \cos\vartheta_\mu$ is

---

[9]Note that this is true even in the presence of $\vec{B}_0$ and in molecules aligned along the direction of $\vec{B}_0$, for example in liquid crystals oriented by the magnetic field.

$$P^{\text{eq}}(u) = \frac{w}{\text{e}^w - \text{e}^{-w}} \text{e}^{uw} \approx \frac{w}{1 - w - 1 + w}(1 + uw) = \frac{1}{2}(1 + uw). \tag{2.113}$$

Consequently, $\mathcal{E}_\mu / k_{\text{B}} T = -uw = 1 - 2P^{\text{eq}}(u)$ and the probability to find a molecule with the rotational kinetic energy $\mathcal{E}_0^{\text{rot}} + \Delta \mathcal{E}^{\text{rot}}$ is proportional to

$$1 - \frac{\Delta \mathcal{E}^{\text{rot}}}{k_{\text{B}} T} = 1 + \frac{\mathcal{E}_\mu}{k_{\text{B}} T} = 2 - 2P^{\text{eq}}(u) = 2(1 - P^{\text{eq}}(u)), \tag{2.114}$$

where the factor of two can be absorbed in the normalization constant.

We have derived that the averaged values of μ_z are weighted by $1 - P^{\text{eq}}(u)$. How does it affect the calculation of M_z? In the expression $\mu_z - P^{\text{eq}}(u)\mu_z$, μ_z in the first term is not weighted by anything and its average (multiplied by the number of magnetic moments per unit volume) is equal to M_z. The average value of the second term has been already calculated in Eqs. 1.23–1.26. It represents the equilibrium value of the magnetization, M^{eq}. Therefore, averaging of μ_z results in $M_z - M^{\text{eq}}$, usually abbreviated as ΔM_z.

Using the same arguments as in Section 2.5.1,

$$\frac{\text{d}\Delta M_z}{\text{d}t} = -\left(\frac{1}{2}b^2 \int_0^\infty \overline{\Theta^\perp(0)\Theta^\perp(t)\text{e}^{-\text{i}(\varphi(t)-\varphi(0))}}\text{e}^{\text{i}\omega_0 t}\text{d}t + \frac{1}{2}b^2 \int_0^\infty \overline{\Theta^\perp(0)\Theta^\perp(t)\text{e}^{\text{i}(\varphi(t)-\varphi(0))}}\text{e}^{-\text{i}\omega_0 t}\text{d}t\right)\Delta M_z \tag{2.115}$$

The relaxation rate R_1 for M_z, known as *longitudinal relaxation rate* in the literature, is the real part[10] of the expression in the parentheses

$$R_1 = b^2 \Re\left\{\int_0^\infty \overline{\Theta^\perp(0)\Theta^\perp(t)\text{e}^{-\text{i}(\varphi(t)-\varphi(0))}}\text{e}^{\text{i}\omega_0 t}\text{d}t + \int_0^\infty \overline{\Theta^\perp(0)\Theta^\perp(t)\text{e}^{\text{i}(\varphi(t)-\varphi(0))}}\text{e}^{-\text{i}\omega_0 t}\text{d}t\right\}. \tag{2.116}$$

If the fluctuations are random and their statistical properties do not change in time, they are *stationary*: the current orientation of the molecule is correlated with the orientation in the past in the same manner as it is correlated with the orientation in the future. Therefore,

$$\int_0^\infty \overline{\Theta^\perp(0)\Theta^\perp(t)\text{e}^{-\text{i}(\varphi(t)-\varphi(0))}}\text{e}^{\text{i}\omega_0 t}\text{d}t = \frac{1}{2}\left(\int_0^\infty \overline{\Theta^\perp(0)\Theta^\perp(t)\text{e}^{-\text{i}(\varphi(t)-\varphi(0))}}\text{e}^{\text{i}\omega_0 t}\text{d}t + \int_{-\infty}^0 \overline{\Theta^\perp(0)\Theta^\perp(t)\text{e}^{-\text{i}(\varphi(t)-\varphi(0))}}\text{e}^{\text{i}\omega_0 t}\text{d}t\right) \tag{2.117}$$

$$= \frac{1}{2}\int_{-\infty}^\infty \overline{\Theta^\perp(0)\Theta^\perp(t)\text{e}^{-\text{i}(\varphi(t)-\varphi(0))}}\text{e}^{\text{i}\omega_0 t}\text{d}t. \tag{2.118}$$

$$\int_0^\infty \overline{\Theta^\perp(0)\Theta^\perp(t)\text{e}^{\text{i}(\varphi(t)-\varphi(0))}}\text{e}^{-\text{i}\omega_0 t}\text{d}t = \frac{1}{2}\left(\int_0^\infty \overline{\Theta^\perp(0)\Theta^\perp(t)\text{e}^{\text{i}(\varphi(t)-\varphi(0))}}\text{e}^{-\text{i}\omega_0 t}\text{d}t + \int_{-\infty}^0 \overline{\Theta^\perp(0)\Theta^\perp(t)\text{e}^{\text{i}(\varphi(t)-\varphi(0))}}\text{e}^{-\text{i}\omega_0 t}\text{d}t\right) \tag{2.119}$$

$$= \frac{1}{2}\int_{-\infty}^\infty \overline{\Theta^\perp(0)\Theta^\perp(t)\text{e}^{\text{i}(\varphi(t)-\varphi(0))}}\text{e}^{-\text{i}\omega_0 t}\text{d}t. \tag{2.120}$$

In isotropic solutions, the motions of molecules are very little affected by magnetic fields. Therefore, the choice of the z axes is arbitrary form the point of the view of the molecule (not of the magnetic moment!). Therefore, the terms with $\Theta^\perp$ can be replaced by those with $\Theta^\parallel$, multiplied by $3/2$ to match the difference between $\overline{\Theta^\parallel(0)^2} = 1/5$ and $\overline{\Theta^\perp(0)^2} = 3/10$:

$$\frac{1}{2}\int_{-\infty}^\infty \overline{\Theta^\perp(0)\Theta^\perp(t)\text{e}^{\mp\text{i}(\varphi(t)-\varphi(0))}}\text{e}^{\pm\text{i}\omega_0 t}\text{d}t = \frac{3}{4}\int_{-\infty}^\infty \overline{\Theta^\parallel(0)\Theta^\parallel(t)}\text{e}^{\pm\text{i}\omega_0 t}\text{d}t. \tag{2.121}$$

Real parts of the integrals in Eq. 2.121 are known as *spectral density functions* $J(\omega)$. Note that the real part of the integral in the right-hand side of Eq. 2.121 is

---

[10]Solving Eq. 2.115 gives

$$\Delta M_z = \Delta M_z(0)\text{e}^{-(R_1 + \text{i}\omega')t} = \Delta M_z(0)\text{e}^{-R_1 t}\text{e}^{\text{i}\omega' t} = \Delta M_z(0)\text{e}^{-R_1 t}\left(\cos\omega' t + \text{i}\sin\omega' t\right),$$

where R_1 and ω' are the real and imaginary parts, respectively, of the expression in the parentheses in Eq. 2.115. Whereas R_1 describes the decay rate of ΔM_z, ω' (much smaller than ω_0), known as the *dynamic frequency shift*, describes an oscillation of ΔM_z, and is usually included into the value of ω_0.

$$\Re\left\{\frac{3}{4}\int\limits_{-\infty}^{\infty}\overline{\Theta^{\parallel}(0)\Theta^{\parallel}(t)}e^{\pm i\omega_0 t}dt\right\} = \frac{3}{4}\int\limits_{-\infty}^{\infty}\overline{\Theta^{\parallel}(0)\Theta^{\parallel}(t)}\cos(\omega_0 t)dt. \tag{2.122}$$

because

$$e^{\pm ix} = \cos x \pm i\sin x. \tag{2.123}$$

Also note that the integral in Eq. 2.47 in Section 2.5.1 can be also included in the definition of the spectral density function if we replace ω_0 by zero:

$$\int\limits_{0}^{\infty}\overline{\Theta^{\parallel}(0)\Theta^{\parallel}(t)}dt = \frac{1}{2}\left(\int\limits_{0}^{\infty}\overline{\Theta^{\parallel}(0)\Theta^{\parallel}(t)}dt + \int\limits_{-\infty}^{0}\overline{\Theta^{\parallel}(0)\Theta^{\parallel}(t)}dt\right) = \frac{1}{2}\int\limits_{-\infty}^{\infty}\overline{\Theta^{\parallel}(0)\Theta^{\parallel}(t)}\cos(0)dt = \frac{1}{2}J(0). \tag{2.124}$$

2.5.6   Bloch equations

The effects of relaxation can be included in the equations describing evolution of the bulk magnetization (Eqs. 1.115–1.117). The obtained set of equations, known as *Bloch equations*, provides a general macroscopic description of NMR for proton and similar nuclei.

$$\frac{dM_x}{dt} = -R_2 M_x - \Omega M_y + \omega_1 \sin\varphi M_z, \tag{2.125}$$

$$\frac{dM_y}{dt} = +\Omega M_x - R_2 M_y - \omega_1 \cos\varphi M_z, \tag{2.126}$$

$$\frac{dM_z}{dt} = -\omega_1 \sin\varphi M_x + \omega_1 \cos\varphi M_y - R_1(M_z - M_z^{\text{eq}}). \tag{2.127}$$

$$\tag{2.128}$$

Lecture 3
Signal acquisition and processing

Literature: Function of an NMR spectrometer is nicely described in L4, K13, or C3.1. More details are provided in B23. Experimental setup is discussed in C3.8.2. Signal averaging is described in L5.2, quadrature detection in L5.7 and LA.5, K13.6, and C3.2.3, Fourier transformation is introduced in K5.1–K5.3.1 and L5.8.1.–L5.8.3, and treated more thoroughly in B8 and C3.3.1. Phase correction is described nicely in K5.3.2–K5.3.4 and discussed also in C3.3.2.3 and L5.8.4–L5.8.5, zero filling is discussed in C3.3.2.1 and K5.5, and apodization is explained in K5.4 and C3.3.2.2.

3.1 NMR experiment

It is not our aim to discuss practical issues of NMR spectroscopy. However, it is useful to have at least a basic idea how NMR signal is acquired and processed before discussing theory of magnetic resonance.

The real NMR experiment closely resembles FM radio broadcast. The mega-hertz radio frequency ω_{radio} plays the role of the *carrier frequency*, and is *frequency-modulated* by the offset, which usually falls in the range of kilo-hertz *audio frequencies*. In a similar fashion, the carrier frequency of the FM broadcast is modulated by the audio frequency of the transmitted signal (voice, music). Like when listening to the radio, we need to know the carrier frequency to tune the receiver, but its value is not interesting. The interesting information about the chemical environment is hidden in the audio-frequency offset. But recall that the numerical value of Ω is arbitrary as it depends on the actual choice of the carrier frequency. What can be interpreted unambiguously, is the constant δ, given just by the electron density. As discussed in Section 1.4, the absolute value of δ is extremely difficult to obtain because the reference $\delta = 0$ represents nuclei with no electrons – definitely not a sample we are used to produce in our labs. Therefore, more accessible references (precession frequencies ω_{ref} of stable chemical compounds) are used instead of the vacuum frequency. The value of δ is then defined as $(\omega - \omega_{\mathrm{ref}})/\omega_{\mathrm{ref}}$ and usually presented in the units of ppm (see Section 1.4).

Setting up the NMR experiment is not a simple task. It includes several steps, listed in Section 3.10.1.

3.2 NMR signal acquisition

Most often, the NMR signal is acquired in a manner called *quadrature detection*. The procedure is described in Section 3.10.2, here we only describe its result. Magnetic field of the rotating magnetization induces electromotive voltage in the detector coil. This electric signal, oscillating and decaying due to the relaxation, is known as the *free induction decay (FID)*. The voltage induced in the detector coil is split into two channels. The high-frequency (radio) component of the signal (oscillating with carrier frequency $-\omega_{\mathrm{radio}}$) is filtered out (*demodulation*). The resulting signal contains only the low-frequency (audio) component (superposition of oscillations with frequency offsets Ω_j of individual nuclei) but with a different phase in each channel. The phase difference between the channels is $\pi/2$, or $90\,^{\circ}$. It is convenient to treat the signals in the individual channels (labeled $a(t)$ and $b(t)$ in this text) as a real and imaginary component of a single complex number, denoted $y(t)$ in this text. If we ignore relaxation, the complex signal can be described as

$$y(t) = a(t) + \mathrm{i}b(t) = \sum_j \left(\mathcal{A}_j \cos(\Omega_j t) + \mathrm{i}\mathcal{A}_j \sin(\Omega_j t) \right) = \sum_j \mathcal{A}_j \mathrm{e}^{\mathrm{i}\Omega_j t}. \tag{3.1}$$

The output of the quadrature receiver is converted to a digital form (*analog-digital conversion*). Therefore, the information obtained from an NMR experiment is a set of complex numbers describing the signal intensities at the time points $t \in \{0, \Delta t, 2\Delta t, \cdots, (N-1)\Delta t\}$.

The NMR signal induced by precession of the magnetization vector is very weak, comparable to the *noise*, generated mostly by random motions of electrons in the receiver coil. Therefore, the NMR experiments are usually repeated several times, adding the signal together. If the experiment is repeated in the same manner n-times, the evolution of the magnetization vector is identical in all repetitions (magnetization is evolving *coherently*), and the sum of the signals from the individual measurements, called *transients*, is simply $ny(t)$. However, the absolute size of the signal is not important, what really matters is the *signal-to-noise* ratio. Therefore, it is also important how noise accumulates when adding signals of separate measurements. The analysis presented in Section 3.10.3 shows that the signal-to-noise ratio is proportional to the square root of the number of summed transients.

3.3 Fourier transformation

The effect of electrons (chemical shift) makes NMR signal much more interesting but also much more complicated. Oscillation of the voltage induced in the receiver coil is not described by a cosine function, but represents a superposition (sum) of several cosine curves (phase-shifted and dumped). It is practically impossible to get the frequencies of the individual cosine functions just by looking at the recorded interferograms. Fortunately, the signal acquired as a function of time can be converted into a frequency dependence using a straightforward mathematical procedure, known as *Fourier transformation*.

It might be useful to present the basic idea of the Fourier transformation in a pictorial form before we describe details of Fourier transformation by mathematical equations. The oscillating red dots in Figure 3.1 represent an NMR signal defined by one frequency ν. Let us assume that the signal
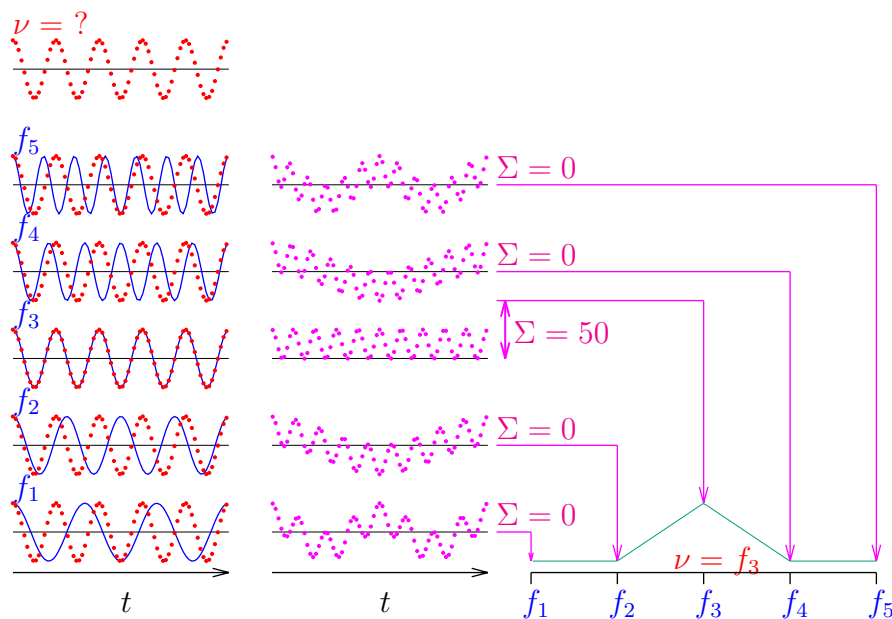
Figure 3.1: The basic idea of Fourier transformation.

oscillates as a cosine function but we do not know the frequency. We generate a testing set of cosine functions of different known frequencies f_j (blue curves in Figure 3.1) and we multiply each blue testing function by the red signal. The resulting product is plotted as magenta dots in Figure 3.1. Then we sum the values of the magenta points for each testing frequency getting one number (the sum) for each blue function. Finally, we plot these numbers (the sums) as the function of the testing frequency. How does the plot looks like? If the testing frequency differs from ν, the magenta dots oscillate around zero and their sum is close to zero (slightly positive or negative, depending on how many points were summed). But if we are lucky and the testing frequency matches ν (f_3 in Figure 3.1), the result is always positive (we always multiply two positive numbers or two negative numbers). The sum is then also positive, the larger the more points are summed. Therefore, the sum for the matching frequency is much higher than the other sums, making a positive peak in the final green plot (the dependence on f_j). The final plot represents a *frequency spectrum* and the position of the peak immediately identifies the value of the unknown frequency. If the NMR signal is composed of two frequencies, the red dots oscillate in a wild interference patterns, not allowing to get the frequency simply by measuring the period of the oscillation. However, the individual components (if they are sufficiently different) just make several peaks in the final green plot and their frequencies can be easily obtained by reading the positions of the peaks.

Let us now try to describe the Fourier transformation in a bit more mathematical manner (a more detailed discussion is presented in Section 3.10.4). If a *continuous* signal $y(t)$ were recorded using quadrature detection, i.e., stored as complex numbers, it would be appropriate to apply continuous complex Fourier transformation, defined as
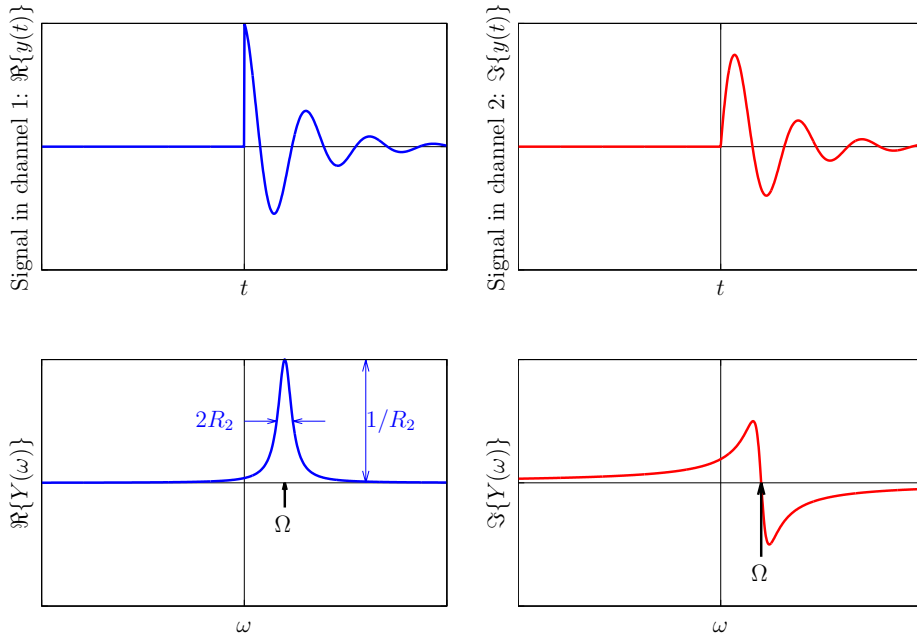
Figure 3.2: Ideal signal detected with a quadrature detection (top) and its Fourier transform (bottom).

$$Y(\omega) = \int\limits_{-\infty}^{\infty} y(t)\mathrm{e}^{-\mathrm{i}\omega t}\mathrm{d}t. \tag{3.2}$$

Important properties of continuous complex Fourier transformation are summarized in Section 3.10.6.

Although the actual NMR signal is not recorded and processed in a continuous manner, the idealized continuous Fourier transformation helps to understand the fundamental relation between the shapes of FID and frequency spectra and reveals important features of signal processing. Therefore, we discuss the continuous Fourier transformation before we proceed to the discrete analysis.

An "ideal signal" (see Figure 3.2) has the form $y(t) = 0$ for $t \leq 0$ and $y(t) = \mathcal{A}\mathrm{e}^{-R_2 t}\mathrm{e}^{\mathrm{i}\Omega t}$ for $t \geq 0$, where $\mathcal{A}$ can be a complex number (*complex amplitude*), including the real amplitude $|\mathcal{A}|$ and the initial phase ϕ_0:

$$\mathcal{A} = |\mathcal{A}|\mathrm{e}^{\mathrm{i}\phi_0}. \tag{3.3}$$

As derived in Section 3.10.5,

Fourier transform of the "ideal" signal is

$$Y(\omega) = \int\limits_{0}^{\infty} \mathcal{A}\mathrm{e}^{-R_2 t}\mathrm{e}^{\mathrm{i}\Omega t}\mathrm{e}^{-\mathrm{i}\omega t}\mathrm{d}t = \mathcal{A}\frac{R_2}{R_2^2 + (\Omega - \omega)^2} + \mathrm{i}\mathcal{A}\frac{\Omega - \omega}{R_2^2 + (\Omega - \omega)^2} \tag{3.4}$$

If $\phi_0 = 0$, the blue term, known as the *absorption line* is a real function ($\Re\{Y(\omega)\}$) having a shape
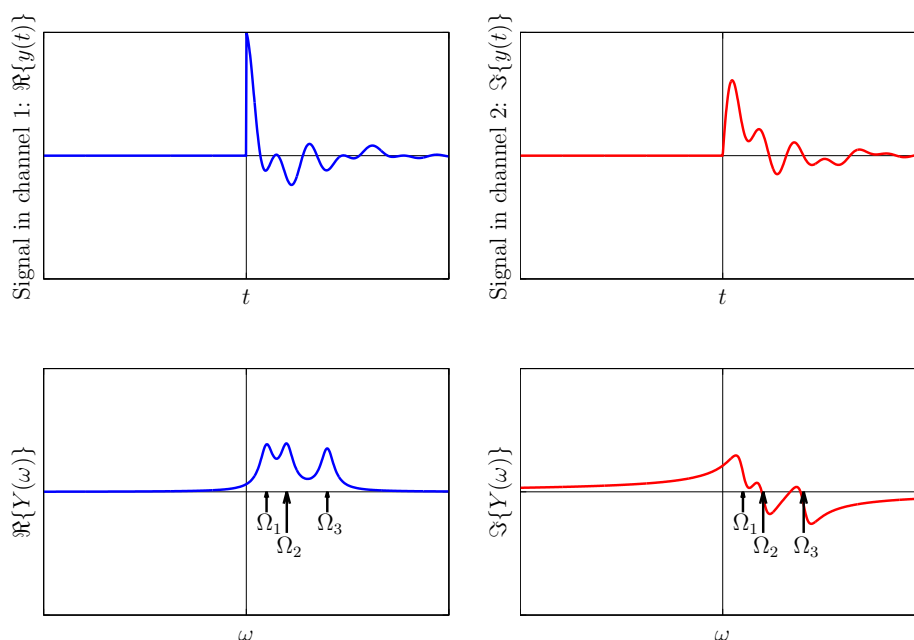
Figure 3.3: Signal (top) and frequency spectrum (bottom) with three precession frequencies.

of the *Lorentz curve* (see Figure 3.2). The shape of the absorption line is given[1] by the relaxation rate R_2:

- Peak height $\propto 1/R_2$ ($Y = Y_{\max}$ at $\omega = \Omega \Rightarrow Y_{\max} = Y(\Omega) = \mathcal{A}/R_2$)

- Linewidth at the half-height $= 2R_2$ ($Y = Y_{\max}/2$ at $\Omega - \omega = \pm R_2$)

The red term, the *dispersion line*, is purely imaginary ($\Im\{Y(\omega)\}$) if $\phi_0 = 0$. Such shape is less convenient in real spectra containing several lines because the broad wings of the dispersion line distort the shape of the neighbouring lines (see Figure 3.2).

Figure 3.3 documents that Fourier transformation allows us to immediately determine several precession frequencies in spectra even if the signal in the time domain (FID) is very difficult to interpret, and that the real (absorption) part of the complex spectrum is much better for such purpose.

Figures 3.4 and 3.5 document the advantage of recording the signal with the quadrature detection, as a complex number. If we take only the signal from the first channel, oscillating as the cosine function if $\phi_0 = 0$ and stored as the real part if the quadrature detection is used (Figure 3.4), and perform the Fourier transformation, we get a spectrum with two peaks with the frequency offsets Ω and $-\Omega$. Such a spectrum does not tell us if the actual Larmor frequency is $\omega_0 = \omega_{\text{radio}} - \Omega$ or $\omega_0 = \omega_{\text{radio}} + \Omega$. If we use the signal from the second channel only, oscillating as the sine function if $\phi_0 = 0$ (Figure 3.5), a spectrum with two peaks is obtained again, the only difference is that the

---

[1]In practice, it is also affected by inhomogeneities of the static magnetic field, increasing the apparent value of R_2. This effect is known as *inhomogeneous broadening*.
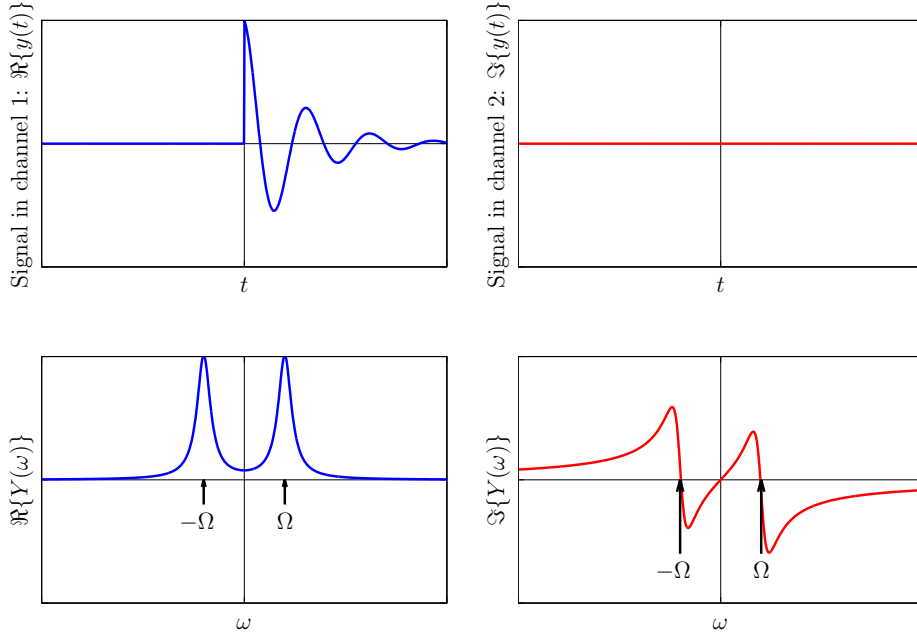
Figure 3.4: A signal detected in the first ("real") channel (top) and its Fourier transform (bottom).

peaks have opposite phases (i.e., their phases differ by $180\,^\circ$). But if we combine both signals, the false peaks at $-\Omega$ disappear because they have opposite signs and cancel each other in the sum of the spectra.

The discussed transformation of a continuous signal is extremely useful for understanding the relation between evolution of the magnetization vector and shape of the peaks observed in the frequency spectra. But in reality, the signal is finite ($t_{\max} < \infty$) and discrete ($\Delta t > 0$):

$$t \in \{ \quad 0, \quad \Delta t, \quad 2\Delta t, \quad \cdots, \quad (N-1)\Delta t \quad \}$$
$$y(t) \in \{ \quad y_0, \quad y_1, \quad y_2, \quad \cdots, \quad y_{N-1} \quad \}$$

As a consequence, the frequency spectrum is also discrete ($\Delta\omega > 0$) and finite (has a defined *spectral width* $N\Delta\omega$):

$$\omega \in \{ \quad 0, \quad \Delta\omega, \quad 2\Delta\omega, \quad \cdots, \quad (N-1)\Delta\omega \quad \}$$
$$Y(\omega) \in \{ \quad Y_0, \quad Y_1, \quad Y_2, \quad \cdots, \quad Y_{N-1} \quad \}$$

The seemingly marginal difference between ideal and real (finite and discrete) signal has several practical consequences, discussed in Sections 3.4 and 3.6.

3.4 Consequence of finite signal acquisition

In reality, the acquisition of signal stops at a finite time $t_{\max}$:

$$Y(\omega) = \int_0^{t_{\max}} \mathcal{A}e^{(i\Omega - R_2)t}e^{-i\omega t}dt = \mathcal{A}\frac{1 - e^{-R_2 t_{\max}}e^{i(\Omega-\omega)t_{\max}}}{R_2 - i(\Omega - \omega)}. \tag{3.5}$$
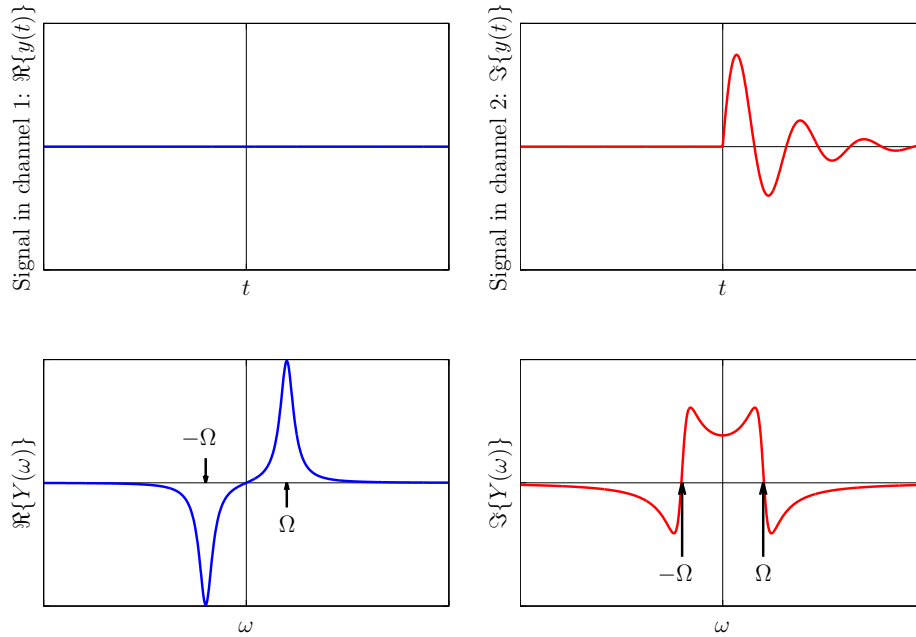
Figure 3.5: A signal detected in the second ("imaginary") channel (top) and its Fourier transform (bottom).

It has some undesirable consequences:

Leakage: Part of the signal is lost, peak height $Y(\Omega) < \mathcal{A}/R_2$.

Truncation artifacts: For $R_2 \to 0$,

$$Y(\omega) = \int\limits_0^{t_{\max}} \mathcal{A}e^{i(\Omega-\omega)t} dt = \mathcal{A}\frac{1 - e^{i(\Omega-\omega)t_{\max}}}{-i(\Omega - \omega)} = \mathcal{A}\frac{\sin(\Omega - \omega)t_{\max}}{\Omega - \omega} + i\mathcal{A}\frac{1 - \cos(\Omega - \omega)t_{\max}}{\Omega - \omega}. \quad (3.6)$$

If the acquisition is stopped before the signal relaxes completely, artifacts (baseline oscillation) appear. In the limit of no relaxation, the real part of the Fourier-transformed signal does not have a pure absorption shape (Lorentz curve), but has a shape of the $\sin(\Omega - \omega)t_{\max}/((\Omega - \omega)t_{\max})$ function (*sinc function*) multiplied by $\mathcal{A}t_{\max}$.

Loss of causality: The finite nature of the acquired signal has also a subtle effect known as the loss of causality. The phenomenon is discussed in detail Section 3.10.7 and a simple way of avoiding its undesired consequences is described in Section 3.7.

3.5 Discrete Fourier transformation

As mentioned in Sections 3.2 and 3.3, the digitized acquired signal is finite ($t_{\max} < \infty$) and discrete ($\Delta t > 0$):

$$t \in \{\quad 0, \quad \Delta t, \quad 2\Delta t, \quad \cdots, \quad (N-1)\Delta t \quad \}$$
$$y(t) \in \{\quad y_0, \quad y_1, \quad y_2, \quad \cdots, \quad y_{N-1} \quad \}$$
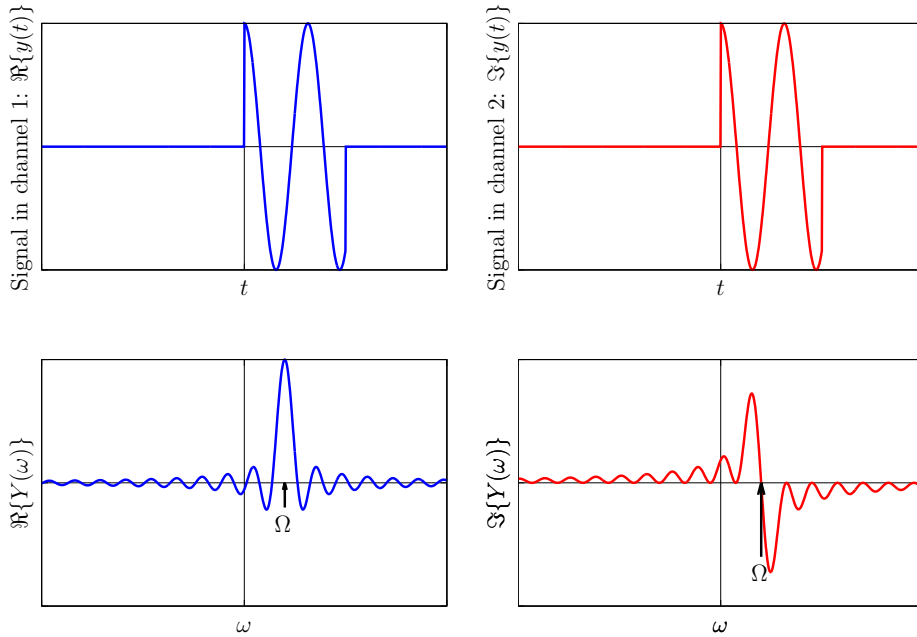
Figure 3.6: Effect of finite acqusition in the limit $R_2 \to 0$.

Therefore, *discrete Fourier transformation* is typically applied, producing digital spectra with the spectral width limited to $N\Delta\omega$

$$\omega \in \{ \quad 0, \quad \Delta\omega, \quad 2\Delta\omega, \quad \cdots, \quad (N-1)\Delta\omega \quad \}$$
$$Y(\omega) \in \{ \quad Y_0, \quad Y_1, \quad Y_2, \quad \cdots, \quad Y_{N-1} \quad \}$$

or, expressing ω as $2\pi f$ (in Hertz)

$$f \in \{ \quad 0, \quad \Delta f, \quad 2\Delta f, \quad \cdots, \quad (N-1)\Delta f \quad \}$$
$$Y(\omega) \in \{ \quad Y_0, \quad Y_1, \quad Y_2, \quad \cdots, \quad Y_{N-1} \quad \}$$

As shown in Section 3.10.8, the values of Δt, Δf and N are not independent in the discrete Fourier transformation, but they are restricted by the relation

$$\Delta f \Delta t = 1/N. \tag{3.7}$$

The consequences of the requirement $\Delta f \Delta t = 1/N$ are:

- spectral width $N\Delta f = 1/\Delta t$, it is defined by the choice of the time increment

- digital resolution $\Delta f = 1/N\Delta t$, it is defined by the choice of the maximum acquisition time

Possible definitions of the discrete Fourier transform with a correct normalization (so that $\Delta f \Delta t = 1/N$) are

$$Y_k = \sum_{j=0}^{N-1} y_j \mathrm{e}^{-\mathrm{i}\frac{2\pi}{N}kj} \qquad y_j = \frac{1}{N} \sum_{k=0}^{N-1} Y_k \mathrm{e}^{\mathrm{i}\frac{2\pi}{N}kj} \tag{3.8}$$

or

$$Y_k = \frac{1}{\sqrt{N}} \sum_{j=0}^{N-1} y_j e^{-i\frac{2\pi}{N}kj} \qquad y_j = \frac{1}{\sqrt{N}} \sum_{k=0}^{N-1} Y_k e^{i\frac{2\pi}{N}kj}. \tag{3.9}$$

3.6 Consequence of discrete signal acquisition

As derived in Section 3.10.9, the discrete "ideal" NMR signal

$$y_j = \mathcal{A} e^{-R_2 j \Delta t} e^{i\Omega j \Delta t} = \mathcal{A} e^{-R_2 j \Delta t} e^{i2\pi \nu j \Delta t} \tag{3.10}$$

has the Fourier transform

$$Y_k = \sum_{j=0}^{N-1} \mathcal{A} e^{-R_2 j \Delta t} e^{i2\pi\nu j \Delta t} e^{-i\frac{2\pi}{N}kj} \Delta t = \mathcal{A}\Delta t \frac{1 - e^{-R_2 N \Delta t} e^{i\pi(N-2k)}}{1 + (1 - R_2\Delta t)e^{-i2\pi\frac{k}{N}}}. \tag{3.11}$$

Since the signal is discrete, the spectral width is limited: $\Delta t > 0 \Rightarrow N\Delta f = 1/\Delta t < \infty$. The consequences of the discrete sampling are, as derived in Section 3.10.9:

Aliasing: A peak of the real frequency $\nu + N\Delta f$ (outside the spectral width) appears at the apparent frequency ν in the spectrum (*Nyquist theorem*: frequencies ν and $\nu + 1/\Delta t$ cannot be distinguished).

Offset: Peak height of the continuous Fourier transform $Y(f) = \mathcal{A}/R_2$ and offset of the continuous Fourier transform $Y(\pm\infty) = 0$. Peak height of the discrete Fourier transform

$$Y_{\frac{N}{2}} = \mathcal{A}\Delta t \frac{1 - e^{-R_2 N \Delta t}}{R_2 \Delta t} \to \mathcal{A}/R_2 \tag{3.12}$$

for $N\Delta t \to \infty$, but offset of the discrete Fourier transform is non-zero. For a sufficiently long acquisition time (compared to the relaxation rate, i.e., $N\Delta t \gg 1/R_2$), the offset is equal to half of the intensity of the signal at the first time point $y(0)$. The aliasing and the offset are depicted in Figure 3.7.

3.7 Zero filling

Routinely, a sequence of N_Z zeros is appended to the recorded signal, mimicking data obtained at time points $N\Delta t$ to $(N + N_Z - 1)\Delta t$:

$$\begin{aligned} t &\in \{\ 0,\ \Delta t, 2\Delta t, \cdots, (N-1)\Delta t\ \} \\ y(t) &\in \{\ y_0,\ y_1,\ y_2,\ \cdots,\ \ \ y_{N-1}\ \ \ \ \} \end{aligned} \tag{3.13}$$

$$\downarrow$$

$$\begin{aligned} t &\in \{\ 0,\ \Delta t, 2\Delta t, \cdots, (N-1)\Delta t, N\Delta t, (N+1)\Delta t, \cdots, (N+N_Z-1)\Delta t\ \} \\ y(t) &\in \{\ y_0,\ y_1,\ y_2,\ \cdots,\ \ \ y_{N-1},\ \ \ \ \ 0,\ \ \ \ \ \ \ \ 0,\ \ \ \ \cdots,\ \ \ \ \ \ \ \ \ 0\ \ \ \ \ \ \ \} \end{aligned} \tag{3.14}$$

This may look like a completely artificial procedure, but there are several practical reasons to do it.
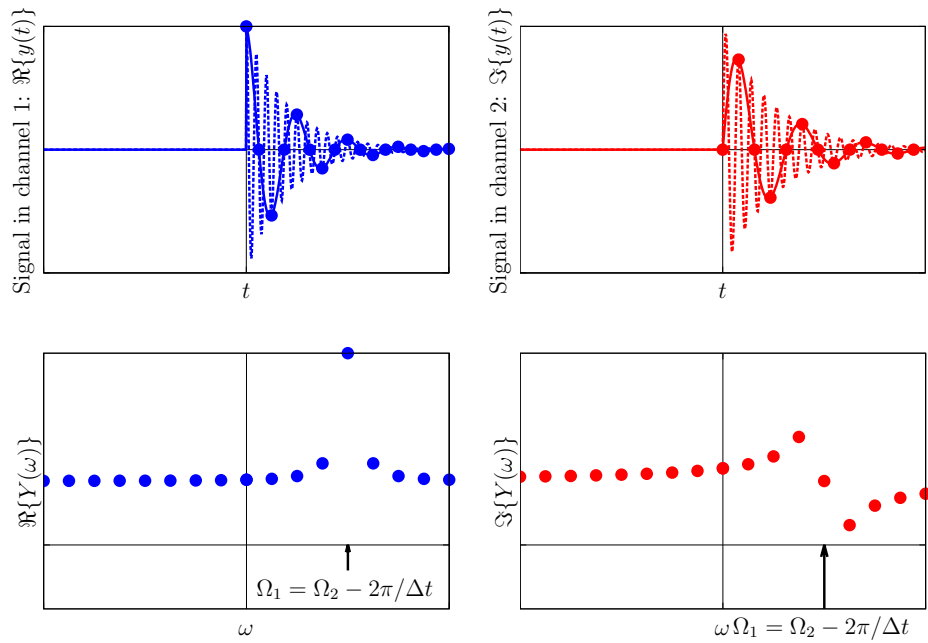
Figure 3.7: Aliasing and offset. If the signal is acquired in discrete time intervals (dots in the top plots), the signals with frequencies different by an integer multiple of $2\pi/\Delta t$, shown by solid (Ω_1) and dotted (Ω_2) lines, cannot be distinguished. Both signals give a peak with the same frequency in the spectrum. This frequency is equal to Ω_1 and to $\Omega_2 - 2\pi/\Delta t$, where $2\pi/\Delta t$ is the width of the spectrum. The discrete nature of the signal also results in a non-zero offset.

1. The very fast computational algorithm of calculating Fourier transform, known as *Cooley–Tukey FFT*, requires the number of time points to be an integer power of 2. If the number of collected time points N is not a power of 2, N_Z zeros are added to the data prior to Fourier transformation so that $N + N_Z$ is an integer power of 2.

2. In order to obtain a spectrum with the full content of information by discrete Fourier transformation, the collected data must be extended by a factor of 2 by zero-filling. This operation reintroduces causality, as it was briefly mentioned in Section 3.4 and is discussed in detail in Section 3.10.7. The important consequence is that the full information content of N experimental complex points (i.e., N points of the real part and N points of the imaginary part, together $2N$ bits of information) is encoded in the spectrum (i.e., in the real part of the Fourier transform, which now consists of $2N$ frequency points because we artificially increased the maximum time from $(N-1)\Delta t$ to $(2N-1)\Delta t$ and therefore narrowed the frequency sampling step Δf from $1/N\Delta t$ to $1/2N\Delta t$).

3. The *digital resolution* Δf, given by $1/(N\Delta t)$, can be improved (narrowed) to $1/((N+N_Z)\Delta t)$ by zero-filling. In this manner, the visual appearance of spectra can be improved by interpolation between data points. Note, however, that adding more than N zeros does not improve the informational content of the spectrum. Although the digital resolution is improved, the real resolution is the same, zero-filling does not help to resolve frequencies that differ less than $1/(N\Delta t)$!

3.8 Phase correction

So-far, we ignored the effect of the initial phase ϕ_0 and analyzed Fourier transforms of NMR signals consisting of a collection of (damped) cosine functions, with zero initial phase. In reality, the signal has a non-zero phase, difficult to predict

$$y(t) = \mathcal{A}e^{-R_2(t+t_0)}e^{i\Omega(t+t_0)} = |\mathcal{A}|e^{-R_2(t+t_0)}e^{i(\Omega(t+t_0)+\phi_0)}. \tag{3.15}$$

The phase has a dramatic impact on the result of the Fourier transformation. Real and imaginary parts are mixtures of absorption and dispersion functions. If we plot the real part as a spectrum, it looks really ugly for a non-zero phase.

For a single frequency, the phase correction is possible (multiplication by the function $e^{-(i\Omega t_0+\phi_0)}$, where t_0 and ϕ_0 are found empirically):

$$|\mathcal{A}|e^{-R_2(t+t_0)}e^{i(\Omega(t+t_0)+\phi_0)}e^{-i(\Omega t_0+\phi_0)} = |\mathcal{A}|e^{-R_2(t+t_0)}e^{i\Omega t}. \tag{3.16}$$

In practice, phase corrections are applied also to signal with more frequencies, as described in Section 3.10.10. The signal is multiplied by a function $e^{-i(\vartheta_0+\vartheta_1\omega)}$, where ϑ_0 and ϑ_1 are *zero-order* and *first-order phase corrections*, respectively. We try to find ϑ_0 and ϑ_1 giving the best-looking spectra. The procedure is a trial-and-error process, but modern computers allow us to vary ϑ_0 and ϑ_1 and repeat the Fourier transformation iteratively in a very short time. Note that phase correction is *always necessary*, but only approximative corrections are possible for a signal with multiple frequencies!
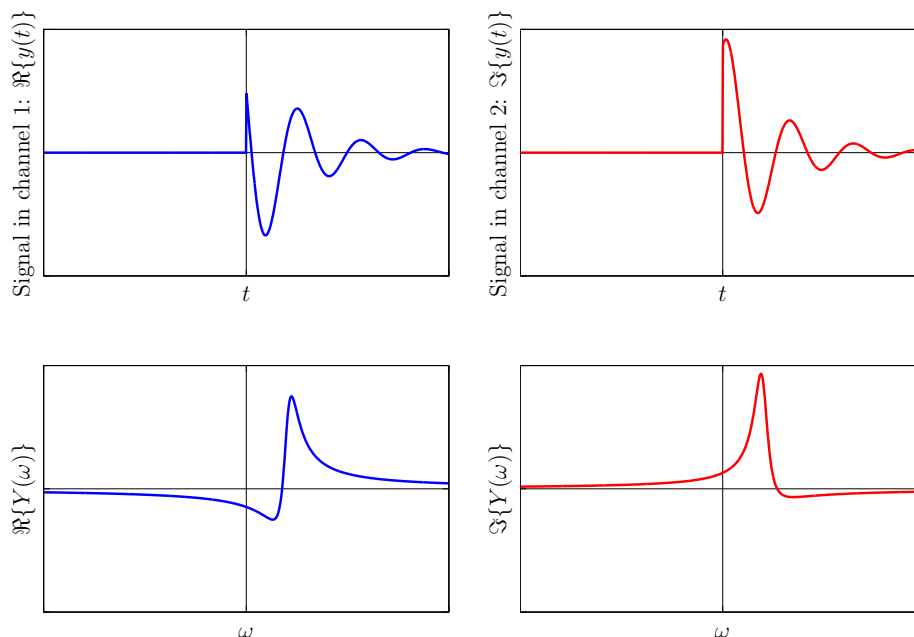
Figure 3.8: A signal with the initial phase of $60\,^\circ$ (top) provides distorted spectra (bottom), unless a phase correction is applied.

3.9 Apodization

The NMR signal is very often multiplied by a so-called *window function* prior to Fourier transformation.[2] This process is known as *apodization*. The goal is to

1. *improve sensitivity.* Due to the relaxation, signal of data acquired at later time points is lower, but the noise is the same. Therefore, the late time points decrease the signal-to-noise ratio. The sensitivity can be improved by discarding or attenuating the late time points.

2. *improve resolution.* As the resolution is given by $1/(N\Delta t)$, resolution is improved if the signal is multiplied by a window function that amplifies the late data points.

3. *suppress truncation artifacts.* We have seen that oscillations of the baseline appear if the data acquisition stops before the signal relaxes to zero (i.e., to the noise level). The desired effect of relaxation can be mimicked by a window function that smoothly converges to zero at $N\Delta t$.

Obviously, the three listed goals are in conflict, and only a compromise can been reached. There is no "best apodization". The choice of the optimal window function depends on the actual needs.

The simplest window function is a *rectangle*: multiplying the signal by a rectangular function equal to 1 for $j\Delta t \leq m\Delta t$ and to 0 for $j\Delta t > m\Delta t$ represents discarding data recorded for times

---

[2]The mathematical expression describing the Fourier-transformed product of two functions, signal and window in our case, is given by the convolution theorem, presented in Section 3.10.6.

longer than $m\Delta t$. It is a very useful way of improving signal-to-noise ratio if the signal relaxed before $m\Delta t$. Otherwise, it produces severe truncation artifacts.

The highest signal-to-noise ratio is provided by a *matched filter* window function. The matched filter has the shape of the envelope of the signal. The matched filter for our ideal signal is $\mathrm{e}^{-R_2 j\Delta t}$. The price paid for the signal-to-noise improvement is a lower resolution: Multiplying $\mathrm{e}^{-R_2 t}\mathrm{e}^{\mathrm{i}\Omega\Delta t}$ by $\mathrm{e}^{-R_2 t}$ obviously doubles the linewidth, given by the decay rate, which is now $2R_2$.

The best balance between resolution and truncation artifacts for an allowed extra line broadening λ is obtained with the *Dolph–Chebyshev* window, defined in Section 3.10.11, which is, however, not used in practice due to its very complex form. Instead, *sine-bell* windows $\sin^p\left(\frac{2\pi-\phi}{N}j+\phi\right)$ are used routinely, usually with the phase $\phi = \pi/2$ (i.e., cosine function) and with the power $p = 1$ or $p = 2$.

HOMEWORK

Describe how finite nature of the NMR signal results in leakage and truncation artifacts (Section 3.4). Derive the equation describing the discrete Fourier transformation of an ideal NMR signal describe the consequences of the discrete nature of the NMR signal (Section 3.10.9).

3.10   SUPPORTING INFORMATION

3.10.1   Setting up NMR experiment

- *Temperature control and calibration.* Temperature affects molecular motions and chemical shifts, it should be controlled carefully to obtain reproducible spectra and to analyze them quantitatively. The sample temperature is controlled by a flow of pre-heated/cooled air or nitrogen gas. The exact temperature inside the sample is not so easy to measure. Usually, spectra of compounds with known temperature dependence of chemical shifts are recorded (e.g. methanol). The temperature is obtained by comparing a difference of two well defined chemical shifts (of methyl and hydroxyl protons in the case of methanol) with its values reported for various temperatures. Purity of the standard samples is a critical issue.

- *Field-frequency lock.* The external magnetic field should be *stationary*. It is achieved by a feedback system known as *field-frequency lock*. A deuterated compound (usually heavy water or other deuterated solvent) is added to the sample and the deuterium frequency is measured continually and kept constant by adjusting electric current in an auxiliary electromagnet. The lock parameters for the particular deuterium compound used are selected and the deuterium spectrometer is switched on before the measurement.

- *Shimming.* The external magnetic field should be also *homogeneous*. The inhomogeneities caused e.g. by the presence of the sample are compensated by adjusting electric current in a set of correction coils called *shims*. This is usually at least partially automated.

- *Tuning.* Each radio-frequency circuit in the probe consists of a receiver coil and two adjustable capacitors. The capacitors should be adjusted for each sample. The *tuning capacitor* of the capacitance C_{T} and the coil of the inductance L make an LC circuit, acting as a resonator. Adjusting the value of C_{T} defines the resonant frequency, which should be equal to the precession frequency of the measured nucleus ω_0. If we neglect the second capacitor, the resonant frequency is $\omega = 1/\sqrt{LC_{\mathrm{T}}}$. The second, *matching capacitor* of the capacitance C_{M} is used to adjust the impedance of the resonator. The radio waves do not travel from the transmitter to the coil through air but through co-axial cables. In order to have minimum of the wave reflected back to the transmitter, the impedance of the resonator (coil circuit) Z_{c}, given by

$$Z_{\mathrm{c}} = \frac{1}{\frac{1}{Z_{\mathrm{M}}} + \frac{1}{Z_{\mathrm{T}} + Z_{\mathrm{L}} + R}} = \frac{1}{\mathrm{i}\omega C_{\mathrm{M}} + \dfrac{1}{\dfrac{1}{\mathrm{i}\omega C_{\mathrm{T}}} + \mathrm{i}\omega L + R}},$$

should match the input impedance Z_{in}. In order to tune the circuit, C_{T} and C_{M} must be adjusted simultaneously to get (i) $Z_{\mathrm{c}} = Z_{\mathrm{in}}$ and (ii) $\omega = \omega_0$.

- *Calibration of pulse duration.* The magnitude of $\vec{B}_1$ cannot be set directly. Therefore, the duration of irradiation rotating $\vec{M}$ by $360\,^\circ$ at the given strength of radio waves is searched for empirically. This duration is equal to $2\pi/\omega_1$ and can be used to calculate ω_1 or $|\vec{B}_1| = \omega_1/\gamma$. As $|\vec{B}_1|$ is proportional to the square root of power P, durations of pulses of radio waves of other strengths need not be calibrated, but can be recalculated. Power is measured in the units of Watt, but the relative power is usually expressed on a logarithmic scale in decibells (dB). One Bell represents a ten-fold attenuation of power

$$\log_{10} \frac{P_2}{P_1} = \text{attenuation/B}.$$

Consequently,

$$10\log_{10} \frac{P_2}{P_1} = \text{attenuation/dB},$$

and

$$20\log_{10} \frac{|\vec{B}_1|_2}{|\vec{B}_1|_1} = 10\log_{10} \frac{|\vec{B}_1|_2^2}{|\vec{B}_1|_1^2} = 10\log_{10} \frac{P_2^2}{P_1^2} = \text{attenuation/dB}. \tag{3.17}$$

3.10.2   Quadrature detection and demodulation

Precession of the magnetization vector in the sample induces an electromotive force (voltage) oscillating with the same frequency ω_0 in the coil of the NMR probe.

The signal generated in the coil and amplified in the preamplifier is split into two channels, labeled a and b here. The signal in each channel is mixed with a reference wave supplied by the radio-frequency synthesizer. The reference waves have the same frequency $-\omega_{\mathrm{radio}}$ in both channels, but their phases are shifted by $90\,^\circ$. Let us assume that the signal oscillates as a cosine function $\cos(\omega_0 t)$ and that

the reference wave in the first channel is a cosine wave $\cos(-\omega_{\text{radio}}t)$ and that the reference wave in the second channel is a sine wave $\sin(-\omega_{\text{radio}}t)$. Mathematically, splitting the signal and mixing it with the reference wave can be described as

$$\cos(\omega_0 t) \rightarrow \begin{cases} \frac{1}{2}\cos(\omega_0 t) \rightarrow \frac{1}{2}\cos(\omega_0 t)\cos(-\omega_{\text{radio}}t) & \text{channel } a \\ \frac{1}{2}\cos(\omega_0 t) \rightarrow \frac{1}{2}\cos(\omega_0 t)\sin(-\omega_{\text{radio}}t) & \text{channel } b \end{cases} \tag{3.18}$$

Basic trigonometric identities show that the result of mixing in the first channel is a sum of a high-frequency cosine wave $\cos((\omega_0 - \omega_{\text{radio}})t)$ and a low-frequency cosine wave $\cos((\omega_0 + \omega_{\text{radio}})t) = \cos(\Omega t)$, while the result of mixing in the second channel is a difference of the corresponding sine waves:

$$\frac{1}{2}\cos(\omega_0 t)\cos(-\omega_{\text{radio}}t) = \frac{1}{4}\cos((\omega_0 - \omega_{\text{radio}})t) + \frac{1}{4}\cos((\omega_0 + \omega_{\text{radio}})t), \tag{3.19}$$

$$\frac{1}{2}\cos(\omega_0 t)\sin(-\omega_{\text{radio}}t) = \frac{1}{4}\sin((\omega_0 - \omega_{\text{radio}})t) - \frac{1}{4}\sin((\omega_0 + \omega_{\text{radio}})t). \tag{3.20}$$

The high-frequency waves are filtered out by a low-pass filter, resulting in signals oscillating with a low frequency $\omega_0 + \omega_{\text{radio}} = \Omega$. The procedure, similar to the demodulation in an ordinary radio receiver, thus produces audio signals in both channels

$$\cos(\omega_0 t) \rightarrow \begin{cases} \frac{1}{2}\cos(\omega_0 t) \rightarrow \frac{1}{2}\cos(\omega_0 t)\cos(-\omega_{\text{radio}}t) \rightarrow \frac{1}{4}\cos(\Omega t) & \text{channel } a \\ \frac{1}{2}\cos(\omega_0 t) \rightarrow \frac{1}{2}\cos(\omega_0 t)\sin(-\omega_{\text{radio}}t) \rightarrow \frac{1}{4}\sin(\Omega t) & \text{channel } b \end{cases} \tag{3.21}$$

The signal also has some amplitude, therefore, we replace the factor of $1/4$ by an amplitude A and write

$$a = A\cos(\Omega t) \qquad b = A\sin(\Omega t). \tag{3.22}$$

The described manipulation is called *quadrature detection* and the unit performing it is called the *receiver*. The outputs of the receiver are converted to digital data (series of numbers describing values of the signal at discrete, equally spaced time points). It is convenient to treat the outputs of the individual channels as a real and imaginary component of a single complex number, but physically they are stored just as series of two numbers in the computer.

A very useful trick is to play with the order of the stored numbers. The four basic options are

data storing option:	$a, \ b$	conventionally labeled:	x
	$b, -a$		y
	$-a, -b$		$-x$
	$-b, \ a$		$-y$

The given storage option is described as the *receiver phase* in the literature. It is not an accident that the same symbols are used for the phase of the radio wave transmitted during the pulse and for the receiver phase. Choosing the right storage option (setting the receiver phase) allows us to remove the effect of changing the pulse phase. For example, a signal recorded immediately after an ideal $90°$ pulse of phase x (by definition) oscillates as $a = A\sin(\Omega t), b = -A\cos(\Omega t)$ (the magnetization starts to rotate from the $-y$ direction). If we run the same experiment but with the y phase of the first pulse, the signal oscillates as $a = A\cos(\Omega t), b = A\sin(\Omega t)$. However, if we use the option y to store the data, the record is the same as in the previous experiment: $b = A\sin(\Omega t), -a = -A\cos(\Omega t)$. We see that the same signal is obtained if the receiver phase matches the transmitter phase.

3.10.3 Noise accumulation

Here we analyze accumulation of the noise in repeated signal acquisition. The related physics is discussed later in Section 7.12.4. The noise $U_{\text{noise}}(t)$ is random and so its average[3] $\langle U_{\text{noise}}(t) \rangle = 0$. The size of the noise is typically defined by the *root-mean-square* $\sqrt{\langle U_{\text{noise}}(t)^2 \rangle}$. Sum of the noise from n independent experiments is

$$\sqrt{\left\langle \left(U_{\text{noise},1}(t) + U_{\text{noise},2}(t) + \cdots + U_{\text{noise},n}(t) \right)^2 \right\rangle}. \tag{3.23}$$

All terms like $\langle 2U_{\text{noise},1}(t)U_{\text{noise},2}(t) \rangle$ are equal to zero because the random motions of electrons in the individual experiments are not correlated (are independent). Therefore, calculation of the square in Eq. 3.23 simplifies to

$$\sqrt{\left\langle \left(U_{\text{noise},1}(t) + U_{\text{noise},2}(t) + \cdots + U_{\text{noise},n}(t) \right)^2 \right\rangle} = \sqrt{\langle U_{\text{noise},1}(t)^2 \rangle + \langle U_{\text{noise},2}(t)^2 \rangle + \cdots + \langle U_{\text{noise},n}(t)^2 \rangle}. \tag{3.24}$$

We can also assume that the root-mean-square is the same in all experiments, and write it as $\sqrt{\langle U_{\text{noise}}(t)^2 \rangle}$. The sum of the noise can be then calculated as

$$\sqrt{n\langle U_{\text{noise}}(t)^2 \rangle} = \sqrt{n}\sqrt{\langle U_{\text{noise}}(t)^2 \rangle}. \tag{3.25}$$

---

[3]To avoid writing the integrals defining averaging, we indicate the time average by the angled brackets.

We can now calculate the signal-to-noise ratio as

$$\frac{nU_{\text{measured}}(t)}{\sqrt{n}\sqrt{\langle U_{\text{noise}}(t)^2\rangle}} = \sqrt{n}\frac{U_{\text{measured}}(t)}{\sqrt{\langle U_{\text{noise}}(t)^2\rangle}}. \tag{3.26}$$

3.10.4 Mathematical description of Fourier transformation

We start with a special case of a signal which can be described by a sum of cosine functions with frequencies that are integer multiples of some small frequency increment $\Delta\omega$. All such cosine functions must have the same value at time t and $t + 2\pi/\Delta\omega$: the whole signal is periodic with the period $2\pi/\Delta\omega$. If we record such a signal using quadrature detection, we obtain

$$y(t) = \sum_{j=-\infty}^{\infty} \mathcal{A}_j e^{i\omega_j t} = \sum_{j=-\infty}^{\infty} \mathcal{A}_j e^{ij\Delta\omega t}. \tag{3.27}$$

The mentioned periodicity allows us to determine $\mathcal{A}_k$ by calculating the integrals

$$\int_0^{\frac{2\pi}{\Delta\omega}} y(t)e^{-i\omega_k t}dt = \sum_{j=-\infty}^{\infty} \mathcal{A}_j \int_0^{\frac{2\pi}{\Delta\omega}} e^{i(j-k)\Delta\omega t}dt = \frac{2\pi}{\Delta\omega}\mathcal{A}_k \tag{3.28}$$

(All integrated functions are periodic and their integrals are therefore equal to zero with the exception of the case when $k = j$, which is a constant function).

The same result is obtained for any integration limits which differ by $2\pi/\Delta\omega$, e.g.

$$\int_{-\frac{\pi}{\Delta\omega}}^{+\frac{\pi}{\Delta\omega}} y(t)e^{-i\omega_k t}dt = \sum_{j=-\infty}^{\infty} \mathcal{A}_j \int_{-\frac{\pi}{\Delta\omega}}^{+\frac{\pi}{\Delta\omega}} e^{i(j-k)\Delta\omega t}dt = \frac{2\pi}{\Delta\omega}\mathcal{A}_k \tag{3.29}$$

We can now continue in two different directions. We can describe the signal as it is actually measured, not as a continuous function of time, but as a discrete series of points sampled in time increments Δt. Then, the integral in Eq. 3.28 is replaced by summation of a finite number of measured signal points:

$$Y_k = \sum_{j=0}^{N-1} y_j e^{-ik\Delta\omega j\Delta t}\Delta t, \tag{3.30}$$

where $Y_k = \frac{2\pi}{\Delta\omega}\mathcal{A}_k$. As the time and frequency are treated in the same manner, we can also define the inverse operation

$$y_j = \sum_{k=0}^{N-1} Y_k e^{ik\Delta\omega j\Delta t}\Delta\omega. \tag{3.31}$$

This way of the signal analysis, discussed in more details in Section 3.5, handles the signal as it is measured in reality. It is also instructive to follow the other direction and to increase the period $2\pi/\Delta\omega$ by decreasing $\Delta\omega$. The series of ω_k becomes a continuous variable ω and $\pi/\Delta\omega \to \infty$ if $\Delta\omega \to 0$. The sum in Eq. 3.27 is replaced by the integral

$$y(t) = \frac{1}{2\pi}\int_{-\infty}^{\infty} Y(\omega)e^{i\omega t}d\omega \tag{3.32}$$

and the integral in Eq. 3.29 becomes

$$Y(\omega) = \int_{-\infty}^{\infty} y(t)e^{-i\omega t}dt. \tag{3.33}$$

If we apply Eq. 3.33 to a function $y(t)$ and Eq. 3.32 to the obtained result, we should get back the function $y(t)$. Such a double transformation can be written as

$$y(t) = \frac{1}{2\pi}\int_{-\infty}^{\infty} Y(\omega)e^{i\omega t}d\omega = \frac{1}{2\pi}\int_{-\infty}^{\infty} e^{i\omega t}d\omega \int_{-\infty}^{\infty} y(t')e^{-i\omega t'}dt' = \int_{-\infty}^{\infty} y(t')dt'\frac{1}{2\pi}\int_{-\infty}^{\infty} e^{i\omega(t-t')}d\omega. \tag{3.34}$$

This requires the second integral to be equal to 2π for $t' = t$ and to zero for $t' \neq t$. Therefore, the integral can be used to define the *delta* function

$$\delta(t - t') = \frac{1}{2\pi} \int\limits_{-\infty}^{\infty} e^{i\omega(t-t')} d\omega. \tag{3.35}$$

An alternative definition including a factor of $1/\sqrt{2\pi}$ in $\mathcal{A}_j$

$$y(t) = \sum_{j=-\infty}^{\infty} \frac{\mathcal{A}_j}{\sqrt{2\pi}} e^{i\omega_j t} = \sum_{j=-\infty}^{\infty} \frac{\mathcal{A}_j}{\sqrt{2\pi}} e^{ij\Delta\omega t}, \tag{3.36}$$

$$Y(\omega) = \frac{1}{\sqrt{2\pi}} \int\limits_{-\infty}^{\infty} y(t) e^{-i\omega t} dt, \tag{3.37}$$

$$y(t) = \frac{1}{\sqrt{2\pi}} \int\limits_{-\infty}^{\infty} Y(\omega) e^{i\omega t} d\omega. \tag{3.38}$$

is equally acceptable.

3.10.5   Fourier transformation of an ideal NMR signal

Let us assume that an ideal NMR signal has the form $\mathcal{A}e^{(i(\Omega-\omega)-R_2)t}$. Its Fourier transformation can be calculated easily as

$$Y(\omega) = \int\limits_{-\infty}^{\infty} y(t) e^{-i\omega t} dt = \int\limits_{0}^{\infty} \mathcal{A}e^{(i(\Omega-\omega)-R_2)t} dt = \frac{-\mathcal{A}}{i(\Omega-\omega)-R_2} = \mathcal{A}\frac{1}{R_2-i(\Omega-\omega)}\frac{R_2+i(\Omega-\omega)}{R_2+i(\Omega-\omega)} = \mathcal{A}\frac{R_2+i(\Omega-\omega)}{R_2^2+(\Omega-\omega)^2} \tag{3.39}$$

3.10.6   Properties of continuous Fourier transformation

The continuous Fourier transformation has several important properties:

- *Parseval's theorem* $\int\limits_{-\infty}^{\infty} |y(t)|^2 dt = \frac{1}{2\pi} \int\limits_{-\infty}^{\infty} |Y(\omega)|^2 d\omega$

  A conservation law, documents that the signal energy (information content) is preserved by the Fourier transformation.

- *Linearity* $\int\limits_{-\infty}^{\infty} (y(t) + z(t)) e^{-i\omega t} dt = Y(\omega) + Z(\omega)$

  It documents that a sum of periodic functions (difficult to be distinguished in the time domain) can be converted to a sum of resonance peaks (easily distinguishable in the frequency domain if the resonance frequencies differ).

- *Convolution* $\int\limits_{-\infty}^{\infty} (y(t) \cdot z(t)) e^{-i\omega t} dt = \int\limits_{-\infty}^{\infty} Y(\omega) Z(\omega - \omega') d\omega'$

  It provides mathematical description of apodization (Section 3.9)

- *Time shift* $\int\limits_{-\infty}^{\infty} y(t - t_0) e^{-i\omega t} dt = Y(\omega) e^{-i\omega t_0}$

  It shows that time delays result in frequency-dependent phase shifts in the frequency domain (Section 3.8)

- *Frequency modulation* $\int\limits_{-\infty}^{\infty} y(t) e^{i\omega_0 t} e^{-i\omega t} dt = Y(\omega - \omega_0)$

  It shows that the apparent frequencies can be shifted after acquisition.

- *Causality* $\int\limits_{-\infty}^{\infty} y(t) e^{-i\omega t} dt = \int\limits_{0}^{\infty} y(t) e^{-i\omega t} dt$

  It says that no signal is present before the radio-wave pulse (this is why we can start integration at $t = 0$ or $t = -\infty$, $y(t) = 0$ for $t < 0$). This provides an extra piece of information allowing us to reconstruct the imaginary part of the signal from the real one and vice versa (Figure 3.9 and Section 3.10.7).

3.10.7   Causality and reconstruction of imaginary signal

The consequence of causality mentioned at the end of Section 3.10.6 is rather subtle. As mentioned above, the NMR signal is recorded in two channels, as a real and imaginary part of a complex number. It is because Fourier transformation of a cosine (or sine) function gives a symmetric (or antisymmetric) spectrum with two frequency peaks and thus does not allow us to distinguish frequencies higher than the carrier frequency from those lower than the carrier frequency. Once we have the transformed complex signal in the frequency domain, we can ask whether we need both its parts (real and imaginary). It looks like we do because the inverse Fourier transformation of just the real (imaginary) part produces a symmetric (antisymmetric) picture in the time domain (the second row in Figure 3.9). But the causality tells us that this is not a problem because we know that there is no signal left from the zero time – the symmetry does not bother us because we know that we can reconstruct the time signal simply by discarding the left half of the inverse Fourier image (the third row in Figure 3.9). The time signal reconstructed from the real part of the frequency spectrum only can be then Fourier transformed to provide the missing imaginary part of the frequency spectrum. The time signal can be reconstructed from the imaginary part of the frequency spectrum in the same manner (although this is not done typically). This discussion shows that the real and imaginary parts of the frequency spectrum are not independent but carry the same information.

However, it should be emphasized that the causality principle does not apply to the NMR signal as it is acquired. In reality, the signal is *finite*, i.e., it is acquisition is stopped at $t_{\max} < \infty$. Therefore, our generalization to Eq. 3.32 does not correspond to the reality: when the Fourier transformation of really acquired signal is performed, the upper limit of integration is not infinity but $t_{\max}$. The transformation is mathematically equivalent to Eq. 3.28, with $t_{\max} = 2\pi/\Delta\omega = 1/\Delta f$. Therefore, the signal can be classified as *periodic*[4] with the period $t_{\max} = 2\pi/\Delta\omega = 1/\Delta f$. The real and imaginary parts of the integral are independent series of real and imaginary components of the coefficients $\mathcal{A}_k$ in Eq. 3.28, which contradicts the causality principle (the real and imaginary parts of a causal signal are dependent, as discussed above).

In order to introduce causality, *zero filling* has to be applied to the acquired signal, as described in Section 3.7. We take the signal as a function $y(t)$ defined in the range $0 \leq t \leq t_{\max}$. We extend $y(t)$ to a function $y^{\mathrm{ZF}}(t)$ defined in a range $-t_{\max} \leq t \leq t_{\max}$ by setting

$$y^{\mathrm{ZF}}(t) = \begin{cases} 0 & \text{for } -t_{\max} \leq t \leq 0 \\ y(t) & \text{for } 0 \leq t \leq t_{\max} \end{cases} \tag{3.40}$$

The extended function $y^{\mathrm{ZF}}(t)$ fulfills the requirement of causality (there is no signal before applying the radio-wave pulse at $t = 0$). As a consequence, the $\Re\{Y^{\mathrm{ZF}}(t)\}$ and $\Im\{Y^{\mathrm{ZF}}(t)\}$ are not independent, and each of them carries the full information. In practice, $y^{\mathrm{ZF}}(t)$ is constructed in a slightly different manner (see Section 3.7):

$$y^{\mathrm{ZF}}(t) = \begin{cases} y(t) & \text{for } 0 \leq t \leq t_{\max} \\ 0 & \text{for } t_{\max} \leq t \leq 2t_{\max} \end{cases} \tag{3.41}$$

Both variants (zeros before $t =$ and zeros after $t_{\max}$) are mathematically equivalent because $y(t)$ defined in the range $0 \leq t \leq t_{\max}$ has the periodic nature. Increasing $2t_{\max}$ in Eq. 3.41 to a higher number does not have any effect on the information content of $\Re\{Y^{\mathrm{ZF}}(t)\}$ and $\Im\{Y^{\mathrm{ZF}}(t)\}$.

3.10.8   Spectral width, resolution, and sampling

We may try to define the discrete Fourier transform as

$$Y_k = \sum_{j=0}^{N-1} y_j \mathrm{e}^{-\mathrm{i}k\Delta\omega j\Delta t}\Delta t = \sum_{j=0}^{N-1} y_j \mathrm{e}^{-\mathrm{i}2\pi\Delta f \Delta t k j}\Delta t, \tag{3.42}$$

$$y_j = \sum_{k=0}^{N-1} Y_k \mathrm{e}^{\mathrm{i}k\Delta\omega j\Delta t}\Delta t = \sum_{k=0}^{N-1} Y_k \mathrm{e}^{\mathrm{i}2\pi\Delta f \Delta t k j}\Delta f. \tag{3.43}$$

However, there is a catch here. It turns out that Δt and Δf are not independent, but closely related. The transformation can be written in a matrix form as

$$\begin{pmatrix} Y_0 \\ Y_1 \\ Y_2 \\ \vdots \\ Y_{N-1} \end{pmatrix} = \underbrace{\begin{pmatrix} F_{0,0} & F_{0,1} & F_{0,2} & \ldots F_{0,N-1} \\ F_{1,0} & F_{1,1} & F_{1,2} & \ldots F_{1,N-1} \\ F_{2,0} & F_{2,1} & F_{2,2} & \ldots F_{2,N-1} \\ \vdots & \vdots & \vdots & \ddots\vdots \\ F_{N-1,0} & F_{N-1,1} & F_{N-1,2} & \ldots F_{N-1,N-1} \end{pmatrix}}_{\hat{F}} \begin{pmatrix} y_0 \\ y_1 \\ y_2 \\ \vdots \\ y_{N-1} \end{pmatrix} \Delta t, \tag{3.44}$$

where the elements of the matrix $\hat{F}$ are $F_{jk} = \mathrm{e}^{-\mathrm{i}2\pi\Delta f \Delta t \cdot k \cdot j}$.

---

[4]Note that the signal is really acquired in a periodic manner in practice. The experiment is repeated several times in order to accumulate data and improve the signal-to-noise ratio. The repeated experiments start from some steady state, not from equilibrium because we do not let the relaxation to act for an infinite time.
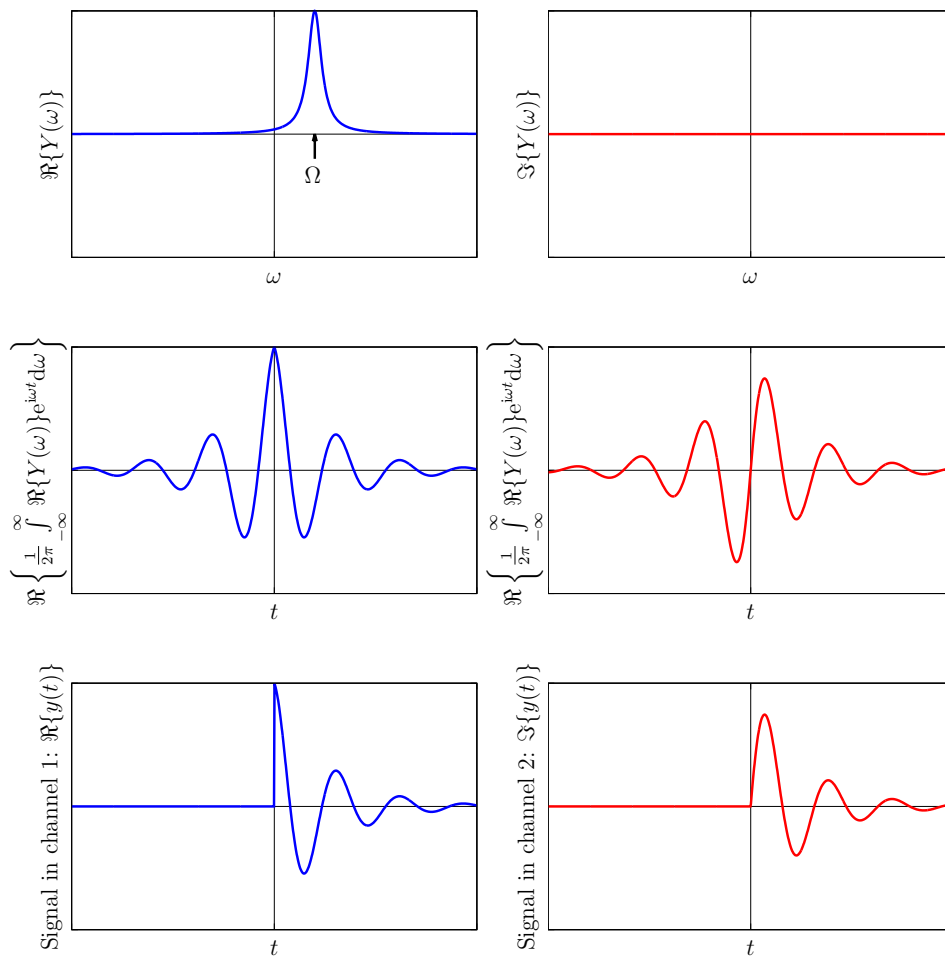
Figure 3.9: Causality of NMR signal. If we take a frequency spectrum, discard its imaginary part (the first row), and perform the inverse Fourier transformation, we do not get the original signal (starting at $t = 0$), but a set of symmetric (real part) and antisymmetric (imaginary part) functions predicting non-zero signal before $t = 0$ (the second row). However, we can apply our knowledge that no signal was present before $t = 0$ and multiply the left half of the predicted signal by zero. This recovers the actual signal (the third row). Fourier transformation of this signal provides both real and imaginary parts of the spectrum, as shown in Figure 3.2.

Let us now try to transform Y_k back to the time domain:

$$
\begin{pmatrix} y_0 \\ y_1 \\ y_2 \\ \vdots \\ y_{N-1} \end{pmatrix} = \underbrace{\begin{pmatrix} F_{0,0}^{-1} & F_{0,1}^{-1} & F_{0,2}^{-1} & \dots F_{0,N-1}^{-1} \\ F_{1,0}^{-1} & F_{1,1}^{-1} & F_{1,2}^{-1} & \dots F_{1,N-1}^{-1} \\ F_{2,0}^{-1} & F_{2,1}^{-1} & F_{2,2}^{-1} & \dots F_{2,N-1}^{-1} \\ \vdots & \vdots & \vdots & \ddots \vdots \\ F_{N-1,0}^{-1} & F_{N-1,1}^{-1} & F_{N-1,2}^{-1} & \dots F_{N-1,N-1}^{-1} \end{pmatrix}}_{\hat{F}^{-1}} \begin{pmatrix} Y_0 \\ Y_1 \\ Y_2 \\ \vdots \\ Y_{N-1} \end{pmatrix} \Delta f,
\tag{3.45}
$$

where the elements of the matrix $\hat{F}^{-1}$ are $F_{jk}^{-1} = \mathrm{e}^{+\mathrm{i}2\pi\Delta f\Delta t \cdot k\cdot j}$. Substituting from Eq. 3.44,

$$
\begin{pmatrix} y_0 \\ y_1 \\ y_2 \\ \vdots \\ y_{N-1} \end{pmatrix} = \begin{pmatrix} F_{0,0}^{-1} & F_{0,1}^{-1} & F_{0,2}^{-1} & \dots F_{0,N-1}^{-1} \\ F_{1,0}^{-1} & F_{1,1}^{-1} & F_{1,2}^{-1} & \dots F_{1,N-1}^{-1} \\ F_{2,0}^{-1} & F_{2,1}^{-1} & F_{2,2}^{-1} & \dots F_{2,N-1}^{-1} \\ \vdots & \vdots & \vdots & \ddots \vdots \\ F_{N-1,0}^{-1} & F_{N-1,1}^{-1} & F_{N-1,2}^{-1} & \dots F_{N-1,N-1}^{-1} \end{pmatrix} \begin{pmatrix} F_{0,0} & F_{0,1} & F_{0,2} & \dots F_{0,N-1} \\ F_{1,0} & F_{1,1} & F_{1,2} & \dots F_{1,N-1} \\ F_{2,0} & F_{2,1} & F_{2,2} & \dots F_{2,N-1} \\ \vdots & \vdots & \vdots & \ddots \vdots \\ F_{N-1,0} & F_{N-1,1} & F_{N-1,2} & \dots F_{N-1,N-1} \end{pmatrix} \begin{pmatrix} y_0 \\ y_1 \\ y_2 \\ \vdots \\ y_{N-1} \end{pmatrix} \Delta f\Delta t.
\tag{3.46}
$$

In order to get the original signal, the product of the transformation matrices, $\hat{F}^{-1}\hat{F}$ multiplied by $\Delta f\Delta t$, must be a unit matrix:

$$
\begin{pmatrix} F_{0,0}^{-1} & F_{0,1}^{-1} & F_{0,2}^{-1} & \dots F_{0,N-1}^{-1} \\ F_{1,0}^{-1} & F_{1,1}^{-1} & F_{1,2}^{-1} & \dots F_{1,N-1}^{-1} \\ F_{2,0}^{-1} & F_{2,1}^{-1} & F_{2,2}^{-1} & \dots F_{2,N-1}^{-1} \\ \vdots & \vdots & \vdots & \ddots \vdots \\ F_{N-1,0}^{-1} & F_{N-1,1}^{-1} & F_{N-1,2}^{-1} & \dots F_{N-1,N-1}^{-1} \end{pmatrix} \begin{pmatrix} F_{0,0} & F_{0,1} & F_{0,2} & \dots F_{0,N-1} \\ F_{1,0} & F_{1,1} & F_{1,2} & \dots F_{1,N-1} \\ F_{2,0} & F_{2,1} & F_{2,2} & \dots F_{2,N-1} \\ \vdots & \vdots & \vdots & \ddots \vdots \\ F_{N-1,0} & F_{N-1,1} & F_{N-1,2} & \dots F_{N-1,N-1} \end{pmatrix} \Delta f\Delta t = \begin{pmatrix} 1 & 0 & 0 & \dots & 0 \\ 0 & 1 & 0 & \dots & 0 \\ 0 & 0 & 1 & \dots & 0 \\ \vdots & \vdots & \vdots & \ddots & \vdots \\ 0 & 0 & 0 & \dots & 1 \end{pmatrix}.
\tag{3.47}
$$

According to the matrix multiplication rule, the jl-element of the product $\hat{F}^{-1}\hat{F}$ is given by

$$
\sum_{k=0}^{N-1} \mathrm{e}^{-\mathrm{i}2\pi\Delta f\Delta t(jk-kl)}\Delta t.
\tag{3.48}
$$

Clearly, the exponential terms in the sums representing the diagonal elements ($j = l$) are equal to $\mathrm{e}^{-\mathrm{i}2\pi\Delta f\Delta t(jk-kj)}\Delta t = \mathrm{e}^0 = 1$. Therefore, the diagonal elements (sums of N terms $\mathrm{e}^0 = 1$) are equal to N. Obviously, we need to set $N\Delta f\Delta t = 1$ to get the elements of the product $\hat{F}^{-1}\hat{F}$ equal to one.

What about the off-diagonal elements? For $N\Delta f\Delta t = 1$, the elements of $\hat{F}^{-1}\hat{F}$ are equal to

$$
\sum_{k=0}^{N-1} \mathrm{e}^{-\mathrm{i}\frac{2\pi}{N}(j-l)k}\Delta t.
\tag{3.49}
$$

The complex numbers in the sum can be visualized as points in the Gauss plane (plane of complex numbers) with the phase of $2\pi k(l-j)/N$. Let us assume that N is an integer power of two ($N = 2^n$, a typical choice in discrete Fourier transform). Then all numbers in the series are symmetrically distributed in the Gauss plane. As a consequence, their sum is equal to zero (they cancel each other). We can therefore conclude that setting $N\Delta f\Delta t = 1$ ensures that the product $\hat{F}^{-1}\hat{F}$ is a unit matrix.

3.10.9 Discrete ideal signal

In order to compare the discrete and continuous Fourier transformation quantitatively, we directly replace $\mathrm{d}t$ by Δt and integration by summation in Eq. 3.5. The ideal NMR signal converted to the digital form has the Fourier transform

$$
Y_k = \sum_{j=0}^{N-1} \mathcal{A}\mathrm{e}^{-R_2 j\Delta t}\mathrm{e}^{\mathrm{i}2\pi\nu j\Delta t}\mathrm{e}^{-\mathrm{i}\frac{2\pi}{N}kj}\Delta t.
\tag{3.50}
$$

The summation formula[5]

---

[5]The summation formula can be derived easily. Write the sum

$$
z^0 + z^1 + z^2 + \dots + z^{N-1} = \sum_{j=0}^{N-1} z^j
$$

$$\sum_{j=0}^{N-1} z^j = \frac{1-z^N}{1-z} \tag{3.51}$$

helps us to evaluate the sum. For the sake of simplicity, let us assume that the carrier frequency is chosen so that the peak is in the middle of the spectrum

$$\nu = \frac{1}{2}N\Delta f = \frac{1}{2\Delta t}. \tag{3.52}$$

Then, z and z^N in the summation formula are

$$z = e^{-R_2\Delta t}e^{i2\pi\left(\frac{1}{2}-\frac{k}{N}\right)} = \underbrace{e^{-R_2\Delta t}}_{1-R_2\Delta t}\underbrace{e^{i\pi}}_{-1}e^{-i2\pi\frac{k}{N}} = -(1-R_2\Delta t)e^{-i2\pi\frac{k}{N}}, \tag{3.53}$$

$$z^N = e^{-R_2N\Delta t}e^{i\pi(N-2k)}. \tag{3.54}$$

Note that we replaced $e^{-R_2\Delta t}$ by the Taylor series in Eq. 3.53, and neglected terms higher than linear in $R_2\Delta t$ because Δt is usually much shorter than $1/R_2$. Therefore,

$$Y_k = \mathcal{A}\Delta t\frac{1-e^{-R_2N\Delta t}e^{i\pi(N-2k)}}{1+(1-R_2\Delta t)e^{-i2\pi\frac{k}{N}}}. \tag{3.55}$$

The consequences of the discrete nature of the signal are:

Aliasing: If we add a value of $N\Delta f$ to the frequency which was originally in the middle of the frequency spectrum ($\frac{1}{2}N\Delta f = \frac{1}{2\Delta t}$), i.e. add N to $k = N/2$ in Eq. 3.11, the last exponent in the sum in Eq. 3.11 changes from $i\pi j$ to $i3\pi j$, i.e. by one period (2π), and the transformed signal (the spectrum) does not change. In general, a peak of the real frequency $\nu + N\Delta f$ (outside the spectral width) appears at the apparent frequency ν in the spectrum (*Nyquist theorem*: frequencies ν and $\nu + 1/\Delta t$ cannot be distinguished).

Offset: Peak height of the continuous Fourier transform $Y(f) = \mathcal{A}/R_2$ and offset of the continuous Fourier transform $Y(\pm\infty) = 0$. Peak height of the discrete Fourier transform.

$$Y_{\frac{N}{2}} = \mathcal{A}\Delta t\frac{1-e^{-R_2N\Delta t}}{R_2\Delta t} \rightarrow \mathcal{A}/R_2 \tag{3.56}$$

for $N\Delta t \rightarrow \infty$, but offset of the discrete Fourier transform

$$Y_0 = \mathcal{A}\Delta t\frac{1-e^{-R_2N\Delta t}e^{iN\pi}}{2-R_2\Delta t} \rightarrow \frac{1}{2}\mathcal{A}\Delta t = \frac{1}{2}y_0\Delta t \tag{3.57}$$

for $N\Delta t \rightarrow \infty$ and $\Delta t \rightarrow 0$. The offset of discrete Fourier transform is non-zero, equal to half of the intensity of the signal at the first time point $y(0)$ if the signal was acquired sufficiently long to relax completely ($N\Delta t \gg 1/R_2$).

3.10.10 Zero- and first-order phase corrections

Let us assume that the acquired signal was created by a set of rotating magnetization vectors that differ in Ω and that started to rotate at some unspecified time $-t_0$ (i.e., before the acquisition started at $t = 0$) with the same unspecified phase ϕ_0. For the sake of simplicity, we assume that all magnetization vectors relax exponentially with the same rate constant R_2. Each such magnetization vector produces a signal

$$y_n(t) = |\mathcal{A}_n|e^{-R_2(t+t_0)}e^{i(\Omega_n(t+t_0)+\phi_0)}. \tag{3.58}$$

We multiply the whole signal, i.e., each $y_n(t)$, by the correction function $e^{-i(\vartheta_0+\vartheta_1\omega)}$

$$y_n(t)e^{-i(\vartheta_0+\vartheta_1\omega)} = |\mathcal{A}_n|e^{-R_2(t+t_0)}e^{i(\Omega_n(t+t_0)+\phi_0)}e^{-i(\vartheta_0+\vartheta_1\omega)} = |\mathcal{A}_n|e^{-R_2(t+t_0)}e^{i(\Omega_n(t+t_0)+\phi_0-\vartheta_0-\vartheta_1\omega)}. \tag{3.59}$$

The Fourier transform of such modified signal is

---

and multiply it by $(1-z)$:

$$(1-z)(z^0+z^1+z^2+\cdots+z^{N-1}) = z^0-z^1+z^1-z^2+z^2+\cdots-z^{N-1}+z^{N-1}-z^N = 1-z^N = (1-z)\sum_{j=0}^{N-1} z^j.$$

Divide the last equation on the previous line by $(1-z)$ to obtain the summation formula.

$$|\mathcal{A}_n| \int\limits_{-\infty}^{\infty} e^{-R_2(t+t_0)} e^{i(\Omega_n(t+t_0)+\phi_0-\vartheta_0-\vartheta_1\omega)} e^{-i\omega t} dt = |\mathcal{A}_n| \int\limits_{-\infty}^{\infty} e^{-R_2(t+t_0)} e^{i(\Omega_n(t+t_0)+\phi_0-\vartheta_0-\vartheta_1\omega-\omega t)} dt. \tag{3.60}$$

This expression does not change if we multiply it by $1 = e^{i(\omega t_0-\omega t_0)}$.

$$|\mathcal{A}_n| \int\limits_{-\infty}^{\infty} e^{-R_2(t+t_0)} e^{i(\Omega_n(t+t_0)+\phi_0-\vartheta_0-\vartheta_1\omega-\omega t)} dt = |\mathcal{A}_n| \int\limits_{-\infty}^{\infty} e^{-R_2(t+t_0)} e^{i(\Omega_n(t+t_0)+\phi_0-\vartheta_0-\vartheta_1\omega+\omega t_0-\omega(t+t_0))} dt. \tag{3.61}$$

Note that changing the variable from t to $t + t_0$ does not change the Fourier transform (the integral) because $dt = d(t + t_0)$ and the integration limits are $-\infty$ and ∞ in both cases

$$|\mathcal{A}_n| \int\limits_{-\infty}^{\infty} e^{-R_2(t+t_0)} e^{i(\Omega_n(t+t_0)+\phi_0-\vartheta_0-\vartheta_1\omega+\omega t_0-\omega(t+t_0))} d(t+t_0) = |\mathcal{A}_n| \underbrace{e^{i(\phi_0-\vartheta_0+\omega(t_0-\vartheta_1))}}_{\substack{=1 \\ \text{if } \phi_0=\vartheta_0 \text{ and } t_0=\vartheta_1}} \underbrace{\int\limits_{-\infty}^{\infty} e^{-R_2(t+t_0)} e^{i(\Omega_n(t+t_0)} e^{-\omega(t+t_0))} d(t+t_0)}_{Y_n(\omega)}.$$

$$\tag{3.62}$$

As we can see, the effects of the initial phase and time shift are removed by multiplying the signal with $e^{-i(\vartheta_0+\vartheta_1\omega)}$ if we succeed to find the first-order phase correction $\vartheta_0 = \phi_0$ and the second-order phase correction $\vartheta_1 = t_0$.

3.10.11   Dolph–Chebyshev window

The Dolph–Chebyshev window function is defined as

$$\frac{1}{\sqrt{N}} \sum_{k=0}^{N-1} \frac{\cos\left(2(N-1)\arccos\frac{\cos(\pi k/N)}{\cos(\pi\lambda\Delta t/2)}\right)}{\cosh\left(2(N-1)\text{arccosh}\frac{1}{\cos(\pi\lambda\Delta t/2)}\right)} e^{i\frac{2\pi}{N}kj}. \tag{3.63}$$

Part II

Quantum description

Lecture 4
Review of quantum mechanics

Literature: This chapter starts with a brief review of the quantum mechanics. Textbooks covering this topic represent the best source of information. Brown presents in B9 a useful review of the classical mechanics, usually missing in the quantum mechanics textbooks (assuming that students learnt the classical mechanics earlier, which is true in the case of students of physics, but not so often in the case of chemistry or biology students), and reviews the quantum mechanics in B13, B15, and B16. B1–B5 provides overview of the relevant mathematical tools. NMR books also provide some introduction. Keeler reviews the quantum mechanics in a very understandable fashion, using the concept of the spin from the very beginning (K3.2 and K6). Levitt proceeds more like us (L6–7). A condensed summary is presented in C2.1 (short, rigorous, but not a good start for a novice).

4.1 Wave function and state of the system

This course should not provide explanation of principles of the quantum mechanics, it should build on an already acquired knowledge. Nevertheless, we briefly review basics of the quantum mechanics in this lecture because in the following lectures, we use the quantum mechanical approach to describe NMR.

The quantum mechanics was introduced because the Newton mechanics did not described experiments correctly. Yet, knowledge of the classical mechanics is very helpful in discussions of various ideas and approaches of the quantum mechanics. Those who did not have chance to study the Hamiltonian and Lagrangian mechanics in other courses may find a short summary of issues related to our topic (NMR) in Sections 4.9.1–4.9.3.

The quantum mechanics is postulated, not derived. It can be only tested experimentally. The basic differences between the Newton and quantum mechanics are listed below.

- *Newton mechanics*: coordinates x, y, z and moments $\vec{p}$ of all particles describe all properties of the current state and all future states

- *Quantum mechanics*: wave function Ψ describes all properties of the current state and all future states

---

We postulate that the state of the system is completely described by a *wave function*.

The two-slit (Young) experiment may serve as an example of motivation to use the quantum mechanics to describe experimental results. The experiment (presumably known to the reader) asks the question whether the studied microscopic objects (e.g. electrons) are particles or waves. The answer is "Particles, but with probabilities combined like waves".[1] The wave function used to describe the studied object can be interpreted as a (complex) probability amplitude $\Psi = Ce^{i\Phi}$. The (real) probability density is then $\rho = \Psi^*\Psi = |\Psi|^2 = |C|^2$ and the probability of finding single particle in volume L^3 is $\int_0^L \int_0^L \int_0^L \Psi^*\Psi \mathrm{d}x\mathrm{d}y\mathrm{d}z$. We see that calculating a probability includes a calculation of square of the complex probability amplitude. Definitions of square values of different mathematical objects and the notation used in quantum mechanics are listed in Section 4.9.4. In particular, the quantum-mechanical notation includes a convention to write

$$|\Psi\rangle \equiv \Psi, \qquad \langle\Psi| \equiv \Psi^*, \qquad \langle\Psi|\Psi\rangle \equiv \int_0^L \int_0^L \int_0^L \Psi^*\Psi \mathrm{d}x\mathrm{d}y\mathrm{d}z. \tag{4.1}$$

The wave function of a free particle moving in direction x (coordinate frame can be always chosen so that x is the direction of motion of a free particle) can be written as

$$\Psi = Ce^{i2\pi(\frac{x}{\lambda} - \frac{t}{T})} = Ce^{\frac{i}{\hbar}(px - \mathcal{E}t)}, \tag{4.2}$$

where $h = 2\pi\hbar$ is the Planck's constant, $p = mv$ is the momentum (along x), and $\mathcal{E}$ is the (kinetic) energy. Note that Ψ corresponds to a *monochromatic wave* with period equal to $h/\mathcal{E}$, wavelength equal to h/p, and a complex amplitude C (it may contain a phase factor $e^{i\phi}$).

4.2 Superposition and localization in space

Note that a monochromatic wave function describes exactly what is p of the particle (Figure 4.1A,B), but does not say anything about the *position* of the particle because $\rho = \Psi^*\Psi = |C|$ is the same for any x (the distribution of the probability is constant from $x = -\infty$ to $x = \infty$, Figure 4.1C). A wave function describing a particle (more) localized in space can be obtained by *superposition* of monochromatic waves (Figure 4.2).

$$\Psi(x,t) = c_1 \underbrace{\mathcal{A}e^{\frac{i}{\hbar}(p_1 x - \mathcal{E}_1 t)}}_{\psi_1} + c_2 \underbrace{\mathcal{A}e^{\frac{i}{\hbar}(p_2 x - \mathcal{E}_2 t)}}_{\psi_2} + \cdots \tag{4.3}$$

We postulate that if possible states of our system are described by the wave functions $\psi_1, \psi_2, \ldots$, their linear combination also describes a possible state of the system.

Note that monochromatic waves are *orthogonal* and can be normalized (Section 4.9.5).

---

[1] Quantum field theory provides more elegant description of fundamental "particles" than presented in this text. However, the relations presented in this text can be recovered from the quantum field approach.
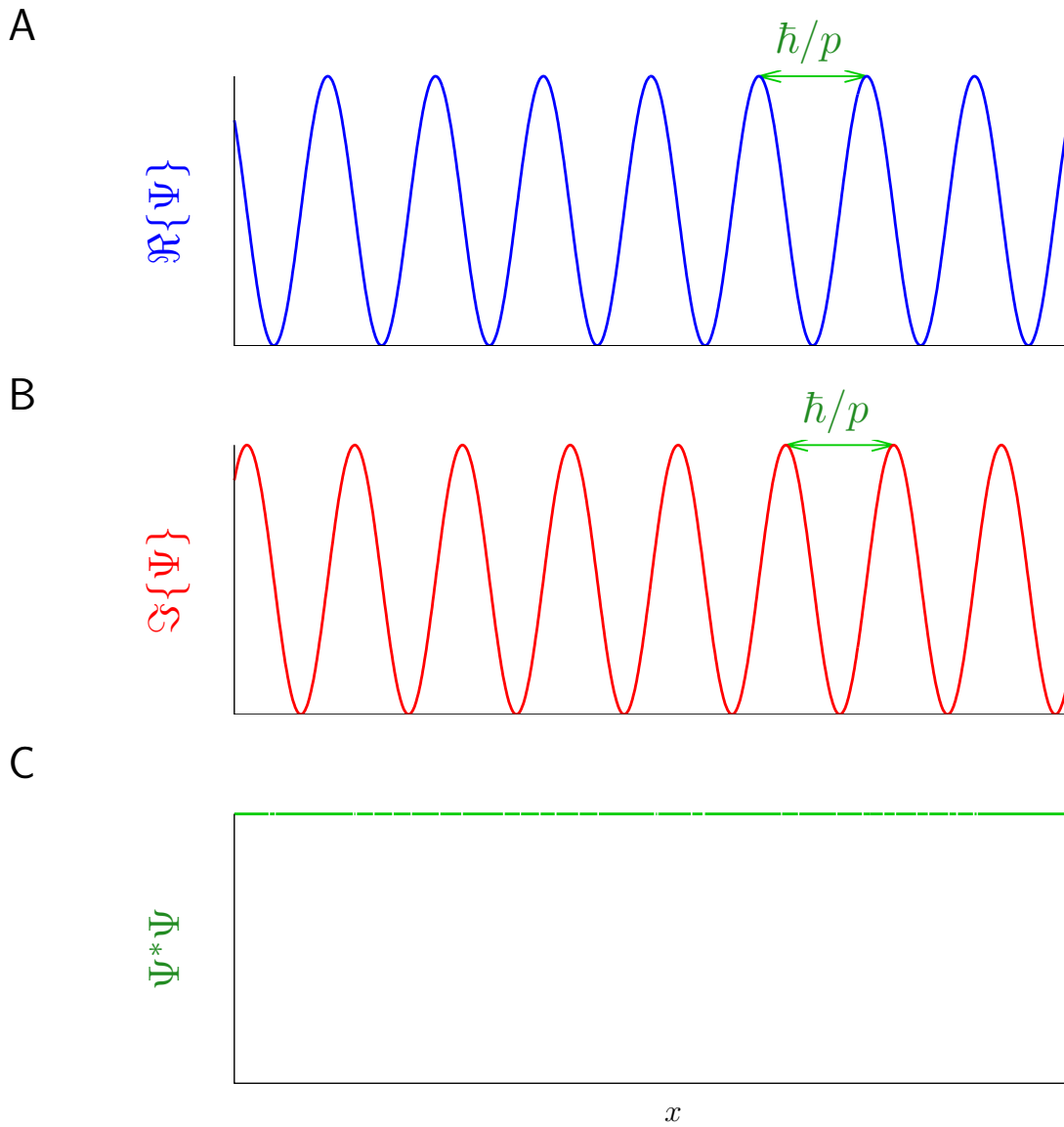
Figure 4.1: Free particle described by a monochromatic wave function Ψ. The real and imaginary parts of the wave function are plotted in Panels A and B, respectively, the probability density $\rho = \Psi^*\Psi$ is plotted in Panel C. Note that the wavelength and consequently the value of the momentum p is sharply defined (A,B), but the position of the particle is completely undefined (C).

A
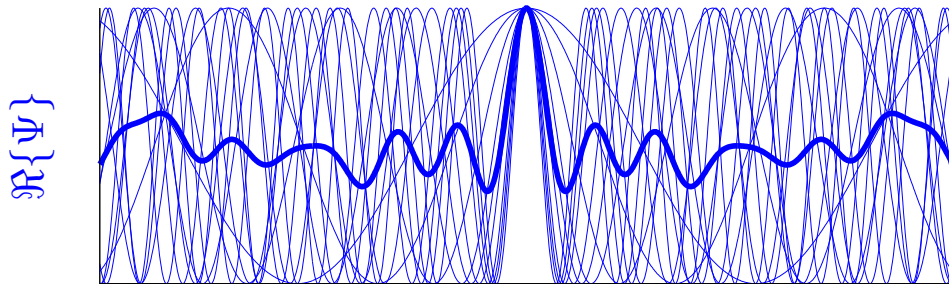
B
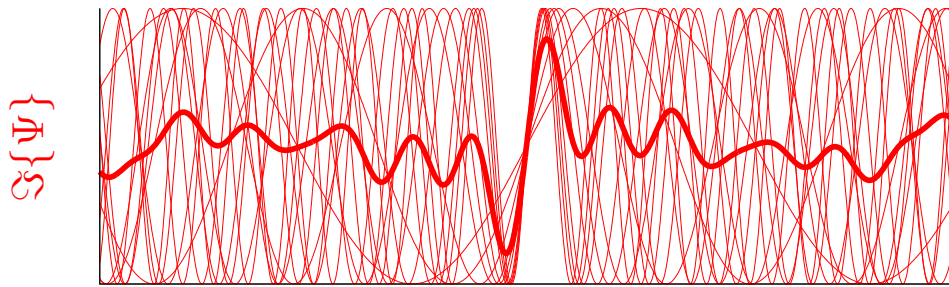
C
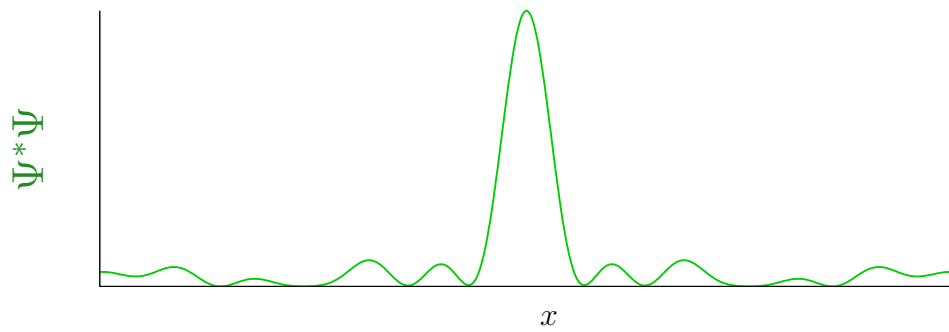
Figure 4.2: Free particle described by a superposition of ten monochromatic wave functions of the same amplitude. The real and imaginary parts of the monochromatic wave functions (thin lines) and of the final wave function Ψ (normalized to have the same amplitude as the monochromatic wave functions, thick line) are plotted in Panels A and B, respectively, the probability density $\rho = \Psi^*\Psi$ is plotted in Panel C. Note that the position of the particle starts to be defined by the maximum of $\rho = \Psi^*\Psi$, but the wavelength and consequently the value of the momentum p is no longer well defined (A,B).

4.3 Operators and possible results of measurement

We postulated that the wave function contains a complete information about the system, but how can we extract this information from the wave function?

> We postulate that any measurable property is represented by an Hermitian operator (acting on the wave function) and that result of a measurement must be one of eigenvalues of the operator.

The term *eigenvalue* and a related term *eigenfunction* are explained and an example is given in Section 4.9.6. An operator $\hat{A}$ is called *Hermitian* if

$$\langle \Psi | \hat{A}\Psi \rangle = \langle \hat{A}\Psi | \Psi \rangle \equiv \langle \Psi | \hat{A} | \Psi \rangle. \tag{4.4}$$

In this text, we usually write operators with "hats", like $\hat{A}$. Writing $\hat{A}\Psi$ means "take function Ψ and modify it as described by $\hat{A}$". It is *not* a multiplication: $\hat{A}\Psi \neq \hat{A} \cdot \Psi$, $\hat{A}$ is not a number but an instruction what to do with Ψ!

A recipe to calculate *possible results of a measurement* is:

1. Identify the operator representing what you measure ($\hat{A}$)

2. Find all eigenfunctions $|\psi_1\rangle, |\psi_2\rangle, \ldots$ of the operator and use them as an *orthonormal basis*[2] for Ψ: $|\Psi\rangle = c_1|\psi_1\rangle + c_2|\psi_2\rangle + \ldots$

3. Calculate individual eigenvalues A_j as

$$\langle \psi_j | \hat{A}\psi_j \rangle = \langle \psi_j | A_j \cdot \psi_j \rangle = A_j \underbrace{\langle \psi_j | \psi_j \rangle}_{=1} = A_j. \tag{4.5}$$

The first equation in 4.5 follows from the definition of eigenfunctions. A_j is just a number and can be factored out of the brackets (representing integration or summation) as described by the second equation. The number A_j is the eigenvalue of $\hat{A}$ for $|\psi_j\rangle$. The last equation in 4.5 reflects orthonormality of $|\psi_j\rangle$. If $\hat{A}$ is Hermitian, the same result must be obtained by calculating

$$\langle \hat{A}\psi_j | \psi_j \rangle = \langle A_j^* \cdot \psi_j | \psi_j \rangle = A_j^* \underbrace{\langle \psi_j | \psi_j \rangle}_{=1} = A_j^*, \tag{4.6}$$

i.e. A_j must be equal to its complex conjugate A_j^*. This is true only for real numbers. As a result of measurement is always a real number, the eigenvalues must be real numbers. This is why operators representing a measurable quantity must be Hermitian.

4.4 Expected result of measurement

Eq. 4.5 tells us what are the *possible* results of a measurement, but it does not say which value *is actually measured.* We can only calculate probabilities of getting individual eigenvalues and predict the expected result of the measurement.

---

[2]The term "orthonormal basis" is described in Section 4.9.5.

> We postulate that the expected result of measuring a quantity A represented by an operator $\hat{A}$ in a state of the system described by a wave function Ψ is
>
> $$\langle A \rangle = \langle \Psi | \hat{A} | \Psi \rangle. \tag{4.7}$$

There are three ways how to do the calculation described by Eq. 4.7:

1. Express Ψ, calculate its complex conjugate $\Psi^* \equiv \langle \Psi |$, calculate $\hat{A}\Psi \equiv |\hat{A}\Psi\rangle$, and in the manner of Eq. 4.79

$$\langle A \rangle = \langle \Psi | \hat{A} | \Psi \rangle \equiv \langle \Psi | (\hat{A}\Psi) \rangle = \int\limits_{-\infty}^{\infty} \Psi^*(x, \dots) \hat{A} \Psi(x, \dots) \mathrm{d}x \dots. \tag{4.8}$$

Three dots in Eq. 4.8 tell us that for anything else than a single free particle (with zero spin) we integrate over all degrees of freedom, not just over x.

2. Find eigenfunctions $\psi_1, \psi_2, \dots$ of $\hat{A}$ and write Ψ as their linear combination $\Psi = c_1\psi_1 + c_2\psi_2 + \cdots$ (use the eigenfunctions as an *orthonormal basis* for Ψ). Due to the orthonormality of the basis functions, the result of Eq. 4.8 is $\langle A \rangle = c_1^* c_1 A_1 + c_2^* c_2 A_2 + \cdots$, where $A_1, A_2, \dots$ are eigenvalues of $\hat{A}$. We see that $\langle A \rangle$ is a *weighted average* of eigenvalues A_j with the weights equal to the squares of the coefficients ($c_j^* c_j = |c_j|^2$). The same result is obtained if we calculate

$$\langle A \rangle = \begin{pmatrix} c_1^* & c_2^* & \cdots \end{pmatrix} \begin{pmatrix} A_1 & 0 & \cdots \\ 0 & A_2 & \cdots \\ \vdots & \vdots & \ddots \end{pmatrix} \begin{pmatrix} c_1 \\ c_2 \\ \vdots \end{pmatrix}. \tag{4.9}$$

We see that we can replace (i) operators by two-dimensional diagonal matrices, with eigenvalues forming the diagonal, and (ii) wave functions by one-dimensional matrices (known as the *state vectors*) composed of the coefficients c_j. Eq. 4.9 shows calculation of the expected results of the measurement of A using the *matrix representation* of the operators and the wave functions. The matrix representation is a big simplification because it allows us to calculate $\langle A \rangle$ without knowing how the operator $\hat{A}$ and its eigenfunctions look like! We just need the eigenvalues and coefficients c_j. This simplification is possible because the right coefficients are defined by the right choice of the basis.

3. Write Ψ as a linear combination of basis functions $\psi_1', \psi_2', \dots$ (not necessarily eigenfunctions of $\hat{A}$)

$$\Psi = c_1'\psi_1' + c_2'\psi_2' + \cdots \tag{4.10}$$

Build a two-dimensional matrix $\hat{P}'$ from the products of the coefficients $c_j'^* c_k'$:

$$\hat{P}' = \begin{pmatrix} c_1' c_1'^* & c_1' c_2'^* & \cdots \\ c_2' c_1'^* & c_2' c_2'^* & \cdots \\ \vdots & \vdots & \ddots \end{pmatrix}. \tag{4.11}$$

Multiply the matrix $\hat{P}'$ by a matrix[3] $\hat{A}'$ representing the operator $\hat{A}$ in the basis $\psi_1', \psi_1', \ldots$. The sum of the diagonal elements (called *trace*) of the resulting matrix $\hat{P}'\hat{A}'$ is equal[4] to the expected value $\langle A \rangle$

$$\langle A \rangle = \mathrm{Tr}\{\hat{P}'\hat{A}'\}. \tag{4.12}$$

Why should we use such a bizarre way of calculating the expected value of A when it can be calculated easily from Eq. 4.9? The answer is that Eq. 4.12 is *more general*. We can use the same basis for operators with different sets of eigenfunctions.

For the sake of completeness, we should point out that the quantum mechanics must also somehow describe result of a measurement that has been already done and that gave us one value of A. We need an operator that identifies the wave function describing the state corresponding to the measured value A_m. Such operator is called the *projection operator* $\hat{P}_m$ and its form is derived in Section 4.9.9.

> We postulate that if A_m is the result of measuring A in the state described by $|\Psi\rangle$, then the state immediately after the measurement is described by $\hat{P}_m|\Psi\rangle / \sqrt{\langle\Psi|\hat{P}_m|\Psi\rangle}$, where $\hat{P}_m$ is the projection operator associated with A_m.

---

[3]How can we get a matrix representation of an operator with eigenfunctions different from the basis? The complete set of N functions defines an abstract N-dimensional space ($N = \infty$ for free particles!). The wave function Ψ is represented by a vector in this space built from coefficients $c_1', c_2', \ldots$, as described by Eq. 4.10, and a change of the basis is described as a rotation in this space. The same rotation describes how the matrix representing the operator $\hat{A}$ changes upon changing the basis. Note that the matrix is not diagonal if the basis functions are not eigenfunctions of $\hat{A}$.

[4]The trace of the product $\hat{P}'\hat{A}'$ is equal to

$$\begin{pmatrix} c_1'^* & c_2'^* & \cdots \end{pmatrix} \begin{pmatrix} A_{11}' & A_{12}' & \cdots \\ A_{21}' & A_{22}' & \cdots \\ \vdots & \vdots & \ddots \end{pmatrix} \begin{pmatrix} c_1 \\ c_2 \\ \vdots \end{pmatrix},$$

but it must be also equal to

$$\begin{pmatrix} c_1'^* & c_2'^* & \cdots \end{pmatrix} \begin{pmatrix} A_{11}'^* & A_{12}'^* & \cdots \\ A_{21}'^* & A_{22}'^* & \cdots \\ \vdots & \vdots & \ddots \end{pmatrix} \begin{pmatrix} c_1 \\ c_2 \\ \vdots \end{pmatrix}$$

because $\hat{A}$ is Hermitian. This shows that the diagonal elements of matrices representing Hermitian operators must be real numbers $A_{jj}'^* = A_{jj}'$ and the off-diagonal elements must be such complex numbers that $A_{jk}'^* = A_{kj}'$.

4.5 Operators of position and momentum, commutators

We need to find operators in order to describe measurable quantities. Let us start with the most fundamental quantities, the *position* of a particle x and the *momentum* $p = mv$, that completely describe studied systems in the Newton mechanics. Their operators are defined in terms of their *mutual relation*. Therefore, we first discuss a general relation of two operators. If we apply two operators subsequently to the same wave function, the order of the operators sometimes does not matter

$$\hat{A}\hat{B}f = \hat{B}\hat{A}f \quad \Rightarrow \quad \hat{A}\hat{B}f - \hat{B}\hat{A}f = 0. \tag{4.13}$$

However, sometimes the order of the operators makes a difference

$$\hat{A}\hat{B}f \neq \hat{B}\hat{A}f \quad \Rightarrow \quad \hat{A}\hat{B}f - \hat{B}\hat{A}f \neq 0. \tag{4.14}$$

The difference of the operators can be viewed as a new operator $(\hat{A}\hat{B} - \hat{B}\hat{A})$ known as the *commutator* and written as

$$\hat{A}\hat{B}f - \hat{B}\hat{A}f = (\hat{A}\hat{B} - \hat{B}\hat{A})f = [\hat{A}, \hat{B}]f. \tag{4.15}$$

A non-zero commutator tells us that the quantities represented by $\hat{A}$ and $\hat{B}$ are not independent and cannot be measured exactly at the same time.

> We postulate that the operators of the position and of the momentum obey the relations
>
> $$[\hat{r}_j, \hat{p}_k] = i\hbar\delta_{jk} \qquad [\hat{r}_j, \hat{r}_k] = [\hat{p}_j, \hat{p}_k] = 0. \tag{4.16}$$

Note that we only postulate relations between the operators. Various choices of expressing the operators are possible and correct as long as Eq. 4.16 holds. A frequently used choice is described below.

The wave function $\Psi(x, t)$ defined by Eq. 4.3 is a function of the position of the particle, not of the momentum (it is a sum of contributions of *all* possible momenta). If we define the basis as a set of functions $\psi_j = \Psi(x_j, t)$ for all possible positions x_j, the operator of the position is simply *multiplication by the value of the coordinate* describing the given position (see Section 4.9.7). Operators of the positions in the y and z directions are defined in the same manner.

$$\hat{x} \equiv x \cdot \qquad \hat{y} \equiv y \cdot \qquad \hat{z} \equiv z \cdot \tag{4.17}$$

In Section 4.9.6, an operator of the momentum of a particle moving in the x direction is obtained by calculating $\partial\Psi/\partial x$ (Eq. 4.87). If a particle moves in a general direction, operators of components of the momentum vector are derived in the same manner.

$$\hat{p}_x \equiv -\mathrm{i}\hbar\frac{\partial}{\partial x}, \tag{4.18}$$

$$\hat{p}_y \equiv -\mathrm{i}\hbar\frac{\partial}{\partial y}, \tag{4.19}$$

$$\hat{p}_z \equiv -\mathrm{i}\hbar\frac{\partial}{\partial z}. \tag{4.20}$$

It is shown in Section 4.9.8 that such a choice is compatible with the postulate described by Eq. 4.16. Note that the commutator relations described in Section 4.9.8 follow from the way how we defined Ψ in Eq. 4.3. However, we can also use Eq. 4.16 as the fundamental definition and Eq. 4.3 as its consequence. This is how we postulate the definition of the position and momentum operators here.

4.6   Operator of energy and equation of motion

The arguments presented in Section 4.9.10 show that the eigenvalues of the total (kinetic and potential) energy of a free particle can be obtained by calculating $\partial\Psi/\partial t$. If the particles experience forces that depend only on the coordinates (and can be calculated as gradients of the potential energy), the sum of the kinetic and potential energy is equal to the Hamiltonian $\mathcal{H}$ in the classical mechanics (Section 4.9.1). The same term is used for the corresponding quantum mechanical operator, labeled $\hat{H}$.

The association of the Hamiltonian (energy operator) with the time derivative makes the Hamiltonian essential for the analysis of the dynamics of systems in the quantum mechanics:

We postulate that evolution of a system in time is given by the Hamiltonian:

$$\mathrm{i}\hbar\frac{\partial\Psi}{\partial t} = \hat{H}\Psi. \tag{4.21}$$

Note that our first postulate (the wave function completely describes the system, including its future) requires that the wave equation contains only the first time derivative (not e.g. the second time derivative). The explanation is provided in Section 4.9.11.

Eq. 4.21 can be also written for the matrix representations of Ψ and $\hat{H}$. If the eigenfunctions of $\hat{H}$ are used as a basis ($\Psi = c_1(t)\psi_1 + c_2(t)\psi_2 + \cdots$), the time-independent eigenfunctions ψ_j can be factored out from $\partial\Psi/\partial t$ (left-hand side) and Ψ (right-hand side), and canceled, giving

$$\mathrm{i}\hbar\frac{\mathrm{d}}{\mathrm{d}t}\begin{pmatrix} c_1 \\ c_2 \\ \vdots \end{pmatrix} = \begin{pmatrix} \mathcal{E}_1 & 0 & \cdots \\ 0 & \mathcal{E}_2 & \cdots \\ \vdots & \vdots & \ddots \end{pmatrix}\begin{pmatrix} c_1 \\ c_2 \\ \vdots \end{pmatrix}, \tag{4.22}$$

which is simply a set of independent differential equations

$$\frac{\mathrm{d}c_j}{\mathrm{d}t} = -\mathrm{i}\frac{\mathcal{E}_j}{\hbar}c_j \quad \Rightarrow \quad c_j = a_j\mathrm{e}^{-\mathrm{i}\frac{\mathcal{E}_j}{\hbar}t}, \tag{4.23}$$

where the (possibly complex) integration constant a_j is given by the value of c_j at $t = 0$.

Note that the coefficients c_j evolve, but the products $c_j^* c_j = |a_j|^2$ do not change in time. Each product $c_j^* c_j$ describes the probability that the system is in the state with the energy equal to the eigenvalue $\mathcal{E}_j$, described by an eigenfunction ψ_j.

- States corresponding to the eigenfunctions of the Hamiltonian are *stationary* (do not vary in time).

- Only stationary states can be described by the *energy level diagram.*

Since our goal is the quantum description of NMR, it is useful to see how is the evolution of a wave function influenced by the magnetic fields. Therefore, we list the equations of motions for wave functions describing a free particle, a particle in an electric field, and a particle in an electric and magnetic field. All three variants are known as the *Schrödinger equation.*

- *Free particle.* As shown in Section 4.9.10, a wave function describing a free particle evolves as

$$
i\hbar \frac{\partial \Psi}{\partial t} = \underbrace{\left(-\frac{\hbar^2}{2m} \left(\frac{\partial^2}{\partial x^2} + \frac{\partial^2}{\partial x^2} + \frac{\partial^2}{\partial x^2} \right) \right)}_{\hat{H}} \Psi. \tag{4.24}
$$

- *Charged particle in an electric field.* Electric forces depend only on the position of the charge in the electrical field. Therefore, the electric potential energy can be described as $QV(x, y, z)$, where Q is the electric charge and $V(x, y, z)$ is an electrostatic potential. As follows from the classical mechanics (Section 4.9.1), and is also shown in Section 4.9.10, the effect of an electric field is accounted for simply by adding the electric potential energy $\mathcal{E}_{\text{pot}}(x, y, z) = QV(x, y, z)$ to the Hamiltonian

$$
i\hbar \frac{\partial \Psi}{\partial t} = \underbrace{\left(-\frac{\hbar^2}{2m} \left(\frac{\partial^2}{\partial x^2} + \frac{\partial^2}{\partial y^2} + \frac{\partial^2}{\partial z^2} \right) + QV(x, y, z) \right)}_{\hat{H}} \Psi. \tag{4.25}
$$

- *Charged particle in an electromagnetic field.* The real challenge is to describe the effect of the magnetic field on the evolution in time. The problem is that the magnetic force does not depend solely on the position in the field, but also on the *velocity* of the charge (Eq. 4.53). This case is analyzed in detail in Section 4.9.2, showing that the effect of the magnetic field can be described by the *vector potential*, a vector quantity that can be used to define the magnetic induction $\vec{B} = \vec{\nabla} \times \vec{A} = \left(\frac{\partial A_z}{\partial y} - \frac{\partial A_y}{\partial z}, \frac{\partial A_x}{\partial z} - \frac{\partial A_z}{\partial x}, \frac{\partial A_y}{\partial x} - \frac{\partial A_x}{\partial y} \right)$. As shown in Section 4.9.2, the vector potential modifies the momentum $\vec{p} \to \vec{p} - Q\vec{A}$ and the resulting wave equation is

$$
i\hbar \frac{\partial \Psi}{\partial t} = \underbrace{\left(\frac{1}{2m} \left(\left(i\hbar \frac{\partial}{\partial x} + QA_x \right)^2 + \left(i\hbar \frac{\partial}{\partial y} + QA_y \right)^2 + \left(i\hbar \frac{\partial}{\partial z} + QA_z \right)^2 \right) + QV(x, y, z) \right)}_{\hat{H}} \Psi.
$$

$$\tag{4.26}$$

4.7 Operator of angular momentum

In order to understand NMR experiments, we also need to describe the *rotation* in space. The fundamental quantity related to the rotation is the *angular momentum.* In a search for its operator, we start from what we know, from the position and momentum operators. We use the classical physics and just replace the values of the coordinates and of the momentum components by their operators.

The classical definition of the vector of the angular momentum $\vec{L}$ is

$$\vec{L} = \vec{r} \times \vec{p}. \tag{4.27}$$

The vector product represents the following set of equations:

$$L_x = r_y p_z - r_z p_y, \tag{4.28}$$
$$L_y = r_z p_x - r_x p_z, \tag{4.29}$$
$$L_z = r_x p_y - r_y p_x. \tag{4.30}$$

Going to the operators

$$\hat{L}_x = \hat{r}_y \hat{p}_z - \hat{r}_z \hat{p}_y = -i\hbar y \frac{\partial}{\partial z} + i\hbar z \frac{\partial}{\partial y}, \tag{4.31}$$

$$\hat{L}_y = \hat{r}_z \hat{p}_x - \hat{r}_x \hat{p}_z = -i\hbar z \frac{\partial}{\partial x} + i\hbar x \frac{\partial}{\partial z}, \tag{4.32}$$

$$\hat{L}_z = \hat{r}_x \hat{p}_y - \hat{r}_y \hat{p}_x = -i\hbar x \frac{\partial}{\partial y} + i\hbar y \frac{\partial}{\partial x}, \tag{4.33}$$

$$\hat{L}^2 = \hat{L}_x^2 + \hat{L}_y^2 + \hat{L}_z^2. \tag{4.34}$$

As shown in Section 4.9.12

$$[\hat{L}_x, \hat{L}_y] = i\hbar \hat{L}_z, \tag{4.35}$$

$$[\hat{L}_y, \hat{L}_z] = i\hbar \hat{L}_x, \tag{4.36}$$

$$[\hat{L}_z, \hat{L}_x] = i\hbar \hat{L}_y, \tag{4.37}$$

but

$$[\hat{L}^2, \hat{L}_x] = [\hat{L}^2, \hat{L}_y] = [\hat{L}^2, \hat{L}_z] = 0. \tag{4.38}$$

Note that

- Two components of the angular momentum cannot be measured exactly at the same time.

- Eqs. 4.35–4.38 can be used as a definition of the angular momentum operators if the position and momentum operators are not available.[5]

The relationship between the angular momentum and the rotation is discussed in Sections 4.9.13. Eigenvalues and eigenfunctions of the commuting operators $\hat{L}^2$ and $\hat{L}_z$ are derived in Sections 4.9.14 and 4.9.15, respectively.

4.8   Operator of orbital magnetic moment

Knowing the operator of the angular momentum, we can easily define the operators of the orbital magnetic moment.

A moving charged particle can be viewed as an electric current. The classical definition of the magnetic moment of a charged particle travelling in a circular path (orbit) is (Section 0.6.2)

$$\vec{\mu} = \frac{Q}{2}(\vec{r} \times \vec{v}) = \frac{Q}{2m}(\vec{r} \times \vec{p}) = \frac{Q}{2m}\vec{L} = \gamma\vec{L}, \tag{4.39}$$

where Q is the charge of the particle, m is the mass of the particle, $\vec{v}$ is the velocity of the particle, and γ is known as the *magnetogyric ratio (constant)*.[6]

Therefore, we can write the operators

$$\hat{\mu}_x = \gamma\hat{L}_x \qquad \hat{\mu}_y = \gamma\hat{L}_y \qquad \hat{\mu}_z = \gamma\hat{L}_z \qquad \hat{\mu}^2 = \gamma^2\hat{L}^2. \tag{4.40}$$

Finally, we can define the operator of the energy (Hamiltonian) of a magnetic moment in a magnetic field. Classically, the energy of a magnetic moment $\vec{\mu}$ in a magnetic field of the induction $\vec{B}$ is $\mathcal{E} = -\vec{\mu} \cdot \vec{B}$. Accordingly, the Hamiltonian of the interactions of an orbital magnetic moment with a magnetic field is

$$\hat{H} = -B_x\hat{\mu}_x - B_y\hat{\mu}_y - B_z\hat{\mu}_z = -\gamma\left(B_x\hat{L}_x + B_y\hat{L}_y + B_z\hat{L}_z\right) = -\frac{Q}{2m}\left(B_x\hat{L}_x + B_y\hat{L}_y + B_z\hat{L}_z\right). \tag{4.41}$$

In contrast to the operators of the orbital angular momentum and of the magnetic moment, the derivation of the intrinsic angular momentum, known as the *spin*, and of the associated magnetic moment, requires a more fundamental (and much more demanding) approach. We discuss such approach in the next Lecture.

HOMEWORK

As a preparation for the next lecture, derive the Dirac equation (Section 5.7.3), and check if you understand why the $\hat{\gamma}$ matrices in Dirac equation (Eq. 5.2) can have the required properties, whereas numbers cannot (Section 5.7.4).

---

[5]Eqs. 4.35–4.38 are sometimes written in a condensed form as $[\hat{L}_j, \hat{L}_k] = i\hbar\epsilon_{jkl}\hat{L}_l$ and $[\hat{L}^2, \hat{L}_j] = 0$, where $j, k, l \in \{x, y, z\}$ and $\epsilon_{jkl} = 1$ for $jkl = xyz$ or any even permutation of x, y, z in ϵ_{xyz} (even number of exchanges of subscripts x, y, z in ϵ_{xyz}, e.g. ϵ_{yzx} is obtained by two exchanges: first $x \leftrightarrow y$ and subsequently $x \leftrightarrow z$), $\epsilon_{jkl} = -1$ for any odd permutation of x, y, z in ϵ_{xyz}, $\epsilon_{jkl} = 0$ for two or three identical subscripts (e.g. ϵ_{xyy}).

[6]The term *gyromagnetic ratio* is also used.

4.9 SUPPORTING INFORMATION

4.9.1 Classical mechanics: Newton, Lagrange, Hamilton

Newton's laws describe mechanics using *forces*. In the presence of a force $\vec{F}$, motion of a particle of a mass m is described by the second Newton's law

$$\vec{F} = m\vec{a} = \frac{\mathrm{d}\vec{p}}{\mathrm{d}t}. \tag{4.42}$$

As an alternative, the Newton mechanics can be reformulated in terms of *energies*. The total kinetic energy of a body consisting of N particles is

$$\mathcal{E}_{\mathrm{kin}} = \frac{1}{2}m\sum_{k=1}^{N} \vec{v}_k \cdot \vec{v}_k \tag{4.43}$$

and depends only on the velocities of the particles $\vec{v}_k$, not on their positions $\vec{r}_k$. The total kinetic energy can be related to the accelerations as follows

$$\frac{\partial \mathcal{E}_{\mathrm{kin}}}{\partial v_{kl}} = \frac{1}{2}m(2v_{kl}) = mv_{kl} = p_{kl}, \tag{4.44}$$

$$ma_{kl} = \frac{\mathrm{d}}{\mathrm{d}t}(mv_{kl}) = \frac{\mathrm{d}p_{kl}}{\mathrm{d}t} = \frac{\mathrm{d}}{\mathrm{d}t}\frac{\partial \mathcal{E}_{\mathrm{kin}}}{\partial v_{kl}}, \tag{4.45}$$

where k is the particle number and l is the direction (x, y, or z). In the presence of forces that depend only on the coordinates (x, y, or z) and can be calculated as gradients of potential energy, the formulation of the second Newton's law is straightforward

$$\frac{\mathrm{d}p_{kl}}{\mathrm{d}t} = \frac{\mathrm{d}}{\mathrm{d}t}\frac{\partial \mathcal{E}_{\mathrm{kin}}}{\partial v_{kl}} = \frac{\partial \mathcal{E}_{\mathrm{pot}}}{\partial r_{kl}} = F_{kl}. \tag{4.46}$$

Since our $\mathcal{E}_{\mathrm{kin}}$ depends only on velocities and not on position in space, and $\mathcal{E}_{\mathrm{pot}}$ depends only on position in space and not on velocities, $\mathcal{E}_{\mathrm{kin}}$ and $\mathcal{E}_{\mathrm{pot}}$ can be combined into one variable called *Lagrangian* $\mathcal{L}$:

$$0 = \frac{\mathrm{d}p_{kl}}{\mathrm{d}t} - F_{kl} = \frac{\mathrm{d}}{\mathrm{d}t}\frac{\partial \mathcal{E}_{\mathrm{kin}}}{\partial v_{kl}} - \frac{\partial \mathcal{E}_{\mathrm{pot}}}{\partial r_{kl}} = \frac{\mathrm{d}}{\mathrm{d}t}\frac{\partial(\mathcal{E}_{\mathrm{kin}} - \mathcal{E}_{\mathrm{pot}})}{\partial v_{kl}} - \frac{\partial(\mathcal{E}_{\mathrm{kin}} - \mathcal{E}_{\mathrm{pot}})}{\partial r_{kl}} \equiv \frac{\mathrm{d}}{\mathrm{d}t}\frac{\partial \mathcal{L}}{\partial v_{kl}} - \frac{\partial \mathcal{L}}{\partial r_{kl}}. \tag{4.47}$$

A set of Eq. 4.47 for all values of k and l ($3N$ combinations) describes well a set of N free particles, which has $3N$ degrees of freedom. If the mutual positions of particles are constrained by C constrains (e.g. atoms in a molecule), the number of degrees of freedom is lower ($3N - C$) and the number of equations can be reduced. It is therefore desirable to replace the $3N$ values of r_{kl} by $3N - C$ values of *generalized coordinates* q_j. Each value of r_{kl} is then a combination of q_j values, and

$$\mathrm{d}r_{kl} = \sum_{j=1}^{3N-C} \frac{\partial r_{kl}}{\partial q_j}\mathrm{d}q_j, \tag{4.48}$$

and (if the constraints do not depend on time)

$$v_{kl} = \frac{\mathrm{d}r_{kl}}{\mathrm{d}t} = \sum_{j=1}^{3N-C} \frac{\partial r_{kl}}{\partial q_j}\frac{\mathrm{d}q_j}{\mathrm{d}t} \equiv \sum_{j=1}^{3N-C} \frac{\partial r_{kl}}{\partial q_j}\dot{q}_j, \tag{4.49}$$

where the dot represents time derivative. The equation of motion can be thus rewritten as

$$\frac{\mathrm{d}}{\mathrm{d}t}\frac{\partial \mathcal{L}}{\partial \dot{q}_j} = \frac{\partial \mathcal{L}}{\partial q_j}. \tag{4.50}$$

We obtained Eq. 4.50 starting from the second Newton's law. However, mechanics can be also built in the opposite direction, starting from the following statement. *Equation of motion describing a physical process that starts at time t_1 and ends at time t_2 must be such that the integral $\int_{t_1}^{t_2} \mathcal{L}\mathrm{d}t$ is stationary, in other words, that the variation of the integral is zero.* This statement is known as the *least action principle* and, using calculus of variation (as nicely described in The Feynman Lectures on Physics, Vol. 2, Chapter 19), Eq. 4.50 can be derived from it.[7] There is, however, no general rule how to express the Lagrangian as an explicit function of generalized coordinates and velocities. Finding the Lagrangian may be a demanding task, requiring experience and physical intuition.

---

[7]Richard Feynman showed that quantum mechanics can be reformulated by using

$$\mathrm{e}^{\mathrm{i}\int_{t_1}^{t_2}\mathcal{L}/\hbar\mathrm{d}t}$$

as a probability amplitude (*path integral approach*).

Lagrangian can be converted to yet another energy-related function, known as *Hamiltonian*. Lagrangian and Hamiltonian are related by the *Legendre transformation* (see Section 4.9.3).

$$\mathcal{H}(q_j, p_j) + \mathcal{L}(q_j, \dot{q}_j) = \sum_j (p_j \cdot \dot{q}_j), \tag{4.51}$$

where

$$p_j = \frac{\partial \mathcal{L}}{\partial \dot{q}_j}. \tag{4.52}$$

For our set of N unconstrained particles exposed to forces that do not depend on the particle velocities, $q_j = r_{kl}$ and $p_j = \frac{\partial \mathcal{L}}{\partial \dot{q}_j}$ is the linear momentum of the k-th particle in the direction l (cf. Eq. 4.44) and the Hamiltonian is simply the sum of total kinetic and potential energy ($\mathcal{H} = \mathcal{E}_{\text{kin}} + \mathcal{E}_{\text{pot}}$). In general, p_j is called the *canonical momentum*.

The introduction of Lagrangian and Hamiltonian approaches may seem to be an unnecessarily complication of the description of classical mechanics. However, Hamiltonians and Lagrangians become essential when we search for quantum mechanical description of particles observed in magnetic resonance experiments because Hamiltonian describes evolution of quantum states in time.[8]

4.9.2 Lagrangian and Hamiltonian including magnetism

Derivation of the Hamiltonian (classical or quantum) for magnetic particles in magnetic fields is much more demanding because the magnetic force depends on the velocity of moving charged particles. Therefore, velocity enters the Lagrangian not only through the kinetic energy and the canonical momentum is no longer identical with the linear momentum. We start our analysis by searching for a classical Lagrangian describing motion of a charged particle in a magnetic field, and then convert it to the Hamiltonian using Legendre transformation.

We know that the Lagrangian should give us the Lorentz force

$$\vec{F} = Q(\vec{E} + \vec{v} \times \vec{B}). \tag{4.53}$$

We know that a velocity-independent force is a gradient of the corresponding potential energy. For the electric force,

$$\vec{F} = \vec{\nabla}\mathcal{E}_{\text{el}} = Q\vec{\nabla}V, \tag{4.54}$$

where the electric potential energy $\mathcal{E}_{\text{el}}$ and the electric potential V are scalar quantities. Intuitively, we expect the magnetic force to be also a gradient of some scalar quantity (some sort of magnetic potential energy or magnetic potential). The magnetic force is given by $Q\vec{v} \times \vec{B}$, so the magnetic energy should be proportional to the velocity. But the velocity is a vector quantity, not a scalar. We may guess that the scalar quantity resembling the electric potential may be a scalar product of velocity with another vector. This tells us that the search for the electromagnetic Lagrangian is a search for a vector that, when included in the Lagrangian, correctly reproduces the Lorentz force, expressed in terms of $\vec{E}$ and $\vec{B}$ in Eq. 4.53. The information about $\vec{E}$ and $\vec{B}$ can be extracted from the following Maxwell equations

$$\vec{\nabla} \cdot \vec{B} = 0 \tag{4.55}$$

$$\vec{\nabla} \times \vec{E} = -\frac{\partial \vec{B}}{\partial t}, \tag{4.56}$$

but we have to employ our knowledge of vector algebra to handle the divergence in Eq. 4.55 and the curl in Eq. 4.56.

First, note that we look for a scalar product, but Eq. 4.53 contains a vector product. The useful identity $\vec{a} \times (\vec{b} \times \vec{c}) = \vec{b}(\vec{a} \cdot \vec{c}) - (\vec{a} \cdot \vec{b})\vec{c}$ tells us that it would be nice to replace $\vec{B}$ with a curl of another vector because it would give us, after inserting in Eq. 4.53, the desired gradient of scalar product:

$$\vec{v} \times (\vec{\nabla} \times \vec{A}) = \vec{\nabla}(\vec{v} \cdot \vec{A}) - (\vec{v} \cdot \vec{\nabla})\vec{A}). \tag{4.57}$$

The vector $\vec{A}$ is a so-called *vector potential*.

Another identity says that $\vec{a} \cdot (\vec{a} \times \vec{b}) = 0$ for any vectors $\vec{a}$ and $\vec{b}$ because $\vec{a} \times \vec{b} \perp \vec{a}$. As a consequence, we can really replace $\vec{B}$ by a curl (rotation) of some vector $\vec{A}$ because $\vec{\nabla} \cdot (\vec{\nabla} \times \vec{A}) = 0$ as required by Eq. 4.55. The first step thus gives us a new definition of $\vec{B}$

$$\vec{B} = \vec{\nabla} \times \vec{A} \tag{4.58}$$

which can be inserted into Eq. 4.53

$$\vec{F} = Q(\vec{E} + \vec{v} \times \vec{B}) = Q(\vec{E} + \vec{v} \times (\vec{\nabla} \times \vec{A})), \tag{4.59}$$

and using the aforementioned identity $\vec{a} \times (\vec{b} \times \vec{c}) = \vec{b}(\vec{a} \cdot \vec{c}) - (\vec{a} \cdot \vec{b})\vec{c}$,

---

[8]The Hamiltonian can be also used to describe time evolution in classical mechanics.

$$\vec{F} = Q(\vec{E} + \vec{v} \times \vec{B}) = Q(\vec{E} + \vec{v} \times (\vec{\nabla} \times \vec{A})) = Q(\vec{E} + \vec{\nabla}(\vec{v} \cdot \vec{A}) - (\vec{v} \cdot \vec{\nabla})\vec{A}). \tag{4.60}$$

Second, we use our new definition of $\vec{B}$ and rewrite Eq. 4.56 as

$$0 = \frac{\partial \vec{B}}{\partial t} + \vec{\nabla} \times \vec{E} = \vec{\nabla} \times \frac{\partial \vec{A}}{\partial t} + \vec{\nabla} \times \vec{E} = \vec{\nabla} \times \left(\frac{\partial \vec{A}}{\partial t} + \vec{E} \right). \tag{4.61}$$

Third, we notice that for any vector $\vec{a}$ and constant c, $\vec{a} \times (c\vec{a}) = 0$ because $\vec{a} \parallel c\vec{a}$. As a consequence, we can replace $(\partial \vec{A}/\partial t + \vec{E})$ by a gradient of some scalar V because $\vec{\nabla} \times (\vec{\nabla}(\partial \vec{A}/\partial t + \vec{E})) = \vec{\nabla} \times (-\vec{\nabla}V) = 0$ as required by Eq. 4.56. The scalar V is the well-known electric potential and allows us to express $\vec{E}$ as w combine

$$\vec{E} = -\frac{\partial \vec{A}}{\partial t} - \vec{\nabla}V. \tag{4.62}$$

which can be also inserted into Eq. 4.53

$$\vec{F} = Q(\vec{E} + \vec{v} \times \vec{B}) = Q\left(-\frac{\partial \vec{A}}{\partial t} - \vec{\nabla}V + \vec{\nabla}(\vec{v} \cdot \vec{A}) - (\vec{v} \cdot \vec{\nabla})\vec{A} \right). \tag{4.63}$$

Finally, we notice that

$$\frac{\mathrm{d}\vec{A}}{\mathrm{d}t} = \frac{\partial \vec{A}}{\partial t} + \frac{\partial \vec{A}}{\partial x}\frac{\mathrm{d}x}{\mathrm{d}t} + \frac{\partial \vec{A}}{\partial y}\frac{\mathrm{d}y}{\mathrm{d}t} + \frac{\partial \vec{A}}{\partial z}\frac{\mathrm{d}z}{\mathrm{d}t} = \frac{\partial \vec{A}}{\partial t} + \left(\vec{v} \cdot \vec{\nabla} \right)\vec{A} \quad \Rightarrow \quad \frac{\partial \vec{A}}{\partial t} = \frac{\mathrm{d}\vec{A}}{\mathrm{d}t} - \left(\vec{v} \cdot \vec{\nabla} \right)\vec{A}, \tag{4.64}$$

which shows that $\left(\vec{v} \cdot \vec{\nabla} \right)\vec{A}$ in Eq. 4.63 can be can be included into $\mathrm{d}\vec{A}/\mathrm{d}t$

$$\vec{F} = Q(\vec{E} + \vec{v} \times \vec{B}) = Q\left(-\frac{\partial \vec{A}}{\partial t} - \vec{\nabla}V + \vec{\nabla}(\vec{v} \cdot \vec{A}) - (\vec{v} \cdot \vec{\nabla})\vec{A} \right) = Q\left(-\frac{\mathrm{d}\vec{A}}{\mathrm{d}t} - \vec{\nabla}V + \vec{\nabla}(\vec{v} \cdot \vec{A}) \right). \tag{4.65}$$

Let us now try to write $\mathcal{L}$ as

$$\mathcal{L} = \mathcal{E}_{\mathrm{kin}} - \mathcal{E}_{\mathrm{el}} + \mathcal{E}_{\mathrm{magn}} = \frac{1}{2}mv^2 - QV + \mathcal{E}_{\mathrm{magn}}, \tag{4.66}$$

where $\mathcal{E}_{\mathrm{el}}$ is a typical potential energy dependent on position but not on speed, and $\mathcal{E}_{\mathrm{magn}}$ can depend on both position and speed. For this Lagrangian,

$$\frac{\partial \mathcal{L}}{\partial x} = \frac{\partial \mathcal{E}_{\mathrm{el}}}{\partial x} + \frac{\partial \mathcal{E}_{\mathrm{magn}}}{\partial x} = -Q\frac{\partial V}{\partial x} + \frac{\partial \mathcal{E}_{\mathrm{magn}}}{\partial x} \tag{4.67}$$

$$\frac{\mathrm{d}}{\mathrm{d}t}\frac{\partial \mathcal{L}}{\partial v_x} = \frac{\mathrm{d}}{\mathrm{d}t}\left(\frac{\partial \mathcal{E}_{\mathrm{kin}}}{\partial v_x} + \frac{\partial \mathcal{E}_{\mathrm{magn}}}{\partial v_x} \right) = ma_x + \frac{\mathrm{d}}{\mathrm{d}t}\frac{\partial \mathcal{E}_{\mathrm{magn}}}{\partial v_x}. \tag{4.68}$$

If we use $\mathcal{E}_{\mathrm{magn}} = Q\vec{v} \cdot \vec{A}$, Eqs. 4.67 and 4.68 with Eq. 4.50 for $q = x$ give us

$$ma_x = -Q\left(\frac{\mathrm{d}A_x}{\mathrm{d}t} - \frac{\partial V}{\partial x} + \frac{\partial(\vec{v} \cdot \vec{A})}{\partial x} \right) \tag{4.69}$$

and a sum with similar y- and z-components is equal to the Lorentz force

$$m\vec{a} = F = Q\left(-\frac{\mathrm{d}\vec{A}}{\mathrm{d}t} - \vec{\nabla}V + \vec{\nabla}(\vec{v} \cdot \vec{A}) \right) = Q(\vec{E} + \vec{v} \times \vec{B}). \tag{4.70}$$

We have found that our (classical and non-relativistic) Lagrangian has the form

$$\mathcal{L} = \frac{1}{2}mv^2 - QV + Q(\vec{v} \cdot \vec{A}). \tag{4.71}$$

According to Eq. 4.52, the canonical momentum has the following components

$$p_x = \frac{\partial \mathcal{L}}{\partial v_x} = mv_x + QA_x \qquad p_y = \frac{\partial \mathcal{L}}{\partial v_y} = mv_y + QA_y \qquad p_z = \frac{\partial \mathcal{L}}{\partial v_z} = mv_y + QA_z. \tag{4.72}$$

The Hamiltonian can be obtained as usually as the Legendre transform

$$\mathcal{H} = \sum_{j=x,y,z} p_j v_j - \mathcal{L} = \vec{p} \cdot \vec{v} - \mathcal{L} = \vec{p} \cdot \vec{v} - \frac{1}{2}mv^2 + QV - Q(\vec{v} \cdot \vec{A}). \tag{4.73}$$

In order to express $\mathcal{H}$ as a function of $\vec{p}$, we express $\vec{v}$ as $(\vec{p} - Q\vec{A})/m$:

$$\mathcal{H} = \frac{\vec{p} \cdot (\vec{p} - Q\vec{A})}{m} - \frac{(\vec{p} - Q\vec{A})^2}{2m} + QV - \frac{Q(\vec{p} - Q\vec{A}) \cdot \vec{A}}{m} = \frac{2\vec{p} \cdot (\vec{p} - Q\vec{A}) - (\vec{p} - Q\vec{A})^2 - 2Q(\vec{p} - Q\vec{A}) \cdot \vec{A}}{2m} + QV$$

$$= \frac{2p^2 - 2Q\vec{p} \cdot \vec{A} - p^2 + 2Q\vec{p} \cdot \vec{A} - Q^2A^2 - 2Q\vec{p} \cdot \vec{A} + 2Q^2A^2}{2m} + QV = \frac{p^2 - 2Q\vec{p} \cdot \vec{A} + Q^2A^2}{2m} + QV = \frac{(\vec{p} - Q\vec{A})^2}{2m} + QV. \tag{4.74}$$

We use Eq. 4.74 in Section 5.7.8 as a starting point of quantum mechanical description of the spin magnetic moment.

4.9.3 Legendre transformation

The Legendre transformation has a simple graphical representation (Figure 4.3). If we plot (Figure 4.3A) a function of a variable x, e.g. $f(x)$, slope at a certain value of $x = \xi$ is equal to $s(\xi) = (\partial f/\partial x)_\xi$. A tangent line $y(\xi)$ touching the plotted f for $x = \xi$ is described by the slope $s(\xi)$ and intercept $g(\xi)$ as $y = g + s(\xi)x$. The value of the intercept for all possible values of ξ can be expressed as a function of the slope $g(s) = y(\xi) - s(\xi)\xi = f(\xi) - s(\xi)\xi$ (y and f are equal at $x = \xi$ because they touch each other). If we identify x with $\dot{q}$, f with $\mathcal{L}$, and $-g$ with $\mathcal{H}$ (Figure 4.3B), we get Eq. 4.51 for a one-dimensional case ($j = 1$). The inverse Legendre transformation is defined in a similar manner for the function $g(s)$ and its slope t at $s = \sigma$ (Figure 4.3C), or for $-g = \mathcal{H}$ and $f = \mathcal{L}$ (Figure 4.3D).

4.9.4 Calculating square

Recall how "square" is calculated for various mathematical objects: for a real number $c^2 = cc$, for a complex number $|c|^2 = cc^*$, for vector $\vec{v}$ composed of N real numbers $v_1, v_2, \ldots$, which can be written in a matrix form as a row or column of the numbers $v_1, v_2, \ldots$,

$$|v|^2 = \vec{v} \cdot \vec{v} = v_1 v_1 + v_2 v_2 + \cdots = \sum_{j=1}^{N} v_j v_j = \begin{pmatrix} v_1 & v_2 & \cdots \end{pmatrix} \begin{pmatrix} v_1 \\ v_2 \\ \vdots \end{pmatrix}, \tag{4.75}$$

for a vector $\vec{v}$ composed of N complex numbers $c_1 = a_1 + \mathrm{i}b_1, c_2 = a_2 + \mathrm{i}b_2, \ldots$

$$|v|^2 = \vec{v}^\dagger \cdot \vec{v} = c_1^* c_1 + c_2^* c_2 + \cdots = \sum_{j=1}^{N} c_j^* c_j = \sum_{j=1}^{N} (a_j - \mathrm{i}b_j)(a_j + \mathrm{i}b_j) = \begin{pmatrix} c_1^* & c_2^* & \cdots \end{pmatrix} \begin{pmatrix} c_1 \\ c_2 \\ \vdots \end{pmatrix} = \begin{pmatrix} a_1 - \mathrm{i}b_1 & a_2 - \mathrm{i}b_2 & \cdots \end{pmatrix} \begin{pmatrix} a_1 + \mathrm{i}b_1 \\ a_2 + \mathrm{i}b_2 \\ \vdots \end{pmatrix},$$
$$\tag{4.76}$$

for a (continuous and possibly complex) function

$$\int_{-\infty}^{\infty} f^*(x)f(x)\mathrm{d}x \tag{4.77}$$

(function can be viewed as a vector of infinite number of infinitely "dense" elements, summation is therefore replaced by integration). Paul Dirac introduced the following notation: $|v\rangle$, $|f\rangle$ is a vector v or function f, respectively, and

$$\langle v|v \rangle = \vec{v}^\dagger \cdot \vec{v} = \sum_{j=1}^{N} v_j^* v_j, \tag{4.78}$$

$$\langle f|f \rangle = \int_{-\infty}^{\infty} f^*(x)f(x)\mathrm{d}x. \tag{4.79}$$
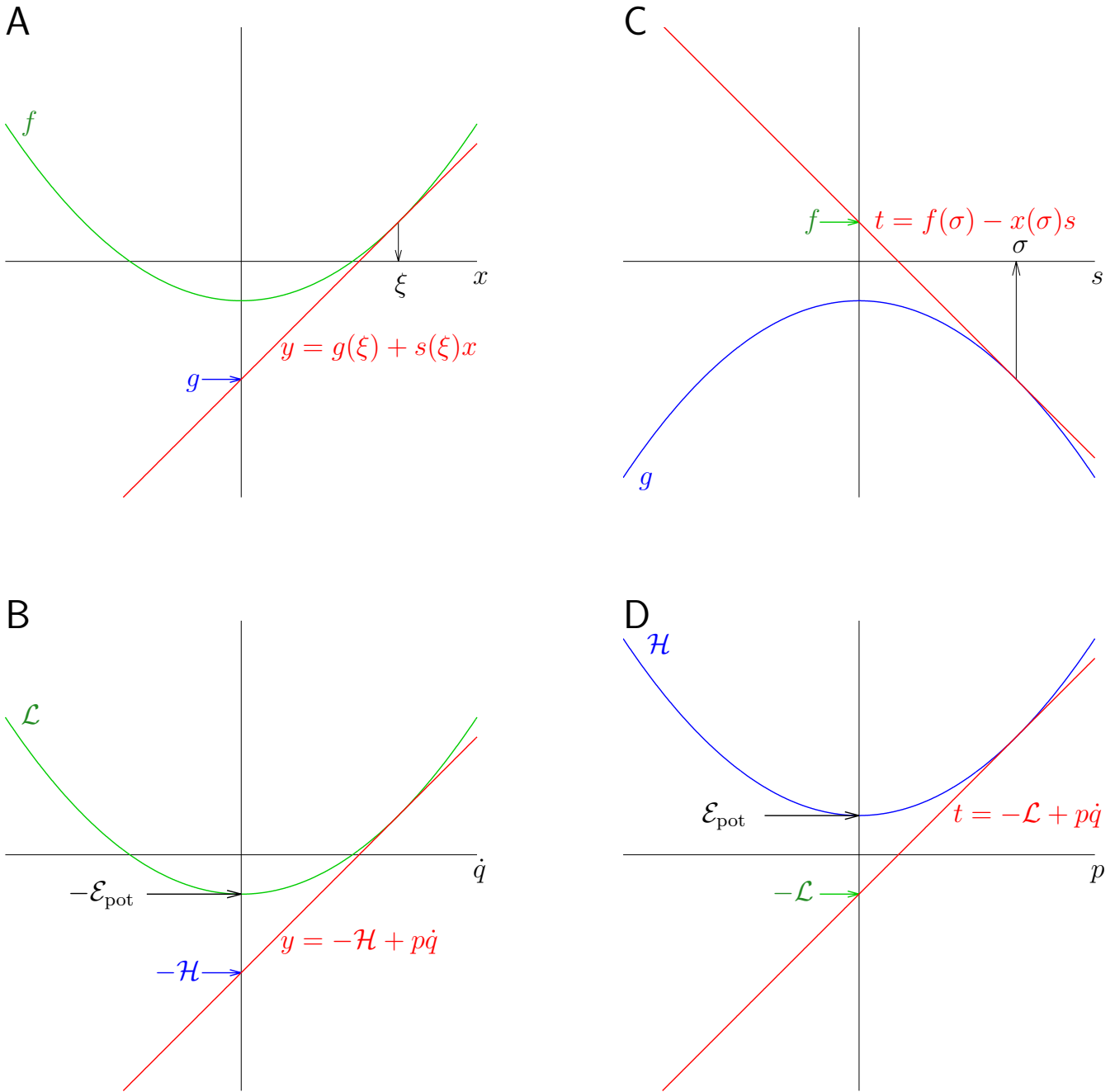
Figure 4.3: Legendre transformation of a general function $f(x)$ (A) and of one-dimensional Lagrangian $\mathcal{L}$ (B), and inverse Legendre transformation of a general function $g(s)$ of one-dimensional Lagrangian $\mathcal{L}$ and Hamiltonian $\mathcal{H}$ (D). The transformation is presented for a Lagrangian $\mathcal{L}$ and a Hamiltonian $\mathcal{H}$ describing forces independent of the velocity.

4.9.5 Orthogonality and normalization of monochromatic waves

Note that monochromatic waves are *orthogonal*, i.e., a scalar product of two waves differing in p is equal to zero:

$$\langle\psi_1|\psi_2\rangle = \int\limits_{-\infty}^{\infty} \psi_1^*\psi_2 \mathrm{d}x = \int\limits_{-\infty}^{\infty} \mathcal{A}^*\mathrm{e}^{-\frac{\mathrm{i}}{\hbar}(p_1 x - \mathcal{E}_1 t)}\mathcal{A}\mathrm{e}^{\frac{\mathrm{i}}{\hbar}(p_2 x - \mathcal{E}_2 t)}\mathrm{d}x = |\mathcal{A}|^2 \mathrm{e}^{\frac{\mathrm{i}}{\hbar}(\mathcal{E}_1-\mathcal{E}_2)t}\int\limits_{-\infty}^{\infty}\mathrm{e}^{\frac{\mathrm{i}}{\hbar}(p_1-p_2)x}\mathrm{d}x =$$

$$|\mathcal{A}|^2 \mathrm{e}^{\frac{\mathrm{i}}{\hbar}(\mathcal{E}_1-\mathcal{E}_2)t}\int\limits_{-\infty}^{\infty}\cos\frac{(p_1-p_2)x}{\hbar}\mathrm{d}x + \mathrm{i}|\mathcal{A}|^2 \mathrm{e}^{\frac{\mathrm{i}}{\hbar}(\mathcal{E}_1-\mathcal{E}_2)t}\int\limits_{-\infty}^{\infty}\sin\frac{(p_1-p_2)x}{\hbar}\mathrm{d}x = 0 \tag{4.80}$$

unless $p_1 = p_2$ (positive and negative parts of sine and cosine functions cancel each other during integration, with the exception of $\cos 0 = 1$).

Values of $\mathcal{A}$ can be also *normalized* to give the result of Eq. 4.80 equal to 1 if $p_1 = p_2$ and $\mathcal{E}_1 = \mathcal{E}_2$. The requirement $\langle\psi_1|\psi_2\rangle = 0$ for $p_1 \neq p_2, \mathcal{E}_1 \neq \mathcal{E}_2$ and $\langle\psi_1|\psi_2\rangle = 1$ for $p_1 = p_2, \mathcal{E}_1 = \mathcal{E}_2$ can be written using the *delta function* (see Section 3.10.4):

$$|\mathcal{A}|^2\int\limits_{-\infty}^{\infty}\mathrm{e}^{\frac{\mathrm{i}}{\hbar}(p_1-p_2)x}\mathrm{d}x = \delta(p_1-p_2), \tag{4.81}$$

taken into account the fact that $\mathrm{e}^{\frac{\mathrm{i}}{\hbar}(\mathcal{E}_1-\mathcal{E}_2)t} = 1$ for $\mathcal{E}_1 = \mathcal{E}_2$. Repeating the analysis presented in Section 3.10.4 (replacing ω by $p/\hbar$, and t by x) shows that

$$|\mathcal{A}|^2\int\limits_{-\infty}^{\infty}\mathrm{e}^{\frac{\mathrm{i}}{\hbar}(p_1-p_2)x}\mathrm{d}x = \frac{1}{\sqrt{2\pi\hbar}}\int\limits_{-\infty}^{\infty}\mathrm{e}^{\frac{\mathrm{i}}{\hbar}(p_1-p_2)x}\mathrm{d}x = h^{-\frac{1}{2}}\int\limits_{-\infty}^{\infty}\mathrm{e}^{\frac{\mathrm{i}}{\hbar}(p_1-p_2)x}\mathrm{d}x = \delta(p_1-p_2) \tag{4.82}$$

(cf. Eqs. 3.35 and 3.37). The procedure can be extended to the three-dimensional case, where all three coordinates of the momentum vectors $\vec{p}_1$ and $\vec{p}_2$ must be equal to get non-zero $\langle\psi_1|\psi_2\rangle$. This can be written as

$$\langle\psi_1|\psi_2\rangle = h^{-\frac{3}{2}}\int\limits_{-\infty}^{\infty}\int\limits_{-\infty}^{\infty}\int\limits_{-\infty}^{\infty}\mathrm{e}^{\frac{\mathrm{i}}{\hbar}(\vec{p}_1-\vec{p}_2)\cdot\vec{r}}\mathrm{d}\vec{r} = h^{-\frac{3}{2}}\int\limits_{-\infty}^{\infty}\mathrm{e}^{\frac{\mathrm{i}}{\hbar}(p_{1,x}-p_{2,x})x}\mathrm{d}x\int\limits_{-\infty}^{\infty}\mathrm{e}^{\frac{\mathrm{i}}{\hbar}(p_{1,y}-p_{2,y})y}\mathrm{d}y\int\limits_{-\infty}^{\infty}\mathrm{e}^{\frac{\mathrm{i}}{\hbar}(p_{1,z}-p_{2,z})z}\mathrm{d}z$$

$$= \delta(\vec{p}_1-\vec{p}_2) = \delta(p_{1,x}-p_{2,x})\cdot\delta(p_{1,y}-p_{2,y})\cdot\delta(p_{1,z}-p_{2,z}). \tag{4.83}$$

In the language of algebra, the complete set of normalized monochromatic waves constitutes an *orthonormal basis* for wave functions, in a similar way as unit vectors $\vec{i},\vec{j},\vec{k}$ are the orthonormal basis for all vectors in the Cartesian coordinate system x,y,z.

Also, Ψ (linear combination of $\psi_1,\psi_2,\dots$) can be normalized based on the condition

$$\int\limits_{-\infty}^{\infty}\Psi^*\Psi\mathrm{d}x = P = 1 \tag{4.84}$$

(if a particle exists, it must be somewhere). It requires

$$\int\limits_{-\infty}^{\infty}(c_1^*c_1 + c_2^*c_2 + \cdots)\mathrm{d}x = 1. \tag{4.85}$$

4.9.6 Eigenfunctions and eigenvalues, operator of momentum

In order to understand what quantum mechanics says about measurable properties of the studied system, let us ask a question: How can we get the value of a momentum of a free particle described by Eq. 4.3? What operation should be applied to $\Psi(x)$ (a function of x) in order to get the value of the momentum? Calculation of $\partial\Psi/\partial x$ gives us a clue:

$$\frac{\partial\Psi}{\partial x} = c_1\frac{\partial}{\partial x}\mathrm{e}^{\frac{\mathrm{i}}{\hbar}(p_1 x - \mathcal{E}_1 t)} + c_2\frac{\partial}{\partial x}\mathrm{e}^{\frac{\mathrm{i}}{\hbar}(p_2 x - \mathcal{E}_2 t)} + \cdots = \frac{\mathrm{i}}{\hbar}p_1 c_1\mathrm{e}^{\frac{\mathrm{i}}{\hbar}(p_1 x - \mathcal{E}_1 t)} + \frac{\mathrm{i}}{\hbar}p_2 c_2\mathrm{e}^{\frac{\mathrm{i}}{\hbar}(p_2 x - \mathcal{E}_2 t)} + \cdots \tag{4.86}$$

It implies that

$$-\mathrm{i}\hbar\frac{\partial}{\partial x}\mathrm{e}^{\frac{\mathrm{i}}{\hbar}(p_1 x - \mathcal{E}_1 t)} = p_1\mathrm{e}^{\frac{\mathrm{i}}{\hbar}(p_1 x - \mathcal{E}_1 t)}, \quad -\mathrm{i}\hbar\frac{\partial}{\partial x}\mathrm{e}^{\frac{\mathrm{i}}{\hbar}(p_2 x - \mathcal{E}_2 t)} = p_2\mathrm{e}^{\frac{\mathrm{i}}{\hbar}(p_2 x - \mathcal{E}_2 t)},\dots \tag{4.87}$$

We see that

1. Calculation of the partial derivative of any monochromatic wave and multiplying the result by $-i\hbar$ gives us the same wave just multiplied by a constant. The instruction to calculate the partial derivative and multiply the result by $-i\hbar$ is an example of an *operator*. If application of the operator to a function gives the same function, only multiplied by a constant, the function is called *eigenfunction* of the operator and the constant is called *eigenvalue* of the operator.

2. The eigenvalues are well-defined, measurable physical quantities – possible values of the momentum along x.

3. The eigenvalues can be obtained by applying the operator to the eigenfunctions and multiplying the results by the complex conjugates of the eigenfunctions, e.g.

$$p_1 = e^{-\frac{i}{\hbar}(p_1 x - \mathcal{E}_1 t)} \left(-i\hbar \frac{\partial}{\partial x} e^{\frac{i}{\hbar}(p_1 x - \mathcal{E}_1 t)} \right) = e^{-\frac{i}{\hbar}(p_1 x - \mathcal{E}_1 t)} p_1 e^{\frac{i}{\hbar}(p_1 x - \mathcal{E}_1 t)} = p_1 \underbrace{e^{-\frac{i}{\hbar}(p_1 x - \mathcal{E}_1 t)} e^{\frac{i}{\hbar}(p_1 x - \mathcal{E}_1 t)}}_{=1}. \tag{4.88}$$

4.9.7 Operator of position

The question we ask now is: What operation should I apply to Ψ (a function of x) in order to get the value of its coordinate? When $-i\hbar\partial/\partial x$ is used as an operator of momentum (in the x direction), applied to $\Psi(x)$, multiplication by the coordinate x is an operator of the position of the particle (in the x direction). To see how the operator acts, let us write $\Psi(x,t)$ as a series of the values $\Psi(x_j,t)$ for all possible positions x_j.[9] Then, the product $x\Psi(x,t)$ can be written as

$$x \cdot \Psi(x,t) = \begin{pmatrix} x_1 c_1 e^{\frac{i}{\hbar}(p_1 x_1 - \mathcal{E}_1 t)} + x_1 c_2 e^{\frac{i}{\hbar}(p_2 x_1 - \mathcal{E}_2 t)} + x_1 c_3 e^{\frac{i}{\hbar}(p_3 x_1 - \mathcal{E}_3 t)} + \cdots \\ x_2 c_1 e^{\frac{i}{\hbar}(p_1 x_2 - \mathcal{E}_1 t)} + x_2 c_2 e^{\frac{i}{\hbar}(p_2 x_2 - \mathcal{E}_2 t)} + x_2 c_3 e^{\frac{i}{\hbar}(p_3 x_2 - \mathcal{E}_3 t)} + \cdots \\ x_3 c_1 e^{\frac{i}{\hbar}(p_1 x_3 - \mathcal{E}_1 t)} + x_3 c_2 e^{\frac{i}{\hbar}(p_2 x_3 - \mathcal{E}_2 t)} + x_3 c_3 e^{\frac{i}{\hbar}(p_3 x_3 - \mathcal{E}_3 t)} + \cdots \\ \vdots \end{pmatrix} = \begin{pmatrix} x_1 \cdot \Psi(x_1) \\ x_2 \cdot \Psi(x_2) \\ x_3 \cdot \Psi(x_3) \\ \vdots \end{pmatrix}. \tag{4.89}$$

If the position of the particle is e.g. x_2,

$$\Psi(x_2,t) = \begin{pmatrix} 0 \\ c_1 e^{\frac{i}{\hbar}(p_1 x_2 - \mathcal{E}_1 t)} + c_2 e^{\frac{i}{\hbar}(p_2 x_2 - \mathcal{E}_2 t)} + c_3 e^{\frac{i}{\hbar}(p_3 x_2 - \mathcal{E}_3 t)} + \cdots \\ 0 \\ \vdots \end{pmatrix} = \begin{pmatrix} 0 \\ \Psi(x_2) \\ 0 \\ \vdots \end{pmatrix} \tag{4.90}$$

and $x \cdot \Psi(x,t)$ for $x = x_2$ is

$$x_2 \cdot \Psi(x_2,t) = \begin{pmatrix} 0 \\ x_2 \left(c_1 e^{\frac{i}{\hbar}(p_1 x_2 - \mathcal{E}_1 t)} + c_2 e^{\frac{i}{\hbar}(p_2 x_2 - \mathcal{E}_2 t)} + c_3 e^{\frac{i}{\hbar}(p_3 x_2 - \mathcal{E}_3 t)} + \cdots \right) \\ 0 \\ \vdots \end{pmatrix} = \begin{pmatrix} 0 \\ x_2 \cdot \Psi(x_2) \\ 0 \\ \vdots \end{pmatrix}. \tag{4.91}$$

We see that multiplication of $\Psi(x_2,t)$ by x_2 results in $x_2\Psi(x_2)$, i.e., $\Psi(x_2)$ is an eigenfunction of the operator $\hat{x} = x\cdot$ and x_2 is the corresponding eigenvalue.

Note that multiplication by p_j does not work in the same way! We could multiply $\Psi(x_2)$ by x_2 because $\Psi(x_2)$ does not depend on any other value of the x coordinate. However, $\Psi(x_2)$ depends on all possible values of p. On the other hand, the partial derivative $\partial\Psi/\partial x$ in Eq 4.86 gave us each monochromatic wave multiplied by its value of p and ensured that the monochromatic waves acted as eigenfunctions.

4.9.8 Commutation relations of the position and momentum operators

It is easy to check that subsequently applied operators related to different coordinates commute. For example

$$\hat{x}\hat{y}\Psi = xy\Psi = yx\Psi = \hat{y}\hat{x}\Psi, \tag{4.92}$$

$$\hat{p}_x\hat{p}_y\Psi = -\hbar^2 \frac{\partial^2 \Psi}{\partial x \partial y} = -\hbar^2 \frac{\partial^2 \Psi}{\partial y \partial x} = \hat{p}_y\hat{p}_x\Psi, \tag{4.93}$$

or

---

[9]We write the continuous function $\Psi(x)$ as a vector formally containing distinct elements $\Psi(x_1), \Psi(x_2), \ldots$. In a similar fashion, we write x as a vector containing a series of all values of the coordinate x: $x_1, x_2, \ldots$.

$$\hat{x}\hat{p}_y\Psi = -\mathrm{i}\hbar x \frac{\partial \Psi}{\partial y} = -\mathrm{i}\hbar\left(\frac{\partial(x\Psi)}{\partial y}\right) = \hat{p}_y\hat{x}\Psi. \tag{4.94}$$

However,

$$\hat{x}\hat{p}_x\Psi = -\mathrm{i}\hbar x \frac{\partial \Psi}{\partial x} \tag{4.95}$$

but

$$\hat{p}_x\hat{x}\Psi = -\mathrm{i}\hbar\frac{\partial(x\Psi)}{\partial x} = -\mathrm{i}\hbar\Psi - \mathrm{i}\hbar x\frac{\partial \Psi}{\partial x}. \tag{4.96}$$

We see that

- commutators of operators of a coordinate and the momentum component in the same direction are equal to $\mathrm{i}\hbar$ (i.e., multiplication of Ψ by the factor $\mathrm{i}\hbar$),

- all other position and coordinate operators commute,

in agreement with Eq. 4.16.

4.9.9 Projection operator

Let us assume that the state of the studied system immediately before measuring a quantity A was described by the wave function $|\Psi\rangle$, expressed in the basis of orthogonal eigenfunctions of $\hat{A}$ as

$$|\Psi\rangle = c_1|\psi_1\rangle + c_2|\psi_2\rangle + \cdots = |c_1|\mathrm{e}^{\mathrm{i}\phi_1}|\psi_1\rangle + |c_2|\mathrm{e}^{\mathrm{i}\phi_2}|\psi_2\rangle + \cdots \tag{4.97}$$

The measurement provided a value $A_m = c_m c_m^* = |c_m|^2$, one of eigenvalues of $\hat{A}$. Let us also assume that all eigenvalues are different. Application of the operator $|\psi_m\rangle\langle\psi_m|/|c_m|^2$ to $|\Psi\rangle$ gives

$$\frac{1}{|c_m|}|\psi_m\rangle\langle\psi_m|\Psi\rangle = \frac{1}{|c_m|}|\psi_m\rangle\langle\psi_m|(c_1|\psi_1\rangle + \cdots + c_m|\psi_m\rangle + \cdots) = \frac{1}{|c_m|}c_m|\psi_m\rangle = \frac{1}{|c_m|}|c_m|\mathrm{e}^{\mathrm{i}\phi_m}|\psi_m\rangle = \mathrm{e}^{\mathrm{i}\phi_m}|\psi_m\rangle, \tag{4.98}$$

where $\mathrm{e}^{\mathrm{i}\phi_m}|\psi_m\rangle$ describes the state immediately after the measurement.

If n different eigenfunctions $|\psi_{m,1}\rangle, |\psi_{m,2}\rangle, \ldots |\psi_{m,n}\rangle$ have the same eigenvalue $|c_m|$, Eq. 4.98 is modified to

$$= \frac{\sum_{j=1}^{n}|\psi_{m,j}\rangle\langle\psi_{m,j}|}{\sqrt{n}|c_m|}\left(c_1|\psi_1\rangle + \cdots + \sum_{j=1}^{n}c_{m,j}|\psi_{m,j}\rangle + \cdots\right) = \frac{1}{\sqrt{n}|c_m|}|c_m|\sum_{j=1}^{n}\mathrm{e}^{\mathrm{i}\phi_{m,j}}|\psi_{m,j}\rangle = \sum_{j=1}^{n}\frac{\mathrm{e}^{\mathrm{i}\phi_{m,j}}}{\sqrt{n}}|\psi_{m,j}\rangle, \tag{4.99}$$

where the final sum (linear combination of eigenfunctions $|\psi_{m,j}\rangle$) describes the state immediately after the measurement.

The operator $\hat{P}_m = \sum_{j=1}^{n}|\psi_{m,j}\rangle\langle\psi_{m,j}|$ is known as the *projection operator*, and the normalization constant can be defined using the relation

$$\langle\Psi|\hat{P}_m|\Psi\rangle = \left(c_1^*\langle\psi_1| + \cdots + \sum_{j=1}^{n}c_{m,j}^*\langle\psi_{m,j}| + \cdots\right)\sum_{j=1}^{n}|\psi_{m,j}\rangle\langle\psi_{m,j}|\left(c_1|\psi_1\rangle + \cdots + \sum_{j=1}^{n}c_{m,j}|\psi_{m,j}\rangle + \cdots\right) = n|c_m|^2. \tag{4.100}$$

4.9.10 Schrödinger equation

We obtained the operator of momentum by calculating $\partial\Psi/\partial x$. What happens if we calculate $\partial\Psi/\partial t$?

$$\frac{\partial\Psi}{\partial t} = c_1\frac{\partial}{\partial t}e^{\frac{i}{\hbar}(p_1 x - \mathcal{E}_1 t)} + c_2\frac{\partial}{\partial t}e^{\frac{i}{\hbar}(p_2 x - \mathcal{E}_2 t)} + \cdots = -\frac{i}{\hbar}\mathcal{E}_1 c_1 e^{\frac{i}{\hbar}(p_1 x - \mathcal{E}_1 t)} - \frac{i}{\hbar}\mathcal{E}_2 c_2 e^{\frac{i}{\hbar}(p_2 x - \mathcal{E}_2 t)} - \cdots \tag{4.101}$$

and consequently

$$i\hbar\frac{\partial}{\partial t}e^{\frac{i}{\hbar}(p_1 x - \mathcal{E}_1 t)} = \mathcal{E}_1 e^{\frac{i}{\hbar}(p_1 x - \mathcal{E}_1 t)}, \quad i\hbar\frac{\partial}{\partial t}e^{\frac{i}{\hbar}(p_2 x - \mathcal{E}_2 t)} = \mathcal{E}_2 e^{\frac{i}{\hbar}(p_2 x - \mathcal{E}_2 t)}, \quad \cdots \tag{4.102}$$

1. First, we obtain the *operator of energy* from Eq. 4.102, in analogy to Eq. 4.87.

2. The second achievement is Eq. 4.101 itself. Energy of free particles is just the kinetic energy (by definition, "free" particles do not experience any forces). Therefore, all energies $\mathcal{E}_j$ in the right-hand side of Eq. 4.101 can be written as

$$\mathcal{E}_j = \frac{mv_j^2}{2} = \frac{p_j^2}{2m}, \tag{4.103}$$

resulting in

$$\frac{\partial\Psi}{\partial t} = -\frac{i}{\hbar}\left(\frac{p_1^2}{2m}c_1 e^{\frac{i}{\hbar}(p_1 x - \mathcal{E}_1 t)} + \frac{p_2^2}{2m}c_2 e^{\frac{i}{\hbar}(p_2 x - \mathcal{E}_2 t)} + \cdots\right). \tag{4.104}$$

But an equation with the p_j^2 terms can be also obtained by calculating

$$\frac{1}{2m}\frac{\partial^2\Psi}{\partial x^2} = \frac{1}{2m}\frac{\partial}{\partial x}\frac{\partial\Psi}{\partial x} = -\frac{1}{\hbar^2}\left(\frac{p_1^2}{2m}c_1 e^{\frac{i}{\hbar}(p_1 x - \mathcal{E}_1 t)} + \frac{p_2^2}{2m}c_2 e^{\frac{i}{\hbar}(p_2 x - \mathcal{E}_2 t)} + \cdots\right). \tag{4.105}$$

Comparison of Eqs. 4.104 and 4.105 gives us the *equation of motion*

$$i\hbar\frac{\partial\Psi}{\partial t} = -\frac{\hbar^2}{2m}\frac{\partial^2\Psi}{\partial x^2}. \tag{4.106}$$

If we extend our analysis to particles experiencing a time-independent potential energy $\mathcal{E}_{\text{pot}}(x,y,z)$, the energy will be given by

$$\mathcal{E}_j = \frac{p_j^2}{2m} + \mathcal{E}_{\text{pot}} \tag{4.107}$$

where p_j is now the absolute value of a momentum vector $\vec{p}_j$ (we have to consider all three direction x, y, z because particles change direction of motion in the presence of a potential). The time derivative of Ψ is now

$$\frac{\partial\Psi}{\partial t} = -\frac{i}{\hbar}\left(\frac{p_1^2}{2m}c_1 e^{\frac{i}{\hbar}(\vec{p}_1\vec{r} - \mathcal{E}_1 t)} + \frac{p_2^2}{2m}c_2 e^{\frac{i}{\hbar}(\vec{p}_2\vec{r} - \mathcal{E}_2 t)} + \cdots\right) - \frac{i}{\hbar}\mathcal{E}_{\text{pot}}(\vec{r})\Psi \tag{4.108}$$

and

$$\left(\frac{p_1^2}{2m}c_1 e^{\frac{i}{\hbar}(\vec{p}_1\vec{r} - \mathcal{E}_1 t)} + \frac{p_2^2}{2m}c_2 e^{\frac{i}{\hbar}(\vec{p}_2\vec{r} - \mathcal{E}_2 t)} + \cdots\right) = -\frac{\hbar^2}{2m}\left(\frac{\partial^2\Psi}{\partial x^2} + \frac{\partial^2\Psi}{\partial x^2} + \frac{\partial^2\Psi}{\partial x^2}\right). \tag{4.109}$$

Substituting Eq. 4.109 into Eq. 4.108 gives us the famous Schrödinger equation

$$i\hbar\frac{\partial\Psi}{\partial t} = \underbrace{\left(-\frac{\hbar^2}{2m}\left(\frac{\partial^2}{\partial x^2} + \frac{\partial^2}{\partial x^2} + \frac{\partial^2}{\partial x^2}\right) + \mathcal{E}_{\text{pot}}(x,y,z)\right)}_{\hat{H}}\Psi. \tag{4.110}$$

In our case, the Hamiltonian is expressed in terms of the linear momentum $\vec{p} = m\vec{v}$. This is sufficient to describe action of forces that depend only on the position in space and can be therefore calculated as the gradients of the potential energy (e.g. electric forces). However, using the linear momentum does not allow us to describe forces that depend on velocities of the particles (e.g., magnetic forces). Therefore, the *canonical* (or *generalized*) momentum should be used in general. The canonical momentum is defined by the Lagrange mechanics, reviewed in Section 4.9.1. We return to the description of a particle in a magnetic field in Section 5.7.8.

4.9.11 Limitation of wave equation to first time derivative

Before saying what a wave equation must fulfill in order to describe evolution of a quantum state in time, let us review similar requirements for the equation of motion in Newton mechanics. In the classical Newton mechanics, the state of the system is fully described by the coordinates x, y, z and momenta mv_x, mv_y, mv_z of the particles. Therefore, the solution of the equation of motion must depend only on the starting values of the coordinates and momenta, not on any additional parameter. What does it say about the equation of motion itself? It can contain only first and second derivatives in time. Why? Because:

- Solutions of equation containing only $\partial x/\partial t$ require the knowledge of $x(t = 0) = x(0)$.

For example, solution of

$$\frac{\partial x}{\partial t} + kx = 0 \tag{4.111}$$

is $x = x(0)\mathrm{e}^{-kt}$, i.e., it depends only on $x(0)$.

- Solutions of equation containing only $\partial x/\partial t$ and $\partial^2 x/\partial t^2$ require the knowledge of $x(0)$ and $\partial x/\partial t(t = 0) = v_x(0)$.

For example, let us look at the wave equation

$$\frac{\partial^2 x}{\partial t^2} + \omega^2 x = 0. \tag{4.112}$$

Note that this equation corresponds to the second Newton's law, with $-m\omega^2 x$ being the force (for the sake of simplicity assumed not to change in time). The solution is well known, but we can derive it easily because we know how to play with operators:

$$\frac{\partial^2 x}{\partial t^2} + \omega^2 x = \frac{\partial}{\partial t}\left(\frac{\partial}{\partial t}x\right) + \omega^2 x = \left(\left(\frac{\partial}{\partial t}\right)^2 + \omega^2\right)x = \left(\frac{\partial}{\partial t} + \mathrm{i}\omega\right)\left(\frac{\partial}{\partial t} - \mathrm{i}\omega\right)x = 0. \tag{4.113}$$

Obviously, there are two solutions of the equation

$$\left(\frac{\partial}{\partial t} - \mathrm{i}\omega\right)x_+ = 0 \quad \Rightarrow \quad x_+ = C_+\mathrm{e}^{\mathrm{i}\omega t} = C_+(\cos(\omega t) + \mathrm{i}\sin(\omega t)) \qquad \left(\frac{\partial}{\partial t} + \mathrm{i}\omega\right)x_- = 0 \quad \Rightarrow \quad x_- = C_-\mathrm{e}^{-\mathrm{i}\omega t} = C_-(\cos(\omega t) - \mathrm{i}\sin(\omega t)), \tag{4.114}$$

but the solution must be also any linear combination of x_+ and x_- because $0 + 0 = 0$:

$$x = A_+x_+ + A_-x_- = \underbrace{(A_+C_+ + A_-C_-)}_{C_1}\cos(\omega t) + \underbrace{\mathrm{i}(A_+C_+ - A_-C_-)}_{C_2}\sin(\omega t) = C_1\cos(\omega t) + C_2\sin(\omega t). \tag{4.115}$$

Consequently, the velocity

$$v_x = \frac{\partial x}{\partial t} = C_1\frac{\partial\cos(\omega t)}{\partial t} + C_2\frac{\partial\sin(\omega t)}{\partial t} = -\omega C_1\sin(\omega t) + \omega C_2\cos(\omega t). \tag{4.116}$$

It is clear that the so-far unknown parameters C_1 and C_2 can be obtained by calculating x and v_x at $t = 0$

$$\cos(0) = 1, \quad \sin(0) = 0 \quad \Rightarrow \quad x(0) = C_1 \quad v_x(0) = \omega C_2 \tag{4.117}$$

and that the evolution of x and v_x depends only on $x(0)$ and $v_x(0)$, as required in Newton mechanics:

$$x(t) = x(0)\cos(\omega t) + \frac{v_x(0)}{\omega}\sin(\omega t) \qquad v_x(t) = v_x(0)\cos(\omega t) - \omega \cdot x(0)\sin(\omega t). \tag{4.118}$$

- Solutions of equations containing higher than second time derivative of x require knowledge of the initial values of higher than first time derivatives of x.

For example, let us inspect

$$\frac{\partial^3 x}{\partial t^3} + \omega^3 x = 0 \tag{4.119}$$

Following the same strategy as in Eq. 4.113

$$\frac{\partial^3 x}{\partial t^3} + \lambda^3 x = \left(\frac{\partial}{\partial t} + \lambda\right)\left(\frac{\partial^2}{\partial t^2} - \frac{\partial}{\partial t}\lambda + \lambda^2\right)x = \left(\frac{\partial}{\partial t} + \lambda\right)\left(\frac{\partial^2}{\partial t^2} - 2\frac{\partial}{\partial t}\frac{\lambda}{2} + \frac{1}{4}\lambda^2 + \frac{3}{4}\lambda^2\right)x = \left(\frac{\partial}{\partial t} + \lambda\right)\left(\left(\frac{\partial}{\partial t} - \frac{\lambda}{2}\right)^2 + \frac{3}{4}\lambda^2\right)x =$$

$$\left(\frac{\partial}{\partial t}+\lambda\right)\left(\left(\frac{\partial}{\partial t}-\frac{\lambda}{2}\right)^2-\left(\mathrm{i}\frac{\sqrt{3}}{2}\lambda\right)^2\right)x=\left(\frac{\partial}{\partial t}+\lambda\right)\left(\frac{\partial}{\partial t}-\frac{1+\mathrm{i}\sqrt{3}}{2}\lambda\right)\left(\frac{\partial}{\partial t}-\frac{1-\mathrm{i}\sqrt{3}}{2}\lambda\right)x=0, \tag{4.120}$$

which has three solutions

$$x_0=C_0\mathrm{e}^{-\lambda t}, \qquad x_+=C_+\mathrm{e}^{\frac{1+\mathrm{i}\sqrt{3}\lambda}{2}t}, \qquad x_-=C_-\mathrm{e}^{\frac{1-\mathrm{i}\sqrt{3}\lambda}{2}t} \tag{4.121}$$

and any of their linear combinations is also a valid solution

$$x=A_0x_0+A_+x_++A_-x_-=C_1\mathrm{e}^{-\lambda t}+C_2\mathrm{e}^{\frac{1+\mathrm{i}\sqrt{3}\lambda}{2}t}+C_3\mathrm{e}^{\frac{1-\mathrm{i}\sqrt{3}\lambda}{2}t} \tag{4.122}$$

where $C_1=A_0C_0, C_2=A_+C_+, C_3=A_-C_-$. In order to determine C_1, C_2, and C_3, we need three initial conditions, not only $x(0)$ and $v_x(0)$, but also the initial acceleration $a(0)=\partial^2x/\partial t^2$. However, the acceleration should not represent an additional degree of freedom. In Newton mechanics, the acceleration should be completely defined by the initial coordinates and velocities, and by forces that are already incorporated in the constants in the equation. Therefore, the equation containing the third time derivative is not a Newton's equation of motion.

After making sure that we understand the Newton mechanics, we can return to the quantum mechanics. We have postulated that the wave function Ψ contains the *complete* information about the studied particle (or system in general). In contrast to the Newton mechanics, we must require that the wave equation describing the evolution of the system must depend only on Ψ at $t=0$. Therefore, our wave function must contain only first derivative in time. If it contained e.g. also $\partial^2\Psi/\partial t^2$, the evolution in time would depend also on $\partial\Psi/\partial t$ at $t=0$, which is against our first postulate.

Another problem of an equation containing second time derivative is related to our interpretation of the wave function. We interpret $\Psi(x,y,z)^*\Psi(x,y,z)$ as a distribution of the probability that the particle's coordinates are x,y,z. How is this related to the wave equation? The Schrödinger's equation Eq. 4.24 and its complex conjugate are

$$\mathrm{i}\hbar\frac{\partial\Psi}{\partial t}=\hat{H}\Psi \qquad -\mathrm{i}\hbar\frac{\partial\Psi^*}{\partial t}=\hat{H}^*\Psi^*. \tag{4.123}$$

When we multiply the equations by Ψ^* and Ψ, respectively, subtract them, and divide the result by $\mathrm{i}\hbar$, we obtain

$$\Psi^*\frac{\partial\Psi}{\partial t}+\Psi\frac{\partial\Psi^*}{\partial t}=\frac{1}{\mathrm{i}\hbar}(\Psi^*\hat{H}\Psi-\Psi\hat{H}^*\Psi^*)$$
$$\frac{\partial(\Psi^*\Psi)}{\partial t}=\frac{1}{\mathrm{i}\hbar}(\Psi^*\hat{H}\Psi-\Psi\hat{H}^*\Psi^*). \tag{4.124}$$

If we assume that a free particle does not move (has a zero momentum and therefore zero Hamiltonian), we find that

$$\frac{\partial(\Psi^*\Psi)}{\partial t}=0. \tag{4.125}$$

The result is expected, if the particle does not move, $\rho=\Psi^*\Psi$ does not change in time. But if we repeat the procedure with the equations containing the second time derivative (i.e., when the operator $\mathrm{i}\hbar\partial/\partial t$ is applied twice)

$$-\hbar^2\frac{\partial^2\Psi}{\partial t^2}=\hat{H}\Psi \qquad -\hbar^2\frac{\partial^2\Psi^*}{\partial t^2}=\hat{H}^*\Psi^*, \tag{4.126}$$

we get

$$-\Psi^*\frac{\partial^2\Psi}{\partial t^2}+\Psi\frac{\partial^2\Psi^*}{\partial t^2}=\frac{1}{\hbar^2}(\Psi^*\hat{H}\Psi-\Psi\hat{H}^*\Psi^*)$$
$$\frac{\partial}{\partial t}\left(\Psi\frac{\partial\Psi^*}{\partial t}\right)-\frac{\partial}{\partial t}\left(\Psi^*\frac{\partial\Psi}{\partial t}\right)=\frac{1}{\hbar^2}(\Psi^*\hat{H}\Psi-\Psi\hat{H}^*\Psi^*)$$
$$\frac{\partial}{\partial t}\left(\Psi\frac{\partial\Psi^*}{\partial t}-\Psi^*\frac{\partial\Psi}{\partial t}\right)=\frac{1}{\hbar^2}(\Psi^*\hat{H}\Psi-\Psi\hat{H}^*\Psi^*). \tag{4.127}$$

If we now assume that a free particle does not move (has a zero momentum and therefore zero Hamiltonian), the conserved quantity is not $\Psi^*\Psi$, but $\Psi\frac{\partial\Psi^*}{\partial t}-\Psi^*\frac{\partial\Psi}{\partial t}$, containing both Ψ and its time derivative. This contradicts our interpretation of the wave function as a probability amplitude.

4.9.12 Commutators of angular momentum operators

The operators of angular momentum components are

$$\hat{L}_x = \hat{r}_y \hat{p}_z - \hat{r}_z \hat{p}_y = -i\hbar y \frac{\partial}{\partial z} + i\hbar z \frac{\partial}{\partial y}, \tag{4.128}$$

$$\hat{L}_y = \hat{r}_z \hat{p}_x - \hat{r}_x \hat{p}_z = -i\hbar z \frac{\partial}{\partial x} + i\hbar x \frac{\partial}{\partial z}, \tag{4.129}$$

$$\hat{L}_z = \hat{r}_x \hat{p}_y - \hat{r}_y \hat{p}_x = -i\hbar x \frac{\partial}{\partial y} + i\hbar y \frac{\partial}{\partial x}, \tag{4.130}$$

$$\hat{L}^2 = \hat{L}_x^2 + \hat{L}_y^2 + \hat{L}_z^2. \tag{4.131}$$

Therefore,

$$[\hat{L}_x, \hat{L}_y] = (\hat{r}_y \hat{p}_z - \hat{r}_z \hat{p}_y)(\hat{r}_z \hat{p}_x - \hat{r}_x \hat{p}_z) - (\hat{r}_z \hat{p}_x - \hat{r}_x \hat{p}_z)(\hat{r}_y \hat{p}_z - \hat{r}_z \hat{p}_y)$$

$$= \hat{r}_y \hat{p}_z \hat{r}_z \hat{p}_x - \hat{r}_z \hat{p}_y \hat{r}_z \hat{p}_x - \hat{r}_y \hat{p}_z \hat{r}_x \hat{p}_z + \hat{r}_z \hat{p}_y \hat{r}_x \hat{p}_z - \hat{r}_z \hat{p}_x \hat{r}_y \hat{p}_z + \hat{r}_x \hat{p}_z \hat{r}_y \hat{p}_z + \hat{r}_z \hat{p}_x \hat{r}_z \hat{p}_y - \hat{r}_x \hat{p}_z \hat{r}_z \hat{p}_y \tag{4.132}$$

The commutation relations postulated in Eq. 4.16 allow us to exchange some of the operators and write first the operators that commute

$$[\hat{L}_x, \hat{L}_y] = \hat{r}_y \hat{p}_x \hat{p}_z \hat{r}_z {\color{red}- \hat{r}_z \hat{r}_z \hat{p}_x \hat{p}_y} {\color{red}- \hat{r}_x \hat{r}_y \hat{p}_z \hat{p}_z} + \hat{r}_x \hat{p}_y \hat{r}_z \hat{p}_z - \hat{r}_y \hat{p}_x \hat{r}_z \hat{p}_z {\color{red}+ \hat{r}_x \hat{r}_y \hat{p}_z \hat{p}_z} {\color{red}+ \hat{r}_z \hat{r}_z \hat{p}_x \hat{p}_y} - \hat{r}_x \hat{p}_y \hat{p}_z \hat{r}_z \tag{4.133}$$

The red terms cancel each other and using Eq. 4.16

$$[\hat{L}_x, \hat{L}_y] = (\hat{r}_y \hat{p}_x - \hat{r}_x \hat{p}_y)(\hat{p}_z \hat{r}_z - \hat{r}_z \hat{p}_z) = (-\hat{L}_z)(-i\hbar) = i\hbar \hat{L}_z. \tag{4.134}$$

The other commutators can be derived in the same manner.

It is also useful to calculate commutators of the following combinations of operators

$$\hat{L}_x + i\hat{L}_y = \hat{L}_+ \qquad \hat{L}_x - i\hat{L}_y = \hat{L}_- : \tag{4.135}$$

$$[\hat{L}_+, \hat{L}_-] = [\hat{L}_x + i\hat{L}_y, \hat{L}_x - i\hat{L}_y] = [\hat{L}_x, \hat{L}_x] + [\hat{L}_y, \hat{L}_y] + i[\hat{L}_y, \hat{L}_x] - i[\hat{L}_x, \hat{L}_y] = -2i[\hat{L}_x, \hat{L}_y] = -2i(i\hbar \hat{L}_z) = 2\hbar \hat{L}_z \tag{4.136}$$

$$[\hat{L}_z, \hat{L}_+] = [\hat{L}_z, \hat{L}_x + i\hat{L}_y] = [\hat{L}_z, \hat{L}_x] + i[\hat{L}_z, \hat{L}_y] = i\hbar \hat{L}_y + i(-i\hbar \hat{L}_x) = \hbar \hat{L}_x + i\hbar \hat{L}_y = \hbar \hat{L}_+ \tag{4.137}$$

$$[\hat{L}_z, \hat{L}_-] = [\hat{L}_z, \hat{L}_x - i\hat{L}_y] = [\hat{L}_z, \hat{L}_x] - i[\hat{L}_z, \hat{L}_y] = i\hbar \hat{L}_y - i(-i\hbar \hat{L}_x) = \hbar \hat{L}_x - i\hbar \hat{L}_y = -\hbar \hat{L}_- \tag{4.138}$$

$$[\hat{L}^2, \hat{L}_\pm] = [\hat{L}^2, \hat{L}_x \pm i\hat{L}_y] = [\hat{L}^2, \hat{L}_x] \pm i[\hat{L}^2, \hat{L}_y] = 0. \tag{4.139}$$

4.9.13 Angular momentum and rotation

To see the relation between angular momentum and rotation in space, we first find eigenvalues $L_{z,k}$ and eigenfunctions ψ_k of $\hat{L}_z$. As described in B15.3 (and in textbooks discussing quantum mechanics), the operator $\hat{L}_z$ written in the spherical coordinates (r, ϑ, φ) is

$$\hat{L}_z = -i\hbar \frac{\partial}{\partial \varphi} \tag{4.140}$$

and we can assume that the part of its eigenfunctions dependent on the coordinate φ (azimuth) can be separated: $\psi_k = Q(r, \vartheta) R_k(\varphi)$. Eigenvalues and eigenfunctions of $\hat{L}_z$ are defined by

$$\hat{L}_z \psi_k = L_{z,k} \psi_k, \tag{4.141}$$

$$-i\hbar \frac{\partial (Q R_k)}{\partial \varphi} = L_{z,k}(Q R_k), \tag{4.142}$$

$$-i\hbar Q \frac{\mathrm{d} R_k}{\mathrm{d}\varphi} = L_{z,k} Q R_k, \tag{4.143}$$

$$-i\hbar \frac{\mathrm{d} \ln R_k}{\mathrm{d}\varphi} = L_{z,k}, \tag{4.144}$$

$$R_k = \mathrm{e}^{i \frac{L_{z,k}}{\hbar} \varphi}. \tag{4.145}$$

Note that $\psi_k(\varphi)$ and $\psi_k(\varphi + 2\pi k)$ are equal for any integer k:

$$e^{i\frac{L_{z,k}}{\hbar}(\varphi+2\pi)} = e^{i\frac{L_{z,k}}{\hbar}\varphi} \quad \underbrace{\cdot e^{i2\pi\frac{L_{z,k}}{\hbar}}}_{\substack{= 1 \\ \text{if } \frac{L_{z,k}}{\hbar} \text{ is integer}}} \tag{4.146}$$

Therefore,

- value of the z-component of the angular momentum must be an integer multiple of $\hbar$.

There is a close relation between the angular momentum operators and description of rotation in quantum mechanics. In order to illustrate the relation, we repeat the analysis that was presented in Section 1.5.9 for a rotating magnetization vector. Now we analyze simply rotation of a point in space.

Rotation of a point defined by the position vector $\vec{r}$ about an axis given by the angular frequency vector $\vec{\omega}$ can be described as

$$\frac{\mathrm{d}\vec{r}}{\mathrm{d}t} = \vec{\omega} \times \vec{r}, \tag{4.147}$$

or more explicitly

$$\frac{\mathrm{d}r_x}{\mathrm{d}t} = \omega_y r_z - \omega_z r_y, \tag{4.148}$$

$$\frac{\mathrm{d}r_y}{\mathrm{d}t} = \omega_z r_x - \omega_x r_z, \tag{4.149}$$

$$\frac{\mathrm{d}r_z}{\mathrm{d}t} = \omega_x r_y - \omega_y r_x. \tag{4.150}$$

If a coordinate frame is chosen so that $\vec{\omega} = (0, 0, \omega)$

$$\frac{\mathrm{d}r_x}{\mathrm{d}t} = -\omega r_y, \tag{4.151}$$

$$\frac{\mathrm{d}r_y}{\mathrm{d}t} = \omega r_x, \tag{4.152}$$

$$\frac{\mathrm{d}r_z}{\mathrm{d}t} = 0. \tag{4.153}$$

We already know (see Section 1.5.9) that such a set of equation can be solved easily: multiply the second equation by i and add it to the first equation or subtract it from the first equation.

$$\frac{\mathrm{d}(r_x + ir_y)}{\mathrm{d}t} = \omega(-r_y + ir_x) = +i\omega(r_x + ir_y), \tag{4.154}$$

$$\frac{\mathrm{d}(r_x - ir_y)}{\mathrm{d}t} = \omega(-r_y - ir_x) = -i\omega(r_x - ir_y), \tag{4.155}$$

$$r_x + ir_y = C_+ e^{+i\omega t}, \tag{4.156}$$

$$r_x - ir_y = C_- e^{-i\omega t}, \tag{4.157}$$

where the integration constants $C_+ = r_x(0) + ir_y(0) = re^{i\phi_0}$ and $C_- = r_x(0) - ir_y(0) = re^{-i\phi_0}$ are given by the initial phase ϕ_0 of $\vec{r}$ in the coordinate system:

$$r_x + ir_y = re^{+i(\omega t + \phi_0)} = r(\cos(\omega t + \phi_0) + i(\sin(\omega t + \phi_0)), \tag{4.158}$$

$$r_x - ir_y = re^{-i(\omega t + \phi_0)} = r(\cos(\omega t + \phi_0) - i(\sin(\omega t + \phi_0)). \tag{4.159}$$

The angle of rotation φ is obviously given by ωt.

$$r_x + ir_y = re^{+i\phi_0}e^{+i\varphi} = (r_x(0) + ir_y(0))e^{+i\varphi}, \tag{4.160}$$

$$r_x - ir_y = re^{-i\phi_0}e^{-i\varphi} = (r_x(0) - ir_y(0))e^{-i\varphi}. \tag{4.161}$$

Comparison with Eq. 4.145 documents the relation between $\hat{L}_z$ and rotation:

- The eigenfunction of $\hat{L}_z$ with the eigenvalue $\hat{L}_z = \hbar$ describes counterclockwise rotation of a vector about z.

This conclusion of course applies to any vector $\vec{a}$. We have used the complex numbers to describe rotation already in Section 1.5.4. In order to describe a general rotation in space, we have to address also rotation about another axis, e.g. y (see Section 1.5.3). The relation between the rotation about the y axis and the operator $\hat{L}_y$ is less obvious because $\hat{L}_y$ has a more complicated form in the spherical coordinates (cf B15.3)

$$\hat{L}_y = \mathrm{i}\hbar \left(-\cos\varphi \frac{\partial}{\partial\vartheta} + \cot\theta \sin\varphi \frac{\partial}{\partial\vartheta} \right). \tag{4.162}$$

The matrix describing the rotation about y is presented in Section 1.5.4.

4.9.14   Eigenvalues of angular momentum operators

In the preceding section, we have found that eigenfunctions of $\hat{L}_z$ describe rotation about z and that eigenvalues of $\hat{L}_z$ are integer multiples of $\hbar$. In this section, we complete the description of the eigenvalues of $\hat{L}_z$ and of $\hat{L}^2$. Determination of eigenvalues of angular momentum operators is very important for describing electron configuration of atoms (atomic orbitals) and solving issues related to molecular rotation (e.g. infrared spectroscopy). The motivation to include its discussion here is to explain notation that is also used in some areas of NMR spectroscopy (NMR of nuclei with spin number higher than 1/2). A reader who is not interested in such issues (that are not directly discussed in this course) may skip this section and Section 4.9.15 without loosing information important for the following lectures.

A set of eigenvalues L_j^2 of the operator $\hat{L}^2$ is given by a set of equations

$$\hat{L}^2 \psi_j = L_j^2 \psi_j, \tag{4.163}$$

where ψ_j are individual eigenfunctions of $\hat{L}^2$. The same applies to $\hat{L}_z$ and its eigenfunctions ψ_k:

$$\hat{L}_z \psi_k = L_{z,k} \psi_k. \tag{4.164}$$

As $\hat{L}^2$ and $\hat{L}_z$ commute ($[\hat{L}^2, \hat{L}_z] = 0$), their eigenvalues can be evaluated simultaneously, using the same eigenfunction. The j-th eigenfunction of $\hat{L}^2$ can be also the k-th eigenfunction of $\hat{L}_z$. Here we denote such simultaneous eigenfunctions as $\psi_{j,k}$. To relate the eigenvalues, we use the Pythagorean theorem

$$\hat{L}^2 = \hat{L}_x^2 + \hat{L}_y^2 + \hat{L}_z^2 \quad \Rightarrow \quad (\hat{L}_x^2 + \hat{L}_y^2)\psi_{j,k} = (\hat{L}^2 - \hat{L}_z^2)\psi_{j,k} = \hat{L}^2\psi_{j,k} - \hat{L}_z(\hat{L}_z\psi_{j,k}) = (L_j^2 - L_{z,k}^2)\psi_{j,k}. \tag{4.165}$$

Because $L_j^2 - L_{z,k}^2$ are eigenvalues of a square operator $\hat{L}_x^2 + \hat{L}_y^2$, they cannot be negative. Therefore, $L_{z,k}^2$ cannot exceed L_j^2.

In the next step, we take advantage of the operators $\hat{L}_+$ and $\hat{L}_-$ introduced in Eq. 4.135. As $\hat{L}^2$ and $\hat{L}_\pm$ commute,

$$\hat{L}^2 \hat{L}_+ \psi_{j,k} = \hat{L}_+ \hat{L}^2 \psi_{j,k} = \hat{L}_+(L_j^2 \psi_{j,k}) = L_j^2(\hat{L}_+ \psi_{j,k}) \tag{4.166}$$

$$\hat{L}^2 \hat{L}_- \psi_{j,k} = \hat{L}_- \hat{L}^2 \psi_{j,k} = \hat{L}_-(L_j^2 \psi_{j,k}) = L_j^2(\hat{L}_- \psi_{j,k}) \tag{4.167}$$

According to Eqs. 4.137 and 4.138

$$[\hat{L}_z, \hat{L}_+] = \hat{L}_z\hat{L}_+ - \hat{L}_+\hat{L}_z = +\hbar\hat{L}_+ \quad \Rightarrow \quad \hat{L}_z\hat{L}_+ = \hat{L}_+\hat{L}_z + \hbar\hat{L}_+ \tag{4.168}$$

$$[\hat{L}_z, \hat{L}_-] = \hat{L}_z\hat{L}_- - \hat{L}_-\hat{L}_z = -\hbar\hat{L}_- \quad \Rightarrow \quad \hat{L}_z\hat{L}_- = \hat{L}_-\hat{L}_z - \hbar\hat{L}_- \tag{4.169}$$

and therefore

$$\hat{L}_z\hat{L}_+\psi_{j,k} = \hat{L}_+\hat{L}_z\psi_{j,k} + \hbar\hat{L}_+\psi_{j,k} = \hat{L}_+(L_{z,k}\psi_{j,k}) + \hbar\hat{L}_+\psi_{j,k} = (L_{z,k} + \hbar)(\hat{L}_+\psi_{j,k}) \tag{4.170}$$

$$\hat{L}_z\hat{L}_-\psi_{j,k} = \hat{L}_-\hat{L}_z\psi_{j,k} - \hbar\hat{L}_-\psi_{j,k} = \hat{L}_-(L_{z,k}\psi_{j,k}) - \hbar\hat{L}_-\psi_{j,k} = (L_{z,k} - \hbar)(\hat{L}_-\psi_{j,k}). \tag{4.171}$$

This tells us that the operator $\hat{L}_+$ converts $\psi_{j,k}$ to another eigenfunction of $\hat{L}_z$, to an eigenfunction associated with the eigenvalue $L_{z,k} + \hbar$, i.e. with the eigenvalue associated with $\psi_{j,k}$ increased by $\hbar$. But we already know (Eq. 4.146), that $\hbar$ is the difference between two successive eigenvalues of $\hat{L}_z$. Therefore, the eigenfunction created by application of $\hat{L}_+$ to $\psi_{j,k}$ can be called $C_+\psi_{j,k+1}$:

$$\hat{L}_+\psi_{j,k} = C_+\psi_{j,k+1}, \tag{4.172}$$

where C_+ is a so-far unknown coefficient that cancels out in Eq. 4.170. If we insert $\psi_{j,k+1}$ into Eq. 4.170, we obtain $\psi_{j,k+2}$ and so on. But we cannot play this game forever because we know that $L_{z,k}^2$ cannot exceed L_j^2. There must be some maximum value $k_{\max}$ which cannot be increased any further:

$$\hat{L}_+ \psi_{j,k_{\max}} = 0 \cdot \psi_{j,k_{\max}}. \tag{4.173}$$

In a very similar way, $\hat{L}_-$ decreases k down to $k_{\min}$:

$$\hat{L}_- \psi_{j,k_{\min}} = 0 \cdot \psi_{j,k_{\min}}. \tag{4.174}$$

We now apply $\hat{L}_-$ to $\hat{L}_+ \psi_{j,k_{\max}}$ and $\hat{L}_+$ to $\hat{L}_- \psi_{j,k_{\min}}$:

$$\hat{L}_- \hat{L}_+ \psi_{j,k_{\max}} = (\hat{L}_x - \mathrm{i}\hat{L}_y)(\hat{L}_x + \mathrm{i}\hat{L}_y)\psi_{j,k_{\max}} = (\hat{L}_x^2 + \hat{L}_y^2 + \mathrm{i}(\hat{L}_x\hat{L}_y - \hat{L}_y\hat{L}_x))\psi_{j,k_{\max}} = (\hat{L}^2 - \hat{L}_z^2 + \mathrm{i}([\hat{L}_x,\hat{L}_y]))\psi_{j,k_{\max}}$$
$$= (\hat{L}^2 - \hat{L}_z^2 + \mathrm{i}(\mathrm{i}\hbar\hat{L}_z))\psi_{j,k_{\max}} = (\hat{L}^2 - \hat{L}_z^2 - \hbar\hat{L}_z)\psi_{j,k_{\max}} = (L_j^2 - L_{z,k_{\max}}^2 - \hbar L_{z,k_{\max}})\psi_{j,k_{\max}} \tag{4.175}$$

$$\hat{L}_+ \hat{L}_- \psi_{j,k_{\min}} = (\hat{L}_x + \mathrm{i}\hat{L}_y)(\hat{L}_x - \mathrm{i}\hat{L}_y)\psi_{j,k_{\min}} = (\hat{L}_x^2 + \hat{L}_y^2 - \mathrm{i}(\hat{L}_x\hat{L}_y - \hat{L}_y\hat{L}_x))\psi_{j,k_{\min}} = (\hat{L}^2 - \hat{L}_z^2 - \mathrm{i}([\hat{L}_x,\hat{L}_y]))\psi_{j,k_{\min}}$$
$$= (\hat{L}^2 - \hat{L}_z^2 - \mathrm{i}(\mathrm{i}\hbar\hat{L}_z))\psi_{j,k_{\min}} = (\hat{L}^2 - \hat{L}_z^2 + \hbar\hat{L}_z)\psi_{j,k_{\min}} = (L_j^2 - L_{z,k_{\min}}^2 + \hbar L_{z,k_{\min}})\psi_{j,k_{\min}}. \tag{4.176}$$

Comparison with Eqs. 4.173 and 4.174 requires

$$L_j^2 - L_{z,k_{\max}}^2 - \hbar L_{z,k_{\max}} = 0 \tag{4.177}$$
$$L_j^2 - L_{z,k_{\min}}^2 + \hbar L_{z,k_{\min}} = 0. \tag{4.178}$$

Subtracting the Eq. 4.177 from Eq. 4.178,

$$L_{z,k_{\max}}^2 - L_{z,k_{\min}}^2 + \hbar L_{z,k_{\max}} + \hbar L_{z,k_{\min}} = (L_{z,k_{\max}} - L_{z,k_{\min}})(L_{z,k_{\max}} + L_{z,k_{\min}}) + \hbar(L_{z,k_{\max}} + \hbar L_{z,k_{\min}}) =$$
$$(L_{z,k_{\max}} + L_{z,k_{\min}})(L_{z,k_{\max}} - L_{z,k_{\min}} + \hbar) = 0. \tag{4.179}$$

Obviously, $(L_{z,k_{\max}} + L_{z,k_{\min}})$ or $(L_{z,k_{\max}} - L_{z,k_{\min}} + \hbar)$ must be equal to zero. Because $L_{z,k_{\max}} \geq L_{z,k_{\min}}$, the only possible solution is $L_{z,k_{\max}} + L_{z,k_{\min}} = 0$. But the difference $L_{z,k_{\max}} - L_{z,k_{\min}}$ is also restricted. As successive values of $L_{z,k}$ differ by $\hbar$ (Eq. 4.146), $L_{z,k_{\max}} - L_{z,k_{\min}}$ must be also a multiple of $\hbar$. Both conditions are fulfilled for $L_{z,k_{\max}} = +j\hbar$ and $L_{z,k_{\min}} = -j\hbar$, where j is integer or half-integer. Considering what we learned about angular momentum and rotation in Section 4.9.13, the half-integer values seem to be allowed mathematically but not physically (terms with half-integer values of the rotation angles do not appear in matrices $\mathscr{D}^j$ describing rotations of vectors and tensors). However, we find a meaningful physical interpretation of $j = 1/2$ in the following lecture.

Substituting $L_{z,k_{\max}} = +j\hbar$ into Eq. 4.177 defines

$$L_j^2 = j^2\hbar^2 + j\hbar^2 = j(j+1)\hbar^2. \tag{4.180}$$

For such an eigenvalue of $\hat{L}^2$, the possible eigenvalues of $\hat{L}_z$ are

$$-j\hbar, -(j-1)\hbar, -(j-2)\hbar, \dots, (j-2)\hbar, (j-1)\hbar, j\hbar. \tag{4.181}$$

Our last task is to evaluate C_+ in Eq. 4.172 and a similar coefficient C_- for $\hat{L}_- \psi_{j,k} = C_- \psi_{j,k-1}$. We start by evaluating $|C_+|^2$, which requires calculation of the complex conjugate of the (in general complex) coefficient C_+. We express the complex conjugate taking advantage of the fact that operators and eigenfunctions can be represented by vectors and matrices.

$$(C_+ \psi_{j,k})^* = (\hat{L}_+ |\psi_{j,k}\rangle)^\dagger = \langle\psi_{j,k}|\hat{L}_+^\dagger = \langle\psi_{j,k}|\hat{L}_-, \tag{4.182}$$

where $|\psi_{j,k}\rangle$ and $\langle\psi_{j,k}|$ are treated as a column and row vector, respectively, and $\hat{L}_+$ and $\hat{L}_-$ as mutually transposed square matrices. Then,

$$|C_+ \psi_{j,k}|^2 = \langle\psi_{j,k}|\hat{L}_- \hat{L}_+|\psi_{j,k}\rangle = \langle\psi_{j,k}|\hat{L}^2 - \hat{L}_z^2 - \hbar\hat{L}_z|\psi_{j,k}\rangle = j(j+1)\hbar^2 - m(m+1)\hbar^2. \tag{4.183}$$

In a similar manner,

$$|C_- \psi_{j,k}|^2 = \langle\psi_{j,k}|\hat{L}_+ \hat{L}_-|\psi_{j,k}\rangle = \langle\psi_{j,k}|\hat{L}^2 - \hat{L}_z^2 + \hbar\hat{L}z|\psi_{j,k}\rangle = j(j+1)\hbar^2 - m(m-1)\hbar^2. \tag{4.184}$$

The absolute values of C_+ and C_- are

$$|C_+| = \hbar\sqrt{j(j+1)\hbar^2 - m(m+1)}, \tag{4.185}$$
$$|C_-| = \hbar\sqrt{j(j+1)\hbar^2 - m(m-1)}. \tag{4.186}$$

The phases of C_+ and C_- are not restricted. We can therefore set them to zero and define C_+ and C_- as real numbers

$$C_+ = \hbar\sqrt{j(j+1)\hbar^2 - m(m+1)}, \tag{4.187}$$
$$C_- = \hbar\sqrt{j(j+1)\hbar^2 - m(m-1)}. \tag{4.188}$$

4.9.15 Eigenfunctions of angular momentum operators

After evaluation of eigenvalues of $\hat{L}^2$ and $\hat{L}_z$, we can proceed to the determination of the eigenfunctions $\psi_{j,k}$. We have already found eigenfunctions of $\hat{L}_z$ in Section 4.9.13 (Eq. 4.145). In order to find wave functions that are simultaneously eigenfunctions of $\hat{L}^2$ and $\hat{L}_z$, we have to express both operators in spherical coordinates. For $\hat{L}_z$, it has been done already in Eq. 4.140, for $\hat{L}^2$, the desired algebraic expression is (see e.g. B15.3)

$$\hat{L}^2 = -\frac{\hbar^2}{\sin\vartheta}\left(\frac{\partial}{\partial\vartheta}\left(\sin\vartheta\frac{\partial}{\partial\vartheta}\right) + \frac{\partial}{\partial\varphi}\left(\frac{1}{\sin\vartheta}\frac{\partial}{\partial\varphi}\right)\right). \tag{4.189}$$

We have therefore to solve a set of equations

$$\hat{L}_z\psi_{j,k} = -\mathrm{i}\hbar\frac{\partial}{\partial\varphi}\psi_{j,k} = L_{z,k}\psi_{j,k} = k\hbar\psi_{j,k}, \tag{4.190}$$

$$\hat{L}^2\psi_{j,k} = -\frac{\hbar^2}{\sin\vartheta}\left(\frac{\partial}{\partial\vartheta}\left(\sin\vartheta\frac{\partial}{\partial\vartheta}\right) + \frac{\partial}{\partial\varphi}\left(\frac{1}{\sin\vartheta}\frac{\partial}{\partial\varphi}\right)\right)\psi_{j,k} = L_j\psi_{j,k} = j(j+1)\hbar^2\psi_{j,k}. \tag{4.191}$$

If $\psi_{j,k} = Q_{j,k}(r,\vartheta)R_{j,k}(\varphi)$,

$$-\mathrm{i}Q_{j,k}\frac{\partial}{\partial\varphi}R_{j,k} = kQ_{j,k}R_{j,k}, \tag{4.192}$$

$$-\frac{R_{j,k}}{\sin\vartheta}\left(\frac{\partial}{\partial\vartheta}\left(\sin\vartheta\frac{\partial Q_{j,k}}{\partial\vartheta}\right) + \frac{Q_{j,k}}{\sin\vartheta}\frac{\partial^2 R_{j,k}}{\partial\varphi^2}\right) = j(j+1)Q_{j,k}R_{j,k}. \tag{4.193}$$

The first equation has been already solved in Section 4.9.13, yielding ((Eq. 4.145)

$$R_{j,k} = R_k = \mathrm{e}^{\mathrm{i}k\varphi}. \tag{4.194}$$

We can use this solution to calculate $\partial^2 R_k/\partial\varphi^2$

$$\frac{\partial^2 R_k}{\partial\varphi^2} = \frac{\partial^2 \mathrm{e}^{\mathrm{i}k\varphi}}{\partial\varphi^2} = -k^2\mathrm{e}^{\mathrm{i}k\varphi} = -k^2 R_k \tag{4.195}$$

and insert it into Eq. 4.193:

$$-\frac{R_k}{\sin\vartheta}\left(\frac{\mathrm{d}}{\mathrm{d}\vartheta}\left(\sin\vartheta\frac{\mathrm{d}Q_{j,k}}{\mathrm{d}\vartheta}\right) - \frac{Q_{j,k}}{\sin\vartheta}k^2 R_k\right) = j(j+1)Q_{j,k}R_k \tag{4.196}$$

$$\frac{1}{\sin\vartheta}\frac{\mathrm{d}}{\mathrm{d}\vartheta}\left(\sin\vartheta\frac{\mathrm{d}Q_{j,k}}{\mathrm{d}\vartheta}\right) + \left(j(j+1) - \frac{k^2}{\sin^2\vartheta}\right)Q_{j,k} = 0 \tag{4.197}$$

$$(1-u^2)\frac{\mathrm{d}^2 Q_{j,k}}{\mathrm{d}u^2} - 2u\frac{\mathrm{d}Q_{j,k}}{\mathrm{d}u} + \frac{j(j+1)(1-u^2) - k^2}{1-u^2}Q_{j,k} = 0, \tag{4.198}$$

where the substitution $u = \cos\vartheta$ (and $\partial u = -\sin\vartheta\partial\vartheta$) was used on the last line. This equation has the same form as Eq. 2.55 derived in Section 2.5.3. A simplified version of Eq. 2.55 was solved in Section 2.5.4, where the solution was searched for in a form of a series of powers of u. Solving the complete equation is more difficult due to the presence of the $(1-u^2)^{-1}$ factor in the term proportional to $Q_{j,k}$. In order to cope with the $(1-u^2)^{-1}$ factor, we notice that each differentiation of a function multiplied by a so-far undefined power of $(1-u^2)$ produces terms with the power decreased by one (in addition to other terms). We may hope that this compensates for the opposite trend in Eq. 4.198: $Q_{j,k}$ is associated with $(1-u^2)^{-1}$, the first derivative of $Q_{j,k}$ with $(1-u^2)^0$, the second derivative of $Q_{j,k}$ with $(1-u^2)^1$. This motivates us to look for solutions in a form

$$Q_{j,k} = (1-u^2)^s \sum_{l=0}^{\infty} a_l u^l, \tag{4.199}$$

with the first derivative

$$\frac{\mathrm{d}Q_{j,k}}{\mathrm{d}u} = (1-u^2)^s \frac{\mathrm{d}}{\mathrm{d}u}\sum_{l=0}^{\infty} a_l u^l - 2us(1-u^2)^{s-1}\sum_{l=0}^{\infty} a_l u^l = (1-u^2)^s \sum_{l=0}^{\infty} la_l u^{l-1} - 2s(1-u^2)^{s-1}\sum_{l=0}^{\infty} a_l u^{l+1} \tag{4.200}$$

and the second derivative

$$\frac{\mathrm{d}^2 Q_{j,k}}{\mathrm{d}u^2} = (1-u^2)^s \frac{\mathrm{d}}{\mathrm{d}u} \sum_{l=0}^{\infty} l a_l u^{l-1} - 2s(1-u^2)^{s-1} \frac{\mathrm{d}}{\mathrm{d}u} \sum_{l=0}^{\infty} a_l u^{l+1} - 2us(1-u^2)^{s-1} \sum_{l=0}^{\infty} l a_l u^{l-1} + 4us(s-1)(1-u^2)^{s-2} \sum_{l=0}^{\infty} a_l u^{l+1}$$

$$= (1-u^2)^s \sum_{l=0}^{\infty} l(l-1) a_l u^{l-2} - 2s(1-u^2)^{s-1} \sum_{l=0}^{\infty} (2l+1) a_l u^l + 4s(s-1)(1-u^2)^{s-2} \sum_{l=0}^{\infty} a_l u^{l+2} \tag{4.201}$$

Substituting $Q_{j,k}$, $\frac{\mathrm{d}Q_{j,k}}{\mathrm{d}u}$, and $\frac{\mathrm{d}^2 Q_{j,k}}{\mathrm{d}u^2}$ into Eq. 4.198,

$$(1-u^2)\left((1-u^2)^s \sum_{l=0}^{\infty} l(l-1) a_l u^{l-2} - 2s(1-u^2)^{s-1} \sum_{l=0}^{\infty} (2l+1) a_l u^l + 4s(s-1)(1-u^2)^{s-2} \sum_{l=0}^{\infty} a_l u^{l+2}\right)$$

$$-2u\left((1-u^2)^s \sum_{l=0}^{\infty} l a_l u^{l-1} - 2s(1-u^2)^{s-1} \sum_{l=0}^{\infty} a_l u^{l+1}\right)$$

$$+\frac{j(j+1)(1-u^2)-k^2}{1-u^2}(1-u^2)^s \sum_{l=0}^{\infty} a_l u^l = 0. \tag{4.202}$$

Now we use the u and $1-u^2$ factors to adjust the exponents in the sums to u^l

$$(1-u^2)^s \sum_{l=0}^{\infty} l(l-1) a_l u^{l-2} - (1-u^2)^s \sum_{l=0}^{\infty} l(l-1) a_l u^l - 2s(1-u^2)^s \sum_{l=0}^{\infty} (2l+1) a_l u^l + 4s(s-1)(1-u^2)^{s-1} u^2 \sum_{l=0}^{\infty} a_l u^l$$

$$-2(1-u^2)^s \sum_{l=0}^{\infty} l a_l u^l + 4s(1-u^2)^{s-1} u^2 \sum_{l=0}^{\infty} a_l u^l$$

$$+j(j+1)(1-u^2)^s \sum_{l=0}^{\infty} a_l u^l - k^2(1-u^2)^{s-1} \sum_{l=0}^{\infty} a_l u^l = 0. \tag{4.203}$$

We succeeded except for the first sum. We factor out $(1-u^2)^s$ and combine all terms into one sum

$$(1-u^2)^s \sum_{l=0}^{\infty} \left\{ l(l-1) a_l u^{l-2} + \left[-l(l-1) - 2s(2l+1) - 2l + j(j+1) + \frac{4s(s-1)u^2 + 4su^2 - k^2}{1-u^2} \right] a_l u^l \right\} = 0 \tag{4.204}$$

$$(1-u^2)^s \sum_{l=0}^{\infty} u^l \left\{ l(l-1) a_l u^{l-2} + \left[-l^2 - 4sl - 2s - l + j(j+1) + \frac{4s^2 u^2 - k^2}{1-u^2} \right] a_l u^l \right\} = 0. \tag{4.205}$$

This equation is satisfied if $(1-u^2)^s$ or the sum is equal to zero for every value of l. Let us first inspect solutions for $l=0$

$$(1-u^2)^s \left\{ 0 + \left[-2s + j(j+1) + \frac{4s^2 u^2 - k^2}{1-u^2} \right] a_0 \right\} = 0. \tag{4.206}$$

This must be true for any u, including $u=1$ or $u=-1$ (solutions for $u=\cos\vartheta=1$, i.e., $\theta=0$, and $u=\cos\vartheta=-1$, i.e., $\theta=\pi$). But $u=\pm1$ makes the denominator in the last term to tend to zero. Such singularities must be checked carefully. If $u=\pm1$, all terms in the sum multiplied by $(1-u^2)^s$ are zero, except for the last one. The last term approaches infinity unless the numerator (equal to $4s^2 - k^2$ for $u=\pm1$) is equal to zero. Therefore, the conditions

$$4s^2 = k^2 \qquad \Rightarrow s = \frac{|k|}{2} \tag{4.207}$$

must be fulfilled in order to satisfy Eq. 4.206 for $a_0 \neq 0$. The inspection of the boundary conditions (the singularities at $\theta=0$ and $\theta=\pi$) thus provided the so-far unknown value of s.

We now return to Eq. 4.205 and move the exponents in the first sum to u^l. We proceed as in Section 2.5.4. The first two terms of the first sum are equal to zero because the first term includes multiplication by $l=0$ and the second term includes multiplication by $l-1=0$ for $l=1$. Therefore, starting summation from $l=2$ does not change anything.

$$\sum_{l=0}^{\infty} l(l-1) a_l u^{l-2} = \sum_{l=2}^{\infty} l(l-1) a_l u^{l-2}. \tag{4.208}$$

Decreasing the index l in this sum by two moves u^{l-2} to u^l, as desired.

$$\sum_{l=2}^{\infty} l(l-1)a_l u^{l-2} = \sum_{l=0}^{\infty}(l+2)(l+1)a_{l+2}u^l. \tag{4.209}$$

We factor out u^l

$$(1-u^2)^{|k|/2}\sum_{l=0}^{\infty}u^l\left\{(l+2)(l+1)a_{l+2}+\left[-l^2-2|k|l-|k|-l+j(j+1)+\frac{k^2u^2-k^2}{1-u^2}\right]a_l\right\}=0 \tag{4.210}$$

$$(1-u^2)^{|k|/2}\sum_{l=0}^{\infty}u^l\left\{(l+2)(l+1)a_{l+2}-\left[l^2+2|k|l+|k|+l+k^2-j(j+1)\right]a_l\right\}=0 \tag{4.211}$$

$$(1-u^2)^{|k|/2}\sum_{l=0}^{\infty}u^l\left\{(l+2)(l+1)a_{l+2}-\left[(|k|+l)(|k|+l+1)-j(j+1)\right]a_l\right\}=0 \tag{4.212}$$

and obtain a recurrence formula very similar to Eq. 2.71

$$a_{l+2}=\frac{(l+|k|)(l+|k|+1)-j(j+1)}{(l+2)(l+1)}a_l. \tag{4.213}$$

Therefore, we can express the series $\sum_{l=0}^{\infty}a_l u^l$ as

$$\sum_{l=0}^{\infty}a_l u^l = a_0\left(1+\frac{(|k|)(|k|+1)-j(j+1)}{1\cdot 2}u^2+\frac{(|k|)(|k|+1)-j(j+1)}{1\cdot 2}\cdot\frac{(|k|+2)(|k|+3)-j(j+1)}{3\cdot 4}u^4+\dots\right)$$
$$+a_1\left(u+\frac{(|k|+1)(|k|+2)-j(j+1)}{2\cdot 3}u^3+\frac{(|k|+1)(|k|+2)-j(j+1)}{2\cdot 3}\cdot\frac{(|k|+3)(|k|+4)-j(j+1)}{4\cdot 5}u^5+\dots\right) \tag{4.214}$$

The recurrence formula also tells us that every value of l satisfying the condition $l+|k|=j$, i.e., $l=j-|k|$, terminates one of the series in the parenthesis because

$$a_{j-|k|+2}=\frac{(j-|k|+|k|)(j-|k|+|k|+1)-j(j+1)}{(j-|k|+2)(j-|k|+1)}a_{j-|k|}=\frac{0}{(j-|k|+2)(j-|k|+1)}a_{j-|k|}=0. \tag{4.215}$$

We can therefore express all solutions $Q_{j,k}$ using the same approach as in Section 2.5.4. For each combination of j and k, one of the series in Eq. 4.214 is terminated at $l=j-|k|$ and the other one grows to infinity. To keep the whole sum finite, the so-far undetermined coefficient multiplying the unterminated series is set to zero. For example, if $l=j-|k|$ occurs in the series following a_0, then a_1 is set to zero, and vice versa. The coefficient multiplying the terminated series is determined by the normalization condition, as discussed below. In this manner, we can find, step-by-step, all solutions of $Q_{j,k}$ as possible *finite* sums multiplied by $(1-u^2)^{|k|/2}=\sin^{|k|}\vartheta$ with the corresponding value of $|k|$. The first solutions are listed in Table 4.1. The complete eigenfunctions are the products $R_{j,k}Q_{j,k}=Y_{j,k}$, called *spherical harmonics*. They are orthogonal, often normalized (by setting the values of a_0 and a_1) so that the integral of the square of $Y_{j,k}$ over all possible orientations is unity:

$$\int_0^{2\pi}\mathrm{d}\varphi\int_0^{\pi}\sin\vartheta\mathrm{d}\vartheta\ Y_{j,k}^*(\varphi,\vartheta)Y_{j',k'}(\varphi,\vartheta)=\int_0^{2\pi}\mathrm{d}\varphi\int_{-1}^{1}\mathrm{d}u\ Y_{j,k}^*(\varphi,u)Y_{j',k'}(\varphi,u)=\delta_{jj'}\delta_{kk'}. \tag{4.216}$$

The derived eigenfunctions deserve some remarks

- Spherical harmonics $Y_{j,k}(\vartheta,\varphi)$ describe simultaneous eigenfunctions of $\hat{L}^2$ and $\hat{L}_z$ for all integer eigenvalues $j\hbar$, but not for the half-integer eigenvalues $j\hbar$. Spherical harmonics are eigenfunctions of *orbital angular momentum*. The half-integer eigenvalues $j\hbar$ and the corresponding eigenfunctions are discussed in the next lecture when the *spin angular momentum* is introduced.

- Spherical harmonics describe the angular dependence of the familiar atomic orbitals (derived for hydrogen).

- As expected for eigenfunctions of operator $\hat{L}_z$, the square $Y_{j,k}^*(\varphi,\vartheta)Y_{j,k}(\varphi,\vartheta)$ depends only on ϑ, not on φ (note that $\hat{L}_z$ represents projection of $\vec{L}$ on the z axis).

- Comparison of Tables 1.1 and 4.1 reveals a close relation between the spherical harmonics and Wigner matrix elements: except for the normalization factor, $Y_{j,k}(\vartheta,\varphi)$ is equal to $\mathscr{D}_{k,0}^j$

Table 4.1: Eigenfunctions of the operators $\hat{L}^2$ and $\hat{L}_z$.

j	k	l	recurrence	$Q_{j,k}$	$\psi_{j,k}$
0	0	$0 = j - |k|$	$a_2 = 0 \cdot a_0 \Rightarrow a_1 = 0$	a_0	$Y_{0,0} = \sqrt{\frac{1}{4\pi}}$
1	0	0	$a_2 = \frac{-2}{1 \cdot 2} \cdot a_0$		
		$1 = j - |k|$	$a_3 = 0 \cdot a_1 \Rightarrow a_0 = 0$	$a_1 u = a_1 \cos \vartheta$	$Y_{1,0} = \sqrt{\frac{3}{4\pi}} \cos \vartheta$
1	± 1	$1 = j - |k|$	$a_2 = 0 \cdot a_0 \Rightarrow a_1 = 0$	$a_0 \sqrt{1 - u^2} = a_0 \sin \vartheta$	$Y_{1,\pm 1} = \mp \sqrt{\frac{3}{8\pi}} \mathrm{e}^{\pm \mathrm{i}\varphi} \sin \vartheta$
2	0	0	$a_2 = \frac{-6}{1 \cdot 2} \cdot a_0$		
		1	$a_3 = \frac{-4}{2 \cdot 3} \cdot a_1$		
		$2 = j - |k|$	$a_4 = 0 \cdot a_2 \Rightarrow a_1 = 0$	$a_0 \left(1 - 3u^2\right) = a_0 \left(1 - 3\cos^2 \vartheta\right)$	$Y_{2,0} = \sqrt{\frac{5}{16\pi}} \left(3\cos^2 \vartheta - 1\right)$
2	± 1	0	$a_2 = \frac{-4}{1 \cdot 2} \cdot a_0$		
2	± 1	$1 = j - |k|$	$a_3 = 0 \cdot a_1 \Rightarrow a_0 = 0$	$a_1 \sqrt{1 - u^2}\, u = a_1 \sin \vartheta \cos \vartheta$	$Y_{2,\pm 1} = \mp \sqrt{\frac{15}{8\pi}} \mathrm{e}^{\pm \mathrm{i}\varphi} \sin \vartheta \cos \vartheta$
2	± 2	$0 = j - |k|$	$a_2 = 0 \cdot a_0 \Rightarrow a_1 = 0$	$a_0(1 - u^2) = a_0 \sin^2 \vartheta$	$Y_{2,\pm 2} = \sqrt{\frac{15}{32\pi}} \mathrm{e}^{\pm 2\mathrm{i}\varphi} \sin^2 \vartheta$
3	0	0	$a_2 = \frac{-12}{1 \cdot 2} \cdot a_0$		
		1	$a_3 = \frac{-10}{2 \cdot 3} \cdot a_1$		
		2	$a_4 = \frac{-6}{3 \cdot 4} \cdot a_2$		
		$3 = j - |k|$	$a_5 = 0 \cdot a_3 \Rightarrow a_0 = 0$	$a_1 \frac{3u - 5u^3}{3} = a_1 \frac{3\cos \vartheta - 5\cos^3 \vartheta}{3}$	$Y_{3,0} = \sqrt{\frac{7}{16\pi}} \left(5\cos^3 \vartheta - 3\cos \vartheta\right)$
3	± 1	0	$a_2 = \frac{-4}{1 \cdot 2} \cdot a_0$		
3	± 1	1	$a_3 = \frac{-6}{2 \cdot 3} \cdot a_1$		
3	± 1	$2 = j - |k|$	$a_4 = 0 \cdot a_2 \Rightarrow a_1 = 0$	$a_0 \sqrt{1 - u^2}(1 - 5u^2) = a_0 \sin \vartheta \left(1 - 5\cos^2 \vartheta\right)$	$Y_{3,\pm 1} = \mp \sqrt{\frac{21}{64\pi}} \mathrm{e}^{\pm \mathrm{i}\varphi} \sin \vartheta \left(5\cos^2 \vartheta - 1\right)$
3	± 2	0	$a_2 = \frac{-6}{1 \cdot 2} \cdot a_0$		
3	± 2	$1 = j - |k|$	$a_3 = 0 \cdot a_1 \Rightarrow a_0 = 0$	$a_1 (1 - u^2) u = a_1 \sin^2 \vartheta \cos \vartheta$	$Y_{3,\pm 2} = \sqrt{\frac{105}{32\pi}} \mathrm{e}^{\pm 2\mathrm{i}\varphi} \sin^2 \vartheta \cos \vartheta$
3	± 3	$0 = j - |k|$	$a_2 = 0 \cdot a_0 \Rightarrow a_1 = 0$	$a_0 \sqrt{(1 - u^2)^3} = a_0 \sin^3 \vartheta$	$Y_{3,\pm 3} = \mp \sqrt{\frac{35}{64\pi}} \mathrm{e}^{\pm 3\mathrm{i}\varphi} \sin^3 \vartheta$

- Wigner matrices can be used to express $Y_{j,k}(\vartheta, \varphi)$ in different coordinate frames. The transformations are not limited to $j = 0, 1, 2$, discussed in Section 1.5.4. Wigner derived a general form of the transformation matrix applicable to eigenfunctions associated with all eigenvalues $j\hbar$ (including the half-integer j). The elements of the general Wigner matrix are given by

$$\mathrm{e}^{-\mathrm{i}k\varphi} d^j_{k,k'}(\vartheta) \mathrm{e}^{-\mathrm{i}k'\chi} = \mathrm{e}^{-\mathrm{i}(k\varphi + k'\chi)} \sqrt{(j+k)!(j-k)!(j+k')!(j-k')!} \sum_l \frac{(-1)^{k-k'+l} \left(\cos \frac{-\vartheta}{2}\right)^{2j-k+k'-2l} \left(\sin \frac{-\vartheta}{2}\right)^{k-k'+2l}}{(j-k-l)!l!(k-k'+l)!(j+k'-l)!},$$

(4.217)

where l are integer values $l \geq 0$, $l \leq j - k$, $l \leq j + k'$, and $l \geq k' - k$ so that the factorials are computed from non-negative numbers.

Lecture 5
Spin

Literature: Introduction to the special theory of relativity can be found in B10, but relativistic quantum mechanics is not discussed in the literature recommended for this course or in general physical chemistry textbooks (despite the important role of spin in chemistry). Therefore, more background information is presented here than in the other chapters. NMR can be correctly described if the spin is introduced *ad hoc*. The purpose of Section 5.7.3 is to show how the spin emerges naturally. Origin of nuclear magnetism is touched in L1.3 and L1.4. Quantum mechanics of spin angular momentum is reviewed in K6, L7, and L10.

5.1 Dirac equation

The angular momentum discussed in Section 4.7 is associated with the change of direction of a moving particle. However, the theory discussed so-far does not explain the experimental observation that even point-like particles moving along straight lines possess a well defined angular momentum, so-called *spin*.

The origin of the spin is a consequence of the symmetry of Nature that is taken into account in the theory of relativity. The Schrödinger equation is not relativistic and does not describe the spin naturally. In this lecture, we describe spin using relativistic quantum mechanics, a theory which is in agreement with two fundamental postulates of the special theory of relativity (see Sections 5.7.1 and 5.7.2 for review of the special theory of relativity):

> The laws of physics are invariant (i.e. identical) in all inertial systems (non-accelerating frames of reference).

> The speed of light in a vacuum is the same for all observers, regardless of the motion of the light source.

The arguments presented in Sections 5.7.3 and 5.7.4 lead to the wave equation

$$\left(i\hbar \frac{\partial}{\partial t} \hat{\gamma}^0 + ic\hbar \frac{\partial}{\partial x} \hat{\gamma}^1 + ic\hbar \frac{\partial}{\partial y} \hat{\gamma}^2 + ic\hbar \frac{\partial}{\partial z} \hat{\gamma}^3 - m_0 c^2 \hat{1} \right) \Psi = 0, \tag{5.1}$$

where $\hat{\gamma}^j$ are the following 4×4 matrices

$$\hat{\gamma}^0 = \begin{pmatrix} 1 & 0 & 0 & 0 \\ 0 & 1 & 0 & 0 \\ 0 & 0 & -1 & 0 \\ 0 & 0 & 0 & -1 \end{pmatrix} \qquad \hat{\gamma}^1 = \begin{pmatrix} 0 & 0 & 0 & 1 \\ 0 & 0 & 1 & 0 \\ 0 & -1 & 0 & 0 \\ -1 & 0 & 0 & 0 \end{pmatrix} \qquad \hat{\gamma}^2 = \begin{pmatrix} 0 & 0 & 0 & -i \\ 0 & 0 & i & 0 \\ 0 & i & 0 & 0 \\ -i & 0 & 0 & 0 \end{pmatrix} \qquad \hat{\gamma}^3 = \begin{pmatrix} 0 & 0 & 1 & 0 \\ 0 & 0 & 0 & -1 \\ -1 & 0 & 0 & 0 \\ 0 & 1 & 0 & 0 \end{pmatrix}.$$

$$(5.2)$$

The presented matrices $\hat{\gamma}^j$ represent only one possible choice, but it is a good choice for describing NMR as as the following sections show.

The solution of Eq. 5.1 is a wave function consisting of four components

$$\Psi = \begin{pmatrix} \psi_1 \\ \psi_2 \\ \psi_3 \\ \psi_4 \end{pmatrix}.$$

$$(5.3)$$

The explicit form of the solution for a free particle is presented in Section 5.7.6. Note that the solution is written as a four-component vector, but the indices 1, 2, 3, 4 are not related to time and space coordinate. Instead, they represent *new degrees of freedom*, distinguishing different spin states and particles from antiparticles.

When postulated by Dirac, Eq. 5.1 naturally explained the behavior of particles with spin number 1/2 and predicted existence of antiparticles, discovered a few years later. Relation of Eq. 5.1 to the non-relativistic Schrödinger equation is described in Section 5.7.7.

After describing the free particle, we should move to the description of particles interacting with their surroundings, in particular with the electromagnetic fields. Strictly speaking, both spin-1/2 particles and the fields should be treated in the same manner, i.e., as quantum particles or, more precisely, as states of various quantum fields. Such approach is reviewed in Engelke, *Concepts Magn. Reson.* **36(A)** (2010) 266-339, DOI 10.1002/cmr.a.20166. However, the energy of the electromagnetic quanta (photons) used in NMR spectroscopy is low and their number is very high. As a consequence, the quantum and classical[1] description of the fields give almost identical results. As we try to keep the theoretical description as simple as possible in this text, we follow with the classical description of the electromagnetic field.[2]

5.2   Operator of the spin magnetic moment

The Dirac equation allows us to find the operator of the spin magnetic moment. We start by deriving the Hamiltonian describing the energy of the spin magnetic moment in a magnetic field (Section 5.7.8). In a limit of energies much lower than the rest-mass energy $m_0 c^2$, the Hamiltonian is

---

[1]Here, "classical" means "non-quantum, but relativistic" because the Maxwell equations are consistent with the special theory of relativity.

[2]A consequence of the classical treatment of the electromagnetic fields is that we derive a value of the magnetogyric ratio slightly lower than observed and predicted by the fully quantum approach. This fact is mentioned in Section 5.6.

$$\hat{H} \approx \left(\frac{1}{2m_0} \left(\left(i\hbar\frac{\partial}{\partial x} + QA_x \right)^2 + \left(i\hbar\frac{\partial}{\partial y} + QA_y \right)^2 + \left(i\hbar\frac{\partial}{\partial z} + QA_z \right)^2 \right) + QV \right) \begin{pmatrix} 1 & 0 \\ 0 & 1 \end{pmatrix}$$

$$-\frac{\hbar Q}{2m_0} \left(B_x \begin{pmatrix} 0 & 1 \\ 1 & 0 \end{pmatrix} + B_y \begin{pmatrix} 0 & -i \\ i & 0 \end{pmatrix} + B_z \begin{pmatrix} 1 & 0 \\ 0 & -1 \end{pmatrix} \right). \quad (5.4)$$

The Hamiltonian contains a part (shown in green on the first line) which is identical with the non-relativistic Hamiltonian in the Schrödinger equation describing a particle in an electromagnetic field (Eq. 4.26), but it also contains a new part (shown in red on the second line), which appears only in the relativistic treatment (and survives the simplification to the low-energy limit). This "relativistic" component closely resembles the Hamiltonian of the interaction of the orbital magnetic moment with the magnetic field (Eq. 4.41) and, as we discuss below, has all properties expected for the Hamiltonian of the *spin* magnetic moment, despite the fact that we analyze a point-like particle which cannot spin. Comparison of Eqs. 5.4 and 4.41 helps us to identify the operator of the components of the *spin magnetic moment*:

$$\hat{\mu}_x = \frac{\hbar Q}{2m_0} \begin{pmatrix} 0 & 1 \\ 1 & 0 \end{pmatrix}, \quad (5.5)$$

$$\hat{\mu}_y = \frac{\hbar Q}{2m_0} \begin{pmatrix} 0 & -i \\ i & 0 \end{pmatrix}, \quad (5.6)$$

$$\hat{\mu}_z = \frac{\hbar Q}{2m_0} \begin{pmatrix} 1 & 0 \\ 0 & -1 \end{pmatrix}. \quad (5.7)$$

5.3 Operators of spin angular momentum

Our final task is to find the operators of the components of the *spin angular momentum*, which also gives us the value of the magnetogyric ratio. Eq. 5.4 itself is not sufficient because it does not say which constants belong to the spin angular momentum and which constitute the magnetogyric ratio. We cannot use the classical definition either because our case does not have a classical counterpart. But we can use

- the general relation between magnetic moment and angular momentum $\vec{\mu} = \gamma\vec{L}$ and

- the commutation relations Eqs. 4.35–4.38, which define operators of x, y, z components of *any* angular momentum.

In order to distinguish it from the orbital angular momentum $\vec{L}$, we label the spin angular momentum $\vec{I}$, whereas we use the symbol $\vec{\mu}$ for the spin magnetic moment. The operators of μ_x, μ_y, μ_z are given by

$$\hat{\mu}_x = \gamma\hat{I}_x, \qquad \hat{\mu}_x = \gamma\hat{I}_y, \qquad \hat{\mu}_x = \gamma\hat{I}_z, \quad (5.8)$$

and the operators of I_x, I_y, I_z must fulfill the same commutation relations as the operators of L_x, L_y, L_z:

$$\hat{I}_x\hat{I}_y - \hat{I}_y\hat{I}_x = i\hbar\hat{I}_z, \qquad \hat{I}_y\hat{I}_z - \hat{I}_z\hat{I}_y = i\hbar\hat{I}_x, \qquad \hat{I}_z\hat{I}_x - \hat{I}_x\hat{I}_z = i\hbar\hat{I}_y. \tag{5.9}$$

Following the classical definition $\vec{\mu} = \gamma\vec{L}$, we can express the operators $\hat{I}_x$, $\hat{I}_y$, $\hat{I}_z$ as $\hat{\mu}_x/\gamma$, $\hat{\mu}_x/\gamma$, $\hat{\mu}_x/\gamma$, respectively, where $\hat{\mu}_x$, $\hat{\mu}_x$, $\hat{\mu}_x$ are already defined by Eqs. 5.5–5.7. As shown in Section 5.7.9, the commutation relations summarized in Eq. 5.9 require that the magnetogyric ratio differs by a factor of 2 from the value for orbital magnetic moment:

$$\gamma = 2\frac{Q}{2m}. \tag{5.10}$$

When we divide definitions of $\hat{\mu}_x$, $\hat{\mu}_x$, $\hat{\mu}_x$ by this value of γ, we obtain the definition of the spin operators

$$\hat{I}_x = \frac{\hbar}{2}\begin{pmatrix} 0 & 1 \\ 1 & 0 \end{pmatrix} \qquad \hat{I}_y = \frac{\hbar}{2}\begin{pmatrix} 0 & -i \\ i & 0 \end{pmatrix} \qquad \hat{I}_z = \frac{\hbar}{2}\begin{pmatrix} 1 & 0 \\ 0 & -1 \end{pmatrix} \qquad \hat{I}^2 = \frac{3\hbar^2}{4}\begin{pmatrix} 1 & 0 \\ 0 & 1 \end{pmatrix}. \tag{5.11}$$

5.4 Eigenfunctions and eigenvalues of $\hat{I}_z$

The fact that $\hat{I}_z$ is diagonal tells us that we have written the matrix representations of the operators of the spin angular momentum in the basis formed by the eigenfunctions of $\hat{I}_z$. This basis is a good choice if the matrix representing Hamiltonian is also diagonal in this basis and, therefore, eigenfunctions of $\hat{I}_z$ are the same as eigenfunctions of the Hamiltonian.[3] These eigenfunctions can be

$$\sqrt{\frac{1}{h^3}}\begin{pmatrix} \psi \\ 0 \end{pmatrix} = \sqrt{\frac{1}{h^3}}\,\psi\begin{pmatrix} 1 \\ 0 \end{pmatrix}, \qquad \sqrt{\frac{1}{h^3}}\begin{pmatrix} 0 \\ \psi \end{pmatrix} = \sqrt{\frac{1}{h^3}}\,\psi\begin{pmatrix} 0 \\ 1 \end{pmatrix}, \tag{5.12}$$

i.e., the two-component variants of the free-particle wave functions from Eq. 5.179 in the low-energy approximation (the explicit form of the four-component wave function and the normalization factor $h^{-3/2}$ are described in Section 5.7.6). The normalization coefficient $h^{-3/2}$ and ψ can be canceled out in the eigenvalue equations and the eigenfunctions can be replaced by the vectors

$$\begin{pmatrix} 1 \\ 0 \end{pmatrix}, \qquad \begin{pmatrix} 0 \\ 1 \end{pmatrix} \tag{5.13}$$

corresponding to the first and second wave functions in Eq. 5.179.

The states represented by the eigenfunctions of $\hat{I}_z$ (*eigenstates*) are traditionally called states α and β and are further discussed in Section 5.5. The eigenfunctions of $\hat{I}_z$ are usually labeled as $|\alpha\rangle$ or $|\uparrow\rangle$ and $|\beta\rangle$ or $|\downarrow\rangle$:

---

[3]This is a good choice because such eigenfunctions represent states that are stationary, as was shown in Section 4.6 an is further discussed in Section 5.5.

$$\hat{I}_z|\alpha\rangle = +\frac{\hbar}{2}|\alpha\rangle \qquad \hat{I}_z|\uparrow\rangle = +\frac{\hbar}{2}|\uparrow\rangle \qquad \frac{\hbar}{2}\begin{pmatrix}1 & 0\\ 0 & -1\end{pmatrix}\begin{pmatrix}1\\ 0\end{pmatrix} = +\frac{\hbar}{2}\begin{pmatrix}1\\ 0\end{pmatrix}, \tag{5.14}$$

$$\hat{I}_z|\beta\rangle = -\frac{\hbar}{2}|\beta\rangle \qquad \hat{I}_z|\downarrow\rangle = -\frac{\hbar}{2}|\downarrow\rangle \qquad \frac{\hbar}{2}\begin{pmatrix}1 & 0\\ 0 & -1\end{pmatrix}\begin{pmatrix}0\\ 1\end{pmatrix} = -\frac{\hbar}{2}\begin{pmatrix}0\\ 1\end{pmatrix}. \tag{5.15}$$

The physical significance of the found eigenvalues $\pm\hbar/2$ is discussed in Section 5.7.10.

Note that the vectors used to represent $|\alpha\rangle$ and $|\beta\rangle$ in Eqs. 5.14 and 5.15 are not the only choice. Vectors in Eqs. 5.14 and 5.15 have a phase set to zero (they are made of real numbers). Any other phase ϕ would work as well, e.g.

$$\begin{pmatrix}1\\ 0\end{pmatrix} \rightarrow \begin{pmatrix}e^{i\phi}\\ 0\end{pmatrix}. \tag{5.16}$$

The postulates of quantum mechanics, discussed in the preceding lecture, tell us that measurement of spin angular momentum or spin magnetic moment of a single particle is limited by *quantum indeterminacy*, described bellow and shown in Figure 5.1.

- If the particle is in state $|\alpha\rangle$, the result of measuring I_z is *always* $+\hbar/2$. The expected value is

$$\langle I_z\rangle = \langle\alpha|I_z|\alpha\rangle = \begin{pmatrix}1 & 0\end{pmatrix}\frac{\hbar}{2}\begin{pmatrix}1 & 0\\ 0 & -1\end{pmatrix}\begin{pmatrix}1\\ 0\end{pmatrix} = +\frac{\hbar}{2}. \tag{5.17}$$

- If the particle is in state $|\beta\rangle$, the result of measuring I_z is *always* $-\hbar/2$. The expected value is

$$\langle I_z\rangle = \langle\beta|I_z|\beta\rangle = \begin{pmatrix}0 & 1\end{pmatrix}\frac{\hbar}{2}\begin{pmatrix}1 & 0\\ 0 & -1\end{pmatrix}\begin{pmatrix}0\\ 1\end{pmatrix} = -\frac{\hbar}{2}. \tag{5.18}$$

- Any state $c_\alpha|\alpha\rangle + c_\beta|\beta\rangle$ is possible, but the result of a single measurement of I_z is *always* $+\hbar/2$ or $-\hbar/2$. However, the expected value of I_z is

$$\langle I_z\rangle = \langle\alpha|I_z|\beta\rangle = \begin{pmatrix}c_\alpha^* & c_\beta^*\end{pmatrix}\frac{\hbar}{2}\begin{pmatrix}1 & 0\\ 0 & -1\end{pmatrix}\begin{pmatrix}c_\alpha\\ c_\beta\end{pmatrix} = (|c_\alpha|^2 - |c_\beta|^2)\frac{\hbar}{2}. \tag{5.19}$$

Wave functions $|\alpha\rangle$ and $|\beta\rangle$ are *not* eigenfunctions of $\hat{I}_x$ or $\hat{I}_y$. Eigenfunctions of $\hat{I}_x$ and $\hat{I}_y$ are presented in Section 5.7.11

5.5 Evolution, eigenstates and energy levels

Knowledge of the Hamiltonian allows us to describe how the studied system evolves. We have learnt in Section 4.6 that states corresponding to eigenfuctions, i.e., the *eigenstates*, are stationary. This is shown for the eigenfunctions of $\hat{I}_z$ in Section 5.7.12 and in Figure 5.2. If the system is in the stationary state, its eigenvalue does not change in time. Therefore, a system in a state described by
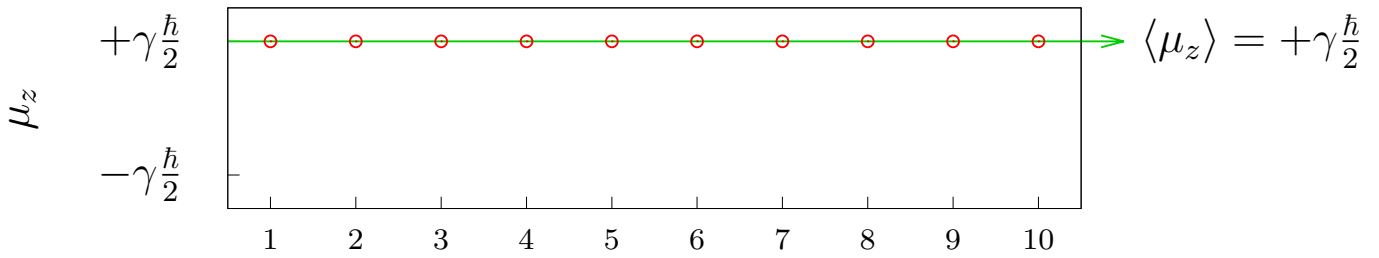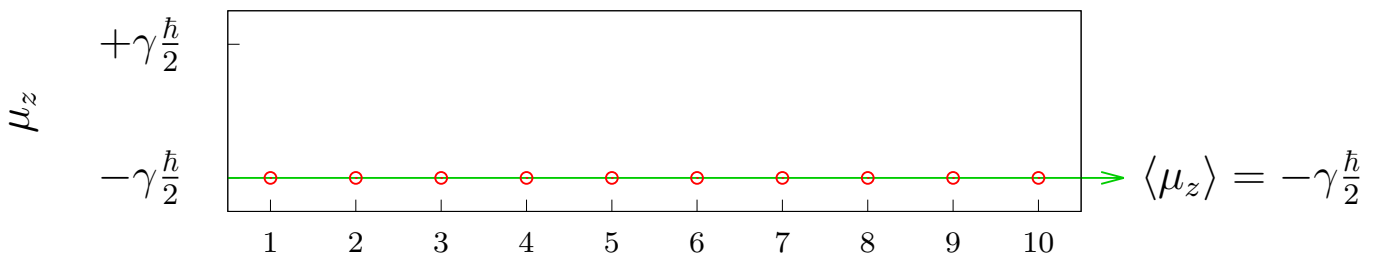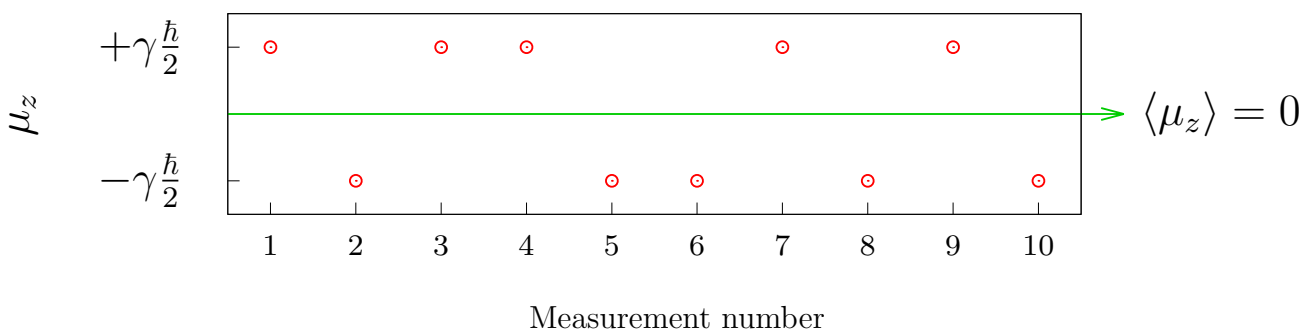
Figure 5.1: Plot of hypothetical results of individual measurements of the z components of the magnetic moment of a spin-1/2 particle in a vertical magnetic field $\vec{B}_0$. Individual measured values (equal to one of eigenvalues of $\hat{\mu}_z$) and average measured values (equal to the expectation value $\langle\mu_z\rangle$) are shown as red circles and green arrows, respectively, for a particle in the α eigenstate (A), in the β eigenstate (B) and in the superposition state described by $\frac{1}{\sqrt{2}}|\alpha\rangle + \frac{1}{\sqrt{2}}|\beta\rangle$ (C).

an eigenfunction of the Hamiltonian can be associated with a certain eigenvalue of the Hamiltonian, i.e., with a certain *energy*.

> The states described by basis functions which are eigenfunctions of the Hamiltonian do not evolve (are stationary). It makes sense to draw *energy level diagram* for such states, with energy of each state given by the corresponding eigenvalue of the Hamiltonian. Energy of the $|\alpha\rangle$ state is $-\hbar\omega_0/2$ and energy of the $|\beta\rangle$ state is $+\hbar\omega_0/2$. The measurable quantity is the energy difference $\hbar\omega_0$, corresponding to the angular frequency ω_0.

In general, the studied system can be present in a state that is not described by a single eigenfunction, but by a linear combination (superposition) of eigenfunctions. A shown in Section 5.7.13 and in Figure 5.2, such a *superposition state* evolves in time and cannot be associated with a single energy.

> The states described by basis functions different from eigenfunctions of the Hamiltonian are not stationary but oscillate between $|\alpha\rangle$ and $|\beta\rangle$ with the angular frequency ω_1, given by the difference of the eigenvalues of the Hamiltonian ($-\hbar\omega_1/2$ and $\hbar\omega_1/2$).

It should be stressed that eigenstates of individual magnetic moments are not eigenstates of the macroscopic ensembles of nuclear magnetic moments. Eigenstates of individual magnetic moments do not determine the possible result of measurement of bulk magnetization. We present the correct description of large ensembles in the next lecture.

Our ability to analyze evolution of the coefficients c_α and c_β also allows us to describe rigorously the effect of radio waves on the spin states. Detailed analysis presented in Sections 5.7.14–5.7.18 shows that equations describing weak fields oscillating in one direction (a physically realistic model of a radio wave) have the same form as equations describing rotating fields (such fields are not applied in reality, but equations describing their effects on spin states have simple analytical solutions).

5.6 Real particles

Eq. 5.4, used to derive the value of γ, describes interaction of a particle with an external electromagnetic field. However, charged particles are themselves sources of electromagnetic fields. Therefore, γ is not exactly twice $Q/2m$. In general, the value of γ is

$$\gamma = g\frac{Q}{2m}, \tag{5.20}$$

where the constant g include corrections for interactions of the particle with its own field (and other effects). For electron, the corrections are small and easy to calculate in the fully quantum approach (*quantum electrodynamics*). The current theoretical prediction is $g = 2.0023318361(10)$, compared to a recent experimental measured value of $g = 2.0023318416(13)$. On the other hand, "corrections" for the constituents of atomic nuclei, quarks, are two orders of magnitude higher than the basic value of 2! It is because quarks are not "bare" as electrons, they are confined in protons and nucleons, "dressed" by interactions, not only electromagnetic, but mostly strong nuclear with gluon. Therefore, the magnetogyric ratio of the proton is difficult to calculate and we rely on its experimental value. Everything is even more complicated when we go to higher nuclei, consisting of multiple protons and neutrons. In such cases, adding spin angular momenta represents another level

A $|\Psi\rangle(t=0) = |\alpha\rangle; \quad \hat{H} = -\gamma B_0 \hat{I}_z = \omega_0 \hat{I}_z$
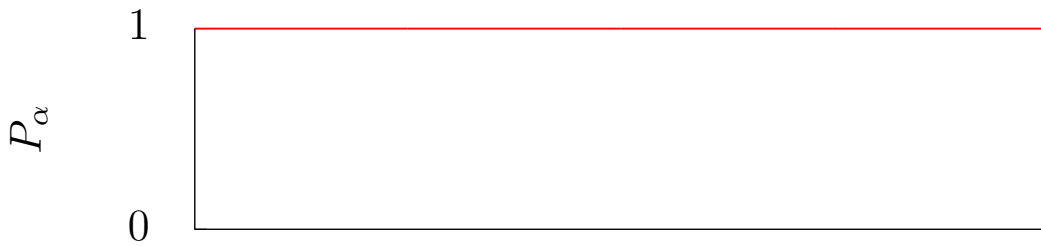
B $|\Psi\rangle(t=0) = |\beta\rangle; \quad \hat{H} = -\gamma B_0 \hat{I}_z = \omega_0 \hat{I}_z$
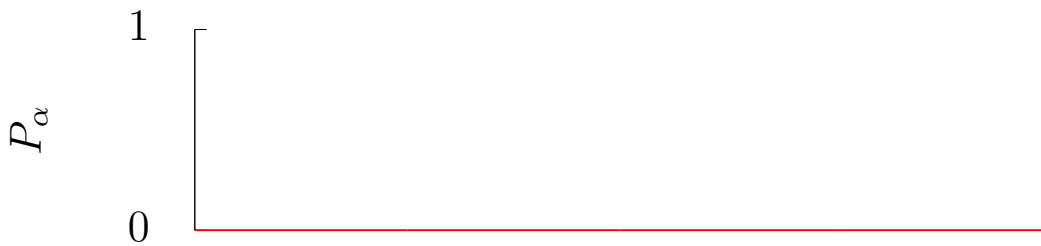
C $|\Psi\rangle(t=0) = |\alpha\rangle; \quad \hat{H} = -\gamma B_1 \hat{I}_x = \omega_1 \hat{I}_x$
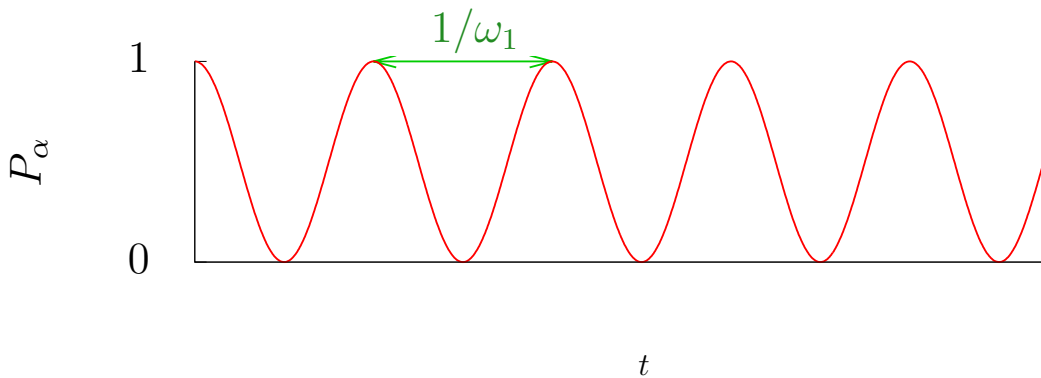
Figure 5.2: Evolution of the probability P_α that a spin-1/2 particle is found in the α state: for a particle in a vertical magnetic field $\vec{B}_0$ and in the α eigenstate at $t = 0$ (A), for a particle in a vertical magnetic field $\vec{B}_0$ and in the β eigenstate at $t = 0$ (B), and for a particle in a horizontal magnetic field $\vec{B}_1$ and in the α state at $t = 0$ (C). The states α and β are represented by eigenfunctions of $\hat{I}_z$ (Panels A and B), but $|\alpha\rangle$ is not an eigenfunction of $\hat{I}_x$.

Table 5.1: Values of the magnetogyric ratios of selected nuclei

Nucleus	magnetogyric ratio
$^{1}_{1}$H	$267.513 \times 10^6 \, \text{rad.s}^{-1}.\text{T}^{-1}$
$^{13}_{6}$C	$67.262 \times 10^6 \, \text{rad.s}^{-1}.\text{T}^{-1}$
$^{15}_{7}$N	$-27.116 \times 10^6 \, \text{rad.s}^{-1}.\text{T}^{-1}$
$^{19}_{9}$F	$251.662 \times 10^6 \, \text{rad.s}^{-1}.\text{T}^{-1}$
$^{31}_{15}$P	$108.291 \times 10^6 \, \text{rad.s}^{-1}.\text{T}^{-1}$
electron	$176\,085.952 \times 10^6 \, \text{rad.s}^{-1}.\text{T}^{-1}$

of complexity. Fortunately, all equations derived for the electron also apply to nuclei with the same eigenvalues of spin magnetic moments (spin-1/2 nuclei), if the value of γ is replaced by the correct value for the given nucleus.[4] Magnetogyric ratios of the nuclei observed most frequently are listed in Table 5.1.

HOMEWORK

Check that you understand how commutators of the operator of the orbital angular momentum are derived (Section 4.9.12) and derive the Hamiltonian of the spin magnetic moment (Section 5.7.8).

---

[4]NMR in organic chemistry and biochemistry is usually limited to spin-1/2 nuclei because signal decays too fast if the spin number is grater than 1/2.

5.7 SUPPORTING INFORMATION

5.7.1 Special theory of relativity

The first postulate of the special theory of relativity says that physical laws have the same form in all inertial coordinate frames. Two inertial frames can differ in the orientation in space. Vectors expressed in one frame can be transformed to those in another frame using relations presented in Section 1.5.3. But two inertial frames can also differ in velocity. For example, we may describe one coordinate system as *stationary* and another one as moving with a constant velocity $\vec{v}$. Galileo proposed that velocity in the stationary system is a vector sum of the velocity in the moving system and of $\vec{v}$. If we describe velocity in the stationary system as $\mathrm{d}\vec{r}/\mathrm{d}t$ (change of the position $\vec{r}$ in time), and velocity in the moving system as $\mathrm{d}\vec{r}'/\mathrm{d}t$, we can write the *Galilean transformation* as

$$\frac{\mathrm{d}\vec{r}}{\mathrm{d}t} = \frac{\mathrm{d}\vec{r}'}{\mathrm{d}t} + \vec{v}. \tag{5.21}$$

Note that both $\mathrm{d}\vec{r}$ and $\mathrm{d}\vec{r}'$ are differentiated with respect to the same time t. Galileo expected that time is a global parameter, same in all systems.

$$\mathrm{d}t = \mathrm{d}t'. \tag{5.22}$$

Eqs. 5.21 and 5.22 obviously imply

$$\mathrm{d}\vec{r} = \mathrm{d}\vec{r}' + \vec{v}\mathrm{d}t. \tag{5.23}$$

We can use the direction of $\vec{v}$ to define the x axis and to write for individual coordinates

$$\mathrm{d}x = \mathrm{d}x' + v\mathrm{d}t \tag{5.24}$$
$$\mathrm{d}y = \mathrm{d}y' \tag{5.25}$$
$$\mathrm{d}z = \mathrm{d}z' \tag{5.26}$$

The Galilean transformation yields correct results for v much slower than the speed of light c.

The second postulate of the special theory of relativity says that the value of c is the same in all inertial coordinate frames. This contradicts the Galilean transformation and another transformation relations must be searched for. The relations that satisfy both postulates of the special theory are known as *Lorentz transformation*. We are not going to derive them rigorously, but we present simple arguments that point to them (without proving the assumptions that we make).

If anything moves with a constant speed $\vec{u}$ in the stationary system, or $\vec{u}'$ in a moving system,

$$\mathrm{d}\vec{r} = \vec{u}\mathrm{d}t \quad \Rightarrow \quad \mathrm{d}r^2 - u^2\mathrm{d}t^2 = \mathrm{d}x^2 + \mathrm{d}y^2 + \mathrm{d}z^2 - u^2\mathrm{d}t^2 = 0 \tag{5.27}$$

and

$$\mathrm{d}\vec{r}' = \vec{u}'\mathrm{d}t' \quad \Rightarrow \quad \mathrm{d}r'^2 - u'^2\mathrm{d}t'^2 = \mathrm{d}x'^2 + \mathrm{d}y'^2 + \mathrm{d}z'^2 - u'^2\mathrm{d}t'^2 = 0, \tag{5.28}$$

where the expression with squares do not depend on the directions of $\vec{u}$ and $\vec{u}'$. Note that we are ready to accept that time may be different in the coordinate frames (we distinguish t' from t).

We know that the Galilean transformation $\mathrm{d}\vec{r} = \mathrm{d}\vec{r}' + \vec{v}\mathrm{d}t$ is correct for low speeds. Therefore, we can assume that for $u = 0$ and $u' = 0$

$$\mathrm{d}r^2 - u^2\mathrm{d}t^2 = \mathrm{d}r^2 = \mathrm{d}x^2 + \mathrm{d}y^2 + \mathrm{d}z^2 = \mathrm{d}r'^2 - u'^2\mathrm{d}t'^2 = \mathrm{d}r'^2 = k_x\left(\mathrm{d}x - v\mathrm{d}t\right)^2 + k_y\mathrm{d}y^2 + k_z\mathrm{d}z^2, \tag{5.29}$$

where the unknown coefficients k_x, k_y, and k_z must tend to one for $v \ll c$.

The second postulate of the special theory of relativity requires that for $u = |u| = c$

$$\mathrm{d}r^2 - |u|^2\mathrm{d}t^2 = \mathrm{d}r^2 - c^2\mathrm{d}t^2 = \mathrm{d}x^2 + \mathrm{d}y^2 + \mathrm{d}z^2 - c^2\mathrm{d}t^2 = 0 \tag{5.30}$$

but also

$$\mathrm{d}r'^2 - |u'|^2\mathrm{d}t'^2 = \mathrm{d}r'^2 - c^2\mathrm{d}t'^2 = \mathrm{d}x'^2 + \mathrm{d}y'^2 + \mathrm{d}z'^2 - c^2\mathrm{d}t'^2 = 0. \tag{5.31}$$

Combination of Eqs. 5.29–5.31 gives

$$\mathrm{d}x^2 + \mathrm{d}y^2 + \mathrm{d}z^2 - c^2\mathrm{d}t^2 = k_x\left(\mathrm{d}x - v\mathrm{d}t\right)^2 + k_y\mathrm{d}y^2 + k_z\mathrm{d}z^2 - c^2\mathrm{d}t'^2 = k_x\left(\mathrm{d}x^2 - \textcolor{red}{2v\mathrm{d}x\mathrm{d}t} + v^2\mathrm{d}t^2\right) + k_y\mathrm{d}y^2 + k_z\mathrm{d}z^2 - c^2\mathrm{d}t'^2. \tag{5.32}$$

Obviously, $\mathrm{d}t'$ cannot be equal to $\mathrm{d}t$, but the transformation of $\mathrm{d}t$ must generate a term that would cancel the red term in Eq. 5.32. We can guess that the following relation does what we need:

$$\mathrm{d}t' = \sqrt{k_x}\left(\mathrm{d}t - \frac{1}{c^2}v\mathrm{d}x\right) \quad \Rightarrow \quad \mathrm{d}t'^2 = k_x\left(\mathrm{d}t^2 - \frac{2}{c^2}v\mathrm{d}x\mathrm{d}t + \frac{1}{c^4}v^2\mathrm{d}x^2\right). \tag{5.33}$$

Plugging this into Eq. 5.32,

$$\mathrm{d}x^2 + \mathrm{d}y^2 + \mathrm{d}z^2 - c^2\mathrm{d}t^2 = k_x\left(\mathrm{d}x^2 - 2v\mathrm{d}x\mathrm{d}t + v^2\mathrm{d}t^2\right) + k_y\mathrm{d}y^2 + k_z\mathrm{d}z^2 - k_x\left(c^2\mathrm{d}t^2 - 2v\mathrm{d}x\mathrm{d}t + \frac{1}{c^2}v^2\mathrm{d}x^2\right)$$

$$= k_x\left(\mathrm{d}x^2 + v^2\mathrm{d}t^2 - c^2\mathrm{d}t^2 - \frac{v^2}{c^2}\mathrm{d}x^2\right) + k_y\mathrm{d}y^2 + k_z\mathrm{d}z^2 = k_x\left(1 - \frac{v^2}{c^2}\right)\left(\mathrm{d}x^2 - c^2\mathrm{d}t^2\right) + k_y\mathrm{d}y^2 + k_z\mathrm{d}z^2$$

$$. \tag{5.34}$$

The left-hand side is equal to the right-hand side if $k_y = k_z = 1$ and $k_x = 1/(1 - v^2/c^2)$. In summary, the transformation consistent with both postulates of special theory of relativity is

$$ct' = \frac{ct - vx/c}{\sqrt{1 - v^2/c^2}} = +\frac{1}{\sqrt{1 - v^2/c^2}}ct - \frac{v/c}{\sqrt{1 - v^2/c^2}}x = +\frac{c}{\sqrt{c^2 - v^2}}ct - \frac{v}{\sqrt{c^2 - v^2}}x, \tag{5.35}$$

$$x' = \frac{x - vt}{\sqrt{1 - v^2/c^2}} = -\frac{v/c}{\sqrt{1 - v^2/c^2}}ct + \frac{1}{\sqrt{1 - v^2/c^2}}x = -\frac{v}{\sqrt{c^2 - v^2}}ct + \frac{c}{\sqrt{c^2 - v^2}}x, \tag{5.36}$$

$$y' = y, \tag{5.37}$$

$$z' = z, \tag{5.38}$$

where the direction of $\vec{v}$ defines the x axis. Transformations between inertial coordinate systems with other directions of $\vec{v}$ are described in Section 1.5.3. For example, transformation to a coordinate system where $\vec{v}$ has a different orientation in the xy plane ($v'_x = v\cos\varphi$, $v'_y = -v\sin\varphi$) corresponds to a rotation of the coordinate frame about the z axis by the azimuth angle φ:

$$ct' = ct, \tag{5.39}$$

$$x' = +(\cos\varphi)x + (\sin\varphi)y = +\frac{v'_x}{v}x - \frac{v'_y}{v}y = +\frac{v'_x}{\sqrt{v'^2_x + v'^2_y}}x - \frac{v'_y}{\sqrt{v'^2_x + v'^2_y}}y, \tag{5.40}$$

$$y' = -(\sin\varphi)x + (\cos\varphi)y = +\frac{v'_y}{v}x + \frac{v'_x}{v}y = +\frac{v'_y}{\sqrt{v'^2_x + v'^2_y}}x + \frac{v'_x}{\sqrt{v'^2_x + v'^2_y}}y, \tag{5.41}$$

$$z' = z, \tag{5.42}$$

Note that time and space coordinates are not independent in the special theory of relativity (as they were in the Newton mechanics). Eqs. 5.30 and 5.31 tell us that

$$\mathrm{d}x^2 + \mathrm{d}y^2 + \mathrm{d}y^2 - c^2\mathrm{d}t^2 = \mathrm{d}x'^2 + \mathrm{d}y'^2 + \mathrm{d}z'^2 - c^2\mathrm{d}t'^2. \tag{5.43}$$

If the first system is stationary, i.e., the position $\vec{r}$ does not change, then $\mathrm{d}x = \mathrm{d}y = \mathrm{d}y = 0$ and

$$c^2\mathrm{d}t^2 = c^2\mathrm{d}t_0^2 = c^2\mathrm{d}t'^2 - \mathrm{d}x'^2 - \mathrm{d}y'^2 - \mathrm{d}z'^2. \tag{5.44}$$

The time measured in the stationary system is called *proper time*, we label it t_0, and it describes difference in time between two events that occur at the same position. The quantity $c^2\mathrm{d}t^2 - \mathrm{d}x^2 - \mathrm{d}y^2 - \mathrm{d}z^2$, called *space-time interval*, is *invariant* (the same in all inertial frames), equal to $c^2\mathrm{d}t_0^2$.

Eq. 5.44 is analogous to the Pythagorean theorem in a four-dimensional space, called *space-time*, consisting of time and three space dimensions. Events in the space-time are described by *four-vectors* (ct, x, y, z). Note however, that the space-time does not have Euclidean geometry as the familiar three-dimensional space of the x, y, z dimensions. This is why the minus signs appear in Eq. 5.44, in contrast to the Pythagorean theorem $r^2 = x^2 + y^2 + z^2$. Square in the space-time is calculated as

$$c^2\mathrm{d}t_0^2 = \begin{pmatrix} cdt & \mathrm{d}x & \mathrm{d}y & \mathrm{d}z \end{pmatrix} \begin{pmatrix} 1 & 0 & 0 & 0 \\ 0 & -1 & 0 & 0 \\ 0 & 0 & -1 & 0 \\ 0 & 0 & 0 & -1 \end{pmatrix} \begin{pmatrix} cdt \\ \mathrm{d}x \\ \mathrm{d}y \\ \mathrm{d}z \end{pmatrix} = c^2\mathrm{d}t^2 - \mathrm{d}x^2 - \mathrm{d}y^2 - \mathrm{d}z^2. \tag{5.45}$$

Transformation of four-vectors can be described by four-dimensional matrices, obtained by extending the three-dimensional matrices of Section 1.5.3 to the time dimension. For example, the transformations discussed above (change of velocity in the x direction and rotation in the xy plane) can be described as

$$
\begin{pmatrix} ct' \\ x' \\ y' \\ z' \end{pmatrix} = \begin{pmatrix} +\frac{1}{\sqrt{1-v^2/c^2}} & -\frac{v/c}{\sqrt{1-v^2/c^2}} & 0 & 0 \\ -\frac{v/c}{\sqrt{1-v^2/c^2}} & +\frac{1}{\sqrt{1-v^2/c^2}} & 0 & 0 \\ 0 & 0 & 1 & 0 \\ 0 & 0 & 0 & 1 \end{pmatrix} \begin{pmatrix} ct \\ x \\ y \\ z \end{pmatrix} = \begin{pmatrix} +\frac{c}{\sqrt{c^2-v^2}} & -\frac{v}{\sqrt{c^2-v^2}} & 0 & 0 \\ -\frac{v}{\sqrt{c^2-v^2}} & +\frac{c}{\sqrt{c^2-v^2}} & 0 & 0 \\ 0 & 0 & 1 & 0 \\ 0 & 0 & 0 & 1 \end{pmatrix} \begin{pmatrix} ct \\ x \\ y \\ z \end{pmatrix} \tag{5.46}
$$

and

$$
\begin{pmatrix} ct' \\ x' \\ y' \\ z' \end{pmatrix} = \begin{pmatrix} 1 & 0 & 0 & 0 \\ 0 & +\cos\varphi & +\sin\varphi & 0 \\ 0 & -\sin\varphi & +\cos\varphi & 0 \\ 0 & 0 & 0 & 1 \end{pmatrix} \begin{pmatrix} ct \\ x \\ y \\ z \end{pmatrix} = \begin{pmatrix} 1 & 0 & 0 & 0 \\ 0 & +\frac{v'_x}{\sqrt{v_x'^2+v_y'^2}} & -\frac{v'_y}{\sqrt{v_x'^2+v_y'^2}} & 0 \\ 0 & +\frac{v'_y}{\sqrt{v_x'^2+v_y'^2}} & +\frac{v'_x}{\sqrt{v_x'^2+v_y'^2}} & 0 \\ 0 & 0 & 0 & 1 \end{pmatrix} \begin{pmatrix} ct \\ x \\ y \\ z \end{pmatrix}, \tag{5.47}
$$

respectively.

5.7.2 Relativistic momentum and energy

According to the first postulate of special theory of relativity, the second Newton's law

$$
\vec{F} = \frac{\mathrm{d}\vec{p}}{\mathrm{d}t} \tag{5.48}
$$

must have the same form in all inertial frames. In the Newton mechanics, the momentum $\vec{p} = m\mathrm{d}\vec{r}/\mathrm{d}t$, where the velocity $\mathrm{d}\vec{r}/\mathrm{d}t$ is measured differently in different frames. In order to keep the second Newton's law the same in all inertial frames, momentum is defined in the special theory of relativity as

$$
\vec{p} = m_0 \frac{\mathrm{d}\vec{r}}{\mathrm{d}t_0} = m_0 \frac{\mathrm{d}\vec{r}}{\mathrm{d}t}\frac{\mathrm{d}t}{\mathrm{d}t_0} = \frac{m_0\vec{u}}{\sqrt{1-u^2/c^2}}, \tag{5.49}
$$

where $\vec{u} = \mathrm{d}\vec{r}/\mathrm{d}t$ is the velocity in the reference frame, not a velocity of the reference frame relative to another coordinate frame. Eq 5.35 was used to evaluate $\mathrm{d}t = \mathrm{d}t_0/\sqrt{1-u^2/c^2}$ (note that $\mathrm{d}x = 0$ for a stationary system). By writing m_0, we stress that we use the mass measured in the stationary system (the *rest mass*[5]).

Let us assume that the work done by a force along a certain path is converted to the kinetic energy:

$$
\mathcal{E}_{\mathrm{kin}} = -W_{12} = \int_{\vec{r}_1}^{\vec{r}_2} \vec{F} \cdot \mathrm{d}\vec{r} = \int_{t_1}^{t_2} \frac{\mathrm{d}\vec{p}}{\mathrm{d}t} \cdot \vec{u}\,\mathrm{d}t = \int_{t_1}^{t_2} \frac{\mathrm{d}}{\mathrm{d}t}\left(\frac{m_0\vec{u}}{\sqrt{1-u^2/c^2}}\right) \cdot \vec{u}\,\mathrm{d}t = m_0 \int_0^{u_2} u\,\mathrm{d}\left(\frac{u}{\sqrt{1-u^2/c^2}}\right), \tag{5.50}
$$

where the velocity increased from zero to u_2. The final integral is well suited for integration by parts (*per partes*):

$$
\mathcal{E}_{\mathrm{kin}} = m_0 \int_0^{u_2} u\,\mathrm{d}\left(\frac{u}{\sqrt{1-u^2/c^2}}\right) = m_0 \frac{u_2^2}{\sqrt{1-u_2^2/c^2}} - m_0 \int_0^{u_2} \frac{u}{\sqrt{1-u^2/c^2}}\mathrm{d}u. \tag{5.51}
$$

We notice that

$$
\frac{\mathrm{d}\left(1-u^2/c^2\right)^{\frac{1}{2}}}{\mathrm{d}u} = -\frac{u}{c^2}\left(1-u^2/c^2\right)^{-\frac{1}{2}} \quad \Rightarrow \quad -\frac{u}{\sqrt{1-u^2/c^2}}\mathrm{d}u = c^2\mathrm{d}\sqrt{1-u^2/c^2} \tag{5.52}
$$

and consequently

$$
\mathcal{E}_{\mathrm{kin}} = m_0 \frac{u_2^2}{\sqrt{1-u_2^2/c^2}} + m_0 c^2 \int_1^{\sqrt{1-u_2^2/c^2}} \mathrm{d}\sqrt{1-u^2/c^2} = m_0 \frac{u_2^2}{\sqrt{1-u_2^2/c^2}} + m_0 c^2\sqrt{1-u_2^2/c^2} - m_0 c^2 = m_0 \frac{u_2^2 + c^2 - u_2^2}{\sqrt{1-u_2^2/c^2}} - m_0 c^2
$$

$$
= \frac{m_0 c^2}{\sqrt{1-u_2^2/c^2}} - m_0 c^2 \tag{5.53}
$$

---

[5]Some old textbooks talk about a "relativistic mass", in contrast to the rest mass. As the concept of the relativistic mass was confusing, it has been abandoned. Therefore, it should be sufficient to talk about *the mass* as an invariant quantity without stressing that it is the rest mass. Nevertheless, we use the symbol m_0 here to remind us that the mass is constant and to avoid any possible confusion.

Relabeling the final velocity $u_2 \to u$,

$$\mathcal{E}_{\text{kin}} = \frac{m_0 c^2}{\sqrt{1 - u^2/c^2}} - m_0 c^2, \tag{5.54}$$

or

$$\frac{m_0 c^2}{\sqrt{1 - u^2/c^2}} = \mathcal{E}_t = \mathcal{E}_{\text{kin}} + m_0 c^2, \tag{5.55}$$

where $\mathcal{E}_t = m_0 c^2/\sqrt{1 - u^2/c^2}$ has the form of the total energy, consisting of $\mathcal{E}_{\text{kin}}$ and Einstein's famous $m_0 c^2$, playing the role of a potential energy. We can now compare the relativistic definitions of the momentum and of the energy:

$$\mathcal{E}_t = \frac{m_0 c^2}{\sqrt{1 - u^2/c^2}} \quad \Rightarrow \mathcal{E}_t^2 = \frac{m_0^2 c^4}{1 - u^2/c^2} \tag{5.56}$$

$$\vec{p} = \frac{m_0 \vec{u}}{\sqrt{1 - u^2/c^2}} \quad \Rightarrow p^2 = \frac{m_0^2 u^2}{1 - u^2/c^2}. \tag{5.57}$$

This comparison shows that

$$\mathcal{E}_t^2 - p^2 c^2 = \frac{m_0^2 c^4 - m_0^2 u^2 c^2}{1 - u^2/c^2} = \frac{m_0^2 c^4 \left(1 - u^2/c^2\right)}{1 - u^2/c^2} = m_0^2 c^4. \tag{5.58}$$

Note that both m_0 (the rest mass) and c are identical in all inertial frames (m_0 by definition, c by the second postulate of the special theory of relativity). We have found another *invariant*, the difference $\mathcal{E}_t^2 - p^2 c^2$, which is the same in all inertial coordinate frames. This invariant is the space-time square of the *momentum four-vector* $(\mathcal{E}_t, cp_x, cp_y, cp_z)$.

5.7.3 Relativistic quantum mechanics

We found in Section 5.7.2 that the special theory of relativity requires that the quantity $\mathcal{E}_t^2 - p^2 c^2$ is equal to the invariant $m_0^2 c^4$. This can be written as

$$- \mathcal{E}_t^2 + c^2 p_x^2 + c^2 p_y^2 + c^2 p_z^2 + m_0^2 c^4 = 0 \tag{5.59}$$

Let us look for an operator which represents the quantity $-\mathcal{E}_t^2 + c^2 p_x^2 + c^2 p_y^2 + c^2 p_z^2 + m_0^2 c^4$. We know that for a monochromatic wave function

$$\psi = e^{\frac{i}{\hbar}(p_x x + p_y y + p_z z - \mathcal{E}_t t)}, \tag{5.60}$$

partial derivatives of ψ serve as operators of energy and momentum:

$$i\hbar \frac{\partial \psi}{\partial x} = -p_x \psi \qquad i\hbar \frac{\partial \psi}{\partial y} = -p_y \psi \qquad i\hbar \frac{\partial \psi}{\partial z} = -p_z \psi \qquad i\hbar \frac{\partial \psi}{\partial t} = \mathcal{E}_t \psi. \tag{5.61}$$

Therefore, the operator of $-\mathcal{E}_t^2 + c^2 p_x^2 + c^2 p_y^2 + c^2 p_z^2 + m_0^2 c^4$ should have a form

$$\hbar^2 \frac{\partial^2}{\partial t^2} - c^2 \hbar^2 \frac{\partial^2}{\partial z^2} - c^2 \hbar^2 \frac{\partial^2}{\partial x^2} - c^2 \hbar^2 \frac{\partial^2}{\partial y^2} + (m_0 c^2)^2. \tag{5.62}$$

Eq. 5.62 fulfills the requirements of the special theory of relativity, but it contains the second time derivative. As discussed in Section 4.9.11, an attempt to use Eq. 5.62 to describe evolution of the quantum system in time is not consistent with our first postulate of quantum mechanics and with our interpretation of $\Psi^* \Psi$ as the probability density. Therefore, we look for an operator that contains only the first time derivative and allows us to formulate the equation(s) of motion that is in agreement with the special theory of relativity and with the postulates of quantum mechanics. As this problem is not easy to solve, we will proceed step by step. Let us first assume that particles do not move, i.e., $\vec{p} = 0$. Then, Eq. 5.59 simplifies to

$$- \mathcal{E}_t^2 + m_0^2 c^4 = 0, \tag{5.63}$$

which can be written as

$$(-\mathcal{E}_t + m_0 c^2)(\mathcal{E}_t + m_0 c^2) = 0, \tag{5.64}$$

Using the operator of energy,

$$\hbar^2 \frac{\partial^2 \psi}{\partial t^2} + (m_0 c^2)^2 \psi = \left(-\mathcal{E}_t^2 + m_0^2 c^4\right) \psi = 0 \tag{5.65}$$

132

if ψ is an eigenfunction of the energy operator. The operator of $-\mathcal{E}_t^2 + m_0^2 c^4$ (let us call it $\hat{O}^2$) can be obtained by a subsequent application of operators $\hat{O}^+$ and $\hat{O}^-$ that provide the following equations of motion:

$$\left(i\hbar\frac{\partial}{\partial t} - m_0 c^2\right)\psi = \hat{O}^+\psi = 0, \tag{5.66}$$

$$\left(-i\hbar\frac{\partial}{\partial t} - m_0 c^2\right)\psi = \hat{O}^-\psi = 0. \tag{5.67}$$

The operators $\hat{O}^-$ and $\hat{O}^+$ can be viewed as "square roots" of $\hat{O}^2$:

$$\hat{O}^2\psi \equiv \hbar^2\frac{\partial^2\psi}{\partial t^2} + (m_0 c^2)^2\psi = \left(i\hbar\frac{\partial}{\partial t} - m_0 c^2\right)\left(-i\hbar\frac{\partial}{\partial t} - m_0 c^2\right)\psi = \hat{O}^+\left(\hat{O}^-\psi\right)0. \tag{5.68}$$

What are the eigenfuctions? One solution is a wave described by Eq. 5.60 with $p_x = p_y = p_z = 0$. We can prove it by checking that calculating the time derivatives give us the eigenvalues (see the green terms in the following equation):

$$\left(i\hbar\frac{\partial}{\partial t} - m_0 c^2\right)\left(-i\hbar\frac{\partial}{\partial t} - m_0 c^2\right)e^{\frac{i}{\hbar}(-\mathcal{E}_t t)} = \left(i\hbar\frac{\partial}{\partial t} - m_0 c^2\right)\left(-\mathcal{E}_t - m_0 c^2\right)e^{\frac{i}{\hbar}(-\mathcal{E}_t t)}$$

$$= \left(-\mathcal{E}_t - m_0 c^2\right)\left(i\hbar\frac{\partial}{\partial t} - m_0 c^2\right)e^{\frac{i}{\hbar}(-\mathcal{E}_t t)} = \left(-\mathcal{E}_t - m_0 c^2\right)\left(\mathcal{E}_t - m_0 c^2\right)e^{\frac{i}{\hbar}(-\mathcal{E}_t t)} = \left(m_0^2 c^4 - \mathcal{E}_t^2\right)e^{\frac{i}{\hbar}(-\mathcal{E}_t t)} = 0. \tag{5.69}$$

But the complex conjugate of the wave described by Eq. 5.60 is another possible solution:

$$\left(i\hbar\frac{\partial}{\partial t} - m_0 c^2\right)\left(-i\hbar\frac{\partial}{\partial t} - m_0 c^2\right)e^{\frac{i}{\hbar}(\mathcal{E}_t t)} = \left(i\hbar\frac{\partial}{\partial t} - m_0 c^2\right)\left(\mathcal{E}_t - m_0 c^2\right)e^{\frac{i}{\hbar}(\mathcal{E}_t t)}$$

$$= \left(\mathcal{E}_t - m_0 c^2\right)\left(i\hbar\frac{\partial}{\partial t} - m_0 c^2\right)e^{\frac{i}{\hbar}(\mathcal{E}_t t)} = \left(\mathcal{E}_t - m_0 c^2\right)\left(-\mathcal{E}_t - m_0 c^2\right)e^{\frac{i}{\hbar}(\mathcal{E}_t t)} = \left(m_0^2 c^4 - \mathcal{E}_t^2\right)e^{\frac{i}{\hbar}(\mathcal{E}_t t)} = 0. \tag{5.70}$$

The second eigenfunction can be interpreted as a particle with a positive energy moving backwards in time, or as an *antiparticle* moving forward in time.

Let us now turn our attention to particles that can move ($\vec{p} \neq 0$). For the most interesting particles as electron or quarks, the operator $\hat{O}^2$ should have the form described by Eq. 5.62

$$\hat{O}^2\psi = \left(\hbar^2\frac{\partial^2}{\partial t^2} - c^2\hbar^2\frac{\partial^2}{\partial z^2} - c^2\hbar^2\frac{\partial^2}{\partial x^2} - c^2\hbar^2\frac{\partial^2}{\partial y^2} + (m_0 c^2)^2\right)\psi. \tag{5.71}$$

Let us try to find "square roots" of the operator $\hat{O}^2$ for a particle with a momentum $\vec{p}$. In Eq. 5.68, $\hat{O}^+$ and $\hat{O}^-$ were complex conjugates. A similar choice for a particle with a momentum $\vec{p}$, i.e.,[6]

$$\hat{O}^+\psi = \left(i\hbar\frac{\partial}{\partial t} + ic\hbar\frac{\partial}{\partial x} + ic\hbar\frac{\partial}{\partial y} + ic\hbar\frac{\partial}{\partial z} - m_0 c^2\right)\psi \tag{5.72}$$

$$\hat{O}^-\psi = \left(-i\hbar\frac{\partial}{\partial t} - ic\hbar\frac{\partial}{\partial x} - ic\hbar\frac{\partial}{\partial y} - ic\hbar\frac{\partial}{\partial z} - m_0 c^2\right)\psi \tag{5.73}$$

gives

$$\hat{O}^-\hat{O}^+\psi = \hat{O}^2\psi = \begin{array}{lllll} \hbar^2\frac{\partial^2\psi}{\partial t^2} & +c\hbar^2\frac{\partial\psi}{\partial t}\frac{\partial\psi}{\partial x} & +c\hbar^2\frac{\partial\psi}{\partial t}\frac{\partial\psi}{\partial y} & +c\hbar^2\frac{\partial\psi}{\partial t}\frac{\partial\psi}{\partial z} & -im_0 c^2\hbar\frac{\partial\psi}{\partial t} \\ +c\hbar^2\frac{\partial\psi}{\partial x}\frac{\partial\psi}{\partial t} & +\hbar^2\frac{\partial^2\psi}{\partial x^2} & +c\hbar^2\frac{\partial\psi}{\partial x}\frac{\partial\psi}{\partial y} & +c\hbar^2\frac{\partial\psi}{\partial x}\frac{\partial\psi}{\partial z} & -im_0 c^3\hbar\frac{\partial\psi}{\partial x} \\ +c\hbar^2\frac{\partial\psi}{\partial y}\frac{\partial\psi}{\partial t} & +c\hbar^2\frac{\partial\psi}{\partial y}\frac{\partial\psi}{\partial x} & +\hbar^2\frac{\partial^2\psi}{\partial y^2} & +c\hbar^2\frac{\partial\psi}{\partial y}\frac{\partial\psi}{\partial z} & -im_0 c^3\hbar\frac{\partial\psi}{\partial y} \\ +c\hbar^2\frac{\partial\psi}{\partial z}\frac{\partial\psi}{\partial t} & +c\hbar^2\frac{\partial\psi}{\partial z}\frac{\partial\psi}{\partial x} & +c\hbar^2\frac{\partial\psi}{\partial z}\frac{\partial\psi}{\partial y} & +\hbar^2\frac{\partial^2\psi}{\partial z^2} & -im_0 c^3\hbar\frac{\partial\psi}{\partial z} \\ +im_0 c^2\hbar\frac{\partial\psi}{\partial t} & +im_0 c^3\hbar\frac{\partial\psi}{\partial x} & +im_0 c^3\hbar\frac{\partial\psi}{\partial y} & +im_0 c^3\hbar\frac{\partial\psi}{\partial z} & +(m_0 c^2)^2\psi \end{array} \tag{5.74}$$

with the correct five square terms shown in blue, but also with additional twelve unwanted mixed terms shown in red (the green terms for t, x, y, z cancel each other.

As the second trial, let us try (naïvely) to get rid of the unwanted mixed terms by introducing coefficients γ_j that hopefully cancel them:

---

[6] It make sense to look for an operator which depends on time and space coordinates in a similar manner because time and space play similar roles in quantum mechanics. As the first time derivative is our requirement, the equation should contain also the first derivatives $\partial/\partial x, \partial/\partial y, \partial/\partial z$.

$$\hat{O}^+\psi = \left(\mathrm{i}\hbar\frac{\partial}{\partial t}\gamma_0 + \mathrm{i}c\hbar\frac{\partial}{\partial x}\gamma_1 + \mathrm{i}c\hbar\frac{\partial}{\partial y}\gamma_2 + \mathrm{i}c\hbar\frac{\partial}{\partial z}\gamma_3 - m_0 c^2\right)\psi$$

(5.75)

$$\hat{O}^-\psi = \left(-\mathrm{i}\hbar\frac{\partial}{\partial t}\gamma_0 - \mathrm{i}c\hbar\frac{\partial}{\partial x}\gamma_1 - \mathrm{i}c\hbar\frac{\partial}{\partial y}\gamma_2 - \mathrm{i}c\hbar\frac{\partial}{\partial z}\gamma_3 - m_0 c^2\right)\psi.$$

(5.76)

Then,

$$
\begin{aligned}
\hat{O}^-\hat{O}^+\psi = \hat{O}^2\psi = &\ \gamma_0^2\hbar^2\frac{\partial^2\psi}{\partial t^2} && +\gamma_0\gamma_1 c\hbar^2\frac{\partial\psi}{\partial t}\frac{\partial\psi}{\partial x} && +\gamma_0\gamma_2 c\hbar^2\frac{\partial\psi}{\partial t}\frac{\partial\psi}{\partial y} && +\gamma_0\gamma_3 c\hbar^2\frac{\partial\psi}{\partial t}\frac{\partial\psi}{\partial z} && {\color{green}-\mathrm{i}\gamma_0 m_0 c^2\hbar\frac{\partial\psi}{\partial t}} \\
&+\gamma_1\gamma_0 c\hbar^2\frac{\partial\psi}{\partial x}\frac{\partial\psi}{\partial t} && +\gamma_1^2\hbar^2\frac{\partial^2\psi}{\partial x^2} && +\gamma_1\gamma_2 c\hbar^2\frac{\partial\psi}{\partial x}\frac{\partial\psi}{\partial y} && +\gamma_1\gamma_3 c\hbar^2\frac{\partial\psi}{\partial x}\frac{\partial\psi}{\partial z} && {\color{green}-\mathrm{i}\gamma_1 m_0 c^3\hbar\frac{\partial\psi}{\partial x}} \\
&+\gamma_2\gamma_0 c\hbar^2\frac{\partial\psi}{\partial y}\frac{\partial\psi}{\partial t} && +\gamma_2\gamma_1 c\hbar^2\frac{\partial\psi}{\partial y}\frac{\partial\psi}{\partial x} && +\gamma_2^2\hbar^2\frac{\partial^2\psi}{\partial y^2} && +\gamma_2\gamma_3 c\hbar^2\frac{\partial\psi}{\partial y}\frac{\partial\psi}{\partial z} && {\color{green}-\mathrm{i}\gamma_2 m_0 c^3\hbar\frac{\partial\psi}{\partial y}} \\
&+\gamma_3\gamma_0 c\hbar^2\frac{\partial\psi}{\partial z}\frac{\partial\psi}{\partial t} && +\gamma_3\gamma_1 c\hbar^2\frac{\partial\psi}{\partial z}\frac{\partial\psi}{\partial x} && +\gamma_3\gamma_2 c\hbar^2\frac{\partial\psi}{\partial z}\frac{\partial\psi}{\partial y} && +\gamma_3^2\hbar^2\frac{\partial^2\psi}{\partial z^2} && {\color{green}-\mathrm{i}\gamma_3 m_0 c^3\hbar\frac{\partial\psi}{\partial z}} \\
&{\color{green}+\mathrm{i}\gamma_0 m_0 c^2\hbar\frac{\partial\psi}{\partial t}} && {\color{green}+\mathrm{i}\gamma_1 m_0 c^3\hbar\frac{\partial\psi}{\partial x}} && {\color{green}+\mathrm{i}\gamma_2 m_0 c^3\hbar\frac{\partial\psi}{\partial y}} && {\color{green}+\mathrm{i}\gamma_3 m_0 c^3\hbar\frac{\partial\psi}{\partial z}} && +(m_0 c^2)^2\psi.
\end{aligned}
$$

(5.77)

Obviously, the green terms with $-\mathrm{i}\gamma_j m_0 c^2\hbar$ cancel each other, which removes eight unwanted terms. Can we also remove the remaining dozen of unwanted mixed derivative terms? In order to do it, we need the following conditions to be fulfilled:

$$\gamma_0^2 = 1,$$

(5.78)

$$\gamma_1^2 = -1 \qquad \gamma_2^2 = -1 \qquad \gamma_3^2 = -1$$

(5.79)

and

$$\gamma_j\gamma_k + \gamma_k\gamma_j = 0 \text{ for } j \neq k.$$

(5.80)

These conditions are clearly in conflict. The first four condition require γ_j to be ± 1 or $\pm\mathrm{i}$, but the last condition requires them to be zero. There are no complex numbers that allow us to get the correct operator $\hat{O}^2$. However, there are mathematical objects that can fulfil the listed conditions simultaneously. Such objects are *matrices*.

Let us replace the coefficients γ_j in Eqs. 5.75–5.75 by matrices[7] $\hat{\gamma}^j$:

$$\hat{O}^+\Psi = \left(\mathrm{i}\hbar\frac{\partial}{\partial t}\hat{\gamma}^0 + \mathrm{i}c\hbar\frac{\partial}{\partial x}\hat{\gamma}^1 + \mathrm{i}c\hbar\frac{\partial}{\partial y}\hat{\gamma}^2 + \mathrm{i}c\hbar\frac{\partial}{\partial z}\hat{\gamma}^3 - m_0 c^2\hat{1}\right)\Psi = 0$$

(5.81)

$$\hat{O}^-\Psi = \left(-\mathrm{i}\hbar\frac{\partial}{\partial t}\hat{\gamma}^0 - \mathrm{i}c\hbar\frac{\partial}{\partial x}\hat{\gamma}^1 - \mathrm{i}c\hbar\frac{\partial}{\partial y}\hat{\gamma}^2 - \mathrm{i}c\hbar\frac{\partial}{\partial z}\hat{\gamma}^3 - m_0 c^2\hat{1}\right)\Psi = 0.$$

(5.82)

As $\hat{\gamma}^j$ are matrices, the wave function must be a *vector* composed of several waves ψ_k. This is emphasized by changing ψ (representing a monochromatic wave) to Ψ (representing a vector of monochromatic waves) in the equations.

We need a set of four matrices $\hat{\gamma}^j$ with the following properties:

$$\hat{\gamma}^0 \cdot \hat{\gamma}^0 = \hat{1},$$

(5.83)

$$\hat{\gamma}^1 \cdot \hat{\gamma}^1 = -\hat{1} \qquad \hat{\gamma}^2 \cdot \hat{\gamma}^2 = -\hat{1} \qquad \hat{\gamma}^3 \cdot \hat{\gamma}^3 = -\hat{1}$$

(5.84)

and

$$\hat{\gamma}^j \cdot \hat{\gamma}^k + \hat{\gamma}^k \cdot \hat{\gamma}^j = \hat{0} \text{ for } j \neq k.$$

(5.85)

In addition, there is a physical restriction. We know that the operator of energy (Hamiltonian) is

$$\hat{H} = \mathrm{i}\hbar\frac{\partial}{\partial t}.$$

(5.86)

We can get the *Dirac Hamiltonian* by multiplying Eq. 5.81 by $\hat{\gamma}^0$ from left:

$$\mathrm{i}\hbar\frac{\partial}{\partial t}\hat{1}\Psi = \left(-\mathrm{i}c\hbar\frac{\partial}{\partial x}\hat{\gamma}^0 \cdot \hat{\gamma}^1 - \mathrm{i}c\hbar\frac{\partial}{\partial y}\hat{\gamma}^0 \cdot \hat{\gamma}^2 - \mathrm{i}c\hbar\frac{\partial}{\partial z}\hat{\gamma}^0 \cdot \hat{\gamma}^3 + m_0 c^2\hat{\gamma}^0\right)\Psi.$$

(5.87)

---

[7]In relativistic quantum mechanics, these matrices can be treated as four components of a *four-vector*. There are two types of four-vectors (contravariant and covariant) which transform differently. There is a convention to distinguish these two types by writing components of covariant vectors with lower indices and components of contravariant vectors with upper indices. To keep this convention, we label the gamma matrices with upper indices, do not confuse them with the power!

Operator of any measurable quantity must be *Hermitian* ($\langle\psi|\hat{O}\psi\rangle = \langle\hat{O}\psi|\psi\rangle$) in order to give real values of the measured quantity (see Section 4.3). Since the terms in the Hamiltonian are proportional to $\hat{\gamma}^0$ or to $\hat{\gamma}^0 \cdot \hat{\gamma}^j$, all these matrices must be Hermitian (the elements in the j-th row and k-th column must be equal to the complex conjugates of the elements in the k-th row and j-th column for each j and k, see footnote 4 in Lecture 4.).

5.7.4 Finding the matrices

Our task is to find Hermitian matrices fulfilling the criteria imposed by Eqs. 5.83–5.85. We have a certain liberty in choosing the matrices. A matrix equation is nothing else than a set of equations. One of the matrices can be always chosen to be diagonal. Let us assume that $\hat{\gamma}^0$ is diagonal.[8] How should the diagonal elements of $\hat{\gamma}^0$ look like? In order to fulfill Eq. 5.83, the elements must be $+1$ or -1.

Another requirement follows from a general property of matrix multiplication: Trace (sum of the diagonal elements) of the matrix product $\hat{A} \cdot \hat{B}$ is the same as that of $\hat{B} \cdot \hat{A}$. Let us assume that $\hat{A} = \hat{\gamma}^j$ and $\hat{B} = \hat{\gamma}^0 \cdot \hat{\gamma}^j$. Then,

$$\mathrm{Tr}\{\hat{\gamma}^j \cdot \hat{\gamma}^0 \cdot \hat{\gamma}^j\} = \mathrm{Tr}\{\hat{\gamma}^j \cdot \hat{\gamma}^j \cdot \hat{\gamma}^0\}. \tag{5.88}$$

But Eq. 5.85 tells us that $\hat{\gamma}^0 \cdot \hat{\gamma}^j = -\hat{\gamma}^j \cdot \hat{\gamma}^0$. Therefore, the left-hand side of Eq. 5.88 can be written as $\mathrm{Tr}\{\hat{\gamma}^j \cdot (-\hat{\gamma}^j) \cdot \hat{\gamma}^0\}$, resulting in

$$-\mathrm{Tr}\{\hat{\gamma}^j \cdot \hat{\gamma}^j \cdot \hat{\gamma}^0\} = \mathrm{Tr}\{\hat{\gamma}^j \cdot \hat{\gamma}^j \cdot \hat{\gamma}^0\}, \tag{5.89}$$

and using Eq. 5.84

$$\mathrm{Tr}\{\hat{\gamma}^0\} = -\mathrm{Tr}\{\hat{\gamma}^0\}. \tag{5.90}$$

It can be true only if the trace is equal to zero. Consequently, the diagonal of $\hat{\gamma}^0$ must contain the same number of $+1$ and -1 elements. It also tells us that the dimension of the $\hat{\gamma}^j$ matrices must be even. Can they be two-dimensional?

No, for the following reason. The four $\hat{\gamma}^j$ matrices must be linearly independent, and it is impossible to find four linearly independent 2×2 matrices so that all fulfill Eq. 5.85.[9]

Is it possible to find four-dimensional $\hat{\gamma}^j$ matrices? Yes. We start by choosing

$$\hat{\gamma}^0 = \begin{pmatrix} 1 & 0 & 0 & 0 \\ 0 & 1 & 0 & 0 \\ 0 & 0 & -1 & 0 \\ 0 & 0 & 0 & -1 \end{pmatrix} \tag{5.91}$$

(the diagonal must contain two $+1$ elements and two -1 elements, their order is arbitrary, but predetermines forms of the other matrices).

Being diagonal, $\hat{\gamma}^0$ is of course Hermitian. The $\hat{\gamma}^0 \cdot \hat{\gamma}^j$ products

$$\begin{pmatrix} 1 & 0 & 0 & 0 \\ 0 & 1 & 0 & 0 \\ 0 & 0 & -1 & 0 \\ 0 & 0 & 0 & -1 \end{pmatrix} \cdot \begin{pmatrix} \gamma^j_{1,1} & \gamma^j_{1,2} & \gamma^j_{1,3} & \gamma^j_{1,4} \\ \gamma^j_{2,1} & \gamma^j_{2,2} & \gamma^j_{2,3} & \gamma^j_{2,4} \\ \gamma^j_{3,1} & \gamma^j_{3,2} & \gamma^j_{3,3} & \gamma^j_{3,4} \\ \gamma^j_{4,1} & \gamma^j_{4,2} & \gamma^j_{4,3} & \gamma^j_{4,4} \end{pmatrix} = \begin{pmatrix} \gamma^j_{1,1} & \gamma^j_{1,2} & \gamma^j_{1,3} & \gamma^j_{1,4} \\ \gamma^j_{2,1} & \gamma^j_{2,2} & \gamma^j_{2,3} & \gamma^j_{2,4} \\ -\gamma^j_{3,1} & -\gamma^j_{3,2} & -\gamma^j_{3,3} & -\gamma^j_{3,4} \\ -\gamma^j_{4,1} & -\gamma^j_{4,2} & -\gamma^j_{4,3} & -\gamma^j_{4,4} \end{pmatrix} \tag{5.92}$$

must be also Hermitian, i.e.,

$$\begin{pmatrix} \gamma^j_{1,1} & \gamma^j_{1,2} & \gamma^j_{1,3} & \gamma^j_{1,4} \\ \gamma^j_{2,1} & \gamma^j_{2,2} & \gamma^j_{2,3} & \gamma^j_{2,4} \\ -\gamma^j_{3,1} & -\gamma^j_{3,2} & -\gamma^j_{3,3} & -\gamma^j_{3,4} \\ -\gamma^j_{4,1} & -\gamma^j_{4,2} & -\gamma^j_{4,3} & -\gamma^j_{4,4} \end{pmatrix} = \begin{pmatrix} (\gamma^j_{1,1})^* & (\gamma^j_{2,1})^* & -(\gamma^j_{3,1})^* & -(\gamma^j_{4,1})^* \\ (\gamma^j_{1,2})^* & (\gamma^j_{2,2})^* & -(\gamma^j_{3,2})^* & -(\gamma^j_{4,2})^* \\ (\gamma^j_{1,3})^* & (\gamma^j_{2,3})^* & -(\gamma^j_{3,3})^* & -(\gamma^j_{4,3})^* \\ (\gamma^j_{1,4})^* & (\gamma^j_{2,4})^* & -(\gamma^j_{3,4})^* & -(\gamma^j_{4,4})^* \end{pmatrix}. \tag{5.93}$$

---

[8] This is a good choice because it results in a diagonal matrix representing the Hamiltonian, which is convenient.

[9] If the $\hat{\gamma}^j$ matrices are linearly independent, they can be used as a basis. If they constitute a basis, there must exist a linear combination of $\hat{\gamma}^j$ giving any 2×2 matrix, e.g., the unit matrix $\hat{1}$: $\hat{1} = c_0\hat{\gamma}^0 + c_1\hat{\gamma}^1 + c_2\hat{\gamma}^2 + c_3\hat{\gamma}^3$. Let us now multiply this equation by $\hat{\gamma}^0$ from left (and use Eq. 5.83)

$$\hat{\gamma}^0 = c_0\hat{1} + c_1\hat{\gamma}^0 \cdot \hat{\gamma}^1 + c_2\hat{\gamma}^0 \cdot \hat{\gamma}^2 + c_3\hat{\gamma}^0 \cdot \hat{\gamma}^3,$$

then from right

$$\hat{\gamma}^0 = c_0\hat{1} + c_1\hat{\gamma}^1 \cdot \hat{\gamma}^0 + c_2\hat{\gamma}^2 \cdot \hat{\gamma}^0 + c_3\hat{\gamma}^3 \cdot \hat{\gamma}^0,$$

and sum both equations. If the matrices fulfill Eq. 5.85, the result must be $2\hat{\gamma}^0 = 2c_0\hat{1}$, but this cannot be true because we need $\hat{\gamma}^0$ with a zero trace and the trace of the unit matrix $\hat{1}$ is obviously not zero.

At the same time, Eq. 5.85 requires $\hat{\gamma}^0 \cdot \hat{\gamma}^j = -\hat{\gamma}^j \cdot \hat{\gamma}^0$

$$
\begin{pmatrix} \gamma_{1,1}^j & \gamma_{1,2}^j & \gamma_{1,3}^j & \gamma_{1,4}^j \\ \gamma_{2,1}^j & \gamma_{2,2}^j & \gamma_{2,3}^j & \gamma_{2,4}^j \\ -\gamma_{3,1}^j & -\gamma_{3,2}^j & -\gamma_{3,3}^j & -\gamma_{3,4}^j \\ -\gamma_{4,1}^j & -\gamma_{4,2}^j & -\gamma_{4,3}^j & -\gamma_{4,4}^j \end{pmatrix} = - \begin{pmatrix} \gamma_{1,1}^j & \gamma_{1,2}^j & \gamma_{1,3}^j & \gamma_{1,4}^j \\ \gamma_{2,1}^j & \gamma_{2,2}^j & \gamma_{2,3}^j & \gamma_{2,4}^j \\ \gamma_{3,1}^j & \gamma_{3,2}^j & \gamma_{3,3}^j & \gamma_{3,4}^j \\ \gamma_{4,1}^j & \gamma_{4,2}^j & \gamma_{4,3}^j & \gamma_{4,4}^j \end{pmatrix} \cdot \begin{pmatrix} 1 & 0 & 0 & 0 \\ 0 & 1 & 0 & 0 \\ 0 & 0 & -1 & 0 \\ 0 & 0 & 0 & -1 \end{pmatrix} = \begin{pmatrix} -\gamma_{1,1}^j & -\gamma_{1,2}^j & \gamma_{1,3}^j & \gamma_{1,4}^j \\ -\gamma_{2,1}^j & -\gamma_{2,2}^j & \gamma_{2,3}^j & \gamma_{2,4}^j \\ -\gamma_{3,1}^j & -\gamma_{3,2}^j & \gamma_{3,3}^j & \gamma_{3,4}^j \\ -\gamma_{4,1}^j & -\gamma_{4,2}^j & \gamma_{4,3}^j & \gamma_{4,4}^j \end{pmatrix},
\tag{5.94}
$$

which is possible only if the red elements are equal to zero. Eq. 5.93 shows that the blue elements form two adjoint 2×2 matrices for each $j > 0$:

$$
\hat{\gamma}^j = \begin{pmatrix} 0 & 0 & \gamma_{1,3}^j & \gamma_{1,4}^j \\ 0 & 0 & \gamma_{2,3}^j & \gamma_{2,4}^j \\ \gamma_{3,1}^j & \gamma_{3,2}^j & 0 & 0 \\ \gamma_{4,1}^j & \gamma_{4,2}^j & 0 & 0 \end{pmatrix} = \begin{pmatrix} 0 & 0 & \gamma_{1,3}^j & \gamma_{1,4}^j \\ 0 & 0 & \gamma_{2,3}^j & \gamma_{2,4}^j \\ -(\gamma_{1,3}^j)^* & -(\gamma_{2,3}^j)^* & 0 & 0 \\ -(\gamma_{1,4}^j)^* & -(\gamma_{2,4}^j)^* & 0 & 0 \end{pmatrix} = \begin{pmatrix} \hat{0} & \hat{\sigma}^j \\ -(\hat{\sigma}^j)^\dagger & \hat{0} \end{pmatrix}.
\tag{5.95}
$$

Now we use Eqs. 5.84 and 5.85 to find the actual forms of three $\hat{\sigma}^j$ (and consequently $\hat{\gamma}^j$) matrices for $j > 0$. Eq. 5.84 requires

$$
\begin{pmatrix} \hat{0} & \hat{\sigma}^j \\ -(\hat{\sigma}^j)^\dagger & \hat{0} \end{pmatrix} \cdot \begin{pmatrix} \hat{0} & \hat{\sigma}^j \\ -(\hat{\sigma}^j)^\dagger & \hat{0} \end{pmatrix} = \begin{pmatrix} -\hat{\sigma}^j \cdot (\hat{\sigma}^j)^\dagger & \hat{0} \\ \hat{0} & -(\hat{\sigma}^j)^\dagger \cdot \hat{\sigma}^j \end{pmatrix} = - \begin{pmatrix} \hat{1} & \hat{0} \\ \hat{0} & \hat{1} \end{pmatrix} = \begin{pmatrix} -\hat{1} & \hat{0} \\ \hat{0} & -\hat{1} \end{pmatrix},
\tag{5.96}
$$

i.e.,

$$
\hat{\sigma}^j \cdot (\hat{\sigma}^j)^\dagger = (\hat{\sigma}^j)^\dagger \cdot \hat{\sigma}^j = \hat{1}
\tag{5.97}
$$

Eq. 5.97 is obviously true if the $\hat{\sigma}^j$ matrices are Hermitian ($\hat{\sigma}^j = (\hat{\sigma}^j)^\dagger$), i.e. $\sigma_{m,n}^j = (\sigma_{n,m}^j)^*$. It implies that the $\hat{\sigma}^j$ matrices have the following form:

$$
\hat{\sigma}^j = \begin{pmatrix} a_j & c_j \\ c_j^* & b_j \end{pmatrix},
\tag{5.98}
$$

where a_j and b_j are real, and c_j is complex. Eq. 5.97 can be then written as

$$
\hat{\sigma}^j \cdot (\hat{\sigma}^j)^\dagger = \hat{\sigma}^j \cdot \hat{\sigma}^j = \begin{pmatrix} a_j & c_j \\ c_j^* & b_j \end{pmatrix} \cdot \begin{pmatrix} a_j & c_j \\ c_j^* & b_j \end{pmatrix} = \begin{pmatrix} a_j^2 + |c_j|^2 & (a_j + b_j)c_j \\ (a_j + b_j)c_j^* & b_j^2 + |c_j|^2 \end{pmatrix} = \begin{pmatrix} 1 & 0 \\ 0 & 1 \end{pmatrix}.
\tag{5.99}
$$

The off-diagonal terms of the product matrix must be equal to zero, which is true if $a_j = -b_j$ or $|c_j| = 0$. In the former case, matrices $\hat{\sigma}^j$ can be written as

$$
\hat{\sigma}^j = \begin{pmatrix} \sqrt{1 - |c_j|^2} & c_j \\ c_j^* & -\sqrt{1 - |c_j|^2} \end{pmatrix},
\tag{5.100}
$$

in the latter case, there are only two possibilities how to construct the $\hat{\sigma}^j$ matrix:

$$
\hat{\sigma}^j = \begin{pmatrix} 1 & 0 \\ 0 & 1 \end{pmatrix} \quad \text{or} \quad \hat{\sigma}^j = \begin{pmatrix} 1 & 0 \\ 0 & -1 \end{pmatrix}
\tag{5.101}
$$

(note that $|c_j|^2 = 0 \Rightarrow a_j^2 = b_j^2 = 1$.) Eq. 5.85 shows that the second option is correct. Eq. 5.85 requires

$$
\begin{pmatrix} \hat{0} & \hat{\sigma}^j \\ -(\hat{\sigma}^j)^\dagger & \hat{0} \end{pmatrix} \cdot \begin{pmatrix} \hat{0} & \hat{\sigma}^k \\ -(\hat{\sigma}^k)^\dagger & \hat{0} \end{pmatrix} + \begin{pmatrix} \hat{0} & \hat{\sigma}^k \\ -(\hat{\sigma}^k)^\dagger & \hat{0} \end{pmatrix} \cdot \begin{pmatrix} \hat{0} & \hat{\sigma}^j \\ -(\hat{\sigma}^j)^\dagger & \hat{0} \end{pmatrix} = - \begin{pmatrix} \hat{\sigma}^j \cdot (\hat{\sigma}^k)^\dagger + \hat{\sigma}^k \cdot (\hat{\sigma}^j)^\dagger & \hat{0} \\ \hat{0} & (\hat{\sigma}^j)^\dagger \cdot \hat{\sigma}^k + (\hat{\sigma}^k)^\dagger \cdot \hat{\sigma}^j \end{pmatrix} = \begin{pmatrix} \hat{0} & \hat{0} \\ \hat{0} & \hat{0} \end{pmatrix},
\tag{5.102}
$$

therefore no $\hat{\sigma}^j$ can be a unit matrix.

As Eq. 5.101 unambiguously defines one sigma matrix (let us call it $\hat{\sigma}^3$), the other two ($\hat{\sigma}^1$ and $\hat{\sigma}^2$) are given by Eq. 5.100. According to Eq. 5.102, $\hat{\sigma}^j \cdot (\hat{\sigma}^k)^\dagger + \hat{\sigma}^k \cdot (\hat{\sigma}^j)^\dagger = \hat{\sigma}^j \hat{\sigma}^k + \hat{\sigma}^k \hat{\sigma}^j = \hat{0}$ and consequently,

$$
\begin{pmatrix} 1 & 0 \\ 0 & -1 \end{pmatrix} \cdot \begin{pmatrix} \sqrt{1 - |c_j|^2} & c_j \\ c_j^* & -\sqrt{1 - |c_j|^2} \end{pmatrix} + \begin{pmatrix} \sqrt{1 - |c_j|^2} & c_j \\ c_j^* & -\sqrt{1 - |c_j|^2} \end{pmatrix} \cdot \begin{pmatrix} 1 & 0 \\ 0 & -1 \end{pmatrix} = \begin{pmatrix} 2\sqrt{1 - |c_j|^2} & 0 \\ 0 & -2\sqrt{1 - |c_j|^2} \end{pmatrix} = \begin{pmatrix} 0 & 0 \\ 0 & 0 \end{pmatrix},
\tag{5.103}
$$

showing that $|c_j|^2 = 1$ and the diagonal elements of $\hat{\sigma}^1$ and $\hat{\sigma}^2$ are equal to zero. Therefore, these equations can be written as

$$
\hat{\sigma}^1 = \begin{pmatrix} 0 & e^{i\phi_1} \\ e^{-i\phi_1} & 0 \end{pmatrix} \qquad \hat{\sigma}^2 = \begin{pmatrix} 0 & e^{i\phi_2} \\ e^{-i\phi_2} & 0 \end{pmatrix}
\tag{5.104}
$$

According to Eq. 5.102, $\hat{\sigma}^j \hat{\sigma}^k + \hat{\sigma}^k \hat{\sigma}^j = \hat{0}$ and therefore

$$\begin{pmatrix} 0 & e^{i\phi_1} \\ e^{-i\phi_1} & 0 \end{pmatrix} \cdot \begin{pmatrix} 0 & e^{i\phi_2} \\ e^{-i\phi_2} & 0 \end{pmatrix} + \begin{pmatrix} 0 & e^{i\phi_2} \\ e^{-i\phi_2} & 0 \end{pmatrix} \cdot \begin{pmatrix} 0 & e^{i\phi_1} \\ e^{-i\phi_1} & 0 \end{pmatrix} = \begin{pmatrix} e^{i(\phi_1-\phi_2)} + e^{-i(\phi_1-\phi_2)} & 0 \\ 0 & e^{-i(\phi_1-\phi_2)} + e^{i(\phi_1-\phi_2)} \end{pmatrix} =$$

$$\begin{pmatrix} 2\cos(\phi_1 - \phi_2) & 0 \\ 0 & 2\cos(\phi_1 - \phi_2) \end{pmatrix} = \begin{pmatrix} 0 & 0 \\ 0 & 0 \end{pmatrix}. \tag{5.105}$$

The off-diagonal elements of the sum of the matrix products are equal to zero if the phases differ by $\pi/2$. Choosing $\phi_1 = 0$, the set of three sigma matrices is

$$\hat{\sigma}^1 = \begin{pmatrix} 0 & 1 \\ 1 & 0 \end{pmatrix} \qquad \hat{\sigma}^2 = \begin{pmatrix} 0 & -i \\ i & 0 \end{pmatrix} \qquad \hat{\sigma}^3 = \begin{pmatrix} 1 & 0 \\ 0 & -1 \end{pmatrix} \tag{5.106}$$

and the set of the four gamma matrices is

$$\hat{\gamma}^0 = \begin{pmatrix} 1 & 0 & 0 & 0 \\ 0 & 1 & 0 & 0 \\ 0 & 0 & -1 & 0 \\ 0 & 0 & 0 & -1 \end{pmatrix} \qquad \hat{\gamma}^1 = \begin{pmatrix} 0 & 0 & 0 & 1 \\ 0 & 0 & 1 & 0 \\ 0 & -1 & 0 & 0 \\ -1 & 0 & 0 & 0 \end{pmatrix} \qquad \hat{\gamma}^2 = \begin{pmatrix} 0 & 0 & 0 & -i \\ 0 & 0 & i & 0 \\ 0 & i & 0 & 0 \\ -i & 0 & 0 & 0 \end{pmatrix} \qquad \hat{\gamma}^3 = \begin{pmatrix} 0 & 0 & 1 & 0 \\ 0 & 0 & 0 & -1 \\ -1 & 0 & 0 & 0 \\ 0 & 1 & 0 & 0 \end{pmatrix}. \tag{5.107}$$

With the help of the $\hat{\gamma}^j$ matrices, we can modify our definition of $\hat{O}^+$ and $\hat{O}^-$ to get the correct operator $\hat{O}^2$:

$$\left(i\hbar \frac{\partial}{\partial t} \begin{pmatrix} 1 & 0 & 0 & 0 \\ 0 & 1 & 0 & 0 \\ 0 & 0 & -1 & 0 \\ 0 & 0 & 0 & -1 \end{pmatrix} + ic\hbar \frac{\partial}{\partial z} \begin{pmatrix} 0 & 0 & 1 & 0 \\ 0 & 0 & 0 & -1 \\ -1 & 0 & 0 & 0 \\ 0 & 1 & 0 & 0 \end{pmatrix} + ic\hbar \frac{\partial}{\partial x} \begin{pmatrix} 0 & 0 & 0 & 1 \\ 0 & 0 & 1 & 0 \\ 0 & -1 & 0 & 0 \\ -1 & 0 & 0 & 0 \end{pmatrix} + ic\hbar \frac{\partial}{\partial y} \begin{pmatrix} 0 & 0 & 0 & -i \\ 0 & 0 & i & 0 \\ 0 & i & 0 & 0 \\ -i & 0 & 0 & 0 \end{pmatrix} \right.$$
$$\left. - m_0 c^2 \begin{pmatrix} 1 & 0 & 0 & 0 \\ 0 & 1 & 0 & 0 \\ 0 & 0 & 1 & 0 \\ 0 & 0 & 0 & 1 \end{pmatrix} \right) \begin{pmatrix} \psi_1 \\ \psi_2 \\ \psi_3 \\ \psi_4 \end{pmatrix} = \hat{O}^+ \Psi = 0,$$
$$\tag{5.108}$$

$$\left(-i\hbar \frac{\partial}{\partial t} \begin{pmatrix} 1 & 0 & 0 & 0 \\ 0 & 1 & 0 & 0 \\ 0 & 0 & -1 & 0 \\ 0 & 0 & 0 & -1 \end{pmatrix} - ic\hbar \frac{\partial}{\partial z} \begin{pmatrix} 0 & 0 & 1 & 0 \\ 0 & 0 & 0 & -1 \\ -1 & 0 & 0 & 0 \\ 0 & 1 & 0 & 0 \end{pmatrix} - ic\hbar \frac{\partial}{\partial x} \begin{pmatrix} 0 & 0 & 0 & 1 \\ 0 & 0 & 1 & 0 \\ 0 & -1 & 0 & 0 \\ -1 & 0 & 0 & 0 \end{pmatrix} - ic\hbar \frac{\partial}{\partial y} \begin{pmatrix} 0 & 0 & 0 & -i \\ 0 & 0 & i & 0 \\ 0 & i & 0 & 0 \\ -i & 0 & 0 & 0 \end{pmatrix} \right.$$
$$\left. - m_0 c^2 \begin{pmatrix} 1 & 0 & 0 & 0 \\ 0 & 1 & 0 & 0 \\ 0 & 0 & 1 & 0 \\ 0 & 0 & 0 & 1 \end{pmatrix} \right) \begin{pmatrix} \psi_1 \\ \psi_2 \\ \psi_3 \\ \psi_4 \end{pmatrix} = \hat{O}^- \Psi = 0.$$
$$\tag{5.109}$$

5.7.5 Dirac equation and spin angular momentum

Introducing matrices means that we do not have a single equation of motion, but a set of four equations for four coupled wave functions. The complete wave function Ψ therefore consists of four components. We are used to call arrays of numbers *vectors*. However, Ψ is not a four-vector in our four-dimensional physical spacetime. The four components of Ψ have nothing to do with time and the three spatial dimensions x, y, z. We have to treat Ψ as a new physical entity and explore how it behaves.

An important question is how Ψ transforms. In Section 5.7.1, we described that the relation between coordinates in two inertial systems must be the Lorentz transformation, so that the physical laws and the value of the vacuum speed of light c are the same in both coordinate frames. As we claim that the Dirac equation is a general equation of motion, it must have the same form (be *invariant*) in different inertial coordinate systems. This can be analyzed for a general Lorentz transformation in a mathematically elegant manner, but here we explore just the rotation about the axis z.

Let us write the Dirac equation Eq. 5.108 shortly as

$$\left(i\hbar \frac{\partial}{\partial t} \hat{\gamma}^0 + ic\hbar \frac{\partial}{\partial x} \hat{\gamma}^1 + ic\hbar \frac{\partial}{\partial y} \hat{\gamma}^2 + ic\hbar \frac{\partial}{\partial z} \hat{\gamma}^3 - m_0 c^2 \hat{1} \right) \Psi = 0. \tag{5.110}$$

Then we express the Dirac equation in a coordinate frame rotated about the z axis by an angle $-\varphi$, as described for the *passive rotation* in Section 1.5.3.

$$\left(i\hbar \frac{\partial}{\partial t'} \hat{\gamma}^0 + ic\hbar \frac{\partial}{\partial x'} \hat{\gamma}^1 + ic\hbar \frac{\partial}{\partial y'} \hat{\gamma}^2 + ic\hbar \frac{\partial}{\partial z'} \hat{\gamma}^3 - m_0 c^2 \hat{1} \right) \Psi' = 0. \tag{5.111}$$

First, we have to evaluate the partial derivatives in the rotated coordinate frame. Let us to assume that we differentiate some function $f(t, x, y, z)$. Change of the coordinates means that we have to differentiate according to new coordinates t', x', y', z'. Eq. 5.47,

$$\begin{pmatrix} ct' \\ x' \\ y' \\ z' \end{pmatrix} = \begin{pmatrix} 1 & 0 & 0 & 0 \\ 0 & +\cos\varphi & +\sin\varphi & 0 \\ 0 & -\sin\varphi & +\cos\varphi & 0 \\ 0 & 0 & 0 & 1 \end{pmatrix} \begin{pmatrix} ct \\ x \\ y \\ z \end{pmatrix}, \tag{5.112}$$

shows that the new (primed) coordinates depend on the original ones. Therefore, the new partial derivatives can be calculated using the chain rule:

$$\frac{\partial f}{\partial t'} = \frac{\partial f}{\partial t}\frac{\partial t}{\partial t'} + \frac{\partial f}{\partial x}\frac{\partial x}{\partial t'} + \frac{\partial f}{\partial y}\frac{\partial y}{\partial t'} + \frac{\partial f}{\partial z}\frac{\partial z}{\partial t'} \tag{5.113}$$

$$\frac{\partial f}{\partial x'} = \frac{\partial f}{\partial t}\frac{\partial t}{\partial x'} + \frac{\partial f}{\partial x}\frac{\partial x}{\partial x'} + \frac{\partial f}{\partial y}\frac{\partial y}{\partial x'} + \frac{\partial f}{\partial z}\frac{\partial z}{\partial x'} \tag{5.114}$$

$$\frac{\partial f}{\partial y'} = \frac{\partial f}{\partial t}\frac{\partial t}{\partial y'} + \frac{\partial f}{\partial x}\frac{\partial x}{\partial y'} + \frac{\partial f}{\partial y}\frac{\partial y}{\partial y'} + \frac{\partial f}{\partial z}\frac{\partial z}{\partial y'} \tag{5.115}$$

$$\frac{\partial f}{\partial z'} = \frac{\partial f}{\partial t}\frac{\partial t}{\partial z'} + \frac{\partial f}{\partial x}\frac{\partial x}{\partial z'} + \frac{\partial f}{\partial y}\frac{\partial y}{\partial z'} + \frac{\partial f}{\partial z}\frac{\partial z}{\partial z'} \tag{5.116}$$

In order to proceed, we need the values $\partial x/\partial x'$ etc. We notice that differentiation of Eq. 5.112 provides the inverse partial derivatives:

$$\frac{\partial t'}{\partial t} = 1 \qquad \frac{\partial t'}{\partial x} = 0 \qquad \frac{\partial t'}{\partial y} = 0 \qquad \frac{\partial t'}{\partial z} = 0 \tag{5.117}$$

$$\frac{\partial x'}{\partial t} = 0 \qquad \frac{\partial x'}{\partial x} = +\cos\varphi \qquad \frac{\partial x'}{\partial y} = +\sin\varphi \qquad \frac{\partial x'}{\partial z} = 0 \tag{5.118}$$

$$\frac{\partial y'}{\partial t} = 0 \qquad \frac{\partial y'}{\partial x} = -\sin\varphi \qquad \frac{\partial y'}{\partial y} = +\cos\varphi \qquad \frac{\partial y'}{\partial z} = 0 \tag{5.119}$$

$$\frac{\partial z'}{\partial t} = 0 \qquad \frac{\partial z'}{\partial x} = 0 \qquad \frac{\partial z'}{\partial y} = 0 \qquad \frac{\partial z'}{\partial z} = 1 \tag{5.120}$$

It suggests that we should differentiate the inverse transformation to Eq. 5.112. The inverse transformation can be obtained easily by changing φ to $-\varphi$:

$$\begin{pmatrix} ct \\ x \\ y \\ z \end{pmatrix} = \begin{pmatrix} 1 & 0 & 0 & 0 \\ 0 & +\cos\varphi & -\sin\varphi & 0 \\ 0 & +\sin\varphi & +\cos\varphi & 0 \\ 0 & 0 & 0 & 1 \end{pmatrix} \begin{pmatrix} ct' \\ x' \\ y' \\ z' \end{pmatrix}. \tag{5.121}$$

We write the individual equations of the inverse transformation:

$$ct = ct' \tag{5.122}$$

$$x = +\cos\varphi\, x' - \sin\varphi\, y' \tag{5.123}$$

$$y = +\sin\varphi\, x' + \cos\varphi\, y' \tag{5.124}$$

$$z = z' \tag{5.125}$$

Now we can evaluate

$$\frac{\partial t}{\partial t'} = 1 \qquad \frac{\partial t}{\partial x'} = 0 \qquad \frac{\partial t}{\partial y'} = 0 \qquad \frac{\partial t}{\partial z'} = 0 \tag{5.126}$$

$$\frac{\partial x}{\partial t'} = 0 \qquad \frac{\partial x}{\partial x'} = +\cos\varphi \qquad \frac{\partial x}{\partial y'} = -\sin\varphi \qquad \frac{\partial x}{\partial z'} = 0 \tag{5.127}$$

$$\frac{\partial y}{\partial t'} = 0 \qquad \frac{\partial y}{\partial x'} = +\sin\varphi \qquad \frac{\partial y}{\partial y'} = +\cos\varphi \qquad \frac{\partial y}{\partial z'} = 0 \tag{5.128}$$

$$\frac{\partial z}{\partial t'} = 0 \qquad \frac{\partial z}{\partial x'} = 0 \qquad \frac{\partial z}{\partial y'} = 0 \qquad \frac{\partial z}{\partial z'} = 1 \tag{5.129}$$

and

$$\frac{\partial f}{\partial t'} = \frac{\partial f}{\partial t} \tag{5.130}$$

$$\frac{\partial f}{\partial x'} = +\cos\varphi \; \frac{\partial f}{\partial x} - \sin\varphi \; \frac{\partial f}{\partial y} \tag{5.131}$$

$$\frac{\partial f}{\partial y'} = +\sin\varphi \; \frac{\partial f}{\partial x} + \cos\varphi \; \frac{\partial f}{\partial y} \tag{5.132}$$

$$\frac{\partial f}{\partial z'} = \frac{\partial f}{\partial z} \tag{5.133}$$

or

$$\begin{pmatrix} \frac{\partial}{\partial t'} \\ \frac{\partial}{\partial x'} \\ \frac{\partial}{\partial y'} \\ \frac{\partial}{\partial z'} \end{pmatrix} = \begin{pmatrix} 1 & 0 & 0 & 0 \\ 0 & +\cos\varphi & -\sin\varphi & 0 \\ 0 & +\sin\varphi & +\cos\varphi & 0 \\ 0 & 0 & 0 & 1 \end{pmatrix} \begin{pmatrix} \frac{\partial}{\partial t} \\ \frac{\partial}{\partial x} \\ \frac{\partial}{\partial y} \\ \frac{\partial}{\partial z} \end{pmatrix}. \tag{5.134}$$

Therefore, Eq. 5.111 can be rewritten as

$$\left(i\hbar \frac{\partial}{\partial t}\hat{\gamma}^0 + ic\hbar \left(\cos\varphi \frac{\partial}{\partial x} - \sin\varphi \frac{\partial}{\partial y} \right) \hat{\gamma}^2 + ic\hbar \left(\sin\varphi \frac{\partial}{\partial x} + \cos\varphi \frac{\partial}{\partial y} \right) \hat{\gamma}^2 + ic\hbar \frac{\partial}{\partial z}\hat{\gamma}^3 - m_0 c^2 \hat{1} \right) \Psi' = 0. \tag{5.135}$$

After expressing the operator (the expression in the parenthesis in Eq. 5.111) in the rotated coordinate system, we have to pay attention to the four-component object introduced by the Dirac equation, to Φ. We know that *scalar* quantities do not change when we rotate the coordinate frame. An example is a plane-wave solution Ψ of the Schrödinger equation, which contains the scalar product of coordinates and angular momentum. We also know that vectors change as described by Eq. 5.47. But what about Ψ?. At this moment, we do not know how Ψ transforms. Therefore, we write Ψ' using a so-far undefined transformation matrix $\hat{S}$:

$$\left(i\hbar \frac{\partial}{\partial t}\hat{\gamma}^0 + ic\hbar \left(\cos\varphi \frac{\partial}{\partial x} - \sin\varphi \frac{\partial}{\partial y} \right) \hat{\gamma}^1 + ic\hbar \left(\sin\varphi \frac{\partial}{\partial x} + \cos\varphi \frac{\partial}{\partial y} \right) \hat{\gamma}^2 + ic\hbar \frac{\partial}{\partial z}\hat{\gamma}^3 - m_0 c^2 \hat{1} \right) \hat{S}\Psi = 0, \tag{5.136}$$

$$\left(i\hbar \frac{\partial}{\partial t}\hat{\gamma}^0\hat{S} + ic\hbar \left(\cos\varphi \frac{\partial}{\partial x} - \sin\varphi \frac{\partial}{\partial y} \right) \hat{\gamma}^1\hat{S} + ic\hbar \left(\sin\varphi \frac{\partial}{\partial x} + \cos\varphi \frac{\partial}{\partial y} \right) \hat{\gamma}^2\hat{S} + ic\hbar \frac{\partial}{\partial z}\hat{\gamma}^3\hat{S} - m_0 c^2 \hat{S} \right) \Psi = 0. \tag{5.137}$$

We then multiply the equation from left by the inverse matrix to $\hat{S}$ (we can move it after the partial derivatives because it is a constant matrix):

$$\left(i\hbar \frac{\partial}{\partial t}\hat{S}^{-1}\hat{\gamma}^0\hat{S} + ic\hbar \left(\cos\varphi \frac{\partial}{\partial x} - \sin\varphi \frac{\partial}{\partial y} \right) \hat{S}^{-1}\hat{\gamma}^1\hat{S} + ic\hbar \left(\sin\varphi \frac{\partial}{\partial x} + \cos\varphi \frac{\partial}{\partial y} \right) \hat{S}^{-1}\hat{\gamma}^2\hat{S} + ic\hbar \frac{\partial}{\partial z}\hat{S}^{-1}\hat{\gamma}^3\hat{S} - m_0 c^2 \hat{1} \right) \Psi = 0, \tag{5.138}$$

$$\left(i\hbar \frac{\partial}{\partial t}\hat{S}^{-1}\hat{\gamma}^0\hat{S} + ic\hbar \frac{\partial}{\partial x}\hat{S}^{-1} \left(\cos\varphi\hat{\gamma}^1 + \sin\varphi\hat{\gamma}^2 \right) \hat{S} + ic\hbar \frac{\partial}{\partial y}\hat{S}^{-1} \left(-\sin\varphi\hat{\gamma}^1 + \cos\varphi\hat{\gamma}^2 \right) \hat{S} + ic\hbar \frac{\partial}{\partial z}\hat{S}^{-1}\hat{\gamma}^3\hat{S} - m_0 c^2 \hat{1} \right) \Psi = 0. \tag{5.139}$$

The Dirac equation must be invariant. Therefore, Eqs. 5.110 and 5.139 must be identical for any φ. It requires

$$\hat{S}^{-1}\hat{\gamma}^0\hat{S} = \hat{\gamma}^0 \tag{5.140}$$

$$\hat{S}^{-1} \left(\cos\varphi\hat{\gamma}^1 + \sin\varphi\hat{\gamma}^2 \right) \hat{S} = \hat{\gamma}^1 \tag{5.141}$$

$$\hat{S}^{-1} \left(-\sin\varphi\hat{\gamma}^1 + \cos\varphi\hat{\gamma}^2 \right) \hat{S} = \hat{\gamma}^2 \tag{5.142}$$

$$\hat{S}^{-1}\hat{\gamma}^3\hat{S} = \hat{\gamma}^3. \tag{5.143}$$

We multiply Eq. 5.142 by the imaginary unit, and then add it to Eq. 5.141 and subtract it from Eq. 5.141:

$$\hat{S}^{-1} \left(\cos\varphi \left(\hat{\gamma}^1 + i\hat{\gamma}^2 \right) - i\sin\varphi \left(\hat{\gamma}^1 + i\hat{\gamma}^2 \right) \right) \hat{S} = \hat{S}^{-1} \left(e^{-i\varphi} \left(\hat{\gamma}^1 + i\hat{\gamma}^2 \right) \right) \hat{S} = \hat{\gamma}^1 + i\hat{\gamma}^2 \tag{5.144}$$

$$\hat{S}^{-1} \left(\cos\varphi \left(\hat{\gamma}^1 - i\hat{\gamma}^2 \right) + i\sin\varphi \left(\hat{\gamma}^1 - i\hat{\gamma}^2 \right) \right) \hat{S} = \hat{S}^{-1} \left(e^{+i\varphi} \left(\hat{\gamma}^1 - i\hat{\gamma}^2 \right) \right) \hat{S} = \hat{\gamma}^1 - i\hat{\gamma}^2. \tag{5.145}$$

Now we multiply the first equation by $e^{+i\varphi}$ and the second equation by $e^{-i\varphi}$:

$$\hat{S}^{-1}\left(\hat{\gamma}^1 + i\hat{\gamma}^2\right)\hat{S} = e^{+i\varphi}\left(\hat{\gamma}^1 + i\hat{\gamma}^2\right) \tag{5.146}$$

$$\hat{S}^{-1}\left(\hat{\gamma}^1 - i\hat{\gamma}^2\right)\hat{S} = e^{-i\varphi}\left(\hat{\gamma}^1 - i\hat{\gamma}^2\right). \tag{5.147}$$

This is a remarkable result. The right-hand sides of the equations contain the factors $e^{\pm i\varphi}$ multiplying the combinations of the matrices $\hat{\gamma}^1 \pm i\hat{\gamma}^2$. The exponential factors $e^{\pm i\varphi}$ described rotation of magnetization about z in Section 1.5.9, where they multiplied the combinations $M_x \pm iM_y$, and rotation of a general vector $\vec{r}$ about z in Section 4.9.13, where they multiplied the combinations $r_x \pm ir_y$. We can therefore conclude that the right-hand sides of the equations describe rotation about the axis z by an angle φ. But then also the left-hand sides of the equations must describe rotation about the axis z. In other words, the so-far unknown matrix $\hat{S}$ must have the same effect on the gamma matrices as the rotation matrix $\hat{R}$ has on the matrix representing the tensor $\hat{T}$ in Eq. 1.50. But remember that we first introduced $\hat{S}$ as a matrix transforming the four-component quantity Ψ.

What does it mean? We have written Eq. 5.111 so that it represents the Dirac equation for a system that rotates. We then expressed explicitly how rotation changes the terms in the parentheses in Eq. 5.111. Finally, we have found out that the solution of the Dirac equation, Ψ, must also rotate to keep the Dirac equation invariant. But any rotating object must have an angular momentum. We see that Ψ carrying all available information about a point-like particle such as electron, described by the Dirac equation, must possess an angular momentum. Our analysis did not include any assumption that the electron is moving along a curved path. It tells us that the angular momentum of Ψ is *not* an orbital angular momentum. It must be an angular momentum associated with the particle itself, an angular momentum called *spin*, regardless of the point-like nature of the described particle.

5.7.6 Plane wave solutions of the Dirac equation

Let us now describe solutions of the Dirac equations for particles such as a free electron. The operators $\hat{O}^+$ and $\hat{O}^-$ consist of partial derivative operators summarized in Eq. 5.61, and Eq. 5.61 also shows that a monochromatic plane wave $\psi = e^{\frac{i}{\hbar}(p_x x + p_y y + p_z z - \mathcal{E}_t t)}$ is an eigenfunction of the partial derivative operators, with the eigenvalues equal to $\mathcal{E}_t, p_x, p_y, p_z$. The wave ψ is also an eigenfunction of the operator $\hat{O}^2$ described by Eq. 5.62

$$\hat{O}^2\psi = \left(\hbar^2\frac{\partial^2}{\partial t^2} - c^2\hbar^2\frac{\partial^2}{\partial z^2} - c^2\hbar^2\frac{\partial^2}{\partial x^2} - c^2\hbar^2\frac{\partial^2}{\partial y^2} + (m_0 c^2)^2\right)e^{\frac{i}{\hbar}(p_x x + p_y y + p_z z - \mathcal{E}_s t)} = (-\mathcal{E}_s^2 + c^2 p^2 + (m_0 c^2)^2)\psi, \tag{5.148}$$

providing the expected eigenvalue $-\mathcal{E}_s^2 + c^2 p^2 + (m_0 c^2)^2$. The requirement of the special theory of relativity

$$-\mathcal{E}_s^2 + c^2 p^2 + (m_0 c^2)^2 = 0 \quad \Rightarrow \quad \mathcal{E}_s^2 = c^2 p^2 + (m_0 c^2)^2 \tag{5.149}$$

allows for two possible values of energy $\mathcal{E}_s$, one with a positive sign and another one with a negative sign

$$\mathcal{E}_s = \pm\sqrt{c^2 p^2 + (m_0 c^2)^2} = \pm\mathcal{E}_t. \tag{5.150}$$

We have labeled the energy $\mathcal{E}_s$ in order to reserve the symbol $\mathcal{E}_t$ for always positive $\sqrt{c^2 p^2 + (m_0 c^2)^2}$.

We check if a vector consisting of functions ψ multiplied by different coefficients w_j (i.e., $\psi_j = w_j\psi$) is a solution of the Dirac equation

$$\left(i\hbar\frac{\partial}{\partial t}\begin{pmatrix}1&0&0&0\\0&1&0&0\\0&0&-1&0\\0&0&0&-1\end{pmatrix} + ic\hbar\frac{\partial}{\partial z}\begin{pmatrix}0&0&1&0\\0&0&0&-1\\-1&0&0&0\\0&1&0&0\end{pmatrix} + ic\hbar\frac{\partial}{\partial x}\begin{pmatrix}0&0&0&1\\0&0&1&0\\0&-1&0&0\\-1&0&0&0\end{pmatrix} + ic\hbar\frac{\partial}{\partial y}\begin{pmatrix}0&0&0&-i\\0&0&i&0\\0&i&0&0\\-i&0&0&0\end{pmatrix}\right.$$
$$\left.-m_0 c^2\begin{pmatrix}1&0&0&0\\0&1&0&0\\0&0&1&0\\0&0&0&1\end{pmatrix}\right)\begin{pmatrix}w_1\psi\\w_2\psi\\w_3\psi\\w_4\psi\end{pmatrix} = \hat{O}^+\Psi = 0, \tag{5.151}$$

$$\left(-i\hbar\frac{\partial}{\partial t}\begin{pmatrix}1&0&0&0\\0&1&0&0\\0&0&-1&0\\0&0&0&-1\end{pmatrix} - ic\hbar\frac{\partial}{\partial z}\begin{pmatrix}0&0&1&0\\0&0&0&-1\\-1&0&0&0\\0&1&0&0\end{pmatrix} - ic\hbar\frac{\partial}{\partial x}\begin{pmatrix}0&0&0&1\\0&0&1&0\\0&-1&0&0\\-1&0&0&0\end{pmatrix} - ic\hbar\frac{\partial}{\partial y}\begin{pmatrix}0&0&0&-i\\0&0&i&0\\0&i&0&0\\-i&0&0&0\end{pmatrix}\right.$$
$$\left.-m_0 c^2\begin{pmatrix}1&0&0&0\\0&1&0&0\\0&0&1&0\\0&0&0&1\end{pmatrix}\right)\begin{pmatrix}w_1\psi\\w_2\psi\\w_3\psi\\w_4\psi\end{pmatrix} = \hat{O}^-\Psi = 0, \tag{5.152}$$

or shortly

$$\left(\mathrm{i}\hbar\frac{\partial}{\partial t}\hat{\gamma}^0 + \mathrm{i}c\hbar\frac{\partial}{\partial x}\hat{\gamma}^1 + \mathrm{i}c\hbar\frac{\partial}{\partial y}\hat{\gamma}^2 + \mathrm{i}c\hbar\frac{\partial}{\partial z}\hat{\gamma}^3 - m_0c^2\hat{1}\right)\begin{pmatrix} w_1\psi \\ w_2\psi \\ w_3\psi \\ w_4\psi \end{pmatrix} = \hat{O}^+\Psi = 0 \tag{5.153}$$

$$\left(-\mathrm{i}\hbar\frac{\partial}{\partial t}\hat{\gamma}^0 - \mathrm{i}c\hbar\frac{\partial}{\partial x}\hat{\gamma}^1 - \mathrm{i}c\hbar\frac{\partial}{\partial y}\hat{\gamma}^2 - \mathrm{i}c\hbar\frac{\partial}{\partial z}\hat{\gamma}^3 - m_0c^2\hat{1}\right)\begin{pmatrix} w_1\psi \\ w_2\psi \\ w_3\psi \\ w_4\psi \end{pmatrix} = \hat{O}^-\Psi = 0. \tag{5.154}$$

For our wavefunction,

$$\hat{O}^+\Psi = \begin{pmatrix} (\mathcal{E}_s - m_0c^2)w_1 & +0 & -cp_z w_3 & -c(p_x - \mathrm{i}p_y)w_4 \\ 0 & +(\mathcal{E}_s - m_0c^2)w_2 & -c(p_x + \mathrm{i}p_y)w_3 & +cp_z w_4 \\ cp_z w_1 & +c(p_x - \mathrm{i}p_y)w_2 & -(\mathcal{E}_s + m_0c^2)w_3 & +0 \\ c(p_x + \mathrm{i}p_y)w_1 & -cp_z w_2 & +0 & -(\mathcal{E}_s + m_0c^2)w_4 \end{pmatrix}\psi = 0. \tag{5.155}$$

The values of w_j are partially restrained by Eq. 5.155, but partially depend on the choice of the coordinate frame. One set of solution is such that one of the coefficients w_j is set to zero and another one to a normalization constant N in each solution. The normalization constant can be determined as discussed in Section 4.9.5 by requiring

$$\int\limits_{-\infty}^{\infty}\int\limits_{-\infty}^{\infty}\int\limits_{-\infty}^{\infty}\begin{pmatrix} w_1^*\psi^* & w_2^*\psi^* & w_3^*\psi^* & w_4^*\psi^* \end{pmatrix}\begin{pmatrix} w_1\psi \\ w_2\psi \\ w_3\psi \\ w_4\psi \end{pmatrix}\mathrm{d}x\mathrm{d}y\mathrm{d}z = (w_1w_1^* + w_2w_2^* + w_3w_3^* + w_4w_4^*)\underbrace{\int\limits_{-\infty}^{\infty}\int\limits_{-\infty}^{\infty}\int\limits_{-\infty}^{\infty}\psi\psi^*\mathrm{d}x\mathrm{d}y\mathrm{d}z}_{h^3} = 1, \tag{5.156}$$

where we define the probability as a "square" of the vector Ψ.

Let us find the first solution Ψ_1 by setting $w_{1,1} = N$ and $w_{2,1} = 0$. Eq. 5.155 then corresponds to a set of four equations

$$\begin{array}{llll} (\mathcal{E}_s - m_0c^2)N & +0 & -cp_z w_{3,1} & -c(p_x - \mathrm{i}p_y)w_{4,1} & = 0, \\ 0 & +0 & -c(p_x + \mathrm{i}p_y)w_{3,1} & +cp_z w_{4,1} & = 0, \\ cp_z N & +0 & -(\mathcal{E}_s + m_0c^2)w_{3,1} & +0 & = 0, \\ c(p_x + \mathrm{i}p_y)N & -0 & +0 & -(\mathcal{E}_s + m_0c^2)w_{4,1} & = 0. \end{array} \tag{5.157}$$

The third and fourth equation immediately provides the value of $w_{3,1}$ and $w_{4,1}$, respectively:

$$w_{3,1} = N\frac{cp_z}{E_s + m_0c^2} \qquad w_{4,1} = N\frac{c(p_x + \mathrm{i}p_y)}{\mathcal{E}_s + m_0c^2}. \tag{5.158}$$

The solution is

$$\Psi_1 = N\begin{pmatrix} \psi \\ 0 \\ \frac{cp_z}{\mathcal{E}_s + m_0c^2}\psi \\ \frac{c(p_x + \mathrm{i}p_y)}{\mathcal{E}_s + m_0c^2}\psi \end{pmatrix} \tag{5.159}$$

and the normalization condition is

$$N^2\left(1 + \frac{c^2p_z^2}{(\mathcal{E}_s + m_0c^2)^2} + \frac{c^2(p_x^2 + p_y^2)}{(\mathcal{E}_s + m_0c^2)^2}\right)\int\limits_{-\infty}^{\infty}\int\limits_{-\infty}^{\infty}\int\limits_{-\infty}^{\infty}\psi^*\psi\,\mathrm{d}x\mathrm{d}y\mathrm{d}z = N^2\left(1\hat{1} + \frac{c^2p_z^2}{(\mathcal{E}_s + m_0c^2)^2} + \frac{c^2(p_x^2 + p_y^2)}{(\mathcal{E}_s + m_0c^2)^2}\right)h^3$$

$$= N^2\left(\frac{(\mathcal{E}_s + m_0c^2)^2 + c^2p^2}{(\mathcal{E}_s + m_0c^2)^2}\right)h^3 = N^2\left(\frac{\mathcal{E}_s^2 + 2\mathcal{E}_s m_0c^2 + m_0^2c^4 + c^2p^2}{(\mathcal{E}_s + m_0c^2)^2}\right)h^3 = N^2\left(\frac{2\mathcal{E}_s^2 + 2\mathcal{E}_s m_0c^2}{(\mathcal{E}_s + m_0c^2)^2}\right)h^3 = N^2\left(\frac{2\mathcal{E}_s}{\mathcal{E}_s + m_0c^2}\right)h^3 = 1. \tag{5.160}$$

Therefore,

$$N = \sqrt{\frac{\mathcal{E}_t + m_0c^2}{2\mathcal{E}_t h^3}} \tag{5.161}$$

and

$$\Psi_1 = \sqrt{\frac{\mathcal{E}_t + m_0 c^2}{2\mathcal{E}_t h^3}} \begin{pmatrix} 1 \\ 0 \\ \frac{cp_z}{\mathcal{E}_t + m_0 c^2} \\ \frac{c(p_x + \mathrm{i}p_y)}{\mathcal{E}_t + m_0 c^2} \end{pmatrix} \mathrm{e}^{\frac{\mathrm{i}}{\hbar}(p_x x + p_y y + p_z z - \mathcal{E}_t t)}. \tag{5.162}$$

Here, the energy $\mathcal{E}_s$ is a positive number $\mathcal{E}_s = \mathcal{E}_t = +\sqrt{p^2 c^2 + m_0^2 c^4}$ (otherwise $N \to \infty$ for slow motions, $p \to 0$).
The second solution Ψ_2 is obtained by setting $w_{2,2} = N$ and $w_{1,2} = 0$

$$\begin{array}{llll} 0 & +0 & -cp_z w_{3,2} & -c(p_x - \mathrm{i}p_y)w_{4,2} & = 0, \\ 0 & +(\mathcal{E}_s - m_0 c^2)N & -c(p_x + \mathrm{i}p_y)w_{3,2} & +cp_z w_{4,2} & = 0, \\ 0 & +c(p_x - \mathrm{i}p_y)N & -(\mathcal{E}_s + m_0 c^2)w_{3,2} & +0 & = 0, \\ 0 & -cp_z N & +0 & -(\mathcal{E}_s + m_0 c^2)w_{4,2} & = 0, \end{array} \tag{5.163}$$

$$w_{3,2} = N \frac{c(p_x + \mathrm{i}p_y)}{E_s + m_0 c^2} \qquad w_{4,2} = N \frac{-cp_z}{E_s + m_0 c^2}, \tag{5.164}$$

giving the same normalization condition. Therefore,

$$\Psi_2 = \sqrt{\frac{\mathcal{E}_t + m_0 c^2}{2\mathcal{E}_t h^3}} \begin{pmatrix} 0 \\ 1 \\ \frac{c(p_x + \mathrm{i}p_y)}{\mathcal{E}_t + m_0 c^2} \\ \frac{-cp_z}{\mathcal{E}_t + m_0 c^2} \end{pmatrix} \mathrm{e}^{\frac{\mathrm{i}}{\hbar}(p_x x + p_y y + p_z z - \mathcal{E}_t t)} \tag{5.165}$$

with $\mathcal{E}_s = \mathcal{E}_t = +\sqrt{p^2 c^2 + m_0^2 c^4}$.
The third solution Ψ_3 is obtained by setting $w_{3,3} = N$ and $w_{4,3} = 0$

$$\begin{array}{llll} (\mathcal{E}_s - m_0 c^2)w_{1,3} & +0 & -cp_z N & +0 = 0, \\ 0 & +(E_s - m_0 c^2)w_{2,3} & -c(p_x + \mathrm{i}p_y)N & +0 = 0, \\ cp_z w_{1,3} & +c(p_x - \mathrm{i}p_y)w_{2,3} & -(\mathcal{E}_s + m_0 c^2)N & +0 = 0, \\ c(p_x + \mathrm{i}p_y)w_{1,3} & -cp_z w_{2,3} & +0 & +0 = 0. \end{array} \tag{5.166}$$

The values of $w_{1,3}$ and $w_{2,3}$ are calculated from the first two equations. Keeping the same sign of the mass term,

$$w_{1,3} = N \frac{-c(p_x + \mathrm{i}p_y)}{-E_s + m_0 c^2} \qquad w_{2,3} = N \frac{-cp_z}{-E_s + m_0 c^2}, \tag{5.167}$$

Now the normalization condition is

$$N^2 \left(1 + \frac{c^2 p_z^2}{(-\mathcal{E}_s + m_0 c^2)^2} + \frac{c^2(p_x^2 + p_y^2)}{(-\mathcal{E}_s + m_0 c^2)^2} \right) \int\limits_{-\infty}^{\infty} \int\limits_{-\infty}^{\infty} \int\limits_{-\infty}^{\infty} \psi^* \psi \mathrm{d}x \mathrm{d}y \mathrm{d}z = N^2 \left(1 + \frac{c^2 p_z^2}{(-\mathcal{E}_s + m_0 c^2)^2} + \frac{c^2(p_x^2 + p_y^2)}{(-\mathcal{E}_s + m_0 c^2)^2} \right) h^3$$

$$= N^2 \left(\frac{(-\mathcal{E}_s + m_0 c^2)^2 + c^2 p^2}{(-\mathcal{E}_s + m_0 c^2)^2} \right) h^3 = N^2 \left(\frac{\mathcal{E}_s^2 - 2\mathcal{E}_s m_0 c^2 + m_0^2 c^4 + c^2 p^2}{(-\mathcal{E}_s + m_0 c^2)^2} \right) h^3 = N^2 \left(\frac{2\mathcal{E}_s^2 - 2\mathcal{E}_s m_0 c^2}{(-\mathcal{E}_s + m_0 c^2)^2} \right) h^3 = N^2 \left(\frac{-2\mathcal{E}_s}{-\mathcal{E}_s + m_0 c^2} \right) h^3 = 1. \tag{5.168}$$

Therefore,

$$N = \sqrt{\frac{-\mathcal{E}_s + m_0 c^2}{-2\mathcal{E}_s h^3}} \tag{5.169}$$

and

$$\Psi_3 = \sqrt{\frac{-\mathcal{E}_s + m_0 c^2}{-2\mathcal{E}_s h^3}} \begin{pmatrix} \hat{1} \frac{-cp_z}{-\mathcal{E}_s + m_0 c^2} \\ \frac{-c(p_x + \mathrm{i}p_y)}{-\mathcal{E}_s + m_0 c^2} \\ 1 \\ 0 \end{pmatrix} \mathrm{e}^{\frac{\mathrm{i}}{\hbar}(p_x x + p_y y + p_z z - \mathcal{E}_s t)} = \sqrt{\frac{\mathcal{E}_t + m_0 c^2}{2\mathcal{E}_t h^3}} \begin{pmatrix} \hat{1} \frac{-cp_z}{\mathcal{E}_t + m_0 c^2} \\ \frac{-c(p_x + \mathrm{i}p_y)}{\mathcal{E}_t + m_0 c^2} \\ 1 \\ 0 \end{pmatrix} \mathrm{e}^{\frac{\mathrm{i}}{\hbar}(p_x x + p_y y + p_z z + \mathcal{E}_t t)}. \tag{5.170}$$

Here, the energy $\mathcal{E}_s$ is a negative number $\mathcal{E}_s = -\mathcal{E}_t = -\sqrt{p^2 c^2 + m_0^2 c^4}$ (otherwise $N \to \infty$ for slow motions, $p \to 0$). The fourth solution Ψ_4 is obtained by setting $w_{4,4} = N$ and $w_{3,4} = 0$

$$
\begin{aligned}
(\mathcal{E}_s - m_0 c^2) w_{1,4} &+0 &+0 &-c(p_x - \mathrm{i}p_y)N &= 0, \\
0 &+(\mathcal{E}_s - m_0 c^2) w_{2,4} &+0 +cp_z N & &= 0, \\
cp_z w_{1,4} &+c(p_x - \mathrm{i}p_y) w_{2,4} &+0 +0 & &= 0, \\
c(p_x + \mathrm{i}p_y) w_{1,4} &-cp_z w_{2,4} &+0 -(\mathcal{E}_s + m_0 c^2)N & &= 0
\end{aligned}
\tag{5.171}
$$

$$
w_{1,4} = N \frac{-c(p_x + \mathrm{i}p_y)}{-E_s + m_0 c^2} \qquad w_{2,4} = N \frac{cp_z}{-E_s + m_0 c^2},
\tag{5.172}
$$

with the same normalization condition as the third solution. Therefore,

$$
\Psi_4 = \sqrt{\frac{-\mathcal{E}_s + m_0 c^2}{-2\mathcal{E}_s h^3}}
\begin{pmatrix}
\frac{-c(p_x+\mathrm{i}p_y)}{-\mathcal{E}_s+m_0 c^2} \\
\frac{-cp_z}{-\mathcal{E}_s+m_0 c^2} \\
0 \\
1
\end{pmatrix}
\mathrm{e}^{\frac{\mathrm{i}}{\hbar}(p_x x + p_y y + p_z z - \mathcal{E}_s t)}
\tag{5.173}
$$

with $\mathcal{E}_s = -\mathcal{E}_t = -\sqrt{p^2 c^2 + m_0^2 c^4}$.

The negative energy has some strange implications. For example, the plane wave ψ should propagate with the rate $\vec{c}$. The value of c is given by $c = \lambda/T = \mathcal{E}_t/|p|$ and the direction should be given by the momentum vector $\vec{p}$

$$
\vec{c} = \frac{\mathcal{E}_s}{|p|} \frac{\vec{p}}{|p|} = \frac{\mathcal{E}_s \vec{p}}{p^2}.
\tag{5.174}
$$

Changing the sign of $\mathcal{E}_s$ also changes direction of motion. However, note that opposite directions of the vectors of momentum give the same p^2:

$$
p^2 = \vec{p} \cdot \vec{p} \qquad p^2 = -\vec{p} \cdot (-\vec{p}).
\tag{5.175}
$$

We can therefore use $-\vec{p}$ in the wavefunction with the negative energy $\mathcal{E}_s = -\mathcal{E}_t$. Such wavefunction is complex conjugate of ψ describing the first two states

$$
\mathrm{e}^{\frac{\mathrm{i}}{\hbar}(-p_x x - p_y y - p_z z - \mathcal{E}_s t)} = \mathrm{e}^{\frac{\mathrm{i}}{\hbar}(-p_x x - p_y y - p_z z + \mathcal{E}_t t)} = \mathrm{e}^{-\frac{\mathrm{i}}{\hbar}(p_x x + p_y y + p_z z - \mathcal{E}_t t)} = \psi^*.
\tag{5.176}
$$

and it is also an eigenfunction of $\hat{O}^2$

$$
\hat{O}^2 \psi^* = \left(\hbar^2 \frac{\partial^2}{\partial t^2} - c^2 \hbar^2 \frac{\partial^2}{\partial z^2} - c^2 \hbar^2 \frac{\partial^2}{\partial x^2} - c^2 \hbar^2 \frac{\partial^2}{\partial y^2} + (m_0 c^2)^2 \right) \mathrm{e}^{-\frac{\mathrm{i}}{\hbar}(p_x x + p_y y + p_z z - \mathcal{E}_t t)} = (-\mathcal{E}_t^2 + c^2 p^2 + (m_0 c^2)^2)\psi^*.
\tag{5.177}
$$

When we change the signs of p_x, p_y, and p_z in the coefficients $w_{j,3}$ and $w_{j,4}$, we can express the solutions of the Dirac equation in a general form

$$
\Psi =
\begin{pmatrix}
u_1 \psi \\
u_2 \psi \\
v_1 \psi^* \\
v_2 \psi^*
\end{pmatrix},
\tag{5.178}
$$

where

$$
\Psi_1 = N
\begin{pmatrix}
\psi \\
0 \\
\frac{cp_z}{\mathcal{E}_t+m_0 c^2}\psi^* \\
\frac{c(p_x+\mathrm{i}p_y)}{\mathcal{E}_t+m_0 c^2}\psi^*
\end{pmatrix},
\qquad
\Psi_2 = N
\begin{pmatrix}
0 \\
\psi \\
\frac{c(p_x-\mathrm{i}p_y)}{\mathcal{E}_t+m_0 c^2}\psi^* \\
\frac{-cp_z}{\mathcal{E}_t+m_0 c^2}\psi^*
\end{pmatrix},
\qquad
\Psi_3 = N
\begin{pmatrix}
\frac{cp_z}{\mathcal{E}_t+m_0 c^2}\psi \\
\frac{c(p_x+\mathrm{i}p_y)}{\mathcal{E}_t+m_0 c^2}\psi \\
\psi^* \\
0
\end{pmatrix},
\qquad
\Psi_4 = N
\begin{pmatrix}
\frac{c(p_x-\mathrm{i}p_y)}{\mathcal{E}_t+m_0 c^2}\psi \\
\frac{-cp_z}{\mathcal{E}_t+m_0 c^2}\psi \\
0 \\
\psi^*
\end{pmatrix},
\tag{5.179}
$$

$$
N = \sqrt{\frac{\mathcal{E}_t + m_0 c^2}{2\mathcal{E}_t h^3}},
\tag{5.180}
$$

and

$$
\psi = \mathrm{e}^{\frac{\mathrm{i}}{\hbar}(p_x x + p_y y + p_z z - \mathcal{E}_t t)}.
\tag{5.181}
$$

5.7.7 Relation between Dirac and Schrödinger equations

How is the Dirac equation related to the Schrödinger equation? We came to the Schrödinger equation using the relation $\mathcal{E}_{\mathrm{kin}} = p^2/2m$ (energy of a free particle, i.e., kinetic energy). Let us now try to relate the kinetic energy $\mathcal{E}_{\mathrm{kin}}$ to the total energy $\mathcal{E}_t$ of the relativistic treatment. We know that mass contributes to $\mathcal{E}_t$ as m_0c^2. We can assume that in the absence of an electromagnetic field, the total energy of a free particle consists of the mass contribution m_0c^2 (*rest energy*) and of $\mathcal{E}_{\mathrm{kin}}$. Therefore, the square of the total energy should be

$$\mathcal{E}_t^2 = (m_0c^2 + \mathcal{E}_{\mathrm{kin}})^2 = (m_0c^2)^2 + 2\mathcal{E}_{\mathrm{kin}}(m_0c^2) + \mathcal{E}_{\mathrm{kin}}^2. \tag{5.182}$$

As a next step, we divide the square of the total energy by the square of the mass contribution

$$\frac{\mathcal{E}_t^2}{(m_0c^2)^2} = \frac{(m_0c^2)^2 + 2\mathcal{E}_{\mathrm{kin}}(m_0c^2) + \mathcal{E}_{\mathrm{kin}}^2}{(m_0c^2)^2} = 1 + 2\frac{\mathcal{E}_{\mathrm{kin}}}{m_0c^2} + \frac{\mathcal{E}_{\mathrm{kin}}^2}{(m_0c^2)^2}. \tag{5.183}$$

If the speed of the particle is low, $\mathcal{E}_{\mathrm{kin}}^2 \ll (m_0c^2)^2$, and the last term can be neglected

$$\frac{\mathcal{E}_t^2}{(m_0c^2)^2} \approx 1 + 2\frac{\mathcal{E}_{\mathrm{kin}}}{m_0c^2}. \tag{5.184}$$

But Eq. 5.59 also tells us that

$$\mathcal{E}_t^2 = (m_0c^2)^2 + c^2p^2 \quad \Rightarrow \quad \frac{\mathcal{E}_t^2}{(m_0c^2)^2} = 1 + \frac{c^2p^2}{(m_0c^2)^2}. \tag{5.185}$$

Comparison of the right-hand sides of Eqs. 5.184 and 5.185 shows that

$$2\frac{\mathcal{E}_{\mathrm{kin}}}{m_0c^2} = \frac{c^2p^2}{(m_0c^2)^2} \quad \Rightarrow \quad \mathcal{E}_{\mathrm{kin}} = \frac{p^2}{2m_0}. \tag{5.186}$$

We see that the approximation for low speeds led us to the relation defining the kinetic energy as in the Schrödinger equation. Therefore, Schrödinger equation can be viewed as a low-speed limit of the Dirac equation. We use similar arguments more rigorously in Section 5.7.8 when we relate Dirac and Schrödinger Hamiltonian in the presence of the electromagnetic field.

5.7.8 Hamiltonian of spin magnetic moment

Our next goal is to find Hamiltonian for a relativistic charged particle in a magnetic field. When we compare the classical Hamiltonian of a particle in an electromagnetic field (Eq. 4.74) with the classical Hamiltonian of a free particle $\mathcal{H} = (\vec{p})^2/(2m)$ outside the field, we see that the presence of an electromagnetic field requires the following modifications:

$$\mathcal{H} \to \mathcal{H} - QV \qquad \vec{p} \to \vec{p} - Q\vec{A}, \tag{5.187}$$

Accordingly, the operators of energy and momentum in the quantum description change to

$$\mathrm{i}\hbar\frac{\partial}{\partial t} \to \mathrm{i}\hbar\frac{\partial}{\partial t} - QV \qquad -\mathrm{i}\hbar\frac{\partial}{\partial x} \to -\mathrm{i}\hbar\frac{\partial}{\partial x} - QA_x \qquad -\mathrm{i}\hbar\frac{\partial}{\partial y} \to -\mathrm{i}\hbar\frac{\partial}{\partial y} - QA_y \qquad -\mathrm{i}\hbar\frac{\partial}{\partial z} \to -\mathrm{i}\hbar\frac{\partial}{\partial z} - QA_z. \tag{5.188}$$

This modifies Eq. 5.87 to

$$\left(\mathrm{i}\hbar\frac{\partial}{\partial t} - QV\right)\hat{1}\Psi = \left(-c\left(\mathrm{i}\hbar\frac{\partial}{\partial x} + QA_x\right)\hat{\gamma}^0\hat{\gamma}^1 - c\left(\mathrm{i}\hbar\frac{\partial}{\partial y} + QA_y\right)\hat{\gamma}^0\hat{\gamma}^2 - c\left(\mathrm{i}\hbar\frac{\partial}{\partial z} + QA_z\right)\hat{\gamma}^0\hat{\gamma}^3 + m_0c^2\hat{\gamma}^0\right)\Psi, \tag{5.189}$$

where $\hat{1}$ is a 4×4 unit matrix. In order to obtain an expression comparable to Eq. 4.26 (nonrelativistic Schrödinger equation), we apply the operator $(\mathrm{i}\hbar\partial/\partial t - QV)$ twice

$$\left(i\hbar\frac{\partial}{\partial t} - QV\right)\left(i\hbar\frac{\partial}{\partial t} - QV\right)\hat{1}\Psi = \left(i\hbar\frac{\partial}{\partial t} - QV\right)^2\hat{1}\Psi$$

$$= \left(c^2\left(i\hbar\frac{\partial}{\partial x} + QA_x\right)^2\hat{\gamma}^0\hat{\gamma}^1\hat{\gamma}^0\hat{\gamma}^1 + c^2\left(i\hbar\frac{\partial}{\partial y} + QA_y\right)^2\hat{\gamma}^0\hat{\gamma}^2\hat{\gamma}^0\hat{\gamma}^2 + c^2\left(i\hbar\frac{\partial}{\partial z} + QA_z\right)^2\hat{\gamma}^0\hat{\gamma}^3\hat{\gamma}^0\hat{\gamma}^3 + m_0^2c^4\hat{\gamma}^0\hat{\gamma}^0\right)\Psi$$

$$-m_0c^3\left(\left(i\hbar\frac{\partial}{\partial x} + QA_x\right)\hat{\gamma}^0\hat{\gamma}^1\hat{\gamma}^0 + \left(i\hbar\frac{\partial}{\partial y} + QA_y\right)\hat{\gamma}^0\hat{\gamma}^2\hat{\gamma}^0 + \left(i\hbar\frac{\partial}{\partial z} + QA_z\right)\hat{\gamma}^0\hat{\gamma}^3\hat{\gamma}^0\right)\Psi$$

$$-m_0c^3\left(\left(i\hbar\frac{\partial}{\partial x} + QA_x\right)\hat{\gamma}^0\hat{\gamma}^0\hat{\gamma}^1 + \left(i\hbar\frac{\partial}{\partial y} + QA_y\right)\hat{\gamma}^0\hat{\gamma}^0\hat{\gamma}^2 + \left(i\hbar\frac{\partial}{\partial z} + QA_z\right)\hat{\gamma}^0\hat{\gamma}^0\hat{\gamma}^3\right)\Psi$$

$$+c^2\left(\left(i\hbar\frac{\partial}{\partial x} + QA_x\right)\left(i\hbar\frac{\partial}{\partial y} + QA_y\right)\hat{\gamma}^0\hat{\gamma}^1\hat{\gamma}^0\hat{\gamma}^2 + \left(i\hbar\frac{\partial}{\partial y} + QA_y\right)\left(i\hbar\frac{\partial}{\partial x} + QA_x\right)\hat{\gamma}^0\hat{\gamma}^2\hat{\gamma}^0\hat{\gamma}^1\right)\Psi$$

$$+c^2\left(\left(i\hbar\frac{\partial}{\partial y} + QA_y\right)\left(i\hbar\frac{\partial}{\partial z} + QA_z\right)\hat{\gamma}^0\hat{\gamma}^2\hat{\gamma}^0\hat{\gamma}^3 + \left(i\hbar\frac{\partial}{\partial z} + QA_z\right)\left(i\hbar\frac{\partial}{\partial y} + QA_y\right)\hat{\gamma}^0\hat{\gamma}^3\hat{\gamma}^0\hat{\gamma}^2\right)\Psi$$

$$+c^2\left(\left(i\hbar\frac{\partial}{\partial z} + QA_z\right)\left(i\hbar\frac{\partial}{\partial x} + QA_x\right)\hat{\gamma}^0\hat{\gamma}^3\hat{\gamma}^0\hat{\gamma}^1 + \left(i\hbar\frac{\partial}{\partial x} + QA_x\right)\left(i\hbar\frac{\partial}{\partial z} + QA_z\right)\hat{\gamma}^0\hat{\gamma}^1\hat{\gamma}^0\hat{\gamma}^3\right)\Psi. \tag{5.190}$$

We use the properties of the gamma matrices (Eqs. 5.83–5.85) to simplify the equation. In particular, we invert of the order of matrices in the products

$$\hat{\gamma}^0\hat{\gamma}^j\hat{\gamma}^0 = -(\hat{\gamma}^0\hat{\gamma}^0)\hat{\gamma}^j = -\hat{\gamma}^j, \tag{5.191}$$

$$\hat{\gamma}^0\hat{\gamma}^j\hat{\gamma}^0\hat{\gamma}^j = -(\hat{\gamma}^0\hat{\gamma}^0)(\hat{\gamma}^j\hat{\gamma}^j) = -(\hat{1})(-\hat{1}) = \hat{1}, \tag{5.192}$$

$$\hat{\gamma}^0\hat{\gamma}^j\hat{\gamma}^0\hat{\gamma}^k = -(\hat{\gamma}^0\hat{\gamma}^0)(\hat{\gamma}^j\hat{\gamma}^k) = -(\hat{1})(\hat{\gamma}^j\hat{\gamma}^k) = -\hat{\gamma}^j\hat{\gamma}^k = \hat{\gamma}^k\hat{\gamma}^j \tag{5.193}$$

and obtain

$$\left(i\hbar\frac{\partial}{\partial t} - QV\right)^2\hat{1}\Psi = \left(c^2\left(i\hbar\frac{\partial}{\partial x} + QA_x\right)^2\hat{1} + c^2\left(i\hbar\frac{\partial}{\partial y} + QA_y\right)^2\hat{1} + c^2\left(i\hbar\frac{\partial}{\partial z} + QA_z\right)^2\hat{1} + m_0^2c^4\hat{1}\right)\Psi$$

$$+m_0c^3\left(\left(i\hbar\frac{\partial}{\partial x} + QA_x\right)\hat{\gamma}^1 + \left(i\hbar\frac{\partial}{\partial y} + QA_y\right)\hat{\gamma}^2 + \left(i\hbar\frac{\partial}{\partial z} + QA_z\right)\hat{\gamma}^3\right)\Psi$$

$$-m_0c^3\left(\left(i\hbar\frac{\partial}{\partial x} + QA_x\right)\hat{\gamma}^1 + \left(i\hbar\frac{\partial}{\partial y} + QA_y\right)\hat{\gamma}^2 + \left(i\hbar\frac{\partial}{\partial z} + QA_z\right)\hat{\gamma}^3\right)\Psi$$

$$-c^2\left(\left(i\hbar\frac{\partial}{\partial x} + QA_x\right)\left(i\hbar\frac{\partial}{\partial y} + QA_y\right) - \left(i\hbar\frac{\partial}{\partial y} + QA_y\right)\left(i\hbar\frac{\partial}{\partial x} + QA_x\right)\right)\hat{\gamma}^1\hat{\gamma}^2\Psi$$

$$-c^2\left(\left(i\hbar\frac{\partial}{\partial y} + QA_y\right)\left(i\hbar\frac{\partial}{\partial z} + QA_z\right) - \left(i\hbar\frac{\partial}{\partial z} + QA_z\right)\left(i\hbar\frac{\partial}{\partial y} + QA_y\right)\right)\hat{\gamma}^2\hat{\gamma}^3\Psi$$

$$-c^2\left(\left(i\hbar\frac{\partial}{\partial z} + QA_z\right)\left(i\hbar\frac{\partial}{\partial x} + QA_x\right) - \left(i\hbar\frac{\partial}{\partial x} + QA_x\right)\left(i\hbar\frac{\partial}{\partial z} + QA_z\right)\right)\hat{\gamma}^3\hat{\gamma}^1\Psi, \tag{5.194}$$

where the second line and the third line cancel each other. To proceed, we need to evaluate the products of operators on the last three lines. Let us look at one of the lines more closely

$$-c^2\left(\left(i\hbar\frac{\partial}{\partial x} + QA_x\right)\left(i\hbar\frac{\partial}{\partial y} + QA_y\right) - \left(i\hbar\frac{\partial}{\partial y} + QA_y\right)\left(i\hbar\frac{\partial}{\partial x} + QA_x\right)\right)\hat{\gamma}^1\hat{\gamma}^2\Psi \tag{5.195}$$

and analyze the operator part (green) and the wave function part (blue) separately. We start by the green operator (to emphasize that we work with the operator, we apply it to some arbitrary function, labeled ψ). The green operator is composed of linear operators, we have to apply them twice (we must be very careful with the differentiation)

$$\left(\left(i\hbar\frac{\partial}{\partial x} + QA_x\right)\left(i\hbar\frac{\partial}{\partial y} + QA_y\right) - \left(i\hbar\frac{\partial}{\partial y} + QA_y\right)\left(i\hbar\frac{\partial}{\partial x} + QA_x\right)\right)\psi =$$

$$-\hbar^2\left(\frac{\partial}{\partial x}\frac{\partial\psi}{\partial y} - \frac{\partial}{\partial y}\frac{\partial\psi}{\partial x}\right) + Q^2(A_xA_y - A_yA_x)\psi + i\hbar Q\left(\frac{\partial(A_y\psi)}{\partial x} + A_x\frac{\partial\psi}{\partial y} - \frac{\partial(A_x\psi)}{\partial y} - A_y\frac{\partial\psi}{\partial x}\right). \tag{5.196}$$

The first two terms on the second line cancel each other because $\partial^2\psi/\partial x\partial y = \partial^2\psi/\partial y\partial x$ and $A_xA_y = A_yA_x$ (A_x, A_y are numbers, not operators). Then we apply the chain rule to calculate the partial derivatives of $A_x\psi$ and $A_y\psi$:

$$\mathrm{i}\hbar Q\left(\frac{\partial(A_y\psi)}{\partial x}+A_x\frac{\partial\psi}{\partial y}-\frac{\partial(A_x\psi)}{\partial y}-A_y\frac{\partial\psi}{\partial x}\right)=\mathrm{i}\hbar Q\left(\frac{\partial A_y}{\partial x}\psi+A_y\frac{\partial\psi}{\partial x}+A_x\frac{\partial\psi}{\partial y}-\frac{\partial A_x}{\partial y}\psi-A_x\frac{\partial\psi}{\partial y}-A_y\frac{\partial\psi}{\partial x}\right)=\mathrm{i}\hbar Q\left(\frac{\partial A_y}{\partial x}-\frac{\partial A_x}{\partial y}\right)\psi.$$
(5.197)

Note that the resulting difference of partial derivatives in the parentheses is nothing else but the z component of the rotation (formally a vector product) of the definition of $\vec{B}$ in Eq. 4.58. Therefore, we can write

$$-\hbar^2\left(\frac{\partial}{\partial x}\frac{\partial\psi}{\partial y}-\frac{\partial}{\partial y}\frac{\partial\psi}{\partial x}\right)+Q^2(A_xA_y-A_yA_x)\psi+\mathrm{i}\hbar Q\left(\frac{\partial(A_y\psi)}{\partial x}+A_x\frac{\partial\psi}{\partial y}-\frac{\partial(A_x\psi)}{\partial y}-A_y\frac{\partial\psi}{\partial x}\right)=\mathrm{i}\hbar Q\left(\frac{\partial A_y}{\partial x}-\frac{\partial A_x}{\partial y}\right)\psi=\mathrm{i}\hbar QB_z\psi.$$
(5.198)

The combinations on the last two lines of Eq. 5.194 are obtained in the same manner.

In addition to the combinations of the operators evaluated above, the last three lines of Eq. 5.194 also contain the products $\hat{\gamma}^1\hat{\gamma}^2$, $\hat{\gamma}^2\hat{\gamma}^3$, and $\hat{\gamma}^3\hat{\gamma}^1$. They can be calculated from Eq. 5.95

$$\hat{\gamma}^1\hat{\gamma}^2=\begin{pmatrix}\hat{0}&\hat{\sigma}^1\\-\hat{\sigma}^1&\hat{0}\end{pmatrix}\begin{pmatrix}\hat{0}&\hat{\sigma}^2\\-\hat{\sigma}^2&\hat{0}\end{pmatrix}=-\begin{pmatrix}\hat{\sigma}^1\hat{\sigma}^2&\hat{0}\\\hat{0}&\hat{\sigma}^1\hat{\sigma}^2\end{pmatrix}=-\mathrm{i}\begin{pmatrix}\hat{\sigma}^3&\hat{0}\\\hat{0}&\hat{\sigma}^3\end{pmatrix},$$
(5.199)

$$\hat{\gamma}^2\hat{\gamma}^3=\begin{pmatrix}\hat{0}&\hat{\sigma}^2\\-\hat{\sigma}^2&\hat{0}\end{pmatrix}\begin{pmatrix}\hat{0}&\hat{\sigma}^3\\-\hat{\sigma}^3&\hat{0}\end{pmatrix}=-\begin{pmatrix}\hat{\sigma}^2\hat{\sigma}^3&\hat{0}\\\hat{0}&\hat{\sigma}^2\hat{\sigma}^3\end{pmatrix}=-\mathrm{i}\begin{pmatrix}\hat{\sigma}^1&\hat{0}\\\hat{0}&\hat{\sigma}^1\end{pmatrix},$$
(5.200)

$$\hat{\gamma}^3\hat{\gamma}^1=\begin{pmatrix}\hat{0}&\hat{\sigma}^3\\-\hat{\sigma}^3&\hat{0}\end{pmatrix}\begin{pmatrix}\hat{0}&\hat{\sigma}^1\\-\hat{\sigma}^1&\hat{0}\end{pmatrix}=-\begin{pmatrix}\hat{\sigma}^3\hat{\sigma}^1&\hat{0}\\\hat{0}&\hat{\sigma}^3\hat{\sigma}^1\end{pmatrix}=-\mathrm{i}\begin{pmatrix}\hat{\sigma}^2&\hat{0}\\\hat{0}&\hat{\sigma}^2\end{pmatrix},$$
(5.201)

where the following important properties of the $\hat{\sigma}^j$ matrices were used in the lasts steps:

$$\hat{\sigma}^1\hat{\sigma}^2=\begin{pmatrix}0&1\\1&0\end{pmatrix}\begin{pmatrix}0&-\mathrm{i}\\\mathrm{i}&0\end{pmatrix}=\begin{pmatrix}\mathrm{i}&0\\0&-\mathrm{i}\end{pmatrix}=\mathrm{i}\hat{\sigma}^3$$
(5.202)

$$\hat{\sigma}^2\hat{\sigma}^3=\begin{pmatrix}0&-\mathrm{i}\\\mathrm{i}&0\end{pmatrix}\begin{pmatrix}1&0\\0&-1\end{pmatrix}=\begin{pmatrix}0&\mathrm{i}\\\mathrm{i}&0\end{pmatrix}=\mathrm{i}\hat{\sigma}^1$$
(5.203)

$$\hat{\sigma}^3\hat{\sigma}^1=\begin{pmatrix}1&0\\0&-1\end{pmatrix}\begin{pmatrix}0&1\\1&0\end{pmatrix}=\begin{pmatrix}0&1\\-1&0\end{pmatrix}=\mathrm{i}\hat{\sigma}^2.$$
(5.204)

Note that we have written the 4×4 matrices $\hat{\gamma}^j\hat{\gamma}^k$ in a *block-diagonal* form, using 2×2 matrices $\hat{\sigma}^l$ and $\hat{0}$.

After inserting everything into Eq. 5.194, we get

$$\left(\mathrm{i}\hbar\frac{\partial}{\partial t}-QV\right)^2\begin{pmatrix}\hat{1}&\hat{0}\\\hat{0}&\hat{1}\end{pmatrix}\Psi=\left(c^2\left(\mathrm{i}\hbar\frac{\partial}{\partial x}+QA_x\right)^2+c^2\left(\mathrm{i}\hbar\frac{\partial}{\partial y}+QA_y\right)^2+c^2\left(\mathrm{i}\hbar\frac{\partial}{\partial z}+QA_z\right)^2+m_0^2c^4\right)\begin{pmatrix}\hat{1}&\hat{0}\\\hat{0}&\hat{1}\end{pmatrix}\Psi$$

$$-c^2\hbar Q\left(B_x\begin{pmatrix}\hat{\sigma}^1&\hat{0}\\\hat{0}&\hat{\sigma}^1\end{pmatrix}+B_y\begin{pmatrix}\hat{\sigma}^2&\hat{0}\\\hat{0}&\hat{\sigma}^2\end{pmatrix}+B_z\begin{pmatrix}\hat{\sigma}^3&\hat{0}\\\hat{0}&\hat{\sigma}^3\end{pmatrix}\right)\Psi.$$
(5.205)

To emphasize the block-diagonal form of the equation, we use 2×2 matrices $\hat{1}$ (unit matrix) and $\hat{0}$ (zero matrix) to write the 4×4 unit matrices on the first line (note that the same symbol $\hat{1}$ represents a 4×4 matrix above and a 2×2 matrix here and below).

Now we have a relativistic equation describing our particle in an electromagnetic field. Let us now separate the mass contribution to the energy from the operator $\mathrm{i}\hbar\partial/\partial t$ and let us call the difference $\hat{H}$ (it becomes clear soon why we choose the same symbol as the symbol used for the Hamiltonian in the Schrödinger equation):

$$\hat{H}=\mathrm{i}\hbar\frac{\partial}{\partial t}-m_0c^2,$$
(5.206)

Eq. 5.205 can be rewritten as

$$\left(\hat{H}+m_0c^2-QV\right)^2\begin{pmatrix}\hat{1}&\hat{0}\\\hat{0}&\hat{1}\end{pmatrix}\Psi=\left((\hat{H}-QV)^2+2m_0c^2(\hat{H}-QV)+\textcolor{red}{m_0^2c^4}\right)\begin{pmatrix}\hat{1}&\hat{0}\\\hat{0}&\hat{1}\end{pmatrix}\Psi=$$

$$\left(c^2\left(\mathrm{i}\hbar\frac{\partial}{\partial x}+QA_x\right)^2+c^2\left(\mathrm{i}\hbar\frac{\partial}{\partial y}+QA_y\right)^2+c^2\left(\mathrm{i}\hbar\frac{\partial}{\partial z}+QA_z\right)^2+\textcolor{red}{m_0^2c^4}\right)\begin{pmatrix}\hat{1}&\hat{0}\\\hat{0}&\hat{1}\end{pmatrix}\Psi$$

$$-c^2\hbar Q\left(B_x\begin{pmatrix}\hat{\sigma}^1&\hat{0}\\\hat{0}&\hat{\sigma}^1\end{pmatrix}+B_y\begin{pmatrix}\hat{\sigma}^2&\hat{0}\\\hat{0}&\hat{\sigma}^2\end{pmatrix}+B_z\begin{pmatrix}\hat{\sigma}^3&\hat{0}\\\hat{0}&\hat{\sigma}^3\end{pmatrix}\right)\Psi,$$
(5.207)

where the two red terms $m_0^2 c^4$ cancel each other. Dividing both sides of the equation by $2m_0 c^2$ gives

$$\left(\frac{(\hat{H} - QV)^2}{2m_0 c^2} + \hat{H} - QV \right) \begin{pmatrix} \hat{1} & \hat{0} \\ \hat{0} & \hat{1} \end{pmatrix} \Psi =$$

$$\frac{1}{2m_0} \left(\left(i\hbar \frac{\partial}{\partial x} + QA_x \right)^2 + \left(i\hbar \frac{\partial}{\partial y} + QA_y \right)^2 + \left(i\hbar \frac{\partial}{\partial z} + QA_z \right)^2 \right) \begin{pmatrix} \hat{1} & \hat{0} \\ \hat{0} & \hat{1} \end{pmatrix} \Psi$$

$$- \frac{\hbar Q}{2m_0} \left(B_x \begin{pmatrix} \hat{\sigma}^1 & \hat{0} \\ \hat{0} & \hat{\sigma}^1 \end{pmatrix} + B_y \begin{pmatrix} \hat{\sigma}^2 & \hat{0} \\ \hat{0} & \hat{\sigma}^2 \end{pmatrix} + B_z \begin{pmatrix} \hat{\sigma}^3 & \hat{0} \\ \hat{0} & \hat{\sigma}^3 \end{pmatrix} \right) \Psi. \tag{5.208}$$

Note that the rest energy of particles $m_0 c^2$ is huge. Unless the eigenvalue of $\hat{H}$ is very large (which is not expected in a standard NMR experiment), the first term with $m_0 c^2$ in the denominator can be safely neglected. For the same reason, the factors $\pm c p_z / (\mathcal{E}_t + m_0 c^2)$ and $c(p_x \pm i p_y) / (\mathcal{E}_t + m_0 c^2)$ in Eq. 5.179 are close to zero for $v \ll c$.

The derived matrix equation represent a set of four equations for four unknowns. The block-diagonal form of all matrices reveals that the first two equations and the last two equations can be solved separately. Therefore, we obtain identical sets of two equations describing particles and antiparticles:

$$\hat{H} \begin{pmatrix} u_1 \psi \\ u_2 \psi \end{pmatrix} \approx \left(\frac{1}{2m_0} \left(\left(i\hbar \frac{\partial}{\partial x} + QA_x \right)^2 + \left(i\hbar \frac{\partial}{\partial y} + QA_y \right)^2 + \left(i\hbar \frac{\partial}{\partial z} + QA_z \right)^2 \right) + QV \right) \hat{1} - \frac{\hbar Q}{2m_0} \left(B_x \hat{\sigma}^1 + B_y \hat{\sigma}^2 + B_z \hat{\sigma}^3 \right) \right) \begin{pmatrix} u_1 \psi \\ u_2 \psi \end{pmatrix}, \tag{5.209}$$

$$\hat{H} \begin{pmatrix} v_1 \psi^* \\ v_2 \psi^* \end{pmatrix} \approx \left(\frac{1}{2m_0} \left(\left(i\hbar \frac{\partial}{\partial x} + QA_x \right)^2 + \left(i\hbar \frac{\partial}{\partial y} + QA_y \right)^2 + \left(i\hbar \frac{\partial}{\partial z} + QA_z \right)^2 \right) + QV \right) \hat{1} - \frac{\hbar Q}{2m_0} \left(B_x \hat{\sigma}^1 + B_y \hat{\sigma}^2 + B_z \hat{\sigma}^3 \right) \right) \begin{pmatrix} v_1 \psi^* \\ v_2 \psi^* \end{pmatrix}, \tag{5.210}$$

where we described the wave functions using the notation introduced in Eq. 5.178. In both matrix equations, the terms multiplied by $\hat{1}$ constitute the Hamiltonian of the non-relativistic Schrödinger equation (Eq. 4.26), and the terms with the $\hat{\sigma}^j$ matrices appear only in our relativistic equations.

5.7.9 Spin magnetogyric ratio

The value of the magnetogyric ratio for the spin magnetic moment can be derived by inserting the expressions defining operators of spin magnetic moment components (Eqs. 5.5–5.7) into the commutation relation (Eq. 5.9), e.g.

$$\hat{I}_x \hat{I}_y - \hat{I}_y \hat{I}_x = \frac{\hat{\mu}_x}{\gamma} \frac{\hat{\mu}_y}{\gamma} - \frac{\hat{\mu}_y}{\gamma} \frac{\hat{\mu}_x}{\gamma} = \frac{1}{\gamma^2} \left(\frac{\hbar Q}{2m_0} \right)^2 \left(\begin{pmatrix} 0 & 1 \\ 1 & 0 \end{pmatrix} \begin{pmatrix} 0 & -i \\ i & 0 \end{pmatrix} - \begin{pmatrix} 0 & -i \\ i & 0 \end{pmatrix} \begin{pmatrix} 0 & 1 \\ 1 & 0 \end{pmatrix} \right) = \frac{1}{\gamma^2} \left(\frac{\hbar Q}{2m_0} \right)^2 \left(\begin{pmatrix} i & 0 \\ 0 & -i \end{pmatrix} - \begin{pmatrix} -i & 0 \\ 0 & i \end{pmatrix} \right)$$

$$= i \frac{2}{\gamma^2} \left(\frac{\hbar Q}{2m_0} \right)^2 \begin{pmatrix} 1 & 0 \\ 0 & -1 \end{pmatrix} \tag{5.211}$$

The commutation relation Eq. 5.9 requires that

$$\hat{I}_x \hat{I}_y - \hat{I}_y \hat{I}_x = i \frac{2}{\gamma^2} \left(\frac{\hbar Q}{2m_0} \right)^2 \begin{pmatrix} 1 & 0 \\ 0 & -1 \end{pmatrix} = i\hbar \hat{I}_z = i \frac{\hbar}{\gamma} \left(\frac{\hbar Q}{2m_0} \right) \begin{pmatrix} 1 & 0 \\ 0 & -1 \end{pmatrix} \quad \Rightarrow \quad \frac{2}{\gamma} \frac{\hbar Q}{2m_0} a = 1 \quad \Rightarrow \quad \gamma = 2 \frac{\hbar Q}{2m_0}. \tag{5.212}$$

5.7.10 The factor of one half in the eigenvalues of $\hat{I}_z$

The eigenvalues $\pm \hbar/2$ are closely related to the fact that spin is a relativistic effect. Special relativity requires that the Dirac equation must not change if we rotate the coordinate frame or if it moves with a constant speed (Lorentz transformation). This is true in general, but for the sake of simplicity, we just check rotation about the z axis.

We start by writing explicitly the Dirac equation as a set of four equations[10]

---

[10]Note that we use the form of the Dirac equation which directly defines the relativistic Hamiltonian (Eq. 5.87).

$$i\hbar\frac{\partial(u_1\psi)}{\partial t} = -ic\hbar\frac{\partial(v_1\psi^*)}{\partial z} - ic\hbar\frac{\partial(v_2\psi^*)}{\partial x} + ic\hbar\frac{\partial(iv_2\psi^*)}{\partial y} + m_0c^2u_1\psi, \tag{5.213}$$

$$i\hbar\frac{\partial(u_2\psi)}{\partial t} = +ic\hbar\frac{\partial(v_2\psi^*)}{\partial z} - ic\hbar\frac{\partial(v_1\psi^*)}{\partial x} - ic\hbar\frac{\partial(iv_1\psi^*)}{\partial y} + m_0c^2u_2\psi, \tag{5.214}$$

$$i\hbar\frac{\partial(v_1\psi^*)}{\partial t} = -ic\hbar\frac{\partial(u_1\psi)}{\partial z} - ic\hbar\frac{\partial(u_2\psi)}{\partial x} + ic\hbar\frac{\partial(iu_2\psi)}{\partial y} - m_0c^2v_1\psi^*, \tag{5.215}$$

$$i\hbar\frac{\partial(v_2\psi^*)}{\partial t} = +ic\hbar\frac{\partial(u_2\psi)}{\partial z} - ic\hbar\frac{\partial(u_1\psi)}{\partial x} - ic\hbar\frac{\partial(iu_1\psi)}{\partial y} - m_0c^2v_2\psi^*. \tag{5.216}$$

Let us assume that we have an original coordinate frame t, x, y, z and a rotated frame t', x', y', z'. If we rotate about z by an angle φ,

$$t' = t \tag{5.217}$$
$$z' = z \tag{5.218}$$
$$x' = (\cos\varphi)x - (\sin\varphi)y \tag{5.219}$$
$$y' = (\sin\varphi)x + (\cos\varphi)y \tag{5.220}$$

and

$$\frac{\partial f}{\partial t} = \frac{\partial f}{\partial t'} \tag{5.221}$$

$$\frac{\partial f}{\partial z} = \frac{\partial f}{\partial z'} \tag{5.222}$$

$$\frac{\partial f}{\partial x} = \frac{\partial x'}{\partial x}\frac{\partial f}{\partial x'} + \frac{\partial y'}{\partial x}\frac{\partial f}{\partial y'} = \cos\varphi\frac{\partial f}{\partial x'} + \sin\varphi\frac{\partial f}{\partial y'} \tag{5.223}$$

$$\frac{\partial f}{\partial y} = \frac{\partial x'}{\partial y}\frac{\partial f}{\partial x'} + \frac{\partial y'}{\partial y}\frac{\partial f}{\partial y'} = -\sin\varphi\frac{\partial f}{\partial x'} + \cos\varphi\frac{\partial f}{\partial y'} \tag{5.224}$$

and consequently

$$\frac{\partial f}{\partial x} + i\frac{\partial f}{\partial y} = e^{-i\varphi}\left(\frac{\partial f}{\partial x'} + i\frac{\partial f}{\partial y'}\right), \tag{5.225}$$

$$\frac{\partial f}{\partial x} - i\frac{\partial f}{\partial y} = e^{i\varphi}\left(\frac{\partial f}{\partial x'} - i\frac{\partial f}{\partial y'}\right). \tag{5.226}$$

We also need to transform the wavefunction Ψ to the rotated frame. We already know (Eqs. 4.160 and 4.161) that rotation of a complex function f by an angle ϕ can be written as $f' = fe^{i\phi}$. Let us assume that each of component of Ψ rotates by some angle $(\varphi_1, \varphi_2, \varphi_3, \varphi_4,)$ – the key step of our analysis will be to relate values of these angles the actual angle of rotating the coordinate frames φ.

Now we have everything that we need to write the set of Eqs. 5.213–5.216 in the rotated coordinate frame:

$$i\hbar\frac{\partial(e^{i\varphi_1}u_1'\psi')}{\partial t'} = -ic\hbar\frac{\partial(e^{i\varphi_3}v_1'\psi'^*)}{\partial z'} - ic\hbar\frac{\partial(e^{i(\varphi_4+\varphi)}v_2'\psi'^*)}{\partial x'} + ic\hbar\frac{\partial(ie^{i(\varphi_4+\varphi)}v_2'\psi'^*)}{\partial y'} + m_0c^2e^{i\varphi_1}u_1'\psi', \tag{5.227}$$

$$i\hbar\frac{\partial(e^{i\varphi_2}u_2'\psi')}{\partial t'} = +ic\hbar\frac{\partial(e^{i\varphi_4}v_2'\psi'^*)}{\partial z'} - ic\hbar\frac{\partial(e^{i(\varphi_3-\varphi)}v_1'\psi'^*)}{\partial x'} - ic\hbar\frac{\partial(ie^{i(\varphi_3-\varphi)}v_1'\psi'^*)}{\partial y'} + m_0c^2e^{i\varphi_2}u_2'\psi', \tag{5.228}$$

$$i\hbar\frac{\partial(e^{i\varphi_3}v_1'\psi'^*)}{\partial t'} = -ic\hbar\frac{\partial(e^{i\varphi_1}u_1'\psi')}{\partial z'} - ic\hbar\frac{\partial(e^{i(\varphi_2+\varphi)}u_2'\psi')}{\partial x'} + ic\hbar\frac{\partial(ie^{i(\varphi_2+\varphi)}u_2'\psi')}{\partial y'} - m_0c^2e^{i\varphi_3}v_1'\psi'^*, \tag{5.229}$$

$$i\hbar\frac{\partial(e^{i\varphi_4}v_2'\psi'^*)}{\partial t'} = +ic\hbar\frac{\partial(e^{i\varphi_2}u_2'\psi')}{\partial z'} - ic\hbar\frac{\partial(e^{i(\varphi_1-\varphi)}u_1'\psi')}{\partial x'} - ic\hbar\frac{\partial(ie^{i(\varphi_1-\varphi)}u_1'\psi')}{\partial y'} - m_0c^2e^{i\varphi_4}v_2'\psi'^*. \tag{5.230}$$

According to the first postulate of the special theory of relativity, Eqs. 5.227–5.230 must have the same form as Eqs. 5.213–5.216. In other words, we must eliminate the complex exponential expressions from Eqs. 5.227–5.230. Let us first multiply both sides of the first equation by $e^{-i\varphi_1}$, both sides of the second equation by $e^{-i\varphi_2}$, both sides of the third equation by $e^{-i\varphi_3}$, and both sides of the last equation by $e^{-i\varphi_4}$:

$$i\hbar\frac{\partial(u_1'\psi')}{\partial t'} = -ic\hbar\frac{\partial(e^{i(\varphi_3-\varphi_1)}v_1'\psi'^*)}{\partial z'} - ic\hbar\frac{\partial(e^{i(\varphi_4-\varphi_1+\varphi)}v_2'\psi'^*)}{\partial x'} + ic\hbar\frac{\partial(ie^{i(\varphi_4-\varphi_1+\varphi)}v_2'\psi'^*)}{\partial y'} + m_0c^2u_1'\psi', \tag{5.231}$$

$$i\hbar\frac{\partial(u_2'\psi')}{\partial t'} = +ic\hbar\frac{\partial(e^{i(\varphi_4-\varphi_2)}v_2'\psi'^*)}{\partial z'} - ic\hbar\frac{\partial(e^{i(\varphi_3-\varphi_2-\varphi)}v_1'\psi'^*)}{\partial x'} - ic\hbar\frac{\partial(ie^{i(\varphi_3-\varphi_2-\varphi)}v_1'\psi'^*)}{\partial y'} + m_0c^2u_2'\psi', \tag{5.232}$$

$$i\hbar\frac{\partial(v_1'\psi'^*)}{\partial t'} = -ic\hbar\frac{\partial(e^{i(\varphi_1-\varphi_3)}u_1'\psi')}{\partial z'} - ic\hbar\frac{\partial(e^{i(\varphi_2-\varphi_3+\varphi)}u_2'\psi')}{\partial x'} + ic\hbar\frac{\partial(ie^{i(\varphi_2-\varphi_3+\varphi)}u_2'\psi')}{\partial y'} - m_0c^2v_1'\psi'^*, \tag{5.233}$$

$$i\hbar\frac{\partial(v_2'\psi'^*)}{\partial t'} = +ic\hbar\frac{\partial(e^{i(\varphi_2-\varphi_4)}u_2'\psi')}{\partial z'} - ic\hbar\frac{\partial(e^{i(\varphi_1-\varphi_4-\varphi)}u_1'\psi')}{\partial x'} - ic\hbar\frac{\partial(ie^{i(\varphi_1-\varphi_4-\varphi)}u_1'\psi')}{\partial y'} - m_0c^2v_2'\psi'^*. \tag{5.234}$$

This cleared the t' and m_0 terms. The exponential expressions disappear from the z' term if $\varphi_1 = \varphi_3$ and $\varphi_2 = \varphi_4$ (i.e., if the rotation of $u_1\psi$ and $v_1\psi^*$ is identical and the same applies to $u_2\psi$ and $v_2\psi^*$). In order to fix the x' and y' terms, we assume that $\varphi_1 = -\varphi_2$ and $\varphi_3 = -\varphi_4$, i.e., that the rotation of $u_1\psi$ and $u_2\psi$ is opposite and the same applies to $v_1\psi^*$ and $v_2\psi^*$. This implies that $u_1\psi$ and $u_2\psi$ describe states with opposite spins (and $v_1\psi^*$ and $v_2\psi^*$ too). Then, $u_1'\psi'$ and $v_1'\psi'^*$ in the x' and y' terms are multiplied by $e^{i(2\varphi_1-\varphi)}$, and $u_2'\psi'$ and $v_2'\psi'^*$ in the x' and y' terms are multiplied by $e^{-i(2\varphi_1-\varphi)}$. In both cases, the exponential expressions disappear (are equal to one) if $\varphi_1 = \varphi/2$. What does it mean? If we rotate the coordinate system by a certain angle, the components of the wavefunction rotate only by half of this angle! The function describing rotation of the wavefunction about z has the form

$$R_j = e^{i\frac{I_{z,j}}{\hbar}\frac{\varphi}{2}}. \tag{5.235}$$

This looks very similar to Eq. 4.145, but with one important difference: rotation by 2π ($360°$) does not give the same eigenfunction R_j as no rotation ($\varphi = 0$), but changes its sign. Only rotation by 4π ($720°$) reverts the system to the initial state!

Eq. 4.145 tells us that the eigenvalues of the operator of the spin angular momentum are half-integer multiples of $\hbar$:

$$I_{z,1} = \frac{\hbar}{2} \qquad I_{z,2} = -\frac{\hbar}{2}. \tag{5.236}$$

5.7.11 Eigenfunctions of $\hat{I}_x$ and $\hat{I}_y$

Eigenfunctions of $\hat{I}_x$ are the following linear combinations of $|\alpha\rangle$ and $|\beta\rangle$:

$$\frac{1}{\sqrt{2}}|\alpha\rangle + \frac{1}{\sqrt{2}}|\beta\rangle = \frac{1}{\sqrt{2}}\begin{pmatrix}1\\1\end{pmatrix} \equiv |\rightarrow\rangle, \tag{5.237}$$

$$-\frac{i}{\sqrt{2}}|\alpha\rangle + \frac{i}{\sqrt{2}}|\beta\rangle = \frac{1}{\sqrt{2}}\begin{pmatrix}-i\\i\end{pmatrix} \equiv |\leftarrow\rangle, \tag{5.238}$$

or these linear combinations multiplied by a phase factor $e^{i\phi}$. E.g., state vectors multiplied by $e^{i\pi/2} = i$ are

$$|\rightarrow\rangle = e^{i\pi/2}\frac{1}{\sqrt{2}}\begin{pmatrix}1\\1\end{pmatrix} = i\frac{1}{\sqrt{2}}\begin{pmatrix}1\\1\end{pmatrix} = \frac{1}{\sqrt{2}}\begin{pmatrix}i\\i\end{pmatrix}, \qquad |\leftarrow\rangle = e^{i\pi/2}\frac{1}{\sqrt{2}}\begin{pmatrix}-i\\i\end{pmatrix} = i\frac{1}{\sqrt{2}}\begin{pmatrix}-i\\i\end{pmatrix} = \frac{1}{\sqrt{2}}\begin{pmatrix}1\\-1\end{pmatrix}. \tag{5.239}$$

Eigenvalues are again $\hbar/2$ and $-\hbar/2$:

$$\hat{I}_x|\rightarrow\rangle = +\frac{\hbar}{2}|\rightarrow\rangle \qquad \frac{\hbar}{2}\begin{pmatrix}0&1\\1&0\end{pmatrix}\frac{1}{\sqrt{2}}\begin{pmatrix}1\\1\end{pmatrix} = +\frac{\hbar}{2}\cdot\frac{1}{\sqrt{2}}\begin{pmatrix}1\\1\end{pmatrix}, \tag{5.240}$$

$$\hat{I}_x|\leftarrow\rangle = +\frac{\hbar}{2}|\leftarrow\rangle \qquad \frac{\hbar}{2}\begin{pmatrix}0&1\\1&0\end{pmatrix}\frac{1}{\sqrt{2}}\begin{pmatrix}-i\\i\end{pmatrix} = -\frac{\hbar}{2}\cdot\frac{1}{\sqrt{2}}\begin{pmatrix}-i\\i\end{pmatrix}. \tag{5.241}$$

Eigenfunctions of $\hat{I}_y$ are the following linear combinations of $|\alpha\rangle$ and $|\beta\rangle$:

$$\frac{1-i}{2}|\alpha\rangle + \frac{1+i}{2}|\beta\rangle = \frac{1}{2}\begin{pmatrix}1-i\\1+i\end{pmatrix} \equiv |\otimes\rangle, \tag{5.242}$$

$$-\frac{1+i}{2}|\alpha\rangle + \frac{1-i}{2}|\beta\rangle = \frac{1}{2}\begin{pmatrix}1+i\\1-i\end{pmatrix} \equiv |\odot\rangle, \tag{5.243}$$

or these linear combinations multiplied by a phase factor $e^{i\phi}$. E.g., state vectors multiplied by $e^{i\pi/4} = (1+i)/\sqrt{2}$ are

$$|\otimes\rangle = \mathrm{e}^{\mathrm{i}\pi/4}\frac{1}{2}\begin{pmatrix}1-\mathrm{i}\\1+\mathrm{i}\end{pmatrix} = \frac{1+\mathrm{i}}{\sqrt{2}}\frac{1}{2}\begin{pmatrix}1-\mathrm{i}\\1+\mathrm{i}\end{pmatrix} = \frac{1}{\sqrt{2}}\begin{pmatrix}1\\\mathrm{i}\end{pmatrix}, \qquad |\odot\rangle = \mathrm{e}^{\mathrm{i}\pi/4}\frac{1}{2}\begin{pmatrix}1+\mathrm{i}\\1-\mathrm{i}\end{pmatrix} = \frac{1+\mathrm{i}}{\sqrt{2}}\frac{1}{2}\begin{pmatrix}1+\mathrm{i}\\1-\mathrm{i}\end{pmatrix} = \frac{1}{\sqrt{2}}\begin{pmatrix}\mathrm{i}\\1\end{pmatrix}. \tag{5.244}$$

Eigenvalues are again $\hbar/2$ and $-\hbar/2$:

$$\hat{I}_y|\otimes\rangle = +\frac{\hbar}{2}|\otimes\rangle \qquad \frac{\hbar}{2}\begin{pmatrix}0 & -\mathrm{i}\\\mathrm{i} & 0\end{pmatrix}\frac{1}{2}\begin{pmatrix}1-\mathrm{i}\\1+\mathrm{i}\end{pmatrix} = +\frac{\hbar}{2}\cdot\frac{1}{2}\begin{pmatrix}1-\mathrm{i}\\1+\mathrm{i}\end{pmatrix}, \tag{5.245}$$

$$\hat{I}_y|\odot\rangle = -\frac{\hbar}{2}|\odot\rangle \qquad \frac{\hbar}{2}\begin{pmatrix}0 & -\mathrm{i}\\\mathrm{i} & 0\end{pmatrix}\frac{1}{2}\begin{pmatrix}1+\mathrm{i}\\1-\mathrm{i}\end{pmatrix} = -\frac{\hbar}{2}\cdot\frac{1}{2}\begin{pmatrix}1+\mathrm{i}\\1-\mathrm{i}\end{pmatrix}. \tag{5.246}$$

An operator representing angular momentum pointing in a general direction, described by angles ϑ (inclination) and φ (azimuth) can be written as

$$\hat{I}_z\cos\vartheta + \hat{I}_x\sin\vartheta\cos\varphi + \hat{I}_y\sin\vartheta\sin\varphi. \tag{5.247}$$

Its eigenvalue are again $\hbar/2$ and $-\hbar/2$ and its eigenfunctions are

$$|\vartheta,\varphi\rangle = \begin{pmatrix}\cos\frac{\vartheta}{2}\mathrm{e}^{-\mathrm{i}\frac{\varphi}{2}}\\\sin\frac{\vartheta}{2}\mathrm{e}^{+\mathrm{i}\frac{\varphi}{2}}\end{pmatrix}, \qquad |\vartheta+\pi,\varphi\rangle = \begin{pmatrix}-\sin\frac{\vartheta}{2}\mathrm{e}^{-\mathrm{i}\frac{\varphi}{2}}\\\cos\frac{\vartheta}{2}\mathrm{e}^{+\mathrm{i}\frac{\varphi}{2}}\end{pmatrix} \tag{5.248}$$

or the vectors described by Eq. 5.248 multiplied by a phase factor $\mathrm{e}^{\mathrm{i}\phi}$, e.g.

$$|\vartheta,\varphi\rangle = \begin{pmatrix}\cos\frac{\vartheta}{2}\\\sin\frac{\vartheta}{2}\mathrm{e}^{\mathrm{i}\varphi}\end{pmatrix}, \qquad |\vartheta+\pi,\varphi\rangle = \begin{pmatrix}-\sin\frac{\vartheta}{2}\\\cos\frac{\vartheta}{2}\mathrm{e}^{\mathrm{i}\varphi}\end{pmatrix}. \tag{5.249}$$

5.7.12   Stationary states and energy level diagram

In the presence of a homogeneous magnetic field $\vec{B}_0 = (0,0,B_0)$, the evolution of the system is given by the Hamiltonian $\hat{H} = -\gamma B_0\hat{I}_z$. The Schrödinger equation is then

$$\mathrm{i}\hbar\frac{\partial}{\partial t}\begin{pmatrix}c_\alpha\\c_\beta\end{pmatrix} = -\gamma B_0\frac{\hbar}{2}\begin{pmatrix}1 & 0\\0 & -1\end{pmatrix}\begin{pmatrix}c_\alpha\\c_\beta\end{pmatrix}, \tag{5.250}$$

which is a set of two equations with separated variables

$$\frac{\mathrm{d}c_\alpha}{\mathrm{d}t} = +\mathrm{i}\frac{\gamma B_0}{2}c_\alpha, \tag{5.251}$$

$$\frac{\mathrm{d}c_\beta}{\mathrm{d}t} = -\mathrm{i}\frac{\gamma B_0}{2}c_\beta, \tag{5.252}$$

with the solution

$$c_\alpha = c_\alpha(t=0)\mathrm{e}^{+\mathrm{i}\frac{\gamma B_0}{2}t} = c_\alpha(t=0)\mathrm{e}^{-\mathrm{i}\frac{\omega_0}{2}t}, \tag{5.253}$$

$$c_\beta = c_\beta(t=0)\mathrm{e}^{-\mathrm{i}\frac{\gamma B_0}{2}t} = c_\beta(t=0)\mathrm{e}^{+\mathrm{i}\frac{\omega_0}{2}t}. \tag{5.254}$$

If the initial state is $|\alpha\rangle$, $c_\alpha(t=0) = 1$, $c_\beta(t=0) = 0$, and

$$c_\alpha = \mathrm{e}^{-\mathrm{i}\frac{\omega_0}{2}t}, \tag{5.255}$$

$$c_\beta = 0. \tag{5.256}$$

Note that the evolution changes only the phase factor, but the system stays in state $|\alpha\rangle$ (all vectors described by Eq. 5.16 correspond to state $|\alpha\rangle$). It can be shown by calculating the probability that the system is in the $|\alpha\rangle$ or $|\beta\rangle$ state.

$$P_\alpha = c_\alpha^* c_\alpha = \mathrm{e}^{+\mathrm{i}\frac{\omega_0}{2}t}\mathrm{e}^{-\mathrm{i}\frac{\omega_0}{2}t} = 1, \tag{5.257}$$

$$P_\beta = c_\beta^* c_\beta = 0. \tag{5.258}$$

If the initial state is $|\beta\rangle$, $c_\alpha(t=0) = 0$, $c_\beta(t=0) = 1$, and

$$c_\alpha = 0, \tag{5.259}$$

$$c_\beta = \mathrm{e}^{+\mathrm{i}\frac{\omega_0}{2}t}. \tag{5.260}$$

Again, the evolution changes only the phase factor, but the system stays in state $|\beta\rangle$. The probability that the system is in the $|\alpha\rangle$ or $|\beta\rangle$ state is

$$P_\alpha = c_\alpha^* c_\alpha = 0, \tag{5.261}$$

$$P_\beta = c_\beta^* c_\beta = \mathrm{e}^{-\mathrm{i}\frac{\omega_0}{2}t}\mathrm{e}^{+\mathrm{i}\frac{\omega_0}{2}t} = 1. \tag{5.262}$$

Let us summarize results of our analysis. If evolving wave functions are eigenfunctions of the Hamiltonian describing the evolution:

- The probability of finding the system in a given state do not change the state is *stationary*.

- Only the phase factors of the coefficients constituting the state vector change with a frequencies equal to the eigenvalues of the Hamiltonian divided by $\hbar$ (Eqs. 5.253 and 5.254).

- The eigenvalues of the Hamiltonian represent energies of the individual eigenstates. Such energies can be plotted as the *energy level diagram*.

5.7.13   Oscillatory states

We now analyze evolution of states described by other wave functions that eigenfunctions of the Hamiltonian. We can continue the discussion of the previous section (evolution of evolution of $|\alpha\rangle$ and $|\beta\rangle$ due to $\hat{H} = -\gamma B_0 \hat{I}_z$) and change either the wave function or the Hamiltonian. We start by the latter option, which is easier.

In the presence of a homogeneous magnetic field $\vec{B}_1 = (B_1, 0, 0)$, the evolution of the system is given by the Hamiltonian $\hat{H} = -\gamma B_0 \hat{I}_x$. The Schrödinger equation is then

$$\mathrm{i}\hbar\frac{\partial}{\partial t}\begin{pmatrix} c_\alpha \\ c_\beta \end{pmatrix} = -\gamma B_1 \frac{\hbar}{2}\begin{pmatrix} 0 & 1 \\ 1 & 0 \end{pmatrix}\begin{pmatrix} c_\alpha \\ c_\beta \end{pmatrix}, \tag{5.263}$$

which is a set of two equations

$$\frac{\mathrm{d}c_\alpha}{\mathrm{d}t} = \mathrm{i}\frac{\gamma B_1}{2}c_\beta, \tag{5.264}$$

$$\frac{\mathrm{d}c_\beta}{\mathrm{d}t} = \mathrm{i}\frac{\gamma B_1}{2}c_\alpha. \tag{5.265}$$

These equations have similar structure as Eqs. 4.151 and 4.152. Adding and subtracting them leads to the solution

$$c_\alpha + c_\beta = C_+ \mathrm{e}^{+\mathrm{i}\frac{\gamma B_1}{2}t} = C_+ \mathrm{e}^{-\mathrm{i}\frac{\omega_1}{2}t}, \tag{5.266}$$

$$c_\alpha - c_\beta = C_- \mathrm{e}^{-\mathrm{i}\frac{\gamma B_1}{2}t} = C_- \mathrm{e}^{+\mathrm{i}\frac{\omega_1}{2}t}. \tag{5.267}$$

If the initial state is $|\alpha\rangle$, $c_\alpha(t=0) = 1$, $c_\beta(t=0) = 0$, $C_+ = C_- = 1$, and

$$c_\alpha = \cos\left(\frac{\omega_1}{2}t\right), \tag{5.268}$$

$$c_\beta = -\mathrm{i}\sin\left(\frac{\omega_1}{2}t\right). \tag{5.269}$$

Probability that the system is in the $|\alpha\rangle$ or $|\beta\rangle$ state is calculated as

$$P_\alpha = c_\alpha^* c_\alpha = \cos^2\left(\frac{\omega_1}{2}t\right) = \frac{1}{2} + \frac{1}{2}\cos(\omega_1 t), \tag{5.270}$$

$$P_\beta = c_\beta^* c_\beta = \sin^2\left(\frac{\omega_1}{2}t\right) = \frac{1}{2} - \frac{1}{2}\cos(\omega_1 t). \tag{5.271}$$

If the initial state is $|\beta\rangle$, $c_\alpha(t=0) = 0$, $c_\beta(t=0) = 1$, $C_+ = 1$, $C_- = -1$, and

$$c_\alpha = -\mathrm{i}\sin\left(\frac{\omega_1}{2}t\right),\tag{5.272}$$

$$c_\beta = \cos\left(\frac{\omega_1}{2}t\right).\tag{5.273}$$

Probability that the system is in the $|\alpha\rangle$ or $|\beta\rangle$ state is calculated as

$$P_\alpha = c_\alpha^* c_\alpha = \sin^2\left(\frac{\omega_1}{2}t\right) = \frac{1}{2} - \frac{1}{2}\cos(\omega_1 t),\tag{5.274}$$

$$P_\beta = c_\beta^* c_\beta = \cos^2\left(\frac{\omega_1}{2}t\right) = \frac{1}{2} + \frac{1}{2}\cos(\omega_1 t).\tag{5.275}$$

In both cases, the system oscillates between the $|\alpha\rangle$ and $|\beta\rangle$ states.

Now we return to the Hamiltonian of the vertical field $\hat{H} = -\gamma B_0 \hat{I}_z$, but analyze the evolution of superposition states called $|\rightarrow\rangle$ and $|\leftarrow\rangle$ in Section 5.7.11. The Schrödinger equation has in this case the same form as in Section 5.7.12 with the solution

$$c_\alpha = c_\alpha(t=0)\mathrm{e}^{+\mathrm{i}\frac{\gamma B_0}{2}t} = c_\alpha(t=0)\mathrm{e}^{-\mathrm{i}\frac{\omega_0}{2}t},\tag{5.276}$$

$$c_\beta = c_\beta(t=0)\mathrm{e}^{-\mathrm{i}\frac{\gamma B_0}{2}t} = c_\beta(t=0)\mathrm{e}^{+\mathrm{i}\frac{\omega_0}{2}t}.\tag{5.277}$$

We are interested in evolution of a wave function that can be described as

$$|\Psi\rangle = c_\rightarrow |\rightarrow\rangle + c_\leftarrow |\leftarrow\rangle.\tag{5.278}$$

According to Eqs. 5.251 and 5.252,

$$c_\rightarrow = \frac{c_\alpha}{\sqrt{2}} + \frac{c_\beta}{\sqrt{2}}\tag{5.279}$$

$$c_\leftarrow = -\mathrm{i}\frac{c_\alpha}{\sqrt{2}} + \mathrm{i}\frac{c_\beta}{\sqrt{2}}.\tag{5.280}$$

If the initial state is $|\rightarrow\rangle$, $c_\alpha(t=0) = 1/\sqrt{2}$, $c_\beta(t=0) = 1/\sqrt{2}$, and

$$c_\rightarrow = \frac{1}{2}\mathrm{e}^{-\mathrm{i}\frac{\omega_0}{2}t} + \frac{1}{2}\mathrm{e}^{+\mathrm{i}\frac{\omega_0}{2}t} = \cos\left(\frac{\omega_0}{2}t\right)\tag{5.281}$$

$$c_\leftarrow = -\frac{\mathrm{i}}{2}\mathrm{e}^{-\mathrm{i}\frac{\omega_0}{2}t} + \frac{\mathrm{i}}{2}\mathrm{e}^{+\mathrm{i}\frac{\omega_0}{2}t} = -\sin\left(\frac{\omega_0}{2}t\right).\tag{5.282}$$

Probability that the system is in the $|\rightarrow\rangle$ or $|\leftarrow\rangle$ state is calculated as

$$P_\rightarrow = c_\rightarrow^* c_\rightarrow = \cos^2\left(\frac{\omega_0}{2}t\right) = \frac{1}{2} + \frac{1}{2}\cos(\omega_0 t),\tag{5.283}$$

$$P_\leftarrow = c_\leftarrow^* c_\leftarrow = \sin^2\left(\frac{\omega_0}{2}t\right) = \frac{1}{2} - \frac{1}{2}\cos(\omega_0 t).\tag{5.284}$$

5.7.14 Evolution in general alternating magnetic fields

Bloch and Siegert analyzed in Phys. Rev. 57 (1940) 522–527 a general case of evolution of spin states in a magnetic field $\vec{B}$ whose x and y component alternate with the frequency ω_radio. The analysis is not simple and the main purpose of discussing it here is to explain why the effect of radio waves is usually described approximatively, assuming presence of rotating magnetic fields, instead of a much more realistic description using fields oscillating in one direction.

The Schrödinger equation describing evolution in the general field $\vec{B} = (B_x, B_y, B_z)$ is

$$\mathrm{i}\hbar\frac{\partial\psi}{\partial t} = \hat{H}\psi = -\gamma B_z \hat{I}_z \psi - \gamma B_x \hat{I}_x \psi - \gamma B_y \hat{I}_y \psi\tag{5.285}$$

$$\mathrm{i}\hbar\frac{\partial}{\partial t}\begin{pmatrix} c_\alpha \\ c_\beta \end{pmatrix} = -\gamma\frac{\hbar}{2}\left(B_z\begin{pmatrix} 1 & 0 \\ 0 & -1 \end{pmatrix}\begin{pmatrix} c_\alpha \\ c_\beta \end{pmatrix} + B_x\begin{pmatrix} 0 & 1 \\ 1 & 0 \end{pmatrix}\begin{pmatrix} c_\alpha \\ c_\beta \end{pmatrix} + \mathrm{i}B_x\begin{pmatrix} 0 & -1 \\ 1 & 0 \end{pmatrix}\begin{pmatrix} c_\alpha \\ c_\beta \end{pmatrix}\right). \tag{5.286}$$

Written as a set of two equations,

$$\frac{\mathrm{d}c_\alpha}{\mathrm{d}t} = +\mathrm{i}\frac{\gamma}{2}\left(B_z c_\alpha + (B_x - \mathrm{i}B_y)c_\beta\right), \tag{5.287}$$

$$\frac{\mathrm{d}c_\beta}{\mathrm{d}t} = -\mathrm{i}\frac{\gamma}{2}\left(-B_z c_\beta + (B_x + \mathrm{i}B_y)c_\alpha\right). \tag{5.288}$$

The coefficients c_α and c_β are not independent because $c_\alpha c_\alpha^* + c_\beta c_\beta^* = 1$. Therefore, we can combine them into a single variable and then solve one equation instead of two. Bloch and Siegert divided both equations by c_β and introduced a variable $u = c_\alpha/c_\beta$:

$$\frac{1}{c_\beta}\frac{\mathrm{d}c_\alpha}{\mathrm{d}t} = +\mathrm{i}\frac{\gamma}{2}\left(B_z u + (B_x - \mathrm{i}B_y)\right), \tag{5.289}$$

$$\frac{1}{c_\beta}\frac{\mathrm{d}c_\beta}{\mathrm{d}t} = -\mathrm{i}\frac{\gamma}{2}\left(-B_z + (B_x + \mathrm{i}B_y)u\right). \tag{5.290}$$

We multiply the second equation by u and subtract it from the first one

$$\frac{1}{c_\beta}\frac{\mathrm{d}c_\alpha}{\mathrm{d}t} - u\frac{1}{c_\beta}\frac{\mathrm{d}c_\beta}{\mathrm{d}t} = \mathrm{i}\frac{\gamma}{2}\left(2B_z u + (B_x - \mathrm{i}B_y) - (B_x + \mathrm{i}B_y)u^2\right). \tag{5.291}$$

The time derivative of u is

$$\frac{\mathrm{d}u}{\mathrm{d}t} = \frac{\mathrm{d}}{\mathrm{d}t}\frac{c_\alpha}{c_\beta} = \frac{\frac{\mathrm{d}c_\alpha}{\mathrm{d}t}c_\beta - c_\alpha\frac{\mathrm{d}c_\beta}{\mathrm{d}t}}{c_\beta^2} = \frac{1}{c_\beta}\frac{\mathrm{d}c_\alpha}{\mathrm{d}t} - u\frac{1}{c_\beta}\frac{\mathrm{d}c_\beta}{\mathrm{d}t} \tag{5.292}$$

Inserting the result into Eq. 5.291,

$$\frac{\mathrm{d}u}{\mathrm{d}t} = \mathrm{i}\frac{\gamma}{2}\left(2B_z u + (B_x - \mathrm{i}B_y) - (B_x + \mathrm{i}B_y)u^2\right). \tag{5.293}$$

We assume that the longitudinal component of $\vec{B}$ is the static magnetic field $\vec{B}_0$ and that the transverse component of $\vec{B}$ is composed of two counterrotating fields with general amplitudes and phases:

$$B_z = B_0, \tag{5.294}$$

$$B_x + \mathrm{i}B_y = B_1 e^{\mathrm{i}(\omega_{\mathrm{radio}}t+\phi_1)} + B_2 e^{-\mathrm{i}(\omega_{\mathrm{radio}}t+\phi_2)}, \tag{5.295}$$

$$B_x - \mathrm{i}B_y = B_1 e^{-\mathrm{i}(\omega_{\mathrm{radio}}t+\phi_1)} + B_2 e^{\mathrm{i}(\omega_{\mathrm{radio}}t+\phi_2)}. \tag{5.296}$$

Then,

$$\frac{\mathrm{d}u}{\mathrm{d}t} = \mathrm{i}\frac{\gamma}{2}\left(2B_0 + B_1 e^{\mathrm{i}(\omega_{\mathrm{radio}}t+\phi_1)} + B_2 e^{-\mathrm{i}(\omega_{\mathrm{radio}}t+\phi_2)} - \left(B_1 e^{-\mathrm{i}(\omega_{\mathrm{radio}}t+\phi_1)} + B_2 e^{\mathrm{i}(\omega_{\mathrm{radio}}t+\phi_2)}\right)u^2\right), \tag{5.297}$$

$$\frac{\mathrm{d}u}{\mathrm{d}t} = -\mathrm{i}\left(\omega_0 u + \frac{\omega_1}{2}e^{\mathrm{i}(\omega_{\mathrm{radio}}t+\phi_1)} + \frac{\omega_2}{2}e^{-\mathrm{i}(\omega_{\mathrm{radio}}t+\phi_2)} - \left(\frac{\omega_1}{2}e^{-\mathrm{i}(\omega_{\mathrm{radio}}t+\phi_1)} + \frac{\omega_2}{2}e^{\mathrm{i}(\omega_{\mathrm{radio}}t+\phi_2)}\right)u^2\right). \tag{5.298}$$

We multiply both sides by $\frac{\omega_1}{2}e^{-\mathrm{i}(\omega_{\mathrm{radio}}t+\phi_1)}$ and introduce a new variable

$$w = \frac{\omega_1}{2}e^{-\mathrm{i}(\omega_{\mathrm{radio}}t+\phi_1)}u \tag{5.299}$$

with the time derivative

$$\frac{\mathrm{d}w}{\mathrm{d}t} = -\mathrm{i}\omega_{\mathrm{radio}}\frac{\omega_1}{2}e^{-\mathrm{i}(\omega_{\mathrm{radio}}t+\phi_1)} + \frac{\omega_1}{2}e^{-\mathrm{i}(\omega_{\mathrm{radio}}t+\phi_1)}\frac{\mathrm{d}u}{\mathrm{d}t} \tag{5.300}$$

We obtain

$$\frac{\mathrm{d}w}{\mathrm{d}t} = -\mathrm{i}\left((\omega_0 + \omega_{\mathrm{radio}})w + \frac{\omega_1^2}{4}\left(1 + \frac{\omega_2}{\omega_1}e^{-\mathrm{i}(2\omega_{\mathrm{radio}}t+\phi_1+\phi_2)}\right) - \left(1 + \frac{\omega_2}{\omega_1}e^{\mathrm{i}(2\omega_{\mathrm{radio}}t+\phi_1+\phi_2)}\right)w^2\right). \tag{5.301}$$

To simplify the right-hand side, we use the definition of the frequency offset $\Omega = \omega_0 + \omega_{\text{radio}}$ (see Section 1.5.8) and write $2\omega_{\text{radio}}t + \phi_1 + \phi_2 = 2\omega_{\text{radio}}t + \phi$ as Φ:

$$\frac{\mathrm{d}w}{\mathrm{d}t} = -\mathrm{i}\left(\Omega w + \frac{\omega_1^2}{4}\left(1 + \frac{\omega_2}{\omega_1}\mathrm{e}^{-\mathrm{i}\Phi}\right) - \left(1 + \frac{\omega_2}{\omega_1}\mathrm{e}^{\mathrm{i}\Phi}\right)w^2\right) = \mathrm{i}\left(1 + \frac{\omega_2}{\omega_1}\mathrm{e}^{\mathrm{i}\Phi}\right)\left(w^2 - \frac{\Omega}{1 + \frac{\omega_2}{\omega_1}\mathrm{e}^{\mathrm{i}\Phi}}\ w - \frac{\omega_1^2}{4}\frac{1 + \frac{\omega_2}{\omega_1}\mathrm{e}^{-\mathrm{i}\Phi}}{1 + \frac{\omega_2}{\omega_1}\mathrm{e}^{\mathrm{i}\Phi}}\right). \qquad (5.302)$$

To proceed, we note that

$$\frac{\mathrm{d}\cot\eta}{\mathrm{d}\eta} = \frac{\mathrm{d}}{\mathrm{d}\eta}\frac{\cos\eta}{\sin\eta} = \frac{-\sin^2\eta - \cos^2\eta}{\sin^2\eta} = -\left(1 + \cot^2\eta\right). \qquad (5.303)$$

We try to modify Eq. 5.302 to resemble Eq. 5.303. We rewrite the left-hand side as

$$\frac{\mathrm{d}w}{\mathrm{d}t} = \frac{\mathrm{d}w}{\mathrm{d}\eta}\frac{\mathrm{d}\eta}{\mathrm{d}t} \qquad (5.304)$$

and complete the square in the right-hand side:

$$\frac{\mathrm{d}w}{\mathrm{d}\eta}\frac{\mathrm{d}\eta}{\mathrm{d}t} = \mathrm{i}\left(1 + \frac{\omega_2}{\omega_1}\mathrm{e}^{\mathrm{i}\Phi}\right)\left(\left(w - \frac{1}{2}\frac{\Omega}{1 + \frac{\omega_2}{\omega_1}\mathrm{e}^{\mathrm{i}\Phi}}\right)^2 - \frac{1}{4}\frac{\Omega^2 + \omega_1^2\left(1 + \frac{\omega_2}{\omega_1}\mathrm{e}^{-\mathrm{i}\Phi}\right)\left(1 + \frac{\omega_2}{\omega_1}\mathrm{e}^{\mathrm{i}\Phi}\right)}{\left(1 + \frac{\omega_2}{\omega_1}\mathrm{e}^{\mathrm{i}\Phi}\right)^2}\right), \qquad (5.305)$$

$$\frac{\mathrm{d}w}{\mathrm{d}\eta}\frac{\mathrm{d}\eta}{\mathrm{d}t} = -\frac{\mathrm{i}}{4}\frac{\Omega^2 + \omega_1^2\left(1 + \frac{\omega_2}{\omega_1}\mathrm{e}^{-\mathrm{i}\Phi}\right)\left(1 + \frac{\omega_2}{\omega_1}\mathrm{e}^{\mathrm{i}\Phi}\right)}{1 + \frac{\omega_2}{\omega_1}\mathrm{e}^{\mathrm{i}\Phi}}\left(1 - \frac{4\left(1 + \frac{\omega_2}{\omega_1}\mathrm{e}^{\mathrm{i}\Phi}\right)^2}{\Omega^2 + \omega_1^2\left(1 + \frac{\omega_2}{\omega_1}\mathrm{e}^{-\mathrm{i}\Phi}\right)\left(1 + \frac{\omega_2}{\omega_1}\mathrm{e}^{\mathrm{i}\Phi}\right)}\left(w - \frac{1}{2}\frac{\Omega}{1 + \frac{\omega_2}{\omega_1}\mathrm{e}^{\mathrm{i}\Phi}}\right)^2\right). \qquad (5.306)$$

We can identify

$$\cot^2\eta = -\frac{4\left(1 + \frac{\omega_2}{\omega_1}\mathrm{e}^{\mathrm{i}\Phi}\right)^2}{\Omega^2 + \omega_1^2\left(1 + \frac{\omega_2}{\omega_1}\mathrm{e}^{-\mathrm{i}\Phi}\right)\left(1 + \frac{\omega_2}{\omega_1}\mathrm{e}^{\mathrm{i}\Phi}\right)}\left(w - \frac{1}{2}\frac{\Omega}{1 + \frac{\omega_2}{\omega_1}\mathrm{e}^{\mathrm{i}\Phi}}\right)^2 \qquad (5.307)$$

and consequently

$$\cot\eta = \mathrm{i}\frac{2\left(1 + \frac{\omega_2}{\omega_1}\mathrm{e}^{\mathrm{i}\Phi}\right)}{\sqrt{\Omega^2 + \omega_1^2\left(1 + \frac{\omega_2}{\omega_1}\mathrm{e}^{-\mathrm{i}\Phi}\right)\left(1 + \frac{\omega_2}{\omega_1}\mathrm{e}^{\mathrm{i}\Phi}\right)}}\left(w - \frac{1}{2}\frac{\Omega}{1 + \frac{\omega_2}{\omega_1}\mathrm{e}^{\mathrm{i}\Phi}}\right) = \mathrm{i}\frac{2\left(1 + \frac{\omega_2}{\omega_1}\mathrm{e}^{\mathrm{i}\Phi}\right)}{\lambda}\left(w - \frac{1}{2}\frac{\Omega}{1 + \frac{\omega_2}{\omega_1}\mathrm{e}^{\mathrm{i}\Phi}}\right) \qquad (5.308)$$

$$w = \frac{1}{2}\frac{\Omega - \mathrm{i}\lambda\cot\eta}{1 + \frac{\omega_2}{\omega_1}\mathrm{e}^{\mathrm{i}\Phi}} = \frac{1}{2}\frac{\Omega + \lambda\frac{\cos\eta}{\mathrm{i}\sin\eta}}{1 + \frac{\omega_2}{\omega_1}\mathrm{e}^{\mathrm{i}\Phi}} = \frac{1}{2}\frac{\Omega + \lambda\frac{\mathrm{e}^{\mathrm{i}\eta}+\mathrm{e}^{-\mathrm{i}\eta}}{\mathrm{e}^{\mathrm{i}\eta}-\mathrm{e}^{-\mathrm{i}\eta}}}{1 + \frac{\omega_2}{\omega_1}\mathrm{e}^{\mathrm{i}\Phi}}, \qquad (5.309)$$

where

$$\lambda = \sqrt{\Omega^2 + \omega_1^2\left(1 + \frac{\omega_2}{\omega_1}\mathrm{e}^{-\mathrm{i}\Phi}\right)\left(1 + \frac{\omega_2}{\omega_1}\mathrm{e}^{\mathrm{i}\Phi}\right)} = \sqrt{\Omega^2 + \omega_1^2 + \omega_2^2 + 2\omega_1\omega_2\cos\Phi} = \sqrt{\Omega^2 + \omega_1^2 + \omega_2^2 + 2\omega_1\omega_2\cos(2\omega_{\text{radio}}t + \phi)}. \qquad (5.310)$$

The solution should be obtained by inserting Eq. 5.309 into Eq. 5.306. Before we try it for the general field, we check a simpler solution for $\omega_2 = 0$.

5.7.15   Evolution in rotating magnetic fields

A magnetic field composed of $\vec{B}_0$ and of a component rotating about the z can be completely described by $B_0 = B_z$ and a single rotating field $B_1\mathrm{e}^{\mathrm{i}\omega_{\text{radio}}t+\phi_1} = B_x + \mathrm{i}B_y$. The absence of the $\omega_2 = -\gamma B_2$ term simplifies Eq. 5.306 to

$$\frac{\mathrm{d}w}{\mathrm{d}\eta}\frac{\mathrm{d}\eta}{\mathrm{d}t} = -\frac{\mathrm{i}}{4}\left(\Omega^2 + \omega_1^2\right)\left(1 + \cot^2\eta\right) = -\frac{\mathrm{i}}{4}\lambda_0^2\left(1 + \cot^2\eta\right) \qquad (5.311)$$

and Eq. 5.309 to

$$w = \frac{1}{2}\Omega - \frac{\mathrm{i}}{2}\lambda_0\cot\eta = \frac{1}{2}\Omega + \frac{1}{2}\lambda_0\frac{\cos\eta}{\mathrm{i}\sin\eta} = \frac{1}{2}\Omega + \frac{1}{2}\lambda_0\frac{\mathrm{e}^{\mathrm{i}\eta}+\mathrm{e}^{-\mathrm{i}\eta}}{\mathrm{e}^{\mathrm{i}\eta}-\mathrm{e}^{-\mathrm{i}\eta}}, \qquad (5.312)$$

where $\lambda_0 = \sqrt{\Omega^2 + \omega_1^2}$ is constant (time-independent). Differentiation of Eq. 5.312 is then simply

$$\frac{\mathrm{d}w}{\mathrm{d}\eta} = \frac{\mathrm{d}}{\mathrm{d}\eta}\left(\frac{1}{2}\Omega - \frac{\mathrm{i}}{2}\lambda_0 \cot \eta\right) = -\frac{\mathrm{i}}{2}\lambda_0 \frac{\mathrm{d}\cot \eta}{\mathrm{d}\eta} = \frac{\mathrm{i}}{2}\lambda_0^2\left(1 + \cot^2 \eta\right) \tag{5.313}$$

because both Ω and λ_0 are constants. Inserting the result into Eq. 5.311 gives

$$\frac{\mathrm{d}w}{\mathrm{d}\eta}\frac{\mathrm{d}\eta}{\mathrm{d}t} = \frac{\mathrm{i}}{2}\lambda_0\left(1 + \cot^2 \eta\right)\frac{\mathrm{d}\eta}{\mathrm{d}t} = -\frac{\mathrm{i}}{4}\lambda_0^2\left(1 + \cot^2 \eta\right). \tag{5.314}$$

Evaluation of η is then a matter of straightforward integration

$$\int_{\eta_0}^{\eta}\mathrm{d}\eta' = -\int_0^t \frac{1}{2}\lambda_0 \mathrm{d}t' = -\frac{1}{2}\lambda_0 t \qquad \eta = \eta_0 - \frac{1}{2}\lambda_0 t. \tag{5.315}$$

Inserting to Eq. 5.312 and returning to the variable u,

$$u = \frac{2w}{\omega_1}\mathrm{e}^{\mathrm{i}(\omega_{\mathrm{radio}}t+\phi_1)} = \left(\frac{\Omega}{\omega_1} - \mathrm{i}\frac{\lambda_0}{\omega_1}\cot \eta\right)\mathrm{e}^{\mathrm{i}(\omega_{\mathrm{radio}}t+\phi_1)} = \left(\frac{\Omega}{\omega_1} + \frac{\lambda_0}{\omega_1}\frac{\mathrm{e}^{\mathrm{i}\eta} + \mathrm{e}^{-\mathrm{i}\eta}}{\mathrm{e}^{\mathrm{i}\eta} - \mathrm{e}^{-\mathrm{i}\eta}}\right)\mathrm{e}^{\mathrm{i}(\omega_{\mathrm{radio}}t+\phi_1)}, \tag{5.316}$$

$$u^* = \frac{2w^*}{\omega_1}\mathrm{e}^{-\mathrm{i}(\omega_{\mathrm{radio}}t+\phi_1)} = \left(\frac{\Omega}{\omega_1} + \mathrm{i}\frac{\lambda_0}{\omega_1}\cot \eta\right)\mathrm{e}^{-\mathrm{i}(\omega_{\mathrm{radio}}t+\phi_1)} = \left(\frac{\Omega}{\omega_1} - \frac{\lambda_0}{\omega_1}\frac{\mathrm{e}^{\mathrm{i}\eta} + \mathrm{e}^{-\mathrm{i}\eta}}{\mathrm{e}^{\mathrm{i}\eta} - \mathrm{e}^{-\mathrm{i}\eta}}\right)\mathrm{e}^{-\mathrm{i}(\omega_{\mathrm{radio}}t+\phi_1)}, \tag{5.317}$$

and

$$uu^* = \frac{4ww^*}{\omega_1^2} = \frac{1}{\omega_1^2}\left(\Omega + \mathrm{i}\lambda_0\cot\eta\right)\left(\Omega - \mathrm{i}\lambda_0\cot\eta\right) = \frac{\Omega^2}{\omega_1^2} + \frac{\Omega^2 + \omega_1^2}{\omega_1^2}\frac{\cos^2\eta}{\sin^2\eta} = \frac{\Omega^2 + \omega_1^2\cos^2\eta}{\omega_1^2\sin^2\eta} = \frac{\Omega^2 + \omega_1^2 - \omega_1^2\sin^2\eta}{\omega_1^2\sin^2\eta} = \frac{\Omega^2 + \omega_1^2}{\omega_1^2\sin^2\eta} - 1, \tag{5.318}$$

This allows us to calculate P_α and P_β:

$$P_\alpha = c_\alpha^* c_\alpha = uu^* c_\beta^* c_\beta = uu^*(1 - P_\alpha) \qquad \Rightarrow \qquad P_\alpha = \frac{uu^*}{1 + uu*} = 1 - \frac{\omega_1^2\sin^2\eta}{\Omega^2 + \omega_1^2}, \qquad P_\beta = 1 - P_\alpha = 1 - \frac{uu^*}{1 + uu^*} = \frac{1}{1 + uu^*} = \frac{\omega_1^2\sin^2\eta}{\Omega^2 + \omega_1^2}. \tag{5.319}$$

The derived equations include results of Section 5.7.12 for $\omega_1 = 0$ and of Section 5.7.13 for $\Omega = 0$.

The last issue discussed in this section is determination of the integration factor η_0. The value of η_0 depends on the initial conditions. For example, if we start from $P_\alpha = 1$ at $t = 0$, $\sin\eta(t = 0)$ and consequently $\eta(t = 0)$ must be zero. As $\eta = \eta_0 - \lambda_0 t/2$, η_0 must be zero to give $\eta(t = 0) = 0$. With the boundary condition $P_\alpha = 1$ at $t = 0$, the variable u is determined by

$$u = \frac{2w}{\omega_1}\mathrm{e}^{\mathrm{i}(\omega_{\mathrm{radio}}t+\phi_1)} = \left(\frac{\Omega}{\omega_1} - \mathrm{i}\frac{\lambda_0}{\omega_1}\cot\frac{\lambda_0}{2}t\right)\mathrm{e}^{\mathrm{i}(\omega_{\mathrm{radio}}t+\phi_1)} = \left(\frac{\Omega}{\omega_1} + \frac{\lambda_0}{\omega_1}\frac{\mathrm{e}^{-\mathrm{i}\frac{\lambda_0}{2}t} + \mathrm{e}^{\mathrm{i}\frac{\lambda_0}{2}t}}{\mathrm{e}^{-\mathrm{i}\frac{\lambda_0}{2}t} - \mathrm{e}^{\mathrm{i}\frac{\lambda_0}{2}t}}\right)\mathrm{e}^{\mathrm{i}(\omega_{\mathrm{radio}}t+\phi_1)}$$

$$= \left(\frac{\Omega}{\omega_1} + \frac{\lambda_0}{\omega_1}\frac{\mathrm{e}^{-\mathrm{i}\lambda_0 t} + 1}{\mathrm{e}^{-\mathrm{i}\lambda_0 t} - 1}\right)\mathrm{e}^{\mathrm{i}(\omega_{\mathrm{radio}}t+\phi_1)} = \frac{\frac{\lambda_0 + \Omega_0}{\omega_1}\mathrm{e}^{-\mathrm{i}\lambda_0 t} + \frac{\lambda_0 - \Omega_0}{\omega_1}}{\mathrm{e}^{-\mathrm{i}\lambda_0 t} - 1}\mathrm{e}^{\mathrm{i}(\omega_{\mathrm{radio}}t+\phi_1)} = \frac{\frac{\lambda_0 + \Omega_0}{\omega_1}\mathrm{e}^{-\mathrm{i}\frac{\lambda_0}{2}t} + \frac{\lambda_0 - \Omega_0}{\omega_1}\mathrm{e}^{+\mathrm{i}\frac{\lambda_0}{2}t}}{\mathrm{e}^{-\mathrm{i}\frac{\lambda_0}{2}t} - \mathrm{e}^{+\mathrm{i}\frac{\lambda_0}{2}t}}\mathrm{e}^{\mathrm{i}(\omega_{\mathrm{radio}}t+\phi_1)}. \tag{5.320}$$

Consequently (taking into account that $\lambda_0 = \sqrt{\Omega^2 + \omega_1^2}$ and $\sin^2(-x) = \sin^2 x$),

$$P_\beta = \frac{1}{1 + uu^*} = \frac{\omega_1^2}{\Omega^2 + \omega_1^2}\sin^2\frac{\sqrt{\Omega^2 + \omega_1^2}}{2}t, \qquad P_\alpha = 1 - P_\beta = 1 - \frac{\omega_1^2}{\Omega^2 + \omega_1^2}\sin^2\frac{\sqrt{\Omega^2 + \omega_1^2}}{2}t. \tag{5.321}$$

which serves us as a reference when discussing the general case in the next section.

5.7.16   Evolution in non-rotating magnetic fields

In general, w is (Eq. 5.309)

$$w = \frac{1}{2}\frac{\Omega - \mathrm{i}\lambda\cot\eta}{1 + \frac{\omega_2}{\omega_1}\mathrm{e}^{\mathrm{i}\Phi}} = \frac{1}{2\left(1 + \frac{\omega_2}{\omega_1}\mathrm{e}^{\mathrm{i}\Phi}\right)}\left(\Omega + \lambda\frac{\mathrm{e}^{\mathrm{i}\eta} + \mathrm{e}^{-\mathrm{i}\eta}}{\mathrm{e}^{\mathrm{i}\eta} - \mathrm{e}^{-\mathrm{i}\eta}}\right) = \frac{(\lambda + \Omega)\,\mathrm{e}^{\mathrm{i}\eta} + (\lambda - \Omega)\,\mathrm{e}^{-\mathrm{i}\eta}}{\left(1 + \frac{\omega_2}{\omega_1}\mathrm{e}^{\mathrm{i}\Phi}\right)\mathrm{e}^{\mathrm{i}\eta} - \mathrm{e}^{-\mathrm{i}\eta}} = \frac{(\lambda + \Omega)\,\mathrm{e}^{2\mathrm{i}\eta} + (\lambda - \Omega)}{2\left(1 + \frac{\omega_2}{\omega_1}\mathrm{e}^{\mathrm{i}\Phi}\right)\left(\mathrm{e}^{2\mathrm{i}\eta} - 1\right)} \tag{5.322}$$

In the presence of $\omega_2 = -\gamma B_2$, differentiation of w defined by Eq. 5.309 is far from simple because $\Phi = 2\omega_{\text{radio}}t + \phi_1 + \phi_2$ and $\lambda = \sqrt{\Omega^2 + \omega_1^2 + \omega_2^2 + 2\omega_1\omega_2\cos\Phi}$ are not constants, but time-dependent functions. To follow the analysis by Bloch and Siegert, we "hide" the time-dependence in a single quantity denoted ξ in the following text. We express u using w defined by Eq. 5.309

$$u = \frac{1}{\omega_1}\frac{\Omega - i\lambda\cot\eta}{1 + \frac{\omega_2}{\omega_1}e^{i\Phi}}e^{i(\omega_{\text{radio}}t+\phi_1)} = \frac{\frac{\lambda+\Omega}{\omega_1}e^{2i\eta} + \frac{\lambda-\Omega}{\omega_1}}{\left(1 + \frac{\omega_2}{\omega_1}e^{i\Phi}\right)\left(e^{2i\eta} - 1\right)}e^{i(\omega_{\text{radio}}t+\phi_1)} \tag{5.323}$$

and require, in analogy with Eq. 5.320, that it is equal to

$$u = \frac{\frac{\lambda_0+\Omega}{\omega_1}\,\Xi\,e^{-i\lambda_0 t} + \frac{\lambda_0-\Omega}{\omega_1}}{\left(\Xi\,e^{-i\lambda_0 t} - 1\right)}e^{i(\omega_{\text{radio}}t+\phi_1)} = \frac{\frac{\lambda_0+\Omega}{\omega_1}\,e^{i\xi}\,e^{-i\lambda_0 t} + \frac{\lambda_0-\Omega}{\omega_1}}{\left(e^{i\xi}\,e^{-i\lambda_0 t} - 1\right)}e^{i(\omega_{\text{radio}}t+\phi_1)} = \frac{\frac{\lambda_0+\Omega}{\omega_1}e^{i\frac{\xi-\lambda_0 t}{2}} + \frac{\lambda_0-\Omega}{\omega_1}e^{-i\frac{\xi-\lambda_0 t}{2}}}{e^{i\frac{\xi-\lambda_0 t}{2}} - e^{-i\frac{\xi-\lambda_0 t}{2}}}e^{i(\omega_{\text{radio}}t+\phi_1)}, \tag{5.324}$$

where $\Xi = e^{i\xi}$ is a time-dependent factor to be determined (note that any Ξ can be written as $e^{i\xi}$ if we allow ξ to be a complex quantity). The following rearrangements confirm that Ξ can be really expressed analytically as a function of well-defined Φ and the unknown quantity η.

$$\frac{\frac{1}{1+\frac{\omega_2}{\omega_1}e^{i\Phi}}\frac{\lambda+\Omega}{\omega_1}e^{2i\eta} + \frac{1}{1+\frac{\omega_2}{\omega_1}e^{i\Phi}}\frac{\lambda-\Omega}{\omega_1}}{e^{2i\eta} - 1} = \frac{\frac{\lambda_0+\Omega}{\omega_1}\,\Xi\,e^{-i\lambda_0 t} + \frac{\lambda_0-\Omega}{\omega_1}}{\Xi\,e^{-i\lambda_0 t} - 1} \tag{5.325}$$

$$\left(\Xi\,e^{-i\lambda_0 t} - 1\right)\left(\frac{1}{1+\frac{\omega_2}{\omega_1}e^{i\Phi}}\frac{\lambda+\Omega}{\omega_1}e^{2i\eta} + \frac{1}{1+\frac{\omega_2}{\omega_1}e^{i\Phi}}\frac{\lambda-\Omega}{\omega_1}\right) = \left(\frac{\lambda_0+\Omega}{\omega_1}\,\Xi\,e^{-i\lambda_0 t} + \frac{\lambda_0-\Omega}{\omega_1}\right)\left(e^{2i\eta} - 1\right) \tag{5.326}$$

$$\Xi\,e^{-i\lambda_0 t}\left(\frac{1}{1+\frac{\omega_2}{\omega_1}e^{i\Phi}}\frac{\lambda+\Omega}{\omega_1}e^{2i\eta} + \frac{1}{1+\frac{\omega_2}{\omega_1}e^{i\Phi}}\frac{\lambda-\Omega}{\omega_1} - \frac{\lambda_0+\Omega}{\omega_1}\left(e^{2i\eta} - 1\right)\right) = \frac{1}{1+\frac{\omega_2}{\omega_1}e^{i\Phi}}\frac{\lambda+\Omega}{\omega_1}e^{2i\eta} + \frac{1}{1+\frac{\omega_2}{\omega_1}e^{i\Phi}}\frac{\lambda-\Omega}{\omega_1} + \frac{\lambda_0-\Omega}{\omega_1}\left(e^{2i\eta} - 1\right) \tag{5.327}$$

$$\Xi = e^{i\lambda_0 t}\frac{\left(\frac{\lambda+\Omega}{\omega_1+\omega_2 e^{i\Phi}} + \frac{\lambda_0-\Omega}{\omega_1}\right)e^{2i\eta} + \frac{\lambda-\Omega}{\omega_1+\omega_2 e^{i\Phi}} - \frac{\lambda_0-\Omega}{\omega_1}}{\left(\frac{\lambda+\Omega}{\omega_1+\omega_2 e^{i\Phi}} - \frac{\lambda_0+\Omega}{\omega_1}\right)e^{2i\eta} + \frac{\lambda-\Omega}{\omega_1+\omega_2 e^{i\Phi}} + \frac{\lambda_0+\Omega}{\omega_1}} \tag{5.328}$$

Determination of Ξ is demanding. Therefore, we postpone it to Sections 5.7.17 and 5.7.18 and present here only the solution. For the sake of simplicity, the solution for the most interesting case of a field *oscillating in one direction* (i.e., for $\omega_2 = \omega_1$) is summarized below, a more general is derived in Sections 5.7.17 and 5.7.18.

- It is possible to find sufficiently accurate approximation of ξ for oscillating fields much weaker than the static field $B_1 \ll B_0$. If the alternating fields oscillate close to resonance, this also implies $\omega_1 \ll \omega_{\text{radio}}$.

- The solution can be found as a series expansion of ξ in powers of $\omega_1/\omega_{\text{radio}}$. The second-order approximation is sufficient for standard NMR experiments.

- Using this approximation, ξ, u, P_α, and P_β can be evaluated.

- The solution is greatly simplified if we are interested only in average results of repeated experiments and assume that phase factors dependent on the actual beginning of the measurement average to zero.

- As $\omega_1/\omega_{\text{radio}} \ll 1$, the terms proportional to $(\omega_1/\omega_{\text{radio}})^2$ can be neglected in the expressions defining the average values of P_β and of $P_\alpha = 1 - P_\beta$. Then,

$$\overline{P}_\beta \approx \frac{\omega_1^2}{\omega_1^2 + \left(\Omega - \frac{\omega_1^2}{4\omega_{\text{radio}}}\right)^2}\sin^2\frac{\sqrt{\omega_1^2 + \left(\Omega - \frac{\omega_1^2}{4\omega_{\text{radio}}}\right)^2}}{2}t. \tag{5.329}$$

We see that in a field of radio waves oscillating in one direction with frequency close to ω_0 and amplitude much lower than B_0, the equation describing evolution of $\overline{P}_\beta$ has the same form as the equation describing evolution of P_β in a rotating field (Eq. 5.321). The only difference is a small[11] *Bloch-Siegert shift* of the frequency offset (by $\omega_1^2/(4\omega_{\text{radio}})$). This justifies the common practice to approximate the effects of radio waves by effects of rotating fields.

---

[11]The shift by $\omega_1^2/(4\omega_{\text{radio}})$ changes Ω from $\Omega = \omega_0 + \omega_{\text{radio}}$ to $\Omega = \omega_0 + \omega_{\text{radio}} - \omega_1^2/(4\omega_{\text{radio}}) = \omega_0 + \omega_{\text{radio}}(1 - (\omega_1/(2\omega_{\text{radio}}))^2)$. The relative change is thus proportional to $(\omega_1/(2\omega_{\text{radio}}))^2$

5.7.17 Modifying factor ξ in description of non-rotating fields

In order to determine Ξ in terms of known parameters, we convert u expressed in Eq. 5.324 to w, and evaluated its square and time derivative

$$\frac{2w}{\omega_1} = ue^{-\mathrm{i}(\omega_{\mathrm{radio}}t+\phi_1)} = \frac{\frac{\lambda_0+\Omega}{\omega_1}\Xi\,e^{-\mathrm{i}\lambda_0 t}+\frac{\lambda_0-\Omega}{\omega_1}}{\Xi\,e^{-\mathrm{i}\lambda_0 t}-1} = \frac{\frac{\lambda_0+\Omega}{\omega_1}\Xi\left(e^{-\mathrm{i}\lambda_0 t}-1\right)+\frac{\lambda_0+\Omega}{\omega_1}+\frac{\lambda_0-\Omega}{\omega_1}}{\Xi\,e^{-\mathrm{i}\lambda_0 t}-1} = \frac{\lambda_0+\Omega}{\omega_1}+\frac{2\lambda_0}{\omega_1}\frac{1}{\Xi\,e^{-\mathrm{i}\lambda_0 t}-1}, \quad (5.330)$$

$$w = \frac{\frac{\lambda_0+\Omega}{2}\Xi\,e^{-\mathrm{i}\lambda_0 t}+\frac{\lambda_0-\Omega}{2}}{\Xi\,e^{-\mathrm{i}\lambda_0 t}-1} = \frac{\frac{\lambda_0+\Omega}{2}\Xi\left(e^{-\mathrm{i}\lambda_0 t}-1\right)+\frac{\lambda_0+\Omega}{2}+\frac{\lambda_0-\Omega}{\omega_1}}{\Xi\,e^{-\mathrm{i}\lambda_0 t}-1} = \frac{\lambda_0+\Omega}{2}+\frac{\lambda_0}{\Xi\,e^{-\mathrm{i}\lambda_0 t}-1}, \quad (5.331)$$

$$w^2 = \left(\frac{\lambda_0+\Omega}{2}+\frac{\lambda_0}{\Xi\,e^{-\mathrm{i}\lambda_0 t}-1}\right)^2 = \left(\frac{\lambda_0+\Omega}{2}\right)^2+\frac{(\lambda_0+\Omega)\lambda_0}{\Xi\,e^{-\mathrm{i}\lambda_0 t}-1}+\frac{\lambda_0^2}{\left(\Xi\,e^{-\mathrm{i}\lambda_0 t}-1\right)^2}, \quad (5.332)$$

$$\frac{\mathrm{d}w}{\mathrm{d}t} = \lambda_0\frac{\mathrm{d}}{\mathrm{d}t}\frac{1}{\Xi\,e^{-\mathrm{i}\lambda_0 t}-1} = -\lambda_0\frac{\frac{\mathrm{d}\Xi}{\mathrm{d}t}e^{-\mathrm{i}\lambda_0 t}-\mathrm{i}\lambda_0\Xi\,e^{-\mathrm{i}\lambda_0 t}}{\left(\Xi\,e^{-\mathrm{i}\lambda_0 t}-1\right)^2} = \mathrm{i}\frac{\lambda_0^2\Xi\,e^{-\mathrm{i}\lambda_0 t}}{\left(\Xi\,e^{-\mathrm{i}\lambda_0 t}-1\right)^2}-\frac{\lambda_0 e^{-\mathrm{i}\lambda_0 t}}{\left(\Xi\,e^{-\mathrm{i}\lambda_0 t}-1\right)^2}\frac{\mathrm{d}\Xi}{\mathrm{d}t}, \quad (5.333)$$

and insert them into Eq. 5.302:

$$\frac{\mathrm{d}w}{\mathrm{d}t} = -\mathrm{i}\left(\Omega w+\frac{\omega_1^2}{4}\left(1+\frac{\omega_2}{\omega_1}e^{-\mathrm{i}\Phi}\right)-\left(1+\frac{\omega_2}{\omega_1}e^{\mathrm{i}\Phi}\right)w^2\right) \quad (5.334)$$

$$\mathrm{i}\frac{\lambda_0^2\Xi\,e^{-\mathrm{i}\lambda_0 t}}{\left(\Xi\,e^{-\mathrm{i}\lambda_0 t}-1\right)^2}-\frac{\lambda_0 e^{-\mathrm{i}\lambda_0 t}}{\left(\Xi\,e^{-\mathrm{i}\lambda_0 t}-1\right)^2}\frac{\mathrm{d}\Xi}{\mathrm{d}t} =$$

$$-\mathrm{i}\left(\frac{\Omega(\lambda_0+\Omega)}{2}+\frac{\Omega\lambda_0}{\Xi\,e^{-\mathrm{i}\lambda_0 t}-1}+\frac{\omega_1^2}{4}\left(1+\frac{\omega_2}{\omega_1}e^{-\mathrm{i}\Phi}\right)-\left(1+\frac{\omega_2}{\omega_1}e^{\mathrm{i}\Phi}\right)\left(\left(\frac{\lambda_0+\Omega}{2}\right)^2+\frac{(\lambda_0+\Omega)\lambda_0}{\Xi\,e^{-\mathrm{i}\lambda_0 t}-1}+\frac{\lambda_0^2}{\left(\Xi\,e^{-\mathrm{i}\lambda_0 t}-1\right)^2}\right)\right). \quad (5.335)$$

Then we separate $\mathrm{d}\Xi/\mathrm{d}t$

$$\frac{\mathrm{d}\Xi}{\mathrm{d}t} = \mathrm{i}\left(\lambda_0\Xi+\frac{\Omega(\lambda_0+\Omega)}{2}\frac{\left(\Xi\,e^{-\mathrm{i}\lambda_0 t}-1\right)^2}{\lambda_0 e^{-\mathrm{i}\lambda_0 t}}+\Omega\frac{\Xi\,e^{-\mathrm{i}\lambda_0 t}-1}{e^{-\mathrm{i}\lambda_0 t}}+\frac{\omega_1^2}{4}\left(1+\frac{\omega_2}{\omega_1}e^{-\mathrm{i}\Phi}\right)\frac{\left(\Xi\,e^{-\mathrm{i}\lambda_0 t}-1\right)^2}{\lambda_0 e^{-\mathrm{i}\lambda_0 t}}\right.$$
$$\left.-\left(1+\frac{\omega_2}{\omega_1}e^{\mathrm{i}\Phi}\right)\left(\left(\frac{\lambda_0+\Omega}{2}\right)^2\frac{\left(\Xi\,e^{-\mathrm{i}\lambda_0 t}-1\right)^2}{\lambda_0 e^{-\mathrm{i}\lambda_0 t}}+(\lambda_0+\Omega)\frac{\Xi\,e^{-\mathrm{i}\lambda_0 t}-1}{e^{-\mathrm{i}\lambda_0 t}}+\frac{\lambda_0}{e^{-\mathrm{i}\lambda_0 t}}\right)\right), \quad (5.336)$$

and simplify the right-hand side as much as possible in a series of routine steps:

$$\frac{\mathrm{d}\Xi}{\mathrm{d}t} = \mathrm{i}\left(\left(\frac{2\Omega\lambda_0+2\Omega^2+\omega_1^2-(\lambda_0^2+2\Omega\lambda_0+\Omega^2)}{4}+\frac{\omega_1^2}{4}\frac{\omega_2}{\omega_1}e^{-\mathrm{i}\Phi}-\frac{\omega_2}{\omega_1}e^{\mathrm{i}\Phi}\frac{\lambda_0^2+2\Omega\lambda_0+\Omega^2}{4}\right)\frac{\left(\Xi\,e^{-\mathrm{i}\lambda_0 t}-1\right)^2}{\lambda_0 e^{-\mathrm{i}\lambda_0 t}}\right.$$
$$\left.\left(\Omega-(\lambda_0+\Omega)-\frac{\omega_2}{\omega_1}e^{\mathrm{i}\Phi}(\lambda_0+\Omega)\right)\frac{\Xi\,e^{-\mathrm{i}\lambda_0 t}-1}{e^{-\mathrm{i}\lambda_0 t}}+\lambda_0\Xi-\frac{\lambda_0}{e^{-\mathrm{i}\lambda_0 t}}-\frac{\omega_2}{\omega_1}e^{\mathrm{i}\Phi}\frac{\lambda_0}{e^{-\mathrm{i}\lambda_0 t}}\right), \quad (5.337)$$

$$\frac{\mathrm{d}\Xi}{\mathrm{d}t} = \mathrm{i}\left(\left(\frac{2\Omega\lambda_0+2\Omega^2+\omega_1^2-(\Omega^2+\omega_1^2+2\Omega\lambda_0+\Omega^2)}{4}+\frac{\omega_1^2}{4}\frac{\omega_2}{\omega_1}e^{-\mathrm{i}\Phi}-\frac{\omega_2}{\omega_1}e^{\mathrm{i}\Phi}\frac{\lambda_0^2+2\Omega\lambda_0+\Omega^2}{4}\right)\frac{\left(\Xi\,e^{-\mathrm{i}\lambda_0 t}-1\right)^2}{\lambda_0 e^{-\mathrm{i}\lambda_0 t}}\right.$$
$$\left.-\lambda_0\frac{\Xi\,e^{-\mathrm{i}\lambda_0 t}-1}{e^{-\mathrm{i}\lambda_0 t}}-\frac{\omega_2}{\omega_1}e^{\mathrm{i}\Phi}(\lambda_0+\Omega)\frac{\Xi\,e^{-\mathrm{i}\lambda_0 t}-1}{e^{-\mathrm{i}\lambda_0 t}}+\lambda_0\frac{\Xi\,e^{-\mathrm{i}\lambda_0 t}-1}{e^{-\mathrm{i}\lambda_0 t}}-\frac{\omega_2}{\omega_1}e^{\mathrm{i}\Phi}\frac{\lambda_0}{e^{-\mathrm{i}\lambda_0 t}}\right), \quad (5.338)$$

$$\frac{\mathrm{d}\Xi}{\mathrm{d}t} = \mathrm{i}\left(\frac{\omega_1\omega_2}{4\lambda_0}\left(e^{-\mathrm{i}\Phi}-e^{\mathrm{i}\Phi}\left(\frac{\lambda_0+\Omega}{\omega_1}\right)^2\right)\frac{\left(\Xi\,e^{-\mathrm{i}\lambda_0 t}-1\right)^2}{e^{-\mathrm{i}\lambda_0 t}}-\frac{\omega_2}{\omega_1}e^{\mathrm{i}\Phi}\frac{(\lambda_0+\Omega)\Xi\,e^{-\mathrm{i}\lambda_0 t}-\Omega}{e^{-\mathrm{i}\lambda_0 t}}\right), \quad (5.339)$$

$$\frac{\mathrm{d}\Xi}{\mathrm{d}t} = \mathrm{i}\left(\frac{\omega_1\omega_2}{4\lambda_0}\left(e^{-\mathrm{i}\Phi}-e^{\mathrm{i}\Phi}\left(\frac{\lambda_0+\Omega}{\omega_1}\right)^2\right)\left(\Xi^2 e^{-\mathrm{i}\lambda_0 t}-2\Xi+e^{\mathrm{i}\lambda_0 t}\right)-\frac{\omega_2}{\omega_1}e^{\mathrm{i}\Phi}(\lambda_0+\Omega)\Xi+\frac{\omega_2}{\omega_1}e^{\mathrm{i}\Phi}\Omega e^{\mathrm{i}\lambda_0 t}\right), \quad (5.340)$$

$$\frac{\mathrm{d}\Xi}{\mathrm{d}t} = \mathrm{i}\frac{\omega_1\omega_2}{4\lambda_0}\left(e^{-\mathrm{i}\Phi}\left(\Xi^2 e^{-\mathrm{i}\lambda_0 t}-2\Xi+e^{\mathrm{i}\lambda_0 t}\right)-e^{\mathrm{i}\Phi}\left(\left(\frac{\lambda_0+\Omega}{\omega_1}\right)^2\left(\Xi^2 e^{-\mathrm{i}\lambda_0 t}-2\Xi+e^{\mathrm{i}\lambda_0 t}\right)+\frac{4\lambda_0^2+4\Omega\lambda_0}{\omega_1^2}\Xi-\frac{4\Omega\lambda_0}{\omega_1^2}e^{\mathrm{i}\lambda_0 t}\right)\right), \quad (5.341)$$

$$\frac{\mathrm{d}\Xi}{\mathrm{d}t} = \mathrm{i}\frac{\omega_1\omega_2}{4\lambda_0}\left(\left(\mathrm{e}^{-\mathrm{i}\Phi} - \left(\frac{\lambda_0+\Omega}{\omega_1}\right)^2\mathrm{e}^{\mathrm{i}\Phi}\right)\Xi^2\mathrm{e}^{-\mathrm{i}\lambda_0 t} - 2\left(\mathrm{e}^{-\mathrm{i}\Phi} - \frac{\Omega^2+\omega_1^2+2\Omega\lambda_0+\Omega^2-2(\Omega^2+\omega_1^2)-2\Omega\lambda_0}{\omega_1^2}\mathrm{e}^{\mathrm{i}\Phi}\right)\Xi\right.$$

$$\left. + \left(\mathrm{e}^{-\mathrm{i}\Phi} - \frac{\lambda_0^2+2\Omega\lambda_0+\Omega^2-4\Omega\lambda_0}{\omega_1^2}\mathrm{e}^{\mathrm{i}\Phi}\right)\mathrm{e}^{\mathrm{i}\lambda_0 t}\right),\tag{5.342}$$

$$\frac{\mathrm{d}\Xi}{\mathrm{d}t} = \mathrm{i}\frac{\omega_1\omega_2}{4\lambda_0}\left(\left(\mathrm{e}^{-\mathrm{i}\Phi} - \left(\frac{\lambda_0+\Omega}{\omega_1}\right)^2\mathrm{e}^{\mathrm{i}\Phi}\right)\Xi^2\mathrm{e}^{-\mathrm{i}\lambda_0 t} - 2\left(\mathrm{e}^{-\mathrm{i}\Phi}+\mathrm{e}^{\mathrm{i}\Phi}\right)\Xi + \left(\mathrm{e}^{-\mathrm{i}\Phi} - \left(\frac{\lambda_0-\Omega}{\omega_1}\right)^2\mathrm{e}^{\mathrm{i}\Phi}\right)\mathrm{e}^{\mathrm{i}\lambda_0 t}\right).\tag{5.343}$$

We express the complex quantity Ξ as $\mathrm{e}^{\mathrm{i}\xi}$, where ξ is also a complex time-dependent function. Then

$$\frac{\mathrm{d}\Xi}{\mathrm{d}t} = \frac{\mathrm{d}(\mathrm{i}\xi)}{\mathrm{d}t}\mathrm{e}^{\mathrm{i}\xi} = \mathrm{i}\Xi\frac{\mathrm{d}\xi}{\mathrm{d}t}\tag{5.344}$$

Dividing Eq. 5.343 by $\mathrm{i}\Xi$ gives

$$\frac{\mathrm{d}\xi}{\mathrm{d}t} = \frac{\omega_1\omega_2}{4\lambda_0}\left(\left(\mathrm{e}^{-\mathrm{i}\Phi} - \left(\frac{\lambda_0+\Omega}{\omega_1}\right)^2\mathrm{e}^{\mathrm{i}\Phi}\right)\mathrm{e}^{\mathrm{i}(\xi-\lambda_0 t)} - 2\left(\mathrm{e}^{-\mathrm{i}\Phi}+\mathrm{e}^{\mathrm{i}\Phi}\right) + \left(\mathrm{e}^{-\mathrm{i}\Phi} - \left(\frac{\lambda_0-\Omega}{\omega_1}\right)^2\mathrm{e}^{\mathrm{i}\Phi}\right)\mathrm{e}^{-\mathrm{i}(\xi-\lambda_0 t)}\right).\tag{5.345}$$

This differential equation cannot be solved by direct integration because the variables t and ξ are not separated. But we proceed anyway

$$\int_0^\xi \mathrm{d}\xi' = \frac{\omega_1\omega_2}{4\lambda_0}\int_0^t\left(\mathrm{e}^{-\mathrm{i}\Phi} - \left(\frac{\lambda_0+\Omega}{\omega_1}\right)^2\mathrm{e}^{\mathrm{i}\Phi}\right)\mathrm{e}^{\mathrm{i}(\xi-\lambda_0 t')}\mathrm{d}t' - \frac{\omega_1\omega_2}{2\lambda_0}\int_0^t\left(\mathrm{e}^{-\mathrm{i}\Phi}+\mathrm{e}^{\mathrm{i}\Phi}\right)\mathrm{d}t' + \frac{\omega_1\omega_2}{4\lambda_0}\int_0^t\left(\mathrm{e}^{-\mathrm{i}\Phi} - \left(\frac{\lambda_0-\Omega}{\omega_1}\right)^2\mathrm{e}^{\mathrm{i}\Phi}\right)\mathrm{e}^{-\mathrm{i}(\xi-\lambda_0 t')}\mathrm{d}t',$$
$$\tag{5.346}$$

applying the boundary condition $P_\alpha = 1 \Rightarrow u \to \infty \Rightarrow \Xi = 1$ and $\xi = 0$ at $t = 0$ (see Eq. 5.324). Only the middle integral of the right-hand side can be evaluated

$$-\frac{\omega_1\omega_2}{2\lambda_0}\int_0^t\left(\mathrm{e}^{-\mathrm{i}\Phi}+\mathrm{e}^{\mathrm{i}\Phi}\right)\mathrm{d}t' = -\frac{\omega_1\omega_2}{\lambda_0}\int_0^t\cos\Phi\,\mathrm{d}t' = -\frac{\omega_1\omega_2}{\lambda_0}\int_\phi^\Phi\frac{\mathrm{d}t'}{\mathrm{d}\Phi'}\cos\Phi\,\mathrm{d}\Phi' = -\frac{\omega_1\omega_2}{2\lambda_0\omega_{\mathrm{radio}}}\int_\phi^\Phi\cos\Phi\,\mathrm{d}\Phi' = -\varepsilon\int_\phi^\Phi\cos\Phi\,\mathrm{d}\Phi'$$

$$= \varepsilon(\sin\phi - \sin\Phi) = \varepsilon(\sin\phi - \sin(2\omega_{\mathrm{radio}}t + \phi)),\tag{5.347}$$

where ε is a dimensionless constant

$$\varepsilon = \frac{\omega_1\omega_2}{2\omega_{\mathrm{radio}}\sqrt{\Omega^2+\omega_1}}.\tag{5.348}$$

The other two integrals can be modified, but not solved, in the same manner

$$\frac{\omega_1\omega_2}{4\lambda_0}\int_0^t\left(\mathrm{e}^{-\mathrm{i}\Phi} - \left(\frac{\lambda_0\pm\Omega}{\omega_1}\right)^2\mathrm{e}^{\mathrm{i}\Phi}\right)\mathrm{e}^{\pm\mathrm{i}(\xi-\lambda_0 t')}\mathrm{d}t' = \frac{\omega_1\omega_2}{4\lambda_0}\int_\phi^\Phi\left(\frac{\mathrm{e}^{-\mathrm{i}\Phi'}}{2\omega_{\mathrm{radio}}} - \left(\frac{\lambda_0\pm\Omega}{\omega_1}\right)^2\frac{\mathrm{e}^{\mathrm{i}\Phi'}}{2\omega_{\mathrm{radio}}}\right)\mathrm{e}^{\pm\mathrm{i}\left(\xi-\lambda_0\frac{\Phi'-\phi}{2\omega_{\mathrm{radio}}}\right)}\mathrm{d}\Phi'$$

$$= \frac{\omega_1\omega_2}{8\lambda_0\omega_{\mathrm{radio}}}\int_\phi^\Phi\left(\mathrm{e}^{-\mathrm{i}\Phi'} - \left(\frac{\lambda_0\pm\Omega}{\omega_1}\right)^2\mathrm{e}^{\mathrm{i}\Phi'}\right)\mathrm{e}^{\pm\mathrm{i}\left(\xi-\lambda_0\frac{\Phi'-\phi}{2\omega_{\mathrm{radio}}}\right)}\mathrm{d}\Phi' = \varepsilon\int_\phi^\Phi\frac{1}{4}\left(\mathrm{e}^{-\mathrm{i}\Phi'} - \left(\frac{\lambda_0\pm\Omega}{\omega_1}\right)^2\mathrm{e}^{\mathrm{i}\Phi'}\right)\mathrm{e}^{\pm\mathrm{i}\left(\xi-\lambda_0\frac{\Phi'-\phi}{2\omega_{\mathrm{radio}}}\right)}\mathrm{d}\Phi'.\tag{5.349}$$

In summary, we have found that the time-dependent factor ξ is defined by

$$\xi = \varepsilon\left(\sin\phi - \sin\Phi + \frac{1}{4}\int_\phi^\Phi\left(\left(\mathrm{e}^{-\mathrm{i}\Phi'} - \left(\frac{\lambda_0+\Omega}{\omega_1}\right)^2\mathrm{e}^{\mathrm{i}\Phi'}\right)\mathrm{e}^{\mathrm{i}\left(\xi-\lambda_0\frac{\Phi'-\phi}{2\omega_{\mathrm{radio}}}\right)} + \left(\mathrm{e}^{-\mathrm{i}\Phi'} - \left(\frac{\lambda_0-\Omega}{\omega_1}\right)^2\mathrm{e}^{\mathrm{i}\Phi'}\right)\mathrm{e}^{-\mathrm{i}\left(\xi-\lambda_0\frac{\Phi'-\phi}{2\omega_{\mathrm{radio}}}\right)}\right)\mathrm{d}\Phi'\right).$$
$$\tag{5.350}$$

This definition is only implicit, because ξ is present also in the integral in the right-hand side.

5.7.18 Factor ξ approximated by power series expansion

Bloch and Siegert noticed that the constant ε plays a critical role in Eq. 5.350. The function ξ depends on ε and, if ε is sufficiently small, this dependence can be approximated as a power series

$$\xi = \xi_0 + \varepsilon\xi_1 + \varepsilon^2\xi_2 + \dots \tag{5.351}$$

In other words, we assume that $\xi \approx \xi_0$ and add corrections $\varepsilon\xi_1$, $\varepsilon^2\xi_2$, etc. to improve accuracy of the approximation. If $\varepsilon \ll 1$ is, the higher powers of ε are even smaller and already low powers provide good approximation. When is ε sufficiently small? Eq. 5.348 shows that on resonance (i.e., for $\Omega = 0$),

$$\varepsilon \leq \frac{\omega_2}{2\omega_{\text{radio}}}. \tag{5.352}$$

We see that $\varepsilon \ll 1$ if $\omega_2 \ll \omega_{\text{radio}}$, it is not necessary to have $\omega_2 \ll \omega_1$! This shows that our approximation is well applicable for counter-rotating fields with $B_1 = B_2$ (and therefore $\omega_2 = \omega_1$) and with $\phi_1{=}\phi_2$ that add up to a field *oscillating in one direction*:

$$B_1 e^{i(\omega_{\text{radio}}t+\phi_1)} + B_1 e^{-i(\omega_{\text{radio}}t+\phi_1)} = 2B_1\cos(\omega_{\text{radio}}t + \phi_1). \tag{5.353}$$

For $\omega_2 \ll \omega_{\text{radio}}$, we can replace ξ in Eq. 5.350 by $\xi = \xi_0 + \varepsilon\xi_1 + \varepsilon^2\xi_2 + \dots$ and compare the terms with the same powers of ε to determine the functions $\xi_0, \xi_1, \xi_2, \dots$. As ξ is a time-dependent function, we should also check how it evolves in time. The oscillatory terms like $e^{-i\omega t}$ (where ω is a constant) stay within the range ± 1 even if $t \to \infty$. However, as we show below, the integral in Eq. 5.350 also yields linear terms. Therefore, we have to express ξ as a sum of oscillatory components (labeled by the symbol $\sim$ and including also constant contributions) and components linearly increasing in time (labeled by the symbol $\angle$):

$$\xi = \xi^\sim + \xi^\angle t = \xi_0^{\widetilde{}} + \varepsilon\xi_1^{\widetilde{}} + \varepsilon^2\xi_2^{\widetilde{}} + \dots + \xi_0^\angle t + \varepsilon\xi_1^\angle t + \varepsilon^2\xi_2^\angle t + \dots \tag{5.354}$$

Eq. 5.350 with the power expansion of the left-hand side is

$$\xi = \xi_0^{\widetilde{}} + \varepsilon\xi_1^{\widetilde{}} + \varepsilon^2\xi_2^{\widetilde{}} + \dots + \xi_0^\angle t + \varepsilon\xi_1^\angle t + \varepsilon^2\xi_2^\angle t + \dots = \varepsilon\left(\sin\phi - \sin\Phi\right) +$$

$$\frac{\varepsilon}{4}\int_\phi^\Phi \left(\left(e^{-i\Phi'} - \left(\frac{\lambda_0+\Omega}{\omega_1}\right)^2 e^{i\Phi'}\right) e^{i\xi^\sim} e^{i(\xi^\angle - \lambda_0)\frac{\Phi'-\phi}{2\omega_{\text{radio}}}} + \left(e^{-i\Phi'} - \left(\frac{\lambda_0-\Omega}{\omega_1}\right)^2 e^{i\Phi'}\right) e^{-i\xi^\sim} e^{-i(\xi^\angle - \lambda_0)\frac{\Phi'-\phi}{2\omega_{\text{radio}}}} \right) d\Phi'$$

$$= \varepsilon\left(\sin\phi - \sin\Phi\right) +$$

$$\frac{1}{4}\int_\phi^\Phi \left(\left(e^{-i\Phi'} - \left(\frac{\lambda_0+\Omega}{\omega_1}\right)^2 e^{i\Phi'}\right) \varepsilon e^{i\xi^\sim} e^{i\Lambda\Phi'} e^{-i\Lambda\phi} + \left(e^{-i\Phi'} - \left(\frac{\lambda_0-\Omega}{\omega_1}\right)^2 e^{i\Phi'}\right) \varepsilon e^{-i\xi^\sim} e^{-i\Lambda\Phi'} e^{i\Lambda\phi} \right) d\Phi', \tag{5.355}$$

where

$$\Lambda = \frac{\xi^\angle - \lambda_0}{2\omega_{\text{radio}}}. \tag{5.356}$$

We have already evaluated (from the initial condition) $\xi_0 = \xi(t=0) = 0$. Therefore, we can skip the constant ξ_0 part in the expansion. To determine the higher terms, we replace the time-dependent exponential functions $e^{\pm i\xi^\sim}$ by a power series[12]

$$e^{\pm i(\varepsilon\xi_1^{\widetilde{}} + \varepsilon^2\xi_2^{\widetilde{}} + \dots)} = 1 \pm i\left(\varepsilon\xi_1^{\widetilde{}} + \varepsilon^2\xi_2^{\widetilde{}} + \dots\right) - \left(\frac{1}{2}\varepsilon^2\left(\xi_1^{\widetilde{}}\right)^2 + \dots\right) \tag{5.357}$$

and consequently

$$\varepsilon e^{\pm i\xi^\sim + \dots} = \varepsilon \pm i\varepsilon^2\xi_1^{\widetilde{}} + \dots. \tag{5.358}$$

Equating terms linear in ε, we determine ξ_1

$$\xi_1 = \xi_1^{\widetilde{}} + \xi_1^\angle t = \xi_1^{\widetilde{}} + \xi_1^\angle \frac{\Phi-\phi}{2\omega_{\text{radio}}} =$$

$$\sin\phi - \sin\Phi + \frac{1}{4}\left(\int_\phi^\Phi \left(e^{-i\Phi'} - \left(\frac{\lambda_0+\Omega}{\omega_1}\right)^2 e^{i\Phi'}\right) e^{i\Lambda\Phi'} e^{-i\Lambda\phi} + \left(e^{-i\Phi'} - \left(\frac{\lambda_0-\Omega}{\omega_1}\right)^2 e^{i\Phi'}\right) e^{-i\Lambda\Phi'} e^{i\Lambda\phi} \right) d\Phi' =$$

$$\sin\phi - \sin\Phi + \frac{1}{4}\left(\int_\phi^\Phi e^{-i(1-\Lambda)\Phi'} e^{-i\Lambda\phi} + e^{-i(1+\Lambda)\Phi'} e^{i\Lambda\phi} - \left(\frac{\lambda_0+\Omega}{\omega_1}\right)^2 e^{i(1+\Lambda)\Phi'} e^{-i\Lambda\phi} - \left(\frac{\lambda_0-\Omega}{\omega_1}\right)^2 e^{i(1-\Lambda)\Phi'} e^{i\Lambda\phi} \right) d\Phi' = \sin\phi - \sin\Phi +$$

---

[12]Note that $e^x = 1 + \frac{x}{1!} + \frac{x^2}{2!} + \frac{x^3}{3!} + \dots$

$$\frac{\mathrm{i}}{4}\left(\overbrace{\frac{\mathrm{e}^{-\mathrm{i}(1-\Lambda)\Phi}\mathrm{e}^{-\mathrm{i}\Lambda\phi}}{1-\Lambda}}^{\mathcal{F}_-^*}-\mathrm{e}^{-\mathrm{i}\phi}+\overbrace{\frac{\mathrm{e}^{-\mathrm{i}(1+\Lambda)\Phi}\mathrm{e}^{\mathrm{i}\Lambda\phi}}{1+\Lambda}}^{\mathcal{F}_+^*}-\mathrm{e}^{-\mathrm{i}\phi}+\left(\frac{\lambda_0+\Omega}{\omega_1}\right)^2\overbrace{\frac{\mathrm{e}^{\mathrm{i}(1+\Lambda)\Phi}\mathrm{e}^{-\mathrm{i}\Lambda\phi}}{1+\Lambda}}^{\mathcal{F}_+}-\mathrm{e}^{\mathrm{i}\phi}+\left(\frac{\lambda_0-\Omega}{\omega_1}\right)^2\overbrace{\frac{\mathrm{e}^{\mathrm{i}(1-\Lambda)\Phi}\mathrm{e}^{\mathrm{i}\Lambda\phi}}{1-\Lambda}}^{\mathcal{F}_-}-\mathrm{e}^{\mathrm{i}\phi}\right)=$$

$$\sin\phi-\sin(2\omega_{\mathrm{radio}}t+\phi)+\frac{\mathrm{i}\mathrm{e}^{-\mathrm{i}\phi}}{4}\left(\frac{\mathrm{e}^{-2\mathrm{i}(1-\Lambda)\omega_{\mathrm{radio}}t}-1}{1-\Lambda}+\frac{\mathrm{e}^{-2\mathrm{i}(1+\Lambda)\omega_{\mathrm{radio}}t}-1}{1+\Lambda}\right)+$$

$$\frac{\mathrm{i}\mathrm{e}^{\mathrm{i}\phi}}{4}\left(\left(\frac{\lambda_0+\Omega}{\omega_1}\right)^2\frac{\mathrm{e}^{2\mathrm{i}(1+\Lambda)\omega_{\mathrm{radio}}t}-1}{1+\Lambda}+\left(\frac{\lambda_0-\Omega}{\omega_1}\right)^2\frac{\mathrm{e}^{2\mathrm{i}(1-\Lambda)\omega_{\mathrm{radio}}t}-1}{1-\Lambda}\right). \tag{5.359}$$

The integration produces only oscillatory terms or constant terms (those depending on ϕ only), implying that $\xi_1^{\angle}=0$. Note that all terms depend on ϕ values of these terms are arbitrary because the value of ϕ depends on the choice of $t=0$. If a series of independent experiments is run, the ϕ-dependent terms average to zero. Therefore, such terms must be evaluated in order to proceed to the next order of approximation, but they themselves do not contribute to the results of repeated experiments. Another feature of the solution is that the result of the integration can be written in terms of two time-dependent functions, denoted $\mathcal{F}_+$, $\mathcal{F}_-$ and written in blue, and their complex conjugates, denoted $\mathcal{F}_+^*$, $\mathcal{F}_-^*$ and written in red. We use this fact when we evaluate $\xi_2^{\angle}$ in the next step.

Equating terms quadratic in ε, we determine ξ_2

$$\xi_2=\xi_2^{\widetilde{}}+\xi_2^{\angle}t=\xi_2^{\widetilde{}}+\xi_2^{\angle}\frac{\Phi-\phi}{2\omega_{\mathrm{radio}}}=$$

$$\frac{\mathrm{i}}{4}\int_\phi^\Phi\xi_1^{\widetilde{}}\left(\left(\mathrm{e}^{-\mathrm{i}\Phi'}-\left(\frac{\lambda_0+\Omega}{\omega_1}\right)^2\mathrm{e}^{\mathrm{i}\Phi'}\right)\mathrm{e}^{\mathrm{i}\Lambda\Phi'}\mathrm{e}^{-\mathrm{i}\Lambda\phi}-\left(\mathrm{e}^{-\mathrm{i}\Phi'}-\left(\frac{\lambda_0-\Omega}{\omega_1}\right)^2\mathrm{e}^{\mathrm{i}\Phi'}\right)\mathrm{e}^{-\mathrm{i}\Lambda\Phi'}\mathrm{e}^{\mathrm{i}\Lambda\phi}\right)\mathrm{d}\Phi'=$$

$$\frac{\mathrm{i}}{4}\int_\phi^\Phi\xi_1^{\widetilde{}}\left(\mathrm{e}^{-\mathrm{i}(1-\Lambda)\Phi'}\mathrm{e}^{-\mathrm{i}\Lambda\phi}-\mathrm{e}^{-\mathrm{i}(1+\Lambda)\Phi'}\mathrm{e}^{\mathrm{i}\Lambda\phi}-\left(\frac{\lambda_0+\Omega}{\omega_1}\right)^2\mathrm{e}^{\mathrm{i}(1+\Lambda)\Phi'}\mathrm{e}^{-\mathrm{i}\Lambda\phi}+\left(\frac{\lambda_0-\Omega}{\omega_1}\right)^2\mathrm{e}^{\mathrm{i}(1-\Lambda)\Phi'}\mathrm{e}^{\mathrm{i}\Lambda\phi}\right)\mathrm{d}\Phi' \tag{5.360}$$

The function to be integrated is a product of the following expressions:

$$\xi_1^{\widetilde{}}=\sin\phi-\sin\Phi+\frac{\mathrm{i}}{4}\left(\frac{\mathcal{F}_-^*-\mathrm{e}^{-\mathrm{i}\phi}}{1-\Lambda}+\frac{\mathcal{F}_+^*-\mathrm{e}^{-\mathrm{i}\phi}}{1+\Lambda}+\left(\frac{\lambda_0+\Omega}{\omega_1}\right)^2\frac{\mathcal{F}_+-\mathrm{e}^{\mathrm{i}\phi}}{1+\Lambda}+\left(\frac{\lambda_0-\Omega}{\omega_1}\right)^2\frac{\mathcal{F}_--\mathrm{e}^{\mathrm{i}\phi}}{1-\Lambda}\right)=$$

$$\frac{\mathrm{i}}{4}\left(2\mathrm{e}^{-\mathrm{i}\phi}-2\mathrm{e}^{\mathrm{i}\phi}-2\mathrm{e}^{-\mathrm{i}\Phi}+2\mathrm{e}^{\mathrm{i}\Phi}+\frac{\mathcal{F}_-^*-\mathrm{e}^{-\mathrm{i}\phi}}{1-\Lambda}+\frac{\mathcal{F}_+^*-\mathrm{e}^{-\mathrm{i}\phi}}{1+\Lambda}+\left(\frac{\lambda_0+\Omega}{\omega_1}\right)^2\frac{\mathcal{F}_+-\mathrm{e}^{\mathrm{i}\phi}}{1+\Lambda}+\left(\frac{\lambda_0-\Omega}{\omega_1}\right)^2\frac{\mathcal{F}_--\mathrm{e}^{\mathrm{i}\phi}}{1-\Lambda}\right)$$

and

$$\frac{\mathrm{i}}{4}\left(\mathcal{F}_-^*-\mathcal{F}_+^*-\left(\frac{\lambda_0+\Omega}{\omega_1}\right)^2\mathcal{F}_++\left(\frac{\lambda_0-\Omega}{\omega_1}\right)^2\mathcal{F}_-\right).$$

This product consists of three types of terms:

1. *Constant terms.* Their integration produces a linear function, i.e., the $\xi_2^{\angle}t$ component of ξ_2.

2. *Terms that oscillate in time but do not depend on the phase ϕ.* Their integration yields oscillatory and constant terms, i.e., contributions to $\xi_2^{\widetilde{}}$.

3. *Oscillatory ϕ-dependent terms.* Their integration also yields oscillatory and constant terms (contributions to $\xi_2^{\widetilde{}}$). However, values of these terms are arbitrary and do not contribute to a description of repeated experiments because they depend on the choice of $t=0$ as mentioned when we discussed the obtained ξ_1 factor. As we stop our approximation at the second order of the power series expansion, we do not need the ϕ-dependent terms to calculate corrections of higher orders and neglect them in our analysis.

We use the following relations to identify the constant and oscillatory ϕ-independent terms.

$$\mathcal{F}_\pm\mathcal{F}_\pm^*\ =\ 1 \tag{5.361}$$

$$\mathcal{F}_\pm\mathrm{e}^{-\mathrm{i}\phi}=\mathrm{e}^{+\mathrm{i}\Phi}\mathrm{e}^{\pm\mathrm{i}\Lambda\Phi}\mathrm{e}^{\mp\mathrm{i}\Lambda\phi}\cdot\mathrm{e}^{-\mathrm{i}\phi}=\mathrm{e}^{+2\mathrm{i}(1\pm\Lambda)\omega_{\mathrm{radio}}t}\qquad\mathcal{F}_\pm^*\mathrm{e}^{+\mathrm{i}\phi}=\mathrm{e}^{-\mathrm{i}\Phi}\mathrm{e}^{\mp\mathrm{i}\Lambda\Phi}\mathrm{e}^{\pm\mathrm{i}\Lambda\phi}\cdot\mathrm{e}^{+\mathrm{i}\phi}=\mathrm{e}^{-2\mathrm{i}(1\pm\Lambda)\omega_{\mathrm{radio}}t} \tag{5.362}$$

$$\mathcal{F}_\pm\mathrm{e}^{-\mathrm{i}\Phi}=\mathrm{e}^{+\mathrm{i}\Phi}\mathrm{e}^{\pm\mathrm{i}\Lambda\Phi}\mathrm{e}^{\mp\mathrm{i}\Lambda\phi}\cdot\mathrm{e}^{-\mathrm{i}\Phi}=\mathrm{e}^{\pm2\mathrm{i}\Lambda\omega_{\mathrm{radio}}t}\qquad\mathcal{F}_\pm^*\mathrm{e}^{+\mathrm{i}\Phi}=\mathrm{e}^{-\mathrm{i}\Phi}\mathrm{e}^{\mp\mathrm{i}\Lambda\Phi}\mathrm{e}^{\pm\mathrm{i}\Lambda\phi}\cdot\mathrm{e}^{+\mathrm{i}\Phi}=\mathrm{e}^{\mp2\mathrm{i}\Lambda\omega_{\mathrm{radio}}t}. \tag{5.363}$$

Eqs. 5.362 and 5.363 tell us that we have to inspect all terms of the product obtained by multiplying a red function by a blue function, or vice versa.

$$\int_\phi^\Phi \frac{\mathcal{F}_-^* - \mathcal{F}_+^*}{16}\left(2\mathrm{e}^{\mathrm{i}\phi} - 2\mathrm{e}^{\mathrm{i}\Phi'} - \left(\frac{\lambda_0 + \Omega}{\omega_1}\right)^2 \frac{\mathcal{F}_+ - \mathrm{e}^{\mathrm{i}\phi}}{1 + \Lambda} - \left(\frac{\lambda_0 - \Omega}{\omega_1}\right)^2 \frac{\mathcal{F}_- - \mathrm{e}^{\mathrm{i}\phi}}{1 - \Lambda}\right)\mathrm{d}\Phi'$$

$$+ \frac{1}{16}\int_\phi^\Phi \left(\left(\frac{\lambda_0 + \Omega}{\omega_1}\right)^2 \mathcal{F}_+ - \left(\frac{\lambda_0 - \Omega}{\omega_1}\right)^2 \mathcal{F}_-\right)\left(2\mathrm{e}^{-\mathrm{i}\phi} - 2\mathrm{e}^{-\mathrm{i}\Phi'} + \frac{\mathcal{F}_-^* - \mathrm{e}^{-\mathrm{i}\phi}}{1 - \Lambda} + \frac{\mathcal{F}_+^* - \mathrm{e}^{-\mathrm{i}\phi}}{1 + \Lambda}\right)\mathrm{d}\Phi' \tag{5.364}$$

$$= \frac{\omega_\mathrm{radio}}{4}\int_0^t \left(\left(\frac{\lambda_0 + \Omega}{\omega_1}\right)^2 \frac{1}{1 + \Lambda} - \left(\frac{\lambda_0 - \Omega}{\omega_1}\right)^2 \frac{1}{1 - \Lambda}\right)\mathrm{d}t'$$

$$+ \frac{\omega_\mathrm{radio}}{8}\int_0^t \mathrm{e}^{+2\mathrm{i}\Lambda\omega_\mathrm{radio}t'}\left(2\left(\mathrm{e}^{-2\mathrm{i}\omega_\mathrm{radio}t'} - 1\right) + \left(\left(\frac{\lambda_0 + \Omega}{\omega_1}\right)^2 \frac{1}{1 + \Lambda} + \left(\frac{\lambda_0 - \Omega}{\omega_1}\right)^2 \frac{1}{1 - \Lambda}\right)\mathrm{e}^{-2\mathrm{i}\omega_\mathrm{radio}t'} - \left(\frac{\lambda_0 + \Omega}{\omega_1}\right)^2 \frac{1}{1 + \Lambda}\right)\mathrm{d}t'$$

$$- \frac{\omega_\mathrm{radio}}{8}\int_0^t \mathrm{e}^{-2\mathrm{i}\Lambda\omega_\mathrm{radio}t'}\left(2\left(\mathrm{e}^{-2\mathrm{i}\omega_\mathrm{radio}t'} - 1\right) + \left(\left(\frac{\lambda_0 + \Omega}{\omega_1}\right)^2 \frac{1}{1 + \Lambda} + \left(\frac{\lambda_0 - \Omega}{\omega_1}\right)^2 \frac{1}{1 - \Lambda}\right)\mathrm{e}^{-2\mathrm{i}\omega_\mathrm{radio}t'} - \left(\frac{\lambda_0 - \Omega}{\omega_1}\right)^2 \frac{1}{1 - \Lambda}\right)\mathrm{d}t'$$

$$+ \frac{\omega_\mathrm{radio}}{8}\int_0^t \left(\left(\frac{\lambda_0 + \Omega}{\omega_1}\right)^2 \frac{1}{1 + \Lambda} - \left(\frac{\lambda_0 - \Omega}{\omega_1}\right)^2 \frac{1}{1 - \Lambda}\right)\mathrm{d}t'$$

$$+ \frac{\omega_\mathrm{radio}}{8}\int_0^t \mathrm{e}^{+2\mathrm{i}\Lambda\omega_\mathrm{radio}t'}\left(2\left(\frac{\lambda_0 + \Omega}{\omega_1}\right)^2\left(\mathrm{e}^{+2\mathrm{i}\omega_\mathrm{radio}t'} - 1\right) - \left(\frac{\lambda_0 + \Omega}{\omega_1}\right)^2\left(\frac{1}{1 + \Lambda} + \frac{1}{1 - \Lambda}\right)\mathrm{e}^{+2\mathrm{i}\omega_\mathrm{radio}t'} + \left(\frac{\lambda_0 + \Omega}{\omega_1}\right)^2 \frac{1}{1 - \Lambda}\right)\mathrm{d}t'$$

$$- \frac{\omega_\mathrm{radio}}{8}\int_0^t \mathrm{e}^{-2\mathrm{i}\Lambda\omega_\mathrm{radio}t'}\left(2\left(\frac{\lambda_0 - \Omega}{\omega_1}\right)^2\left(\mathrm{e}^{-2\mathrm{i}\omega_\mathrm{radio}t'} - 1\right) - \left(\frac{\lambda_0 - \Omega}{\omega_1}\right)^2\left(\frac{1}{1 + \Lambda} + \frac{1}{1 - \Lambda}\right)\mathrm{e}^{+2\mathrm{i}\omega_\mathrm{radio}t'} + \left(\frac{\lambda_0 - \Omega}{\omega_1}\right)^2 \frac{1}{1 + \Lambda}\right)\mathrm{d}t'. \tag{5.365}$$

We combine terms with the same s in the exponents $\mathrm{e}^{2s\mathrm{i}\Lambda\omega_\mathrm{radio}t'}$

$$\xi_2 = \frac{\omega_\mathrm{radio}}{4}\int_0^t \left(\left(\frac{\lambda_0 + \Omega}{\omega_1}\right)^2 \frac{1}{1 + \Lambda} - \left(\frac{\lambda_0 - \Omega}{\omega_1}\right)^2 \frac{1}{1 - \Lambda}\right)\mathrm{d}t'$$

$$- \frac{\omega_\mathrm{radio}}{8}\int_0^t \mathrm{e}^{+2\mathrm{i}\Lambda\omega_\mathrm{radio}t'}\left\{\left(\frac{\lambda_0 + \Omega}{\omega_1}\right)^2\left(\frac{1}{1 - \Lambda} - \frac{1}{1 + \Lambda}\right) + 2\left(\left(\frac{\lambda_0 + \Omega}{\omega_1}\right)^2 + 1\right)\right.$$

$$\left. + \left(\frac{\lambda_0 + \Omega}{\omega_1}\right)^2\left(\frac{1}{1 + \Lambda} + \frac{1}{1 - \Lambda} - 2\right)\mathrm{e}^{+2\mathrm{i}\omega_\mathrm{radio}t'} - \left(\left(\frac{\lambda_0 + \Omega}{\omega_1}\right)^2 \frac{1}{1 + \Lambda} + \left(\frac{\lambda_0 - \Omega}{\omega_1}\right)^2 \frac{1}{1 - \Lambda} + 2\right)\mathrm{e}^{-2\mathrm{i}\omega_\mathrm{radio}t'}\right\}\mathrm{d}t'$$

$$+ \frac{\omega_\mathrm{radio}}{8}\int_0^t \mathrm{e}^{+2\mathrm{i}\Lambda\omega_\mathrm{radio}t'}\left\{\left(\frac{\lambda_0 - \Omega}{\omega_1}\right)^2\left(\frac{1}{1 + \Lambda} - \frac{1}{1 - \Lambda}\right) + 2\left(\left(\frac{\lambda_0 + \Omega}{\omega_1}\right)^2 + 1\right)\right.$$

$$\left. + \left(\frac{\lambda_0 - \Omega}{\omega_1}\right)^2\left(\frac{1}{1 + \Lambda} + \frac{1}{1 - \Lambda} - 2\right)\mathrm{e}^{+2\mathrm{i}\omega_\mathrm{radio}t'} - \left(\left(\frac{\lambda_0 + \Omega}{\omega_1}\right)^2 \frac{1}{1 + \Lambda} + \left(\frac{\lambda_0 - \Omega}{\omega_1}\right)^2 \frac{1}{1 - \Lambda} + 2\right)\mathrm{e}^{-2\mathrm{i}\omega_\mathrm{radio}t'}\right\}\mathrm{d}t'. \tag{5.366}$$

In order to simplify Eq. 5.366, we examine the value of

$$\Lambda = \frac{\xi^{\angle} - \lambda_0}{2\omega_\mathrm{radio}} = \frac{\varepsilon\xi_1^{\angle} + \varepsilon^2\xi_2^{\angle} + \cdots - \lambda_0}{2\omega_\mathrm{radio}}. \tag{5.367}$$

We have determined that $\xi_1^{\angle} = 0$. Therefore, Λ at the examined level of approximation (including corrections up to quadratic in ε),

$$\Lambda = \frac{\varepsilon^2\xi_2^{\angle} - \lambda_0}{2\omega_\mathrm{radio}} = \frac{\omega_1^2\omega_2^2\xi_2^{\angle}}{2\lambda_0^2\omega_\mathrm{radio}^3} - \frac{\lambda_0}{2\omega_\mathrm{radio}} = \frac{\omega_1^2}{\Omega^2 + \omega_1^2}\frac{\omega_2^2\xi_2^{\angle}}{2\omega_\mathrm{radio}^3} - \frac{\omega_1}{2\omega_\mathrm{radio}}\sqrt{1 + \frac{\Omega^2}{\omega_1^2}}. \tag{5.368}$$

Our approximation is applicable only for ω_{radio} much higher than ω_2 or ω_1 (recall that $\omega_2 = \omega_1$ for the most interesting example of a field oscillating in one direction). The ratios $\omega_1/\omega_{\text{radio}}$ and $\omega_2/\omega_{\text{radio}}$ in Eq. 5.368 indicate that $\Lambda \ll 1$. For $\Lambda \ll 1$, $1 + \Lambda \approx 1 - \Lambda \approx 1$. Consequently, the red terms Eq. 5.366 are negligible, and the green expression simplifies to $4(\Omega^2 + \omega_1^2)/\omega_1^2$, which allows us to further simplify the integral by in the next step

$$\xi_2 = \frac{\omega_{\text{radio}}}{4} \int_0^t \left(\left(\frac{\lambda_0 + \Omega}{\omega_1}\right)^2 - \left(\frac{\lambda_0 - \Omega}{\omega_1}\right)^2 \right) \mathrm{d}t'$$

$$+ \frac{\omega_{\text{radio}}}{4} \int_0^t \left\{ \mathrm{e}^{-2\mathrm{i}\Lambda\omega_{\text{radio}}t'} \left(\left(\frac{\lambda_0 - \Omega}{\omega_1}\right)^2 + 1 \right) - \mathrm{e}^{+2\mathrm{i}\Lambda\omega_{\text{radio}}t'} \left(\left(\frac{\lambda_0 + \Omega}{\omega_1}\right)^2 + 1 \right) \right\} \mathrm{d}t'$$

$$+ \frac{\omega_{\text{radio}}}{2} \int_0^t \frac{\Omega^2 + \omega_1^2}{\omega_1^2} \left(\mathrm{e}^{-2\mathrm{i}(1-\Lambda)\omega_{\text{radio}}t'} - \mathrm{e}^{-2\mathrm{i}(1+\Lambda)\omega_{\text{radio}}t'} \right) \mathrm{d}t' \tag{5.369}$$

because the green exponential factors cancel each other for $\Lambda \ll 1$. Neglecting the last line, the integration yields

$$\xi_2 = \xi_2^{\angle} t + \xi_2^{\sim} = \frac{\omega_{\text{radio}}}{4} \left(\left(\frac{\lambda_0 + \Omega}{\omega_1}\right)^2 - \left(\frac{\lambda_0 - \Omega}{\omega_1}\right)^2 \right) [t']_0^t$$

$$+ \frac{\omega_{\text{radio}}}{4} \left(\left(\frac{\lambda_0 - \Omega}{\omega_1}\right)^2 + 1 \right) \frac{\left[\mathrm{e}^{-2\mathrm{i}\Lambda\omega_{\text{radio}}t'}\right]_0^t}{-2\mathrm{i}\Lambda\omega_{\text{radio}}} - \frac{\omega_{\text{radio}}}{4} \left(\left(\frac{\lambda_0 + \Omega}{\omega_1}\right)^2 + 1 \right) \frac{\left[\mathrm{e}^{+2\mathrm{i}\Lambda\omega_{\text{radio}}t'}\right]_0^t}{2\mathrm{i}\Lambda\omega_{\text{radio}}}$$

$$= \frac{\omega_{\text{radio}}}{4} \left(\left(\frac{\lambda_0 + \Omega}{\omega_1}\right)^2 - \left(\frac{\lambda_0 - \Omega}{\omega_1}\right)^2 \right) t + \frac{\mathrm{i}}{8\Lambda} \left\{ \left(\left(\frac{\lambda_0 + \Omega}{\omega_1}\right)^2 + 1 \right) \left(\mathrm{e}^{+2\mathrm{i}\Lambda\omega_{\text{radio}}t} - 1 \right) + \left(\left(\frac{\lambda_0 - \Omega}{\omega_1}\right)^2 + 1 \right) \left(\mathrm{e}^{-2\mathrm{i}\Lambda\omega_{\text{radio}}t} - 1 \right) \right\} \tag{5.370}$$

$$= \omega_{\text{radio}} \frac{\lambda_0 \Omega}{\omega_1^2} t +$$

$$\frac{\mathrm{i}}{8\Lambda} \left(\left(\frac{\lambda_0 + \Omega}{\omega_1}\right)^2 + 1 \right) (\cos(2\Lambda\omega_{\text{radio}}t) + \mathrm{i}\sin(2\Lambda\omega_{\text{radio}}t) - 1) + \frac{\mathrm{i}}{8\Lambda} \left(\left(\frac{\lambda_0 - \Omega}{\omega_1}\right)^2 + 1 \right) (\cos(2\Lambda\omega_{\text{radio}}t) - \mathrm{i}\sin(2\Lambda\omega_{\text{radio}}t) - 1) \tag{5.371}$$

$$= \omega_{\text{radio}} \frac{\lambda_0 \Omega}{\omega_1^2} t + \frac{\mathrm{i}}{8\Lambda} \left(\left(\frac{\lambda_0 + \Omega}{\omega_1}\right)^2 + \left(\frac{\lambda_0 - \Omega}{\omega_1}\right)^2 + 2 \right) (\cos(2\Lambda\omega_{\text{radio}}t) - 1) - \frac{1}{8\Lambda} \left(\left(\frac{\lambda_0 + \Omega}{\omega_1}\right)^2 - \left(\frac{\lambda_0 - \Omega}{\omega_1}\right)^2 \right) \sin(2\Lambda\omega_{\text{radio}}t) \tag{5.372}$$

$$= \omega_{\text{radio}} \frac{\lambda_0 \Omega}{\omega_1^2} t + \frac{\mathrm{i}}{8\Lambda} \left(\frac{\lambda_0 + \Omega}{\omega_1} + \frac{\lambda_0 - \Omega}{\omega_1} \right)^2 (\cos(2\Lambda\omega_{\text{radio}}t) - 1) - \frac{1}{8\Lambda} \frac{4\lambda_0 \Omega}{\omega_1^2} \sin(2\Lambda\omega_{\text{radio}}t) \tag{5.373}$$

$$= \omega_{\text{radio}} \frac{\lambda_0 \Omega}{\omega_1^2} t + \frac{\mathrm{i}}{2\Lambda} \frac{\lambda_0^2}{\omega_1^2} (\cos(2\Lambda\omega_{\text{radio}}t) - 1) - \frac{1}{2\Lambda} \frac{\lambda_0 \Omega}{\omega_1^2} \sin(2\Lambda\omega_{\text{radio}}t). \tag{5.374}$$

We easily identify $\xi_2^{\angle}$ and $\xi_2^{\sim}$ as the red and blue expressions. We are now ready to express the factor $\Xi = \mathrm{e}^{\mathrm{i}\xi}$ as

$$\mathrm{e}^{\mathrm{i}\xi} = \mathrm{e}^{\mathrm{i}\varepsilon^2 \xi_2} = \mathrm{e}^{\mathrm{i}\frac{\omega_2^2}{2\omega_{\text{radio}}}\frac{\Omega}{\lambda_0}t - \overbrace{\frac{1}{2\Lambda}\left(\frac{\omega_2}{2\omega_{\text{radio}}}\right)^2 (\cos(2\Lambda\omega_{\text{radio}}t) - 1)}^{2f} - \mathrm{i}\overbrace{\frac{1}{2\Lambda}\left(\frac{\omega_2}{2\omega_{\text{radio}}}\right)^2 \frac{\Omega}{\lambda_0} \sin(2\Lambda\omega_{\text{radio}}t)}^{2g}} = \mathrm{e}^{\mathrm{i}\frac{\omega_2^2}{2\omega_{\text{radio}}}\frac{\Omega}{\lambda_0}t - 2f - 2\mathrm{i}g} \tag{5.375}$$

and

$$\mathrm{e}^{\mathrm{i}\frac{\xi - \lambda_0 t}{2}} = \mathrm{e}^{\mathrm{i}\left(\frac{\omega_2^2}{4\omega_{\text{radio}}}\frac{\Omega}{\lambda_0} - \frac{\lambda_0}{2}\right)t - \overbrace{\frac{1}{4\Lambda}\left(\frac{\omega_2}{2\omega_{\text{radio}}}\right)^2 (\cos(2\Lambda\omega_{\text{radio}}t) - 1)}^{f} - \mathrm{i}\overbrace{\frac{1}{4\Lambda}\left(\frac{\omega_2}{2\omega_{\text{radio}}}\right)^2 \frac{\Omega}{\lambda_0} \sin(2\Lambda\omega_{\text{radio}}t)}^{g}} = \mathrm{e}^{\mathrm{i}\Lambda\omega_{\text{radio}}t - f - \mathrm{i}g}, \tag{5.376}$$

where we simplified notation by introducing real functions f and g. Using the notation, we can express $\overline{P}_\beta = 1 - \overline{P}_\alpha$ from the last term in Eq. 5.324 (the horizontal bars indicate that $\overline{P}_\beta$ and $\overline{P}_\alpha$ are averages for a large number of measurements with random phases ϕ)

$$uu^* = \frac{\frac{\lambda_0 + \Omega}{\omega_1}\mathrm{e}^{\mathrm{i}\Lambda\omega_{\text{radio}}t}\mathrm{e}^{-f-\mathrm{i}g} + \frac{\lambda_0 - \Omega}{\omega_1}\mathrm{e}^{-\mathrm{i}\Lambda\omega_{\text{radio}}t}\mathrm{e}^{f+\mathrm{i}g}}{\mathrm{e}^{\mathrm{i}\Lambda\omega_{\text{radio}}t}\mathrm{e}^{-f-\mathrm{i}g} - \mathrm{e}^{-\mathrm{i}\Lambda\omega_{\text{radio}}t}\mathrm{e}^{f+\mathrm{i}g}} \cdot \frac{\frac{\lambda_0 + \Omega}{\omega_1}\mathrm{e}^{-\mathrm{i}\Lambda\omega_{\text{radio}}t}\mathrm{e}^{-f+\mathrm{i}g} + \frac{\lambda_0 - \Omega}{\omega_1}\mathrm{e}^{\mathrm{i}\Lambda\omega_{\text{radio}}t}\mathrm{e}^{f-\mathrm{i}g}}{\mathrm{e}^{-\mathrm{i}\Lambda\omega_{\text{radio}}t}\mathrm{e}^{-f+\mathrm{i}g} - \mathrm{e}^{\mathrm{i}\Lambda\omega_{\text{radio}}t}\mathrm{e}^{f-\mathrm{i}g}}$$

$$= \frac{\left(\frac{\lambda_0+\Omega}{\omega_1}\right)^2 e^{-2f} + \left(\frac{\lambda_0-\Omega}{\omega_1}\right)^2 e^{2f} + \frac{\lambda_0^2-\Omega^2}{\omega_1^2}\left(e^{2i\Lambda\omega_{\text{radio}}t}e^{-2ig} + e^{-2i\Lambda\omega_{\text{radio}}t}e^{2ig}\right)}{e^{-2f} + e^{2f} - e^{2i\Lambda\omega_{\text{radio}}t}e^{-2ig} - e^{-2i\Lambda\omega_{\text{radio}}t}e^{2ig}}$$

$$= \frac{\frac{\lambda_0^2+\Omega^2}{\omega_1^2}\left(e^{-2f}+e^{2f}\right) + \frac{2\lambda_0\Omega}{\omega_1^2}\left(e^{-2f}-e^{2f}\right) + e^{2i\Lambda\omega_{\text{radio}}t}e^{-2ig} + e^{-2i\Lambda\omega_{\text{radio}}t}e^{2ig}}{e^{-2f}+e^{2f}-\left(e^{2i\Lambda\omega_{\text{radio}}t}e^{-2ig}+e^{-2i\Lambda\omega_{\text{radio}}t}e^{2ig}\right)} \tag{5.377}$$

$$1-uu^* = \frac{\left(\frac{\lambda_0^2+\Omega^2}{\omega_1^2}+1\right)\left(e^{-2f}+e^{2f}\right)+\frac{2\lambda_0\Omega}{\omega_1^2}\left(e^{-2f}-e^{2f}\right)}{e^{-2f}+e^{2f}-\left(e^{2i\Lambda\omega_{\text{radio}}t}e^{-2ig}+e^{-2i\Lambda\omega_{\text{radio}}t}e^{2ig}\right)} = \frac{2\frac{\lambda_0^2}{\omega_1^2}\left(e^{-2f}+e^{2f}\right)+\frac{2\lambda_0\Omega}{\omega_1^2}\left(e^{-2f}-e^{2f}\right)}{e^{-2f}+e^{2f}-\left(e^{2i\Lambda\omega_{\text{radio}}t}e^{-2ig}+e^{-2i\Lambda\omega_{\text{radio}}t}e^{2ig}\right)}. \tag{5.378}$$

To proceed, we look at f and g more closely. Knowing the explicit expression of $\xi_2^{\angle}$ (Eq. 5.374), we can calculate Λ from Eq. 5.368

$$\Lambda = \frac{\varepsilon^2\xi_2^{\angle}}{2\omega_{\text{radio}}} - \frac{\lambda_0}{2\omega_{\text{radio}}} = \frac{1}{2}\left(\frac{\omega_2}{2\omega_{\text{radio}}}\right)^2\frac{\Omega}{\lambda_0} - \frac{\lambda_0}{2\omega_{\text{radio}}} = -\frac{\lambda_0}{2\omega_{\text{radio}}}\left(1 - \frac{\omega_2^2\Omega}{4\omega_{\text{radio}}\lambda_0^2}\right). \tag{5.379}$$

Inserting the expressed Λ to Eq. 5.376,

$$\frac{1}{4\Lambda}\left(\frac{\omega_2}{2\omega_{\text{radio}}}\right)^2 = \frac{\left(\frac{\omega_2}{2\omega_{\text{radio}}}\right)^2}{2\left(\frac{\omega_2}{2\omega_{\text{radio}}}\right)^2\frac{\Omega}{\lambda_0} - 2\frac{\lambda_0}{\omega_{\text{radio}}}} = \frac{1}{2}\frac{1}{\frac{\Omega}{\lambda_0} - \left(\frac{2\omega_{\text{radio}}}{\omega_2}\right)^2\frac{\lambda_0}{\omega_{\text{radio}}}} = \frac{1}{2}\frac{1}{\frac{\Omega}{\sqrt{\Omega^2+\omega_1^2}} - 4\frac{\omega_{\text{radio}}}{\omega_2}\frac{\omega_1}{\omega_2}\frac{\sqrt{\Omega^2+\omega_1^2}}{\omega_1}}. \tag{5.380}$$

Since we assumed that $\omega_2 \ll \omega_{\text{radio}}$, this expression and consequently f and g are much smaller than unity[13]

$$\frac{1}{4\Lambda}\left(\frac{\omega_2}{2\omega_{\text{radio}}}\right)^2 = \frac{1}{2}\frac{1}{\frac{\Omega}{\sqrt{\Omega^2+\omega_1^2}} - 4\frac{\omega_{\text{radio}}}{\omega_2}\frac{\omega_1}{\omega_2}\frac{\sqrt{\Omega^2+\omega_1^2}}{\omega_1}} \approx -\frac{1}{8}\cdot\frac{\omega_2}{\omega_{\text{radio}}}\cdot\frac{\omega_2}{\omega_1}\cdot\frac{\omega_1}{\sqrt{\Omega^2+\omega_1^2}} \ll 1. \tag{5.381}$$

We can therefore express e^f and e^{ig} as power series and safely ignore higher than linear terms

$$e^f \approx 1+f, \qquad e^{ig} \approx 1+ig \tag{5.382}$$

This simplifies Eq. 5.378 to

$$1-uu^* = \frac{4\frac{\lambda_0^2}{\omega_1^2} - 8\frac{\lambda_0\Omega}{\omega_1^2}f}{2-\left(e^{2i\Lambda\omega_{\text{radio}}t}+e^{-2i\Lambda\omega_{\text{radio}}t}\right)+2ig\left(e^{2i\Lambda\omega_{\text{radio}}t}-e^{-2i\Lambda\omega_{\text{radio}}t}\right)} = \frac{\lambda_0^2}{\omega_1^2}\cdot\frac{2-4\frac{\Omega}{\lambda_0}f}{1-\cos(2\Lambda\omega_{\text{radio}}t)-2g\sin(2\Lambda\omega_{\text{radio}}t)}. \tag{5.383}$$

and

$$\overline{P}_\beta = \frac{1}{1-uu^*} = \frac{\omega_1^2}{\lambda_0^2}\cdot\frac{1-\cos(2\Lambda\omega_{\text{radio}}t)-2g\sin(2\Lambda\omega_{\text{radio}}t)}{2-4\frac{\Omega}{\lambda_0}f}. \tag{5.384}$$

Writing f and g explicitly,

$$\overline{P}_\beta = \frac{1}{1-uu^*} = \frac{\omega_1^2}{\lambda_0^2}\cdot\frac{1-\cos(2\Lambda\omega_{\text{radio}}t)-\frac{1}{2\Lambda}\left(\frac{\omega_2}{2\omega_{\text{radio}}}\right)^2\frac{\Omega}{\lambda_0}\sin^2(2\Lambda\omega_{\text{radio}}t)}{2+\frac{1}{\Lambda}\left(\frac{\omega_2}{2\omega_{\text{radio}}}\right)^2\frac{\Omega}{\lambda_0}(1-\cos(2\Lambda\omega_{\text{radio}}t))}. \tag{5.385}$$

Using the identities $\cos(2x) = \cos^2 x - \sin^x = 1 - 2\sin^2 x$ and $\sin(2x) = 2\sin x\cos x$,

$$\overline{P}_\beta = \frac{\omega_1^2}{\lambda_0^2}\cdot\frac{2\sin^2(\Lambda\omega_{\text{radio}}t)-\frac{2}{\Lambda}\left(\frac{\omega_2}{2\omega_{\text{radio}}}\right)^2\frac{\Omega}{\lambda_0}\sin^2(\Lambda\omega_{\text{radio}}t)\cos^2(\Lambda\omega_{\text{radio}}t)}{2+\frac{2}{\Lambda}\left(\frac{\omega_2}{2\omega_{\text{radio}}}\right)^2\frac{\Omega}{\lambda_0}\sin^2(\Lambda\omega_{\text{radio}}t)} = \frac{\omega_1^2}{\lambda_0^2}\sin^2(\Lambda\omega_{\text{radio}}t)\cdot\frac{1-\frac{1}{\Lambda}\left(\frac{\omega_2}{2\omega_{\text{radio}}}\right)^2\frac{\Omega}{\lambda_0}\cos^2(\Lambda\omega_{\text{radio}}t)}{1+\frac{1}{\Lambda}\left(\frac{\omega_2}{2\omega_{\text{radio}}}\right)^2\frac{\Omega}{\lambda_0}\sin^2(\Lambda\omega_{\text{radio}}t)}$$

---

[13]Taking into account that $\Omega \le \lambda\sqrt{\Omega^2+\omega_1^2}$, $\omega_1 \le \lambda\sqrt{\Omega^2+\omega_1^2}$, and that ω_2 is not substantially greater than ω_1 (in the most relevant case of linear oscillations $\omega_2 = \omega_1$).

$$= \frac{\omega_1^2}{\lambda_0^2} \sin^2(\Lambda\omega_{\text{radio}}t) \cdot \frac{1 - \frac{1}{\Lambda}\left(\frac{\omega_2}{2\omega_{\text{radio}}}\right)^2 \frac{\Omega}{\lambda_0} \cos^2(\Lambda\omega_{\text{radio}}t)}{1 + \frac{1}{\Lambda}\left(\frac{\omega_2}{2\omega_{\text{radio}}}\right)^2 \frac{\Omega}{\lambda_0} \sin^2(\Lambda\omega_{\text{radio}}t)} \cdot \frac{1 - \frac{1}{\Lambda}\left(\frac{\omega_2}{2\omega_{\text{radio}}}\right)^2 \frac{\Omega}{\lambda_0} \sin^2(\Lambda\omega_{\text{radio}}t)}{1 - \frac{1}{\Lambda}\left(\frac{\omega_2}{2\omega_{\text{radio}}}\right)^2 \frac{\Omega}{\lambda_0} \sin^2(\Lambda\omega_{\text{radio}}t)}$$

$$= \frac{\omega_1^2}{\lambda_0^2} \sin^2(\Lambda\omega_{\text{radio}}t) \cdot \frac{1 - \frac{1}{\Lambda}\left(\frac{\omega_2}{2\omega_{\text{radio}}}\right)^2 \frac{\Omega}{\lambda_0} + \frac{1}{\Lambda^2}\left(\frac{\omega_2}{2\omega_{\text{radio}}}\right)^4 \left(\frac{\Omega}{\lambda_0}\right)^2 \sin^2(\Lambda\omega_{\text{radio}}t)\cos^2(\Lambda\omega_{\text{radio}}t)}{1 - \frac{1}{\Lambda^2}\left(\frac{\omega_2}{2\omega_{\text{radio}}}\right)^4 \left(\frac{\Omega}{\lambda_0}\right)^2 \sin^4(\Lambda\omega_{\text{radio}}t)}, \tag{5.386}$$

where the blue term was obtained using the Pythagorean identity $\cos^2 x + \sin^2 x = 1$. The terms containing the very small factors printed in red can be safely neglected, yielding an equation closely resembling Eq 5.321

$$\overline{P}_\beta \approx \frac{\omega_1^2}{\lambda_0^2}\left(1 - \frac{1}{\Lambda}\left(\frac{\omega_2}{2\omega_{\text{radio}}}\right)^2 \frac{\Omega}{\lambda_0}\right)\sin^2(\Lambda\omega_{\text{radio}}t) = \frac{\omega_1^2}{\lambda_0^2}\left(1 - \frac{\omega_2^2}{2\omega_{\text{radio}}}\frac{\Omega}{2\Lambda\omega_{\text{radio}}\lambda_0}\right)\sin^2(\Lambda\omega_{\text{radio}}t). \tag{5.387}$$

Using Eq. 5.379,

$$2\Lambda\omega_{\text{radio}}\lambda_0 = -\left(\omega_1^2 + \Omega^2 - \frac{\omega_2^2}{4\omega_{\text{radio}}}\Omega\right) \tag{5.388}$$

and

$$(2\Lambda\omega_{\text{radio}})^2 = \frac{\left(\omega_1^2 + \Omega^2 - \frac{\omega_2^2}{4\omega_{\text{radio}}}\Omega\right)^2}{\omega_1^2 + \Omega^2} = \frac{\left(\omega_1^2 + \Omega^2\right)^2 - \frac{\omega_2^2}{2\omega_{\text{radio}}}\Omega\left(\omega_1^2 + \Omega^2\right) + \frac{\omega_2^4}{16\omega_{\text{radio}}^2}\Omega^2}{\omega_1^2 + \Omega^2} = \omega_1^2 + \Omega^2 - \frac{\omega_2^2}{2\omega_{\text{radio}}}\Omega + \frac{\omega_2^4}{16\omega_{\text{radio}}^2}\frac{\Omega^2}{\omega_1^2 + \Omega^2}$$

$$= \omega_1^2 + \left(\Omega - \frac{\omega_2^2}{4\omega_{\text{radio}}}\right)^2 - \frac{\omega_2^4}{16\omega_{\text{radio}}^2} + \frac{\omega_2^4}{16\omega_{\text{radio}}^2}\frac{\Omega^2}{\omega_1^2 + \Omega^2} = \omega_1^2 + \left(\Omega - \frac{\omega_2^2}{4\omega_{\text{radio}}}\right)^2 - \frac{\omega_2^4}{16\omega_{\text{radio}}^2}\frac{\omega_1^2}{\omega_1^2 + \Omega^2}. \tag{5.389}$$

Neglecting the very small red term,

$$\Lambda\omega_{\text{radio}} \approx -\frac{1}{2}\sqrt{\omega_1^2 + \left(\Omega - \frac{\omega_2^2}{4\omega_{\text{radio}}}\right)^2} \tag{5.390}$$

Taking into account that $\sin^2(-x) = \sin^2 x$, we can express $\overline{P}_\beta$ as

$$\overline{P}_\beta \approx \frac{\omega_1^2}{\omega_1^2 + \Omega^2}\left(1 - \frac{\omega_2^2}{2\omega_{\text{radio}}}\frac{\Omega}{\omega_1^2 + \Omega^2 - \frac{\omega_2^2}{4\omega_{\text{radio}}}\Omega}\right)\sin^2\frac{\sqrt{\omega_1^2 + \left(\Omega - \frac{\omega_2^2}{4\omega_{\text{radio}}}\right)^2}}{2}t$$

$$= \frac{\omega_1^2}{\omega_1^2 + \Omega^2}\frac{\omega_1^2 + \Omega^2 + \frac{\omega_2^2}{4\omega_{\text{radio}}}\Omega}{\omega_1^2 + \Omega^2 - \frac{\omega_2^2}{4\omega_{\text{radio}}}\Omega}\sin^2\frac{\sqrt{\omega_1^2 + \left(\Omega - \frac{\omega_2^2}{4\omega_{\text{radio}}}\right)^2}}{2}t \tag{5.391}$$

Multiplying numerator and denominator of the second fraction on the second line by $\omega_1^2 + \Omega^2 - \frac{\omega_2^2}{4\omega_{\text{radio}}}\Omega$, we obtain

$$\overline{P}_\beta \approx \frac{\omega_1^2}{\omega_1^2 + \Omega^2} \frac{\left(\omega_1^2 + \Omega^2\right)^2 - \frac{\omega_2^4}{16\omega_{\rm radio}^2}\Omega^2}{\left(\omega_1^2 + \Omega^2 - \frac{\omega_2^2}{4\omega_{\rm radio}}\Omega\right)^2} \sin^2 \frac{\sqrt{\omega_1^2 + \left(\Omega - \frac{\omega_2^2}{4\omega_{\rm radio}}\right)^2}}{2} t$$

$$= \frac{\omega_1^2}{\omega_1^2 + \Omega^2} \frac{\left(\omega_1^2 + \Omega^2\right)^2 - \frac{\omega_2^4}{16\omega_{\rm radio}^2}\Omega^2}{\left(\omega_1^2 + \Omega^2\right)^2 - \frac{\omega_2^2}{2\omega_{\rm radio}}\Omega\left(\omega_1^2 + \Omega^2\right) + \frac{\omega_2^4}{16\omega_{\rm radio}^2}\Omega^2} \sin^2 \frac{\sqrt{\omega_1^2 + \left(\Omega - \frac{\omega_2^2}{4\omega_{\rm radio}}\right)^2}}{2} t$$

$$= \frac{\omega_1^2}{\left(\omega_1^2 + \Omega^2\right)^2} \frac{\left(\omega_1^2 + \Omega^2\right)^2 - \frac{\omega_2^4}{16\omega_{\rm radio}^2}\Omega^2}{\omega_1^2 + \Omega^2 - \frac{\omega_2^2}{2\omega_{\rm radio}}\Omega + \frac{\omega_2^4}{16\omega_{\rm radio}^2}\frac{\Omega^2}{\omega_1^2 + \Omega^2}} \sin^2 \frac{\sqrt{\omega_1^2 + \left(\Omega - \frac{\omega_2^2}{4\omega_{\rm radio}}\right)^2}}{2} t$$

$$= \frac{\omega_1^2}{\left(\omega_1^2 + \Omega^2\right)^2} \frac{\left(\omega_1^2 + \Omega^2\right)^2 - \frac{\omega_2^4}{16\omega_{\rm radio}^2}\Omega^2}{\omega_1^2 + \left(\Omega - \frac{\omega_2^2}{4\omega_{\rm radio}}\right)^2 - \frac{\omega_2^4}{16\omega_{\rm radio}^2}\frac{\omega_1^2}{\omega_1^2 + \Omega^2}} \sin^2 \frac{\sqrt{\omega_1^2 + \left(\Omega - \frac{\omega_2^2}{4\omega_{\rm radio}}\right)^2}}{2} t. \tag{5.392}$$

Again, we neglect the very small red terms, cancel $\left(\omega_1^2 + \Omega^2\right)^2$ in the denominator and numerator of the first and second fraction, respectively, and obtain

$$\overline{P}_\beta \approx \frac{\omega_1^2}{\omega_1^2 + \left(\Omega - \frac{\omega_2^2}{4\omega_{\rm radio}}\right)^2} \sin^2 \frac{\sqrt{\omega_1^2 + \left(\Omega - \frac{\omega_2^2}{4\omega_{\rm radio}}\right)^2}}{2} t. \tag{5.393}$$

Comparison with Eq 5.321

$$P_\beta = \frac{\omega_1^2}{\omega_1^2 + \Omega^2} \sin^2 \frac{\sqrt{\omega_1^2 + \Omega^2}}{2} t \tag{5.394}$$

reveals that the expression describing the average population $\overline{P}_\beta$ for non-rotating fields (in the approximation keeping terms proportional to $\omega_1/\omega_{\rm radio}$ but neglecting terms proportional to higher powers of $\omega_1/\omega_{\rm radio}$) differs form the expression describing the population P_β for rotating fields only by the frequency shift $\frac{\omega_2^2}{4\omega_{\rm radio}}$.

Lecture 6
Ensemble of non-interacting spins

Literature: A nice short introduction is given in K3.1. The topic is clearly described in K6, L11, C2.2. The mixed state is introduced nicely in B17.2, K6.8, L11.1, and C2.2.2. The general strategy of analyzing NMR experiments is outlined in C2.4. More specific references are given in the individual sections below.

6.1   Mixed state

So far, we worked with systems in so-called *pure states*, when we described the whole studied system by its complete wave function. It is fine if the system consists of one particle or a small number of particles. In the case of a single particle, the wave function $\Psi(x, y, z, c_\alpha)$ depends on the x, y, z coordinates of the particle plus the additional degree of freedom describing the spin state (in terms of the four components of the solution of the Dirac equation). Extending the quantum-mechanical description to more than one particle presents both fundamental and practical problems. A fundamental problem is that particles of the same type cannot be distinguished as in classical mechanics. This issue is briefly discussed in Section 6.7.1. The major practical problem is a high complexity of multiparticle systems. The complete wave function of whole molecule is already very complicated, represented by multidimensional state vectors and their properties are described by operators represented by multidimensional matrices. In the case of macroscopic ensembles of many molecules, the dimensionality of the state vectors and operator matrices is described by astronomic numbers. A typical NMR sample contains approximately 10^{24} particles (electrons, protons, and neutrons). Clearly, we cannot use the brute-force approach requiring determination of the complete wave function. In this lecture, we describe two levels of simplification routinely applied to describe NMR samples.

The *first level of simplification* is separation of the description of spin magnetic moments from the other terms of the wave function. In the NMR spectroscopy, we are interested only in properties of molecules associated with the spins of the observed nuclei. If we assume that motions of the whole molecule, of its atoms, and of electrons and nuclei in the atoms, do not depend on the spin of the observed nucleus, we can divide the complete wave function into the spin wave functions and the wave function describing all the other degrees of freedom. Validity of such assumption is discussed in Section 6.7.2. Based on the arguments presented there, we can conclude that (in most cases except for some relaxation effects) the wave functions (and consequently the Hamiltonians) can be divided into two parts, one dependent on the spin degrees of freedom, and the other one dependent on the

other degrees of freedom that are not important in the NMR spectroscopy. To describe the NMR experiment, it is sufficient to analyze only the spin wave function (the spin state vector). However, the number of dimensions of the spin state vector is extremely high, typically $\sim 10^{23}$, and properties of the large sets of magnetic moments in bulk samples are described by operators represented by matrices of the same dimensionality. Another level of simplification is therefore needed.

The *second level of simplification* is related to the question whether individual magnetic moments can be treated independently. This is possible if the spin Hamiltonian can be decomposed into a sum of operators acting separately on individual nuclear magnetic moments, as shown in Section 6.7.3. If this condition is fulfilled, the spin wave function of the whole ensemble can be decomposed to independent spin wave functions of individual nuclei, and the Hamiltonian has the same eigenfunctions ($|\alpha\rangle, |\beta\rangle$ in the case of a vertical field $\vec{B}_0$) when applied to any of the individual spin wave function. These eigenfunctions can be used as the same basis set for all spin wave functions (state vectors) of individual magnetic moments. Using the same basis for vectors representing spins of different nuclei allows us to use two-dimensional operator matrices (for spin-1/2 nuclei) instead of multidimensional operator matrices. Similar arguments can be applied to the Hamiltonian of magnetic moments in magnetic fields in other directions.

The expected value $\langle A \rangle$ of a quantity A for a single nucleus can be calculated using Eq. 4.12 as a trace of the following product of matrices:

$$\langle A \rangle = \text{Tr} \left\{ \begin{pmatrix} c_\alpha c_\alpha^* & c_\alpha c_\beta^* \\ c_\beta c_\alpha^* & c_\beta c_\beta^* \end{pmatrix} \begin{pmatrix} A_{11} & A_{12} \\ A_{21} & A_{22} \end{pmatrix} \right\}. \tag{6.1}$$

The expected value $\langle A \rangle$ of a quantity A for *multiple nuclei with the same basis* is

$$
\begin{aligned}
\langle A \rangle &= \text{Tr} \left\{ \begin{pmatrix} c_{\alpha,1} c_{\alpha,1}^* & c_{\alpha,1} c_{\beta,1}^* \\ c_{\beta,1} c_{\alpha,1}^* & c_{\beta,1} c_{\beta,1}^* \end{pmatrix} \begin{pmatrix} A_{11} & A_{12} \\ A_{21} & A_{22} \end{pmatrix} + \begin{pmatrix} c_{\alpha,2} c_{\alpha,2}^* & c_{\alpha,2} c_{\beta,2}^* \\ c_{\beta,2} c_{\alpha,2}^* & c_{\beta,2} c_{\beta,2}^* \end{pmatrix} \begin{pmatrix} A_{11} & A_{12} \\ A_{21} & A_{22} \end{pmatrix} + \cdots \right\} \\
&= \text{Tr} \left\{ \left(\begin{pmatrix} c_{\alpha,1} c_{\alpha,1}^* & c_{\alpha,1} c_{\beta,1}^* \\ c_{\beta,1} c_{\alpha,1}^* & c_{\beta,1} c_{\beta,1}^* \end{pmatrix} + \begin{pmatrix} c_{\alpha,2} c_{\alpha,2}^* & c_{\alpha,2} c_{\beta,2}^* \\ c_{\beta,2} c_{\alpha,2}^* & c_{\beta,2} c_{\beta,2}^* \end{pmatrix} + \cdots \right) \begin{pmatrix} A_{11} & A_{12} \\ A_{21} & A_{22} \end{pmatrix} \right\} \\
&= N \text{Tr} \left\{ \underbrace{\begin{pmatrix} \overline{c_\alpha c_\alpha^*} & \overline{c_\alpha c_\beta^*} \\ \overline{c_\beta c_\alpha^*} & \overline{c_\beta c_\beta^*} \end{pmatrix}}_{\hat{\rho}} \underbrace{\begin{pmatrix} A_{11} & A_{12} \\ A_{21} & A_{22} \end{pmatrix}}_{\hat{A}} \right\} = N \text{Tr} \left\{ \hat{\rho} \hat{A} \right\}.
\end{aligned}
\tag{6.2}
$$

The matrix $\hat{\rho}$ is the *(probability) density matrix*, the horizontal bar indicates average over the whole ensemble of nuclei in the sample, and N is the number of non-interacting nuclei described in the same operator basis.

Why probability density? Because the probability $P = \langle \Psi | \Psi \rangle$, the operator of probability can be written as the unit matrix $\hat{1}$: $\langle \Psi | \Psi \rangle \equiv \langle \Psi | \hat{1} | \Psi \rangle$. Therefore, the expectation value of probability can be also calculated using Eq. 4.12 as $\text{Tr}\{\hat{\rho}\hat{1}\} = \text{Tr}\{\hat{\rho}\}$.

The most important features of the mixed-state approach are listed below:

- Two-dimensional basis is sufficient for the whole set of N nuclei (if they do not interact with each other).

Table 6.1: Examples of operators and a density matrix expressed in the same basis. The density matrix is shown in red, the operators are shown in green. The elements of the density matrix are expressed in terms of the $|\vartheta_j, \varphi_j\rangle$ states, as described in Section 6.7.4.

Description of	units	symbol	explicit expression (linear combination of basis matrices)
mixed state	1	$\hat{\rho}$	$1 \times \frac{1}{2}\begin{pmatrix} 1 & 0 \\ 0 & 1 \end{pmatrix} + \overline{\cos\vartheta} \times \frac{1}{2}\begin{pmatrix} 1 & 0 \\ 0 & -1 \end{pmatrix} + \overline{\sin\vartheta\cos\varphi} \times \frac{1}{2}\begin{pmatrix} 0 & 1 \\ 1 & 0 \end{pmatrix} + \overline{\sin\vartheta\sin\varphi} \times \frac{1}{2}\begin{pmatrix} 0 & -i \\ i & 0 \end{pmatrix}$
angular momentum	J s	$\hat{I}_z$	$0 \times \frac{1}{2}\begin{pmatrix} 1 & 0 \\ 0 & 1 \end{pmatrix} + \hbar \times \frac{1}{2}\begin{pmatrix} 1 & 0 \\ 0 & -1 \end{pmatrix} + 0 \times \frac{1}{2}\begin{pmatrix} 0 & 1 \\ 1 & 0 \end{pmatrix} + 0 \times \frac{1}{2}\begin{pmatrix} 0 & -i \\ i & 0 \end{pmatrix}$
magnetic moment	J T^{-1}	$\hat{\mu}_z$	$0 \times \frac{1}{2}\begin{pmatrix} 1 & 0 \\ 0 & 1 \end{pmatrix} + \gamma\hbar \times \frac{1}{2}\begin{pmatrix} 1 & 0 \\ 0 & -1 \end{pmatrix} + 0 \times \frac{1}{2}\begin{pmatrix} 0 & 1 \\ 1 & 0 \end{pmatrix} + 0 \times \frac{1}{2}\begin{pmatrix} 0 & -i \\ i & 0 \end{pmatrix}$
energy	J	$\hat{H}$	$0 \times \frac{1}{2}\begin{pmatrix} 1 & 0 \\ 0 & 1 \end{pmatrix} - \gamma B_z\hbar \times \frac{1}{2}\begin{pmatrix} 1 & 0 \\ 0 & -1 \end{pmatrix} - \gamma B_x\hbar \times \frac{1}{2}\begin{pmatrix} 0 & 1 \\ 1 & 0 \end{pmatrix} - \gamma B_y\hbar \times \frac{1}{2}\begin{pmatrix} 0 & -i \\ i & 0 \end{pmatrix}$

- Statistical approach: the possibility to use a 2D basis is paid by loosing the information about the *microscopic state*. The same density matrix can describe an astronomic number of possible combinations of individual angular momenta which give the same *macroscopic* result. What is described by the density matrix is called the *mixed state*.

- Choice of the basis of the wave function is encoded in the definition of $\hat{\rho}$ (eigenfunctions of $\hat{I}_z$).

- The state is described not by a vector, but by a matrix, $\hat{\rho}$ is a matrix like matrices representing the operators.

- Any 2×2 matrix can be written as a linear combination of four 2×2 matrices. Such four matrices can be used as a *basis* of all 2×2 matrices, including matrices representing operators (in the same manner as two selected 2-component vectors serve as a basis for all 2-component vectors). Examples of such linear combinations are presented in Table 6.1. Note that the density matrix and the operators describe different features, they are clearly distinguished by the coefficients of the linear combinations.

- A good choice of a basis is a set of *orthonormal* matrices.[1]

- *Diagonal elements* of $\hat{\rho}$ (or matrices with diagonal elements only) are known as *populations*. They are discussed in Section 6.2.

- *Off-diagonal elements* (or matrices with diagonal elements only) are known as *coherences*. They are discussed in Section 6.3.

6.2 Populations

Population is a somewhat confusing name of a diagonal element of the probability density matrix, the correct physical interpretation is clearly described in L11.2.

---

[1]Orthonormality for a set of four matrices $\hat{A}_1, \hat{A}_2, \hat{A}_3, \hat{A}_4$ can be defined as $\mathrm{Tr}\{\hat{A}_j^\dagger \hat{A}_k\} = \delta_{jk}$, where j and $k \in \{1, 2, 3, 4\}$, $\delta_{jk} = 1$ for $j = k$ and $\delta_{jk} = 0$ for $j \neq k$, and $\hat{A}_j^\dagger$ is an *adjoint* matrix of $\hat{A}_j$, i.e., matrix obtained from $\hat{A}_j$ by exchanging rows and columns and replacing all numbers with their complex conjugates.

- In a *pure state*, $c_\alpha c_\alpha^*$ is given by the amplitude of c_α: $c_\alpha c_\alpha^* = |c_\alpha|^2$.

- In a *mixed state*, the coefficients $c_{\alpha,j}$ are different for the observed nucleus in each molecule j.

- The *populations* $\overline{c_\alpha c_\alpha^*}$ and $\overline{c_\beta c_\beta^*}$ are real numbers $\overline{|c_\alpha|^2}$ and $\overline{|c_\beta|^2}$, respectively, and their sum is always one.[2]

- If $c_{\alpha,j}$ and $c_{\beta,j}$ describe stationary states, the populations $\overline{c_\alpha c_\alpha^*}$ and $\overline{c_\beta c_\beta^*}$ do not change in time.

- A population $\overline{c_\alpha c_\alpha^*} > 1/2$ describes *longitudinal polarization*, i.e. polarization of magnetic moments in the z direction (the direction of $\vec{B}_0$), an excess of magnetic moments with positive μ_z components. The sum of μ_z of all magnetic moments in the sample divided by the volume of the sample is the z component of the bulk magnetization (M_z).

- The value $\overline{c_\alpha c_\alpha^*} = 1/2$ indicates no net polarization in the direction $\vec{B}_0$ (equal populations of the α and β states). It does not indicate that all spins in the ensemble must be either in the α state or in the β state! The value $\overline{c_\alpha c_\alpha^*} = 1/2$ describes equally well all combinations of superposition states describing sets of magnetic moments pointing in all possible directions as long as their vector sum has a zero z component. Probability that the system contains 50 % spins in the α state and 50 % spins in the β state is actually negligible.

- When $\overline{c_\alpha c_\alpha^*}$ is specified, $\overline{c_\beta c_\beta^*}$ does not carry any additional information because its value is already fully described by the $\overline{c_\alpha c_\alpha^*}$ value: $\overline{c_\beta c_\beta^*} = 1 - \overline{c_\alpha c_\alpha^*}$. It also implies that the real number $\overline{c_\alpha c_\alpha^*}$ carries the same information as the matrix

$$\begin{pmatrix} \overline{c_\alpha c_\alpha^*} & 0 \\ 0 & \overline{c_\beta c_\beta^*} \end{pmatrix} = \begin{pmatrix} \overline{c_\alpha c_\alpha^*} & 0 \\ 0 & 1 - \overline{c_\alpha c_\alpha^*} \end{pmatrix} = \frac{1}{2} \begin{pmatrix} 1 & 0 \\ 0 & 1 \end{pmatrix} + \left(\overline{c_\alpha c_\alpha^*} - \frac{1}{2} \right) \begin{pmatrix} 1 & 0 \\ 0 & -1 \end{pmatrix}.$$

  Consequently, the longitudinal polarization is described equally well by the number $\overline{c_\alpha c_\alpha^*}$ and by the second term contributing to the displayed matrix.

- Graphical representations of quantum mechanical objects are helpful but not perfect. An attempt to visualize the population $\overline{c_\alpha c_\alpha^*}$ is presented in Figure 6.1. The polarization is depicted as one possible distribution of magnetic moments and as a vector describing the bulk magnetization as a result of the longitudinal polarization of magnetic moments.

6.3 Coherence

Coherence is a very important issue in NMR spectroscopy. It is discussed in K6.9, L11.2, C2.6.

- In a *pure state*, $c_\beta c_\alpha^*$ is given by amplitudes and by the difference of phases of c_α and c_β: $c_\beta c_\alpha^* = |c_\alpha||c_\beta|\mathrm{e}^{-\mathrm{i}(\phi_\alpha - \phi_\beta)}$.

---

[2]Note that $\sum_{j=1}^{N}(c_{\alpha,j}c_{\alpha,j}^* + c_{\beta,j}c_{\beta,j}^*) = N$. Therefore, $\overline{c_\alpha c_\alpha^*} + \overline{c_\beta c_\beta^*} = 1$.

- In a *mixed state*, $c_{\alpha,j} = |c_{\alpha,j}|\mathrm{e}^{\mathrm{i}\phi_{\alpha,j}}$ and $c_{\beta,j} = |c_{\beta,j}|\mathrm{e}^{\mathrm{i}\phi_{\beta,j}}$ are different for the observed nucleus in each molecule j.

- The *coherence* $\overline{c_\beta c_\alpha^*}$ is a complex number $|\mathcal{A}|\mathrm{e}^{-\mathrm{i}\Phi} = \overline{|c_\alpha||c_\beta|} \cdot \overline{\mathrm{e}^{-\mathrm{i}(\phi_\alpha - \phi_\beta)}}$. Its amplitude $|\mathcal{A}|$ is $\overline{|c_\alpha||c_\beta|}$ and its phase Φ is given by $\overline{\mathrm{e}^{-\mathrm{i}(\phi_\alpha - \phi_\beta)}} = \overline{\cos(\phi_\alpha - \phi_\beta)} - \mathrm{i}\,\overline{\sin(\phi_\alpha - \phi_\beta)}$.

- In general, the spin magnetic moments in individual molecules are present in various superposition states corresponding to various linear combinations of the $|\alpha\rangle$ and $|\beta\rangle$ eigenstates $(c_{\alpha,j}|\alpha\rangle + c_{\beta,j}|\beta\rangle)$. If there is no macroscopic relationship between the phases $\phi_{\alpha,j}$ and $\phi_{\beta,j}$ in individual molecules, the difference $\phi_{\alpha,j} - \phi_{\beta,j}$ can take any value in the interval $(0, 2\pi)$ with the same probability. Therefore, $\overline{\mathrm{e}^{-\mathrm{i}(\phi_\alpha - \phi_\beta)}} = \overline{\cos(\phi_\alpha - \phi_\beta)} - \mathrm{i}\,\overline{\sin(\phi_\alpha - \phi_\beta)} = 0 + 0 = 0$ because the average values of both sine and cosine functions are zero in the interval $(0, 2\pi)$. Obviously, $\overline{c_\beta c_\alpha^*} = 0$ in such a case, regardless of the amplitudes. Such an ensemble of states is called an *incoherent superposition* of the $|\alpha\rangle$ and $|\beta\rangle$ eigenstates.

- If $\mathrm{e}^{-\mathrm{i}(\phi_{\alpha,j} - \phi_{\beta,j})}$ does not average to zero, a macroscopic relationship exists between the phases $\phi_{\alpha,j}$ and $\phi_{\beta,j}$. Such an ensemble of states is called a *coherent superposition* of the $|\alpha\rangle$ and $|\beta\rangle$ eigenstates. This is why the term *coherence* is used for the off-diagonal elements of the density matrix, whose non-zero values indicate a coherent superposition of the $|\alpha\rangle$ and $|\beta\rangle$ eigenstates, or simply a *coherence* of the system.

- The non-zero coherence $\overline{c_\beta c_\alpha^*}$ describes the *transverse polarization*, i.e. polarization of magnetic moments in the xy plane (a plane perpendicular to $\vec{B}_0$). The magnitude of the transverse polarization is $\overline{|c_\alpha||c_\beta|}$ and its direction is given by the phase of $\overline{c_\beta c_\alpha^*}$. Since the result of polarization of magnetic moments is a bulk magnetization, the direction of the transverse polarization can be described by the x and y components of the magnetization vector $\vec{M}$: $M_x = |M_\perp|\cos\Phi, M_y = |M_\perp|\sin\Phi$, where Φ is the phase of $\overline{c_\beta c_\alpha^*}$ and $M_\perp = \sqrt{M^2 - M_z^2}$.

- If the evolution of the phases $\phi_{\alpha,j}$ and $\phi_{\beta,j}$ is *coherent*, the differences $\phi_{\alpha,j} - \phi_{\beta,j}$ change in time, but identically for all magnetic moments. In such a case, the coherence of the system persists and $\overline{c_\beta c_\alpha^*}$ describes the transverse polarization with a constant magnitude and in the direction specified by the actual value of the phase Φ. Section 6.7.4 describes explicitly how the coherence $\overline{c_\beta c_\alpha^*}$ depends on $\phi_{\alpha,j}$ and $\phi_{\beta,j}$.

- The number $\overline{c_\alpha c_\beta^*}$ does not carry any additional information, it is just a complex conjugate of $\overline{c_\beta c_\alpha^*}$. It also implies that the complex number $\overline{c_\beta c_\alpha^*}$ carries the same information as the matrix

$$\begin{pmatrix} 0 & \overline{c_\alpha c_\beta^*} \\ \overline{c_\beta c_\alpha^*} & 0 \end{pmatrix}.$$

  Consequently, the term *coherence* is used for the complex number $\overline{c_\beta c_\alpha^*}$ as well as for the displayed matrix.

- As $\overline{c_\beta c_\alpha^*}$ is a complex number, it carries information of two real numbers, of its amplitude and phase, or of its real and imaginary components $\overline{|c_\alpha||c_\beta|}\cos\Phi$ and $\mathrm{i}\overline{|c_\alpha||c_\beta|}\sin\Phi$, respectively.
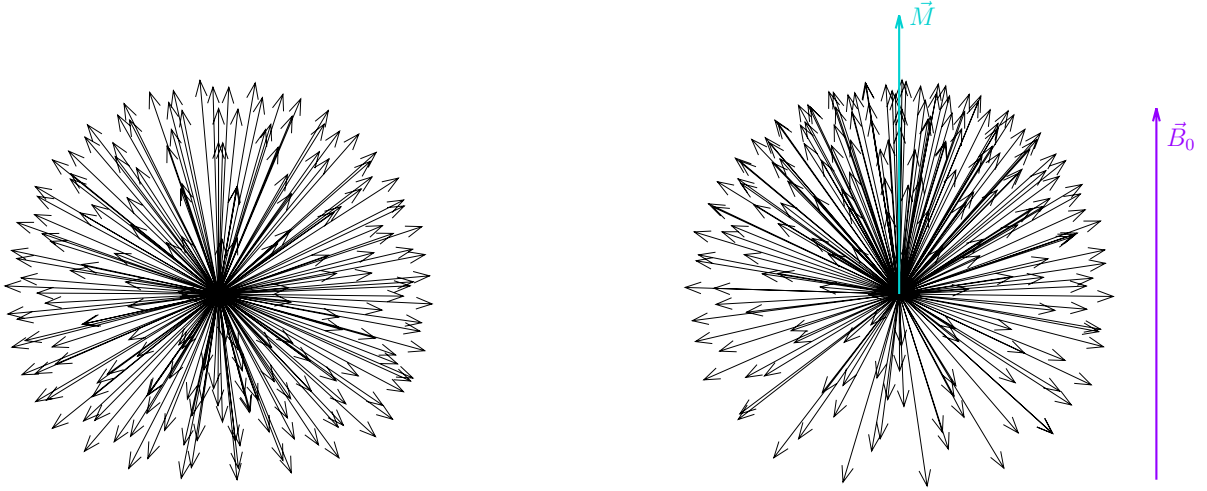
Figure 6.1: Pictorial representation of the populations $\overline{c_\alpha c_\alpha^*} = 1/2$ (left) and $\overline{c_\alpha c_\alpha^*} > 1/2$ (right). The populations are depicted as distributions of magnetic moments (black) and as a magnetization vector (cyan) defining the direction of the longitudinal polarization.

The same information is encoded in purely real and purely imaginary matrices

$$\overline{|c_\alpha||c_\beta|\cos\Phi} \begin{pmatrix} 0 & 1 \\ 1 & 0 \end{pmatrix} \qquad \mathrm{i}\overline{|c_\alpha||c_\beta|\sin\Phi} \begin{pmatrix} 0 & -1 \\ 1 & 0 \end{pmatrix}.$$

- A graphical representation of the coherence $\overline{c_\beta c_\alpha^*}$ is shown in Figure 6.2.

6.4   Basis sets

The usual choices of basis matrices are (C2.7.2):

- *Cartesian operators*, equal to the operators of spin angular momentum divided by $\hbar$. In this text, these matrices are written as $\mathscr{I}_x$, $\mathscr{I}_y$, $\mathscr{I}_z$, $\mathscr{I}_t$. In a similar fashion, we write $\mathscr{H} = \hat{H}/\hbar$ for Hamiltonians with eigenvalues expressed in units of (angular) frequency, not energy. The normalization factor $\sqrt{2}$ is often omitted (then the basis is still orthogonal, but not orthonormal):

$$\sqrt{2}\mathscr{I}_t = \frac{1}{\sqrt{2}} \begin{pmatrix} 1 & 0 \\ 0 & 1 \end{pmatrix} \qquad \sqrt{2}\mathscr{I}_z = \frac{1}{\sqrt{2}} \begin{pmatrix} 1 & 0 \\ 0 & -1 \end{pmatrix}$$

$$\sqrt{2}\mathscr{I}_x = \frac{1}{\sqrt{2}} \begin{pmatrix} 0 & 1 \\ 1 & 0 \end{pmatrix} \qquad \sqrt{2}\mathscr{I}_y = \frac{1}{\sqrt{2}} \begin{pmatrix} 0 & -\mathrm{i} \\ \mathrm{i} & 0 \end{pmatrix}. \tag{6.3}$$
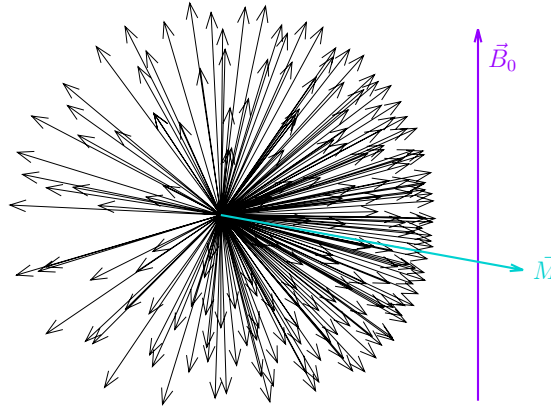
Figure 6.2: Pictorial representation of the coherence $\overline{c_\beta c_\alpha^*}$ as a distribution of magnetic moments (black) and as a magnetization vector (cyan) defining the direction of the transverse polarization.

- Single-element *population*

$$\mathscr{I}_\alpha = \mathscr{I}_t + \mathscr{I}_z = \begin{pmatrix} 1 & 0 \\ 0 & 0 \end{pmatrix} \qquad \mathscr{I}_\beta = \mathscr{I}_t - \mathscr{I}_z = \begin{pmatrix} 0 & 0 \\ 0 & 1 \end{pmatrix} \tag{6.4}$$

  and *transition* operators

$$\mathscr{I}_+ = \mathscr{I}_x + \mathrm{i}\mathscr{I}_y = \begin{pmatrix} 0 & 1 \\ 0 & 0 \end{pmatrix} \qquad \mathscr{I}_- = \mathscr{I}_x - \mathrm{i}\mathscr{I}_y = \begin{pmatrix} 0 & 0 \\ 1 & 0 \end{pmatrix}. \tag{6.5}$$

- A mixed basis

$$\sqrt{2}\mathscr{I}_t = \frac{1}{\sqrt{2}} \begin{pmatrix} 1 & 0 \\ 0 & 1 \end{pmatrix} \qquad \sqrt{2}\mathscr{I}_z = \frac{1}{\sqrt{2}} \begin{pmatrix} 1 & 0 \\ 0 & -1 \end{pmatrix} \qquad \mathscr{I}_+ = \begin{pmatrix} 0 & 1 \\ 0 & 0 \end{pmatrix} \qquad \mathscr{I}_- = \begin{pmatrix} 0 & 0 \\ 1 & 0 \end{pmatrix}. \tag{6.6}$$

6.5 Liouville-von Neumann equation

In order to describe the evolution of mixed states in time, we must find an equation describing how the elements of the density matrix change in time. Derivation of such equation is nicely described in C2.2.3 and reviewed in Section 6.7.5 of our text. The result is

$$\frac{\mathrm{d}\hat{\rho}}{\mathrm{d}t} = \frac{\mathrm{i}}{\hbar}(\hat{\rho}\hat{H} - \hat{H}\hat{\rho}) = \frac{\mathrm{i}}{\hbar}[\hat{\rho}, \hat{H}] = -\frac{\mathrm{i}}{\hbar}[\hat{H}, \hat{\rho}] \tag{6.7}$$

or in the units of (angular) frequency

$$\frac{\mathrm{d}\hat{\rho}}{\mathrm{d}t} = \mathrm{i}(\hat{\rho}\mathscr{H} - \mathscr{H}\hat{\rho}) = \mathrm{i}[\hat{\rho}, \mathscr{H}] = -\mathrm{i}[\mathscr{H}, \hat{\rho}]. \tag{6.8}$$

Eqs. 6.7 and 6.8 are known as the *Liouville-von Neumann equation.*

The Liouville-von Neumann equation can be solved using techniques of linear algebra. However, a very simple geometric solution is possible (K7.3, C2.7.3, L11.8) if the Hamiltonian does not change in time and consists solely of matrices which commute (e.g., $\mathscr{I}_t$ and $\mathscr{I}_z$, but not $\mathscr{I}_x$ and $\mathscr{I}_z$).

The evolution of $\hat{\rho}$ can be described as a *rotation in an abstract three-dimensional operator space* with the dimensions given by $\mathscr{I}_x$, $\mathscr{I}_y$, and $\mathscr{I}_z$, as shown in Section 6.7.6. An example is given in Fig. 6.3.

If the operator $\mathscr{I}_j$, defining the density matrix $\hat{\rho}(t = 0) = c\mathscr{I}_j$, and the operator $\mathscr{I}_l$, defining the Hamiltonian $\mathscr{H} = \omega\mathscr{I}_l$, satisfy the following commutation relation

$$[\mathscr{I}_j, \mathscr{I}_k] = i\mathscr{I}_l, \tag{6.9}$$

where $j, k, l \in \{x, y, z\}$, then the density matrix evolves as

$$\hat{\rho} = c\mathscr{I}_j \quad \longrightarrow \quad c\mathscr{I}_j \cos(\omega t) + c\mathscr{I}_k \sin(\omega t), \tag{6.10}$$

which corresponds to a rotation about $\mathscr{I}_l$ in an abstract three-dimensional space defined by the basis $\mathscr{I}_j, \mathscr{I}_k, \mathscr{I}_l$.
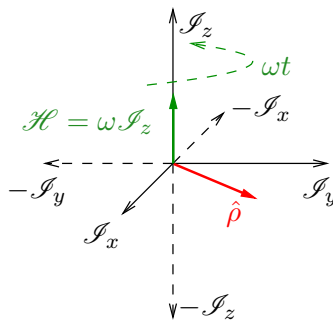
Figure 6.3: Evolution of the density matrix $\hat{\rho} = c\mathscr{I}_x \cos(\omega t) + c\mathscr{I}_y \cos(\omega t)$ under the influence of the Hamiltonian $\mathscr{H} = \omega\mathscr{I}_z$ visualized as a rotations in the space of operators $\mathscr{I}_x, \mathscr{I}_y, \mathscr{I}_z$.

6.6 General strategy of analyzing NMR experiments

The Liouville-von Neumann equation is the most important tool in the analysis of evolution of the spin system during the NMR experiment. The general strategy consists of three steps:

1. Define $\hat{\rho}$ at $t = 0$

2. Describe evolution of $\hat{\rho}$ using the relevant Hamiltonians – this is usually done in several steps

3. Calculate the expectation value of the measured quantity (magnetization components in the x, y plane) according to Eq. 6.2

Obviously, the procedure requires knowledge of

1. relation(s) describing the initial state of the system ($\hat{\rho}(0)$)

2. all Hamiltonians

3. the operator representing the measurable quantity

In the next section, we start from the end and define first the operator of the measurable quantity. Then we spend a lot of time defining all necessary Hamiltonians. Finally, we use the knowledge of the Hamiltonians and basic thermodynamics to describe the initial state.

HOMEWORK

Analyze when we can separate the spin part of the wave function from the non-spin part (Section 6.7.2) and when we can treat individual magnetic moment separately (Section 6.7.3). Following Section 6.7.6, and in particular Eq. 6.61, calculate the density matrix after $25\,\mu$s, starting from the state $\mathscr{I}_y$ and evolving under the influence of the Hamiltonian $\mathscr{H} = \omega_0 \mathscr{I}_z$, where $\omega_0 = \pi \times 10^5\,\text{rad/s}$.

6.7 SUPPORTING INFORMATION

6.7.1 Indistinguishable particles

In the classical mechanics, where particles are described by coordinates and momenta, two particles can be always distinguished by tracking their coordinates. This is not possible in quantum mechanics, where particles are described by wave functions. For example, two electrons in a hydrogen molecule are indistinguishable, it is not possible to tell which electron "originally" belonged to which hydrogen atom. This seemingly innocent quantum mechanical feature has dramatic consequences.

Let us investigate a set of three identical spin-1/2 particles, e.g. electrons. Their state is completely described by a wave function Ψ, which depends on their coordinates and spin degrees of freedom:

$$\Psi(x_1, y_1, z_1, c_{\alpha_1}, x_2, y_2, z_2, c_{\alpha_2}, x_3, y_3, z_3, c_{\alpha_3}). \tag{6.11}$$

The probability density that one particle is in a place and in a spin state described by the coordinates $x_1, y_1, z_1, c_{\alpha_1}$, another one in a place and in a spin state described by the coordinates $x_2, y_2, z_2, c_{\alpha_2}$, and a third one in a place and in a spin state described by the coordinates $x_3, y_3, z_3, c_{\alpha_3}$ is given by $\Psi^*\Psi = |\Psi|^2$:

$$\rho = |\Psi(x_1, y_1, z_1, c_{\alpha_1}, x_2, y_2, z_2, c_{\alpha_2}, x_3, y_3, z_3, c_{\alpha_3})|^2. \tag{6.12}$$

If the particles are indistinguishable, $\Psi^*\Psi = |\Psi|^2$ should not be changed by exchanging the particles because we cannot say which one is which.

$$\rho = |\Psi(x_1, y_1, z_1, c_{\alpha_1}, x_2, y_2, z_2, c_{\alpha_2}, x_3, y_3, z_3, c_{\alpha_3})|^2$$
$$= |\Psi(x_2, y_2, z_2, c_{\alpha_2}, x_1, y_1, z_1, c_{\alpha_1}, x_3, y_3, z_3, c_{\alpha_3})|^2$$

This is true only if the amplitude of Ψ is not affected by the exchange. The phase of Ψ can differ, but only in a limited way. If the exchange $x_1, y_1, z_1, c_{\alpha_1} \leftrightarrow x_2, y_2, z_2, c_{\alpha_2}$ changes Ψ to $\Psi e^{i\Delta\phi}$, then the second exchange $x_1, y_1, z_1, c_{\alpha_1} \leftrightarrow x_2, y_2, z_2, c_{\alpha_2}$ must return Ψ to its original form because we have returned to the initial state:

$$\Psi e^{i\Delta\phi} \to \left(\Psi e^{i\Delta\phi}\right) e^{i\Delta\phi} = \Psi e^{i2\Delta\phi} = \Psi \qquad \Rightarrow \qquad e^{i\Delta\phi} = \pm 1. \tag{6.13}$$

Therefore

$$\Psi(x_1, y_1, z_1, c_{\alpha_1}, x_2, y_2, z_2, c_{\alpha_2}, x_3, y_3, z_3, c_{\alpha_3}) = \pm\Psi(x_2, y_2, z_2, c_{\alpha_2}, x_1, y_1, z_1, c_{\alpha_1}, x_3, y_3, z_3, c_{\alpha_3}). \tag{6.14}$$

The wave functions for spin-1/2 particles always change the sign, they are called *antisymmetric*, whereas wave functions keeping the sign upon particle exchange are called *symmetric*. Note that a possible solution of the Schrödinger's equation may by a linear combination of the "correct" symmetric and antisymmetric wave functions, which is not symmetric or antisymmetric. Then, the symmetric and antisymmetric wave functions, correctly describing the system, must be recovered by finding appropriate linear combinations of the "wrong" solutions. For example, if our function Ψ is not symmetric or antisymmetric, we first write all functions obtained by all possible permutations (exchanges) of the coordinates:

$$
\begin{aligned}
\text{no exchange}: &\ \Psi(x_1, y_1, z_1, c_{\alpha_1}, x_2, y_2, z_2, c_{\alpha_2}, x_3, y_3, z_3, c_{\alpha_3}) \\
\text{1 exchange}: &\ \Psi(x_2, y_2, z_2, c_{\alpha_2}, x_1, y_1, z_1, c_{\alpha_1}, x_3, y_3, z_3, c_{\alpha_3}) \\
\text{1 exchange}: &\ \Psi(x_3, y_3, z_3, c_{\alpha_3}, x_2, y_2, z_2, c_{\alpha_2}, x_1, y_1, z_1, c_{\alpha_1}) \\
\text{1 exchange}: &\ \Psi(x_1, y_1, z_1, c_{\alpha_1}, x_3, y_3, z_3, c_{\alpha_3}, x_2, y_2, z_2, c_{\alpha_2}) \\
\text{2 exchanges}: &\ \Psi(x_2, y_2, z_2, c_{\alpha_2}, x_3, y_3, z_3, c_{\alpha_3}, x_1, y_1, z_1, c_{\alpha_1}) \\
\text{2 exchanges}: &\ \Psi(x_3, y_3, z_3, c_{\alpha_3}, x_1, y_1, z_1, c_{\alpha_1}, x_2, y_2, z_2, c_{\alpha_2})
\end{aligned} \tag{6.15}
$$

Then, the sum of all permuted wave functions is symmetric

$$
\begin{aligned}
\Psi^s = &+ \frac{1}{\sqrt{6}}\Psi(x_1, y_1, z_1, c_{\alpha_1}, x_2, y_2, z_2, c_{\alpha_2}, x_3, y_3, z_3, c_{\alpha_3}) \\
&+ \frac{1}{\sqrt{6}}\Psi(x_2, y_2, z_2, c_{\alpha_2}, x_1, y_1, z_1, c_{\alpha_1}, x_3, y_3, z_3, c_{\alpha_3}) \\
&+ \frac{1}{\sqrt{6}}\Psi(x_3, y_3, z_3, c_{\alpha_3}, x_2, y_2, z_2, c_{\alpha_2}, x_1, y_1, z_1, c_{\alpha_1}) \\
&+ \frac{1}{\sqrt{6}}\Psi(x_1, y_1, z_1, c_{\alpha_1}, x_3, y_3, z_3, c_{\alpha_3}, x_2, y_2, z_2, c_{\alpha_2}) \\
&+ \frac{1}{\sqrt{6}}\Psi(x_2, y_2, z_2, c_{\alpha_2}, x_3, y_3, z_3, c_{\alpha_3}, x_1, y_1, z_1, c_{\alpha_1}) \\
&+ \frac{1}{\sqrt{6}}\Psi(x_3, y_3, z_3, c_{\alpha_3}, x_1, y_1, z_1, c_{\alpha_1}, x_2, y_2, z_2, c_{\alpha_2})
\end{aligned} \tag{6.16}
$$

and the sum of the permuted functions multiplied by $(-1)^n$, where n is the number of exchanges, is antisymmetric

$$
\begin{aligned}
\Psi^{\mathrm{a}} = \; & + \frac{1}{\sqrt{6}} \Psi(x_1, y_1, z_1, c_{\alpha_1}, x_2, y_2, z_2, c_{\alpha_2}, x_3, y_3, z_3, c_{\alpha_3}) \\
& - \frac{1}{\sqrt{6}} \Psi(x_2, y_2, z_2, c_{\alpha_2}, x_1, y_1, z_1, c_{\alpha_1}, x_3, y_3, z_3, c_{\alpha_3}) \\
& - \frac{1}{\sqrt{6}} \Psi(x_3, y_3, z_3, c_{\alpha_3}, x_2, y_2, z_2, c_{\alpha_2}, x_1, y_1, z_1, c_{\alpha_1}) \\
& - \frac{1}{\sqrt{6}} \Psi(x_1, y_1, z_1, c_{\alpha_1}, x_3, y_3, z_3, c_{\alpha_3}, x_2, y_2, z_2, c_{\alpha_2}) \\
& + \frac{1}{\sqrt{6}} \Psi(x_2, y_2, z_2, c_{\alpha_2}, x_3, y_3, z_3, c_{\alpha_3}, x_1, y_1, z_1, c_{\alpha_1}) \\
& + \frac{1}{\sqrt{6}} \Psi(x_3, y_3, z_3, c_{\alpha_3}, x_1, y_1, z_1, c_{\alpha_1}, x_2, y_2, z_2, c_{\alpha_2}).
\end{aligned}
\tag{6.17}
$$

The factor $1/\sqrt{6}$ is a normalization constant, used to obtain $|\Psi^{\mathrm{s}}|^2 = |\Psi^{\mathrm{a}}|^2 = |\Psi|^2$. The symmetry of Ψ^{s} and the antisymmetry of Ψ^{a} can be checked easily. If we switch any pair of particles, the individual contributions Ψ may change. But the exchange of particles changes the given Ψ to another Ψ, which is already present in the sum, with the same sign (in Ψ^{s}) or with the opposite sign (in Ψ^{a}). Therefore, the exchange of particles does not change Ψ^{s} and changes all signs in Ψ^{a}.

The minus signs in Eq. 6.17 require that all indistinguishable particles in a system described by an antisymmetric wave must be in different quantum states (*Pauli exclusion principle*). E.g., if particles 1 and 2 in our three-particle set are in the same state, i.e., if $x_1, y_1, z_1, c_{\alpha_1} = x_2, y_2, z_2, c_{\alpha_2}$, the lines 1 and 2, 3 and 6, and 4 and 5 in Eq. 6.17 cancel each other and the final result is $\Psi^{\mathrm{a}} = 0$. Consequently, $|\Psi^{\mathrm{a}}|^2 = 0$ and the probability of finding the particles anywhere is zero.

Whereas the wave function of a set of indistinguishable particles can change its sign when the particles are exchanged, the Hamiltonian acting on them must stay the same because the Hamiltonian represents the total energy which does not change if we exchange particles. And because the evolution of Ψ is given by the Hamiltonian, a symmetric wave function remains symmetric and an antisymmetric wave function remains antisymmetric during the evolution.

As described in Section 6.1, we usually separate the spatial and spin degrees of freedom:

$$
\Psi = \psi_{\mathrm{non\text{-}spin}}(x_1, y_1, z_1, x_2, y_2, z_2, x_3, y_3, z_3) \cdot \psi_{\mathrm{spin}}(c_{\alpha_1}, c_{\alpha_2}, c_{\alpha_3}).
\tag{6.18}
$$

Note that $\psi_{\mathrm{non\text{-}spin}}$ must be symmetric and ψ_{spin} antisymmetric, to obtain an antisymmetric Ψ.

6.7.2 Separation of spin wave function

The separation of the spin wave function is trivial in the case of a free particle in the low-speed (i.e., low-energy) limit, as shown in Section 5.4:

$$
\Psi = \sqrt{\frac{1}{h^3}} \cdot \mathrm{e}^{\frac{\mathrm{i}}{\hbar} p_x x} \cdot \mathrm{e}^{\frac{\mathrm{i}}{\hbar} p_y y} \cdot \mathrm{e}^{\frac{\mathrm{i}}{\hbar} p_z z} \cdot \begin{pmatrix} c_\alpha \\ c_\beta \end{pmatrix}
\tag{6.19}
$$

Here, we expressed the wave function as a product of the green vector describing the degree of freedom important in NMR spectroscopy, and of a function dependent of the irrelevant degrees of freedom, shown in red.

In molecules, we first have to be able to separate the nuclear component of the wave function from the electronic one. This is possible if we assume that motions of the electrons in the orbitals are (i) much faster then evolution of the nuclear spin states[3] and (ii) little affected by the magnetic moments of nuclei (i.e., if we assume that the magnetic fields of the nuclear magnetic moments are too weak to influence motions of electrons). Then, we can use *shapes*[4] of molecular orbitals as a static description of the distribution probability of electron localization, independent of the actual state of the nuclear spin.

---

[3] In the currently available NMR spectrometers, the frequency of the magnetic moment precession is $\sim 10^9\,\mathrm{s}^{-1}$. The velocity of the electrons in atoms is not sharply defined (a consequence of the commutation relation between $\hat{r}_j$ and $\hat{p}_j$, known as the *Heisenberg's uncertainty principle*). Nevertheless, a rough estimate can be made. In a stationary set of bound particles described by the classical mechanics, the total kinetic and potential energy are related as follows. Since our set of particles is stationary, the time derivative of the quantity $\sum_k (\vec{p}_k \cdot \vec{r}_k)$ is equal to zero. The time derivative can be expressed as $\sum_k (\frac{\mathrm{d}\vec{p}_k}{\mathrm{d}t} \cdot \vec{r}_k + \vec{p}_k \frac{\mathrm{d}\vec{r}_k}{\mathrm{d}t}) = \sum_k (\vec{F}_k \cdot \vec{r}_k + m v_k^2) = \mathcal{E}_{\mathrm{pot}} + 2\mathcal{E}_{\mathrm{kin}} = 0$, where $\vec{r}_k$ is the position vector of the k-th particle, $\vec{p}_k$ is its momentum, $\vec{v}_k$ is its velocity, $\vec{F}_k$ is the force acting on it, $\mathcal{E}_{\mathrm{kin}}$ and $\mathcal{E}_{\mathrm{pot}}$ are the total kinetic and potential energy, respectively. In the case of the electron in the hydrogen atom, $\mathcal{E}_{\mathrm{pot}} = -Q^2/(4\pi\epsilon_0 r)$, where Q is the elementary charge and r is the electron-proton distance, related to the velocity by the uncertainty principle $r_j p_j \sim \hbar$. Therefore, $mv^2 \sim mvQ^2/(4\pi\epsilon_0 \hbar) \Rightarrow v \sim Q^2/(4\pi\epsilon_0 \hbar) \approx c/137$, where c is the speed of light. Considering the size of the atom ($\sim 10^{-10}\,\mathrm{m}$), the "frequency" of the electron is roughly $\sim 10^{16}\,\mathrm{s}^{-1}$ in hydrogen and higher in heavier atoms.

[4] Here, the word "shape" is a synonym for values of the wave function dependent on the x, y, z coordinates in a coordinate frame attached to the molecule, independent of the position and orientation of the molecule as a whole.

176

Second, we have to consider how the nuclear spin wave function depends on the coordinates of the nucleus (to see if the degree of freedom describing the spin state can be separated from the degrees of freedom describing the position). Infrared spectra tell us that vibrations of nuclei in molecules are much faster (roughly $10^{14}\,\mathrm{s}^{-1}$) than the precession of magnetic moments ($\sim 10^9\,\mathrm{s}^{-1}$). Therefore, we can safely use coordinates describing *averaged* positions of nuclei in the molecule. Then, the molecule is defined as a rigid object, and the average coordinates of nuclei define the orientation of the molecule, but also the orientation of the cloud of electrons, discussed above. Instead of investigating the effects of magnetic moments on individual nuclei, it is sufficient to ask how the magnetic moments of nuclei affect the orientation of the molecule. The magnetic fields of the nuclear magnetic moments are weak (the energy of magnetic moments in NMR spectrometers is much lower than the kinetic energy of molecules at the ambient temperature), and we can assume that the influence of the magnetic moments on the orientation of molecules is negligible.[5]

At this moment, we have finished our discussion of the first level of the simplification of quantum mechanical description of magnetic moments in molecules. The second level of simplification is discussed in Section 6.7.3.

6.7.3   Separation of variables

Our task is to find when a wave function ψ_{spin} depending on degrees of freedom of many spins[6] can be treated as a product of wave functions of individual spins $\psi_{\mathrm{spin}} = \psi^{(1)} \cdot \psi^{(2)} \cdot \psi^{(3)} \ldots$, where $\psi^{(j)}$ depends only on the spin degree of freedom of the first nucleus etc. Such separation works if the Hamiltonian can be written as a sum of operators that act only on individual particles (on magnetic moments of nuclei in individual molecules):

$$\hat{H}_{\mathrm{spin}} = \hat{H}^{(1)} + \hat{H}^{(2)} + \hat{H}^{(3)} + \ldots \tag{6.20}$$

$$\hat{H}_{\mathrm{spin}}\psi_{\mathrm{spin}} = (\hat{H}^{(1)} + \hat{H}^{(2)} + \hat{H}^{(3)} + \ldots)\psi^{(1)} \cdot \psi^{(2)} \cdot \psi^{(3)} \ldots = \psi^{(2)} \cdot \psi^{(3)} \cdot \ldots \cdot \hat{H}^{(1)}\psi^{(1)} + \psi^{(1)} \cdot \psi^{(3)} \cdot \ldots \cdot \hat{H}^{(2)}\psi^{(2)} + \psi^{(1)} \cdot \psi^{(2)} \cdot \ldots \cdot \hat{H}^{(3)}\psi^{(3)} + \ldots \tag{6.21}$$

Let us assume (see Section 4.9.10)

$$\hat{H}_{\mathrm{spin}}\psi_{\mathrm{spin}} = \mathcal{E}_{\mathrm{spin}}\psi_{\mathrm{spin}}. \tag{6.22}$$

Then, expressing ψ_{spin} as the product $\psi^{(1)} \cdot \psi^{(2)} \cdot \psi^{(3)} \ldots$ results in

$$\hat{H}_{\mathrm{spin}}\psi_{\mathrm{spin}} = \psi^{(2)} \cdot \psi^{(3)} \cdot \ldots \cdot \hat{H}^{(1)}\psi^{(1)} + \psi^{(1)} \cdot \psi^{(3)} \cdot \ldots \cdot \hat{H}^{(2)}\psi^{(2)} + \psi^{(1)} \cdot \psi^{(2)} \cdot \ldots \cdot \hat{H}^{(3)}\psi^{(3)} + \cdots = \mathcal{E}_{\mathrm{spin}}\psi^{(1)} \cdot \psi^{(2)} \cdot \psi^{(3)} \ldots \tag{6.23}$$

If we divide both sides by $\psi_{\mathrm{spin}} = \psi^{(1)} \cdot \psi^{(2)} \cdot \psi^{(3)} \ldots$,

$$\frac{\hat{H}^{(1)}\psi^{(1)}}{\psi^{(1)}} + \frac{\hat{H}^{(2)}\psi^{(2)}}{\psi^{(2)}} + \frac{\hat{H}^{(3)}\psi^{(3)}}{\psi^{(3)}} + \cdots = \mathcal{E}_{\mathrm{spin}}. \tag{6.24}$$

The right-hand side is the constant $\mathcal{E}_{\mathrm{spin}}$. Therefore, all terms $\hat{H}^{(j)}\psi^{(j)}/\psi^{(j)}$ must be constant if the equation is true for *all* values of the spin degrees of freedom of all nuclei:

$$\frac{\hat{H}^{(1)}\psi^{(1)}}{\psi^{(1)}} = \mathcal{E}^{(1)}, \qquad \frac{\hat{H}^{(2)}\psi^{(2)}}{\psi^{(2)}} = \mathcal{E}^{(2)}, \qquad \frac{\hat{H}^{(3)}\psi^{(3)}}{\psi^{(3)}} = \mathcal{E}^{(3)}, \qquad \ldots$$

$$\Rightarrow \hat{H}^{(1)}\psi^{(1)} = \mathcal{E}^{(1)}\psi^{(1)}, \qquad \hat{H}^{(2)}\psi^{(2)} = \mathcal{E}^{(2)}\psi^{(2)}, \qquad \hat{H}^{(3)}\psi^{(3)} = \mathcal{E}^{(3)}\psi^{(3)},$$
$$\Rightarrow \mathcal{E}^{(1)} + \mathcal{E}^{(2)} + \mathcal{E}^{(3)} + \cdots = \mathcal{E}_{\mathrm{spin}}. \tag{6.25}$$

If the nuclei are *indistinguishable* (see Section 6.7.1), all equations $\hat{H}^{(j)}\psi^{(j)} = \mathcal{E}^{(j)}\psi^{(j)}$ are identical and the superscripts can be omitted

$$\hat{H}\psi = \mathcal{E}\psi. \tag{6.26}$$

Nuclear magnetic moments in all molecules are now described by the same spin wave function ψ and by the same Hamiltonian $\hat{H}$ with eigenvalues $\mathcal{E}_j$ and eigenfunctions ψ_j. For example, we have shown (Section 5.4) that the Hamiltonian representing the energy of a magnetic moment in a vertical magnetic field described by $\vec{B}_0$ is

$$-\frac{\gamma B_0 \hbar}{2}\begin{pmatrix} 1 & 0 \\ 0 & -1 \end{pmatrix} = \omega_0 \frac{\hbar}{2}\begin{pmatrix} 1 & 0 \\ 0 & -1 \end{pmatrix}, \tag{6.27}$$

---

[5]This is a very reasonable assumption in most cases. However, note that it is not true completely: if motions of the magnetic moments and of the molecules were independent, it would be impossible to explain how the magnetic moments reach their equilibrium distribution.

[6]We are now interested in the spin degrees of freedom, but the same arguments can be applied to any variables.

its eigenfunctions are (after separation from the wave functions describing the dependence on x, y, z) the vectors

$$\begin{pmatrix} 1 \\ 0 \end{pmatrix} = |\alpha\rangle, \qquad \begin{pmatrix} 0 \\ 1 \end{pmatrix} = |\beta\rangle, \tag{6.28}$$

and its eigenvalues are

$$-\frac{\gamma B_0 \hbar}{2} = +\omega_0 \frac{\hbar}{2} = \mathcal{E}_\alpha, \qquad +\frac{\gamma B_0 \hbar}{2} = -\omega_0 \frac{\hbar}{2} = \mathcal{E}_\beta, \tag{6.29}$$

respectively. This Hamiltonian and its eigenfunctions can be used to describe all nuclear magnetic moments of a macroscopic sample if *all consequences of interactions of individual magnetic moments* can be described by modifying only the values $\mathcal{E}_\alpha, \mathcal{E}_\beta$ to some $\mathcal{E}'_\alpha, \mathcal{E}'_\beta$ (actually, only the energy differences $\mathcal{E}_\alpha - \mathcal{E}_\beta$ and $\mathcal{E}'_\alpha - \mathcal{E}'_\beta$ are relevant). Such modification may account for the shielding magnetic fields by electrons, variation of the external field $\vec{B}_0$ etc. The modification should be general, i.e., we should be able to use a single expression for $\mathcal{E}'_\alpha - \mathcal{E}'_\beta$ of any magnetic moment in the sample.

6.7.4 Phases and coherences

The coherence $\overline{c_\beta c_\alpha^*}$ with the amplitude $\overline{|c_\alpha||c_\beta|}$ and with a phase Φ describes the *transverse polarization* of magnetic moments. In order to analyze the coherences explicitly, we use an eigenfunction of the operator representing an angular momentum pointing in a general direction, described by angles ϑ (inclination) and φ (azimuth), introduced in Section 5.7.11. The eigenfunction (cf. Eq. 5.248) is the following linear combination (superposition) of the α and β eigenstates of $\hat{I}_z$:

$$|\vartheta_j, \varphi_j\rangle = \begin{pmatrix} \cos\frac{\vartheta_j}{2} e^{-i\frac{\varphi_j}{2}} \\ \sin\frac{\vartheta_j}{2} e^{+i\frac{\varphi_j}{2}} \end{pmatrix} = \begin{pmatrix} c_{\alpha,j} \\ c_{\beta,j} \end{pmatrix} = c_{\alpha,j}|\alpha\rangle + c_{\beta,j}|\beta\rangle. \tag{6.30}$$

If states of all magnetic moments in our ensemble are described by an eigenfunction of this form, the density matrix element $\overline{c_\beta c_\alpha^*}$ is

$$\overline{c_\beta c_\alpha^*} = \overline{\cos\frac{\vartheta}{2}\sin\frac{\vartheta}{2}e^{+i\varphi}} = \frac{1}{2}\overline{\sin\vartheta e^{+i\varphi}}. \tag{6.31}$$

If the distributions of the angles ϑ and φ are independent,

$$\overline{c_\beta c_\alpha^*} = \frac{1}{2}\overline{\sin\vartheta} \cdot \overline{e^{+i\varphi}}. \tag{6.32}$$

What is the physical interpretation of such density matrix elements? If the phase φ is the same for all magnetic moments of the ensemble (it is never true in reality), the direction of the transverse polarization is given by $M_x = |M_\perp|\cos\varphi$ and $M_y = |M_\perp|\sin\varphi$. E.g., $\varphi = 0$ describes the polarization of the magnetic moments in the x direction, $\varphi = \pi/2$ describes the polarization of the magnetic moments in the y direction, etc.

What defines the values of φ_j in real samples? In Section 5.7.12, we analyzed how the phases of the c_α and c_β coefficients *evolve* in a magnetic field described by the Hamiltonian $\hat{H} = -\gamma B_0 \hat{I}_z = \omega_0 \hat{I}_z$. We have found (Eqs. 5.253–5.254) that the phases of both coefficients *rotate* with the frequencies given by the eigenvalues of the Hamiltonian ($\mathcal{E}_\alpha$ and $\mathcal{E}_\beta$):

$$c_\alpha(t) = c_\alpha(t=0)e^{+i\frac{\gamma B_0}{2}t} = \cos\frac{\vartheta}{2}e^{-i\frac{\varphi(t=0)}{2}}e^{+i\frac{\gamma B_0}{2}t} = \cos\frac{\vartheta}{2}e^{-i\frac{\varphi(t=0)}{2}}e^{-i\frac{\omega_0}{2}t} = \cos\frac{\vartheta}{2}e^{-i\frac{\varphi(t=0)}{2}}e^{+i\frac{\mathcal{E}_\alpha}{\hbar}t}, \tag{6.33}$$

$$c_\beta(t) = c_\beta(t=0)e^{-i\frac{\gamma B_0}{2}t} = \sin\frac{\vartheta}{2}e^{+i\frac{\varphi(t=0)}{2}}e^{-i\frac{\gamma B_0}{2}t} = \sin\frac{\vartheta}{2}e^{+i\frac{\varphi(t=0)}{2}}e^{+i\frac{\omega_0}{2}t} = \sin\frac{\vartheta}{2}e^{+i\frac{\varphi(t=0)}{2}}e^{-i\frac{\mathcal{E}_\beta}{\hbar}t}, \tag{6.34}$$

where we have used the explicit forms of $c_\alpha(t=0)$ and $c_\beta(t=0)$ for $|\vartheta, \varphi\rangle$, (cf. Eq. 5.248). Note that the evolution in the magnetic field $\vec{B}_0$ changes only the azimuth φ, not the inclination ϑ.

If all magnetic moments experience the same magnetic field $\vec{B}_0$, the coherence $\overline{c_\beta c_\alpha^*}$ evolves as

$$\overline{c_\beta c_\alpha^*} = \frac{1}{2}\overline{\sin\vartheta}\,\overline{e^{+i\varphi(t=0)}}\,e^{+i\omega_0 t}, \tag{6.35}$$

i.e., all azimuths φ_j evolve with the same angular frequency ω_0.

We have described the evolution of the coherence, but we have not yet specified what defines the distributions of ϑ_j and $\varphi_j(t=0)$, determining $\overline{c_\beta c_\alpha^*}$ at $t=0$, i.e., $\frac{1}{2}\overline{\sin\vartheta}\,\overline{e^{+i\varphi(t=0)}}$. The general answer is that the magnetic field felt by the magnetic moments determines the statistical distribution of ϑ_j and $\varphi_j(t=0)$. A quantitative analysis of various magnetic fields (the external static field $\vec{B}_0$, the influence

of the electrons, the field of the applied radio waves $\vec{B}_0$) is presented in the next lecture.[7] At this moment, we only comment two results that are derived in the next lecture.

The first example is an equilibrium ensemble of magnetic moments in $\vec{B}_0$. At the thermodynamic equilibrium, there is no preferred azimuth of magnetic moments in the vertical field $\vec{B}_0$. Therefore, the state of the system is an incoherent superposition of the eigenstates α and β with $\overline{\mathrm{e}^{+\mathrm{i}\varphi(t=0)}} = 0$ and consequently $\overline{c_\beta c_\alpha^*} = 0$.

The second example is an ensemble of magnetic moments in $\vec{B}_0$ after applying a radio-wave pulse that rotated the bulk magnetization to the direction y (cf. Figure 1.4). In such a case, $M_x = |M|\cos\Phi = 0$ and $M_y = |M|\sin\Phi = |M|$, telling us that $\Phi = \pi/2$ immediately after the pulse. Then, the phase factor starts to rotate with the frequency $\omega_0 = -\gamma B_0$:

$$\mathrm{e}^{\mathrm{i}\Phi} = \overline{\mathrm{e}^{+\mathrm{i}\varphi}} = \overline{\mathrm{e}^{+\mathrm{i}\varphi(t=0)}} \; \mathrm{e}^{+\mathrm{i}\omega_0 t} = \mathrm{e}^{\mathrm{i}\frac{\pi}{2}} \; \mathrm{e}^{+\mathrm{i}\omega_0 t} = \mathrm{e}^{\mathrm{i}\left(\frac{\pi}{2}+\omega_0 t\right)}. \tag{6.36}$$

Now only the magnitude $\frac{1}{2}\overline{\sin\vartheta}$ remains to be specified. In the next lecture, we derive (i) that the magnitude of the transverse polarization after the pulse is equal to the longitudinal polarization before the pulse and (ii) that the longitudinal polarization at the equilibrium is defined by a statistical relation resembling the Boltzmann's law of classical statistical mechanics.

6.7.5 From Schrödinger to Liouville-von Neumann equation

We start with the Schrödinger equation for a single spin in the matrix representation:

$$\mathrm{i}\hbar\frac{\mathrm{d}}{\mathrm{d}t}\begin{pmatrix} c_\alpha \\ c_\beta \end{pmatrix} = \begin{pmatrix} H_{\alpha,\alpha} & H_{\alpha,\beta} \\ H_{\beta,\alpha} & H_{\beta,\beta} \end{pmatrix}\begin{pmatrix} c_\alpha \\ c_\beta \end{pmatrix} = \begin{pmatrix} H_{\alpha,\alpha}c_\alpha + H_{\alpha,\beta}c_\beta \\ H_{\beta,\alpha}c_\alpha + H_{\beta,\beta}c_\beta \end{pmatrix}. \tag{6.37}$$

Note that the Hamiltonian matrix is written in a general form, the basis functions are not necessarily eigenfunctions of the operator. However, the matrix must be *Hermitian*, i.e., $H_{j,k} = H_{k,j}^*$:

$$H_{\alpha,\beta} = H_{\beta,\alpha}^* \qquad H_{\beta,\alpha} = H_{\alpha,\beta}^*. \tag{6.38}$$

If we multiply Eq. 6.37 by the basis functions from left, we obtained the differential equations for c_α and c_β (because the basis functions are orthonormal):

$$(\,1\;0\,)\mathrm{i}\hbar\frac{\mathrm{d}}{\mathrm{d}t}\begin{pmatrix} c_\alpha \\ c_\beta \end{pmatrix} = \mathrm{i}\hbar\frac{\mathrm{d}c_\alpha}{\mathrm{d}t} = H_{\alpha,\alpha}c_\alpha + H_{\alpha,\beta}c_\beta \tag{6.39}$$

$$(\,0\;1\,)\mathrm{i}\hbar\frac{\mathrm{d}}{\mathrm{d}t}\begin{pmatrix} c_\alpha \\ c_\beta \end{pmatrix} = \mathrm{i}\hbar\frac{\mathrm{d}c_\beta}{\mathrm{d}t} = H_{\beta,\alpha}c_\alpha + H_{\beta,\beta}c_\beta. \tag{6.40}$$

In general,

$$\frac{\mathrm{d}c_k}{\mathrm{d}t} = -\frac{\mathrm{i}}{\hbar}\sum_l H_{k,l}c_l \tag{6.41}$$

and its complex conjugate (using Eq. 6.38) is

$$\frac{\mathrm{d}c_k^*}{\mathrm{d}t} = +\frac{\mathrm{i}}{\hbar}\sum_l H_{k,l}^* c_l^* = +\frac{\mathrm{i}}{\hbar}\sum_l H_{l,k}c_l^*. \tag{6.42}$$

Elements of the density matrix consist of the products $c_j c_k^*$. Therefore, we must calculate

$$\frac{\mathrm{d}(c_j c_k^*)}{\mathrm{d}t} = c_j\frac{\mathrm{d}c_k^*}{\mathrm{d}t} + c_k^*\frac{\mathrm{d}c_j}{\mathrm{d}t} = \frac{\mathrm{i}}{\hbar}\sum_l H_{l,k}c_j c_l^* - \frac{\mathrm{i}}{\hbar}\sum_l H_{j,l}c_l c_k^*. \tag{6.43}$$

For multiple nuclei with the same basis,

$$\frac{\mathrm{d}(c_{j,1}c_{k,1}^* + c_{j,2}c_{k,2}^* + \cdots)}{\mathrm{d}t} = c_{j,1}\frac{\mathrm{d}c_{k,1}^*}{\mathrm{d}t} + c_{k,1}^*\frac{\mathrm{d}c_{j,1}}{\mathrm{d}t} + c_{j,2}\frac{\mathrm{d}c_{k,2}^*}{\mathrm{d}t} + c_{k,2}^*\frac{\mathrm{d}c_{j,2}}{\mathrm{d}t} + \cdots \tag{6.44}$$

$$= \frac{\mathrm{i}}{\hbar}\sum_l H_{l,k}(c_{j,1}c_{l,1}^* + c_{j,2}c_{l,2}^* + \cdots) - \frac{\mathrm{i}}{\hbar}\sum_l H_{j,l}(c_{l,1}c_{k,1}^* + c_{l,2}c_{k,2}^* + \cdots). \tag{6.45}$$

Note that

---

[7]Setting the beginning of the time scale is somewhat tricky. Therefore we start the analysis by defining the elements of the density matrix (the distribution of ϑ_j and φ_j) for a *stationary macroscopic state*, when the density matrix does not depend on time. Then we can start to vary the magnetic fields and count the time from the first applied change.

$$\sum_l (c_{j,1} c_{l,1}^* + c_{j,2} c_{l,2}^* + \cdots) H_{l,k} = N \sum_l \rho_{j,l} H_{l,k} \tag{6.46}$$

is the j,k element of the product $N\hat{\rho}\hat{H}$, and

$$\sum_l H_{j,l}(c_{l,1} c_{k,1}^* + c_{l,2} c_{k,2}^* + \cdots) = N \sum_l H_{j,l} \rho_{l,k} \tag{6.47}$$

is the j,k element of the product $N\hat{H}\hat{\rho}$. Therefore, we can write the equation of motion for the whole density matrix as

$$\frac{\mathrm{d}\hat{\rho}}{\mathrm{d}t} = \frac{\mathrm{i}}{\hbar}(\hat{\rho}\hat{H} - \hat{H}\hat{\rho}) = \frac{\mathrm{i}}{\hbar}[\hat{\rho}, \hat{H}] = -\frac{\mathrm{i}}{\hbar}[\hat{H}, \hat{\rho}]. \tag{6.48}$$

6.7.6   Rotation in operator space

Let us look at an example[8] for $\mathscr{H} = \varepsilon_t \mathscr{I}_t + \omega_0 \mathscr{I}_z$ and $\hat{\rho} = c_x \mathscr{I}_x + c_y \mathscr{I}_y + c_z \mathscr{I}_z + c_t \mathscr{I}_t$.

Let us first evaluate the commutators from the Liouville-von Neumann equation:

$\mathscr{I}_t$ is proportional to a unit matrix $\Rightarrow$ it must commute with all matrices:

$$[\mathscr{I}_t, \mathscr{I}_j] = 0 \qquad (j = x, y, z, t). \tag{6.49}$$

Commutators of $\mathscr{I}_z$ are given by the definition of angular momentum operators (Eqs. 4.35–4.38):

$$[\mathscr{I}_z, \mathscr{I}_z] = [\mathscr{I}_z, \mathscr{I}_t] = 0 \qquad [\mathscr{I}_z, \mathscr{I}_x] = \mathrm{i}\mathscr{I}_y \qquad [\mathscr{I}_z, \mathscr{I}_y] = -\mathrm{i}\mathscr{I}_x. \tag{6.50}$$

Let us write the Liouville-von Neumann equation with the evaluated commutators:

$$\frac{\mathrm{d}c_x}{\mathrm{d}t}\mathscr{I}_x + \frac{\mathrm{d}c_y}{\mathrm{d}t}\mathscr{I}_y + \frac{\mathrm{d}c_z}{\mathrm{d}t}\mathscr{I}_z + \frac{\mathrm{d}c_t}{\mathrm{d}t}\mathscr{I}_t = \mathrm{i}\left(-\mathrm{i}\omega_0 c_x \mathscr{I}_y + \mathrm{i}\omega_0 c_y \mathscr{I}_x\right). \tag{6.51}$$

Written in a matrix representation (noticing that c_z and c_t do not evolve because the $c_z \mathscr{I}_z$ and $c_t \mathscr{I}_t$ components of the density matrix commute with both matrices constituting the Hamiltonian),

$$\frac{\mathrm{d}c_x}{\mathrm{d}t}\frac{1}{2}\begin{pmatrix} 0 & 1 \\ 1 & 0 \end{pmatrix} + \frac{\mathrm{d}c_y}{\mathrm{d}t}\frac{1}{2}\begin{pmatrix} 0 & -\mathrm{i} \\ \mathrm{i} & 0 \end{pmatrix} + 0 + 0 = \omega_0 c_x \frac{1}{2}\begin{pmatrix} 0 & -\mathrm{i} \\ \mathrm{i} & 0 \end{pmatrix} - \omega_0 c_y \frac{1}{2}\begin{pmatrix} 0 & 1 \\ 1 & 0 \end{pmatrix}, \tag{6.52}$$

$$\frac{1}{2}\begin{pmatrix} 0 & \frac{\mathrm{d}c_x}{\mathrm{d}t} \\ \frac{\mathrm{d}c_x}{\mathrm{d}t} & 0 \end{pmatrix} + \frac{1}{2}\begin{pmatrix} 0 & -\mathrm{i}\frac{\mathrm{d}c_y}{\mathrm{d}t} \\ \mathrm{i}\frac{\mathrm{d}c_y}{\mathrm{d}t} & 0 \end{pmatrix} + 0 + 0 = \frac{\mathrm{i}}{2}\begin{pmatrix} 0 & -\omega_0 c_x \\ \omega_0 c_x & 0 \end{pmatrix} + \frac{\mathrm{i}}{2}\begin{pmatrix} 0 & \mathrm{i}\omega_0 c_y \\ \mathrm{i}\omega_0 c_y & 0 \end{pmatrix}. \tag{6.53}$$

Adding the matrices,

$$\begin{pmatrix} 0 & \frac{\mathrm{d}(c_x - \mathrm{i}c_y)}{\mathrm{d}t} \\ \frac{\mathrm{d}(c_x + \mathrm{i}c_y)}{\mathrm{d}t} & 0 \end{pmatrix} = \mathrm{i}\omega_0 \begin{pmatrix} 0 & -(c_x - \mathrm{i}c_y) \\ c_x + \mathrm{i}c_y & 0 \end{pmatrix}. \tag{6.54}$$

This corresponds to a set of two differential equations

$$\frac{\mathrm{d}(c_x - \mathrm{i}c_y)}{\mathrm{d}t} = -\mathrm{i}\omega_0(c_x - \mathrm{i}c_y) \tag{6.55}$$

$$\frac{\mathrm{d}(c_x + \mathrm{i}c_y)}{\mathrm{d}t} = +\mathrm{i}\omega_0(c_x + \mathrm{i}c_y) \tag{6.56}$$

with the same structure as Eqs. 4.154 and 4.155. The solution is

$$c_x - \mathrm{i}c_y = (c_x(0) - \mathrm{i}c_y(0))\mathrm{e}^{-\mathrm{i}\omega_0 t} = c_0 \mathrm{e}^{-\mathrm{i}(\omega_0 t + \phi_0)} \tag{6.57}$$

$$c_x + \mathrm{i}c_y = (c_x(0) + \mathrm{i}c_y(0))\mathrm{e}^{+\mathrm{i}\omega_0 t} = c_0 \mathrm{e}^{+\mathrm{i}(\omega_0 t + \phi_0)} \tag{6.58}$$

with the amplitude c_0 and phase ϕ_0 given by the initial conditions. It corresponds to

---

[8]Various Hamiltonians encountered in NMR spectroscopy are discussed in the next lectures. At this moment, take $\mathscr{H} = \varepsilon_t \mathscr{I}_t + \omega_0 \mathscr{I}_z$ just as an example.

$$c_x = c_0 \cos(\omega_0 t + \phi_0) \tag{6.59}$$

$$c_y = c_0 \sin(\omega_0 t + \phi_0). \tag{6.60}$$

We see that coefficients c_x, c_y, c_z play the same roles as coordinates r_x, r_y, r_z in Eqs. 4.151–4.153, respectively, and operators $\mathscr{I}_x$, $\mathscr{I}_y$, $\mathscr{I}_z$ play the same role as unit vectors $\vec{\imath}, \vec{\jmath}, \vec{k}$, defining directions of the axes of the Cartesian coordinate system. Therefore, evolution of $\hat{\rho}$ in our case can be described as a rotation of a three-dimensional vector consisting of the elements c_x, c_y, c_z in an abstract three-dimensional space defined by $\mathscr{I}_x$, $\mathscr{I}_y$, and $\mathscr{I}_z$. In our case, if $\phi = 0$, then $\hat{\rho}(0) = c_0 \mathscr{I}_x + c_z \mathscr{I}_z + c_t \mathscr{I}_t$ and it evolves as

$$c_0 \mathscr{I}_x + c_z \mathscr{I}_z + c_t \mathscr{I}_t \longrightarrow c_0 \mathscr{I}_x \cos(\omega_0 t) + c_0 \mathscr{I}_y \sin(\omega_0 t) + c_z \mathscr{I}_z + c_t \mathscr{I}_t. \tag{6.61}$$

Lecture 7
Chemical shift, one-pulse experiment

Literature: The operator of magnetization is described in C2.4.1, Hamiltonians discussed in L8, thermal equilibrium in L11.3, C2.4.1, K6.8.6, relaxation due to the chemical shift in C5.4.4, K9.10 (very briefly, the quantum approach to relaxation is usually introduced using dipole-dipole interactions as an example). The one-pulse experiment is analyzed in K7.2.1, L11.11 and L11.12.

7.1 Operator of the observed quantity

The quantity observed in the NMR experiment is the *bulk magnetization* $\vec{M}$, i.e., the sum of the magnetic moments of all nuclei divided by volume of the sample, assuming isotropic distribution of the nuclei in the sample. Technically, we observe oscillations in the plane perpendicular to the homogeneous field of the magnet $\vec{B}_0$. The associated oscillations of the magnetic fields of nuclei induce *electromotive force* in the detector coil, as described by Eq. 55. Since a complex signal is usually recorded (see Section 3.2), the operator of complex magnetization $M_+ = M_x + \mathrm{i}M_y$ is used ($M_- = M_x - \mathrm{i}M_y$ can be used as well).

$$\hat{M}_+ = \mathcal{N}\gamma(\hat{I}_x + \mathrm{i}\hat{I}_y) = \mathcal{N}\gamma\hat{I}_+, \tag{7.1}$$

where $\mathcal{N}$ is the number of nuclei in the sample per unit volume.

7.2 Hamiltonian of the static field $\vec{B}_0$

The Hamiltonian of the static homogeneous magnetic field $\vec{B}_0$ can be easily derived from the classical description of energy of a magnetic moment in a magnetic field (Eq. 6):

$$\mathcal{E} = -\vec{\mu} \cdot \vec{B}_0. \tag{7.2}$$

Since $\vec{B}_0$ defines direction of the z axis,

$$\mathcal{E} = -\vec{\mu} \cdot \vec{B}_0 = -\mu_z B_0 = -\gamma B_0 I_z. \tag{7.3}$$

Replacing the value of I_z (z-component of the spin angular momentum) by its operator provides the Hamiltonian:

$$\hat{H}_{0,\text{lab}} = -\gamma B_0 \hat{I}_z. \tag{7.4}$$

7.3 Hamiltonian of the radio field $\vec{B}_1$

Using radio waves in NMR spectroscopy has two consequences. First, frequency of the radio waves defines angular frequency of the *rotating coordinate frame*, used to describe evolution of the distribution of the magnetic moments in the presence, but also in the absence of radio waves. Second, radio waves allow us to change the distribution of the magnetic moments, described by the probability density matrix $\hat{\rho}$.

The oscillating magnetic field of radio waves irradiating the sample is usually approximated by a magnetic field $\vec{B}_1$ rotating with the frequency of the radio waves ω_{radio} (validity of such approximation is discussed in Sections 5.7.14–5.7.18). Evolution of the density matrix is then described in a coordinate frame rotating with the opposite angular frequency $\omega_{\text{rot}} = -\omega_{\text{radio}}$, as described in Section 1.5.6. The x axis of the rotating coordinate frame is defined by the direction of the B_1 vector. The phase ϕ_{rot} of this vector is given by the convention described in Section 1.5.6.

In the rotating coordinate system, frequency of the rotation of the coordinate frame[1] is subtracted from the precession frequency and the difference $\Omega = \omega_0 - \omega_{\text{rot}} = -\gamma B_0 - \omega_{\text{rot}}$ is the frequency offset defining the evolution in the rotating frame in the absence of other fields:[2]

In the absence of other fields than $\vec{B}_0$,

$$\hat{H}_{0,\text{rot}} = (-\gamma B_0 - \omega_{\text{rot}})\hat{I}_z = \Omega\hat{I}_z. \tag{7.5}$$

During irradiation by the radio wave, the magnetic field of the radio wave influences the distribution of the magnetic moments described by $\hat{\rho}$. The Hamiltonian contains an additional term $\hat{H}_{1,\text{rot}}$ describing the effect of the field of the radio waves:

$$\hat{H}_{0,\text{rot}} + \hat{H}_{1,\text{rot}} = (-\gamma B_0 - \omega_{\text{rot}})\hat{I}_z - \gamma B_1 \hat{I}_x = \Omega\hat{I}_z + \omega_1 \hat{I}_x. \tag{7.6}$$

As the radio frequency ω_{radio} (and consequently ω_{rot}) should be close to the precession frequency of the magnetic moments of the observed nuclei, we can assume $|\Omega| \ll |\gamma B_0|$. If the radio frequency is very close to the resonance, $-\gamma B_0 \approx \omega_{\text{rot}}$, $\Omega \ll \omega_1$, and the $\hat{I}_z$ component of the Hamiltonian can be neglected.

The above description is sufficient for a one-dimensional experiment, discussed in this lecture. However, radio waves are applied in several pulses in many NMR experiments. During different pulses, the phase of the radio waves is often shifted. In such a case, it is the phase of the first pulse which defines the x axis of the rotating coordinate frame. In order to be able to analyze the multiple radio pulses later in our course, we now also describe the form of a Hamiltonian of the magnetic field affecting the magnetic moments during irradiation by a wave shifted by $\pi/2$ from the phase of the first pulse:

---

[1] Formally opposite to ω_{radio}.

[2] Note that eigenvalues of such Hamiltonian are not values of the energy in the field $\vec{B}_0$.

$$\hat{H}_{0,\text{rot}} + \hat{H}_{1,\text{rot}} = (-\gamma B_0 - \omega_{\text{rot}})\hat{I}_z - \gamma B_1 \hat{I}_y = \Omega \hat{I}_z + \omega_1 \hat{I}_y. \tag{7.7}$$

Note that such a radio wave (phase shifted by $\pi/2$ from the first pulse) defines the direction of the y axis of the rotating frame. Therefore, a pulse of such a wave is referred to as a y-pulse. In a similar manner, we describe pulses of waves shifted by π or $3\pi/2$ as $-x$ or $-y$ pulses, respectively.

7.4 Hamiltonian of chemical shift

In addition to the external field, magnetic moments are also influenced by magnetic fields of electrons in the molecules. In order to describe our ensemble of spin magnetic moments by a 2×2 density matrix, the interactions with the electrons must modify only eigenvalues, not eigenfunctions of the already introduced Hamiltonians. The concept of the chemical shift tensor, introduced during our classical treatment of the magnetic fields of moving electrons in Section 1.4, allows us to include the chemical shift into the already defined Hamiltonians without changing their eigenfunctions. The values of μ_x, μ_y, and μ_z in the classical equations are simply replaced by the operators $\hat{I}_x$, $\hat{I}_y$, and $\hat{I}_z$:

$$\hat{H}_\delta = -\gamma(\hat{I}_x B_{\text{e},x} + \hat{I}_y B_{\text{e},y} + \hat{I}_z B_{\text{e},z}) = -\gamma(\hat{I}_x \ \hat{I}_y \ \hat{I}_z) \begin{pmatrix} B_{\text{e},x} \\ B_{\text{e},y} \\ B_{\text{e},z} \end{pmatrix} =$$

$$= -\gamma(\hat{I}_x \ \hat{I}_y \ \hat{I}_z) \begin{pmatrix} \delta_{xx} & \delta_{xy} & \delta_{xz} \\ \delta_{yx} & \delta_{yy} & \delta_{yz} \\ \delta_{zx} & \delta_{zy} & \delta_{zz} \end{pmatrix} \begin{pmatrix} B_{0,x} \\ B_{0,y} \\ B_{0,z} \end{pmatrix} = -\gamma \hat{\vec{I}} \cdot \underline{\delta} \cdot \vec{B}_0. \tag{7.8}$$

As we have also learnt in Section 1.4, we can decompose the chemical shift tensor $\underline{\delta}$ into isotropic, axially symmetric and asymmetric (rhombic) components. The corresponding decomposition of the chemical shift Hamiltonian to $\hat{H}_{\delta,\text{i}}$, $\hat{H}_{\delta,\text{a}}$, and $\hat{H}_{\delta,\text{r}}$ is presented in Section 7.12.1. The complete Hamiltonian of a magnetic moment of a nucleus not interacting with magnetic moments of other nuclei in the presence of the static field $\vec{B}_0$ but in the absence of the radio waves is given by

$$\hat{H} = \hat{H}_{0,\text{lab}} + \hat{H}_{\delta,\text{i}} + \hat{H}_{\delta,\text{a}} + \hat{H}_{\delta,\text{r}}. \tag{7.9}$$

If we insert the explicit forms of $\hat{H}_{\delta,\text{i}}$, $\hat{H}_{\delta,\text{a}}$, and $\hat{H}_{\delta,\text{r}}$ (Section 7.12.1) to Eq. 7.9, the Hamiltonian including the chemical shift becomes very complicated. Fortunately, it can be simplified in many cases, as we show in the following sections.

7.5 Secular approximation and averaging

- The components of the induced fields $B_{\text{e},x}$ and $B_{\text{e},y}$ are perpendicular to $\vec{B}_0$. The contributions of $\hat{H}_{\delta,\text{i}}$ are constant and the contributions of $\hat{H}_{\delta,\text{a}}$ and $\hat{H}_{\delta,\text{r}}$ fluctuate with the molecular motions changing values of φ, ϑ, and χ. Since the molecular motions do not resonate (in general) with the precession frequency $-\gamma B_0$, the components $B_{\text{e},x}\hat{I}_x$ and $B_{\text{e},y}\hat{I}_y$ of the Hamiltonian

oscillate (in addition to fluctuations due to the molecular motions) rapidly with a frequency close to $-\gamma B_0$ in the rotating coordinate frame. These oscillations are much faster than the precession about $B_{\mathrm{e},x}$ and $B_{\mathrm{e},y}$ (because the field $\vec{B}_0$ is much larger than $\vec{B}_{\mathrm{e}}$) and effectively average to zero on the timescale longer than $1/(\gamma B_0)$ (typically nanoseconds). Therefore, the $B_{\mathrm{e},x}\hat{I}_x$ and $B_{\mathrm{e},y}\hat{I}_y$ terms can be neglected if the effects on the longer timescales are studied. Such a simplification is known as the *secular approximation*.[3] The secular approximation simplifies the (time-averaged) Hamiltonian to

$$\hat{H} = -\gamma B_0(1 + \delta_{\mathrm{i}} + \delta_{\mathrm{a}}\langle 3\cos^2\vartheta - 1\rangle + \delta_{\mathrm{r}}\langle\cos(2\chi)\sin^2\vartheta\rangle)\hat{I}_z \qquad (7.10)$$

- If the sample is an isotropic liquid, averaging over all molecules of the sample further simplifies the Hamiltonian. As no orientation of the molecule is preferred, all values of χ are equally probable and independent of ϑ. Therefore, the last term in Eq. 7.10 is averaged to zero. Moreover, average values of $Z_x^2 = \cos^2\varphi\sin^2\vartheta$, of $Z_y^2 = \sin^2\varphi\sin^2\vartheta$, and of $Z_z^2 = \cos^2\vartheta$ must be the same because none of the directions x, y, z is preferred. The consequence has been already discussed when we described relaxation classically (Eq. 2.42 in Section 2.5.1): $\overline{(3\cos^2\vartheta - 1)} = 0$ and the anisotropic and rhombic contributions can be neglected.

> The Hamiltonian describing the effects of the static external magnetic field and coherent effects of the electrons in isotropic liquids reduces to
>
> $$\hat{H} = -\gamma B_0(1 + \delta_{\mathrm{i}})\hat{I}_z. \qquad (7.11)$$

Note that the described simplifications can be used only if they are applicable. Eq. 7.11 is valid only in isotropic liquids, not in liquid crystals, stretched gels, polycrystalline powders, monocrystals, etc.! Moreover, Eq. 7.11 does not describe relaxation processes, as discussed in Section 7.7.

7.6 Thermal equilibrium as the initial state

Knowledge of the Hamiltonian allows us to derive the density matrix at the beginning of the experiment. Usually, we start from the thermal equilibrium. If the equilibrium is achieved, phases of individual magnetic moments are random and the magnetic moments precess incoherently. Therefore, the off-diagonal elements (*coherences*) of the equilibrium density matrix (proportional to $\mathscr{I}_x$ and $\mathscr{I}_y$) are equal to zero. Values of the diagonal elements (*populations*) are derived in Section 7.12.2 and the complete equilibrium density matrix is

---

[3]In terms of quantum mechanics, eigenfunctions of $B_{\mathrm{e},x}\hat{I}_x$ and $B_{\mathrm{e},y}\hat{I}_y$ differ from the eigenfunctions of $\hat{H}_{0,\mathrm{lab}}$ ($|\alpha\rangle$ and $|\beta\rangle$). Therefore, the matrix representation of $B_{\mathrm{e},x}\hat{I}_x$ and $B_{\mathrm{e},y}\hat{I}_y$ contains off-diagonal elements. Terms proportional to $\hat{I}_z$ represent so-called *secular* part of the Hamiltonian, which does not change the $|\alpha\rangle$ and $|\beta\rangle$ states (because they are eigenfunctions of $\hat{I}_z$). Terms proportional to $\hat{I}_x$ and $\hat{I}_y$ are *non-secular* because they change the $|\alpha\rangle$ and $|\beta\rangle$ states ($|\alpha\rangle$ and $|\beta\rangle$ are not eigenfunctions of $\hat{I}_x$ or $\hat{I}_y$). However, eigenvalues of $B_{\mathrm{e},x}\hat{I}_x$ and $B_{\mathrm{e},y}\hat{I}_y$, defining the off-diagonal elements, are much smaller than the eigenvalues of $\hat{H}_{0,\mathrm{lab}}$ (because the field $\vec{B}_{\mathrm{e}}$ is much smaller than $\vec{B}_0$). The *secular approximation* represents neglecting such small off-diagonal elements in the matrix representation of the total Hamiltonian and keeping only the diagonal secular terms.

$$\hat{\rho}^{\mathrm{eq}} = \begin{pmatrix} \frac{1}{2} + \frac{\gamma B_0 \hbar}{4k_{\mathrm{B}}T} & 0 \\ 0 & \frac{1}{2} - \frac{\gamma B_0 \hbar}{4k_{\mathrm{B}}T} \end{pmatrix} = \frac{1}{2}\begin{pmatrix} 1 & 0 \\ 0 & 1 \end{pmatrix} + \frac{\gamma B_0 \hbar}{4k_{\mathrm{B}}T}\begin{pmatrix} 1 & 0 \\ 0 & -1 \end{pmatrix} = \mathscr{I}_t + \kappa \mathscr{I}_z, \tag{7.12}$$

where

$$\kappa = \frac{\gamma B_0 \hbar}{2k_{\mathrm{B}}T}. \tag{7.13}$$

Note that we derived the quantum description of a *mixed state.* The difference in two diagonal elements (populations) of the density matrix describes the *longitudinal polarization* of the magnetic moments (their sum is equal to one by definition). Populations do not tell us anything about microscopic states of the individual magnetic moments. The two-dimensional density matrix does not imply that all magnetic moments are in one of two eigenstates!

7.7 Relaxation due to chemical shift anisotropy

The simplified Eq. 7.11 does not describe the effects of fast fluctuations, resulting in the relaxation. In order to derive the quantum description of the relaxation caused by the chemical shift, the Liouville-von Neumann equation must be solved for the complete Hamiltonian including the axial and rhombic contributions. Bloch, Wangsness, and Redfield developed a theory, described in Section 7.12.3, that treats the magnetic moments quantum mechanically and their molecular surroundings classically.[4] The theory provides the same definitions of the rate constants describing relaxation due to chemical shift anisotropy as we derived classically in Section 2.5.1.

$$R_1 = \frac{3}{4}b^2\left(\frac{1}{2}J(\omega_0) + \frac{1}{2}J(-\omega_0)\right) \approx \frac{3}{4}b^2 J(\omega_0), \tag{7.14}$$

$$R_2 = b^2\left(\frac{1}{2}J(0) + \frac{3}{8}J(\omega_0)\right) \approx R_0 + \frac{1}{2}R_1, \tag{7.15}$$

where $b = -2\gamma B_0 \delta_{\mathrm{a}}$ and $J(\omega)$ is the spectral density function introduced in Section 2.3.

7.8 One-pulse experiment

Having the initial form of the density matrix, the Hamiltonians, and the operator of the measured quantity, we can proceed and describe a real NMR experiment for a sample consisting of isolated magnetic moments (not interacting with each other). The basic NMR experiment consists of two parts. In the first part, the radio-wave transmitter is switched on for a short time, needed to rotate the magnetization to the plane perpendicular to the magnetic filed $\vec{B}_0$. Such application of the radio wave is called *excitation pulse.* In the second part, the radio-wave transmitter is switched off but the receiver is switched on in order to detect rotation of the magnetization vector about the direction of

---

[4]The surroundings can be also treated quantum mechanically, as described in Abragam: The principles of nuclear magnetism, Oxford Press 1961, Chapter VIII, Section II.D.

$\vec{B}_0$. We start by describing the density matrix before the experiment, then we analyze evolution of the density matrix during these two periods, evaluate the relaxation rate, and finally we calculate the magnetization contributing to the detected signal.

7.9   One-pulse experiment: excitation

At the beginning of the experiment, the density matrix describes thermal equilibrium (Eq. 7.12):

$$\hat{\rho}(0) = \mathscr{I}_t + \kappa \mathscr{I}_z. \tag{7.16}$$

The Hamiltonian governing evolution of the system during the first part of the experiment consists of coherent and fluctuating terms. The fluctuating contributions result in *relaxation*, described by the relaxation rates R_1 and R_2. The coherent contributions include

$$\mathscr{H} = -\gamma B_0(1 + \delta_{\mathrm{i}})\mathscr{I}_z - \gamma B_1(1 + \delta_{\mathrm{i}})\cos(-\omega_{\mathrm{radio}}t)\mathscr{I}_x - \gamma B_1(1 + \delta_{\mathrm{i}})\sin(-\omega_{\mathrm{radio}}t)\mathscr{I}_y, \tag{7.17}$$

where we have chosen the directions x and y so that the initial phase $\phi_{\mathrm{radio}} = 0$ (see Section 1.5.6). The Hamiltonian simplifies in a coordinate system rotating with $\omega_{\mathrm{rot}} = -\omega_{\mathrm{radio}}$

$$\mathscr{H} = \underbrace{(-\gamma B_0(1 + \delta_{\mathrm{i}}) - \omega_{\mathrm{rot}})}_{\Omega} \mathscr{I}_z + \underbrace{(-\gamma B_1(1 + \delta_{\mathrm{i}}))}_{\omega_1} \mathscr{I}_x, \tag{7.18}$$

but it still contains non-commuting terms ($\mathscr{I}_x$ *vs.* $\mathscr{I}_z$). Let us check what can be neglected to keep only commuting terms, which allows us to solve the Liouville-von Neumann equation using the simple geometric approach.

- The value of ω_1 defines how much of the magnetization is rotated to the x, y plane. The maximum effect is obtained for $\omega_1 \tau_{\mathrm{p}} = \pi/2$, where τ_{p} is the length of the radio-wave pulse. Typical values of τ_{p} for proton are approximately $10\,\mu\mathrm{s}$, corresponding to frequency of rotation of $25\,\mathrm{kHz}$ ($90°$ rotation in $10\,\mu\mathrm{s}$ corresponds to $40\,\mu\mathrm{s}$ for a full circle, $1/40\,\mu\mathrm{s} = 25\,\mathrm{kHz}$).

- Typical values of R_1 are $10^{-1}\,\mathrm{s}^{-1}$ to $10^0\,\mathrm{s}^{-1}$ and typical values of R_2 are $10^{-1}\,\mathrm{s}^{-1}$ to $10^2\,\mathrm{s}^{-1}$ for protons in organic molecules and biomacromolecules. Therefore, effects of relaxations can be safely neglected during τ_{p}.

- When observing a single type of proton (or other nucleus), Ω can be set to zero by the choice of ω_{radio}. However, variation of Ω is what we observe in real samples, containing protons (or other nuclei) with various δ_{i}. The typical range of proton δ_{i} is $10\,\mathrm{ppm}$, corresponding to $5\,\mathrm{kHz}$ at a $500\,\mathrm{MHz}$ spectrometer.[5] The carrier frequency ω_{radio} is often set to the precession frequency of the solvent. In the case of water, it is roughly in the middle of the spectrum ($4.7\,\mathrm{ppm}$ at pH 7). So, we need to cover $\pm 2.5\,\mathrm{kHz}$. We see that $|\Omega| < |\omega_1|$, but the value of $|\Omega|$ is $10\,\%$ of $|\omega_1|$ at the edge of the spectrum, which is not completely negigible.

---

[5]Chosen as a compromise here: spectra of small molecules are usually recorded at $300\,\mathrm{MHz}$–$500\,\mathrm{MHz}$, while spectra of biomacromolecules are recorded at $\geq 500\,\mathrm{MHz}$.

In summary, we see that we can safely ignore fluctuating contributions, but we must be careful when neglecting $\Omega \mathscr{I}_z$. The latter approximation allows us to use the geometric solution of the Liouville-von Neumann equation, but is definitely not perfect for larger Ω resulting in *offset effects*.

Using the simplified Hamiltonian $\mathscr{H} = \omega_1 \mathscr{I}_x$, evolution of $\hat{\rho}$ during τ_{p} can be described as a rotation about the "$\mathscr{I}_x$ axis":

$$\hat{\rho}(0) = \mathscr{I}_t + \kappa \mathscr{I}_z \longrightarrow \hat{\rho}(\tau_{\mathrm{p}}) = \mathscr{I}_t + \kappa(\mathscr{I}_z \cos(\omega_1 \tau_{\mathrm{p}}) - \mathscr{I}_y \sin(\omega_1 \tau_{\mathrm{p}})). \tag{7.19}$$

For a 90° pulse,

$$\hat{\rho}(\tau_{\mathrm{p}}) = \mathscr{I}_t - \kappa \mathscr{I}_y. \tag{7.20}$$

7.10 One-pulse experiment: detection

After switching off the transmitter, $\omega_1 \mathscr{I}_x$ disappears from the Hamiltonian, which now contains only commuting terms. On the other hand, the signal is typically acquired for a relatively long time (0.1 s to 10 s) to achieve a good frequency resolution. Therefore, the relaxation effects cannot be neglected.

The coherent evolution can be described as a rotation about the "$\mathscr{I}_z$ axis" with the angular frequency Ω

$$\hat{\rho}(t) = \mathscr{I}_t + \kappa(-\mathscr{I}_y \cos(\Omega t) + \mathscr{I}_x \sin(\Omega t)). \tag{7.21}$$

The measured quantity M_+ can be expressed as (Eq. 4.12)

$$\langle M_+ \rangle = \mathrm{Tr}\{\hat{\rho}(t)\hat{M}_+\} = \mathcal{N}\gamma\hbar\mathrm{Tr}\{(\mathscr{I}_t + \kappa(-\mathscr{I}_y \cos(\Omega t) + \mathscr{I}_x \sin(\Omega t))\mathscr{I}_+\} \tag{7.22}$$

$$= \mathcal{N}\gamma\hbar\mathrm{Tr}\{\mathscr{I}_t\mathscr{I}_+\} - \mathcal{N}\gamma\hbar\kappa\cos(\Omega t)\mathrm{Tr}\{\mathscr{I}_y\mathscr{I}_+\} + \mathcal{N}\gamma\hbar\kappa\sin(\Omega t)\mathrm{Tr}\{\mathscr{I}_x\mathscr{I}_+\}. \tag{7.23}$$

The final expression includes the following three traces:

$$\mathrm{Tr}\{\mathscr{I}_t\mathscr{I}_+\} = \mathrm{Tr}\left\{ \begin{pmatrix} \frac{1}{2} & 0 \\ 0 & \frac{1}{2} \end{pmatrix} \begin{pmatrix} 0 & 1 \\ 0 & 0 \end{pmatrix} \right\} = \mathrm{Tr}\left\{ \begin{pmatrix} 0 & \frac{1}{2} \\ 0 & 0 \end{pmatrix} \right\} = 0 \tag{7.24}$$

$$\mathrm{Tr}\{\mathscr{I}_x\mathscr{I}_+\} = \mathrm{Tr}\left\{ \begin{pmatrix} 0 & \frac{1}{2} \\ \frac{1}{2} & 0 \end{pmatrix} \begin{pmatrix} 0 & 1 \\ 0 & 0 \end{pmatrix} \right\} = \mathrm{Tr}\left\{ \begin{pmatrix} 0 & 0 \\ 0 & \frac{1}{2} \end{pmatrix} \right\} = \frac{1}{2} \tag{7.25}$$

$$\mathrm{Tr}\{\mathscr{I}_y\mathscr{I}_+\} = \mathrm{Tr}\left\{ \begin{pmatrix} 0 & -\frac{\mathrm{i}}{2} \\ \frac{\mathrm{i}}{2} & 0 \end{pmatrix} \begin{pmatrix} 0 & 1 \\ 0 & 0 \end{pmatrix} \right\} = \mathrm{Tr}\left\{ \begin{pmatrix} 0 & 0 \\ 0 & \frac{\mathrm{i}}{2} \end{pmatrix} \right\} = \frac{\mathrm{i}}{2} \tag{7.26}$$

As mentioned above, relaxation effects should be taken into account when analyzing acquisition of the NMR signal. Including the exponential relaxation term and expressing κ

$$\langle M_+ \rangle = \frac{\mathcal{N}\gamma^2\hbar^2 B_0}{4k_{\mathrm{B}}T}\mathrm{e}^{-R_2 t}(\sin(\Omega t) - \mathrm{i}\cos(\Omega t)), \tag{7.27}$$

which can be rewritten as

$$\langle M_+ \rangle = \frac{\mathcal{N}\gamma^2\hbar^2 B_0}{4k_{\mathrm{B}}T}\mathrm{e}^{-R_2 t}(-\mathrm{i})\left(\cos\left(\Omega t\right) + \mathrm{i}\sin\left(\Omega t\right)\right) = \frac{\mathcal{N}\gamma^2\hbar^2 B_0}{4k_{\mathrm{B}}T}\mathrm{e}^{-R_2 t}\mathrm{e}^{\mathrm{i}\Omega t}\mathrm{e}^{-\mathrm{i}\frac{\pi}{2}}. \qquad (7.28)$$

We know that in order to obtain purely Lorentzian (absorption) real component of the spectrum by Fourier transformation, the signal should evolve as $\mathrm{e}^{-R_2 t}\mathrm{e}^{\mathrm{i}\Omega t}$. We see that the magnetization described by Eq. 7.28 is shifted from the ideal signal by a phase of $-\pi/2$. However, this is true only if the evolution starts *exactly* at $t = 0$. In practice, this is impossible to achieve for various technical reasons (instrumental delays and phase shifts, evolution starts already during τ_{p}, etc.). Therefore, the rotation has an unknown phase shift ϕ (including the $\pi/2$ shift among other contributions), which is removed by an empirical correction during signal processing (corresponding to multiplying Eq. 7.28 by $\mathrm{e}^{\mathrm{i}\pi/2}$). It tells us that we can ignore the phase shift and write the phase-corrected signal as

$$\langle M_+ \rangle = \frac{\mathcal{N}\gamma^2\hbar^2 B_0}{4k_{\mathrm{B}}T}\mathrm{e}^{-R_2 t}(\cos(\Omega t) + \mathrm{i}\sin(\Omega t)) = \frac{\mathcal{N}\gamma^2\hbar^2 B_0}{4k_{\mathrm{B}}T}\mathrm{e}^{-R_2 t}\mathrm{e}^{\mathrm{i}\Omega t}. \qquad (7.29)$$

Knowing the expected magnetization, we can try to describe the one-dimensional NMR spectrum quantitatively. Factors that should be taken into account are listed and analyzed in Sections 7.12.4 and 7.12.5. The analysis shows that the signal-to-noise ratio is proportional to $|\gamma|^{5/2}B_0^{3/2}$ and further influenced by the relaxation, that strongly depends on the temperature.

7.11   Conclusions

In general, the analysis of an ideal one-pulse experiment leads to the following conclusions:

- The analysis of a one-pulse NMR experiment shows that the density matrix evolves as

$$\hat{\rho}(t) \propto \mathscr{I}_x \cos(\Omega t + \phi) + \mathscr{I}_y \sin(\Omega t + \phi) + \text{terms orthogonal to } \mathscr{I}_+, \qquad (7.30)$$

and that the magnetization rotates during signal acquisition as

$$\langle M_+ \rangle = |M_+|\mathrm{e}^{-R_2 t}\mathrm{e}^{\mathrm{i}\Omega t} \qquad (7.31)$$

(with some unimportant phase shift which is empirically corrected).

- Fourier transform gives a complex signal proportional to

$$\frac{\mathcal{N}\gamma^2\hbar^2 B_0}{4k_{\mathrm{B}}T}\left(\frac{R_2}{R_2^2 + (\omega - \Omega)^2} - \mathrm{i}\frac{\omega - \Omega}{R_2^2 + (\omega - \Omega)^2}\right). \qquad (7.32)$$

- The cosine modulation of $\mathscr{I}_x$ can be taken as the real component of the signal and the sine modulation of $\mathscr{I}_y$ can be taken as the imaginary component of the signal:
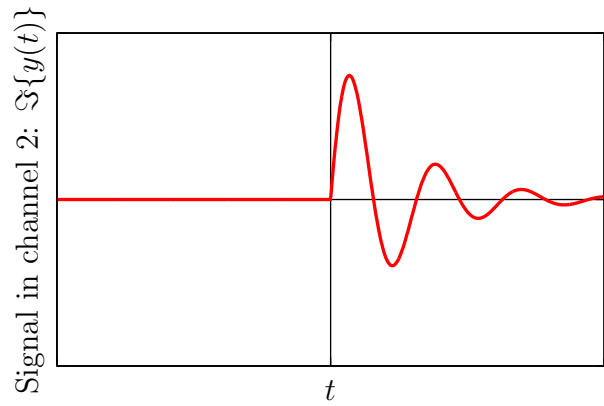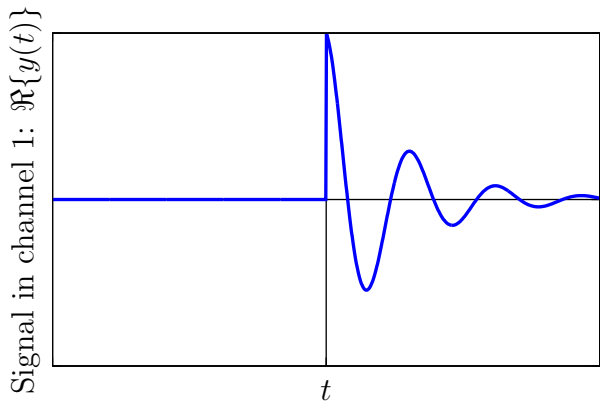
After Fourier transformation:
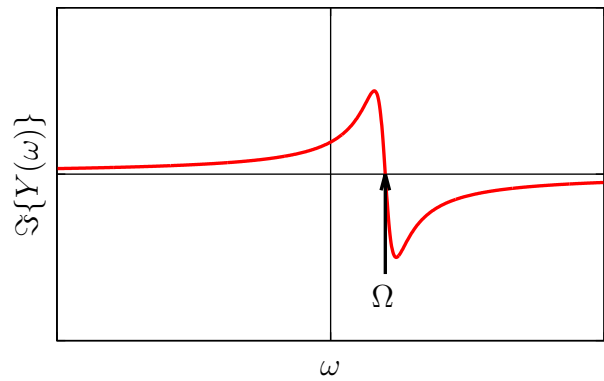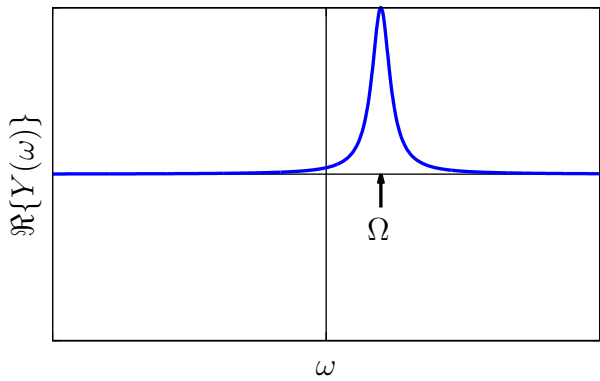
- The signal-to-noise ratio (without relaxation) is proportional to $|\gamma|^{5/2}B_0^{3/2}$, with the optimal temperature given by relaxation properties (close to room temperatures for proteins in aqueous solutions).

HOMEWORK

Analyze the One-pulse experiment (Sections 7.9 and 7.10) and make sure that you understand the conclusions presented in Section 7.11.

7.12 SUPPORTING INFORMATION

7.12.1 Decomposition of chemical shift Hamiltonian

The Hamiltonian of a homogeneous magnetic field aligned with the z-axis of the coordinate frame can be decomposed into

- isotropic contribution, independent of the rotation in space:

$$\hat{H}_{\delta,\mathrm{i}} = -\gamma B_0 \delta_{\mathrm{i}}(\hat{I}_z) \tag{7.33}$$

- axial component, dependent on φ and ϑ:

$$\begin{aligned}
\hat{H}_{\delta,\mathrm{a}} &= -\gamma B_0 \delta_{\mathrm{a}}(3\sin\vartheta\cos\vartheta\cos\varphi\hat{I}_x + 3\sin\vartheta\cos\vartheta\sin\varphi\hat{I}_y + (3\cos^2\vartheta - 1)\hat{I}_z) \\
&= -\gamma B_0 \delta_{\mathrm{a}}(3Z_x Z_z \hat{I}_x + 3Z_y Z_z \hat{I}_y + (3Z_z^2 - 1)\hat{I}_z)
\end{aligned} \tag{7.34}$$

- rhombic component, dependent on φ, ϑ, and χ:

$$\begin{aligned}
\hat{H}_{\delta,\mathrm{r}} = -\gamma B_0 \delta_{\mathrm{r}}(\ &(-(2\cos^2\chi - 1)\sin\vartheta\cos\vartheta\cos\varphi + 2\sin\chi\cos\chi\sin\vartheta\cos\vartheta\sin\varphi)\hat{I}_x + \\
&(-(2\cos^2\chi - 1)\sin\vartheta\cos\vartheta\sin\varphi - 2\sin\chi\cos\chi\sin\vartheta\cos\vartheta\cos\varphi)\hat{I}_y + \\
&((2\cos^2\chi - 1)\sin^2\vartheta)\hat{I}_z)
\end{aligned}$$

$$= \gamma B_0 \delta_{\mathrm{r}}((\cos(2\chi)Z_x - \sin(2\chi)Z_y)Z_z\hat{I}_x + (\cos(2\chi)Z_y + \sin(2\chi)Z_x)Z_z\hat{I}_y + \cos(2\chi)(Z_z^2 - 1)\hat{I}_z) \tag{7.35}$$

7.12.2 Density matrix in thermal equilibrium

We use the mixed state approach to define the state of the sample in thermal equilibrium. In the large ensemble of nuclei observed in NMR, the equilibrium distribution of the magnetic moments is such that their orientations in the x and y directions are equally probable, and the orientation in the z direction (defined by the direction of the magnetic induction of the external homogeneous field $\vec{B}_0$) is slightly favored.

Classically, the energy of individual moments depends only on μ_z:

$$\mathcal{E}_j = -\vec{\mu}_j \cdot \vec{B}_0 = -\mu_{z,j} B_0, \tag{7.36}$$

where j identifies the molecule with the observed nuclear magnetic moment, and the overall energy is $\sum_j \mathcal{E}_j$.

Quantum mechanically, the ensemble of magnetic moments represents a mixed state and the expected value of the energy is given by Eq. 6.2, where $\langle A \rangle = \langle \mathcal{E} \rangle$ and $\hat{A} = \hat{H}$. Note that Eq. 6.2 contains an operator (in our case the Hamiltonian) representing the quantity of interest (in our case the energy) for a *single* magnetic moment, although we calculate the expected value for the whole ensemble. If we use eigenfunctions of $\hat{I}_z$ as the basis (the best choice for magnetic moments in the filed with $\vec{B}_0$ defining the z axis), eigenvalues of $H = -\gamma B_0(1 + \delta_{\mathrm{i}})\hat{I}_z$ are the diagonal elements of the matrix representation of $\hat{H}$:

$$\hat{H} = -\gamma B_0(1 + \delta_{\mathrm{i}})\hat{I}_z = -\gamma B_0(1 + \delta_{\mathrm{i}})\frac{\hbar}{2}\begin{pmatrix} 1 & 0 \\ 0 & -1 \end{pmatrix} = \begin{pmatrix} -\gamma B_0(1 + \delta_{\mathrm{i}})\frac{\hbar}{2} & 0 \\ 0 & +\gamma B_0(1 + \delta_{\mathrm{i}})\frac{\hbar}{2} \end{pmatrix} = \begin{pmatrix} \mathcal{E}_\alpha & 0 \\ 0 & \mathcal{E}_\beta \end{pmatrix}. \tag{7.37}$$

Eq. 6.2 in this case has the form

$$\langle \mathcal{E} \rangle = \mathcal{N}\mathrm{Tr}\left\{ \underbrace{\begin{pmatrix} \overline{c_\alpha c_\alpha^*} & \overline{c_\alpha c_\beta^*} \\ \overline{c_\beta c_\alpha^*} & \overline{c_\beta c_\beta^*} \end{pmatrix}}_{\hat{\rho}} \underbrace{\begin{pmatrix} \mathcal{E}_\alpha & 0 \\ 0 & \mathcal{E}_\beta \end{pmatrix}}_{\hat{H}} \right\} = \mathcal{N}\left(\overline{c_\alpha c_\alpha^*}\,\mathcal{E}_\alpha + \overline{c_\beta c_\beta^*}\,\mathcal{E}_\beta \right) = \mathcal{N}\left(P_\alpha\,\mathcal{E}_\alpha + P_\beta\,\mathcal{E}_\beta \right). \tag{7.38}$$

We see that the expected value of the energy of our mixed state is a weighted average of the energies of the α and β eigenstates of a single magnetic moment. The off-diagonal elements of $\hat{\rho}$, the populations, play a role of *statistical weights* in the derived relation. At the equilibrium, the populations can be evaluated using statistical arguments similar to the Boltzmann law in the classical molecular statistics:

$$P_\alpha^{\mathrm{eq}} = \frac{\mathrm{e}^{-\mathcal{E}_\alpha/k_{\mathrm{B}}T}}{\mathrm{e}^{-\mathcal{E}_\alpha/k_{\mathrm{B}}T} + \mathrm{e}^{-\mathcal{E}_\beta/k_{\mathrm{B}}T}}, \tag{7.39}$$

$$P_\beta^{\mathrm{eq}} = \frac{\mathrm{e}^{-\mathcal{E}_\beta/k_{\mathrm{B}}T}}{\mathrm{e}^{-\mathcal{E}_\alpha/k_{\mathrm{B}}T} + \mathrm{e}^{-\mathcal{E}_\beta/k_{\mathrm{B}}T}}, \tag{7.40}$$

where $k_\mathrm{B} = 1.38064852 \times 10^{-23}\,\mathrm{m^2\,kg\,s^{-2}\,K^{-1}}$ is the Boltzmann constant.

The thermal energy at $0\,^\circ\mathrm{C}$ is more than $10\,000$ times higher than $\gamma B_0 \hbar/2$ for the most sensitive nuclei (protons) at spectrometers with the highest magnetic fields (1.2 GHz in 2021). The effect of the chemical shift is four orders of magnitude lower (roughly $10^{-8}k_\mathrm{B}T$). We see that (i) the effect of the chemical shift δ_i on $\mathcal{E}_\alpha$ and $\mathcal{E}_\beta$ can be safely neglected, and (ii) that the values in the exponents are much lesser than unity. Therefore, we can approximate the exponential terms by a linear expansion

$$\mathrm{e}^{\pm \frac{\gamma B_0 (1+\delta_\mathrm{i})\hbar}{k_\mathrm{B}T}} \approx 1 \pm \frac{\gamma B_0 \hbar}{2k_\mathrm{B}T} \tag{7.41}$$

and calculate the populations as

$$P_\alpha^\mathrm{eq} = \frac{\mathrm{e}^{-\mathcal{E}_\alpha/k_\mathrm{B}T}}{\mathrm{e}^{-\mathcal{E}_\alpha/k_\mathrm{B}T} + \mathrm{e}^{-\mathcal{E}_\beta/k_\mathrm{B}T}} = \frac{1 + \frac{\gamma B_0 \hbar}{2k_\mathrm{B}T}}{1 + \frac{\gamma B_0 \hbar}{2k_\mathrm{B}T} + 1 - \frac{\gamma B_0 \hbar}{2k_\mathrm{B}T}} = \frac{1 + \frac{\gamma B_0 \hbar}{2k_\mathrm{B}T}}{2}, \tag{7.42}$$

$$P_\beta^\mathrm{eq} = \frac{\mathrm{e}^{-\mathcal{E}_\beta/k_\mathrm{B}T}}{\mathrm{e}^{-\mathcal{E}_\alpha/k_\mathrm{B}T} + \mathrm{e}^{-\mathcal{E}_\beta/k_\mathrm{B}T}} = \frac{1 - \frac{\gamma B_0 \hbar}{2k_\mathrm{B}T}}{1 + \frac{\gamma B_0 \hbar}{2k_\mathrm{B}T} + 1 - \frac{\gamma B_0 \hbar}{2k_\mathrm{B}T}} = \frac{1 - \frac{\gamma B_0 \hbar}{2k_\mathrm{B}T}}{2}. \tag{7.43}$$

7.12.3 Bloch-Wangsness-Redfield theory

The Liouville-von Neumann equation describing the relaxing system of magnetic moments interacting with moving electrons in a so-called *interaction frame* (corresponding to the rotating coordinate frame in the classical description) has the form

$$\frac{\mathrm{d}\Delta\hat{\rho}}{\mathrm{d}t} = -\frac{\mathrm{i}}{\hbar}[\hat{H}_{\delta,\mathrm{a}} + \hat{H}_{\delta,\mathrm{r}}, \Delta\hat{\rho}], \tag{7.44}$$

where $\hat{H}_{\delta,\mathrm{a}}$ and $\hat{H}_{\delta,\mathrm{r}}$ are defined by Eqs. 7.34 and 7.35, respectively, and $\Delta\hat{\rho}$ is a difference (expressed in the interaction frame) between the density matrix at the given time and density matrix in the thermodynamic equilibrium. Writing $\Delta\hat{\rho}$ in the same basis as used for the Hamiltoninan,

$$\Delta\hat{\rho} = d_t \hat{I}_t + d_z \hat{I}_z + d_+ \hat{I}_+ \mathrm{e}^{\mathrm{i}\omega_0 t} + d_- \hat{I}_- \mathrm{e}^{-\mathrm{i}\omega_0 t}. \tag{7.45}$$

If the chemical shift is axially symmetric and its size or shape do not change,

$$\frac{\mathrm{d}(d_z \hat{I}_z + d_+ \hat{I}_+ \mathrm{e}^{\mathrm{i}\omega_0 t} + d_- \hat{I}_- \mathrm{e}^{-\mathrm{i}\omega_0 t})}{\mathrm{d}t} = -\frac{\mathrm{i}b}{\hbar}\left[c^z \hat{I}_z + \sqrt{\frac{3}{8}}c^+ \hat{I}_+ \mathrm{e}^{\mathrm{i}\omega_0 t} + \sqrt{\frac{3}{8}}c^- \hat{I}_- \mathrm{e}^{-\mathrm{i}\omega_0 t}, d_z \hat{I}_z + d_+ \hat{I}_+ \mathrm{e}^{\mathrm{i}\omega_0 t} + d_- \hat{I}_- \mathrm{e}^{-\mathrm{i}\omega_0 t}\right], \tag{7.46}$$

where $\hat{I}_\pm \mathrm{e}^{\pm\mathrm{i}\omega_0 t}$ are operators $\hat{I}_\pm = \hat{I}_x \pm \mathrm{i}\hat{I}_y$ in the interaction frame, $\omega_0 = -\gamma B_0(1+\delta_\mathrm{a})$, $b = -2\gamma B_0 \delta_\mathrm{a}$, and

$$c^z = \frac{1}{2}(3\cos^2\vartheta - 1) = \Theta^\| \tag{7.47}$$

$$c^+ = \sqrt{\frac{3}{2}}\sin\vartheta\cos\vartheta\mathrm{e}^{-\mathrm{i}\varphi} = \sqrt{\frac{2}{3}}\Theta^\perp \mathrm{e}^{-\mathrm{i}\varphi} \tag{7.48}$$

$$c^- = \sqrt{\frac{3}{2}}\sin\vartheta\cos\vartheta\mathrm{e}^{+\mathrm{i}\varphi} = \sqrt{\frac{2}{3}}\Theta^\perp \mathrm{e}^{+\mathrm{i}\varphi} \tag{7.49}$$

Analogically to the classical analysis, the evolution can be written as

$$\frac{\mathrm{d}\Delta\hat{\rho}}{\mathrm{d}t} = -\frac{1}{\hbar^2}\int_0^\infty \overline{[\hat{H}_{\delta,\mathrm{a}}(0), [\hat{H}_{\delta,\mathrm{a}}(t), \Delta\hat{\rho}]]}\mathrm{d}t. \tag{7.50}$$

The right-hand side can be simplified dramatically by the *secular approximation*: all terms with $\mathrm{e}^{\pm\mathrm{i}\omega_0 t}$ are averaged to zero because they rapidly oscillate with the angular frequency ω_0. Only terms with $\overline{(c^z)^2}$ and $\overline{c^+ c^-}$ are non zero (both equal to 1/5 at $t_j = 0$).[6] These are the terms with $[\hat{I}_z, [\hat{I}_z, \Delta\hat{\rho}]]$, $[\hat{I}_+, [\hat{I}_-, \Delta\hat{\rho}]]$, and $[\hat{I}_-, [\hat{I}_+, \Delta\hat{\rho}]]$. Moreover, averaging over all molecules makes all three correlation functions identical in isotropic liquids: $\overline{c^z(0)c^z(t)} = \overline{c^+(0)c^-(t)} = \overline{c^-(0)c^+(t)} = \overline{c(0)c(t)}$.

In order to proceed, the double commutators must be expressed. We start with

$$[\hat{I}_z, \hat{I}_\pm] = [\hat{I}_z, \hat{I}_x] \pm \mathrm{i}[\hat{I}_z, \hat{I}_y] = \pm\hbar(\hat{I}_x \pm \mathrm{i}\hat{I}_y) = \pm\hbar\hat{I}_\pm \tag{7.51}$$

---

[6]We have factored out $\sqrt{3/8}$ in order to make $\overline{c^+ c^-} = \overline{(c^z)^2}$.

and

$$[\hat{I}_+, \hat{I}_-] = [\hat{I}_x, \hat{I}_x] - \mathrm{i}[\hat{I}_x, \hat{I}_y] + \mathrm{i}[\hat{I}_y, \hat{I}_x] + [\hat{I}_y, \hat{I}_y] = 2\hbar\hat{I}_z. \tag{7.52}$$

Our goal is to calculate relaxation rates for the expectation values of components parallel (M_z) and perpendicular (M_+ or M_-) to $\vec{B}_0$.

Let us start with M_z. According to Eq. 4.12,

$$\Delta\langle M_z \rangle = \mathrm{Tr}\{\Delta\hat{\rho}\hat{M}_z\} \tag{7.53}$$

where $\Delta\langle M_z \rangle$ is the difference from the expectation value of M_z in equilibrium. The operator of M_z for one magnetic moment observed is (Eq. 7.1)

$$\hat{M}_z = \mathcal{N}\gamma\hat{I}_z, \tag{7.54}$$

where $\mathcal{N}$ is the number of molecules per volume element detected by the spectrometer. Since the basis matrices are orthogonal, products of $\hat{I}_z$ with the components of the density matrix different from $\hat{I}_z$ are equal to zero and the left-hand side of Eq. 7.50 reduces to

$$\frac{\mathrm{d}d_z}{\mathrm{d}t}\hat{I}_z \tag{7.55}$$

when calculating relaxation rate of $\langle M_z \rangle$. In the right-hand side, we need to calculate three double commutators:

$$[\hat{I}_z, [\hat{I}_z, \hat{I}_z]] = 0 \qquad [\hat{I}_+, [\hat{I}_-, \hat{I}_z]] = 2\hbar^2\hat{I}_z \qquad [\hat{I}_-, [\hat{I}_+, \hat{I}_z]] = 2\hbar^2\hat{I}_z \tag{7.56}$$

After substituting into Eq. 7.50,

$$\frac{\mathrm{d}d_z}{\mathrm{d}t}\mathrm{Tr}\{\hat{I}_z\hat{I}_z\} = -\left(\frac{3}{4}b^2\int\limits_0^\infty \overline{c^+(0)c^-(t)}\mathrm{e}^{\mathrm{i}\omega_0 t}\mathrm{d}t + \frac{3}{4}b^2\int\limits_0^\infty \overline{c^-(0)c^+(t)}\mathrm{e}^{-\mathrm{i}\omega_0 t}\mathrm{d}t\right)d_z\mathrm{Tr}\{\hat{I}_z\hat{I}_z\} \tag{7.57}$$

$$\frac{\mathrm{d}\Delta\langle M_z\rangle}{\mathrm{d}t} = -\left(\frac{3}{4}b^2\int\limits_0^\infty \overline{c^+(0)c^-(t)}\mathrm{e}^{\mathrm{i}\omega_0 t}\mathrm{d}t + \frac{3}{4}b^2\int\limits_0^\infty \overline{c^-(0)c^+(t)}\mathrm{e}^{-\mathrm{i}\omega_0 t}\mathrm{d}t\right)\Delta\langle M_z\rangle \tag{7.58}$$

The relaxation rate R_1 for M_z, known as the *longitudinal relaxation rate* in the literature, is the real part of the expression in the parentheses

$$R_1 = \frac{3}{4}b^2\Re\left\{\int\limits_0^\infty \overline{c^+(0)c^-(t)}\mathrm{e}^{\mathrm{i}\omega_0 t}\mathrm{d}t + \int\limits_0^\infty \overline{c^-(0)c^+(t)}\mathrm{e}^{-\mathrm{i}\omega_0 t}\mathrm{d}t\right\} \tag{7.59}$$

As already discussed in the classical description of relaxation, if the fluctuations are random, they are also stationary: the current orientation of the molecule is correlated with the orientation in the past in the same manner as it is correlated with the orientation in the future. Therefore,

$$\int\limits_0^\infty \overline{c^+(0)c^-(t)}\mathrm{e}^{\mathrm{i}\omega_0 t}\mathrm{d}t = \frac{1}{2}\left(\int\limits_0^\infty \overline{c^+(0)c^-(t)}\mathrm{e}^{\mathrm{i}\omega_0 t}\mathrm{d}t + \int\limits_{-\infty}^0 \overline{c^+(0)c^-(t)}\mathrm{e}^{\mathrm{i}\omega_0 t}\mathrm{d}t\right) = \frac{1}{2}\int\limits_{-\infty}^\infty \overline{c^+(0)c^-(t)}\mathrm{e}^{\mathrm{i}\omega_0 t}\mathrm{d}t. \tag{7.60}$$

$$\int\limits_0^\infty \overline{c^-(0)c^+(t)}\mathrm{e}^{-\mathrm{i}\omega_0 t}\mathrm{d}t = \frac{1}{2}\left(\int\limits_0^\infty \overline{c^-(0)c^+(t)}\mathrm{e}^{-\mathrm{i}\omega_0 t}\mathrm{d}t + \int\limits_{-\infty}^0 \overline{c^-(0)c^+(t)}\mathrm{e}^{-\mathrm{i}\omega_0 t}\mathrm{d}t\right) = \frac{1}{2}\int\limits_{-\infty}^\infty \overline{c^-(0)c^+(t)}\mathrm{e}^{-\mathrm{i}\omega_0 t}\mathrm{d}t, \tag{7.61}$$

The right-hand side integrals are identical with the mathematical definition of the Fourier transform of the correlation functions and real parts of such Fourier transforms are the *spectral density functions* $J(\omega)$.

The relaxation rate R_1 can be therefore written in the same form as derived classically:

$$R_1 = \frac{3}{4}b^2\left(\frac{1}{2}J(\omega_0) + \frac{1}{2}J(-\omega_0)\right) \approx \frac{3}{4}b^2 J(\omega_0) \tag{7.62}$$

What is the physical interpretation of the obtained equation? Relaxation of M_z is given by the correlation functions $\overline{c^+(0)c^-(t)}$ and $\overline{c^-(0)c^+(t)}$ describing fluctuations of the components of the chemical shift tensor perpendicular to $\vec{B}_0$ (in the case of an axially symmetric tensor, of the Z_x and Z_y components of the vector defining the symmetry axis $\vec{Z}$). Such fluctuating fields resemble the radio waves with $\vec{B}_1 \perp \vec{B}_0$. If the frequency of such fluctuations matches the precession frequency ω_0, the resonance condition is fulfilled and, for a short time (comparable to the frequency of molecular collisions) when a fluctuation accidentally resonates with ω_0, the $-\gamma B_{\mathrm{e},x}\hat{I}_x$ and/or $-\gamma B_{\mathrm{e},x}\hat{I}_y$ components of the chemical shift Hamiltonian are not completely removed by the secular approximation. In analogy to Eq. 7.19, the $\mathscr{I}_z$ component of $\hat{\rho}$ (and consequently $\langle M_z \rangle$) slightly changes due to $-\gamma B_{\mathrm{e},x}\hat{I}_x$ and/or $-\gamma B_{\mathrm{e},x}\hat{I}_y$.

If the molecular motions are assumed to be completely random and independent of the distribution of magnetic moments, M_z is expected to decay to zero, which does not happen in reality. If the coupling between molecular motions and magnetic moment distribution is described correctly by the quantum theory (see footnote 4), a correlation function is obtained that describes correctly the return of $\hat{\rho}$ to its equilibrium form.[7] This drives the system back to the equilibrium distribution of magnetic moments.

Let us continue with M_+. According to Eq. 4.12,

$$\Delta\langle M_+\rangle \equiv \langle M_+\rangle = \mathrm{Tr}\{\Delta\hat{\rho}\hat{M}_+\} \tag{7.63}$$

The expectation value of M_+ in equilibrium is zero, this is why we do not need to calculate the difference for $\langle M_+\rangle$ and why we did not calculate the difference in the classical analysis.

The operator of M_+ for one magnetic moment observed is

$$\hat{M}_+ = \mathcal{N}\gamma\hat{I}_+ = \mathcal{N}\gamma(\hat{I}_x + \mathrm{i}\hat{I}_y). \tag{7.64}$$

Due to the orthogonality of basis matrices, the left-hand side of Eq. 7.50 reduces to

$$\frac{\mathrm{d}d_+}{\mathrm{d}t}\hat{I}_+\mathrm{e}^{\mathrm{i}\omega_0 t} \tag{7.65}$$

when calculating relaxation rate of $\Delta\langle M_+\rangle \equiv \langle M_+\rangle$. In the right-hand side, we need to calculate three double commutators:

$$[\hat{I}_z,[\hat{I}_z,\hat{I}_+]] = \hbar^2\hat{I}_+ \qquad [\hat{I}_+,[\hat{I}_-,\hat{I}_+]] = 2\hbar^2\hat{I}_+ \qquad [\hat{I}_-,[\hat{I}_+,\hat{I}_+]] = 0. \tag{7.66}$$

After substituting into Eq. 7.50,

$$\frac{\mathrm{d}d_+}{\mathrm{d}t}\mathrm{Tr}\{\hat{I}_-\hat{I}_+\} = -\left(b^2\int_0^\infty \overline{c^z(0)c^z(t)}\mathrm{d}t + \frac{3}{4}b^2\int_0^\infty \overline{c^+(0)c^-(t)}\mathrm{e}^{\mathrm{i}\omega_0 t}\mathrm{d}t\right)d_+\mathrm{Tr}\{\hat{I}_-\hat{I}_+\} \tag{7.67}$$

$$\frac{\mathrm{d}\langle M_+\rangle}{\mathrm{d}t} = -\left(b^2\int_0^\infty \overline{c^z(0)c^z(t)}\mathrm{d}t + \frac{3}{4}b^2\int_0^\infty \overline{c^+(0)c^-(t)}\mathrm{e}^{\mathrm{i}\omega_0 t}\mathrm{d}t\right)\langle M_+\rangle. \tag{7.68}$$

The relaxation rate R_2 for M_+, known as the *transverse relaxation rate* in the literature, is the real part of the expression in the parentheses.

$$R_2 = b^2\int_0^\infty \overline{c^z(0)c^z(t)}\mathrm{d}t + \Re\left\{\frac{3}{4}b^2\int_0^\infty \overline{c^+(0)c^-(t)}\mathrm{e}^{\mathrm{i}\omega_0 t}\mathrm{d}t\right\}. \tag{7.69}$$

Note that the first integral in 7.69 is a real number, equal to R_0 derived by the classical analysis.

Using the same arguments as for M_z,

$$R_2 = b^2\left(\frac{1}{2}J(0) + \frac{3}{8}J(\omega_0)\right) \approx R_0 + \frac{1}{2}R_1. \tag{7.70}$$

What is the physical interpretation of the obtained equation? Two terms in Eq. 7.70 describe two processes contributing to the relaxation of M_+. The first one is the *loss of coherence* with the rate R_0, given by the correlation function $\overline{c^z(0)c^z(t)}$ and describing fluctuations of the components of the chemical shift tensor parallel with $\vec{B}_0$ (of Z_z). This contribution was analyzed in Section 2.5.1 using the classical approach. The second contribution is due to fluctuations of the components of the chemical shift tensor perpendicular to $\vec{B}_0$ (of Z_x and Z_y), returning the magnetization vector $\vec{M}$ to its direction in the thermodynamic equilibrium. These fluctuations renew the equilibrium value of M_z, as described above, but also make the M_x and M_y components to disappear. Note however, that only one correlation function ($\overline{c^+(0)c^-(t)}$) contributes to the relaxation of M_+, while both $\overline{c^+(0)c^-(t)}$ and $\overline{c^-(0)c^+(t)}$ contribute to the relaxation of M_z. Therefore only $R_1/2$, not R_1, contributes to R_2. If we defined R_2 as a relaxation rate of M_-, only $\overline{c^-(0)c^+(t)}$ would contribute.[8]

---

[7]It can be described as $J(\omega_0) = \mathrm{e}^{-\hbar\omega_0/k_\mathrm{B}T}J(-\omega_0)$. In the semi-classical Bloch-Wangsness-Redfield theory, this is taken into account by working with $\Delta\hat{\rho}$ and $\langle\Delta M_z\rangle$ instead of $\hat{\rho}$ and $\langle M_z\rangle$.

[8]Fluctuations with the frequency $+\omega_0$ affect M_+ and fluctuations with the frequency $-\omega_0$ affect M_-, but both affect M_z. Alternatively, we could define R_2 as a relaxation rate of M_x or M_y. Fluctuations of the $B_{\mathrm{e},y}$ component affect M_x but not M_y, while fluctuations of the $B_{\mathrm{e},x}$ component affect M_y but not M_x. On the other hand, both fluctuations of $B_{\mathrm{e},x}$ and $B_{\mathrm{e},y}$ affect M_z. Working with M_+, M_- or M_x, M_y, the relaxation of M_z due to $B_{\mathrm{e},x}$ and $B_{\mathrm{e},y}$ is always twice faster.

7.12.4 Thermal noise of electrical circuits

All NMR measurements are influenced by the thermal noise (also called Johnson noise) generated by random motions of electrons inside electric conductors. In order to analyze the thermal noise, we use a simple model circuit, consisting of two electric devices connected by a cable of the length a. As we are interested only in the effect of the thermal noise, which is described by the electric *resistance*, we can view the devices as two resistors R_1 and R_2. For the sake of simplicity, we assume that both resistors have the same resistance $R_1 = R_2 = R$ and that the cable does not radiate any energy.[9] The thermal motions of electrons in the resistor R_1 generate a randomly fluctuating voltage $U_1(t)$ that propagates through the cable to the resistor R_2. If the cable does not irradiate any energy, all electric energy associated with $U_1(t)$ is absorbed by R_2. The fluctuations of $U_1(t)$ travelling through the cable can be decomposed into a series of standing waves (*vibration modes*) along the cable. The permitted wavelengths of the standing waves are

$$\lambda_j = \frac{2a}{j}, \tag{7.71}$$

where j is an integer number.[10] The corresponding allowed frequencies are

$$f_j = \frac{c}{2a}j, \tag{7.72}$$

where c is the speed of the wave propagation. In NMR spectroscopy, we observe frequencies only in a certain window, selected by the *band-pass filter*. Therefore, we are interested only the vibration modes in this window. If the window is defined as a range between f_0 and $f_0 + \Delta f$, the number of modes in the window is equal to $2a\Delta f/c$.

The statistical thermodynamics shows that the thermal energy of a single mode is (approximately,[11] for sufficiently low frequencies) equal to $k_\mathrm{B}T$. The thermal energy of all modes within the frequency window Δf is $2ak_\mathrm{B}T\Delta f/c$. Half of this energy (i.e., $ak_\mathrm{B}T\Delta f/c$) is generated by the resistor R_1, transmitted by the cable, and absorbed by R_2. The energy arrives at R_2 in the time $\Delta t = a/c$. The power transmitted in this time is

$$P = \frac{ak_\mathrm{B}T\Delta f/c}{\Delta t} = \frac{ak_\mathrm{B}T\Delta f/c}{a/c} = k_\mathrm{B}T\Delta f. \tag{7.73}$$

The power can be also described using the resistance. In general, $P = UI$ and, applying the Ohm's law ($U = RI$), $P = RI^2$. The voltage U_1 generated by the thermal motions of electrons in R_1 produces the current

$$I = \frac{U_1}{R_1 + R_2} = \frac{U_1}{2R} \tag{7.74}$$

and consequently the power

$$P = RI^2 = R\left(\frac{U_1}{2R}\right)^2 = \frac{U_1^2}{4R}. \tag{7.75}$$

By comparing Eqs. 7.73 and 7.75, U_1^2 can be expressed as $U_1^2 = 4Rk_\mathrm{B}T\Delta f$. As U_1 represents the noise voltage, we can define the mean-squared noise voltage as

$$\langle U_\mathrm{noise}^2 \rangle = 4Rk_\mathrm{B}T\Delta f. \tag{7.76}$$

7.12.5 Spectrum and signal-to-noise ratio

In order to describe the one-dimensional NMR spectrum quantitatively, we need to know

1. how is the detected signal related to the magnetization. Here, we analyze a simple experimental setup with a detector coil perpendicular to the external field, and sufficiently far from the sample. In this case, the voltage induced in the coil is described by Eq. 55 (Section 0.5).

2. how is the noise defined. As derived in Section 7.12.4, the mean square of the voltage variance is $\langle U_\mathrm{noise}^2 \rangle = 4Rk_\mathrm{B}T\Delta f$ (Eq. 7.76), where R is the resistance and Δf is the frequency bandwidth of the detector (the range of frequencies actually detected).

3. how is the time-dependent signal converted to a frequency spectrum. Here, the answer is described in Lecture 3, the most important step is the Fourier transformation.

---

[9]Technically, the impedance of the cable matches the impedance of the devices (in our case simply equal to the resistance R). In NMR spectroscopy, we try to match the impedance by setting the capacitance of the *matching capacitor* when tuning the spectrometer before the measurement.

[10]In a similar manner, mechanic waves propagate along the plucked string of a guitar or another string instrument. Very similar arguments led to the formulation of the basic ideas of quantum physics (black body radiation).

[11]The exact value, given by the statistics of a quantum harmonic oscillator, is $hf/(\mathrm{e}^{hf/(k_\mathrm{B}T)} - 1)$.

According Eq. 55, describing the voltage induced in the detector coil in our setup, the amplitude of the induced voltage is

$$|U_{\text{induced}}| = \frac{\mu_0}{4\pi} \frac{2n|\mu|S}{r^3} |\omega_0|, \tag{7.77}$$

where μ_0 is the magnetic permeability of vacuum, r is the coil from the measured sample,[12] n and S are the number of turns and the cross-section area of the coil. The amplitude of the magnetic moment μ, rotating with the frequency ω_0, is equal to the amplitude of the transverse magnetization of the sample, multiplied by the volume sensed by the detector coil. Eq. 7.29 derived in Section 7.10 tells us that the expected value of the magnetization rotating in the plane perpendicular to $\vec{B}_0$ is (in the laboratory coordinate frame)

$$\langle M_+ \rangle = \frac{\mathcal{N}\gamma^2\hbar^2 B_0}{4k_{\text{B}}T} e^{-R_2 t}(\cos(\omega_0 t) + \mathrm{i}\sin(\omega_0 t)) = \frac{\mathcal{N}\gamma^2\hbar^2 B_0}{4k_{\text{B}}T} e^{-R_2 t}e^{\mathrm{i}\omega_0 t}. \tag{7.78}$$

We start our analysis ignoring the relaxation factor $e^{-R_2 t}$. In such a case,

$$|U_{\text{induced}}| = \frac{\mu_0}{4\pi} \frac{2nS}{r^3} \frac{N\gamma^2\hbar^2 B_0}{4k_{\text{B}}T} |\omega_0| = \frac{\mu_0}{4\pi} \frac{2nS}{r^3} \frac{N\gamma^2\hbar^2 B_0}{4k_{\text{B}}T} |\gamma| B_0 = \frac{\mu_0}{4\pi} \left(\frac{\hbar}{2}\right)^2 \frac{2nS}{r^3} \frac{N|\gamma|^3 B_0^2}{k_{\text{B}}T}, \tag{7.79}$$

where N is the number of magnetic moments in the volume sensed by the receiver coil.

As described in Section 3.10.1, the coil (serving both as transmitter and receiver coil) is a part of an LC circuit, acting as a resonator. If the capacitor C_{T}, wired in parallel with the coil, is tuned to the resonance frequency $\omega_0^2 = LC_{\text{T}}$, than it accumulates the energy given by $\frac{1}{2}LI^2$, where I is the current induced in the coil. On the other hand, the coil has also some resistance R_{coil}, and therefore it dissipates a part of the energy as the Joule heat. Balance of the energy accumulation and dissipation is described by the *quality factor* Q, defined as

$$Q = |\omega_0| \frac{\text{energy stored}}{\text{power loss}} = |\omega_0| \frac{\frac{1}{2}LI^2}{\frac{1}{2}R_{\text{coil}}I^2} = |\omega_0| L/R_{\text{coil}}. \tag{7.80}$$

When calculating the parallel impedance of the circuit, the resistance of the coil R_{coil} can be repplaced by a parallel (shunt) resistance of the circuit R

$$R = Q|\omega_0|L \tag{7.81}$$

The amplitude of the voltage actually measured across the coil terminals is

$$|U_{\text{measured}}| = Q|U_{\text{induced}}| = \frac{\mu_0}{4\pi} \left(\frac{\hbar}{2}\right)^2 \frac{2nQS}{r^3} \frac{N|\gamma|^3 B_0^2}{k_{\text{B}}T}. \tag{7.82}$$

Now, we move from the signal amplitude to the frequency spectrum and reintroduce the relaxation. We derived in Section 3.4 (cf. Eq. 3.5) that the height of a peak obtained by the Fourier transformation of a signal with an amplitude $\mathcal{A}$ depends on the relaxation rate R_2 and on the acquisition time $t_{\max}$ as

$$Y_{\max} = \mathcal{A}\frac{1 - e^{-R_2 t_{\max}}}{R_2} = \frac{\mu_0}{4\pi} \left(\frac{\hbar}{2}\right)^2 \frac{2nQS}{r^3} \frac{N|\gamma|^3 B_0^2}{k_{\text{B}}T} \frac{1 - e^{-R_2 t_{\max}}}{R_2}. \tag{7.83}$$

From the practical point of view, it is not important how large is the detected signal (the measured voltage can be amplified or attenuated if needed). The sensitivity of the measurement is given by the signal-to-noise ratio. Therefore, we also need to calculate the noise in the spectrum. According to Eq. 7.76,

$$\langle U_{\text{noise}}^2 \rangle = 4Rk_{\text{B}}T\Delta f = 4Rk_{\text{B}}T\frac{\Delta\omega}{2\pi} \tag{7.84}$$

As the noise voltage fluctuates stochastically, we can describe its correlation function in a similar manner as we described it for the magnetic moment fluctuations in Sections 2.5.1 and 2.5.5, i.e. as $\langle U_{\text{noise}}(0)\, U_{\text{noise}}(t)\rangle$, and calculate also the corresponding spectral density function:

$$J_{\text{noise}}(\omega) = \int_{-\infty}^{\infty} \langle U_{\text{noise}}(0)\, U_{\text{noise}}(t)\rangle e^{-\mathrm{i}\omega t}\mathrm{d}t. \tag{7.85}$$

The inverse Fourier transformation allows us to calculate

$$\langle U_{\text{noise}}(0)\, U_{\text{noise}}(t)\rangle = \frac{1}{2\pi}\int_{-\infty}^{\infty} J_{\text{noise}}(\omega)e^{\mathrm{i}\omega t}\mathrm{d}\omega \tag{7.86}$$

and by setting $t = 0$

---

[12]We assume that this distance is large, which is not true in NMR spectrometers, but later we include the distance in a general parameter defining the geometry.

$$\langle U_{\text{noise}}^2 \rangle = \langle U_{\text{noise}}(0)\, U_{\text{noise}}(0) \rangle = \frac{1}{2\pi} \int\limits_{-\infty}^{\infty} J_{\text{noise}}(\omega)\, \mathrm{d}\omega. \tag{7.87}$$

When applying a band-pass filter[13] selecting only frequencies in the range from ω_{low} to $\omega_{\text{high}} = \omega_{\text{low}} + \Delta\omega$,

$$\langle U_{\text{noise}}^2 \rangle = \langle U_{\text{noise}}(0)\, U_{\text{noise}}(0) \rangle = \frac{1}{2\pi} \int\limits_{-\infty}^{\infty} J_{\text{noise}}(\omega)\, \mathrm{d}\omega = \frac{1}{2\pi} \int\limits_{\omega_{\text{low}}}^{\omega_{\text{low}} + \Delta\omega} J_{\text{noise}}(\omega)\, \mathrm{d}\omega \tag{7.88}$$

because $J_{\text{noise}}(\omega) = 0$ outside the limits ω_{low} and $\omega_{\text{high}} = \omega_{\text{low}} + \Delta\omega$. Comparison with Eq. 7.84, where $4Rk_{\text{B}}T$ is frequency independent, shows that:

$$\langle U_{\text{noise}}^2 \rangle = \frac{1}{2\pi} 4Rk_{\text{B}}T\Delta\omega = \frac{1}{2\pi} 4Rk_{\text{B}}T \int\limits_{\omega_{\text{low}}}^{\omega_{\text{low}}+\Delta\omega} \mathrm{d}\omega = \frac{1}{2\pi} \int\limits_{\omega_{\text{low}}}^{\omega_{\text{low}}+\Delta\omega} 4Rk_{\text{B}}T\, \mathrm{d}\omega = \frac{1}{2\pi} \int\limits_{\omega_{\text{low}}}^{\omega_{\text{low}}+\Delta\omega} J_{\text{noise}}(\omega)\, \mathrm{d}\omega \tag{7.89}$$

and therefore $J_{\text{noise}}(\omega) = 4Rk_{\text{B}}T$. This finding helps us to evaluate how the noise enters the signal-to-noise ratio of the frequency spectrum. The Fourier transform

$$Y_{\text{noise}} = \int\limits_{0}^{t_{\text{max}}} U_{\text{noise}}(t)\mathrm{e}^{-\mathrm{i}\omega t}\, \mathrm{d}t \tag{7.90}$$

is a random quantity that cannot be evaluated easily. However, its mean square can be related to $J_{\text{noise}}(\omega)$ if t_{max} is sufficiently long ($t_{\text{max}} \gg 1/\Delta\omega$):

$$\langle Y_{\text{noise}}^2 \rangle = \int\limits_{0}^{t_{\text{max}}} \mathrm{d}t \int\limits_{0}^{t_{\text{max}}} \langle U_{\text{noise}}(t)U_{\text{noise}}(t-t') \rangle \mathrm{e}^{-\mathrm{i}\omega(t-t')}\, \mathrm{d}t' \approx \frac{1}{2} \int\limits_{0}^{t_{\text{max}}} \mathrm{d}t \int\limits_{-\infty}^{\infty} \langle U_{\text{noise}}(t)U_{\text{noise}}(t-t') \rangle \mathrm{e}^{-\mathrm{i}\omega(t-t')}\, \mathrm{d}t'$$

$$= \frac{1}{2} J_{\text{noise}}(\omega) \int\limits_{0}^{t_{\text{max}}} \mathrm{d}t = 2Rk_{\text{B}}T \int\limits_{0}^{t_{\text{max}}} \mathrm{d}t = 2Rk_{\text{B}}Tt_{\text{max}}. \tag{7.91}$$

We can use Eq. 7.81 to convert R to $|\omega_0|L/Q$. Since the inductance of a solenoid is $L = \mu_0 n^2 S/l$, where l is the length of the solenoid,

$$R = Q|\omega_0|L = \frac{Q|\omega_0|Sn^2}{l} = \frac{Q|\gamma|B_0 Sn^2}{l} \tag{7.92}$$

and

$$\langle Y_{\text{noise}}^2 \rangle = \frac{2Q|\gamma|B_0 k_{\text{B}}TSn^2 t_{\text{max}}}{l}. \tag{7.93}$$

We can now combine Eqs. 7.83 and 7.93, and calculate the signal-to-noise ratio as

$$\text{Signal/noise} = \frac{Y_{\text{max}}}{\sqrt{\langle Y_{\text{noise}}^2 \rangle}} = \frac{\frac{\mu_0}{4\pi}\left(\frac{\hbar}{2}\right)^2 \frac{2nQS}{r^3} \frac{N|\gamma|^3 B_0^2}{k_{\text{B}}T} \frac{1-\mathrm{e}^{-R_2 t_{\text{max}}}}{R_2}}{\sqrt{\frac{2Q|\gamma|B_0 k_{\text{B}}TSn^2 t_{\text{max}}}{l}}} = \frac{\mu_0}{4\pi}\left(\frac{\hbar}{2}\right)^2 \underbrace{\frac{\sqrt{2QV_{\text{coil}}}}{r^3}}_{K} \frac{N|\gamma|^{5/2} B_0^{3/2}}{k_{\text{B}}^{3/2} T^{3/2}} \frac{1-\mathrm{e}^{-R_2(T)t_{\text{max}}}}{R_2(T)t_{\text{max}}^{1/2}}, \tag{7.94}$$

where $V_{\text{coil}} = Sl$ is the coil volume. The signal-to-noise ratio in the spectrum also depends on other tricks applied during signal processing. When deriving Eq. 7.29, we already assumed that the phase correction was applied. Another factor determining the sensitivity of the spectrum in practice is apodization, but we ignore it now for the sake of simplicity. The actual sensitivity is also proportional to square root of the ratio of the time of signal acquisition to the overall time of the experiment.[14]

Eq. 7.94 contains many factors. The blue geometry and construction factors do not deserve much attention as they depend on the actual instrumental setup, and can be replaced by a general parameter K. The green factors are most interesting. They show why NMR spectroscopists like to work with high concentrations (resulting in high N), with high-γ nuclei, and at high-field spectrometers. The total

---

[13]Limiting the detected range of frequencies is important. A completely random noise is present at all frequencies. Without the band-pass filter, this infinite range of frequencies (representing theoretically an infinite noise power) would be aliased (Section 3.6) into the spectral width given by the time increment of the digital signal.

[14]In many experiments (but not necessarily in the one-dimensional experiment), the recycle delay (waiting for the sample to return close to the equilibrium before the next measurement) is much longer than the actual signal acquisition.

acquisition time (purple) and temperature (red) and are set for each experiment. We usually prefer to acquire the signal for $t_{\max} \gg R_2$ in order to avoid truncation artifacts discussed in Section 3.4. However, the noise also accumulates in time, it grows proportional to $\sqrt{t_{\max}}$. Therefore, an optimum $t_{\max}$ should be set (depending on R_2) and/or a well chosen apodization should be applied (Section 3.9). For example, if our $t_{\max}$ is substantially longer than R_2 and we decide to prolong it further, we accumulate only the noise without acquiring any additional signal. The temperature is also a factor that can be controlled easily. At the first glance, lower temperatures seem to be beneficial. However, the dependence of the signal-to-noise ratio on the relaxation rate R_2 introduces also additional dependence on the temperature and, in the case of the relaxation caused by the chemical shift anisotropy, on γB_0. The relaxation seriously reduces the sensitivity of the detection of the magnetic moment precession in large, rigid molecules. In such molecules, the major contribution to R_2 is the loss of coherence (we labeled its rate R_0 in Section 2.2). As shown in Section 2.2, in a large rigid spherical molecule,

$$\frac{1}{R_2} \approx \frac{6D^{\mathrm{rot}}}{b^2} = \frac{3k_{\mathrm{B}}T}{4\pi r^3 \eta(T) b^2}. \tag{7.95}$$

When inserted to Eq. 7.94, $1/R_2$ may seem to change the temperature dependence to $1/T^{1/2}$. However, the temperature dependence of the water viscosity in Eq. 7.95 influences $1/R_2$ more than the linear temperature dependence of the numerator. Therefore, the temperature dependence of sensitivity on the temperature has a maximum (interestingly close to the room temperature for medium-size proteins in aqueous solutions).

The factor $1/b^2$ in Eq. 7.95 is equal to $1/(\gamma B_0 \delta_{\mathrm{a}})^2$ for the for chemical shift anisotropy. It suggests that the signal-to-noise ratio should *decrease* with increasing B_0. However, the relaxation in most chemical groups of molecules is dominated by other mechanisms than the chemical shift anisotropy, in particular by the dipole-dipole interactions with magnetic moments of nearby protons. As the dipole-dipole interactions do not depend on B_0, a high field usually *increases* the signal-to-noise ratio. Nevertheless, Eq. 7.95 warns us that using a high magnetic field does not always improves the sensitivity. For example, the relaxation due to the chemical shift anisotropy reduces sensitivity at high fields in the case of ^{13}C nuclei in sp^2 hybridization without attached protons (e.g. in carbonyl groups).

It should be stressed that when deriving Eq. 12.4.9, we made many simplifications. We neglected the effect of the preamplifier, resistance of the sample, and assumed that the receiver coil and sample have the same temperature. In the most sensitive NMR probes, the motions of the electrons are suppressed by cooling the receiver coil to a very low temperature, approximately $20\,\mathrm{K}$. Therefore, we have to include the sample and coil temperature separately. If the effect of preamplifier is included, we get a bit more complex relation

$$\mathrm{Signal/noise} = \frac{Y_{\max}}{\sqrt{\langle Y_{\mathrm{noise}}^2 \rangle}} = \frac{\mu_0}{4\pi} \left(\frac{\hbar}{2} \right)^2 \; K \; \frac{N |\gamma|^{5/2} B_0^{3/2}}{k_{\mathrm{B}}^{3/2} T_{\mathrm{sample}} \sqrt{(T_{\mathrm{coil}} + T_{\mathrm{sample}} R'/R + (1 + R'/R)\, T')}} \; \frac{1 - \mathrm{e}^{-R_2(T) t_{\max}}}{R_2(T) t_{\max}^{1/2}}, \tag{7.96}$$

where R is the resistance of the coil, R' is the resistance induced by the sample in the coil (proportional to the conductivity and therefore to the ionic strength of the sample), and T' is the so called noise temperature of the amplifier.[15]

The numerical values given by Eqs. 7.94 and 7.96 are of little practical use. However, it is useful to notice how sensitivity depends on individual factors (temperature, field, magnetogyric ratio of the observed nucleus).

---

[15]The input noise is amplified by the factor $(1 + T'/T)G$, where G is the gain of the preamplifier.

Lecture 8
Dipolar coupling, product operators

Literature: The product operator formalism for multi-spin systems is described in B17.4, B18, C2.5.1, C2.7, L15. The dipole-dipole Hamiltonian is discussed in L9.3. Relaxation is described in K9, L19–L20, C5 in different manners. All texts are excellent. It is very helpful to read them all if you really want to get an insight. However, relaxation is a difficult topic and absorbing the information requires a lot of time.

8.1 Dipolar coupling

So far, we analyzed effects of various fields on nuclear magnetic moments, but we assumed that individual magnetic moments are independent and their properties can be described by operators composed of two-dimensional matrices. In this lecture, we take into account also mutual interactions – interactions with fields generated by magnetic moments of other nuclei.

As usually, we start by the classical description of the interaction. If spin magnetic moments of two spin-1/2 nuclei interact with each other, the magnetic moment of nucleus 1 is influenced by the magnetic field $\vec{B}_2$ of the magnetic moment of nucleus 2. The analysis presented in Section 8.9.1 shows that the magnetic field of nucleus 2 contributes to the magnetic field at the position of nucleus 1 as

$$\begin{pmatrix} B_{2,x} \\ B_{2,y} \\ B_{2,z} \end{pmatrix} = \frac{\mu_0}{4\pi r^5} \begin{pmatrix} 3r_x^2 - r^2 & 3r_x r_y & 3r_x r_z \\ 3r_x r_y & 3r_y^2 - r^2 & 3r_y r_z \\ 3r_x r_z & 3r_y r_z & 3r_z^2 - r^2 \end{pmatrix} \cdot \begin{pmatrix} \mu_{2x} \\ \mu_{2y} \\ \mu_{2z} \end{pmatrix}, \tag{8.1}$$

where r_j are components of a vector describing mutual positions of the nuclei in space. A graphical representation of the effect of $\vec{B}_2$ on nucleus 1 and of its dependence on the orientation of the nuclei (given by the orientation of the molecule) is presented in Figure 8.1. The matrix in Eq. 8.1 can be viewed as a representation of the tensor of the dipolar interactions. In contrast to the chemical shift tensor, the tensor of dipolar interactions does not have any isotropic or rhombic component.

Having the classical description of the interaction of two magnetic dipolar moments, derivation of the quantum mechanical Hamiltonian is easy, as shown in Section 8.9.1. The result of Eq. 8.1 is inserted into the general relation $\mathcal{E}_D = -\vec{\mu}_1 \cdot \vec{B}_2$, the magnetic moments are expressed by the angular momenta ($\vec{\mu}_1 = \gamma_1 \vec{I}_1$, $\vec{\mu}_2 = \gamma_2 \vec{I}_2$), and the energy and angular momentum components are replaced by the corresponding operators. The result is
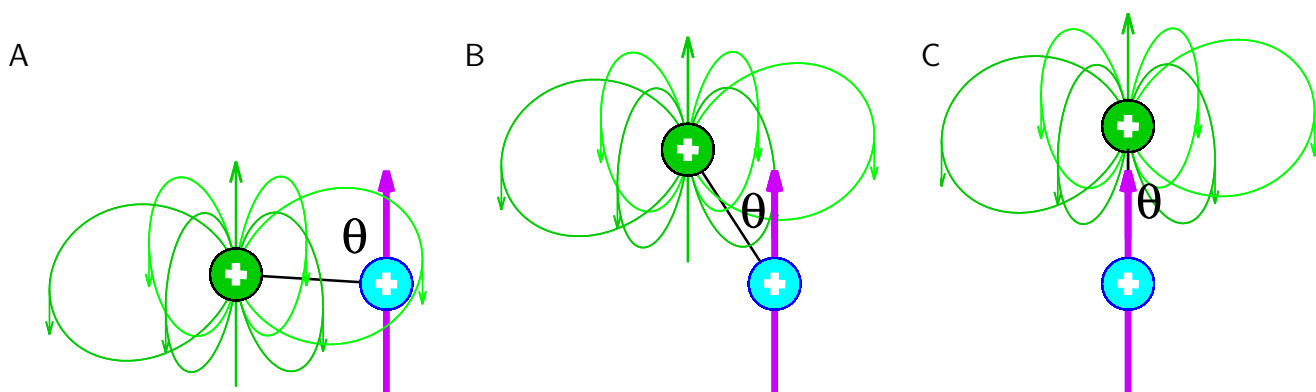
Figure 8.1: A, Classical description of the interaction of a spin magnetic moment of the observed nucleus (shown in cyan) with a spin magnetic moment of another nucleus (shown in green). The thick purple arrow represents $\vec{B}_0$, the thin green induction lines represent the magnetic field $\vec{B}_2$ of the green nucleus (the small green arrows indicate its direction). The black line represents the internuclear vector $\vec{r}$. As the molecule rotates, the cyan nucleus moves from a position where the field of the spin magnetic moment of the green nucleus $\vec{B}_2$ has the opposite direction than $\vec{B}_0$ (A), through a position where $\vec{B}_2$ is perpendicular to $\vec{B}_0$ (B), to the position where $\vec{B}_2$ has the same direction as $\vec{B}_0$ (C).

$$
\begin{aligned}
\hat{H}_D = & -\frac{\mu_0 \gamma_1 \gamma_2}{4\pi r^5} \begin{pmatrix} \hat{I}_{1x} & \hat{I}_{1y} & \hat{I}_{1z} \end{pmatrix} \begin{pmatrix} 3r_x^2 - r^2 & 3r_x r_y & 3r_x r_z \\ 3r_x r_y & 3r_y^2 - r^2 & 3r_y r_z \\ 3r_x r_z & 3r_y r_z & 3r_z^2 - r^2 \end{pmatrix} \begin{pmatrix} \hat{I}_{2x} \\ \hat{I}_{2y} \\ \hat{I}_{2z} \end{pmatrix} \\
= & -\frac{\mu_0}{4\pi r^3} \left((3r_x^2 - r^2)\hat{I}_{1x}\hat{I}_{2x} + (3r_y^2 - r^2)\hat{I}_{1y}\hat{I}_{2y} + (3r_z^2 - r^2)\hat{I}_{1z}\hat{I}_{2z} + \right. \\
& \left. 3r_x r_y \hat{I}_{1x}\hat{I}_{2y} + 3r_x r_z \hat{I}_{1x}\hat{I}_{2z} + 3r_y r_z \hat{I}_{1y}\hat{I}_{2z} + 3r_y r_x \hat{I}_{1y}\hat{I}_{2x} + 3r_z r_x \hat{I}_{1z}\hat{I}_{2x} + 3r_z r_y \hat{I}_{1z}\hat{I}_{2y} \right). \quad (8.2)
\end{aligned}
$$

After defining the Hamiltonian of the dipole-dipole interaction, we can ask how is the total Hamiltonian representing the energy of the magnetic moment pairs influenced by the dipolar coupling. In the absence of radio waves,[1] the energy of the magnetic moment pairs depends on $\vec{B}_0$, on the chemical shifts δ_1 and δ_2 of the coupled nuclei, and on the dipolar coupling. The corresponding Hamiltonian consists of the isotropic component $\hat{H}_0$, and of an anisotropic part including axial and rhombic components of the chemical shift Hamiltonian and of the Hamiltonian representing the dipolar coupling, $\hat{H}_D$. The complete Hamiltonian $\hat{H}_D$ described by Eq. 8.2 is rather complex. However, it can be often greatly simplified, as discussed in Section 8.9.2. The *secular approximation* depends on whether the precession frequencies of the interacting magnetic moments are identical or different. In the former case, $\hat{H}_D$ simplifies to

$$
\hat{H}_D = -\frac{\mu_0 \gamma_1 \gamma_2}{4\pi r^3} \frac{3\langle \cos^2 \vartheta \rangle - 1}{2} \left(2\hat{I}_{1z}\hat{I}_{2z} - \hat{I}_{1x}\hat{I}_{2x} - \hat{I}_{1y}\hat{I}_{2y} \right), \quad (8.3)
$$

---

[1]We assume that the field of the irradiating radio waves is much stronger than the dipolar interactions of nuclear magnetic moments. Therefore, we neglect the effect of the dipolar coupling during the short radio wave pulses.

in the latter case, to

$$\hat{H}_D = -\frac{\mu_0 \gamma_1 \gamma_2}{4\pi r^3} \frac{3\langle \cos^2 \vartheta \rangle - 1}{2} \left(2\hat{I}_{1z}\hat{I}_{2z} \right).$$

(8.4)

As derived in Section 8.9.1, $\hat{H}_D$ depends on the orientation of the molecule like the anisotropic component of the chemical shift. It implies that whole $\hat{H}_D$ averages to zero in isotropic liquids (Section 8.9.2).

The Hamiltonian representing the energy of an ensemble of pairs of directly interacting spin dipolar magnetic moments in $\vec{B}_0$ reduces in isotropic liquids to

$$\hat{H} = -\gamma_1 B_0 (1 + \delta_{i,1})\hat{I}_{1z} - \gamma_2 B_0 (1 + \delta_{i,2})\hat{I}_{2z}.$$

(8.5)

The simplified Eq. 8.5 is valid only in isotropic liquids and does not describe relaxation processes. The effect of $\hat{H}_D$ is huge in solid state NMR and can be also be measured e.g. in liquid crystals or mechanically stretched gels. Last but not least, dipole-dipole interactions result in strong relaxation effects, discussed in Section 8.7.

8.2 Quantum states of magnetic moment pairs

We know how to construct the Hamiltonian of the dipole-dipole interactions from the operators $\hat{I}_{1x}, \hat{I}_{1y}, \hat{I}_{1z}, \hat{I}_{2x}, \hat{I}_{2y}, \hat{I}_{2z}$, but we still did not describe the explicit forms of these operators or of the wave function the Hamiltonian acts on. To fill this gap in our knowledge, we look for a vector representing the wave function of coupled magnetic moments. Although we are concerned with direct dipole-dipole interactions in this Lecture, we try to formulate our conclusions so that they apply to various couplings of nuclear magnetic moments in general.

We first describe a quantum state of a pair of *non-interacting* spin-1/2 nuclei. The wave function Ψ of such a pair of particles can be decomposed into the spin-part and a part dependent on the other degrees of freedom (spatial coordinates of the nuclei). The spin part can be further separated into a product of wave functions dependent on the spin degrees of freedom of the individual nuclei:

$$\Psi = \psi_{\text{non-spin}}(x_1, y_1, z_1, x_2, y_2, z_2) \cdot \psi_{\text{spin}}(c_{\alpha,1}, c_{\alpha,2}) = \psi_{\text{non-spin}} \cdot \psi_{1,\text{spin}} \cdot \psi_{2,\text{spin}}.$$

(8.6)

Writing explicitly first $\psi_{1,\text{spin}}$

$$\Psi = \psi_{\text{non-spin}} \cdot \begin{pmatrix} c_{\alpha,1} \\ c_{\beta,1} \end{pmatrix} \cdot \psi_{2,\text{spin}} = \psi_{\text{non-spin}} \cdot \begin{pmatrix} c_{\alpha,1}\psi_{2,\text{spin}} \\ c_{\beta,1}\psi_{2,\text{spin}} \end{pmatrix}$$

(8.7)

and then $\psi_{2,\text{spin}}$

$$\Psi = \psi_{\text{non-spin}} \cdot \begin{pmatrix} c_{\alpha,1} \begin{pmatrix} c_{\alpha,2} \\ c_{\beta,2} \end{pmatrix} \\ c_{\beta,1} \begin{pmatrix} c_{\alpha,2} \\ c_{\beta,2} \end{pmatrix} \end{pmatrix} = \psi_{\text{non-spin}} \cdot \begin{pmatrix} c_{\alpha,1}c_{\alpha,2} \\ c_{\alpha,1}c_{\beta,2} \\ c_{\beta,1}c_{\alpha,2} \\ c_{\beta,1}c_{\beta,2} \end{pmatrix} \equiv \psi_{\text{non-spin}} \cdot \begin{pmatrix} c_{\alpha\alpha} \\ c_{\alpha\beta} \\ c_{\beta\alpha} \\ c_{\beta\beta} \end{pmatrix},$$

(8.8)

we obtain a four-component wave function built as a *direct product*[2] (or *Kronecker product*) of two-component wave functions (state vectors) of single spin magnetic moments:

$$
\begin{pmatrix} c_{\alpha,1} \\ c_{\beta,1} \end{pmatrix} \otimes \begin{pmatrix} c_{\alpha,2} \\ c_{\beta,2} \end{pmatrix} = \begin{pmatrix} c_{\alpha,1} \begin{pmatrix} c_{\alpha,2} \\ c_{\beta,2} \end{pmatrix} \\ c_{\beta,1} \begin{pmatrix} c_{\alpha,2} \\ c_{\beta,2} \end{pmatrix} \end{pmatrix} = \begin{pmatrix} c_{\alpha,1} c_{\alpha,2} \\ c_{\alpha,1} c_{\beta,2} \\ c_{\beta,1} c_{\alpha,2} \\ c_{\beta,1} c_{\beta,2} \end{pmatrix} \equiv \begin{pmatrix} c_{\alpha\alpha} \\ c_{\alpha\beta} \\ c_{\beta\alpha} \\ c_{\beta\beta} \end{pmatrix}.
\tag{8.9}
$$

A detailed analysis of the four-component wavefunction is presented in Section 8.9.3 (for non-interacting and interacting magnetic moments). Here, we only summarize the results of the analysis. In the eigenequation, $\psi_{\text{non-spin}}$ is canceled out (see Section 5.4). The introduced four-component function is written in a basis of vectors that are simultaneous eigenfuctions of the angular momentum operators $\hat{I}_1^2, \hat{I}_2^2, \hat{I}_{1z}, \hat{I}_{2z}$. If the magnetic moments are independent, $\hat{I}_1^2 = \hat{I}_2^2$, $\hat{I}_{1z} = \hat{I}_{2z}$, and the pair can be described in a two-component basis of the eigenfunctions of $\hat{I}_z = \hat{I}_{1z} = \hat{I}_{2z}$ (and of $\hat{I}^2 = \hat{I}_1^2 = \hat{I}_2^2$), as described in Section 6.1.

If the magnetic moments of the pair interact, they cannot be described in the two-component basis of independent spin magnetic moments. The state of the first spin depends on the state of the second spin. Therefore, the probability density matrix describing *a large ensemble* of pairs that interact mutually, but are isolated from other pairs, must be four-dimensional, built from coefficients of the wave function in Eq. 8.8. In other words, we can use the mixed-state approach, but we must describe the pair of the interacting magnetic moments and its four states as one entity. Furthermore, the Hamiltonian of dipolar interactions (Eq. 8.2) is built from operators representing *products* of individual components of the interacting magnetic moments. Let us now look for a basis that fulfils these requirements.

8.3 Product operators

The wave function (state vector) describing a single interacting pair of magnetic moments is four-dimensional. Therefore, the density matrix that describes an ensemble of such interacting pairs, and consists of averaged combinations of the elements of the four-dimensional state vector, is a 4×4 matrix

$$
\hat{\rho} = \begin{pmatrix} \overline{c_{\alpha\alpha} c_{\alpha\alpha}^*} & \overline{c_{\alpha\alpha} c_{\alpha\beta}^*} & \overline{c_{\alpha\alpha} c_{\beta\alpha}^*} & \overline{c_{\alpha\alpha} c_{\beta\beta}^*} \\ \overline{c_{\alpha\beta} c_{\alpha\alpha}^*} & \overline{c_{\alpha\beta} c_{\alpha\beta}^*} & \overline{c_{\alpha\beta} c_{\beta\alpha}^*} & \overline{c_{\alpha\beta} c_{\beta\beta}^*} \\ \overline{c_{\beta\alpha} c_{\alpha\alpha}^*} & \overline{c_{\beta\alpha} c_{\alpha\beta}^*} & \overline{c_{\beta\alpha} c_{\beta\alpha}^*} & \overline{c_{\beta\alpha} c_{\beta\beta}^*} \\ \overline{c_{\beta\beta} c_{\alpha\alpha}^*} & \overline{c_{\beta\beta} c_{\alpha\beta}^*} & \overline{c_{\beta\beta} c_{\beta\alpha}^*} & \overline{c_{\beta\beta} c_{\beta\beta}^*} \end{pmatrix}.
\tag{8.10}
$$

---

[2]Direct product $\hat{A} \otimes \hat{B}$ is a mathematical operation when each element of the matrix $\hat{A}$ is multiplied by the whole matrix $\hat{B}$:

$$
\hat{A} \otimes \hat{B} = \begin{pmatrix} A_{11} & A_{12} \\ A_{21} & A_{22} \end{pmatrix} \otimes \begin{pmatrix} B_{11} & B_{12} \\ B_{21} & B_{22} \end{pmatrix} = \begin{pmatrix} A_{11} \begin{pmatrix} B_{11} & B_{12} \\ B_{21} & B_{22} \end{pmatrix} & A_{12} \begin{pmatrix} B_{11} & B_{12} \\ B_{21} & B_{22} \end{pmatrix} \\ A_{21} \begin{pmatrix} B_{11} & B_{12} \\ B_{21} & B_{22} \end{pmatrix} & A_{22} \begin{pmatrix} B_{11} & B_{12} \\ B_{21} & B_{22} \end{pmatrix} \end{pmatrix} = \begin{pmatrix} A_{11}B_{11} & A_{11}B_{12} & A_{12}B_{11} & A_{12}B_{12} \\ A_{11}B_{21} & A_{11}B_{22} & A_{12}B_{21} & A_{12}B_{22} \\ A_{21}B_{11} & A_{21}B_{12} & A_{22}B_{11} & A_{22}B_{12} \\ A_{21}B_{21} & A_{21}B_{22} & A_{22}B_{21} & A_{22}B_{22} \end{pmatrix}
$$

A basis used for such density matrices and for operators acting on the four-dimensional wave function must consist of $4^2 = 16$ matrices.[3] The four-dimensional wave function (state vector) describing the interacting pair of magnetic moments was constructed as a direct product of two-dimensional single-spin state vectors. Not surprisingly,[4] the basis of the 4×4 matrices can be built from direct products of 2×2 basis matrices used for spins without mutual interactions. For example, Cartesian single-spin operators can be used to create a basis for two spins (see Tables 8.1 and 8.2) using the following direct products of normalized basis matrices:

$$\left(\sqrt{2}\,\mathscr{I}_t^{(1)}\right) \otimes \left(\sqrt{2}\,\mathscr{I}_t^{(2)}\right) = \mathscr{I}_t^{(12)} \tag{8.11}$$

$$\left(\sqrt{2}\,\mathscr{I}_x^{(1)}\right) \otimes \left(\sqrt{2}\,\mathscr{I}_t^{(2)}\right) = \mathscr{I}_{1x}^{(12)} \tag{8.12}$$

$$\left(\sqrt{2}\,\mathscr{I}_y^{(1)}\right) \otimes \left(\sqrt{2}\,\mathscr{I}_t^{(2)}\right) = \mathscr{I}_{1y}^{(12)} \tag{8.13}$$

$$\left(\sqrt{2}\,\mathscr{I}_z^{(1)}\right) \otimes \left(\sqrt{2}\,\mathscr{I}_t^{(2)}\right) = \mathscr{I}_{1z}^{(12)} \tag{8.14}$$

$$\left(\sqrt{2}\,\mathscr{I}_t^{(1)}\right) \otimes \left(\sqrt{2}\,\mathscr{I}_x^{(2)}\right) = \mathscr{I}_{2x}^{(12)} \tag{8.15}$$

$$\left(\sqrt{2}\,\mathscr{I}_t^{(1)}\right) \otimes \left(\sqrt{2}\,\mathscr{I}_y^{(2)}\right) = \mathscr{I}_{2y}^{(12)} \tag{8.16}$$

$$\left(\sqrt{2}\,\mathscr{I}_t^{(1)}\right) \otimes \left(\sqrt{2}\,\mathscr{I}_z^{(2)}\right) = \mathscr{I}_{2z}^{(12)} \tag{8.17}$$

$$\left(\sqrt{2}\,\mathscr{I}_x^{(1)}\right) \otimes \left(\sqrt{2}\,\mathscr{I}_x^{(2)}\right) = 2\mathscr{I}_{1x}\mathscr{I}_{2x}^{(12)} \tag{8.18}$$

$$\left(\sqrt{2}\,\mathscr{I}_x^{(1)}\right) \otimes \left(\sqrt{2}\,\mathscr{I}_y^{(2)}\right) = 2\mathscr{I}_{1x}\mathscr{I}_{2y}^{(12)} \tag{8.19}$$

$$\left(\sqrt{2}\,\mathscr{I}_x^{(1)}\right) \otimes \left(\sqrt{2}\,\mathscr{I}_z^{(2)}\right) = 2\mathscr{I}_{1x}\mathscr{I}_{2z}^{(12)} \tag{8.20}$$

$$\left(\sqrt{2}\,\mathscr{I}_y^{(1)}\right) \otimes \left(\sqrt{2}\,\mathscr{I}_x^{(2)}\right) = 2\mathscr{I}_{1y}\mathscr{I}_{2x}^{(12)} \tag{8.21}$$

$$\left(\sqrt{2}\,\mathscr{I}_y^{(1)}\right) \otimes \left(\sqrt{2}\,\mathscr{I}_y^{(2)}\right) = 2\mathscr{I}_{1y}\mathscr{I}_{2y}^{(12)} \tag{8.22}$$

$$\left(\sqrt{2}\,\mathscr{I}_y^{(1)}\right) \otimes \left(\sqrt{2}\,\mathscr{I}_z^{(2)}\right) = 2\mathscr{I}_{1y}\mathscr{I}_{2z}^{(12)} \tag{8.23}$$

$$\left(\sqrt{2}\,\mathscr{I}_z^{(1)}\right) \otimes \left(\sqrt{2}\,\mathscr{I}_x^{(2)}\right) = 2\mathscr{I}_{1z}\mathscr{I}_{2x}^{(12)} \tag{8.24}$$

$$\left(\sqrt{2}\,\mathscr{I}_z^{(1)}\right) \otimes \left(\sqrt{2}\,\mathscr{I}_y^{(2)}\right) = 2\mathscr{I}_{1z}\mathscr{I}_{2y}^{(12)} \tag{8.25}$$

$$\left(\sqrt{2}\,\mathscr{I}_z^{(1)}\right) \otimes \left(\sqrt{2}\,\mathscr{I}_z^{(2)}\right) = 2\mathscr{I}_{1z}\mathscr{I}_{2z}^{(12)}, \tag{8.26}$$

where the numbers in parentheses specify which nuclei constitute the spin system described by the given matrix (these numbers are not written in practice). The matrices on the right-hand side

---

[3]In general, the density matrix for n states is a $n \times n$ matrix. Basis used for such density matrices must consist of 4^n matrices.

[4]The relation between the construction of the state vectors and of operators acting on them is described by the group theory. It follows from the analysis of the rotation of the state vectors and operators acting on them that the coupling between the state vectors and between the operators is the same.

are known as *product operators*. Note that $2\mathscr{I}_t$, equal to[5] $\hat{1}$, is not written in the product operators for the sake of simplicity. Note also that e.g. $\mathscr{I}_x^{(1)}$ and $\mathscr{I}_x^{(2)}$ are the same 2×2 matrices, but $\mathscr{I}_{1x}^{(12)}$ and $\mathscr{I}_{2x}^{(12)}$ are different 4×4 matrices. Basis matrices for more nuclei are derived in the same manner, a more detailed discussion is presented in Section 12.4.5.

The basis presented in Eqs. 8.11–8.26 represents one of many possible choices. Other choices are presented in Section 8.9.4.

8.4   Density matrix of a two-spin system

The introduced formal description of the density matrix would be useless if we did not understand its physical significance. Interpretation of the 4×4 density matrix requires more care than the interpretation of its two-dimensional version. In general, the density matrix $\hat{\rho}$ is a linear combination of 16 basis matrices $\mathscr{B}_j$ (the actual forms of $\mathscr{B}_j$ depend on the chosen basis):

$$\hat{\rho} = \sum_{j=1}^{16} C_j \mathscr{B}_j \tag{8.27}$$

Each basis matrix $\mathscr{B}_j$ describes one feature of the mixed state (e.g., longitudinal polarization of the first magnetic moment) and the coefficients C_j specify how much the given feature contributes to the mixed state. Below, we interpret the individual matrices of a commonly used Cartesian basis. Although we discuss direct dipole-dipole interaction in this Lecture, the interpretation of the Cartesian matrices is general and applicable to other interactions between the magnetic moments. The description of the matrices is also summarized in Tables 8.1 and 8.2.

The Cartesian basis contains four diagonal matrices. Like in the two-dimensional case, the diagonal elements of $\hat{\rho}$ and diagonal matrices describe the *longitudinal polarization* of the magnetic moments. The sum of the diagonal elements is equal to one, like in the two-dimensional density matrix. Therefore, we have three independent *populations*. Two of them, corresponding to contributions of matrices labeled $\mathscr{I}_{1z}$ and $\mathscr{I}_{2z}$, describe *separately* longitudinal magnetic moment polarization of nuclei 1 and 2, respectively. Contribution of the third diagonal matrix, $2\mathscr{I}_{1z}\mathscr{I}_{2z}$, describes *correlation* between μ_{1z} and μ_{2z}, how much the longitudinal polarization of $\vec{\mu}_1$ is influenced by the longitudinal polarization of $\vec{\mu}_2$, and vice versa.

Twelve off-diagonal elements or matrices composed of them are called *coherences*. Only six off-diagonal elements are independent because each element below the diagonal has its complex conjugate above the diagonal. Note, however, that coherences are complex quantities. The six independent off-diagonal elements thus represent twelve real numbers. Therefore, none of twelve purely real or purely imaginary matrices in Table 8.2 is redundant. The coherences corresponding to contributions of matrices $\mathscr{I}_{1x}$ and $\mathscr{I}_{2x}$, respectively, describe the *transverse polarization in the direction x* of magnetic moments of nuclei 1 and 2, regardless of the state of the other nucleus. Contributions of $\mathscr{I}_{1y}$ and $\mathscr{I}_{2y}$ describe transverse polarization in the direction y in the same manner. A contribution of $2\mathscr{I}_{1x}\mathscr{I}_{2z}$ describes how the transverse polarization of $\vec{\mu}_1$ in the x direction depends on the longitudinal polarization of $\vec{\mu}_2$. The dependence of the transverse polarization of $\vec{\mu}_2$ in the x direction

---

[5]$\hat{1}$ is a 2×2 unit matrix in the case of $\mathscr{I}_t^{(1)}$ or $\mathscr{I}_t^{(2)}$, and a 4×4 unit matrix in the case of $\mathscr{I}_t^{(1)}$.

Table 8.1: Contributions to the two-spin density matrix describing the uniform distribution and longitudinal polarizations of spin magnetic moments $\vec{\mu}_1$ and $\vec{\mu}_2$. In the graphical representation, the left and right distribution corresponds to of superimposed $\vec{\mu}_1$ and $\vec{\mu}_2$, respectively. The uniform distribution is shown in black. In order to visualize the correlation of the longitudinal polarization, the following color-coding is used. In the case of the longitudinal polarization of $\vec{\mu}_1$, magnetic moments of nucleus 1 in 10% molecules with most polarized $\vec{\mu}_1$ are shown in cyan, and magnetic moments of nucleus 2 *in the same molecules* are shown in green. In the case of the longitudinal polarization of $\vec{\mu}_2$, magnetic moments of nucleus 2 in 10% molecules with most polarized $\vec{\mu}_2$ are shown in green, and magnetic moments of nucleus 1 *in the same molecules* are shown in cyan. The chosen distributions of orientation symbolize the *trend* of the polarization represented by the given matrix, the depicted degree of polarization is lower than the degree corresponding to the actual matrices: basis matrices describe either no polarization (the uniform distribution of orientations) or complete polarization (identical orientations, i.e., a single arrow in the plot).

Matrix	graph	description
$\mathscr{I}_t = \frac{1}{2}\begin{pmatrix} +1 & 0 & 0 & 0 \\ 0 & +1 & 0 & 0 \\ 0 & 0 & +1 & 0 \\ 0 & 0 & 0 & +1 \end{pmatrix}$		no polarization of $\vec{\mu}_1$ or $\vec{\mu}_2$
$\mathscr{I}_{1z} = \frac{1}{2}\begin{pmatrix} +1 & 0 & 0 & 0 \\ 0 & +1 & 0 & 0 \\ 0 & 0 & -1 & 0 \\ 0 & 0 & 0 & -1 \end{pmatrix}$		longitudinal polarization of $\vec{\mu}_1$ regardless of $\vec{\mu}_2$
$\mathscr{I}_{2z} = \frac{1}{2}\begin{pmatrix} +1 & 0 & 0 & 0 \\ 0 & -1 & 0 & 0 \\ 0 & 0 & +1 & 0 \\ 0 & 0 & 0 & -1 \end{pmatrix}$		longitudinal polarization of $\vec{\mu}_2$ regardless of $\vec{\mu}_1$
$2\mathscr{I}_{1z}\mathscr{I}_{2z} = \frac{1}{2}\begin{pmatrix} +1 & 0 & 0 & 0 \\ 0 & -1 & 0 & 0 \\ 0 & 0 & -1 & 0 \\ 0 & 0 & 0 & +1 \end{pmatrix}$		correlation of longitudinal polarizations of $\vec{\mu}_1$ and $\vec{\mu}_2$

on the longitudinal polarization of $\vec{\mu}_1$ is given by the contribution $2\mathscr{I}_{1z}\mathscr{I}_{2x}$. The same applies to $2\mathscr{I}_{1y}\mathscr{I}_{2z}, 2\mathscr{I}_{1z}\mathscr{I}_{2y}$ and to direction y. Finally, contributions of $2\mathscr{I}_{1x}\mathscr{I}_{2x}$, $2\mathscr{I}_{1y}\mathscr{I}_{2y}$, $2\mathscr{I}_{1x}\mathscr{I}_{2y}$, and $2\mathscr{I}_{1y}\mathscr{I}_{2x}$ describe mutual correlation of transverse polarizations of $\vec{\mu}_1$ and $\vec{\mu}_2$.

8.5 Commutators of product operators

The Liouville-von Neumann equation can be written for coupled magnetic moments in the same form as for spins without mutual interactions (Eq. 6.8):

$$\frac{\mathrm{d}\hat{\rho}}{\mathrm{d}t} = \mathrm{i}(\hat{\rho}\mathscr{H} - \mathscr{H}\hat{\rho}) = \mathrm{i}[\hat{\rho}, \mathscr{H}] = -\mathrm{i}[\mathscr{H}, \hat{\rho}], \tag{8.28}$$

but the density matrix and the Hamiltonian are now[6] 4×4 matrices. Also Eqs. 6.9 and 6.10 can be generalized to the product operators. The same simple geometric solution of the Liouville-von Neumann equation is possible if the Hamiltonian does not vary in time and consists of commuting matrices only. However, the operator space is now 16-dimensional. Therefore, the appropriate three-dimensional subspace must be selected for each rotation. The subspaces are defined by the

---

[6]In general, Eq. 6.8 is valid for $n \times n$ matrices describing ensembles of n mutually interacting nuclei.

Table 8.2: Contributions to the two-spin density matrix describing coherences (see Table 8.1 for color coding).

Matrix	graph	description
$\mathscr{I}_{1x} = \frac{1}{2}\begin{pmatrix} 0 & 0 & +1 & 0 \\ 0 & 0 & 0 & +1 \\ +1 & 0 & 0 & 0 \\ 0 & +1 & 0 & 0 \end{pmatrix}$		transverse polarization of $\vec{\mu}_1$ in direction x, regardless of $\vec{\mu}_2$
$2\mathscr{I}_{1x}\mathscr{I}_{2z} = \frac{1}{2}\begin{pmatrix} 0 & 0 & +1 & 0 \\ 0 & 0 & 0 & -1 \\ +1 & 0 & 0 & 0 \\ 0 & -1 & 0 & 0 \end{pmatrix}$		correlation between transverse polarization of $\vec{\mu}_1$ in direction x and longitudinal polarization of $\vec{\mu}_2$
$\mathscr{I}_{1y} = \frac{\mathrm{i}}{2}\begin{pmatrix} 0 & 0 & -1 & 0 \\ 0 & 0 & 0 & -1 \\ +1 & 0 & 0 & 0 \\ 0 & +1 & 0 & 0 \end{pmatrix}$		transverse polarization of $\vec{\mu}_1$ in direction y, regardless of $\vec{\mu}_2$
$2\mathscr{I}_{1y}\mathscr{I}_{2z} = \frac{\mathrm{i}}{2}\begin{pmatrix} 0 & 0 & -1 & 0 \\ 0 & 0 & 0 & +1 \\ +1 & 0 & 0 & 0 \\ 0 & -1 & 0 & 0 \end{pmatrix}$		correlation between transverse polarization of $\vec{\mu}_1$ in direction y and longitudinal polarization of $\vec{\mu}_2$
$\mathscr{I}_{2x} = \frac{1}{2}\begin{pmatrix} 0 & +1 & 0 & 0 \\ +1 & 0 & 0 & 0 \\ 0 & 0 & 0 & +1 \\ 0 & 0 & +1 & 0 \end{pmatrix}$		transverse polarization of $\vec{\mu}_2$ in direction x, regardless of $\vec{\mu}_1$
$2\mathscr{I}_{1z}\mathscr{I}_{2x} = \frac{1}{2}\begin{pmatrix} 0 & +1 & 0 & 0 \\ +1 & 0 & 0 & 0 \\ 0 & 0 & 0 & -1 \\ 0 & 0 & -1 & 0 \end{pmatrix}$		correlation between transverse polarization of $\vec{\mu}_2$ in direction x and longitudinal polarization of $\vec{\mu}_1$
$\mathscr{I}_{2y} = \frac{\mathrm{i}}{2}\begin{pmatrix} 0 & -1 & 0 & 0 \\ +1 & 0 & 0 & 0 \\ 0 & 0 & 0 & -1 \\ 0 & 0 & +1 & 0 \end{pmatrix}$		transverse polarization of $\vec{\mu}_2$ in direction y, regardless of $\vec{\mu}_1$
$2\mathscr{I}_{1z}\mathscr{I}_{2y} = \frac{\mathrm{i}}{2}\begin{pmatrix} 0 & -1 & 0 & 0 \\ +1 & 0 & 0 & 0 \\ 0 & 0 & 0 & +1 \\ 0 & 0 & -1 & 0 \end{pmatrix}$		correlation between transverse polarization of $\vec{\mu}_2$ in direction y and longitudinal polarization of $\vec{\mu}_1$
$2\mathscr{I}_{1x}\mathscr{I}_{2x} = \frac{1}{2}\begin{pmatrix} 0 & 0 & 0 & +1 \\ 0 & 0 & +1 & 0 \\ 0 & +1 & 0 & 0 \\ +1 & 0 & 0 & 0 \end{pmatrix}$		correlation between transverse polarization of $\vec{\mu}_1$ and $\vec{\mu}_2$ in direction x
$2\mathscr{I}_{1y}\mathscr{I}_{2y} = \frac{1}{2}\begin{pmatrix} 0 & 0 & 0 & -1 \\ 0 & 0 & +1 & 0 \\ 0 & +1 & 0 & 0 \\ -1 & 0 & 0 & 0 \end{pmatrix}$		correlation between transverse polarization of $\vec{\mu}_1$ and $\vec{\mu}_2$ in direction y
$2\mathscr{I}_{1x}\mathscr{I}_{2y} = \frac{\mathrm{i}}{2}\begin{pmatrix} 0 & 0 & 0 & -1 \\ 0 & 0 & +1 & 0 \\ 0 & -1 & 0 & 0 \\ +1 & 0 & 0 & 0 \end{pmatrix}$		correlation between transverse polarization of $\vec{\mu}_1$ in direction x and transverse polarization of $\vec{\mu}_2$ in direction y
$2\mathscr{I}_{1y}\mathscr{I}_{2x} = \frac{\mathrm{i}}{2}\begin{pmatrix} 0 & 0 & 0 & -1 \\ 0 & 0 & -1 & 0 \\ 0 & +1 & 0 & 0 \\ +1 & 0 & 0 & 0 \end{pmatrix}$		correlation between transverse polarization of $\vec{\mu}_1$ in direction y and transverse polarization of $\vec{\mu}_2$ in direction x

commutation relations derived in Section 8.9.5. The relations (applicable to any set of n^2 operators of spin systems consisting of n spin-1/2 nuclei) are described by the following equations:

$$[\mathscr{I}_{nx}, \mathscr{I}_{ny}] = i\mathscr{I}_{nz} \qquad [\mathscr{I}_{ny}, \mathscr{I}_{nz}] = i\mathscr{I}_{nx} \qquad [\mathscr{I}_{nz}, \mathscr{I}_{nx}] = i\mathscr{I}_{ny} \tag{8.29}$$

$$[\mathscr{I}_{nj}, 2\mathscr{I}_{nk}\mathscr{I}_{n'l}] = 2[\mathscr{I}_{nj}, \mathscr{I}_{nk}]\mathscr{I}_{n'l} \tag{8.30}$$

$$[2\mathscr{I}_{nj}\mathscr{I}_{n'l}, 2\mathscr{I}_{nk}\mathscr{I}_{n'm}] = [\mathscr{I}_{nj}, \mathscr{I}_{nk}]\delta_{lm} + [\mathscr{I}_{n'l}, \mathscr{I}_{n'm}]\delta_{jk}, \tag{8.31}$$

where n and n' specify the nucleus, $j, k, l, m \in \{x, y, z\}$, and $\delta_{jk} = 1$ for $j = k$ and $\delta_{jk} = 0$ for $j \neq k$. Since the dipolar interactions do not have coherent effects in isotropic liquids, we postpone the discussion of the rotations in the product operator space to Section 10.4, where we discuss interactions that are not averaged to zero in isotropic samples.

8.6 Operator of the observed quantity for more nuclei

In order to describe the observed signal for a system of n different nuclei, Eq. 7.1, defining the operator of complex magnetization, must be slightly modified

$$\hat{M}_+ = \sum_n \mathcal{N}\gamma_n(\hat{I}_{nx} + i\hat{I}_{ny}) = \sum_n \mathcal{N}\gamma_n\hat{I}_{n+}, \tag{8.32}$$

where the index n distinguishes different types of nuclei. In the case of the magnetic moment pairs discussed in this Lecture, $n = 2$.

8.7 Dipolar relaxation

As mentioned above, dipole-dipole interactions do not have coherent effects (do not influence the measured values of precession frequencies) in isotropic liquids. On the other hand, the dipole-dipole interactions represent a very important source of relaxation.

Rotation of the molecule (and internal motions) change the orientation of the inter-nuclear vector and cause fluctuations of the field of the magnetic moment $\vec{\mu}_2$ sensed by the magnetic moment $\vec{\mu}_1$. It leads to the loss of the coherence in the same manner as described for the anisotropic part of the chemical shift (cf. Eqs 1.109 and 8.56). However, the relaxation effects of the dipole-dipole interactions are more complex, reflecting the higher complexity of the Hamiltonian of the dipolar coupling. A detailed analysis is presented in Section 8.9.6. The analysis shows how molecular motions determine constants R_{a1}, R_{a2}, R_x, $R_{2,1}$, and $R_{2,2}$ in the following relaxation equations:

$$\frac{\mathrm{d}\Delta\langle M_{1z}\rangle}{\mathrm{d}t} = -R_{\mathrm{a}1}\Delta\langle M_{1z}\rangle - R_{\mathrm{x}}\Delta\langle M_{2z}\rangle, \tag{8.33}$$

$$\frac{\mathrm{d}\Delta\langle M_{2z}\rangle}{\mathrm{d}t} = -R_{\mathrm{a}2}\Delta\langle M_{2z}\rangle - R_{\mathrm{x}}\Delta\langle M_{1z}\rangle, \tag{8.34}$$

$$\frac{\mathrm{d}\langle M_{1+}\rangle}{\mathrm{d}t} = -R_{2,1}\langle M_{1+}\rangle, \tag{8.35}$$

$$\frac{\mathrm{d}\langle M_{2+}\rangle}{\mathrm{d}t} = -R_{2,2}\langle M_{2+}\rangle. \tag{8.36}$$

The values of the relaxation rates and their dependence are discussed in Section 8.9.7. Here we mention only two features that directly affect the experiment described in the next Lecture.

- Eqs. 8.33 and 8.34 reveal an important feature of the relaxation due to the dipole-dipole interactions. Return to the equilibrium polarization of nucleus 1 depends also on the actual polarization *of nucleus 2*. This effect, resembling chemical kinetics of a reversible reaction, is known as the *cross-relaxation*, or the *nuclear Overhauser effect* (NOE), and is described by the *cross-relaxation constant* R_{x}. The value of R_{x} is proportional to r^{-6} and thus provides information about inter-atomic distances. NOE is a useful tool in analysis of small molecules and the most important source of structural information for large biological molecules.

- Eqs. 8.35 and 8.36 have a similar form as those describing the transverse relaxation due to the chemical shift anisotropy (Section 7.7). In real samples, contributions to the relaxation due to the chemical shift anisotropy and due to the dipole-dipole interactions (often with several spin magnetic moments close in space) are combined. The constants R_1 and R_2 (and other) are therefore sums of the relaxation rate constants described here and in Section 7.7. At moderate $\vec{B}_0$ fields (up to 15–20 T, depending on the molecule), the relaxation of $^1\mathrm{H}$ in unlabeled molecules and of $^{13}\mathrm{C}$ and $^{15}\mathrm{N}$ in CH_n and NH_n groups of $^{13}\mathrm{C}/^{15}\mathrm{N}$ labeled molecules is usually dominated by dipole-dipole interactions with protons.

8.8 Thermal equilibrium with dipolar coupling

As shown in Section 8.9.8, if we neglect the chemical shifts ($\delta_{\mathrm{i},1} \ll 1, \delta_{\mathrm{i},2} \ll 1$), the density matrix describing two different nuclei coupled only through dipolar interactions is

$$\hat{\rho}^{\mathrm{eq}} = \begin{pmatrix} \frac{1}{4} + \frac{\gamma_1 B_0 \hbar}{8k_{\mathrm{B}}T} + \frac{\gamma_2 B_0 \hbar}{8k_{\mathrm{B}}T} & 0 & 0 & 0 \\ 0 & \frac{1}{4} + \frac{\gamma_1 B_0 \hbar}{8k_{\mathrm{B}}T} - \frac{\gamma_2 B_0 \hbar}{8k_{\mathrm{B}}T} & 0 & 0 \\ 0 & 0 & \frac{1}{4} - \frac{\gamma_1 B_0 \hbar}{8k_{\mathrm{B}}T} + \frac{\gamma_2 B_0 \hbar}{8k_{\mathrm{B}}T} & 0 \\ 0 & 0 & 0 & \frac{1}{4} - \frac{\gamma_1 B_0 \hbar}{8k_{\mathrm{B}}T} - \frac{\gamma_2 B_0 \hbar}{8k_{\mathrm{B}}T} \end{pmatrix} \tag{8.37}$$

$$= \frac{1}{4}\begin{pmatrix} 1 & 0 & 0 & 0 \\ 0 & 1 & 0 & 0 \\ 0 & 0 & 1 & 0 \\ 0 & 0 & 0 & 1 \end{pmatrix} + \frac{\gamma_1 B_0 \hbar}{8k_{\mathrm{B}}T}\begin{pmatrix} +1 & 0 & 0 & 0 \\ 0 & +1 & 0 & 0 \\ 0 & 0 & -1 & 0 \\ 0 & 0 & 0 & -1 \end{pmatrix} + \frac{\gamma_2 B_0 \hbar}{8k_{\mathrm{B}}T}\begin{pmatrix} +1 & 0 & 0 & 0 \\ 0 & -1 & 0 & 0 \\ 0 & 0 & +1 & 0 \\ 0 & 0 & 0 & -1 \end{pmatrix} \tag{8.38}$$

$$= \frac{1}{2} \left(\mathscr{I}_t + \kappa_1 \mathscr{I}_{1z} + \kappa_2 \mathscr{I}_{2z} \right), \tag{8.39}$$

where

$$\kappa_j = \frac{\gamma_j B_0 \hbar}{2 k_{\mathrm{B}} T}. \tag{8.40}$$

HOMEWORK

To prepare for the next lecture, analyze evolution of the density matrix described in Section 9.2.

8.9   SUPPORTING INFORMATION

8.9.1   Tensor and Hamiltonian of dipolar coupling

As shown in Section 4.9.2, magnetic induction can be expressed as a curl (rotation) of the vector potential ($\vec{B} = \vec{\nabla} \times \vec{A}$). Therefore, the magnetic induction of the field of nucleus $\vec{B}_2$ is given by the classical electrodynamics as

$$\vec{B}_2 = \vec{\nabla} \times \vec{A}_2, \tag{8.41}$$

where

$$\vec{\nabla} \equiv \left(\frac{\partial}{\partial x}, \frac{\partial}{\partial y}, \frac{\partial}{\partial z} \right). \tag{8.42}$$

Let us assume (classically) that the source of the magnetic moment of nucleus 2 is a current loop. It can be derived from Maxwell equations[7] that the vector potential $\vec{A}_2$ in a distance much larger than radius of the loop is

$$\vec{A}_2 = \frac{\mu_0}{4\pi} \frac{\vec{\mu}_2 \times \vec{r}}{r^3}, \tag{8.43}$$

where $\vec{r}$ is a vector defining the mutual position of nuclei 1 and 2 (inter-nuclear vector). The individual components of $\vec{A}_2$ are

$$A_{2,x} = \frac{\mu_0}{4\pi} \left(\mu_{2y} \frac{r_z}{r^3} - \mu_{2z} \frac{r_y}{r^3} \right), \tag{8.44}$$

$$A_{2,y} = \frac{\mu_0}{4\pi} \left(\mu_{2z} \frac{r_x}{r^3} - \mu_{2x} \frac{r_z}{r^3} \right), \tag{8.45}$$

$$A_{2,z} = \frac{\mu_0}{4\pi} \left(\mu_{2x} \frac{r_y}{r^3} - \mu_{2y} \frac{r_x}{r^3} \right). \tag{8.46}$$

Calculation of $\vec{B}_2$ thus includes two vector products

$$\vec{B}_2 = \frac{\mu_0}{4\pi} \vec{\nabla} \times \frac{\vec{\mu}_2 \times \vec{r}}{r^3}. \tag{8.47}$$

As a consequence, each component of $\vec{B}_2$ depends on all components of $\vec{\mu}_2$:

$$B_{2,x} = \frac{\mu_0}{4\pi} \left(\frac{\partial A_{2,z}}{\partial r_y} - \frac{\partial A_{2,y}}{\partial r_z} \right) = \frac{\mu_0}{4\pi} \left(\mu_{2x} \left(\frac{\partial}{\partial r_y} \frac{r_y}{r^3} + \frac{\partial}{\partial r_z} \frac{r_z}{r^3} \right) - \mu_{2y} \frac{\partial}{\partial r_y} \frac{r_x}{r^3} - \mu_{2z} \frac{\partial}{\partial r_z} \frac{r_x}{r^3} \right), \tag{8.48}$$

$$B_{2,y} = \frac{\mu_0}{4\pi} \left(\frac{\partial A_{2,x}}{\partial r_z} - \frac{\partial A_{2,z}}{\partial r_x} \right) = \frac{\mu_0}{4\pi} \left(\mu_{2y} \left(\frac{\partial}{\partial r_z} \frac{r_z}{r^3} + \frac{\partial}{\partial r_x} \frac{r_x}{r^3} \right) - \mu_{2z} \frac{\partial}{\partial r_z} \frac{r_y}{r^3} - \mu_{2x} \frac{\partial}{\partial r_x} \frac{r_y}{r^3} \right), \tag{8.49}$$

$$B_{2,z} = \frac{\mu_0}{4\pi} \left(\frac{\partial A_{2,y}}{\partial r_x} - \frac{\partial A_{2,x}}{\partial r_y} \right) = \frac{\mu_0}{4\pi} \left(\mu_{2z} \left(\frac{\partial}{\partial r_x} \frac{r_x}{r^3} + \frac{\partial}{\partial r_y} \frac{r_y}{r^3} \right) - \mu_{2x} \frac{\partial}{\partial r_x} \frac{r_z}{r^3} - \mu_{2y} \frac{\partial}{\partial r_y} \frac{r_z}{r^3} \right). \tag{8.50}$$

To proceed, we have to evaluate the partial derivatives $\frac{\partial}{\partial r_j} \frac{r_j}{r^3}$ and $\frac{\partial}{\partial r_j} \frac{r_k}{r^3}$:

$$\frac{\partial}{\partial r_j} \frac{r_j}{r^3} = \frac{\partial}{\partial r_j} \frac{r_j}{\left(\sqrt{r_x^2 + r_y^2 + r_z^2} \right)^3} = \frac{\partial}{\partial r_j} \frac{r_j}{\left(r_x^2 + r_y^2 + r_z^2 \right)^{3/2}} = \frac{1 \cdot r^3 - r_j \cdot \frac{3}{2} r \cdot 2 r_j}{r^6} = \frac{1}{r^3} - \frac{3 r_j^2}{r^5}, \tag{8.51}$$

$$\frac{\partial}{\partial r_j} \frac{r_k}{r^3} = \frac{\partial}{\partial r_j} \frac{r_k}{\left(\sqrt{r_x^2 + r_y^2 + r_z^2} \right)^3} \frac{\partial}{\partial r_j} \frac{r_k}{\left(r_x^2 + r_y^2 + r_z^2 \right)^{3/2}} = \frac{0 \cdot r^3 - r_k \cdot \frac{3}{2} r \cdot 2 r_j}{r^6} = -\frac{3 r_j r_k}{r^5} \tag{8.52}$$

After inserting the partial derivatives from Eqs. 8.51 and 8.52 to Eqs. 8.48–8.50,

$$B_{2,x} = \frac{\mu_0}{4\pi r^5} ((3 r_x^2 - r^2) \mu_{2x} + 3 r_x r_y \mu_{2y} + 3 r_x r_z \mu_{2z}) \tag{8.53}$$

$$B_{2,y} = \frac{\mu_0}{4\pi r^5} (3 r_x r_y \mu_{2x} + (3 r_y^2 - r^2) \mu_{2y} + 3 r_y r_z \mu_{2z}) \tag{8.54}$$

$$B_{2,z} = \frac{\mu_0}{4\pi r^5} (3 r_x r_z \mu_{2x} + 3 r_y r_z \mu_{2y} + (3 r_z^2 - r^2) \mu_{2z}), \tag{8.55}$$

---

[7]The derivation is presented in The Feynman Lectures on Physics, Vol. 2, Chapter 14 (the general description is presented in Section 14.2. and the current loop is discussed in Section 14.5), using an analogy with the description of the electric dipole in Section 14.3. of Vol. 2.

which can by described by a matrix equation

$$\begin{pmatrix} B_{2,x} \\ B_{2,y} \\ B_{2,z} \end{pmatrix} = \frac{\mu_0}{4\pi r^5} \begin{pmatrix} 3r_x^2 - r^2 & 3r_x r_y & 3r_x r_z \\ 3r_x r_y & 3r_y^2 - r^2 & 3r_y r_z \\ 3r_x r_z & 3r_y r_z & 3r_z^2 - r^2 \end{pmatrix} \cdot \begin{pmatrix} \mu_{2x} \\ \mu_{2y} \\ \mu_{2z} \end{pmatrix}. \tag{8.56}$$

The matrix in Eq. 8.56 represents a tensor describing the geometric relations of the dipolar coupling and has the same form as the matrix in Eq. 1.109, describing the anisotropic contribution to the chemical shift tensor: the vector defining the symmetry axis of the chemical shift tensor $\vec{Z}$ is just replaced with the inter-nuclear vector $\vec{r}$ in Eq. 8.56. Like the anisotropic part of the chemical shift tensor, the matrix in Eq. 8.56 simplifies to

$$\frac{\mu_0}{4\pi r^3} \begin{pmatrix} -1 & 0 & 0 \\ 0 & -1 & 0 \\ 0 & 0 & 2 \end{pmatrix} \tag{8.57}$$

in a coordinate system with axis $z \parallel \vec{r}$. Rotation to the laboratory frame is described by angles φ and ϑ defining orientation of $\vec{r}$ in the laboratory frame

$$\begin{pmatrix} -1 & 0 & 0 \\ 0 & -1 & 0 \\ 0 & 0 & 2 \end{pmatrix} \longrightarrow \frac{1}{r^2} \begin{pmatrix} 3r_x^2 - r^2 & 3r_x r_y & 3r_x r_z \\ 3r_x r_y & 3r_y^2 - r^2 & 3r_y r_z \\ 3r_x r_z & 3r_y r_z & 3r_z^2 - r^2 \end{pmatrix}, \tag{8.58}$$

where $r_x = r\sin\vartheta\cos\varphi$, $r_y = r\sin\vartheta\sin\varphi$, and $r_z = r\cos\vartheta$.

As usually, Hamiltonian of the dipolar coupling can be obtained using the classical description of the energy. Classical electrodynamics tells us that the energy of the interaction of the magnetic moment of nucleus 1 with the field generated by the magnetic moment of nucleus 2, described by Eq. 8.56 is

$$\begin{aligned} \mathcal{E}_D = -\vec{\mu}_1 \cdot \vec{B}_2 = -\frac{\mu_0}{4\pi r^3} \big(\quad & (3r_x^2 - r^2)\mu_{1x}\mu_{2x} + (3r_y^2 - r^2)\mu_{1y}\mu_{2y} + (3r_z^2 - r^2)\mu_{1z}\mu_{2z} + \\ + \ & 3r_x r_y \mu_{1x}\mu_{2y} + 3r_x r_z \mu_{1x}\mu_{2z} + 3r_y r_z \mu_{1y}\mu_{2z} \\ + \ & 3r_y r_x \mu_{1y}\mu_{2x} + 3r_z r_x \mu_{1z}\mu_{2x} + 3r_z r_y \mu_{1z}\mu_{2y} \big). \end{aligned} \tag{8.59}$$

Describing the magnetic moments by the operators $\hat{\mu}_{1j}\gamma_1 \hat{I}_{1j}$ and $\hat{\mu}_{2,j}\gamma_1 \hat{I}_{2,j}$, where j is x, y, and z, the Hamiltonian of dipolar coupling $\hat{H}_D$ can be written as

$$\begin{aligned} \hat{H}_D = -\frac{\mu_0}{4\pi r^3} \big(\quad & (3r_x^2 - r^2)\hat{I}_{1x}\hat{I}_{2x} + (3r_y^2 - r^2)\hat{I}_{1y}\hat{I}_{2y} + (3r_z^2 - r^2)\hat{I}_{1z}\hat{I}_{2z} + \\ + \ & 3r_x r_y \hat{I}_{1x}\hat{I}_{2y} + 3r_x r_z \hat{I}_{1x}\hat{I}_{2z} + 3r_y r_z \hat{I}_{1y}\hat{I}_{2z} \\ + \ & 3r_y r_x \hat{I}_{1y}\hat{I}_{2x} + 3r_z r_x \hat{I}_{1z}\hat{I}_{2x} + 3r_z r_y \hat{I}_{1z}\hat{I}_{2y} \big) \end{aligned}$$

$$= -\frac{\mu_0 \gamma_1 \gamma_2}{4\pi r^5} \big(\hat{I}_{1x} \ \hat{I}_{1y} \ \hat{I}_{1z} \big) \begin{pmatrix} 3r_x^2 - r^2 & 3r_x r_y & 3r_x r_z \\ 3r_x r_y & 3r_y^2 - r^2 & 3r_y r_z \\ 3r_x r_z & 3r_y r_z & 3r_z^2 - r^2 \end{pmatrix} \begin{pmatrix} \hat{I}_{2x} \\ \hat{I}_{2y} \\ \hat{I}_{2z} \end{pmatrix} = \hat{\vec{I}}_1 \cdot \underline{D} \cdot \hat{\vec{I}}_2, \tag{8.60}$$

where $\underline{D}$ is the tensor of direct dipole-dipole interactions (dipolar coupling).

The Hamiltonian can be written in spherical coordinates as

$$\begin{aligned} \hat{H}_D = -\frac{\mu_0 \gamma_1 \gamma_2}{4\pi r^3} \quad \big(& (3\sin^2\vartheta\cos^2\varphi - 1)\hat{I}_{1x}\hat{I}_{2x} + (3\sin^2\vartheta\sin^2\varphi - 1)\hat{I}_{1y}\hat{I}_{2y} + (3\cos^2\vartheta - 1)\hat{I}_{1z}\hat{I}_{2z} + \\ + \ & 3\sin^2\vartheta\sin\varphi\cos\varphi\hat{I}_{1x}\hat{I}_{2y} + 3\sin\vartheta\cos\vartheta\cos\varphi\hat{I}_{1x}\hat{I}_{2z} + 3\sin\vartheta\cos\vartheta\sin\varphi\hat{I}_{1y}\hat{I}_{2z} \\ + \ & 3\sin^2\vartheta\sin\varphi\cos\varphi\hat{I}_{1y}\hat{I}_{2x} + 3\sin\vartheta\cos\vartheta\cos\varphi\hat{I}_{1z}\hat{I}_{2x} + 3\sin\vartheta\cos\vartheta\sin\varphi\hat{I}_{1z}\hat{I}_{2y} \big). \end{aligned} \tag{8.61}$$

8.9.2 Secular approximation and averaging of dipolar Hamiltonian

Like the chemical-shift Hamiltonian, the Hamiltonian of dipolar coupling can be simplified in many cases.

- Magnetic moments with the same γ *and* chemical shift precess about the z axis with *the same precession frequency*. In addition to the precession, the magnetic moments move with random molecular motions, described by re-orientation of $\vec{r}$. In a coordinate system rotating with the common precession frequency, $\vec{r}$ quickly rotates about the z axis in addition to the random molecular motions. On a time scale longer than nanoseconds, the rapid oscillations of r_x, r_y, and r_z are neglected (secular approximation). The values of r_x^2 and r_y^2 do not oscillate about zero, but about a value $\langle r_x^2 \rangle = \langle r_y^2 \rangle$, which is equal to[8] $(r^2 - \langle r_z^2 \rangle)/2$ because $\langle r_x^2 + r_y^2 + r_z^2 \rangle = \langle r^2 \rangle = r^2$. Therefore, the secular approximation (i.e., neglecting the oscillations and keeping the average values) simplifies the Hamiltonian to

$$\hat{H}_D = -\frac{\mu_0 \gamma_1 \gamma_2}{4\pi r^5} \left(3\langle r_z^2 \rangle - r^2 \right) \left(\hat{I}_{1z} \hat{I}_{2z} - \frac{1}{2} \hat{I}_{1x} \hat{I}_{2x} - \frac{1}{2} \hat{I}_{1y} \hat{I}_{2y} \right) = -\frac{\mu_0 \gamma_1 \gamma_2}{4\pi r^3} \frac{3\langle \cos^2 \vartheta \rangle - 1}{2} \left(2\hat{I}_{1z} \hat{I}_{2z} - \hat{I}_{1x} \hat{I}_{2x} - \hat{I}_{1y} \hat{I}_{2y} \right). \quad (8.62)$$

- Magnetic moments with different γ and/or chemical shift precess with *different precession frequencies*. Therefore, the x and y components of $\vec{\mu}_2$ rapidly oscillate in a frame rotating with the precession frequency of $\vec{\mu}_1$ and vice versa. When neglecting the oscillating terms (secular approximation), the Hamiltonian reduces to

$$\hat{H}_D = -\frac{\mu_0 \gamma_1 \gamma_2}{4\pi r^5} \left(3\langle r_z^2 \rangle - r^2 \right) \hat{I}_{1z} \hat{I}_{2z} = -\frac{\mu_0 \gamma_1 \gamma_2}{4\pi r^3} \frac{3\langle \cos^2 \vartheta \rangle - 1}{2} 2\hat{I}_{1z} \hat{I}_{2z}. \quad (8.63)$$

- Averaging over all molecules in isotropic liquids has the same effect as described for the anisotropic part of the chemical shielding tensor because both tensors have the same form. Terms with different coordinates average to zero because they contain products of sine and cosine functions of 2ϑ, φ and 2φ. As the angles ϑ and φ are independent, their functions average independently. And as 2ϑ and φ can have in isotropic liquids any value in the interval $(0, 2\pi)$ with equal probability, the averages of their sine and cosine functions are equal to zero

$$\overline{r_x r_y} = \overline{3 \sin^2 \vartheta \sin \varphi \cos \varphi} = \overline{\frac{3}{2}(1 - \cos(2\vartheta)) \cdot \frac{1}{2} \sin(2\varphi)} = \frac{3}{4}\overline{\sin(2\varphi)} - \frac{3}{4}\overline{\cos(2\vartheta) \cdot \sin(2\varphi)} = 0 - 0 \cdot 0 = 0, \quad (8.64)$$

$$\overline{r_x r_z} = \overline{3 \sin \vartheta \cos \vartheta \cos \varphi} = \overline{\frac{3}{2}(\sin(2\vartheta)) \cdot \cos \varphi} = \frac{3}{4}\overline{\sin(2\vartheta)} \cdot \overline{\cos \varphi} = 0 \cdot 0 = 0, \quad (8.65)$$

$$\overline{r_y r_z} = \overline{3 \sin \vartheta \cos \vartheta \sin \varphi} = \overline{\frac{3}{2}(\sin(2\vartheta)) \cdot \sin \varphi} = \frac{3}{4}\overline{\sin(2\vartheta)} \cdot \overline{\sin \varphi} = 0 \cdot 0 = 0. \quad (8.66)$$

The terms with the same coordinates are identical because no direction is preferred:

$$\overline{r_x^2} = \overline{r_y^2} = \overline{r_z^2}. \quad (8.67)$$

Finally,

$$r_x^2 + r_y^2 + r_z^2 = r^2 \Rightarrow \overline{r_x^2 + r_y^2 + r_z^2} = \overline{3r_j^2} = r^2 \Rightarrow \overline{3r_j^2 - r^2} = 0. \quad (8.68)$$

8.9.3 Interacting and non-interacting magnetic moments

We have decomposed a wave function of a pair of magnetic moments to (Eq. 8.8)

$$\Psi = \psi_{\text{non-spin}} \cdot \begin{pmatrix} c_{\alpha,1} \begin{pmatrix} c_{\alpha,2} \\ c_{\beta,2} \end{pmatrix} \\ c_{\beta,1} \begin{pmatrix} c_{\alpha,2} \\ c_{\beta,2} \end{pmatrix} \end{pmatrix} = \psi_{\text{non-spin}} \cdot \begin{pmatrix} c_{\alpha,1} c_{\alpha,2} \\ c_{\alpha,1} c_{\beta,2} \\ c_{\beta,1} c_{\alpha,2} \\ c_{\beta,1} c_{\beta,2} \end{pmatrix} \equiv \psi_{\text{non-spin}} \cdot \begin{pmatrix} c_{\alpha\alpha} \\ c_{\alpha\beta} \\ c_{\beta\alpha} \\ c_{\beta\beta} \end{pmatrix}, \quad (8.69)$$

What tells us if we can describe the state of the individual magnetic moments in the two-dimensional basis $|\alpha\rangle, |\beta\rangle$? We inspect eigenfunctions and eigenvalues of the Hamiltonian including the influence of $\vec{B}_0$, chemical shifts, and dipolar coupling, in the secular approximation:

$$\hat{H} = -\gamma_1 B_0 (1 + \delta_{\text{i},1}) \hat{I}_{1z} - \gamma_2 B_0 (1 + \delta_{\text{i},2}) \hat{I}_{2z} - \frac{\mu_0 \gamma_1 \gamma_2}{4\pi r^3} \frac{3\langle \cos^2 \vartheta \rangle - 1}{2} \left(2\hat{I}_{1z} \hat{I}_{2z} - \hat{I}_{1x} \hat{I}_{2x} - \hat{I}_{1y} \hat{I}_{2y} \right)$$

$$= \omega_{0,1} \hat{I}_{1z} + \omega_{0,2} \hat{I}_{2z} + D \left(2\hat{I}_{1z} \hat{I}_{2z} - \hat{I}_{1x} \hat{I}_{2x} - \hat{I}_{1y} \hat{I}_{2y} \right) \quad (8.70)$$

---

[8]Note that $\langle r_x^2 \rangle = \langle r_y^2 \rangle \neq \langle r_z^2 \rangle$ in general.

If the magnetic moments are too distant to interact mutually ($r \to \infty \Rightarrow D \to 0$), the Hamiltonian simplifies to a sum of two operators acting separately on each magnetic moment

$$\hat{H} = \omega_{0,1}\hat{I}_{1z} + \omega_{0,2}\hat{I}_{2z}. \tag{8.71}$$

As discussed in Section 6.7.3, the action of such Hamiltonian can be described by two independent eigenequations

$$\omega_{0,1}\hat{I}_{1z}\psi^{(1)} = \mathcal{E}_D^{(1)}\psi^{(1)} \qquad \omega_{0,2}\hat{I}_{2z}\psi^{(2)} = \mathcal{E}_D^{(2)}\psi^{(2)}. \tag{8.72}$$

Since $\hat{I}_{1z}$ and $\hat{I}_{1z}$ are represented by diagonal matrices, the eigenfunctions for a pair of magnetic moments can be found immediately:

$$\frac{\omega_{0,1}\hbar}{2}\begin{pmatrix} 1 & 0 & 0 & 0 \\ 0 & 1 & 0 & 0 \\ 0 & 0 & -1 & 0 \\ 0 & 0 & 0 & -1 \end{pmatrix} \cdot \begin{pmatrix} 1\begin{pmatrix} c_{\alpha,2} \\ c_{\beta,2} \end{pmatrix} \\ 0\begin{pmatrix} c_{\alpha,2} \\ c_{\beta,2} \end{pmatrix} \end{pmatrix} = +\frac{\omega_{0,1}\hbar}{2}\begin{pmatrix} 1\begin{pmatrix} c_{\alpha,2} \\ c_{\beta,2} \end{pmatrix} \\ 0\begin{pmatrix} c_{\alpha,2} \\ c_{\beta,2} \end{pmatrix} \end{pmatrix} \qquad \frac{\omega_{0,2}\hbar}{2}\begin{pmatrix} 1 & 0 & 0 & 0 \\ 0 & -1 & 0 & 0 \\ 0 & 0 & 1 & 0 \\ 0 & 0 & 0 & -1 \end{pmatrix}\begin{pmatrix} c_{\alpha,1}\begin{pmatrix} 1 \\ 0 \end{pmatrix} \\ c_{\beta,1}\begin{pmatrix} 1 \\ 0 \end{pmatrix} \end{pmatrix} = +\frac{\omega_{0,2}\hbar}{2}\begin{pmatrix} c_{\alpha,1}\begin{pmatrix} 1 \\ 0 \end{pmatrix} \\ c_{\beta,1}\begin{pmatrix} 1 \\ 0 \end{pmatrix} \end{pmatrix}$$

$$\frac{\omega_{0,1}\hbar}{2}\begin{pmatrix} 1 & 0 & 0 & 0 \\ 0 & 1 & 0 & 0 \\ 0 & 0 & -1 & 0 \\ 0 & 0 & 0 & -1 \end{pmatrix} \cdot \begin{pmatrix} 0\begin{pmatrix} c_{\alpha,2} \\ c_{\beta,2} \end{pmatrix} \\ 1\begin{pmatrix} c_{\alpha,2} \\ c_{\beta,2} \end{pmatrix} \end{pmatrix} = -\frac{\omega_{0,1}\hbar}{2}\begin{pmatrix} 0\begin{pmatrix} c_{\alpha,2} \\ c_{\beta,2} \end{pmatrix} \\ 1\begin{pmatrix} c_{\alpha,2} \\ c_{\beta,2} \end{pmatrix} \end{pmatrix} \qquad \frac{\omega_{0,2}\hbar}{2}\begin{pmatrix} 1 & 0 & 0 & 0 \\ 0 & -1 & 0 & 0 \\ 0 & 0 & 1 & 0 \\ 0 & 0 & 0 & -1 \end{pmatrix}\begin{pmatrix} c_{\alpha,1}\begin{pmatrix} 0 \\ 1 \end{pmatrix} \\ c_{\beta,1}\begin{pmatrix} 0 \\ 1 \end{pmatrix} \end{pmatrix} = -\frac{\omega_{0,2}\hbar}{2}\begin{pmatrix} c_{\alpha,1}\begin{pmatrix} 0 \\ 1 \end{pmatrix} \\ c_{\beta,1}\begin{pmatrix} 0 \\ 1 \end{pmatrix} \end{pmatrix},$$

$$\tag{8.73}$$

or, using direct products,

$$\frac{\omega_{0,1}\hbar}{2}\left(\begin{pmatrix} 1 & 0 \\ 0 & -1 \end{pmatrix} \otimes \begin{pmatrix} 1 & 0 \\ 0 & 1 \end{pmatrix}\right) \cdot \left(\begin{pmatrix} 1 \\ 0 \end{pmatrix} \otimes \begin{pmatrix} c_{\alpha,2} \\ c_{\beta,2} \end{pmatrix}\right) = +\frac{\omega_{0,1}\hbar}{2}\begin{pmatrix} 1 \\ 0 \end{pmatrix} \otimes \begin{pmatrix} c_{\alpha,2} \\ c_{\beta,2} \end{pmatrix}$$

$$\frac{\omega_{0,1}\hbar}{2}\left(\begin{pmatrix} 1 & 0 \\ 0 & -1 \end{pmatrix} \otimes \begin{pmatrix} 1 & 0 \\ 0 & 1 \end{pmatrix}\right) \cdot \left(\begin{pmatrix} 0 \\ 1 \end{pmatrix} \otimes \begin{pmatrix} c_{\alpha,2} \\ c_{\beta,2} \end{pmatrix}\right) = -\frac{\omega_{0,1}\hbar}{2}\begin{pmatrix} 0 \\ 1 \end{pmatrix} \otimes \begin{pmatrix} c_{\alpha,2} \\ c_{\beta,2} \end{pmatrix}, \tag{8.74}$$

$$\frac{\omega_{0,1}\hbar}{2}\begin{pmatrix} 1 & 0 \\ 0 & -1 \end{pmatrix} \cdot \begin{pmatrix} 1 \\ 0 \end{pmatrix}\psi^{(2)} = +\frac{\omega_{0,1}\hbar}{2}\begin{pmatrix} 1 \\ 0 \end{pmatrix}\psi^{(2)}$$

$$\frac{\omega_{0,1}\hbar}{2}\begin{pmatrix} 1 & 0 \\ 0 & -1 \end{pmatrix} \cdot \begin{pmatrix} 0 \\ 1 \end{pmatrix}\psi^{(2)} = -\frac{\omega_{0,1}\hbar}{2}\begin{pmatrix} 0 \\ 1 \end{pmatrix}\psi^{(2)}, \tag{8.75}$$

$$\frac{\omega_{0,1}\hbar}{2}\begin{pmatrix} 1 & 0 \\ 0 & -1 \end{pmatrix} \cdot \begin{pmatrix} 1 \\ 0 \end{pmatrix} = +\frac{\omega_{0,1}\hbar}{2}\begin{pmatrix} 1 \\ 0 \end{pmatrix}$$

$$\frac{\omega_{0,1}\hbar}{2}\begin{pmatrix} 1 & 0 \\ 0 & -1 \end{pmatrix} \cdot \begin{pmatrix} 0 \\ 1 \end{pmatrix} = -\frac{\omega_{0,1}\hbar}{2}\begin{pmatrix} 0 \\ 1 \end{pmatrix} \tag{8.76}$$

for the first magnetic moment, and

$$\frac{\omega_{0,2}\hbar}{2}\left(\begin{pmatrix} 1 & 0 \\ 0 & 1 \end{pmatrix} \otimes \begin{pmatrix} 1 & 0 \\ 0 & -1 \end{pmatrix}\right) \cdot \left(\begin{pmatrix} c_{\alpha,1} \\ c_{\beta,1} \end{pmatrix} \otimes \begin{pmatrix} 1 \\ 0 \end{pmatrix}\right) = +\frac{\omega_{0,2}\hbar}{2}\begin{pmatrix} c_{\alpha,1} \\ c_{\beta,1} \end{pmatrix} \otimes \begin{pmatrix} 1 \\ 0 \end{pmatrix}$$

$$\frac{\omega_{0,2}\hbar}{2}\left(\begin{pmatrix} 1 & 0 \\ 0 & 1 \end{pmatrix} \otimes \begin{pmatrix} 1 & 0 \\ 0 & -1 \end{pmatrix}\right) \cdot \left(\begin{pmatrix} c_{\alpha,1} \\ c_{\beta,1} \end{pmatrix} \otimes \begin{pmatrix} 0 \\ 1 \end{pmatrix}\right) = -\frac{\omega_{0,2}\hbar}{2}\begin{pmatrix} c_{\alpha,1} \\ c_{\beta,1} \end{pmatrix} \otimes \begin{pmatrix} 0 \\ 1 \end{pmatrix}, \tag{8.77}$$

$$\frac{\omega_{0,2}\hbar}{2}\begin{pmatrix} 1 & 0 \\ 0 & -1 \end{pmatrix} \cdot \begin{pmatrix} 1 \\ 0 \end{pmatrix}\psi^{(1)} = +\frac{\omega_{0,2}\hbar}{2}\begin{pmatrix} 1 \\ 0 \end{pmatrix}\psi^{(1)}$$

$$\frac{\omega_{0,2}\hbar}{2}\begin{pmatrix} 1 & 0 \\ 0 & -1 \end{pmatrix} \cdot \begin{pmatrix} 0 \\ 1 \end{pmatrix}\psi^{(1)} = -\frac{\omega_{0,2}\hbar}{2}\begin{pmatrix} 0 \\ 1 \end{pmatrix}\psi^{(1)}, \tag{8.78}$$

$$\frac{\omega_{0,2}\hbar}{2}\begin{pmatrix} 1 & 0 \\ 0 & -1 \end{pmatrix} \cdot \begin{pmatrix} 1 \\ 0 \end{pmatrix} = +\frac{\omega_{0,2}\hbar}{2}\begin{pmatrix} 1 \\ 0 \end{pmatrix}$$

$$\frac{\omega_{0,2}\hbar}{2}\begin{pmatrix} 1 & 0 \\ 0 & -1 \end{pmatrix} \cdot \begin{pmatrix} 0 \\ 1 \end{pmatrix} = -\frac{\omega_{0,2}\hbar}{2}\begin{pmatrix} 0 \\ 1 \end{pmatrix} \tag{8.79}$$

for the second magnetic moment.

We see that the eigenfunctions of Eq. 8.76 are $\begin{pmatrix} 1 \\ 0 \end{pmatrix}$ and $\begin{pmatrix} 0 \\ 1 \end{pmatrix}$ for any $\psi^{(2)} = \begin{pmatrix} c_{\alpha,2} \\ c_{\beta,2} \end{pmatrix}$, and that the eigenfunctions of Eq. 8.79 are also $\begin{pmatrix} 1 \\ 0 \end{pmatrix}$ and $\begin{pmatrix} 0 \\ 1 \end{pmatrix}$ for any $\psi^{(1)} = \begin{pmatrix} c_{\alpha,1} \\ c_{\beta,1} \end{pmatrix}$. The energy differences, given by the differences of the eigenvalues, are $\omega_{0,1}\hbar$ and $\omega_{0,2}\hbar$. As

Eq. 8.76 does not depend on $\psi^{(2)}$ and Eq. 8.79 does not depend on $\psi^{(1)}$, the original set of four equations, represented by the 4-dimensional matrices, was redundant. If the nuclei are identical, the left and right equations can be replaced by a single equation with $\omega_{0,1} = \omega_{0,2} = \omega_0$ (cf. treatment of indistinguishable nuclei in Section 6.7.3). Such case is equivalent to the mixed state described by the 2×2 density matrix in Section 6.1.

If the magnetic moments interact $(D \neq 0)$ and the Hamiltonian cannot be simplified to Eq. 8.71, we have to work with four-dimensional matrices and state vectors. The Hamiltonian then has the following matrix representation

$$\hat{H} = \hbar \begin{pmatrix} \frac{\omega_{0,1}+\omega_{0,2}}{2} + \frac{D}{2} & 0 & 0 & 0 \\ 0 & \frac{\omega_{0,1}-\omega_{0,2}}{2} - \frac{D}{2} & -D & 0 \\ 0 & -D & -\frac{\omega_{0,1}-\omega_{0,2}}{2} + \frac{D}{2} & 0 \\ 0 & 0 & 0 & -\frac{\omega_{0,1}+\omega_{0,2}}{2} + \frac{D}{2} \end{pmatrix}. \tag{8.80}$$

If $\omega_{0,1}$ and $\omega_{0,2}$ differ substantially, the secular approximation allows us to neglect also the $-\hat{I}_{1x}\hat{I}_{2x} - \hat{I}_{1y}\hat{I}_{2y}$ terms and to obtain a diagonal Hamiltonian matrix

$$\hat{H} \approx \hbar \begin{pmatrix} \frac{\omega_{0,1}+\omega_{0,2}}{2} + \frac{D}{2} & 0 & 0 & 0 \\ 0 & \frac{\omega_{0,1}-\omega_{0,2}}{2} - \frac{D}{2} & 0 & 0 \\ 0 & 0 & -\frac{\omega_{0,1}-\omega_{0,2}}{2} + \frac{D}{2} & 0 \\ 0 & 0 & 0 & -\frac{\omega_{0,1}+\omega_{0,2}}{2} + \frac{D}{2} \end{pmatrix} \tag{8.81}$$

with four-dimensional eigenvectors

$$\begin{pmatrix} 1 \\ 0 \\ 0 \\ 0 \end{pmatrix}, \qquad \begin{pmatrix} 0 \\ 1 \\ 0 \\ 0 \end{pmatrix}, \qquad \begin{pmatrix} 0 \\ 0 \\ 1 \\ 0 \end{pmatrix}, \qquad \begin{pmatrix} 0 \\ 0 \\ 0 \\ 1 \end{pmatrix}. \tag{8.82}$$

If $\omega_{0,1}$ and $\omega_{0,2}$ are similar, the off-diagonal elements warn us that the vectors listed above (direct products of $|\alpha\rangle$ and $|\beta\rangle$) are no longer eigenfunctions of the Hamiltonian in Eq 8.81. Note that the analysis presented in this Lecture and in the following Lectures *cannot be applied to such spin systems.* We return to the interacting magnetic moments with very similar $\omega_{0,1}$ and $\omega_{0,2}$ in the end of our course (Section 12.2).

8.9.4 Product operator bases

The basis presented in Tables 8.1 and 8.2 is used most frequently in NMR spectroscopy, but other choices are better suited for certain applications. Here, we briefly review several commonly used orthonormal bases of two-spin systems and comment their advantages.

- *Cartesian product operator basis* is presented in Tables 8.1 and 8.2, and in a condensed version in Table 8.3. The basis matrices are written as $2\mathscr{I}_{nj}\mathscr{I}_{n'k}$, where n and n' specify the nucleus and $j, k \in \{x, y, z, t\}$, but the unit matrix $2\mathscr{I}_{nt}$ is usually not written in the product. As discussed in Section 8.4, the Cartesian product operator basis is well suited to describe contributions (*populations* and *coherences*) to the probability density matrix $\hat{\rho}$. Also, certain matrices after multiplication by appropriate physical constants represent operators of components of spin angular momentum, magnetic moment, and consequently constituents of various Hamiltonians.

- Coefficients C_j describing contributions of *single-element product operator basis* to the density matrix (Table 8.4) are equal to individual elements of the density matrix. The basis matrices are written as $\mathscr{I}_{1j}\mathscr{I}_{2k} = \mathscr{I}_j^{(1)} \otimes \mathscr{I}_k^{(2)}$, where 1 and 2 specify the nucleus and $j, k \in \{\alpha, \beta, +, -\}$. The relationship between Cartesian and single-element product operator bases is given by Eqs. 6.5 and 6.4, applied to each $\mathscr{I}_j^{(n)}$ matrix in the product:

$$\mathscr{I}_\alpha^{(n)} = \mathscr{I}_t^{(n)} + \mathscr{I}_z^{(n)} \qquad \mathscr{I}_\beta^{(n)} = \mathscr{I}_t^{(n)} - \mathscr{I}_z^{(n)} \qquad \mathscr{I}_+^{(n)} = \mathscr{I}_x^{(n)} + \mathrm{i}\mathscr{I}_y^{(n)} \qquad \mathscr{I}_-^{(n)} = \mathscr{I}_x^{(n)} - \mathrm{i}\mathscr{I}_y^{(n)} \tag{8.83}$$

$$\mathscr{I}_x^{(n)} = \frac{1}{2}\left(\mathscr{I}_+^{(n)} + \mathscr{I}_-^{(n)}\right) \qquad \mathscr{I}_y^{(n)} = -\frac{\mathrm{i}}{2}\left(\mathscr{I}_+^{(n)} - \mathscr{I}_-^{(n)}\right) \qquad \mathscr{I}_z^{(n)} = \frac{1}{2}\left(\mathscr{I}_\alpha^{(n)} - \mathscr{I}_\beta^{(n)}\right) \qquad \mathscr{I}_t^{(n)} = \frac{1}{2}\left(\mathscr{I}_\alpha^{(n)} + \mathscr{I}_\beta^{(n)}\right) \tag{8.84}$$

- *Shift product operator basis*, presented in Table 8.5, can be viewed as a combination of the previous two choices. The basis matrices are direct products of the normalized matrices $\mathscr{I}_+^{(n)}$, $\mathscr{I}_-^{(n)}$, $\sqrt{2}\mathscr{I}_z^{(n)}$, and $\sqrt{2}\mathscr{I}_t^{(n)}$. The shift product operators directly reflect the coherence between spin states. The value of $j+k$ in $\mathscr{I}_{nj}\mathscr{I}_{n'k}$ distinguishes *single-quantum* $(j+k = \pm 1)$, *zero-quantum* $(j+k = 0)$, and *double-quantum* $(j+k = \pm 2)$ coherences.

- *Irreducible spherical tensor operators*, presented in Table 8.6, are useful when rotation (of molecules, chemical groups) needs to be taken into account (e.g., when analyzing stochastic motions resulting in relaxation).

$$\mathscr{I}_{0,0}^{(00)} = \mathscr{I}_t \tag{8.85}$$

$$\mathscr{I}_{1,-1}^{(10)} = \frac{1}{\sqrt{2}}(\mathscr{I}_{1x} - \mathrm{i}\mathscr{I}_{1y}) = \mathscr{I}_{1-} \tag{8.86}$$

$$\mathscr{I}_{1,0}^{(10)} = \mathscr{I}_{1z} = \mathscr{I}_{10} \tag{8.87}$$

$$\mathscr{I}_{1,+1}^{(10)} = -\frac{1}{\sqrt{2}}(\mathscr{I}_{1x} + \mathrm{i}\mathscr{I}_{1y}) = -\mathscr{I}_{1+} \tag{8.88}$$

$$\mathscr{I}_{1,-1}^{(02)} = \frac{1}{\sqrt{2}}(\mathscr{I}_{2x} - \mathrm{i}\mathscr{I}_{2y}) = \mathscr{I}_{2-} \tag{8.89}$$

$$\mathscr{I}_{1,0}^{(02)} = \mathscr{I}_{2z} = \mathscr{I}_{20} \tag{8.90}$$

$$\mathscr{I}_{1,+1}^{(02)} = -\frac{1}{\sqrt{2}}(\mathscr{I}_{2x} + \mathrm{i}\mathscr{I}_{2y}) = -\mathscr{I}_{2+} \tag{8.91}$$

$$\mathscr{I}_{0,0}^{(12)} = -\frac{2}{\sqrt{3}}(\mathscr{I}_{1x}\mathscr{I}_{2x} + \mathscr{I}_{1y}\mathscr{I}_{2y} + \mathscr{I}_{1z}\mathscr{I}_{2z}) = -\frac{1}{\sqrt{3}}(\mathscr{I}_{1-}\mathscr{I}_{2+} + \mathscr{I}_{10}\mathscr{I}_{20} + \mathscr{I}_{1+}\mathscr{I}_{2-}) \tag{8.92}$$

$$\mathscr{I}_{1,-1}^{(12)} = -(\mathscr{I}_{1x}\mathscr{I}_{2z} - \mathscr{I}_{1z}\mathscr{I}_{2x} - \mathrm{i}(\mathscr{I}_{1y}\mathscr{I}_{2z} - \mathscr{I}_{1z}\mathscr{I}_{2y})) = -\frac{1}{\sqrt{2}}(\mathscr{I}_{1-}\mathscr{I}_{20} - \mathscr{I}_{10}\mathscr{I}_{2-}) \tag{8.93}$$

$$\mathscr{I}_{1,0}^{(12)} = \sqrt{2}\mathrm{i}(\mathscr{I}_{1x}\mathscr{I}_{2y} - \mathscr{I}_{1y}\mathscr{I}_{2x}) = -\frac{1}{\sqrt{2}}(\mathscr{I}_{1+}\mathscr{I}_{2-} - \mathscr{I}_{1-}\mathscr{I}_{2+}) \tag{8.94}$$

$$\mathscr{I}_{1,+1}^{(12)} = -(\mathscr{I}_{1x}\mathscr{I}_{2z} - \mathscr{I}_{1z}\mathscr{I}_{2x} + \mathrm{i}(\mathscr{I}_{1y}\mathscr{I}_{2z} - \mathscr{I}_{1z}\mathscr{I}_{2y})) = -\frac{1}{\sqrt{2}}(\mathscr{I}_{1+}\mathscr{I}_{20} - \mathscr{I}_{10}\mathscr{I}_{2+}) \tag{8.95}$$

$$\mathscr{I}_{2,-2}^{(12)} = \mathscr{I}_{1x}\mathscr{I}_{2x} - \mathscr{I}_{1y}\mathscr{I}_{2y} - \mathrm{i}(\mathscr{I}_{1x}\mathscr{I}_{2y} + \mathscr{I}_{1y}\mathscr{I}_{2x}) = \mathscr{I}_{1-}\mathscr{I}_{2-} \tag{8.96}$$

$$\mathscr{I}_{2,-1}^{(12)} = +(\mathscr{I}_{1x}\mathscr{I}_{2z} + \mathscr{I}_{1z}\mathscr{I}_{2x} - \mathrm{i}(\mathscr{I}_{1y}\mathscr{I}_{2z} + \mathscr{I}_{1z}\mathscr{I}_{2y})) = +\frac{1}{\sqrt{2}}(\mathscr{I}_{1-}\mathscr{I}_{20} + \mathscr{I}_{10}\mathscr{I}_{2-}) \tag{8.97}$$

$$\mathscr{I}_{2,0}^{(12)} = -\sqrt{\frac{2}{3}}(\mathscr{I}_{1x}\mathscr{I}_{2x} + \mathscr{I}_{1y}\mathscr{I}_{2y} - 2\mathscr{I}_{1z}\mathscr{I}_{2z}) = -\frac{1}{\sqrt{6}}(\mathscr{I}_{1-}\mathscr{I}_{2+} - 2\mathscr{I}_{10}\mathscr{I}_{20} + \mathscr{I}_{1+}\mathscr{I}_{2-}) \tag{8.98}$$

$$\mathscr{I}_{2,+1}^{(12)} = -(\mathscr{I}_{1x}\mathscr{I}_{2z} + \mathscr{I}_{1z}\mathscr{I}_{2x} + \mathrm{i}(\mathscr{I}_{1y}\mathscr{I}_{2z} + \mathscr{I}_{1z}\mathscr{I}_{2y})) = -\frac{1}{\sqrt{2}}(\mathscr{I}_{1+}\mathscr{I}_{20} + \mathscr{I}_{10}\mathscr{I}_{2+}) \tag{8.99}$$

$$\mathscr{I}_{2,+2}^{(12)} = \mathscr{I}_{1x}\mathscr{I}_{2x} - \mathscr{I}_{1y}\mathscr{I}_{2y} + \mathrm{i}(\mathscr{I}_{1x}\mathscr{I}_{2y} + \mathscr{I}_{1y}\mathscr{I}_{2x}) = \mathscr{I}_{1+}\mathscr{I}_{2+} \tag{8.100}$$

8.9.5   Deriving commutators of product operators

The product operators are direct products of 2×2 matrices $\mathscr{I}_x, \mathscr{I}_y, \mathscr{I}_z, \mathscr{I}_t,$. Therefore, commutators of product operators can be derived from the their relations and from the general properties of the direct product of matrices. In general expressions used in this section letters j, k, l, m replace one of the subscript x, y, z (but not t), n, n' distinguish nuclei (1 or 2), and $\delta_{jk} = 1$ for $j = k$, and $\delta_{jk} = 1$ for $j \neq k$.

Products of the 2×2 matrices $\mathscr{I}_x, \mathscr{I}_y, \mathscr{I}_z$ are related in the following manner (cf Eqs. 4.35–4.38)

$$\mathscr{I}_x \cdot \mathscr{I}_y - \mathscr{I}_y \cdot \mathscr{I}_x = [\mathscr{I}_x, \mathscr{I}_y] = \mathrm{i}\mathscr{I}_z, \tag{8.101}$$

$$\mathscr{I}_y \cdot \mathscr{I}_z - \mathscr{I}_z \cdot \mathscr{I}_y = [\mathscr{I}_y, \mathscr{I}_z] = \mathrm{i}\mathscr{I}_x, \tag{8.102}$$

$$\mathscr{I}_z \cdot \mathscr{I}_x - \mathscr{I}_x \cdot \mathscr{I}_z = [\mathscr{I}_z, \mathscr{I}_x] = \mathrm{i}\mathscr{I}_y, \tag{8.103}$$

$$\mathscr{I}_j \cdot \mathscr{I}_k + \mathscr{I}_k \cdot \mathscr{I}_j = \delta_{jk}\mathscr{I}_t. \tag{8.104}$$

The following properties of the direct (Kronecker) products allow us to find the commutation relation also for the product operators.

Table 8.3: Cartesian basis of product operators for a pair of spin-$\frac{1}{2}$ nuclei

$$\mathscr{I}_t = \tfrac{1}{2}\begin{pmatrix} +1 & 0 & 0 & 0 \\ 0 & +1 & 0 & 0 \\ 0 & 0 & +1 & 0 \\ 0 & 0 & 0 & +1 \end{pmatrix} \qquad \mathscr{I}_{1z} = \tfrac{1}{2}\begin{pmatrix} +1 & 0 & 0 & 0 \\ 0 & +1 & 0 & 0 \\ 0 & 0 & -1 & 0 \\ 0 & 0 & 0 & -1 \end{pmatrix} \qquad \mathscr{I}_{2z} = \tfrac{1}{2}\begin{pmatrix} +1 & 0 & 0 & 0 \\ 0 & -1 & 0 & 0 \\ 0 & 0 & +1 & 0 \\ 0 & 0 & 0 & -1 \end{pmatrix} \qquad 2\mathscr{I}_{1z}\mathscr{I}_{2z} = \tfrac{1}{2}\begin{pmatrix} +1 & 0 & 0 & 0 \\ 0 & -1 & 0 & 0 \\ 0 & 0 & -1 & 0 \\ 0 & 0 & 0 & +1 \end{pmatrix}$$

$$\mathscr{I}_{1x} = \tfrac{1}{2}\begin{pmatrix} 0 & 0 & +1 & 0 \\ 0 & 0 & 0 & +1 \\ +1 & 0 & 0 & 0 \\ 0 & +1 & 0 & 0 \end{pmatrix} \qquad 2\mathscr{I}_{1x}\mathscr{I}_{2z} = \tfrac{1}{2}\begin{pmatrix} 0 & 0 & +1 & 0 \\ 0 & 0 & 0 & -1 \\ +1 & 0 & 0 & 0 \\ 0 & -1 & 0 & 0 \end{pmatrix} \qquad \mathscr{I}_{1y} = \tfrac{1}{2}\begin{pmatrix} 0 & 0 & -i & 0 \\ 0 & 0 & 0 & -i \\ +i & 0 & 0 & 0 \\ 0 & +i & 0 & 0 \end{pmatrix} \qquad 2\mathscr{I}_{1y}\mathscr{I}_{2z} = \tfrac{1}{2}\begin{pmatrix} 0 & 0 & -i & 0 \\ 0 & 0 & 0 & +i \\ +i & 0 & 0 & 0 \\ 0 & -i & 0 & 0 \end{pmatrix}$$

$$\mathscr{I}_{2x} = \tfrac{1}{2}\begin{pmatrix} 0 & +1 & 0 & 0 \\ +1 & 0 & 0 & 0 \\ 0 & 0 & 0 & +1 \\ 0 & 0 & +1 & 0 \end{pmatrix} \qquad 2\mathscr{I}_{1z}\mathscr{I}_{2x} = \tfrac{1}{2}\begin{pmatrix} 0 & +1 & 0 & 0 \\ +1 & 0 & 0 & 0 \\ 0 & 0 & 0 & -1 \\ 0 & 0 & -1 & 0 \end{pmatrix} \qquad \mathscr{I}_{2y} = \tfrac{1}{2}\begin{pmatrix} 0 & -i & 0 & 0 \\ +i & 0 & 0 & 0 \\ 0 & 0 & 0 & -i \\ 0 & 0 & +i & 0 \end{pmatrix} \qquad 2\mathscr{I}_{1z}\mathscr{I}_{2y} = \tfrac{1}{2}\begin{pmatrix} 0 & -i & 0 & 0 \\ +i & 0 & 0 & 0 \\ 0 & 0 & 0 & +i \\ 0 & 0 & -i & 0 \end{pmatrix}$$

$$2\mathscr{I}_{1x}\mathscr{I}_{2x} = \tfrac{1}{2}\begin{pmatrix} 0 & 0 & 0 & +1 \\ 0 & 0 & +1 & 0 \\ 0 & +1 & 0 & 0 \\ +1 & 0 & 0 & 0 \end{pmatrix} \qquad 2\mathscr{I}_{1y}\mathscr{I}_{2y} = \tfrac{1}{2}\begin{pmatrix} 0 & 0 & 0 & -1 \\ 0 & 0 & +1 & 0 \\ 0 & +1 & 0 & 0 \\ -1 & 0 & 0 & 0 \end{pmatrix} \qquad 2\mathscr{I}_{1x}\mathscr{I}_{2y} = \tfrac{1}{2}\begin{pmatrix} 0 & 0 & 0 & -i \\ 0 & 0 & +i & 0 \\ 0 & -i & 0 & 0 \\ +i & 0 & 0 & 0 \end{pmatrix} \qquad 2\mathscr{I}_{1y}\mathscr{I}_{2x} = \tfrac{1}{2}\begin{pmatrix} 0 & 0 & 0 & -i \\ 0 & 0 & -i & 0 \\ 0 & +i & 0 & 0 \\ +i & 0 & 0 & 0 \end{pmatrix}$$

Table 8.4: Single-element basis of product operators for a pair of spin-$\frac{1}{2}$ nuclei

$$\mathscr{I}_{1\alpha}\mathscr{I}_{2\alpha} = \begin{pmatrix} 1&0&0&0 \\ 0&0&0&0 \\ 0&0&0&0 \\ 0&0&0&0 \end{pmatrix} \qquad \mathscr{I}_{1\alpha}\mathscr{I}_{2\beta} = \begin{pmatrix} 0&0&0&0 \\ 0&1&0&0 \\ 0&0&0&0 \\ 0&0&0&0 \end{pmatrix} \qquad \mathscr{I}_{1\beta}\mathscr{I}_{2\alpha} = \begin{pmatrix} 0&0&0&0 \\ 0&0&0&0 \\ 0&0&1&0 \\ 0&0&0&0 \end{pmatrix} \qquad \mathscr{I}_{1\beta}\mathscr{I}_{2\beta} = \begin{pmatrix} 0&0&0&0 \\ 0&0&0&0 \\ 0&0&0&0 \\ 0&0&0&1 \end{pmatrix}$$

$$\mathscr{I}_{1\alpha}\mathscr{I}_{2+} = \begin{pmatrix} 0&1&0&0 \\ 0&0&0&0 \\ 0&0&0&0 \\ 0&0&0&0 \end{pmatrix} \qquad \mathscr{I}_{1\alpha}\mathscr{I}_{2-} = \begin{pmatrix} 0&0&0&0 \\ 1&0&0&0 \\ 0&0&0&0 \\ 0&0&0&0 \end{pmatrix} \qquad \mathscr{I}_{1\beta}\mathscr{I}_{2+} = \begin{pmatrix} 0&0&0&0 \\ 0&0&0&0 \\ 0&0&0&1 \\ 0&0&0&0 \end{pmatrix} \qquad \mathscr{I}_{1\beta}\mathscr{I}_{2-} = \begin{pmatrix} 0&0&0&0 \\ 0&0&0&0 \\ 0&0&0&0 \\ 0&0&1&0 \end{pmatrix}$$

$$\mathscr{I}_{1+}\mathscr{I}_{2\alpha} = \begin{pmatrix} 0&0&1&0 \\ 0&0&0&0 \\ 0&0&0&0 \\ 0&0&0&0 \end{pmatrix} \qquad \mathscr{I}_{1-}\mathscr{I}_{2\alpha} = \begin{pmatrix} 0&0&0&0 \\ 0&0&0&0 \\ 1&0&0&0 \\ 0&0&0&0 \end{pmatrix} \qquad \mathscr{I}_{1+}\mathscr{I}_{2\beta} = \begin{pmatrix} 0&0&0&0 \\ 0&0&0&1 \\ 0&0&0&0 \\ 0&0&0&0 \end{pmatrix} \qquad \mathscr{I}_{1-}\mathscr{I}_{2\beta} = \begin{pmatrix} 0&0&0&0 \\ 0&0&0&0 \\ 0&0&0&0 \\ 0&1&0&0 \end{pmatrix}$$

$$\mathscr{I}_{1+}\mathscr{I}_{2+} = \begin{pmatrix} 0&0&0&1 \\ 0&0&0&0 \\ 0&0&0&0 \\ 0&0&0&0 \end{pmatrix} \qquad \mathscr{I}_{1+}\mathscr{I}_{2-} = -\begin{pmatrix} 0&0&0&0 \\ 0&0&1&0 \\ 0&0&0&0 \\ 0&0&0&0 \end{pmatrix} \qquad \mathscr{I}_{1-}\mathscr{I}_{2+} = -\begin{pmatrix} 0&0&0&0 \\ 0&0&0&0 \\ 0&1&0&0 \\ 0&0&0&0 \end{pmatrix} \qquad \mathscr{I}_{1-}\mathscr{I}_{2-} = \begin{pmatrix} 0&0&0&0 \\ 0&0&0&0 \\ 0&0&0&0 \\ 1&0&0&0 \end{pmatrix}$$

Table 8.5: Shift product operator basis for a pair of spin-$\frac{1}{2}$ nuclei

$$\mathscr{I}_t = \frac{1}{2} \begin{pmatrix} 1\ 0\ 0\ 0 \\ 0\ 1\ 0\ 0 \\ 0\ 0\ 1\ 0 \\ 0\ 0\ 0\ 1 \end{pmatrix}$$

$$\mathscr{I}_{1+} = \frac{1}{\sqrt{2}} \begin{pmatrix} 0\ 0\ 1\ 0 \\ 0\ 0\ 0\ 1 \\ 0\ 0\ 0\ 0 \\ 0\ 0\ 0\ 0 \end{pmatrix} \qquad \mathscr{I}_{2+} = \frac{1}{\sqrt{2}} \begin{pmatrix} 0\ 1\ 0\ 0 \\ 0\ 0\ 0\ 0 \\ 0\ 0\ 0\ 1 \\ 0\ 0\ 0\ 0 \end{pmatrix}$$

$$\mathscr{I}_{10} = \frac{1}{2} \begin{pmatrix} +1 & 0 & 0 & 0 \\ 0 & +1 & 0 & 0 \\ 0 & 0 & -1 & 0 \\ 0 & 0 & 0 & -1 \end{pmatrix} \qquad \mathscr{I}_{20} = \frac{1}{2} \begin{pmatrix} +1 & 0 & 0 & 0 \\ 0 & -1 & 0 & 0 \\ 0 & 0 & +1 & 0 \\ 0 & 0 & 0 & -1 \end{pmatrix}$$

$$\mathscr{I}_{1-} = \frac{1}{\sqrt{2}} \begin{pmatrix} 0\ 0\ 0\ 0 \\ 0\ 0\ 0\ 0 \\ 1\ 0\ 0\ 0 \\ 0\ 1\ 0\ 0 \end{pmatrix} \qquad \mathscr{I}_{2-} = \frac{1}{\sqrt{2}} \begin{pmatrix} 0\ 0\ 0\ 0 \\ 1\ 0\ 0\ 0 \\ 0\ 0\ 0\ 0 \\ 0\ 0\ 1\ 0 \end{pmatrix}$$

$$\mathscr{I}_{1+}\mathscr{I}_{2+} = \begin{pmatrix} 0\ 0\ 0\ 1 \\ 0\ 0\ 0\ 0 \\ 0\ 0\ 0\ 0 \\ 0\ 0\ 0\ 0 \end{pmatrix}$$

$$\mathscr{I}_{1+}\mathscr{I}_{20} = \frac{1}{\sqrt{2}} \begin{pmatrix} 0\ 0\ +1 & 0 \\ 0\ 0\ 0 & -1 \\ 0\ 0\ 0 & 0 \\ 0\ 0\ 0 & 0 \end{pmatrix} \qquad \mathscr{I}_{10}\mathscr{I}_{2+} = \frac{1}{\sqrt{2}} \begin{pmatrix} 0 & +1 & 0 & 0 \\ 0 & 0 & 0 & 0 \\ 0 & 0 & 0 & -1 \\ 0 & 0 & 0 & 0 \end{pmatrix}$$

$$\mathscr{I}_{1+}\mathscr{I}_{2-} = \begin{pmatrix} 0\ 0\ 0\ 0 \\ 0\ 0\ 1\ 0 \\ 0\ 0\ 0\ 0 \\ 0\ 0\ 0\ 0 \end{pmatrix} \qquad \mathscr{I}_{10}\mathscr{I}_{20} = \frac{1}{2} \begin{pmatrix} +1 & 0 & 0 & 0 \\ 0 & -1 & 0 & 0 \\ 0 & 0 & -1 & 0 \\ 0 & 0 & 0 & +1 \end{pmatrix} \qquad \mathscr{I}_{1-}\mathscr{I}_{2+} = \begin{pmatrix} 0\ 0\ 0\ 0 \\ 0\ 0\ 0\ 0 \\ 0\ 1\ 0\ 0 \\ 0\ 0\ 0\ 0 \end{pmatrix}$$

$$\mathscr{I}_{10}\mathscr{I}_{2-} = \frac{1}{\sqrt{2}} \begin{pmatrix} 0\ 0 & 0\ 0 \\ +1\ 0 & 0\ 0 \\ 0\ 0 & 0\ 0 \\ 0\ 0 & -1\ 0 \end{pmatrix} \qquad \mathscr{I}_{1-}\mathscr{I}_{20} = \frac{1}{\sqrt{2}} \begin{pmatrix} 0 & 0\ 0\ 0 \\ 0 & 0\ 0\ 0 \\ +1 & 0\ 0\ 0 \\ 0 & -1\ 0\ 0 \end{pmatrix}$$

$$\mathscr{I}_{1-}\mathscr{I}_{2-} = \begin{pmatrix} 0\ 0\ 0\ 0 \\ 0\ 0\ 0\ 0 \\ 0\ 0\ 0\ 0 \\ 1\ 0\ 0\ 0 \end{pmatrix}$$

Table 8.6: Basis of irreducible spherical operators for a pair of spin-$\frac{1}{2}$ nuclei

$$\mathscr{I}_{1,-1}^{(10)} = \frac{1}{\sqrt{2}} \begin{pmatrix} 0 & 0\ 0\ 0 \\ 0 & 0\ 0\ 0 \\ +1 & 0\ 0\ 0 \\ 0 & +1\ 0\ 0 \end{pmatrix} \qquad \mathscr{I}_{1,-1}^{(02)} = \frac{1}{\sqrt{2}} \begin{pmatrix} 0\ 0 & 0\ 0 \\ +1\ 0 & 0\ 0 \\ 0\ 0 & 0\ 0 \\ 0\ 0 & +1\ 0 \end{pmatrix}$$

$$\mathscr{I}_{0,0}^{(00)} = \frac{1}{2} \begin{pmatrix} +1 & 0 & 0 & 0 \\ 0 & +1 & 0 & 0 \\ 0 & 0 & +1 & 0 \\ 0 & 0 & 0 & +1 \end{pmatrix} \quad \mathscr{I}_{1,0}^{(10)} = \frac{1}{2} \begin{pmatrix} +1 & 0 & 0 & 0 \\ 0 & +1 & 0 & 0 \\ 0 & 0 & -1 & 0 \\ 0 & 0 & 0 & -1 \end{pmatrix} \quad \mathscr{I}_{1,0}^{(02)} = \frac{1}{2} \begin{pmatrix} +1 & 0 & 0 & 0 \\ 0 & -1 & 0 & 0 \\ 0 & 0 & +1 & 0 \\ 0 & 0 & 0 & -1 \end{pmatrix}$$

$$\mathscr{I}_{1,+1}^{(10)} = -\frac{1}{\sqrt{2}} \begin{pmatrix} 0\ 0 & +1 & 0 \\ 0\ 0 & 0 & +1 \\ 0\ 0 & 0 & 0 \\ 0\ 0 & 0 & 0 \end{pmatrix} \qquad \mathscr{I}_{1,+1}^{(02)} = -\frac{1}{\sqrt{2}} \begin{pmatrix} 0 & +1 & 0 & 0 \\ 0 & 0 & 0 & 0 \\ 0 & 0 & 0 & +1 \\ 0 & 0 & 0 & 0 \end{pmatrix}$$

$$\mathscr{I}_{2,-2}^{(12)} = \begin{pmatrix} 0\ 0\ 0\ 0 \\ 0\ 0\ 0\ 0 \\ 0\ 0\ 0\ 0 \\ +1\ 0\ 0\ 0 \end{pmatrix}$$

$$\mathscr{I}_{1,-1}^{(12)} = \frac{1}{2} \begin{pmatrix} 0 & 0 & 0\ 0 \\ +1 & 0 & 0\ 0 \\ -1 & 0 & 0\ 0 \\ 0 & +1 & -1\ 0 \end{pmatrix} \qquad \mathscr{I}_{2,-1}^{(12)} = \frac{1}{2} \begin{pmatrix} 0 & 0 & 0\ 0 \\ +1 & 0 & 0\ 0 \\ +1 & 0 & 0\ 0 \\ 0 & -1 & -1\ 0 \end{pmatrix}$$

$$\mathscr{I}_{0,0}^{(12)} = \frac{1}{2\sqrt{3}} \begin{pmatrix} +1 & 0 & 0 & 0 \\ 0 & -1 & +2 & 0 \\ 0 & +2 & -1 & 0 \\ 0 & 0 & 0 & +1 \end{pmatrix} \quad \mathscr{I}_{1,0}^{(12)} = \frac{1}{\sqrt{2}} \begin{pmatrix} 0 & 0 & 0\ 0 \\ 0 & 0 & -1\ 0 \\ 0 & +1 & 0\ 0 \\ 0 & 0 & 0\ 0 \end{pmatrix} \quad \mathscr{I}_{2,0}^{(12)} = \frac{1}{\sqrt{6}} \begin{pmatrix} +1 & 0 & 0 & 0 \\ 0 & -1 & -1 & 0 \\ 0 & -1 & -1 & 0 \\ 0 & 0 & 0 & +1 \end{pmatrix}$$

$$\mathscr{I}_{1,+1}^{(12)} = \frac{1}{2} \begin{pmatrix} 0 & +1 & -1 & 0 \\ 0 & 0 & 0 & +1 \\ 0 & 0 & 0 & -1 \\ 0 & 0 & 0 & 0 \end{pmatrix} \qquad \mathscr{I}_{2,+1}^{(12)} = \frac{1}{2} \begin{pmatrix} 0 & -1 & -1 & 0 \\ 0 & 0 & 0 & +1 \\ 0 & 0 & 0 & +1 \\ 0 & 0 & 0 & 0 \end{pmatrix}$$

$$\mathscr{I}_{2,+2}^{(12)} = \begin{pmatrix} 0\ 0\ 0 & +1 \\ 0\ 0\ 0 & 0 \\ 0\ 0\ 0 & 0 \\ 0\ 0\ 0 & 0 \end{pmatrix}$$

$$(\hat{A} \otimes \hat{B}) + (\hat{A} \otimes \hat{C}) = \hat{A} \otimes (\hat{B} + \hat{C}), \tag{8.105}$$

$$(\hat{A} \otimes \hat{B}) \cdot (\hat{C} \otimes \hat{D}) = (\hat{A} \cdot \hat{C}) \otimes (\hat{B} \cdot \hat{D}). \tag{8.106}$$

First, we derive commutation relations among operators of the form $\mathscr{I}_{nj}$. Eq. 8.105 shows that

$$2\mathscr{I}_t \otimes (\mathscr{I}_j \cdot \mathscr{I}_k) \pm 2\mathscr{I}_t \otimes (\mathscr{I}_k \cdot \mathscr{I}_j) = 2\mathscr{I}_t \otimes (\mathscr{I}_j \cdot \mathscr{I}_k \pm \mathscr{I}_k \cdot \mathscr{I}_j), \tag{8.107}$$

$$2(\mathscr{I}_j \cdot \mathscr{I}_k) \otimes \mathscr{I}_t \pm 2(\mathscr{I}_j \cdot \mathscr{I}_k) \otimes \mathscr{I}_t = 2(\mathscr{I}_j \cdot \mathscr{I}_k \pm \mathscr{I}_k \cdot \mathscr{I}_j) \otimes \mathscr{I}_t. \tag{8.108}$$

Therefore, the relations among $\mathscr{I}_{1x}, \mathscr{I}_{1y}, \mathscr{I}_{1z}$ and $\mathscr{I}_{2x}, \mathscr{I}_{2y}, \mathscr{I}_{2z}$ can be obtained simply by replacing subscripts x, y, z in Eqs. 8.101–8.104 by the subscripts $1x, 1y, 1z$ and $2x, 2y, 2z$. This is written in a concise form in Eq. 8.29.

Second, we derive commutation relations between operators $\mathscr{I}_{nj}$ and $2\mathscr{I}_{nk}\mathscr{I}_{n'l}$. Their commutator is

$$[\mathscr{I}_{nj}, 2\mathscr{I}_{nk}\mathscr{I}_{n'l}] = 2\mathscr{I}_{nj}\mathscr{I}_{nk}\mathscr{I}_{n'l} - 2\mathscr{I}_{nk}\mathscr{I}_{n'l}\mathscr{I}_{nj}. \tag{8.109}$$

Eq. 8.106 implies

$$\mathscr{I}_{1j}\mathscr{I}_{2k} = (\mathscr{I}_j \otimes \mathscr{I}_t) \cdot (\mathscr{I}_t \otimes \mathscr{I}_k) = (\mathscr{I}_j \cdot \mathscr{I}_t) \otimes (\mathscr{I}_t \cdot \mathscr{I}_k) = \frac{1}{4}\mathscr{I}_j \otimes \mathscr{I}_k, \tag{8.110}$$

$$\mathscr{I}_{2k}\mathscr{I}_{1j} = (\mathscr{I}_t \otimes \mathscr{I}_k) \cdot (\mathscr{I}_j \otimes \mathscr{I}_t) = (\mathscr{I}_t \cdot \mathscr{I}_j) \otimes (\mathscr{I}_k \cdot \mathscr{I}_t) = \frac{1}{4}\mathscr{I}_j \otimes \mathscr{I}_k. \tag{8.111}$$

Therefore, $\mathscr{I}_{1j}\mathscr{I}_{2k} - \mathscr{I}_{2k}\mathscr{I}_{1j} = 0$, i.e., $\mathscr{I}_{1j}$ and $\mathscr{I}_{2k}$ (operators of magnetic moment components of *different* nuclei) *commute* and can be applied in any order:

$$\mathscr{I}_{1j}\mathscr{I}_{2k} = \mathscr{I}_{2k}\mathscr{I}_{1j} \tag{8.112}$$

This allows us to switch the last two operators in Eq. 8.109 and obtain the relation described by Eq. 8.30:

$$2\mathscr{I}_{nj}\mathscr{I}_{nk}\mathscr{I}_{n'l} - 2\mathscr{I}_{nk}\mathscr{I}_{n'l}\mathscr{I}_{nj} = 2\mathscr{I}_{nj}\mathscr{I}_{nk}\mathscr{I}_{n'l} - 2\mathscr{I}_{nk}\mathscr{I}_{nj}\mathscr{I}_{n'l} = 2[\mathscr{I}_{nj}, \mathscr{I}_{nk}]\mathscr{I}_{n'l}. \tag{8.113}$$

Third, we derive commutation relations between operators $2\mathscr{I}_{nj}\mathscr{I}_{n'l}$ and $2\mathscr{I}_{nk}\mathscr{I}_{n'm}$

$$[2\mathscr{I}_{nj}\mathscr{I}_{n'l}, 2\mathscr{I}_{nk}\mathscr{I}_{n'm}] = 4\mathscr{I}_{nj}\mathscr{I}_{n'l}\mathscr{I}_{nk}\mathscr{I}_{n'm} - 4\mathscr{I}_{nk}\mathscr{I}_{n'm}\mathscr{I}_{nj}\mathscr{I}_{n'l}. \tag{8.114}$$

We start by switching the commuting operators of magnetic moment components of different nuclei $\mathscr{I}_{n'l}, \mathscr{I}_{nk}$ and $\mathscr{I}_{n'm}\mathscr{I}_{nj}$.

$$[2\mathscr{I}_{nj}\mathscr{I}_{n'l}, 2\mathscr{I}_{nk}\mathscr{I}_{n'm}] = 4\mathscr{I}_{nj}\mathscr{I}_{nk}\mathscr{I}_{n'l}\mathscr{I}_{n'm} - 4\mathscr{I}_{nk}\mathscr{I}_{nj}\mathscr{I}_{n'm}\mathscr{I}_{n'l}. \tag{8.115}$$

Then we use Eqs. 8.101–8.104 to express

$$2\mathscr{I}_{nj}\mathscr{I}_{nk} = (\mathscr{I}_{nj}\mathscr{I}_{nk} - \mathscr{I}_{nk}\mathscr{I}_{nj}) + (\mathscr{I}_{nj}\mathscr{I}_{nk} + \mathscr{I}_{nk}\mathscr{I}_{nj}) = [\mathscr{I}_{nj}, \mathscr{I}_{nk}] + \delta_{jk}\mathscr{I}_t, \tag{8.116}$$

$$-2\mathscr{I}_{nk}\mathscr{I}_{nj} = (\mathscr{I}_{nj}\mathscr{I}_{nk} - \mathscr{I}_{nk}\mathscr{I}_{nj}) - (\mathscr{I}_{nj}\mathscr{I}_{nk} + \mathscr{I}_{nk}\mathscr{I}_{nj}) = [\mathscr{I}_{nj}, \mathscr{I}_{nk}] - \delta_{jk}\mathscr{I}_t, \tag{8.117}$$

$$2\mathscr{I}_{n'l}\mathscr{I}_{n'm} = (\mathscr{I}_{n'l}\mathscr{I}_{n'm} - \mathscr{I}_{n'm}\mathscr{I}_{n'l}) + (\mathscr{I}_{n'l}\mathscr{I}_{n'm} + \mathscr{I}_{n'm}\mathscr{I}_{n'l}) = [\mathscr{I}_{n'l}, \mathscr{I}_{n'm}] + \delta_{lm}\mathscr{I}_t, \tag{8.118}$$

$$-2\mathscr{I}_{n'm}\mathscr{I}_{n'l} = (\mathscr{I}_{n'l}\mathscr{I}_{n'm} - \mathscr{I}_{n'm}\mathscr{I}_{n'l}) - (\mathscr{I}_{n'l}\mathscr{I}_{n'm} + \mathscr{I}_{n'm}\mathscr{I}_{n'l}) = [\mathscr{I}_{n'l}, \mathscr{I}_{n'm}] - \delta_{lm}\mathscr{I}_t. \tag{8.119}$$

Inserting the obtained expressions into Eq. 8.115 results in Eq. 8.31

$$[2\mathscr{I}_{nj}\mathscr{I}_{n'l}, 2\mathscr{I}_{nk}\mathscr{I}_{n'm}] = 4\mathscr{I}_{nj}\mathscr{I}_{nk}\mathscr{I}_{n'l}\mathscr{I}_{n'm} - 4\mathscr{I}_{nk}\mathscr{I}_{nj}\mathscr{I}_{n'm}\mathscr{I}_{n'l} =$$

$$([\mathscr{I}_{nj}, \mathscr{I}_{nk}] + \delta_{jk}\mathscr{I}_t)([\mathscr{I}_{n'l}, \mathscr{I}_{n'm}] + \delta_{lm}\mathscr{I}_t) - ([\mathscr{I}_{nj}, \mathscr{I}_{nk}] - \delta_{jk}\mathscr{I}_t)([\mathscr{I}_{n'l}, \mathscr{I}_{n'm}] - \delta_{lm}\mathscr{I}_t) = [\mathscr{I}_{nj}, \mathscr{I}_{nk}]\delta_{lm} + [\mathscr{I}_{n'l}, \mathscr{I}_{n'm}]\delta_{jk}. \tag{8.120}$$

Note that

$$j = k \Rightarrow \quad [\mathscr{I}_{nj}, \mathscr{I}_{nk}] = 0, \quad \delta_{jk} = 1 \tag{8.121}$$

$$l = m \Rightarrow \quad [\mathscr{I}_{n'l}, \mathscr{I}_{n'm}] = 0, \quad \delta_{lm} = 1. \tag{8.122}$$

8.9.6 Dipole-dipole relaxation: derivation

The Bloch-Wangsness-Redfield theory (see Section 7.12.3) describes also the relaxation due to the dipole-dipole interactions. The Liouville-von Neumann equation has the same form as Eq. 7.44, only the chemical shift Hamiltonian is replaced by the Hamiltonian describing the interactions of spin magnetic moments:

$$\frac{\mathrm{d}\Delta\hat{\rho}}{\mathrm{d}t} = -\frac{\mathrm{i}}{\hbar}[\hat{H}_D, \Delta\hat{\rho}], \tag{8.123}$$

In order to describe the dipole-dipole relaxation on the quantum level, it is useful to work in spherical coordinates and to convert the product operators constituting the Hamiltonian $\hat{H}_D$ to a different basis. The operators $\hat{I}_{1x}\hat{I}_{2z}, \hat{I}_{1y}\hat{I}_{2z}, \hat{I}_{1z}\hat{I}_{2x}, \hat{I}_{1z}\hat{I}_{2y}$ are transformed using the relation $\hat{I}_{\pm} = \hat{I}_x \pm \mathrm{i}\hat{I}_y$):

$$\hat{I}_{1x}\hat{I}_{2z} = \frac{1}{2}(+\hat{I}_{1+}\hat{I}_{2z} + \hat{I}_{1-}\hat{I}_{2z}), \tag{8.124}$$

$$\hat{I}_{1y}\hat{I}_{2z} = \frac{\mathrm{i}}{2}(-\hat{I}_{1+}\hat{I}_{2z} + \hat{I}_{1-}\hat{I}_{2z}), \tag{8.125}$$

$$\hat{I}_{1z}\hat{I}_{2x} = \frac{1}{2}(+\hat{I}_{1z}\hat{I}_{2+} + \hat{I}_{1z}\hat{I}_{2-}), \tag{8.126}$$

$$\hat{I}_{1z}\hat{I}_{2y} = \frac{\mathrm{i}}{2}(-\hat{I}_{1z}\hat{I}_{2+} + \hat{I}_{1z}\hat{I}_{2-}). \tag{8.127}$$

Since

$$\cos\varphi + \mathrm{i}\sin\varphi = \mathrm{e}^{\mathrm{i}\varphi}, \tag{8.128}$$
$$\cos\varphi - \mathrm{i}\sin\varphi = \mathrm{e}^{-\mathrm{i}\varphi}, \tag{8.129}$$

$$3\sin\vartheta\cos\vartheta(\hat{I}_{1x}\hat{I}_{2z}\cos\varphi + \hat{I}_{1y}\hat{I}_{2z}\sin\varphi + \hat{I}_{1z}\hat{I}_{2x}\cos\varphi + \hat{I}_{1z}\hat{I}_{2y}\sin\varphi).$$
$$= \frac{3}{2}\sin\vartheta\cos\vartheta(\hat{I}_{1+}\hat{I}_{2z}\mathrm{e}^{-\mathrm{i}\varphi} + \hat{I}_{1-}\hat{I}_{2z}\mathrm{e}^{\mathrm{i}\varphi} + \hat{I}_{1z}\hat{I}_{2+}\mathrm{e}^{-\mathrm{i}\varphi} + \hat{I}_{1z}\hat{I}_{2-}\mathrm{e}^{\mathrm{i}\varphi}) \tag{8.130}$$

The $\hat{I}_{1x}\hat{I}_{2x}, \hat{I}_{1y}\hat{I}_{2y}, \hat{I}_{1x}\hat{I}_{2y}, \hat{I}_{1y}\hat{I}_{2x}$ are transformed in a similar fashion

$$\hat{I}_{1x}\hat{I}_{2y} = \frac{\mathrm{i}}{4}(+\hat{I}_{1+}\hat{I}_{2-} - \hat{I}_{1-}\hat{I}_{2+} - \hat{I}_{1+}\hat{I}_{2+} + \hat{I}_{1-}\hat{I}_{2-}),$$

$$\hat{I}_{1y}\hat{I}_{2x} = \frac{\mathrm{i}}{4}(-\hat{I}_{1+}\hat{I}_{2-} + \hat{I}_{1-}\hat{I}_{2+} - \hat{I}_{1+}\hat{I}_{2+} + \hat{I}_{1-}\hat{I}_{2-}),$$

$$\hat{I}_{1x}\hat{I}_{2x} = \frac{1}{4}(+\hat{I}_{1+}\hat{I}_{2-} + \hat{I}_{1-}\hat{I}_{2+} + \hat{I}_{1+}\hat{I}_{2+} + \hat{I}_{1-}\hat{I}_{2-}),$$

$$\hat{I}_{1y}\hat{I}_{2y} = \frac{1}{4}(+\hat{I}_{1+}\hat{I}_{2-} + \hat{I}_{1-}\hat{I}_{2+} - \hat{I}_{1+}\hat{I}_{2+} - \hat{I}_{1-}\hat{I}_{2-}),$$

and

$$3\sin^2\vartheta(\hat{I}_{1x}\hat{I}_{2x}\cos^2\varphi + \hat{I}_{1y}\hat{I}_{2y}\sin^2\varphi + \hat{I}_{1x}\hat{I}_{2y}\sin\varphi\cos\varphi + \hat{I}_{1y}\hat{I}_{2x}\sin\varphi\cos\varphi) - (\hat{I}_{1x}\hat{I}_{2x} + \hat{I}_{1y}\hat{I}_{2y})$$

$$= \frac{3}{4}\sin^2\vartheta \, (\ \hat{I}_{1+}\hat{I}_{2-}(\cos^2\varphi + \sin^2\varphi + \mathrm{i}\sin\varphi\cos\varphi - \mathrm{i}\sin\varphi\cos\varphi)$$
$$+\hat{I}_{1-}\hat{I}_{2+}(\cos^2\varphi + \sin^2\varphi - \mathrm{i}\sin\varphi\cos\varphi + \mathrm{i}\sin\varphi\cos\varphi)$$
$$+\hat{I}_{1+}\hat{I}_{2+}(\cos^2\varphi - \sin^2\varphi - \mathrm{i}\sin\varphi\cos\varphi - \mathrm{i}\sin\varphi\cos\varphi)$$
$$+\hat{I}_{1-}\hat{I}_{2-}(\cos^2\varphi - \sin^2\varphi + \mathrm{i}\sin\varphi\cos\varphi + \mathrm{i}\sin\varphi\cos\varphi) \ )$$
$$-\frac{1}{4}(2\hat{I}_{1+}\hat{I}_{2-} + 2\hat{I}_{1-}\hat{I}_{2+})$$
$$= \frac{1}{4}\hat{I}_{1+}\hat{I}_{2-}(3\sin^2\vartheta - 2) + \frac{1}{4}\hat{I}_{1-}\hat{I}_{2+}(3\sin^2\vartheta - 2)$$
$$+\frac{3}{4}\hat{I}_{1+}\hat{I}_{2+}\sin^2\vartheta\mathrm{e}^{-\mathrm{i}2\varphi} + \frac{3}{4}\hat{I}_{1-}\hat{I}_{2-}\sin^2\vartheta\mathrm{e}^{\mathrm{i}2\varphi}$$
$$= -\frac{1}{4}\hat{I}_{1+}\hat{I}_{2-}(3\cos^2\vartheta - 1) - \frac{1}{4}\hat{I}_{1-}\hat{I}_{2+}(3\cos^2\vartheta - 1)$$
$$+\frac{3}{4}\hat{I}_{1+}\hat{I}_{2+}\sin^2\vartheta\mathrm{e}^{-\mathrm{i}2\varphi} + \frac{3}{4}\hat{I}_{1-}\hat{I}_{2-}\sin^2\vartheta\mathrm{e}^{\mathrm{i}2\varphi}. \tag{8.131}$$

Using Eqs. 8.130 and 8.131 and moving to the interaction frame ($\hat{I}_{n\pm} \to \hat{I}_{n\pm}\mathrm{e}^{\pm\mathrm{i}\omega_{0,n}t}$), Eq. 8.61 is converted to

$$
\begin{aligned}
\hat{H}_D^I = -\frac{\mu_0\gamma_1\gamma_2}{4\pi r^3} \Big(&\hat{I}_{1z}\hat{I}_{2z}(3\cos^2\vartheta - 1) \\
&-\frac{1}{4}\hat{I}_{1+}\hat{I}_{2-}(3\cos^2\vartheta-1)\mathrm{e}^{\mathrm{i}(\omega_{0,1}-\omega_{0,2})t} - \frac{1}{4}\hat{I}_{1-}\hat{I}_{2+}(3\cos^2\vartheta-1)\mathrm{e}^{-\mathrm{i}(\omega_{0,1}-\omega_{0,2})t} \\
&+\frac{3}{2}\hat{I}_{1+}\hat{I}_{2z}\sin\vartheta\cos\vartheta\mathrm{e}^{-\mathrm{i}\varphi}\mathrm{e}^{\mathrm{i}(\omega_{0,1})t} + \frac{3}{2}\hat{I}_{1-}\hat{I}_{2z}\sin\vartheta\cos\vartheta\mathrm{e}^{\mathrm{i}\varphi}\mathrm{e}^{-\mathrm{i}(\omega_{0,1})t} \\
&+\frac{3}{2}\hat{I}_{1z}\hat{I}_{2+}\sin\vartheta\cos\vartheta\mathrm{e}^{-\mathrm{i}\varphi}\mathrm{e}^{\mathrm{i}(\omega_{0,2})t} + \frac{3}{2}\hat{I}_{1z}\hat{I}_{2-}\sin\vartheta\cos\vartheta\mathrm{e}^{\mathrm{i}\varphi}\mathrm{e}^{-\mathrm{i}(\omega_{0,2})t} \\
&+\frac{3}{4}\hat{I}_{1+}\hat{I}_{2+}\sin^2\vartheta\mathrm{e}^{-\mathrm{i}2\varphi}\mathrm{e}^{\mathrm{i}(\omega_{0,1}+\omega_{0,2})t} + \frac{3}{4}\hat{I}_{1-}\hat{I}_{2-}\sin^2\vartheta\mathrm{e}^{\mathrm{i}2\varphi}\mathrm{e}^{-\mathrm{i}(\omega_{0,1}+\omega_{0,2})t} \Big) \\
= -b \Big(&2c^{zz}\hat{I}_{1z}\hat{I}_{2z} - \frac{1}{2}c^{+-}\hat{I}_{1+}\hat{I}_{2-} - \frac{1}{2}c^{-+}\hat{I}_{1-}\hat{I}_{2+} \\
&+ \sqrt{\frac{3}{2}}\left(c^{+z}\hat{I}_{1+}\hat{I}_{2z} + c^{-z}\hat{I}_{1-}\hat{I}_{2z} + c^{z+}\hat{I}_{1z}\hat{I}_{2+} + c^{z-}\hat{I}_{1z}\hat{I}_{2-} + c^{++}\hat{I}_{1+}\hat{I}_{2+} + c^{--}\hat{I}_{1-}\hat{I}_{2-}\right) \Big).
\end{aligned}
\tag{8.132}
$$

The difference of the density matrix from its equilibrium form, written in a bases including the operators used to define $\hat{H}_D$, is in general

$$
\begin{aligned}
\Delta\hat{\rho} = &d_t\hat{I}_t + d_{1z}\hat{I}_{1z} + d_{1+}\hat{I}_{1+} + d_{1-}\hat{I}_{1-} + d_{2z}\hat{I}_{2z} + d_{2+}\hat{I}_{2+} + d_{2-}\hat{I}_{2-} \\
&+ d_{zz}\hat{I}_{1z}\hat{I}_{2z} + d_{+-}\hat{I}_{1+}\hat{I}_{2-} + d_{-+}\hat{I}_{1-}\hat{I}_{2+} + d_{+z}\hat{I}_{1+}\hat{I}_{2z} + d_{-z}\hat{I}_{1-}\hat{I}_{2z} + d_{z+}\hat{I}_{1z}\hat{I}_{2+} + d_{z-}\hat{I}_{1z}\hat{I}_{2-} + d_{++}\hat{I}_{1+}\hat{I}_{2+} + d_{--}\hat{I}_{1-}\hat{I}_{2-}.
\end{aligned}
\tag{8.133}
$$

However, here we analyze only evolution of $d_{1z}\hat{I}_{1z}$, $d_{2z}\hat{I}_{2z}$, $d_{1+}\hat{I}_{1+}$, needed to describe relaxation of $\Delta\langle M_{1z}\rangle$, $\Delta\langle M_{1z}\rangle$, and $\langle M_{1+}\rangle$. Similarly to Eq. 7.50, the dipole-dipole relaxation is described by

$$
\frac{\mathrm{d}\Delta\hat{\rho}}{\mathrm{d}t} = -\frac{1}{\hbar^2}\int_0^\infty \overline{[\hat{H}_D(0), [\hat{H}_D(t), \Delta\hat{\rho}]]}\mathrm{d}t.
\tag{8.134}
$$

The right-hand side can be simplified dramatically by the *secular approximation* as in Eq. 7.50: all terms with $\mathrm{e}^{\pm\mathrm{i}\omega_{0,n}t}$ are averaged to zero. Only terms with $\overline{(c^{zz})^2}$, $\overline{c^{z+}c^{z-}}$, $\overline{c^{+z}c^{-z}}$, $\overline{c^{+-}c^{-+}}$, and $\overline{c^{++}c^{--}}$ are non zero (all equal to $1/5$ at $t_j = 0$).[9] This reduces the number of double commutators to be expressed from 81 to 9 for each density matrix component. The double commutators needed to describe relaxation rates of the contributions of the first nucleus to the magnetization $\langle M_{1z}\rangle$ and $\langle M_{1+}\rangle$ are

$$
\left[\hat{I}_{1z}\hat{I}_{2z}, [\hat{I}_{1z}\hat{I}_{2z}, \hat{I}_{1z}]\right] = 0,
\tag{8.135}
$$

$$
\left[\hat{I}_{1-}\hat{I}_{2+}, [\hat{I}_{1+}\hat{I}_{2-}, \hat{I}_{1z}]\right] = \hbar^2(\hat{I}_{1z} - \hat{I}_{2z}),
\tag{8.136}
$$

$$
\left[\hat{I}_{1+}\hat{I}_{2-}, [\hat{I}_{1-}\hat{I}_{2+}, \hat{I}_{1z}]\right] = \hbar^2(\hat{I}_{1z} - \hat{I}_{2z}),
\tag{8.137}
$$

$$
\left[\hat{I}_{1+}\hat{I}_{2z}, [\hat{I}_{1-}\hat{I}_{2z}, \hat{I}_{1z}]\right] = \frac{1}{2}\hbar^2\hat{I}_{1z},
\tag{8.138}
$$

$$
\left[\hat{I}_{1-}\hat{I}_{2z}, [\hat{I}_{1+}\hat{I}_{2z}, \hat{I}_{1z}]\right] = \frac{1}{2}\hbar^2\hat{I}_{1z},
\tag{8.139}
$$

$$
\left[\hat{I}_{1z}\hat{I}_{2+}, [\hat{I}_{1z}\hat{I}_{2-}, \hat{I}_{1z}]\right] = 0,
\tag{8.140}
$$

$$
\left[\hat{I}_{1z}\hat{I}_{2-}, [\hat{I}_{1z}\hat{I}_{2+}, \hat{I}_{1z}]\right] = 0,
\tag{8.141}
$$

$$
\left[\hat{I}_{1+}\hat{I}_{2+}, [\hat{I}_{1-}\hat{I}_{2-}, \hat{I}_{1z}]\right] = \hbar^2(\hat{I}_{1z} + \hat{I}_{2z}),
\tag{8.142}
$$

$$
\left[\hat{I}_{1-}\hat{I}_{2-}, [\hat{I}_{1+}\hat{I}_{2+}, \hat{I}_{1z}]\right] = \hbar^2(\hat{I}_{1z} + \hat{I}_{2z}),
\tag{8.143}
$$

---

[9]Averaging over all molecules makes all correlation functions identical in isotropic liquids.

$$\left[\hat{I}_{1z}\hat{I}_{2z},[\hat{I}_{1z}\hat{I}_{2z},\hat{I}_{2z}]\right] = 0, \tag{8.144}$$

$$\left[\hat{I}_{1-}\hat{I}_{2+},[\hat{I}_{1+}\hat{I}_{2-},\hat{I}_{2z}]\right] = \hbar^2(\hat{I}_{2z} - \hat{I}_{1z}), \tag{8.145}$$

$$\left[\hat{I}_{1+}\hat{I}_{2-},[\hat{I}_{1-}\hat{I}_{2+},\hat{I}_{2z}]\right] = \hbar^2(\hat{I}_{2z} - \hat{I}_{1z}), \tag{8.146}$$

$$\left[\hat{I}_{1+}\hat{I}_{2z},[\hat{I}_{1-}\hat{I}_{2z},\hat{I}_{2z}]\right] = \frac{1}{2}\hbar^2\hat{I}_{2z}, \tag{8.147}$$

$$\left[\hat{I}_{1-}\hat{I}_{2z},[\hat{I}_{1+}\hat{I}_{2z},\hat{I}_{2z}]\right] = \frac{1}{2}\hbar^2\hat{I}_{2z}, \tag{8.148}$$

$$\left[\hat{I}_{1z}\hat{I}_{2+},[\hat{I}_{1z}\hat{I}_{2-},\hat{I}_{2z}]\right] = 0, \tag{8.149}$$

$$\left[\hat{I}_{1z}\hat{I}_{2-},[\hat{I}_{1z}\hat{I}_{2+},\hat{I}_{2z}]\right] = 0, \tag{8.150}$$

$$\left[\hat{I}_{1+}\hat{I}_{2+},[\hat{I}_{1-}\hat{I}_{2-},\hat{I}_{2z}]\right] = \hbar^2(\hat{I}_{2z} + \hat{I}_{1z}), \tag{8.151}$$

$$\left[\hat{I}_{1-}\hat{I}_{2-},[\hat{I}_{1+}\hat{I}_{2+},\hat{I}_{2z}]\right] = \hbar^2(\hat{I}_{2z} + \hat{I}_{1z}), \tag{8.152}$$

$$\left[\hat{I}_{1z}\hat{I}_{2z},[\hat{I}_{1z}\hat{I}_{2z},\hat{I}_{1+}]\right] = \frac{1}{4}\hbar^2\hat{I}_{1+}, \tag{8.153}$$

$$\left[\hat{I}_{1+}\hat{I}_{2-},[\hat{I}_{1-}\hat{I}_{2+},\hat{I}_{1+}]\right] = \hbar^2\hat{I}_{1+}, \tag{8.154}$$

$$\left[\hat{I}_{1-}\hat{I}_{2+},[\hat{I}_{1+}\hat{I}_{2-},\hat{I}_{1+}]\right] = 0, \tag{8.155}$$

$$\left[\hat{I}_{1+}\hat{I}_{2z},[\hat{I}_{1-}\hat{I}_{2z},\hat{I}_{1+}]\right] = \frac{1}{2}\hbar^2\hat{I}_{1+}, \tag{8.156}$$

$$\left[\hat{I}_{1-}\hat{I}_{2z},[\hat{I}_{1+}\hat{I}_{2z},\hat{I}_{1+}]\right] = 0, \tag{8.157}$$

$$\left[\hat{I}_{1z}\hat{I}_{2+},[\hat{I}_{1z}\hat{I}_{2-},\hat{I}_{1+}]\right] = \frac{1}{2}\hbar^2\hat{I}_{1+}, \tag{8.158}$$

$$\left[\hat{I}_{1z}\hat{I}_{2-},[\hat{I}_{1z}\hat{I}_{2+},\hat{I}_{1+}]\right] = \frac{1}{2}\hbar^2\hat{I}_{1+}, \tag{8.159}$$

$$\left[\hat{I}_{1+}\hat{I}_{2+},[\hat{I}_{1-}\hat{I}_{2-},\hat{I}_{1+}]\right] = 0, \tag{8.160}$$

$$\left[\hat{I}_{1-}\hat{I}_{2-},[\hat{I}_{1+}\hat{I}_{2+},\hat{I}_{1+}]\right] = \frac{1}{2}\hbar^2\hat{I}_{1+}. \tag{8.161}$$

The relaxation rates can be then derived as described for the relaxation due to the chemical shift in Section 7.12.3. For ΔM_{1z},

$$\langle\Delta M_{1z}\rangle = \text{Tr}\{\Delta\hat{\rho}\hat{M}_{1z}\} = \mathcal{N}\gamma\text{Tr}\{\Delta\hat{\rho}\hat{I}_{1z}\}. \tag{8.162}$$

As discussed in Section 7.12.3, the orthogonality of basis matrices reduces the left-hand side of Eq. 8.134 to

$$\frac{\mathrm{d}d_{1z}}{\mathrm{d}t}\hat{I}_{1z}. \tag{8.163}$$

Expressing the terms with the non-zero double commutators in the right-hand side of Eq. 8.134 results in six integrals

$$\frac{\mathrm{d}d_{1z}}{\mathrm{d}t}\text{Tr}\{\hat{I}_{1z}\hat{I}_{1z}\} = -\left(\frac{1}{4}b^2\int\limits_0^\infty\overline{c^{+-}(0)c^{-+}(t)}\mathrm{e}^{\mathrm{i}(\omega_{0,1}-\omega_{0,2})t}\mathrm{d}t + \frac{1}{4}b^2\int\limits_0^\infty\overline{c^{-+}(0)c^{+-}(t)}\mathrm{e}^{-\mathrm{i}(\omega_{0,1}-\omega_{0,2})t}\mathrm{d}t\right)d_{1z}(\text{Tr}\{\hat{I}_{1z}\hat{I}_{1z}\} - \text{Tr}\{\hat{I}_{2z}\hat{I}_{2z}\})$$

$$-\left(\frac{3}{4}b^2\int\limits_0^\infty\overline{c^{+z}(0)c^{-z}(t)}\mathrm{e}^{\mathrm{i}\omega_{0,1}t}\mathrm{d}t + \frac{3}{4}b^2\int\limits_0^\infty\overline{c^{-z}(0)c^{+z}(t)}\mathrm{e}^{-\mathrm{i}\omega_{0,1}t}\mathrm{d}t\right)d_{1z}\text{Tr}\{\hat{I}_{1z}\hat{I}_{1z}\}$$

$$-\left(\frac{3}{2}b^2\int\limits_0^\infty\overline{c^{++}(0)c^{--}(t)}\mathrm{e}^{\mathrm{i}(\omega_{0,1}+\omega_{0,2})t}\mathrm{d}t + \frac{3}{2}b^2\int\limits_0^\infty\overline{c^{--}(0)c^{++}(t)}\mathrm{e}^{-\mathrm{i}(\omega_{0,1}+\omega_{0,2})t}\mathrm{d}t\right)(d_{1z}(\text{Tr}\{\hat{I}_{1z}\hat{I}_{1z}\} + \text{Tr}\{\hat{I}_{2z}\hat{I}_{2z}\})).$$

$$\tag{8.164}$$

As both sides of the equation contain the same coefficients, $d_{nz}\mathrm{Tr}\{\hat{I}_{nz}\hat{I}_{nz}\}$ can be converted to $\Delta\langle M_{nz}\rangle$:

$$\frac{\mathrm{d}\Delta\langle M_{1z}\rangle}{\mathrm{d}t} = -\left(\frac{1}{4}b^2\int_0^\infty \overline{c^{+-}(0)c^{-+}(t)}\mathrm{e}^{\mathrm{i}(\omega_{0,1}-\omega_{0,2})t}\mathrm{d}t + \frac{1}{4}b^2\int_0^\infty \overline{c^{-+}(0)c^{+-}(t)}\mathrm{e}^{-\mathrm{i}(\omega_{0,1}-\omega_{0,2})t}\mathrm{d}t\right)(\Delta\langle M_{1z}\rangle - \Delta\langle M_{2z}\rangle)$$

$$- \left(\frac{3}{4}b^2\int_0^\infty \overline{c^{+z}(0)c^{-z}(t)}\mathrm{e}^{\mathrm{i}\omega_{0,1}t}\mathrm{d}t + \frac{3}{4}b^2\int_0^\infty \overline{c^{-z}(0)c^{+z}(t)}\mathrm{e}^{-\mathrm{i}\omega_{0,1}t}\mathrm{d}t\right)\Delta\langle M_{1z}\rangle$$

$$- \left(\frac{3}{2}b^2\int_0^\infty \overline{c^{++}(0)c^{--}(t)}\mathrm{e}^{\mathrm{i}(\omega_{0,1}+\omega_{0,2})t}\mathrm{d}t + \frac{3}{2}b^2\int_0^\infty \overline{c^{--}(0)c^{++}(t)}\mathrm{e}^{-\mathrm{i}(\omega_{0,1}+\omega_{0,2})t}\mathrm{d}t\right)(\Delta\langle M_{1z}\rangle + \Delta\langle M_{2z}\rangle). \quad (8.165)$$

If the fluctuations are random and consequently stationary, the current orientation of the molecule is correlated with the orientation in the past in the same manner as it is correlated with the orientation in the future (see Section 7.12.3), and the bounds of the integrals can be changed

$$\frac{\mathrm{d}\Delta\langle M_{1z}\rangle}{\mathrm{d}t} = -\left(\frac{1}{8}b^2\int_{-\infty}^\infty \overline{c^{+-}(0)c^{-+}(t)}\mathrm{e}^{\mathrm{i}(\omega_{0,1}-\omega_{0,2})t}\mathrm{d}t + \frac{1}{8}b^2\int_{-\infty}^\infty \overline{c^{-+}(0)c^{+-}(t)}\mathrm{e}^{-\mathrm{i}(\omega_{0,1}-\omega_{0,2})t}\mathrm{d}t\right)(\Delta\langle M_{1z}\rangle - \Delta\langle M_{2z}\rangle)$$

$$- \left(\frac{3}{8}b^2\int_{-\infty}^\infty \overline{c^{+z}(0)c^{-z}(t)}\mathrm{e}^{\mathrm{i}\omega_{0,1}t}\mathrm{d}t + \frac{3}{8}b^2\int_{-\infty}^\infty \overline{c^{-z}(0)c^{+z}(t)}\mathrm{e}^{-\mathrm{i}\omega_{0,1}t}\mathrm{d}t\right)\Delta\langle M_{1z}\rangle$$

$$- \left(\frac{3}{4}b^2\int_{-\infty}^\infty \overline{c^{++}(0)c^{--}(t)}\mathrm{e}^{\mathrm{i}(\omega_{0,1}+\omega_{0,2})t}\mathrm{d}t + \frac{3}{4}b^2\int_{-\infty}^\infty \overline{c^{--}(0)c^{++}(t)}\mathrm{e}^{-\mathrm{i}(\omega_{0,1}+\omega_{0,2})t}\mathrm{d}t\right)(\Delta\langle M_{1z}\rangle + \Delta\langle M_{2z}\rangle). \quad (8.166)$$

Collecting the real parts of integrals preceding $\Delta\langle M_z\rangle$ of the same nucleus, noting that they are identical with the definitions of the spectral density functions, and assuming $J(\omega) \approx J(-\omega)$,

$$\frac{\mathrm{d}\Delta\langle M_{1z}\rangle}{\mathrm{d}t} = -\frac{1}{8}b^2(2J(\omega_{0,1}-\omega_{0,2}) + 6J(\omega_{0,1}) + 12J(\omega_{0,1}+\omega_{0,2}))\Delta\langle M_{1z}\rangle$$

$$+ \frac{1}{8}b^2(2J(\omega_{0,1}-\omega_{0,2}) - 12J(\omega_{0,1}+\omega_{0,2}))\Delta\langle M_{2z}\rangle$$

$$= -R_{\mathrm{a}1}\Delta\langle M_{1z}\rangle - R_{\mathrm{x}}\Delta\langle M_{2z}\rangle. \quad (8.167)$$

The corresponding expression for relaxation of $\Delta\langle M_{2z}\rangle$ is obtained in the same manner (or simply by switching subscripts 1 and 2 in the result):

$$\frac{\mathrm{d}\Delta\langle M_{2z}\rangle}{\mathrm{d}t} = -\frac{1}{8}b^2(2J(\omega_{0,2}-\omega_{0,1}) + 6J(\omega_{0,2}) + 12J(\omega_{0,2}+\omega_{0,1}))\Delta\langle M_{2z}\rangle$$

$$+ \frac{1}{8}b^2(2J(\omega_{0,2}-\omega_{0,1}) - 12J(\omega_{0,2}+\omega_{0,1}))\Delta\langle M_{1z}\rangle$$

$$= -R_{\mathrm{a}2}\Delta\langle M_{2z}\rangle - R_{\mathrm{x}}\Delta\langle M_{1z}\rangle. \quad (8.168)$$

The same approach is applied to M_{1+}.

$$\Delta\langle M_{1+}\rangle \equiv \langle M_{1+}\rangle = \mathrm{Tr}\{\Delta\hat{\rho}\hat{M}_{1+}\}. \quad (8.169)$$

The operator of M_{1+} for one magnetic moment observed is

$$\hat{M}_{1+} = \mathcal{N}\gamma_1\hat{I}_{1+} = \mathcal{N}\gamma_1(\hat{I}_{1x} + \mathrm{i}\hat{I}_{1y}). \quad (8.170)$$

Due to the orthogonality of basis matrices, the left-hand side of Eq. 8.134 reduces to

$$\frac{\mathrm{d}d_{1+}}{\mathrm{d}t}\hat{I}_{1+}\mathrm{e}^{\mathrm{i}\omega_{0,1}t} \quad (8.171)$$

The terms with the non-zero double commutators in the right-hand side of Eq. 8.134 give six integrals

$$\frac{\mathrm{d}d_{1+}}{\mathrm{d}t}\mathrm{Tr}\{\hat{I}_{1-}\hat{I}_{1+}\} = -b^2\left(\int\limits_0^\infty \overline{c^{zz}(0)c^{zz}(t)}\mathrm{d}t + \frac{3}{4}\int\limits_0^\infty \overline{c^{z+}(0)c^{z-}(t)}\mathrm{e}^{\mathrm{i}\omega_{0,2}t}\mathrm{d}t + \frac{3}{4}\int\limits_0^\infty \overline{c^{z-}(0)c^{z+}(t)}\mathrm{e}^{-\mathrm{i}\omega_{0,2}t}\mathrm{d}t\right.$$

$$\left. + \frac{1}{4}\int\limits_0^\infty \overline{c^{+-}(0)c^{-+}(t)}\mathrm{e}^{\mathrm{i}(\omega_{0,1}-\omega_{0,2})t}\mathrm{d}t + \frac{3}{4}\int\limits_0^\infty \overline{c^{+z}(0)c^{-z}(t)}\mathrm{e}^{\mathrm{i}\omega_{0,1}t}\mathrm{d}t + \frac{3}{2}\int\limits_0^\infty \overline{c^{--}(0)c^{++}(t)}\mathrm{e}^{-\mathrm{i}(\omega_{0,1}+\omega_{0,2})t}\mathrm{d}t\right)d_{1+}\mathrm{Tr}\{\hat{I}_{1-}\hat{I}_{1+}\}.$$

$$(8.172)$$

The same coefficients in both sides of the equation allow us to replace $d_{1+}\mathrm{Tr}\{\hat{I}_{1-}\hat{I}_{1+}\}$ by $\langle M_{1+}\rangle$:

$$\frac{\langle M_{1+}\rangle}{\mathrm{d}t} = -b^2\left(\int\limits_0^\infty \overline{c^{zz}(0)c^{zz}(t)}\mathrm{d}t + \frac{3}{4}\int\limits_0^\infty \overline{c^{z+}(0)c^{z-}(t)}\mathrm{e}^{\mathrm{i}\omega_{0,2}t}\mathrm{d}t + \frac{3}{4}\int\limits_0^\infty \overline{c^{z-}(0)c^{z+}(t)}\mathrm{e}^{-\mathrm{i}\omega_{0,2}t}\mathrm{d}t\right.$$

$$\left. + \frac{1}{4}\int\limits_0^\infty \overline{c^{+-}(0)c^{-+}(t)}\mathrm{e}^{\mathrm{i}(\omega_{0,1}-\omega_{0,2})t}\mathrm{d}t + \frac{3}{4}\int\limits_0^\infty \overline{c^{+z}(0)c^{-z}(t)}\mathrm{e}^{\mathrm{i}\omega_{0,1}t}\mathrm{d}t + \frac{3}{2}\int\limits_0^\infty \overline{c^{--}(0)c^{++}(t)}\mathrm{e}^{-\mathrm{i}(\omega_{0,1}+\omega_{0,2})t}\mathrm{d}t\right)\langle M_{1+}\rangle.$$

$$(8.173)$$

Like in the expression for $\Delta\langle M_{1z}\rangle$, the bounds of the integrals can be changed

$$\frac{\langle M_{1+}\rangle}{\mathrm{d}t} = -b^2\left(\frac{1}{2}\int\limits_{-\infty}^\infty \overline{c^{zz}(0)c^{zz}(t)}\mathrm{d}t + \frac{3}{8}\int\limits_{-\infty}^\infty \overline{c^{z+}(0)c^{z-}(t)}\mathrm{e}^{\mathrm{i}\omega_{0,2}t}\mathrm{d}t + \frac{3}{8}\int\limits_{-\infty}^\infty \overline{c^{z-}(0)c^{z+}(t)}\mathrm{e}^{-\mathrm{i}\omega_{0,2}t}\mathrm{d}t\right.$$

$$\left. + \frac{1}{8}\int\limits_{-\infty}^\infty \overline{c^{+-}(0)c^{-+}(t)}\mathrm{e}^{\mathrm{i}(\omega_{0,1}-\omega_{0,2})t}\mathrm{d}t + \frac{3}{8}\int\limits_{-\infty}^\infty \overline{c^{+z}(0)c^{-z}(t)}\mathrm{e}^{\mathrm{i}\omega_{0,1}t}\mathrm{d}t + \frac{3}{4}\int\limits_{-\infty}^\infty \overline{c^{--}(0)c^{++}(t)}\mathrm{e}^{-\mathrm{i}(\omega_{0,1}+\omega_{0,2})t}\mathrm{d}t\right)\langle M_{1+}\rangle$$

$$(8.174)$$

and the real parts of the integrals can be identified with the spectral density values (assuming $J(\omega) \approx J(-\omega)$), providing the final equation describing relaxation of the transverse magnetization of the first nucleus:

$$\frac{\mathrm{d}\langle M_{1+}\rangle}{\mathrm{d}t} = -\frac{1}{8}b^2(4J(0)+6J(\omega_{0,2})+J(\omega_{0,1}-\omega_{0,2})+3J(\omega_{0,2})+6J(\omega_{0,1}+\omega_{0,2}))\langle M_{1+}\rangle = -R_{2,1}\langle M_{1+}\rangle = -\left(R_{0,1}+\frac{1}{2}R_{\mathrm{a}1}\right)\langle M_{1+}\rangle. \quad (8.175)$$

8.9.7 Dipole-dipole relaxation: discussion

The following equations, derived in Section 8.9.6, describe relaxation due to the dipole-dipole interactions in a pair of nuclei separated by a constant distance r:

$$\frac{\mathrm{d}\Delta\langle M_{1z}\rangle}{\mathrm{d}t} = -\frac{1}{8}b^2(2J(\omega_{0,1}-\omega_{0,2})+6J(\omega_{0,1})+12J(\omega_{0,1}+\omega_{0,2}))\Delta\langle M_{1z}\rangle$$

$$+ \frac{1}{8}b^2(2J(\omega_{0,1}-\omega_{0,2})-12J(\omega_{0,1}+\omega_{0,2}))\Delta\langle M_{2z}\rangle$$

$$= -R_{\mathrm{a}1}\Delta\langle M_{1z}\rangle - R_{\mathrm{x}}\Delta\langle M_{2z}\rangle, \quad (8.176)$$

$$\frac{\mathrm{d}\Delta\langle M_{2z}\rangle}{\mathrm{d}t} = -\frac{1}{8}b^2(2J(\omega_{0,1}-\omega_{0,2})+6J(\omega_{0,2})+12J(\omega_{0,1}+\omega_{0,2}))\Delta\langle M_{2z}\rangle$$

$$+ \frac{1}{8}b^2(2J(\omega_{0,1}-\omega_{0,2})-12J(\omega_{0,1}+\omega_{0,2}))\Delta\langle M_{1z}\rangle$$

$$= -R_{\mathrm{a}2}\Delta\langle M_{2z}\rangle - R_{\mathrm{x}}\Delta\langle M_{1z}\rangle, \quad (8.177)$$

$$\frac{\mathrm{d}\langle M_{1+}\rangle}{\mathrm{d}t} = -\frac{1}{8}b^2(4J(0)+6J(\omega_{0,2})+J(\omega_{0,1}-\omega_{0,2})+3J(\omega_{0,1})+6J(\omega_{0,1}+\omega_{0,2}))\langle M_{1+}\rangle$$

$$= -R_{2,1}\langle M_{1+}\rangle = -\left(R_{0,1}+\frac{1}{2}R_{\mathrm{a}1}\right)\langle M_{1+}\rangle, \quad (8.178)$$

where

$$b = -\frac{\mu_0 \gamma_1 \gamma_2 \hbar}{4\pi r^3}. \tag{8.179}$$

The relaxation rate R_1 of the dipole-dipole relaxation is the rate of relaxation of the z-component of the total magnetization $\langle M_z \rangle = \langle M_{1z} \rangle + \langle M_{2z} \rangle$. R_1 is derived by solving the set of Eqs. 8.176 and 8.177. The solution is simple if $J(\omega_{0,1}) = J(\omega_{0,2}) = J(\omega_0) \Rightarrow R_{a1} = R_{a2} = R_a$ (this is correct e.g. if both nuclei have the same γ, if the molecule rotates as a sphere, and if internal motions are negligible or identical for both nuclei).[10] Then,

$$\frac{\mathrm{d}\Delta\langle M_z \rangle}{\mathrm{d}t} = -\frac{1}{8}b^2(6J(\omega_0) + 24J(2\omega_0))\Delta\langle M_z \rangle = -\underbrace{(R_a + R_x)}_{R_1}\Delta\langle M_z \rangle. \tag{8.180}$$

There are several remarkable differences between relaxation due to the chemical shift anisotropy and dipole-dipole interactions:

- The relaxation constant $R_{0,1}$, describing the loss of coherence of the first magnetic moment, depends on $J(0)$ like in the case of the relaxation due to the chemical shift anisotropy. It is a result of changing position of $\vec{\mu}_1$ in the magnetic field of $\vec{\mu}_2$ as the molecule moves (Figure 8.2A). However, $R_{0,1}$ contains also an additional term, depending on the frequency of *the other* magnetic moment, $3b^2 J(\omega_{0,2})/4$. This term has the following physical significance. The field generated by the second magnetic moment depends on its state. For example, $\vec{\mu}_2$ in a pure $|\alpha\rangle$ state[11] reduces the field and consequently precession frequency of $\vec{\mu}_1$ if the internuclear vector is horizontal (Figure 8.1A), whereas $\vec{\mu}_2$ in a pure $|\beta\rangle$ state has the opposite effect.[12] If the molecule rotates about the vertical axis with a frequency that is for a short time close to $\omega_{0,2}$, $\vec{\mu}_1$ stays (for the short time) in a place where the magnetic field of of $\vec{\mu}_2$ pulls it in the z direction (Figure 8.2B). A macroscopic consequence of such short and stochastic resonance of the rate of molecular rotation with $\omega_{0,2}$ is redistribution of $\vec{\mu}_2$ changing the average value of $\mu_{2,z}$ (longitudinal polarization of $\vec{\mu}_2$). Fluctuations of $\omega_{0,1}$ due to the stochastic changes of the longitudinal polarization of $\vec{\mu}_2$ (described by $J(\omega_{0,2})$) contribute to the loss of coherence of $\vec{\mu}_1$.[13]

- The rate constants describing the return to the equilibrium polarization is more complex than for the chemical shift anisotropy relaxation. In addition to the $3b^2 J(\omega_{0,1})/4$ term, describing effect of stochastic molecular motions resonating with the precession frequency of $\vec{\mu}_1$ (Figure 8.2C), the *auto-relaxation rate* R_{a1} contains terms depending on the sum and difference of the precession frequency of $\vec{\mu}_1$ and $\vec{\mu}_2$. These terms account for temporary resonance of random molecular rotation with the mutual difference in the precession of $\vec{\mu}_1$ and $\vec{\mu}_2$. For example, if the molecule rotates for a short time about the vertical axis with an angular frequency ω_{mol} which is accidentally close to $\omega_{0,1} + \omega_{0,2}$, the precession of $\vec{\mu}_2$ combined with the molecular rotation resonates with the precession of $\vec{\mu}_1$ (see examples in Figure 8.2D,E). Quantum mechanically, such effects are described by the orientation-dependent coefficients preceding $2\hat{I}_{1x}\hat{I}_{2x}, 2\hat{I}_{1y}\hat{I}_{2y}, 2\hat{I}_{1x}\hat{I}_{2y}, 2\hat{I}_{1y}\hat{I}_{2x}$ components in $\hat{H}_D$, contributing to $J(\omega_{0,1} \pm \omega_{0,2})$.

- As mentioned in Section 8.7, return to the equilibrium polarization of nucleus 1 depends also on the actual polarization *of nucleus 2*. The *cross-relaxation* is a cause of the *nuclear Overhauser effect* (NOE), and its dependence on r (approximately proportional to r^{-6}) allow us to measure distances between hydrogen atoms in molecules.

8.9.8 Two magnetic moments in thermal equilibrium

The initial density matrix describing an ensemble of pairs of nuclear magnetic moments is derived in a similar manner as outlined in Section 7.12.2 for an ensemble of isolated nuclei. Again, we start from the thermal equilibrium and use the Hamiltonian. The difference from the case of isolated nuclei is that Hamiltonian must be represented by a 4×4 density matrix in order to describe a pair of mutually interacting nuclei. If secular approximation is applicable, the matrix representation of the Hamiltonian is diagonal. In general, the Hamiltonian should include effects of the external field $\vec{B}_0$, of chemical shifts of both nuclei, and of their coupling. However, the dipolar coupling in isotropic liquids is averaged to zero. It is therefore sufficient to write the total Hamiltonian as

---

[10]The general solution gives $R_1 = \frac{1}{2}\left(R_{a1} + R_{a2} + \sqrt{(R_{a1} - R_{a2})^2 + 4R_x^2}\right)$.

[11]Note that we mentioned the $|\alpha\rangle$ and $|\beta\rangle$ eigenstates as an example, $\vec{\mu}_2$ can be in reality in many superposition states.

[12]The interaction is described here for nuclei with positive γ_1 and γ_2, e.g. protons.

[13]Such changes have a similar effect as the *chemical or conformational exchange*, modifying the size of the chemical shift tensor (the chemical/conformational exchange was briefly discussed in Section 2.4). Therefore, $3b^2 J(\omega_{0,2})/4$ adds to R_0 like the exchange contribution.

$$\hat{H} = -\gamma_1 B_0(1+\delta_{i,1})\hat{I}_{1z} - \gamma_2 B_0(1+\delta_{i,2})\hat{I}_{2z} = -\gamma_1 B_0(1+\delta_{i,1})\frac{\hbar}{2}\begin{pmatrix} 1 & 0 & 0 & 0 \\ 0 & 1 & 0 & 0 \\ 0 & 0 & -1 & 0 \\ 0 & 0 & 0 & -1 \end{pmatrix} - \gamma_2 B_0(1+\delta_{i,2})\frac{\hbar}{2}\begin{pmatrix} 1 & 0 & 0 & 0 \\ 0 & -1 & 0 & 0 \\ 0 & 0 & 1 & 0 \\ 0 & 0 & 0 & -1 \end{pmatrix}$$

$$= \frac{B_0\hbar}{2}\begin{pmatrix} -\gamma_1(1+\delta_{i,1})-\gamma_2(1+\delta_{i,2}) & 0 & 0 & 0 \\ 0 & -\gamma_1(1+\delta_{i,1})+\gamma_2(1+\delta_{i,2}) & 0 & 0 \\ 0 & 0 & +\gamma_1(1+\delta_{i,1})-\gamma_2(1+\delta_{i,2}) & 0 \\ 0 & 0 & 0 & +\gamma_1(1+\delta_{i,1})+\gamma_2(1+\delta_{i,2}) \end{pmatrix}$$

$$= \begin{pmatrix} \mathcal{E}_{\alpha\alpha} & 0 & 0 & 0 \\ 0 & \mathcal{E}_{\alpha\beta} & 0 & 0 \\ 0 & 0 & \mathcal{E}_{\beta\alpha} & 0 \\ 0 & 0 & 0 & \mathcal{E}_{\beta\beta} \end{pmatrix}, \tag{8.181}$$

where the diagonal elements (eigenvalues) are the energies of the eigenstates of a single pair of magnetic moments.

As explained for the isolated nuclei, the off-diagonal elements of the equilibrium density matrix (coherences) are equal to zero. The four diagonal elements (populations) represent statistical weights in the relation describing the expected energy of the ensemble of pairs of coupled magnetic moments

$$\langle\mathcal{E}\rangle = P_{\alpha\alpha}\mathcal{E}_{\alpha\alpha} + P_{\alpha\beta}\mathcal{E}_{\alpha\beta} + P_{\beta\alpha}\mathcal{E}_{\beta\alpha} + P_{\beta\beta}\mathcal{E}_{\beta\beta}, \tag{8.182}$$

The values of the populations are obtained as described in Section 7.12.2:

$$P_{\alpha\alpha}^{\text{eq}} = \frac{e^{-\mathcal{E}_{\alpha\alpha}/k_{\mathrm{B}}T}}{e^{-\mathcal{E}_{\alpha\alpha}/k_{\mathrm{B}}T} + e^{-\mathcal{E}_{\alpha\beta}/k_{\mathrm{B}}T} + e^{-\mathcal{E}_{\beta\alpha}/k_{\mathrm{B}}T} + e^{-\mathcal{E}_{\beta\beta}/k_{\mathrm{B}}T}} \approx \frac{1-\frac{\mathcal{E}_{\alpha\alpha}}{k_{\mathrm{B}}T}}{4}, \tag{8.183}$$

$$P_{\alpha\beta}^{\text{eq}} = \frac{e^{-\mathcal{E}_{\alpha\beta}/k_{\mathrm{B}}T}}{e^{-\mathcal{E}_{\alpha\alpha}/k_{\mathrm{B}}T} + e^{-\mathcal{E}_{\alpha\beta}/k_{\mathrm{B}}T} + e^{-\mathcal{E}_{\beta\alpha}/k_{\mathrm{B}}T} + e^{-\mathcal{E}_{\beta\beta}/k_{\mathrm{B}}T}} \approx \frac{1-\frac{\mathcal{E}_{\alpha\beta}}{k_{\mathrm{B}}T}}{4}, \tag{8.184}$$

$$P_{\beta\alpha}^{\text{eq}} = \frac{e^{-\mathcal{E}_{\beta\alpha}/k_{\mathrm{B}}T}}{e^{-\mathcal{E}_{\alpha\alpha}/k_{\mathrm{B}}T} + e^{-\mathcal{E}_{\alpha\beta}/k_{\mathrm{B}}T} + e^{-\mathcal{E}_{\beta\alpha}/k_{\mathrm{B}}T} + e^{-\mathcal{E}_{\beta\beta}/k_{\mathrm{B}}T}} \approx \frac{1-\frac{\mathcal{E}_{\beta\alpha}}{k_{\mathrm{B}}T}}{4}, \tag{8.185}$$

$$P_{\beta\beta}^{\text{eq}} = \frac{e^{-\mathcal{E}_{\beta\beta}/k_{\mathrm{B}}T}}{e^{-\mathcal{E}_{\alpha\alpha}/k_{\mathrm{B}}T} + e^{-\mathcal{E}_{\alpha\beta}/k_{\mathrm{B}}T} + e^{-\mathcal{E}_{\beta\alpha}/k_{\mathrm{B}}T} + e^{-\mathcal{E}_{\beta\beta}/k_{\mathrm{B}}T}} \approx \frac{1-\frac{\mathcal{E}_{\beta\beta}}{k_{\mathrm{B}}T}}{4}, \tag{8.186}$$

and neglecting the small contributions of chemical shifts ($\delta_{i,n} \ll 1$)

$$P_{\alpha\alpha}^{\text{eq}} \approx \frac{1-\frac{\mathcal{E}_{\alpha\alpha}}{k_{\mathrm{B}}T}}{4} = \frac{1}{4} + \gamma_1(1+\delta_{i,1})\frac{B_0\hbar}{8k_{\mathrm{B}}T} + \gamma_2(1+\delta_{i,2})\frac{B_0\hbar}{8k_{\mathrm{B}}T} \approx \frac{1}{4} + \gamma_1\frac{B_0\hbar}{8k_{\mathrm{B}}T} + \gamma_2\frac{B_0\hbar}{8k_{\mathrm{B}}T}, \tag{8.187}$$

$$P_{\alpha\beta}^{\text{eq}} \approx \frac{1-\frac{\mathcal{E}_{\alpha\beta}}{k_{\mathrm{B}}T}}{4} = \frac{1}{4} + \gamma_1(1+\delta_{i,1})\frac{B_0\hbar}{8k_{\mathrm{B}}T} - \gamma_2(1+\delta_{i,2})\frac{B_0\hbar}{8k_{\mathrm{B}}T} \approx \frac{1}{4} + \gamma_1\frac{B_0\hbar}{8k_{\mathrm{B}}T} - \gamma_2\frac{B_0\hbar}{8k_{\mathrm{B}}T}, \tag{8.188}$$

$$P_{\beta\alpha}^{\text{eq}} \approx \frac{1-\frac{\mathcal{E}_{\beta\alpha}}{k_{\mathrm{B}}T}}{4} = \frac{1}{4} - \gamma_1(1+\delta_{i,1})\frac{B_0\hbar}{8k_{\mathrm{B}}T} + \gamma_2(1+\delta_{i,2})\frac{B_0\hbar}{8k_{\mathrm{B}}T} \approx \frac{1}{4} - \gamma_1\frac{B_0\hbar}{8k_{\mathrm{B}}T} + \gamma_2\frac{B_0\hbar}{8k_{\mathrm{B}}T}, \tag{8.189}$$

$$P_{\beta\beta}^{\text{eq}} \approx \frac{1-\frac{\mathcal{E}_{\beta\beta}}{k_{\mathrm{B}}T}}{4} = \frac{1}{4} - \gamma_1(1+\delta_{i,1})\frac{B_0\hbar}{8k_{\mathrm{B}}T} - \gamma_2(1+\delta_{i,2})\frac{B_0\hbar}{8k_{\mathrm{B}}T} \approx \frac{1}{4} - \gamma_1\frac{B_0\hbar}{8k_{\mathrm{B}}T} - \gamma_2\frac{B_0\hbar}{8k_{\mathrm{B}}T}. \tag{8.190}$$

$$\tag{8.191}$$

Figure 8.2: Illustration how random molecular motions resonating with five characteristic frequencies affect $\vec{\mu}_1 = \vec{\mu}_C$ in the CH bond in a 500 MHz spectrometer ($\vec{B}_0 = 11.75$ T). The first diagram in each row shows positions of the nuclei (^{13}C in green, ^{1}H in cyan), the second diagram shows orientation of the coordinate frame, the following diagrams are snapshots of the orientations of magnetic moments shown as arrows (^{13}C in green, ^{1}H in cyan) in a magnetic field of the neighbour (shown as force lines). The red arrow indicates the direction of the change of the orientation of the influenced magnetic moment, but the actual change is very small (not observable in the pictures) in the short depicted period of 4 ns. The molecule is assumed to rotate with a constant frequency for 4 ns. A, $\vec{\mu}_C$ oriented horizontally, $\vec{\mu}_2 = \vec{\mu}_H$ oriented vertically, ^{13}C in the yz plane, ^{1}H in the center of the coordinate system. Rotation at any frequency about a horizontal axis varies precession frequency of $\vec{\mu}_C$ about $\vec{B}_0$ and results in the loss of coherence of ^{13}C. B, $\vec{\mu}_H$ oriented horizontally, $\vec{\mu}_C$ oriented vertically, ^{1}H above the xy plane, ^{13}C in the center of the coordinate system. Rotation at ω_H about a horizontal axis pulls $\vec{\mu}_H$ up (red arrow pointing up in the given coordinate frame) in the magnetic fields of $\vec{\mu}_C$. This reorientation of $\vec{\mu}_H$ (observed only at time much longer than the depicted period of 4 ns) influences the effect of the J-coupling. C, $\vec{\mu}_C$ oriented horizontally, $\vec{\mu}_H$ oriented vertically, ^{13}C above the xy plane, ^{1}H in the center of the coordinate system. Rotation at ω_C about a horizontal axis pulls $\vec{\mu}_C$ up (red arrow pointing up in the given coordinate frame) in the magnetic fields of $\vec{\mu}_H$. D, $\vec{\mu}_C$ oriented horizontally, $\vec{\mu}_H$ oriented horizontally, ^{13}C close to the z axis, ^{1}H in the center of the coordinate system. Rotation at $\omega_H + \omega_C$ about a vertical axis pulls $\vec{\mu}_C$ up (red arrow pointing up in the given coordinate frame) in the magnetic fields of $\vec{\mu}_H$. E, $\vec{\mu}_C$ oriented horizontally, $\vec{\mu}_H$ oriented horizontally, ^{13}C in the yz plane, ^{1}H in the center of the coordinate system. Rotation at $\omega_H - \omega_C$ about a horizontal axis pulls μ_C up (red arrow pointing mostly up in the given coordinate frame) in the magnetic fields of μ_H. The reorientation of μ_C in Panels C–E (observed only at time much longer than the depicted period of 4 ns) contributes to the return of the distribution of the ^{13}C magnetic moments to the thermal equilibrium.

Lecture 9
Two-dimensional spectroscopy, NOESY

Literature: A very nice explanation of the principles of two-dimensional spectroscopy can be found in K8.1–K8.2. The States-Haberkorn-Ruben method and other approaches to frequency discrimination are explained in K8.12, L5.9.4, and C4.3.4. The idea of 2D spectroscopy, but for a different type of experiment (COSY) is also presented in C4.1, L5.6 and L5.9.

9.1   Two-dimensional spectroscopy

NMR spectroscopy based on the application of short radio-wave pulses gives us an opportunity to display frequencies of multiple magnetic moments in multiple dimensions of a single multidimensional spectrum. The great advantage of this approach is the possibility to immediately see various *correlations* among the observed nuclear magnetic moments and use this information in the structural analysis of the studied molecule. When working with large molecules (proteins, nucleic acids), spectra with three and more frequency dimensions are recorded routinely. In our course, we analyze only two-dimensional experiments, but we try to understand in detail how various correlations of interacting magnetic moments are encoded in the spectra. Before we reach this point, we have to learn the basic principle.

In order to explain principles of 2D spectroscopy, we first analyze an experiment consisting of three 90° pulses and two delays preceding the data acquisition. Later we learn that this experiment is abbreviated NOESY and serves as a source of information about interatomic distances, but now we use it just as a simple example. The application of three radio-wave pulse is already an advanced experimental approach, deserving a clear formal presentation. The experiment can be described as

$$_{\mathrm{a}}(\pi/2)_{x\mathrm{b}} - t_1 -_{\mathrm{c}} (\pi/2)_{x\mathrm{d}} - \tau_{\mathrm{m}} -_{\mathrm{e}} (\pi/2)_{x\mathrm{f}} - t_2(\mathrm{acquire}).$$

However, a pictorial representation shown in Figure 9.1 is more usual and practical.

In the drawing presented in Figure 9.1, each application of radio waves is represented by a black rectangle. In our experiments, all rectangles have the same width because all pulses have the same duration. Later we discuss experiments that combine 90° and 180°. In schemes of such experiments, 90° and 180° pulses are represented by narrow and wide rectangles, respectively. Durations of the delays between the pulses are described by time variables t_1 and τ_{m}, the time-dependence of the acquired signal is labeled t_2. In our analysis, we describe the density matrix just before and after the pulses, as indicated by red letters "a" to "f" in Figure 9.1.
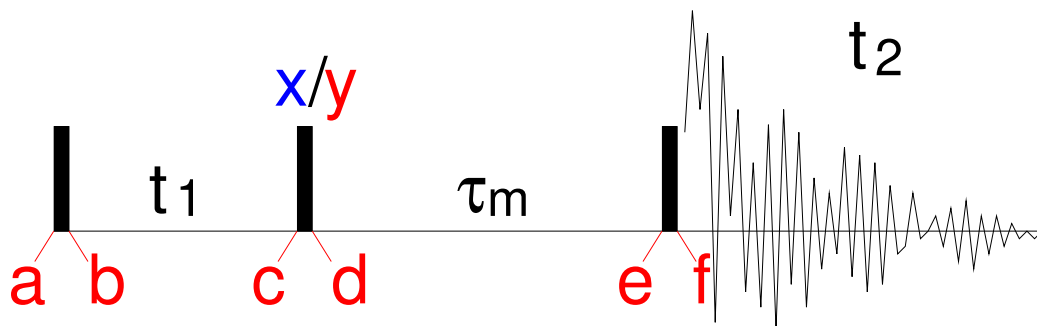
Figure 9.1: Schematic drawing of a two-dimensional NMR experiment. The symbols are explain in the text.

9.2 Evolution in the absence of dipolar coupling

We start with an analysis for two non-interacting magnetic moments, e.g. of two protons that have different chemical shift $\delta_{i,1}$ and $\delta_{i,2}$, and are far from each other in a molecule.[1] The pair of protons is an example of a homonuclear system, where all nuclei have the same magnetogyric ratio γ. Before we analyze evolution of the density matrix in a 2D experiment, we must define its initial form. Like in the case of the isolated nuclear magnetic moments, we assume that the experiments starts from thermal equilibrium. Therefore, we use $\hat{\rho}^{\mathrm{eq}}$, derived in Sections 8.8 and 8.9.8, as $\hat{\rho}(t = 0)$ If we neglect the very small effect of different chemical shifts in Eq. 8.39, the values of κ are also the same for both protons. As in the one-pulse experiment, we follow the coherent evolution of $\hat{\rho}$ step-by-step, and add the effect of relaxation *ad hoc*.

- $\hat{\rho}(a) = \frac{1}{2}\mathscr{I}_t + \frac{1}{2}\kappa(\mathscr{I}_{1z} + \mathscr{I}_{2z})$
  We start from the thermal equilibrium described by Eq. 8.39. Note that the matrices are different than for the single-spin mixed state, but the constant is the same. Moreover, only $\mathscr{I}_t, \mathscr{I}_{1z}, \mathscr{I}_{2z}$ contribute to $\hat{\rho}(a)$. If the magnetic moments do not interact, no $2\mathscr{I}_{1j}\mathscr{I}_{2k}$ operator (where $j, k \in x, y, z$) contributes to any Hamiltonian. As a consequence, the $\mathscr{I}_{1z}$ and $\mathscr{I}_{2z}$ components of the density matrix evolve separately, following the same rules as described for $\mathscr{I}_z$. Therefore, we can use Eq. 6.10 to analyze the evolution, we just repeat the analysis twice for $\mathscr{I}_{1z}$ and $\mathscr{I}_{2z}$, treating both as $\mathscr{I}_z$ in Eq. 6.10.

- $\hat{\rho}(b) = \frac{1}{2}\mathscr{I}_t + \frac{1}{2}\kappa(-\mathscr{I}_{1y} - \mathscr{I}_{2y})$
  Here we describe the effect of the 90° pulse. For a detailed analysis, see the one-pulse experiment.

- $\hat{\rho}(c) = \frac{1}{2}\mathscr{I}_t + \frac{1}{2}\kappa\left(-\cos(\Omega_1 t_1)\mathscr{I}_{1y} + \sin(\Omega_1 t_1)\mathscr{I}_{1x} - \cos(\Omega_2 t_1)\mathscr{I}_{2y} + \sin(\Omega_2 t_1)\mathscr{I}_{2x}\right)$
  Here we describe evolution during t_1 exactly as in the one-pulse experiment. To keep the equations short, we replace the trigonometric terms describing the evolution by (time-dependent) coefficients c_{11}, c_{21}, s_{11}, and s_{21}:
  $\hat{\rho}(c) = \frac{1}{2}\mathscr{I}_t + \frac{1}{2}\kappa\left(-c_{11}\mathscr{I}_{1y} + s_{11}\mathscr{I}_{1x} - c_{21}\mathscr{I}_{2y} + s_{21}\mathscr{I}_{2x}\right)$

---

[1]Protons in propynal (H–C≡C–CO–H) may serve as an example.

The coefficients c_{11}, c_{21}, s_{11}, and s_{21} deserve some attention. First, note that the first subscript specifies the nucleus and the second subscript specifies the time period (so-far, it is always 1 because we have analyzed only the evolution during t_1). Second, we include the effect of teh relaxation into the coefficients:

$c_{11} \rightarrow \mathrm{e}^{-R_{2,1}t_1} \cos(\Omega_1 t_1)$ $s_{11} \rightarrow \mathrm{e}^{-R_{2,1}t_1} \sin(\Omega_1 t_1)$
$c_{21} \rightarrow \mathrm{e}^{-R_{2,2}t_1} \cos(\Omega_2 t_1)$ $s_{21} \rightarrow \mathrm{e}^{-R_{2,2}t_1} \sin(\Omega_2 t_1)$

- $\hat{\rho}(\mathrm{d}) = \frac{1}{2}\mathscr{I}_t + \frac{1}{2}\kappa\left(-c_{11}\mathscr{I}_{1z} + s_{11}\mathscr{I}_{1x} - c_{21}\mathscr{I}_{2z} + s_{21}\mathscr{I}_{2x}\right)$
  Here we analyze the effect of the second 90° pulse, similarly to the step a $\rightarrow$ b. The x-pulse does not affect the x magnetization, but rotates the $-y$ magnetization further to $-z$. The final magnetization is parallel with $\vec{B}_0$, but the equilibrium polarization is inverted.

- $\hat{\rho}(\mathrm{e}) = ?$
  This is a new case, it should be analyzed carefully. Here we perform the analysis for a large molecule such as a small protein: In proteins, M_x, M_y relax with $R_2 > 10\,\mathrm{s}^{-1}$ and M_z with $R_1 \approx 1\,\mathrm{s}^{-1}$. The delay τ_{m} is usually longer than 0.1 s. Let us assume $\tau_{\mathrm{m}} = 0.2\,\mathrm{s}$ and $R_2 = 20\,\mathrm{s}^{-1}$. After 0.2 s, $\mathrm{e}^{-R_2\tau_{\mathrm{m}}} = \mathrm{e}^{-20\times0.2} = \mathrm{e}^{-4} \approx 0.02$. We see that M_x, M_y relaxes almost completely. Therefore, $\mathscr{I}_{1x}, \mathscr{I}_{1y}, \mathscr{I}_{2x}, \mathscr{I}_{2y}$ can be neglected. On the other hand, $\mathrm{e}^{-R_1\tau_{\mathrm{m}}} = \mathrm{e}^{-1\times0.2} = \mathrm{e}^{-0.2} \approx 0.82$. We see that M_z does not relax too much. Therefore, we continue the analysis with $\mathscr{I}_{1z}, \mathscr{I}_{2z}$. The $\mathscr{I}_{1z}, \mathscr{I}_{2z}$ terms do not evolve because they commute with $\mathscr{H} = \Omega_1\mathscr{I}_{1z} + \Omega_2\mathscr{I}_{2z}$. Consequently,
  $\hat{\rho}(\mathrm{e}) = \frac{1}{2}\mathscr{I}_t + \frac{1}{2}\kappa\left(-\mathrm{e}^{-R_{1,1}\tau_{\mathrm{m}}}c_{11}\mathscr{I}_{1z} - \mathrm{e}^{-R_{1,2}\tau_{\mathrm{m}}}c_{21}\mathscr{I}_{2z}\right) = \frac{1}{2}\mathscr{I}_t - \mathcal{A}_1\mathscr{I}_{1z} - \mathcal{A}_2\mathscr{I}_{2z}$.
  We further simplified the notation by introducing the factors $\mathcal{A}_1$ and $\mathcal{A}_2$. Again, we include the relaxation effects into $\mathcal{A}_1$ and $\mathcal{A}_2$ when we express the measurable signal:
  $\mathcal{A}_1 \rightarrow \frac{\kappa}{2}\mathrm{e}^{-R_{1,1}\tau_{\mathrm{m}}}c_{11} = \frac{\kappa}{2}\mathrm{e}^{-R_{1,1}\tau_{\mathrm{m}}}\mathrm{e}^{-R_{2,1}t_1}\cos(\Omega_1 t_1)$
  $\mathcal{A}_2 \rightarrow \frac{\kappa}{2}\mathrm{e}^{-R_{1,2}\tau_{\mathrm{m}}}c_{21} = \frac{\kappa}{2}\mathrm{e}^{-R_{1,2}\tau_{\mathrm{m}}}\mathrm{e}^{-R_{2,2}t_1}\cos(\Omega_2 t_1)$

- $\hat{\rho}(\mathrm{f}) = \frac{1}{2}\mathscr{I}_t + \mathcal{A}_1\mathscr{I}_{1y} + \mathcal{A}_2\mathscr{I}_{2y}$
  Here we analyze the effect of the third pulse, in the same manner as we analyzed the first pulse.

- $\hat{\rho}(t_2) = \frac{1}{2}\mathscr{I}_t + \mathcal{A}_1(\cos(\Omega_1 t_2)\mathscr{I}_{1y} - \sin(\Omega_1 t_2)\mathscr{I}_{1x}) + \mathcal{A}_2(\cos(\Omega_2 t_2)\mathscr{I}_{2y} - \sin(\Omega_2 t_2)\mathscr{I}_{2x})$
  In the last step, we analyze the evolution during the data acquisition.

9.3 Signal modulation in a two-dimensional experiment

Having $\hat{\rho}(t_2)$, we can calculate $\langle M_+ \rangle$. As the size of the matrices increased, it is more convenient to use the orthonormality of the basis than to calculate all matrix products. It follows from the definition of orthonormal matrices (see footnote 1 in Section 6.1) that for the two-spin matrices

$$\mathrm{Tr}\left\{\mathscr{I}_{nx}(\mathscr{I}_{nx} + \mathrm{i}\mathscr{I}_{ny})\right\} = 1, \tag{9.1}$$

$$\mathrm{Tr}\left\{\mathscr{I}_{ny}(\mathscr{I}_{nx} + \mathrm{i}\mathscr{I}_{ny})\right\} = \mathrm{i}, \tag{9.2}$$

and traces of products with other matrices are zero. Applying the orthonormality relations to the product of $\hat{M}_+$ with the obtained $\hat{\rho}(t_2)$ and introducing the relaxation, we get

$$
\begin{aligned}
\langle M_+ \rangle &= \mathrm{Tr}\{\hat{\rho}(t_2)\hat{M}_+\} \\
&= \mathcal{N}\gamma\hbar\left(\mathcal{A}_1(\mathrm{e}^{-R_{2,1}t_2}\cos(\Omega_1 t_2)\mathrm{Tr}\left\{\mathscr{I}_{1y}(\mathscr{I}_{1+}+\mathscr{I}_{2+})\right\}-\mathrm{e}^{-R_{2,1}t_2}\sin(\Omega_1 t_2)\mathrm{Tr}\left\{\mathscr{I}_{1x}(\mathscr{I}_{1+}+\mathscr{I}_{2+})\right\}\right) \\
&\quad +\mathcal{A}_2(\mathrm{e}^{-R_{2,2}t_2}\cos(\Omega_2 t_2)\mathrm{Tr}\left\{\mathscr{I}_{2y}(\mathscr{I}_{1+}+\mathscr{I}_{2+})\right\}-\mathrm{e}^{-R_{2,2}t_2}\sin(\Omega_2 t_2)\mathrm{Tr}\left\{\mathscr{I}_{2x}(\mathscr{I}_{1+}+\mathscr{I}_{2+})\right\})) \\
&= \mathcal{N}\gamma\hbar\mathcal{A}_1\left(\mathrm{i}\mathrm{e}^{-R_{2,1}t_2}\cos(\Omega_1 t_2)-\mathrm{e}^{-R_{2,1}t_2}\sin(\Omega_1 t_2)\right) \\
&\quad + \mathcal{N}\gamma\hbar\mathcal{A}_2\left(\mathrm{i}\mathrm{e}^{-R_{2,2}t_2}\cos(\Omega_2 t_2)-\mathrm{e}^{-R_{2,2}t_2}\sin(\Omega_2 t_2)\right).
\end{aligned}
\tag{9.3}
$$

Note that the resulting phase is shifted by $\pi/2$ similarly to Eq. 7.27, but in the opposite direction. After applying the phase correction, the Fourier transformation of the signal provides spectrum in the form (cf. Eq. 7.32)

$$
\overbrace{\mathcal{N}\gamma\hbar\left(\underbrace{\frac{\mathcal{A}_1 R_{2,1}}{R_{2,1}^2+(\omega-\Omega_1)^2}+\frac{\mathcal{A}_2 R_{2,2}}{R_{2,2}^2+(\omega-\Omega_2)^2}}_{\Re\{Y(\omega)\}}\right)}-\mathrm{i}\mathcal{N}\gamma\hbar\left(\underbrace{\frac{\mathcal{A}_1(\omega-\Omega_1)}{R_{2,1}^2+(\omega-\Omega_1)^2}+\frac{\mathcal{A}_2(\omega-\Omega_2)}{R_{2,2}^2+(\omega-\Omega_2)^2}}_{\Im\{Y(\omega)\}}\right).
\tag{9.4}
$$
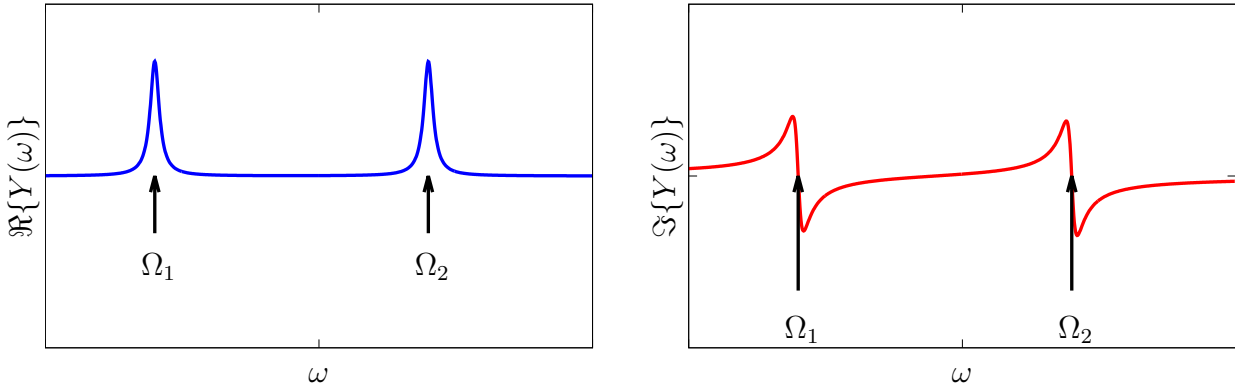
In the one-dimensional experiment, $\mathcal{A}_1$ and $\mathcal{A}_2$ just scale the peak height. However, they depend on the length of the delay t_1 in our two-dimensional experiment. If the measurement is repeated many times and t_1 is increased by an increment Δt each time, the obtained series of 1D spectra is *amplitude modulated* by $c_{11}=\mathrm{e}^{-R_{2,1}t_2}\cos(\Omega_1 t_1)$ and $c_{21}=\mathrm{e}^{-R_{2,2}t_2}\cos(\Omega_2 t_1)$. Since the data are stored in a computer in a digital form, they can be treated as a two-dimensional array (table), depending on the real time t_2 in one direction and on the length of the incremented delay t_1 in the other directions. These directions are referred to as the *direct dimension* and the *indirect dimension*. The Fourier transformation can be performed in each dimension providing the *direct frequency dimension* and the *indirect frequency dimension*.

Since we acquire the signal as a series of complex numbers, it is useful to introduce the complex numbers in the indirect dimension as well. The advantage of such spectrum is that the positive and negative values of the frequency offset can be distinguished in both dimensions. Several protocols
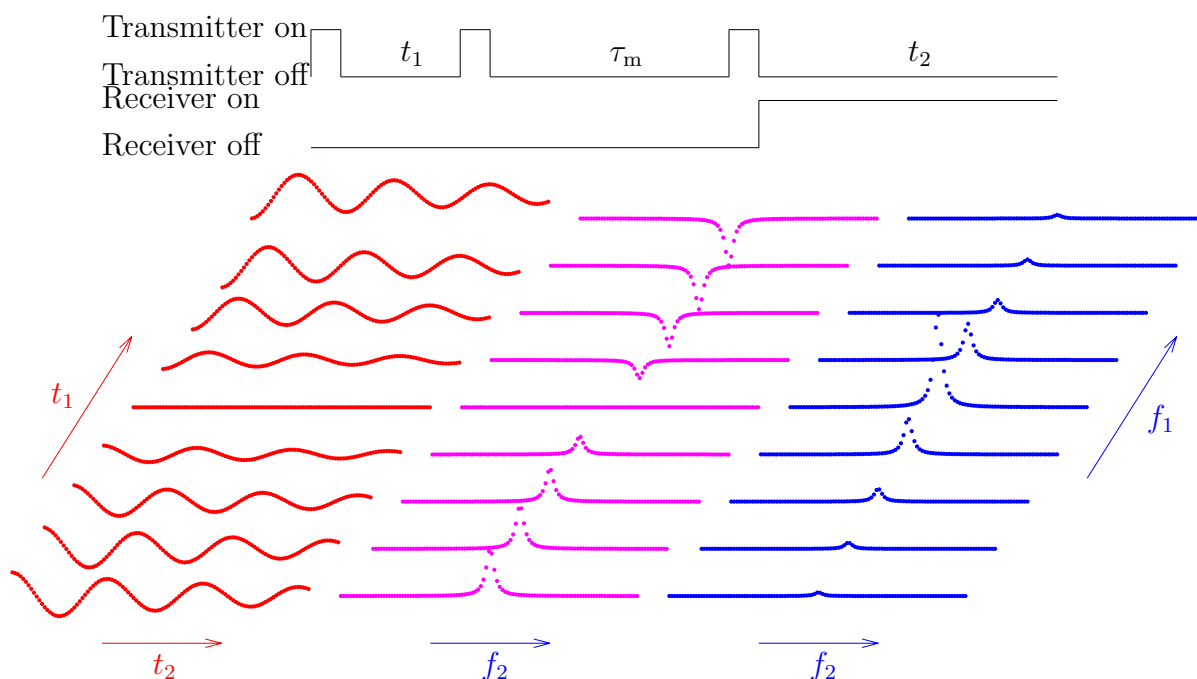
Figure 9.2: Principle of two-dimensional spectroscopy (experiment NOESY). The acquired signal is shown in red, the signal after the Fourier transformation in the direct dimension is shown in magenta, and the signal after the Fourier transformation in both dimensions is shown in blue.

that discriminate the positive and negative frequency offsets in the indirect dimension are routinely used. The frequency discrimination approaches are based on shifting phases of certain radio-wave pulses. The method introduced by States, Haberkorn, and Ruben is described in Section 9.5.1. It should be mentioned that phases are also changed in another manner, called *phase cycling*, in NMR experiments. We discuss phase cycling later and describe recording two-dimensional signal arrays in its full complexity in Section 11.7.

9.4 NOESY

If the two-dimensional spectra looked exactly as described in the preceding section, they would not be very useful because they would not bring any new information. The same frequencies would be measured in the direct and indirect dimension and all peaks would be found along the diagonal of the spectrum. What makes the experiment really useful is the interaction between the magnetic moments during τ_m. Such approach is known as the nuclear Overhauser effect spectroscopy (NOESY) and is used frequently to measure distances between protons in molecules.

As described by Eq. 8.33, the relaxation of nucleus 1 is influenced by the state of nucleus 2 (and vice versa):

$$-\frac{\mathrm{d}\Delta\langle M_{1z}\rangle}{\mathrm{d}t} = R_{\mathrm{a}1}\Delta\langle M_{1z}\rangle + R_{\mathrm{x}}\Delta\langle M_{2z}\rangle \tag{9.5}$$

$$-\frac{\mathrm{d}\Delta\langle M_{2z}\rangle}{\mathrm{d}t} = R_{\mathrm{a}2}\Delta\langle M_{2z}\rangle + R_{\mathrm{x}}\Delta\langle M_{1z}\rangle. \tag{9.6}$$

This set of equations is solved and the solution is analyzed in Section 9.5.2. The analysis shows that the amplitudes $\mathcal{A}_1$ and $\mathcal{A}_2$ depend on *both frequencies* Ω_1 and Ω_2 (contain both c_{11} and c_{21}). Therefore, the spectrum contains both diagonal peaks (with the frequencies of the given magnetic moment in both dimensions) and off-diagonal *cross-peaks* (with the frequencies of the given magnetic moment in the direct dimension and the frequency of its interaction partner in the indirect dimension).

The presence of the cross-peaks provides very useful *qualitative information* about the studied molecules. It tells us which nuclei are close in space. Such knowledge of spatial proximity often allows us to assign measured frequencies to the hydrogen atoms in the studied molecule. But we often go further and analyze the intensities of the cross-peaks *quantitatively*. As shown in Section 9.5.3, the height of the NOESY cross-peaks $Y_{\max}$ depends on two factors: on the dynamics of the molecule and on the distance of the interacting nuclei. Depending on the motions on the molecules, the peak height can be positive or negative. If the molecular motions are slow, the cross-peaks have the same sign as diagonal peaks. However, if the molecular motions are fast (e.g., if the molecule is small), the sign is opposite. Obviously, there is a range of molecular motions that make the peak height close to zero. In such case, other NMR techniques than NOESY should be applied. If the dynamics of the molecule is favorable (sufficiently fast or slow), the dependence on the distance between the interacting nuclei can be used to estimate distances in the molecule. For short τ_{m}, the cross-peak height is approximately proportional to r^{-6}. The studied molecules (especially large molecules like proteins or nucleic acid fragments) often contain pairs of protons with a well-defined geometry. For example, the distance between geminal protons in the CH_2 group is $0.17\,\mathrm{nm}$, distances between protons in the *ortho-* and *meta-* positions in aromatic rings are $0.25\,\mathrm{nm}$ and $0.42\,\mathrm{nm}$, respectively. Such distances can be used as a reference for the measurement of unknown distances. If we assume that two protons have similar dynamics as a reference pair of protons, the ratio of the heights[2] of the cross-peaks of the investigated and reference proton pairs is

$$\frac{Y_{\max}}{Y_{\max,\mathrm{ref}}} = \left(\frac{r_{\mathrm{ref}}}{r}\right)^6. \tag{9.7}$$

Therefore, the unknown distance r can be calculated as

$$r = r_{\mathrm{ref}}\ \sqrt[6]{\frac{Y_{\max,\mathrm{ref}}}{Y_{\max}}}. \tag{9.8}$$

It is quite remarkable that the dipole-dipole interaction allows us to measure distances nine orders of magnitude shorter than the wavelength of the used electromagnetic waves.

---

[2]Volume (integral) of the peak gives more accurate distances because it is not influenced by the relaxation during measurement. On the other hand, measurement of peak volumes may be difficult in crowded spectra of large molecules.

HOMEWORK

Analyze the intensities of the NOESY cross-peaks (Sections 9.4, 9.5.2, and 9.5.3, using Eqs. 8.33–8.34 from Section 8.7.)

9.5 SUPPORTING INFORMATION

9.5.1 States-Haberkorn-Ruben method of processing hypercomplex data

It is possible to introduce the complex numbers in the indirect dimension by repeating the measurement twice for each value of t_1, each time with a different phase of the radio waves applied during the second pulse. We describe the procedure for a pair of non-interacting spin-1/2 nuclei. First we acquire the signal with the second pulse applied with the same phase as the first pulse. Such a phase is labeled x in the NMR literature. Then, we repeat the acquisition with the phase of the radio waves shifted by $90°$ during the second pulse. Such a phase is labeled y in the literature. The former case was analyzed in Section 9.2. In the latter case, the $\mathscr{I}_{1y}$ and $\mathscr{I}_{2y}$ components are not affected and relax during τ_m, while the $\mathscr{I}_{1x}$ and $\mathscr{I}_{2x}$ are rotated to $-\mathscr{I}_{1z}$ and $-\mathscr{I}_{2z}$, respectively, and converted to the measurable signal by the third pulse. Because the $\mathscr{I}_{1x}$ and $\mathscr{I}_{2x}$ coherences are modulated by s_{11} and s_{21}, the amplitudes (labeled here $\mathcal{B}_1$ and $\mathcal{B}_2$) oscillate as a sine function, in the even spectra (unlike the amplitudes $\mathcal{A}_1, \mathcal{A}_2$ of the odd spectra, oscillating as a cosine function). So, we obtain cosine amplitude modulation in odd spectra and sine amplitude modulation in even spectra:

$\mathcal{B}_1 \to \frac{\kappa}{2} e^{-R_{1,1}\tau_m} s_{11} = \frac{\kappa}{2} e^{-R_{1,1}\tau_m} e^{-R_{2,1}t_1} \sin(\Omega_1 t_1)$

$\mathcal{B}_2 \to \frac{\kappa}{2} e^{-R_{1,2}\tau_m} s_{21} = \frac{\kappa}{2} e^{-R_{1,2}\tau_m} e^{-R_{2,2}t_1} \sin(\Omega_2 t_1)$.

Processing of the complete data starts by complex Fourier transformation in the direct (t_2) dimension providing two sets of 1D spectra, cosine amplitude-modulated in t_1

$$\overbrace{\mathcal{N}\gamma\hbar\left(\frac{\mathcal{A}_1 R_{2,1}}{R_{2,1}^2 + (\omega_2 - \Omega_1)^2} + \frac{\mathcal{A}_2 R_{2,2}}{R_{2,2}^2 + (\omega_2 - \Omega_2)^2}\right)}^{\Re\{y_1(t_1)\}\Re\{Y_2(\omega_2)\}} - \overbrace{\mathrm{i}\mathcal{N}\gamma\hbar\left(\frac{\mathcal{A}_1(\omega_2 - \Omega_1)}{R_{2,1}^2 + (\omega_2 - \Omega_1)^2} + \frac{\mathcal{A}_2(\omega_2 - \Omega_2)}{R_{2,2}^2 + (\omega_2 - \Omega_2)^2}\right)}^{\Re\{y_1(t_1)\}\Im\{Y_2(\omega_2)\}} \tag{9.9}$$

and sine amplitude-modulated in t_1

$$\overbrace{\mathcal{N}\gamma\hbar\left(\frac{\mathcal{B}_1 R_{2,1}}{R_{2,1}^2 + (\omega_2 - \Omega_1)^2} + \frac{\mathcal{B}_2 R_{2,2}}{R_{2,2}^2 + (\omega_2 - \Omega_2)^2}\right)}^{\Im\{y_1(t_1)\}\Re\{Y_2(\omega_2)\}} - \overbrace{\mathrm{i}\mathcal{N}\gamma\hbar\left(\frac{\mathcal{B}_1(\omega_2 - \Omega_1)}{R_{2,1}^2 + (\omega_2 - \Omega_1)^2} + \frac{\mathcal{B}_2(\omega_2 - \Omega_2)}{R_{2,2}^2 + (\omega_2 - \Omega_2)^2}\right)}^{\Im\{y_1(t_1)\}\Im\{Y_2(\omega_2)\}}. \tag{9.10}$$

The cosine amplitude-modulated and sine amplitude-modulated *real components* of the obtained 1D spectra, respectively, are then treated as the real and imaginary component of the complex signal in the indirect dimension.

$$\overbrace{\mathcal{N}\gamma\hbar\left(\frac{\mathcal{A}_1 R_{2,1}}{R_{2,1}^2 + (\omega_2 - \Omega_1)^2} + \frac{\mathcal{A}_2 R_{2,2}}{R_{2,2}^2 + (\omega_2 - \Omega_2)^2}\right)}^{\Re\{y_1(t_1)\}\Re\{Y_2(\omega_2)\}} + \overbrace{\mathrm{i}\mathcal{N}\gamma\hbar\left(\frac{\mathcal{B}_1 R_{2,1}}{R_{2,1}^2 + (\omega_2 - \Omega_1)^2} + \frac{\mathcal{B}_2 R_{2,2}}{R_{2,2}^2 + (\omega_2 - \Omega_2)^2}\right)}^{\Im\{y_1(t_1)\}\Re\{Y_2(\omega_2)\}} \tag{9.11}$$

$$= \mathcal{N}\gamma\hbar\left(\frac{(\mathcal{A}_1 + \mathrm{i}\mathcal{B}_1)R_{2,1}}{R_{2,1}^2 + (\omega_2 - \Omega_1)^2} + \frac{(\mathcal{A}_2 + \mathrm{i}\mathcal{B}_2)R_{2,2}}{R_{2,2}^2 + (\omega_2 - \Omega_2)^2}\right) \tag{9.12}$$

$$= \frac{\mathcal{N}\gamma^2\hbar^2 B_0}{4k_B T}\left(e^{-R_{1,1}\tau_m} e^{-R_{2,1}t_1}\cos(\Omega_1 t_1)\frac{R_{2,1}}{R_{2,1}^2 + (\omega_2 - \Omega_1)^2} + e^{-R_{1,2}\tau_m} e^{-R_{2,2}t_1}\cos(\Omega_2 t_1)\frac{R_{2,2}}{R_{2,2}^2 + (\omega_2 - \Omega_2)^2}\right)$$
$$+ \mathrm{i}\,\frac{\mathcal{N}\gamma^2\hbar^2 B_0}{4k_B T}\left(e^{-R_{1,1}\tau_m} e^{-R_{2,1}t_1}\sin(\Omega_1 t_1)\frac{R_{2,1}}{R_{2,1}^2 + (\omega_2 - \Omega_1)^2} + e^{-R_{1,2}\tau_m} e^{-R_{2,2}t_1}\sin(\Omega_2 t_1)\frac{R_{2,2}}{R_{2,2}^2 + (\omega_2 - \Omega_2)^2}\right) \tag{9.13}$$

$$= \frac{\mathcal{N}\gamma^2\hbar^2 B_0}{4k_B T}\left(e^{-R_{1,1}\tau_m} e^{-R_{2,1}t_1}e^{\mathrm{i}\Omega_1 t_1}\frac{R_{2,1}}{R_{2,1}^2 + (\omega_2 - \Omega_1)^2} + e^{-R_{1,2}\tau_m} e^{-R_{2,2}t_1}e^{\mathrm{i}\Omega_2 t_1}\frac{R_{2,2}}{R_{2,2}^2 + (\omega_2 - \Omega_2)^2}\right) \tag{9.14}$$

The complex Fourier transformation in t_1 yields a spectrum

$$\frac{\mathcal{N}\gamma^2\hbar^2 B_0}{4k_B T}\left(e^{-R_{1,1}\tau_m}\frac{R_{2,1}}{R_{2,1}^2 + (\omega_1 - \Omega_1)^2}\cdot\frac{R_{2,1}}{R_{2,1}^2 + (\omega_2 - \Omega_1)^2} + e^{-R_{1,2}\tau_m}\frac{R_{2,2}}{R_{2,2}^2 + (\omega_1 - \Omega_2)^2}\cdot\frac{R_{2,2}}{R_{2,2}^2 + (\omega_2 - \Omega_2)^2}\right)$$
$$+ \mathrm{i}\,\frac{\mathcal{N}\gamma^2\hbar^2 B_0}{4k_B T}\left(e^{-R_{1,1}\tau_m}\frac{\omega_1 - \Omega_1}{R_{2,1}^2 + (\omega_1 - \Omega_1)^2}\cdot\frac{R_{2,1}}{R_{2,1}^2 + (\omega_2 - \Omega_1)^2} + e^{-R_{1,2}\tau_m}\frac{\omega_1 - \Omega_2}{R_{2,2}^2 + (\omega_1 - \Omega_2)^2}\cdot\frac{R_{2,2}}{R_{2,2}^2 + (\omega_2 - \Omega_2)^2}\right), \tag{9.15}$$

where the positive and negative values of the frequency offset are distinguished in both dimensions.

Schematically, the States-Haberkorn-Ruben method can be summarized as

$$y_1(t_1) \cdot y_2(t_2) = (\Re\{y_1(t_1)\} + \mathrm{i}\Im\{y_1(t_1)\}) \;\cdot\; (\Re\{y_2(t_2)\} + \mathrm{i}\Im\{y_2(t_2)\})$$

$$\downarrow \text{ Complex Fourier transformation in } t_2$$

$$(\Re\{y_1(t_1)\} + \mathrm{i}\Im\{y_1(t_1)\}) \;\cdot\; (\Re\{Y_2(\omega_2)\} + \mathrm{i}\Im\{Y_2(\omega_2)\})$$

$$\downarrow \text{ Discard imaginary component in } \omega_2$$

$$(\Re\{y_1(t_1)\} + \mathrm{i}\Im\{y_1(t_1)\}) \;\cdot\; \Re\{Y_2(\omega_2)\}$$

$$\downarrow \text{ Complex Fourier transformation in } t_1$$

$$(\Re\{Y_1(\omega_1)\} + \mathrm{i}\Im\{Y_1(\omega_1)\}) \;\cdot\; \Re\{Y_2(\omega_2)\} = \Re\{Y_1(\omega_1)\}\Re\{Y_2(\omega_2)\} + \mathrm{i}\,\Im\{Y_1(\omega_1)\}\Re\{Y_2(\omega_2)\} \tag{9.16}$$

Note that without separating the real component in ω_2 from the imaginary one prior to the second Fourier transformation a spectrum with a phase-twisted line-shape is obtained:

$$y_1(t_1) \cdot y_2(t_2) = (\Re\{y_1(t_1)\} + \mathrm{i}\Im\{y_1(t_1)\}) \;\cdot\; (\Re\{y_2(t_2)\} + \mathrm{i}\Im\{y_2(t_2)\})$$

$$\downarrow \text{ Complex Fourier transformation in } t_2$$

$$(\Re\{y_1(t_1)\} + \mathrm{i}\Im\{y_1(t_1)\}) \;\cdot\; (\Re\{Y_2(\omega_2)\} + \mathrm{i}\Im\{Y_2(\omega_2)\})$$

$$\downarrow \text{ Complex Fourier transformation in } t_1$$

$$(\Re\{Y_1(\omega_1)\} + \mathrm{i}\Im\{Y_1(\omega_1)\}) \;\cdot\; (\Re\{Y_2(\omega_2)\} + \mathrm{i}\Im\{Y_2(\omega_2)\})$$

$$= \underbrace{\Re\{Y_1(\omega_1)\}\Re\{Y_2(\omega_2)\} - \Im\{Y_1(\omega_1)\}\Im\{Y_2(\omega_2)\}}_{\text{real}} + \mathrm{i}\,\underbrace{(\Re\{Y_1(\omega_1)\}\Im\{Y_2(\omega_2)\} + \Im\{Y_1(\omega_1)\}\Re\{Y_2(\omega_2)\})}_{\text{imaginary}} \tag{9.17}$$

with the real part having the following form (for each peak)

$$\frac{\mathcal{N}\gamma^2\hbar^2 B_0}{4k_{\mathrm{B}}T}\mathrm{e}^{-R_{1,n}\tau_{\mathrm{m}}}\left(\frac{R_{2,n}}{R_{2,n}^2 + (\omega_1 - \Omega_n)^2} \cdot \frac{R_{2,n}}{R_{2,n}^2 + (\omega_2 - \Omega_n)^2} - \frac{\omega_1 - \Omega_n}{R_{2,n}^2 + (\omega_1 - \Omega_n)^2} \cdot \frac{\omega_2 - \Omega_n}{R_{2,n}^2 + (\omega_2 - \Omega_n)^2}\right), \tag{9.18}$$

which is *not* an absorption Lorentz function (due to the presence of the red term).

9.5.2 Quantitative analysis of cross-relaxation in NOESY

As described by Eqs. 8.33–8.34, relaxation of nucleus 1 is influenced by the state of nucleus 2 (and vice versa):

$$-\frac{\mathrm{d}\Delta\langle M_{1z}\rangle}{\mathrm{d}t} = R_{\mathrm{a}1}\Delta\langle M_{1z}\rangle + R_{\mathrm{x}}\Delta\langle M_{2z}\rangle \tag{9.19}$$

$$-\frac{\mathrm{d}\Delta\langle M_{2z}\rangle}{\mathrm{d}t} = R_{\mathrm{a}2}\Delta\langle M_{2z}\rangle + R_{\mathrm{x}}\Delta\langle M_{1z}\rangle. \tag{9.20}$$

The analysis greatly simplifies if the auto-relaxation rates are identical for both magnetic moments.[3] Then,

$$-\frac{\mathrm{d}\Delta\langle M_{1z}\rangle}{\mathrm{d}t} = R_{\mathrm{a}}\Delta\langle M_{1z}\rangle + R_{\mathrm{x}}\Delta\langle M_{2z}\rangle, \tag{9.21}$$

$$-\frac{\mathrm{d}\Delta\langle M_{2z}\rangle}{\mathrm{d}t} = R_{\mathrm{a}}\Delta\langle M_{2z}\rangle + R_{\mathrm{x}}\Delta\langle M_{1z}\rangle. \tag{9.22}$$

Such set of differential equations can be solved easily by adding and subtracting the equations

$$-\frac{\mathrm{d}(\Delta\langle M_{1z}\rangle + \Delta\langle M_{2z}\rangle)}{\mathrm{d}t} = (R_{\mathrm{a}} + R_{\mathrm{x}})(\Delta\langle M_{1z}\rangle + \Delta\langle M_{2z}\rangle) \quad \Rightarrow \quad (\Delta\langle M_{1z}\rangle + \Delta\langle M_{2z}\rangle) = (\Delta\langle M_{1z}\rangle(t_1) + \Delta\langle M_{2z}\rangle(t_1))\mathrm{e}^{-(R_{\mathrm{a}}+R_{\mathrm{x}})\tau_{\mathrm{m}}}, \tag{9.23}$$

$$-\frac{\mathrm{d}(\Delta\langle M_{1z}\rangle - \Delta\langle M_{2z}\rangle)}{\mathrm{d}t} = (R_{\mathrm{a}} - R_{\mathrm{x}})(\Delta\langle M_{1z}\rangle - \Delta\langle M_{2z}\rangle) \quad \Rightarrow \quad (\Delta\langle M_{1z}\rangle - \Delta\langle M_{2z}\rangle) = (\Delta\langle M_{1z}\rangle(t_1) - \Delta\langle M_{2z}\rangle(t_1))\mathrm{e}^{-(R_{\mathrm{a}}-R_{\mathrm{x}})\tau_{\mathrm{m}}}. \tag{9.24}$$

---

[3]This is a reasonable assumption for protons with similar dynamics and in similar chemical environment.

Returning back to $\Delta\langle M_{1z}\rangle$ and $\Delta\langle M_{2z}\rangle$,

$$\Delta\langle M_{1z}\rangle = \frac{(\Delta\langle M_{1z}\rangle + \Delta\langle M_{2z}\rangle) + (\Delta\langle M_{1z}\rangle - \Delta\langle M_{2z}\rangle)}{2} = \mathrm{e}^{-R_\mathrm{a}\tau_\mathrm{m}}\left(\Delta\langle M_{1z}\rangle(t_1)\frac{\mathrm{e}^{-R_\mathrm{x}\tau_\mathrm{m}} + \mathrm{e}^{+R_\mathrm{x}\tau_\mathrm{m}}}{2} + \Delta\langle M_{2z}\rangle(t_1)\frac{\mathrm{e}^{-R_\mathrm{x}\tau_\mathrm{m}} - \mathrm{e}^{+R_\mathrm{x}\tau_\mathrm{m}}}{2}\right),$$
(9.25)

$$\Delta\langle M_{2z}\rangle = \frac{(\Delta\langle M_{1z}\rangle + \Delta\langle M_{2z}\rangle) - (\Delta\langle M_{1z}\rangle - \Delta\langle M_{2z}\rangle)}{2} = \mathrm{e}^{-R_\mathrm{a}\tau_\mathrm{m}}\left(\Delta\langle M_{1z}\rangle(t_1)\frac{\mathrm{e}^{-R_\mathrm{x}\tau_\mathrm{m}} - \mathrm{e}^{+R_\mathrm{x}\tau_\mathrm{m}}}{2} + \Delta\langle M_{2z}\rangle(t_1)\frac{\mathrm{e}^{-R_\mathrm{x}\tau_\mathrm{m}} + \mathrm{e}^{+R_\mathrm{x}\tau_\mathrm{m}}}{2}\right).$$
(9.26)

Therefore, the amplitudes $\mathcal{A}_1$ and $\mathcal{A}_2$ in our two-dimensional experiment are

$$\mathcal{A}_1 = \frac{\kappa}{2}\mathrm{e}^{-R_2 t_1}\mathrm{e}^{-R_\mathrm{a}\tau_\mathrm{m}}\left(\cos(\underbrace{\Omega_1}_{\text{diag}} t_1)\frac{\mathrm{e}^{-R_\mathrm{x}\tau_\mathrm{m}} + \mathrm{e}^{+R_\mathrm{x}\tau_\mathrm{m}}}{2} + \cos(\underbrace{\Omega_2}_{\text{cross}} t_1)\frac{\mathrm{e}^{-R_\mathrm{x}\tau_\mathrm{m}} - \mathrm{e}^{+R_\mathrm{x}\tau_\mathrm{m}}}{2}\right),$$
(9.27)

$$\mathcal{A}_1 = \frac{\kappa}{2}\mathrm{e}^{-R_2 t_1}\mathrm{e}^{-R_\mathrm{a}\tau_\mathrm{m}}\left(\cos(\underbrace{\Omega_1}_{\text{cross}} t_1)\frac{\mathrm{e}^{-R_\mathrm{x}\tau_\mathrm{m}} - \mathrm{e}^{+R_\mathrm{x}\tau_\mathrm{m}}}{2} + \cos(\underbrace{\Omega_2}_{\text{diag}} t_1)\frac{\mathrm{e}^{-R_\mathrm{x}\tau_\mathrm{m}} + \mathrm{e}^{+R_\mathrm{x}\tau_\mathrm{m}}}{2}\right).$$
(9.28)

We see that $\mathcal{A}_1$ depends not only on Ω_1 but also on Ω_2 (and vice versa).

9.5.3 Intensity of NOESY cross-peaks

The intensity (measured as peak height or peak integral, i.e., volume) of the cross-peaks is proportional to the amplitudes $\mathcal{A}_1$ and $\mathcal{A}_2$. Here we analyze how $\mathcal{A}_1$ and $\mathcal{A}_2$ decay during τ_m. Eq. 9.23 tells us that the overall loss of signal, proportional to $\Delta\langle M_{1z}\rangle(\tau_\mathrm{m}) + \Delta\langle M_{2z}\rangle(\tau_\mathrm{m})$, due to the R_1 relaxation is given by $\mathrm{e}^{-(R_\mathrm{a}+R_\mathrm{x})\tau_\mathrm{m}}$. This effect is called the "leakage". The intensities of the cross-peaks are given by the factor

$$-\frac{1}{2}\left(\mathrm{e}^{R_\mathrm{x}\tau_\mathrm{m}} - \mathrm{e}^{-R_\mathrm{x}\tau_\mathrm{m}}\right)\mathrm{e}^{-R_\mathrm{a}\tau_\mathrm{m}}.$$
(9.29)

For short τ_m, Taylor expansion can be applied. Neglecting higher terms, $\mathrm{e}^{R_\mathrm{x}\tau_\mathrm{m}} - \mathrm{e}^{-R_\mathrm{x}\tau_\mathrm{m}} \approx 1 + R_\mathrm{x}\tau_\mathrm{m} - 1 + R_\mathrm{x}\tau_\mathrm{m} = 2R_\mathrm{x}\tau_\mathrm{m}$ and $\mathrm{e}^{-R_\mathrm{a}\tau_\mathrm{m}}$ is close to one. Therefore, the expression describing the cross-peak intensities can be approximated as

$$-\frac{1}{2}\left(\mathrm{e}^{R_\mathrm{x}\tau_\mathrm{m}} - \mathrm{e}^{-R_\mathrm{x}\tau_\mathrm{m}}\right)\mathrm{e}^{-R_\mathrm{a}\tau_\mathrm{m}} \approx -R_\mathrm{x}\tau_\mathrm{m}$$
(9.30)

and R_x can be expressed explicitly using Eqs. 8.176, 8.177, and 8.179

$$-\frac{1}{2}\left(\mathrm{e}^{R_\mathrm{x}\tau_\mathrm{m}} - \mathrm{e}^{-R_\mathrm{x}\tau_\mathrm{m}}\right)\mathrm{e}^{-R_\mathrm{a}\tau_\mathrm{m}} \approx -R_\mathrm{x}\tau_\mathrm{m} = \left(\frac{\mu_0}{8\pi}\right)^2\frac{\gamma^4\hbar^2}{r^6}(J(0) - 6J(2\omega_0))\tau_\mathrm{m},$$
(9.31)

where the difference of the precession frequencies due to different chemical shifts was neglected (assuming $\omega_{0,1} = \omega_{0,2} = \omega_0$ because $\gamma_1 = \gamma_2$ and $|\omega_{0,1} - \omega_{0,2}|$ is $\sim 10^{-5}\omega_{0,1}$ or lower). The obtained result shows that the cross-peak intensity is proportional to r^{-6} and to $J(0) - 6J(2\omega_0)$ in the linear approximation. In order to investigate the impact of the dependence on $J(0) - 6J(2\omega_0)$, we calculate the spectral density function for a simple correlation function of a rigid spherical molecule (Eq. 2.3):

$$J(\omega) = \Re\left\{\int_{-\infty}^{\infty}\frac{1}{5}\mathrm{e}^{-t/\tau_\mathrm{C}}\mathrm{e}^{-\mathrm{i}\omega t}\mathrm{d}t\right\} = 2\Re\left\{\int_0^{\infty}\frac{1}{5}\mathrm{e}^{-\frac{\mathrm{i}\omega\tau_\mathrm{C}+1}{\tau_\mathrm{C}}t}\mathrm{d}t\right\} = \frac{2}{5}\Re\left\{\frac{\tau_\mathrm{C}}{\mathrm{i}\omega\tau_\mathrm{C}+1}\right\} = \frac{2}{5}\Re\left\{\frac{\tau_\mathrm{C}}{1+\mathrm{i}\omega\tau_\mathrm{C}}\frac{1-\mathrm{i}\omega\tau_\mathrm{C}}{1-\mathrm{i}\omega\tau_\mathrm{C}}\right\} = \frac{2}{5}\frac{\tau_\mathrm{C}}{1+(\omega\tau_\mathrm{C})^2}.$$
(9.32)

Setting $\omega = 0$, we obtain $J(0) = \frac{2}{5}\tau_\mathrm{C}$.

If the molecular motions are slow, τ_C is long and $2\omega_0\tau_\mathrm{C} \gg 1 \Rightarrow J(2\omega_0) \ll \frac{2}{5}\tau_\mathrm{C} \Rightarrow J(0) > 6J(2\omega_0)$. Therefore the cross-peak intensity proportional to $J(0) - 6J(2\omega_0)$ is positive (i.e., cross-peaks have the same sign as diagonal peaks).

If the molecular motions are fast, $2\omega_0\tau_\mathrm{C} \ll 1 \Rightarrow J(2\omega_0) \approx \frac{2}{5}\tau_\mathrm{C} \Rightarrow J(0) = \frac{2}{5}\tau_\mathrm{C} < 6J(2\omega_0) \approx 6 \times \frac{2}{5}\tau_\mathrm{C}$. Therefore the cross-peak intensity proportional to $J(0) - 6J(2\omega_0)$ is negative (i.e., cross-peaks and diagonal peaks have the opposite sign).

Lecture 10
J-coupling, spin echoes

Literature: The through-bond coupling (J-coupling) is described in L14 and L15, the Hamiltonian is presented in L9.4 and J-coupled spins are described in L14.2, L14.3, and L14.5. Spin echoes are nicely described in K7.8 and also presented in LA.10.

10.1   Through-bond coupling

Magnetic moments of nuclei connected by covalent bonds interact also indirectly, via interactions with magnetic moments of the electrons of the bonds. This type of interaction is known as the *J-coupling, through-bond coupling,* or *indirect spin-spin coupling.* A magnetic moment μ_2 is a source of a magnetic field that perturbs the distribution of electron magnetic moments. Such a distortion (perturbation of the electron spin states or modification of electron orbital magnetic moments by altering the magnetic field felt by the electrons) modifies the magnetic field at the site of μ_1. The fact that such indirect interaction exists is itself not surprising. But it is less obvious (and was surprising when first observed) why the indirect interaction *is not averaged to zero* in isotropic liquids. The indirect interaction is just a series of direct interactions of different magnetic moments (of the nuclei and of the electrons). We derived in Section 8.9.2 that the effect of a direct interaction of two magnetic dipoles is averaged to zero in isotropic liquids. Should not the whole series of interactions be averaged to zero, when each interaction in the series seems to be?

Before we discuss this mystery, we write down a general form of a Hamiltonian representing a contribution of the coupling to the magnetic energy of a pair of interacting nuclear magnetic moments. For example, if nucleus 2 generates (indirectly, via interactions with the electrons as descried above) a field $\vec{B}_2$ at the site of nucleus 1, then coupling with $\vec{\mu}_2$ contributes to the energy of the magnetic moment $\vec{\mu}_1$ by $-\vec{\mu}_1 \cdot \vec{B}_2$. We can assume that each component of the field felt by magnetic moment 1 (e.g. of ^{1}H) somehow depends on all components of magnetic moment 2 (e.g. of ^{13}C), in a similar manner as we described the through-space direct dipole-dipole coupling. Therefore, it should be possible to describe the indirect interaction by a tensor (like chemical shift or dipolar coupling):

$$\hat{H}_J = \frac{2\pi}{\hbar} (\, \hat{I}_{1x} \ \hat{I}_{1y} \ \hat{I}_{1z} \,) \begin{pmatrix} J_{xx} & J_{xy} & J_{xz} \\ J_{yx} & J_{yy} & J_{yz} \\ J_{zx} & J_{zy} & J_{zz} \end{pmatrix} \begin{pmatrix} \hat{I}_{2x} \\ \hat{I}_{2y} \\ \hat{I}_{2z} \end{pmatrix} = \frac{2\pi}{\hbar} \hat{\vec{I}}_1 \cdot \underline{J} \cdot \hat{\vec{I}}_2. \tag{10.1}$$

To proceed, we should investigate the physical origin of the interaction. As discussed in Sec-

tion 10.10.1, the major contribution to the J-coupling in most molecules is an interaction mediated by electrons occurring *at the same positions* as the nuclei. Obviously, the interaction of such electrons with the nuclei does not change as the molecule rotates. As a consequence, the J-tensor has a dominant isotropic (orientation-independent) component, whereas the anisotropic part is usually small (and difficult to distinguish from the dipolar coupling). Therefore, only the isotropic component of the tensor is considered and the anisotropic component is neglected in practice. The isotropic component is defined as described in Section 1.5.7 for the chemical shift tensor:[1]

$$2\pi \begin{pmatrix} J_{XX} & 0 & 0 \\ 0 & J_{YY} & 0 \\ 0 & 0 & J_{ZZ} \end{pmatrix} = 2\pi \frac{J_{XX} + J_{YY} + J_{ZZ}}{3} \begin{pmatrix} 1 & 0 & 0 \\ 0 & 1 & 0 \\ 0 & 0 & 1 \end{pmatrix} = 2\pi J \begin{pmatrix} 1 & 0 & 0 \\ 0 & 1 & 0 \\ 0 & 0 & 1 \end{pmatrix}. \tag{10.2}$$

The unit matrix tells us that we can replace the tensor $\underline{J}$ (represented by a 3 matrix) in the Hamiltonian by a *scalar* value (single number) J. Accordingly, the J-coupling is often called the *scalar coupling* (implying that the anisotropic component is neglected).

The actual coupling between nuclei connected by chemical bonds is due to interactions of magnetic moments of electrons that (i) can be found with non-zero probabilities at the nuclei, and (ii) contribute to the covalent bonds between the nuclei. Wave functions of electrons in a simple σ-bond are discussed in Section 10.10.2.

The value of the constant J can be positive or negative, it depends on the actual distribution of electrons, and its calculation requires advanced quantum chemistry methods. The factor of 2π reflects the convention to express J in the units of Hz. Note that the J-coupling does not depend on the external magnetic field $\vec{B}_0$. Therefore, it does not make sense to express J in relative units (ppm). The proton-proton J-coupling is significant (exceeding 10 Hz) up to three bonds and observable for 4 or 5 bonds in special cases (planar geometry like in aromatic systems). Interactions of other nuclei are weaker, but the one-bond couplings are always significant (as strong as 700 Hz for ^{31}P-^{1}H, 140 Hz to 200 Hz for ^{13}C-^{1}H, -90 Hz for ^{15}N-^{1}H in amides, 30 Hz to 60 Hz for ^{13}C-^{13}C, -10 Hz to -15 Hz for ^{13}C-^{15}N). Typical values of two-bond (^2J) and three-bond (^3J) ^{1}H-^{1}H couplings are -15 Hz and 0 Hz to 20 Hz, respectively. As the value of J is given by the distribution of electrons in bonds, it reports the local geometry of the molecule. In particular, three-bond J-couplings can be used to measure torsion angles in molecules.

The J-coupling has a quantum origin, but its influence on evolution of magnetic moments can be described classically, as shown in Sections 10.10.3 and 10.10.5.

10.2   Secular approximation, averaging, and relaxation

If the anisotropic part of the J-tensor is neglected, the J-coupling does not depend on the orientation (the *scalar* coupling) and no ensemble averaging is needed. The secular approximation is applied like in the case of the dipolar coupling.

---

[1] Note that it is sufficient to consider only the average of the diagonal elements of the tensor $J = (J_{XX}+J_{YY}+J_{ZZ})/3$ if the anisotropy $(2J_{ZZ} - J_{YY} - J_{XX})/6$ and rhombicity $(J_{XX} - J_{YY})/2$ are equal to zero.
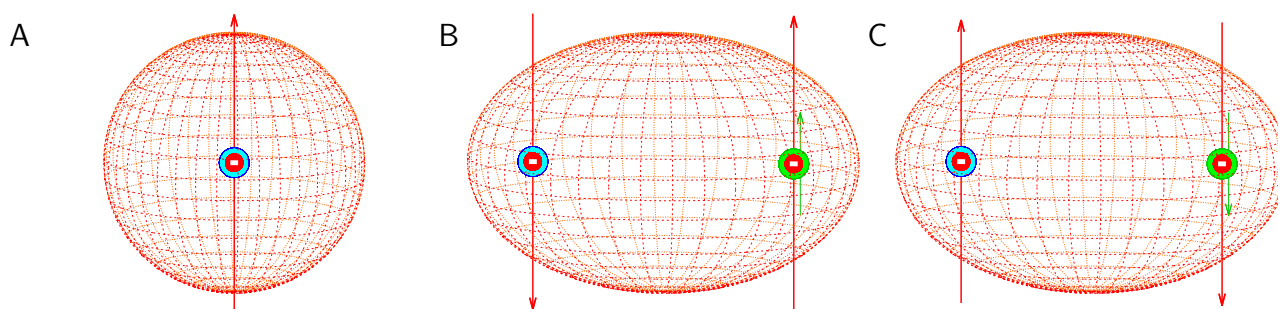
Figure 10.1: *J*-coupling. A, the probability of finding an electron in the hydrogen atom at particular coordinates is described by the probability density ρ. The probability density described by the orbital 1s (depicted as a sphere) has a non-zero value at the position of the nucleus (shown in cyan). Therefore, there is a non-zero probability of finding the electron (red circle) exactly at the site of the nucleus. The field produced at the site of the nucleus by the electron's magnetic moment (red arrow) does not depend on the orientation of the atom if the positions of the nucleus and of the electron coincide. Therefore, the interaction of the nucleus with the electron is not averaged to zero if the atom rotates isotropically. B and C, the probability density described by the sigma orbitals (depicted as an ellipsoid) in molecules has also non-zero values at the sites of nuclei. The spin state of the electrons in the bonding sigma orbital is a superposition of the $|\alpha\rangle \otimes |\beta\rangle$ and $|\beta\rangle \otimes |\alpha|$ eigenstates (indicated by the opposite direction of the red arrows), perturbed by the magnetic moment of the nuclei. The parallel orientation of the magnetic moments is energetically favorable for a nucleus and an electron sharing its position.

The Hamiltonian of the *scalar coupling*, i.e., of the *J*-coupling with the small anisotropic contribution neglected, has one of the following forms.

- In the case of magnetic moments with the same γ *and* chemical shift, precessing about the z axis with *the same precession frequency*,

$$\hat{H}_J = \frac{\pi}{\hbar}\left(2\hat{I}_{1z}\hat{I}_{2z} + 2\hat{I}_{1x}\hat{I}_{2x} + 2\hat{I}_{1y}\hat{I}_{2y}\right). \tag{10.3}$$

This case is called *strong coupling* and is discussed in Lecture 12.

- In the case of magnetic moments with different γ and/or chemical shift, precessing about the z axis with *different precession frequencies*,

$$\hat{H}_J = \frac{2\pi}{\hbar}\hat{I}_{1z}\hat{I}_{2z} = \frac{\pi}{\hbar}\left(2\hat{I}_{1z}\hat{I}_{2z}\right). \tag{10.4}$$

This case is called *weak coupling*. Only the weak coupling Hamiltonian is considered in Lectures 10 and 11.

In principle, the anisotropic part of the *J*-tensor would contribute to the relaxation like the anisotropic part of the chemical shift tensor, but it is small and usually neglected. The scalar coupling (described by the isotropic part of the *J*-tensor) does not depend on the orientation. Therefore, it can contribute to the relaxation only through a conformational or chemical exchange. Conformational effects are usually small: one-bond and two-bond couplings do not depend on torsion angles and

three-bond coupling constants are small. In summary, the relaxation due to the J-coupling is rarely observed. However, the J-coupling influences relaxation of the sample in another way. As described in Section 10.5, the J-coupling creates density matrix components relaxing with different rates than $\mathscr{I}_{1+}$ and $\mathscr{I}_{2+}$, analyzed in Sections 8.7 and 8.9.6.

10.3   Homo- and heteronuclear magnetic moment pairs

So far, we did not distinguish *homonuclear* pairs of magnetic moments (magnetic moments of the same type of nuclei, e.g., two protons) and *heteronuclear* pairs of magnetic moments (magnetic moments of different isotopes, e.g., proton and ^{13}C). It is useful to distinguish these two cases when we analyze advanced NMR experiments. Although the density matrix has the same form in both cases, the Hamiltonians describing the effects of radio waves may differ. The reason is technical. Differences in the chemical shifts are usually small and allow us to irradiate the sample by a radio wave with a frequency sufficiently close to the precession frequencies of both nuclei. Therefore, the resonance conditions can be matched reasonably well for both nuclei and they are affected by the radio waves in a similar manner. On the other hand, the precession frequencies of different isotopes differ substantially and the frequency of the radio waves can resonate only with one of the isotopes. As a consequence, each of the magnetic moments of the pair is affected selectively, which is frequently exploited in the NMR experiments.

In order to distinguish the heteronuclear systems from homonuclear ones in our written notes, we save the symbols $\mathscr{I}_{1j}$ and $\mathscr{I}_{2j}$ for homonuclear pairs (most often two protons) and use symbols $\mathscr{I}_j$ and $\mathscr{S}_j$ for operators of nucleus 1 and 2, respectively, if $\gamma_1 \neq \gamma_2$. Both labeling systems are mixed if we describe more complex chemical groups. For example, we use symbols $\mathscr{I}_{1j}$, $\mathscr{I}_{2j}$, and $\mathscr{S}_j$ for the operators representing contributions to density matrix describing (mixed) states of nuclear magnetic moments in the ^{13}C^{1}H$_2$ group.

10.4   Density matrix evolution in the presence of J-coupling

In order to extend the description of NMR experiments to J-coupled pairs of nuclear magnetic moments, we should update the analysis of the density matrix evolution derived in the previous lectures. As always, the analysis starts by the definition of the initial density matrix form. Derivation of the density matrix in the thermal equilibrium, presented in Section 10.10.6, is very similar to that described for two nuclei interacting through space (dipolar coupling) in Section 8.8. In principle, the diagonal elements of the density matrix are slightly influenced by the J-coupling, but this influence is at least five orders of magnitude weaker than the dominant effect of the external magnetic field $\vec{B}_0$. Therefore, the J-coupling contribution can be neglected together with the effect of the chemical shifts, and the same equilibrium density matrix can be used as the starting point of the analysis of NMR experiments in the presence of J-coupling, as it was used for systems with no or dipolar coupling:

$$\hat{\rho}^{\text{eq}} = \frac{1}{2} \left(\mathscr{I}_t + \kappa_1 \mathscr{I}_{1z} + \kappa_2 \mathscr{I}_{2z} \right), \tag{10.5}$$
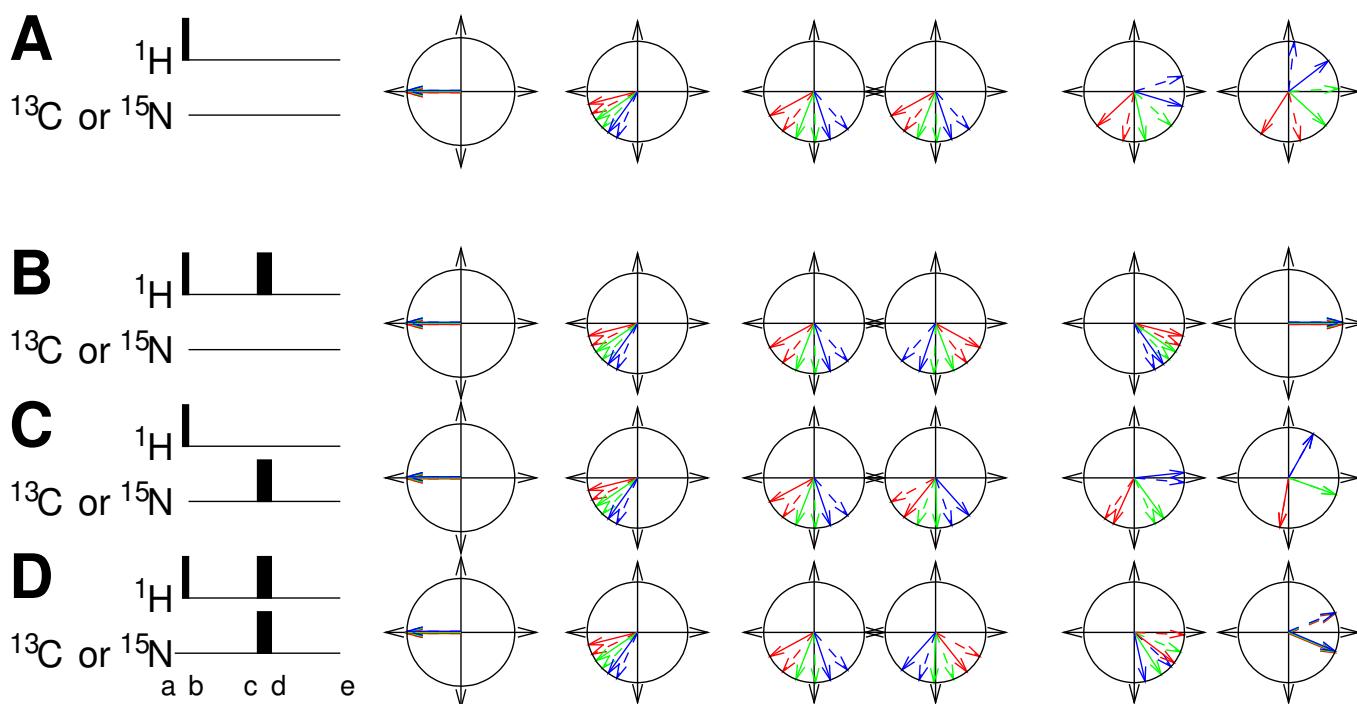
Figure 10.2: Graphical analysis of evolution of density matrix for ^{1}H (nucleus 1) and ^{13}C (nucleus 2) in an isolated –CH– group. In individual rows, evolution of coherences is shown for three protons (distinguished by colors) with slightly different precession frequency due to the different chemical shifts δ_i. The protons are bonded to ^{13}C. Solid arrows represent fractions of proton magnetization in 10 % molecules with ^{13}C magnetic moments most polarized in the direction of $\vec{B}_0$. Dashed arrow represent fractions of proton magnetization in 10 % molecules with ^{13}C magnetic moments most aligned in the opposite direction. The first column shows the arrows at the beginning of the echo (after the initial 90° pulse at the proton frequency), the second column shows the arrows in the middle of the first delay τ, the third and fourth columns show the arrows immediately before and after the 180° pulse(s) in the middle of the echo, respectively, the fifths column shows the arrows in the middle of the second delay τ, the sixth column shows the arrows at the end of the echo. Row A corresponds to an experiment when no 180° pulse is applied, row B corresponds to the echo with the 180° pulse applied at the proton frequency, row C corresponds to the echo with the 180° pulse applied at the ^{13}C frequency, and row D corresponds to the echo with the 180° pulses applied at both frequencies (see the schematic drawings in left part of the figure). The x-axis points down, the y-axis points to the right.

where

$$\kappa_j = \frac{\gamma_j B_0 \hbar}{2 k_{\mathrm{B}} T}. \tag{10.6}$$

In the case of a *homonuclear* pair of magnetic moments (e.g., of two J-coupled protons), $\kappa_1 = \kappa_2 = \kappa$ because $\gamma_1 = \gamma_2$.

Also the second step, the analysis of the effect of the 90° radio wave pulse (see the schematic drawing in Figure 10.2A), gives the same result as for the uncoupled systems. Again, the reason is that the fields indirectly produced by the coupled magnetic moments are too weak (much weaker than the radio-frequency field) to have a noticeable effect during the short pulse. Therefore, our analysis of the evolution in the presence of the J-coupling starts from $\hat{\rho}(\mathrm{b}) = \frac{1}{2}\mathscr{I}_t + \frac{1}{2}\kappa(-\mathscr{I}_{1y} - \mathscr{I}_{2y})$, where the letter "b" refers to the labeling of the time course in Figure 10.2.

In the presence of the J-coupling, the general Hamiltonian describing the evolution after a $90°$ pulse is complicated even in a coordinate system rotating with $\omega_{\text{rot}} = -\omega_{\text{radio}}$

$$\mathcal{H} = \underbrace{-\gamma_1 B_0(1 + \delta_{\text{i},1})}_{\Omega_1} \mathcal{I}_{1z} \underbrace{-\gamma_2 B_0(1 + \delta_{\text{i},2})}_{\Omega_2} \mathcal{I}_{2z} + \pi J \left(2\mathcal{I}_{1z}\mathcal{I}_{2z} + 2\mathcal{I}_{1x}\mathcal{I}_{2x} + 2\mathcal{I}_{1y}\mathcal{I}_{2y}\right). \qquad (10.7)$$

However, if the precession frequencies differ, the secular approximation simplifies the Hamiltonian to a form where all components commute:

$$\mathcal{H} = \underbrace{-\gamma_1 B_0(1 + \delta_{\text{i},1})}_{\Omega_1} \mathcal{I}_{1z} \underbrace{-\gamma_2 B_0(1 + \delta_{\text{i},2})}_{\Omega_2} \mathcal{I}_{2z} + \pi J\, 2\mathcal{I}_{1z}\mathcal{I}_{2z}. \qquad (10.8)$$

In such case, Eq. 6.9 can be applied and the Liouville-von Neumann equation can be solved geometrically as rotations in three-dimensional subspaces of the 16-dimensional operator space. The relevant subspaces are defined by the commutation relations summarized in Eqs. 8.29–8.31 and presented graphically in Figure 10.3. Graphical description of rotations in the 16D operator space of a heteronuclear pair is derived from Figure 10.3 by changing $\mathcal{I}_{1j}$ to $\mathcal{I}_j$ and $\mathcal{I}_{2j}$ to $\mathcal{S}_j$, or vice versa (see Figure 10.4). Rotations described by different components of the Hamiltonian are independent and can be performed consecutively, in any order.

For a density matrix $\hat{\rho}(\text{b}) = \frac{1}{2}\mathcal{I}_t + \frac{1}{2}\kappa(-\mathcal{I}_{1y} - \mathcal{I}_{2y})$ after a $90°$ pulse, the evolution due to the chemical shift (described by Ω_1 and Ω_2) and J-coupling (described by πJ) can be analyzed as follows

$$\mathcal{I}_t \longrightarrow \mathcal{I}_t \longrightarrow \mathcal{I}_t \longrightarrow \mathcal{I}_t \qquad (10.9)$$

$$-\mathcal{I}_{1y} \longrightarrow \begin{cases} -c_1\mathcal{I}_{1y} \longrightarrow -c_1\mathcal{I}_{1y} \longrightarrow \begin{cases} -c_1 c_J\ \mathcal{I}_{1y} \\ +c_1 s_J\ 2\mathcal{I}_{1x}\mathcal{I}_{2z} \end{cases} \\ +s_1\mathcal{I}_{1x} \longrightarrow +s_1\mathcal{I}_{1x} \longrightarrow \begin{cases} +s_1 c_J\ \mathcal{I}_{1x} \\ +s_1 s_J\ 2\mathcal{I}_{1y}\mathcal{I}_{2z} \end{cases} \end{cases}$$

$$(10.10)$$

$$-\mathcal{I}_{2y} \longrightarrow -\mathcal{I}_{2y} \longrightarrow \begin{cases} -c_2\mathcal{I}_{2y} \longrightarrow \begin{cases} -c_2 c_J\ \mathcal{I}_{2y} \\ +c_2 s_J\ 2\mathcal{I}_{2x}\mathcal{I}_{1z} \end{cases} \\ +s_2\mathcal{I}_{2x} \longrightarrow \begin{cases} +s_2 c_J\ \mathcal{I}_{2x} \\ +s_2 s_J\ 2\mathcal{I}_{2y}\mathcal{I}_{1z} \end{cases} \end{cases} \qquad (10.11)$$

where the first (cyan) arrows represent a rotation "about" $\mathcal{I}_{1z}$ by the angle $\Omega_1 t$, the second (green) arrows represent a rotation "about" $\mathcal{I}_{2z}$ by the angle $\Omega_2 t$, the third (red) arrows represent a rotation "about" $2\mathcal{I}_{1z}\mathcal{I}_{2z}$ by the angle $\pi J t$, and

$$c_1 = \cos(\Omega_1 t) \qquad s_1 = \sin(\Omega_1 t) \qquad (10.12)$$
$$c_2 = \cos(\Omega_2 t) \qquad s_2 = \sin(\Omega_2 t) \qquad (10.13)$$
$$c_J = \cos(\pi J t) \qquad s_J = \sin(\pi J t). \qquad (10.14)$$
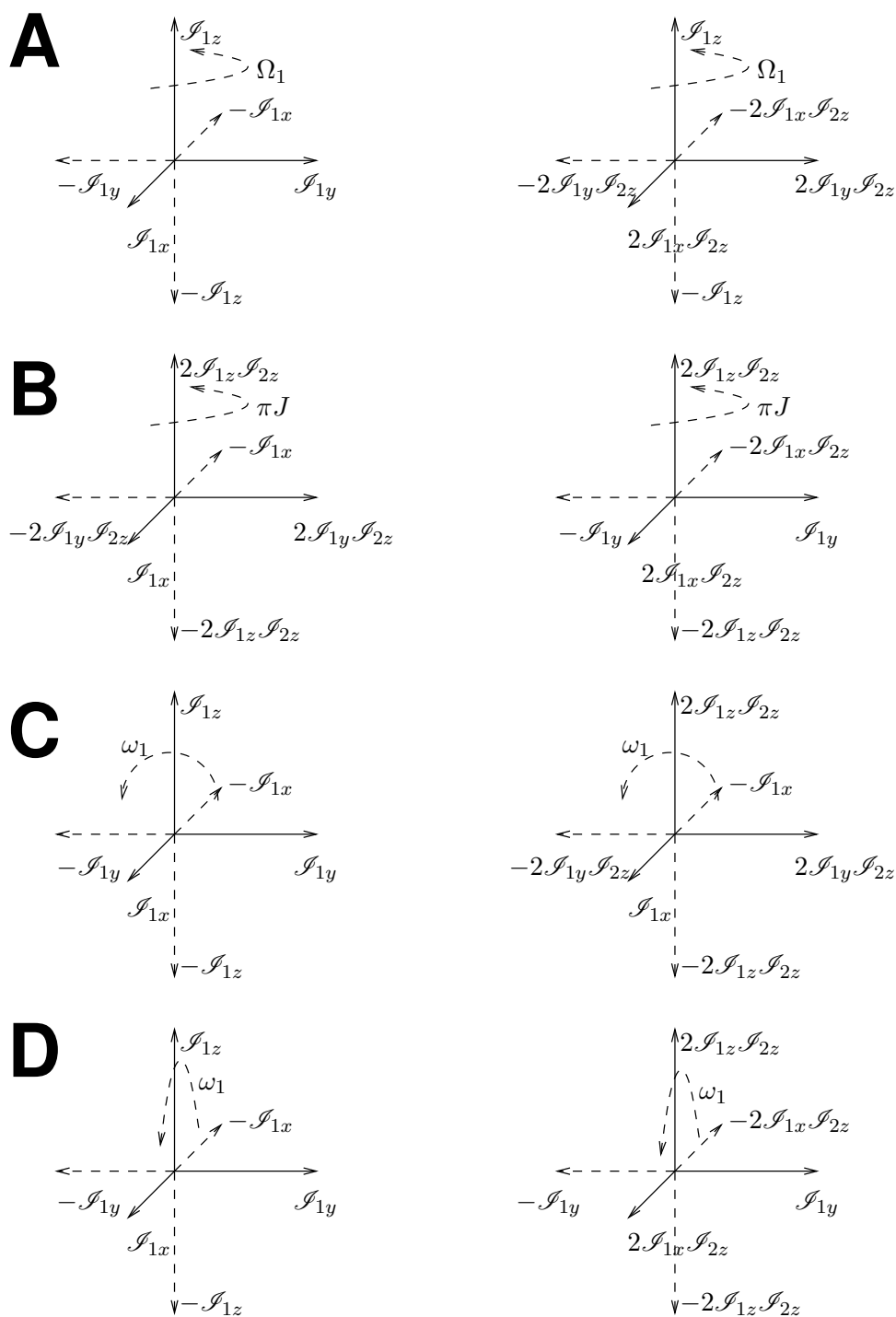
Figure 10.3: Rotations in product operator space. A, effects of the Hamiltonian describing the chemical shift; B, effects of the Hamiltonian describing the J coupling; C, effects of the Hamiltonian describing the radio wave pulses with the phase 0 (x); D effects of the Hamiltonian describing the radio wave pulses with the phase $\pi/2$ (y). The rotations are shown for the magnetic moment 1, a similar diagram for the magnetic moment 2 can be obtained by switching the subscripts 1 and 2 of the operators $\mathscr{I}_{1j}$ and $\mathscr{I}_{2k}$.
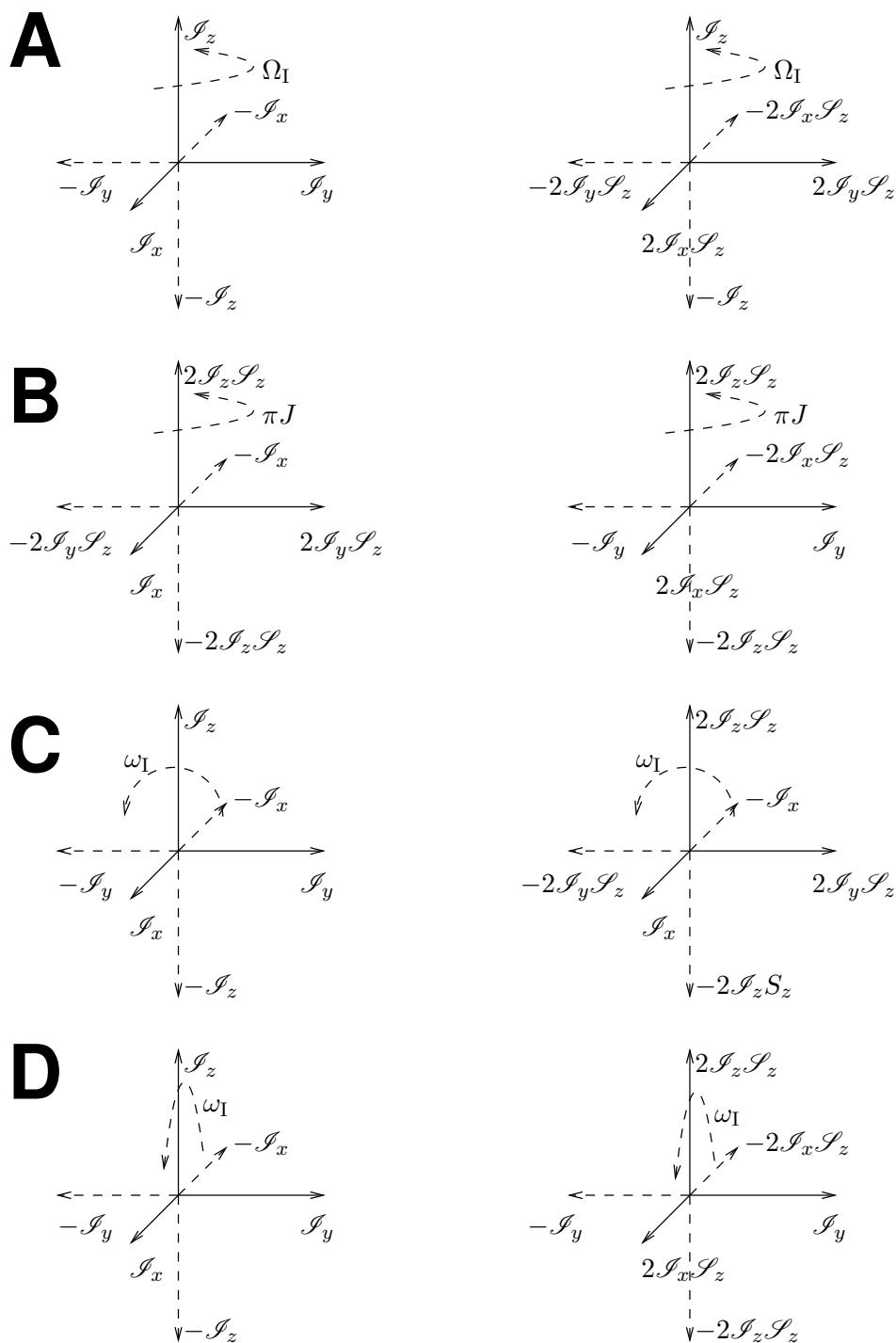
Figure 10.4: Rotations in heteronuclear product operator space. A, effects of the Hamiltonian describing the chemical shift; B, effects of the Hamiltonian describing the J coupling; C, effects of the Hamiltonian describing the radio wave pulses with the phase 0 (x); D effects of the Hamiltonian describing the radio wave pulses with the phase $\pi/2$ (y).

As mentioned above, the same result is obtained if we first "rotate about" $2\mathscr{I}_{1z}\mathscr{I}_{2z}$, and then "about" $\mathscr{I}_{1z}$ or $\mathscr{I}_{2z}$.

The described analysis can be further simplified if we use pairs of arrows to represent the product operators contributing to $\hat{\rho}$. In this representation, the *direction* of the arrows specifies the *transverse polarization of the observed magnetic moment* and the *style* of the arrows (solid or dashed) specifies the *longitudinal polarization of the coupled neighbor*. Pairs of arrows with the *same orientations* represent coherences $\mathscr{I}_{1x}$, $\mathscr{I}_{1y}$, $\mathscr{I}_{2x}$, $\mathscr{I}_{2y}$, describing transverse polarizations regardless of the neighbor's longitudinal polarizations. Pairs of arrows with the *opposite orientations* represent coherences $2\mathscr{I}_{1x}\mathscr{I}_{2z}$, $2\mathscr{I}_{1y}\mathscr{I}_{2z}$, $2\mathscr{I}_{2x}\mathscr{I}_{1z}$, $2\mathscr{I}_{2y}\mathscr{I}_{1z}$, describing correlations of transverse polarizations with the neighbor's longitudinal polarizations. For example,

etc.

The evolution due to the chemical shift, described by the Hamiltonian components $\Omega_1\mathscr{I}_{1z}$ and $\Omega_2\mathscr{I}_{2z}$ is represented by *simultaneous rotation* of the arrows (solid and dashed arrows rotate by the same angle $\Omega_1 t$ or $\Omega_2 t$ in the *same direction*). The evolution due to the J-coupling, described by the Hamiltonian component $\pi J\, 2\mathscr{I}_{1z}\mathscr{I}_{2z}$ is represented by the *mutual rotation* of the arrows (solid and dashed arrows rotate by the same angle πJt in the *opposite direction*). 180° pulses flip the arrows about the axes given by the phases of the pulses. More details are discussed in Section 10.10.7.

10.5 Signal in the presence of the J-coupling

The last step is the evaluation of the expectation value of the transverse magnetization. Only $\mathscr{I}_{1x}$, $\mathscr{I}_{1y}$, $\mathscr{I}_{2x}$, $\mathscr{I}_{2y}$ contribute to the expected value of M_+, giving a non-zero trace when multiplied by $\hat{I}_+$ (taking the advantage of using the orthonormal basis, see Section 9.3):

$$\text{Tr}\left\{\mathscr{I}_{1x}(\mathscr{I}_{1x}+\mathrm{i}\mathscr{I}_{1y})\right\} = \text{Tr}\left\{\mathscr{I}_{2x}(\mathscr{I}_{2x}+\mathrm{i}\mathscr{I}_{2y})\right\} = 1, \tag{10.15}$$

$$\text{Tr}\left\{\mathscr{I}_{1y}(\mathscr{I}_{1x}+\mathrm{i}\mathscr{I}_{1y})\right\} = \text{Tr}\left\{\mathscr{I}_{2y}(\mathscr{I}_{2x}+\mathrm{i}\mathscr{I}_{2y})\right\} = \mathrm{i}, \tag{10.16}$$

Well-known trigonometric relations $\cos(a\pm b) = \cos a \cos b \mp \sin a \sin b$ and $\sin(a\pm b) = \sin a \cos b \pm \cos a \sin b$ allow us to convert the products $c_n c_J$ (modulating $\mathscr{I}_{ny}$) and $s_n c_J$ (modulating $\mathscr{I}_{nx}$) in Eqs. 10.10–10.11 to sums of cosine and sine functions, respectively:

$$c_1 c_J = \frac{1}{2}\cos((\Omega_1+\pi J)t) + \frac{1}{2}\cos((\Omega_1-\pi J)t) \tag{10.17}$$

$$s_1 c_J = \frac{1}{2}\sin((\Omega_1+\pi J)t) + \frac{1}{2}\sin((\Omega_1-\pi J)t) \tag{10.18}$$

$$c_2 c_J = \frac{1}{2}\cos((\Omega_2+\pi J)t) + \frac{1}{2}\cos((\Omega_2-\pi J)t) \tag{10.19}$$

$$s_2 c_J = \frac{1}{2}\sin((\Omega_2+\pi J)t) + \frac{1}{2}\sin((\Omega_2-\pi J)t) \tag{10.20}$$

The expected value of M_+ calculated from the complete density matrix is then

$$\langle M_+ \rangle = \mathrm{Tr}\left\{\hat{\rho}(t)\hat{M}_+\right\} = \mathcal{N}\gamma\hbar\mathrm{Tr}\left\{\hat{\rho}(t)(\mathscr{I}_{1x} + \mathrm{i}\mathscr{I}_{1y} + \mathscr{I}_{2x} + \mathrm{i}\mathscr{I}_{2y})\right\}$$

$$= -\mathrm{i}\mathcal{N}\gamma\hbar\frac{\kappa}{4}\left(\cos((\Omega_1 + \pi J)t) + \cos((\Omega_1 - \pi J)t) + \cos((\Omega_2 + \pi J)t) + \cos((\Omega_2 - \pi J)t)\right)$$

$$+ \mathcal{N}\gamma\hbar\frac{\kappa}{4}\left(\sin((\Omega_1 + \pi J)t) + \sin((\Omega_1 - \pi J)t) + \sin((\Omega_2 + \pi J)t) + \sin((\Omega_2 - \pi J)t)\right)$$

$$= \mathcal{N}\gamma\hbar\frac{\kappa}{4}(-\mathrm{i})\left(\cos((\Omega_1 - \pi J)t) + \mathrm{i}\sin((\Omega_1 - \pi J)t) + \cos((\Omega_1 + \pi J)t) + \mathrm{i}\sin((\Omega_1 + \pi J)t)\right)$$

$$+ \mathcal{N}\gamma\hbar\frac{\kappa}{4}(-\mathrm{i})\left(\cos((\Omega_2 - \pi J)t) + \mathrm{i}\sin((\Omega_2 - \pi J)t) + \cos((\Omega_2 + \pi J)t) + \mathrm{i}\sin((\Omega_2 + \pi J)t)\right)$$

$$= \frac{\mathcal{N}\gamma^2\hbar^2 B_0}{8k_\mathrm{B}T}\mathrm{e}^{-\mathrm{i}\frac{\pi}{2}}\left(\mathrm{e}^{\mathrm{i}(\Omega_1 - \pi J)t} + \mathrm{e}^{\mathrm{i}(\Omega_1 + \pi J)t} + \mathrm{e}^{\mathrm{i}(\Omega_2 - \pi J)t} + \mathrm{e}^{\mathrm{i}(\Omega_2 + \pi J)t}\right) \tag{10.21}$$

At this moment, we should also include the relaxation. We have analyzed the relaxation in Sections 7.7, 7.12.3, and 8.7, 8.9.6. However, the density matrix in the presence of the J-coupling evolves into new terms $2\mathscr{I}_{1x}\mathscr{I}_{2z}$, $2\mathscr{I}_{1y}\mathscr{I}_{2z}$, $2\mathscr{I}_{1z}\mathscr{I}_{2x}$, and $2\mathscr{I}_{1z}\mathscr{I}_{2y}$, and these terms relax differently. Their relaxation rates can be derived using the Bloch-Wangsness-Redfield approach, but we do not do it in this course. If both dipole-dipole interactions and chemical shift anisotropy contribute to the relaxation, another complication appears: the relaxation of $\mathscr{I}_{1+}$ depends on $2\mathscr{I}_{1+}\mathscr{I}_{2z}$ and vice versa, and the same applies to $\mathscr{I}_{2+}$ and $2\mathscr{I}_{1z}\mathscr{I}_{2+}$.[2] To keep our analysis as simple as possible, we (i) assume that the contribution of the chemical shift anisotropy is negligible, (ii) describe relaxation of the inter-converting $\hat{\rho}$ contributions $\mathscr{I}_{1+}$, $2\mathscr{I}_{1+}\mathscr{I}_{2z}$ and $\mathscr{I}_{2+}$, $2\mathscr{I}_{1z}\mathscr{I}_{2+}$ by average rate constants, and (iii) assume that the average rate constants are identical for both nuclei (we use the symbol $\overline{R}_2$).

Including the relaxation and applying a phase shift by $90\,^\circ$, we obtain the description of the time evolution of the expected value of M_+

$$\langle M_+ \rangle = \frac{\mathcal{N}\gamma^2\hbar^2 B_0}{8k_\mathrm{B}T}\mathrm{e}^{-\overline{R}_2 t}\left(\mathrm{e}^{\mathrm{i}(\Omega_1 - \pi J)t} + \mathrm{e}^{\mathrm{i}(\Omega_1 + \pi J)t} + \mathrm{e}^{\mathrm{i}(\Omega_2 - \pi J)t} + \mathrm{e}^{\mathrm{i}(\Omega_2 + \pi J)t}\right) \tag{10.22}$$

which gives four peaks in the spectrum after the Fourier transformation:

---

[2]The mutual dependence of relaxation is described by constants known as *cross-correlated cross-relaxation* rate constants, resembling R_x in Eqs. 8.33 and 8.34.

$$\frac{\mathcal{N}\gamma^2\hbar^2 B_0}{8k_\mathrm{B}T} \left(\frac{\overline{R}_2}{\overline{R}_2^2 + (\omega - \Omega_1 + \pi J)^2} + \frac{\overline{R}_2}{\overline{R}_2^2 + (\omega - \Omega_1 - \pi J)^2} \right.$$
$$\left. + \frac{\overline{R}_2}{\overline{R}_2^2 + (\omega - \Omega_2 + \pi J)^2} + \frac{\overline{R}_2}{\overline{R}_2^2 + (\omega - \Omega_2 - \pi J)^2} \right)$$
$$-\mathrm{i}\frac{\mathcal{N}\gamma^2\hbar^2 B_0}{8k_\mathrm{B}T} \left(\frac{\omega - \Omega_1 + \pi J}{\overline{R}_2^2 + (\omega - \Omega_1 + \pi J)^2} + \frac{\omega - \Omega_1 - \pi J}{\overline{R}_2^2 + (\omega - \Omega_1 - \pi J)^2} \right.$$
$$\left. + \frac{\omega - \Omega_2 + \pi J}{\overline{R}_2^2 + (\omega - \Omega_2 + \pi J)^2} + \frac{\omega - \Omega_2 - \pi J}{\overline{R}_2^2 + (\omega - \Omega_2 - \pi J)^2} \right).$$

$$(10.23)$$
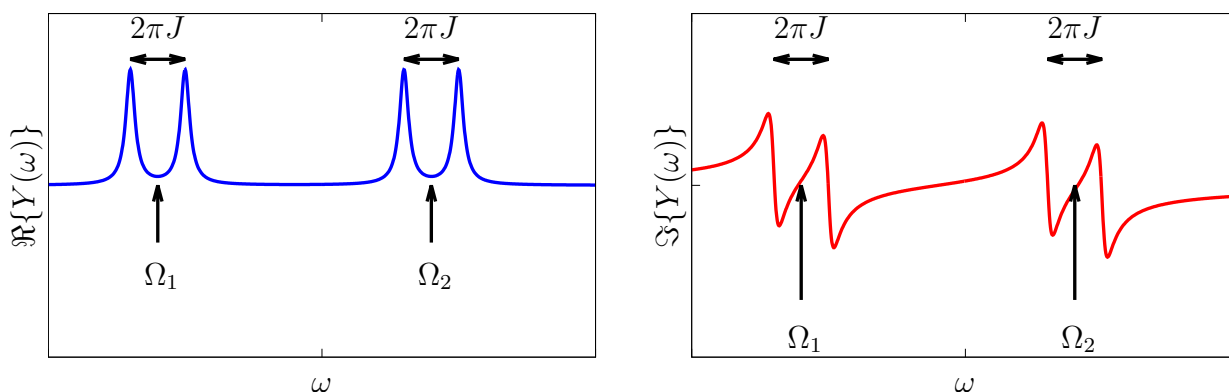
The four peaks in the spectrum form two doublets, one at an average angular frequency Ω_1, the other one at an average angular frequency Ω_2. Both doublets are split by an angular frequency difference $\pi J - (-\pi J) = 2\pi J$, or by the value of J if the frequencies are plotted in Hz.

After describing the spectrum of a homonuclear pair of magnetic moments, we should also mention how spectra of heteronuclear pairs differ from the homonuclear ones. The selective irradiation of either nucleus 1 or nucleus 2 also implies that the peaks of nuclei 1 and 2 are not observed in the same spectrum. The signals of nucleus 1 and nucleus 2 are recorded in two experiments with different frequencies (resonating with the precession frequency of nucleus 1 in one spectrum and of nucleus 2 in the other one) of the radio waves, as shown in Figure 10.5. The sensitivities (signal-to-noise ratios) of the experiments are in the ratio $|\gamma_1/\gamma_2|^{5/2}$ (Eq. 7.94). For example, sensitivity of ^{13}C and ^{15}N spectra is reduced by a factor of 32 (see Figure 10.5) and 300, respectively, compared to proton spectra, even if the molecules contain 100 % ^{13}C and ^{15}N isotopes.

10.6 Spin echoes

In many NMR experiments, the J-coupling is not just detected, but creatively employed to deliberately change quantum states (mixed states) of the studied system. Such a manipulation resembles
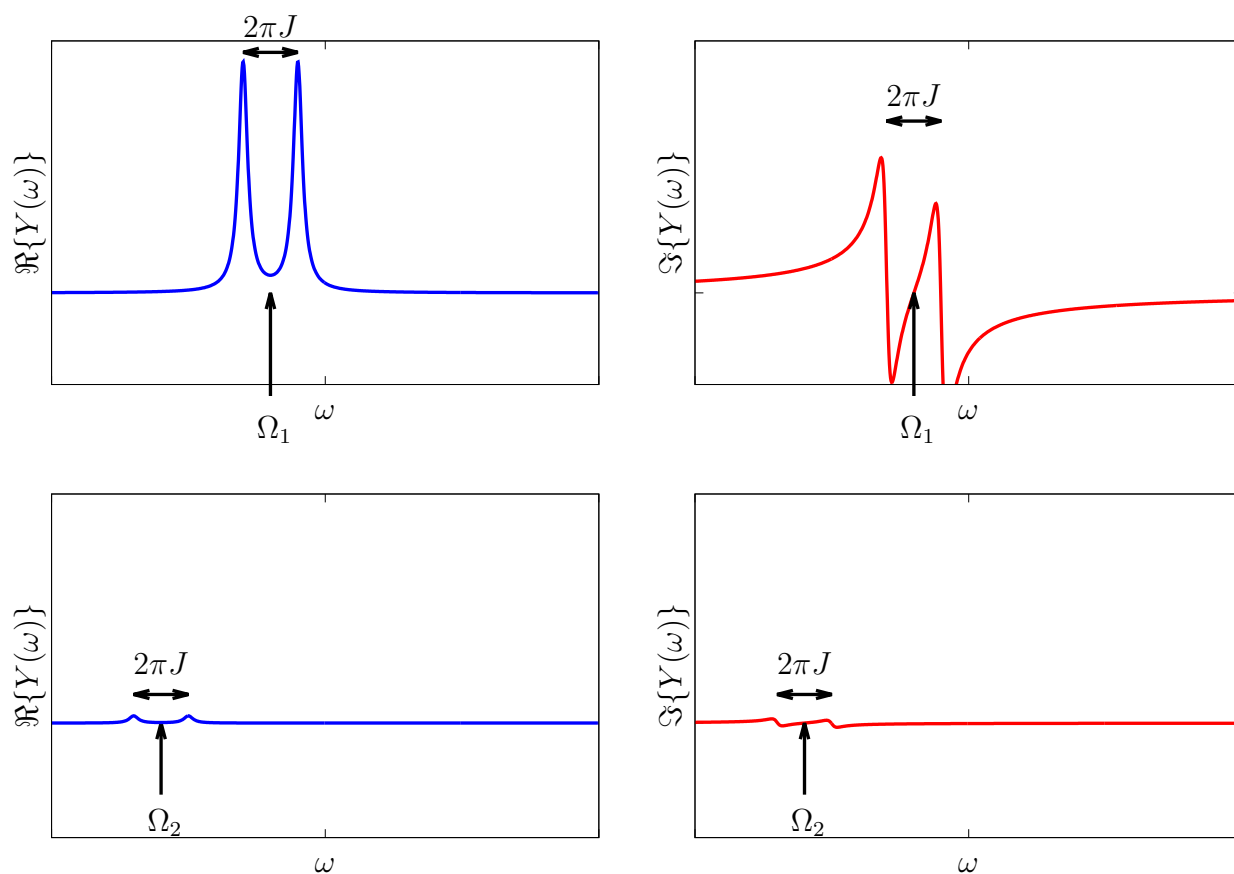
Figure 10.5: Spectra of a heteronuclear pair. Top, real and imaginary component of a spectrum recorded after applying a radio wave pulse close to the precession frequency of nucleus 1. Bottom, real and imaginary component of a spectrum recorded after applying a radio wave pulse close to the precession frequency of nucleus 2. Note that the frequency offsets Ω_1 and Ω_2 are measured from different carrier frequencies (close to $\omega_{0,1}$ and $\omega_{0,2}$, respectively). The spectra are plotted so that the noise is the same in both spectra, the relative intensities correspond to a pair of ^{1}H (nucleus 1) and ^{13}C (nucleus 2). The value of J is the same in the top and bottom spectra.

the dream of the medieval alchemists, transmutation of chemical elements,[3] and is sometimes called the "spin alchemy".

Spin echoes are basic tools of the spin alchemy, consisting of a $180°$ (π) radio-wave pulse sandwiched by two delays of equal duration τ. In the case of a heteronuclear pair, we can apply the $180°$ pulse selectively to magnetic moment 1, to magnetic moment 2, or simultaneously to both (see Figure 10.2). Such a collection of spin echoes gives us the possibility to control evolution due to the chemical shift and due to the J-coupling separately. In the case of a homonuclear pair, the radio waves affect both magnetic moments simultaneously, as shown in Figure 10.2D.[4]

Below, we analyze three types of spin echoes applied to a heteronucler system (^{1}H and ^{13}C in our example). For the sake of simplicity, we do not discuss relaxation effects, although relaxation is usually observable. On the other hand, we have to extend the analyzed system to see how the echoes affect evolution due to the chemical shift differences. Therefore, we analyze *three pairs with different chemical shifts of the observed nucleus* in.

To see how the echoes influence polarization of the sample, we should compare the effect of the echoes with the free evolution. Evolution of a single homonuclear pair of magnetic moments in the presence of J-coupling was described in Section 10.4. To convert the description to our set of three heteronuclear pairs, we should follow the evolution of a density matrix starting from

$$\hat{\rho}(\text{a}) = \frac{1}{2^5}\mathscr{I}_t + \sum_{n=1}^{3}\frac{1}{2^5}\kappa_1\mathscr{I}_{nz} + \sum_{n=1}^{3}\frac{1}{2^5}\kappa_2\mathscr{S}_{nz}. \tag{10.24}$$

However, complexity of such analysis might obscure the effects of the analyzed spin echoes. Therefore, we write the evolution for one heteronuclear pair and depict the set of three pairs only in the graphical analysis, as shown in Figure 10.2A.

- $\hat{\rho}(\text{a}) = \frac{1}{2}\mathscr{I}_t + \frac{1}{2}\kappa_1\mathscr{I}_z + \frac{1}{2}\kappa_2\mathscr{S}_z$
  thermal equilibrium, the constants κ_1 and κ_2 are different because the nuclei have different γ.

- $\hat{\rho}(\text{b}) = \frac{1}{2}\mathscr{I}_t - \frac{1}{2}\kappa_1\mathscr{I}_y + \frac{1}{2}\kappa_2\mathscr{S}_z$
  90° pulse applied to nucleus I only

- $\hat{\rho}(\text{e}) = \frac{1}{2}\mathscr{I}_t + \frac{1}{2}\kappa_1\left(-c_1c_J\mathscr{I}_y + s_1c_J\mathscr{I}_x + c_1s_J2\mathscr{I}_x\mathscr{S}_z + s_1s_J2\mathscr{I}_y\mathscr{S}_z\right) + \frac{1}{2}\kappa_2\mathscr{S}_z$
  free evolution during 2τ ($t \to 2\tau$ in c_1 etc.)

---

[3]Transmutation of the mercury isotope $^{197}_{80}$Hg (which can be prepared from the stable isotope $^{198}_{80}$Hg) to a common isotope of gold $^{197}_{79}$Au is a nuclear reaction known as the electron capture: a proton in the nucleus absorbs an inner-shell electron, emits a neutrino ν_e and changes to neutron. Since proton and neutron can be described as different quantum states of an object called nucleon, the transmutation of mercury to gold can be viewed as a change of the quantum state. Interestingly, proton and neutron differ in the *isospin projection* quantum number I_3, whereas the quantum states manipulated in NMR spectroscopy differ in the *spin projection* quantum number s_z. The similar nomenclature is used to emphasize similar symmetry (the same mathematical description) of two different physical phenomena.

[4]If the chemical shift of nuclei in a homonuclear pair differ substantially, a selective application of $180°$ pulses to either magnetic moment is possible. In such a case, the power of the radio waves should be low, and their amplitude is often modulated during the pulse to achieve a higher selectivity (see Section 1.5.11).

The $2\mathscr{I}_x\mathscr{S}_z$, $2\mathscr{I}_y\mathscr{S}_z$ coherences give a zero trace when multiplied by $\mathscr{I}_+$ (they are not measurable per se), but *cannot be ignored* if the pulse sequence continues because they can *evolve* into measurable coherences later (note that the J-coupling Hamiltonian $2\pi J\mathscr{I}_z\mathscr{S}_z$ converts them to $\mathscr{I}_y$, $\mathscr{I}_x$, respectively).

The graphical "double-arrow" analysis in Figure 10.2A shows how the coherences evolve with different chemical shifts (arrows of different colors rotate with different frequency) and how is the evolution influenced by the J-coupling (solid arrows rotate slower[5] than dashed arrows of the same color).

10.7 Refocusing echo

The *refocusing echo* consists of a 90° pulse exciting magnetic moment 1 and a 180° pulse applied to the excited nucleus in the middle of the echo (see the schematic drawing in Figure 10.2B). The middle 180° pulse flips all arrows from left to right (rotation about the vertical axis x by 180°). The faster arrows start to evolve with a handicap at the beginning of the second delay τ and they reach the slower arrows at the end of the echo regardless of the actual speed of rotation.

Even without a detailed analysis of product operators, we see that the final state of the system does not depend on the chemical shift or on the J-coupling: the evolution due to both chemical shift and J-coupling is *refocused* during this echo.

The evolution of the density matrix can be guessed from the graphical analysis. The frequency of the applied radio waves resonates with the proton precession frequency and is far from the precession frequency of ^{13}C. Therefore, the magnetic moments of ^{13}C should stay in their equilibrium distribution, described by $\mathscr{I}_t$ and $\mathscr{S}_z$. The initial state of protons was described (after the 90° pulse) by $-\mathscr{I}_y$ in terms of product operators and by three arrows with the same $-y$ orientation. As all arrows only changed from the $-y$ direction to the $+y$ direction at the end of the echo, we can deduce that the final state of protons is $+\mathscr{I}_y$. Taken together, each pair of magnetic moment ends in the state described by

- $\hat{\rho}(\mathrm{e}) = \frac{1}{2}\mathscr{I}_t + \frac{1}{2}\kappa_1\mathscr{I}_y + \frac{1}{2}\kappa_2\mathscr{S}_z$

10.8 Decoupling echo

The *decoupling echo* consists of a 90° pulse exciting magnetic moment 1 and a 180° pulse applied to the other nucleus in the middle of the echo (see the schematic drawing in Figure 10.2C). The graphical analysis is shown in Figure 10.2C. The middle 180° is applied at the ^{13}C frequency. It does not affect proton coherences, depicted as arrows in Figure 10.2C, but *inverts longitudinal polarizations* (populations) of ^{13}C (solid arrows change to dashed ones and vice versa). The faster arrows become slower, the slower arrows become faster, and they meet at the end of the echo.

Without a detailed analysis of product operators, we see that the final state of the system does not depend on J-coupling (the difference between solid and dashed arrows disappeared) but the

---

[5]This is true for nuclei with $\gamma > 0$.

evolution due to the chemical shift took place (arrows of different colors rotated by different angles $2\Omega_1\tau$). As the effects of the J-coupling are masked, this echo is known as the *decoupling* echo.

We again derive the final density matrix from the graphical analysis. As the arrows at the end of the echo have the same orientations as if the nuclei were not coupled at all, we can deduce that the final state of protons is identical to the density matrix evolving due to the chemical shift only. Magnetic moments of the ^{13}C nuclei were affected only by the middle 180° pulse that *inverted* the longitudinal polarization. The density matrix at the end of the echo is

- $\hat{\rho}(\mathrm{e}) = \frac{1}{2}\mathscr{I}_t + \frac{1}{2}\kappa_1\left(c_1\mathscr{I}_y - s_1\mathscr{I}_x\right) - \frac{1}{2}\kappa_2\mathscr{S}_z$

10.9 Simultaneous echo

The last echo consists of a 90° pulse exciting magnetic moment 1 and 180° pulses applied to both nuclei in the middle of the echo (see the schematic drawing in Figure 10.2D). As both nuclei are affected, thye simultaneous echo can be applied to heteronuclear or homonuclear pairs. The homonuclear version includes one 180° pulse of radio waves with a frequency close to the precession frequency of both magnetic moments. In the heteronuclear variant, two 180° pulses are applied simultaneously to both nuclei. The graphical analysis of the heteronuclear application is shown in Figure 10.2D. The 180° pulses are applied at the ^{1}H and ^{13}C frequencies in the middle of the echo, resulting in a combination of both effects described in Figs. 10.2B and C. The proton pulse flips the arrows representing proton coherences and the ^{13}C pulse inverts the longitudinal polarizations (populations) of ^{13}C nuclei (solid arrows change to dashed ones and vice versa). As a result, the average direction of the dashed and solid arrows is refocused at the end of the echo but the difference due to the coupling is preserved (the handicapped arrows were made slower by the inversion of the longitudinal polarization of ^{13}C).

Without a detailed analysis of the product operators, we see that the effect of the chemical shift is removed (the average direction of arrows of the same color is just reversed), but the final state of the system depends on the J-coupling (the solid and dashed arrows collapsed). We can deduce from the graphical analysis that the final state of the density matrix is obtained by rotation "about" $2\mathscr{I}_z\mathscr{S}_z$, but not "about" $\mathscr{I}_z$ in the product operator space, and by changing the sign of the resulting coherences:

- $\hat{\rho}(\mathrm{e}) = \frac{1}{2}\mathscr{I}_t + \frac{1}{2}\kappa_1\left(c_J\mathscr{I}_y - s_J 2\mathscr{I}_x\mathscr{S}_z\right) - \frac{1}{2}\kappa_2\mathscr{S}_z$

HOMEWORK

Analyze the spin echoes (Sections 10.6–10.9).

10.10 SUPPORTING INFORMATION

10.10.1 Interaction between nuclei mediated by bond electrons

In principle, both orbital and spin magnetic moments of electrons can mediate the J-coupling, but the contribution of the orbital magnetic moments is usually negligible (coupling between hydrogen nuclei in water is an interesting exception). In order to describe the mediation of the J-coupling by the electron spin, we first investigate the interaction between electron and proton in the hydrogen atom.

A classical picture of interactions of nuclear and electronic spin magnetic moments is presented in Figure 10.6. The energy of the interaction between the (spin) magnetic moment of the nucleus $\vec{\mu}_\mathrm{n}$ and the magnetic field generated by the spin magnetic moment of the electron $\vec{B}_\mathrm{e}$ is given by (cf. Eq. 8.47)

$$\mathcal{E} = -\vec{\mu}_\mathrm{n} \cdot \vec{B}_\mathrm{e} = -\frac{\mu_0}{4\pi}\vec{\mu}_\mathrm{n} \cdot \vec{\nabla} \times \frac{\vec{\mu}_\mathrm{e} \times \vec{r}}{r^3} = -\frac{\mu_0}{4\pi}\vec{\mu}_\mathrm{n} \cdot \vec{\nabla} \times \left(\vec{\nabla} \times \frac{\vec{\mu}_\mathrm{e}}{r} \right). \tag{10.25}$$

In principle, the interaction with an electron does not differ from an interaction between two nuclear magnetic moments, described in Sections 8.1 and 8.9.1. Depending on the mutual orientation of the nucleus and the electron, the direction of $\vec{B}_\mathrm{e}$ varies (Figure 10.6A–C). If the distribution of electrons is spherically symmetric, or if the molecules tumble isotropically, the interactions of the spin magnetic moments of the electron and the nucleus average to zero. With one exception, depicted in Figure 10.6D. If the electron is present *exactly* at the nucleus, the vector of the electron spin magnetic moment $\vec{\mu}_\mathrm{e}$ has the same direction as $\vec{B}_\mathrm{e}$ and $\mathcal{E}$ is proportional to the scalar product $-\vec{\mu}_\mathrm{n} \cdot \vec{\mu}_\mathrm{e}$. The exact co-localization of the electron and the nucleus may look strange in the classical physics, but the interaction between the nucleus and an electron *inside* the nucleus can be simulated by a hypothetical current loop giving the correct magnetic moment when treated classically. To include the distribution of the electron around the nucleus into our classical model, the total energy of the integration must be calculated by integrating Eq. 10.25 over the electron coordinates. As mentioned above, the integral tends to zero for $r > 0$ in isotropic samples. However, the integral has a non-zero value in the limit $r \to 0$, as discussed e.g. in Abragam: The principles of nuclear magnetism, Oxford Press 1961, Chapter VI, Section II.A.

Here, we present a quantum-mechanical analysis, following the original paper by Fermi in Z. Phys. 60 (1930) 320–333. Fermi started from the eigenfunctions of the Dirac Hamiltonian for an electron in an electromagnetic field (Eq. 5.189) of nuclei of alkali metals. We investigate the simplest example, the ground state of hydrogen atom. The 1s atomic orbital of the hydrogen atom is particularly interesting because it has a non-zero value in the center, at the place of the nucleus (cf. Figure 10.1A). The eigenfunctions describing an electron in the 1s orbital[6] are

$$\Psi(1\mathrm{s}_{1/2},+1/2) = \frac{1}{\sqrt{\pi}}\left(\frac{\mu_0}{4\pi}\frac{Q^2mc^2}{\hbar^2}\right)^{\frac{3}{2}}\begin{pmatrix} \mathrm{e}^{-\frac{\mu_0}{4\pi}\frac{Q^2mc^2}{\hbar^2}r} \\ 0 \\ \frac{\mathrm{i}}{2}\frac{\mu_0}{4\pi}\frac{Q^2c}{\hbar}\cos\vartheta\,\mathrm{e}^{-\frac{\mu_0}{4\pi}\frac{Q^2mc^2}{\hbar^2}r} \\ \frac{\mathrm{i}}{2}\frac{\mu_0}{4\pi}\frac{Q^2c}{\hbar}\sin\vartheta\mathrm{e}^{\mathrm{i}\varphi}\,\mathrm{e}^{-\frac{\mu_0}{4\pi}\frac{Q^2mc^2}{\hbar^2}r} \end{pmatrix} = \begin{pmatrix} \psi \\ 0 \\ -\frac{\mathrm{i}}{2}\lambda_\mathrm{C}\frac{z}{r}\psi' \\ -\frac{\mathrm{i}}{2}\lambda_\mathrm{C}\frac{x+\mathrm{i}y}{r}\psi' \end{pmatrix}, \tag{10.26}$$

$$\Psi(1\mathrm{s}_{1/2},-1/2) = \frac{1}{\sqrt{\pi}}\left(\frac{\mu_0}{4\pi}\frac{Q^2mc^2}{\hbar^2}\right)^{\frac{3}{2}}\begin{pmatrix} 0 \\ -\mathrm{e}^{-\frac{\mu_0}{4\pi}\frac{Q^2mc^2}{\hbar^2}r} \\ -\frac{\mathrm{i}}{2}\frac{\mu_0}{4\pi}\frac{Q^2c}{\hbar}\sin\vartheta\mathrm{e}^{-\mathrm{i}\varphi}\,\mathrm{e}^{-\frac{\mu_0}{4\pi}\frac{Q^2mc^2}{\hbar^2}r} \\ \frac{\mathrm{i}}{2}\frac{\mu_0}{4\pi}\frac{Q^2c}{\hbar}\cos\vartheta\,\mathrm{e}^{-\frac{\mu_0}{4\pi}\frac{Q^2mc^2}{\hbar^2}r} \end{pmatrix} = \begin{pmatrix} 0 \\ -\psi \\ +\frac{\mathrm{i}}{2}\lambda_\mathrm{C}\frac{x-\mathrm{i}y}{r}\psi' \\ -\frac{\mathrm{i}}{2}\lambda_\mathrm{C}\frac{z}{r}\psi' \end{pmatrix}, \tag{10.27}$$

---

[6]Derivation of the Dirac or Schrödinger orbitals is beyond the scope of our course. It can be found in quantum chemistry textbooks. Here we only use the results, reviewed e.g. by Powel in J. Chem. Educ. 45 (1968) 558–563. Note that we use results of the original derivation for simple Coulombic potential (published in 1928). We ignore corrections of the interaction of the electron with its own field, that has to be made to achieve a good agreement with the experiment.

A   B   C   D
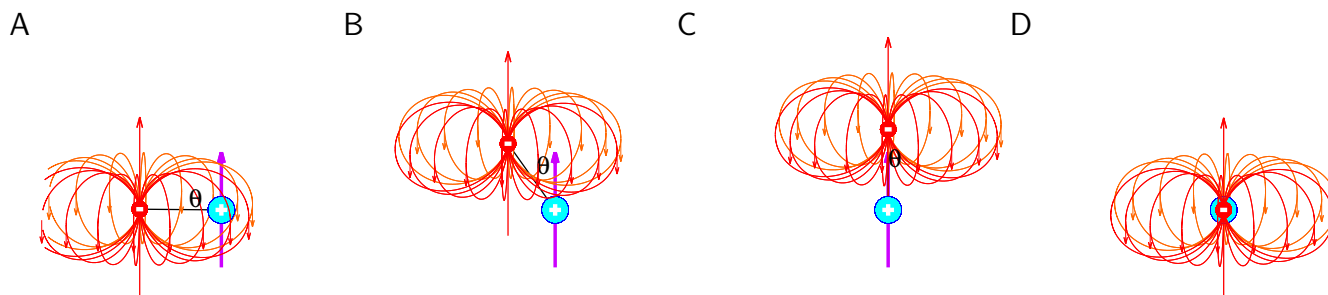
Figure 10.6: Classical description of interactions of nuclear and electronic spin magnetic moments.

where $\lambda_C = \hbar/(mc)$ is known as the Compton wavelength, ψ is the familiar non-relativistic (Schrödinger) orbital 1s, and $\psi' = \mathrm{d}\psi/\mathrm{d}r$. Note that the 1s orbital is a real wave function, i.e. $\psi^* = \psi$.

Contribution of the interaction between the magnetic moments of the nucleus and of the electron to the expected energy can be calculated by applying Eq. 4.8 to the spin magnetic part of the Hamiltonian in Eq. 5.189

$$\mathcal{E} = \int\limits_V \Psi^* Qc \left(-A_{\mathrm{n},x}\hat{\gamma}^0\hat{\gamma}^1 - A_{\mathrm{n},y}\hat{\gamma}^0\hat{\gamma}^2 - A_{\mathrm{n},z}\hat{\gamma}^0\hat{\gamma}^3\right) \Psi \ \mathrm{d}x \ \mathrm{d}y \ \mathrm{d}z, \tag{10.28}$$

where $\vec{A}_{\mathrm{n}}$ is the vector potential of the nucleus. Using Eq. 8.43, the vector potential can be expressed in terms of the nuclear magnetic moment and electron coordinates

$$\mathcal{E} = -\frac{\mu_0 Qc}{4\pi} \int\limits_V \frac{1}{r^3} \Psi^* \left((z\mu_{\mathrm{n},y} - y\mu_{\mathrm{n},z})\hat{\gamma}^0\hat{\gamma}^1 + (x\mu_{\mathrm{n},z} - z\mu_{\mathrm{n},x})\hat{\gamma}^0\hat{\gamma}^2 + (y\mu_{\mathrm{n},x} - x\mu_{\mathrm{n},y})\hat{\gamma}^0\hat{\gamma}^3\right) \Psi \ \mathrm{d}x \ \mathrm{d}y \ \mathrm{d}z. \tag{10.29}$$

The integral with $\Psi(1\mathrm{s}_{1/2}, +1/2)$ includes the following three terms

$$
\begin{aligned}
\Psi^* \frac{z\mu_{\mathrm{n},y} - y\mu_{\mathrm{n},z}}{r^3}\hat{\gamma}^0\hat{\gamma}^1\Psi &= \frac{z\mu_{\mathrm{n},y} - y\mu_{\mathrm{n},z}}{r^3} \begin{pmatrix} \psi & 0 & \frac{\mathrm{i}}{2}\lambda_C\frac{z}{r}\psi' & \frac{\mathrm{i}}{2}\lambda_C\frac{x-\mathrm{i}y}{r}\psi' \end{pmatrix} \begin{pmatrix} 0&0&0&1 \\ 0&0&1&0 \\ 0&1&0&0 \\ 1&0&0&0 \end{pmatrix} \begin{pmatrix} \psi \\ 0 \\ -\frac{\mathrm{i}}{2}\lambda_C\frac{z}{r}\psi' \\ -\frac{\mathrm{i}}{2}\lambda_C\frac{x+\mathrm{i}y}{r}\psi' \end{pmatrix} \\
&= \frac{z\mu_{\mathrm{n},y} - y\mu_{\mathrm{n},z}}{r^3} \begin{pmatrix} \psi & 0 & \frac{\mathrm{i}}{2}\lambda_C\frac{z}{r}\psi' & \frac{\mathrm{i}}{2}\lambda_C\frac{x-\mathrm{i}y}{r}\psi' \end{pmatrix} \begin{pmatrix} -\frac{\mathrm{i}}{2}\lambda_C\frac{x+\mathrm{i}y}{r}\psi' \\ -\frac{\mathrm{i}}{2}\lambda_C\frac{z}{r}\psi' \\ 0 \\ \psi \end{pmatrix} \\
&= \frac{z\mu_{\mathrm{n},y} - y\mu_{\mathrm{n},z}}{r^3} \left(-\frac{\mathrm{i}}{2}\lambda_C\frac{x+\mathrm{i}y}{r}\psi\psi' + \frac{\mathrm{i}}{2}\lambda_C\frac{x-\mathrm{i}y}{r}\psi\psi'\right) = \frac{z\mu_{\mathrm{n},y} - y\mu_{\mathrm{n},z}}{r^3}\lambda_C\frac{y}{r}\psi\psi' = \frac{yz\mu_{\mathrm{n},y} - y^2\mu_{\mathrm{n},z}}{r^4}\lambda_C\psi\psi',
\end{aligned}
\tag{10.30}
$$

$$
\begin{aligned}
\Psi^* \frac{x\mu_{\mathrm{n},z} - z\mu_{\mathrm{n},x}}{r^3}\hat{\gamma}^0\hat{\gamma}^2\Psi &= \frac{x\mu_{\mathrm{n},z} - z\mu_{\mathrm{n},x}}{r^3} \begin{pmatrix} \psi & 0 & \frac{\mathrm{i}}{2}\lambda_C\frac{z}{r}\psi' & \frac{\mathrm{i}}{2}\lambda_C\frac{x-\mathrm{i}y}{r}\psi' \end{pmatrix} \begin{pmatrix} 0&0&0&-\mathrm{i} \\ 0&0&\mathrm{i}&0 \\ 0&-\mathrm{i}&0&0 \\ \mathrm{i}&0&0&0 \end{pmatrix} \begin{pmatrix} \psi \\ 0 \\ -\frac{\mathrm{i}}{2}\lambda_C\frac{z}{r}\psi' \\ -\frac{\mathrm{i}}{2}\lambda_C\frac{x+\mathrm{i}y}{r}\psi' \end{pmatrix} \\
&= \frac{x\mu_{\mathrm{n},z} - z\mu_{\mathrm{n},x}}{r^3} \begin{pmatrix} \psi & 0 & \frac{\mathrm{i}}{2}\lambda_C\frac{z}{r}\psi' & \frac{\mathrm{i}}{2}\lambda_C\frac{x-\mathrm{i}y}{r}\psi' \end{pmatrix} \begin{pmatrix} -\frac{1}{2}\lambda_C\frac{x+\mathrm{i}y}{r}\psi' \\ +\frac{1}{2}\lambda_C\frac{z}{r}\psi' \\ 0 \\ \mathrm{i}\psi \end{pmatrix} \\
&= \frac{x\mu_{\mathrm{n},z} - z\mu_{\mathrm{n},x}}{r^3} \left(-\frac{1}{2}\lambda_C\frac{x+\mathrm{i}y}{r}\psi\psi' - \frac{1}{2}\lambda_C\frac{x-\mathrm{i}y}{r}\psi\psi'\right) = \frac{x\mu_{\mathrm{n},z} - z\mu_{\mathrm{n},x}}{r^3}\lambda_C\frac{-x}{r}\psi\psi' = \frac{xz\mu_{\mathrm{n},x} - x^2\mu_{\mathrm{n},z}}{r^3}\lambda_C\psi\psi',
\end{aligned}
\tag{10.31}
$$

$$
\begin{aligned}
\Psi^* \frac{y\mu_{\mathrm{n},x} - x\mu_{\mathrm{n},y}}{r^3}\hat{\gamma}^0\hat{\gamma}^3\Psi &= \frac{y\mu_{\mathrm{n},x} - x\mu_{\mathrm{n},y}}{r^3} \begin{pmatrix} \psi & 0 & \frac{\mathrm{i}}{2}\lambda_C\frac{z}{r}\psi' & \frac{\mathrm{i}}{2}\lambda_C\frac{x-\mathrm{i}y}{r}\psi' \end{pmatrix} \begin{pmatrix} 0&0&1&0 \\ 0&0&0&-1 \\ 1&0&0&0 \\ 0&-1&0&0 \end{pmatrix} \begin{pmatrix} \psi \\ 0 \\ -\frac{\mathrm{i}}{2}\lambda_C\frac{z}{r}\psi' \\ -\frac{\mathrm{i}}{2}\lambda_C\frac{x+\mathrm{i}y}{r}\psi' \end{pmatrix} \\
&= \frac{y\mu_{\mathrm{n},x} - x\mu_{\mathrm{n},y}}{r^3} \begin{pmatrix} \psi & 0 & \frac{\mathrm{i}}{2}\lambda_C\frac{z}{r}\psi' & \frac{\mathrm{i}}{2}\lambda_C\frac{x-\mathrm{i}y}{r}\psi' \end{pmatrix} \begin{pmatrix} -\frac{\mathrm{i}}{2}\lambda_C\frac{z}{r}\psi' \\ +\frac{\mathrm{i}}{2}\lambda_C\frac{x+\mathrm{i}y}{r}\psi' \\ \psi \\ 0 \end{pmatrix} \\
&= \frac{y\mu_{\mathrm{n},x} - x\mu_{\mathrm{n},y}}{r^3} \left(-\frac{\mathrm{i}}{2}\lambda_C\frac{z}{r}\psi\psi' + \frac{\mathrm{i}}{2}\lambda_C\frac{z}{r}\psi\psi'\right) = 0.
\end{aligned}
\tag{10.32}
$$

Inserting the results of Eqs. 10.30–10.32 into Eq. 10.29,

$$\mathcal{E} = \frac{\mu_0 Qc}{4\pi}\lambda_{\mathrm{C}}\int\limits_V \frac{1}{r^2}\left(\frac{x^2+y^2}{r^2}\mu_{\mathrm{n},z} - \frac{xz}{r^2}\mu_{\mathrm{n},x} - \frac{yz}{r^2}\mu_{\mathrm{n},y}\right)\psi\psi'\ \mathrm{d}x\mathrm{d}y\mathrm{d}z = \frac{\mu_0}{4\pi}\frac{Q\hbar}{m}\int\limits_V \frac{1}{r^2}\left(\frac{r^2-z^2}{r^2}\mu_{\mathrm{n},z} - \frac{xz}{r^2}\mu_{\mathrm{n},x} - \frac{yz}{r^2}\mu_{\mathrm{n},y}\right)\psi\psi'\ \mathrm{d}x\mathrm{d}y\mathrm{d}z.$$

(10.33)

Expressed in the spherical coordinates $x = r\sin\vartheta\cos\varphi$, $y = r\sin\vartheta\sin\varphi$, $z = r\cos\vartheta$, $\mathrm{d}V = \mathrm{d}x\mathrm{d}y\mathrm{d}z = r^2\sin\vartheta\mathrm{d}r\mathrm{d}\vartheta\mathrm{d}\varphi$,

$$\begin{aligned}
\mathcal{E} = {} & \frac{\mu_0}{4\pi}\frac{Q\hbar}{m}\mu_{\mathrm{n},z}\int\limits_0^{2\pi}\mathrm{d}\varphi\int\limits_0^{\pi}\sin\vartheta\mathrm{d}\vartheta(1-\cos^2\vartheta)\int\limits_0^{\infty}\psi(r)\psi'(r)\mathrm{d}r \\
& - \frac{\mu_0}{4\pi}\frac{Q\hbar}{m}\mu_{\mathrm{n},x}\int\limits_0^{2\pi}\mathrm{d}\varphi\cos\varphi\int\limits_0^{\pi}\sin\vartheta\mathrm{d}\vartheta\sin\vartheta\int\limits_0^{\infty}\psi(r)\psi'(r)\mathrm{d}r \\
& - \frac{\mu_0}{4\pi}\frac{Q\hbar}{m}\mu_{\mathrm{n},y}\int\limits_0^{2\pi}\mathrm{d}\varphi\sin\varphi\int\limits_0^{\pi}\sin\vartheta\mathrm{d}\vartheta\sin\vartheta\int\limits_0^{\infty}\psi(r)\psi'(r)\mathrm{d}r
\end{aligned}$$

(10.34)

Only the first term differs from zero because $\cos\varphi$ and $\sin\varphi$ are periodic functions and their integrals over the whole period

$$\int\limits_0^{2\pi}\mathrm{d}\varphi\cos\varphi = 0,\qquad \int\limits_0^{2\pi}\mathrm{d}\varphi\sin\varphi = 0.$$

(10.35)

The first term can be evaluated using the substitution $u = \cos\vartheta$, $\mathrm{d}u = -\sin\vartheta\mathrm{d}\vartheta$, and noting that

$$\frac{\mathrm{d}\rho(r)}{\mathrm{d}r} = \frac{\mathrm{d}|\psi(r)|^2}{\mathrm{d}r} \equiv \frac{\mathrm{d}\psi^2(r)}{\mathrm{d}r} = 2\psi\frac{\mathrm{d}\psi(r)}{\mathrm{d}r} = 2\psi(r)\psi'(r),$$

(10.36)

where $\rho(r)$ is the probability density of finding the electron at the distance r from the nucleus.
Therefore,

$$\mathcal{E} = \frac{\mu_0}{4\pi}\frac{Q\hbar}{m}\mu_{\mathrm{n},z}\int\limits_0^{2\pi}\mathrm{d}\varphi\int\limits_0^{\pi}\sin\vartheta\mathrm{d}\vartheta(1-\cos^2\vartheta)\int\limits_0^{\infty}\psi(r)\psi'(r)\mathrm{d}r = \frac{\mu_0}{4\pi}\frac{Q\hbar}{m}\mu_{\mathrm{n},z}2\pi\int\limits_{-1}^{1}(1-u^2)\mathrm{d}u\int\limits_{\rho(0)}^{\rho(\infty)}\frac{\mathrm{d}\rho(r)}{2} = \frac{\mu_0}{4\pi}\frac{Q\hbar}{m}\mu_{\mathrm{n},z}2\pi\left[u-\frac{u^3}{3}\right]_{-1}^{1}\left[\frac{\rho}{2}\right]_{\rho(0)}^{\rho(\infty)}.$$

(10.37)

As the probability of finding the electron at an infinite distance from the nucleus tends to zero,

$$\mathcal{E} = \frac{\mu_0}{4\pi}\frac{Q\hbar}{m}\mu_{\mathrm{n},z}\pi\left(2-\frac{2^3}{3}\right)\left(0-\frac{\rho(0)}{2}\right) = -\frac{\mu_0}{4\pi}\frac{Q\hbar}{m}\mu_{\mathrm{n},z}\frac{4\pi}{3}\rho(0) = -\frac{\mu_0 Q\hbar}{3m}\mu_{\mathrm{n},z}\rho(0).$$

(10.38)

Note that $Q\hbar/2m$ is the eigenvalue of the component of the magnetic moment of the electron parallel to the magnetic field. This time, it is the magnetic field of the nucleus ($\vec{B}_0$ does not play any role here). If we use the direction of $\vec{\mu}_{\mathrm{n}}$ as the z-axis of our coordinate system,

$$\mathcal{E} = -\frac{2}{3}\mu_0\rho(0)\vec{\mu}_{\mathrm{n}}\cdot\vec{\mu}_{\mathrm{e}}.$$

(10.39)

Accordingly, the corresponding Hamiltonian is

$$\hat{H}_{\mathrm{F}} = -\frac{2}{3}\mu_0\gamma_{\mathrm{n}}\gamma_{\mathrm{e}}\rho(0)\left(\hat{\vec{I}}_{\mathrm{n}}\cdot\hat{\vec{I}}_{\mathrm{e}}\right),$$

(10.40)

where $\hat{\vec{I}}_{\mathrm{n}}$ and $\hat{\vec{I}}_{\mathrm{e}}$ are operators of the spin of the nucleus and the electron, respectively, γ_{n} and γ_{e} are magnetogyric ratios of the spin of the nucleus and the electron, respectively, and the integral is equal to one inside the nucleus and to zero outside the nucleus. This type of interaction is known as the *Fermi contact interaction* and does not depend on the orientation of the molecule in the magnetic field, as documented by the scalar product in Eq. 10.40.

We can now proceed from the nucleus-electron interactions to interactions between two sigma-bonded nuclei mediated by electrons of the bond. The electrons in the bonding sigma orbital also have non-zero probability density at the positions of the nuclei (Figure 10.7). If the nuclei did not have any magnetic moments, the eigenfunction of the electrons is the linear combination $\frac{1}{\sqrt{2}}|\alpha\rangle\otimes|\beta\rangle - \frac{1}{\sqrt{2}}|\beta\rangle\otimes|\alpha\rangle$, as discussed in Section 10.10.2 and shown schematically in Figure 10.7A. Due to the Fermi interaction, the parallel orientation of the nuclear and electron spin magnetic moments (Figure 10.7B) has a lower energy and the opposite orientation (Figure 10.7C) has a higher energy than the unperturbed stationary state. Thus the orientation of the magnetic moment of the first nucleus is indirectly influenced by the orientation of the second magnetic moment: the energy is proportional to the scalar product $\vec{\mu}_1\cdot\vec{\mu}_2$, where $\vec{\mu}_1$ and $\vec{\mu}_2$ are the nuclear magnetic moments. The exact value of the energy depends on the actual distribution of the electrons in the bonding orbital, the calculation
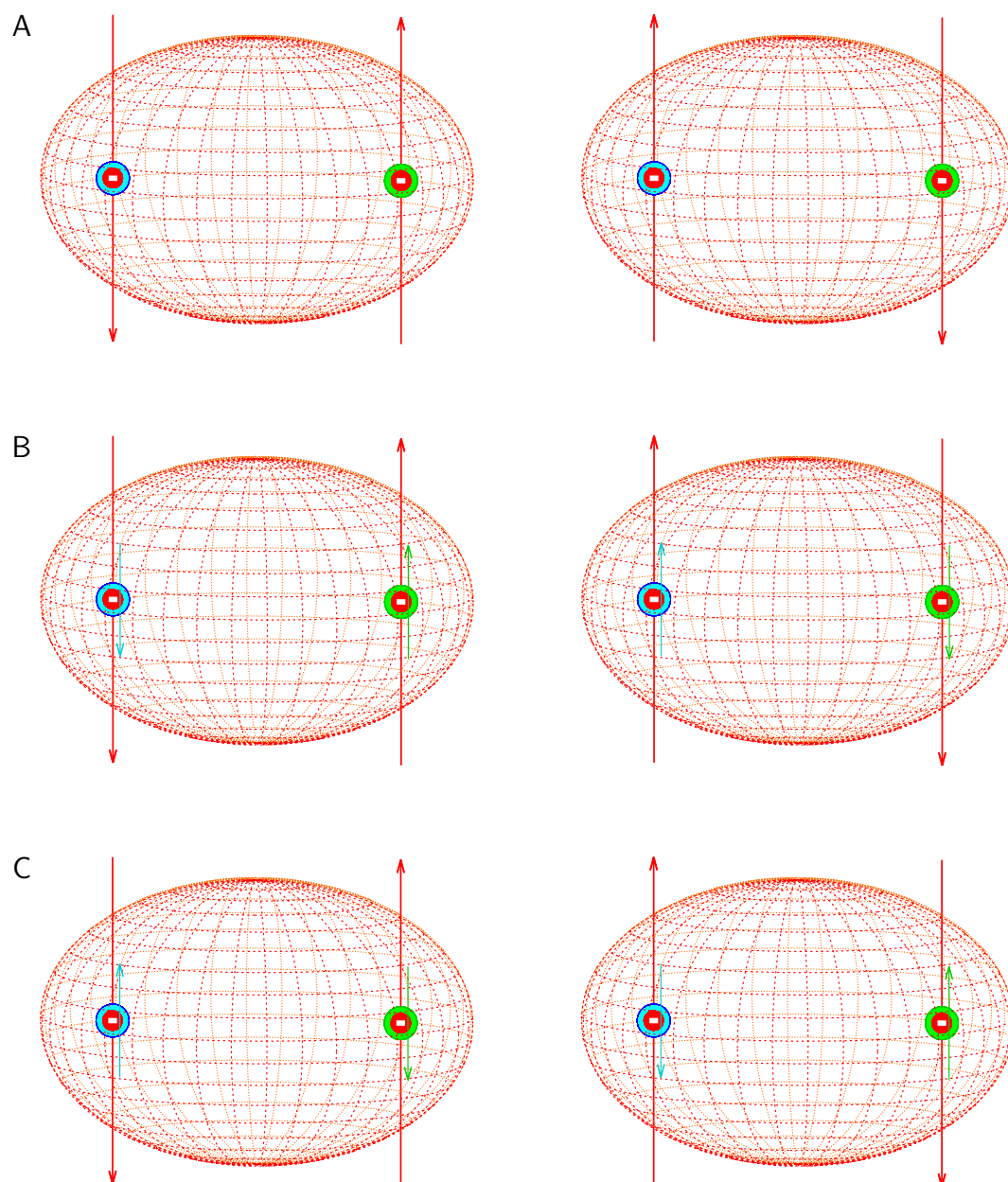
Figure 10.7: *J*-coupling. A, the stationary spin state of the electrons in the bonding sigma orbital without nuclear magnetic moments is a superposition of the $|\alpha\rangle \otimes |\beta\rangle$ and $|\beta\rangle \otimes \alpha|$ eigenstates (indicated by the opposite direction of the red arrows). B, energetically favorable state of electrons interacting with nuclear magnetic moments (green and cyan arrows). C, energetically unfavorable state of electrons interacting with nuclear magnetic moments.

of the energy requires advanced quantum chemical methods. Such methods can be applied to more complex systems too. In general, the described indirect interaction is described by the Hamiltonian

$$\hat{H}_J = \frac{2\pi}{\hbar}(\hat{I}_{1x}\hat{I}_{2x} + \hat{I}_{1y}\hat{I}_{2y} + \hat{I}_{1z}\hat{I}_{2z}), \tag{10.41}$$

where $2\pi J$ is a constant describing the strength of the indirect, electron mediated interaction and $\hat{I}_{nj}$ are operators of the components of the angular momenta of the nuclei.

10.10.2   Two electrons in a sigma orbital

A wave function describing two electrons must be antisymmetric, as stated in Section 6.7.1. Assuming that the spin degrees of freedom can be separated (see the discussion in Sections 6.1 and 6.7.3), we can decompose the wave function (i) into a symmetric non-spin part σ^{s} and an antisymmetric spin part ψ^{a}, or (ii) to an antisymmetric non-spin part σ^{a} and a symmetric spin part ψ^{s}. We try to express the spin wave function in a suitable basis. In the case of a single particle in a field described by the Hamiltonian $-\gamma B_0 \hat{I}_z$, we used a basis consisting of eigenfunctions of the operator $\hat{I}_z$, i.e., the eigenvectors $|\alpha\rangle = \begin{pmatrix} 1 \\ 0 \end{pmatrix}$ and $|\beta\rangle = \begin{pmatrix} 0 \\ 1 \end{pmatrix}$. These eigenvectors are also eigenfunctions of the operator of I^2 because the matrix representation of $\hat{I}^2$ is proportional to the unit matrix (see Eq. 5.11) and $\hat{1}\psi = \psi$ for any ψ. For a pair of two electrons, we could use the eigenfunctions of $\hat{I}_{1z}$, $\hat{I}_1^2$, $\hat{I}_{2z}$, and $\hat{I}_2^2$ (i.e., eigenvectors listed in Eq. 8.82). However, it is more useful to chose eigenfunctions of operators representing the z-component and the square of the *total spin angular momentum* $\vec{I} = \vec{I}_1 + \vec{I}_2$, in combination with $\hat{I}_1^2$ and $\hat{I}_2^2$. Note that all operators of the set $\hat{I}_1^2$, $\hat{I}_2^2$, $\hat{I}^2$, and $\hat{I}_z$ commute (the first two operators are proportional to the unit matrix that commutes with any matrix of the same size, commutation of the last two operators is given by Eq. 4.38). The explicit forms of the chosen operators are obtained using the matrix representations of the product operators in Tables 8.1 and 8.2:

$$\hat{I}_1^2 \psi_k = \frac{3\hbar^2}{4} \begin{pmatrix} 1 & 0 & 0 & 0 \\ 0 & 1 & 0 & 0 \\ 0 & 0 & 1 & 0 \\ 0 & 0 & 0 & 1 \end{pmatrix} \begin{pmatrix} c_{1k} \\ c_{2k} \\ c_{3k} \\ c_{4k} \end{pmatrix}, \tag{10.42}$$

$$\hat{I}_2^2 \psi_k = \frac{3\hbar^2}{4} \begin{pmatrix} 1 & 0 & 0 & 0 \\ 0 & 1 & 0 & 0 \\ 0 & 0 & 1 & 0 \\ 0 & 0 & 0 & 1 \end{pmatrix} \begin{pmatrix} c_{1k} \\ c_{2k} \\ c_{3k} \\ c_{4k} \end{pmatrix}, \tag{10.43}$$

$$\hat{I}^2 \psi_k = \left(\hat{\vec{I}}_1 + \hat{\vec{I}}_2 \right)^2 \psi_k = \left(\hat{I}_1^2 + \hat{I}_2^2 + 2\hat{\vec{I}}_1 \cdot \hat{\vec{I}}_2 \right) \psi_k =$$

$$= \left(\hat{I}_1^2 + \hat{I}_2^2 + 2\hat{I}_{1x}\hat{I}_{2x} + 2\hat{I}_{1y}\hat{I}_{2y} + 2\hat{I}_{1z}\hat{I}_{2z} \right) \psi_k = \hbar^2 \begin{pmatrix} 2 & 0 & 0 & 0 \\ 0 & 1 & 1 & 0 \\ 0 & 1 & 1 & 0 \\ 0 & 0 & 0 & 2 \end{pmatrix} \begin{pmatrix} c_{1k} \\ c_{2k} \\ c_{3k} \\ c_{4k} \end{pmatrix}, \tag{10.44}$$

$$\hat{I}_z \psi_k = \left(\hat{I}_{1z} + \hat{I}_{2z} \right) \psi_k = \hbar \begin{pmatrix} 1 & 0 & 0 & 0 \\ 0 & 0 & 0 & 0 \\ 0 & 0 & 0 & 0 \\ 0 & 0 & 0 & 1 \end{pmatrix} \begin{pmatrix} c_{1k} \\ c_{2k} \\ c_{3k} \\ c_{4k} \end{pmatrix}. \tag{10.45}$$

The eigenfunctions of $\hat{I}_{1z}$, $\hat{I}_1^2$, $\hat{I}_{2z}$, and $\hat{I}_2^2$ clearly cannot be eigenfunctions of the operator $\hat{I}^2$, represented by a non-diagonal matrix. Therefore, we have to look for a new basis, where the operator $\hat{I}^2$ is represented by a diagonal matrix $\hat{I}'^2$. For this purpose, we use a procedure that is not very elegant, but does not require any special approaches of matrix algebra.

From the mathematical point of view, we have to find a *transformation* matrix $\hat{T}$ so that

$$\hat{T}\hat{I}'^2 = \hat{I}^2 \hat{T}. \tag{10.46}$$

Then, the *diagonalized* matrix $\hat{I}'^2$ representing the $\hat{I}^2$ operator is obtained by multiplying the equation from left by a matrix $\hat{T}^{-1}$, inverse to $\hat{T}$ (i.e., $\hat{T}^{-1}\hat{T} = \hat{1}$):

$$\mathscr{H}' = \hat{T}^{-1}\mathscr{H}\hat{T}. \tag{10.47}$$

Multiplying by $\hat{T}$ from left gives

$$\hat{T}\mathscr{H}' = \mathscr{H}\hat{T}. \tag{10.48}$$

The desired eigenvalues are diagonal elements of the *diagonalized* matrix

$$\begin{pmatrix} \lambda_1' & 0 & 0 & 0 \\ 0 & \lambda_2' & 0 & 0 \\ 0 & 0 & \lambda_3' & 0 \\ 0 & 0 & 0 & \lambda_4' \end{pmatrix}. \tag{10.49}$$

The eigenvalues λ_k' and eigenvectors $|\psi_k'\rangle$ can be obtained by comparing the eigenvalue equation

$$\mathscr{H}'|\psi_k'\rangle = \omega_k'|\psi_k'\rangle \tag{10.50}$$

with the left-hand side of Eq. 10.48

$$\hat{T}\mathscr{H}' = \begin{pmatrix} T_{11} & T_{12} & T_{13} & T_{14} \\ T_{21} & T_{22} & T_{23} & T_{24} \\ T_{31} & T_{32} & T_{33} & T_{34} \\ T_{41} & T_{42} & T_{43} & T_{44} \end{pmatrix} \begin{pmatrix} \lambda_1' & 0 & 0 & 0 \\ 0 & \lambda_2' & 0 & 0 \\ 0 & 0 & \lambda_3' & 0 \\ 0 & 0 & 0 & \lambda_4' \end{pmatrix} = \begin{pmatrix} \lambda_1'T_{11} & \lambda_2'T_{12} & \lambda_3'T_{13} & \lambda_4'T_{14} \\ \lambda_1'T_{21} & \lambda_2'T_{22} & \lambda_3'T_{23} & \lambda_4'T_{24} \\ \lambda_1'T_{31} & \lambda_2'T_{32} & \lambda_3'T_{33} & \lambda_4'T_{34} \\ \lambda_1'T_{41} & \lambda_2'T_{42} & \lambda_3'T_{43} & \lambda_4'T_{44} \end{pmatrix}. \tag{10.51}$$

The eigenvalue equation can be written as a set of four equations for $k = 1, 2, 3, 4$

$$\mathscr{H}'|\psi_k'\rangle = \hbar^2 \begin{pmatrix} 2 & 0 & 0 & 0 \\ 0 & 1 & 1 & 0 \\ 0 & 1 & 1 & 0 \\ 0 & 0 & 0 & 2 \end{pmatrix} \begin{pmatrix} T_{1k} \\ T_{2k} \\ T_{3k} \\ T_{4k} \end{pmatrix} = \hbar^2 \begin{pmatrix} 2T_{1k} \\ T_{2k} + T_{3k} \\ T_{2k} + T_{3k} \\ 2T_{4k} \end{pmatrix} = \lambda_k' \begin{pmatrix} T_{1k} \\ T_{2k} \\ T_{3k} \\ T_{4k} \end{pmatrix} = \lambda_k'|\psi_k'\rangle. \tag{10.52}$$

The first row of the middle equality allows us to identify

$$\lambda_1' = 2\hbar^2 \tag{10.53}$$

if we set $T_{21} = T_{31} = T_{41} = 0$, i.e.,

$$|\psi_1'\rangle = \begin{pmatrix} T_{11} \\ 0 \\ 0 \\ 0 \end{pmatrix}. \tag{10.54}$$

Similarly,

$$\lambda_4' = 2\hbar^2 \tag{10.55}$$

for

$$|\psi_4'\rangle = \begin{pmatrix} 0 \\ 0 \\ 0 \\ T_{44} \end{pmatrix}. \tag{10.56}$$

The λ_2' and λ_3' values can be calculated from the equations

$$\lambda_k'T_{2k} = \hbar^2(T_{2k} + T_{3k}) \tag{10.57}$$
$$\lambda_k'T_{3k} = \hbar^2(T_{2k} + T_{3k}), \tag{10.58}$$

(setting $T_{12} = T_{42} = T_{13} = T_{43} = 0$).
T_{3k} can be expressed from the first equation

$$T_{3k} = \frac{\lambda_k' - \hbar^2}{\hbar^2} T_{2k} \tag{10.59}$$

and inserted into the second equation

$$\lambda_k' \frac{\lambda_k' - \hbar^2}{\hbar^2} T_{2k} = (\lambda_k' - \hbar^2)T_{2k} + \hbar^2 T_{2k} = \lambda_k' T_{2k}, \tag{10.60}$$

$$(\lambda_k')^2 - 2\hbar^2\lambda_k' = \lambda_k'(\lambda_k' - 2\hbar^2) = 0, \tag{10.61}$$

directly giving

$$\lambda_2' = 0, \qquad \lambda_3' = 2\hbar^2. \tag{10.62}$$

We have identified all diagonal elements of the diagonalized operator

$$\hat{I}'^2 = 2\hbar^2 \begin{pmatrix} 1 & 0 & 0 & 0 \\ 0 & 0 & 0 & 0 \\ 0 & 0 & 1 & 0 \\ 0 & 0 & 0 & 1 \end{pmatrix}. \tag{10.63}$$

The new basis is given by Eqs. 10.57, 10.58, and the normalization condition

$$\langle \psi'_k | \psi'_k \rangle = 1 \Rightarrow \sum_{j=1}^{4} T_{jk}^2 = 1. \tag{10.64}$$

The normalization condition immediately defines $T_{11} = T_{44} = 1$.
Substituting λ'_2 into Eqs. 10.57 and 10.58 gives

$$T_{22} + T_{32} = 0 \quad \Rightarrow \quad T_{22} = -T_{32}. \tag{10.65}$$

The normalization condition $1 = T_{22}^2 + T_{32}^2 = 2T_{22}^2$ requires

$$T_{22} = \frac{1}{\sqrt{2}}, \quad T_{32} = -\frac{1}{\sqrt{2}}. \tag{10.66}$$

Substituting λ'_3 into Eqs. 10.57 and 10.58 gives

$$2\hbar^2 T_{23} = \hbar^2 (T_{23} + T_{33}) \tag{10.67}$$
$$2\hbar^2 T_{33} = \hbar^2 (T_{23} + T_{33}) \tag{10.68}$$
$$\Rightarrow \quad T_{23} = T_{33}. \tag{10.69}$$

$$\Rightarrow \quad T_{23} = T_{23}. \tag{10.70}$$

The normalization condition $1 = T_{23}^2 + T_{33}^2 = 2T_{23}^2$ requires

$$T_{23} = \frac{1}{\sqrt{2}}, \quad T_{33} = \frac{1}{\sqrt{2}}. \tag{10.71}$$

Taken together, the new basis consists of the following eigenvectors

$$|\psi'_1\rangle = \begin{pmatrix} 1 \\ 0 \\ 0 \\ 0 \end{pmatrix} = |\alpha\rangle \otimes |\alpha\rangle, \ |\psi'_2\rangle = \begin{pmatrix} 0 \\ \frac{1}{\sqrt{2}} \\ -\frac{1}{\sqrt{2}} \\ 0 \end{pmatrix} = \frac{1}{\sqrt{2}}(|\alpha\rangle \otimes |\beta\rangle - |\beta\rangle \otimes |\alpha\rangle), \ |\psi'_3\rangle = \begin{pmatrix} 0 \\ \frac{1}{\sqrt{2}} \\ \frac{1}{\sqrt{2}} \\ 0 \end{pmatrix} = \frac{1}{\sqrt{2}}(|\alpha\rangle \otimes |\beta\rangle + |\beta\rangle \otimes |\alpha\rangle), \ |\psi'_4\rangle = \begin{pmatrix} 0 \\ 0 \\ 0 \\ 1 \end{pmatrix} = |\beta\rangle \otimes |\beta\rangle. \tag{10.72}$$

Among them, $|\psi'_1\rangle$, $|\psi'_3\rangle$, and $|\psi'_4\rangle$, are symmetric and are multiplied by the antisymmetric σ^{a}, whereas $|\psi'_2\rangle$ is antisymmetric and is multiplied by the symmetric σ^{s}. Calculations of the non-spin functions σ^{a} and σ^{s} is not easy[7] and requires advanced quantum chemistry. The result of such calculation is the *bonding sigma orbital* σ^{s} with a lower energy and the *antibonding sigma orbital* σ^{s} with a higher energy. Therefore, we are interested in $\sigma^{\mathrm{s}}|\psi'_2\rangle = \sigma^{\mathrm{s}}(|\alpha\rangle \otimes |\beta\rangle - |\beta\rangle \otimes |\alpha\rangle)/\sqrt{2}$ if we study the ground state of the molecule. The corresponding eigenvalues are $3\hbar^2/4$ for $\hat{I}_1^2$ and $\hat{I}_1^2$, zero for $\hat{I}^2$ and $\hat{I}_z$.

10.10.3 Classical analysis of two J-coupled polarizations

Although the physical origin of the J-coupling is a consequence of quantum behavior of electrons, the evolution of the macroscopic magnetization can be described classically. We have described precession of a magnetic moment $\vec{\mu}$ in a magnetic field $\vec{B}$ as (Eq. 51)

$$\frac{\mathrm{d}\vec{\mu}}{\mathrm{d}t} = \vec{\omega} \times \vec{\mu} = -\gamma \vec{B} \times \vec{\mu}. \tag{10.73}$$

As $\vec{\mu} = \gamma \vec{L}$,

$$\frac{\mathrm{d}\vec{L}}{\mathrm{d}t} = \vec{\omega} \times \vec{L} = -\gamma \vec{B} \times \vec{L}. \tag{10.74}$$

---

[7]The major difficulty is a mutual interaction of the electron charges.

We assume that the magnetic moment is placed in a strong homogeneous magnetic field $\vec{B}_0$ defining the direction of the axis z (a typical case in NMR). On sufficiently long time scales, effects of other, weaker fields, average to zero, unless the weak fields are oriented along $\vec{B}_0$ or rotate with a frequency close to $-\gamma \vec{B}_0$ (secular approximation). Therefore, orbital magnetic moments of electrons modify the field B_0 only by adding a small chemical shift, which can be described by changing B_0 to $(1+\delta)B_0$. If two magnetic moments are coupled, they are influenced not only by the external field $\vec{B}_0$, but also by a field proportional to the neighbor's magnetic moment

$$\frac{\mathrm{d}\vec{L}_1}{\mathrm{d}t} = -\gamma_1 \left((1+\delta_1)\vec{B}_0 + \zeta\vec{L}_2\right) \times \vec{L}_1 = -\gamma_1(1+\delta_1)\vec{B}_0 \times \vec{L}_1 + \zeta\vec{L}_2 \times \vec{L}_1 = -\gamma_1(1+\delta_1)\vec{B}_0 \times \vec{L}_1 - \zeta\vec{L}_1 \times \vec{L}_2 \tag{10.75}$$

$$\frac{\mathrm{d}\vec{L}_2}{\mathrm{d}t} = -\gamma_2 \left((1+\delta_2)\vec{B}_0 + \zeta\vec{L}_1\right) \times \vec{L}_2 = -\gamma_2(1+\delta_2)\vec{B}_0 \times \vec{L}_2 + \zeta\vec{L}_1 \times \vec{L}_2, \tag{10.76}$$

where ζ is a so far undefined coupling constant. As magnitudes of nuclear magnetic moments differ only in γ_1, γ_2, while $|L_1| = |L_2| = L$, we can divide both sides of the equations by L, and analyze rotation of dimensionless vectors $\vec{r}_1 = (x_1, y_1, z_1)$ and $\vec{r}_2 = (x_2, y_2, z_2)$, describing orientations of $\vec{\mu}_1$ and $\vec{\mu}_2$, respectively:

$$\frac{\mathrm{d}\vec{r}_1}{\mathrm{d}t} = -\gamma_1(1+\delta_1)\vec{B}_0 \times \vec{r}_1 - \zeta L\vec{r}_1 \times \vec{r}_2 = \vec{\omega}_{0,1} \times \vec{r}_1 - \pi J\vec{r}_1 \times \vec{r}_2 \tag{10.77}$$

$$\frac{\mathrm{d}\vec{r}_2}{\mathrm{d}t} = -\gamma_2(1+\delta_2)\vec{B}_0 \times \vec{r}_2 + \zeta L\vec{r}_1 \times \vec{r}_2 = \vec{\omega}_{0,2} \times \vec{r}_2 + \pi J\vec{r}_1 \times \vec{r}_2, \tag{10.78}$$

where we introduced the traditional symbols $\omega_{0,1}$, $\omega_{0,2}$, and πJ.
Writing the vector products explicitly,

$$\frac{\mathrm{d}x_1}{\mathrm{d}t} = -\omega_{0,1}y_1 - \pi Jy_1z_2 + \pi Jz_1y_2 \tag{10.79}$$

$$\frac{\mathrm{d}y_1}{\mathrm{d}t} = +\omega_{0,1}x_1 + \pi Jx_1z_2 - \pi Jz_1x_2 \tag{10.80}$$

$$\frac{\mathrm{d}z_1}{\mathrm{d}t} = -\pi Jx_1y_2 + \pi Jy_1x_2 \tag{10.81}$$

and

$$\frac{\mathrm{d}x_2}{\mathrm{d}t} = -\omega_{0,2}y_2 + \pi Jy_1z_2 - \pi Jz_1y_2 \tag{10.82}$$

$$\frac{\mathrm{d}y_2}{\mathrm{d}t} = +\omega_{0,2}x_2 - \pi Jx_1z_2 + \pi Jz_1x_2 \tag{10.83}$$

$$\frac{\mathrm{d}z_2}{\mathrm{d}t} = +\pi Jx_1y_2 - \pi Jy_1x_2. \tag{10.84}$$

In the case of the weak J-coupling, evolution on sufficiently long time scales is influenced only by vertical magnetic fields(secular approximation). Therefore, it is sufficient to neglect the effect of the horizontal fields (πJy_2 acting on $\vec{\mu}_1$ and πJy_1 acting on $\vec{\mu}_2$) and analyze only rotations about the z axis. The equations simplify to

$$\frac{\mathrm{d}x_1}{\mathrm{d}t} = -\omega_{0,1}y_1 - \pi Jy_1z_2 \tag{10.85}$$

$$\frac{\mathrm{d}y_1}{\mathrm{d}t} = +\omega_{0,1}x_1 + \pi Jx_1z_2 \tag{10.86}$$

$$\frac{\mathrm{d}z_1}{\mathrm{d}t} = 0 \tag{10.87}$$

and

$$\frac{\mathrm{d}x_2}{\mathrm{d}t} = -\omega_{0,2}y_2 - \pi Jz_1y_2 \tag{10.88}$$

$$\frac{\mathrm{d}y_2}{\mathrm{d}t} = +\omega_{0,2}x_2 + \pi Jz_1x_2 \tag{10.89}$$

$$\frac{\mathrm{d}z_2}{\mathrm{d}t} = 0. \tag{10.90}$$

In the NMR spectroscopy, we do not observe individual magnetic moments, but the bulk magnetization defined as

$$\vec{M}_n = \mathcal{N}\overline{\vec{\mu}_n} = \mathcal{N}\gamma_n\overline{\vec{L}_n} = \mathcal{N}\gamma_n L\overline{\vec{r}_n}, \tag{10.91}$$

where the bar indicates an ensemble average. Therefore, the ensemble-averaged terms $\overline{x_n}$, $\overline{x_n z_{n'}}$, $\overline{y_n}$, $\overline{y_n z_{n'}}$ should be followed to describe the evolution of weakly coupled magnetizations:

$$\frac{\mathrm{d}\overline{x_1}}{\mathrm{d}t} = -\omega_{0,1}\overline{y_1} - \pi J\overline{y_1 z_2} \tag{10.92}$$

$$\frac{\mathrm{d}\overline{y_1}}{\mathrm{d}t} = +\omega_{0,1}\overline{x_1} + \pi J\overline{x_1 z_2} \tag{10.93}$$

and

$$\frac{\mathrm{d}\overline{x_2}}{\mathrm{d}t} = -\omega_{0,2}\overline{y_2} - \pi J\overline{z_1 y_2} \tag{10.94}$$

$$\frac{\mathrm{d}\overline{y_2}}{\mathrm{d}t} = +\omega_{0,2}\overline{x_2} + \pi J\overline{z_1 x_2}. \tag{10.95}$$

We have two pairs of differential equations describing temporal changes of $\overline{x_1}, \overline{y_1}$ and $\overline{x_2}, \overline{y_2}$, but each pair includes four variables $(\overline{x_1}, \overline{y_1}, \overline{x_1 z_2}, \overline{y_1 z_2}$ and $\overline{x_2}, \overline{y_2}, \overline{z_1 x_2}, \overline{z_1 y_2})$. Therefore, we should look for another source of information about the temporal changes of the terms $\overline{x_1 z_2}, \overline{y_1 z_2}, \overline{z_1 x_2}, \overline{z_1 y_2}$. We take advantage of the fact that the motion of the magnetic moments in our case is rotation about the z axis. We will describe rotation of $\vec{\mu}_1$ and $\vec{\mu}_2$ in the spinor representation, introduced in Section 1.5.5. We express $\vec{r}_1$ and $\vec{r}_2$ in spherical coordinates

$$
\begin{aligned}
x_1 &= \sin\vartheta_1\cos\varphi_1 & x_2 &= \sin\vartheta_2\cos\varphi_2, \\
y_1 &= \sin\vartheta_1\sin\varphi_1 & y_2 &= \sin\vartheta_2\sin\varphi_2, \\
z_1 &= \cos\vartheta_1 & z_2 &= \cos\vartheta_2
\end{aligned} \tag{10.96}
$$

and represent the orientations by two-dimensional spinors according to Eq. 1.75

$$
\begin{pmatrix} a_1 \\ b_1 \end{pmatrix} = \begin{pmatrix} \cos\frac{\vartheta_1}{2}\mathrm{e}^{-\mathrm{i}\frac{\varphi_1}{2}} \\ \sin\frac{\vartheta_1}{2}\mathrm{e}^{+\mathrm{i}\frac{\varphi_1}{2}} \end{pmatrix} \qquad \begin{pmatrix} a_2 \\ b_2 \end{pmatrix} = \begin{pmatrix} \cos\frac{\vartheta_2}{2}\mathrm{e}^{-\mathrm{i}\frac{\varphi_2}{2}} \\ \sin\frac{\vartheta_2}{2}\mathrm{e}^{+\mathrm{i}\frac{\varphi_2}{2}} \end{pmatrix}. \tag{10.97}
$$

As we checked in Section 1.5.5, the spinor components really represent orientation vectors:

$$a_n a_n^* + b_n b_n^* = \cos^2\frac{\vartheta_n}{2} + \sin^2\frac{\vartheta_n}{2} = 1, \tag{10.98}$$

$$a_n a_n^* - b_n b_n^* = \cos^2\frac{\vartheta_n}{2} - \sin^2\frac{\vartheta_n}{2} = \cos\vartheta_n = z_n, \tag{10.99}$$

$$a_n b_n^* + b_n a_n^* = \sin\frac{\vartheta_n}{2}\cos\frac{\vartheta_n}{2}\left(\mathrm{e}^{-\mathrm{i}\varphi_n} + \mathrm{e}^{+\mathrm{i}\varphi_n}\right) = \sin\vartheta_n\cos\varphi_n = x_n, \tag{10.100}$$

$$a_n b_n^* - b_n a_n^* = \sin\frac{\vartheta_n}{2}\cos\frac{\vartheta_n}{2}\left(\mathrm{e}^{-\mathrm{i}\varphi_n} - \mathrm{e}^{+\mathrm{i}\varphi_n}\right) = -\mathrm{i}\sin\vartheta_n\sin\varphi_n = -\mathrm{i}y_n, \tag{10.101}$$

where $n = 1$ or $n = 2$. Combining the components of $\vec{r}_1$ and $\vec{r}_2$, we express the ensemble-averaged terms of Eqs. 10.92–10.95

$$\overline{x_1} = \overline{x_1 \cdot 1} = \overline{(a_1 b_1^* + b_1 a_1^*)(a_2 a_2^* + b_2 b_2^*)} = \overline{a_1 a_2 b_1^* a_2^*} + \overline{b_1 a_2 a_1^* a_2^*} + \overline{a_1 b_2 b_1^* b_2^*} + \overline{b_1 b_2 a_1^* b_2^*} = u_1 + u_1^* + v_1 + v_1^*, \tag{10.102}$$

$$-\overline{\mathrm{i}y_1} = -\overline{\mathrm{i}y_1 \cdot 1} = \overline{(a_1 b_1^* - b_1 a_1^*)(a_2 a_2^* + b_2 b_2^*)} = \overline{a_1 a_2 b_1^* a_2^*} - \overline{b_1 a_2 a_1^* a_2^*} + \overline{a_1 b_2 b_1^* b_2^*} - \overline{b_1 b_2 a_1^* b_2^*} = u_1 - u_1^* + v_1 - v_1^*, \tag{10.103}$$

$$\overline{x_1 z_2} = \overline{x_1 \cdot z_2} = \overline{(a_1 b_1^* + b_1 a_1^*)(a_2 a_2^* - b_2 b_2^*)} = \overline{a_1 a_2 b_1^* a_2^*} + \overline{b_1 a_2 a_1^* a_2^*} - \overline{a_1 b_2 b_1^* b_2^*} - \overline{b_1 b_2 a_1^* b_2^*} = u_1 + u_1^* - v_1 - v_1^*, \tag{10.104}$$

$$-\overline{\mathrm{i}y_1 z_2} = -\overline{\mathrm{i}y_1 \cdot z_2} = \overline{(a_1 b_1^* - b_1 a_1^*)(a_2 a_2^* - b_2 b_2^*)} = \overline{a_1 a_2 b_1^* a_2^*} - \overline{b_1 a_2 a_1^* a_2^*} - \overline{a_1 b_2 b_1^* b_2^*} + \overline{b_1 b_2 a_1^* b_2^*} = u_1 - u_1^* - v_1 + v_1^*, \tag{10.105}$$

$$\overline{x_2} = \overline{1 \cdot x_2} = \overline{(a_1 a_1^* + b_1 b_1^*)(a_2 b_2^* + b_2 a_2^*)} = \overline{a_1 a_2 a_1^* b_2^*} + \overline{b_1 a_2 b_1^* b_2^*} + \overline{a_1 b_2 a_1^* a_2^*} + \overline{b_1 b_2 b_1^* a_2^*} = u_2 + v_2 + u_2^* + v_2^*, \tag{10.106}$$

$$-\overline{\mathrm{i}y_1} = -\overline{1 \cdot \mathrm{i}y_2} = \overline{(a_1 a_1^* + b_1 b_1^*)(a_2 b_2^* - b_2 a_2^*)} = \overline{a_1 a_2 a_1^* b_2^*} + \overline{b_1 a_2 b_1^* b_2^*} - \overline{a_1 b_2 a_1^* a_2^*} - \overline{b_1 b_2 b_1^* a_2^*} = u_2 + v_2 - u_2^* - v_2^*, \tag{10.107}$$

$$\overline{z_1 x_2} = \overline{z_1 \cdot x_2} = \overline{(a_1 a_1^* - b_1 b_1^*)(a_2 b_2^* + b_2 a_2^*)} = \overline{a_1 a_2 a_1^* b_2^*} - \overline{b_1 a_2 b_1^* b_2^*} + \overline{a_1 b_2 a_1^* a_2^*} - \overline{b_1 b_2 b_1^* a_2^*} = u_2 - v_2 + u_2^* - v_2^*, \tag{10.108}$$

$$-\overline{\mathrm{i}z_1 y_2} = -\overline{\mathrm{i}z_1 \cdot y_2} = \overline{(a_1 a_1^* - b_1 b_1^*)(a_2 b_2^* - b_2 a_2^*)} = \overline{a_1 a_2 a_1^* b_2^*} - \overline{b_1 a_2 b_1^* b_2^*} - \overline{a_1 b_2 a_1^* a_2^*} + \overline{b_1 b_2 b_1^* a_2^*} = u_2 - v_2 - u_2^* + v_2^*, \tag{10.109}$$

The variables of the equations of motion Eqs. 10.92–10.95 are linear combinations of ensemble-averaged producst of the spinor components a_n, b_n, and of their complex conjugates. Note that the constituents of the ensemble-averaged products can be written a four components of a larger spinor

$$\begin{pmatrix} a_1 \\ b_1 \end{pmatrix} \otimes \begin{pmatrix} a_2 \\ b_2 \end{pmatrix} = \begin{pmatrix} a_1 a_2 \\ a_1 b_2 \\ b_1 a_2 \\ b_1 b_2 \end{pmatrix}. \tag{10.110}$$

Our goal is to describe how the orientations evolve in time. Since we decided to use a four-component spinor to represent the distributions of $\vec{L}_1$ and $\vec{L}_2$, we first describe a change of a spinor representing a single pair of $\vec{L}_1$ and $\vec{L}_2$. Such a change is described by some transformation matrix

$$\begin{pmatrix} a_1' a_2' \\ a_1' b_2' \\ b_1' a_2' \\ b_1' b_2' \end{pmatrix} = \begin{pmatrix} T_{aa\to aa} & T_{ab\to aa} & T_{ba\to aa} & T_{bb\to aa} \\ T_{aa\to ab} & T_{ab\to ab} & T_{ba\to ab} & T_{bb\to ab} \\ T_{aa\to ba} & T_{ab\to ba} & T_{ba\to ba} & T_{bb\to ba} \\ T_{aa\to bb} & T_{ab\to bb} & T_{ba\to bb} & T_{bb\to bb} \end{pmatrix} \begin{pmatrix} a_1 a_2 \\ a_1 b_2 \\ b_1 a_2 \\ b_1 b_2 \end{pmatrix}. \tag{10.111}$$

The spinor components are complex numbers and therefore the components of the transformation matrix are in general complex numbers as well. We can write the complex components of the transformation matrix in the exponential form

$$\begin{pmatrix} a_1' a_2' \\ a_1' b_2' \\ b_1' a_2' \\ b_1' b_2' \end{pmatrix} = \begin{pmatrix} A_{aa\to aa}e^{-i\varphi_{aa\to aa}/2} & A_{ab\to aa}e^{-i\varphi_{ab\to aa}/2} & A_{ba\to aa}e^{-i\varphi_{ba\to aa}/2} & A_{bb\to aa}e^{-i\varphi_{bb\to aa}/2} \\ A_{aa\to ab}e^{-i\varphi_{aa\to ab}/2} & A_{ab\to ab}e^{-i\varphi_{ab\to ab}/2} & A_{ba\to ab}e^{-i\varphi_{ba\to ab}/2} & A_{bb\to ab}e^{-i\varphi_{bb\to ab}/2} \\ A_{aa\to ba}e^{-i\varphi_{aa\to ba}/2} & A_{ab\to ba}e^{-i\varphi_{ab\to ba}/2} & A_{ba\to ba}e^{-i\varphi_{ba\to ba}/2} & A_{bb\to ba}e^{-i\varphi_{bb\to ba}/2} \\ A_{aa\to bb}e^{-i\varphi_{aa\to bb}/2} & A_{ab\to bb}e^{-i\varphi_{ab\to bb}/2} & A_{ba\to bb}e^{-i\varphi_{ba\to bb}/2} & A_{bb\to bb}e^{-i\varphi_{bb\to bb}/2} \end{pmatrix} \begin{pmatrix} a_1 a_2 \\ a_1 b_2 \\ b_1 a_2 \\ b_1 b_2 \end{pmatrix}, \tag{10.112}$$

where the phases $\varphi_{aa\to aa}$ etc. change the azimuths φ_1 and φ_2 of the vectors $\vec{r}_1$ and $\vec{r}_2$ and the amplitudes $A_{aa\to aa}$ change the inclinations ϑ_1 and ϑ_2 of the vectors $\vec{r}_1$ and $\vec{r}_2$, respectively.

We proceed to the evolution of the whole distributions of $\vec{L}_1$ and $\vec{L}_2$ in large ensembles of molecules. We write the ensemble averages $\overline{z_1}$, $\overline{z_2}$, and $\overline{z_1 z_2}$ as combinations of the spinor components:

$$\overline{z_1} = \overline{z_1 \cdot 1} = \overline{(a_1 a_1^* - b_1 b_1^*)(a_2 a_2^* + b_2 b_2^*)} = \overline{a_1 a_2 a_1^* a_2^*} - \overline{b_1 a_2 b_1^* a_2^*} + \overline{a_1 b_2 a_1^* b_2^*} - \overline{b_1 b_2 b_1^* b_2^*} = \overline{|a_1|^2|a_2|^2} - \overline{|b_1|^2|a_2|^2} + \overline{|a_1|^2|b_2|^2} - \overline{|b_1|^2|b_2|^2}, \tag{10.113}$$

$$\overline{z_2} = \overline{1 \cdot z_2} = \overline{(a_1 a_1^* + b_1 b_1^*)(a_2 a_2^* - b_2 b_2^*)} = \overline{a_1 a_2 a_1^* a_2^*} + \overline{b_1 a_2 b_1^* a_2^*} - \overline{a_1 b_2 a_1^* b_2^*} - \overline{b_1 b_2 b_1^* b_2^*} = \overline{|a_1|^2|a_2|^2} + \overline{|b_1|^2|a_2|^2} - \overline{|a_1|^2|b_2|^2} - \overline{|b_1|^2|b_2|^2}, \tag{10.114}$$

$$\overline{z_1 z_2} = \overline{z_1 \cdot z_2} = \overline{(a_1 a_1^* - b_1 b_1^*)(a_2 a_2^* - b_2 b_2^*)} = \overline{a_1 a_2 a_1^* a_2^*} - \overline{b_1 a_2 b_1^* a_2^*} - \overline{a_1 b_2 a_1^* b_2^*} + \overline{b_1 b_2 b_1^* b_2^*} = \overline{|a_1|^2|a_2|^2} - \overline{|b_1|^2|a_2|^2} - \overline{|a_1|^2|b_2|^2} + \overline{|b_1|^2|b_2|^2}. \tag{10.115}$$

Of course, the following combination is always constant

$$1 = 1 \cdot 1 = \overline{(a_1 a_1^* + b_1 b_1^*)(a_2 a_2^* + b_2 b_2^*)} = \overline{a_1 a_2 a_1^* a_2^*} + \overline{b_1 a_2 b_1^* a_2^*} + \overline{a_1 b_2 a_1^* b_2^*} + \overline{b_1 b_2 b_1^* b_2^*} = \overline{|a_1|^2|a_2|^2} + \overline{|b_1|^2|a_2|^2} + \overline{|a_1|^2|b_2|^2} + \overline{|b_1|^2|b_2|^2}. \tag{10.116}$$

As mentioned above, it is sufficient to analyze only effects of vertical fields for a weak J-coupling. Such fields do not change the ensemble-averaged z components of $\vec{L}_1$ and $\vec{L}_2$: $\overline{z_1}' = \overline{z_1}$, $\overline{z_2}' = \overline{z_2}$, but also $\overline{z_1 z_2}' = \overline{z_1 z_2}$, where $\overline{z_1}'$, $\overline{z_2}'$, and $\overline{z_1 z_2}'$ are the ensemble-averaged z components of $\vec{L}_1$, $\vec{L}_2$, and their product, respectively, after some evolution of the magnetic moment distributions.

All four combinations described by Eqs. 10.113–10.116 are constant when the spinor evolves due to vertical fields. As a consequence, *each of the following terms* must remain constant: $\overline{a_1 a_2 a_1^* a_2^*}$, $\overline{b_1 a_2 b_1^* a_2^*}$, $\overline{a_1 b_2 a_1^* b_2^*}$, and $\overline{b_1 b_2 b_1^* b_2^*}$. Let us now explore how these terms transform. We start with $\overline{a_1 a_2 a_1^* a_2^*}$, consisting of the spinor components $a_1 a_2$ and of its complex conjugates. A general transformation matrix transforms $a_1 a_2$ as

$$a_1' a_2' = T_{aa\to aa}a_1 a_2 + T_{ab\to aa}a_1 b_2 + T_{ba\to aa}b_1 a_2 + T_{bb\to aa}b_1 b_2. \tag{10.117}$$

Therefore,

$$\overline{a_1' a_2' a_1^{*\prime} a_2^{*\prime}} = \overline{(T_{aa\to aa}a_1 a_2 + T_{ab\to aa}a_1 b_2 + T_{ba\to aa}b_1 a_2 + T_{bb\to aa}b_1 b_2)(T_{aa\to aa}^* a_1^* a_2^* + T_{ab\to aa}^* a_1^* b_2^* + T_{ba\to aa}^* b_1^* a_2^* + T_{bb\to aa}^* b_1^* b_2^*)}. \tag{10.118}$$

In general, the transformation describes two types of motions: *stochastic motions*, influencing each magnetic moment differently, and *coherent motions* with the same effect on all magnetic moments. But we decided to describe only the coherent effect of the J-coupling in this section and to neglect relaxation, i.e., to neglect the stochastic motions. Therefore, we expect only coherent effects described by $T_{aa\to aa}$ etc. that are the same for magnetic moments in all molecules and can be thus factored out of the ensemble averaging:

$$
\overline{a'_1 a'_2 a_1^{*\prime} a_2^{*\prime}} = + T_{aa\to aa}T^*_{aa\to aa}\overline{a_1 a_2 a_1^* a_2^*} + T_{aa\to aa}T^*_{ab\to aa}\overline{a_1 a_2 a_1^* b_2^*} + T_{aa\to aa}T^*_{ba\to aa}\overline{a_1 a_2 b_1^* a_2^*} + T_{aa\to aa}T^*_{bb\to aa}\overline{a_1 a_2 b_1^* b_2^*}
$$
$$
+ T_{ab\to aa}T^*_{aa\to aa}\overline{a_1 b_2 a_1^* a_2^*} + T_{ab\to aa}T^*_{ab\to aa}\overline{a_1 b_2 a_1^* b_2^*} + T_{ab\to aa}T^*_{ba\to aa}\overline{a_1 b_2 b_1^* a_2^*} + T_{ab\to aa}T^*_{bb\to aa}\overline{a_1 b_2 b_1^* b_2^*}
$$
$$
+ T_{ba\to aa}T^*_{aa\to aa}\overline{b_1 a_2 a_1^* a_2^*} + T_{ba\to aa}T^*_{ab\to aa}\overline{b_1 a_2 a_1^* b_2^*} + T_{ba\to aa}T^*_{ba\to aa}\overline{b_1 a_2 b_1^* a_2^*} + T_{ba\to aa}T^*_{bb\to aa}\overline{b_1 a_2 b_1^* b_2^*}
$$
$$
+ T_{bb\to aa}T^*_{aa\to aa}\overline{b_1 b_2 a_1^* a_2^*} + T_{bb\to aa}T^*_{ab\to aa}\overline{b_1 b_2 a_1^* b_2^*} + T_{bb\to aa}T^*_{ba\to aa}\overline{b_1 b_2 b_1^* a_2^*} + T_{bb\to aa}T^*_{bb\to aa}\overline{b_1 b_2 b_1^* b_2^*}.
$$

$$(10.119)$$

But we know that $\overline{a'_1 a'_2 a_1^{*\prime} a_2^{*\prime}} = \overline{a_1 a_2 a_1^* a_2^*}$ because $\overline{a_1 a_2 a_1^* a_2^*}$ should remain constant. This requires $|T_{aa\to aa}|^2 = 1$ and all other combinations $T_{aa\to jk}T^*_{aa\to lm} = 0$. This is true only if the square $T_{aa\to aa}T^*_{aa\to aa} = |T_{aa\to aa}|^2 = 1$, requiring $A_{aa\to aa} = 1$, and all other amplitudes $A_{aa\to ab} = A_{aa\to ba} = A_{aa\to bb} = 0$. Similar arguments for $\overline{b_1 a_2 b_1^* a_2^*}$ $\overline{a_1 b_2 a_1^* b_2^*}$, and $\overline{b_1 b_2 b_1^* b_2^*}$ lead to the conclusion that $A_{aa\to aa} = A_{ab\to ab} = A_{ba\to ba} = A_{bb\to bb} = 1$ and all other amplitudes are equal to zero. Therefore, the transformation matrix has the form

$$
\begin{pmatrix} T_{aa\to aa} & T_{ab\to aa} & T_{ba\to aa} & T_{bb\to aa} \\ T_{aa\to ab} & T_{ab\to ab} & T_{ba\to ab} & T_{bb\to ab} \\ T_{aa\to ba} & T_{ab\to ba} & T_{ba\to ba} & T_{bb\to ba} \\ T_{aa\to bb} & T_{ab\to bb} & T_{ba\to bb} & T_{bb\to bb} \end{pmatrix} = \begin{pmatrix} e^{-i\varphi_{aa\to aa}/2} & 0 & 0 & 0 \\ 0 & e^{-i\varphi_{ab\to ab}/2} & 0 & 0 \\ 0 & 0 & e^{-i\varphi_{ba\to ba}/2} & 0 \\ 0 & 0 & 0 & e^{-i\varphi_{bb\to bb}/2} \end{pmatrix} \equiv \begin{pmatrix} e^{-i\frac{\varphi_{aa}}{2}} & 0 & 0 & 0 \\ 0 & e^{-i\frac{\varphi_{ab}}{2}} & 0 & 0 \\ 0 & 0 & e^{-i\frac{\varphi_{ba}}{2}} & 0 \\ 0 & 0 & 0 & e^{-i\frac{\varphi_{bb}}{2}} \end{pmatrix}.
$$

$$(10.120)$$

Since we need only the diagonal terms, we simplified the notation by replacing $\varphi_{aa\to aa}$ with φ_{aa} etc. We see that we can write the transformation of the spinor by vertical fields as

$$
\begin{pmatrix} a'_1 a'_2 \\ a'_1 b'_2 \\ b'_1 a'_2 \\ b'_1 b'_2 \end{pmatrix} = \begin{pmatrix} e^{-i\frac{\varphi_{aa}}{2}} & 0 & 0 & 0 \\ 0 & e^{-i\frac{\varphi_{ab}}{2}} & 0 & 0 \\ 0 & 0 & e^{-i\frac{\varphi_{ba}}{2}} & 0 \\ 0 & 0 & 0 & e^{-i\frac{\varphi_{bb}}{2}} \end{pmatrix} \begin{pmatrix} a_1 a_2 \\ a_1 b_2 \\ b_1 a_2 \\ b_1 b_2 \end{pmatrix}.
$$

$$(10.121)$$

Note that the effect of the vertical fields is limited to the phases φ_{jk} changing the azimuths φ_1 and φ_2, i.e., to rotations about z, as expected.

We started the classical analysis of the J-coupling by describing the evolution of the magnetization by the differential equations Eqs. 10.92–10.95. Therefore, we also convert Eq. 10.121 to a differential equation. The differential equation describing the evolution of the spinor can be derived by analyzing the rotation for a small time increment dt:

$$
\begin{pmatrix} a'_1 a'_2 \\ a'_1 b'_2 \\ b'_1 a'_2 \\ b'_1 b'_2 \end{pmatrix} = \begin{pmatrix} a_1 a_2 + d(a_1 a_2) \\ a_1 b_2 + d(a_1 b_2) \\ b_1 a_2 + d(b_1 a_2) \\ b_1 b_2 + d(b_1 b_2) \end{pmatrix} = \begin{pmatrix} e^{-i\frac{d\varphi_{aa}}{2}} & 0 & 0 & 0 \\ 0 & e^{-i\frac{d\varphi_{ab}}{2}} & 0 & 0 \\ 0 & 0 & e^{-i\frac{d\varphi_{ba}}{2}} & 0 \\ 0 & 0 & 0 & e^{-i\frac{d\varphi_{bb}}{2}} \end{pmatrix} \begin{pmatrix} a_1 a_2 \\ a_1 b_2 \\ b_1 a_2 \\ b_1 b_2 \end{pmatrix}.
$$

$$(10.122)$$

As $dt \to 0$, the exponential terms can be replaced by $1 - id\varphi_{aa}/2$, $1 - id\varphi_{ab}/2$, $1 - id\varphi_{ba}/2$, and $1 - id\varphi_{ab}/2$, respectively (Taylor's expansion), and the equation can be written as

$$
\begin{pmatrix} d(a_1 a_2) \\ d(a_1 b_2) \\ d(b_1 a_2) \\ d(b_1 b_2) \end{pmatrix} = \begin{pmatrix} 1 - i\frac{d\varphi_{aa}}{2} & 0 & 0 & 0 \\ 0 & 1 - i\frac{d\varphi_{ab}}{2} & 0 & 0 \\ 0 & 0 & 1 - i\frac{d\varphi_{ba}}{2} & 0 \\ 0 & 0 & 0 & 1 - i\frac{d\varphi_{bb}}{2} \end{pmatrix} \begin{pmatrix} a_1 a_2 \\ a_1 b_2 \\ b_1 a_2 \\ b_1 b_2 \end{pmatrix} - \begin{pmatrix} a_1 a_2 \\ a_1 b_2 \\ b_1 a_2 \\ b_1 b_2 \end{pmatrix} =
$$

$$(10.123)$$

$$
\begin{pmatrix} 1 - i\frac{d\varphi_{aa}}{2} & 0 & 0 & 0 \\ 0 & 1 - i\frac{d\varphi_{ab}}{2} & 0 & 0 \\ 0 & 0 & 1 - i\frac{d\varphi_{ba}}{2} & 0 \\ 0 & 0 & 0 & 1 - i\frac{d\varphi_{bb}}{2} \end{pmatrix} \begin{pmatrix} a_1 a_2 \\ a_1 b_2 \\ b_1 a_2 \\ b_1 b_2 \end{pmatrix} - \begin{pmatrix} 1 & 0 & 0 & 0 \\ 0 & 1 & 0 & 0 \\ 0 & 0 & 1 & 0 \\ 0 & 0 & 0 & 1 \end{pmatrix} \begin{pmatrix} a_1 a_2 \\ a_1 b_2 \\ b_1 a_2 \\ b_1 b_2 \end{pmatrix} = \begin{pmatrix} -i\frac{d\varphi_{aa}}{2} & 0 & 0 & 0 \\ 0 & -i\frac{d\varphi_{ab}}{2} & 0 & 0 \\ 0 & 0 & -i\frac{d\varphi_{ba}}{2} & 0 \\ 0 & 0 & 0 & -i\frac{d\varphi_{bb}}{2} \end{pmatrix} \begin{pmatrix} a_1 a_2 \\ a_1 b_2 \\ b_1 a_2 \\ b_1 b_2 \end{pmatrix}.
$$

$$(10.124)$$

Dividing by dt yields

$$
\frac{d}{dt} \begin{pmatrix} a_1 a_2 \\ a_1 b_2 \\ b_1 a_2 \\ b_1 b_2 \end{pmatrix} = \begin{pmatrix} -i\frac{d\varphi_{aa}}{2dt} & 0 & 0 & 0 \\ 0 & -i\frac{d\varphi_{ab}}{2dt} & 0 & 0 \\ 0 & 0 & -i\frac{d\varphi_{ba}}{2dt} & 0 \\ 0 & 0 & 0 & -i\frac{d\varphi_{bb}}{2dt} \end{pmatrix} \begin{pmatrix} a_1 a_2 \\ a_1 b_2 \\ b_1 a_2 \\ b_1 b_2 \end{pmatrix}.
$$

$$(10.125)$$

In order to identify the time derivatives $\mathrm{d}\varphi_{aa}/\mathrm{d}t$, $\mathrm{d}\varphi_{ab}/\mathrm{d}t$, $\mathrm{d}\varphi_{ba}/\mathrm{d}t$, and $\mathrm{d}\varphi_{bb}/\mathrm{d}t$, we use Eq. 10.125 to express the time derivatives of u_1, v_1, u_2, and v_2.

$$\frac{\mathrm{d}u_1}{\mathrm{d}t} = \overline{\frac{\mathrm{d}(a_1 a_2)}{\mathrm{d}t} b_1^* a_2^* + a_1 a_2 \frac{\mathrm{d}(b_1^* a_2^*)}{\mathrm{d}t}} = -\mathrm{i}\frac{\mathrm{d}\varphi_{aa}}{2\mathrm{d}t}\overline{a_1 a_2 b_1^* a_2^*} + \mathrm{i}\frac{\mathrm{d}\varphi_{ba}}{2\mathrm{d}t}\overline{a_1 a_2 b_1^* a_2^*} = -\mathrm{i}\left(\frac{\mathrm{d}\varphi_{aa}}{2\mathrm{d}t} - \frac{\mathrm{d}\varphi_{ba}}{2\mathrm{d}t}\right) u_1, \tag{10.126}$$

$$\frac{\mathrm{d}v_1}{\mathrm{d}t} = \overline{\frac{\mathrm{d}(a_1 b_2)}{\mathrm{d}t} b_1^* b_2^* + a_1 b_2 \frac{\mathrm{d}(b_1^* b_2^*)}{\mathrm{d}t}} = -\mathrm{i}\frac{\mathrm{d}\varphi_{ab}}{2\mathrm{d}t}\overline{a_1 b_2 b_1^* b_2^*} + \mathrm{i}\frac{\mathrm{d}\varphi_{bb}}{2\mathrm{d}t}\overline{a_1 a_2 b_1^* b_2^*} = -\mathrm{i}\left(\frac{\mathrm{d}\varphi_{ab}}{2\mathrm{d}t} - \frac{\mathrm{d}\varphi_{bb}}{2\mathrm{d}t}\right) v_1, \tag{10.127}$$

$$\frac{\mathrm{d}u_2}{\mathrm{d}t} = \overline{\frac{\mathrm{d}(a_1 a_2)}{\mathrm{d}t} a_1^* b_2^* + a_1 a_2 \frac{\mathrm{d}(a_1^* b_2^*)}{\mathrm{d}t}} = -\mathrm{i}\frac{\mathrm{d}\varphi_{aa}}{2\mathrm{d}t}\overline{a_1 a_2 a_1^* b_2^*} + \mathrm{i}\frac{\mathrm{d}\varphi_{ba}}{2\mathrm{d}t}\overline{a_1 a_2 a_1^* b_2^*} = -\mathrm{i}\left(\frac{\mathrm{d}\varphi_{aa}}{2\mathrm{d}t} - \frac{\mathrm{d}\varphi_{ab}}{2\mathrm{d}t}\right) u_2, \tag{10.128}$$

$$\frac{\mathrm{d}v_2}{\mathrm{d}t} = \overline{\frac{\mathrm{d}(b_1 a_2)}{\mathrm{d}t} b_1^* b_2^* + b_1 a_2 \frac{\mathrm{d}(b_1^* b_2^*)}{\mathrm{d}t}} = -\mathrm{i}\frac{\mathrm{d}\varphi_{ba}}{2\mathrm{d}t}\overline{b_1 a_2 b_1^* b_2^*} + \mathrm{i}\frac{\mathrm{d}\varphi_{bb}}{2\mathrm{d}t}\overline{b_1 a_2 b_1^* b_2^*} = -\mathrm{i}\left(\frac{\mathrm{d}\varphi_{ba}}{2\mathrm{d}t} - \frac{\mathrm{d}\varphi_{bb}}{2\mathrm{d}t}\right) v_2. \tag{10.129}$$

The time derivatives of the complex conjugates are obtained easily by changing the sign of the imaginary unit

$$\frac{\mathrm{d}u_1^*}{\mathrm{d}t} = = +\mathrm{i}\left(\frac{\mathrm{d}\varphi_{aa}}{2\mathrm{d}t} - \frac{\mathrm{d}\varphi_{ba}}{2\mathrm{d}t}\right) u_1^*, \tag{10.130}$$

$$\frac{\mathrm{d}v_1^*}{\mathrm{d}t} = = +\mathrm{i}\left(\frac{\mathrm{d}\varphi_{ab}}{2\mathrm{d}t} - \frac{\mathrm{d}\varphi_{bb}}{2\mathrm{d}t}\right) v_1^*, \tag{10.131}$$

$$\frac{\mathrm{d}u_2^*}{\mathrm{d}t} = = +\mathrm{i}\left(\frac{\mathrm{d}\varphi_{aa}}{2\mathrm{d}t} - \frac{\mathrm{d}\varphi_{ab}}{2\mathrm{d}t}\right) u_2^*, \tag{10.132}$$

$$\frac{\mathrm{d}v_2^*}{\mathrm{d}t} = = +\mathrm{i}\left(\frac{\mathrm{d}\varphi_{ba}}{2\mathrm{d}t} - \frac{\mathrm{d}\varphi_{bb}}{2\mathrm{d}t}\right) v_2^*. \tag{10.133}$$

Now we use Eqs. 10.102–10.109 to substitute $\overline{x_1}, \overline{y_1}, \overline{x_1 z_2}, \overline{y_1 z_2}$ and $\overline{x_2}, \overline{y_2}, \overline{z_1 x_2}, \overline{z_1 y_2}$ by u_n, v_n, u_n^*, v_n^* in Eqs. 10.92–10.95:

$$\frac{\mathrm{d}(u_1 + u_1^* + v_1 + v_1^*)}{\mathrm{d}t} = -\mathrm{i}\left(\frac{\mathrm{d}\varphi_{aa}}{2\mathrm{d}t} - \frac{\mathrm{d}\varphi_{ba}}{2\mathrm{d}t}\right)(u_1 - u_1^*) - \mathrm{i}\left(\frac{\mathrm{d}\varphi_{ab}}{2\mathrm{d}t} - \frac{\mathrm{d}\varphi_{bb}}{2\mathrm{d}t}\right)(v_1 - v_1^*) = -\mathrm{i}\left(\omega_{0,1} + \pi J\right)(u_1 - u_1^*) - \mathrm{i}\left(\omega_{0,1} - \pi J\right)(v_1 - v_1^*), \tag{10.134}$$

$$\frac{\mathrm{d}(u_2 + u_2^* + v_2 + v_2^*)}{\mathrm{d}t} = -\mathrm{i}\left(\frac{\mathrm{d}\varphi_{aa}}{2\mathrm{d}t} - \frac{\mathrm{d}\varphi_{ab}}{2\mathrm{d}t}\right)(u_2 - u_2^*) - \mathrm{i}\left(\frac{\mathrm{d}\varphi_{ba}}{2\mathrm{d}t} - \frac{\mathrm{d}\varphi_{bb}}{2\mathrm{d}t}\right)(v_2 - v_2^*) = -\mathrm{i}\left(\omega_{0,2} + \pi J\right)(u_2 - u_2^*) - \mathrm{i}\left(\omega_{0,2} - \pi J\right)(v_2 - v_2^*). \tag{10.135}$$

We immediately see that

$$\omega_{0,1} + \pi J = \frac{\omega_{aa} - \omega_{ba}}{2}, \tag{10.136}$$

$$\omega_{0,1} - \pi J = \frac{\omega_{ab} - \omega_{bb}}{2}, \tag{10.137}$$

$$\omega_{0,2} + \pi J = \frac{\omega_{aa} - \omega_{ab}}{2}, \tag{10.138}$$

$$\omega_{0,2} - \pi J = \frac{\omega_{ba} - \omega_{bb}}{2}. \tag{10.139}$$

This allows us to solve Eqs. 10.126–10.133

$$\frac{\mathrm{d}u_1}{\mathrm{d}t} = -\mathrm{i}\left(\omega_{0,1} + \pi J\right) u_1 \quad \Rightarrow \quad u_1 = u_{10}\mathrm{e}^{-\mathrm{i}(\omega_{0,1}+\pi J)t} = \overline{a_{10} b_{10}^* a_{20} a_{20}^*}\,\mathrm{e}^{-\mathrm{i}(\omega_{0,1}+\pi J)t} = \overline{\sin\frac{\vartheta_{10}}{2}\cos\frac{\vartheta_{10}}{2}\mathrm{e}^{-\mathrm{i}\varphi_{10}}\cos^2\frac{\vartheta_{20}}{2}}\,\mathrm{e}^{-\mathrm{i}(\omega_{0,1}+\pi J)t}, \tag{10.140}$$

$$\frac{\mathrm{d}v_1}{\mathrm{d}t} = -\mathrm{i}\left(\omega_{0,1} - \pi J\right) v_1 \quad \Rightarrow \quad v_1 = v_{10}\mathrm{e}^{-\mathrm{i}(\omega_{0,1}-\pi J)t} = \overline{a_{10} b_{10}^* b_{20} b_{20}^*}\,\mathrm{e}^{-\mathrm{i}(\omega_{0,1}-\pi J)t} = \overline{\sin\frac{\vartheta_{10}}{2}\cos\frac{\vartheta_{10}}{2}\mathrm{e}^{-\mathrm{i}\varphi_{10}}\sin^2\frac{\vartheta_{20}}{2}}\,\mathrm{e}^{-\mathrm{i}(\omega_{0,1}-\pi J)t}, \tag{10.141}$$

$$\frac{\mathrm{d}u_2}{\mathrm{d}t} = -\mathrm{i}\left(\omega_{0,2} + \pi J\right) u_2 \quad \Rightarrow \quad u_2 = u_{20}\mathrm{e}^{-\mathrm{i}(\omega_{0,2}+\pi J)t} = \overline{a_{20} b_{20}^* a_{20} a_{20}^*}\,\mathrm{e}^{-\mathrm{i}(\omega_{0,2}+\pi J)t} = \overline{\sin\frac{\vartheta_{20}}{2}\cos\frac{\vartheta_{20}}{2}\mathrm{e}^{-\mathrm{i}\varphi_{20}}\cos^2\frac{\vartheta_{20}}{2}}\,\mathrm{e}^{-\mathrm{i}(\omega_{0,2}+\pi J)t}, \tag{10.142}$$

$$\frac{\mathrm{d}v_2}{\mathrm{d}t} = -\mathrm{i}\left(\omega_{0,2} - \pi J\right) v_2 \quad \Rightarrow \quad v_2 = v_{20}\mathrm{e}^{-\mathrm{i}(\omega_{0,2}-\pi J)t} = \overline{a_{20} b_{20}^* b_{20} b_{20}^*}\,\mathrm{e}^{-\mathrm{i}(\omega_{0,2}-\pi J)t} = \overline{\sin\frac{\vartheta_{20}}{2}\cos\frac{\vartheta_{20}}{2}\mathrm{e}^{-\mathrm{i}\varphi_{20}}\sin^2\frac{\vartheta_{20}}{2}}\,\mathrm{e}^{-\mathrm{i}(\omega_{0,2}-\pi J)t}, \tag{10.143}$$

where $u_{n0}, v_{n0}, a_{n0}, b_{n0}, \vartheta_{n0}$, and φ_{n0} are the initial values of $u_n, v_n, a_n, b_n, \vartheta_n$, and φ_n, respectively. Using the standard trigonometric relations $\sin(2\vartheta) = 2\sin\vartheta\cos\vartheta$, $\cos(2\vartheta) = \cos^2\vartheta - \sin^2\vartheta = 2\cos^2\vartheta - 1$, definitions of spherical coordinates, and the Euler formula $e^{\pm i\varphi} = \cos\varphi \pm i\sin\varphi$,

$$
\begin{aligned}
u_1 &= \frac{1}{4}\overline{\sin\vartheta_{10}(\cos\varphi_{10} - i\sin\varphi_{10})(1+\cos\vartheta_{20})}e^{-i(\omega_{0,1}+\pi J)t} = \frac{1}{4}\overline{(x_{10}-iy_{10})(1+z_{20})}(\cos((\omega_{0,1}+\pi J)t) - i\sin((\omega_{0,1}+\pi J)t)) \\
&= \frac{1}{4}\overline{(x_{10}-iy_{10}+x_{10}z_{20}-iy_{10}z_{20})}\cos((\omega_{0,1}+\pi J)t) + \frac{1}{4}\overline{(-ix_{10}-y_{10}-ix_{10}z_{20}-y_{10}z_{20})}\sin((\omega_{0,1}+\pi J)t),
\end{aligned}
\tag{10.144}
$$

$$
\begin{aligned}
v_1 &= \frac{1}{4}\overline{\sin\vartheta_{10}(\cos\varphi_{10}-i\sin\varphi_{10})(1-\cos\vartheta_{20})}e^{-i(\omega_{0,1}-\pi J)t} = \frac{1}{4}\overline{(x_{10}-iy_{10})(1-z_{20})}(\cos((\omega_{0,1}+\pi J)t) - i\sin((\omega_{0,1}+\pi J)t)) \\
&= \frac{1}{4}\overline{(x_{10}-iy_{10}-x_{10}z_{20}+iy_{10}z_{20})}\cos((\omega_{0,1}-\pi J)t) + \frac{1}{4}\overline{(-ix_{10}-y_{10}+ix_{10}z_{20}+y_{10}z_{20})}\sin((\omega_{0,1}-\pi J)t).
\end{aligned}
\tag{10.145}
$$

Changing the sign of the imaginary unit,

$$
u_1^* = \frac{1}{4}\overline{(x_{10}+iy_{10}+x_{10}z_{20}+iy_{10}z_{20})}\cos((\omega_{0,1}+\pi J)t) + \frac{1}{4}\overline{(ix_{10}-y_{10}+ix_{10}z_{20}-y_{10}z_{20})}\sin((\omega_{0,1}+\pi J)t),
\tag{10.146}
$$

$$
v_1^* = \frac{1}{4}\overline{(x_{10}+iy_{10}-x_{10}z_{20}-iy_{10}z_{20})}\cos((\omega_{0,1}-\pi J)t) + \frac{1}{4}\overline{(ix_{10}-y_{10}+ix_{10}z_{20}+y_{10}z_{20})}\sin((\omega_{0,1}-\pi J)t).
\tag{10.147}
$$

Note that knowing the time evolution of u_1, u_1^*, v_1, and v_1^*, we can also write the differential equations describing the evolution of $\overline{x_1 z_2}$ and $\overline{y_1 z_2}$:

$$
\begin{aligned}
\frac{d\left(\overline{x_1 z_2} - i\overline{y_1 z_2}\right)}{dt} &= \frac{d(u_1 - v_1)}{dt} = -i(\omega_{0,1}+\pi J)u_1 + i(\omega_{0,1}-\pi J)v_1 = -i\omega_{0,1}(u_1-v_1) - i\pi J(u_1+v_1) \\
&= -i\omega_{0,1}\left(\overline{x_1 z_2} - i\overline{y_1 z_2}\right) - i\pi J\left(\overline{x_1} - i\overline{y_1}\right),
\end{aligned}
\tag{10.148}
$$

$$
\begin{aligned}
\frac{d\left(\overline{x_1 z_2} + i\overline{y_1 z_2}\right)}{dt} &= \frac{d(u_1^* - v_1^*)}{dt} = +i(\omega_{0,1}+\pi J)u_1^* - i(\omega_{0,1}-\pi J)v_1^* = +i\omega_{0,1}(u_1^*-v_1^*) + i\pi J(u_1^*+v_1^*) \\
&= +i\omega_{0,1}\left(\overline{x_1 z_2} + i\overline{y_1 z_2}\right) + i\pi J\left(\overline{x_1} + i\overline{y_1}\right).
\end{aligned}
\tag{10.149}
$$

The sum and the difference of these equations give

$$
\frac{d\overline{x_1 z_2}}{dt} = -\omega_{0,1}\overline{y_1 z_2} - \pi J\overline{y_1}
\tag{10.150}
$$

$$
\frac{d\overline{y_1 z_2}}{dt} = +\omega_{0,1}\overline{x_1 z_2} + \pi J\overline{x_1}.
\tag{10.151}
$$

The evolution of u_2, u_2^*, v_2, and v_2^* and consequently of $\overline{z_1 x_2}$ and $\overline{z_1 y_2}$ can be described in the same fashion.

We are now ready to analyze the evolution of the magnetization. In a first example, we examine the magnetization of the first nucleus in a heteronuclear pair after a $90°$ excitation pulse. $M_{1+} = M_{1x} + iM_{1y}$ is proportional to $\overline{x_1 + iy_1} = 2(u_1^* + v_1^*)$. After the $90°$ excitation pulse, the magnetic moments are polarized in the $-y$ direction. Therefore, $\overline{x_{10}} = 0$. If we assume that the equilibrium distributions of $\vec{\mu}_1$ and $\vec{\mu}_2$ are almost independent, then

$$
\overline{y_{10}z_{20}} = \overline{y_{10}} \cdot \overline{z_{20}} \ll \overline{y_{10}}
\tag{10.152}
$$

because the magnetic moments are very little polarized under the typical circumstances ($\overline{z_{20}} \ll 1$). We can therefore write

$$
\overline{x_1 + iy_1} = 2(u_1^* + v_1^*) = \frac{\overline{y_{10}}}{2}\left(i\cos((\omega_{0,1}+\pi J)t) + i\cos((\omega_{0,1}-\pi J)t) - \sin((\omega_{0,1}+\pi J)t) - \sin((\omega_{0,1}-\pi J)t)\right)
$$

$$
= i\frac{\overline{y_{10}}}{2}\left(\cos((\omega_{0,1}+\pi J)t) + \cos((\omega_{0,1}-\pi J)t) + i\sin((\omega_{0,1}+\pi J)t) + i\sin((\omega_{0,1}-\pi J)t)\right) = \frac{\overline{y_{10}}}{2}\underbrace{e^{i\frac{\pi}{2}}}_{i}\left(e^{i(\omega_{0,1}+\pi J)t} + e^{i(\omega_{0,1}-\pi J)t}\right),
\tag{10.153}
$$

which is the same result as obtained by analyzing the density matrix.

In a second example, we assume that M_{1+} first evolved for $t = 1/(2J)$. Then,

$$
\overline{x_1 + iy_1}\left(t = \frac{1}{2J}\right) = \frac{\overline{y_{10}}}{2}e^{+i\frac{\pi}{2}}\left(e^{+i\frac{\omega_{0,1}}{2J}+i\frac{\pi}{2}} + e^{+i\frac{\omega_{0,1}}{2J}-i\frac{\pi}{2}}\right) = \frac{\overline{y_{10}}}{2}e^{+i\frac{\omega_{0,1}}{2J}}\left(e^{+i\pi} + e^0\right) = \frac{\overline{y_{10}}}{2}e^{+i\frac{\omega_{0,1}}{2J}}(-1+1) = 0,
\tag{10.154}
$$

$$\overline{x_1 - \mathrm{i}y_1}\left(t = \frac{1}{2J}\right) = \frac{\overline{y_{10}}}{2}\mathrm{e}^{-\mathrm{i}\frac{\pi}{2}}\left(\mathrm{e}^{-\mathrm{i}\frac{\omega_{0,1}}{2J}-\mathrm{i}\frac{\pi}{2}} + \mathrm{e}^{-\mathrm{i}\frac{\omega_{0,1}}{2J}+\mathrm{i}\frac{\pi}{2}}\right) = \frac{\overline{y_{10}}}{2}\mathrm{e}^{-\mathrm{i}\frac{\omega_{0,1}}{2J}}\left(\mathrm{e}^{-\mathrm{i}\pi} + \mathrm{e}^0\right) = \frac{\overline{y_{10}}}{2}\mathrm{e}^{-\mathrm{i}\frac{\omega_{0,1}}{2J}}(-1+1) = 0, \qquad (10.155)$$

where we used $\mathrm{e}^{\mathrm{i}\frac{\pi}{2}} = \mathrm{i}$ and $\mathrm{e}^{\pm\mathrm{i}\pi} = -1$. As both $\overline{x_1 + \mathrm{i}y_1}$ and $\overline{x_1 - \mathrm{i}y_1}$ are equal to zero at $t = 1/(2J)$, $\overline{x_1} = \overline{y_1} = 0$ at $t = 1/(2J)$.
On the other hand,

$$\overline{x_1 z_2} = u_1 + u_1^* - v_1 - v_1^* = -\frac{\overline{y_{10}}}{2}\sin((\omega_{0,1} + \pi J)t) + \frac{\overline{y_{10}}}{2}\sin((\omega_{0,1} - \pi J)t), \qquad (10.156)$$

where we again neglected $\overline{y_{10}z_{20}} \ll \overline{y_{10}}$, and

$$\overline{x_1 z_2}\left(t = \frac{1}{2J}\right) = \frac{\overline{y_{10}}}{2}\left(-\sin\left(\frac{\omega_{0,1}}{2J} + \frac{\pi}{2}\right) + \sin\left(\frac{\omega_{0,1}}{2J} - \frac{\pi}{2}\right)\right) = -\overline{y_{10}}\cos\frac{\omega_{0,1}}{2J} \qquad (10.157)$$

because $\sin(\varphi \pm \pi/2) = \pm\cos\varphi$.
If we continue in a rotating coordinate frame and $\vec{M}_1$ is exactly on resonance ($\omega_{0,1} \to \Omega_1 = 0$),

$$\overline{x_1 z_2}\left(t = \frac{1}{2J}\right) = -\overline{y_{10}}. \qquad (10.158)$$

If we start to count time from this moment,[8] $\overline{x_{10}}' = \overline{y_{10}}' = 0$ and $\overline{x_{10}z_{20}}' = -\overline{y_{10}}' = 0$ but $\overline{y_{10}z_{20}}' \neq 0$. M_{1+} then evolves (Eqs. 10.146–10.147) as

$$\overline{x_1 + \mathrm{i}y_1} = 2(u_1^* + v_1^*) = \frac{\overline{y_{10}z_{20}}'}{2}\left(\mathrm{i}\cos((\omega_{0,1} + \pi J)t) - \mathrm{i}\cos((\omega_{0,1} - \pi J)t) - \sin((\omega_{0,1} + \pi J)t) + \sin((\omega_{0,1} - \pi J)t)\right)$$

$$= \mathrm{i}\frac{\overline{y_{10}z_{20}}'}{2}\left(\cos((\omega_{0,1} + \pi J)t) - \cos((\omega_{0,1} - \pi J)t) + \mathrm{i}\sin((\omega_{0,1} + \pi J)t) - \mathrm{i}\sin((\omega_{0,1} - \pi J)t)\right) = \frac{\overline{y_{10}z_{20}}'}{2}\mathrm{e}^{\mathrm{i}\frac{\pi}{2}}\left(\mathrm{e}^{\mathrm{i}(\omega_{0,1} + \pi J)t} - \mathrm{e}^{\mathrm{i}(\omega_{0,1} - \pi J)t}\right). \qquad (10.159)$$

We obtain the same result, corresponding to *anti-phase peaks*, as obtain in Section 11.2 by the analysis of the density matrix.

10.10.4 Comparison of classical and quantum analysis of J-coupling

We now try to compare how the classical analysis presented in Section 10.10.3 and quantum mechanical analysis describe relationship between energy of stationary states and precession frequency. We start by the classical treatment. We assume that a magnetic moment is placed in a strong homogeneous magnetic field $\vec{B}_0$ defining the direction of the axis z (a typical case in NMR). On sufficiently long time scales, effects of other, weaker fields, average to zero, unless the weak fields are oriented along $\vec{B}_0$ or rotate with a frequency close to $-\gamma\vec{B}_0$ (secular approximation).

Position of $\vec{\mu}$ in a magnetic field $\vec{B}$, composed of $\vec{B}_0$ and a z-component of an additional weak field, changes as $\vec{\mu}$ precesses about the z-axis with a frequency (Eq. 20)

$$\omega = -\gamma B_z = -\gamma|B|. \qquad (10.160)$$

The only exceptions are two *stationary states*, when $\vec{\mu}$ is oriented in the same direction as $\vec{B}$ or in the direction opposite to $\vec{B}$. The former stationary state of $\vec{\mu}$ (labeled here as $\vec{\mu}_a$) corresponds to a spinor with $a = 1$ and $b = 0$ (therefore, $z = aa^* - bb^* = 1$) and has an energy (Eqs. 6 and 19)

$$\mathcal{E}_a = -\vec{B}\cdot\vec{\mu}_a = -\gamma\vec{B}\cdot\vec{L}_a = -\gamma B_z L_{a,z} = \omega L_{a,z} = -\omega L. \qquad (10.161)$$

The latter stationary state of $\vec{\mu}$ (labeled here as $\vec{\mu}_b = -\vec{\mu}_a$) corresponds to a spinor with $a = 0$ and $b = 1$ (therefore, $z = aa^* - bb^* = -1$) and has an energy

$$\mathcal{E}_b = -\vec{B}\cdot\vec{\mu}_b = -\gamma\vec{B}\cdot\vec{L}_b = -\gamma B_z L_{b,z} = \omega L_{b,z} = +\omega|L|. \qquad (10.162)$$

If we compare Eqs.10.160, 10.161, and 10.162, we obtain

$$\mathcal{E}_b - \mathcal{E}_a = \omega(\omega L_{b,z} - \omega L_{a,z}) = \omega\Delta L_z = \omega(2|L|). \qquad (10.163)$$

As we have described in Section 5.5, relativistic quantum mechanics also reveals existence of two quantum states ($|\alpha\rangle$ and $|\beta\rangle$) of a spin magnetic moment of an electron (and similar particles) in a homogeneous magnetic field. A result of measuring z-component of spin angular momentum must be one of two eigenvalues of the operator $\hat{I}_z$, i.e., $+\hbar/2$ or $-\hbar/2$, related to two eigenvalues of the spin Hamiltonian $\hat{H} = -\gamma B_z\hat{I}_z$:

$$\mathcal{E}_\alpha = -\gamma B_z I_{\alpha,z} = -\gamma B_z\frac{\hbar}{2}, \qquad (10.164)$$

---

[8]We label the values at $t = 1/(2J)$ as $\overline{x_{10}}', \overline{y_{10}}', \overline{x_{10}z_{20}}', \overline{y_{10}z_{20}}'$.

$$\mathcal{E}_\beta = -\gamma B_z I_{\beta,z} = +\gamma B_z \frac{\hbar}{2}. \tag{10.165}$$

The energy difference $\mathcal{E}_\beta - \mathcal{E}_\alpha$ is related to the precession frequency of a spin magnetic moment in a general (superposition) state as

$$\mathcal{E}_\beta - \mathcal{E}_\alpha = -\gamma B_z(I_{\beta,z} - I_{\alpha,z}) = \omega(I_{\beta,z} - I_{\alpha,z}) = \omega \Delta I_z = \omega \hbar. \tag{10.166}$$

We see that the classical and quantum results differ only in the value of ΔL_z (equal to $2|L|$) vs. ΔI_z (equal to $\hbar = 2|I|/\sqrt{3}$).

10.10.5 J-coupling compared to classical coupled oscillators

To see relation between J-coupling and coupling discussed in classical physics, we analyze obviously classical coupled systems: two coupled oscillators or pendulums. Let us consider two equal masses m attached to walls with springs of the stiffness $k_1 = k_2 = k$ and connected with another spring of the stiffness k_{12}:

$$| \cdots\cdots k_1 \cdots\cdots (m) \cdots\cdots k_{12} \cdots\cdots (m) \cdots\cdots k_2 \cdots\cdots |$$

The horizontal displacements x_1 and x_2, respectively, of the masses from their equilibrium positions can be calculated from the second Newton's law:

$$F_1 = ma_1 = m\frac{\mathrm{d}^2 x_1}{\mathrm{d}t^2} \qquad F_2 = ma_2 = m\frac{\mathrm{d}^2 x_2}{\mathrm{d}t^2}. \tag{10.167}$$

If both masses move together ($x_1 = x_2$), the middle spring does not get stretched or compressed and both masses just experience the forces of the outer springs

$$F_1 = -k_1 x_1 = -k x_1 \qquad F_2 = -k_2 x_2 = -k x_2. \tag{10.168}$$

As $x_1 = x_2$, both masses experience the same force $F_1 = F_2$. Therefore,

$$F_1 + F_2 = m\frac{\mathrm{d}^2 x_+}{\mathrm{d}t^2} = -k x_+, \qquad F_1 - F_2 = 0 = m\frac{\mathrm{d}^2 x_-}{\mathrm{d}t^2} = -k x_- \tag{10.169}$$

where $x_+ = x_1 + x_2$ and $x_- = x_1 - x_2$. The second derivatives of sine and cosine functions are proportional to the sine and cosine functions themselves:

$$\frac{\mathrm{d}^2}{\mathrm{d}t^2}\sin(\omega_+ t) = \frac{\mathrm{d}}{\mathrm{d}t}\left(\frac{\mathrm{d}\sin(\omega_+ t)}{\mathrm{d}t}\right) = \frac{\mathrm{d}}{\mathrm{d}t}(\omega_+ \cos(\omega_+ t)) = -\omega_+^2 \sin(\omega_+ t), \tag{10.170}$$

$$\frac{\mathrm{d}^2}{\mathrm{d}t^2}\cos(\omega_+ t) = \frac{\mathrm{d}}{\mathrm{d}t}\left(\frac{\mathrm{d}\cos(\omega_+ t)}{\mathrm{d}t}\right) = \frac{\mathrm{d}}{\mathrm{d}t}(-\omega_+ \sin(\omega_+ t)) = -\omega_+^2 \cos(\omega_+ t). \tag{10.171}$$

The solution of our differential equation can be thus written in a form

$$x_+ = A_+ \sin(\omega_+ t) + B_+ \cos(\omega_+ t). \tag{10.172}$$

The coefficients A_+, B_+ can be obtained from the initial conditions. If we start measurement from the time when both masses pass their equilibrium positions ($x_1 = x_2 = 0$ at $t = 0$),

$$x_+(t = 0) = 0 = A_+ \sin(0) + B_+ \cos(0) = B_+ \tag{10.173}$$

and

$$x_+ = A_+ \sin(\omega_+ t). \tag{10.174}$$

Differentiation

$$\frac{\mathrm{d}^2 x_+}{\mathrm{d}t^2} = A_+ \frac{\mathrm{d}^2 \sin(\omega_+ t)}{\mathrm{d}t^2} = -A_+ \omega_+^2 \sin(\omega_+ t) = -\omega_+^2 x_+ = -\frac{k}{m} x_+ \tag{10.175}$$

shows that

$$\omega_+ = \sqrt{\frac{k}{m}}. \tag{10.176}$$

Motions of individual masses can be back-calculated from the evaluated x_+ and from the fact that $x_- = 0$:

$$x_1 = \frac{1}{2}(x_+ + x_-) = \frac{A_+}{2}\sin(\omega_+ t), \qquad x_2 = \frac{1}{2}(x_+ - x_-) = \frac{A_+}{2}\sin(\omega_+ t). \tag{10.177}$$

If the masses move exactly in the opposite directions (anti-phase), the stiffness of the middle spring k_{12} increases the forces $F_1 = -F_2$ experienced by both masses

$$F_1 = -(k_1 + k_{12})x_1 = -(k + k_{12})x_1 \qquad\qquad F_2 = -F_1 = (k_2 + k_{12})x_2 = (k + k_{12})x_2 \qquad (10.178)$$

and

$$F_1 - F_2 = m\frac{\mathrm{d}^2 x_-}{\mathrm{d}t^2} = -(k + 2k_{12})x_-, \qquad\qquad F_1 + F_2 = 0 = m\frac{\mathrm{d}^2 x_+}{\mathrm{d}t^2}. \qquad (10.179)$$

The solution is

$$x_- = A_- \sin(\omega_- t) + B_- \cos(\omega_- t). \qquad (10.180)$$

If we start again from equilibrium positions ($x_1 = x_2 = 0$ at $t = 0$),

$$x_-(t = 0) = 0 = A_- \sin(0) + B_- \cos(0) = B_-, \qquad (10.181)$$

$$x_- = A_- \sin(\omega_- t), \qquad (10.182)$$

$$\frac{\mathrm{d}^2 x_-}{\mathrm{d}t^2} = A_- \frac{\mathrm{d}^2 \sin(\omega_- t)}{\mathrm{d}t^2} = -A_- \omega_-^2 \sin(\omega_- t) = -\omega_-^2 x_- = -\frac{k + 2k_{12}}{m} x_-, \qquad (10.183)$$

and

$$\omega_- = \sqrt{\frac{k + 2k_{12}}{m}}. \qquad (10.184)$$

Motions of individual masses are now calculated from the evaluated x_- and from the fact that $x_+ = 0$:

$$x_1 = \frac{1}{2}(x_+ + x_-) = +\frac{A_-}{2}\sin(\omega_+ t), \qquad\qquad x_2 = \frac{1}{2}(x_+ - x_-) = -\frac{A_-}{2}\sin(\omega_+ t). \qquad (10.185)$$

The two discussed modes of motions (in-phase and anti-phase oscillations) are *stationary*. The masses move with constant frequencies and amplitudes. All other modes (e.g. starting with the left mass in the equilibrium and the right mass displaced) exhibit *beats*, double oscillations with combinations of ω_+ and ω_-.

For example, if we start from

$$x_1(0) = A, \qquad\qquad x_2(0) = 0, \qquad (10.186)$$

the initial conditions are

$$x_+(0) = A_+ \sin(\omega_+ 0) + B_+ \cos(\omega_+ 0) = x_1(0) + x_2(0) = \frac{A}{2}, \qquad\qquad x_-(0) = A_- \sin(\omega_- 0) + B_- \cos(\omega_- 0) = x_1(0) - x_2(0) = \frac{A}{2}, \quad (10.187)$$

telling us that $A_+ = A_- = 0$ and $B_+ = B_- = A$. The individual masses move as

$$\begin{aligned}
x_1 &= \frac{1}{2}(x_+ + x_-) = \frac{A}{2}\left(\cos(\omega_+ t) + \cos(\omega_- t)\right) = \frac{A}{2}\left(\cos\left(\frac{\omega_+ + \omega_-}{2}t + \frac{\omega_+ - \omega_-}{2}t\right) + \cos\left(\frac{\omega_+ + \omega_-}{2}t - \frac{\omega_+ - \omega_-}{2}t\right)\right) \\
&= A\left(\cos\left(\frac{\omega_+ + \omega_-}{2}t\right)\cos\left(\frac{\omega_+ - \omega_-}{2}t\right)\right)
\end{aligned} \qquad (10.188)$$

and

$$\begin{aligned}
x_2 &= \frac{1}{2}(x_+ - x_-) = \frac{A}{2}\left(\cos(\omega_+ t) - \cos(\omega_- t)\right) = \frac{A}{2}\left(\cos\left(\frac{\omega_+ + \omega_-}{2}t + \frac{\omega_+ - \omega_-}{2}t\right) - \cos\left(\frac{\omega_+ + \omega_-}{2}t - \frac{\omega_+ - \omega_-}{2}t\right)\right) \\
&= A\left(\sin\left(\frac{\omega_+ + \omega_-}{2}t\right)\sin\left(\frac{\omega_+ - \omega_-}{2}t\right)\right).
\end{aligned} \qquad (10.189)$$

If $k_{12} \ll k$, ω_+ and ω_- are similar and

$$\frac{\omega_+ - \omega_-}{2} \ll \frac{\omega_+ + \omega_-}{2}. \qquad (10.190)$$

The second cosine in equations describing motions of the individual masses represents a second, slow oscillation of the rapidly oscillating positions.

Analysis of two coupled pendulums (connected with a spring of the stiffness k_{12}) yields the same solution (for small swing angles), k/m is just replaced by g/l (gravitational acceleration divided by the length of the pendulum).

How are the coupled oscillators or pendulums related to J-coupling? If we further differentiate Eq. 10.125 we obtain second-order equations of the same form as those describing the second Newton's law for the coupled oscillators. For example,

$$\frac{\mathrm{d}^2(a_1 a_2)}{\mathrm{d}t^2} = \frac{\mathrm{d}}{\mathrm{d}t}\left(\frac{\mathrm{d}(a_1 a_2)}{\mathrm{d}t}\right) = \left(\mathrm{i}\frac{-\omega_{0,1} - \omega_{0,2} - \pi J}{2}\right)\left(\mathrm{i}\frac{-\omega_{0,1} - \omega_{0,2} - \pi J}{2}\right) a_1 a_2, = -\left(\frac{\omega_{0,1} + \omega_{0,2} + \pi J}{2}\right)^2 a_1 a_2. \tag{10.191}$$

As described above, the general form of the solution is

$$a_1 a_2 = A_{aa}\sin\left(\frac{\omega_{0,1} + \omega_{0,2} + \pi J}{2}\right) + B_{aa}\cos\left(\frac{\omega_{0,1} + \omega_{0,2} + \pi J}{2}\right). \tag{10.192}$$

The coefficients A_{aa} and B_{aa} can be determined by comparing Eq. 10.192 with the solution obtained earlier (Eq. **??**):

$$a_1 a_2 = a_1(0)a_2(0)\mathrm{e}^{\mathrm{i}\frac{-\omega_{0,1}-\omega_{0,2}-\pi J}{2}t} = \underbrace{a_1(0)a_2(0)}_{B_{aa}}\cos\left(\frac{\omega_{0,1} + \omega_{0,2} + \pi J}{2}\right)\underbrace{-\mathrm{i}a_1(0)a_2(0)}_{A_{aa}}\sin\left(\frac{\omega_{0,1} + \omega_{0,2} + \pi J}{2}\right). \tag{10.193}$$

We see that evolution of magnetic moments due to the J-coupling can be described by the same equations as coupled oscillation. The only difference is that the coefficients A_{aa} and B_{aa} are complex numbers (note that the spinor components $a_1(0)$ and $a_2(0)$ are complex numbers in general).

10.10.6   Two J-coupled nuclei in thermal equilibrium

Before we analyze evolution of the density matrix in a 2D experiment, we must define its initial form. Again, we start from the thermal equilibrium and use the Hamiltonian. The difference from the case of isolated nuclei is that we need to define a 4×4 density matrix in order to describe a pair of mutually interacting nuclei. As explained above, the off-diagonal elements of the equilibrium density matrix (proportional to $\mathscr{I}_x$ and $\mathscr{I}_y$) are equal to zero. The four diagonal elements describe average populations of four stationary states of a system composed of (isolated) nuclear pairs: $\alpha\alpha$, $\alpha\beta$, $\beta\alpha$, and $\beta\beta$. These populations are:

$$P_{\alpha\alpha}^{\mathrm{eq}} = \frac{\mathrm{e}^{-\mathcal{E}_{\alpha\alpha}/k_{\mathrm{B}}T}}{\mathrm{e}^{-\mathcal{E}_{\alpha\alpha}/k_{\mathrm{B}}T} + \mathrm{e}^{-\mathcal{E}_{\alpha\beta}/k_{\mathrm{B}}T} + \mathrm{e}^{-\mathcal{E}_{\beta\alpha}/k_{\mathrm{B}}T} + \mathrm{e}^{-\mathcal{E}_{\beta\beta}/k_{\mathrm{B}}T}} \approx \frac{1 - \frac{\mathcal{E}_{\alpha\alpha}}{k_{\mathrm{B}}T}}{4}, \tag{10.194}$$

$$P_{\alpha\beta}^{\mathrm{eq}} = \frac{\mathrm{e}^{-\mathcal{E}_{\alpha\beta}/k_{\mathrm{B}}T}}{\mathrm{e}^{-\mathcal{E}_{\alpha\alpha}/k_{\mathrm{B}}T} + \mathrm{e}^{-\mathcal{E}_{\alpha\beta}/k_{\mathrm{B}}T} + \mathrm{e}^{-\mathcal{E}_{\beta\alpha}/k_{\mathrm{B}}T} + \mathrm{e}^{-\mathcal{E}_{\beta\beta}/k_{\mathrm{B}}T}} \approx \frac{1 - \frac{\mathcal{E}_{\alpha\beta}}{k_{\mathrm{B}}T}}{4}, \tag{10.195}$$

$$P_{\beta\alpha}^{\mathrm{eq}} = \frac{\mathrm{e}^{-\mathcal{E}_{\beta\alpha}/k_{\mathrm{B}}T}}{\mathrm{e}^{-\mathcal{E}_{\alpha\alpha}/k_{\mathrm{B}}T} + \mathrm{e}^{-\mathcal{E}_{\alpha\beta}/k_{\mathrm{B}}T} + \mathrm{e}^{-\mathcal{E}_{\beta\alpha}/k_{\mathrm{B}}T} + \mathrm{e}^{-\mathcal{E}_{\beta\beta}/k_{\mathrm{B}}T}} \approx \frac{1 - \frac{\mathcal{E}_{\beta\alpha}}{k_{\mathrm{B}}T}}{4}, \tag{10.196}$$

$$P_{\beta\beta}^{\mathrm{eq}} = \frac{\mathrm{e}^{-\mathcal{E}_{\beta\beta}/k_{\mathrm{B}}T}}{\mathrm{e}^{-\mathcal{E}_{\alpha\alpha}/k_{\mathrm{B}}T} + \mathrm{e}^{-\mathcal{E}_{\alpha\beta}/k_{\mathrm{B}}T} + \mathrm{e}^{-\mathcal{E}_{\beta\alpha}/k_{\mathrm{B}}T} + \mathrm{e}^{-\mathcal{E}_{\beta\beta}/k_{\mathrm{B}}T}} \approx \frac{1 - \frac{\mathcal{E}_{\beta\beta}}{k_{\mathrm{B}}T}}{4}. \tag{10.197}$$

In principle, the total Hamiltonian also includes the term $\hat{H}_J$, which describes the J coupling and which is not averaged to zero.

$$\hat{H} = -\gamma_1 B_0(1 + \delta_{\mathrm{i},1})\hat{I}_{1z} - \gamma_2 B_0(1 + \delta_{\mathrm{i},2})\hat{I}_{2z} + \frac{2\pi}{\hbar}\hat{I}_{1z}\hat{I}_{2z} = \tag{10.198}$$

$$-\gamma_1 B_0(1 + \delta_{\mathrm{i},1})\frac{\hbar}{2}\begin{pmatrix} 1 & 0 & 0 & 0 \\ 0 & 1 & 0 & 0 \\ 0 & 0 & -1 & 0 \\ 0 & 0 & 0 & -1 \end{pmatrix} - \gamma_2 B_0(1 + \delta_{\mathrm{i},2})\frac{\hbar}{2}\begin{pmatrix} 1 & 0 & 0 & 0 \\ 0 & -1 & 0 & 0 \\ 0 & 0 & 1 & 0 \\ 0 & 0 & 0 & -1 \end{pmatrix} + \frac{\pi J}{2}\frac{\hbar}{2}\begin{pmatrix} 1 & 0 & 0 & 0 \\ 0 & -1 & 0 & 0 \\ 0 & 0 & -1 & 0 \\ 0 & 0 & 0 & 1 \end{pmatrix}. \tag{10.199}$$

where the diagonal elements (eigenvalues) are the energies of the individual states. Therefore, the populations (diagonal elements of the density matrix) should be given by

$$P_{\alpha\alpha}^{\text{eq}} \approx \frac{1 - \frac{\mathcal{E}_{\alpha\alpha}}{k_{\text{B}}T}}{4} = \frac{1}{4} + \gamma_1(1 + \delta_{\text{i},1})\frac{B_0\hbar}{8k_{\text{B}}T} + \gamma_2(1 + \delta_{\text{i},2})\frac{B_0\hbar}{8k_{\text{B}}T} - \frac{\pi J\hbar}{16k_{\text{B}}T},$$ (10.200)

$$P_{\alpha\beta}^{\text{eq}} \approx \frac{1 - \frac{\mathcal{E}_{\alpha\beta}}{k_{\text{B}}T}}{4} = \frac{1}{4} + \gamma_1(1 + \delta_{\text{i},1})\frac{B_0\hbar}{8k_{\text{B}}T} - \gamma_2(1 + \delta_{\text{i},2})\frac{B_0\hbar}{8k_{\text{B}}T} + \frac{\pi J\hbar}{16k_{\text{B}}T},$$ (10.201)

$$P_{\beta\alpha}^{\text{eq}} \approx \frac{1 - \frac{\mathcal{E}_{\beta\alpha}}{k_{\text{B}}T}}{4} = \frac{1}{4} - \gamma_1(1 + \delta_{\text{i},1})\frac{B_0\hbar}{8k_{\text{B}}T} + \gamma_2(1 + \delta_{\text{i},2})\frac{B_0\hbar}{8k_{\text{B}}T} + \frac{\pi J\hbar}{16k_{\text{B}}T},$$ (10.202)

$$P_{\beta\beta}^{\text{eq}} \approx \frac{1 - \frac{\mathcal{E}_{\beta\beta}}{k_{\text{B}}T}}{4} = \frac{1}{4} - \gamma_1(1 + \delta_{\text{i},1})\frac{B_0\hbar}{8k_{\text{B}}T} - \gamma_2(1 + \delta_{\text{i},2})\frac{B_0\hbar}{8k_{\text{B}}T} - \frac{\pi J\hbar}{16k_{\text{B}}T}.$$ (10.203)

$$ $$ (10.204)

However, the values of J in typical organic compounds are at least five orders of magnitude lower than the frequencies measured even at low-field magnets. As a consequence, the contribution of J-coupling can be safely neglected, and the initial density matrix is identical to that derived for a pair of nuclei interacting through space (Eq. 8.39).

10.10.7   Coherences depicted as double arrows
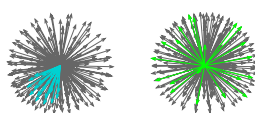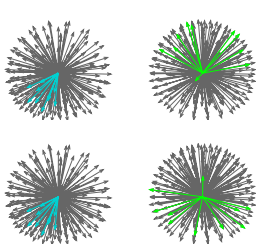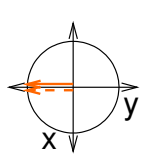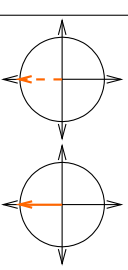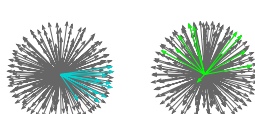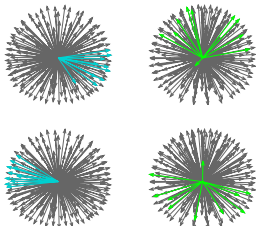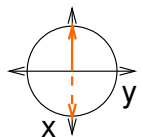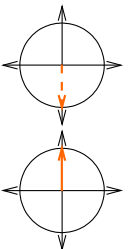
Algebraic analysis of the corresponding density matrix evolution is straightforward, but somewhat tedious. An alternative graphical analysis using "double arrows" was mentioned in Section 10.4 and used in Figure 10.2. Here we discus the "double arrow" visualization in more detail.
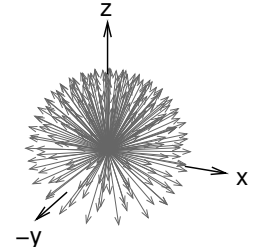
We have introduced a graphical representation of the product operators (density matrix contributions) in Table 8.2, where the contribution of each coherence is visualized as a colored plot of the magnetic moment distributions. Two examples are shown in the second column of Table 10.1. The third column of Table 10.1 explains the difference between the depicted coherences. On one hand, the $-\mathscr{I}_{1y}$ coherence describes the transverse polarization of $\vec{\mu}_1$ regardless of the distribution of $\vec{\mu}_2$. Therefore, we observe the transverse polarization of $\vec{\mu}_1$ (highlighted cyan arrows of most polarized $\vec{\mu}_1$) in the same direction if we look at a fraction of molecules with $\vec{\mu}_2$ pointing mostly up or mostly down (highlighted green arrows of $\vec{\mu}_2$). On the other hand, the $2\mathscr{I}_{1x}\mathscr{I}_{2z}$ coherence describes the correlation of the transverse polarization of $\vec{\mu}_1$ with the longitudinal polarization of $\vec{\mu}_2$. Therefore, we observe the transverse polarization of $\vec{\mu}_1$ (cyan arrows) in the *opposite directions* if we look at a fraction of molecules with $\vec{\mu}_2$ pointing mostly up or mostly down (green arrows).

In order to depict the transverse polarization of three magnetic moments in a single diagram, the graphical representation is further simplified in the fourth column. Directions of the orange arrows in the fourth column show the transverse polarization of $\vec{\mu}_1$ whereas the style (dashed or solid) of the arrows describes the longitudinal polarization of $\vec{\mu}_2$ (up or down, respectively) in the same fraction of molecules. The solid and dashed arrows can be viewed as vectors of partial magnetizations, and are thus affected by the radio waves in the same way as the magnetization vectors: $180°$ pulses with the $\pm x$ phases flip the arrows about the x axis, whereas $180°$ pulses with the $\pm y$ phases flip the arrows about the y axis. Our graphical analysis can be thus viewed as an extension of the *vector model*, presented e.g. by Keeler in K4.

As described in Section 10.4, the evolution due to the chemical shift is represented by *simultaneous rotation* of the arrows (solid and dashed arrows rotate by the same angle $\Omega_1 t$ or $\Omega_2 t$ in the *same direction*). The evolution due to the J-coupling is represented by *mutual rotation* of the arrows (solid and dashed arrows rotate by the same angle $\pi J t$ in the *opposite direction*). The evolution of coherences of $\vec{\mu}_1$ in the presence of chemical shift, J-coupling, or both is depicted in Figures 10.8–10.10, respectively. Figure 10.11 shows the evolution of the coherences described by the double arrows for various signs of Ω_1 and J, and relates them to the spectra plotted according to the standard conventions.

Table 10.1: Examples of two graphical representations of coherences: as distributions (used in Table 8.2) and as arrows (used in Figure 10.2). The color coding of distributions is similar to that used in Tables 8.1–8.2. Cyan arrows represent magnetic moments resonating with the applied radio wave (magnetic moments of ^{1}H in our example) most aligned along the $-y$ direction. Green arrows represent magnetic moments that do not resonate with the radio frequency (magnetic moments of ^{13}C or ^{15}N in our example) in the same molecules. The solid and dashed orange arrows presented in the last two columns correspond to partial distributions of proton magnetic moments, shown in cyan in the third column. The direction of the arrow is given by the average direction of the cyan arrows, the type (dashed or solid) of the arrow is given by the average direction of the green arrows in the third column (up or down, respectively). The orientation of axes in the schematic drawings of the magnetic moment distributions is shown below the table.

Coherence contributing to $\hat{\rho}$ in addition to $\mathscr{I}_t$	depicted as distributions: selected molecules with $\vec{\mu}$ of ^{1}H closest to $-y$ (in-phase) or closest to x (anti-phase)	decomposed distributions based on $\vec{\mu}$ of ^{13}C/^{15}N being closer to $+z$ vs. to $-z$ in the selected molecules	depicted as arrows	decomposed arrows
$-\mathscr{I}_{1y} = -\frac{\mathrm{i}}{2}\begin{pmatrix} 0 & 0 & -1 & 0 \\ 0 & 0 & 0 & -1 \\ +1 & 0 & 0 & 0 \\ 0 & +1 & 0 & 0 \end{pmatrix}$				
$2\mathscr{I}_{1x}\mathscr{I}_{2z} = \frac{1}{2}\begin{pmatrix} 0 & 0 & +1 & 0 \\ 0 & 0 & 0 & -1 \\ +1 & 0 & 0 & 0 \\ 0 & -1 & 0 & 0 \end{pmatrix}$				

Figure 10.8: Coherence evolution due to the chemical shift in the absence of *J*-coupling ($J = 0$). Several snapshots of evolving coherences are shown in the circles in the middle. Evolution of the $\mathscr{I}_{1x}$ and $\mathscr{I}_{1y}$ coherences is plotted above the snapshots. Evolution of the $2\mathscr{I}_{1x}\mathscr{I}_{2z}$ and $2\mathscr{I}_{1y}\mathscr{I}_{2z}$ coherences is plotted below the snapshots. The blue bar coincides with the transverse polarization of magnetic moments (cyan arrow), size of which is preserved in the presence of the chemical shifts and in the absence of *J*-coupling. The $2\mathscr{I}_{1x}\mathscr{I}_{2z}$ and $2\mathscr{I}_{1y}\mathscr{I}_{2z}$ coherences do not evolve as $s_J = \sin(\pi J t) = 0$.
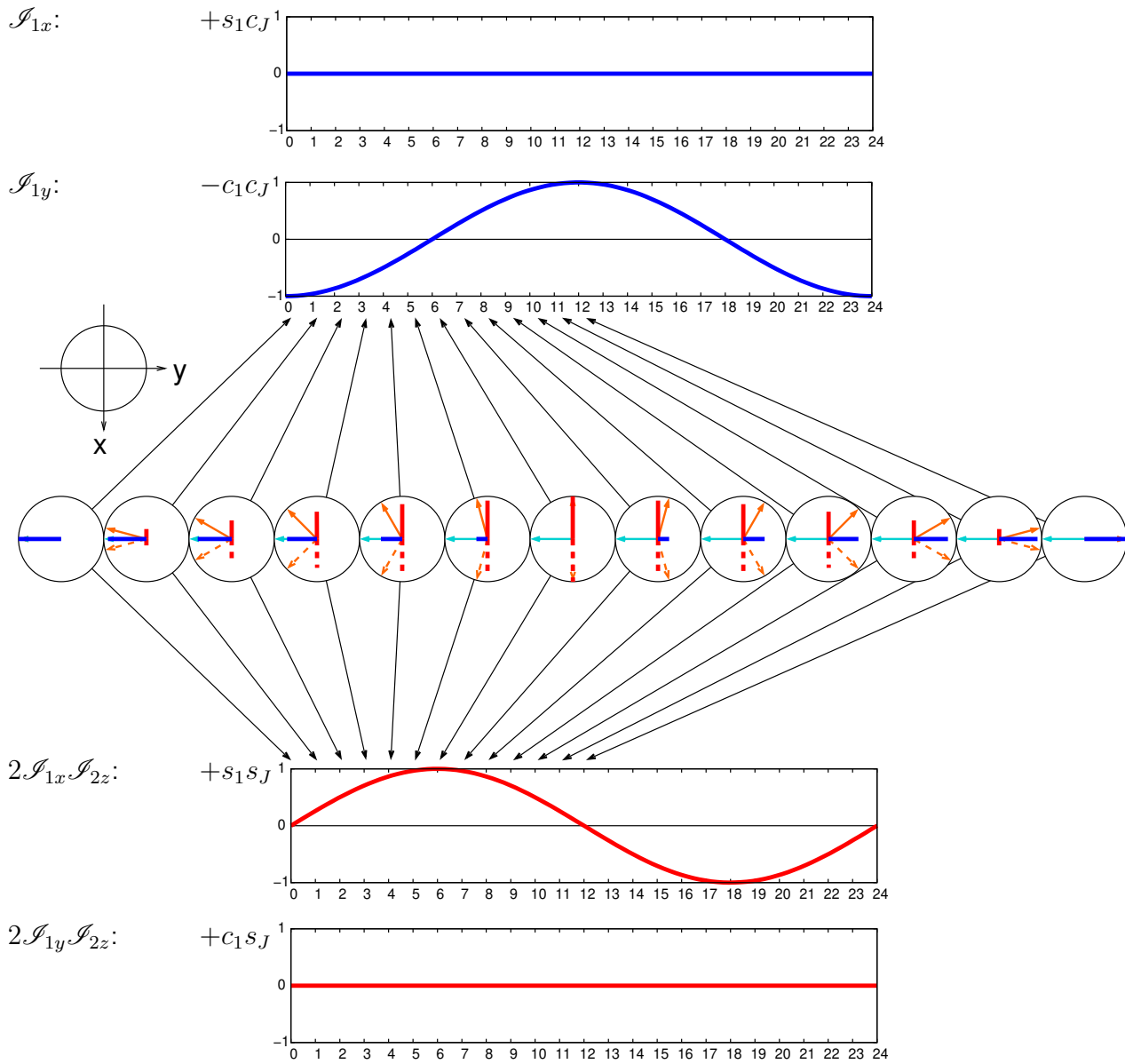
Figure 10.9: Coherence evolution due to the J-coupling for $\Omega_1 = 0$. Several snapshots of evolving coherences are shown in the circles in the middle. Evolution of the $\mathscr{I}_{1x}$ and $\mathscr{I}_{1y}$ coherences is plotted above the snapshots. Evolution of the $2\mathscr{I}_{1x}\mathscr{I}_{2z}$ and $2\mathscr{I}_{1y}\mathscr{I}_{2z}$ coherences is plotted below the snapshots. The $-\mathscr{I}_{1y}$ coherence (blue bar) evolves into the $2\mathscr{I}_{1x}\mathscr{I}_{2z}$ coherences (red bars). The orientation of the $2\mathscr{I}_{1x}\mathscr{I}_{2z}$ coherence is given by the direction of the dashed bar. The direction of the transverse polarization in the absence of the J-coupling is shown as the cyan arrow. The solid and dashed arrows, used in this text to describe evolution of coherences, are shown in orange. The blue and red bars are projections of the orange arrows to the directions parallel and perpendicular to the cyan arrow.
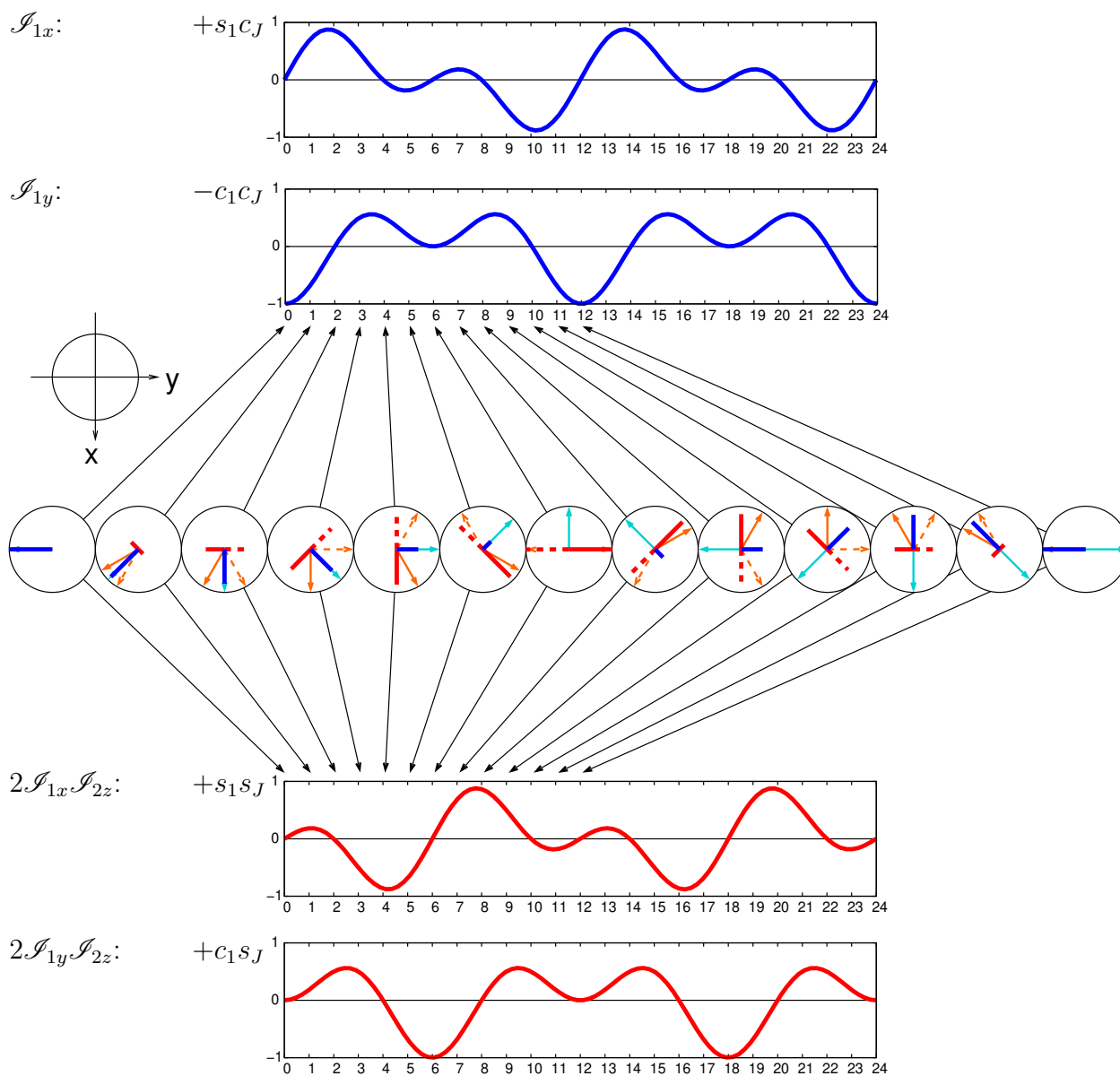
Figure 10.10: Coherence evolution due to the chemical shift and J-coupling. Several snapshots of evolving coherences are shown in the circles in the middle. Evolution of the $\mathscr{I}_{1x}$ and $\mathscr{I}_{1y}$ coherences is plotted above the snapshots. Evolution of the $2\mathscr{I}_{1x}\mathscr{I}_{2z}$ and $2\mathscr{I}_{1y}\mathscr{I}_{2z}$ coherences is plotted below the snapshots. The orientation of the transverse $\vec{\mu}_1$ polarization uncorrelated with the $\vec{\mu}_2$ longitudinal polarization is given by the direction of the blue bar. The orientations of the transverse $\vec{\mu}_1$ polarizations correlated with the $\vec{\mu}_2$ polarization in the $+z$ and $-z$ direction are given by the direction of the dashed and solid red bars, respectively. The direction of the transverse polarization in the absence of the J-coupling is shown as the cyan arrow. The solid and dashed arrows, used in this text to describe evolution of coherences, are shown in orange. The blue and red bars are projections of the orange arrows to the directions parallel and perpendicular to the cyan arrow.
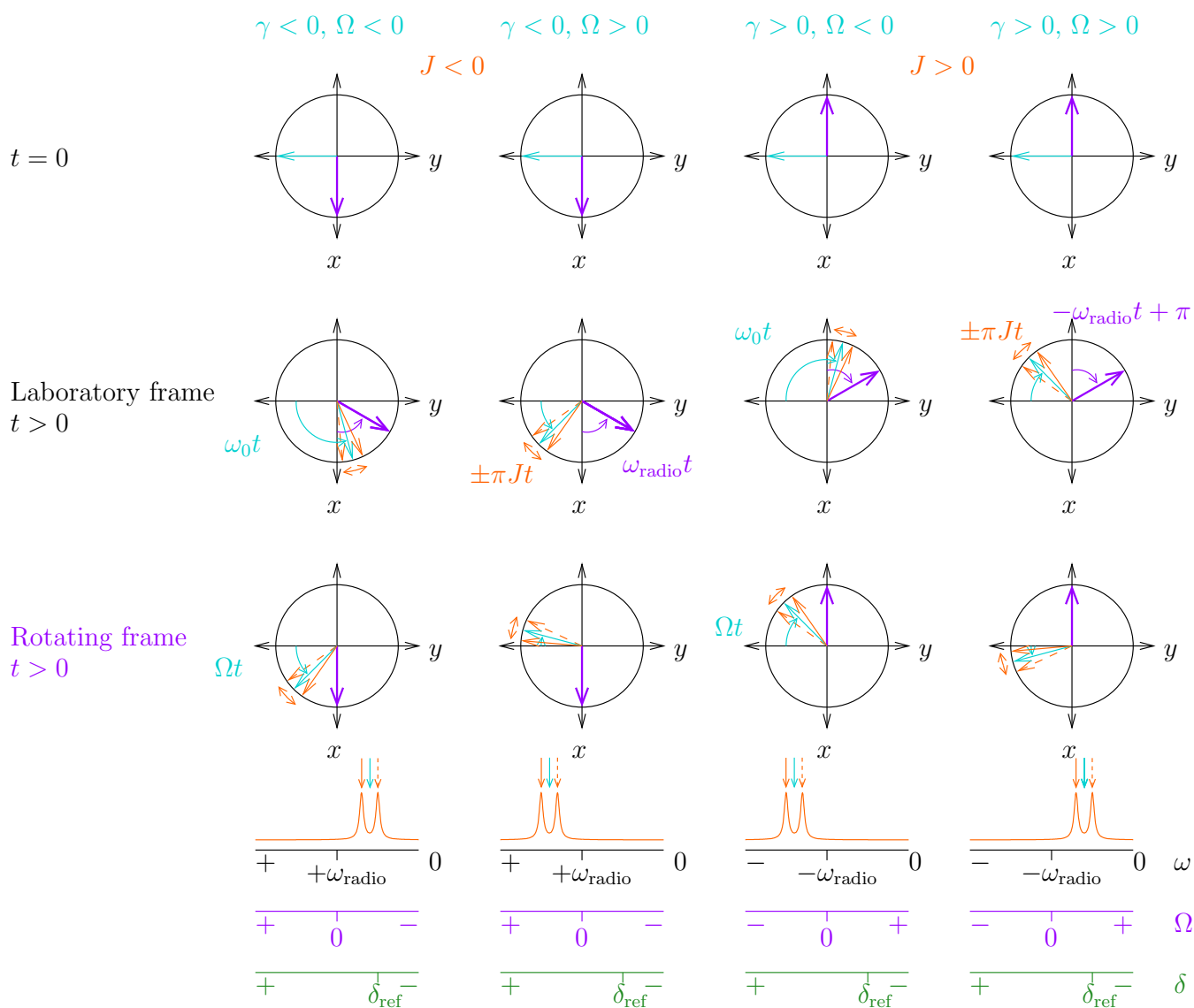
Figure 10.11: Conventions used in NMR spectroscopy when describing the effect of radio-wave pulses and the evolution of coherences, and when presenting the spectra. Evolution of coherences symbolized by the solid and dashed orange arrows (introduced in Table 10.1) for nuclei with different signs of γ and Ω is shown in the circles. The first row of circles represents the polarization immediately after applying a very short $90°$ radio-wave pulse (at $t = 0$). The second and third row show directions of coherences and of $\vec{B}_1$ at time t the laboratory and rotating coordinate frame, respectively. The direction of the transverse polarization in the absence of the J-coupling is shown as the cyan arrow. The z axis is defined by the direction of $\vec{B}_0$. The oscillating radio-wave magnetic field is decomposed into two counter-rotating components. The purple arrows indicate the direction of the resonant component $\vec{B}_1$ ($+\vec{B}_{\text{radio}}$ for $\gamma < 0$ and $-\vec{B}_{\text{radio}}$ for $\gamma > 0$). The absolute value of $\vec{B}_0$ is supposed to be much greater that the amplitude of $\vec{B}_1$. Note the convention to add a phase of $180°$ to the direction of $\vec{B}_1$ (i.e., to revert the direction) for $\gamma > 0$. The resulting spectra (after Fourier transformation and applying the necessary phase correction, which is $90°$ in the presented cases), are plotted below the circles. Arrows above the spectra assign individual peaks to the solid and dashed arrows. Note the convention to plot the frequency axis from the right to the left for nuclei with $\gamma < 0$.

Lecture 11
Correlated spectroscopy using J-coupling

Literature: INEPT, HSQC, and APT experiments are nicely described in K7.10, K8.7, and K12.4.4., respectively. INEPT is discussed in detail in L16.3., HSQC in C7.1.1. Decoupling trains are reviewed in C3.5. COSY is described in detail in L16.1, C6.2.1., and K8.3 (with a detailed discussion of DQF-COSY in K8.4).

11.1 Through-bond correlation

Correlated spectroscopy greatly extends the benefits of NMR. We have described in Section 9.4 how the dipolar coupling allows us to correlate frequencies of nuclei (usually protons) that are close in space. The distance-dependence of the mentioned NOESY experiment is a great advantage as it provides a structural information (the interatomic distance). However, the dependence of the signal on the *a priori* unknown distances in molecules makes the interpretation of NOESY spectra difficult. In many cases, it is desirable to introduce a correlation mediated by an interaction that depends only on a presence of a covalent bond between the observed nuclei. The one-bond J-coupling (usually between ^{13}C or ^{15}N and attached protons) is an ideal choice. The one-bond coupling constants are almost identical in all C–H bonds in molecules, and the same applies to N–H, C–C, C=C, etc. It is therefore possible to design experiments where *identical* one-bond J-coupling provides the *correlation*, and the *variable* chemical shift provides the *resolution*.

Design of *heteronuclear correlation experiments* is facilitated by the possibility to apply radio-wave pulses selectively affecting only one nucleus. Spin echoes can be used to separate the effect of the J-coupling from that of the chemical shift. In the following section, we first introduce a pulse sequence INEPT based on the simultaneous echo (Sections 11.2–11.3). It can be used as a building block of multidimensional correlated experiments, but also as a one-dimensional experiment utilizing the J-coupling to increase sensitivity of the measurement of the magnetization of nuclei with low γ. Another application of the simultaneous echo, known as APT (attached proton test) and useful for analysis of the CH$_n$ groups, is presented in Section 11.10.1. Then we describe the most popular heteronuclear correlation experiment HSQC, built of the INEPT modules (Sections 11.5–11.8). Finally, we discuss the use of J-coupling in the *homonuclear correlated spectroscopy* (Section 11.9).

11.2 INEPT

INEPT is a heteronuclear NMR experiment based on the simultaneous echo. It differs from the simple simultaneous echo in two issues:

- The length of the delay τ is set to $1/4|J|$

- The echo is followed by two 90° radio wave pulses, one applied at the same frequency as the excitation pulse (the 90° pulse preceding the echo) – this one must be phase-shifted by 90° from the excitation pulse, and the other one applied at the precession frequency of the other nucleus (^{13}C or ^{15}N in Fig. 11.1).

With $\tau = 1/4|J|$, $2\pi\tau = \pi/2$, $c_J = 0$, $s_J = 1$ if $J > 0$, and $s_J = -1$ if $J < 0$. Therefore, the density matrix at the end of the echo is[1]

$\hat{\rho}(e) = \frac{1}{2}\mathscr{I}_t - \frac{1}{2}\kappa_1\left(2\mathscr{I}_x\mathscr{S}_z\right) - \frac{1}{2}\kappa_2\mathscr{S}_z$

$\longrightarrow \hat{\rho}(f) = \frac{1}{2}\mathscr{I}_t + \frac{1}{2}\kappa_1\left(2\mathscr{I}_z\mathscr{S}_z\right) - \frac{1}{2}\kappa_2\mathscr{S}_z$ after the first pulse and

$\longrightarrow \hat{\rho}(g) = \frac{1}{2}\mathscr{I}_t - \frac{1}{2}\kappa_1\left(2\mathscr{I}_z\mathscr{S}_y\right) + \frac{1}{2}\kappa_2\mathscr{S}_y$ after the second pulse.

If the experiment continues by acquisition, the density matrix evolves as

$$\mathscr{I}_t \longrightarrow \mathscr{I}_t \longrightarrow \mathscr{I}_t \tag{11.1}$$

$$-2\mathscr{I}_z\mathscr{S}_y \longrightarrow \begin{cases} -c_2\, 2\mathscr{I}_z\mathscr{S}_y \longrightarrow \begin{cases} -c_2 c_J\, 2\mathscr{I}_z\mathscr{S}_y \\ +c_2 s_J\, \mathscr{S}_x \end{cases} \\ +s_2\, 2\mathscr{I}_x\mathscr{S}_z \longrightarrow \begin{cases} +s_2 c_J\, 2\mathscr{I}_z\mathscr{S}_x \\ +s_2 s_J\, \mathscr{S}_y \end{cases} \end{cases} \tag{11.2}$$

$$\mathscr{S}_y \longrightarrow \begin{cases} +c_2\mathscr{S}_y \longrightarrow \begin{cases} +c_2 c_J\, \mathscr{S}_y \\ -c_2 s_J\, 2\mathscr{S}_x\mathscr{I}_z \end{cases} \\ -s_2\mathscr{S}_x \longrightarrow \begin{cases} -s_2 c_J\, \mathscr{S}_x \\ -s_2 s_J\, 2\mathscr{S}_y\mathscr{I}_z \end{cases} \end{cases} \tag{11.3}$$

Both the "blue" coherence $2\mathscr{I}_z\mathscr{S}_y$ and the "green" coherence $\mathscr{S}_y$ evolve into "measurable" product operators, giving non-zero trace when multiplied by $\mathscr{S}_+$. Note that all components of $\hat{\rho}(g)$ commute with $\mathscr{I}_z$. Therefore, the chemical shift of the first nucleus (Hamiltonian $\Omega_1\mathscr{I}_z$) does not contribute to the density matrix evolution.

Evaluation of the expected value of the magnetization must take into account the instrumental set up used in the heteronuclear experiments. Only frequencies of the observed nucleus pass the audio filters of the NMR spectrometer (see footnote 13 in Section 7.12.5). Therefore, the detected transverse magnetization is represented by the operator

$$\hat{M}_{2+} = \mathcal{N}\gamma_2\hbar\mathscr{S}_+ = \mathcal{N}\gamma_2\hbar\left(\mathscr{S}_x + \mathrm{i}\mathscr{S}_y\right). \tag{11.4}$$

---

[1]The analysis is done for $J > 0$. If $J < 0$ (e.g. for one-bond ^{1}H-^{15}N coupling), all blue terms have the opposite sign.
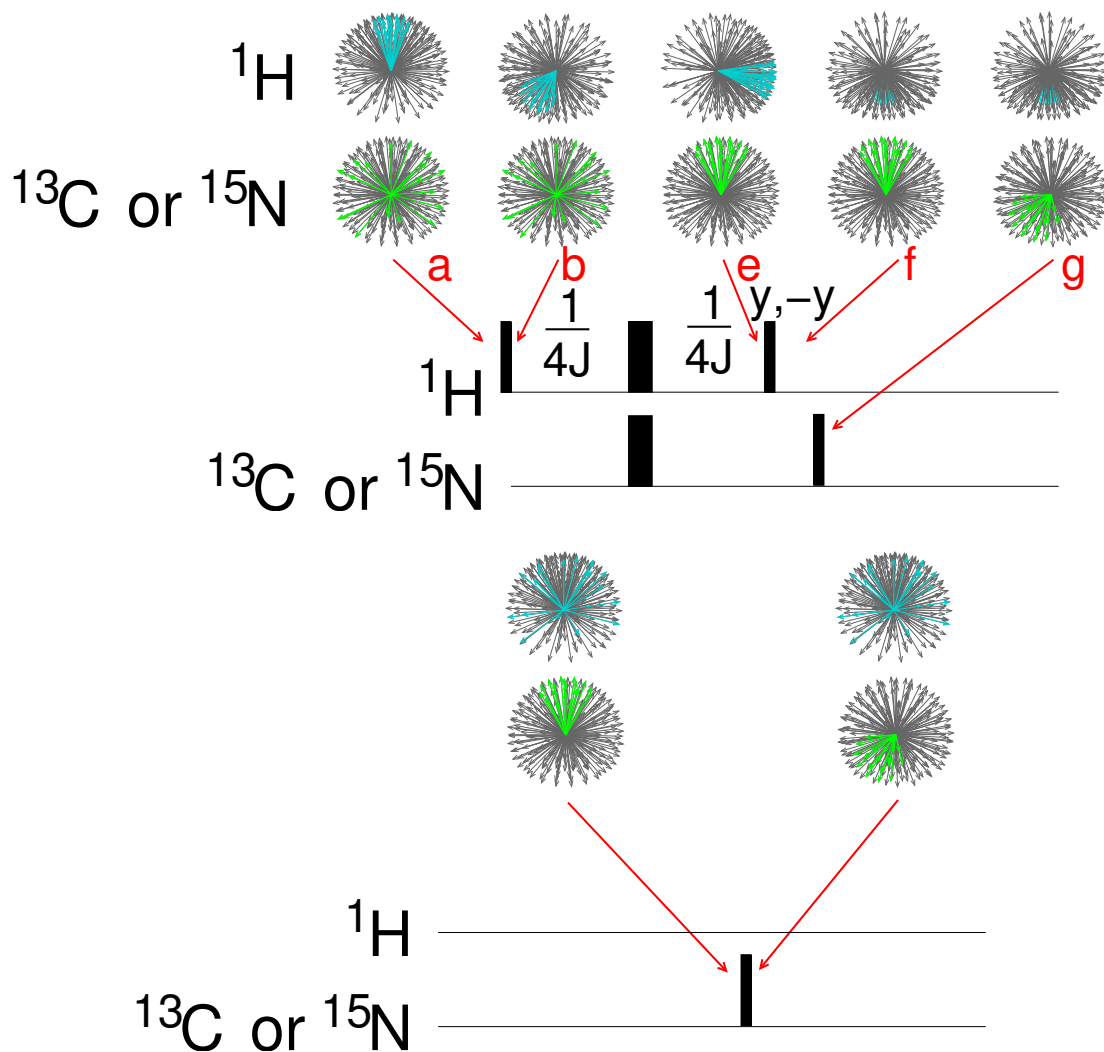
Figure 11.1: INEPT pulse sequence applied to ^{1}H and ^{13}C or ^{15}N (top) and direct excitation of ^{13}C or ^{15}N (bottom). The narrow and wide rectangles represent 90° and 180° radio wave pulses, respectively. The label $y, -y$ above the pulse indicates application of phase cycling to the labeled pulse (irradiation by a radio wave with the phases alternating between values of 90° and 270°, relative to the first pulse in the sequence, in subsequent measurements). Distributions of magnetic moments corresponding to the density matrix contributions other than $\mathscr{I}_t$ are shown schematically above the pulse sequences for time instants labeled by the red letters and arrows. For a better visibility, the distributions are shown in a coordinate frame rotated by 90° counterclockwise about z, compared with the orientation used in Table 8.2.

As discussed in Section 10.5, only products of $\mathscr{S}_x$, $\mathscr{S}_y$, $\mathscr{S}_x$, $\mathscr{S}_y$ with $\mathscr{S}_+$ have non-zero traces:

$$\mathrm{Tr}\left\{\mathscr{S}_x(\mathscr{S}_x + \mathrm{i}\mathscr{S}_y)\right\} = \mathrm{Tr}\left\{\mathscr{S}_x(\mathscr{S}_x + \mathrm{i}\mathscr{S}_y)\right\} = 1, \tag{11.5}$$

$$\mathrm{Tr}\left\{\mathscr{S}_y(\mathscr{S}_x + \mathrm{i}\mathscr{S}_y)\right\} = \mathrm{Tr}\left\{\mathscr{S}_y(\mathscr{S}_x + \mathrm{i}\mathscr{S}_y)\right\} = \mathrm{i}, \tag{11.6}$$

The expected value of M_{2+} is therefore

$$\langle M_{2+}\rangle = \mathrm{Tr}\left\{\hat\rho(t)\hat M_{2+}\right\} = \mathcal{N}\gamma_2\hbar\mathrm{Tr}\left\{\hat\rho(t)(\mathscr{S}_x + \mathrm{i}\mathscr{S}_y)\right\} = \mathcal{N}\gamma_2\hbar\left(\frac{\kappa_1}{2}(c_2 s_J + \mathrm{i}s_2 s_J) + \frac{\kappa_2}{2}(-s_2 c_J + \mathrm{i}c_2 c_J)\right).$$

The trigonometric relations $\cos(a\pm b) = \cos a\cos b \mp \sin a\sin b$ and $\sin(a\pm b) = \sin a\cos b \pm \cos a\sin b$ allow us to convert the products $c_2 s_J$, $s_2 s_J$ $s_2 c_J$, and $c_2 c_J$ to goniometric functions of $(\Omega_2 - \pi J)t$ and $(\Omega_2 + \pi J)t$

$$\langle M_{2+}\rangle = \mathcal{N}\gamma_2\hbar\frac{\kappa_1}{4}\left(-\sin((\Omega_1 - \pi J)t) + \sin((\Omega_1 + \pi J)t) + \mathrm{i}\cos((\Omega_1 - \pi J)t) - \mathrm{i}\cos((\Omega_1 + \pi J)t)\right) +$$

$$\mathcal{N}\gamma_2\hbar\frac{\kappa_2}{4}\left(-\sin((\Omega_1 - \pi J)t) - \sin((\Omega_1 + \pi J)t) + \mathrm{i}\cos((\Omega_1 - \pi J)t) + \mathrm{i}\cos((\Omega_1 + \pi J)t)\right)$$

$$= \mathcal{N}\gamma_2\hbar\frac{\kappa_1}{4}\mathrm{i}\left(\cos((\Omega_1 - \pi J)t) + \mathrm{i}\sin((\Omega_1 - \pi J)t) - \cos((\Omega_1 + \pi J)t) - \mathrm{i}\sin((\Omega_1 + \pi J)t)\right) +$$

$$\mathcal{N}\gamma_2\hbar\frac{\kappa_2}{4}\mathrm{i}\left(\cos((\Omega_1 - \pi J)t) + \mathrm{i}\sin((\Omega_1 - \pi J)t) + \cos((\Omega_1 + \pi J)t) + \mathrm{i}\sin((\Omega_1 + \pi J)t)\right)$$

$$= \frac{\mathcal{N}\gamma_1\gamma_2\hbar}{8k_\mathrm{B}T}\mathrm{e}^{\mathrm{i}\frac{\pi}{2}}\left(\mathrm{e}^{\mathrm{i}(\Omega_1 - \pi J)t} - \mathrm{e}^{\mathrm{i}(\Omega_1 + \pi J)t}\right) + \frac{\mathcal{N}\gamma_2^2\hbar}{8k_\mathrm{B}T}\mathrm{e}^{\mathrm{i}\frac{\pi}{2}}\left(\mathrm{e}^{\mathrm{i}(\Omega_1 - \pi J)t} + \mathrm{e}^{\mathrm{i}(\Omega_1 + \pi J)t}\right), \tag{11.7}$$

where the unimportant red terms are removed by the phase correction. After including the relaxation with the simplifications introduced in Section 10.5,

$$\langle M_{2+}\rangle = \frac{\mathcal{N}\gamma_2\hbar}{8k_\mathrm{B}T}\mathrm{e}^{-\overline{R_2}t}\left(\gamma_1\left(\mathrm{e}^{\mathrm{i}(\Omega_1 - \pi J)t} - \mathrm{e}^{\mathrm{i}(\Omega_1 + \pi J)t}\right) + \gamma_2\left(\mathrm{e}^{\mathrm{i}(\Omega_1 - \pi J)t} + \mathrm{e}^{\mathrm{i}(\Omega_1 + \pi J)t}\right)\right). \tag{11.8}$$

The real part of the spectrum obtained by the Fourier transformation is

$$\Re\{Y(\omega)\} = \frac{\mathcal{N}\gamma_2^2\hbar^2 B_0}{8k_\mathrm{B}T}\left(+\frac{\gamma_1\overline{R_2}}{\overline{R_2}^2 + (\omega - \Omega_2 + \pi J)^2} - \frac{\gamma_1\overline{R_2}}{\overline{R_2}^2 + (\omega - \Omega_2 - \pi J)^2}\right) +$$

$$\frac{\mathcal{N}\gamma_2^2\hbar^2 B_0}{8k_\mathrm{B}T}\left(+\frac{\gamma_2\overline{R_2}}{\overline{R_2}^2 + (\omega - \Omega_2 + \pi J)^2} + \frac{\gamma_2\overline{R_2}}{\overline{R_2}^2 + (\omega - \Omega_2 - \pi J)^2}\right) \tag{11.9}$$

- The "blue" coherence $2\mathscr{I}_z\mathscr{S}_y$ gives a signal with the *opposite phases* of the peaks at $\Omega_2 - \pi J$ and $\Omega_2 + \pi J$. Accordingly, it is called the *anti-phase* coherence.

- The "green" coherence $\mathscr{S}_y$ gives a signal with the *same phase* of the peaks at $\Omega_2 - \pi J$ and $\Omega_2 + \pi J$. Accordingly, it is called the *in-phase* coherence.
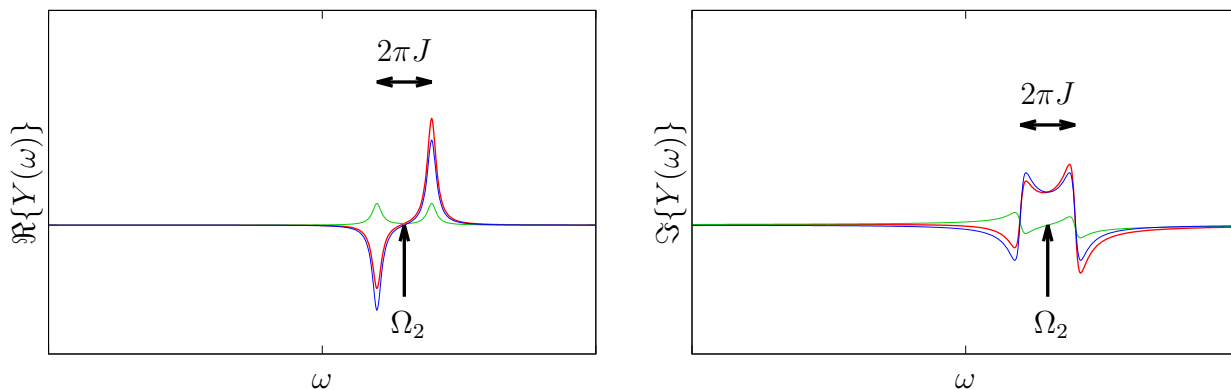
Figure 11.2: Real (left) and imaginary (right) components of an INEPT spectrum of a ^{1}H–^{13}C pair. The blue and green curves are contributions of the INEPT transfer and direct excitation to the final spectrum (red). Note that the direct contribution makes the final peak heights slightly unbalanced. The blue spectrum is obtained if the phase cycling is applied, the direct measurement of ^{13}C magnetization provides the green spectrum. The scale is the same as in Figure 10.5.

- More importantly, the "blue" coherence $2\mathscr{I}_z\mathscr{S}_y$ gives a signal proportional to $|\gamma_1|$ while the "green" coherence $\mathscr{S}_y$ gives a signal proportional to $|\gamma_2|$. The amplitude of the "green" signal corresponds to the amplitude of a regular 1D ^{15}N spectrum. The "blue" signal "inherited" the amplitude with $|\gamma_1|$ from the excited nucleus, proton. In the case of ^{1}H and ^{15}N, $|\gamma_1|$ is approximately ten times higher than $|\gamma_2|$. Therefore, the blue signal is an order of magnitude stronger. This is why this experiment is called *Insensitive Nuclei Enhanced by Polarization Transfer (INEPT)*.

11.3   Phase cycling

As described in the previous section, the "blue" and "green" signals of different origins (evolving from the "blue" coherence $2\mathscr{I}_z\mathscr{S}_y$ and from the "green" coherence $\mathscr{S}_y$) are combined in the INEPT experiment. It results in different heights of the $\Omega_2 - \pi J$ and $\Omega_2 + \pi J$ peaks in the INEPT spectrum (Figure 11.2). The "blue" and "green" signals can be separated if we repeat the measurement twice with the phase of the proton y pulse shifted by $180\,°$(i.e., with the $-y$ phase). The mentioned pulse converts the $2\mathscr{I}_x\mathscr{S}_z$ operator in $\hat{\rho}(\mathrm{e})$ to $-2\mathscr{I}_z\mathscr{S}_z$ if the relative phase of the radio wave is $+90\,°$ (y), but to $+2\mathscr{I}_z\mathscr{S}_z$ if the phase is $-90\,°$ $(-y)$: $\hat{\rho}(\mathrm{e}) = \frac{1}{2}\mathscr{I}_t - \frac{1}{2}\kappa_1\left(2\mathscr{I}_x\mathscr{S}_z\right) - \frac{1}{2}\kappa_2\mathscr{S}_z \longrightarrow$
$\hat{\rho}(\mathrm{f}) = \frac{1}{2}\mathscr{I}_t \pm \frac{1}{2}\kappa_1\left(2\mathscr{I}_z\mathscr{S}_z\right) - \frac{1}{2}\kappa_2\mathscr{S}_z \longrightarrow$
$\hat{\rho}(\mathrm{g}) = \frac{1}{2}\mathscr{I}_t \mp \frac{1}{2}\kappa_1\left(2\mathscr{I}_z\mathscr{S}_y\right) + \frac{1}{2}\kappa_2\mathscr{S}_y$
Such alteration of the phase does not affect the "green" signal, but changes the sign of the "blue" signal. If we subtract the spectra, we obtain a pure "blue" signal. This trick, repeating acquisition with different phases, is known as the *phase cycling* and is used routinely in the NMR spectroscopy to remove unwanted signals.

11.4 Simplified analysis

When analyzing more advanced NMR experiments, tracking the complete density matrix evolution may be very demanding. In practice, the analysis is simplified (i) by working with the already known effects of the complete building blocks (spin echoes, INEPT) and (ii) by ignoring the evolution of the density matrix contributions that cannot influence the measured transverse magnetization. The latter simplification is based on the following considerations (presented for a heteronuclear pair of magnetic moments).

- Only product operators representing the *uncorrelated transverse polarizations* ($\mathscr{I}_x$, $\mathscr{I}_y$, $\mathscr{S}_x$, $\mathscr{S}_y$), known as the *in-phase single-quantum coherences*, directly contribute to the measurable signal. Furthermore, only the signal oscillating relatively close to the carrier frequency of the radio waves passes the audio filters of the spectrometer (see footnote 13 in Section 7.12.5). Therefore, the operator of the measured quantity represents only the actually detected transverse magnetization (M_{1+} in our case). This limits the coherences contributing to the signal to $\mathscr{I}_x$, $\mathscr{I}_y$ (if nucleus 1 is detected). Only traces of their products with $\hat{M}_+$ are not zero. The coherences $\mathscr{S}_x$, $\mathscr{S}_y$ can be converted to the "measurable" operators $\mathscr{I}_x$, $\mathscr{I}_y$ by a combination of the J-coupling and 90° pulses.

- Product operators representing *transverse polarizations correlated with the longitudinal polarizations*, known as the *anti-phase single-quantum coherences* ($2\mathscr{I}_x\mathscr{S}_z$, $2\mathscr{I}_y\mathscr{S}_z$ if nucleus 1 is detected), do not contribute to the measurable signal (traces of their products with $\hat{M}_{1+}$ are equal to zero), but they can evolve to the "measurable" in-phase single-quantum coherences if the J-coupling is present (without application of any radio-wave pulses).

- Conversion of the operators $2\mathscr{I}_z\mathscr{S}_x$, $2\mathscr{I}_z\mathscr{S}_y$ to the single-quantum coherences of the measured nucleus 1 requires evolution of the J-coupling and application of a 90° pulse (at the precession frequency of nucleus 1).

- Product operators representing *two[2] correlated transverse polarizations* ($2\mathscr{I}_x\mathscr{S}_x$, $2\mathscr{I}_y\mathscr{S}_y$, $2\mathscr{I}_x\mathscr{S}_y$, $2\mathscr{I}_y\mathscr{S}_x$), known as *multiple-quantum coherences*, do not contribute to the measurable signal (traces of their products with $\hat{M}_{1+}$ are equal to zero), and can be converted to the "measurable" in-phase single quantum coherences only by applying a 90° pulse and by a subsequent action of the J-coupling.

- Product operators representing the *longitudinal polarizations* ($\mathscr{I}_z$, $\mathscr{S}_z$, $2\mathscr{I}_z\mathscr{S}_z$), known as the *populations*, do not contribute to the measurable signal (traces of their products with $\hat{M}_{1+}$ are equal to zero), and can be converted to single quantum coherences only by applying a 90° pulse ($\mathscr{I}_z$) and, in the case of $\mathscr{S}_z$ and $2\mathscr{I}_z\mathscr{S}_z$, by a subsequent action of the J-coupling.

- The product operator $\mathscr{I}_t$ never evolves to a measurable coherence because it commutes with all Hamiltonians. It can be ignored right from the beginning.

---

[2] In spin systems consisting of more than two coupled magnetic moments, product operators representing more than two correlated transverse polarizations also belong to this category.

Based on the arguments discussed above, all operators other than $\mathscr{I}_x$, $\mathscr{I}_y$, $2\mathscr{I}_x\mathscr{S}_z$, $2\mathscr{I}_y\mathscr{S}_z$ can be ignored *after the last 90° pulse* applied at the frequency of the given nucleus.

11.5   HSQC

Heteronuclear Single-Quantum Correlation (HSQC) spectroscopy is a 2D experiment using the *J*-coupling to correlate frequencies of two magnetic moments with different γ (Figure 11.3A). The experiment consists of

- excitation pulse, usually applied at the proton frequency

- INEPT module, transferring the polarization to the coupled nucleus (usually ^{15}N or ^{13}C)

- evolution period of incremented duration t_1, introducing the signal modulation by the frequency of the other nucleus

- another INEPT module, transferring the polarization back to proton

- signal acquisition

We now analyze the evolution of the density matrix during the HSQC experiments using the simplified approach described in Section 11.4.

- After a 90° pulse at the proton frequency, the polarization is transferred to the other nucleus (usually ^{15}N or ^{13}C). The density matrix at the end of the INEPT is
$\hat{\rho}(\mathrm{f}) = \frac{1}{2}\mathscr{I}_t - \frac{1}{2}\kappa_1\left(2\mathscr{I}_z\mathscr{S}_y\right) + \frac{1}{2}\kappa_2\mathscr{S}_y$

- During an echo with a decoupling 180° pulse at the proton frequency (the cyan pulse in Figure 11.3, top), anti-phase single quantum coherences evolve according to the chemical shift
$\hat{\rho}(\mathrm{f}) \longrightarrow \hat{\rho}(\mathrm{g}) = \frac{1}{2}\mathscr{I}_t + \frac{1}{2}\kappa_1\left(c_{21}2\mathscr{I}_z\mathscr{S}_y - s_{21}2\mathscr{I}_z\mathscr{S}_x\right) + \frac{1}{2}\kappa_2\left(c_{21}\mathscr{S}_y - s_{21}\mathscr{S}_x\right)$.
The coefficients c_{21} and s_{21}, respectively, include the $\cos(\Omega_2 t_1)$ and $\sin(\Omega_2 t_1)$ factors, as described in Section 9.2.

- Two 90° pulses convert $2\mathscr{I}_z\mathscr{S}_y$ to $-2\mathscr{I}_y\mathscr{S}_z$ and $-2\mathscr{I}_z\mathscr{S}_x$ to $2\mathscr{I}_y\mathscr{S}_x$. The magenta operator is a contribution to the density matrix representing a *multiple-quantum coherence*, which can be converted to a "measurable" in-phase single quantum coherence only by applying a 90° pulse (and by a subsequent action of the *J*-coupling). Since our pulse sequence does not contain any more 90° pulses, we ignore $2\mathscr{I}_y\mathscr{S}_x$. The 90° pulse applied at the precession frequency of ^{13}C or ^{15}N converts $\mathscr{S}_y$ to the longitudinal polarization $\mathscr{S}_z$. The $\mathscr{S}_x$ is not affected by the 90° pulses applied with the 0° (x) phase. As the pulse sequence does not contain any more 90° pulses, we can ignore the green terms. Also, we ignore the red term $\mathscr{I}_t$ which never evolves to a measurable coherence because it commutes with all Hamiltonians. The density matrix can be written as
$\hat{\rho}(\mathrm{h}) = -\frac{1}{2}\kappa_1 c_{21}2\mathscr{I}_y\mathscr{S}_z +$ unmeasurable contributions.

- The last echo allows the J-coupling to evolve but refocuses the evolution due to the chemical shift. If the delays $\tau = 1/4J$, the measurable components of the density matrix evolve to $\frac{1}{2}\kappa_1 \cos(\Omega_2 t_1)\mathscr{I}_x$ (rotation "about" $2\mathscr{I}_z\mathscr{S}_z$ by $90\,^\circ$ and change of the sign by the last $180°$ pulse applied at the proton frequency):
  $\hat{\rho}(\text{i}) = \frac{1}{2}\kappa_1 c_{21}\mathscr{I}_x +$ unmeasurable contributions

- During acquisition, both chemical shift and J-coupling evolve in the experiment depicted in Figure 11.3A:

$$\frac{1}{2}\kappa_1 c_{21}\mathscr{I}_x \longrightarrow \begin{cases} +\frac{1}{2}\kappa_1 c_{21} c_{12}\ \mathscr{I}_x \longrightarrow \begin{cases} +\frac{1}{2}\kappa_1 c_{21} c_{12} c_J\ \mathscr{I}_x \\ +\frac{1}{2}\kappa_1 c_{21} c_{12} s_J\ 2\mathscr{I}_y\mathscr{S}_z \end{cases} \\ +\frac{1}{2}\kappa_1 c_{21} s_{12}\ \mathscr{I}_y \longrightarrow \begin{cases} +\frac{1}{2}\kappa_1 c_{21} s_{12} c_J\ \mathscr{I}_y \\ -\frac{1}{2}\kappa_1 c_{21} s_{12} s_J\ 2\mathscr{I}_x\mathscr{S}_z \end{cases} \end{cases} \tag{11.10}$$

The HSQC experiments are usually two-dimensional. The second dimension is introduced by repeating the measurement with t_1 being incremented. Moreover, each increment is measured twice with a different phase of one of the $90°$ radio-wave pulses applied to ^{13}C or ^{15}N (labeled in Figure 11.3 by writing x/y above the pulse, do not confuse with the label x, y in Figure 11.1 that indicates phase cycling, i.e. storing a single record obtained by adding or subtracting data acquired with a different phase). In the records acquired with the phase shifted by $90°$ (y), the pulses influence the density matrix as follows:

- The density matrix at the end of the first INEPT applied with the $90°$ ^{13}C (or ^{15}N) pulse shifted by $90°$ (y) is
  $\hat{\rho}(\text{f}) = \frac{1}{2}\mathscr{I}_t + \frac{1}{2}\kappa_1\left(2\mathscr{I}_z\mathscr{S}_x\right) - \frac{1}{2}\kappa_2\mathscr{S}_x$

- During the echo with a decoupling $180°$ pulse at the proton frequency (the cyan pulse in Figure 11.3, top), anti-phase single quantum coherences evolve according to the chemical shift
  $\hat{\rho}(\text{f}) \longrightarrow \hat{\rho}(\text{g}) = \frac{1}{2}\mathscr{I}_t - \frac{1}{2}\kappa_1\left(c_{21}2\mathscr{I}_z\mathscr{S}_x + s_{21}2\mathscr{I}_z\mathscr{S}_y\right) - \frac{1}{2}\kappa_2\left(c_{21}\mathscr{S}_x + s_{21}\mathscr{S}_y\right)$.

- Two $90°$ pulses convert $-2\mathscr{I}_z\mathscr{S}_x$ to $-2\mathscr{I}_y\mathscr{S}_z$ and $-2\mathscr{I}_z\mathscr{S}_y$ to $-2\mathscr{I}_y\mathscr{S}_y$. The $90°$ pulse applied at the precession frequency of ^{13}C or ^{15}N with a phase shift of $90\,^\circ$ (y) converts $-\mathscr{S}_x$ to $\mathscr{S}_z$ and leaves $-\mathscr{S}_y$ untouched. As discussed above, only $2\mathscr{I}_y\mathscr{S}_z$ evolves to a measurable coherence:
  $\hat{\rho}(\text{h}) = -\frac{1}{2}\kappa_1 s_{21}2\mathscr{I}_y\mathscr{S}_z +$ unmeasurable contributions

The density matrix then evolves as described above for the records acquired with the phase $0\,^\circ$ (x), the only difference is the factor s_{21} instead of c_{21}:

$$\frac{1}{2}\kappa_1 s_{21}\mathscr{I}_x \longrightarrow \begin{cases} +\frac{1}{2}\kappa_1 s_{21} c_{12}\ \mathscr{I}_x \longrightarrow \begin{cases} +\frac{1}{2}\kappa_1 s_{21} c_{12} c_J\ \mathscr{I}_x \\ +\frac{1}{2}\kappa_1 s_{21} c_{12} s_J\ 2\mathscr{I}_y\mathscr{S}_z \end{cases} \\ +\frac{1}{2}\kappa_1 s_{21} s_{12}\ \mathscr{I}_y \longrightarrow \begin{cases} +\frac{1}{2}\kappa_1 s_{21} s_{12} c_J\ \mathscr{I}_y \\ -\frac{1}{2}\kappa_1 s_{21} s_{12} s_J\ 2\mathscr{I}_x\mathscr{S}_z \end{cases} \end{cases} \tag{11.11}$$

The subsequent records acquired with the $0°$ (x) and $90°$ (y) phases of the $90°$ ^{13}C or ^{15}N pulse are stored as real (modulated by $c_{21} = \cos(\Omega_2 t_1)$) and imaginary (modulated by $s_{21} = \sin(\Omega_2 t_1)$) component of a complex signal, respectively, like in the NOESY experiment.

As described in Section 10.5, we continue by calculating the trace of $\hat{\rho}(t_2)\hat{M}_{1+}$ and including relaxation (with different rates $\overline{R}_{2,1}$ and $\overline{R}_{2,2}$ in the direct and indirect dimensions,[3] respectively). The result shows that the expected value of M_{1+} evolves as

$$\langle M_{1+} \rangle = \frac{\mathcal{N}\gamma_1{}^2 \hbar^2 B_0}{8 k_{\mathrm{B}} T} \mathrm{e}^{-\overline{R}_{2,2} t_1} \mathrm{e}^{-\overline{R}_{2,1} t_2} \cos(\Omega_2 t_1) \left(\mathrm{e}^{\mathrm{i}(\Omega_1 - \pi J) t_2} + \mathrm{e}^{\mathrm{i}(\Omega_1 + \pi J) t_2} \right) \tag{11.12}$$

for the $0°$ (x) phase of the $90°$ ^{13}C or ^{15}N pulse, and as

$$\langle M_{1+} \rangle = \frac{\mathcal{N}\gamma_1{}^2 \hbar^2 B_0}{8 k_{\mathrm{B}} T} \mathrm{e}^{-\overline{R}_{2,2} t_1} \mathrm{e}^{-\overline{R}_{2,1} t_2} \sin(\Omega_2 t_1) \left(\mathrm{e}^{\mathrm{i}(\Omega_1 - \pi J) t_2} + \mathrm{e}^{\mathrm{i}(\Omega_1 + \pi J) t_2} \right) \tag{11.13}$$

for the $90°$ (y) phase of the $90°$ ^{13}C or ^{15}N pulse.

The last step is conversion of the data to a two-dimensional spectrum, described already in Section 9.5.1. We first perform the Fourier transformation in t_2 for each t_1 and each phase ($0°$ and $90°$) of the $90°$ ^{13}C or ^{15}N pulse. Then we take the real parts of the (correctly phased) one-dimensional spectra and combine them in an array containing two 1D spectra per each t_1 value, one with the c_{21} modulation and the other one with the s_{21} modulation. We combine c_{21} and s_{21} as $c_{21} + \mathrm{i}s_{21} = \mathrm{e}^{\mathrm{i}\Omega_2 t_1}$ and perform the Fourier transformation in t_1. The real part of the obtained spectrum (real in both dimensions) is

$$\Re\{Y(\omega)\} = \frac{\mathcal{N}\gamma_1{}^2 \hbar^2 B_0}{8 k_{\mathrm{B}} T} \frac{\overline{R}_{2,2}^2}{\overline{R}_{2,1}^2 + (\omega - \Omega_1)^2} \left(\frac{\overline{R}_{2,1}^2}{\overline{R}_{2,1}^2 + (\omega - \Omega_2 + \pi J)^2} + \frac{\overline{R}_{2,1}^2}{\overline{R}_{2,1}^2 + (\omega - \Omega_2 - \pi J)^2} \right) \tag{11.14}$$

11.6 Decoupling trains

If we perform the experiments as depicted in Figure 11.3A and analyzed above, we obtain a 2D spectrum with peaks at the frequency offset Ω_2 in the indirect dimension and a doublet at $\Omega_1 \pm \pi J$ in the direct (proton) dimension (Figure 11.4). Note that the splitting by $\pm \pi J$ was removed by the cyan decoupling pulse in the indirect dimension. Splitting of peaks in the direct dimension is undesirable, but the remedy is not simple. We acquire signal in the real time and cannot remove the splitting by a decoupling echo. In principle, we can divide the acquisition time into short fragments and apply a 180° pulse at the frequency of ^{13}C (or ^{15}N) in the middle of each such echo (green pulses

---

[3]The relaxation rates differ because single-quantum coherences of ^{13}C or ^{15}N evolve during t_1, whereas proton single-quantum coherences evolve during t_2. Moreover, the single-quantum coherences oscillate between the in-phase and the anti-phase terms during t_1 and t_2, and the relaxation rates of the in-phase and of the anti-phase single-quantum coherences differ as described in Section 10.5. The actually observed relaxation rates $\overline{R}_{2,1}$ and $\overline{R}_{2,2}$ are averages of the in-phase and anti-phase values, despite the fact that (i) the density matrix is purely anti-phase (consisting of $2\mathscr{I}_z\mathscr{S}_x$ and $2\mathscr{I}_z\mathscr{S}_y$ operators) at the end of t_1 (due to the presence of the cyan decoupling pulse) and that (ii) only the in-phase ($\mathscr{I}_x$ and $\mathscr{I}_y$) coherence contributes to the signal in t_2.

286
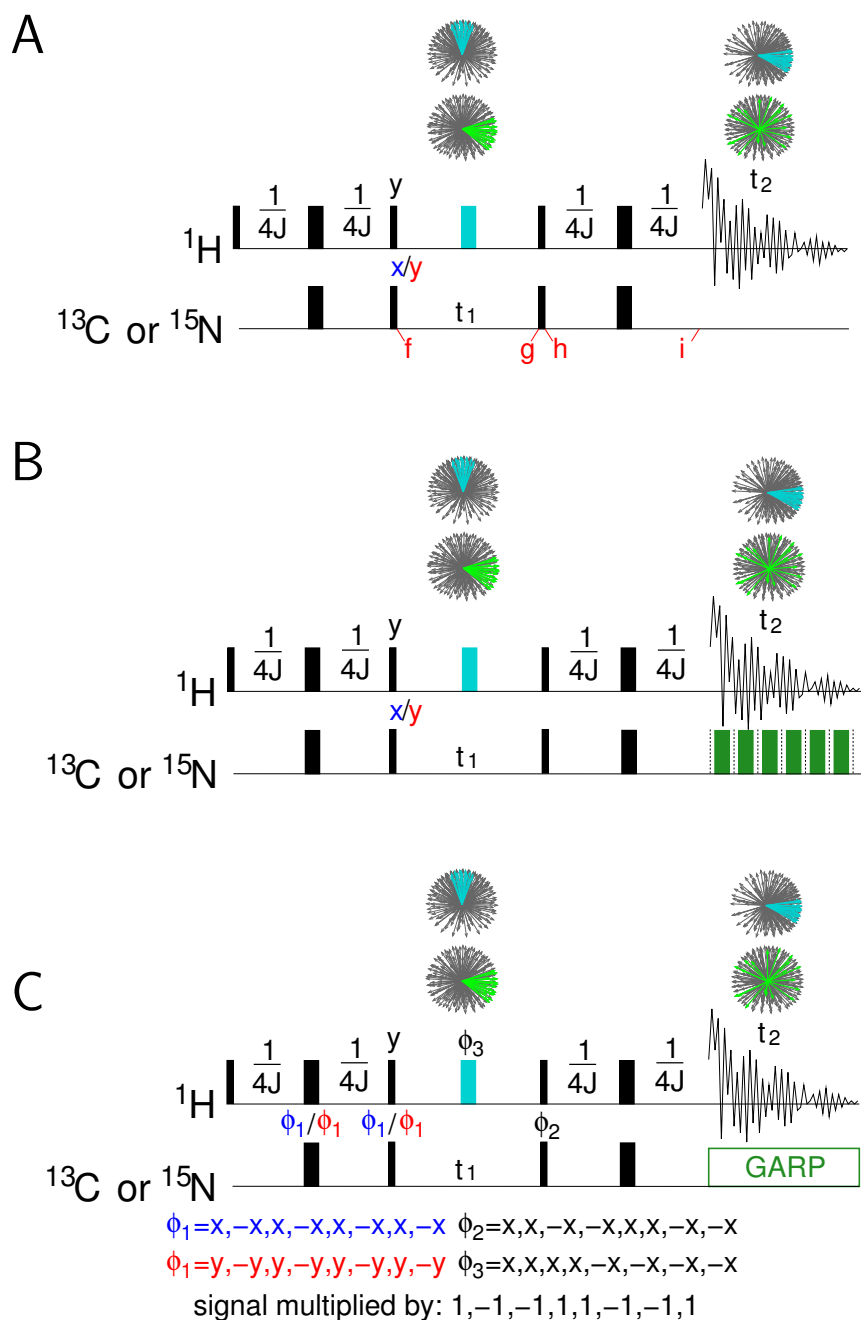
Figure 11.3: HSQC experiment. A, basic HSQC pulse sequence. B, general idea of the decoupling in the direct dimension. C, standard presentation of the HSQC pulse sequence with decoupling in the direct dimension and phase cycling. The decoupling pulse applied to proton and to ^{13}C (or ^{15}N) are shown in cyan and green, respectively. The label x/y indicates repeated acquisition with the phase of the given pulse set first to $0°$ (x) and than to $90°$ (y), in order to obtain cosine-modulated and sine-modulated 1D records for each t_1 increment. In panel C, the pulses with cycled phases are labeled ϕ_1, ϕ_2, ϕ_3, and the actual phases during the cycles are listed below the sequence. In order to add signals with the same signs, the individual signals acquired during the phase cycles are multiplied by the +1 or −1 factors as indicated below the sequence. Other symbols are used as explained in Figure 11.1.

in Figure 11.3B). In practice, imperfections of such a long series of echoes, affecting especially the magnetic moments with large Ω_2, are significant. However, more sophisticated series of pulses have a much better performance. Typical examples of decoupling pulse sequences are

- WALTZ - a series of 90°, 180°, and 270° pulses with the phase of $0\,°$ (x), or $180\,°$ $(-x)$, repeating in complex patterns

- DIPSI - a similar series of pulses with non-integer rotation angles

- GARP - computer-optimized sequence of pulses with non-integer rotation angles and phases.

In the schematic drawings of pulse sequences, the decoupling (and other) trains of many pulses are depicted as rectangles with abbreviations of the used sequences (Figure 11.3C).

11.7   Signal summation and arraying in 2D spectroscopy

Phases of pulses during NMR experiments really run in practice alternate in order to suppress unwanted signals. The unwanted signals may be due to magnetic moments really present in the sample (of water protons, of ^{13}C or ^{15}N nuclei without protons attached) or due to various artifacts. An example of an HSQC sequence including such *phase cycling* is presented in Figure 11.3C. When phase cycling is applied, the experiments are repeated for each increment of t_1 with different phases of some radio-wave pulses, and the acquired signals are combined. Repeating the measurements of course extends the overall time of the experiments. However, this drawback is not as serious as it may appear. In many cases, the sensitivity of the measurement requires to sum results of several measurements anyway, in order to achieve a sufficient signal-to-noise ratio. Usually, the signals recorded with individual settings of the phases are not stored separately but directly added to the data acquired with the preceding phase setting. The phase of the desired signal acquired with different phases of the pulses may vary. Therefore, the phase of the acquired signal has to be adjusted before it is added to the sum of the signals recorded in the previous runs. In the example shown in Figure 11.3C, the phases of the signal acquired in the second, third, sixth, and seventh runs are shifted by $180\,°$, which corresponds to changing the sign of the signal. Therefore, the signals detected in the aforementioned runs are multiplied by -1 before they are added to the overall signal.

When the phase cycling is applied in a two-dimensional experiment, as discussed in this section, we should carefully distinguish different purposes of repeating the data acquisition:

- In order to apply the *phase cycling* and to *improve signal-to-noise ratio*, the signal is acquired repeatedly with various phases of certain radio-wave pulses. The individual signals are called *transients* or *scans* in the NMR literature. Usually, the transients (scans) are not stored separately, but combined (summed after a necessary phase adjustment). Quadrature receivers of standard NMR spectrometers supply two output signals with phases shifted by $90\,°$, therefore each transient represents a *complex signal* with the *real* and the *imaginary* component.

- In order to introduce the *second dimension*, the signal is acquired repeatedly with an increasing (or decreasing) length of the delay t_1. The individual signals are called *increments* in the NMR
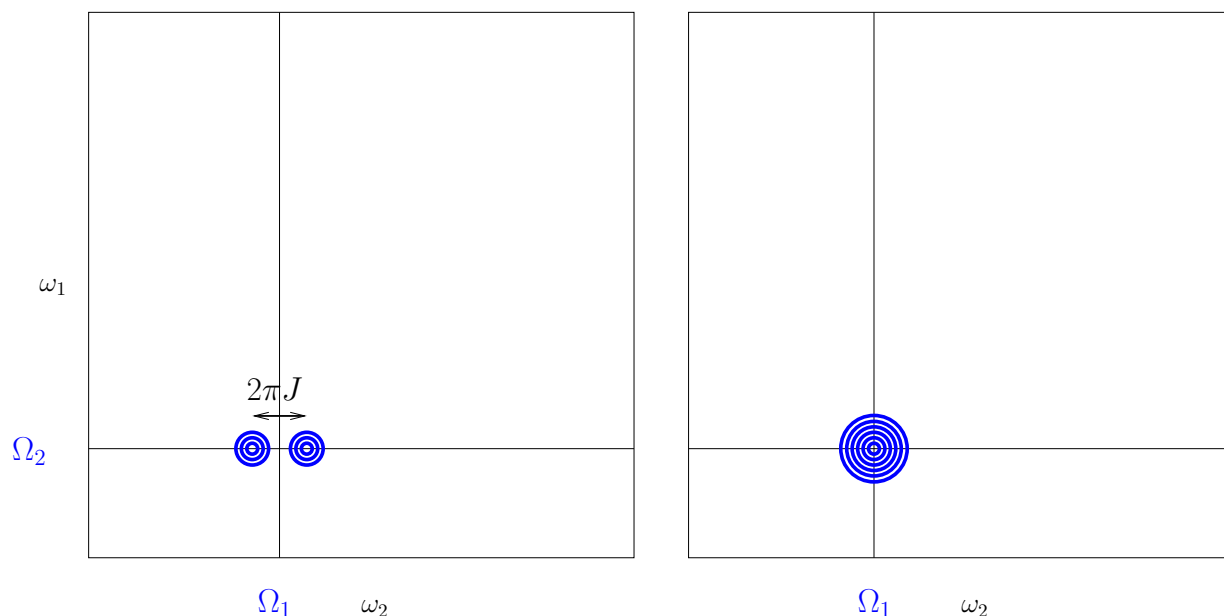
Figure 11.4: HSQC spectrum of a ^{1}H–^{13}C (or ^{1}H–^{15}N) pair. The two-dimensional peaks are displayed as contour plots. Frequency offsets of the proton and ^{13}C (or ^{15}N) are Ω_1 and Ω_2, respectively. The left spectrum was obtained using the pulse sequence shown in Figure 11.3A, the right spectrum was acquired with the decoupling applied in the direct dimension (Figure 11.3B,C).

literature. The increments are stored separately as an *array* of one-dimensional data (data matrix). Each increment is stored as two signals (sums of transients) with phases shifted by 90°, providing (after an appropriate phase correction) the *real* and the *imaginary* component of the data in the *direct dimension*.

- In order to achieve the *frequency discrimination* in the *indirect dimension* (using the States-Haberkorn-Ruben method described in Section 9.5.1), each increment is recorded twice with a different phase of a certain pulse. The individual increments are called *cosine modulated* and *sine modulated* in the NMR literature. The States-Haberkorn-Ruben method of frequency discrimination is based on changing a pulse phase (like the phase cycling), but (unlike the phase cycling) data collected with different phases are stored separately. The real components of the cosine- and sine-modulated increments provide the real and imaginary component of the data in the *indirect dimension* as described in Section 9.5.1.

11.8 Benefits of HSQC

At the and of the discussion of the HSQC experiment, we summarize the advantages of recording a 2D HSQC spectrum instead of 1D proton and ^{13}C or ^{15}N spectra.

- The ^{13}C or ^{15}N frequency is measured with a *high sensitivity* (higher by $|\gamma_1/\gamma_2|^{5/2}$ than provided by the direct detection, cf. Section 7.12.5).

- Expansion to the second dimension and reducing the number of peaks in the spectrum (only ^{13}C or ^{15}N-bonded protons and only protonated ^{13}C or ^{15}N nuclei are visible) provides a *high resolution*.

- The ^{1}H-^{13}C and ^{1}H-^{15}N correlation is an *important structural information* (it tells us which proton is attached to which ^{13}C or ^{15}N).

11.9 COSY

We started the discussion of experiments based on the J-coupling with the heteronuclear correlation because they are easier to analyze. The basic (and very popular) *homonuclear* experiment is COSY (COrrelated SpectroscopY). Its pulse sequence is very simple, consisting of only two 90° pulses separated by an incremented delay t_1 (which provides the second dimension), but the evolution of the density matrix is relatively complex. Here, we analyze the evolution for a pair of interacting nuclei (protons). During t_2 (signal acquisition), we discuss only the components of the density matrix that contribute to the measurable signal. The complete analysis is summarized in Table 11.1.

- $\hat{\rho}(\mathrm{a}) = \frac{1}{2}\mathscr{I}_t + \frac{1}{2}\kappa(\mathscr{I}_{1z} + \mathscr{I}_{2z})$
  thermal equilibrium, the matrices are different than for the non-interacting spin, but the constant is the same.

- $\hat{\rho}(\mathrm{b}) = \frac{1}{2}\mathscr{I}_t + \frac{1}{2}\kappa(-\mathscr{I}_{1y} - \mathscr{I}_{2y})$
  90° pulse, see the one-pulse experiment

- $\hat{\rho}(\mathrm{c}) = \frac{1}{2}\mathscr{I}_t$
  $+\frac{1}{2}\kappa(-c_{11}c_{J1}\mathscr{I}_{1y} + s_{11}c_{J1}\mathscr{I}_{1x} + c_{11}s_{J1}2\mathscr{I}_{1x}\mathscr{I}_{2z} + s_{11}s_{J1}2\mathscr{I}_{1y}\mathscr{I}_{2z})$
  $+\frac{1}{2}\kappa(-c_{21}c_{J1}\mathscr{I}_{2y} + s_{21}c_{J1}\mathscr{I}_{2x} + c_{21}s_{J1}2\mathscr{I}_{1z}\mathscr{I}_{2x} + s_{21}s_{J1}2\mathscr{I}_{1z}\mathscr{I}_{2y})$,
  where $c_{11} = \cos(\Omega_1 t_1)$, $s_{11} = \sin(\Omega_1 t_1)$, $c_{21} = \cos(\Omega_2 t_1)$, $s_{21} = \sin(\Omega_2 t_1)$, $c_{J1} = \cos(\pi J t_1)$, and $s_{J1} = \sin(\pi J t_1)$ – evolution of the chemical shift and coupling.

- The second 90° pulse creates the following coherences
  $\hat{\rho}(\mathrm{d}) = \frac{1}{2}\mathscr{I}_t$
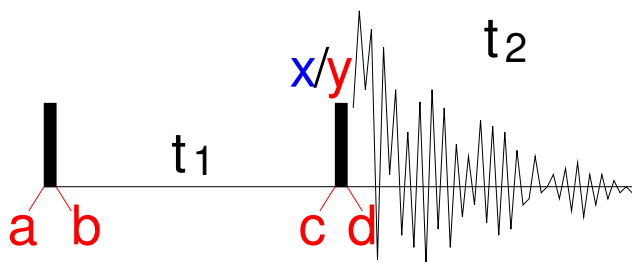
Figure 11.5: COSY pulse sequence. The rectangles represent 90° radio wave pulses applied at a frequency sufficiently close to the precession frequencies of both interacting magnetic moments.

$$+\tfrac{1}{2}\kappa(-c_{11}c_{J1}\mathscr{I}_{1z}+\boxed{s_{11}c_{J1}\mathscr{I}_{1x}}-c_{11}s_{J1}2\mathscr{I}_{1x}\mathscr{I}_{2y}-\boxed{s_{11}s_{J1}2\mathscr{I}_{1z}\mathscr{I}_{2y}})$$

$$+\tfrac{1}{2}\kappa(-c_{21}c_{J1}\mathscr{I}_{2z}+\boxed{s_{21}c_{J1}\mathscr{I}_{2x}}-c_{21}s_{J1}2\mathscr{I}_{1y}\mathscr{I}_{2x}-\boxed{s_{21}s_{J1}2\mathscr{I}_{1y}\mathscr{I}_{2z}}).$$

The red terms contain population operators, not coherences, they do not contribute to the signal. The green terms contain in-phase single-quantum coherences, only they give non-zero trace when multiplied with $\hat{M}_+ \propto (\mathscr{I}_{1x}+\mathrm{i}\mathscr{I}_{1y}+\mathscr{I}_{2x}+\mathrm{i}\mathscr{I}_{2y})$. The blue terms contain anti-phase single-quantum coherences, they do not contribute to the signal directly, but they evolve into in-phase coherences during the acquisition due to the J-coupling. The magenta terms contain multiple-quantum coherences. They do not contribute to the signal, but can be converted to single-quantum coherences by 90° pulses.[4] Such pulses are not applied in the discussed pulse sequence, but are used in some versions of the experiment.

- The terms in black frames evolve with the chemical shift of the first nucleus during acquisition:

$$\boxed{s_{11}c_{J1}\mathscr{I}_{1x} \to s_{11}c_{J1}c_{12}c_{J2}\mathscr{I}_{1x} + s_{11}c_{J1}s_{12}c_{J2}\mathscr{I}_{1y}+ \text{ unmeasurable anti-phase coherences}}$$

$$\boxed{-s_{21}s_{J1}2\mathscr{I}_{1y}\mathscr{I}_{2z} \to s_{21}s_{J1}c_{12}s_{J2}\mathscr{I}_{1x} + s_{21}s_{J1}s_{12}s_{J2}\mathscr{I}_{1y}+ \text{ unmeasurable anti-phase coherences}},$$

where $c_{n2} = \cos(\Omega_n t_2)$, $s_{n2} = \sin(\Omega_n t_2)$, $c_{J2} = \cos(\pi J t_2)$, and $s_{J2} = \sin(\pi J t_2)$. Using the following trigonometric relations

$$c_{nk}c_{Jk} = \frac{c_{nk}^- + c_{nk}^+}{2} \quad s_{nk}s_{Jk} = \frac{c_{nk}^- - c_{nk}^+}{2} \quad c_{nk}s_{Jk} = \frac{-s_{nk}^- + s_{nk}^+}{2} \quad s_{nk}c_{Jk} = \frac{s_{nk}^- + s_{nk}^+}{2}, \quad (11.15)$$

where $c_{nk}^\pm = \cos((\Omega_n \pm \pi J)t_k)$ and $s_{nk}^\pm = \sin((\Omega_n \pm \pi J)t_k)$, the terms contributing to the signal can be written as

$$\frac{\kappa}{8}\left(\underbrace{(s_{11}^- + s_{11}^+)(c_{12}^- + c_{12}^+)}_{[\Omega_1,\Omega_1]} + \underbrace{(c_{21}^- - c_{21}^+)(-s_{12}^- + s_{12}^+)}_{[\Omega_2,\Omega_1]}\right)\mathscr{I}_{1x} + \frac{\kappa}{8}\left(\underbrace{(s_{11}^- + s_{11}^+)(s_{12}^- + s_{12}^+)}_{[\Omega_1,\Omega_1]} + \underbrace{(c_{21}^- - c_{21}^+)(c_{12}^- - c_{12}^+)}_{[\Omega_2,\Omega_1]}\right)\mathscr{I}_{1y}$$

The $\mathscr{I}_{1x}$ and $\mathscr{I}_{1y}$ coherences provide the real and imaginary component of the complex signal acquired in the direct dimension (t_2).

- Evaluation of the traces of $\hat{M}_+\hat{\rho}(t_2)$ gives the following modulation of the signal:

$$\underbrace{(s_{11}^- + s_{11}^+)\left(\mathrm{e}^{\mathrm{i}(\Omega_1 - \pi J)t_2} + \mathrm{e}^{\mathrm{i}(\Omega_1 + \pi J)t_2}\right)}_{[\Omega_1,\Omega_1]} + \mathrm{i}\underbrace{(c_{21}^- - c_{21}^+)\left(\mathrm{e}^{\mathrm{i}(\Omega_1 - \pi J)t_2} - \mathrm{e}^{\mathrm{i}(\Omega_1 + \pi J)t_2}\right)}_{[\Omega_2,\Omega_1]}.$$

The imaginary unit in front of the blue term can be written as $\mathrm{e}^{\mathrm{i}\pi/2}$. The phase correction of the whole signal by $-\pi/2$ (mathematically equivalent to multiplication by $-\mathrm{i}$ results in

$$-\mathrm{i}\underbrace{(s_{11}^- + s_{11}^+)\left(\mathrm{e}^{\mathrm{i}(\Omega_1 - \pi J)t_2} + \mathrm{e}^{\mathrm{i}(\Omega_1 + \pi J)t_2}\right)}_{[\Omega_1,\Omega_1]} + \underbrace{(c_{21}^- - c_{21}^+)\left(\mathrm{e}^{\mathrm{i}(\Omega_1 - \pi J)t_2} - \mathrm{e}^{\mathrm{i}(\Omega_1 + \pi J)t_2}\right)}_{[\Omega_2,\Omega_1]}. \quad (11.16)$$

Note that the phase correction cannot remove the phase shift of $\pi/2$ from the whole signal: either green or blue part is always multiplied by the imaginary unit (equivalent to $\mathrm{e}^{\mathrm{i}\pi/2}$). As a

---

[4]We have not analyzed the evolution of the multiple quantum coherences so far. To do it, it is sufficient (i) to recognize that the multiple quantum coherences commute with $2\mathscr{I}_{1z}\mathscr{I}_{2z}$ (therefore they are not influenced by the weak J-coupling), and (ii) to analyze the "rotation" of individual constituents of the product operators (e.g. of $\mathscr{I}_{1x}$ and $\mathscr{I}_{2y}$) "about" $\mathscr{I}_{nj}$ individually and calculate the product of the results of the rotation.

consequence, the blue and green parts of the signal result in peaks of different shapes (one of a convenient absorption shape and the other one of an undesirable dispersion shape).

The imaginary signal in the indirect dimension is obtained by repeating the acquisition for each increment of t_1 with a different phase of the second $90°$ pulse (shifted by $90°$, which corresponds to the direction y in the rotating coordinate system).

- The second $90°$ pulse with the y phase creates the following coherences

$$\hat{\rho}(\mathrm{d}) = \tfrac{1}{2}\mathscr{I}_t$$
$$+\tfrac{1}{2}\kappa(-\boxed{c_{11}c_{J1}\mathscr{I}_{1y}}-s_{11}c_{J1}\mathscr{I}_{1z}-\boxed{c_{11}s_{J1}2\mathscr{I}_{1z}\mathscr{I}_{2x}}+s_{11}s_{J1}2\mathscr{I}_{1y}\mathscr{I}_{2x})$$
$$+\tfrac{1}{2}\kappa(-\boxed{c_{21}c_{J1}\mathscr{I}_{2y}}-s_{21}c_{J1}\mathscr{I}_{2z}-\boxed{c_{21}s_{J1}2\mathscr{I}_{1x}\mathscr{I}_{2z}}+s_{21}s_{J1}2\mathscr{I}_{1x}\mathscr{I}_{2y}).$$

- The terms in black frames evolve with the chemical shift of the first nucleus during acquisition:

$$\boxed{-c_{11}c_{J1}\mathscr{I}_{1y} \to c_{11}c_{J1}s_{12}c_{J2}\mathscr{I}_{1x} - c_{11}c_{J1}c_{12}c_{J2}\mathscr{I}_{1y}+ \text{ unmeasurable anti-phase coherences}}$$

$$\boxed{-s_{21}s_{J1}2\mathscr{I}_{1x}\mathscr{I}_{2z} \to c_{21}s_{J1}s_{12}s_{J2}\mathscr{I}_{1x} - c_{21}s_{J1}c_{12}s_{J2}\mathscr{I}_{1y}+ \text{ unmeasurable anti-phase coherences}}.$$

The terms contributing to the signal can be written as

$$\left(\underbrace{(c_{11}^- + c_{11}^+)(s_{12}^- + s_{12}^+)}_{[\Omega_1,\Omega_1]} + \underbrace{(-s_{21}^- - s_{21}^+)(c_{12}^- - c_{12}^+)}_{[\Omega_2,\Omega_1]}\right)\mathscr{I}_{1x} - \left(\underbrace{(c_{11}^- + c_{11}^+)(c_{12}^- + c_{12}^+)}_{[\Omega_1,\Omega_1]} + \underbrace{(-s_{21}^- + s_{21}^+)(-s_{12}^- + s_{12}^+)}_{[\Omega_2,\Omega_1]}\right)\mathscr{I}_{1y}.$$

- Evaluation of the traces of $\hat{M} + \hat{\rho}(t_2)$ gives the following modulation of the signal:

$$-\mathrm{i}\underbrace{(c_{11}^- + c_{11}^+)\left(\mathrm{e}^{\mathrm{i}(\Omega_1-\pi J)t_2} + \mathrm{e}^{\mathrm{i}(\Omega_1+\pi J)t_2}\right)}_{[\Omega_1,\Omega_1]} - \underbrace{(s_{21}^- - s_{21}^+)\left(\mathrm{e}^{\mathrm{i}(\Omega_1-\pi J)t_2} - \mathrm{e}^{\mathrm{i}(\Omega_1+\pi J)t_2}\right)}_{[\Omega_2,\Omega_1]}$$

Again, the green part of the signal is shifted by $\pi/2$ from the blue one (multiplied by $-\mathrm{i}$), and this difference in phases cannot be removed by any phase correction. If we apply the same phase correction as for the experiment with the x phase of the second pulse, we obtain

$$- \underbrace{(c_{11}^- + c_{11}^+)\left(\mathrm{e}^{\mathrm{i}(\Omega_1-\pi J)t_2} + \mathrm{e}^{\mathrm{i}(\Omega_1+\pi J)t_2}\right)}_{[\Omega_1,\Omega_1]} + \mathrm{i}\underbrace{(s_{21}^- - s_{21}^+)\left(\mathrm{e}^{\mathrm{i}(\Omega_1-\pi J)t_2} - \mathrm{e}^{\mathrm{i}(\Omega_1+\pi J)t_2}\right)}_{[\Omega_2,\Omega_1]} \qquad (11.17)$$

- Now we combine signals obtained with the different phases of the second pulse. The Fourier transformation (with respect to the real time course during measurement, labeled t_2 here) of the signal obtained with the phase x (Eq. 11.16) after introducing the relaxation yields a series of one-dimensional spectra with the following shape:

$$- \mathrm{i}(s_{11}^- + s_{11}^+)\underbrace{\left(\frac{\overline{R}_{2,1}}{\overline{R}_{2,1}^2 + (\Omega_1 - \pi J - \omega_2)^2} + \frac{\overline{R}_{2,1}}{\overline{R}_{2,1}^2 + (\Omega_1 + \pi J - \omega_2)^2} + \frac{\mathrm{i}(\Omega_1 - \pi J - \omega_2)}{\overline{R}_{2,1}^2 + (\Omega_1 - \pi J - \omega_2)^2} + \frac{\mathrm{i}(\Omega_1 + \pi J - \omega_2)}{\overline{R}_{2,1}^2 + (\Omega_1 + \pi J - \omega_2)^2}\right)}_{[\Omega_1,\Omega_1]}$$

$$+ (c_{21}^- - c_{21}^+)\underbrace{\left(\frac{\overline{R}_{2,1}}{\overline{R}_{2,1}^2 + (\Omega_1 - \pi J - \omega_2)^2} - \frac{\overline{R}_{2,1}}{\overline{R}_{2,1}^2 + (\Omega_1 + \pi J - \omega_2)^2} + \frac{\mathrm{i}(\Omega_1 - \pi J - \omega_2)}{\overline{R}_{2,1}^2 + (\Omega_1 - \pi J - \omega_2)^2} - \frac{\mathrm{i}(\Omega_1 + \pi J - \omega_2)}{\overline{R}_{2,1}^2 + (\Omega_1 + \pi J - \omega_2)^2}\right)}_{[\Omega_2,\Omega_1]}.$$

$$(11.18)$$

292

Separating the real and imaginary parts provides

$$
+ \underbrace{(s_{11}^- + s_{11}^+) \left(\frac{(\Omega_1 - \pi J - \omega_2)}{\overline{R}_{2,1}^2 + (\Omega_1 - \pi J - \omega_2)^2} + \frac{(\Omega_1 + \pi J - \omega_2)}{\overline{R}_{2,1}^2 + (\Omega_1 + \pi J - \omega_2)^2} - \mathrm{i} \left(\frac{\overline{R}_{2,1}}{\overline{R}_{2,1}^2 + (\Omega_1 - \pi J - \omega_2)^2} + \frac{\overline{R}_{2,1}}{\overline{R}_{2,1}^2 + (\Omega_1 + \pi J - \omega_2)^2} \right) \right)}_{[\Omega_1, \Omega_1]}
$$

$$
+ \underbrace{(c_{21}^- - c_{21}^+) \left(\frac{\overline{R}_{2,1}}{\overline{R}_{2,1}^2 + (\Omega_1 - \pi J - \omega_2)^2} - \frac{\overline{R}_{2,1}}{\overline{R}_{2,1}^2 + (\Omega_1 + \pi J - \omega_2)^2} + \mathrm{i} \left(\frac{(\Omega_1 - \pi J - \omega_2)}{\overline{R}_{2,1}^2 + (\Omega_1 - \pi J - \omega_2)^2} - \frac{(\Omega_1 + \pi J - \omega_2)}{\overline{R}_{2,1}^2 + (\Omega_1 + \pi J - \omega_2)^2} \right) \right)}_{[\Omega_2, \Omega_1]}.
$$

$$(11.19)$$

In a similar manner, the Fourier transformation of the signal obtained with the phase y (Eq. 11.17) provides a series of one-dimensional spectra with the following shape:

$$
- \underbrace{(c_{11}^- + c_{11}^+) \left(\frac{\overline{R}_{2,1}}{\overline{R}_{2,1}^2 + (\Omega_1 - \pi J - \omega_2)^2} + \frac{\overline{R}_{2,1}}{\overline{R}_{2,1}^2 + (\Omega_1 + \pi J - \omega_2)^2} + \frac{\mathrm{i}(\Omega_1 - \pi J - \omega_2)}{\overline{R}_{2,1}^2 + (\Omega_1 - \pi J - \omega_2)^2} + \frac{\mathrm{i}(\Omega_1 + \pi J - \omega_2)}{\overline{R}_{2,1}^2 + (\Omega_1 + \pi J - \omega_2)^2} \right)}_{[\Omega_1, \Omega_1]}
$$

$$
+ \underbrace{\mathrm{i}(s_{21}^- - s_{21}^+) \left(\frac{\overline{R}_{2,1}}{\overline{R}_{2,1}^2 + (\Omega_1 + \pi J - \omega_2)^2} - \frac{\overline{R}_{2,1}}{\overline{R}_{2,1}^2 + (\Omega_1 - \pi J + \omega_2)^2} + \frac{\mathrm{i}(\Omega_1 - \pi J - \omega_2)}{\overline{R}_{2,1}^2 + (\Omega_1 - \pi J - \omega_2)^2} - \frac{\mathrm{i}(\Omega_1 + \pi J - \omega_2)}{\overline{R}_{2,1}^2 + (\Omega_1 + \pi J - \omega_2)^2} \right)}_{[\Omega_2, \Omega_1]}.
$$

$$(11.20)$$

We wish to use the signal obtained with the phase y as an imaginary component. Therefore, we factor out the imaginary unit and then separate the real and imaginary parts

$$
- \mathrm{i} \underbrace{(c_{11}^- + c_{11}^+) \left(\frac{(\Omega_1 - \pi J - \omega_2)}{\overline{R}_{2,1}^2 + (\Omega_1 - \pi J - \omega_2)^2} + \frac{(\Omega_1 + \pi J - \omega_2)}{\overline{R}_{2,1}^2 + (\Omega_1 + \pi J - \omega_2)^2} - \mathrm{i} \left(\frac{\overline{R}_{2,1}}{\overline{R}_{2,1}^2 + (\Omega_1 - \pi J - \omega_2)^2} + \frac{\overline{R}_{2,1}}{\overline{R}_{2,1}^2 + (\Omega_1 + \pi J - \omega_2)^2} \right) \right)}_{[\Omega_1, \Omega_1]}
$$

$$
+ \mathrm{i} \underbrace{(s_{21}^- - s_{21}^+) \left(\frac{\overline{R}_{2,1}}{\overline{R}_{2,1}^2 + (\Omega_1 - \pi J - \omega_2)^2} - \frac{\overline{R}_{2,1}}{\overline{R}_{2,1}^2 + (\Omega_1 + \pi J - \omega_2)^2} + \mathrm{i} \left(\frac{(\Omega_1 - \pi J - \omega_2)}{\overline{R}_{2,1}^2 + (\Omega_1 - \pi J - \omega_2)^2} - \frac{(\Omega_1 + \pi J - \omega_2)}{\overline{R}_{2,1}^2 + (\Omega_1 + \pi J - \omega_2)^2} \right) \right)}_{[\Omega_2, \Omega_1]}.
$$

$$(11.21)$$

As described in Section 9.5.1, the *hypercomplex* signal is obtained by (i) discarding the imaginary parts and (ii) processing the signals recorded with the x and y phases of the second pulse as real and imaginary components

$$+ \left((s_{11}^- + s_{11}^+) + \mathrm{i}(c_{11}^- + c_{11}^+)\right) \left(\underbrace{\frac{(\Omega_1 - \pi J - \omega_2)}{\overline{R}_{2,1}^2 + (\Omega_1 - \pi J - \omega_2)^2} + \frac{(\Omega_1 + \pi J - \omega_2)}{\overline{R}_{2,1}^2 + (\Omega_1 + \pi J - \omega_2)^2}}_{[\Omega_1, \Omega_1]} \right)$$

$$+ \left((c_{21}^- - c_{21}^+) + \mathrm{i}(s_{21}^- - s_{21}^+)\right) \left(\underbrace{\frac{\overline{R}_{2,1}}{\overline{R}_{2,1}^2 + (\Omega_1 - \pi J - \omega_2)^2} - \frac{\overline{R}_{2,1}}{\overline{R}_{2,1}^2 + (\Omega_1 + \pi J - \omega_2)^2}}_{[\Omega_2, \Omega_1]} \right).$$

$$(11.22)$$

When we express the obtained complex numbers in the exponential form and write the $-\mathrm{i}$ multiplying the green terms as $\mathrm{e}^{-\mathrm{i}\pi/2}$,

$$+ \mathrm{e}^{-\mathrm{i}\frac{\pi}{2}} \left(\mathrm{e}^{\mathrm{i}(\Omega_1 - \pi J)t_1} + \mathrm{e}^{\mathrm{i}(\Omega_1 + \pi J)t_1} \right) \left(\underbrace{\frac{(\Omega_1 - \pi J - \omega_2)}{\overline{R}_{2,1}^2 + (\Omega_1 - \pi J - \omega_2)^2} + \frac{(\Omega_1 + \pi J - \omega_2)}{\overline{R}_{2,1}^2 + (\Omega_1 + \pi J - \omega_2)^2}}_{[\Omega_1, \Omega_1]} \right)$$

$$+ \left(\mathrm{e}^{\mathrm{i}(\Omega_2 - \pi J)t_1} - \mathrm{e}^{\mathrm{i}(\Omega_2 + \pi J)t_1} \right) \left(\underbrace{\frac{\overline{R}_{2,1}}{\overline{R}_{2,1}^2 + (\Omega_1 - \pi J - \omega_2)^2} - \frac{\overline{R}_{2,1}}{\overline{R}_{2,1}^2 + (\Omega_1 + \pi J - \omega_2)^2}}_{[\Omega_2, \Omega_1]} \right),$$

$$(11.23)$$

we see that the green and blue parts differ in phase also in the indirect t_1 dimension. After the second Fourier transformation, we obtain a two-dimensional spectrum with the intensity of the real part proportional to

$$+ \frac{\mathcal{N}\gamma^2\hbar^2 B_0}{16 k_{\mathrm{B}} T} \underbrace{\left(\frac{(\Omega_1 - \pi J - \omega_1)}{\overline{R}_{2,1}^2 + (\Omega_1 - \pi J - \omega_1)^2} + \frac{(\Omega_1 + \pi J - \omega_1)}{\overline{R}_{2,1}^2 + (\Omega_1 + \pi J - \omega_1)^2} \right) \left(\frac{(\Omega_1 - \pi J - \omega_2)}{\overline{R}_{2,1}^2 + (\Omega_1 - \pi J - \omega_2)^2} + \frac{(\Omega_1 + \pi J - \omega_2)}{\overline{R}_{2,1}^2 + (\Omega_1 + \pi J - \omega_2)^2} \right)}_{[\Omega_1, \Omega_1]}$$

$$+ \frac{\mathcal{N}\gamma^2\hbar^2 B_0}{16 k_{\mathrm{B}} T} \underbrace{\left(\frac{\overline{R}_{2,2}}{\overline{R}_{2,2}^2 + (\Omega_2 - \pi J - \omega_1)^2} - \frac{\overline{R}_{2,2}}{\overline{R}_{2,2}^2 + (\Omega_2 + \pi J - \omega_1)^2} \right) \left(\frac{\overline{R}_{2,1}}{\overline{R}_{2,1}^2 + (\Omega_1 - \pi J - \omega_2)^2} - \frac{\overline{R}_{2,1}}{\overline{R}_{2,1}^2 + (\Omega_1 + \pi J - \omega_2)^2} \right)}_{[\Omega_2, \Omega_1]},$$

$$(11.24)$$

where $\overline{R}_{2,1}$ and $\overline{R}_{2,2}$ are the average relaxation rates of proton 1 and 2, respectively (ignoring the differences in the relaxation of different coherences).

- The green component of the signal evolves with the same chemical shift in both dimensions, providing a *diagonal* signal (at the frequencies $[\Omega_1, \Omega_1]$ in the 2D spectrum). The blue (originally anti-phase) component of the signal also evolves with Ω_1 in the direct dimension (t_2), but with Ω_2 in the indirect dimension (t_1). It provides an *off-diagonal* signal, a *cross-peak* at

frequencies $[\Omega_2, \Omega_1]$ in the 2D spectrum. As the phases of the blue and green components differ by $90°$, either diagonal peaks or cross-peaks have the undesirable dispersion shape (it is not possible to phase both diagonal peaks and cross-peaks, they always have their phases differing by $90°$, even when the spectrum is processed correctly following the protocol described in Section 9.5.1). Typically, the spectrum is phased so that the cross-peaks have a nice absorptive shape corresponding to Eq. 11.26 (see Figure 11.6) because they carry a useful chemical information: they show which protons are connected by 2 or 3 covalent bonds.

- The diagonal peaks are not interesting, but their dispersive shape may obscure cross-peaks close to the diagonal. The problem with the phase can be solved if one more $90°$ pulse is introduced. Such a pulse converts the magenta multiple-quantum coherences to anti-phase single-quantum coherences, which evolve into the measurable signal. The point is that other coherences can be removed by phase cycling. The obtained spectrum contains diagonal peaks and cross-peaks, but (in contrast to the simple two-pulse variant of the COSY experiment) both diagonal peaks and cross-peaks have the same phase.[5] This version of the experiment, known as *double-quantum filtered* COSY (DQF-COSY), is analyzed in Section 11.10.2. Its disadvantage is a lower sensitivity – we lose a half of the signal.

- Also, note that each peak is split into doublets in both dimensions. More complex multiplets are obtained if more than two nuclei are coupled. The distance of peaks in the multiplets is given by the interaction constant J. In the case of nuclei connected by three bonds, J depends on the torsion angle defined by these three bonds. So, COSY spectra can be used to determine torsion angles in the molecule.

- The terms in the cyan frames evolve with the chemical shift of the second nucleus during the acquisition as

$$s_{21}c_{J1}\mathscr{I}_{2x} \rightarrow s_{21}c_{J1}c_{12}c_{J2}\mathscr{I}_{2x} + s_{21}c_{J1}s_{12}c_{J2}\mathscr{I}_{2y} + \text{ unmeasurable anti-phase coherences}$$

$$-s_{11}s_{J1}2\mathscr{I}_{1z}\mathscr{I}_{2y} \rightarrow s_{11}s_{J1}c_{12}s_{J2}\mathscr{I}_{2x} + s_{11}s_{J1}s_{12}s_{J2}\mathscr{I}_{2y} + \text{ unmeasurable anti-phase coherences}$$

and give a similar type of signal for the other nucleus:

$$+ \frac{\mathcal{N}\gamma^2\hbar^2 B_0}{16k_{\mathrm{B}}T} \underbrace{\left(\frac{(\Omega_2 - \pi J - \omega_1)}{\overline{R}_{2,2}^2 + (\Omega_2 + \pi J - \omega_1)^2} + \frac{(\Omega_2 + \pi J - \omega_1)}{\overline{R}_{2,2}^2 + (\Omega_2 - \pi J - \omega_1)^2} \right) \left(\frac{(\Omega_2 - \pi J - \omega_2)}{\overline{R}_{2,2}^2 + (\Omega_2 + \pi J - \omega_2)^2} + \frac{(\Omega_2 + \pi J - \omega_2)}{\overline{R}_{2,2}^2 + (\Omega_2 - \pi J - \omega_2)^2} \right)}_{[\Omega_1,\Omega_1]}$$

$$+ \frac{\mathcal{N}\gamma^2\hbar^2 B_0}{16k_{\mathrm{B}}T} \underbrace{\left(\frac{\overline{R}_{2,1}}{\overline{R}_{2,1}^2 + (\Omega_1 + \pi J - \omega_1)^2} - \frac{\overline{R}_{2,1}}{\overline{R}_{2,1}^2 + (\Omega_1 - \pi J - \omega_1)^2} \right) \left(\frac{\overline{R}_{2,2}}{\overline{R}_{2,2}^2 + (\Omega_2 + \pi J - \omega_2)^2} - \frac{\overline{R}_{2,2}}{\overline{R}_{2,2}^2 + (\Omega_2 - \pi J - \omega_2)^2} \right)}_{[\Omega_2,\Omega_1]},$$

$$(11.25)$$

This signal represents the other diagonal and off-diagonal peak in the spectrum.

---

[5]We cannot use phase cycling to remove the green terms resulting in the unwanted diagonal peaks because phase cycling can distinguish multiple-quantum coherences from single-quantum ones, but it cannot distinguish anti-phase single quantum coherences from in-phase single quantum coherences.

Table 11.1: Evolution of the density matrix during the COSY experiment. Modulations of the density matrix components (omitting the $\kappa/2$ factor and the $\mathscr{I}_t$ component) having the origin in $\mathscr{I}_{1z}$ and $\mathscr{I}_{2z}$ are shown in black and cyan, respectively. The product operators are color-coded as in the text.

Real in t_1:

	$\hat\rho(a)$	$\hat\rho(b)$	$\hat\rho(c)$	$\hat\rho(d)$	$\hat\rho(t2)$	Tr$\{\hat\rho(t2)(\mathscr{I}_{1x}+\mathscr{I}_{2x}+\mathrm{i}\mathscr{I}_{1y}+\mathrm{i}\mathscr{I}_{2y})\}$
$\mathscr{I}_{1z}$	$+1$	0	0	$-c_{11}c_{J1}$	$+c_{11}c_{J1}$	0
$\mathscr{I}_{1x}$		0	$+s_{11}c_{J1}$	$+s_{11}c_{J1}$	$+s_{11}c_{J1}c_{12}c_{J2}+s_{21}s_{J1}c_{12}s_{J2}$	$+s_{11}c_{J1}c_{12}c_{J2}+s_{21}s_{J1}c_{12}s_{J2}$
$\mathscr{I}_{1y}$		-1	$-c_{11}c_{J1}$	0	$+s_{11}c_{J1}s_{12}c_{J2}+s_{21}s_{J1}s_{12}s_{J2}$	$\mathrm{i}(+s_{11}c_{J1}s_{12}c_{J2}+s_{21}s_{J1}s_{12}s_{J2})$
$2\mathscr{I}_{1y}\mathscr{I}_{2z}$			$+s_{11}s_{J1}$	$-s_{21}s_{J1}$	$+s_{11}c_{J1}c_{12}s_{J2}-s_{21}s_{J1}c_{12}c_{J2}$	0
$2\mathscr{I}_{1x}\mathscr{I}_{2z}$			$+c_{11}s_{J1}$	0	$-s_{11}c_{J1}s_{12}s_{J2}+s_{21}s_{J1}s_{12}c_{J2}$	0
$2\mathscr{I}_{1x}\mathscr{I}_{2y}$				$-c_{11}s_{J1}$	$-c_{11}s_{J1}c_{12}c_{22}+c_{21}s_{J1}s_{12}s_{22}$	0
$2\mathscr{I}_{1x}\mathscr{I}_{2x}$					$+c_{11}s_{J1}c_{12}s_{22}+c_{21}s_{J1}s_{12}c_{22}$	0
$2\mathscr{I}_{1y}\mathscr{I}_{2y}$					$-c_{21}s_{J1}c_{12}s_{22}-c_{11}s_{J1}s_{12}c_{22}$	0
$2\mathscr{I}_{1y}\mathscr{I}_{2x}$				$-c_{21}s_{J1}$	$-c_{21}s_{J1}c_{12}c_{22}+c_{11}s_{J1}s_{12}s_{22}$	0
$2\mathscr{I}_{1z}\mathscr{I}_{2x}$			$+c_{21}s_{J1}$	0	$-s_{21}c_{J1}s_{22}s_{J2}+s_{11}s_{J1}s_{22}c_{J2}$	0
$2\mathscr{I}_{1z}\mathscr{I}_{2y}$			$+s_{21}s_{J1}$	$-s_{11}s_{J1}$	$+s_{21}c_{J1}c_{22}s_{J2}-s_{11}s_{J1}c_{22}c_{J2}$	0
$\mathscr{I}_{2y}$		-1	$-c_{21}c_{J1}$	0	$+s_{21}c_{J1}s_{22}c_{J2}+s_{11}s_{J1}s_{22}s_{J2}$	$\mathrm{i}(+s_{21}c_{J1}s_{22}c_{J2}+s_{11}s_{J1}s_{22}s_{J2})$
$\mathscr{I}_{2x}$		0	$+s_{21}c_{J1}$	$+s_{21}c_{J1}$	$+s_{21}c_{J1}c_{22}c_{J2}+s_{11}s_{J1}c_{22}s_{J2}$	$+s_{21}c_{J1}c_{22}c_{J2}+s_{11}s_{J1}c_{22}s_{J2}$
$\mathscr{I}_{2z}$	$+1$	0	0	$-c_{21}c_{J1}$	$+c_{21}c_{J1}$	0

Imaginary in t_1:

	$\hat\rho(a)$	$\hat\rho(b)$	$\hat\rho(c)$	$\hat\rho(d)$	$\hat\rho(t_2)$	
$\mathscr{I}_{1z}$	$+1$	0	0	$-s_{11}c_{J1}$	$+s_{11}c_{J1}$	0
$\mathscr{I}_{1x}$		0	$+s_{11}c_{J1}$	0	$+c_{11}c_{J1}s_{12}c_{J2}+c_{21}s_{J1}s_{12}s_{J2}$	$+c_{11}c_{J1}s_{12}c_{J2}+c_{21}s_{J1}s_{12}s_{J2}$
$\mathscr{I}_{1y}$		-1	$-c_{11}c_{J1}$	$-c_{11}c_{J1}$	$-c_{11}c_{J1}c_{12}c_{J2}-c_{21}s_{J1}c_{12}s_{J2}$	$\mathrm{i}(-c_{11}c_{J1}c_{12}c_{J2}-c_{21}s_{J1}c_{12}s_{J2})$
$2\mathscr{I}_{1y}\mathscr{I}_{2z}$			$+s_{11}s_{J1}$	0	$+c_{11}c_{J1}s_{12}s_{J2}-c_{21}s_{J1}s_{12}c_{J2}$	0
$2\mathscr{I}_{1x}\mathscr{I}_{2z}$			$+c_{11}s_{J1}$	$-c_{21}s_{J1}$	$+c_{11}c_{J1}c_{12}s_{J2}-c_{21}s_{J1}c_{12}c_{J2}$	0
$2\mathscr{I}_{1x}\mathscr{I}_{2y}$				$+s_{11}s_{J1}$	$+s_{11}s_{J1}c_{12}c_{22}+c_{21}s_{J1}s_{12}s_{22}$	0
$2\mathscr{I}_{1x}\mathscr{I}_{2x}$					$-s_{11}s_{J1}c_{12}s_{22}-s_{21}s_{J1}s_{12}c_{22}$	0
$2\mathscr{I}_{1y}\mathscr{I}_{2y}$					$+s_{21}s_{J1}c_{12}s_{22}+s_{11}s_{J1}s_{12}c_{22}$	0
$2\mathscr{I}_{1y}\mathscr{I}_{2x}$				$+s_{21}s_{J1}$	$+s_{21}s_{J1}c_{12}c_{22}+c_{11}s_{J1}s_{12}s_{22}$	0
$2\mathscr{I}_{1z}\mathscr{I}_{2x}$			$+c_{21}s_{J1}$	$-c_{11}s_{J1}$	$+c_{21}c_{J1}c_{22}s_{J2}-c_{11}s_{J1}c_{22}c_{J2}$	0
$2\mathscr{I}_{1z}\mathscr{I}_{2y}$			$+s_{21}s_{J1}$	0	$+c_{21}c_{J1}s_{22}s_{J2}-c_{11}s_{J1}s_{22}c_{J2}$	0
$\mathscr{I}_{2y}$		-1	$-c_{21}c_{J1}$	$-c_{21}c_{J1}$	$-c_{21}c_{J1}c_{22}c_{J2}-c_{11}s_{J1}c_{22}s_{J2}$	$\mathrm{i}(-c_{21}c_{J1}c_{22}c_{J2}-c_{11}s_{J1}c_{22}s_{J2})$
$\mathscr{I}_{2x}$		0	$+s_{21}c_{J1}$	0	$+c_{21}c_{J1}s_{22}c_{J2}+c_{11}s_{J1}s_{22}s_{J2}$	$+c_{21}c_{J1}s_{22}c_{J2}+c_{11}s_{J1}s_{22}s_{J2}$
$\mathscr{I}_{2z}$	$+1$	0	0	$-s_{21}c_{J1}$	$+s_{21}c_{J1}$	0
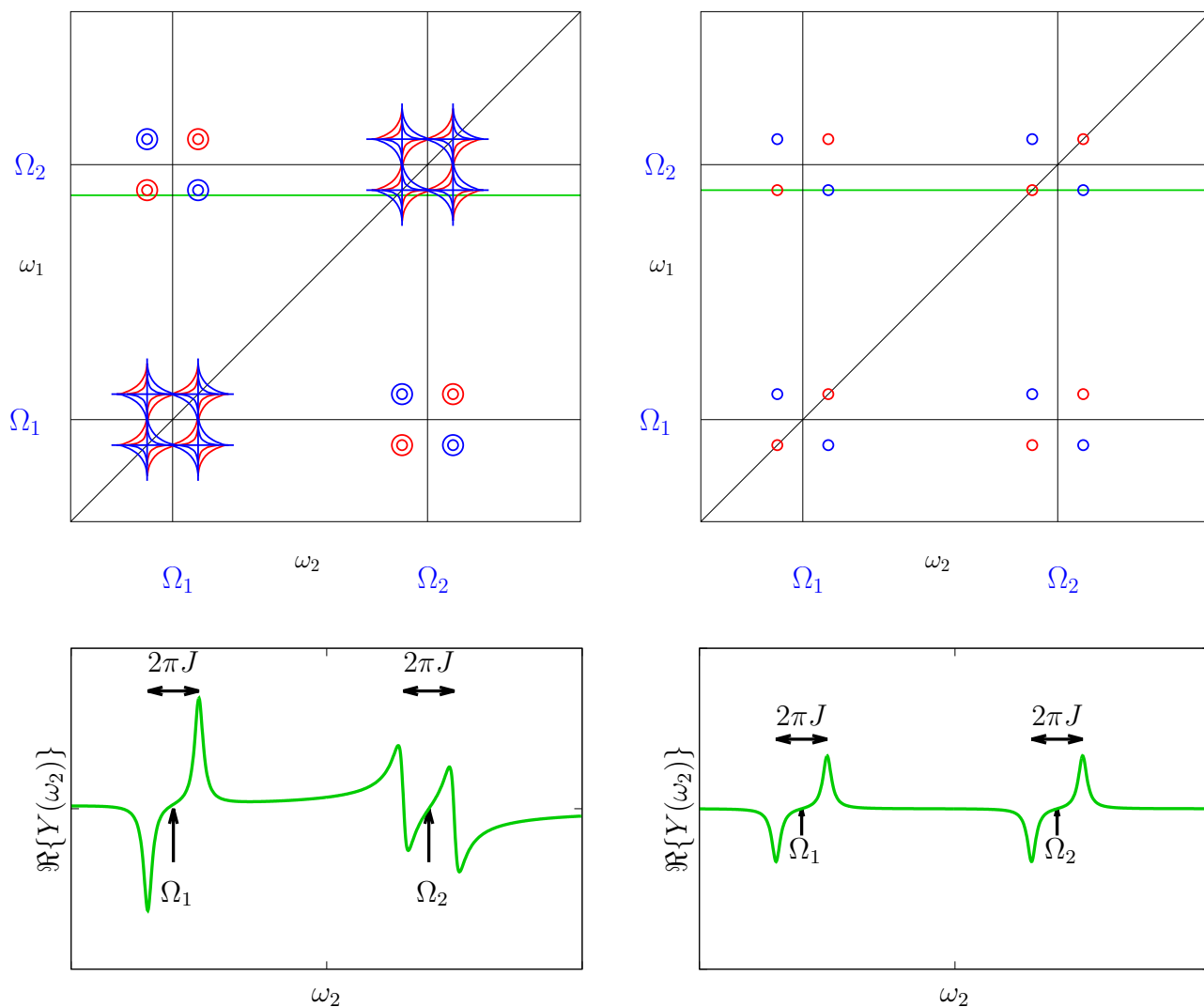
Figure 11.6: COSY spectrum of a ^{1}H–^{1}H pair. The two-dimensional peaks are displayed as contour plots, the positive and negative contours are shown in blue and red, respectively. A one-dimensional slice taken from the 2D spectrum at the position indicated by the green line is displayed below the 2D plot. Frequency offsets of the protons are Ω_1 and Ω_2. The left spectra were obtained by the pulse sequence displayed in Figure 11.5, the right spectra by the pulse sequence DQF-COSY.

HOMEWORK

Analyze the COSY experiment (Section 11.9).

11.10 SUPPORTING INFORMATION

11.10.1 APT

The attached proton test (APT) is useful for analysis of systems with multiple protons, most often CH_n (C, CH, CH_2, CH_3). The experiment consists of ^{13}C excitation, simultaneous echo (discussed in Section 10.9), and ^{13}C acquisition with proton decoupling. In the following analysis, the ^{13}C operators are labeled $\mathscr{S}_x$, $\mathscr{S}_y$, $\mathscr{S}_z$, and relaxation is ignored for the sake of simplicity.

- $\hat{\rho}(a) = \frac{1}{2^n}\mathscr{I}_t + \frac{\kappa_1}{2^n}\sum_{k=1}^{n}(\mathscr{I}_{kz}) + \frac{\kappa_2}{2^n}\mathscr{S}_z$

  The probability density matrix at equilibrium is described in a similar manner as for one or two magnetic moments, the extension to the multinuclear system is reflected by the scaling constant $1/2^n$, where n is the number of protons attached to ^{13}C.

- $\hat{\rho}(b) = \frac{1}{2^n}\mathscr{I}_t + \frac{\kappa_1}{2^n}\sum_{k=1}^{n}(\mathscr{I}_{kz}) - \frac{\kappa_2}{2^n}\mathscr{S}_y$

  Excitation of ^{13}C is an analogy of cases discussed above.

- Understanding the next step is critical for the analysis. The general conclusions of Section 10.9 apply, but the actual form of the density matrix must be derived for each system. The general conclusions are: evolution of Ω_2 (^{13}C frequency offset) due tho the ^{13}C chemical shift is refocused, J-coupling evolves for 2τ as $\cos(2\pi J\tau)$ and $\sin(2\pi J\tau)$, nucleus 1 (proton) is never excited (no proton $90°$ pulse), therefore only $\mathscr{I}_{kz}$ contributions are present for protons.

- The actual analysis for $^{13}CH_2$ and $^{13}CH_3$ groups requires extension of the density matrix to $2^{n+1} \times 2^{n+1}$ dimensions. Construction of the basis matrices for such 4^{n+1}-dimensional operator space involves additional direct products with the matrices $\mathscr{I}_t$, $\mathscr{I}_x$, $\mathscr{I}_y$, $\mathscr{I}_z$. Evolution of the $2^{n+1} \times 2^{n+1}$ matrices is governed by their commutation rules, three-dimensional subspaces where "rotations" of operators take place are defined by these commutation rules (Eqs. 8.29–8.31).

- When the rules are applied, the analysis gives

  $$\hat{\rho}(e) = \frac{1}{2^n}\mathscr{I}_t + \frac{\kappa_1}{2^n}\sum_{k=1}^{n}(\mathscr{I}_{kz}) + \frac{\kappa_2}{2^n}\begin{cases} n=0: & \mathscr{S}_y \\ n=1: & c\mathscr{S}_y - s2\mathscr{I}_{1z}\mathscr{S}_x \\ n=2: & c^2\mathscr{S}_y - sc(2\mathscr{I}_{1z}\mathscr{S}_x + 2\mathscr{I}_{2z}\mathscr{S}_x) - s^2 4\mathscr{I}_{1z}\mathscr{I}_{2z}\mathscr{S}_y \\ n=3: & c^3\mathscr{S}_y - sc^2(2\mathscr{I}_{1z}\mathscr{S}_x + 2\mathscr{I}_{2z}\mathscr{S}_x + 2\mathscr{I}_{3z}\mathscr{S}_x) \\ & -s^2 c(4\mathscr{I}_{1z}\mathscr{I}_{2z}\mathscr{S}_y + 4\mathscr{I}_{1z}\mathscr{I}_{3z}\mathscr{S}_y + 4\mathscr{I}_{2z}\mathscr{I}_{3z}\mathscr{S}_y) \\ & +s^3 8\mathscr{I}_{1z}\mathscr{I}_{2z}\mathscr{I}_{3z}\mathscr{S}_x \end{cases}$$

  where $s = \sin(2\pi J\tau)$ and $c = \cos(2\pi J\tau)$.

- Since decoupling is applied during acquisition, only the $\mathscr{S}_y$ coherences give a measurable signal. Note that the fact that the proton decoupling is used tells us in advance that the terms containing $\mathscr{I}_{kz}$ need not be analyzed. Therefore the knowledge of exact commutation rules is not necessary, the only important conclusion is that the observable contributions to the density matrix are modulated by $\cos^n(2\pi J\tau)$ for CH_n. During acquisition, these terms evolve under the influence of chemical shift, exactly like in a one-pulse experiment. If τ is set to $\tau = 2J$, then $c = \cos\pi = -1$. Therefore, signals of C and CH_2 are positive and signals of CH and CH_3 are negative $\Rightarrow$ useful chemical information.

11.10.2 Double-quantum filtered COSY

The double-quantum filtered variant of the COSY experiment (DQF-COSY) provides spectra with the same phases of diagonal peaks and cross peaks. The modification of the experiment consists of (i) adding a third $90°$ pulse and (ii) phase cycle of the first two pulses (Figure 11.7). In DQF-COSY, the initial density matrix
$\hat{\rho}(a) = \frac{1}{2}(\mathscr{I}_t + \kappa\mathscr{I}_{1z} + \kappa\mathscr{I}_{2z})$
evolves as shown in Table 11.2. The experiment is repeated for times with different phases of the radio waves (see values ϕ_1 and ϕ_2 in Table 11.2). As the consecutive measured records are subtracted before storing the data (indicated by the multiplying factor m in Table 11.2), contribution of all coherences are canceled except for the multiple-quantum terms $2\mathscr{I}_{1x}\mathscr{I}_{1y}$ and $2\mathscr{I}_{1y}\mathscr{I}_{1x}$. It is therefore sufficient to analyze only the following component of $\hat{\rho}(d)$:
$\hat{\rho}(d) = \frac{\kappa}{2}(\frac{1}{2}(c_{11}s_{J1} + c_{21}s_{J1})2\mathscr{I}_{1x}\mathscr{I}_{1y} + \frac{1}{2}(c_{11}s_{J1} + c_{21}s_{J1})2\mathscr{I}_{1y}\mathscr{I}_{1x})$
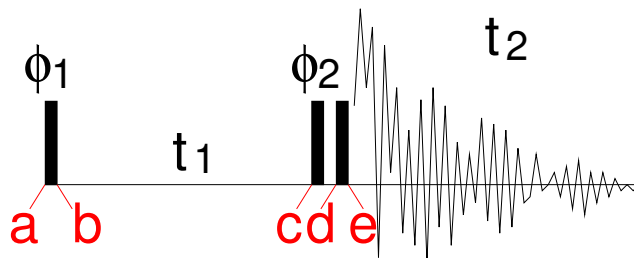
Figure 11.7: DQF-COSY pulse sequence. The rectangles represent 90° radio wave pulses applied at a frequency sufficiently close to the precession frequencies of both interacting magnetic moments. The symbols ϕ_1 and ϕ_2 represent a phase cycle $x, y, -x, -y$. The hypercomplex spectrum is obtained by repeating the measurement for each t_1 increment with ϕ_2 advanced by $90°$ (see Table 11.2).

Table 11.2: Evolution of the density matrix during DQF-COSY. Modulations of the density matrix components (omitting the $\kappa/2$ factor and the $\mathscr{I}_t$ component) having the origin in $\mathscr{I}_{1z}$ and $\mathscr{I}_{2z}$ are shown in black and cyan, respectively. The lines labeled ϕ_1 and ϕ_2 show phase cycles of the first two radio-wave pulses (cf. Figure 11.7). The multiplier m indicates whether the data recorded with the given phases are stored as positive $(+)$ or negative $(-)$ numbers. The modulations after the second pulse averaged by the phase cycle are presented in the last column labeled $\frac{1}{4}\sum$. The product operators are color-coded as in Section 11.9.

Real in t_1:

	$\hat\rho$(a)		$\hat\rho$(b)			$\hat\rho$(c)				$\hat\rho$(d)				$m\hat\rho$(d8)				$\frac{1}{4}\sum$
ϕ_1:		$+x$	$+y$	$-x$	$-y$	$+x$	$+y$	$-x$	$-y$	$+x$	$+y$	$-x$	$-y$	$+x$	$+y$	$-x$	$-y$	
ϕ_2:						$+x$	$+y$	$-x$	$-y$	$+x$	$+y$	$-x$	$-y$	$+x$	$+y$	$-x$	$-y$	
m:														$-$	$+$	$-$	$+$	
$\mathscr{I}_{1z}$	$+1$	0	0	0	0	0	0	0	0	$-c_{11}c_{J1}$	$-c_{11}c_{J1}$	$-c_{11}c_{J1}$	$-c_{11}c_{J1}$	$+c_{11}c_{J1}$	$-c_{11}c_{J1}$	$+c_{11}c_{J1}$	$-c_{11}c_{J1}$	0
$\mathscr{I}_{1x}$		0	1	0	-1	$+s_{11}c_{J1}$	$+c_{11}c_{J1}$	$-s_{11}c_{J1}$	$-c_{11}c_{J1}$	$+s_{11}c_{J1}$	0	$-s_{11}c_{J1}$	0	$-s_{11}c_{J1}$	0	$+s_{11}c_{J1}$	0	0
$\mathscr{I}_{1y}$		-1	0	1	0	$-c_{11}c_{J1}$	$+s_{11}c_{J1}$	$+c_{11}c_{J1}$	$-s_{11}c_{J1}$	0	$+s_{11}c_{J1}$	0	$-s_{11}c_{J1}$	0	$+s_{11}c_{J1}$	0	$-s_{11}c_{J1}$	0
$2\mathscr{I}_{1y}\mathscr{I}_{2z}$						$+s_{11}s_{J1}$	$+c_{11}s_{J1}$	$-s_{11}s_{J1}$	$-c_{11}s_{J1}$	$-s_{21}s_{J1}$	0	$+s_{21}s_{J1}$	0	$+s_{21}s_{J1}$	0	$-s_{21}s_{J1}$	0	0
$2\mathscr{I}_{1x}\mathscr{I}_{2z}$						$+c_{11}s_{J1}$	$-s_{11}s_{J1}$	$-c_{11}s_{J1}$	$+s_{11}s_{J1}$	0	$+s_{21}s_{J1}$	0	$-s_{21}s_{J1}$	0	$+s_{21}s_{J1}$	0	$-s_{21}s_{J1}$	
$2\mathscr{I}_{1x}\mathscr{I}_{2y}$										$-c_{11}s_{J1}$	$+c_{21}s_{J1}$	$-c_{11}s_{J1}$	$+c_{21}s_{J1}$	$+c_{11}s_{J1}$	$+c_{21}s_{J1}$	$+c_{11}s_{J1}$	$+c_{21}s_{J1}$	$\frac{+c_{11}s_{J1}+c_{21}s_{J1}}{2}$
$2\mathscr{I}_{1y}\mathscr{I}_{2x}$										$-c_{21}s_{J1}$	$+c_{11}s_{J1}$	$-c_{21}s_{J1}$	$+c_{11}s_{J1}$	$+c_{21}s_{J1}$	$+c_{11}s_{J1}$	$+c_{21}s_{J1}$	$+c_{11}s_{J1}$	$\frac{+c_{21}s_{J1}+c_{11}s_{J1}}{2}$
$2\mathscr{I}_{1z}\mathscr{I}_{2x}$						$+c_{21}s_{J1}$	$-s_{21}s_{J1}$	$-c_{21}s_{J1}$	$+s_{21}s_{J1}$	0	$+s_{11}s_{J1}$	0	$-s_{11}s_{J1}$	0	$+s_{11}s_{J1}$	0	$-s_{11}s_{J1}$	0
$2\mathscr{I}_{1z}\mathscr{I}_{2y}$						$+s_{21}s_{J1}$	$+c_{21}s_{J1}$	$-s_{21}s_{J1}$	$-c_{21}s_{J1}$	$-s_{11}s_{J1}$	0	$+s_{11}s_{J1}$	0	$+s_{11}s_{J1}$	0	$-s_{11}s_{J1}$	0	0
$\mathscr{I}_{2y}$		-1	0	1	0	$-c_{21}c_{J1}$	$+s_{21}c_{J1}$	$+c_{21}c_{J1}$	$-s_{21}c_{J1}$	0	$+s_{11}c_{J1}$	0	$-s_{11}c_{J1}$	0	$+s_{11}c_{J1}$	0	$-s_{11}c_{J1}$	0
$\mathscr{I}_{2x}$		0	1	0	-1	$+s_{21}c_{J1}$	$+c_{21}c_{J1}$	$-s_{21}c_{J1}$	$-c_{21}c_{J1}$	$+s_{21}c_{J1}$	0	$-s_{21}c_{J1}$	0	$-s_{21}c_{J1}$	0	$+s_{21}c_{J1}$	0	0
$\mathscr{I}_{2z}$	$+1$	0	0	0	0	0	0	0	0	$-c_{21}c_{J1}$	$-c_{21}c_{J1}$	$-c_{21}c_{J1}$	$-c_{21}c_{J1}$	$+c_{21}c_{J1}$	$-c_{21}c_{J1}$	$+c_{21}c_{J1}$	$-c_{21}c_{J1}$	0

Imaginary in t_1:

	$\hat\rho$(a)		$\hat\rho$(b)			$\hat\rho$(c)				$\hat\rho$(d)				$m\hat\rho$(d)				$\frac{1}{4}\sum$
ϕ_1:		$+x$	$+y$	$-x$	$-y$	$+x$	$+y$	$-x$	$-y$	$+x$	$+y$	$-x$	$-y$	$+x$	$+y$	$-x$	$-y$	
ϕ_2:						$+y$	$-x$	$-y$	$+x$	$+y$	$-x$	$-y$	$+x$	$+y$	$-x$	$-y$	$+x$	
m:														$-$	$+$	$-$	$+$	
$\mathscr{I}_{1z}$	$+1$	0	0	0	0	0	0	0	0	$-s_{11}c_{J1}$	$-s_{11}c_{J1}$	$-s_{11}c_{J1}$	$-s_{11}c_{J1}$	$+s_{11}c_{J1}$	$-s_{11}c_{J1}$	$+s_{11}c_{J1}$	$-s_{11}c_{J1}$	0
$\mathscr{I}_{1x}$		0	1	0	-1	$+s_{11}c_{J1}$	$+c_{11}c_{J1}$	$-s_{11}c_{J1}$	$-c_{11}c_{J1}$	0	$+c_{11}c_{J1}$	0	$-c_{11}c_{J1}$	0	$+c_{11}c_{J1}$	0	$-c_{11}c_{J1}$	0
$\mathscr{I}_{1y}$		-1	0	1	0	$-c_{11}c_{J1}$	$+s_{11}c_{J1}$	$+c_{11}c_{J1}$	$-s_{11}c_{J1}$	$-c_{11}c_{J1}$	0	$+c_{11}c_{J1}$	0	$+c_{11}c_{J1}$	0	$-c_{11}c_{J1}$	0	0
$2\mathscr{I}_{1y}\mathscr{I}_{2z}$						$+s_{11}s_{J1}$	$+c_{11}s_{J1}$	$-s_{11}s_{J1}$	$-c_{11}s_{J1}$	0	$-c_{21}s_{J1}$	0	$+c_{21}s_{J1}$	0	$-c_{21}s_{J1}$	0	$+c_{21}s_{J1}$	0
$2\mathscr{I}_{1x}\mathscr{I}_{2z}$						$+c_{11}s_{J1}$	$-s_{11}s_{J1}$	$-c_{11}s_{J1}$	$+s_{11}s_{J1}$	$-s_{21}s_{J1}$	0	$+s_{21}s_{J1}$	0	$+s_{21}s_{J1}$	0	$-s_{21}s_{J1}$	0	0
$2\mathscr{I}_{1x}\mathscr{I}_{2y}$										$+s_{11}s_{J1}$	$-s_{21}s_{J1}$	$+s_{11}s_{J1}$	$-s_{21}s_{J1}$	$-s_{11}s_{J1}$	$-s_{21}s_{J1}$	$-s_{11}s_{J1}$	$-s_{21}s_{J1}$	$\frac{-s_{11}s_{J1}-s_{21}s_{J1}}{2}$
$2\mathscr{I}_{1y}\mathscr{I}_{2x}$										$+s_{21}s_{J1}$	$-s_{11}s_{J1}$	$+s_{21}s_{J1}$	$-s_{11}s_{J1}$	$-s_{21}s_{J1}$	$-s_{11}s_{J1}$	$-s_{21}s_{J1}$	$-s_{11}s_{J1}$	$\frac{-s_{21}s_{J1}-s_{11}s_{J1}}{2}$
$2\mathscr{I}_{1z}\mathscr{I}_{2x}$						$+c_{21}s_{J1}$	$-s_{21}s_{J1}$	$-c_{21}s_{J1}$	$+s_{21}s_{J1}$	$-c_{11}s_{J1}$	0	$+c_{11}s_{J1}$	0	$+c_{11}s_{J1}$	0	$-c_{11}s_{J1}$	0	0
$2\mathscr{I}_{1z}\mathscr{I}_{2y}$						$+s_{21}s_{J1}$	$+c_{21}s_{J1}$	$-s_{21}s_{J1}$	$-c_{21}s_{J1}$	0	$-c_{11}s_{J1}$	0	$+c_{11}s_{J1}$	0	$-c_{11}s_{J1}$	0	$+c_{11}s_{J1}$	0
$\mathscr{I}_{2y}$		-1	0	1	0	$-c_{21}c_{J1}$	$+s_{21}c_{J1}$	$+c_{21}c_{J1}$	$-s_{21}c_{J1}$	$-c_{21}c_{J1}$	0	$+c_{21}c_{J1}$	0	$+c_{21}c_{J1}$	0	$-c_{21}c_{J1}$	0	0
$\mathscr{I}_{2x}$		0	1	0	-1	$+s_{21}c_{J1}$	$+c_{21}c_{J1}$	$-s_{21}c_{J1}$	$-c_{21}c_{J1}$	0	$+c_{11}c_{J1}$	0	$-c_{11}c_{J1}$	0	$+c_{11}c_{J1}$	0	$-c_{11}c_{J1}$	0
$\mathscr{I}_{2z}$	$+1$	0	0	0	0	0	0	0	0	$-s_{21}c_{J1}$	$-s_{21}c_{J1}$	$-s_{21}c_{J1}$	$-s_{21}c_{J1}$	$+s_{21}c_{J1}$	$-s_{21}c_{J1}$	$+s_{21}c_{J1}$	$-s_{21}c_{J1}$	0

$$+\frac{\mathcal{N}\gamma^2\hbar^2 B_0}{16k_{\mathrm{B}}T}\left(\frac{(\Omega_1-\pi J-\omega_1)}{\overline{R}_{2,1}^2+(\Omega_1-\pi J-\omega_1)^2}+\frac{(\Omega_1+\pi J-\omega_1)}{\overline{R}_{2,1}^2+(\Omega_1+\pi J-\omega_1)^2}\right)\left(\frac{(\Omega_1-\pi J-\omega_2)}{\overline{R}_{2,1}^2+(\Omega_1-\pi J-\omega_2)^2}+\frac{(\Omega_1+\pi J-\omega_2)}{\overline{R}_{2,1}^2+(\Omega_1+\pi J-\omega_2)^2}\right)$$
$$\underbrace{}_{[\Omega_1,\Omega_1]}$$

$$+\frac{\mathcal{N}\gamma^2\hbar^2 B_0}{16k_{\mathrm{B}}T}\left(\frac{\overline{R}_{2,2}}{\overline{R}_{2,2}^2+(\Omega_2-\pi J-\omega_1)^2}-\frac{\overline{R}_{2,2}}{\overline{R}_{2,2}^2+(\Omega_2+\pi J-\omega_1)^2}\right)\left(\frac{\overline{R}_{2,1}}{\overline{R}_{2,1}^2+(\Omega_1-\pi J-\omega_2)^2}-\frac{\overline{R}_{2,1}}{\overline{R}_{2,1}^2+(\Omega_1+\pi J-\omega_2)^2}\right),$$
$$\underbrace{}_{[\Omega_2,\Omega_1]}$$

$$(11.26)$$

It is converted by the third 90° pulse to
$\hat{\rho}(\mathrm{e}) = \frac{\kappa}{2}(\frac{1}{2}(c_{11}s_{J1}+c_{21}s_{J1})2\mathscr{I}_{1x}\mathscr{I}_{1z} + \frac{1}{2}(c_{11}s_{J1}+c_{21}s_{J1})2\mathscr{I}_{1z}\mathscr{I}_{1x})$,
which evolves during t_2 as
$\hat{\rho}(t_2) = \frac{\kappa}{2}(\frac{1}{2}(c_{11}s_{J1}+c_{21}s_{J1})c_{12}s_{J2}\mathscr{I}_{1y} - \frac{1}{2}(c_{11}s_{J1}+c_{21}s_{J1})s_{12}s_{J2}\mathscr{I}_{1x} + \frac{1}{2}(c_{11}s_{J1}+c_{21}s_{J1})c_{22}s_{J2}\mathscr{I}_{2y} - \frac{1}{2}(c_{11}s_{J1}+c_{21}s_{J1})s_{22}s_{J2}\mathscr{I}_{2x})$
plus unmeasurable anti-quantum coherences.

Considering orthogonality of the matrices,

$$\mathrm{Tr}\{\hat{\rho}(t_2)(\mathscr{I}_{1x} + \mathrm{i}\mathscr{I}_{1y} + \mathscr{I}_{2x} + \mathrm{i}\mathscr{I}_{2y})\} =$$
$$\frac{\kappa}{2}(\mathrm{i}\frac{1}{2}(c_{11}s_{J1}+c_{21}s_{J1})c_{12}s_{J2} - \frac{1}{2}(c_{11}s_{J1}+c_{21}s_{J1})s_{12}s_{J2} + \mathrm{i}\frac{1}{2}(c_{11}s_{J1}+c_{21}s_{J1})c_{22}s_{J2} - \frac{1}{2}(c_{11}s_{J1}+c_{21}s_{J1})s_{22}s_{J2}). \quad (11.27)$$

Using the trigonometric relations (Eq. 11.15), the averaged signal (i.e., the signal recorded for the full phase cycle, divided by four) is proportional to

$$\mathrm{Tr}\{\hat{\rho}(t_2)(\mathscr{I}_{1x} + \mathrm{i}\mathscr{I}_{1y} + \mathscr{I}_{2x} + \mathrm{i}\mathscr{I}_{2y})\}$$
$$= \frac{\kappa}{4}(\mathrm{i}(c_{11}s_{J1}+c_{21}s_{J1})c_{12}s_{J2} - (c_{11}s_{J1}+c_{21}s_{J1})s_{12}s_{J2} + \mathrm{i}(c_{11}s_{J1}+c_{21}s_{J1})c_{22}s_{J2} - (c_{11}s_{J1}+c_{21}s_{J1})s_{22}s_{J2})$$
$$= \mathrm{i}\frac{\kappa}{4}\left(\frac{-s_{11}^-+s_{11}^+}{2}\frac{-s_{12}^-+s_{12}^+}{2} + \frac{-s_{21}^-+s_{21}^+}{2}\frac{-s_{12}^-+s_{12}^+}{2} + \frac{-s_{11}^-+s_{11}^+}{2}\frac{-s_{22}^-+s_{22}^+}{2} + \frac{-s_{21}^-+s_{21}^+}{2}\frac{-s_{22}^-+s_{22}^+}{2}\right.$$
$$\left.-\mathrm{i}\left(\frac{-s_{11}^-+s_{11}^+}{2}\frac{c_{12}^--c_{12}^+}{2} + \frac{-s_{21}^-+s_{21}^+}{2}\frac{c_{12}^--c_{12}^+}{2} + \frac{-s_{11}^-+s_{11}^+}{2}\frac{c_{22}^--c_{22}^+}{2} + \frac{-s_{21}^-+s_{21}^+}{2}\frac{c_{22}^--c_{22}^+}{2}\right)\right)$$

$$(11.28)$$

In order to obtain a hypercomplex two-dimensional spectrum, the measurements is repeated with ϕ_2 advanced by 90° for each t_1 increment. The components of $\hat{\rho}(\mathrm{d})$ contributing to the signal, $= -\frac{\kappa}{2}(\frac{1}{2}(s_{11}s_{J1}+s_{21}s_{J1})2\mathscr{I}_{1x}\mathscr{I}_{1y} + (s_{11}s_{J1}+s_{21}s_{J1})2\mathscr{I}_{1y}\mathscr{I}_{1x})$
are converted by the third 90° pulse to
$\hat{\rho}(\mathrm{e}) = -\frac{\kappa}{2}(\frac{1}{2}(s_{11}s_{J1}+s_{21}s_{J1})2\mathscr{I}_{1x}\mathscr{I}_{1z} + \frac{1}{2}(s_{11}s_{J1}+s_{21}s_{J1})2\mathscr{I}_{1z}\mathscr{I}_{1x})$,
which evolves during t_2 as
$\hat{\rho}(t_2) = -\frac{\kappa}{2}(\frac{1}{2}(s_{11}s_{J1}+s_{21}s_{J1})c_{12}s_{J2}\mathscr{I}_{1y} - \frac{1}{2}(s_{11}s_{J1}+s_{21}s_{J1})s_{12}s_{J2}\mathscr{I}_{1x} + \frac{1}{2}(s_{11}s_{J1}+s_{21}s_{J1})c_{22}s_{J2}\mathscr{I}_{2y} - \frac{1}{2}(s_{11}s_{J1}+s_{21}s_{J1})s_{22}s_{J2}\mathscr{I}_{2x})$
plus unmeasurable anti-quantum coherences.

Considering orthogonality of the matrices,

$$\mathrm{Tr}\{\hat{\rho}(t_2)(\mathscr{I}_{1x} + \mathrm{i}\mathscr{I}_{1y} + \mathscr{I}_{2x} + \mathrm{i}\mathscr{I}_{2y})\} =$$
$$-\frac{\kappa}{2}(\mathrm{i}\frac{1}{2}(s_{11}s_{J1}+s_{21}s_{J1})c_{12}s_{J2} - \frac{1}{2}(s_{11}s_{J1}+s_{21}s_{J1})s_{12}s_{J2} + \mathrm{i}\frac{1}{2}(s_{11}s_{J1}+s_{21}s_{J1})c_{22}s_{J2} - \frac{1}{2}(s_{11}s_{J1}+s_{21}s_{J1})s_{22}s_{J2}). \quad (11.29)$$

Including the factor of two and using the trigonometric relations (Eq. 11.15),

$$\mathrm{Tr}\{\hat{\rho}(t_2)(\mathscr{I}_{1x} + \mathrm{i}\mathscr{I}_{1y} + \mathscr{I}_{2x} + \mathrm{i}\mathscr{I}_{2y})\}$$
$$= -\frac{\kappa}{4}(\mathrm{i}(s_{11}s_{J1}+s_{21}s_{J1})c_{12}s_{J2} - (s_{11}s_{J1}+s_{21}s_{J1})s_{12}s_{J2} + \mathrm{i}(s_{11}s_{J1}+s_{21}s_{J1})c_{22}s_{J2} - (s_{11}s_{J1}+s_{21}s_{J1})s_{22}s_{J2})$$
$$= -\mathrm{i}\frac{\kappa}{4}\left(\frac{c_{11}^--c_{11}^+}{2}\frac{-s_{12}^-+s_{12}^+}{2} + \frac{c_{21}^--c_{21}^+}{2}\frac{-s_{12}^-+s_{12}^+}{2} + \frac{c_{11}^--c_{11}^+}{2}\frac{-s_{22}^-+s_{22}^+}{2} + \frac{c_{21}^--c_{21}^+}{2}\frac{-s_{22}^-+s_{22}^+}{2}\right.$$
$$\left.-\mathrm{i}\left(\frac{c_{11}^--c_{11}^+}{2}\frac{c_{12}^--c_{12}^+}{2} + \frac{c_{21}^--c_{21}^+}{2}\frac{c_{12}^--c_{12}^+}{2} + \frac{c_{11}^--c_{11}^+}{2}\frac{c_{22}^--c_{22}^+}{2} + \frac{c_{21}^--c_{21}^+}{2}\frac{c_{22}^--c_{22}^+}{2}\right)\right)$$

$$(11.30)$$

Introducing relaxation, applying phase correction, and performing Fourier transformation in the direct dimension, discarding the imaginary component (see Section 9.5.1), multiplying Eq. 11.30 by "i" and combining it with Eq. 11.28, introducing relaxation and performing Fourier transformation in the indirect dimension provides a signal with the real part proportional to

$$
+ \underbrace{\frac{\mathcal{N}\gamma^2\hbar^2 B_0}{32k_{\mathrm{B}}T} \left(\frac{\overline{R}_{2,1}}{\overline{R}_{2,1}^2 + (\omega_1 - \Omega_1 + \pi J)^2} - \frac{\overline{R}_{2,1}}{\overline{R}_{2,1}^2 + (\omega_1 - \Omega_1 - \pi J)^2} \right) \left(\frac{\overline{R}_{2,1}}{\overline{R}_{2,1}^2 + (\omega_2 - \Omega_1 + \pi J)^2} - \frac{\overline{R}_{2,1}}{\overline{R}_{2,1}^2 + (\omega_2 - \Omega_1 - \pi J)^2} \right)}_{[\Omega_1,\Omega_1]}
$$

$$
+ \underbrace{\frac{\mathcal{N}\gamma^2\hbar^2 B_0}{32k_{\mathrm{B}}T} \left(\frac{\overline{R}_{2,2}}{\overline{R}_{2,2}^2 + (\omega_1 - \Omega_2 + \pi J)^2} - \frac{\overline{R}_{2,2}}{\overline{R}_{2,2}^2 + (\omega_1 - \Omega_2 - \pi J)^2} \right) \left(\frac{\overline{R}_{2,1}}{\overline{R}_{2,1}^2 + (\omega_2 - \Omega_1 + \pi J)^2} - \frac{\overline{R}_{2,1}}{\overline{R}_{2,1}^2 + (\omega_2 - \Omega_1 - \pi J)^2} \right)}_{[\Omega_2,\Omega_1]}
$$

$$
+ \underbrace{\frac{\mathcal{N}\gamma^2\hbar^2 B_0}{32k_{\mathrm{B}}T} \left(\frac{\overline{R}_{2,2}}{\overline{R}_{2,2}^2 + (\omega_1 - \Omega_2 + \pi J)^2} - \frac{\overline{R}_{2,2}}{\overline{R}_{2,2}^2 + (\omega_1 - \Omega_2 - \pi J)^2} \right) \left(\frac{\overline{R}_{2,2}}{\overline{R}_{2,2}^2 + (\omega_2 - \Omega_2 + \pi J)^2} - \frac{\overline{R}_{2,2}}{\overline{R}_{2,2}^2 + (\omega_2 - \Omega_2 - \pi J)^2} \right)}_{[\Omega_1,\Omega_1]}
$$

$$
+ \underbrace{\frac{\mathcal{N}\gamma^2\hbar^2 B_0}{32k_{\mathrm{B}}T} \left(\frac{\overline{R}_{2,1}}{\overline{R}_{2,1}^2 + (\omega_1 - \Omega_1 + \pi J)^2} - \frac{\overline{R}_{2,1}}{\overline{R}_{2,1}^2 + (\omega_1 - \Omega_1 - \pi J)^2} \right) \left(\frac{\overline{R}_{2,2}}{\overline{R}_{2,2}^2 + (\omega_2 - \Omega_2 + \pi J)^2} - \frac{\overline{R}_{2,2}}{\overline{R}_{2,2}^2 + (\omega_2 - \Omega_2 - \pi J)^2} \right)}_{[\Omega_2,\Omega_1]}.
$$

$$(11.31)$$

The terms with the same indices of Ω represent diagonal peaks with a Lorentzian absorption shape at $[\Omega_1, \Omega_1]$ and $[\Omega_2, \Omega_2]$ and the terms with different indices represent cross-peaks with a Lorentzian absorption shape at $[\Omega_2, \Omega_1]$ and $[\Omega_1, \Omega_2]$. Comparison with Eqs. 11.26 and 11.25 shows that (i) a phase shift between diagonal peaks and cross-peaks is present only in standard COSY but not in DQF-COSY, and (ii) the DQF-COSY signal intensity is half of the value obtained in standard COSY. The spectrum is plotted in Figure 11.6. Note that diagonal peaks and cross-peaks have the same phase (form anti-phase doublets).

Lecture 12
Strong coupling, TOCSY

Literature: The strong coupling for a pair of nuclei is discussed in K12.1, L14.1-L14.3, C2.5.2, and analyzed in detail in LA.8. The idea of the magnetic equivalence is presented in K12.2, L14.4 (for two nuclei), L17.5 (in larger molecules, with some details discussed in LA.9). The TOCSY experiment discussed in Section 12.3 (mixing the $\mathscr{I}_{ny}$ coherences) is described in L18.14, another variant (mixing the $\mathscr{I}_{nz}$ coherences) is presented in K8.11, C4.2.1.2, and C6.5.

12.1 Strong J-coupling

We have seen in Section 10.2 that the secular approximation substantially simplifies the Hamiltonian of the J-coupling if γ and/or the chemical shifts differ (the *weak coupling*). However, the description of the system of interacting nuclei changes dramatically if $\gamma_1 = \gamma_2$ and chemical shifts are similar (the *strong coupling*). We now analyze how a density matrix describing a strongly coupled pair of magnetic moments evolves in a one-pulse 1D NMR experiment.

As usually, the density matrix at the beginning of the experiment is given by the thermal equilibrium. As mentioned in Section 10.10.6, the effect of the J-coupling on the populations is negligible. Therefore, the initial form of the density matrix and its form after the 90° excitation pulse are the same as in the case of a weak coupling:

$$\hat{\rho}(\text{b}) = \frac{1}{2}\mathscr{I}_t - \frac{\kappa}{2}\mathscr{I}_{1y} - \frac{\kappa}{2}\mathscr{I}_{2y}. \tag{12.1}$$

In order to describe the evolution of $\hat{\rho}$, we need to know the Hamiltonian. For a pair of nuclei, the Hamiltonian (expressed in the rotating coordinate frame) is given by Eq. 10.3. In the presence of very similar chemical shifts

$$\mathscr{H} = +\Omega_1\mathscr{I}_{1z} + \Omega_2\mathscr{I}_{2z} + \pi J\left(2\mathscr{I}_{1x}\mathscr{I}_{2x} + 2\mathscr{I}_{1y}\mathscr{I}_{2y} + 2\mathscr{I}_{1z}\mathscr{I}_{2z}\right). \tag{12.2}$$

In this Hamiltonian, $\mathscr{I}_{1z}$ and $\mathscr{I}_{2z}$ do not commute with $2\mathscr{I}_{1x}\mathscr{I}_{2x}$ and $2\mathscr{I}_{1y}\mathscr{I}_{2y}$. Therefore, we cannot analyze the evolution of the density matrix by analyzing effects of individual components of the Hamiltonian separately and in any order, as we did in the case of the weak coupling Hamiltonian $\Omega_1\mathscr{I}_{1z} + \Omega_2\mathscr{I}_{2z} + \pi J \cdot 2\mathscr{I}_{1z}\mathscr{I}_{2z}$ consisting of three mutually commuting components.

If we use matrices listed in Tables 8.1 and 8.2, the matrix representation of the Hamiltonian is

$$\mathscr{H} = \begin{pmatrix} \frac{\Omega_1+\Omega_2}{2} + \frac{\pi}{2}J & 0 & 0 & 0 \\ 0 & \frac{\Omega_1-\Omega_2}{2} - \frac{\pi}{2}J & \pi J & 0 \\ 0 & \pi J & -\frac{\Omega_1-\Omega_2}{2} - \frac{\pi}{2}J & 0 \\ 0 & 0 & 0 & -\frac{\Omega_1+\Omega_2}{2} + \frac{\pi}{2}J \end{pmatrix}. \tag{12.3}$$

Obviously, the matrix is not diagonal. In order to find the eigenvalues of the Hamiltonian, corresponding to the frequencies observed in the spectra, we have to find a new basis where the Hamiltonian is represented by a diagonal matrix. This is done in Section 12.4.1. The diagonalized matrix $\mathscr{H}'$ can be written as a linear combination of matrices listed in Table 8.1

$$\mathscr{H}' = \Omega_1' \mathscr{I}_{1z} + \Omega_2' \mathscr{I}_{2z} + \pi J \cdot 2\mathscr{I}_{1z}\mathscr{I}_{2z}, \tag{12.4}$$

where

$$\Omega_1' = \frac{1}{2}\left(\Omega_1 + \Omega_2 + \sqrt{(\Omega_1 - \Omega_2)^2 + 4\pi^2 J^2}\right) \tag{12.5}$$

$$\Omega_2' = \frac{1}{2}\left(\Omega_1 + \Omega_2 - \sqrt{(\Omega_1 - \Omega_2)^2 + 4\pi^2 J^2}\right). \tag{12.6}$$

We see that $\mathscr{H}'$ consists of the same product operators as the Hamiltonian describing the weak J-coupling, only the frequencies differ. The density matrix $\hat{\rho}(b)$ and the operator of the measured quantity $\hat{M}_+$ should be also expressed in the basis found in Section 12.4.1. The transformed density matrix $\hat{\rho}'$ consists of the same product operators as the density matrix in the original basis, they are just combined with different coefficients. We can thus repeat the analysis presented for the weak J-coupling in Section 10.4 using the same rotations in the operators space as presented in Figure 10.3. The analysis of a strongly J-coupled system differs only in three issues: (i) we start to rotate from a different combination of product operators, (ii) the angles of rotations differ, being given by the frequencies Ω_1', Ω_2' instead of the frequency offsets Ω_1, Ω_2, and (iii) we have to calculate a trace of the density matrix multiplied by the transformed operator of the transverse magnetization, $\hat{M}_+'$. The analysis is presented in Section 12.4.2. The Fourier transform of the result (Eq. 12.52) is

$$\begin{aligned}
\Re\{Y(\omega)\} = {} & \left(1 - \frac{2\pi J}{\sqrt{(\Omega_1 - \Omega_2)^2 + 4\pi^2 J^2}}\right) \frac{\mathcal{N}\gamma^2\hbar^2 B_0}{8k_{\mathrm{B}}T} \frac{\overline{R}_2}{\overline{R}_2^2 + (\Omega_2' - \pi J - \omega)^2} \\
& + \left(1 + \frac{2\pi J}{\sqrt{(\Omega_1 - \Omega_2)^2 + 4\pi^2 J^2}}\right) \frac{\mathcal{N}\gamma^2\hbar^2 B_0}{8k_{\mathrm{B}}T} \frac{\overline{R}_2}{\overline{R}_2^2 + (\Omega_2' + \pi J - \omega)^2} \\
& + \left(1 + \frac{2\pi J}{\sqrt{(\Omega_1 - \Omega_2)^2 + 4\pi^2 J^2}}\right) \frac{\mathcal{N}\gamma^2\hbar^2 B_0}{8k_{\mathrm{B}}T} \frac{\overline{R}_2}{\overline{R}_2^2 + (\Omega_1' - \pi J - \omega)^2} \\
& + \left(1 - \frac{2\pi J}{\sqrt{(\Omega_1 - \Omega_2)^2 + 4\pi^2 J^2}}\right) \frac{\mathcal{N}\gamma^2\hbar^2 B_0}{8k_{\mathrm{B}}T} \frac{\overline{R}_2}{\overline{R}_2^2 + (\Omega_1' + \pi J - \omega)^2}
\end{aligned}$$

$$
\Im\{Y(\omega)\} = \mathrm{i}\left(1 - \frac{2\pi J}{\sqrt{(\Omega_1 - \Omega_2)^2 + 4\pi^2 J^2}}\right) \frac{\mathcal{N}\gamma^2\hbar^2 B_0}{8k_\mathrm{B}T} \frac{\Omega_2' - \pi J - \omega}{\overline{R}_2^2 + (\Omega_2' - \pi J - \omega)^2}
$$

$$
+\mathrm{i}\left(1 + \frac{2\pi J}{\sqrt{(\Omega_1 - \Omega_2)^2 + 4\pi^2 J^2}}\right) \frac{\mathcal{N}\gamma^2\hbar^2 B_0}{8k_\mathrm{B}T} \frac{\Omega_2' + \pi J - \omega}{\overline{R}_2^2 + (\Omega_2' + \pi J - \omega)^2}
$$

$$
+\mathrm{i}\left(1 + \frac{2\pi J}{\sqrt{(\Omega_1 - \Omega_2)^2 + 4\pi^2 J^2}}\right) \frac{\mathcal{N}\gamma^2\hbar^2 B_0}{8k_\mathrm{B}T} \frac{\Omega_1' - \pi J - \omega}{\overline{R}_2^2 + (\Omega_1' - \pi J - \omega)^2}
$$

$$
+\mathrm{i}\left(1 - \frac{2\pi J}{\sqrt{(\Omega_1 - \Omega_2)^2 + 4\pi^2 J^2}}\right) \frac{\mathcal{N}\gamma^2\hbar^2 B_0}{8k_\mathrm{B}T} \frac{\Omega_1' + \pi J - \omega}{\overline{R}_2^2 + (\Omega_1' + \pi J - \omega)^2}. \tag{12.7}
$$

Spectra for three different values of $|\Omega_1 - \Omega_2|$ are plotted in Figure 12.1. The following features distinguish spectra of strongly coupled nuclear magnetic moments from those of weakly coupled pairs:

- The centers of doublets of peaks of individual nuclei are shifted from the precession frequencies of the nuclei Ω_1 and Ω_2 by a factor of $\pm\left(\Omega_1 - \Omega_2 - \sqrt{(\Omega_1 - \Omega_2)^2 + 4\pi^2 J^2}\right)/2$.

- The intensities of the inner peaks of the doublet of doublets are increased and the intensities of the outer peaks are decreased by a factor of $2\pi J/\sqrt{(\Omega_1 - \Omega_2)^2 + 4\pi^2 J^2}$.

The square root $\sqrt{(\Omega_1 - \Omega_2)^2 + 4\pi^2 J^2}$ specifies the limit between the *weak* and the *strong* J-coupling. If $|\Omega_1 - \Omega_2| \gg 2\pi|J|$, the factors modifying the peak intensities are negligible and the J-coupling is considered *weak*. The other limit, $|\Omega_1 - \Omega_2| \to 0$, deserves a special attention and is discussed in more details in the next section.

12.2 Magnetic equivalence

If two interacting nuclear magnetic moments have the same precession frequencies (due to a molecular symmetry[1] or accidentally), and if they are not distinguished by different couplings to other nuclei, they are *magnetically equivalent.*

Following the trends in Figure 12.1 suggests that only one peak appears in a spectrum of a pair of magnetically equivalent nuclei. This explains why we do not observe e.g. splitting due to the relatively large J-coupling of protons in water ($|^2J| \approx 7$ Hz).

From the theoretical point of view, a pair of magnetically equivalent nuclei represents a fundamentally different system than a pair of weakly coupled nuclei (even for the identical J constant). The eigenstates of the Hamiltonian of the magnetically equivalent nuclei in $\vec{B}_0$ are not direct products of the $|\alpha\rangle$ and $|\beta\rangle$ eigenstates (as we described in Section 8.9.3). The pair of magnetically equivalent

---

[1]Nuclei can be inequivalent even if the whole molecule is symmetric (i.e., achiral). The existence of a plane of symmetry is not sufficient, the plane must bisect the particular pair of nuclei. Otherwise, the nuclei are *diastereotopic* and magnetically inequivalent.
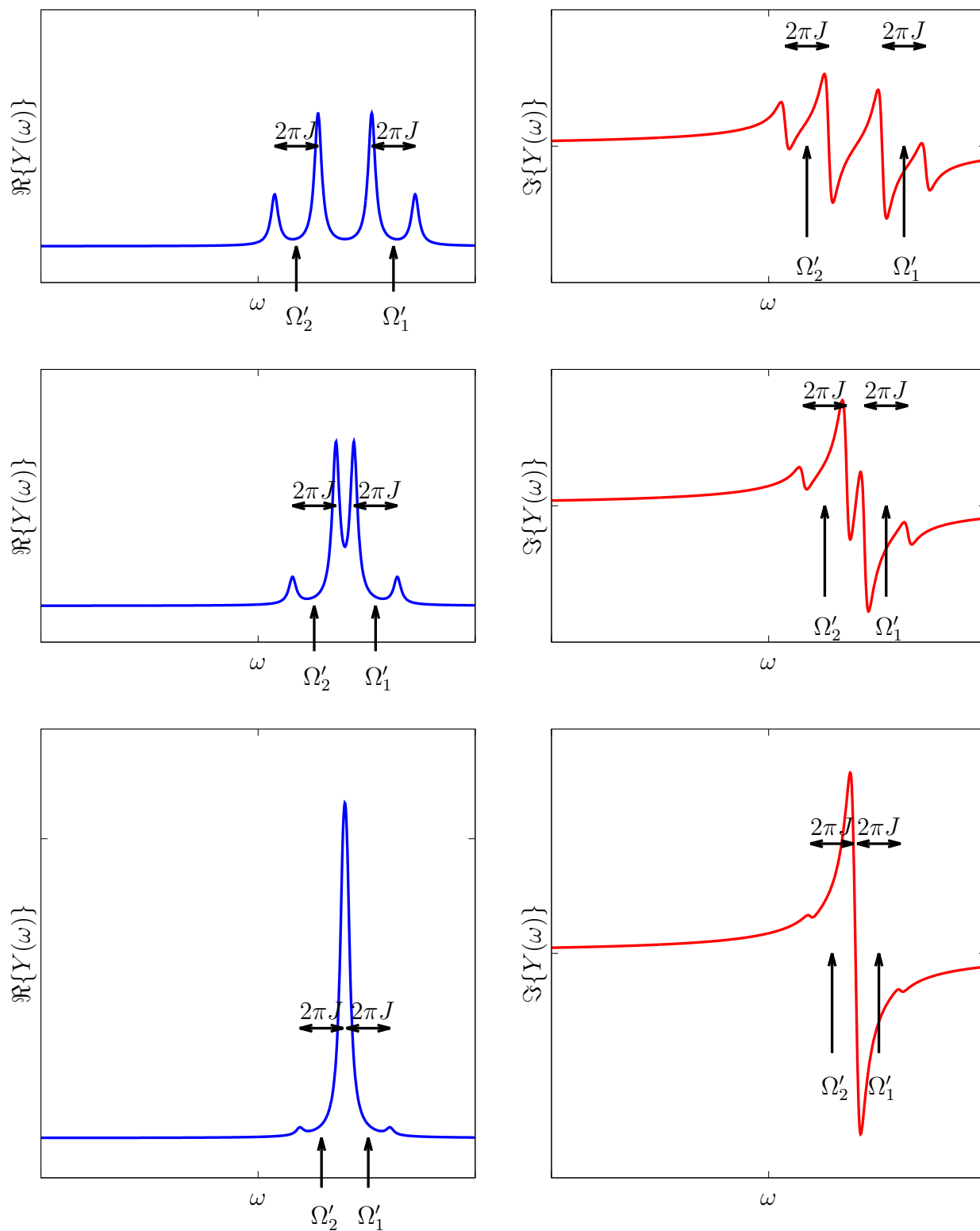
Figure 12.1: One-dimensional spectra of strongly J-coupled ^{1}H–^{1}H pairs. The spectra are plotted for $\Omega_1 - \Omega_2 = 4\pi J$ (top), $\Omega_1 - \Omega_2 = 2\pi J$ (middle), and $\Omega_1 - \Omega_2 = 0.8\pi J$ (bottom).

Table 12.1: Eigenvalues of selected operators for a pair of magnetically equivalent nuclei. The operators $\hat{I}_1^2$, $\hat{I}_1^2$, $\hat{I}'^2$, and $\hat{I}'_z$ are defined in Section 10.10.2, $\mathscr{H}' = (\omega_0 + \pi J)\mathscr{I}_{1z} + (\omega_0 - \pi J)\mathscr{I}_{2z} + \pi J \cdot 2\mathscr{I}_{1z}\mathscr{I}_{2z}$.

Eigenfunction	$\hat{I}_1^2$	$\hat{I}_2^2$	$\hat{I}'^2$	$\hat{I}'_z$	$\mathscr{H}'$
$|\alpha\rangle \otimes |\alpha\rangle$	$3\hbar^2/4$	$3\hbar^2/4$	$2\hbar^2$	$+\hbar$	$+\omega_0 + \frac{\pi}{2}J$
$\frac{1}{\sqrt{2}}|\alpha\rangle \otimes |\beta\rangle + \frac{1}{\sqrt{2}}|\beta\rangle \otimes |\alpha\rangle$	$3\hbar^2/4$	$3\hbar^2/4$	$2\hbar^2$	0	$+\frac{\pi}{2}J$
$\frac{1}{\sqrt{2}}|\alpha\rangle \otimes |\beta\rangle - \frac{1}{\sqrt{2}}|\beta\rangle \otimes |\alpha\rangle$	$3\hbar^2/4$	$3\hbar^2/4$	0	0	$-\frac{3\pi}{2}J$
$|\beta\rangle \otimes |\beta\rangle$	$3\hbar^2/4$	$3\hbar^2/4$	$2\hbar^2$	$-\hbar$	$-\omega_0 + \frac{\pi}{2}J$

nuclei is similar to a pair of electrons discussed in Section 10.10.2. The eigenfunctions and eigenvalues for important operators are listed in Table 12.1.

The eigenfunctions help us to understand the difference between quantum states of non-interacting or weakly J-coupled pairs on one hand, and magnetically equivalent pairs on the other hand. We have discussed in detail that the stationary states $|\alpha\rangle\otimes|\alpha\rangle$, $|\alpha\rangle\otimes|\beta\rangle$, $|\beta\rangle\otimes|\alpha\rangle$, $|\beta\rangle\otimes|\beta\rangle$ are important in single pairs of nuclei, but are rarely present in large macroscopic ensembles. Now we see that in the case of magnetically equivalent nuclei, $|\alpha\rangle \otimes |\beta\rangle$ and $|\beta\rangle \otimes |\alpha\rangle$ do not even describe stationary states of a single pair. Instead, the stationary states are their combinations.

The eigenvalues of the operator representing the square of the total angular momentum $\hat{I}'^2$ tells us that three eigenstates have the same size of the total angular momentum ($\sqrt{2}\hbar$) and one does not have any angular momentum (and therefore any magnetic moment). The energy differences (eigenvalues of $\mathscr{H}'$ multiplied by $\hbar$) between the three "magnetic states" are the same in isotropic liquids (but they differ if the dipole-dipole coupling is not averaged to zero), which explains why we see only one frequency in the spectrum. The "non-magnetic" state does not have any magnetic moment and thus does not contribute to the observable magnetization.

The analysis is more demanding if a magnetically equivalent pair is a part of a larger molecule. Nevertheless, it can be shown that the J-couplings between magnetically equivalent nuclei in larger molecules do not affect the NMR spectra (Sections 12.4.3 and 12.4.4).

12.3   TOCSY

At the first glance, molecules whose nuclei have very similar chemical shifts (by accident or as a result of a molecular symmetry), and are therefore very strongly J-coupled, seem to represent a special case. However, tricks discussed in the previous lectures allow us to exploit advantages of the magnetic equivalence even if the chemical shifts are very different. We have learnt that we can use a spin echo to suppress the effect of the chemical shift evolution, which is exactly what we need: no chemical shift evolution corresponds to zero difference in the frequency offset. If we apply the simultaneous echo (actually, the only echo applicable to homonuclear pairs) that keeps the J-coupling evolution but refocuses the evolution due to the chemical shift, the state of the system of nuclei at the end of the echo is the same as a state of a system of nuclei with identical chemical shifts. Note, however, that a single application of a spin echo is not sufficient. Our goal is to make the strong coupling
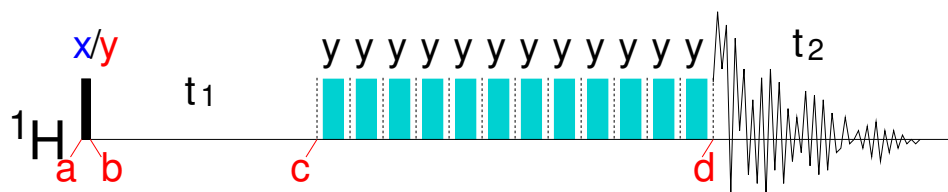
Figure 12.2: TOCSY pulse sequence. The narrow black and wide cyan rectangles, respectively, represent 90° and 180° radio wave pulses applied at a frequency sufficiently close to the precession frequencies of all interacting magnetic moments.

to act continuously for a certain period of time, comparable to $1/(2J)$, not just in one moment. Therefore, we have to apply a series of radio-frequency pulses to keep the strong coupling active for a whole *mixing* period. In principle, a series of very short coupling echoes with very short 180 ° pulses should work (Figure 12.2). However, specially designed sequences of pulses with much weaker offset effects are used in practice.[2] Two-dimensional experiment utilizing a mixing mimicking the strong coupling is known as Totally Correlated Spectroscopy (TOCSY). There are numerous variants of the experiment, here we present only the simplest version (Figure 12.2) illustrating the basic idea.

In order to describe the major advantage of the TOCSY experiment, we analyze a simple system of three nuclei (e.g. three protons) where nuclei 1 and 2 are coupled, nuclei 2 and 3 are also coupled, but there is no coupling between nuclei 1 and 3 (a more general analysis and matrix representations of the product operators for ensembles are presented in Sections 12.4.5–12.4.8). Let us assume that both coupling constants are identical ($J_{12} = J_{23} = J$). Before the TOCSY mixing period, the density matrix of our system evolves like in the NOESY or COSY experiment. The evolution starts from the equilibrium density matrix

$\hat{\rho}(\mathrm{a}) = \frac{1}{4}(\mathscr{I}_t + \kappa\mathscr{I}_{1z} + \kappa\mathscr{I}_{2z} + \kappa\mathscr{I}_{3z})$,

derived in Section 12.4.6 for a general case of N magnetic moments. The starting density matrix is converted to

$\hat{\rho}(\mathrm{b}) = \frac{1}{4}(\mathscr{I}_t - \kappa\mathscr{I}_{1y} - \kappa\mathscr{I}_{2y} - \kappa\mathscr{I}_{3y})$

by a 90° excitation pulse and evolves during the incremented evolution period t_1. For the sake of simplicity, we pay attention to the fate of the coherences modulated by the chemical shift of nucleus 1:

$\hat{\rho}(\mathrm{c}) = -\frac{\kappa}{4}\cos(\Omega_1 t_1)\cos(\pi J t_1)\mathscr{I}_{1y} + \ldots$

Let us assume that the TOCSY pulse train is applied with the 90° or −90° (y or $-y$) phases of the radio waves. As a consequence, the pulses keep the $\mathscr{I}_{1y}$, $\mathscr{I}_{2y}$, $\mathscr{I}_{3y}$ components of the density matrix intact and rotate other coherences "about" the $\mathscr{I}_{ny}$ "axis". Because the trains contain many (hundreds) of pulses, the imperfections of the pulses and stochastic molecular motions randomize the direction of the polarizations in the xz plane (an effect similar to the loss of coherence in the xy plane during the evolution in the $\vec{B}_0$ field). Therefore, we assume that only the $\mathscr{I}_{1y}$, $\mathscr{I}_{2y}$, $\mathscr{I}_{3y}$ coherences, "locked" in the y direction of the rotating frame, survive the TOCSY mixing pulse train.[3]

The Hamiltonian describing the evolution of our simple system during the TOCSY mixing period is

---

[2]Technically, our task is very similar to the decoupling during the acquisition, shown in Section 11.6.

[3]If coherences other than $\mathscr{I}_{ny}$ are not destroyed completely, their contribution can be removed by phase cycling.

$$\mathcal{H}_{\text{TOCSY}} = \pi J \left(2\mathcal{I}_{1x}\mathcal{I}_{2x} + 2\mathcal{I}_{1y}\mathcal{I}_{2y} + 2\mathcal{I}_{1z}\mathcal{I}_{2z} + 2\mathcal{I}_{2x}\mathcal{I}_{3x} + 2\mathcal{I}_{2y}\mathcal{I}_{3y} + 2\mathcal{I}_{2z}\mathcal{I}_{3z} \right). \tag{12.8}$$

Note that the Hamiltonian is fully symmetric in our coordinate system. In our version of the TOCSY experiment, we decided to preserve only the $\mathcal{I}_{ny}$ coherences by the choice of the phase of the applied pulses. However, the Hamiltonian itself acts on $\mathcal{I}_{nx}$, $\mathcal{I}_{ny}$, and $\mathcal{I}_{nz}$ in a completely identical way.[4] Therefore, the effect of the Hamiltonian is called *isotropic mixing* (working equally in all directions).

All components of the Hamiltonian in Eq. 12.8 commute (because the echo removed the chemical shift components) and it is possible to inspect their effects separately. Such analysis is straightforward for two interacting nuclei, but gets complicated for three or more nuclei. Nevertheless, a useful insight can be gained from the inspection of the commutation relations of the $\mathcal{H}_{\text{TOCSY}}$ Hamiltonian, derived in Section 12.4.7. First, $\mathcal{H}_{\text{TOCSY}}$ does not commute with $\mathcal{I}_{1y}$. It tells us that $-\frac{\kappa}{4}\cos(\Omega_1 t_1)\cos(\pi J t_1)\mathcal{I}_{1y}$ partially evolves to other coherences (or populations) during the TOCSY mixing (Eq. 12.69). Second, $\mathcal{H}_{\text{TOCSY}}$ does not commute with $\mathcal{I}_{1y}+\mathcal{I}_{2y}$ either (Eq. 12.72). We see that the lost portion of $-\frac{\kappa}{4}\cos(\Omega_1 t_1)\cos(\pi J t_1)\mathcal{I}_{1y}$ is not completely converted to $-\frac{\kappa}{4}\cos(\Omega_1 t_1)\cos(\pi J t_1)\mathcal{I}_{2y}$. Finally, $\mathcal{H}_{\text{TOCSY}}$ *does* commute[5] with $\mathcal{I}_{1y} + \mathcal{I}_{2y} + \mathcal{I}_{3y}$ (Eq. 12.73). If $\mathcal{I}_{1y} + \mathcal{I}_{2y} + \mathcal{I}_{3y}$ does not change and $\mathcal{I}_{1y}$ is not completely converted to $\mathcal{I}_{2y}$, the missing portion of $\mathcal{I}_{1y}$ must be compensated by formation of $-\frac{\kappa}{4}\cos(\Omega_1 t_1)\cos(\pi J t_1)\mathcal{I}_{3y}$. The fraction of the density matrix converted to $\mathcal{I}_{2y}$ and $\mathcal{I}_{3y}$ depends on the length of the TOCSY pulse train (*mixing time*), on the actual values of the J constants (they are not identical in a real case), on the relaxation, and on the evolution during the pulses (their duration is not negligible compared to the lengths of individual echoes in the train if the goal is to have the echoes as short as possible). In our analysis, we describe the fraction that stays in $\mathcal{I}_{1y}$ by a factor a_{11}, the efficiency of the transfer from nucleus 1 to nucleus 2 by a factor a_{12}, and the efficiency of the transfer from nucleus 1 to nucleus 3 by a factor a_{13}.

A detailed analysis of the evolution of the density matrix (the procedure, presented in Section 12.4.8, is very similar to those described in previous lectures for other 2D experiments) shows that the coherence $\mathcal{I}_{1y}$ provides the following components of the signal (cf. Eq. 12.82)

$$\mathcal{N}\gamma\hbar\frac{\kappa}{16}a_{11}\mathrm{e}^{-\overline{R}_2 t_1}\left(\cos((\Omega_1 - \pi J)t_1) + \cos((\Omega_1 + \pi J)t_1)\right)\mathrm{e}^{-\overline{R}_2 t_2}\left(\mathrm{e}^{-\mathrm{i}(\Omega_1 - \pi J)t_2} + \mathrm{e}^{-\mathrm{i}(\Omega_1 + \pi J)t_2}\right)$$
$$+ \mathcal{N}\gamma\hbar\frac{\kappa}{32}a_{12}\mathrm{e}^{-\overline{R}_2 t_1}\left(\cos((\Omega_1 - \pi J)t_1) + \cos((\Omega_1 + \pi J)t_1)\right)\mathrm{e}^{-\overline{R}_2 t_2}\left(\mathrm{e}^{-\mathrm{i}(\Omega_2 - 2\pi J)t_2} + 2\mathrm{e}^{-\mathrm{i}\Omega_2 t_2} + \mathrm{e}^{-\mathrm{i}(\Omega_2 + 2\pi J)t_2}\right)$$
$$+ \mathcal{N}\gamma\hbar\frac{\kappa}{16}a_{13}\mathrm{e}^{-\overline{R}_2 t_1}\left(\cos((\Omega_1 - \pi J)t_1) + \cos((\Omega_1 + \pi J)t_1)\right)\mathrm{e}^{-\overline{R}_2 t_2}\left(\mathrm{e}^{-\mathrm{i}(\Omega_3 - \pi J)t_2} + \mathrm{e}^{-\mathrm{i}(\Omega_3 + \pi J)t_2}\right). \tag{12.9}$$

After processing the signal as described in Section 9.5.1, these components result in one set of diagonal peaks (at the frequencies close to $[\Omega_1, \Omega_1]$) and in two sets of cross-peaks (Figure 12.3), including peaks close to the frequencies of protons that are not directly J-coupled ($[\Omega_1, \Omega_3]$). This is a fundamental difference between COSY and TOCSY spectra. Appearance of cross-peaks in the

---

[4]We could select $\mathcal{I}_{nx}$ coherences equally well by applying pulses with a phase of $0\,^\circ$ (x). The $\mathcal{I}_{nz}$ can be selected by applying additional 90° before and after the TOCSY pulse train (this approach is described in K8.11 and C6.5). In practice, the pulse trains are optimized for the given purpose.

[5]In general, $\mathcal{H}_{\text{TOCSY}}$ commutes with the operators of all three components I_j of the total angular momentum, where $j \in \{x, y, z\}$ and I_j is a sum of I_{nj} for all nuclei n.
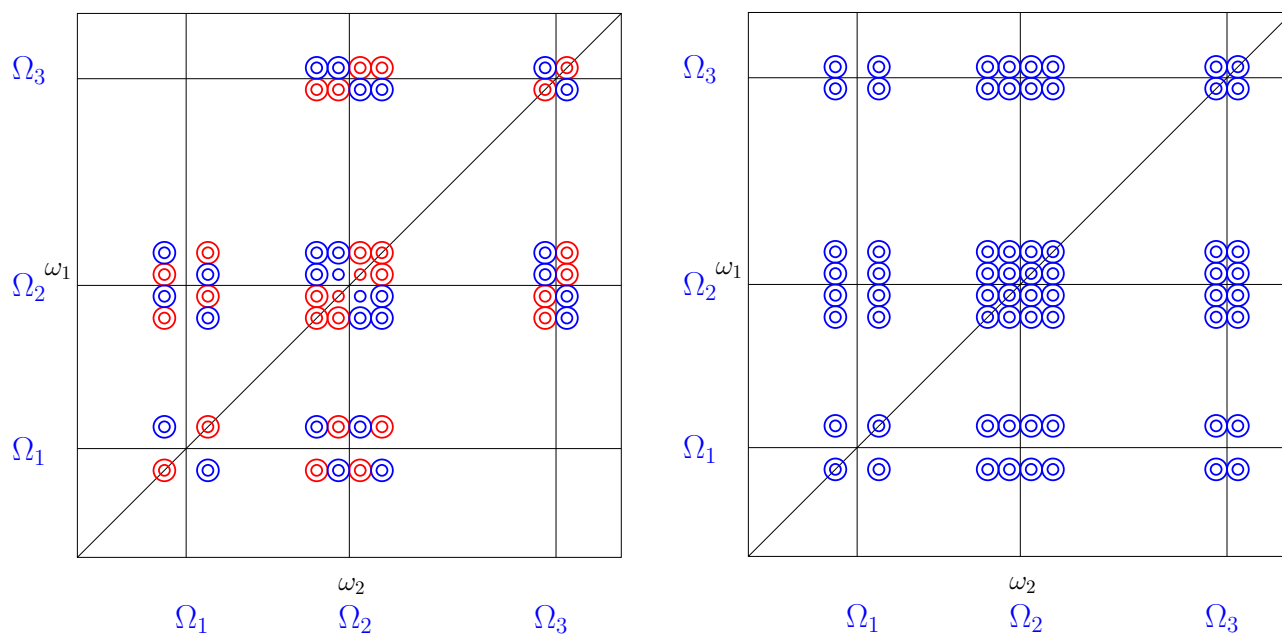
Figure 12.3: DQF-COSY (left) and TOCSY (right) spectra of a molecule with three protons with the J-coupling constants $|J_{12}| > |J_{23}|$ and $J_{13} = 0$. Note the presence of a cross-peak correlating the not coupled protons 1 and 3 in the TOCSY, but not in the DQF-COSY spectrum.

COSY spectra requires a direct J-coupling, whereas cross-peaks in the TOCSY spectra correlate all peaks of a *spin-system* (a network of nuclei connected by J-coupling), even if the coupling of a particular pair is negligible (Figure 12.3). The structural information in COSY and TOCSY spectra is complementary. The TOCSY experiment describes the complete spin systems in a single spectrum, COSY spectra distinguish directly J-coupled nuclei (usually vicinal and geminal protons).

HOMEWORK

Analyze the TOCSY experiment.

12.4 SUPPORTING INFORMATION

12.4.1 Diagonalization of the J-coupling Hamiltonian matrix

The matrix representation of the Hamiltonian describing the chemical shift and the strong J-coupling, written in the basis constructed from the α and β states of the interacting nuclei (i.e., $|\alpha\alpha\rangle$, $|\beta\alpha\rangle$, $|\alpha\beta\rangle$, $|\beta\beta\rangle$), is

$$\mathscr{H} = \frac{\pi}{2} \begin{pmatrix} \Sigma + J & 0 & 0 & 0 \\ 0 & \Delta - J & 2J & 0 \\ 0 & 2J & -\Delta - J & 0 \\ 0 & 0 & 0 & -\Sigma + J \end{pmatrix}, \tag{12.10}$$

where $\Sigma = (\omega_{0,1} + \omega_{0,2})/\pi$ and $\Delta = (\omega_{0,1} - \omega_{0,2})/\pi$. We are looking for a new, diagonal matrix representation of our Hamiltonian $\mathscr{H}'$. A similar task is solved in Section 10.10.2, the matrix in Eq. 12.10 just has more complicated elements. From the mathematical point of view, the *diagonalization* of our Hamiltonian can be described using a transformation matrix $\hat{T}$:

$$\mathscr{H}' = \hat{T}^{-1}\mathscr{H}\hat{T}. \tag{12.11}$$

Multiplying by $\hat{T}$ from left gives

$$\hat{T}\mathscr{H}' = \mathscr{H}\hat{T}. \tag{12.12}$$

The desired eigenvalues ω'_k and eigenvectors $|\psi'_k\rangle$ can be obtained by comparing the eigenvalue equation

$$\mathscr{H}'|\psi'_k\rangle = \omega'_k|\psi'_k\rangle \tag{12.13}$$

with the left-hand side of Eq. 12.12

$$\begin{pmatrix} T_{11} & T_{12} & T_{13} & T_{14} \\ T_{21} & T_{22} & T_{23} & T_{24} \\ T_{31} & T_{32} & T_{33} & T_{34} \\ T_{41} & T_{42} & T_{43} & T_{44} \end{pmatrix} \begin{pmatrix} \omega'_1 & 0 & 0 & 0 \\ 0 & \omega'_2 & 0 & 0 \\ 0 & 0 & \omega'_3 & 0 \\ 0 & 0 & 0 & \omega'_4 \end{pmatrix} = \begin{pmatrix} \omega'_1 T_{11} & \omega'_2 T_{12} & \omega'_3 T_{13} & \omega'_4 T_{14} \\ \omega'_1 T_{21} & \omega'_2 T_{22} & \omega'_3 T_{23} & \omega'_4 T_{24} \\ \omega'_1 T_{31} & \omega'_2 T_{32} & \omega'_3 T_{33} & \omega'_4 T_{34} \\ \omega'_1 T_{41} & \omega'_2 T_{42} & \omega'_3 T_{43} & \omega'_4 T_{44} \end{pmatrix}. \tag{12.14}$$

The eigenvalue equation can be written as a set of four equations for $k = 1, 2, 3, 4$

$$\mathscr{H}'|\psi'_k\rangle = \frac{\pi}{2} \begin{pmatrix} \Sigma + J & 0 & 0 & 0 \\ 0 & \Delta - J & 2J & 0 \\ 0 & 2J & -\Delta - J & 0 \\ 0 & 0 & 0 & -\Sigma + J \end{pmatrix} \begin{pmatrix} T_{1k} \\ T_{2k} \\ T_{3k} \\ T_{4k} \end{pmatrix} = \frac{\pi}{2} \begin{pmatrix} (\Sigma + J)T_{1k} \\ (\Delta - J)T_{2k} + 2JT_{3k} \\ 2JT_{2k} - (\Delta + J)T_{3k} \\ (-\Sigma + J)T_{4k} \end{pmatrix} = \omega'_k \begin{pmatrix} T_{1k} \\ T_{2k} \\ T_{3k} \\ T_{4k} \end{pmatrix} = \omega'_k|\psi'_k\rangle. \tag{12.15}$$

The first row of the middle equality allows us to identify

$$\omega'_1 = \frac{\pi}{2}(\Sigma + J) = \frac{\omega_{0,1} + \omega_{0,2}}{2} + \frac{\pi}{2}J \tag{12.16}$$

if we set $T_{21} = T_{31} = T_{41} = 0$, i.e.,

$$|\psi'_1\rangle = \begin{pmatrix} T_{11} \\ 0 \\ 0 \\ 0 \end{pmatrix}. \tag{12.17}$$

Similarly,

$$\omega'_4 = \frac{\pi}{2}(-\Sigma + J) = -\frac{\omega_{0,1} + \omega_{0,2}}{2} + \frac{\pi}{2}J \tag{12.18}$$

for

$$|\psi'_4\rangle = \begin{pmatrix} 0 \\ 0 \\ 0 \\ T_{44} \end{pmatrix}. \tag{12.19}$$

The ω'_2 and ω'_3 values can be calculated from the equations

$$2\omega'_k T_{2k} = \pi(\Delta - J)T_{2k} + 2\pi J T_{3k}, \tag{12.20}$$

$$2\omega'_k T_{3k} = 2\pi J T_{2k} - \pi(\Delta + J)T_{3k} \tag{12.21}$$

(setting $T_{12} = T_{42} = T_{13} = T_{43} = 0$).
T_{3k} can be expressed from the first equation

$$T_{3k} = \frac{2\omega'_k + \pi(J - \Delta)}{2\pi J} T_{2k} \tag{12.22}$$

and inserted into the second equation

$$(2\omega'_k + \pi(J + \Delta))(2\omega'_k + \pi(J - \Delta))T_{2k} = (2\pi J)^2 T_{2k}, \tag{12.23}$$

directly giving

$$\omega'_k = -\frac{\pi}{2}\left(J \pm \sqrt{4J^2 + \Delta^2}\right). \tag{12.24}$$

Choosing

$$\omega'_2 = -\frac{\pi}{2}\left(J - \sqrt{4J^2 + \Delta^2}\right) = \frac{\sqrt{(\omega_{0,1} - \omega_{0,2})^2 + 4\pi^2 J^2}}{2} - \frac{\pi}{2}J \tag{12.25}$$

and

$$\omega'_3 = -\frac{\pi}{2}\left(J + \sqrt{4J^2 + \Delta^2}\right) = -\frac{\sqrt{(\omega_{0,1} - \omega_{0,2})^2 + 4\pi^2 J^2}}{2} - \frac{\pi}{2}J \tag{12.26}$$

completely defines the diagonalized Hamiltonian

$$\mathscr{H}' = \frac{\pi}{2}\begin{pmatrix} \Sigma + J & 0 & 0 & 0 \\ 0 & \sqrt{\Delta^2 + 4J^2} - J & 0 & 0 \\ 0 & 0 & -\sqrt{\Delta^2 + 4J^2} - J & 0 \\ 0 & 0 & 0 & -\Sigma + J \end{pmatrix} = \frac{\omega'_{0,1}}{2}\begin{pmatrix} 1 & 0 & 0 & 0 \\ 0 & 1 & 0 & 0 \\ 0 & 0 & -1 & 0 \\ 0 & 0 & 0 & -1 \end{pmatrix} + \frac{\omega'_{0,1}}{2}\begin{pmatrix} 1 & 0 & 0 & 0 \\ 0 & -1 & 0 & 0 \\ 0 & 0 & 1 & 0 \\ 0 & 0 & 0 & -1 \end{pmatrix} + \pi J\begin{pmatrix} 1 & 0 & 0 & 0 \\ 0 & -1 & 0 & 0 \\ 0 & 0 & -1 & 0 \\ 0 & 0 & 0 & 1 \end{pmatrix}$$

$$= \omega'_{0,1}\mathscr{I}_{1z} + \omega'_{0,2}\mathscr{I}_{2z} + \pi J 2 \mathscr{I}_{1z}\mathscr{I}_{2z}, \tag{12.27}$$

where

$$\omega'_{0,1} = \frac{\pi}{2}(\Sigma + \sqrt{\Delta^2 + 4J^2}) = \frac{1}{2}\left(\omega_{0,1} + \omega_{0,2} + \sqrt{(\omega_{0,1} - \omega_{0,2})^2 + 4\pi^2 J^2}\right), \tag{12.28}$$

$$\omega'_{0,2} = \frac{\pi}{2}(\Sigma - \sqrt{\Delta^2 + 4J^2}) = \frac{1}{2}\left(\omega_{0,1} + \omega_{0,2} - \sqrt{(\omega_{0,1} - \omega_{0,2})^2 + 4\pi^2 J^2}\right). \tag{12.29}$$

The new basis is given by Eqs. 12.20, 12.21, and by the normalization condition

$$\langle\psi'_k|\psi'_k\rangle = 1 \Rightarrow \sum_{j=1}^{4} T_{jk}^2 = 1. \tag{12.30}$$

The normalization conditions immediately defines $T_{11} = T_{44} = 1$. Substituting ω'_2 into Eqs. 12.20 and 12.21, respectively, gives

$$\frac{T_{32}}{T_{22}} = \frac{\sqrt{4J^2 + \Delta^2} - \Delta}{2J}, \tag{12.31}$$

$$\frac{T_{22}}{T_{32}} = \frac{\sqrt{4J^2 + \Delta^2} + \Delta}{2J}. \tag{12.32}$$

Consequently,

$$\frac{T_{32}^2}{T_{22}^2} = \frac{\sqrt{4J^2 + \Delta^2} - \Delta}{\sqrt{4J^2 + \Delta^2} + \Delta} \tag{12.33}$$

and applying the normalization condition $T_{32}^2 = 1 - T_{22}^2$

$$\frac{1 + T_{22}^2}{T_{22}^2} = \frac{\sqrt{4J^2 + \Delta^2} - \Delta}{\sqrt{4J^2 + \Delta^2} + \Delta} \tag{12.34}$$

defines

$$T_{22}^2 = \frac{1}{1 - \frac{\sqrt{4J^2 + \Delta^2} - \Delta}{\sqrt{4J^2 + \Delta^2} + \Delta}} = \frac{\sqrt{4J^2 + \Delta^2} + \Delta}{2\sqrt{4J^2 + \Delta^2}} \tag{12.35}$$

and

$$T_{32}^2 = 1 - T_{22}^2 = \frac{\sqrt{4J^2 + \Delta^2} - \Delta}{2\sqrt{4J^2 + \Delta^2}}. \tag{12.36}$$

Similarly, T_{23}^2 and T_{33}^2 can be calculated by substituting ω_3' into Eqs. 12.20 and 12.21:

$$T_{23}^2 = \frac{\sqrt{4J^2 + \Delta^2} - \Delta}{2\sqrt{4J^2 + \Delta^2}} \tag{12.37}$$

$$T_{33}^2 = \frac{\sqrt{4J^2 + \Delta^2} + \Delta}{2\sqrt{4J^2 + \Delta^2}}. \tag{12.38}$$

If we use

$$T_{22} = T_{33} = \sqrt{\frac{1}{2} + \frac{\Delta}{2\sqrt{4J^2 + \Delta^2}}} \equiv c_\xi, \quad T_{23} = \sqrt{\frac{1}{2} - \frac{\Delta}{2\sqrt{4J^2 + \Delta^2}}} \equiv s_\xi, \quad T_{32} = -\sqrt{\frac{1}{2} + \frac{\Delta}{2\sqrt{4J^2 + \Delta^2}}} \equiv -s_\xi, \tag{12.39}$$

we obtain a transformation matrix

$$\hat{T} = \begin{pmatrix} 1 & 0 & 0 & 0 \\ 0 & c_\xi & -s_\xi & 0 \\ 0 & s_\xi & c_\xi & 0 \\ 0 & 0 & 0 & 1 \end{pmatrix}, \tag{12.40}$$

which is its own inverse ($\hat{T}^{-1} = \hat{T} \Rightarrow \hat{T}^{-1}\hat{T} = \hat{T}\hat{T} = \hat{1}$). Later, we also use the following relations between c_ξ and s_ξ:

$$c_\xi^2 + s_\xi^2 = \frac{1}{2} + \frac{\Delta}{2\sqrt{4J^2 + \Delta^2}} + \frac{1}{2} - \frac{\Delta}{2\sqrt{4J^2 + \Delta^2}} = 1 \tag{12.41}$$

$$2c_\xi s_\xi = 2\sqrt{\frac{1}{4} - \frac{\Delta^2}{4(4J^2 + \Delta^2)}} = \sqrt{\frac{4J^2 + \Delta^2 - \Delta^2}{4J^2 + \Delta^2}} = \frac{2J}{\sqrt{4J^2 + \Delta^2}}. \tag{12.42}$$

Finally, the new basis consists of the following eigenvectors

$$|\psi_1'\rangle = \begin{pmatrix} 1 \\ 0 \\ 0 \\ 0 \end{pmatrix}, \quad |\psi_2'\rangle = \begin{pmatrix} 0 \\ \sqrt{\frac{1}{2} + \frac{\Delta}{2\sqrt{4J^2+\Delta^2}}} \\ \sqrt{\frac{1}{2} - \frac{\Delta}{2\sqrt{4J^2+\Delta^2}}} \\ 0 \end{pmatrix} \equiv \begin{pmatrix} 0 \\ c_\xi \\ s_\xi \\ 0 \end{pmatrix}, \quad |\psi_3'\rangle = \begin{pmatrix} 0 \\ -\sqrt{\frac{1}{2} - \frac{\Delta}{2\sqrt{4J^2+\Delta^2}}} \\ \sqrt{\frac{1}{2} + \frac{\Delta}{2\sqrt{4J^2+\Delta^2}}} \\ 0 \end{pmatrix} \equiv \begin{pmatrix} 0 \\ -s_\xi \\ c_\xi \\ 0 \end{pmatrix}, \quad |\psi_4'\rangle = \begin{pmatrix} 0 \\ 0 \\ 0 \\ 1 \end{pmatrix}. \tag{12.43}$$

We can also use the transformation matrix to express the density matrix ($\hat{\rho}' = \hat{T}\hat{\rho}\hat{T}$) and the operator of the measured quantity ($\hat{M}_+' = \hat{T}\hat{M}_+\hat{T}$) in the new basis (cf. Eq. 12.11). In particular, we are interested in the transformed operators $\mathscr{I}_{1y}' + \mathscr{I}_{2y}'$ and $\mathscr{I}_{1+}' + \mathscr{I}_{2+}' = \mathscr{I}_{1x}' + \mathscr{I}_{2x}' + \mathrm{i}(\mathscr{I}_{1y}' + \mathscr{I}_{2y}')$:

$$\mathscr{I}_{1y}' + \mathscr{I}_{2y}' = \hat{T}(\mathscr{I}_{1y} + \mathscr{I}_{2y})\hat{T} = \begin{pmatrix} 1 & 0 & 0 & 0 \\ 0 & c_\xi & -s_\xi & 0 \\ 0 & s_\xi & c_\xi & 0 \\ 0 & 0 & 0 & 1 \end{pmatrix} \frac{\mathrm{i}}{2} \begin{pmatrix} 0 & -1 & -1 & 0 \\ 1 & 0 & 0 & -1 \\ 1 & 0 & 0 & -1 \\ 0 & 1 & 1 & 0 \end{pmatrix} \begin{pmatrix} 1 & 0 & 0 & 0 \\ 0 & c_\xi & -s_\xi & 0 \\ 0 & s_\xi & c_\xi & 0 \\ 0 & 0 & 0 & 1 \end{pmatrix} = \frac{\mathrm{i}}{2} \begin{pmatrix} 0 & -(c_\xi + s_\xi) & -(c_\xi - s_\xi) & 0 \\ c_\xi + s_\xi & 0 & 0 & -(c_\xi + s_\xi) \\ c_\xi - s_\xi & 0 & 0 & -(c_\xi - s_\xi) \\ 0 & c_\xi + s_\xi & c_\xi - s_\xi & 0 \end{pmatrix}$$

$$= c_\xi \frac{\mathrm{i}}{2} \begin{pmatrix} 0 & -1 & -1 & 0 \\ +1 & 0 & 0 & -1 \\ +1 & 0 & 0 & -1 \\ 0 & +1 & +1 & 0 \end{pmatrix} + s_\xi \frac{\mathrm{i}}{2} \begin{pmatrix} 0 & -1 & +1 & 0 \\ +1 & 0 & 0 & -1 \\ -1 & 0 & 0 & +1 \\ 0 & +1 & -1 & 0 \end{pmatrix} = c_\xi(\mathscr{I}_{1y} + \mathscr{I}_{2y}) + s_\xi(2\mathscr{I}_{1z}\mathscr{I}_{2y} - 2\mathscr{I}_{1y}\mathscr{I}_{2z}), \tag{12.44}$$

$$\mathscr{I}'_{1x} + \mathscr{I}'_{2x} = \hat{T}(\mathscr{I}_{1x} + \mathscr{I}_{2x})\hat{T} = \begin{pmatrix} 1 & 0 & 0 & 0 \\ 0 & c_\xi & -s_\xi & 0 \\ 0 & s_\xi & c_\xi & 0 \\ 0 & 0 & 0 & 1 \end{pmatrix} \frac{1}{2}\begin{pmatrix} 0 & 1 & 1 & 0 \\ 1 & 0 & 0 & 1 \\ 1 & 0 & 0 & 1 \\ 0 & 1 & 1 & 0 \end{pmatrix} \begin{pmatrix} 1 & 0 & 0 & 0 \\ 0 & c_\xi & -s_\xi & 0 \\ 0 & s_\xi & c_\xi & 0 \\ 0 & 0 & 0 & 1 \end{pmatrix} = \frac{1}{2}\begin{pmatrix} 0 & c_\xi+s_\xi & c_\xi-s_\xi & 0 \\ c_\xi+s_\xi & 0 & 0 & c_\xi+s_\xi \\ c_\xi-s_\xi & 0 & 0 & c_\xi-s_\xi \\ 0 & c_\xi+s_\xi & c_\xi-s_\xi & 0 \end{pmatrix}$$

$$= c_\xi \frac{1}{2}\begin{pmatrix} 0 & +1 & +1 & 0 \\ +1 & 0 & 0 & +1 \\ +1 & 0 & 0 & +1 \\ 0 & +1 & +1 & 0 \end{pmatrix} + s_\xi \frac{1}{2}\begin{pmatrix} 0 & +1 & -1 & 0 \\ +1 & 0 & 0 & +1 \\ -1 & 0 & 0 & -1 \\ 0 & +1 & -1 & 0 \end{pmatrix} = c_\xi(\mathscr{I}_{1x}+\mathscr{I}_{2x}) + s_\xi(2\mathscr{I}_{1z}\mathscr{I}_{2x} - 2\mathscr{I}_{1x}\mathscr{I}_{2z}), \tag{12.45}$$

$$\mathscr{I}'_{1+} + \mathscr{I}'_{2+} = \begin{pmatrix} 0 & c_\xi+s_\xi & c_\xi-s_\xi & 0 \\ 0 & 0 & 0 & c_\xi+s_\xi \\ 0 & 0 & 0 & c_\xi-s_\xi \\ 0 & 0 & 0 & 0 \end{pmatrix} = c_\xi(\mathscr{I}_{1x}+\mathscr{I}_{2x}+i\mathscr{I}_{1y}+i\mathscr{I}_{2y}) + s_\xi(2\mathscr{I}_{1z}\mathscr{I}_{2x} - 2\mathscr{I}_{1x}\mathscr{I}_{2z} + i2\mathscr{I}_{1z}\mathscr{I}_{2y} - i2\mathscr{I}_{1y}\mathscr{I}_{2z}) \tag{12.46}$$

12.4.2 Strong J-coupling and density matrix evolution

When the density matrix at the beginning of the evolution is written in the new basis (where the Hamiltonian matrix is diagonal), it consists of multiple contributions. We analyze its evolution separately for the operators contributing to the signal of individual nuclei, and write the progress of the analysis in a table. The density matrix can be divided as

$$\hat{\rho}' = -\frac{\kappa}{2}\mathscr{I}'_{1y} - \frac{\kappa}{2}\mathscr{I}'_{2y} = \hat{\rho}'_1 + \hat{\rho}'_2 \tag{12.47}$$

Starting with $\hat{\rho}'_1$,

Contribution	$\hat{\rho}'_1$(b)	$\xrightarrow{\omega'_{0,1}\mathscr{I}_{1z}}$	$\xrightarrow{\pi J\cdot 2\mathscr{I}_{1z}\mathscr{I}_{2z}}$		$\mathrm{Tr}\{\hat{\rho}'_1(t)\mathscr{I}'_{1+}\}$
$\mathscr{I}_{1y}$	$+\frac{\kappa}{2}c_\xi$	$+\frac{\kappa}{2}c_\xi c'_1$	$+\frac{\kappa}{2}c_\xi c'_1 c_J + \frac{\kappa}{2}s_\xi s'_1 s_J$	$+i\frac{\kappa}{2}c_\xi^2 c'_1 c_J + i\frac{\kappa}{2}c_\xi s_\xi s'_1 s_J$	$\left.\right\} = i\frac{\kappa}{2}\left(c'_1 c_J + \frac{2J}{\sqrt{4J^2+\Delta^2}}s'_1 s_J\right)$
$2\mathscr{I}_{1y}\mathscr{I}_{2z}$	$-\frac{\kappa}{2}s_\xi$	$-\frac{\kappa}{2}s_\xi c'_1$	$-\frac{\kappa}{2}s_\xi c'_1 c_J - \frac{\kappa}{2}c_\xi s'_1 s_J$	$+i\frac{\kappa}{2}s_\xi^2 c'_1 c_J + i\frac{\kappa}{2}c_\xi s_\xi s'_1 s_J$	
$\mathscr{I}_{1x}$	0	$-\frac{\kappa}{2}c_\xi s'_1$	$-\frac{\kappa}{2}c_\xi s'_1 c_J + \frac{\kappa}{2}s_\xi c'_1 s_J$	$-\frac{\kappa}{2}c_\xi^2 s'_1 c_J + \frac{\kappa}{2}c_\xi s_\xi c'_1 s_J$	$\left.\right\} = -\frac{\kappa}{2}\left(s'_1 c_J - \frac{2J}{\sqrt{4J^2+\Delta^2}}c'_1 s_J\right)$
$2\mathscr{I}_{1x}\mathscr{I}_{2z}$	0	$+\frac{\kappa}{2}s_\xi s'_1$	$+\frac{\kappa}{2}s_\xi s'_1 c_J - \frac{\kappa}{2}c_\xi c'_1 s_J$	$-\frac{\kappa}{2}s_\xi^2 s'_1 c_J + \frac{\kappa}{2}c_\xi s_\xi c'_1 s_J$	

Using the following trigonometric relations

$$c'_1 c_J = \frac{c'^-_1 + c'^+_1}{2} \quad s'_1 s_J = \frac{c'^-_1 - c'^+_1}{2} \quad c'_1 s_J = \frac{-s'^-_1 + s'^+_1}{2} \quad s'_1 c_J = \frac{s'^-_1 + s'^+_1}{2}, \tag{12.48}$$

where $c'^\pm_1 = \cos((\omega'_{0,1} - \omega_{\mathrm{rot}} \pm \pi J)t) = \cos((\Omega'_1 \pm \pi J)t)$ and $s'^\pm_1 = \sin((\omega'_{0,1} - \omega_{\mathrm{rot}} \pm \pi J)t) = \sin((\Omega'_1 \pm \pi J)t)$ ($\omega_{\mathrm{rot}} = -\omega_{\mathrm{radio}}$),

$$\mathrm{Tr}\{\hat{\rho}'_1(t)\mathscr{I}'_{1+}\} = i\frac{\kappa}{2}\left(c'_1 c_J + \frac{2J}{\sqrt{4J^2+\Delta^2}}s'_1 s_J\right) - \frac{\kappa}{2}\left(s'_1 c_J - \frac{2J}{\sqrt{4J^2+\Delta^2}}c'_1 s_J\right)$$

$$= i\frac{\kappa}{2}\left(\frac{c'^-_1 + c'^+_1}{2} + \frac{2J}{\sqrt{4J^2+\Delta^2}}\frac{c'^-_1 - c'^+_1}{2}\right) - \frac{\kappa}{2}\left(\frac{s'^-_1 + s'^+_1}{2} + \frac{2J}{\sqrt{4J^2+\Delta^2}}\frac{s'^-_1 - s'^+_1}{2}\right)$$

$$= i\frac{\kappa}{4}\left(\left(1 + \frac{2J}{\sqrt{4J^2+\Delta^2}}\right)c'^-_1 + \left(1 - \frac{2J}{\sqrt{4J^2+\Delta^2}}\right)c'^+_1 + i\left(\left(1 + \frac{2J}{\sqrt{4J^2+\Delta^2}}\right)s'^-_1 + \left(1 - \frac{2J}{\sqrt{4J^2+\Delta^2}}\right)s'^+_1\right)\right)$$

$$= \frac{\kappa}{4}e^{i\frac{\pi}{2}}\left(\left(1 + \frac{2J}{\sqrt{4J^2+\Delta^2}}\right)e^{i(\Omega'_1-\pi J)t} + \left(1 - \frac{2J}{\sqrt{4J^2+\Delta^2}}\right)e^{i(\Omega'_1+\pi J)t}\right). \tag{12.49}$$

We now repeat the analysis for nucleus 2.

Contribution	$\hat{\rho}'_2$(b)	$\xrightarrow{\omega'_{0,2}\mathscr{I}_{2z}}$	$\xrightarrow{\pi J\cdot 2\mathscr{I}_{1z}\mathscr{I}_{2z}}$		$\mathrm{Tr}\{\hat{\rho}'_2(t)\mathscr{I}'_{2+}\}$
$\mathscr{I}_{2y}$	$+\frac{\kappa}{2}c_\xi$	$+\frac{\kappa}{2}c_\xi c'_2$	$+\frac{\kappa}{2}c_\xi c'_2 c_J - \frac{\kappa}{2}s_\xi s'_2 s_J$	$+i\frac{\kappa}{2}c_\xi^2 c'_2 c_J - i\frac{\kappa}{2}c_\xi s_\xi s'_2 s_J$	$\left.\right\} = i\frac{\kappa}{2}\left(c'_2 c_J - \frac{2J}{\sqrt{4J^2+\Delta^2}}s'_2 s_J\right)$
$2\mathscr{I}_{1z}\mathscr{I}_{2y}$	$+\frac{\kappa}{2}s_\xi$	$+\frac{\kappa}{2}s_\xi c'_2$	$+\frac{\kappa}{2}s_\xi c'_2 c_J - \frac{\kappa}{2}c_\xi s'_2 s_J$	$+i\frac{\kappa}{2}s_\xi^2 c'_2 c_J - i\frac{\kappa}{2}c_\xi s_\xi s'_2 s_J$	
$\mathscr{I}_{2x}$	0	$-\frac{\kappa}{2}c_\xi s'_2$	$-\frac{\kappa}{2}c_\xi s'_2 c_J - \frac{\kappa}{2}s_\xi c'_2 s_J$	$-\frac{\kappa}{2}c_\xi^2 s'_2 c_J - \frac{\kappa}{2}c_\xi s_\xi c'_2 s_J$	$\left.\right\} = -\frac{\kappa}{2}\left(s'_2 c_J + \frac{2J}{\sqrt{4J^2+\Delta^2}}c'_2 s_J\right)$
$2\mathscr{I}_{1z}\mathscr{I}_{2x}$	0	$-\frac{\kappa}{2}s_\xi s'_2$	$-\frac{\kappa}{2}s_\xi s'_2 c_J - \frac{\kappa}{2}c_\xi c'_2 s_J$	$-\frac{\kappa}{2}s_\xi^2 s'_2 c_J - \frac{\kappa}{2}c_\xi s_\xi c'_2 s_J$	

Using the following trigonometric relations

$$c'_2 c_J = \frac{c'^-_2 + c'^+_2}{2} \quad s'_2 s_J = \frac{c'^-_2 - c'^+_2}{2} \quad c'_2 s_J = \frac{-s'^-_2 + s'^+_2}{2} \quad s'_2 c_J = \frac{s'^-_2 + s'^+_2}{2}, \tag{12.50}$$

where $c_2'^{\pm} = \cos((\omega_{0,2}' - \omega_{\text{rot}} \pm \pi J)t) = \cos((\Omega_2' \pm \pi J)t)$ and $s_2'^{\pm} = \sin((\omega_{0,2}' - \omega_{\text{rot}} \pm \pi J)t) = \sin((\Omega_2' \pm \pi J)t)$,

$$
\begin{aligned}
\text{Tr}\{\hat{\rho}_2'(t)\mathscr{I}_{2+}'\} &= \text{i}\frac{\kappa}{2}\left(c_2'c_J - \frac{2J}{\sqrt{4J^2+\Delta^2}}s_2's_J\right) - \frac{\kappa}{2}\left(s_2'c_J + \frac{2J}{\sqrt{4J^2+\Delta^2}}c_2's_J\right) \\
&= \text{i}\frac{\kappa}{2}\left(\frac{c_2'^- + c_2'^+}{2} - \frac{2J}{\sqrt{4J^2+\Delta^2}}\frac{c_2'^- - c_2'^+}{2}\right) - \frac{\kappa}{2}\left(\frac{s_2'^- + s_2'^+}{2} - \frac{2J}{\sqrt{4J^2+\Delta^2}}\frac{s_2'^- - s_2'^+}{2}\right) \\
&= \text{i}\frac{\kappa}{4}\left(\left(1 - \frac{2J}{\sqrt{4J^2+\Delta^2}}\right)c_2'^- + \left(1 + \frac{2J}{\sqrt{4J^2+\Delta^2}}\right)c_2'^+ + \text{i}\left(\left(1 - \frac{2J}{\sqrt{4J^2+\Delta^2}}\right)s_2'^- + \left(1 + \frac{2J}{\sqrt{4J^2+\Delta^2}}\right)s_2'^+\right)\right) \\
&= \frac{\kappa}{4}\text{e}^{\text{i}\frac{\pi}{2}}\left(\left(1 - \frac{2J}{\sqrt{4J^2+\Delta^2}}\right)\text{e}^{\text{i}(\Omega_2'-\pi J)t} + \left(1 + \frac{2J}{\sqrt{4J^2+\Delta^2}}\right)\text{e}^{\text{i}(\Omega_2'+\pi J)t}\right).
\end{aligned}
\tag{12.51}
$$

Combining the results presented in Eqs. 12.51 and 12.49, applying the phase correction, and including the relaxation, we obtain the following description of the evolution of the signal:

$$
\langle M_+\rangle = \frac{\mathcal{N}\gamma^2\hbar^2 B_0}{8k_{\text{B}}T}\text{e}^{-\overline{R}_2 t}\left((1 - 2c_\xi s_\xi)\,\text{e}^{\text{i}(\Omega_1'-\pi J)t} + (1 + 2c_\xi s_\xi)\,\text{e}^{\text{i}(\Omega_1'+\pi J)t} + (1 + 2c_\xi s_\xi)\,\text{e}^{\text{i}(\Omega_2'-\pi J)t} + (1 - 2c_\xi s_\xi)\,\text{e}^{\text{i}(\Omega_2'+\pi J)t}\right), \tag{12.52}
$$

where $2c_\xi s_\xi = 2J/\sqrt{4J^2+\Delta^2}$.

12.4.3 $\mathscr{H}_J$ and operators of components of total $\vec{I}$ commute

We show that the operator of each component of the total angular momentum (e.g., $\hat{I}_x \propto \mathscr{I}_x = \mathscr{I}_{1x} + \mathscr{I}_{2x} + \mathscr{I}_{3x} + \dots$) commutes with the strong coupling Hamiltonian $\mathscr{H}_J$ for any number of nuclei in the coupled system and for any values of the J constants. For $j = x, k = y, l = z$ or for any cyclic permutation ($j = y, k = z, l = x$ or $j = z, k = x, l = y$),

$$
\begin{aligned}
[\mathscr{I}_j, \mathscr{H}_J] &= \sum_n \sum_{n'\neq n} 2\pi J_{nn'}[\mathscr{I}_{nj}, (\mathscr{I}_{nj}\mathscr{I}_{n'j} + \mathscr{I}_{nk}\mathscr{I}_{n'k} + \mathscr{I}_{nl}\mathscr{I}_{n'l})] \\
&= \sum_n \sum_{n'\neq n} 2\pi J_{nn'}([\mathscr{I}_{nj}, \mathscr{I}_{nk}]\mathscr{I}_{n'k} + [\mathscr{I}_{nj}, \mathscr{I}_{nl}]\mathscr{I}_{n'l}) = \sum_n \sum_{n'\neq n} 2\pi J_{nn'}([\mathscr{I}_{nj}, \mathscr{I}_{nk}]\mathscr{I}_{n'k} - [\mathscr{I}_{nl}, \mathscr{I}_{nj}]\mathscr{I}_{n'l}) \\
&= \sum_n \sum_{n'\neq n} 2\text{i}\pi J_{nn'}(\mathscr{I}_{nl}\mathscr{I}_{n'k} - \mathscr{I}_{nk}\mathscr{I}_{n'l}) = 0,
\end{aligned}
\tag{12.53}
$$

where n and n' are two different nuclei. The commutator is equal to zero because for any pair of nuclei p and q, the term $2\text{i}\pi J_{nn'}(\mathscr{I}_{nl}\mathscr{I}_{n'k} - \mathscr{I}_{nk}\mathscr{I}_{n'l})$ appears twice in the sum, with the opposite sign: once for $n = p$ and $n' = q$ as $2\text{i}\pi J_{pq}(\mathscr{I}_{pl}\mathscr{I}_{qk} - \mathscr{I}_{pk}\mathscr{I}_{ql})$, and once for $n = q$ and $n' = p$ as $2\text{i}\pi J_{pq}(\mathscr{I}_{ql}\mathscr{I}_{pk} - \mathscr{I}_{qk}\mathscr{I}_{pl})$.

12.4.4 J-coupling of magnetically equivalent nuclei

In general, the free evolution of multiple spin-1/2 magnetic moments is governed by the Hamiltonian

$$
\mathscr{H} = \sum_n \omega_{0,n}\mathscr{I}_{nz} + \pi J_{nn'}\sum_n\sum_{n'}(2\mathscr{I}_{nx}\mathscr{I}_{n'x} + 2\mathscr{I}_{ny}\mathscr{I}_{n'y} + 2\mathscr{I}_{nz}\mathscr{I}_{n'z}) = \sum_n \omega_{0,n}\mathscr{I}_{nz} + \mathscr{H}_J \tag{12.54}
$$

If the nuclei are magnetically equivalent,

$$
\mathscr{H} = \omega_0\sum_n \mathscr{I}_{nz} + \mathscr{H}_J = \omega_0\mathscr{I}_z + \mathscr{H}_J, \tag{12.55}
$$

where $\mathscr{I}_z$ and $\mathscr{H}_J$ commute, as shown in Section 12.4.3. Therefore, the effect of chemical shift and J-coupling can be analyzed separately. Note that $\mathscr{H}_J$ commutes also with $\hat{M}_+$, which is proportional to $\mathscr{I}_x + \text{i}\mathscr{I}_y$.

In order to analyze the effect of the J-coupling on the spectrum, we evaluate $\langle M_+\rangle$ as

$$
\langle M_+\rangle = \text{Tr}\{\hat{\rho}\hat{M}_+\} = \sum_j\sum_k \rho_{jk}M_{+jk}, \tag{12.56}
$$

where we expressed the trace explicitly in terms of the elements of the matrices $\hat{\rho}$ and $\hat{M}_+$. If the system evolves due to the J-coupling, $\langle M_+ \rangle$ should change, i.e., the time derivative of $\langle M_+ \rangle$ should differ from zero.

$$\frac{\mathrm{d}\langle M_+ \rangle}{\mathrm{d}t} = \sum_j \sum_k \frac{\mathrm{d}\rho_{jk} M_{+jk}}{\mathrm{d}t} = \mathrm{Tr}\left\{ \frac{\mathrm{d}\hat{\rho}}{\mathrm{d}t} \hat{M}_+ \right\}. \tag{12.57}$$

According to the Liouville-von Neumann equation,

$$\frac{\mathrm{d}\hat{\rho}}{\mathrm{d}t} = \mathrm{i}[\hat{\rho}, \mathscr{H}_J] \quad \Rightarrow \quad \frac{\mathrm{d}\langle M_+ \rangle}{\mathrm{d}t} = \mathrm{i}\mathrm{Tr}\left\{ [\hat{\rho}, \mathscr{H}_J]\hat{M}_+ \right\} = \mathrm{i}\mathrm{Tr}\left\{ \hat{\rho}\mathscr{H}_J\hat{M}_+ \right\} - \mathrm{i}\mathrm{Tr}\left\{ \mathscr{H}_J\hat{\rho}\hat{M}_+ \right\}. \tag{12.58}$$

Because $\mathscr{H}_J$ commutes with $\hat{M}_+$ (and therefore $\mathscr{H}_J\hat{M}_+ = \hat{M}_+\mathscr{H}_J$), and because $\mathrm{Tr}\{\hat{A}\hat{B}\} = \mathrm{Tr}\{\hat{B}\hat{A}\}$,

$$\frac{\mathrm{d}\langle M_+ \rangle}{\mathrm{d}t} = \mathrm{i}\mathrm{Tr}\left\{ \hat{\rho}\hat{M}_+\mathscr{H}_J \right\} - \mathrm{i}\mathrm{Tr}\left\{ \mathscr{H}_J\hat{\rho}\hat{M}_+ \right\} = \mathrm{i}\mathrm{Tr}\left\{ (\hat{\rho}\hat{M}_+)\mathscr{H}_J \right\} - \mathrm{i}\mathrm{Tr}\left\{ \mathscr{H}_J(\hat{\rho}\hat{M}_+) \right\} = \mathrm{i}\mathrm{Tr}\left\{ (\hat{\rho}\hat{M}_+)\mathscr{H}_J \right\} - \mathrm{i}\mathrm{Tr}\left\{ (\hat{\rho}\hat{M}_+)\mathscr{H}_J \right\} = 0. \tag{12.59}$$

We see that $\langle M_+ \rangle$ does not change due to the J-coupling regardless of the actual form of $\hat{\rho}$. This proves that the J-coupling between magnetically equivalent nuclei does not have any effect on the spectrum (is invisible).

12.4.5   Product operators of three and more coupled magnetic moments

Features of the TOCSY experiments are fully manifested only in networks consisting of three or more interacting magnetic moments. Therefore, we need to find product operators for systems of more than two nuclei. We start by the normalized bases of density matrices of isolated magnetic moments, consisting of four operators $\sqrt{2}\mathscr{I}_t, \sqrt{2}\mathscr{I}_x, \sqrt{2}\mathscr{I}_y, \sqrt{2}\mathscr{I}_z$. They can be also written as

$$\frac{1}{\sqrt{2}}\left(2\mathscr{I}_j^{(1)} \right), \tag{12.60}$$

where $j \in \{t, x, y, z\}$ and the superscript (1), not written in practice, emphasizes that we describe a single magnetic moment. Note that all operators $2\mathscr{I}_j^{(1)}$ are represented my matrices with elements equal to 0, ± 1, or $\pm\mathrm{i}$.

We continue by the procedure introduced in Section 8.3. Eqs. 8.11–8.26 describe construction of an orthonormal basis consisting of direct products of operators $\sqrt{2}\mathscr{I}_j$, where $j \in \{t, x, y, z\}$. A general form of Eqs. 8.11–8.26 can be written as

$$2\mathscr{I}_{1j}\mathscr{I}_{2k}^{(12)} = \left(\sqrt{2}\mathscr{I}_j^{(1)} \right) \otimes \left(\sqrt{2}\mathscr{I}_k^{(2)} \right) = \frac{1}{2}\left(2\mathscr{I}_j^{(1)} \right) \otimes \left(2\mathscr{I}_k^{(2)} \right), \tag{12.61}$$

where $j, k \in \{t, x, y, z\}$. The unit matrices $\hat{1} = \left(2\mathscr{I}_t^{(n)} \right)$ are usually not written explicitly.

In a similar manner, 64 operators constituting an orthonormal bases of density matrices of three coupled magnetic moments can be obtained by calculating

$$2\sqrt{2}\mathscr{I}_{1j}\mathscr{I}_{2k}\mathscr{I}_{3l}^{(123)} = \left(\sqrt{2}\mathscr{I}_j^{(1)} \right) \otimes \left(\sqrt{2}\mathscr{I}_k^{(2)} \right) \otimes \left(\sqrt{2}\mathscr{I}_l^{(3)} \right) = \frac{1}{\sqrt{8}}\left(2\mathscr{I}_j^{(1)} \right) \otimes \left(2\mathscr{I}_k^{(2)} \right) \otimes \left(2\mathscr{I}_l^{(3)} \right), \tag{12.62}$$

where $j, k, l \in \{t, x, y, z\}$.

In general, 2^{2N} operators constituting an orthonormal basis of density matrices of N coupled magnetic moments are obtained by calculating

$$\frac{\sqrt{2^N}}{2}\mathscr{I}_{1j}\cdots\mathscr{I}_{Nk}^{(1\cdots N)} = \left(\sqrt{2}\mathscr{I}_j^{(1)} \right) \otimes \cdots \otimes \left(\sqrt{2}\mathscr{I}_k^{(N)} \right) = \frac{1}{\sqrt{2^N}}\left(2\mathscr{I}_j^{(1)} \right) \otimes \cdots \otimes \left(2\mathscr{I}_k^{(N)} \right). \tag{12.63}$$

Note that the operators of angular momentum components divided by $\hbar$, $\mathscr{I}_{nj}$, are orthonormal only for systems of two magnetic moments (together with $\mathscr{I}_t = \frac{1}{2}\hat{1}$ and product operators $2\mathscr{I}_{nj}\mathscr{I}_{n'k}$). In general, product operators of N coupled magnetic moments

$$\frac{2^N}{2}\mathscr{I}_{1j}\cdots\mathscr{I}_{Nk}^{(1\cdots N)} = \frac{1}{2}\left(2\mathscr{I}_j^{(1)} \right) \otimes \cdots \otimes \left(2\mathscr{I}_k^{(N)} \right), \tag{12.64}$$

including $\mathscr{I}_{nj}$, must be multiplied by $2/\sqrt{2^N}$ to be normalized. For example, single-quantum coherences of a set of three magnetic moments are normalized by dividing the product operators $\mathscr{I}_{1x}, 2\mathscr{I}_{1x}\mathscr{I}_{2z}, 4\mathscr{I}_{1x}\mathscr{I}_{2z}\mathscr{I}_{3z}$, etc., by $\sqrt{2}$.

In conclusion, we have to distinguish whether we use the product operator to represent a *physical quantity*, or to serve as a *mathematical object*, i.e., a basis matrix. In the former case, we should use the operator without normalization: e.g., $\mathscr{I}_{nz}$ multiplied by $\hbar$ to represent angular momentum, multiplied by $\gamma\hbar$ to represent magnetic moment, multiplied by $-\gamma B_0\hbar$ to represent energy in the magnetic field $\vec{B}_0$, etc. In the latter case, normalization is useful e.g. when calculating traces of products of matrices.

12.4.6   Three magnetic moments in thermal equilibrium

Derivation of the density matrix describing an ensemble of pairs of nuclear magnetic moments presented in Section 8.9.8 can be easily extended to a sets of N nuclei. As the influence of direct or indirect interaction on the distribution of magnetic moments is negligible in liquid samples, and the impact of the chemical shift is also very small, it is sufficient to consider the Hamiltonian reflecting the effect of the external magnetic field $\vec{B}_0$:

$$\hat{H} = -\sum_{n=1}^{N} \gamma_n B_0 \hat{I}_{nz} = -\sum_{n=1}^{N} \gamma_n B_0 \hbar \mathscr{I}_{nz}. \tag{12.65}$$

The density matrix describing the mixed state in the equilibrium consists of populations

$$P_j^{\mathrm{eq}} = \frac{\mathrm{e}^{-\mathcal{E}_j/k_{\mathrm{B}}T}}{\sum\limits_{k=1}^{2^N} \mathrm{e}^{-\mathcal{E}_k/k_{\mathrm{B}}T}} \approx \frac{1 - \dfrac{\mathcal{E}_j}{k_{\mathrm{B}}T}}{2^N}, \tag{12.66}$$

where $\mathcal{E}_j$ is the eigenvalue of the Hamiltonian corresponding the population P_j. Consequently, the equilibrium density matrix is

$$\hat{\rho}^{\mathrm{eq}} = \frac{1}{2^N}\left(\hat{1} + \sum_{n=1}^{N} \frac{\gamma_n B_0 \hbar}{k_{\mathrm{B}}T}\mathscr{I}_{nz}\right) = \frac{1}{2^{N-1}}\left(\mathscr{I}_t + \sum_{n=1}^{N} \kappa_n \mathscr{I}_{nz}\right), \tag{12.67}$$

where

$$\kappa_n = \frac{\gamma_n B_0 \hbar}{2k_{\mathrm{B}}T}. \tag{12.68}$$

12.4.7   Commutation relations of the TOCSY mixing Hamiltonian

The commutators of the $\mathscr{I}_{jy}$ operators with the $\mathscr{H}_{\mathrm{TOCSY}}$ Hamiltonian for a set of three protons with $J_{12} = J_{23} > 0$ and $J_{13} = 0$ are given by

$$[\mathscr{I}_{1y}, \mathscr{H}_{\mathrm{TOCSY}}] = \pi J[\mathscr{I}_{1y}, 2\mathscr{I}_{1x}\mathscr{I}_{2x} + 2\mathscr{I}_{1y}\mathscr{I}_{2y} + 2\mathscr{I}_{1z}\mathscr{I}_{2z}] = 2\pi J[\mathscr{I}_{1y}, \mathscr{I}_{1x}]\mathscr{I}_{2x} + 2\pi J[\mathscr{I}_{1y}, \mathscr{I}_{1z}]\mathscr{I}_{2z} = -2\mathrm{i}\pi J(\mathscr{I}_{1z}\mathscr{I}_{2x} - \mathscr{I}_{1x}\mathscr{I}_{2z}), \tag{12.69}$$

$$\begin{aligned}[\mathscr{I}_{2y}, \mathscr{H}_{\mathrm{TOCSY}}] &= \pi J[\mathscr{I}_{2y}, 2\mathscr{I}_{1x}\mathscr{I}_{2x} + 2\mathscr{I}_{1y}\mathscr{I}_{2y} + 2\mathscr{I}_{1z}\mathscr{I}_{2z} + 2\mathscr{I}_{2x}\mathscr{I}_{3x} + 2\mathscr{I}_{2y}\mathscr{I}_{3y} + 2\mathscr{I}_{2z}\mathscr{I}_{3z}] \\ &= 2\pi J\mathscr{I}_{1x}[\mathscr{I}_{2y}, \mathscr{I}_{2x}] + 2\pi J\mathscr{I}_{1z}[\mathscr{I}_{2y}, \mathscr{I}_{2z}] + 2\pi J[\mathscr{I}_{2y}, \mathscr{I}_{2x}]\mathscr{I}_{3x} + 2\pi J[\mathscr{I}_{2y}, \mathscr{I}_{2z}]\mathscr{I}_{3z} \\ &= -2\mathrm{i}\pi J(\mathscr{I}_{1x}\mathscr{I}_{2z} - \mathscr{I}_{1z}\mathscr{I}_{2x}) - 2\mathrm{i}\pi J(\mathscr{I}_{2x}\mathscr{I}_{3z} - \mathscr{I}_{2z}\mathscr{I}_{3x}),\end{aligned} \tag{12.70}$$

$$[\mathscr{I}_{3y}, \mathscr{H}_{\mathrm{TOCSY}}] = \pi J[\mathscr{I}_{3y}, 2\mathscr{I}_{2x}\mathscr{I}_{3x} + 2\mathscr{I}_{2y}\mathscr{I}_{3y} + 2\mathscr{I}_{2z}\mathscr{I}_{3z}] = 2\pi J\mathscr{I}_{2x}[\mathscr{I}_{3y}, \mathscr{I}_{3x}] + 2\pi J\mathscr{I}_{2z}[\mathscr{I}_{3y}, \mathscr{I}_{3z}] = -2\mathrm{i}\pi J(\mathscr{I}_{2x}\mathscr{I}_{3z} - \mathscr{I}_{2z}\mathscr{I}_{3x}). \tag{12.71}$$

A sum of the first two commutators (Eqs. 12.69 and 12.70) shows that

$$[\mathscr{I}_{1y} + \mathscr{I}_{2y}, \mathscr{H}_{\mathrm{TOCSY}}] = 2\mathrm{i}\pi J(\mathscr{I}_{2x}\mathscr{I}_{3z} - \mathscr{I}_{2z}\mathscr{I}_{3x}) \tag{12.72}$$

and a sum of all three commutators (Eqs. 12.69–12.71) shows that

$$[\mathscr{I}_{1y} + \mathscr{I}_{2y} + \mathscr{I}_{3y}, \mathscr{H}_{\mathrm{TOCSY}}] = 0 \tag{12.73}$$

in agreement with Eq. 12.53.

12.4.8 Density matrix evolution in the TOCSY experiment

As discussed in Section 12.3, the TOCSY pulse sequence starts by a 90° excitation pulse that converts $\hat{\rho}(\text{a}) = \frac{1}{4}(\mathscr{I}_t + \kappa\mathscr{I}_{1z} + \kappa\mathscr{I}_{2z} + \kappa\mathscr{I}_{3z}) = \frac{1}{4}\mathscr{I}_t + \frac{\kappa}{4}\sum_j \mathscr{I}_{jz}$
to
$\hat{\rho}(\text{b}) = \frac{1}{4}(\mathscr{I}_t - \kappa\mathscr{I}_{1y} - \kappa\mathscr{I}_{2y} - \kappa\mathscr{I}_{3y}) = \frac{1}{4}\mathscr{I}_t - \frac{\kappa}{4}\sum_j \mathscr{I}_{jy}$,

which evolves during the incremented evolution period t_1. An example of a set of nuclei interacting via couplings described by constants $J_{12} = J_{23} = J$ and $J_{13} = 0$ is presented in Section 12.3, here we analyze a general case that evolves (considering only $\mathscr{I}_{jy}$ coherences that survive the TOCSY mixing) as
$\hat{\rho}(\text{c}) = -\frac{\kappa}{4}\sum_j C_{j1}\mathscr{I}_{jy}$,

where

$$C_{11} = \cos(\Omega_1 t_1)\cos(\pi J_{12} t_1)\cos(\pi J_{13} t_1) = \frac{1}{2}\cos(\Omega_1 t_1)(\cos(\pi J_{12} t_1 - \pi J_{13} t_1) - \cos(\pi J_{12} t_1 + \pi J_{13} t_1))$$

$$= \frac{1}{4}(\cos((\Omega_1 - \pi J_{12} - \pi J_{13})t_1) + \cos((\Omega_1 - \pi J_{12} + \pi J_{13})t_1) + \cos((\Omega_1 + \pi J_{12} - \pi J_{13})t_1) + \cos((\Omega_1 + \pi J_{12} + \pi J_{13})t_1))$$

$$C_{21} = \cos(\Omega_2 t_1)\cos(\pi J_{12} t_1)\cos(\pi J_{23} t_1) = \frac{1}{2}\cos(\Omega_2 t_1)(\cos(\pi J_{12} t_1 - \pi J_{23} t_1) - \cos(\pi J_{12} t_1 + \pi J_{23} t_1))$$

$$= \frac{1}{4}(\cos((\Omega_2 - \pi J_{12} - \pi J_{23})t_1) + \cos((\Omega_2 - \pi J_{12} + \pi J_{23})t_1) + \cos((\Omega_2 + \pi J_{12} - \pi J_{23})t_1) + \cos((\Omega_2 + \pi J_{12} + \pi J_{23})t_1))$$

$$C_{31} = \cos(\Omega_3 t_1)\cos(\pi J_{13} t_1)\cos(\pi J_{23} t_1) = \frac{1}{2}\cos(\Omega_3 t_1)(\cos(\pi J_{13} t_1 - \pi J_{23} t_1) - \cos(\pi J_{13} t_1 + \pi J_{23} t_1))$$

$$= \frac{1}{4}(\cos((\Omega_3 - \pi J_{13} - \pi J_{23})t_1) + \cos((\Omega_3 - \pi J_{13} + \pi J_{23})t_1) + \cos((\Omega_3 + \pi J_{13} - \pi J_{23})t_1) + \cos((\Omega_3 + \pi J_{13} + \pi J_{23})t_1)).$$

$$(12.74)$$

The $-\frac{\kappa}{4}C_{j1}\mathscr{I}_{jy}$ components of the density matrix, converted to $\hat{\rho}(\text{d}) = -\frac{\kappa}{4}\sum_j\sum_k a_{jk}C_{j1}\mathscr{I}_{ky}$ during the TOCSY mixing period (see Section 12.3), further evolve during t_2 to
$\hat{\rho}(t_2) = -\frac{\kappa}{4}\sum_j\sum_k a_{jk}C_{j1}(C_{k2}\mathscr{I}_{ky} - S_{k2}\mathscr{I}_{kx})$, where

$$C_{12} = \cos(\Omega_1 t_2)\cos(\pi J_{12} t_2)\cos(\pi J_{13} t_2) = \frac{1}{2}\cos(\Omega_1 t_2)(\cos(\pi J_{12} t_2 - \pi J_{13} t_2) - \cos(\pi J_{12} t_2 + \pi J_{13} t_2))$$

$$= \frac{1}{4}(\cos((\Omega_1 - \pi J_{12} - \pi J_{13})t_2) + \cos((\Omega_1 - \pi J_{12} + \pi J_{13})t_2) + \cos((\Omega_1 + \pi J_{12} - \pi J_{13})t_2) + \cos((\Omega_1 + \pi J_{12} + \pi J_{13})t_2))$$

$$C_{22} = \cos(\Omega_2 t_2)\cos(\pi J_{12} t_2)\cos(\pi J_{23} t_2) = \frac{1}{2}\cos(\Omega_2 t_2)(\cos(\pi J_{12} t_2 - \pi J_{23} t_2) - \cos(\pi J_{12} t_2 + \pi J_{23} t_2))$$

$$= \frac{1}{4}(\cos((\Omega_2 - \pi J_{12} - \pi J_{23})t_2) + \cos((\Omega_2 - \pi J_{12} + \pi J_{23})t_2) + \cos((\Omega_2 + \pi J_{12} - \pi J_{23})t_2) + \cos((\Omega_2 + \pi J_{12} + \pi J_{23})t_2))$$

$$C_{32} = \cos(\Omega_3 t_2)\cos(\pi J_{13} t_2)\cos(\pi J_{23} t_2) = \frac{1}{2}\cos(\Omega_3 t_2)(\cos(\pi J_{13} t_2 - \pi J_{23} t_2) - \cos(\pi J_{13} t_2 + \pi J_{23} t_2))$$

$$= \frac{1}{4}(\cos((\Omega_3 - \pi J_{13} - \pi J_{23})t_2) + \cos((\Omega_3 - \pi J_{13} + \pi J_{23})t_2) + \cos((\Omega_3 + \pi J_{13} - \pi J_{23})t_2) + \cos((\Omega_3 + \pi J_{13} + \pi J_{23})t_2)).$$

$$(12.75)$$

and

$$S_{12} = \sin(\Omega_1 t_2)\cos(\pi J_{12} t_2)\cos(\pi J_{13} t_2) = \frac{1}{2}\sin(\Omega_1 t_2)(\cos(\pi J_{12} t_2 - \pi J_{13} t_2) - \cos(\pi J_{12} t_2 + \pi J_{13} t_2))$$

$$= \frac{1}{4}(\sin((\Omega_1 - \pi J_{12} - \pi J_{13})t_2) + \sin((\Omega_1 - \pi J_{12} + \pi J_{13})t_2) + \sin((\Omega_1 + \pi J_{12} - \pi J_{13})t_2) + \sin((\Omega_1 + \pi J_{12} + \pi J_{13})t_2))$$

$$S_{22} = \sin(\Omega_2 t_2)\cos(\pi J_{12} t_2)\cos(\pi J_{23} t_2) = \frac{1}{2}\sin(\Omega_2 t_2)(\cos(\pi J_{12} t_2 - \pi J_{23} t_2) - \cos(\pi J_{12} t_2 + \pi J_{23} t_2))$$

$$= \frac{1}{4}(\sin((\Omega_2 - \pi J_{12} - \pi J_{23})t_2) + \sin((\Omega_2 - \pi J_{12} + \pi J_{23})t_2) + \sin((\Omega_2 + \pi J_{12} - \pi J_{23})t_2) + \sin((\Omega_2 + \pi J_{12} + \pi J_{23})t_2))$$

$$S_{32} = \sin(\Omega_3 t_2)\cos(\pi J_{13} t_2)\cos(\pi J_{23} t_2) = \frac{1}{2}\sin(\Omega_3 t_2)(\cos(\pi J_{13} t_2 - \pi J_{23} t_2) - \cos(\pi J_{13} t_2 + \pi J_{23} t_2))$$

$$= \frac{1}{4}(\sin((\Omega_3 - \pi J_{13} - \pi J_{23})t_2) + \sin((\Omega_3 - \pi J_{13} + \pi J_{23})t_2) + \sin((\Omega_3 + \pi J_{13} - \pi J_{23})t_2) + \sin((\Omega_3 + \pi J_{13} + \pi J_{23})t_2)).$$

$$(12.76)$$

Considering the orthogonality of the matrices and the normalization used in our analysis,[6] the nonzero traces are

$$\text{Tr}\{\mathscr{I}_{nx}\mathscr{I}_{n+}\} = 2, \quad \text{Tr}\{\mathscr{I}_{ny}\mathscr{I}_{n+}\} = 2\text{i}. \tag{12.77}$$

$$\text{Tr}\{\hat{\rho}(t_2)\hat{M}_+\} = -\mathcal{N}\gamma\hbar\frac{\kappa}{2}\sum_j\sum_k a_{jk}C_{j1}(\text{i}C_{k2} - S_{k2}) = -\text{i}\mathcal{N}\gamma\hbar\frac{\kappa}{2}\sum_j\sum_k a_{jk}C_{j1}(C_{k2} + \text{i}S_{k2}) = -\text{i}\mathcal{N}\gamma\hbar\frac{\kappa}{2}\sum_j\sum_k a_{jk}C_{j1}E_{k2}, \tag{12.78}$$

where

$$E_{12} = C_{12} + \text{i}S_{12} = \frac{1}{4}\left(e^{\text{i}(\Omega_1 - \pi J_{12} - \pi J_{13})t_2} + e^{\text{i}(\Omega_1 - \pi J_{12} + \pi J_{13})t_2} + e^{\text{i}(\Omega_1 + \pi J_{12} - \pi J_{13})t_2} + e^{\text{i}(\Omega_1 + \pi J_{12} + \pi J_{13})t_2}\right)$$

$$E_{22} = C_{22} + \text{i}S_{22} = \frac{1}{4}\left(e^{\text{i}(\Omega_2 - \pi J_{12} - \pi J_{23})t_2} + e^{\text{i}(\Omega_2 - \pi J_{12} + \pi J_{23})t_2} + e^{\text{i}(\Omega_2 + \pi J_{12} - \pi J_{23})t_2} + e^{\text{i}(\Omega_2 + \pi J_{12} + \pi J_{23})t_2}\right)$$

$$E_{32} = C_{32} + \text{i}S_{32} = \frac{1}{4}\left(e^{\text{i}(\Omega_3 - \pi J_{13} - \pi J_{23})t_2} + e^{\text{i}(\Omega_3 - \pi J_{13} + \pi J_{23})t_2} + e^{\text{i}(\Omega_3 + \pi J_{13} - \pi J_{23})t_2} + e^{\text{i}(\Omega_3 + \pi J_{13} + \pi J_{23})t_2}\right). \tag{12.79}$$

As the previously discussed two-dimensional experiments, TOCSY is also applied so that a hypercomplex 2D spectrum is obtained. Therefore, acquisition is repeated for each t_1 increment with the phase of the radio wave shifted by $90°$ (y) during the 90° pulse. The original density matrix
$\hat{\rho}(a) = \frac{1}{4}(\mathscr{I}_t + \kappa\mathscr{I}_{1z} + \kappa\mathscr{I}_{2z} + \kappa\mathscr{I}_{3z}) = \frac{1}{4}\mathscr{I}_t + \frac{\kappa}{4}\sum_j\mathscr{I}_{jz}$
is then converted to
$\hat{\rho}(b) = \frac{1}{4}(\mathscr{I}_t + \kappa\mathscr{I}_{1x} + \kappa\mathscr{I}_{2x} + \kappa\mathscr{I}_{3x}) = \frac{1}{4}\mathscr{I}_t + \frac{\kappa}{4}\sum_j\mathscr{I}_{jx}$,
which evolves during t_1 to the $\mathscr{I}_{jy}$ components, selected during the TOCSY mixing, with the following modulation: $\hat{\rho}(c) = \frac{\kappa}{4}\sum_j S_{j1}\mathscr{I}_{jy}$,

where

$$S_{12} = \sin(\Omega_1 t_2)\cos(\pi J_{12}t_2)\cos(\pi J_{13}t_2) = \frac{1}{2}\cos(\Omega_1 t_2)(\cos(\pi J_{12}t_2 - \pi J_{13}t_2) - \cos(\pi J_{12}t_2 + \pi J_{13}t_2))$$

$$= \frac{1}{4}(\sin((\Omega_1 - \pi J_{12} - \pi J_{13})t_2) + \sin((\Omega_1 - \pi J_{12} + \pi J_{13})t_2) + \sin((\Omega_1 + \pi J_{12} - \pi J_{13})t_2) + \sin((\Omega_1 + \pi J_{12} + \pi J_{13})t_2))$$

$$S_{22} = \sin(\Omega_2 t_2)\cos(\pi J_{12}t_2)\cos(\pi J_{23}t_2) = \frac{1}{2}\sin(\Omega_2 t_2)(\cos(\pi J_{12}t_2 - \pi J_{23}t_2) - \cos(\pi J_{12}t_2 + \pi J_{23}t_2))$$

$$= \frac{1}{4}(\sin((\Omega_2 - \pi J_{12} - \pi J_{23})t_2) + \sin((\Omega_2 - \pi J_{12} + \pi J_{23})t_2) + \sin((\Omega_2 + \pi J_{12} - \pi J_{23})t_2) + \sin((\Omega_2 + \pi J_{12} + \pi J_{23})t_2))$$

$$S_{32} = \cos(\Omega_3 t_2)\cos(\pi J_{13}t_2)\cos(\pi J_{23}t_2) = \frac{1}{2}\cos(\Omega_3 t_2)(\cos(\pi J_{13}t_2 - \pi J_{23}t_2) - \cos(\pi J_{13}t_2 + \pi J_{23}t_2))$$

$$= \frac{1}{4}(\sin((\Omega_3 - \pi J_{13} - \pi J_{23})t_2) + \sin((\Omega_3 - \pi J_{13} + \pi J_{23})t_2) + \sin((\Omega_3 + \pi J_{13} - \pi J_{23})t_2) + \sin((\Omega_3 + \pi J_{13} + \pi J_{23})t_2)). \tag{12.80}$$

The $\frac{\kappa}{4}S_{j1}\mathscr{I}_{jy}$ components of the density matrix, converted to $\hat{\rho}(d) = \frac{\kappa}{4}\sum_j\sum_k a_{jk}S_{j1}\mathscr{I}_{ky}$ during the TOCSY mixing period, evolve during t_2 to
$\hat{\rho}(t_2) = -\frac{\kappa}{4}\sum_j\sum_k a_{jk}S_{j1}(C_{k2}\mathscr{I}_{ky} - S_{k2}\mathscr{I}_{kx})$, and

$$\text{Tr}\{\hat{\rho}(t_2)\hat{M}_+\} = \mathcal{N}\gamma\hbar\frac{\kappa}{2}\sum_j\sum_k a_{jk}S_{j1}(\text{i}C_{k2} - S_{k2}) = \text{i}\mathcal{N}\gamma\hbar\frac{\kappa}{2}\sum_j\sum_k a_{jk}S_{j1}(C_{k2} + \text{i}S_{k2}) = \text{i}\mathcal{N}\gamma\hbar\frac{\kappa}{2}\sum_j\sum_k a_{jk}S_{j1}E_{k2}, \tag{12.81}$$

If we introduce relaxation, apply phase correction and perform Fourier transformation in the direct dimension, discard the imaginary component of the signal, multiply Eq. 12.81 by "i" and combine it with Eq. 12.78, introduce relaxation and perform Fourier transformation in the indirect dimension, we obtain a *hypercomplex* signal with the real component

$$\Re\{Y(\omega_1, \omega_2)\} = \mathcal{N}\gamma\hbar\frac{\kappa}{2}\sum_j\sum_k a_{jk}Y_{j1}Y_{k2}, \tag{12.82}$$

---

[6]As discussed in Section 12.4.5, the product operators listed in Tables 12.2–12.5 differ from normalized basis matrices by a factor of $\sqrt{2}$, resulting in the factor of 2 in the traces $\text{Tr}\{\mathscr{I}_{nx}\mathscr{I}_{n+}\}$ and $\text{Tr}\{\mathscr{I}_{ny}\mathscr{I}_{n+}\}$.

where

$$
\begin{aligned}
Y_{nl} = {} & \frac{1}{4}\frac{\overline{R}_2}{\overline{R}_2^2 + (\Omega_n - \pi J_{nn'} - \pi J_{nn''} - \omega_l)^2} + \frac{1}{4}\frac{\overline{R}_2}{\overline{R}_2^2 + (\Omega_n - \pi J_{nn'} + \pi J_{nn''} - \omega_l)^2} \\
& + \frac{1}{4}\frac{\overline{R}_2}{\overline{R}_2^2 + (\Omega_n + \pi J_{nn'} - \pi J_{nn''} - \omega_l)^2} + \frac{1}{4}\frac{\overline{R}_2}{\overline{R}_2^2 + (\Omega_n + \pi J_{nn'} + \pi J_{nn''} - \omega_l)^2}
\end{aligned}
\tag{12.83}
$$

$(n, n', n'' \in \{1, 2, 3\})$.

12.4.9 Cartesian basis matrices for a three-spin system

Explict forms of the Cartesian basis matrices for a three-spin system are presented in Tables 12.2–12.5.

Table 12.2: Cartesian basis for a three-spin system: population operators. Symbols "+" and "−" stand for +1 and −1, respectively. All operators have to be divided by $\sqrt{2}$ to obtain orthonormal matrices.

$\mathscr{I}_t =$

$$\frac{1}{2}\begin{pmatrix} + & 0 & 0 & 0 & 0 & 0 & 0 & 0 \\ 0 & + & 0 & 0 & 0 & 0 & 0 & 0 \\ 0 & 0 & + & 0 & 0 & 0 & 0 & 0 \\ 0 & 0 & 0 & + & 0 & 0 & 0 & 0 \\ 0 & 0 & 0 & 0 & + & 0 & 0 & 0 \\ 0 & 0 & 0 & 0 & 0 & + & 0 & 0 \\ 0 & 0 & 0 & 0 & 0 & 0 & + & 0 \\ 0 & 0 & 0 & 0 & 0 & 0 & 0 & + \end{pmatrix}$$

$\mathscr{I}_{1z} =$

$$\frac{1}{2}\begin{pmatrix} + & 0 & 0 & 0 & 0 & 0 & 0 & 0 \\ 0 & + & 0 & 0 & 0 & 0 & 0 & 0 \\ 0 & 0 & + & 0 & 0 & 0 & 0 & 0 \\ 0 & 0 & 0 & + & 0 & 0 & 0 & 0 \\ 0 & 0 & 0 & 0 & - & 0 & 0 & 0 \\ 0 & 0 & 0 & 0 & 0 & - & 0 & 0 \\ 0 & 0 & 0 & 0 & 0 & 0 & - & 0 \\ 0 & 0 & 0 & 0 & 0 & 0 & 0 & - \end{pmatrix}$$

$\mathscr{I}_{2z} =$

$$\frac{1}{2}\begin{pmatrix} + & 0 & 0 & 0 & 0 & 0 & 0 & 0 \\ 0 & + & 0 & 0 & 0 & 0 & 0 & 0 \\ 0 & 0 & - & 0 & 0 & 0 & 0 & 0 \\ 0 & 0 & 0 & - & 0 & 0 & 0 & 0 \\ 0 & 0 & 0 & 0 & + & 0 & 0 & 0 \\ 0 & 0 & 0 & 0 & 0 & + & 0 & 0 \\ 0 & 0 & 0 & 0 & 0 & 0 & - & 0 \\ 0 & 0 & 0 & 0 & 0 & 0 & 0 & - \end{pmatrix}$$

$\mathscr{I}_{3z} =$

$$\frac{1}{2}\begin{pmatrix} + & 0 & 0 & 0 & 0 & 0 & 0 & 0 \\ 0 & - & 0 & 0 & 0 & 0 & 0 & 0 \\ 0 & 0 & + & 0 & 0 & 0 & 0 & 0 \\ 0 & 0 & 0 & - & 0 & 0 & 0 & 0 \\ 0 & 0 & 0 & 0 & + & 0 & 0 & 0 \\ 0 & 0 & 0 & 0 & 0 & - & 0 & 0 \\ 0 & 0 & 0 & 0 & 0 & 0 & + & 0 \\ 0 & 0 & 0 & 0 & 0 & 0 & 0 & - \end{pmatrix}$$

$2\mathscr{I}_{1z}\mathscr{I}_{2z} =$

$$\frac{1}{2}\begin{pmatrix} + & 0 & 0 & 0 & 0 & 0 & 0 & 0 \\ 0 & + & 0 & 0 & 0 & 0 & 0 & 0 \\ 0 & 0 & - & 0 & 0 & 0 & 0 & 0 \\ 0 & 0 & 0 & - & 0 & 0 & 0 & 0 \\ 0 & 0 & 0 & 0 & - & 0 & 0 & 0 \\ 0 & 0 & 0 & 0 & 0 & - & 0 & 0 \\ 0 & 0 & 0 & 0 & 0 & 0 & + & 0 \\ 0 & 0 & 0 & 0 & 0 & 0 & 0 & + \end{pmatrix}$$

$2\mathscr{I}_{1z}\mathscr{I}_{3z} =$

$$\frac{1}{2}\begin{pmatrix} + & 0 & 0 & 0 & 0 & 0 & 0 & 0 \\ 0 & - & 0 & 0 & 0 & 0 & 0 & 0 \\ 0 & 0 & + & 0 & 0 & 0 & 0 & 0 \\ 0 & 0 & 0 & - & 0 & 0 & 0 & 0 \\ 0 & 0 & 0 & 0 & - & 0 & 0 & 0 \\ 0 & 0 & 0 & 0 & 0 & + & 0 & 0 \\ 0 & 0 & 0 & 0 & 0 & 0 & - & 0 \\ 0 & 0 & 0 & 0 & 0 & 0 & 0 & + \end{pmatrix}$$

$2\mathscr{I}_{2z}\mathscr{I}_{3z} =$

$$\frac{1}{2}\begin{pmatrix} + & 0 & 0 & 0 & 0 & 0 & 0 & 0 \\ 0 & - & 0 & 0 & 0 & 0 & 0 & 0 \\ 0 & 0 & - & 0 & 0 & 0 & 0 & 0 \\ 0 & 0 & 0 & + & 0 & 0 & 0 & 0 \\ 0 & 0 & 0 & 0 & + & 0 & 0 & 0 \\ 0 & 0 & 0 & 0 & 0 & - & 0 & 0 \\ 0 & 0 & 0 & 0 & 0 & 0 & - & 0 \\ 0 & 0 & 0 & 0 & 0 & 0 & 0 & + \end{pmatrix}$$

$4\mathscr{I}_{1z}\mathscr{I}_{2z}\mathscr{I}_{3z} =$

$$\frac{1}{2}\begin{pmatrix} + & 0 & 0 & 0 & 0 & 0 & 0 & 0 \\ 0 & - & 0 & 0 & 0 & 0 & 0 & 0 \\ 0 & 0 & - & 0 & 0 & 0 & 0 & 0 \\ 0 & 0 & 0 & + & 0 & 0 & 0 & 0 \\ 0 & 0 & 0 & 0 & - & 0 & 0 & 0 \\ 0 & 0 & 0 & 0 & 0 & + & 0 & 0 \\ 0 & 0 & 0 & 0 & 0 & 0 & + & 0 \\ 0 & 0 & 0 & 0 & 0 & 0 & 0 & - \end{pmatrix}$$

Table 12.3: Cartesian basis for a three-spin system: single/triple-quantum operators. Symbols "+" and "−" stand for +1 and −1, respectively. All operators have to be divided by $\sqrt{2}$ to obtain orthonormal matrices.

$4\mathscr{I}_{1x}\mathscr{I}_{2x}\mathscr{I}_{3x} =$

$$\frac{1}{2}\begin{pmatrix} 0 & 0 & 0 & 0 & 0 & 0 & 0 & + \\ 0 & 0 & 0 & 0 & 0 & 0 & + & 0 \\ 0 & 0 & 0 & 0 & 0 & + & 0 & 0 \\ 0 & 0 & 0 & 0 & + & 0 & 0 & 0 \\ 0 & 0 & 0 & + & 0 & 0 & 0 & 0 \\ 0 & 0 & + & 0 & 0 & 0 & 0 & 0 \\ 0 & + & 0 & 0 & 0 & 0 & 0 & 0 \\ + & 0 & 0 & 0 & 0 & 0 & 0 & 0 \end{pmatrix}$$

$4\mathscr{I}_{1x}\mathscr{I}_{2y}\mathscr{I}_{3y} =$

$$\frac{1}{2}\begin{pmatrix} 0 & 0 & 0 & 0 & 0 & 0 & 0 & - \\ 0 & 0 & 0 & 0 & 0 & 0 & - & 0 \\ 0 & 0 & 0 & 0 & 0 & + & 0 & 0 \\ 0 & 0 & 0 & 0 & + & 0 & 0 & 0 \\ 0 & 0 & 0 & + & 0 & 0 & 0 & 0 \\ 0 & 0 & + & 0 & 0 & 0 & 0 & 0 \\ 0 & - & 0 & 0 & 0 & 0 & 0 & 0 \\ - & 0 & 0 & 0 & 0 & 0 & 0 & 0 \end{pmatrix}$$

$4\mathscr{I}_{1y}\mathscr{I}_{2x}\mathscr{I}_{3y} =$

$$\frac{1}{2}\begin{pmatrix} 0 & 0 & 0 & 0 & 0 & 0 & 0 & - \\ 0 & 0 & 0 & 0 & 0 & 0 & + & 0 \\ 0 & 0 & 0 & 0 & 0 & - & 0 & 0 \\ 0 & 0 & 0 & 0 & + & 0 & 0 & 0 \\ 0 & 0 & 0 & + & 0 & 0 & 0 & 0 \\ 0 & 0 & - & 0 & 0 & 0 & 0 & 0 \\ 0 & + & 0 & 0 & 0 & 0 & 0 & 0 \\ - & 0 & 0 & 0 & 0 & 0 & 0 & 0 \end{pmatrix}$$

$4\mathscr{I}_{1y}\mathscr{I}_{2y}\mathscr{I}_{3x} =$

$$\frac{1}{2}\begin{pmatrix} 0 & 0 & 0 & 0 & 0 & 0 & 0 & - \\ 0 & 0 & 0 & 0 & 0 & 0 & + & 0 \\ 0 & 0 & 0 & 0 & 0 & + & 0 & 0 \\ 0 & 0 & 0 & 0 & - & 0 & 0 & 0 \\ 0 & 0 & 0 & - & 0 & 0 & 0 & 0 \\ 0 & 0 & + & 0 & 0 & 0 & 0 & 0 \\ 0 & + & 0 & 0 & 0 & 0 & 0 & 0 \\ - & 0 & 0 & 0 & 0 & 0 & 0 & 0 \end{pmatrix}$$

$4\mathscr{I}_{1x}\mathscr{I}_{2x}\mathscr{I}_{3y} =$

$$\frac{1}{2}\begin{pmatrix} 0 & 0 & 0 & 0 & 0 & 0 & 0 & - \\ 0 & 0 & 0 & 0 & 0 & 0 & + & 0 \\ 0 & 0 & 0 & 0 & 0 & - & 0 & 0 \\ 0 & 0 & 0 & 0 & + & 0 & 0 & 0 \\ 0 & 0 & 0 & - & 0 & 0 & 0 & 0 \\ 0 & 0 & + & 0 & 0 & 0 & 0 & 0 \\ 0 & - & 0 & 0 & 0 & 0 & 0 & 0 \\ + & 0 & 0 & 0 & 0 & 0 & 0 & 0 \end{pmatrix}$$

$4\mathscr{I}_{1x}\mathscr{I}_{2y}\mathscr{I}_{3x} =$

$$\frac{1}{2}\begin{pmatrix} 0 & 0 & 0 & 0 & 0 & 0 & 0 & - \\ 0 & 0 & 0 & 0 & 0 & 0 & - & 0 \\ 0 & 0 & 0 & 0 & 0 & + & 0 & 0 \\ 0 & 0 & 0 & 0 & + & 0 & 0 & 0 \\ 0 & 0 & 0 & - & 0 & 0 & 0 & 0 \\ 0 & 0 & - & 0 & 0 & 0 & 0 & 0 \\ 0 & + & 0 & 0 & 0 & 0 & 0 & 0 \\ + & 0 & 0 & 0 & 0 & 0 & 0 & 0 \end{pmatrix}$$

$4\mathscr{I}_{1y}\mathscr{I}_{2x}\mathscr{I}_{3x} =$

$$\frac{1}{2}\begin{pmatrix} 0 & 0 & 0 & 0 & 0 & 0 & 0 & - \\ 0 & 0 & 0 & 0 & 0 & 0 & - & 0 \\ 0 & 0 & 0 & 0 & 0 & - & 0 & 0 \\ 0 & 0 & 0 & 0 & - & 0 & 0 & 0 \\ 0 & 0 & 0 & + & 0 & 0 & 0 & 0 \\ 0 & 0 & + & 0 & 0 & 0 & 0 & 0 \\ 0 & + & 0 & 0 & 0 & 0 & 0 & 0 \\ + & 0 & 0 & 0 & 0 & 0 & 0 & 0 \end{pmatrix}$$

$4\mathscr{I}_{1y}\mathscr{I}_{2y}\mathscr{I}_{3y} =$

$$\frac{1}{2}\begin{pmatrix} 0 & 0 & 0 & 0 & 0 & 0 & 0 & + \\ 0 & 0 & 0 & 0 & 0 & 0 & - & 0 \\ 0 & 0 & 0 & 0 & 0 & - & 0 & 0 \\ 0 & 0 & 0 & 0 & + & 0 & 0 & 0 \\ 0 & 0 & 0 & - & 0 & 0 & 0 & 0 \\ 0 & 0 & + & 0 & 0 & 0 & 0 & 0 \\ 0 & + & 0 & 0 & 0 & 0 & 0 & 0 \\ - & 0 & 0 & 0 & 0 & 0 & 0 & 0 \end{pmatrix}$$

Table 12.4: Cartesian basis for a three-spin system: single-quantum operators. Symbols "+" and "−" stand for +1 and −1, respectively. All operators have to be divided by $\sqrt{2}$ to obtain orthonormal matrices.

$$\mathscr{I}_{1x} = \frac{1}{2}\begin{pmatrix} 0 & 0 & 0 & 0 & + & 0 & 0 & 0 \\ 0 & 0 & 0 & 0 & 0 & + & 0 & 0 \\ 0 & 0 & 0 & 0 & 0 & 0 & + & 0 \\ 0 & 0 & 0 & 0 & 0 & 0 & 0 & + \\ + & 0 & 0 & 0 & 0 & 0 & 0 & 0 \\ 0 & + & 0 & 0 & 0 & 0 & 0 & 0 \\ 0 & 0 & + & 0 & 0 & 0 & 0 & 0 \\ 0 & 0 & 0 & + & 0 & 0 & 0 & 0 \end{pmatrix}$$

$$2\mathscr{I}_{1x}\mathscr{I}_{2z} = \frac{1}{2}\begin{pmatrix} 0 & 0 & 0 & 0 & + & 0 & 0 & 0 \\ 0 & 0 & 0 & 0 & 0 & + & 0 & 0 \\ 0 & 0 & 0 & 0 & 0 & 0 & - & 0 \\ 0 & 0 & 0 & 0 & 0 & 0 & 0 & - \\ + & 0 & 0 & 0 & 0 & 0 & 0 & 0 \\ 0 & + & 0 & 0 & 0 & 0 & 0 & 0 \\ 0 & 0 & - & 0 & 0 & 0 & 0 & 0 \\ 0 & 0 & 0 & - & 0 & 0 & 0 & 0 \end{pmatrix}$$

$$2\mathscr{I}_{1x}\mathscr{I}_{3z} = \frac{1}{2}\begin{pmatrix} 0 & 0 & 0 & 0 & + & 0 & 0 & 0 \\ 0 & 0 & 0 & 0 & 0 & - & 0 & 0 \\ 0 & 0 & 0 & 0 & 0 & 0 & + & 0 \\ 0 & 0 & 0 & 0 & 0 & 0 & 0 & - \\ + & 0 & 0 & 0 & 0 & 0 & 0 & 0 \\ 0 & - & 0 & 0 & 0 & 0 & 0 & 0 \\ 0 & 0 & + & 0 & 0 & 0 & 0 & 0 \\ 0 & 0 & 0 & - & 0 & 0 & 0 & 0 \end{pmatrix}$$

$$4\mathscr{I}_{1x}\mathscr{I}_{2z}\mathscr{I}_{3z} = \frac{1}{2}\begin{pmatrix} 0 & 0 & 0 & 0 & + & 0 & 0 & 0 \\ 0 & 0 & 0 & 0 & 0 & - & 0 & 0 \\ 0 & 0 & 0 & 0 & 0 & 0 & - & 0 \\ 0 & 0 & 0 & 0 & 0 & 0 & 0 & + \\ + & 0 & 0 & 0 & 0 & 0 & 0 & 0 \\ 0 & - & 0 & 0 & 0 & 0 & 0 & 0 \\ 0 & 0 & - & 0 & 0 & 0 & 0 & 0 \\ 0 & 0 & 0 & + & 0 & 0 & 0 & 0 \end{pmatrix}$$

$$\mathscr{I}_{1y} = \frac{i}{2}\begin{pmatrix} 0 & 0 & 0 & 0 & - & 0 & 0 & 0 \\ 0 & 0 & 0 & 0 & 0 & - & 0 & 0 \\ 0 & 0 & 0 & 0 & 0 & 0 & - & 0 \\ 0 & 0 & 0 & 0 & 0 & 0 & 0 & - \\ + & 0 & 0 & 0 & 0 & 0 & 0 & 0 \\ 0 & + & 0 & 0 & 0 & 0 & 0 & 0 \\ 0 & 0 & + & 0 & 0 & 0 & 0 & 0 \\ 0 & 0 & 0 & + & 0 & 0 & 0 & 0 \end{pmatrix}$$

$$2\mathscr{I}_{1y}\mathscr{I}_{2z} = \frac{i}{2}\begin{pmatrix} 0 & 0 & 0 & 0 & - & 0 & 0 & 0 \\ 0 & 0 & 0 & 0 & 0 & - & 0 & 0 \\ 0 & 0 & 0 & 0 & 0 & 0 & + & 0 \\ 0 & 0 & 0 & 0 & 0 & 0 & 0 & + \\ + & 0 & 0 & 0 & 0 & 0 & 0 & 0 \\ 0 & + & 0 & 0 & 0 & 0 & 0 & 0 \\ 0 & 0 & - & 0 & 0 & 0 & 0 & 0 \\ 0 & 0 & 0 & - & 0 & 0 & 0 & 0 \end{pmatrix}$$

$$2\mathscr{I}_{1y}\mathscr{I}_{3z} = \frac{i}{2}\begin{pmatrix} 0 & 0 & 0 & 0 & - & 0 & 0 & 0 \\ 0 & 0 & 0 & 0 & 0 & + & 0 & 0 \\ 0 & 0 & 0 & 0 & 0 & 0 & - & 0 \\ 0 & 0 & 0 & 0 & 0 & 0 & 0 & + \\ + & 0 & 0 & 0 & 0 & 0 & 0 & 0 \\ 0 & - & 0 & 0 & 0 & 0 & 0 & 0 \\ 0 & 0 & + & 0 & 0 & 0 & 0 & 0 \\ 0 & 0 & 0 & - & 0 & 0 & 0 & 0 \end{pmatrix}$$

$$4\mathscr{I}_{1y}\mathscr{I}_{2z}\mathscr{I}_{3z} = \frac{i}{2}\begin{pmatrix} 0 & 0 & 0 & 0 & - & 0 & 0 & 0 \\ 0 & 0 & 0 & 0 & 0 & + & 0 & 0 \\ 0 & 0 & 0 & 0 & 0 & 0 & + & 0 \\ 0 & 0 & 0 & 0 & 0 & 0 & 0 & - \\ + & 0 & 0 & 0 & 0 & 0 & 0 & 0 \\ 0 & - & 0 & 0 & 0 & 0 & 0 & 0 \\ 0 & 0 & - & 0 & 0 & 0 & 0 & 0 \\ 0 & 0 & 0 & + & 0 & 0 & 0 & 0 \end{pmatrix}$$

$$\mathscr{I}_{2x} = \frac{1}{2}\begin{pmatrix} 0 & 0 & + & 0 & 0 & 0 & 0 & 0 \\ 0 & 0 & 0 & + & 0 & 0 & 0 & 0 \\ + & 0 & 0 & 0 & 0 & 0 & 0 & 0 \\ 0 & + & 0 & 0 & 0 & 0 & 0 & 0 \\ 0 & 0 & 0 & 0 & 0 & 0 & + & 0 \\ 0 & 0 & 0 & 0 & 0 & 0 & 0 & + \\ 0 & 0 & 0 & 0 & + & 0 & 0 & 0 \\ 0 & 0 & 0 & 0 & 0 & + & 0 & 0 \end{pmatrix}$$

$$2\mathscr{I}_{1z}\mathscr{I}_{2x} = \frac{1}{2}\begin{pmatrix} 0 & 0 & + & 0 & 0 & 0 & 0 & 0 \\ 0 & 0 & 0 & + & 0 & 0 & 0 & 0 \\ + & 0 & 0 & 0 & 0 & 0 & 0 & 0 \\ 0 & + & 0 & 0 & 0 & 0 & 0 & 0 \\ 0 & 0 & 0 & 0 & 0 & 0 & - & 0 \\ 0 & 0 & 0 & 0 & 0 & 0 & 0 & - \\ 0 & 0 & 0 & 0 & - & 0 & 0 & 0 \\ 0 & 0 & 0 & 0 & 0 & - & 0 & 0 \end{pmatrix}$$

$$2\mathscr{I}_{2x}\mathscr{I}_{3z} = \frac{1}{2}\begin{pmatrix} 0 & 0 & + & 0 & 0 & 0 & 0 & 0 \\ 0 & 0 & 0 & - & 0 & 0 & 0 & 0 \\ + & 0 & 0 & 0 & 0 & 0 & 0 & 0 \\ 0 & - & 0 & 0 & 0 & 0 & 0 & 0 \\ 0 & 0 & 0 & 0 & 0 & 0 & + & 0 \\ 0 & 0 & 0 & 0 & 0 & 0 & 0 & - \\ 0 & 0 & 0 & 0 & + & 0 & 0 & 0 \\ 0 & 0 & 0 & 0 & 0 & - & 0 & 0 \end{pmatrix}$$

$$4\mathscr{I}_{1z}\mathscr{I}_{2x}\mathscr{I}_{3z} = \frac{1}{2}\begin{pmatrix} 0 & 0 & + & 0 & 0 & 0 & 0 & 0 \\ 0 & 0 & 0 & - & 0 & 0 & 0 & 0 \\ + & 0 & 0 & 0 & 0 & 0 & 0 & 0 \\ 0 & - & 0 & 0 & 0 & 0 & 0 & 0 \\ 0 & 0 & 0 & 0 & 0 & 0 & - & 0 \\ 0 & 0 & 0 & 0 & 0 & 0 & 0 & + \\ 0 & 0 & 0 & 0 & - & 0 & 0 & 0 \\ 0 & 0 & 0 & 0 & 0 & + & 0 & 0 \end{pmatrix}$$

$$\mathscr{I}_{2y} = \frac{i}{2}\begin{pmatrix} 0 & 0 & - & 0 & 0 & 0 & 0 & 0 \\ 0 & 0 & 0 & - & 0 & 0 & 0 & 0 \\ + & 0 & 0 & 0 & 0 & 0 & 0 & 0 \\ 0 & + & 0 & 0 & 0 & 0 & 0 & 0 \\ 0 & 0 & 0 & 0 & 0 & 0 & - & 0 \\ 0 & 0 & 0 & 0 & 0 & 0 & 0 & - \\ 0 & 0 & 0 & 0 & + & 0 & 0 & 0 \\ 0 & 0 & 0 & 0 & 0 & + & 0 & 0 \end{pmatrix}$$

$$2\mathscr{I}_{1z}\mathscr{I}_{2y} = \frac{i}{2}\begin{pmatrix} 0 & 0 & - & 0 & 0 & 0 & 0 & 0 \\ 0 & 0 & 0 & - & 0 & 0 & 0 & 0 \\ + & 0 & 0 & 0 & 0 & 0 & 0 & 0 \\ 0 & + & 0 & 0 & 0 & 0 & 0 & 0 \\ 0 & 0 & 0 & 0 & 0 & 0 & + & 0 \\ 0 & 0 & 0 & 0 & 0 & 0 & 0 & + \\ 0 & 0 & 0 & 0 & - & 0 & 0 & 0 \\ 0 & 0 & 0 & 0 & 0 & - & 0 & 0 \end{pmatrix}$$

$$2\mathscr{I}_{2y}\mathscr{I}_{3z} = \frac{i}{2}\begin{pmatrix} 0 & 0 & - & 0 & 0 & 0 & 0 & 0 \\ 0 & 0 & 0 & + & 0 & 0 & 0 & 0 \\ + & 0 & 0 & 0 & 0 & 0 & 0 & 0 \\ 0 & - & 0 & 0 & 0 & 0 & 0 & 0 \\ 0 & 0 & 0 & 0 & 0 & 0 & - & 0 \\ 0 & 0 & 0 & 0 & 0 & 0 & 0 & + \\ 0 & 0 & 0 & 0 & + & 0 & 0 & 0 \\ 0 & 0 & 0 & 0 & 0 & - & 0 & 0 \end{pmatrix}$$

$$4\mathscr{I}_{1z}\mathscr{I}_{2y}\mathscr{I}_{3z} = \frac{i}{2}\begin{pmatrix} 0 & 0 & - & 0 & 0 & 0 & 0 & 0 \\ 0 & 0 & 0 & + & 0 & 0 & 0 & 0 \\ + & 0 & 0 & 0 & 0 & 0 & 0 & 0 \\ 0 & - & 0 & 0 & 0 & 0 & 0 & 0 \\ 0 & 0 & 0 & 0 & 0 & 0 & + & 0 \\ 0 & 0 & 0 & 0 & 0 & 0 & 0 & - \\ 0 & 0 & 0 & 0 & - & 0 & 0 & 0 \\ 0 & 0 & 0 & 0 & 0 & + & 0 & 0 \end{pmatrix}$$

$$\mathscr{I}_{3x} = \frac{1}{2}\begin{pmatrix} 0 & + & 0 & 0 & 0 & 0 & 0 & 0 \\ + & 0 & 0 & 0 & 0 & 0 & 0 & 0 \\ 0 & 0 & 0 & + & 0 & 0 & 0 & 0 \\ 0 & 0 & + & 0 & 0 & 0 & 0 & 0 \\ 0 & 0 & 0 & 0 & 0 & + & 0 & 0 \\ 0 & 0 & 0 & 0 & + & 0 & 0 & 0 \\ 0 & 0 & 0 & 0 & 0 & 0 & 0 & + \\ 0 & 0 & 0 & 0 & 0 & 0 & + & 0 \end{pmatrix}$$

$$2\mathscr{I}_{1z}\mathscr{I}_{3x} = \frac{1}{2}\begin{pmatrix} 0 & + & 0 & 0 & 0 & 0 & 0 & 0 \\ + & 0 & 0 & 0 & 0 & 0 & 0 & 0 \\ 0 & 0 & 0 & + & 0 & 0 & 0 & 0 \\ 0 & 0 & + & 0 & 0 & 0 & 0 & 0 \\ 0 & 0 & 0 & 0 & 0 & - & 0 & 0 \\ 0 & 0 & 0 & 0 & - & 0 & 0 & 0 \\ 0 & 0 & 0 & 0 & 0 & 0 & 0 & - \\ 0 & 0 & 0 & 0 & 0 & 0 & - & 0 \end{pmatrix}$$

$$2\mathscr{I}_{2z}\mathscr{I}_{3x} = \frac{1}{2}\begin{pmatrix} 0 & + & 0 & 0 & 0 & 0 & 0 & 0 \\ + & 0 & 0 & 0 & 0 & 0 & 0 & 0 \\ 0 & 0 & 0 & - & 0 & 0 & 0 & 0 \\ 0 & 0 & - & 0 & 0 & 0 & 0 & 0 \\ 0 & 0 & 0 & 0 & 0 & + & 0 & 0 \\ 0 & 0 & 0 & 0 & + & 0 & 0 & 0 \\ 0 & 0 & 0 & 0 & 0 & 0 & 0 & - \\ 0 & 0 & 0 & 0 & 0 & 0 & - & 0 \end{pmatrix}$$

$$4\mathscr{I}_{1z}\mathscr{I}_{2z}\mathscr{I}_{3x} = \frac{1}{2}\begin{pmatrix} 0 & + & 0 & 0 & 0 & 0 & 0 & 0 \\ + & 0 & 0 & 0 & 0 & 0 & 0 & 0 \\ 0 & 0 & 0 & - & 0 & 0 & 0 & 0 \\ 0 & 0 & - & 0 & 0 & 0 & 0 & 0 \\ 0 & 0 & 0 & 0 & 0 & - & 0 & 0 \\ 0 & 0 & 0 & 0 & - & 0 & 0 & 0 \\ 0 & 0 & 0 & 0 & 0 & 0 & 0 & + \\ 0 & 0 & 0 & 0 & 0 & 0 & + & 0 \end{pmatrix}$$

$$\mathscr{I}_{3y} = \frac{i}{2}\begin{pmatrix} 0 & - & 0 & 0 & 0 & 0 & 0 & 0 \\ + & 0 & 0 & 0 & 0 & 0 & 0 & 0 \\ 0 & 0 & 0 & - & 0 & 0 & 0 & 0 \\ 0 & 0 & + & 0 & 0 & 0 & 0 & 0 \\ 0 & 0 & 0 & 0 & 0 & - & 0 & 0 \\ 0 & 0 & 0 & 0 & + & 0 & 0 & 0 \\ 0 & 0 & 0 & 0 & 0 & 0 & 0 & - \\ 0 & 0 & 0 & 0 & 0 & 0 & + & 0 \end{pmatrix}$$

$$2\mathscr{I}_{1z}\mathscr{I}_{3y} = \frac{i}{2}\begin{pmatrix} 0 & - & 0 & 0 & 0 & 0 & 0 & 0 \\ + & 0 & 0 & 0 & 0 & 0 & 0 & 0 \\ 0 & 0 & 0 & - & 0 & 0 & 0 & 0 \\ 0 & 0 & + & 0 & 0 & 0 & 0 & 0 \\ 0 & 0 & 0 & 0 & 0 & + & 0 & 0 \\ 0 & 0 & 0 & 0 & - & 0 & 0 & 0 \\ 0 & 0 & 0 & 0 & 0 & 0 & 0 & + \\ 0 & 0 & 0 & 0 & 0 & 0 & - & 0 \end{pmatrix}$$

$$2\mathscr{I}_{2z}\mathscr{I}_{3y} = \frac{i}{2}\begin{pmatrix} 0 & - & 0 & 0 & 0 & 0 & 0 & 0 \\ + & 0 & 0 & 0 & 0 & 0 & 0 & 0 \\ 0 & 0 & 0 & + & 0 & 0 & 0 & 0 \\ 0 & 0 & - & 0 & 0 & 0 & 0 & 0 \\ 0 & 0 & 0 & 0 & 0 & - & 0 & 0 \\ 0 & 0 & 0 & 0 & + & 0 & 0 & 0 \\ 0 & 0 & 0 & 0 & 0 & 0 & 0 & + \\ 0 & 0 & 0 & 0 & 0 & 0 & - & 0 \end{pmatrix}$$

$$4\mathscr{I}_{1z}\mathscr{I}_{2z}\mathscr{I}_{3y} = \frac{i}{2}\begin{pmatrix} 0 & - & 0 & 0 & 0 & 0 & 0 & 0 \\ + & 0 & 0 & 0 & 0 & 0 & 0 & 0 \\ 0 & 0 & 0 & + & 0 & 0 & 0 & 0 \\ 0 & 0 & - & 0 & 0 & 0 & 0 & 0 \\ 0 & 0 & 0 & 0 & 0 & + & 0 & 0 \\ 0 & 0 & 0 & 0 & - & 0 & 0 & 0 \\ 0 & 0 & 0 & 0 & 0 & 0 & 0 & - \\ 0 & 0 & 0 & 0 & 0 & 0 & + & 0 \end{pmatrix}$$

Table 12.5: Cartesian basis for a three-spin system: zero/double-quantum operators. Symbols "+" and "−" stand for +1 and −1, respectively. All operators have to be divided by $\sqrt{2}$ to obtain orthonormal matrices.

$2\mathscr{I}_{1x}\mathscr{I}_{2x} =$

$$\frac{1}{2}\begin{pmatrix} 0 & 0 & 0 & 0 & 0 & 0 & + & 0 \\ 0 & 0 & 0 & 0 & 0 & 0 & 0 & + \\ 0 & 0 & 0 & 0 & + & 0 & 0 & 0 \\ 0 & 0 & 0 & 0 & 0 & + & 0 & 0 \\ 0 & 0 & + & 0 & 0 & 0 & 0 & 0 \\ 0 & 0 & 0 & + & 0 & 0 & 0 & 0 \\ + & 0 & 0 & 0 & 0 & 0 & 0 & 0 \\ 0 & + & 0 & 0 & 0 & 0 & 0 & 0 \end{pmatrix}$$

$2\mathscr{I}_{1y}\mathscr{I}_{2y} =$

$$\frac{1}{2}\begin{pmatrix} 0 & 0 & 0 & 0 & 0 & 0 & - & 0 \\ 0 & 0 & 0 & 0 & 0 & 0 & 0 & - \\ 0 & 0 & 0 & 0 & + & 0 & 0 & 0 \\ 0 & 0 & 0 & 0 & 0 & + & 0 & 0 \\ 0 & 0 & + & 0 & 0 & 0 & 0 & 0 \\ 0 & 0 & 0 & + & 0 & 0 & 0 & 0 \\ - & 0 & 0 & 0 & 0 & 0 & 0 & 0 \\ 0 & - & 0 & 0 & 0 & 0 & 0 & 0 \end{pmatrix}$$

$4\mathscr{I}_{1x}\mathscr{I}_{2x}\mathscr{I}_{3z} =$

$$\frac{1}{2}\begin{pmatrix} 0 & 0 & 0 & 0 & 0 & 0 & + & 0 \\ 0 & 0 & 0 & 0 & 0 & 0 & 0 & - \\ 0 & 0 & 0 & 0 & + & 0 & 0 & 0 \\ 0 & 0 & 0 & 0 & 0 & - & 0 & 0 \\ 0 & 0 & + & 0 & 0 & 0 & 0 & 0 \\ 0 & 0 & 0 & - & 0 & 0 & 0 & 0 \\ + & 0 & 0 & 0 & 0 & 0 & 0 & 0 \\ 0 & - & 0 & 0 & 0 & 0 & 0 & 0 \end{pmatrix}$$

$4\mathscr{I}_{1y}\mathscr{I}_{2y}\mathscr{I}_{3z} =$

$$\frac{1}{2}\begin{pmatrix} 0 & 0 & 0 & 0 & 0 & 0 & - & 0 \\ 0 & 0 & 0 & 0 & 0 & 0 & 0 & + \\ 0 & 0 & 0 & 0 & + & 0 & 0 & 0 \\ 0 & 0 & 0 & 0 & 0 & - & 0 & 0 \\ 0 & 0 & + & 0 & 0 & 0 & 0 & 0 \\ 0 & 0 & 0 & - & 0 & 0 & 0 & 0 \\ - & 0 & 0 & 0 & 0 & 0 & 0 & 0 \\ 0 & + & 0 & 0 & 0 & 0 & 0 & 0 \end{pmatrix}$$

$2\mathscr{I}_{1x}\mathscr{I}_{3x} =$

$$\frac{1}{2}\begin{pmatrix} 0 & 0 & 0 & 0 & 0 & + & 0 & 0 \\ 0 & 0 & 0 & 0 & + & 0 & 0 & 0 \\ 0 & 0 & 0 & 0 & 0 & 0 & 0 & + \\ 0 & 0 & 0 & 0 & 0 & 0 & + & 0 \\ 0 & + & 0 & 0 & 0 & 0 & 0 & 0 \\ + & 0 & 0 & 0 & 0 & 0 & 0 & 0 \\ 0 & 0 & 0 & + & 0 & 0 & 0 & 0 \\ 0 & 0 & + & 0 & 0 & 0 & 0 & 0 \end{pmatrix}$$

$2\mathscr{I}_{1y}\mathscr{I}_{3y} =$

$$\frac{1}{2}\begin{pmatrix} 0 & 0 & 0 & 0 & 0 & - & 0 & 0 \\ 0 & 0 & 0 & 0 & + & 0 & 0 & 0 \\ 0 & 0 & 0 & 0 & 0 & 0 & 0 & - \\ 0 & 0 & 0 & 0 & 0 & 0 & + & 0 \\ 0 & + & 0 & 0 & 0 & 0 & 0 & 0 \\ - & 0 & 0 & 0 & 0 & 0 & 0 & 0 \\ 0 & 0 & 0 & + & 0 & 0 & 0 & 0 \\ 0 & 0 & - & 0 & 0 & 0 & 0 & 0 \end{pmatrix}$$

$4\mathscr{I}_{1x}\mathscr{I}_{2z}\mathscr{I}_{3x} =$

$$\frac{1}{2}\begin{pmatrix} 0 & 0 & 0 & 0 & 0 & + & 0 & 0 \\ 0 & 0 & 0 & 0 & + & 0 & 0 & 0 \\ 0 & 0 & 0 & 0 & 0 & 0 & 0 & - \\ 0 & 0 & 0 & 0 & 0 & 0 & - & 0 \\ 0 & + & 0 & 0 & 0 & 0 & 0 & 0 \\ + & 0 & 0 & 0 & 0 & 0 & 0 & 0 \\ 0 & 0 & 0 & - & 0 & 0 & 0 & 0 \\ 0 & 0 & - & 0 & 0 & 0 & 0 & 0 \end{pmatrix}$$

$4\mathscr{I}_{1y}\mathscr{I}_{2z}\mathscr{I}_{3y} =$

$$\frac{1}{2}\begin{pmatrix} 0 & 0 & 0 & 0 & 0 & - & 0 & 0 \\ 0 & 0 & 0 & 0 & + & 0 & 0 & 0 \\ 0 & 0 & 0 & 0 & 0 & 0 & 0 & + \\ 0 & 0 & 0 & 0 & 0 & 0 & - & 0 \\ 0 & + & 0 & 0 & 0 & 0 & 0 & 0 \\ - & 0 & 0 & 0 & 0 & 0 & 0 & 0 \\ 0 & 0 & 0 & - & 0 & 0 & 0 & 0 \\ 0 & 0 & + & 0 & 0 & 0 & 0 & 0 \end{pmatrix}$$

$2\mathscr{I}_{2x}\mathscr{I}_{3x} =$

$$\frac{1}{2}\begin{pmatrix} 0 & 0 & 0 & + & 0 & 0 & 0 & 0 \\ 0 & 0 & + & 0 & 0 & 0 & 0 & 0 \\ 0 & + & 0 & 0 & 0 & 0 & 0 & 0 \\ + & 0 & 0 & 0 & 0 & 0 & 0 & 0 \\ 0 & 0 & 0 & 0 & 0 & 0 & 0 & + \\ 0 & 0 & 0 & 0 & 0 & 0 & + & 0 \\ 0 & 0 & 0 & 0 & 0 & + & 0 & 0 \\ 0 & 0 & 0 & 0 & + & 0 & 0 & 0 \end{pmatrix}$$

$2\mathscr{I}_{2y}\mathscr{I}_{3y} =$

$$\frac{1}{2}\begin{pmatrix} 0 & 0 & 0 & - & 0 & 0 & 0 & 0 \\ 0 & 0 & + & 0 & 0 & 0 & 0 & 0 \\ 0 & + & 0 & 0 & 0 & 0 & 0 & 0 \\ - & 0 & 0 & 0 & 0 & 0 & 0 & 0 \\ 0 & 0 & 0 & 0 & 0 & 0 & 0 & - \\ 0 & 0 & 0 & 0 & 0 & 0 & + & 0 \\ 0 & 0 & 0 & 0 & 0 & + & 0 & 0 \\ 0 & 0 & 0 & 0 & - & 0 & 0 & 0 \end{pmatrix}$$

$4\mathscr{I}_{1z}\mathscr{I}_{2x}\mathscr{I}_{3x} =$

$$\frac{1}{2}\begin{pmatrix} 0 & 0 & 0 & + & 0 & 0 & 0 & 0 \\ 0 & 0 & + & 0 & 0 & 0 & 0 & 0 \\ 0 & + & 0 & 0 & 0 & 0 & 0 & 0 \\ + & 0 & 0 & 0 & 0 & 0 & 0 & 0 \\ 0 & 0 & 0 & 0 & 0 & 0 & 0 & - \\ 0 & 0 & 0 & 0 & 0 & 0 & - & 0 \\ 0 & 0 & 0 & 0 & 0 & - & 0 & 0 \\ 0 & 0 & 0 & 0 & - & 0 & 0 & 0 \end{pmatrix}$$

$4\mathscr{I}_{1z}\mathscr{I}_{2y}\mathscr{I}_{3y} =$

$$\frac{1}{2}\begin{pmatrix} 0 & 0 & 0 & - & 0 & 0 & 0 & 0 \\ 0 & 0 & + & 0 & 0 & 0 & 0 & 0 \\ 0 & + & 0 & 0 & 0 & 0 & 0 & 0 \\ - & 0 & 0 & 0 & 0 & 0 & 0 & 0 \\ 0 & 0 & 0 & 0 & 0 & 0 & 0 & + \\ 0 & 0 & 0 & 0 & 0 & 0 & - & 0 \\ 0 & 0 & 0 & 0 & 0 & - & 0 & 0 \\ 0 & 0 & 0 & 0 & + & 0 & 0 & 0 \end{pmatrix}$$

$2\mathscr{I}_{1x}\mathscr{I}_{2y} =$

$$\frac{i}{2}\begin{pmatrix} 0 & 0 & 0 & 0 & 0 & 0 & - & 0 \\ 0 & 0 & 0 & 0 & 0 & 0 & 0 & - \\ 0 & 0 & 0 & 0 & + & 0 & 0 & 0 \\ 0 & 0 & 0 & 0 & 0 & + & 0 & 0 \\ 0 & 0 & - & 0 & 0 & 0 & 0 & 0 \\ 0 & 0 & 0 & - & 0 & 0 & 0 & 0 \\ + & 0 & 0 & 0 & 0 & 0 & 0 & 0 \\ 0 & + & 0 & 0 & 0 & 0 & 0 & 0 \end{pmatrix}$$

$2\mathscr{I}_{1y}\mathscr{I}_{2x} =$

$$\frac{i}{2}\begin{pmatrix} 0 & 0 & 0 & 0 & 0 & 0 & - & 0 \\ 0 & 0 & 0 & 0 & 0 & 0 & 0 & - \\ 0 & 0 & 0 & 0 & - & 0 & 0 & 0 \\ 0 & 0 & 0 & 0 & 0 & - & 0 & 0 \\ 0 & 0 & + & 0 & 0 & 0 & 0 & 0 \\ 0 & 0 & 0 & + & 0 & 0 & 0 & 0 \\ + & 0 & 0 & 0 & 0 & 0 & 0 & 0 \\ 0 & + & 0 & 0 & 0 & 0 & 0 & 0 \end{pmatrix}$$

$4\mathscr{I}_{1x}\mathscr{I}_{2y}\mathscr{I}_{3z} =$

$$\frac{i}{2}\begin{pmatrix} 0 & 0 & 0 & 0 & 0 & 0 & - & 0 \\ 0 & 0 & 0 & 0 & 0 & 0 & 0 & + \\ 0 & 0 & 0 & 0 & + & 0 & 0 & 0 \\ 0 & 0 & 0 & 0 & 0 & - & 0 & 0 \\ 0 & 0 & - & 0 & 0 & 0 & 0 & 0 \\ 0 & 0 & 0 & + & 0 & 0 & 0 & 0 \\ + & 0 & 0 & 0 & 0 & 0 & 0 & 0 \\ 0 & - & 0 & 0 & 0 & 0 & 0 & 0 \end{pmatrix}$$

$4\mathscr{I}_{1y}\mathscr{I}_{2x}\mathscr{I}_{3z} =$

$$\frac{i}{2}\begin{pmatrix} 0 & 0 & 0 & 0 & 0 & 0 & - & 0 \\ 0 & 0 & 0 & 0 & 0 & 0 & 0 & + \\ 0 & 0 & 0 & 0 & - & 0 & 0 & 0 \\ 0 & 0 & 0 & 0 & 0 & + & 0 & 0 \\ 0 & 0 & + & 0 & 0 & 0 & 0 & 0 \\ 0 & 0 & 0 & - & 0 & 0 & 0 & 0 \\ + & 0 & 0 & 0 & 0 & 0 & 0 & 0 \\ 0 & - & 0 & 0 & 0 & 0 & 0 & 0 \end{pmatrix}$$

$2\mathscr{I}_{1x}\mathscr{I}_{3y} =$

$$\frac{i}{2}\begin{pmatrix} 0 & 0 & 0 & 0 & 0 & - & 0 & 0 \\ 0 & 0 & 0 & 0 & + & 0 & 0 & 0 \\ 0 & 0 & 0 & 0 & 0 & 0 & 0 & - \\ 0 & 0 & 0 & 0 & 0 & 0 & + & 0 \\ 0 & - & 0 & 0 & 0 & 0 & 0 & 0 \\ + & 0 & 0 & 0 & 0 & 0 & 0 & 0 \\ 0 & 0 & 0 & - & 0 & 0 & 0 & 0 \\ 0 & 0 & + & 0 & 0 & 0 & 0 & 0 \end{pmatrix}$$

$2\mathscr{I}_{1y}\mathscr{I}_{3x} =$

$$\frac{i}{2}\begin{pmatrix} 0 & 0 & 0 & 0 & 0 & - & 0 & 0 \\ 0 & 0 & 0 & 0 & - & 0 & 0 & 0 \\ 0 & 0 & 0 & 0 & 0 & 0 & 0 & - \\ 0 & 0 & 0 & 0 & 0 & 0 & - & 0 \\ 0 & + & 0 & 0 & 0 & 0 & 0 & 0 \\ + & 0 & 0 & 0 & 0 & 0 & 0 & 0 \\ 0 & 0 & 0 & + & 0 & 0 & 0 & 0 \\ 0 & 0 & + & 0 & 0 & 0 & 0 & 0 \end{pmatrix}$$

$4\mathscr{I}_{1x}\mathscr{I}_{2z}\mathscr{I}_{3y} =$

$$\frac{i}{2}\begin{pmatrix} 0 & 0 & 0 & 0 & 0 & - & 0 & 0 \\ 0 & 0 & 0 & 0 & + & 0 & 0 & 0 \\ 0 & 0 & 0 & 0 & 0 & 0 & 0 & + \\ 0 & 0 & 0 & 0 & 0 & 0 & - & 0 \\ 0 & - & 0 & 0 & 0 & 0 & 0 & 0 \\ + & 0 & 0 & 0 & 0 & 0 & 0 & 0 \\ 0 & 0 & 0 & + & 0 & 0 & 0 & 0 \\ 0 & 0 & - & 0 & 0 & 0 & 0 & 0 \end{pmatrix}$$

$4\mathscr{I}_{1y}\mathscr{I}_{2z}\mathscr{I}_{3x} =$

$$\frac{i}{2}\begin{pmatrix} 0 & 0 & 0 & 0 & 0 & - & 0 & 0 \\ 0 & 0 & 0 & 0 & - & 0 & 0 & 0 \\ 0 & 0 & 0 & 0 & 0 & 0 & 0 & + \\ 0 & 0 & 0 & 0 & 0 & 0 & + & 0 \\ 0 & + & 0 & 0 & 0 & 0 & 0 & 0 \\ + & 0 & 0 & 0 & 0 & 0 & 0 & 0 \\ 0 & 0 & 0 & - & 0 & 0 & 0 & 0 \\ 0 & 0 & - & 0 & 0 & 0 & 0 & 0 \end{pmatrix}$$

$2\mathscr{I}_{2x}\mathscr{I}_{3y} =$

$$\frac{i}{2}\begin{pmatrix} 0 & 0 & 0 & - & 0 & 0 & 0 & 0 \\ 0 & 0 & + & 0 & 0 & 0 & 0 & 0 \\ 0 & - & 0 & 0 & 0 & 0 & 0 & 0 \\ + & 0 & 0 & 0 & 0 & 0 & 0 & 0 \\ 0 & 0 & 0 & 0 & 0 & 0 & 0 & - \\ 0 & 0 & 0 & 0 & 0 & 0 & + & 0 \\ 0 & 0 & 0 & 0 & 0 & - & 0 & 0 \\ 0 & 0 & 0 & 0 & + & 0 & 0 & 0 \end{pmatrix}$$

$2\mathscr{I}_{2y}\mathscr{I}_{3x} =$

$$\frac{i}{2}\begin{pmatrix} 0 & 0 & 0 & - & 0 & 0 & 0 & 0 \\ 0 & 0 & - & 0 & 0 & 0 & 0 & 0 \\ 0 & + & 0 & 0 & 0 & 0 & 0 & 0 \\ + & 0 & 0 & 0 & 0 & 0 & 0 & 0 \\ 0 & 0 & 0 & 0 & 0 & 0 & 0 & - \\ 0 & 0 & 0 & 0 & 0 & 0 & - & 0 \\ 0 & 0 & 0 & 0 & 0 & + & 0 & 0 \\ 0 & 0 & 0 & 0 & + & 0 & 0 & 0 \end{pmatrix}$$

$4\mathscr{I}_{1z}\mathscr{I}_{2x}\mathscr{I}_{3y} =$

$$\frac{i}{2}\begin{pmatrix} 0 & 0 & 0 & - & 0 & 0 & 0 & 0 \\ 0 & 0 & 0 & 0 & 0 & 0 & 0 & 0 \\ 0 & - & 0 & 0 & 0 & 0 & 0 & 0 \\ 0 & 0 & 0 & 0 & 0 & 0 & 0 & 0 \\ 0 & 0 & 0 & 0 & 0 & 0 & 0 & 0 \\ 0 & 0 & 0 & 0 & 0 & 0 & - & 0 \\ 0 & 0 & 0 & 0 & 0 & 0 & 0 & 0 \\ 0 & 0 & 0 & 0 & - & 0 & 0 & 0 \end{pmatrix}$$

$4\mathscr{I}_{1z}\mathscr{I}_{2y}\mathscr{I}_{3x} =$

$$\frac{i}{2}\begin{pmatrix} 0 & 0 & 0 & - & 0 & 0 & 0 & 0 \\ 0 & 0 & - & 0 & 0 & 0 & 0 & 0 \\ 0 & + & 0 & 0 & 0 & 0 & 0 & 0 \\ + & 0 & 0 & 0 & 0 & 0 & 0 & 0 \\ 0 & 0 & 0 & 0 & 0 & 0 & 0 & + \\ 0 & 0 & 0 & 0 & 0 & 0 & + & 0 \\ 0 & 0 & 0 & 0 & 0 & - & 0 & 0 \\ 0 & 0 & 0 & 0 & - & 0 & 0 & 0 \end{pmatrix}$$

Lecture 13
Magnetic field gradients

Literature: The use of magnetic field gradients in the NMR spectroscopy is nicely reviewed in K11 (in particular, K11.11–11.14, presented more systematically and in more detail than here) and also presented in L4.7 and L12.4 (with detailed analysis in LA12), C4.3.3., and B19.5. The magnetic resonance imaging is discussed in B22, the basic ideas of slice selection and frequency encoding are also described in L12.5. A very nice introduction has been written by Lars G. Hanson (currently available at http://www.drcmr.dk/).

13.1   Pulsed field gradients in NMR spectroscopy

Resonance frequencies of nuclei depend on the external magnetic field and on properties of the molecule (inherent properties of nuclei and interactions of nuclei with their microscopic environment). The external magnetic field is what we control and the molecular properties is what we study. We try to keep the external magnetic field as homogeneous as possible so that all nuclei feel the same external field $\vec{B}_0$ and their frequencies are modulated by their molecular environment only. Now we learn a trick of the spin alchemy which is based on violating this paradigm. It is possible to create a magnetic field that is inhomogeneous in a controlled way. We will discuss an example when the field is linearly increasing along the z axis (Figure 13.1 left, Sections 13.4.1 and 13.4.2). A *linear gradient of magnetic field* (or simply "a gradient" in the NMR jargon) is applied in the z direction. The nuclei close to the bottom of the sample tube feel a weaker magnetic field and have a lower precession frequency, whereas the nuclei close to the top feel a stronger field and have a higher precession frequency in such case. If we label the gradient in the z direction $\partial B_0/\partial z = G_z$, the frequency offset Ω' at different at different positions is given by

$$\Omega'(z) = \Omega - \gamma G_z z. \tag{13.1}$$

We can say that *the frequency carries information about the position along the z axis.*

If the gradient in the z direction is applied when the total magnetization vector rotates in the xy plane, nuclei at different height of the sample acquire different frequencies of the magnetic moment precession (an analysis of the density matrix evolution is presented in Section 13.4.1). In the individual slices, the coherence is preserved. But after a while, vectors of the local transverse polarization (magnetization) rotating at different frequencies in different slices of the sample would point to all possible directions and they would no longer add up to a measurable total magnetization. We
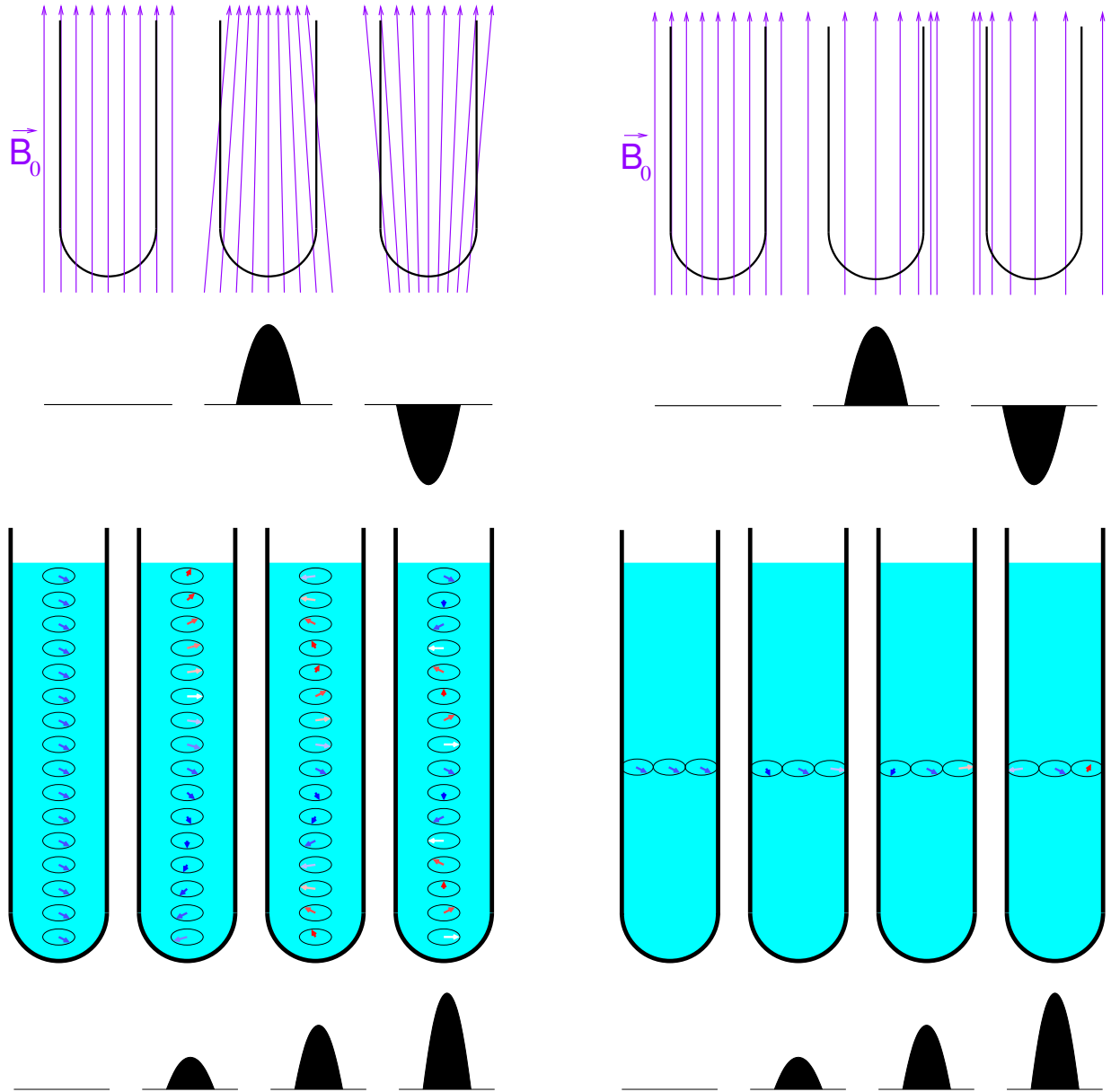
Figure 13.1: Magnetic field gradients in the vertical (z, left) and horizontal (y, right) directions. Top, magnetic induction lines and the corresponding schematic drawings of the gradients (used to present the gradients in pulse sequence diagrams) are shown in purple and black, respectively. Bottom, local transverse polarizations (magnetization) at different positions in the sample tube for increasing gradients (indicated by the black schematic drawings below the sample tubes). The arrows representing the transverse polarizations (magnetization) vectors are color-coded so that blue corresponds to M_x, red corresponds to $-M_x$, and white corresponds to $\pm M_y$. The round shape of the gradient symbols indicates that the gradients were applied with smoothly changing amplitudes as discussed in Section 13.4.2.

can say (i) that the gradient allows us to distinguish magnetic moments in different slices, or (ii) that the gradient destroys the bulk (net) *transverse* magnetization. The longitudinal polarizations are not influenced. We postpone the discussion of the first point of view (selectivity introduced by the gradient) to Section 13.2 and now explore the consequences of the loss of the net transverse magnetization.

At the first glance, it seems that dephasing of coherences and the consequent loss of the signal are completely useless and should be avoided in NMR experiments. It is not true, gradients are very useful if they are applied correctly. The first trick is to apply gradients that destroy coherences we are not interested in. Such gradients have *cleaning* effects and remove unwanted contributions from the spectra.

Another trick is to recover the magnetization back. If we apply the same gradient for the same time, but in the opposite direction $(-z)$ later in the pulse sequence, the magnetic vectors are refocused and the signal appears again. We see how an *echo* can be created from two opposite gradients. There are also other ways of creating gradient echoes, presented in Figure 13.2. Instead of using two opposite gradients, two identical gradients can be applied during the refocusing echo (described in Section 10.7), one in the first half of the echo and the other one in the other half (the left echo in Figure 13.2). The gradients do nothing else but adding another source of frequency variation, on the top of the chemical shift and *J*-coupling effects. Magnetic moments of the nuclei affected by the 180° pulse in the middle of the echo get always refocused, no matter what was the origin of the frequency variability. On the other hand, magnetic moments of nuclei not affected by the 180° pulse (e.g., ^{13}C or ^{15}N nuclei if radio waves are applied at the proton frequency) feel two identical gradients and get dephased. We see the selective cleaning effect of the gradient echo, e.g. preserving the $\mathscr{I}_y$ and $2\mathscr{I}_x\mathscr{S}_z$ coherences but destroying unwanted $\mathscr{S}_x$ and $\mathscr{S}_y$ coherences. Gradients incorporated into the decoupling echo (described in Section 10.8) have exactly the opposite effect (the right echo in Figure 13.2). In this spirit, gradients are frequently added to the echoes in the pulse sequence to clean imperfections of the used pulses.

An application of a cleaning gradient and of gradient echoes in a real NMR experiment is presented in Figure 13.3 (magenta and cyan symbols, respectively). Note that the cleaning (magenta) gradient is applied when no coherence (transverse polarization) should contribute to the density matrix ($\hat{\rho}(\mathrm{d}) = \mathscr{I}_t - \frac{\kappa_1}{2}2\mathscr{I}_z\mathscr{S}_z$, cf. the magnetic moment distribution at "d" in Figure 13.3). The cyan gradients are applied during the simultaneous echoes and refocus coherences that evolve due to the *J*-coupling.

Figure 13.3 also shows another, more tricky use of gradients implemented in an improved version of the HSQC experiment (green and blue/red symbols). The idea is to apply one gradient during the time when the desired coherence rotates in the operator space (and the corresponding transverse polarization rotates in the real space) with the frequency of ^{13}C (or ^{15}N) and the other gradient during the time when the total magnetization rotates with the frequency of protons. In order to do it, we must generate a space in the pulse sequence by including a refocusing echo (a typical example of using refocusing echoes in situation when we need more space but do not want to change the evolution). The two applied gradients are not identical, they change the magnetic fields to a different extent. The deviations of the field must be exactly in the ratio of resonance frequencies of ^{13}C and ^{1}H. Then, the gradients form a *heteronuclear gradient echo*. Note what happens to various coherences of protons. The coherence which contributed to the polarization transfer to ^{13}C and back experiences the gradients as an echo and gets refocused. On the other hand, population of protons
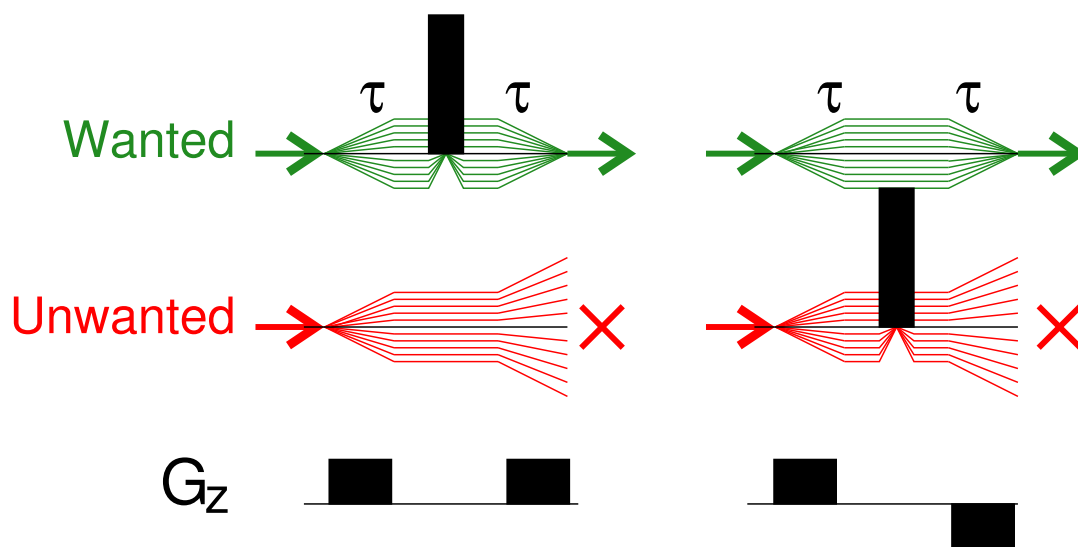
Figure 13.2: Gradient echoes. The black rectangles at the lines labeled "Wanted" and "Unwanted" indicate pluses of radio waves. The black rectangles at the lines labeled G_z indicate magnetic field gradients. Evolution of the phase of the desired and undesired transverse coherence (describing direction of the corresponding transverse polarization) is shown as green and red lines, respectively. Values of the phase at different positions in the sample tubes correspond to the distances of the green and red lines from the central black line.

whose polarization was not transferred to ^{13}C (e.g. protons of water that are not ^{13}C-bonded) feels just two gradients of different strengths and its coherence is destroyed. The gradient echo makes the experiment selective for protons correlated with carbons and suppresses the signal of uncorrelated protons.

13.2 Magnetic resonance imaging

We now explore the selectivity of gradients, mentioned in Section 13.1. During a field gradient in the z direction, the actual precession frequency depends on the position of the molecule along the z axis. This relationship can be used to selectively acquire NMR signal only from molecules in a certain slice perpendicular to the z axis. As discussed in Section 13.4.5, the pulse sequence presented in the right panel of Figure 13.4 allows us to detect the transverse magnetization in an axial slice (perpendicular to z) of a given thickness (the signal is detected from the whole slice but not from outside the slice). The gradient can be also applied in the x and y directions (right part of Figure 13.1). It is therefore possible to select signal in sagittal, coronal, and axial slices of a human body as shown in Figure 13.5.

Gradients also allow us to investigate variations of the local magnetization inside the selected slice. One possibility, called *frequency encoding* and presented in Figure 13.6, is to apply a gradient during the signal acquisition and to convert the frequency of the Fourier-transformed spectrum to the position information. In order to understand the principle, we recall that the direction of the transverse magnetization is described by a phase ϕ having an initial value ϕ_0 and increasing in time as
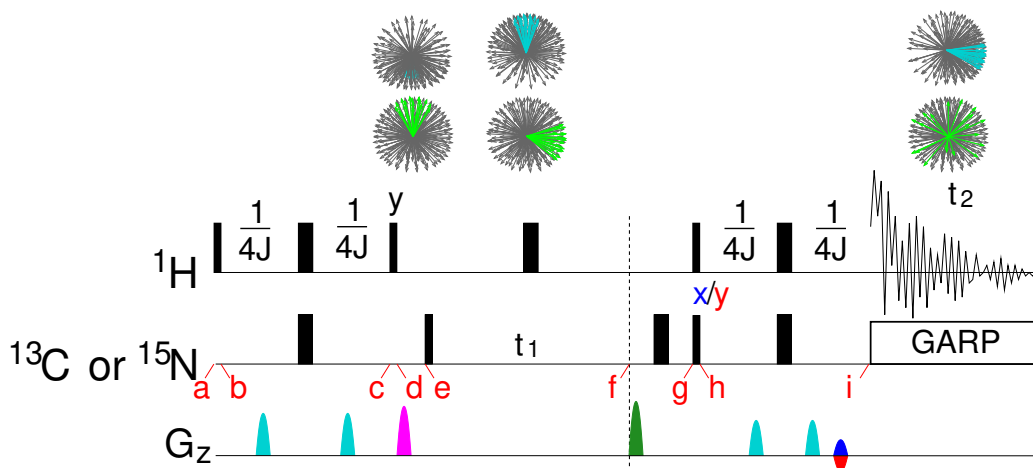
Figure 13.3: Gradient enhanced HSQC experiment. Cleaning gradients and gradient echoes are shown in magenta and cyan, respectively. The heteronuclear gradient echo consists of a gradient shown in green, applied during the refocusing echo between time instants "f" and "g" (when density matrix evolves with the ^{13}C or ^{15}N frequency), and of another gradient applied during the last echo (when density matrix evolves with the proton frequency). The latter gradient is shown in blue for recording the real component of hypercomplex data and in red for recording the imaginary component.
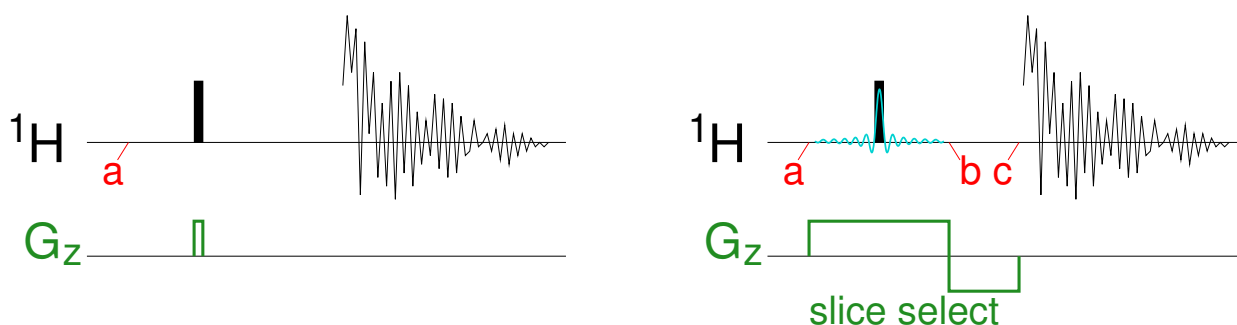
Figure 13.4: Slice selection pulse sequence: the basic idea (left) and real application (right). Gradients of B_0 in the z direction are shown in green. The 90° radio wave pulses are shown schematically as filled black rectangles, the actual modulation of the radio-wave amplitude is depicted in cyan.
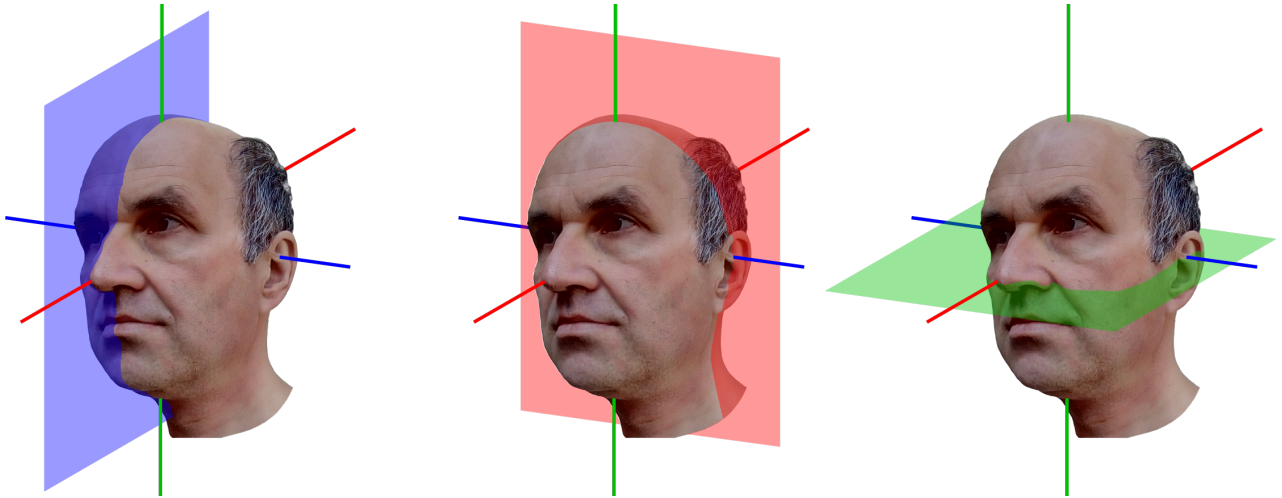
Figure 13.5: Selection of sagittal, coronal, and axial slices by G_x, G_y, and G_z gradients, respectively.

$$\phi(t) = \phi_0 + \Omega't = \phi_0 + (\Omega - \gamma G_x x)t. \tag{13.2}$$

We measure the magnetization in discrete time intervals separated by the time step Δt

$$\phi(t) = \phi_0 + (\Omega - \gamma G_x x)n\Delta t. \tag{13.3}$$

In the standard NMR experiment, no gradient is applied during the signal acquisition ($G_x = 0$). The Fourier transformation then converts the signal varying in time (with the phase growing as $\Omega n\Delta t$) to a spectrum describing how the signal depends on the frequency ω, which is a quantity *reciprocal* to time ($\omega = 2\pi/t$).

In the frequency encoding imaging, we work on resonance ($\Omega = 0$) and typically set ϕ_0 to a convenient value. The signal varies in time as $-\gamma G_x x n\Delta t$. However, we are not interested in how signal changes in time but in its variation in space. Therefore, we can rearrange $(-\gamma G_x x)t$ to $x(-\gamma G_x t) = x k_x$, where k_x has the same meaning as the x component of the wave vector describing the propagation of waves in space. We can treat the measured signal as a set of intensities acquired for a series of incremented values k_x (with the step $\Delta k_x = -\gamma G_x \Delta t$). Therefore, we can write

$$\phi(k_x) = \phi_0 + xn\Delta k_x \tag{13.4}$$

and apply the Fourier transformation to convert the dependence on k_x to the dependence on x, which is a quantity reciprocal to k_x ($x = 2\pi/k_x$). More details are presented in see Section 13.4.6.

Another option, called *phase encoding* and presented in Figure 13.7, is to vary the strength of a gradient applied for a constant time τ_x. In this case, the phase can be still described by Eq. 13.4, but the incrementation step is given by $\Delta k_x = -\gamma \Delta G_x \tau_x$. If we combine the frequency encoding using the gradient G_x with the phase encoding using the gradient G_y, as depicted in the left panel of Figure 13.7, we can image signal variation in the whole selected two-dimensional slice (see Section 13.4.7 for details).
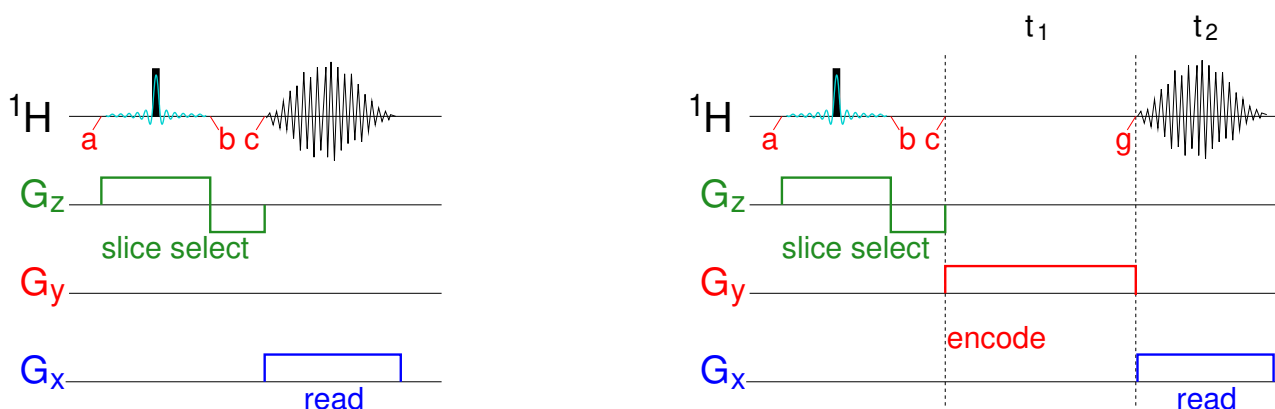
Figure 13.6: Pulse sequences allowing frequency encoded 1D (left) and 2D (right) imaging in the selected slice. Gradients of B_0 in the x, y, and z direction are shown in blue, red, and green, respectively. The 90° radio wave pulses are shown schematically as filled black rectangles, the actual modulation of the radio-wave amplitude is depicted in cyan.

The *slice-selective* imaging techniques, discussed above, have one disadvantage. It is difficult to select a very thin slice. Therefore, the imaging has limited resolution in one dimension. An alternative approach exists that is not restricted in this sense. It is possible to apply gradient encoding to all three dimensions. An example of such a pulse sequence is shown in the right panel in Figure 13.7. However, such a high-resolution 3D imaging is considerably more time consuming. To save time, shorter that 90° pulses are often applied. Such short pulses leave a large portion of the magnetization in the z direction. Therefore, a next short pulse, generating some transverse polarization can be applied immediately after the signal acquisition without the need to wait for the return to the equilibrium. In this fashion, several acquisitions may be performed in one T_R period before the longitudinal magnetization is completely "consumed". This significantly reduces the measurement time.

Reconstruction of the two-dimensional image from frequency- and phase-encoded data can be described in the same manner. Both frequency and phase encoding gradients introduce variation of the magnetic field, and consequently of the precession frequency, in the selected slice (the xy plane in our example). Linear variations of the magnetic field create "waves" of phases of the transverse polarization, as shown in Figures 13.8 and 13.9. The waves propagate in the x or y direction, respectively, if the gradients G_x and G_y are applied separately. Simultaneous application of both gradients generates waves spreading in a direction given by the relative ratio of the gradient strengths (Figure 13.8B). Each imaging experiment consists of a series of measurements with a different setting of the gradients. Each combination of the gradients can be described by two parameters, k_x and k_y, that can be combined in a vector (the vector $\vec{k}$ in Figure 13.8B). The values of k_x and k_y vary as the acquisition time proceeds in the case of the frequency encoding gradient, or as the strength of the phase encoding gradient is incremented (see Sections 13.4.6 and 13.4.7 for details). Each panel in Figure 13.9 represents a phase wave for a particular value of k_x and k_y. In terms of the phase waves, the direction of $\vec{k}$ defines the direction of the wave propagation and the magnitude of $\vec{k}$ says how
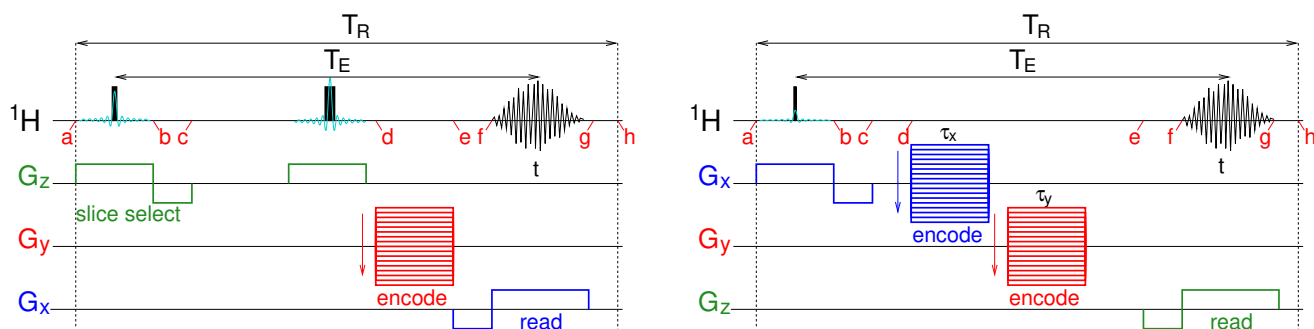
Figure 13.7: Examples of slice-selective 2D imaging experiment, combining phase and frequency encoding (left) and of 3D phase encoding imaging experiment (right). The frequency and phase encode gradients are labeled "read" and "encode" respectively. T_E and T_R are echo time and repetition time, respectively. Gradients of B_0 in the x, y, and z direction are shown in blue, red, and green, respectively. The radio wave pulses ($90°$ in the left panel and $10°$ in the right panel) are shown schematically as filled black rectangles, the actual modulation of the radio-wave amplitude is depicted in cyan. The $180°$ pulse in the left panel creates an echo that refocuses evolution of residual Ω (due to the field inhomogeneity). The first G_x gradient in the right panel allows us to reduce the phase encoding to a limited range of x. Therefore fewer phase encoding steps can be used without problems with aliasing (longer Δk_x can be used to achieve a good resolution by having larger $N_x \Delta k_x$ with lower N_x).

dense the waves are. We see that $\vec{k}$ behaves as a *wave vector* describing any other physical waves (e.g. electromagnetic waves), and we can expect that the signal reconstruction is based on similar principles as the analysis of diffraction patterns providing the structure of the diffracting objects.

Instead of describing the image reconstruction technically (it is done in Sections 13.4.6 and 13.4.7), here we try to get a general idea by inspecting Figure 13.8. For the sake of simplicity, we assume that all observed nuclei have the same chemical shift.[1] Figure 13.8A shows transverse polarization phases in the absence of gradients. The phases are aligned at the beginning of the experiment and move coherently, i.e., do not move at all in the coordinate frame rotating with the frequency $-\omega_{radio}$ (Figure 13.8A). In the absence of the gradients ($k_x = k_y = 0$), the coherent arrangement of the phases depicted in Figure 13.8A does not change (except for relaxation effects and technical imperfections). We therefore record a signal proportional to the number of observed nuclei in the slice and to the magnetic moment distribution in equilibrium (our constant κ). The application of gradients redistributes the phases as shown in Figure 13.8B. Local transverse polarizations (magnetizations) pointing in opposite directions at different sites of the slice cancel each other, and the net transverse magnetization of the whole slice is very small (equal to zero in Figure 13.8B). We see that the gradients greatly reduce the signal in slices with a uniform distribution of the magnetic moments (of the *spin density*). What happens if the magnetic moments (the spin density) are not distributed uniformly, but have some *structure*? For example, if bones (containing much less protons than soft tissues) intersect the slice? If the structure is periodic (e.g. like ribs) and if it has a period and orientation matching the period and direction of the phase waves, the signal may greatly increase because protons are concentrated in the regions of the slice with a similar phase of the transverse

---

[1]The chemical shift differences (e.g. between aliphatic protons of lipids and protons in water) result in artifacts, displacements of the apparent positions of the observed molecules in the image.
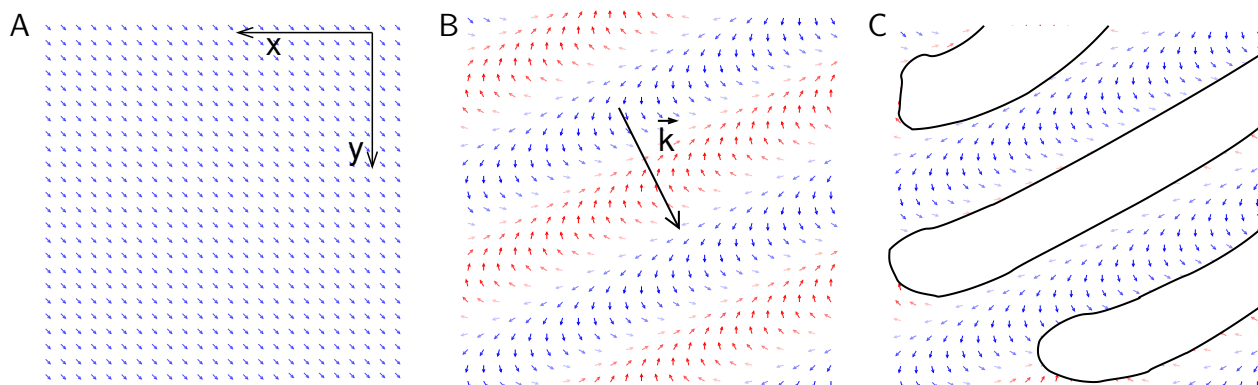
Figure 13.8: Coherent phase distribution (A) and a phase wave generated by the gradients G_x and G_y in selected axial slice with a uniform spin density (B) and with a low-spin density structure (C). The wave vector $\vec{k}$ is depicted in Panel B.

polarization (magnetization). An example is shown in Figure 13.8C.

The example of Figure 13.8C represents an extreme case of signal enhancement. Most structures in the human body are not periodic as the ribs. But any deviation from the uniform distribution of protons perturbs the regular patterns of phase waves resulting in net transverse magnetization close to zero. Each wave interferes with the given structure differently. Therefore, the signal obtained for different k_x and k_y varies. Mathematically, the set of all values of k_x, k_y (and k_z in some experiments) forms a two-dimensional (or three-dimensional) space, called *k-space*. Each combination of gradients represents one point in the k-space. If we plot the values of the signal obtained for different gradient settings in the order of increasing k_x and k_y, we obtain a picture of the imaged object in the k-space. The task of the image reconstruction is to convert this picture into dependence of the spin density on the coordinates x and y. A very simple example is provided in Figure 13.10. Although the signal is calculated only for 25 different $\vec{k}$ values in Figure 13.10, it exhibits some general features. For example, comparison of data collected for shapes with increasing complexity documents that higher values of k_x, k_y (data further from the middle of the k-space) reflect finer structural details.

In reality, there is a straightforward relation between the shape of the imaged object in a real space (described by the coordinates x, y, and z in some experiments) and the shape of the object's picture in the k-space (described by the "coordinates" k_x, k_y, and k_z in some experiments). As shown in Sections 13.4.6 and 13.4.7, the dependence of the signal on the distribution of the magnetic moments (spin density) in the x, y plane (and in space in general) has a form of the Fourier transformation. Therefore, the distribution of the spin density, defining the shape of the object, can be calculated simply by applying the inverse Fourier transformation.

13.3   Weighting

The NMR spectroscopy of diluted chemical compounds is often limited by the inherently low sensitivity of the NMR experiments. However, the highest possible sensitivity is not the ultimate goal of imaging. It is much more important to obtain a *high contrast*. It does not help us to get a very bright
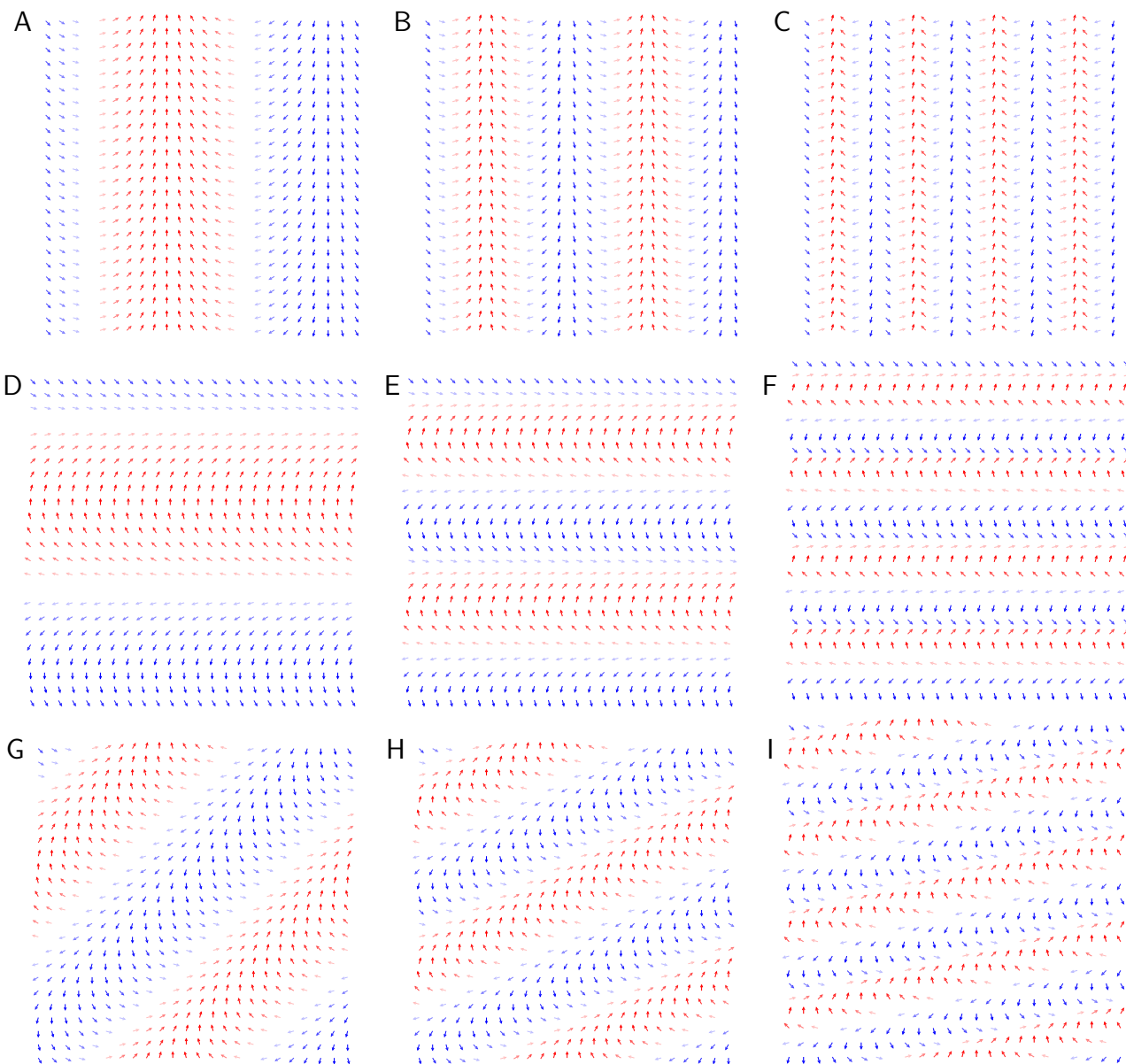
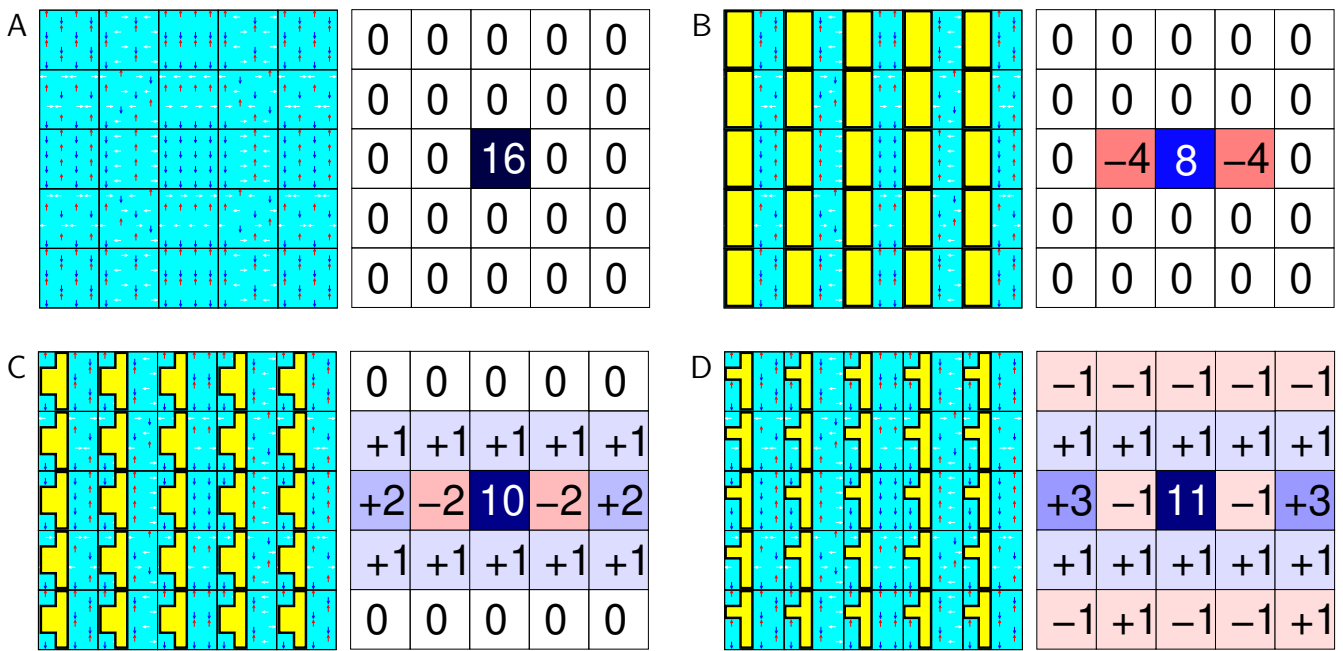Figure 13.9: Phase waves generated in the selected axial slice by the gradients G_x and G_y.

Figure 13.10: A simple example of image reconstruction. In each panel, phase waves (left) and obtained relative signal intensities (right) are shown for 25 different gradient settings (25 small squares). The phases are presented as arrows, color-coded as in Figure 13.1 ($+M_x$ in blue, $-M_x$ in red, $\pm M_y$ in white). The signal intensities are displayed as numbers and corresponding colors (positive and negative intensities are shown in blue and red). Imaging of an object with uniform proton density (A) and with structures of three different shapes (B–D) is presented. Matter with high and low proton density is shown in cyan and yellow, respectively. The depicted waves correspond to the k_x values of $2\Delta k_x$, Δk_x, 0, $-\Delta k_x$, and $-2\Delta k_x$ (top-to-bottom) and to k_y values of $2\Delta k_y$, Δk_y, 0, $-\Delta k_y$, and $-2\Delta k_y$ (right-to-left).

336

image of the human body if we cannot distinguish individual organs and finer structural details. So far, we discussed how magnetic resonance imaging reflects the variations in the local concentration of magnetic moments (spin density). But the signal is also influenced by the relaxation. The relaxation gives us a unique opportunity to distinguish regions of the body where protons are present in similar concentrations but in molecules with different dynamics and consequently different relaxation. Among numerous, often sophisticated imaging techniques, three major approaches can be recognized.

- *Spin density weighting.* The highest possible signal, depending only on the spin density is obtained if the experiment starts from the thermodynamic equilibrium and the transverse relaxation does not decrease the signal significantly. This is the case if (i) the time between the individual measurements is much longer than $1/R_1$ (where R_1 is the relaxation constant of *longitudinal relaxation* which drives the system back to the equilibrium) and (ii) the duration of the experiment is much shorter than $1/R_2$ (where R_2 is the relaxation constant of *transverse relaxation* which is the source of the signal decay). Therefore, the spin density weighted experiments are run with a *short echo time* T_E and a *long repetition time* T_R.

- *T_2 weighting.* The signal strongly depending on the relaxation constant R_2 (or on the relaxation time $T_2 = 1/R_2$) is obtained if (i) the time between the individual measurements is much longer than $1/R_1$ and (ii) the duration of the experiment is such that the differences in the factors $e^{-R_2 T_E}$ of different molecules are most pronounced. Therefore, the T_2 weighted experiments are run with a *long echo time* T_E and a *long repetition time* T_R. As R_2 is mostly given by $J(0)$ and $J(0)$ is proportional to the rotational correlation time (cf. Eq 2.6), the T_2-weighted signal is most attenuated for slowly reorienting molecules (molecules in firm tissues).

- *T_1 weighting.* The signal strongly depending on the relaxation constant R_1 (or on the relaxation time $T_1 = 1/R_1$) is obtained if (i) the time between the individual measurements is comparable to $1/R_1$ and (ii) the duration of the experiment is is much shorter than $1/R_2$. Therefore, the T_1 weighted experiments are run with a *short echo time* T_E and a *short repetition time* T_R. In contrast to R_2, the major contribution to R_1 is $J(\omega_0)$, which has a maximum (in the approximation of Eq. 9.32) for the rotational correlation time equal to $1/\omega_0$, i.e. 3.75 ns at 1 T or 1.25 ns at 3 T. Therefore, the highest contrast of T_1-weighted signal is obtained for molecules with intermediate (low-nanosecond) dynamics (molecules in semi-firm tissues).

13.4 SUPPORTING INFORMATION

13.4.1 Coherence dephasing and slice selection by field gradients

Quantitatively, the magnetic field gradient in the direction z is defined as $G_z = \Delta B_0/\Delta z$. The same applies to gradients applied in other directions: $G_x = \Delta B_0/\Delta x$, $G_y = \Delta B_0/\Delta y$. Note that all gradient describe linear perturbations of the *vertical* magnetic field $\vec{B}_0$. As the precession frequency ω_0, and consequently the frequency offset $\Omega = \omega_0 - \omega_{\rm rot} = \omega_0 - (-\omega_{\rm radio})$, are proportional to B_0, the gradient makes the frequency dependent on the position:

$$\Omega'(x) = \Omega - \gamma G_x x, \quad \Omega'(y) = \Omega - \gamma G_y y, \quad \Omega'(z) = \Omega - \gamma G_z z, \tag{13.5}$$

where we set the origins of the axes x, y, z at the place where the gradient has no effect. For the sake of simplicity, we analyze the effect of the gradients for magnetic moments not influenced by interactions with electrons and other magnetic dipoles (i.e., we assume that all molecules have the same chemical shift and the dipole-dipole and J couplings are not present or can be neglected). We start with a density matrix describing an ensemble of magnetic moments uniformly rotated by a 90° radio wave pulse from the equilibrium distribution $\hat{\rho}(0) = \mathscr{I}_t - \kappa \mathscr{I}_y$ (Figure 13.4). Then we apply a gradient, e.g. in the z direction. The density matrix at evolves as

$$\hat{\rho}(t) = \mathscr{I}_t - \kappa \mathscr{I}_y \overline{\cos(\Omega'(z)t)} + \kappa \mathscr{I}_x \overline{\sin(\Omega'(z)t)} = \mathscr{I}_t - \kappa \mathscr{I}_y \overline{\cos((\Omega - \gamma G_z z)t)} + \kappa \mathscr{I}_x \overline{\sin((\Omega - \gamma G_z z)t)} = \mathscr{I}_t - \kappa \mathscr{I}_y \overline{\cos \phi(z,t)} + \kappa \mathscr{I}_x \overline{\sin \phi(z,t)}, \tag{13.6}$$

where the horizontal bar indicates ensemble averaging. The expected value of the transverse magnetization is

$$\langle M_+ \rangle(t) = \mathrm{Tr}\{\hat{\rho}(t)\hat{M}_+\} = -\mathcal{N} \frac{\gamma^2 \hbar^2 B_0}{2 k_{\rm B} T} \mathrm{Tr}\{\mathscr{I}_y \mathscr{I}_+\} \overline{\cos((\Omega - \gamma G_z z)t)} + \mathcal{N} \frac{\gamma^2 \hbar^2 B_0}{2 k_{\rm B} T} \mathrm{Tr}\{\mathscr{I}_x \mathscr{I}_+\} \overline{\sin((\Omega - \gamma G_z z)t)}$$

$$= \mathcal{N} \frac{\gamma^2 \hbar^2 B_0}{4 k_{\rm B} T} \mathrm{e}^{\mathrm{i}\frac{\pi}{2}} \overline{\mathrm{e}^{\mathrm{i}(\Omega - \gamma G_z z)t}}, \tag{13.7}$$

Performing the phase correction and including the relaxation,

$$\langle M_+ \rangle(t) = \mathcal{N} \frac{\gamma^2 \hbar^2 B_0}{4 k_{\rm B} T} \mathrm{e}^{-R_2 t} \overline{\mathrm{e}^{\mathrm{i}(\Omega t - \gamma G_z z)t}} = \mathcal{N} \frac{\gamma^2 \hbar^2 B_0}{4 k_{\rm B} T} \mathrm{e}^{-R_2 t} \left(\overline{\cos((\Omega - \gamma G_z z)t)} + \overline{\mathrm{i}\sin((\Omega - \gamma G_z z)t)} \right). \tag{13.8}$$

If the gradient is sufficiently strong, the sine and cosine terms oscillate rapidly with frequencies depending on z and their ensemble averages tend to zero. Let us now assume that the gradient is applied not after the 90° pulse, but *during* the excitation pulse. Then, the resonance condition is fulfilled exactly only for a certain value of $\gamma G_z z$ that matches the chemical shift (position-independent frequency offset Ω), $\Omega = \gamma G_z z$. Therefore, the strongest signal is obtained from a slice of the signal at

$$z = \frac{\Omega}{\gamma G_z} = \frac{\omega_0 - \omega_{\rm rot}}{\gamma G_z} = \frac{\omega_0 - (-\omega_{\rm radio})}{\gamma G_z}. \tag{13.9}$$

The reduction of the signal form other vertical positions is given by the excitation profile of the 90° pulse. The thickness of the slice depends on the value of G_z (the stronger G_z the thinner the slice) and the position z can be varied by changing the carrier frequency of the radio wave $\omega_{\rm radio}$. The dependence of the magnetization on the position in the investigated sample is used in different manners in NMR spectroscopy and imaging:

- In NMR spectroscopy of samples with relatively low concentrations of the studied substance, the signal, obtained only from a selected slice would be very low, often below the limit of detection. Usually, a 90° pulse applied in the absence of gradients creates transverse magnetization in the whole sample and a gradient is applied later to de-phase magnetization at different positions. This is the principle of the action of cleaning gradients and gradient echoes destroying coherences that are not interesting. The use of gradients in the NMR spectroscopy is discussed in Section 13.1, and further analyzed in Sections 13.4.2–13.4.3.

- If the concentration of the detected compound is sufficiently high and the transverse magnetization in the selected slice is observable, the signal from different slices can be compared and further investigated. This is interesting especially if the number of magnetic moments per volume element, or the *spin density* $\mathcal{N}(z)$ varies in the z direction. Detection of the magnetization dependent on the spin density in individual selected slices is the basis of slice-selective imaging, described in Sections 13.4.5ff.

13.4.2 Field gradients with smooth amplitude

In NMR pulse sequences, the gradient is usually not switched on and off suddenly. Instead, the linear magnetic field perturbation is increased and decreased in a smooth fashion, following for example a function $\sin(\pi t/\tau_z)$ for a gradient that starts at $t = 0$ and is finished at $t = \tau_z$. In such a case, the total rotation angle of the transverse polarization (the phase ϕ) is

$$\phi(z,t) = \Omega t - \gamma z \frac{\Delta B_0(t = \tau_z/2)}{\Delta z} \int\limits_0^{\tau_z} \sin\frac{\pi t}{\tau_z}\mathrm{d}t. \tag{13.10}$$

Because the ratio

$$\frac{\int\limits_0^t f(t')\mathrm{d}t'}{t} \tag{13.11}$$

is constant (definition of the average value of $f(t)$), it is convenient to absorb the effect of the smooth amplitude of the gradient into the value of G_z:

$$\phi(z,\tau_z) = \Omega\tau_z - \gamma z \underbrace{\frac{\Delta B_0(t = \tau_z/2)}{\Delta z} \frac{\int\limits_0^{\tau_z}\sin\frac{\pi t}{\tau_z}\mathrm{d}t}{\tau_z}}_{G_z} \tau_z = \Omega\tau_z - \gamma G_z z\tau_z. \tag{13.12}$$

The equations describing actions of gradients can be modified for the gradients with a smooth amplitude (*shaped gradients*) by changing t to τ_z.

13.4.3 Coherence selection by pulsed-field gradients

Unwanted coherences can be suppressed by *cleaning gradients* and *gradient echoes*. The principle of cleaning gradients (e.g. the magenta gradient in Figure 13.3) is fairly simple. Phases of magnetizations corresponding to a coherence evolving during the gradient at different vertical positions in the sample are spread to the whole xy plane, resulting in the zero overall transverse magnetization.

The product operator analysis of *gradient echoes* is also straightforward. Let us assume that the density matrix at the beginning of the echoes presented in Figure 13.2 is

$$\hat{\rho}(0) = \mathscr{I}_t - \frac{1}{2}\kappa_1\mathscr{I}_y - \frac{1}{2}\kappa_2\mathscr{S}_y, \tag{13.13}$$

where $\mathscr{I}_y$ is the desired coherence and $\mathscr{S}_y$ is the undesired one. The density matrix at the end of the first delay τ in Figure 13.2 is (cf. Eq. 13.6)

$$\hat{\rho}(t) = \mathscr{I}_t - \frac{1}{2}\kappa_1\overline{\cos(\Omega\tau - \gamma_1 G_z z\tau_z)} + \frac{1}{2}\kappa_1\mathscr{I}_x\overline{\sin(\Omega\tau - \gamma_1 G_z z\tau_z)} - \frac{1}{2}\kappa_2\overline{\cos(\Omega\tau - \gamma_2 G_z z\tau_z)} + \frac{1}{2}\kappa_2\mathscr{I}_x\overline{\sin(\Omega\tau - \gamma_2 G_z z\tau_z)}$$

$$= \mathscr{I}_t - \frac{1}{2}\kappa_1\mathscr{I}_y\overline{c_{11}} + \frac{1}{2}\kappa_1\mathscr{I}_x\overline{s_{11}} - \frac{1}{2}\kappa_1\mathscr{S}_y\overline{c_{21}} + \frac{1}{2}\kappa_1\mathscr{S}_x\overline{s_{21}}. \tag{13.14}$$

The following 180° radio-wave pulse in the left echo in Figure 13.2, influencing only the wanted coherences converts the density matrix to

$$\hat{\rho}(t) = \mathscr{I}_t + \frac{1}{2}\kappa_1\mathscr{I}_y\overline{c_{11}} + \frac{1}{2}\kappa_1\mathscr{I}_x\overline{s_{11}} - \frac{1}{2}\kappa_1\mathscr{S}_y\overline{c_{21}} + \frac{1}{2}\kappa_1\mathscr{S}_x\overline{s_{21}}, \tag{13.15}$$

which evolves during the second delay τ to

$$\hat{\rho}(t) = \mathscr{I}_t + \frac{1}{2}\kappa_1\mathscr{I}_y\overline{(c_{11}c_{12} + s_{11}s_{12})} + \frac{1}{2}\kappa_1\mathscr{I}_x\overline{(c_{11}s_{12} - s_{11}c_{12})} - \frac{1}{2}\kappa_1\mathscr{S}_y\overline{(c_{21}c_{22} - s_{21}s_{22})} + \frac{1}{2}\kappa_1\mathscr{S}_x\overline{(c_{21}s_{22} + s_{21}c_{22})}. \tag{13.16}$$

As the second gradient in the left echo in Figure 13.2 is the same as the first one,

$$\overline{c_{11}c_{12} + s_{11}s_{12}} = \overline{c_{11}^2 + s_{11}^2} = 1 \qquad \overline{c_{11}s_{12} - s_{11}c_{12}} = \overline{c_{11}s_{11} - c_{11}s_{11}} = 0, \tag{13.17}$$

$$\overline{c_{21}c_{22} - s_{21}s_{22}} = \overline{c_{21}^2 - s_{21}^2} \qquad \overline{c_{21}s_{22} + s_{21}c_{22}} = \hat{\rho}(\mathrm{b}) = \frac{1}{2}\mathscr{I}_t - \frac{\kappa}{2}\mathscr{I}_{1y} - \frac{\kappa}{2}\mathscr{I}_{2y}\overline{c_{21}s_{21} + c_{21}s_{21}}, \tag{13.18}$$

and

$$\hat{\rho}(t) = \frac{1}{2}\kappa_1\mathscr{I}_y - \frac{1}{2}\kappa_2\mathscr{S}_y\overline{\cos(\Omega(2\tau) - \gamma_2 G_z z(2\tau_z))} + \frac{1}{2}\kappa_2\mathscr{S}_x\overline{\sin(\Omega(2\tau) - \gamma_2 G_z z(2\tau_z))},$$ (13.19)

where the red terms provide only a very small signal in the selected slice. The $\mathscr{S}_x$ and $\mathscr{S}_y$ symbols may represent a nucleus we are not interested in, or a portion of the coherence of the observed nucleus that is not refocused due to the offset effects. The cyna gradient echoes in Figure 13.3 represent such an application.

Analysis of the right gradient echo in Figure 13.2 is similar. The $180°$ radio-wave pulse following the first delay τ in the right echo in Figure 13.2 influences only the unwanted coherences and converts the density matrix to

$$\hat{\rho}(t) = \mathscr{I}_t - \frac{1}{2}\kappa_1\mathscr{I}_y\overline{c_{11}} + \frac{1}{2}\kappa_1\mathscr{I}_x\overline{s_{11}} + \frac{1}{2}\kappa_1\mathscr{S}_y\overline{c_{21}} + \frac{1}{2}\kappa_1\mathscr{S}_x\overline{s_{21}},$$ (13.20)

which evolves during the second delay τ to

$$\hat{\rho}(t) = \mathscr{I}_t - \frac{1}{2}\kappa_1\mathscr{I}_y\overline{(c_{11}c_{12} - s_{11}s_{12})} + \frac{1}{2}\kappa_1\mathscr{I}_x\overline{(c_{11}s_{12} + s_{11}c_{12})} + \frac{1}{2}\kappa_1\mathscr{S}_y\overline{(c_{21}c_{22} + s_{21}s_{22})} - \frac{1}{2}\kappa_1\mathscr{S}_x\overline{(c_{21}s_{22} - s_{21}c_{22})}.$$ (13.21)

As the second gradients in the right echo in Figure 13.2 has the opposite effect than the first one,

$$\overline{c_{11}c_{12} - s_{11}s_{12}} = \overline{\cos(\Omega\tau - \gamma_1 G_z z\tau_z)\cos(\Omega\tau + \gamma_1 G_z z\tau_z) - \sin(\Omega\tau - \gamma_1 G_z z\tau_z)\sin(\Omega\tau + \gamma_1 G_z z\tau_z)} = \cos(2\Omega\tau),$$ (13.22)

$$\overline{c_{11}s_{12} + s_{11}c_{12}} = \overline{\cos(\Omega\tau - \gamma_1 G_z z\tau_z)\sin(\Omega\tau + \gamma_1 G_z z\tau_z) + \cos(\Omega\tau - \gamma_1 G_z z\tau_z)\sin(\Omega\tau + \gamma_1 G_z z\tau_z)} = \sin(2\Omega\tau),$$ (13.23)

$$\overline{c_{21}c_{22} + s_{21}s_{22}} = \overline{\cos(\Omega\tau - \gamma_1 G_z z\tau_z)\cos(\Omega\tau + \gamma_1 G_z z\tau_z) + \sin(\Omega\tau - \gamma_1 G_z z\tau_z)\sin(\Omega\tau + \gamma_1 G_z z\tau_z)} = \overline{\cos(2\gamma_1 G_z z\tau_z)},$$ (13.24)

$$\overline{c_{21}s_{22} - s_{21}c_{22}} = \overline{\cos(\Omega\tau - \gamma_1 G_z z\tau_z)\sin(\Omega\tau + \gamma_1 G_z z\tau_z) - \sin(\Omega\tau - \gamma_1 G_z z\tau_z)\cos(\Omega\tau + \gamma_1 G_z z\tau_z)} = \overline{\sin(2\gamma_1 G_z z\tau_z)},$$ (13.25)

and

$$\hat{\rho}(t) = -\frac{1}{2}\kappa_1\mathscr{I}_y\cos(2\Omega\tau) + \frac{1}{2}\kappa_1\mathscr{I}_x\sin(2\Omega\tau) + \frac{1}{2}\kappa_2\mathscr{S}_y\overline{\cos(2\gamma_2 G_z z\tau_z)} + \frac{1}{2}\kappa_2\mathscr{S}_x\overline{\sin(2\gamma_2 G_z z\tau_z)},$$ (13.26)

where the red terms again provide only a negligible signal (the averaged sines and cosines tend to zero because the arguments range from $-\pi$ to π). Note that the chemical shift evolution is not refocused because no $180°$ pulse affects the desired coherences in the right echo in Figure 13.2. It suggests that the right gradient echo presented in Figure 13.2 can be used to select the desired coherences during the incremented delays introducing the indirect time dimension (t_1).

13.4.4 Pulsed-field gradients and frequency discrimination

The green and blue gradients in Figure 13.3 (gradient-enhanced HSQC experiment) represent a gradient echo that selects only the coherences that evolve with the frequency of ^{13}C or ^{15}N in t_1 and with the proton frequency in t_2. Following the analysis presented in Section 11.5, the density matrix at point f in Figure 13.3 is

$\hat{\rho}(f) = \frac{1}{2}\mathscr{I}_t + \frac{1}{2}\kappa_1(c_{21}2\mathscr{I}_z\mathscr{S}_y - s_{21}2\mathscr{I}_z\mathscr{S}_x) + \frac{1}{2}\kappa_2(c_{21}\mathscr{S}_y - s_{21}\mathscr{S}_x)$.

The sequence in Figure 13.3 continues by a refocusing echo with the green gradient. The analysis in Section 11.5 shows that the red or green terms do not contribute to the observed signal. Therefore, we analyze here only the fate of the blue terms. Combination of the chemical shift evolution during t_1 and during the gradient echo results in

$\hat{\rho}(g) = \frac{1}{2}\kappa_1(\cos(\Omega_2 t_1)\overline{\sin(\gamma_2 G_{z1}\tau_{z1})} + \sin(\Omega_2 t_1)\overline{\cos(\gamma_2 G_{z1}\tau_{z1})})2\mathscr{I}_z\mathscr{S}_x + \frac{1}{2}\kappa_1(\sin(\Omega_2 t_1)\overline{\sin(\gamma_2 G_{z1}\tau_{z1})} - \cos(\Omega_2 t_1)\overline{\cos(\gamma_2 G_{z1}\tau_{z1})})2\mathscr{I}_z\mathscr{S}_y + \dots$

$= \frac{1}{2}\kappa_1\overline{\sin(\Omega_2 t_1 + \gamma_2 G_{z1}\tau_{z1})}2\mathscr{I}_z\mathscr{S}_x - \frac{1}{2}\kappa_1\overline{\cos(\Omega_2 t_1 + \gamma_2 G_{z1}\tau_{z1})}2\mathscr{I}_z\mathscr{S}_y + \dots$

The following two $90°$ pulses with x phase convert $-2\mathscr{I}_z\mathscr{S}_y$ to $2\mathscr{I}_y\mathscr{S}_z$, which evolves to $\mathscr{I}_x$ during the second INEPT, and $2\mathscr{I}_z\mathscr{S}_x$ to a multiple-quantum coherence $2\mathscr{I}_y\mathscr{S}_x$, which does not contribute to the signal. The chemical shift evolution during the blue gradient combines with the chemical shift evolution during t_2 and results in

$\hat{\rho}(t_2) = \frac{1}{2}\kappa_1\overline{\cos(\Omega_2 t_1 + \gamma_2 G_{z1}\tau_{z1})}\overline{\cos(\Omega_1 t_2 + \gamma_1 G_{z2}\tau_{z2})}\mathscr{I}_x - \frac{1}{2}\kappa_1\overline{\cos(\Omega_2 t_1 + \gamma_2 G_{z1}\tau_{z1})}\overline{\sin(\Omega_1 t_2 + \gamma_1 G_{z2}\tau_{z2})}\mathscr{I}_y + \dots$

$= \frac{1}{4}\kappa_1(\overline{\cos(\Omega_2 t_1 + \Omega_1 t_2 + \gamma_2 G_{z1}\tau_{z1} + \gamma_1 G_{z2}\tau_{z2})} + \overline{\cos(\Omega_2 t_1 - \Omega_1 t_2 + \gamma_2 G_{z1}\tau_{z1} - \gamma_1 G_{z2}\tau_{z2})})\mathscr{I}_x$

$+ \frac{1}{4}\kappa_1(-\overline{\sin(\Omega_2 t_1 + \Omega_1 t_2 + \gamma_2 G_{z1}\tau_{z1} + \gamma_1 G_{z2}\tau_{z2})} + \overline{\sin(\Omega_2 t_1 - \Omega_1 t_2 + \gamma_2 G_{z1}\tau_{z1} - \gamma_1 G_{z2}\tau_{z2})})\mathscr{I}_y + \dots$

Calculating the trace of $\hat{\rho}(t_2)\hat{M}_+$, proportional to $\hat{\rho}(t_2)\mathscr{I}_+$, shows that the observable signal is modulated as

$\frac{1}{4}\kappa_1(\overline{\cos(\Omega_2 t_1 + \Omega_1 t_2 + \gamma_2 G_{z1}\tau_{z1} + \gamma_1 G_{z2}\tau_{z2})} + \overline{\cos(\Omega_2 t_1 - \Omega_1 t_2 + \gamma_2 G_{z1}\tau_{z1} - \gamma_1 G_{z2}\tau_{z2})})$

$+ \frac{1}{4}\kappa_1(-\overline{\sin(\Omega_2 t_1 + \Omega_1 t_2 + \gamma_2 G_{z1}\tau_{z1} + \gamma_1 G_{z2}\tau_{z2})} + \overline{\sin(\Omega_2 t_1 - \Omega_1 t_2 + \gamma_2 G_{z1}\tau_{z1} - \gamma_1 G_{z2}\tau_{z2})})$

$= \frac{1}{4}\left(e^{+i(\Omega_2 t_1)}e^{-i(\Omega_1 t_2)}\overline{e^{+i(\gamma_2 G_{z1}\tau_{z1} - \gamma_1 G_{z2}\tau_{z2})}} + e^{-i(\Omega_2 t_1)}e^{-i(\Omega_1 t_2)}\overline{e^{-i(\gamma_2 G_{z1}\tau_{z1} + \gamma_1 G_{z2}\tau_{z2})}}\right).$

The green and blue gradients make an echo if $+\gamma_2 G_{z1}\tau_{z1} - \gamma_1 G_{z2}\tau_{z2} = 0$ (note that $\hat{\rho}$ evolves with the chemical shift Ω_2, proportional to γ_2, during the green gradient, but with the chemical shift Ω_1, proportional to γ_1, during the blue gradient). With such setting of the gradients, the signal is modulated as

$$e^{+i(\Omega_2 t_1)}e^{-i(\Omega_1 t_2)} + e^{-i(\Omega_2 t_1)}e^{-i(\Omega_1 t_2)}\overline{e^{-i(\gamma_2 G_{z1}\tau_{z1} + \gamma_1 G_{z2}\tau_{z2})}}, \tag{13.27}$$

where the red term results only in a very weak signal in the selected slice. This is a remarkable result, showing that the *frequency discrimination* is achieved without the need to repeat the acquisition with a phase of a 90° pulse shifted by 90° (note that the Fourier transform of $e^{i(\Omega t)}$ is a signal with only one peak at the right frequency Ω). However, the Fourier transformation of the obtained signal yields phase-twisted peaks, as described in Section 9.5.1. Therefore, the acquisition *is repeated* while shifting a phase of the 90° pulse following the green gradient by 90° (the red mark y in Figure 13.3). In the repeated acquisition, the two 90° pulses convert $2\mathscr{I}_z\mathscr{S}_x$ to $2\mathscr{I}_z\mathscr{S}_y$, which evolves to $\mathscr{I}_x$ during the second INEPT, and $2\mathscr{I}_z\mathscr{S}_y$ to a multiple-quantum coherence $2\mathscr{I}_y\mathscr{S}_y$, which does not contribute to the signal. The chemical shift evolution during the second gradient (labeled in red for the repeated experiment) and during t_1

$\hat{\rho}(t_2) = \frac{1}{2}\kappa_1 \overline{\sin(\Omega_2 t_1 + \gamma_2 G_{z1}\tau_{z1})}\cos(\Omega_1 t_2 + \gamma_1 G_{z2}\tau_{z2})\mathscr{I}_x - \frac{1}{2}\kappa_1 \overline{\sin(\Omega_2 t_1 + \gamma_2 G_{z1}\tau_{z1})}\sin(\Omega_1 t_2 + \gamma_1 G_{z2}\tau_{z2})\mathscr{I}_y + \dots$

$= \frac{1}{4}\kappa_1 \overline{(\sin(\Omega_2 t_1 + \Omega_1 t_2 + \gamma_2 G_{z1}\tau_{z1} + \gamma_1 G_{z2}\tau_{z2})} + \overline{\sin(\Omega_2 t_1 - \Omega_1 t_2 + \gamma_2 G_{z1}\tau_{z1} - \gamma_1 G_{z2}\tau_{z2}))}\mathscr{I}_x$

$+ \frac{1}{4}\kappa_1 \overline{(\cos(\Omega_2 t_1 + \Omega_1 t_2 + \gamma_2 G_{z1}\tau_{z1} + \gamma_1 G_{z2}\tau_{z2})} - \overline{\cos(\Omega_2 t_1 - \Omega_1 t_2 + \gamma_2 G_{z1}\tau_{z1} - \gamma_1 G_{z2}\tau_{z2}))}\mathscr{I}_y + \dots$

Calculating the trace of $\hat{\rho}(t_2)\hat{M}_+$, proportional to $\hat{\rho}(t_2)\mathscr{I}_+$, shows that the observable signal is modulated as

$\frac{1}{4}\kappa_1 \overline{(\sin(\Omega_2 t_1 + \Omega_1 t_2 + \gamma_2 G_{z1}\tau_{z1} + \gamma_1 G_{z2}\tau_{z2})} + \overline{\sin(\Omega_2 t_1 - \Omega_1 t_2 + \gamma_2 G_{z1}\tau_{z1} - \gamma_1 G_{z2}\tau_{z2}))}$

$+ \frac{1}{4}\kappa_1 \overline{(\cos(\Omega_2 t_1 + \Omega_1 t_2 + \gamma_2 G_{z1}\tau_{z1} + \gamma_1 G_{z2}\tau_{z2})} - \overline{\cos(\Omega_2 t_1 - \Omega_1 t_2 + \gamma_2 G_{z1}\tau_{z1} - \gamma_1 G_{z2}\tau_{z2}))}$

$= \frac{1}{4}\left(e^{-i(\Omega_2 t_1)}e^{-i(\Omega_1 t_2)}\overline{e^{-i(\gamma_2 G_{z1}\tau_{z1} + \gamma_1 G_{z2}\tau_{z2})}} - e^{+i(\Omega_2 t_1)}e^{-i(\Omega_1 t_2)}\overline{e^{+i(\gamma_2 G_{z1}\tau_{z1} - \gamma_1 G_{z2}\tau_{z2})}}\right)e^{i\pi/2}.$

Now the red gradient is applied in the opposite direction than the blue one. The green and red gradients make an echo if $\gamma_2 G_{z1}\tau_{z1} + \gamma_1 G_{z2}\tau_{z2} = 0$. With such setting of the gradients and after correcting the unimportant phase shift by $\pi/2$ (the last exponential term), the signal is modulated as

$$e^{-i(\Omega_2 t_1)}e^{-i(\Omega_1 t_2)} - e^{+i(\Omega_2 t_1)}e^{-i(\Omega_1 t_2)}\overline{e^{+i(\gamma_2 G_{z1}\tau_{z1} - \gamma_1 G_{z2}\tau_{z2})}}, \tag{13.28}$$

where the red term again results only in a very weak signal in the selected slice. Note that the signal acquired with the "blue" phase of the ^{13}C (or ^{15}N) pulse x (Eq. 13.27) is modulated by frequencies with the opposite signs in the direct and direct dimensions, whereas the signal acquired with the "red" phase of the ^{13}C (or ^{15}N) pulse y (Eq. 13.28) is modulated by frequencies with the same signs in the direct and direct dimensions. Such signals are labeled N and P, or *anti-echo* and *echo*, respectively, in the literature. The sum and the difference of Eqs. 13.27 and 13.28 yield a signal which is cosine and sine modulated, respectively, in the indirect dimension and can be processed as described in Section 9.5.1 to provide the frequency-discriminated, purely absorptive real part of the signal. However, it takes twice as long to acquire the signal of the same size, compared to the discrimination by the States-Haberkorn-Ruben method without the gradient. Therefore, the signal-to-noise ratio is lower by a factor of $\sqrt{2}$ for the same measurement time. A more sophisticated gradient HSQC experiment preserving the original sensitivity (except for some relaxation loss) has been also developed and is used routinely.

13.4.5 Slice-selective imaging

As described in Section 13.4.1, a 90° pulse applied during a gradient G_z fully rotates the magnetization to the xy plane at $z = \Omega/(\gamma G_z)$. The more z differs from $\Omega/(\gamma G_z)$, the lower is the signal.

In practice, we prefer to select signal from a region of a well defined thickness. This is achieved by applying simultaneously the gradient and a radio wave with the amplitude modulated so that magnetic moments with frequencies in a certain interval are rotated by an angle close to 90°, whereas magnetic moments with frequencies outside the selected interval are almost unaffected. The amplitude modulation is achieved by dividing a radio-wave pulse into a series of short pulses with different B_1, as described in Section 1.5.11. The modulation is shown in cyan in Figure 13.4. Then, the resonance condition $-\omega_{\text{radio}} = \omega_0 - \gamma G_z z$ is fulfilled in an interval of z defined by the range of the frequencies affected by the radio-wave pulse. The amplitude-modulated radio-wave pulse is usually relatively long and magnetic moments with different precession frequencies (within the selected range) have enough time to rotate significantly during the pulse. This rotation, of different rates at different vertical positions inside the selected slice, is refocused by a negative gradient. It can be shown that the gradients make an exact echo if the negative gradient corresponds to the second half of the positive gradient (between the middle and end of the amplitude-modulated radio-wave pulse, see Figure 13.4). The exact mathematical prove is not easy, but approximative solutions can be obtained more easily. The first insight can be obtained if we imagine that the chosen range of frequencies was selectively excited by a narrow pulse in the middle of the selection gradient (black bar in Figure 13.4). Then, no transverse magnetization exists before the pulse and the transverse magnetization created by the pulse experiences a gradient echo consisting of the second half of the positive selection gradient and by the negative refocusing gradient.

Such filtering of the signal according to the z coordinate of the observed molecule is the basis of slice-selective imaging techniques. The gradients applied in the x or y direction can be used in the same manner to select slices perpendicular to the x or y axis, respectively. In human body imaging, the coordinate system is used so that G_x, G_y, and G_z selects sagittal, coronal, and axial slices, respectively (see Figure 13.5).

13.4.6 Frequency encoding gradients

We now proceed to the imaging in the slice selected at $z \approx (\omega_0 - (-\omega_{\text{radio}}))/(\gamma G_z)$. In order to describe imaging in the x direction based on the *frequency encoding*, we analyze how the density matrix evolves during the G_x gradient in Figure 13.6. The density matrix at the

beginning of G_x is $\hat{\rho}(\text{c}) = \mathscr{I}_t - \kappa \mathscr{I}_y$ in the selected slice and $\hat{\rho}(\text{c}) = \mathscr{I}_t$ everywhere else. During G_x, $\hat{\rho}(t))$ in the slice evolves as

$$\hat{\rho}(t) = \mathscr{I}_t - \kappa \mathscr{I}_y \overline{\cos((\Omega - \gamma G_x x)t)} + \kappa \mathscr{I}_x \overline{\sin((\Omega - \gamma G_x x)t)}, \tag{13.29}$$

which can be also written as

$$\hat{\rho}(x) = \mathscr{I}_t - \kappa \mathscr{I}_y \overline{\cos((\Omega t - \gamma G_x tx)} + \kappa \mathscr{I}_x \overline{\sin((\Omega t - \gamma G_x tx)} = \mathscr{I}_t - \kappa \mathscr{I}_y \overline{\cos((\Omega t - k_x x)} + \kappa \mathscr{I}_x \overline{\sin((\Omega t - k_x x)}, \tag{13.30}$$

where k_x is the x-component of the *wave vector* $\vec{k}$ in Figure 13.8. Introducing the relaxation and performing the phase correction,

$$\langle M_+ \rangle(t) = \frac{\gamma^2 \hbar^2 B_0}{4 k_B T} e^{-R_2 \tau_z} e^{i\Omega t - R_2 t} \overline{\mathcal{N}(x) e^{-i\gamma G_x x t}}. \tag{13.31}$$

Expressing the ensemble averaging explicitly,

$$\langle M_+ \rangle(t) = \frac{\gamma^2 \hbar^2 B_0}{4 k_B T} e^{-R_2 \tau_z} e^{i\Omega t - R_2 t} \int_0^{L_x} \mathcal{N}(x) e^{-i\gamma G_x x t} \mathrm{d}x = \frac{\gamma^2 \hbar^2 B_0}{4 k_B T} e^{-R_2 \tau_z} e^{i\Omega t - R_2 t} \int_0^{L_x} \mathcal{N}(x) e^{-i k_x x} \mathrm{d}x, \tag{13.32}$$

where L_x is the size of the imaged object in the x direction.

The Fourier transformation of $\langle M_+ \rangle(t)$ gives a spectrum corresponding to

$$Y(\omega) = \frac{\gamma^2 \hbar^2 B_0}{4 k_B T} e^{-R_2 \tau_z} \int_0^{L_x} \mathcal{N}(x) \left(\frac{R_2}{R_2^2 + (\Omega - \gamma G_x x - \omega)^2} + i \frac{\Omega - \gamma G_x x - \omega}{R_2^2 + (\Omega - \gamma G_x x - \omega)^2} \right) \mathrm{d}x, \tag{13.33}$$

with the spatial distribution encoded in the apparent frequency $\Omega' = \Omega - \gamma G_x x$.

In reality, the signal is stored as N discrete data points sampled with a time increment Δt. The value $k_x = \gamma G_x t = \gamma G_x \cdot n \Delta t$ can be written as $n \Delta k_x$, where $\Delta k_x = \gamma G_x \cdot \Delta t$. The sampled time points correspond to $n \Delta t = n \Delta k_x / (\gamma G_x)$. Considering $\Delta t \Delta f = 1/N$ (Eq. 3.7), $\Delta k_x = \gamma G_x / (N \Delta f)$. The second integral in Eq. 13.32 has the form of the Fourier transformation (as $\mathcal{N}(x) = 0$ for $x < 0$ and $x > L$, the integration can be extended to $\pm \infty$). The distribution of the spin density $\mathcal{N}(x)$ can be evaluated at discrete values of $x = j \Delta x$ by the inverse discrete Fourier transformation of the signal sampled at $n \Delta t = n \Delta k_x / (\gamma G_x)$:

$$\mathcal{N}(x) = \mathcal{N}_j = \frac{4 k_B T \Delta k_x}{\gamma^2 \hbar^2 B_0 e^{-R_2 \tau_z}} \sum_{n=0}^{N-1} \langle M_+ \rangle_n e^{-(i\Omega - R_2) \frac{\Delta k_x \cdot n}{\gamma G_x}} e^{i2\pi \frac{j \cdot n}{N}}. \tag{13.34}$$

Note that all features of the discrete Fourier transformation (e.g. aliasing) are relevant for the image reconstruction.

Extending the discussion to the two-dimensional experiment (right panel in Figure 13.6), is straightforward:

$$x = j_x \Delta x \qquad k_x = \gamma G_x t_2 = \gamma G_x \cdot n_x \Delta t_2 \qquad \Delta k_x = \gamma G_x \cdot \Delta t_2 = \gamma G_x / (N_x \Delta f_2) \tag{13.35}$$

$$y = j_y \Delta y \qquad k_y = \gamma G_y t_1 = \gamma G_y \cdot n_y \Delta t_1 \qquad \Delta k_y = \gamma G_y \cdot \Delta t_1 = \gamma G_y / (N_y \Delta f_1), \tag{13.36}$$

and

$$\mathcal{N}(x,y) = \mathcal{N}_{j_x, j_y} = \Delta k_x \Delta k_y \frac{4 k_B T}{\gamma^2 \hbar^2 B_0 e^{-R_2 \tau_z}} \sum_{n_x=0}^{N_x-1} \sum_{n_y=0}^{N_y-1} \langle M_+ \rangle_{n_x, n_y} e^{-(i\Omega - R_2) \left(\frac{\Delta k_x \cdot n_x}{\gamma G_x} + \frac{\Delta k_y \cdot n_y}{\gamma G_y} \right)} e^{i2\pi \left(\frac{j_x \cdot n_x}{N_x} + \frac{j_y \cdot n_y}{N_y} \right)}. \tag{13.37}$$

13.4.7 Phase encoding gradients

In order to describe imaging in the y direction based on the *phase encoding*, we analyze how the density matrix evolves during the G_y gradient in the pulse sequence presented in the left panel in Figure 13.7. The gradient is placed in a refocusing echo of the duration T_E. We ignore the possible phase shift and assume that the density matrix at the beginning of G_y is $\hat{\rho}(\text{d}) = \mathscr{I}_t + \kappa \mathscr{I}_y$ inside the selected slice and $\hat{\rho}(\text{d}) = \mathscr{I}_t$ everywhere else. During G_y, $\hat{\rho}(\text{d})$ evolves to

$$\hat{\rho}(\text{e}) = \mathscr{I}_t + \kappa \mathscr{I}_y \overline{\cos((\Omega - \gamma G_y y)\tau_y)} - \kappa \mathscr{I}_x \overline{\sin((\Omega - \gamma G_y y)\tau_y)}, \tag{13.38}$$

where τ_y is the duration of the gradient. Expressing $\hat{\rho}(\text{e})$ as a function of y,

$$\hat{\rho}(y) = \mathscr{I}_t + \kappa \mathscr{I}_y \overline{\cos((\Omega \tau_y - \gamma G_y \tau_y y)} - \kappa \mathscr{I}_x \overline{\sin((\Omega \tau_y - \gamma G_y \tau_y y)} = \mathscr{I}_t + \kappa \mathscr{I}_y \overline{\cos((\Omega \tau_y - k_y y)} - \kappa \mathscr{I}_x \overline{\sin((\Omega \tau_y - k_y y)}. \tag{13.39}$$

During imaging, τ_y is kept constant and the phase shift $\Omega \tau_y$ is refocused by the echo. The parameter that is varied is the strength of the gradient G_y, gradually decreased from the originally positive value to a negative one by increments ΔG_y.

Then, a negative *pre-phasing* gradient G_x is applied for a time period equal to the half of the total acquisition time $N_x \Delta t/2$. Ignoring the phase shifts $\Omega \tau_x$ and $-\Omega N_x \Delta t/2$ that get refocused at T_E, the density matrix at the beginning of data acquisition is

$$\hat{\rho}(\mathrm{f}) = \mathscr{I}_t + \kappa \mathscr{I}_y \overline{\left(\cos(-\gamma G_y \tau_y y) \cos\left(+\gamma G_x \frac{N_x}{2} \Delta t x \right) - \sin(-\gamma G_y \tau_y y) \sin\left(+\gamma G_x \frac{N_x}{2} \Delta t x \right) \right)}$$
$$- \kappa \mathscr{I}_x \overline{\left(\sin(-\gamma G_y \tau_y y) \cos\left(+\gamma G_x \frac{N_x}{2} \Delta t x \right) - \cos(-\gamma G_y \tau_y y) \sin\left(+\gamma G_x \frac{N_x}{2} \Delta t x \right) \right)} \tag{13.40}$$

and further evolves during the acquisition as

$$\hat{\rho}(x,y) = \mathscr{I}_t + \kappa \mathscr{I}_y \overline{c_x c_y - s_x s_y} - \kappa \mathscr{I}_x \overline{s_x c_y + c_x s_y}, \tag{13.41}$$

where

$$s_x = \sin(k_x x) = -\sin\left(\left(\frac{N_x}{2} - n_x \right) \Delta k_x x \right) \qquad c_x = \cos(k_x x) = \cos\left(\left(\frac{N_x}{2} - n_x \right) \Delta k_x x \right) \tag{13.42}$$

$$s_y = \sin(k_y y) = -\sin\left(\left(\frac{N_y}{2} - n_y \right) \Delta k_y y \right) \qquad c_y = \cos(k_y y) = \cos\left(\left(\frac{N_y}{2} - n_y \right) \Delta k_y y \right) \tag{13.43}$$

$$x = j_x \Delta x \qquad k_x = k_x(0) + \gamma G_x t = -\left(\frac{N_x}{2} - n_x \right) \gamma G_x \Delta t \qquad \Delta k_x = -\gamma G_x \cdot \Delta t = \gamma G_x/(N_x \Delta f) \tag{13.44}$$

$$y = j_y \Delta y \qquad k_y = k_y(0) - n_y \gamma \Delta G_y \tau_y = \left(\frac{N_y}{2} - n_y \right) \gamma \tau_y \Delta G_y \qquad \Delta k_y = -\gamma \Delta G_y \cdot \tau_y. \tag{13.45}$$

The pre-phasing gradient makes the evolution of the density matrix to start from negative k_x and pass $k_x = 0$ in the middle of the experiment. The modulation by $k_x x$ and $k_y y$ thus has the same form.

Using the standard trigonometric relations,

$$\hat{\rho}(x,y) = \mathscr{I}_t + \kappa \mathscr{I}_y \overline{\cos\left(\left(\frac{N_x}{2} - n_x \right) \Delta k_x x + \left(\frac{N_y}{2} - n_y \right) \Delta k_y y \right)} + \kappa \mathscr{I}_x \overline{\sin\left(\left(\frac{N_x}{2} - n_x \right) \Delta k_x x + \left(\frac{N_y}{2} - n_y \right) \Delta k_y y \right)}, \tag{13.46}$$

Introducing the relaxation and performing the phase correction,

$$\langle M_+ \rangle(k_x, k_y) = \frac{\gamma^2 \hbar^2 B_0}{4 k_B T} e^{-R_2 \left(T_E - \left(\frac{N_x}{2} - n_x \right) \frac{\Delta k_x}{\gamma G_x} \right)} \overline{\mathcal{N}(x,y) e^{-i \left(\left(\frac{N_x}{2} - n_x \right) \Delta k_x x + \left(\frac{N_y}{2} - n_y \right) \Delta k_y y \right)}}. \tag{13.47}$$

Expressing the ensemble averaging explicitly,

$$\langle M_+ \rangle(k_x, k_y) = \frac{\gamma^2 \hbar^2 B_0}{4 k_B T} e^{-R_2 \left(T_E - \left(\frac{N_x}{2} - n_x \right) \frac{\Delta k_x}{\gamma G_x} \right)} \int_0^{L_x} \int_0^{L_y} \mathcal{N}(x,y) e^{-i \left(\left(\frac{N_x}{2} - n_x \right) \Delta k_x x + \left(\frac{N_y}{2} - n_y \right) \Delta k_y y \right)} \mathrm{d}x \mathrm{d}y. \tag{13.48}$$

The inverse discrete Fourier transformation converts the signal into the two-dimensional image

$$\mathcal{N}(x,y) = \mathcal{N}_{j_x, j_y} = \frac{4 k_B T \Delta k_x \Delta k_y}{\gamma^2 \hbar^2 B_0 e^{-R_2 T_E}} \sum_{n_x=-\frac{N_x}{2}}^{\frac{N_x}{2}-1} \sum_{n_y=-\frac{N_y}{2}}^{\frac{N_y}{2}-1} \langle M_+ \rangle_{n_x, n_y} e^{-R_2 \left(\frac{N_x}{2} - n_x \right) \frac{\Delta k_x}{\gamma G_x}} e^{i2\pi \left(\frac{j_x \cdot n_x}{N_x} + \frac{j_y \cdot n_y}{N_y} \right)}. \tag{13.49}$$

The analysis can be easily extended to the *three-dimensional* imaging experiment presented in the right panel in Figure 13.7, where two phase-encoding gradients G_x and G_y are applied (the frequency encoding gradient is G_z). The evolution of the density matrix matrix from $\hat{\rho}(\mathrm{d})$ introduces the modulation

$$\hat{\rho}(x,y) = \mathscr{I}_t + \kappa \mathscr{I}_y \overline{c_x c_y c_z - s_x s_y c_z - s_x c_y s_z - c_x c_y c_z} - \kappa \mathscr{I}_x \overline{s_x c_y c_z + c_x s_y c_z + c_x c_y s_z - s_x s_y s_z}, \tag{13.50}$$

where

$$s_x = \sin(k_x x) = -\sin\left(\left(\frac{N_x}{2} - n_x\right)\Delta k_x x\right) \qquad c_x = \cos(k_x x) = \cos\left(\left(\frac{N_x}{2} - n_x\right)\Delta k_x x\right) \tag{13.51}$$

$$s_y = \sin(k_y y) = -\sin\left(\left(\frac{N_y}{2} - n_y\right)\Delta k_y y\right) \qquad c_y = \cos(k_y y) = \cos\left(\left(\frac{N_y}{2} - n_y\right)\Delta k_y y\right) \tag{13.52}$$

$$s_z = \sin(k_z z) = -\sin\left(\left(\frac{N_z}{2} - n_z\right)\Delta k_z z\right) \qquad c_z = \cos(k_z z) = \cos\left(\left(\frac{N_z}{2} - n_z\right)\Delta k_z z\right) \tag{13.53}$$

$$x = j_x\Delta x \qquad k_x = k_x(0) - n_x\gamma\Delta G_x\tau_x = \left(\frac{N_x}{2} - n_x\right)\gamma\tau_x\Delta G_x \qquad \Delta k_x = -\gamma\Delta G_x \cdot \tau_x \tag{13.54}$$

$$y = j_y\Delta y \qquad k_y = k_y(0) - n_y\gamma\Delta G_y\tau_y = \left(\frac{N_y}{2} - n_y\right)\gamma\tau_y\Delta G_y \qquad \Delta k_y = -\gamma\Delta G_y \cdot \tau_y \tag{13.55}$$

$$z = j_z\Delta z \qquad k_z = k_z(0) + \gamma G_z t = -\left(\frac{N_z}{2} - n_z\right)\gamma G_z\Delta t \qquad \Delta k_z = -\gamma G_z \cdot \Delta t = \gamma G_z/(N_z\Delta f). \tag{13.56}$$

The corresponding signal is

$$\langle M_+\rangle(k_x,k_y,k_z) = \frac{\gamma^2\hbar^2 B_0}{4k_B T}\mathrm{e}^{-R_2\left(T_E - \left(\frac{N_z}{2} - n_z\right)\frac{\Delta k_z}{\gamma G_z}\right)}\int\limits_0^{L_x}\int\limits_0^{L_y}\int\limits_0^{L_z}\mathcal{N}(x,y,z)\mathrm{e}^{-\mathrm{i}\left(\left(\frac{N_x}{2}-n_x\right)\Delta k_x x+\left(\frac{N_y}{2}-n_y\right)\Delta k_y y+\left(\frac{N_z}{2}-n_z\right)\Delta k_z z\right)}\mathrm{d}x\mathrm{d}y\mathrm{d}z, \tag{13.57}$$

and the inverse discrete Fourier transformation converts it into the three-dimensional image

$$\mathcal{N}(x,y,z) = \mathcal{N}_{j_x,j_y,j_z} = \frac{4k_B T\Delta k_x\Delta k_y\Delta k_z}{\gamma^2\hbar^2 B_0\mathrm{e}^{-R_2 T_E}}\sum_{n_x=-\frac{N_x}{2}}^{\frac{N_x}{2}-1}\sum_{n_y=-\frac{N_y}{2}}^{\frac{N_y}{2}-1}\sum_{n_z=-\frac{N_z}{2}}^{\frac{N_z}{2}-1}\langle M_+\rangle_{n_x,n_z,n_z}\mathrm{e}^{-R_2\left(\frac{N_z}{2}-n_z\right)\frac{\Delta k_z}{\gamma G_z}}\mathrm{e}^{\mathrm{i}2\pi\left(\frac{j_x\cdot n_x}{N_x}+\frac{j_y\cdot n_y}{N_y}+\frac{j_z\cdot n_z}{N_z}\right)}. \tag{13.58}$$